Thomas J. Bach · Michel Rohmer *Editors*

Isoprenoid Synthesis in Plants and Microorganisms

New Concepts and Experimental Approaches

Springer

Isoprenoid Synthesis in Plants and Microorganisms

Thomas J. Bach • Michel Rohmer
Editors

Isoprenoid Synthesis in Plants and Microorganisms

New Concepts and Experimental Approaches

Springer

Editors
Thomas J. Bach
Département "Réseaux métaboliques"
Institut de Biologie Moléculaire des Plantes (CNRS UPR 2357)
Université de Strasbourg
Strasbourg, France

Michel Rohmer
Institut de Chimie, UMR 7177
Université de Strasbourg
Strasbourg, France

ISBN 978-1-4614-4062-8 ISBN 978-1-4614-4063-5 (eBook)
DOI 10.1007/978-1-4614-4063-5
Springer New York Heidelberg Dordrecht London

Library of Congress Control Number: 2012946735

Printed on acid-free paper

Springer is part of Springer Science+Business Media (www.springer.com)

Preface

There is an increasing number of known metabolites that are derived from the isoprenoid pathways in plants and microorganisms, which are essential in fundamental cellular processes and in whole organisms, but also in ecological interactions. Also, their role in modern industries has spurred an intense research worldwide.

Even though research on isoprenoid synthesis and function is a rapidly developing and rather competitive field, we thought it useful to collect a number of contributions written by true and well-known experts, covering a broad spectrum of aspects. Microorganisms, plants, and even a human parasite are considered. It adds the application of modern techniques in biochemistry and structural biology, not to forget the analysis and identification of a plethora of secondary metabolites.

What aspects will be touched on in this compilation of chapters? More and more the boundaries between different categories of science such as chemistry, biochemistry, molecular and cell biology, and ecology are getting blurred, and this holds true for microbiology versus plant sciences too. In this way, attempts are underway to engineer bacteria and yeast to produce high amounts of a desired metabolite originally identified in medicinal plants of low productivity or to place regulatory and biosynthetic genes under the control of strong and tissue-specific promoters followed by transformation of (crop) plants. This extends even to biosynthesize new, "unnatural" compounds, offering engineered substrates to heterologously expressed enzymes and thus opens new avenues toward the generation of new antibiotics and pharmaceuticals. However, such approaches, including the engineering of whole pathways into yeast and bacterial cells, need to be based on a solid knowledge of biosynthetic pathways and their enzymes involved. A production *in planta* requires a precise knowledge of their intracellular distribution and possible expression in specialized tissues, aiming at enhanced production, for instance, as a consequence of environmental conditions, hormonal treatment, and exposure to biological and chemical stress.

Within the last decade or so, a major focus in the realm of isoprenoid research has been on the alternative methylerythritol phosphate (MEP) pathway, and the classical mevalonic acid (MVA) route has virtually been neglected. Thus, in the compilation of chapters, this one-sided view will be corrected by various contributions. Of course, one major aim in metabolic research is to identify rate-limiting steps in biosynthetic pathways and to

elucidate possible interactions of intermediates with enzymes, causing feedback regulation. Thus, simple overexpression of some enzymes thought of regulating pathways might not always constitute the best method. Structural biology comes into play, not only to elucidate catalytic reaction pathways but also to identify allosteric binding sites and to modify them through genetic engineering, thereby deregulating a pathway for higher productivity. In view of the structural complexity of many isoprenoid-derived vitamins and pharmaceuticals, biological production rather than chemical synthesis is the method of choice. Not so rarely, what is useful in treatment of sickness (saponins, cardenolides, etc.) in the producing organism is just to become toxic to pathogens and other enemies.

Speaking of pharmaceuticals, it is also noteworthy to mention that microbial and plant isoprenoid biosyntheses constitute excellent targets for the development of specific inhibitors and herbicides. As to this aspect, it shall not be neglected that a major human parasite, *Plasmodium falciparum*, the causative agent of malaria, is susceptible to inhibitors of the so-called MVA-independent or MEP pathway, as are a series of humanopathogenic bacteria. The importance of the coexistence of such compartmentalized pathways in plant cells is broadly discussed. Similarly, plant isoprenoid-derived compounds, like the much-studied artemisinin, are still efficient in the treatment of malaria caused by strains that have become resistant to a multitude of synthetic pharmaceuticals. Artemisinin and other drugs of high value, also flavors like geraniol and linalool, are produced by engineered yeast cells.

What about plant hormone biosynthesis and their regulatory action? It should not escape the attention of the reader that most phytohormones are entirely isoprenoids (e.g., gibberellic acids, abscisic acid, brassinosteroids, strigolactones) or contain isoprenoid-derived moieties like natural cytokinins. In signaling chains, we find implicated isoprenylated proteins, even regulating the synthesis and accumulation of secondary products like alkaloids in *Catharanthus roseus*.

Plants can apparently adapt metabolic processes (like the spatially separated MVA and MEP pathways) such that survival is possible under specific stress conditions, especially when attacked by microorganisms and herbivores. Such defense reactions must be rapid and efficient as well. Under these conditions, plants focus on the optimization of metabolic flux rates for the production of suitable phytochemicals, at the expense of general growth and development, and the whole biochemical machinery is adjusted to use all available precursor pools for defense. Interestingly enough, there is evidence for partial crossover of signaling pathways, which leads to the formation of suitably adapted groups of compounds with the highest efficiency against specific enemies. This would involve changing intracellular barriers that separate reactions and key intermediates that are not exchanged under "normal" conditions. Plants emit volatile organic compounds (VOC), many of them being isoprenoids to alert neighboring plants, which react by induction of defense reactions against microbial attack, but also use such signal to attract helper insects and nematodes feeding on herbivores. Trichomes are known to store such VOC, and it is interesting to see how their number and storage capacities depend on biosynthetic pathways and which isozymes are involved.

We do not forget isoprenoid polymers like rubber and how their synthesis is regulated. Even today, the mechanical properties of natural rubber make it absolutely essential for specific industrial products, and there is a fierce search around the world to seek for plants other than *Hevea brasiliensis* that produce rubber and related natural compounds.

Systems biology comes into play in the identification of genes that are co-expressed with known isoprenoid biosynthesis genes under certain conditions and thus helps to identify those that encode enzymes in branch-specific pathways, which opens new avenues in genetic engineering. High-throughput methods, data bank mining, and so forth all require users to ask precise questions that allow the arrangement of large sets of data (which are often of little utility) into something really useful. The same holds true with application of gene silencing techniques, which enable us to eventually identify the biological and metabolic function. Those techniques need to be accompanied by studying metabolic profiles. The combination of these techniques, carried out by well-trained specialists, also in the field of informatics, will certainly put us forward.

The chapters in this book have been arranged in such a way that there is some logical relation between them. In the first part, an overlook is given on isoprenoid biosynthesis in prokaryotic organisms and their enormous biochemical plasticity and adaptation. This then extends to structural biology, namely, the characterization of the entry enzyme into the MEP pathway. Actinomycetes are a primary source of antibiotics, and the various isoprenoid compounds produced are extensively presented. A further contribution focuses on the situation in cyanobacteria, with the focus on the connections between the MEP and pentose phosphate pathways.

The yeast *Saccharomyces cerevisiae* is the vehicle of choice for biotechnological engineering, which is extensively outlined in three chapters. One major product, meanwhile at an industrial scale, is artemisinin, an antimalarial drug. Of course, it fits well to immediately thereafter discuss its production in the plant and how this might be regulated in *Artemisia annua*. As the MEP pathway seems to be essential for the causative parasite *Plasmodium falciparum*, it follows a chapter on the action and efficiency of a MEP pathway inhibitor (fosmidomycin) in treating infected patients.

The next series of chapters is arranged in the order of increasing molecular mass of isoprenoids: semi-, mono-, sesqui-, and up to diterpenes, which leads to a broad discussion on ecological and other functions, including the structural characterization of enzymes like aristolochene synthase. In the context of "defense," the ecological function of C_{16}-terpenes, derivatives of the diterpene geranyl linalool, is discussed, which neatly prepares to talk about the newest addition to the list of phytohormones, carotenoid-derived strigolactones as "a cry to help," but resulting in "fatal attraction" of parasitic plants.

Then already speaking of phytohormones, it seems reasonable to continue with gibberellic acids (GAs) that constitute a major class of diterpenes; their biosynthesis and biological action are extensively presented. When we consider GAs as primary products, it is then necessary to discuss the regulation of pathways leading to primary and secondary products, at least sharing the synthesis of common precursors like IPP and DMAPP, here synthesized via

the MEP pathway. Many such secondary products are stored in specific morphological structures such as trichomes, which present an interesting target for genetic engineering of corresponding plants.

The synthesis of many secondary products can be induced by treatment with the (stress) phytohormone jasmonate, here in the special case of monoterpenoid indole alkaloids in *Catharanthus roseus*, for instance, the pharmacologically important anticancer drugs vinblastine and vincristine. However, there is clear evidence that prenylated proteins are implicated in the signaling chain. The next chapter discusses the role of prenylated proteins, especially their processing by prenylcysteine methylation in abscisic acid (ABA) signaling. In practice, some drought resistance of plants might be increased through affecting this process.

We then go higher in the molecular mass, discussing first polyprenols, like dolichol as cofactor in protein modification by glycosylation. If we go then to polyprenol polymers as secondary products, we arrive at rubber. In *Hevea brasiliensis*, the overall synthesis in latex seems to be regulated at the level of enzymes in the MVA pathway: HMG-CoA synthase and HMG-CoA reductase. But there are other plants that produce rubber, for instance, guayule (*Parthenium argentatum*). Such plants need to be developed into industrial crops.

We again arrive at the MVA pathway, discussing its entry enzymes, acetoacetyl-CoA thiolases, which have biosynthetic and degradative functions. In the same contribution, squalene synthase, the first enzyme committed to the sterol pathway, has been silenced, which results in growth inhibition. Now arrived at the C_{30} level of triterpenes, the biochemistry of phytosterol biochemistry is exemplified with analyzing an important enzymic step, the C4-demethylation, and thereafter of the C22 desaturase reaction in the following chapter. Squalene and squalene epoxide cyclases can be used to produce unnatural cyclic terpenes, perhaps of pharmacological importance.

While phytosterols certainly belong to primary products, triterpenoid compounds like saponins and also cardenolides can be grouped into secondary metabolites; however, their ecological (and pharmacological) importance is evident!

The last chapters focus on the model plant *Arabidopsis thaliana*, going deeply into molecular biology and biochemistry, also with the help of mutants and inhibitors. Of course, some redundancy of information is unavoidable, but various aspects are discussed from different points of view. At the end, the generation of a publicly accessible data bank on all what touches on isoprenoid pathways and regulation in *A. thaliana* is presented.

Of course, a gentle reader is not forced to follow this sequence….

Strasbourg, France — Thomas J. Bach
Strasbourg, France — Michel Rohmer

Contents

Contributors

Ikuro Abe Graduate School of Pharmaceutical Sciences, The University of Tokyo, Bunkyo-ku, Tokyo, Japan

Rudolf K. Allemann School of Chemistry, Cardiff University, Cardiff, UK

Mohammad A. Asadollahi Novo Nordisk Foundation Center for Biosustainability-Technical University of Denmark, Fremtidavej 3, Denmark

Thomas J. Bach Département "Réseaux métaboliques", Institut de Biologie Moléculaire des Plantes (CNRS UPR 2357), Université de Strasbourg, Strasbourg, France

Kirsten R. Benjamin Amyris, Emeryville, CA, USA

Wilhelm Boland Department of Bioorganic Chemistry, Max-Planck-Institute for Chemical Ecology, Jena, Germany

Albert Boronat Department of Molecular Genetics, Centre for Research in Agricultural Genomics (CRAG), CSIC-IRTA-UAB-UB, Barcelona, Spain

Department of Biochemistry and Molecular Biology, University of Barcelona, Barcelona, Spain

Steffen Borrmann Justus-Liebig-Universität Gießen, Institut für Klinische Immunologie und Transfusionsmedizin, Gießen, Germany

Ralph Bours Laboratory of Plant Physiology, Wageningen University, Wageningen, The Netherlands

Florence Bouvier Institut de Biologie Moléculaire des Plantes, CNRS, Strasbourg cedex, France

Harro Bouwmeester Laboratory of Plant Physiology, Wageningen University, Wageningen, The Netherlands

Wolfgang Brandt Abteilung Natur- und Wirkstoffchemie, Leibniz-Institut für Pflanzenbiochemie, Halle (Saale), Germany

Marco Busch Bayer CropScience GmbH, Industriepark Höchst, Frankfurt am Main, Germany

Serge Van Calenbergh Justus-Liebig-Universität Gießen, Institut für Klinische Immunologie und Transfusionsmedizin, Gießen, Germany

Bilal Camara Institut de Biologie Moléculaire des Plantes, CNRS, Strasbourg cedex, France

Narciso Campos Department of Molecular Genetics, Centre for Research in Agricultural Genomics (CRAG) CSIC-IRTA-UAB-UB, Barcelona, Spain

Department of Biochemistry and Molecular Biology, University of Barcelona, Barcelona, Spain

Catarina Cardoso Cropdesign – BASF Plant Sciences, Zwijnaarde, Belgium

Tatsiana Charnikhova Laboratory of Plant Physiology, Wageningen University, Wageningen, The Netherlands

Marc Clastre Biomolécules et Biotechnologies végétales, Université François-Rabelais de Tours Sciences et Techniques, Tours, France

Patricia Claudel UMR SVQV, University of Strasbourg, INRA, Colmar, France

Elizabeth Cordoba Departamento de Biología Molecular, Instituto de Biotecnología Universidad Autónoma de México, Morelos, Mexico

Vincent Courdavault Biomolécules et Biotechnologies végétales, Université François-Rabelais de Tours Sciences et Techniques, Tours, France

Dring N. Crowell Passed away on June 30, 2012

Francis X. Cunningham Jr. Department of Cell Biology and Molecular Genetics, University of Maryland, College Park, MD, USA

Tohru Dairi Graduate School of Engineering, Hokkaido University, Sapporo, Hokkaido, Japan

Sylvain Darnet Institut de Biologie Moléculaire des Plantes, CNRS, Strasbourg cedex, France

Natalia Dudareva Department of Horticulture and Landscape Architecture, Purdue University, West Lafayette, IN, USA

Albert Ferrer Faculty of Pharmacy, Department of Molecular Genetics, Centre for Research in Agricultural Genomics (CRAG) CSIC-IRTA-UAB-UB, Barcelona, Spain

Department of Biochemistry and Molecular Biology, University of Barcelona, Barcelona, Spain

Scott Fickes Amyris Biotechnologies, Emeryville, CA, USA

Marc Fischer UMR SVQV, University of Strasbourg, INRA, Colmar, France

Karl Fisher Amyris Biotechnologies, Emeryville, CA, USA

Daniela S. Floss Abteilung Sekundärstoffwechsel, Leibniz-Institut für Pflanzenbiochemie, Halle (Saale), Germany

Benjamin Fode Albrecht-von Haller-Institute for Plant Sciences, Georg-August-University Göttingen, Göttingen D-37073, Germany

Luca R. Formenti National Food Institute, Kgs Lyngby, Denmark

Elisabeth Gantt Department of Cell Biology and Molecular Genetics, University of Maryland, College Park, MD, USA

R. Raymond Gantt Department of Cell Biology and Molecular Genetics, University of Maryland, College Park, MD, USA

Katrin Gärtner Albrecht-von Haller-Institute for Plant Sciences, Georg-August-University Göttingen, Göttingen D-37073, Germany

Christiane Gatz Albrecht-von Haller-Institute for Plant Sciences, Georg-August-University Göttingen, Göttingen D-37073, Germany

Esther Gerber Department of Genetic Engineering, Deinove Company, Paris, France

Jonathan Gershenzon Department of Biochemistry, Max Planck Institute for Chemical Ecology, Jena, Germany

Nathalie Giglioli-Guivarc'h Biomolécules et Biotechnologies végétales, Université François-Rabelais de Tours Sciences et Techniques, Tours, France

Michael Gutensohn Department of Horticulture and Landscape Architecture, Purdue University, West Lafayette, IN, USA

Michel A. Haring Department of Plant Physiology, Swammerdam Institute for Life Sciences, Amsterdam, The Netherlands

Marie-Andrée Hartmann Département "Réseaux métaboliques", Institut de Biologie Moléculaire des Plantes (CNRS UPR 2357), Université de Strasbourg, Strasbourg, France

Marco Herde Albrecht-von Haller-Institute for Plant Sciences, Georg-August-University Göttingen, GöttingenD-37073, Germany

Department of Biochemistry and Molecular Biology, Michigan State University, East Lansing, MI, USA

Martin Hintz Justus-Liebig-Universität Gießen, Institut für Klinische Immunologie und Transfusionsmedizin, Gießen, Germany

David H. Huizinga Dow AgroSciences LLC, Indianapolis, IN, USA

David Hutchinson Justus-Liebig-Universität Gießen, Institut für Klinische Immunologie und Transfusionsmedizin, Gießen, Germany

Muhammad Jamil Laboratory of Plant Physiology, Wageningen University, Wageningen, The Netherlands

Hassan Jomaa Justus-Liebig-Universität Gießen, Institut für Klinische Immunologie und Transfusionsmedizin, Gießen, Germany

Francis Karst UMR SVQV, University of Strasbourg, INRA, Colmar, France

Wouter Kohlen Department of Plant Physiology, Wageningen University, Wageningen, The Netherlands

Tobias Köllner Department of Biochemistry, Max-Planck-Institute for Chemical Ecology, Jena, Germany

Wolfgang Kreis Lehrstuhl für Pharmazeutische Biologie, Friedrich-Alexander-Universität Erlangen-Nürnberg, Erlangen, Germany

ECROPS, Erlangen Center of Plant Science, Erlangen, Germany

Peter G. Kremsner Justus-Liebig-Universität Gießen, Institut für Klinische Immunologie und Transfusionsmedizin, Gießen, Germany

Gudrun Lange Bayer CropScience GmbH, Industriepark Höchst, Frankfurt am Main, Germany

Michael D. Leavell Amyris Biotechnologies, Emeryville, CA, USA

Bertrand Lell Justus-Liebig-Universität Gießen, Institut für Klinische Immunologie und Transfusionsmedizin, Gießen, Germany

Patricia León Departamento de Biología Molecular, Instituto de Biotecnología Universidad Autónoma de México, Morelos, Mexico

Juan Antonio López-Ráez Soil Microbiology and Symbiotic Systems, Estacion Experimental del Zaidin (CSIC), Granada, Spain

Francesco Loreto CNR – Istituto per la Protezione delle Piante, Sesto Fiorentino (Firenze), Italy

Kerstin Manke Abteilung Sekundärstoffwechsel, Leibniz-Institut für Pflanzenbiochemie, Halle (Saale), Germany

Radoslava Matusova Institute of Plant Genetics and Biotechnology, Slovak Academy of Sciences, Nitra, Slovakia

Jérôme Maury Center for Microbial Biotechnology, DTU-Biosys, Kgs Lyngby, Denmark

Colleen McMahan Crop Improvement and Utilization Unit, Western Regional Research Center, ARS-USDA, Albany, CA, USA

Derek McPhee Amyris Biotechnologies, Emeryville, CA, USA

Sophie Meyer UMR SVQV, University of Strasbourg, INRA, Colmar, France

David J. Miller School of Chemistry, Cardiff University, Cardiff, UK

Masaharu Mizutani Graduate School of Life and Environmental Sciences, Osaka Prefecture University, Sakai, Japan

Sam T. Mugford Department of Metabolic Biology, John Innes Centre, Norwich, UK

Frieder Müller-Uri Lehrstuhl für Pharmazeutische Biologie, Friedrich-Alexander-Universität Erlangen-Nürnberg, Erlangen, Germany

ECROPS, Erlangen Center of Plant Science, Erlangen, Germany

Toshiya Muranaka Department of Biotechnology, Graduate School of Engineering, Osaka University, Osaka, Japan

Dinesh A. Nagegowda Central Institute of Medicinal and Aromatic Plants India, Plant Biotechnology Division, Lucknow, India

Jack D. Newman Amyris Biotechnologies, Emeryville, CA, USA

Jens Nielsen Department of Chemical and Biological Engineering, Chalmers University of Technology, Gothenburg, Sweden

Isabel Nogués CNR – Istituto di Biologia Agroambientale e Forestale, Monterotondo Scalo (Roma), Italy

Daisaku Ohta Graduate School of Life and Environmental Sciences, Osaka Prefecture University, Sakai, Japan

Kiyoshi Ohyama Department of Chemistry and Materials Science, Tokyo Institute of Technology, Meguro, Tokyo, Japan

Regina Ortmann Justus-Liebig-Universität Gießen, Institut für Klinische Immunologie und Transfusionsmedizin, Gießen, Germany

Anne Osbourn Department of Metabolic Biology, John Innes Centre, Norwich, UK

Maryline Oswald UMR SVQV, University of Strasbourg, INRA, Colmar, France

Christopher J. Paddon Amyris Biotechnologies, Emeryville, CA, USA

Heike Paetzold Abteilung Sekundärstoffwechsel, Leibniz-Institut für Pflanzenbiochemie, Halle (Saale), Germany

Reuben J. Peters Department of Biochemistry, Biophysics, and Molecular Biology, Iowa State University, Ames, IA, USA

Douglas J. Pitera Amyris Biotechnologies, Emeryville, CA, USA

Kelly Poliquin Department of Cell Biology and Molecular Genetics, University of Maryland, College Park, MD, USA

Alain Rahier Institut de Biologie Moléculaire des Plantes, CNRS, Strasbourg cedex, France

Armin Reichenberg Justus-Liebig-Universität Gießen, Institut für Klinische Immunologie und Transfusionsmedizin, Gießen, Germany

Manuel Rodríguez-Concepción Department of Molecular Genetics, Centre for Research in Agricultural Genomics (CRAG) CSIC-IRTA-UAB-UB, Barcelona, Spain

Denis Rontein AnaScan, Gréoux les Bains, France

Carolien Ruyter-Spira Laboratory of Plant Physiology, Wageningen University, Wageningen, The Netherlands

Christophe Sallaud Functional and Applied Cereal Group (FAC), Clermont-Ferrand Cedex, France

Michel Schalk Biotechnology Department, Firmenich SA, Geneva, Switzerland

Chris C.N. van Schie Division of Biological Sciences, University of California, San Diego, La Jolla, CA, USA

David Shintani Department of Biochemistry, University of Nevada, Reno, NV, USA

Martin Schlitzer Justus-Liebig-Universität Gießen, Institut für Klinische Immunologie und Transfusionsmedizin, Gießen, Germany

Robert C. Schuurink Department of Plant Physiology, Swammerdam Institute for Life Sciences, Amsterdam, The Netherlands

Andrew John Simkin Faculté de pharmacie Biomolécules et Biotechnologies végétales, Université François-Rabelais de Tours Sciences et Techniques, Tours, France

Nualpun Sirinupong Biochemistry and Molecular Biology, Wayne State University School of Medicine, Detroit, MI, USA

Dieter Strack Abteilung Sekundärstoffwechsel, Leibniz-Institut für Pflanzenbiochemie, Halle (Saale), Germany

Liliana Surmacz Institute of Biochemistry and Biophysics, Polish Academy of Sciences, Warsaw, Poland

Wallie Suvachittanont Faculty of Science Biochemistry Department, Prince of Songkla University, Hat Yai, Songkhla, Thailand

Pluang Suwanmanee Faculty of Science Biology Department, Thaksin University, Songkhla, Thailand

Ewa Swiezewska Institute of Biochemistry and Biophysics, Polish Academy of Sciences, Warsaw, Poland

Dorothea Tholl Department of Biological Sciences, Virginia Tech, Blacksburg, VA, USA

Alain Tissier Leibniz Institute of Plant Biochemistry, Halle (Saale), Germany

Liang Tong Department of Biological Sciences, Columbia University, New York, NY, USA

Melissa Towler Biology and Biotechnology Department, Worcester Polytechnic Institute, Worcester, MA, USA

Gerlinde Usunow Bayer CropScience GmbH, Industriepark Höchst, Frankfurt am Main, Germany

Francel Verstappen Laboratory of Plant Physiology, Wageningen University, Wageningen, The Netherlands

Jessica Vollrath Abteilung Sekundärstoffwechsel, Leibniz-Institut für Pflanzenbiochemie, Halle (Saale), Germany

Eva Vranová Department of Plant Biotechnology, Institute of Plant Sciences, Zurich, Switzerland

Michael H. Walter Abteilung Sekundärstoffwechsel, Leibniz-Institut für Pflanzenbiochemie, Halle (Saale), Germany

Yi Wang Biology and Biotechnology Department, Worcester Polytechnic Institute, Worcester, MA, USA

Pamela Weathers Biology and Biotechnology Department, Worcester Polytechnic Institute, Worcester, MA, USA

Laurent Wentzinger Actelion Pharmaceuticals Ltd, Allschwil, Switzerland

Patrick J. Westfall Amyris Biotechnologies, Emeryville, CA, USA

Maureen Whalen Crop Improvement and Utilization Unit, Western Regional Research Center, ARS-USDA, Albany, CA, USA

Jochen Wiesner Justus-Liebig-Universität Gießen, Institut für Klinische Immunologie und Transfusionsmedizin, Gießen, Germany

Kristin K. Wobbe Chemistry and Biochemistry Department, Worcester Polytechnic Institute, Worcester, MA, USA

Song Xiang Department of Biological Sciences, Columbia University, New York, NY, USA

Isoprenoid Biosynthesis in Prokaryotic Organisms

1

Manuel Rodríguez-Concepción and Albert Boronat

Abstract

Isoprenoids are ubiquitous compounds found in all living organisms. In spite of their remarkable diversity of structures and functions, all isoprenoids derive from a basic five-carbon precursor unit, isopentenyl diphosphate (IPP), and its isomer dimethylallyl diphosphate (DMAPP). Addition of IPP units to DMAPP, catalyzed by prenyltransferases, results in the synthesis of prenyl diphosphates of increasing length which are the starting points of downstream pathways leading to the synthesis of the different isoprenoid end products. For many years, it was accepted that IPP was synthesized from acetyl-CoA through the well-known mevalonate (MVA) pathway. However, an alternative MVA-independent pathway for the biosynthesis of IPP and DMAPP was identified a few years ago in bacteria, algae, and plants. This novel pathway, currently known as the methylerythritol 4-phosphate (MEP) pathway, is widely distributed in nature and is present in most eubacteria. Here, we describe the biological relevance of the main isoprenoid compounds found in prokaryotic organisms and the metabolic origin of the IPP and DMAPP used for their synthesis, with a particular emphasis on those isoprenoids present in the

M. Rodríguez-Concepción (✉)
Department of Molecular Genetics,
Centre for Research in Agricultural Genomics (CRAG)
CSIC-IRTA-UAB-UB, Campus UAB Bellaterra,
Barcelona E-08193, Spain
e-mail: manuel.rodriguez@cragenomica.es

A. Boronat
Department of Molecular Genetics,
Centre for Research in Agricultural Genomics (CRAG)
CSIC-IRTA-UAB-UB, Campus UAB Bellaterra,
Barcelona E-08193, Spain

Department of Biochemistry and Molecular Biology,
Faculty of Biology, University of Barcelona,
Barcelona E-08028, Spain

T.J. Bach and M. Rohmer (eds.), *Isoprenoid Synthesis in Plants and Microorganisms: New Concepts and Experimental Approaches*, DOI 10.1007/978-1-4614-4063-5_1,

model bacteria *Escherichia coli*. Since the MEP pathway is essential in most pathogenic bacteria but is absent in animals (including humans), which synthesize isoprenoids through the MVA pathway, we also describe the recent and increasing interest of the MEP pathway enzymes as targets for the development of new antibiotics.

Keywords
Archaebacteria • Dimethylallyl diphosphate • *Escherichia coli* • Eubacteria • Isoprenoid • Isopentenyl diphosphate • Terpenoid • Mevalonate • Methylerythritol 4-phosphate

1.1 Introduction

Isoprenoids (also known as terpenoids) are ubiquitous compounds found in all living organisms. In spite of their remarkable diversity of structures and functions, all isoprenoids derive from a basic five-carbon precursor unit, isopentenyl diphosphate (IPP), and its isomer dimethylallyl diphosphate (DMAPP) (Fig. 1.1). Addition of IPP units to DMAPP, catalyzed by prenyltransferases, results in the synthesis of prenyl diphosphates of increasing length (e.g., farnesyl diphosphate and geranylgeranyl diphosphate) which are the starting points of downstream pathways leading to the synthesis of the different isoprenoid end products (Fig. 1.2). For many years, it was accepted that IPP was synthesized from acetyl-CoA through the well-known mevalonate (MVA) pathway. However, an alternative MVA-independent pathway for the biosynthesis of IPP and DMAPP was identified a few years ago in bacteria, algae, and plants (Rohmer 1999; Lichtenthaler 1999). This novel pathway, currently known as the methylerythritol 4-phosphate (MEP) pathway (cf. Phillips et al. 2008), is widely distributed in nature and is present in most eubacteria, apicomplexan protozoa (like the malaria parasite *Plasmodium falciparum*), green algae, and higher plants. For a detailed description of the discovery and elucidation of the MEP pathway, we refer to other reviews on this topic (Rodríguez-Concepción and Boronat 2002; Kuzuyama and Seto 2003; Eisenreich et al. 2004; Rohmer 2008).

Here, we describe the biological relevance of the main isoprenoid compounds found in prokaryotic organisms and the metabolic origin of the isoprene units used for their synthesis, with a particular emphasis on those isoprenoids present in the model bacteria *Escherichia coli*. Since the MEP pathway is essential in most pathogenic bacteria but is absent in animals (including humans), which synthesize isoprenoids through the MVA pathway, we also describe the recent and increasing interest of the MEP pathway enzymes as targets for the development of new antibiotics.

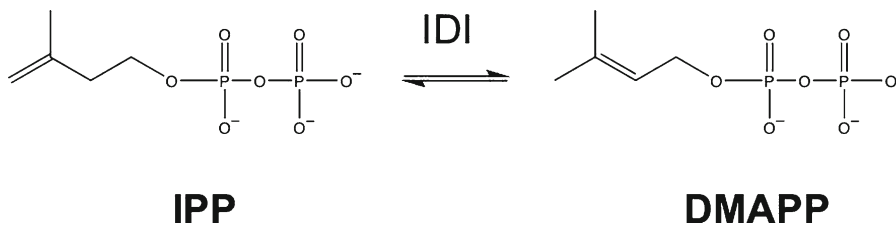

Fig. 1.1 Chemical structure of isopentenyl diphosphate (*IPP*) and dimethylallyl diphosphate (*DMAPP*) and their interconversion by the enzyme isopentenyl diphosphate isomerase (*IDI*)

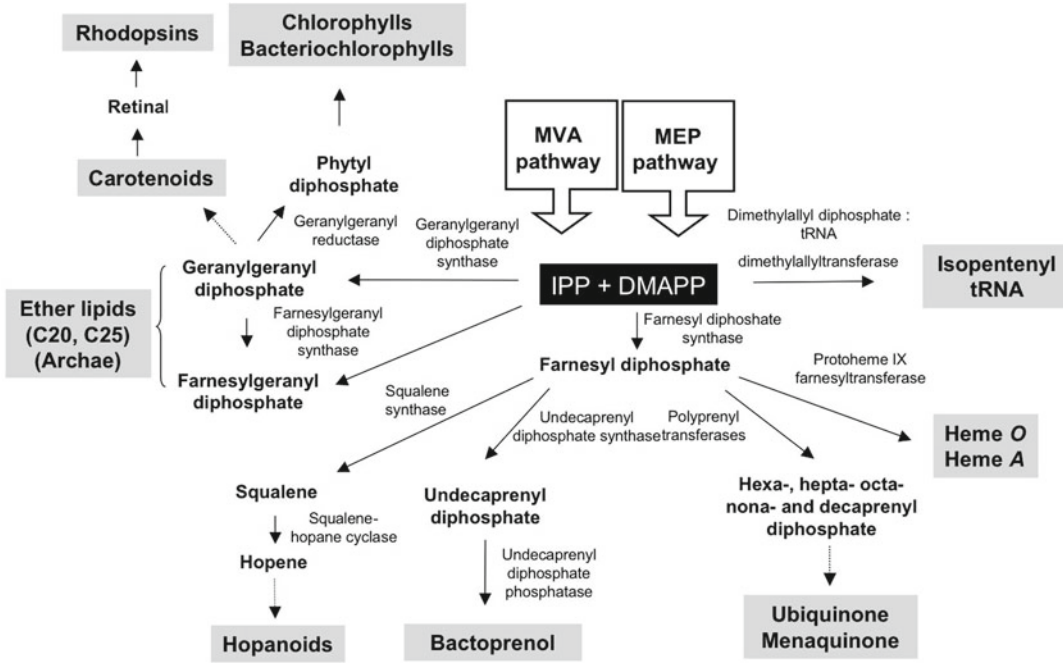

Fig. 1.2 Schematic representation of isoprenoid biosynthesis in prokaryotic organisms

1.2 Biological Relevance of Isoprenoids in the Prokaryotic World

Many isoprenoids play essential roles in a variety of processes that are vital for the growth and survival of prokaryotic organisms. They include, among others, cell wall and membrane biosynthesis, electron transport, and conversion of light into chemical energy. Also, many microorganisms produce isoprenoid secondary metabolites of biotechnological relevance. A number of review articles have recently covered the different strategies and outcomes of the metabolic engineering of isoprenoids in bacteria (Klein-Marcuschamer et al. 2007; Ajikumar et al. 2008; Kirby and Keasling 2008, 2009; Misawa 2011).

1.2.1 Cell Wall Biosynthesis: Bactoprenol

The bacterial cell wall is a rigid structure that surrounds the cytoplasmic membrane and plays an essential role in maintaining the cell shape and preventing the deleterious effect of the internal osmotic pressure. It also serves as a scaffold for anchoring other cell envelope components such as proteins and teichoic acids. Peptidoglycan is the major component of bacterial cell walls and consists in long glycan chains made up of alternating N-acetylglucosamine (GlcNAc) and N-acetylmuramic acid (MurNAc) residues cross-linked together by bridges made of amino acids and amino acid derivatives (Vollmer et al. 2008). The biosynthesis of peptidoglycan is a complex process that involves about 20 reactions that take place in the cytoplasm and the inner and outer sides of the cytoplasmic membrane. A key component in the synthesis of peptidoglycan is undecaprenyl phosphate, also referred to as bactoprenol (Fig. 1.3). This isoprenoid compound is needed for the synthesis and transport of hydrophilic GlcNAc-MurNAc-peptide monomeric units outside the cytoplasmic membrane, the site for peptidoglycan polymerization. Undecaprenyl phosphate derives from undecaprenyl diphosphate, a prenyl diphosphate synthesized from farnesyl diphosphate (FPP) (Fig. 1.2).

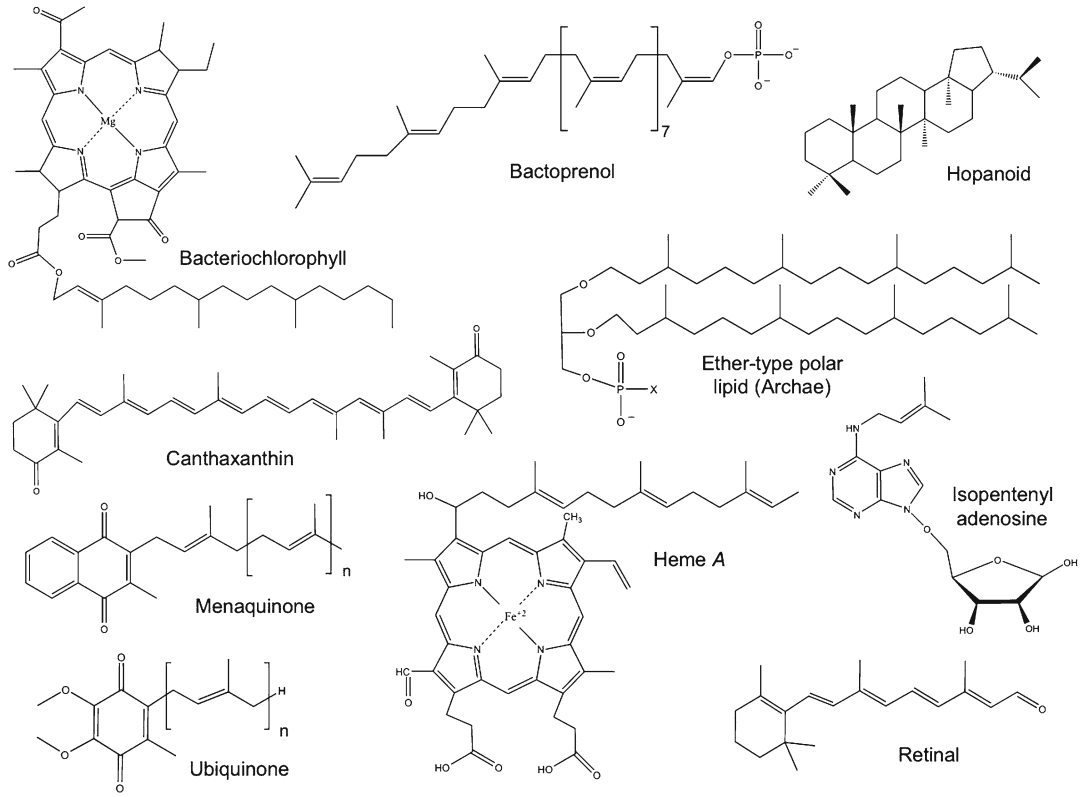

Fig. 1.3 Representative isoprenoids found in prokaryotic organisms

The enzymes involved in bactoprenol biosynthesis are undecaprenyl diphosphate synthase, which adds eight molecules of IPP (in *cis* form) onto FPP and undecaprenyl diphosphate phosphatase, which removes a phosphate group. The genes encoding these enzymes in *E. coli* (*ispU* and *bacA*, respectively) are indicated in Table 1.1. The biosynthesis of bactoprenol and its role in peptidoglycan biosynthesis have recently been reviewed by Bouhss et al. (2008).

1.2.2 Membrane Lipids: Hopanoids and Archaeal Ether-Type Lipids

Biological membranes are composed of lipids and proteins. The main membrane lipids are glycerolipids, composed of a polar head and two hydrophobic alkane groups that are mobile in the interior of the membrane. To regulate membrane fluidity, eukaryotic cells employ sterols (e.g., cholesterol). Since it is known that most prokaryotes lack sterols, the search for alternative molecules playing an equivalent role in prokaryotes has been an ongoing issue during the last decades. It is now well established that many bacteria contain hopanoids, pentacyclic triterpenoid compounds with a structure similar to that of sterols (Fig. 1.3). Hopanoids have been detected in about 30% of all bacteria investigated, including a wide range of Gram-negative and Gram-positive bacteria. Although hopanoids predominantly occur in aerobic bacteria, they have also been found in some facultative anaerobic bacteria. Hopanoids have not been detected in archaebacteria, which produce a particular membrane lipid of isoprenoid nature (see below). The hopanoid skeleton is formed from squalene by the action of squalene-hopene cyclase (Fig. 1.2). Hopanoid chemistry, biosynthesis, function, and distribution have been reviewed by Kannenberg and Poralla (1999).

Table 1.1 Genes encoding isoprenoid biosynthetic enzymes in *E. coli*[a]

Enzyme	Gene	Alternative gene symbol	Minute	Left end	Right end	Cotranscribed with
1-Deoxy-D-xylulose 5-phosphate synthase	*dxs*	*yajP*	9.43	437,539	439,401	*ispA*
1-Deoxy-D-xylulose 5-phosphate reductoisomerase	*dxr*	*ispC, yaeM*	4.17	193,521	194,717	–
2-*C*-methyl-D-erythritol 4-phosphate cytidylyltransferase	*ispD*	*ygbP*	61.85	2,869,802	2,870,512	*ispF*
4-(Cytidine 5′-diphospho)-2-*C*-methyl-D-erythritol kinase	*ispE*	*ipk, ychB*	27.18	1,261,249	1,262,100	–
2*C*-Methyl-D-erythritol 2,4-cyclodiphosphate synthase	*ispF*	*ygbB*	61.84	2,869,323	2,869,802	*ispD*
4-Hydroxy-3-methylbut-2-enyl diphosphate synthase	*ispG*	*gcpE*	56.87	2,638,708	2,639,826	–
4-Hydroxy-3-methylbut-2-enyl diphosphate reductase	*ispH*	*lytB, yaaE*	0.57	26,277	27,227	–
Isopentenyl diphosphate isomerase	*idi*	*ygfV*	65.33	3,031,087	3,031,635	–
Farnesyl diphosphate synthase	*ispA*	–	9.47	439,426	440,325	*dxs*
Octaprenyl-diphosphate synthase	*ispB*	*cel, yhbD*	71.81	3,331,732	3,332,703	–
Undecaprenyl diphosphate synthase	*ispU*	*uppS, rth, yaeS*	4.20	194,903	195,664	–
Undecaprenyl diphosphate phosphatase	*bacA*	*uppP*	69.0	3,201,332	3,202,153	–
Dimethylallyl diphosphate: tRNA dimethylallyltransferase	*miaA*	*trpX*	94.78	4397275	4,398,225	–
Protoheme IX farnesyltransferase	*cyoE*	–	9.61	446,039	446,929	–

[a]EcoGene Website/EcoWeb (http://ecogene.org/index.php)

Archaebacteria are unicellular microorganisms which evolved separately from eubacteria and eukaryotes and that are often found inhabiting extreme environments such as hot springs and salt lakes. They are similar to eubacteria in being prokaryotes (and thus lacking a nucleus) but differ from them in ribosomal structure, the presence of introns (in some species) and in membrane structure and composition. One of the most remarkable features of archaebacteria is the presence of ether-type lipids in their membranes containing hydrocarbon chains of isoprenoid nature (usually C20 phytanyl and C25 farnesylgeranyl groups) linked to *sn*-glycerol 1-phosphate (Fig. 1.3). The C20 prenyl chains may derive from geranylgeranyl diphosphate (GGPP) synthesized from IPP and DMAPP by the action of GGPP synthase (Fig. 1.2). C25 farnesylgeranyl groups are synthesized by farnesylgeranyl diphosphate synthase (Fig. 1.2) either by the consecutive condensation of IPP molecules to DMAPP or to prenyl diphosphates, like GGPP (Boucher et al. 2004). Archaeal polyprenyl diphosphate synthases can also synthesize products of shorter chain lengths. The biosynthesis of ether-type lipids in archaebacteria has recently been reviewed by Koga and Morii (2007).

1.2.3 Electron Transfer: Ubiquinone, Menaquinone, and Heme A

Ubiquinone and menaquinone are lipid-soluble molecules playing important roles in respiration. They are involved in electron transport processes between membrane-bound protein complexes in the respiratory electron-transport chain. Both compounds contain a quinone moiety linked to an isoprenoid side chain (Fig. 1.3). Ubiquinone has a benzoquinone group that is linked to an isoprenoid chain of different length (6–10 isoprene units) depending on the organism. In *E. coli* the isoprenoid side chain of ubiquinone contains 8 isoprene units. Menaquinone has a naphthoquinone ring linked to an isoprene tail, which also contains 8 isoprene units in *E. coli*. Facultative anaerobes, like *E. coli*, use ubiquinone when growing under aerobic conditions and menaquinone under anaerobic conditions. By contrast, many Gram-positive aerobes, such as *Bacillus subtilis*, contain only menaquinone. In *E. coli*, the side chain of ubiquinone and menaquinone is synthesized from FPP by octaprenyl-diphosphate synthase (Fig. 1.2), which is encoded by the essential gene *ispB* (Table 1.1) (Meganathan 2001; Kawamukai 2002).

Cytochromes are membrane-bound proteins also involved in electron-transport processes. Cytochromes contain a prosthetic group, called heme, composed by a heterocyclic porphyrin and a metal ion (usually iron) in a central position. Heme *A* (Fig. 1.3), which is found in cytochrome c and cytochrome c oxidase, is characterized by containing a hydroxyfarnesyl group. *E. coli* has no cytochrome *c* and no equivalent to the mitochondrial complex III (bc_1 complex) or complex IV (cytochrome *c* oxidase). Instead, two enzymes in the *E. coli* cytoplasmic membrane, the cytochromes *bo* and *d*, oxidize ubiquinol and directly reduce molecular oxygen to water. Cytochrome *bo* contains heme O, which only differs from heme A by having a methyl group instead of a formyl group. Heme A is derived from heme B (protoheme IX) with heme O as a probable intermediate (Mogi et al. 1994). The transfer of the farnesyl group from FPP to heme B to form heme O is catalyzed by a farnesyltransferase encoded by the *cyoE* gene in *E. coli* (Table 1.1) (Mogi et al. 1994).

1.2.4 Protein Synthesis: Isopentenyl tRNA

Transfer RNA (tRNA) molecules usually contain modified nucleotides. In almost all the tRNAs reading codons beginning with U, the adenosine at position 37 (adjacent to the 3′ position of the anticodon) is modified to N(6)-(Δ 2)-isopentenyl adenosine (Fig. 1.3) by the action of a tRNA isopentenyltransferase, encoded by the *miaA* gene in *E. coli* (Table 1.1). Homologs of the *E. coli miaA* gene have been detected in other microorganisms. Isopentenyl adenosine increases the efficiency of translation of the modified tRNAs and makes them less sensitive to codon context. Although *miaA* is not essential in *E. coli*, mutants defective

in this gene show increased rates of spontaneous mutations and altered read through and suppression of nonsense codons (Persson et al. 1994).

1.2.5 Phototrophy: Chlorophylls, Bacteriochlorophylls, Rhodopsins, and Carotenoids

Microorganisms can use two mechanisms for the conversion of light into chemical energy. One of them is dependent on photochemical reaction centers that contain chlorophylls or bacteriochlorophylls. The other mechanism employs proteorhodopsins and bacteriorhodopsins, retinal-binding membrane proteins belonging to the rhodopsin family (Bryant and Frigaard 2006).

Like plant chlorophylls, bacterial chlorophylls also contain a long isoprenoid chain (usually phytol) that contributes to their localization in the photosynthetic membranes (Fig. 1.3). The last stage in the biosynthesis of bacterial chlorophylls consists in the addition of the prenyl chain to the corresponding chlorophyllides (Gomez Maqueo Chew and Bryant 2007). It has been proposed that phytol is formed after the addition of a geranylgeraniol group which is later sequentially saturated by geranylgeranyl reductase. However, some evidences suggest that geranylgeranyl reductase can saturate GGPP prior to the transfer of the phytol tail (Fig. 1.2). Although the phytol group is present in most bacterial chlorophylls, other isoprenoids (like farnesyl, geranylgeranyl, and 2,6-phytadienyl groups) have also been reported (Gomez Maqueo Chew and Bryant 2007).

Proteorhodopsins are retinal-binding membrane proteins belonging to the rhodopsin family. Prokaryotic members of this family include energy-conserving transmembrane proton pumps, transmembrane chloride pumps, and photosensors (sensory rhodopsins) (Fuhrman et al. 2008). Originally discovered in archaebacteria, it is currently estimated that a large proportion of marine bacteria contain proteorhodopsin. In Archaea and most bacteria, retinal (Fig. 1.3) is synthesized by the oxidative cleavage of β-carotene. However, recent reports on the characterization of apocarotenoid oxygenases from cyanobacteria have shown that retinal can also be produced by cleavage of some apocarotenoids. At present, the substrate(s) used for retinal production in some bacteria remains an open question (Maresca et al. 2008).

Some photosynthetic bacteria also contain carotenoids, which function primarily as photoprotective pigments but that can also participate in the light harvesting process. Like in plants, bacterial carotenoids are also synthesized from GGPP (Fig. 1.2). Bacterial carotenoid diversity and the biochemical aspects related with their biosynthesis have recently been reviewed by Maresca et al. (2008).

1.2.6 Secondary Metabolism

Prokaryotic organisms produce isoprenoid compounds and derivatives that can be included in the large and diverse family of secondary metabolites. For instance, many nonphotosynthetic bacteria can synthesize carotenoids, some of them of industrial interest (e.g., canthaxanthin and astaxanthin). Since a considerable number of microbial (and plant) carotenoid biosynthetic genes have been cloned over the past few years, it is now possible to engineer carotenoid biosynthesis in noncarotenogenic bacteria like *E. coli*. Excellent reviews describing the biochemistry and the biotechnology of carotenoids in microorganisms are available (Lee and Schmidt-Dannert 2002; Das et al. 2007; Maresca et al. 2008). Another example of prokaryotic secondary metabolites is given by the isoprenoid antibiotics produced by many actinomycete strains (Dairi 2005; Dairi, this volume).

1.3 Origin of Isoprenoid Precursors in Prokaryotic Organisms

For many years, it was accepted that IPP was synthesized through the MVA pathway in all organisms, including microorganisms. However, as indicated above, an alternative pathway for the biosynthesis of IPP (and DMAPP) was identified a few years ago in bacteria, algae, and plants. This novel pathway, known as the MEP pathway,

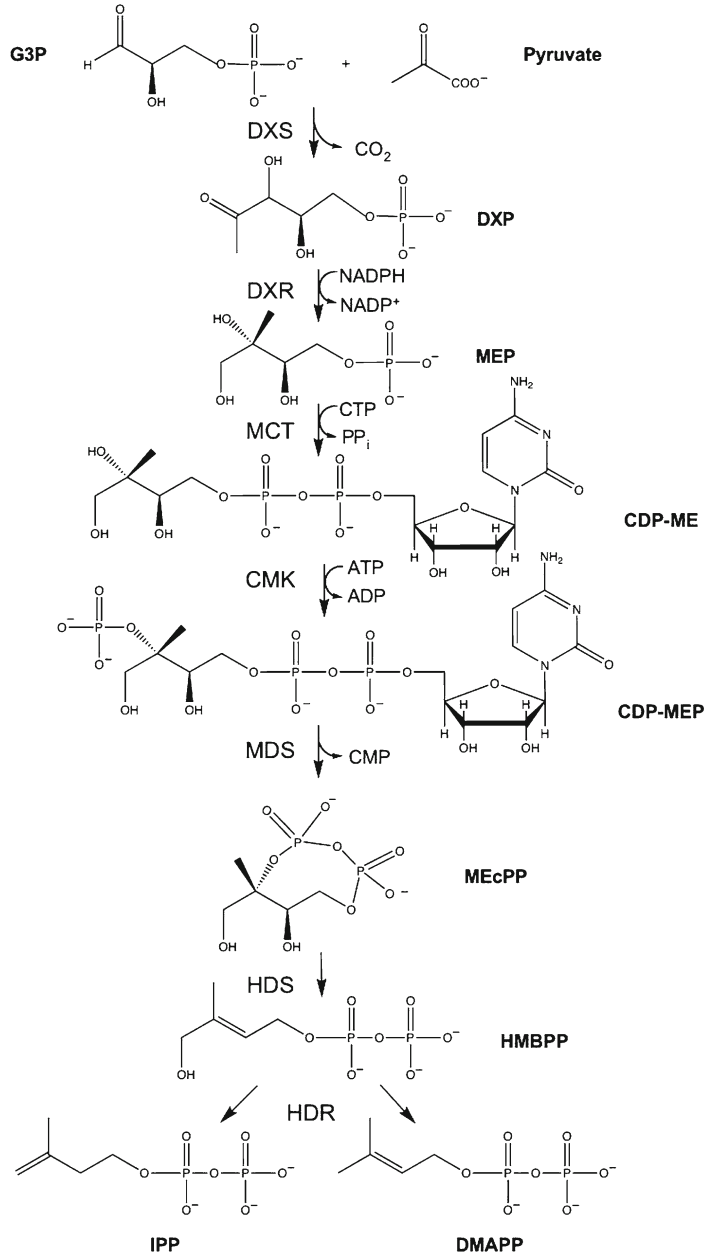

Fig. 1.4 Steps of the MEP pathway leading to the formation of IPP and DMAPP from pyruvate and D-glyceraldehyde 3-phosphate (*G3P*). Acronyms of enzymes and intermediates are described in the text and correspond to those suggested by Phillips et al. (2008)

is widely distributed in nature and is present in most eubacteria (see below).

The first reaction of the MEP pathway (Fig. 1.4) is catalyzed by the enzyme 1-deoxy-D-xylulose 5-phosphate (DXP) synthase (DXS) and involves the condensation of (hydroxyethyl)thiamin derived from pyruvate with the C1 aldehyde group of D-glyceraldehyde 3-phosphate to produce DXP. In the second step, an intramolecular rearrangement and reduction of DXP by the enzyme DXP reductoisomerase (DXR) yields 2-*C*-methyl-D-erythritol 4-phosphate (MEP). As described below, a different oxidoreductase enzyme with a DXR-like (DRL) activity was

recently found in a reduced number of bacteria (Sangari et al. 2010). MEP produced by DXR or DRL is then converted to 2-*C*-methyl-D-erythritol 2,4-cyclodiphosphate by the sequential action of the enzymes 2-*C*-methyl-D-erythritol 4-phosphate cytidylyltransferase (MCT), 4-(cytidine 5′-diphospho)-2-*C*-methyl-D-erythritol kinase (CMK), and 2-*C*-methyl-D-erythritol 2,4-cyclodiphosphate synthase (MDS). An opening reduction of MEcPP ring is catalyzed by the enzyme 4-hydroxy-3-methylbut-2-enyl diphosphate (HMBPP) synthase (HDS), which forms HMBPP. Finally, the enzyme HMBPP reductase (HDR) catalyzes the simultaneous formation of IPP and DMAPP. The functional and structural properties of the different MEP pathway enzymes have recently been reviewed by Hunter (2007).

The MVA pathway (Fig. 1.5) starts with the sequential condensation of three molecules of acetyl-CoA to yield 3-hydroxy-3-methylglutaryl CoA (HMG-CoA) catalyzed by the enzymes acetoacetyl-CoA thiolase (AACT) and HMG-CoA synthase (HMGS). HMG-CoA is then converted to MVA in a functionally irreversible reaction catalyzed by HMG-CoA reductase (HMGR). MVA is sequentially phosphorylated and decarboxylated to generate IPP by the enzymes mevalonate kinase (MVK), 5-phosphomevalonate kinase (PMDK), and 5-diphosphomevalonate decarboxylase (DPMD). As indicated below, some Archaea species contain an alternative version of the MVA pathway involving the last two steps leading to the formation of IPP.

In contrast to the MEP pathway that simultaneously produces both IPP and DMAPP, the MVA pathway can only produce IPP. Thus, the isomerization of IPP to DMAPP, catalyzed by IPP isomerase (IDI) (Fig. 1.1), is an essential reaction in those organisms containing the MVA pathway. Two types of IPP isomerase are currently known. The type I enzyme is found in many eubacteria (including *E. coli*), yeast, and mammals and has been extensively characterized at structural and functional level (Durbecq et al. 2001; Wouters et al. 2003). The type II enzyme was discovered recently in *Streptomyces* sp. (Kaneda et al. 2001) and is known to be present in Archaea and some bacteria, but not in plants and animals (Kuzuyama and Seto 2003; Laupitz et al. 2004). Type I and type II IDI show no sequence similarity and have different cofactor requirements (Kaneda et al. 2001). The crystal structure of type II IDI from *B. subtilis* and *Thermus thermophilus* has recently been resolved by Steinbacher et al. (2003a) and de Ruyck et al. (2008), respectively.

1.4 Distribution of the MEP and MVA Pathways in Microorganisms

The large number of currently available sequenced genomes is providing a clear picture about the distribution of the MEP and MVA pathways in prokaryotic organisms. The distribution of both pathways, as well as that of type I and type II IDIs, in microorganisms belonging to representative groups is shown in Table 1.2. The archaeal genomes sequenced to date have exclusively revealed the presence of genes encoding MVA pathway enzymes. However, with the exception of some *Sulfolobus* species, the genomic analyses have failed to identify the full set of MVA pathway genes in the rest of species. In particular, the genes encoding PMVK and DPMD (Fig. 1.5) are absent in most archaebacteria (Boucher et al. 2004; Lombard and Moreira 2011). In these organisms, the conversion of phosphomevalonate to IPP is achieved through the operation of an alternative route involving the formation of isopentenyl phosphate from phosphomevalonate by phosphomevalonate decarboxylase (PMVD) and further conversion to IPP by IP kinase (IPK) (Fig. 1.5) (Grochowski et al. 2006). Although IPK has been characterized at the biochemical (Chen and Poulter 2010) and structural level (Mabanglo et al. 2010), the PMVD activity is still speculative and needs biochemical confirmation.

As shown in Table 1.2, most eubacteria contain the MEP pathway. Species containing the MVA pathway include the spirochaete *Borrelia burgdorferi* and the Gram-positive cocci *Staphylococcus aureus* and *Streptococcus pneumoniae*. Among the few bacterial species

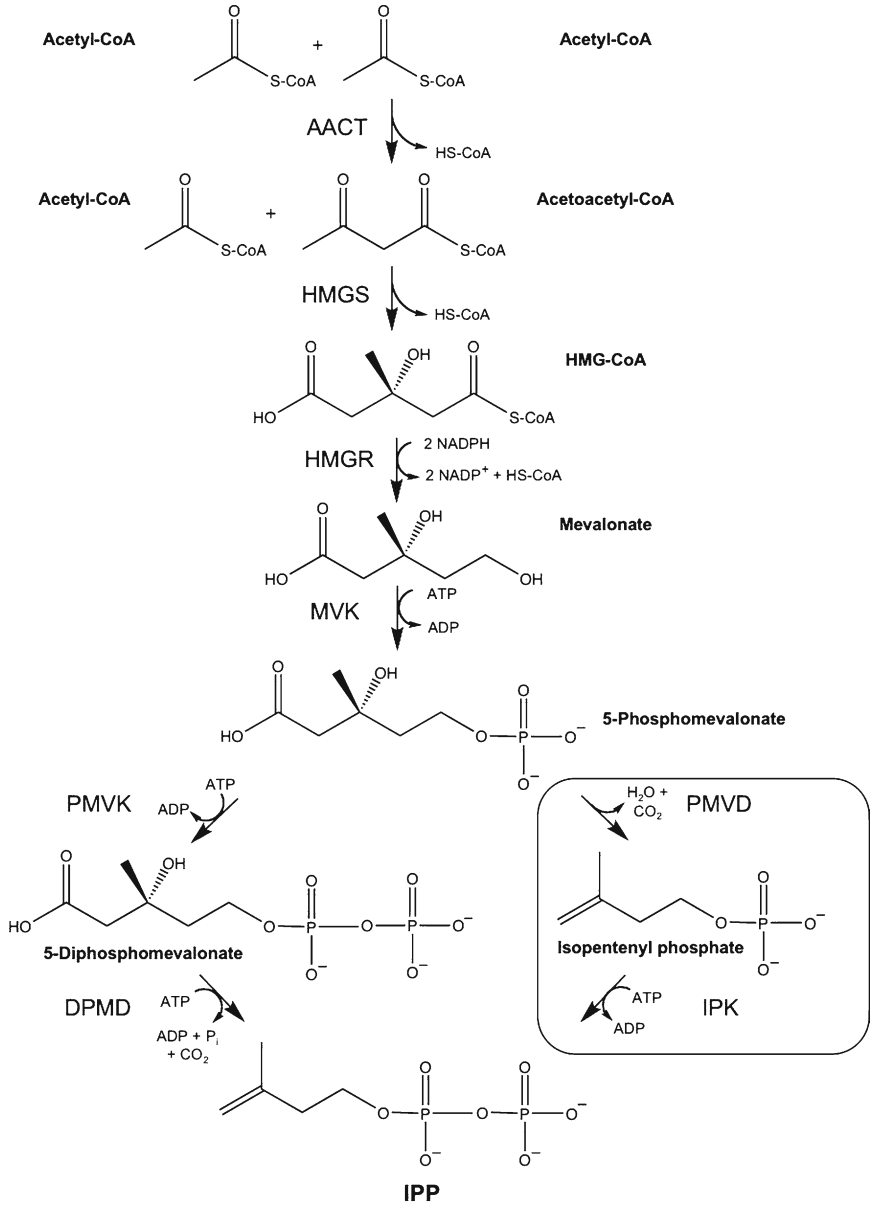

Fig. 1.5 Steps of the MVA pathway leading to the formation of IPP from acetyl-CoA. Acronyms of enzymes and intermediates are described in the text. The modified version of the MVA pathway described in archaebacteria is *boxed*

containing the MVA pathway some of them also have the MEP pathway. Bacteria containing both pathways include *Listeria monocytogenes* and some *Streptomyces* strains. Although all *Streptomyces* use the MEP pathway for the synthesis of essential isoprenoids, some species can additionally use the MVA pathway for the production of secondary metabolites (e.g., antibiotics) (Kuzuyama and Seto 2003). It is interesting to note that some bacteria, like *Rickettsia prowazekii*, lack both isoprenoid pathways. It is likely that, similarly to other obligatory intracellular parasites, *R. prowazekii* uses isoprenoids or precursors provided by the infected host cells.

Table 1.2 Distribution of the MVA and MEP pathways and the genes encoding type I and type II IPP isomerase (IDI) in representative microorganisms

	MEP pathway	MVA pathway	Type I IDI	Type II IDI
Eubacteria				
Aquifex aeolicus	+	–	–	–
Bacillus anthracis	+	–	–	+
Bacillus subtilis	+	–	–	+
Borrelia burgdorferi	–	+	–	+
Brucella abortus	+	–	–	–
Corynebacterium diphtheriae	+	–	+	–
Clostridium acetobutylicum	+	–	+	–
Chlamydia trachomatis	+	–	–	–
Deinococcus radiodurans	+	–	–	+
Escherichia coli	+	–	+	–
Haemophilus influenzae	+	–	–	–
Helicobacter pylori	+	–	–	–
Klebsiella pneumoniae	+	–	–	–
Listeria monocytogenes	+	+	–	+
Mycobacterium tuberculosis	+	–	–	–
Mycoplasma genitalium	+	–	–	–
Neisseria meningitidis	+	–	–	–
Pseudomonas aeruginosa	+	–	+	–
Rickettsia prowazekii	–	–	–	+
Salmonella typhimurium	+	–	+	–
Serratia marcescens	+	–	–	–
Staphylococcus aureus	–	+	–	+
Streptococcus pneumoniae	–	+	–	+
Streptomyces sp. *strain CL190*	+	+	+	+
Synechocystis sp. *PCC 6803*	+	–	–	+
Thermotoga maritima	+	–	–	–
Treponema pallidum	+	–	–	–
Yersinia pestis	+	–	–	–
Vibrio cholerae	+	–	+	–
Archaebacteria				
Archaeoglobus fulgidus	–	+	–	+
Methanococcus jannaschii	–	+	–	+
Pyrococcus furiosus	–	+	–	+

Interestingly, *Brucella abortus* and a number of other related and unrelated bacteria that use the MEP pathway lack DXR but have another DXR-like (DRL) enzyme, which catalyzes the same reaction despite showing no overall homology (Sangari et al. 2010). DRL belongs to a family of previously uncharacterized proteins with oxidoreductase sequence features. The *B. abortus* DRL enzyme was shown to catalyze the NADPH-dependent conversion of DXP into MEP both *in vitro* and *in vivo*, but not as efficiently as *E. coli* DXR. DRL homologues were found in different groups of bacteria with a scattered taxonomic distribution that suggested lateral gene transfer and lineage-specific gene duplications and/or losses, similar to that described for typical MVA and MEP pathway genes (Sangari et al. 2010). Bacteria harboring DRL homologues in their genomes can be grouped in three classes: A (with DRL but not DXR), B (with both DRL and DXR), and C (with DRL but no MEP pathway genes). These observations highlight the

astonishing plasticity of bacterial isoprenoid biosynthesis and open new avenues for research.

Contributing to such plasticity, structurally unrelated type I and II IDI enzymes interconvert IPP and DMAPP albeit with different reaction mechanisms (Rothman et al. 2008; Unno et al. 2009; Sharma et al. 2010). There is no correlation between the presence of type I or type II enzymes and the operation of either the MVA or the MEP pathways (Table 1.2). Interestingly, a large proportion of bacteria containing the MEP pathway do not contain IDI. This may not be surprising considering that the MEP pathway simultaneously produces IPP and DMAPP. Although it is likely that IDI may serve to balance the IPP and DMAPP pools according to particular growth conditions, *E. coli* strains lacking a functional *idi* gene (encoding type I IDI; Table 1.1) do not show any growth phenotype (Hahn et al. 1999; Rodríguez-Concepción et al. 2000). This observation suggests that IDI may also be a dispensable enzyme in bacteria having both the MEP pathway and *idi* genes.

1.5 The MEP Pathway as a Target for the Development of New Antibiotics

The MEP pathway is absent from archaebacteria, fungi, and animals (including humans), which synthesize their isoprenoids exclusively from MVA-derived precursors. By contrast, in some protozoa (including *Plasmodium*, *Cryptosporidium*, *Toxoplasma*, and *Leishmania*), the MEP pathway is the only one synthesizing isoprenoid precursors. Moreover, the MEP pathway is essential for the vast majority of eubacteria that are pathogenic and opportunistic microbes for humans, the main exceptions being *Streptococcus*, *Staphylococcus,* and *Borrelia*. The phylogenetic distribution of the MVA and the MEP pathways immediately suggested the utilization of the MEP pathway as a promising new target for the development of agents against microbial pathogens (many of which are acquiring resistance to currently available drugs). Since the MEP pathway enzymes are highly conserved but show no homology to mammalian proteins (Lange et al. 2000), it was expected that the use of specific inhibitors should result in novel antimicrobial drugs with a broad-spectrum activity and little toxicity to humans. Because of the tools available in *E. coli* due to its use for the elucidation of the pathway, this bacterium appears as an excellent model system for the development of such a new generation of antibiotics targeting the MEP pathway.

1.5.1 The MEP Pathway in *E. Coli*

Soon after the first experimental evidences revealing the existence of an alternative pathway for the synthesis of isoprenoid precursors in bacteria and plants, *E. coli* served as the model organism for the elucidation of this novel pathway. Using a combination of approaches that included microbial genetics, biochemistry, molecular biology, and bioinformatics, all the genes and enzymes of the MEP pathway were identified in *E. coli* in a short period of time (Rodríguez-Concepción and Boronat 2002).

All the genes encoding MEP pathway enzymes in *E. coli* are listed in Table 1.1. With the only exception of *ispD* and *ispF* that are predicted to be included in the same transcription unit, the other MEP pathway genes are found in different chromosomal positions and thus expressed under the control of different promoters. Interestingly, *dxs*, the gene that encodes the first enzyme of the MEP pathway, is present in the operon containing *ispA*, the gene which encodes farnesyl diphosphate synthase. The coexpression of *dxs* and *ispA* suggests a coordinated regulation between the synthesis of IPP/DMAPP and that of FPP, the precursor of the major isoprenoid end products in *E. coli* (Fig. 1.2). Although *dxr* and *ispU* (the gene encoding undecaprenyl diphosphate synthase) are one next to the other in the *E. coli* genome, their expression is predicted to be under the control of different promoters. The other genes of the MEP pathway are expressed individually or in operons containing unrelated genes.

1.5.2 Fosmidomycin, the First Specific Inhibitor of the MEP Pathway

Fosmidomycin (FSM), also known as FR-31564 and 3-(N-formyl-N-hydroxyamino) propylphosphonic acid, was the first compound described to inhibit the MEP pathway. Originally, FSM was identified as a natural antibiotic from *Streptomyces lavendulae* against most Gram-negative and some Gram-positive bacteria (Okuhara et al. 1980). Clinical trials were carried out in the mid-1980s for treating urinary tract infections, but the mechanism of action remained unknown until the end of the decade, when the observation that FSM inhibited the biosynthesis of menaquinone and carotenoids in *Micrococcus luteus* led to propose that the antibiotic targeted isoprenoid biosynthesis (Shigi 1989). The structural similarity of FSM with methylerythrose 4-phosphate, a proposed intermediate in the conversion of DXP into MEP by the enzyme DXR, led to the first experiments demonstrating that FSM is a competitive inhibitor of DXR (Kuzuyama et al. 1998; Zeidler et al. 1998). More recently, the analysis of the crystal structure of DXR in complex with the inhibitor provided stereochemical reasons suggesting that FSM binds substrate-like rather than acting as a transition state analogue (Steinbacher et al. 2003b). FSM also inhibits DRL *in vitro* (Sangari et al. 2010), supporting the conclusion that the reaction mechanism is similar in DXR and DRL.

Different studies have already shown that FSM and derived drugs and prodrugs are efficient tools against the malaria parasites (Jomaa et al. 1999; Rodríguez-Concepción 2004). This, together with their low manufacturing costs and high tolerance and stability, makes them a very attractive class of new antibiotics agents to fight against multidrug-resistant microbes. However, a number of bacteria harboring the MEP pathway can grow normally in the presence of FSM, whereas others can easily develop resistance. For example, Gram-positive mycobacteria are insensitive to FSM despite they only use the MEP pathway for isoprenoid biosynthesis (Dhiman et al. 2005). A recent study (Brown and Parish 2008) has shown that such a resistance is based on the lack of penetration of this hydrophilic inhibitor into the cells due to the highly impervious nature of the hydrophobic mycobacterial cell wall and the lack of the *glpT* gene, encoding a cAMP-dependent glycerol 3-phosphate transporter required for FSM uptake in *E. coli* (Sakamoto et al. 2003). This might also be the case of *B. abortus* cells, which have a DRL enzyme that can be inhibited by FSM, but only showed FSM sensitivity when transformed with the *E. coli glpT* gene (Sangari et al. 2010). Work in *E. coli* has also confirmed that interference with FSM import or export can result in FSM resistance. Thus, *E. coli* mutants defective in the production of cAMP or the GlpT transporter (Sakamoto et al. 2003) or cells overexpressing the *fsr* gene, encoding a putative transmembrane polypeptide with homology to bacterial drug-export proteins (Fujisaki et al. 1996), acquire resistance to FSM.

1.5.3 Identification of New Antibiotics Targeting the MEP Pathway

In addition to FSM, two other main groups of MEP pathway inhibitors have been reported. Phosphonohydroxamic acids 4-(hydroxyamino)-4-oxobutylphosphonic acid and 4-[hydroxy(methyl) amino]-4-oxobutyl phosphonic acid were recently reported as inhibitors of DXR (Kuntz et al. 2005). The latter showed an inhibitory activity towards DXR similar to that of FSM, as well as significant antibacterial activity against *E. coli* cells grown on plates. A second class of inhibitors was identified to target the first step of the MEP pathway, catalyzed by DXS. Clomazone (also known as dimethazone and FMC 57020) is an herbicide that reduces the levels of plastidial isoprenoids in plants similarly to FSM (Lange et al. 2001; Carretero-Paulet et al. 2006). Its breakdown product 5-ketoclomazone (KC) is even more efficient as an inhibitor of plastidial isoprenoid synthesis (Zeidler et al. 2000). Whereas KC is able to inhibit the activity of the DXS enzyme, clomazone itself has no effect *in vitro* (Müller et al. 2000). Because clomazone does not inhibit bacterial growth (Rodríguez-Concepción 2004) but blocks the production of plastidial isoprenoids (Lange et al. 2001; Carretero-Paulet et al. 2006),

it is likely that plants but not bacteria are able to convert clomazone into the active compound KC (which according to IUPAC rules should be named oxoclomazone).

The efficiency of KC as an inhibitor of the MEP pathway in bacteria was recently established (Matsue et al. 2010). In this study, KC showed antibacterial activity against *E. coli* and *Haemophilus influenzae* (although with different inhibitory values), and this activity was suppressed by supplementing the cultures with deoxyxylulose, a free alcohol that can be converted into DXP upon phosphorylation by D-xylulokinase (Wungsintaweekul et al. 2001; Hemmerlin et al. 2006). The kinetics of KC inhibition of purified DXS enzymes from these bacteria was also evaluated (Matsue et al. 2010). KC was found to act as an uncompetitive inhibitor that does not bind to the free enzyme but to the pyruvate-enzyme complex. Even though the antibacterial activity of KC appears to be lower than that of FSM or the well-known antibiotic ampicillin (Matsue et al. 2010), further KC derivatives might eventually be useful to efficiently inhibit the MEP pathway in bacteria and protozoa *in vivo*.

New inhibitors of the MEP pathway are expected to be identified and developed into drugs in the next few years (Rodríguez-Concepción 2004; Rohmer et al. 2004; Obiol-Pardo et al. 2011). To facilitate an effective drug design, genetic, biochemical, and crystallographic approaches should now identify what are the most appropriate pathway enzymes to inhibit and what residues play a relevant structural or catalytic role. Most of this work could be done in a relatively short time by taking advantage of the tools already available in *E. coli*. For example, the use of strains carrying a synthetic MVA operon (which allows them to survive a complete block of the MEP pathway when MVA is present in the growth medium) has led to the identification of several point mutations in the MEP pathway genes leading to a complete loss of enzyme activity (Sauret-Güeto et al. 2003). The same strains were also used to identify the most appropriate targets for future antibiotic design (Sauret-Güeto et al. 2006). Thus, *E. coli* mutants rescuing the otherwise lethal loss of the genes encoding DXS or DXR were found with a relatively high frequency, whereas no mutants were isolated that could rescue the deletion of any of the rest of the pathway genes (Sauret-Güeto et al. 2006). Based on these results, activities other than DXS and even DXR should be targeted to minimize the development of resistance mechanisms in the context of the MEP pathway as a new target for antibiotic and antimalarial agents.

Acknowledgments We thank the collaboration of Marçal Gallemí in the preparation of the figures. Work from our groups was mainly supported by grants from the Spanish Ministerio de Ciencia e Innovación (MICINN) BIO2006-03704 and BIO2009-09523 to A.B. and BIO2011-23680 to M.R.C., all including FEDER funds, and the Generalitat de Catalunya (GC) grant 2009SGR-26. Our work was carried out within the Centre CONSOLIDER on Agrigenomics (funded by MICINN) and Xarxa de Referencia en Biotecnologia (funded by GC).

References

Ajikumar PK, Tyo K, Carlsen S, Mucha O, Phon TH, Stephanopoulos G (2008) Terpenoids: opportunities for biosynthesis of natural product drugs using engineered microorganisms. Mol Pharm 5:167–190

Boucher Y, Kamekura M, Doolittle WF (2004) Origins and evolution of isoprenoid lipid biosynthesis in archaea. Mol Microbiol 52:515–527

Bouhss A, Trunkfield AE, Bugg TD, Mengin-Lecreulx D (2008) The biosynthesis of peptidoglycan lipid-linked intermediates. FEMS Microbiol Rev 32:208–233

Brown AC, Parish T (2008) Dxr is essential in *Mycobacterium tuberculosis* and fosmidomycin resistance is due to a lack of uptake. BMC Microbiol 8:78

Bryant DA, Frigaard NU (2006) Prokaryotic photosynthesis and phototrophy illuminated. Trends Microbiol 14:488–496

Carretero-Paulet L, Cairó A, Botella-Pavía P et al (2006) Enhanced flux through the methylerythritol 4-phosphate pathway in Arabidopsis plants overexpressing deoxyxylulose 5-phosphate reductoisomerase. Plant Mol Biol 62:683–695

Chen M, Poulter CD (2010) Characterization of thermophilic archaeal isopentenyl phosphate kinases. Biochemistry 49:207–217

Dairi J (2005) Studies on biosynthetic genes and enzymes of isoprenoids produced by actinomycetes. J Antibiot (Tokyo) 58:227–243

Das A, Yoon SH, Lee SH, Kim JY, Oh DK, Kim SW (2007) An update on microbial carotenoid production: application of recent metabolic engineering tools. Appl Microbiol Biotechnol 77:505–512

de Ruyck J, Pouyez J, Rothman SC, Poulter D, Wouters J (2008) Crystal structure of type 2 isopentenyl diphosphate isomerase from *Thermus thermophilus* in complex with inorganic pyrophosphate. Biochemistry 47:9051–9053

Dhiman RK, Schaeffer ML, Bailey AM, Testa CA, Scherman H, Crick DC (2005) 1-Deoxy-D-xylulose 5-phosphate reductoisomerase (IspC) from *Mycobacterium tuberculosis*: towards understanding mycobacterial resistance to fosmidomycin. J Bacteriol 187:8395–8402

Durbecq V, Sainz G, Oudjama Y et al (2001) Crystal structure of isopentenyl diphosphate:dimethylallyl diphosphate isomerase. EMBO J 20:1530–1537

Eisenreich W, Bacher A, Arigoni D, Rohdich F (2004) Biosynthesis of isoprenoids via the non-mevalonate pathway. Cell Mol Life Sci 61:1401–1426

Fuhrman JA, Schwalbach MS, Stingl U (2008) Proteorhodopsins: an array of physiological roles? Nat Rev Microbiol 6:488–494

Fujisaki S, Ohnuma S, Horiuchi T et al (1996) Cloning of a gene from *Escherichia coli* that confers resistance to fosmidomycin as a consequence of amplification. Gene 175:83–87

Gomez Maqueo Chew A, Bryant DA (2007) Chlorophyll biosynthesis in bacteria: the origins of structural and functional diversity. Annu Rev Microbiol 61:113–129

Grochowski LL, Xu H, White RH (2006) *Methanocaldococcus jannaschii* uses a modified mevalonate pathway for biosynthesis of isopentenyl diphosphate. J Bacteriol 188:3192–3198

Hahn FM, Hurlburt AP, Poulter CD (1999) *Escherichia coli* open reading frame 696 is *idi*, a nonessential gene encoding isopentenyl diphosphate isomerase. J Bacteriol 181:4499–4504

Hemmerlin A, Tritsch D, Hartmann M et al (2006) A cytosolic Arabidopsis D-xylulose kinase catalyzes the phosphorylation of 1-deoxy-D-xylulose into a precursor of the plastidial isoprenoid pathway. Plant Physiol 142:441–457

Hunter WN (2007) The non-mevalonate pathway of isoprenoid precursor biosynthesis. J Biol Chem 282:21573–21577

Jomaa H, Wiesner J, Sanderbrand S et al (1999) Inhibitors of the nonmevalonate pathway of isoprenoid biosynthesis as antimalarial drugs. Science 285:1573–1576

Kaneda K, Kuzuyama T, Takagi M, Hayakawa Y, Seto H (2001) An unusual isopentenyl diphosphate isomerase found in the mevalonate pathway gene cluster from *Streptomyces* sp. strain CL190. Proc Natl Acad Sci USA 98:932–937

Kannenberg EL, Poralla K (1999) Hopanoid biosynthesis and function in bacteria. Naturwissenschaften 86: 168–176

Kawamukai M (2002) Biosynthesis, bioproduction and novel roles of ubiquinone. J Biosci Bioeng 94: 511–517

Kirby J, Keasling JD (2008) Metabolic engineering of microorganisms for isoprenoid production. Nat Prod Rep 25:656–661

Kirby J, Keasling JD (2009) Biosynthesis of plant isoprenoids: perspectives for microbial engineering. Annu Rev Plant Biol 60:335–355

Klein-Marcuschamer D, Ajikumar PK, Stephanopoulos G (2007) Engineering microbial cell factories for biosynthesis of isoprenoid molecules: beyond lycopene. Trends Biotechnol 25:417–424

Koga Y, Morii H (2007) Biosynthesis of ether-type polar lipids in archaea and evolutionary considerations. Microbiol Mol Biol Rev 71:97–120

Kuntz L, Tritsch D, Grosdemange-Billiard C et al (2005) Isoprenoid biosynthesis as a target for antibacterial and antiparasitic drugs: phosphonohydroxamic acids as inhibitors of deoxyxylulose phosphate reductoisomerase. Biochem J 386:127–135

Kuzuyama T, Seto H (2003) Diversity of the biosynthesis of the isoprene units. Nat Prod Rep 20:171–183

Kuzuyama T, Shimizu T, Takahashi S, Seto H (1998) Fosmidomycin, a specific inhibitor of 1-deoxy-D-xylulose 5-phosphate reductoisomerase in the nonmevalonate pathway for terpenoid biosynthesis. Tetrahedron Lett 39:7913–7916

Lange BM, Rujan T, Martin W, Croteau R (2000) Isoprenoid biosynthesis: the evolution of two ancient and distinct pathways across genomes. Proc Natl Acad Sci USA 97:13172–13177

Lange BM, Ketchum RE, Croteau RB (2001) Isoprenoid biosynthesis. Metabolite profiling of peppermint oil gland secretory cells and application to herbicide target analysis. Plant Physiol 127:305–314

Laupitz R, Hecht S, Amslinger S et al (2004) Biochemical characterization of *Bacillus subtilis* type II isopentenyl diphosphate isomerase, and phylogenetic distribution of isoprenoid biosynthesis pathways. Eur J Biochem 271:2658–2669

Lee PC, Schmidt-Dannert C (2002) Metabolic engineering towards biotechnological production of carotenoids in microorganisms. Appl Microbiol Biotechnol 60:1–11

Lichtenthaler HK (1999) The 1-deoxy-D-xylulose-5-phosphate pathway of isoprenoid biosynthesis in plants. Annu Rev Plant Physiol Plant Mol Biol 50:47–65

Lombard J, Moreira D (2011) Origins and early evolution of the mevalonate pathway of isoprenoid biosynthesis in the three domains of life. Mol Biol Evol 28:87–99

Mabanglo MF, Schubert HL, Chen M, Hill CP, Poulter CD (2010) X-ray structures of isopentenyl phosphate kinase. ACS Chem Biol 5:517–527

Maresca JA, Graham JE, Bryant DA (2008) The biochemical basis for structural diversity in the carotenoids of chlorophototrophic bacteria. Photosynth Res 97: 121–140

Matsue Y, Mizuno H, Tomita T et al (2010) The herbicide ketoclomazone inhibits 1-deoxy-D-xylulose 5-phosphate synthase in the 2-*C*-methyl-D-erythritol 4-phosphate pathway and shows antibacterial activity against *Haemophilus influenzae*. J Antibiot (Tokyo) 63: 583–588

Meganathan R (2001) Ubiquinone biosynthesis in microorganisms. FEMS Microbiol Lett 203:131–139

Misawa N (2011) Pathway engineering for functional isoprenoids. Curr Opin Biotechnol 22:1–7

Mogi T, Saiki K, Anraku Y (1994) Biosynthesis and functional role of haem O and haem A. Mol Microbiol 14:391–398

Müller C, Schwender J, Zeidler J, Lichtenthaler HK (2000) Properties and inhibition of the first two enzymes of the non-mevalonate pathway of isoprenoid biosynthesis. Biochem Soc Trans 28:792–793

Obiol-Pardo C, Rubio-Martinez J, Imperial S (2011) The methylerythritol phosphate (MEP) pathway for isoprenoid biosynthesis as a target for the development of new drugs against tuberculosis. Curr Med Chem 18:1325–1338

Okuhara M, Kuroda Y, Goto T et al (1980) Studies on new phosphonic acid antibiotics. III. Isolation and characterization of FR-31564, FR-32863 and FR-33289. J Antibiot (Tokyo) 33:24–28

Persson BC, Esberg B, Olafsson O, Björk GR (1994) Synthesis and function of isopentenyl adenosine derivatives in tRNA. Biochimie 76:1152–1160

Phillips MA, León P, Boronat A, Rodríguez-Concepción M (2008) The plastidial MEP pathway: unified nomenclature and resources. Trends Plant Sci 13:619–623

Rodríguez-Concepción M (2004) The MEP pathway: a new target for the development of herbicides, antibiotics and antimalarial drugs. Curr Pharm Des 10: 2391–2400

Rodríguez-Concepción M, Boronat A (2002) Elucidation of the methylerythritol phosphate pathway for isoprenoid biosynthesis in bacteria and plastids. A metabolic milestone achieved through genomic. Plant Physiol 130:1079–1089

Rodríguez-Concepción M, Campos N, Lois ML et al (2000) Genetic evidence of branching in the isoprenoid pathway for the production of isopentenyl diphosphate and dimethylallyl diphosphate in *Escherichia coli*. FEBS Lett 473:328–332

Rohmer M (1999) The discovery of a mevalonate-independent pathway for isoprenoid biosynthesis in bacteria, algae and higher plants. Nat Prod Rep 16:565–574

Rohmer M (2008) From molecular fossils of bacterial hopanoids to the formation of isoprene units: discovery and elucidation of the methylerythritol phosphate pathway. Lipids 43:1095–1107

Rohmer M, Grosdemange-Billiard C, Seemann M, Tritsch D (2004) Isoprenoid biosynthesis as a novel target for antibacterial and antiparasitic drugs. Curr Opin Investig Drugs 5:154–162

Rothman SC, Johnston JB, Lee S, Walker JR, Poulter CD (2008) Type II isopentenyl diphosphate isomerase: irreversible inactivation by covalent modification of flavin. J Am Chem Soc 130:4906–4913

Sakamoto Y, Furukawa S, Ogihara H, Yamasaki M (2003) Fosmidomycin resistance in adenylate cyclase deficient (cya) mutants of *Escherichia coli*. Biosci Biotechnol Biochem 67:2030–2033

Sangari FJ, Pérez-Gil J, Carretero-Paulet L, García-Lobo JM, Rodríguez-Concepción M (2010) A new family of enzymes catalyzing the first committed step of the methylerythritol 4-phosphate (MEP) pathway for isoprenoid biosynthesis in bacteria. Proc Natl Acad Sci USA 107:14081–14086

Sauret-Güeto S, Ramos-Valdivia A, Ibáñez E, Boronat A, Rodríguez-Concepción M (2003) Identification of lethal mutations in *Escherichia coli* genes encoding enzymes of the methylerythritol phosphate pathway. Biochem Biophys Res Commun 307:408–415

Sauret-Güeto S, Urós EM, Ibáñez E, Boronat A, Rodríguez-Concepción M (2006) A mutant pyruvate dehydrogenase E1 subunit allows survival of *Escherichia coli* strains defective in 1-deoxy-D-xylulose 5-phosphate synthase. FEBS Lett 580:736–740

Sharma NK, Pan JJ, Poulter CD (2010) Type II isopentenyl diphosphate isomerase: probing the mechanism with alkyne/allene diphosphate substrate analogues. Biochemistry 49:6228–6233

Shigi Y (1989) Inhibition of bacterial isoprenoid synthesis by fosmidomycin, a phosphonic acid-containing antibiotic. J Antimicrob Chemother 24:131–145

Steinbacher S, Kaiser J, Gerhardt S, Eisenreich W, Huber R, Bacher A, Rohdich F (2003a) Crystal structure of the type II isopentenyl diphosphate:dimethylallyl diphosphate isomerase from *Bacillus subtilis*. J Mol Biol 329:973–982

Steinbacher S, Kaiser J, Eisenreich W, Huber R, Bacher A, Rohdich F (2003b) Structural basis of fosmidomycin action revealed by the complex with 2-C-methyl-D-erythritol 4-phosphate synthase (IspC). Implications for the catalytic mechanism and anti-malaria drug development. J Biol Chem 278:18401–18407

Unno H, Yamashita S, Ikeda Y et al (2009) New role of flavin as a general acid–base catalyst with no redox function in type 2 isopentenyl-diphosphate isomerase. J Biol Chem 284:9160–9167

Vollmer W, Blanot D, de Pedro MA (2008) Peptidoglycan structure and architecture. FEMS Microbiol Rev 32:149–167

Wouters J, Oudjama Y, Barkley SJ, Tricot C, Stalon V, Droogmans L, Poulter CD (2003) Catalytic mechanism of *E. coli* isopentenyl diphosphate isomerase involves Cys67, Glu116 and Tyr104 as suggested by crystal structures of complexes with transition state analogues and irreversible inhibitors. J Biol Chem 278:11903–11908

Wungsintaweekul J, Herz S, Hecht S, Eisenreich W, Feicht R, Rohdich F, Bacher A, Zenk MH (2001) Phosphorylation of 1-deoxy-D-xylulose by D-xylulokinase of *Escherichia coli*. Eur J Biochem 268:310–316

Zeidler J, Schwender J, Müller C et al (1998) Inhibition of the non-mevalonate 1-deoxy-D-xylulose-5-phosphate pathway of plant isoprenoid biosynthesis by fosmidomycin. Z Naturforsch 53c:980–986

Zeidler J, Schwender J, Müller C, Lichtenthaler HK (2000) The non-mevalonate isoprenoid biosynthesis of plants as a test system for drugs against malaria and pathogenic bacteria. Biochem Soc Trans 28:796–798

1-Deoxy-D-Xylulose 5-Phosphate Synthase (DXS), a Crucial Enzyme for Isoprenoids Biosynthesis

2

Song Xiang, Gerlinde Usunow, Gudrun Lange, Marco Busch, and Liang Tong

Abstract

Isopentenyl pyrophosphate (IPP) and its isomer dimethylallyl pyrophosphate (DMAPP) are the common precursors for the synthesis of all isoprenoids. While IPP and DMAPP are produced by the mevalonate pathway in archaea, fungi, and animals, they are synthesized by a mevalonate-independent pathway in most bacteria, algae, and plant plastids. DXS (1-deoxy-D-xylulose 5-phosphate synthase) catalyzes the first and the rate-limiting step of the mevalonate-independent pathway and is an attractive target for the development of novel antibiotics, antimalarials, and herbicides. Crystal structures of DXS from *E. coli* and *D. radiodurans*, in complex with the coenzyme thiamine pyrophosphate (TPP), show that the enzyme contains three domains (I, II, and III), which share homology to the equivalent domains in transketolase and the E1 subunit of pyruvate dehydrogenase. However, DXS has a novel arrangement of these domains in the monomer and the dimer as compared to the other enzymes. The active site of DXS is located at the interface of domains I and II in the same monomer. The coenzyme TPP is mostly buried in the complex, but the C2 atom of its thiazolium ring is exposed to a solvent-accessible tunnel that is likely the substrate-binding site.

Keywords

Isoprenoids • Thiamine pyrophosphate • Protein structure • Transketolase • Pyruvate dehydrogenase • Herbicides • Ketoclomazone • Fosmidomycin

2.1 Introduction

Isoprenoids are a class of extraordinarily diverse natural products and have important functions in all living organisms (Dubey et al. 2003; Eisenreich et al. 2004; Rodríguez-Concepción and Boronat 2002; Sacchettini and Poulter 1997). To date,

S. Xiang • L. Tong (✉)
Department of Biological Sciences,
Columbia University, New York, NY 10027, USA
e-mail: ltong@columbia.edu

G. Usunow • G. Lange • M. Busch
Bayer CropScience GmbH, Industriepark Höchst,
Frankfurt am Main 65926, Germany

T.J. Bach and M. Rohmer (eds.), *Isoprenoid Synthesis in Plants and Microorganisms: New Concepts and Experimental Approaches*, DOI 10.1007/978-1-4614-4063-5_2,

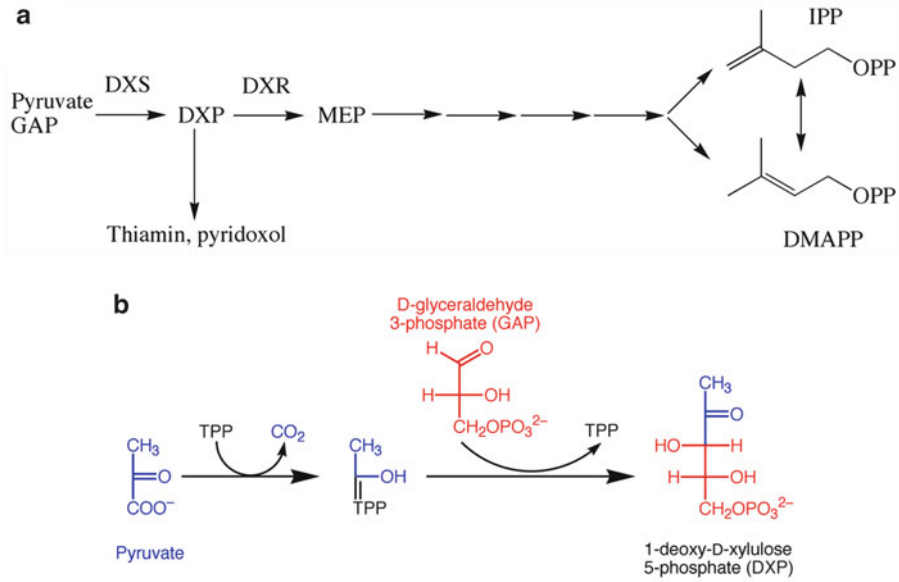

Fig. 2.1 DXS and the mevalonate-independent pathway. (**a**) The mevalonate-independent pathway of IPP and DMAPP biosynthesis. *GAP,* glyceraldehyde 3-phosphate*; DXP,* 1-deoxy-D-xylulose 5-phosphate*; DXS,* DXP synthase*; DXR,* DXP reductoisomerase*; MEP,* 2-*C*-methyl-D-erythritol 4-phosphate. (**b**) The reaction catalyzed by DXS. The covalent intermediate between pyruvate and thiamine diphosphate (*TPP*) is also shown

more than some 30,000–50,000 isoprenoids have been identified from natural sources (cf. Keasling 2010), and some of the well-known compounds include β-carotene, lycopene, cholesterol, chlorophyll, taxol, and dolichol. Because of their important functions, there is considerable interest in increasing the natural production of isoprenoids through genetic engineering or other methods (Enfissi et al. 2005; Tao et al. 2006; Yoon et al. 2007).

Despite their chemical and functional diversity, isoprenoids are synthesized from two common precursors with five carbon atoms, isopentenyl pyrophosphate (IPP) and its isomer dimethylallyl pyrophosphate (DMAPP) (Fig. 2.1a). It has long been known that IPP can be generated from the mevalonate pathway, using acetyl-CoA as the precursor. Recent studies have revealed a mevalonate-independent pathway for IPP biosynthesis in most bacteria, algae, and plant chloroplasts (Fig. 2.1a) (Bouvier et al. 1998; Dubey et al. 2003; Eisenreich et al. 2004; Lange et al. 1998, 2000; Lois et al. 1998; Rodríguez-Concepción and Boronat 2002; Sprenger et al. 1997). This pathway is also called the MEP pathway since 2-*C*-methyl-D-erythritol 4-phosphate (MEP) is its first committed precursor (Fig. 2.1a). As the mevalonate-independent pathway is absent in animals, it represents a promising target for the development of novel antibiotics, antimalarials, herbicides, and other drugs. The herbicide fosmidomycin functions by inhibiting the second enzyme (DXR) in this pathway (Fig. 2.1a) (cf. Lichtenthaler 2000), and it also has activity against malarial infection in an animal model (Jomaa et al. 1999). Although absent in humans, the mevalonate-independent pathway is highly expressed in cohabitating microbiota in the human intestines (Gill et al. 2006).

1-deoxy-D-xylulose 5-phosphate synthase (DXS) catalyzes the first and the rate-limiting reaction in the mevalonate-independent pathway, which involves the condensation of glyceraldehyde 3-phosphate (GAP) and pyruvate (Fig. 2.1b) (Bouvier et al. 1998; Estévez et al. 2001; Harker and Bramley 1999; Lange et al. 1998; Lois et al. 1998, 2000; Matthews and Wurtzel 2000; Sprenger et al. 1997). The 1-deoxy-D-xylulose

5-phosphate (DXP) product of this reaction is also used for the biosynthesis of thiamine (vitamin B_1) and pyridoxol (vitamin B_6) (Fig. 2.1a) (Begley et al. 1999; Hill et al. 1996). DXS requires the coenzyme thiamine diphosphate (TPP), which is believed to form a covalent adduct with the pyruvate substrate as an intermediate in the reaction (Fig. 2.1b).

The *dxs* gene is essential for bacteria (*E. coli*) and plants (Estévez et al. 2001; Mandel et al. 1996). Disruption of this gene in *Arabidopsis* produces an albino phenotype, due to the lack of chlorophylls and carotenoids. Moreover, the herbicide clomazone is believed to function through its metabolite, ketoclomazone, which is an inhibitor of DXS (Lichtenthaler 2000; Meyer et al. 2003; Müller et al. 2000; Zeidler et al. 2000). This demonstrates that DXS may be a proven target for the development of novel herbicides (Zeidler et al. 2000).

2.2 Sequence Conservation of DXS

DXS is highly conserved in plants and bacteria, with 45% or greater amino acid sequence conservation between any pair of enzymes (Fig. 2.2). The conservation of plant DXS proteins is even higher, for example, tomato and *A. thaliana* DXS share 84% amino acid sequence identity (Fig. 2.2).

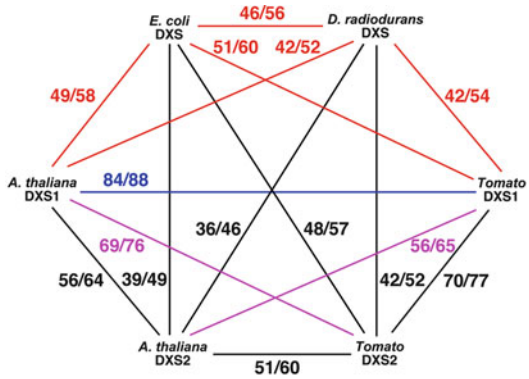

Fig. 2.2 Amino acid sequence conservation of DXS proteins from different organisms. For each pairwise comparison, the first number is the percent sequence identity, and the second number the percent sequence similarity

The conservation among bacterial DXS is relatively weaker; for example, there is 46% sequence identity between *E. coli* and *Deinococcus radiodurans* DXS (Fig. 2.2). This pattern of sequence conservation can also be recognized from a phylogenetic analysis (Fig. 2.3). The plant DXS proteins are clustered together, while the bacterial proteins are more widely dispersed (Fig. 2.3).

Recent studies suggest that most plants contain more than one *dxs* gene (Kim et al. 2006; Paetzold et al. 2010; Walter et al. 2007; Walter et al. 2002, Leon and Cordoba, this volume; Walter et al., this volume). DXS1 (or simply DXS) has similar function compared to those in bacteria. DXS2 (and DXS3) can be in different tissues or different compartments in the plant cell, and their exact biological functions remain to be characterized in most cases. The different DXS isoforms in the same plant share 50–70% amino acid sequence identity (Fig. 2.2). The DXS2 proteins of different plants share roughly 50% identity, suggesting weaker conservation as compared to the DXS1 proteins.

DXS also shares weak sequence homology (about 20% identity) with transketolase and pyruvate dehydrogenase E1 subunit (Bouvier et al. 1998; Lange et al. 1998; Lois et al. 1998; Mandel et al. 1996; Querol et al. 2001; Sprenger et al. 1997). All of these enzymes require the cofactor TPP and catalyze similar biochemical reactions. Nonetheless, the sequence of DXS is significantly distinct from these other enzymes, and it represents a novel class of transketolase-like proteins (Lois et al. 1998; Sprenger et al. 1997).

2.3 Overall Structure of DXS

The crystal structures of *D. radiodurans* and *E. coli* DXS have been reported recently (Fig. 2.4a, b) (Xiang et al. 2007). The overall structures of the two bacterial DXS proteins are similar, consistent with their sequence conservation. The root mean square (rms) distance between equivalent Cα atoms of the two structures is 0.7 Å. The *E. coli* DXS protein was crystallized only after undergoing proteolysis, which removed

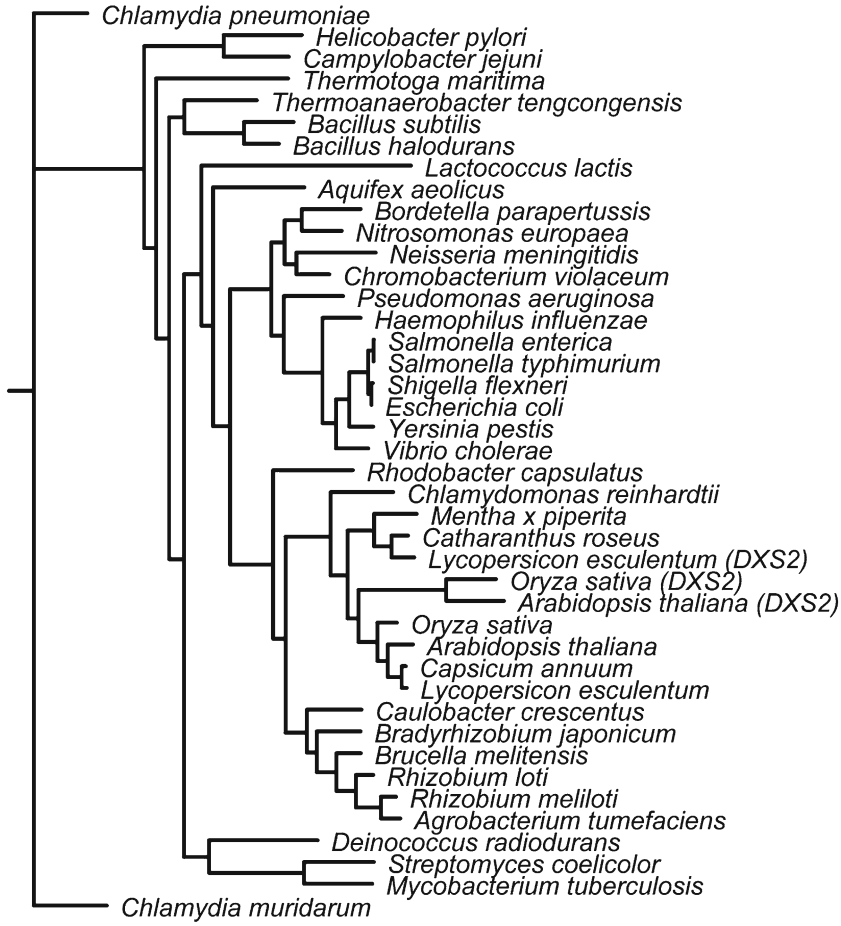

Fig. 2.3 A phylogenetic tree for DXS proteins from different organisms

two loop segments of the protein (Xiang et al. 2007). One of these segments is located near the active site of the enzyme, and the proteolysis caused some structural disturbance in this region. On the other hand, *D. radiodurans* DXS was crystallized without the need for proteolysis, and its structure contains intact active sites.

The DXS monomer contains three domains (Fig. 2.4a, b). All of them have the α/β-fold, with a central, mostly parallel β-sheet that is sandwiched by α helices. Domain I (residues 1–319, numbered based on the *E. coli* DXS sequence) contains five parallel β-strands, flanked on one side by two α-helices and on the other by three major α-helices connected by several smaller ones (Fig. 2.4c). A number of extended surface segments exists in domain I, contributing to its larger size. They are located at the N-terminus (residues 1–49), after the first strand (residues 81–122) and between the fourth and the fifth strands (residues 184–250). Domain II (residues 321–493) contains a six-stranded β-sheet, sandwiched by three α-helices on either side (Fig. 2.4d). Domain III (residues 494–629) contains a five-stranded β-sheet, in which β1 is antiparallel to β2-β5. This central β-sheet is sandwiched by two α-helices on one side and three α-helices on the other (Fig. 2.4e).

Tightly associated dimers were identified in the *E. coli* and *D. radiodurans* DXS crystals (Figs. 2.4a, b), consistent with gel filtration and static light scattering experiments and previous studies (Hahn et al. 2001; Kuzuyama et al. 2000). Each monomer contributes more than 3,900 Å^2

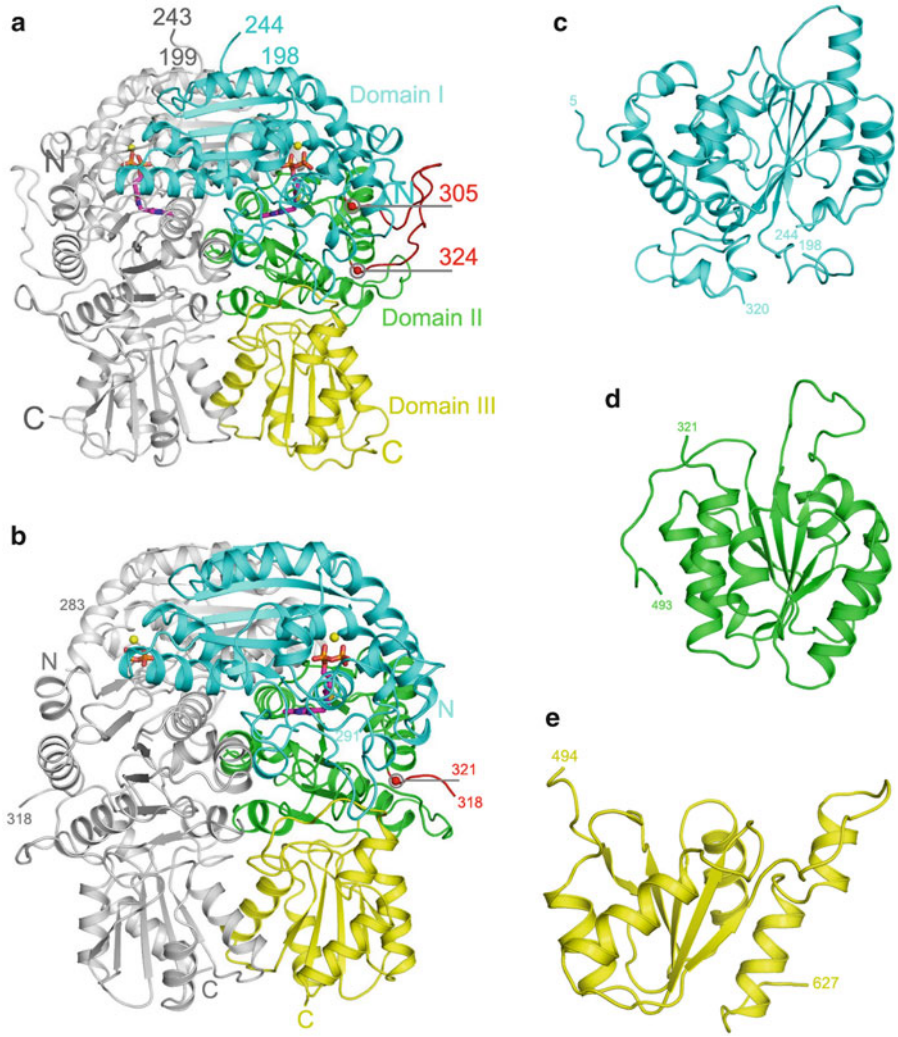

Fig. 2.4 Crystal structures of DXS. (**a**) Schematic drawing of the structure of the *D. radiodurans* DXS dimer. The three domains of one monomer are colored *cyan*, *green*, and *yellow*, respectively, and the linker between domains I and II is colored *red*. The other monomer is colored gray. TPP is shown as a stick model in magenta. (**b**) Structure of *E. coli* DXS dimer, in the same orientation and color scheme as panel A. (**c**) Schematic drawing of domain I of *D. radiodurans* DXS. (**d**) Schematic drawing of domain II of *D. radiodurans* DXS. (**e**) Schematic drawing of domain III of *D. radiodurans* DXS. All structure figures were produced with PyMol (DeLano 2002)

of buried surface area to the dimer interface, corresponding to more than 17% of the total accessible surface area of the monomer. About 67% of the interactions at the interface are hydrophobic. The dimer interface also contains 32 hydrogen bonds and 2 salt bridges, as calculated by the protein-protein interaction server (Jones and Thornton 1996). The dimers of *E. coli* and *D. radiodurans* DXS are very similar, with rms distance of 1.0 Å for their equivalent Cα atoms.

2.4 Structural Homologs and a Novel Dimer Organization in DXS

The structure of DXS displays significant similarity to that of transketolase (TK, Fig. 2.5a) (Nikkola et al. 1994), pyruvate dehydrogenase E1 subunit (PDH, Fig. 2.5b) (Arjunan et al. 2002), and 2-oxoisovalerate dehydrogenase (Aevarsson et al. 1999), despite their low sequence conservation.

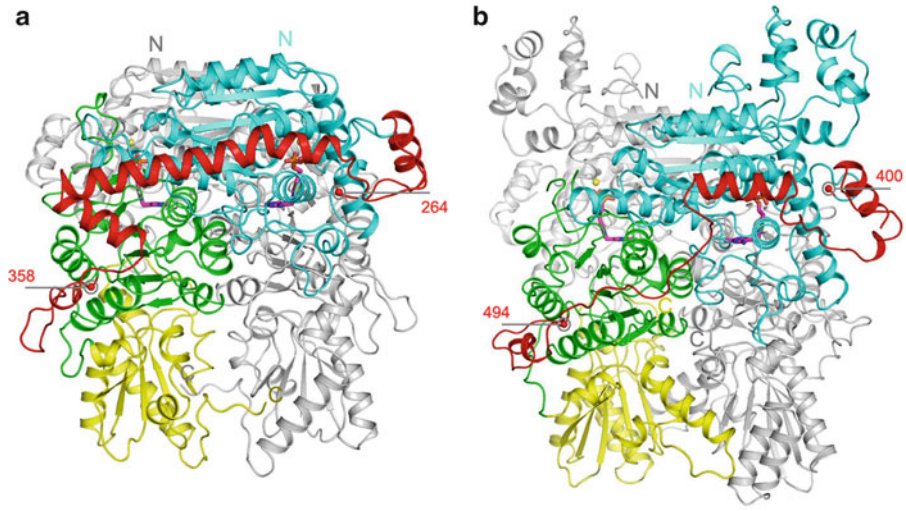

Fig. 2.5 Crystal structures of transketolase and pyruvate dehydrogenase E1 subunit. (**a**) Schematic drawing of the structure of yeast transketolase dimer (Nikkola et al. 1994). (**b**) Structure of *E. coli* pyruvate dehydrogenase E1 subunit dimer (Arjunan et al. 2002)

After structural alignment of the DXS and TK dimers, the rms distance between their equivalent Cα atoms is 1.8 Å for the *E. coli* and *D. radiodurans* DXS. The rms distance between DXS and PDH is about 2.5 Å for their equivalent Cα atoms.

In the dimers of TK and PDH, domain I of one monomer is located directly above domains II and III of the other monomer (Fig. 2.5a, b). A long linker of about 95 residues connects domains I and II across these dimers. In 2-oxoisovalerate dehydrogenase, domain I is a separate subunit, and the protein is a heterotetramer.

In contrast, the linker between domains I and II is much shorter in DXS, with only about 20 residues (Fig. 2.4a). A novel domain arrangement is observed in the structure of DXS, where domain I of one monomer is located directly above domains II and III of the same monomer (Fig. 2.4a). The crystal structures of DXS therefore represent the first observations of a different domain arrangement in TK-like proteins.

Structural information on DXS, TK, PDH, and 2-oxoisovalerate dehydrogenase demonstrates three possible modes of dimerization among these enzymes. The two-subunit form, as exemplified by 2-oxoisovalerate dehydrogenase, might be the precursor of these enzymes. There are two different ways of linking the subunits in this heterotetramer, and both types of linker segment have been adopted by nature.

2.5 The Active Site of DXS

Domains I and II in the DXS monomer are oriented with the C-terminal ends of their central β-sheets pointed toward each other (Fig. 2.6a). The DXS active site is located at the interface between these two domains. The TPP cofactor is bound at this position and is buried deeply inside the protein. Its C2 atom is located at the end of a tunnel opening to the protein surface, consistent with its role in the reaction (see below). Residues in the active site are highly conserved among DXS proteins from bacteria and plants, many of which are also conserved in other TK-like proteins (Table 2.1). In the DXS dimer, the active site is formed by residues from the same monomer, with no direct contribution from the other monomer. In TK and PDH the active site is formed by both monomers in the dimer, due to the different domain organizations.

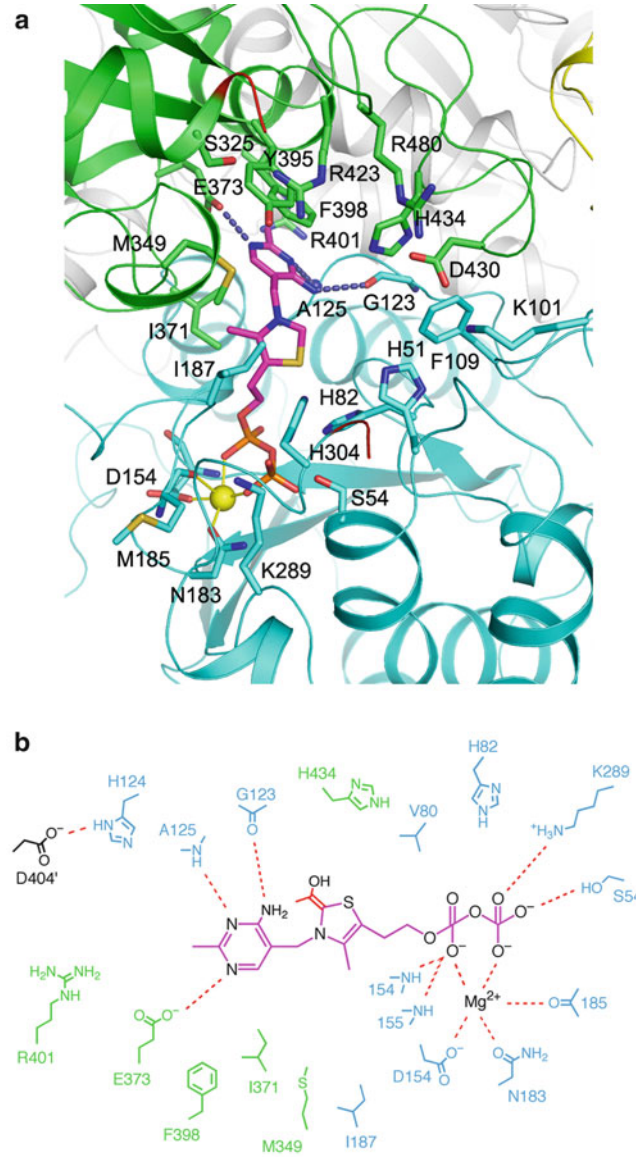

Fig. 2.6 The active site of DXS. (**a**) Structure of the active site of *D. radiodurans* DXS. The TPP molecule is shown in *magenta*. (**b**) Schematic drawing of the interactions between TPP (in adduct with pyruvate) and the active site of DXS. Residues in domain I are colored *cyan*, and those in domain II in *green*. Residue Asp404 is from the other monomer and is shown in *black*

The TPP molecule is accommodated in the active site in a V conformation (Pletcher et al. 1977), with torsion angles Φ_T (rotation around the N3-C_{bridge} bound) of about 100° and Ψ_p (rotation around the C5′-C_{bridge} bound) of about −55° (Fig. 2.6a), which is observed in all TPP-dependent enzymes (Aevarsson et al. 1999; Arjunan et al. 2002; Nikkola et al. 1994). In this conformation, the 4′-amino group is brought into close proximity of the C2 atom in the thiazolium ring (Fig. 2.6a), helping to deprotonate it and activate the cofactor.

The pyrophosphate moiety of TPP interacts with residues from domain I of DXS (Fig. 2.6a). A Mg^{2+} ion is coordinated by the pyrophosphate group and by the side chains of Asp154 (residues numbered according to the *D. radiodurans* DXS sequence) and Asn183 as well as the carbonyl atom of Met185 (Fig. 2.6b). The octahedral coordination of the Mg^{2+} ion would be completed

Table 2.1 Residues in the TPP binding site of DXS and related enzymes

E. coli DXS	*D. radiodurans* DXS	*A. thaliana* DXS	Yeast transketolase	*E. coli* pyruvate dehydrogenase E1 subunit
Ser52	Ser54	Ser118	Ala33	Ser109
His80	**His82**	**His146**	**His69**	**His142**
Gly121	Gly123	Gly187	Gly116	Val192
Ser123	Ala125	Ser189	Leu118	Met194
Asp152	**Asp154**	**Asp208**	**Asp157**	**Asp230**
Asn181	Asn183	Asn247	Asn187	Asn260
Met183	Met185	Val250	Ile189	Gln262
Lys284	Lys289	Lys364	Ile250	Lys392
Ile368	**Ile371**	**Ile448**	**Ile416**	**Ile569**
Glu370	**Glu373**	**Glu450**	**Glu418**	**Glu571**
Phe395	**Phe398**	**Phe475**	**Phe445**	**Phe602**
Arg398	Arg401	Arg478	Tyr448	Arg606

Residues conserved among all five enzymes are in bold face

by a water molecule, which is observed in the crystal structures of TK and PDH (Arjunan et al. 2002; Nikkola et al. 1994). The pyrophosphate group is also anchored to the protein through many hydrogen-bonding interactions, including the side chains of Ser54 and Lys289 as well as the main-chain amide of Asp154 and Gly155 (Fig. 2.6b). The Gly153-Asp154-Gly155–Asn183 sequence in DXS is consistent with the conserved TPP binding motif of GDG-X(25–30)-N (Hawkins et al. 1989).

The thiazolium and the aminopyrimidine rings of TPP form numerous interactions with DXS, primarily with domain II (Fig. 2.6a). On one side of the active site, the thiazolium ring has van der Waals interactions with the side chains of Ile187 and Met349, and the aminopyrimidine ring has π-stacking interactions with the Phe398 side chain (Fig. 2.6b). On the other side of the active site, the side chain of Ile371 interacts with both rings. The three nitrogen atoms on the aminopyrimidine ring are recognized by hydrogen-bonding interactions with the enzyme, including the carbonyl oxygen of Gly123, the main-chain amide of Ala125, and the side chain of the conserved Glu373 residue (Fig. 2.6b). The hydrogen-bonding interaction between the N1′ atom and the glutamate side chain has been proposed to induce tautomerization of the aminopyrimidine ring, converting the 4′ amino group to an imino group, which consequently facilitates the deprotonation of the C2 atom (Schellenberger 1998). In DXS, this conserved Glu373 residue also forms an ion pair with the side chain of Arg401.

Although DXS and TK/PDH adopt different domain arrangements, the active sites of these enzymes are conserved (Table 2.1), and they catalyze similar reactions. This similarity is underscored by the fact that loss of DXS function in *E. coli* can be compensated by a mutation (E636Q) in PDH (Sauret-Güeto et al. 2006). Therefore, the different domain arrangements in these enzymes do not seem to be functionally important. They nevertheless indicate that DXS represents a novel class of the TK-like proteins.

2.6 Reaction Mechanism and Substrate-Binding Modes

The reactions catalyzed by TPP-dependent enzymes have been well characterized (Schellenberger 1998). In the first step of the reaction, the donor substrate (pyruvate in the case of DXS) reacts with the C2 atom of TPP, forming a semistable intermediate (Fig. 2.7). This adduct isomerizes between the α-carbanion and the enamine states. In the second step, the adduct is transferred to the acceptor substrate (GAP in the case of DXS). Extensive studies of the reaction mechanism have been carried out on TK. The crystal structure of the enzyme in complex with the reaction intermediate has been determined (Fiedler et al. 2002), and the structure of the complex with

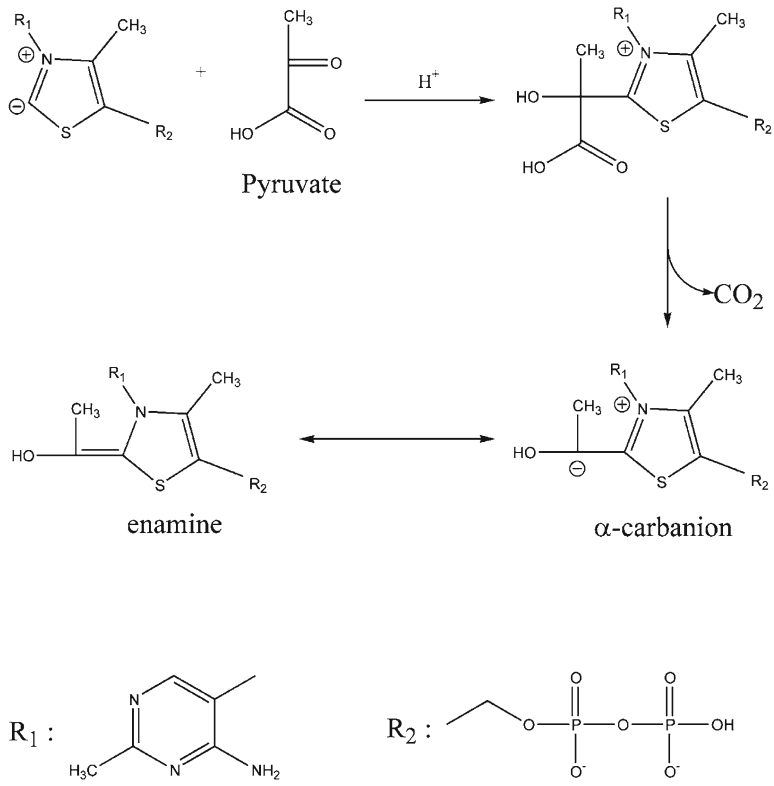

Fig. 2.7 Mechanism for the formation of the adduct between the C2 atom of TPP and pyruvate (Adapted from Fiedler et al. 2002)

the acceptor substrate erythrose 4-phosphate has also been reported (Nilsson et al. 1997).

Based on structural studies of TK, we modeled the covalent adduct (in the enamine state) and the acceptor substrate GAP into the active site of DXS (Fig. 2.8a). Introducing the adduct to the active site does not cause any steric clashes with the protein, consistent with the fact that no conformational changes were observed upon formation of the adduct in TK (Fiedler et al. 2002). The GAP molecule is modeled into the active site tunnel and is expected to interact with residues His51, His304, Tyr395, Arg423, Asp430, and Arg480 (Fig. 2.8b). The positively charged side chains of Arg423 and Arg480 may bind the phosphate group of the GAP molecule, which is also exposed to the solvent. Biochemical studies have shown that glyceraldehyde can also serve as a substrate for DXS (Lois et al. 1998). This property of DXS had for instance been used to prepare ^{14}C-labeled DX for incorporation experiments using tobacco BY-2 cells (Hemmerlin et al. 2003) and for the characterization of a cytosolic xylulose kinase in *Arabidopsis*, converting exogenous DX into DXP, which is then translocated into plastids and integrated into the MEP pathway (Hemmerlin et al. 2006). In a recent kinetic study, DXS from *E. coli* was shown to accept pyruvate as second substrate and could even generate acetolactate, indicative of some substrate promiscuity, most possibly due to some flexibility in the acceptor substrate-binding pocket (Brammer and Meyers 2009).

This model is supported by biochemical studies. His49 of *E. coli* DXS (equivalent to His51 in *D. radiodurans* DXS) has been reported to be essential for its function (Querol et al. 2001). The equivalent residue in TK is His30 (Table 2.2), which may play a role in proton transfer during the reaction (Nikkola et al. 1994). In the model, His51 is involved in GAP binding and is also located in the proximity of the adduct on the C2

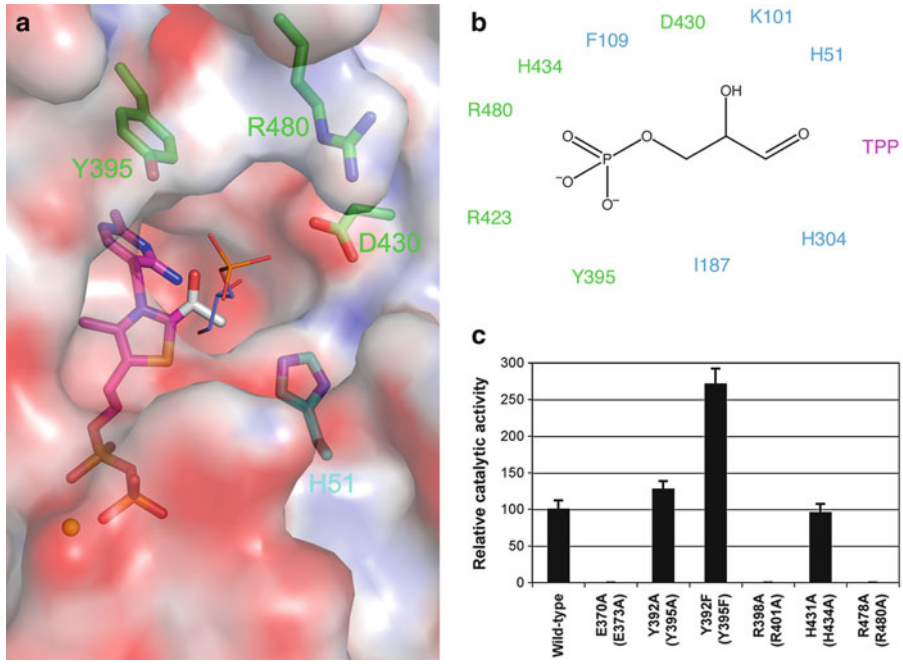

Fig. 2.8 Putative substrate-binding modes of DXS. (**a**) wwwwMolecular surface of *D. radiodurans* DXS in the active site region, colored based on electrostatic potential. A model for the binding mode of the pyruvate adduct and GAP is shown in *white* and *blue*, respectively. (**b**) Schematic drawing of the possible binding site for GAP in the active site of DXS. (**c**) Relative catalytic activity of active site mutants of *E. coli* DXS. The activity of the wild-type enzyme is set at 100. The residue numbers in parenthesis are for *D. radiodurans* DXS

Table 2.2 Residues in the putative GAP binding site of DXS

E. coli DXS	*D. radiodurans* DXS	*A. thaliana* DXS	Yeast transketolase	*E. coli* pyruvate dehydrogenase E1 subunit
His49	**His51**	**His115**	**His30**	**His106**
Arg99	Lys101	Arg165	Arg94	Arg166
Phe107	Phe109	Phe173	His103	Tyr177
Ile185	Ile187	Leu252	Ile191	Leu264
Ser322	Ser325	Thr402	Arg359	Thr495
Met346	Met349	Met426	Leu383	Glu522
Gly349	Gly352	Gly429	Ser386	Thr525
Tyr392	Tyr395	Tyr472	Phe442	Tyr599
Arg420	Arg423	Arg500	His469	Thr627
Asp427	Asp430	Asp507	Asp477	Glu636
His431	**His434**	**His511**	**His481**	**His640**
Arg478	Arg480	Arg558	Arg528	Asn693

Residues conserved among all five enzymes are in bold face

atom of TPP. The *dxs*-null mutant is rescued by a mutation in PDH, E636Q (Sauret-Güeto et al. 2006). The equivalent residue in DXS, Asp430, is located in the active site tunnel and is expected to interact with the GAP molecule. The E636Q mutation in PDH might therefore change the substrate specificity of PDH and compensate for the loss of DXS activity. It remains to be determined whether this mutant can catalyze the DXS reaction.

Mutations of other residues in the active site, including Glu373, Arg401, and Arg480, can also disrupt catalysis (Fig. 2.8c). The data indicate important functional roles for these residues in the catalysis by DXS and are consistent with the structural observations. In comparison, mutations of Tyr392 and His431 have little impact on DXS activity.

2.7 Future Perspectives

The crystal structures of *E. coli* and *D. radiodurans* DXS have greatly enhanced our understanding of this important enzyme. It can be expected that the plant DXS enzymes will have a similar overall structure as the bacterial enzymes, due to their significant sequence conservation. The molecular mechanism for the inhibitory activity of ketoclomazone (oxoclomazone) remains to be determined, however. Structural information on this complex will provide additional help for the design and optimization of potent DXS inhibitors.

References

Aevarsson A, Seger K, Turley S, Sokatch JR, Hol WG (1999) Crystal structure of 2-oxoisovalerate and dehydrogenase and the architecture of 2-oxo acid dehydrogenase multienzyme complexes. Nat Struct Biol 6:785–792

Arjunan P, Nemeria N, Brunskill A et al (2002) Structure of the pyruvate dehydrogenase multienzyme complex E1 component from *Escherichia coli* at 1.85 A resolution. Biochemistry 41:5213–5221

Brammer LA, Meyers CF (2009) Revealing substrate promiscuity of 1-deoxy-D-xylulose 5-phosphate synthase. Org Lett 11:4748–4751

Begley TP, Downs DM, Ealick SE et al (1999) Thiamin biosynthesis in prokaryotes. Arch Microbiol 171: 293–300

Bouvier F, d'Harlingue A, Suire C, Backhaus RA, Camara B (1998) Dedicated roles of plastid transketolases during the early onset of isoprenoid biogenesis in pepper fruits1. Plant Physiol 117:1423–1431

DeLano WL (2002) The Pymol manual. DeLano Scientific, San Carlos

Dubey VS, Bhalla R, Luthra R (2003) An overview of the non-mevalonate pathway for terpenoid biosynthesis in plants. J Biosci 28:637–646

Eisenreich W, Bacher A, Arigoni D, Rohdich F (2004) Biosynthesis of isoprenoids via the non-mevalonate pathway. Cell Mol Life Sci 61:1401–1426

Enfissi EM, Fraser PD, Lois LM, Boronat A, Schuch W, Bramley PM (2005) Metabolic engineering of the mevalonate and non-mevalonate isopentenyl diphosphate-forming pathways for the production of health-promoting isoprenoids in tomato. Plant Biotechnol 3:17–27

Estévez JM, Cantero A, Reindl A, Reichler S, León P (2001) 1-Deoxy-D-xylulose-5-phosphate synthase, a limiting enzyme for plastidic isoprenoid biosynthesis in plants. J Biol Chem 276:22901–22909

Fiedler E, Thorell S, Sandalova T, Golbik R, König S, Schneider G (2002) Snapshot of a key intermediate in enzymatic thiamin catalysis: crystal structure of the α-carbanion of (α, β-dihydroxyethyl)-thiamin diphosphate in the active site of transketolase from Saccharomyces cerevisiae. Proc Natl Acad Sci USA 99:591–595

Gill SR, Pop M, Deboy RT, Eckburg PB et al (2006) Metagenomic analysis of the human distal gut microbiome. Science 312:1355–1359

Hahn FM, Eubanks LM, Testa CA, Blagg BSJ, Baker JA, Poulter CD (2001) 1-Deoxy-D-xylulose 5-phosphate synthase, the gene product of open reading frame (ORF) 2816 and ORF 2895 in *Rhodobacter capsulatus*. J Bacteriol 183:1–11

Harker M, Bramley PM (1999) Expression of prokaryotic 1-deoxy-D-xylulose-5-phosphatases in *Escherichia coli* increases carotenoid and ubiquinone biosynthesis. FEBS Lett 448:115–119

Hawkins CF, Borges A, Perham RN (1989) A common structural motif in thiamin pyrophosphate-binding enzymes. FEBS Lett 255:77–82

Hemmerlin A, Hoeffler J-F, Meyer O et al (2003) Cross-talk between the cytosolic mevalonate and the plastidial methylerythritol phosphate pathways in tobacco bright yellow-2 cells. J Biol Chem 278: 26666–26676

Hemmerlin A, Tritsch D, Hartmann M et al (2006) A cytosolic Arabidopsis D-xylulose kinase catalyzes the phosphorylation of 1-deoxy-D-xylulose into a precursor of the plastidial isoprenoid pathway. Plant Physiol 142:441–457

Hill RE, Himmeldirk K, Kennedy IA et al (1996) The biogenetic anatomy of vitamin B6. A 13C NMR investigation of the biosynthesis of pyridoxol in *Escherichia coli*. J Biol Chem 271:30426–30435

Jomaa H, Wiesner J, Sanderbrand S et al (1999) Inhibitors of the nonmevalonate pathway of isoprenoid biosynthesis as antimalarial drugs. Science 285:1573–1576

Jones S, Thornton JM (1996) Principles of protein–protein interactions. Proc Natl Acad Sci USA 93:13–20

Keasling JD (2010) Microbial production of isoprenoids. In: Timmis KN (ed) Handbook of hydrocarbon and lipid microbiology, part 27. Springer, Berlin/ Heidelberg, pp 2951–2966

Kim SM, Kuzuyama T, Chang YJ, Song KS, Kim SU (2006) Identification of class 2 1-deoxy-D-xylulose 5-phosphate synthase and 1-deoxy-D-xylulose 5-phosphate reductoisomerase genes from *Ginkgo biloba* and their transcription in embryo culture with respect to ginkgolide biosynthesis. Planta Med 72:234–240

Kuzuyama T, Takagi M, Takahashi S, Seto H (2000) Cloning and characterization of 1-deoxy-D-xylulose 5-phosphate synthase from *Streptomyces* sp. Strain CL190, which uses both the mevalonate and nonmevalonate pathways for isopentenyl diphosphate biosynthesis. J Bacteriol 182:891–897

Lange BM, Wildung MR, McCaskill D, Croteau R (1998) A family of transketolases that directs isoprenoid biosynthesis via a mevalonate-independent pathway. Proc Natl Acad Sci USA 95:2100–2104

Lange BM, Rujan T, Martin W, Croteau R (2000) Isoprenoid biosynthesis: the evolution of two ancient and distinct pathways across genomes. Proc Natl Acad Sci USA 97:13172–13177

Lichtenthaler HK (2000) Non-mevalonate isoprenoid biosynthesis: enzymes, genes and inhibitors. Biochem Soc Trans 28:785–789

Lois LM, Campos N, Putra SR, Danielsen K, Rohmer M, Boronat A (1998) Cloning and characterization of a gene from *Escherichia coli* encoding a transketolase-like enzyme that catalyzes the synthesis of D-1-deoxyxylulose 5-phosphate, a common precursor for isoprenoid, thiamin, and pyridoxol biosynthesis. Proc Natl Acad Sci USA 95:2105–2110

Lois LM, Rodríguez-Concepción M, Gallego F, Campos N, Boronat A (2000) Carotenoid biosynthesis during tomato fruit development: regulatory role of 1-deoxy-D-xylulose 5-phosphate synthase. Plant J 22:503–513

Mandel MA, Feldmann KA, Herrera-Estrella L, Rocha-Sosa M, León P (1996) *CLA1*, a novel gene required for chloroplast development, is highly conserved in evolution. Plant J 9:649–658

Matthews PD, Wurtzel ET (2000) Metabolic engineering of carotenoid accumulation in *Escherichia coli* by modulation of the isoprenoid precursor pool with expression of deoxyxylulose phosphate synthase. Appl Microbiol Biotechnol 53:396–400

Meyer O, Grosdemange-Billiard C, Tritsch D, Rohmer M (2003) Isoprenoid biosynthesis via the MEP pathway. Synthesis of (3*R*,4*S*)-3,4-dihydroxy-5-oxohexylphophonic acid, an isosteric analogue of 1-deoxy-D-xylulose 5-phosphate, the substrate of the 1-deoxy-D-xylulose 5-phosphate reducto-isomerase. Org Biomol Chem 1:4367–4372

Müller C, Schwender J, Zeidler J, Lichtenthaler HK (2000) Properties and inhibition of the first two enzymes of the non-mevalonate pathway of isoprenoid biosynthesis. Biochem Soc Trans 28:792–793

Nikkola M, Lindqvist Y, Schneider G (1994) Refined structure of transketolase from *Saccharomyces cerevisiae* at 2.0 A resolution. J Mol Biol 238:387–404

Nilsson U, Meshalkina L, Lindqvist Y, Schneider G (1997) Examination of substrate binding in thiamin diphosphate-dependent transketolase by protein crystallography and site-directed mutagenesis. J Biol Chem 272:1864–1869

Paetzold H, Garms S, Bartram S et al (2010) The isogene 1-deoxy-D-xylulose 5-phosphate synthase 2 controls isoprenoid profiles, precursor pathway allocation, and density of tomato trichomes. Mol Plant 3(5):904–916

Pletcher J, Sax M, Blank G, Wood M (1977) Stereochemistry of intermediates in thiamine catalysis. 2. Crystal structure of DL-2-(alpha-hydroxybenzyl) thiamine chloride hydrochloride trihydrate. J Am Chem Soc 99:1396–1403

Querol J, Rodríguez-Concepción M, Boronat A, Imperial S (2001) Essential role of residue H49 for activity of *Escherichia coli* 1-deoxy-D-xylulose 5-phosphate synthase, the enzyme catalyzing the first step of the 2-*C*-methyl-D-erythritol 4-phosphate pathway for isoprenoid synthesis. Biochem Biophys Res Commun 289:155–160

Rodríguez-Concepción M, Boronat A (2002) Elucidation of the methylerythritol phosphate pathway for isoprenoid biosynthesis in bacteria and plastids. A metabolic milestone achieved through genomics. Plant Physiol 130:1079–1089

Sacchettini JC, Poulter CD (1997) Creating isoprenoid diversity. Science 277:1788–1789

Sauret-Güeto S, Urós EM, Ibáñez E, Boronat A, Rodríguez-Concepción M (2006) A mutant pyruvate dehydrogenase E1 subunit allows survival of *Escherichia coli* strains defective in 1-deoxy-D-xylulose 5-phosphate synthase. FEBS Lett 580:736–740

Schellenberger A (1998) Sixty years of thiamin diphosphate biochemistry. Biochim Biophys Acta 1385: 177–186

Sprenger GA, Schorken U, Wiegert T et al (1997) Identification of a thiamin-dependent synthase in *Escherichia coli* required for the formation of the 1-deoxy-D-xylulose 5-phosphate precursor to isoprenoids, thiamin, and pyridoxol. Proc Natl Acad Sci USA 94:12857–12862

Tao L, Wagner LW, Rouvière PE, Cheng O (2006) Metabolic engineering for synthesis of aryl carotenoids in *Rhodococcus*. Appl Microbiol Biotechnol 70:222–228

Walter MH, Hans J, Strack D (2002) Two distantly related genes encoding 1-deoxy-D-xylulose 5-phosphate synthases: differential regulation in shoots and apocarotenoid-accumulating mycorrhizal roots. Plant J 31: 243–254

Walter MH, Floß DS, Hans J, Fester T, Strack D (2007) Apocarotenoid biosynthesis in arbuscular mycorrhizal roots: contributions from methylerythritol phosphate pathway isogenes and tools for its manipulation. Phytochemistry 68:130–138

Xiang S, Usunow G, Lange G, Busch M, Tong L (2007) Crystal structure of 1-deoxy-D-xylulose 5-phosphate synthase, a crucial enzyme for isoprenoids biosynthesis. J Biol Chem 282:2676–2682

Yoon SH, Park HM, Kim JE et al (2007) Increased β-carotene production in recombinant *Escherichia coli* harboring an engineered isoprenoid precursor pathway with mevalonate addition. Biotechnol Prog 23:599–605

Zeidler J, Schwender J, Müller C, Lichtenthaler HK (2000) The non-mevalonate isoprenoid biosynthesis of plants as a test system for drugs against malaria and pathogenic bacteria. Biochem Soc Trans 28:796–798

Biosynthetic Genes and Enzymes of Isoprenoids Produced by Actinomycetes

3

Tohru Dairi

Abstract

Most isoprenoids have been isolated from eukaryotes such as plants and fungi. However, actinomycete strains, which are known to produce many kinds of nonribosomal peptides and polyketides, were also reported to produce isoprenoids. We now realize that many actinomycete strains possess many isoprenoid biosynthetic genes since genome data base has enabled us to examine the presence of candidate genes. Moreover, by *in vitro* assay with recombinant enzymes and heterologous expression of the gene cluster, we can know structures of metabolites synthesized by the gene product. In many cases, isoprenoid moieties of compounds produced by actinomycetes are attached to other moieties, such as a polyketide, an aromatic ring, an amino acid, etc., that are synthesized via pathways independent of isoprenoid synthesis to give the so-called isoprenoid hybrid compounds, in contrast to eukaryotic isoprenoids, which usually have cyclic structures that are formed by cyclization of GDP, FDP, and GGDP. The structures of prokaryotic isoprenoids, therefore, are unique and different from those of eukaryotic origin. In this chapter, a structural diversity of isoprenoids produced by actinomycetes is summarized together with biosynthetic genes and enzymes responsible for them.

Keywords

Actinomycetes • Monoterpene • Sesquiterpene • Diterpene • Cyclic isoprenoids • Hybrid isoprenoids • MEP pathway • Mevalonate pathway

T. Dairi (✉)
Graduate School of Engineering, Hokkaido University,
N13, W8, Sapporo, Hokkaido 060-8628, Japan
e-mail: dairi@eng.hokudai.ac.jp

T.J. Bach and M. Rohmer (eds.), *Isoprenoid Synthesis in Plants and Microorganisms: New Concepts and Experimental Approaches*, DOI 10.1007/978-1-4614-4063-5_3,

3.1 Introduction

Isoprenoids form the largest single family of compounds found in nature with over 25,000 known examples and contain industrially useful compounds (Connolly and Hill 1992; Dewick 2002). Most of these compounds have been isolated from eukaryotes such as plants and fungi. However, actinomycete strains have recently been reported to produce many types of isoprenoids with unique structures different from those of eukaryotic origin (Dairi 2005). Among actinomycete strains, some strains were demonstrated to possess the mevalonate (MVA) pathway via which isopentenyl diphosphate (IPP), the common precursor of isoprenoids is biosynthesized, though all actinomycete strains are equipped with the 2-*C*-methyl-D-erythritol 4-phosphate (MEP) pathway for the formation of IPP. We have cloned and analyzed the MVA pathway gene clusters and their flanking regions from actinomycete producers of isoprenoid compounds. Most of MVA pathway clusters contained genes coding for mevalonate kinase (MK), mevalonate diphosphate decarboxylase (MDPD), phosphomevalonate kinase (PMK), type 2 IPP isomerase, HMG-CoA reductase (HMGR), HMG-CoA synthase (HMGS), and a new type of an acetoacetyl-CoA synthesizing enzyme (see Sect. 3.2.2). The order of each of the open reading frames (ORFs) is also the same, and the respective homologous ORFs show more than 60% amino acid identity with each other. In contrast to this conservative gene organization, the biosynthetic gene cluster of each of the downstream isoprenoid compounds was located just upstream and/or downstream of the MVA pathway gene cluster. These facts suggested that all the actinomycete strains possessing both the MVA and MEP pathways produce isoprenoid compounds and that the biosynthetic genes of one of these isoprenoids usually exist adjacent to the MVA pathway gene cluster. In contrast, actinomycetes possessing only the MEP pathway also produce a plethora of isoprenoid compounds, and their biosynthetic genes were cloned by using specific strategies. Moreover, whole-genome sequencing has uncovered dozens of candidate genes for isoprenoid biosyntheses in the genome of actinomycete strains. Among them, several genes were characterized by examining the corresponding recombinant enzymes. In this chapter, these studies on biosynthetic genes and enzymes of isoprenoids produced by actinomycetes are summarized.

3.2 MVA Pathway in Actinomycetes

3.2.1 Discovery of the MVA Pathway in Actinomycetes

Actinomycete strains have been known to produce several isoprenoid compounds such as 2-methylisoborneol, geosmin, squalene-hopene, etc. However, not much attention had been paid on the biosynthesis of these compounds, especially on the origin of IPP, until the existence of the MEP pathway in *E. coli* was reported (Kuzuyama and Seto 2003). After that, almost all microorganisms except for some lactobacilli were shown to utilize the MEP pathway, and the MEP pathway genes and enzymes from *Streptomyces* strains were also characterized (Kuzuyama et al. 2000). However, by a tracer experiment, Seto et al. (1996) noticed that naphterpin, a polyketide-isoprenoid hybrid compound produced by *Streptomyces* sp. CL190, was synthesized via the MVA pathway. In contrast, the prenyl side chain of menaquinone, an essential compound for respiration, was mainly synthesized by IPP derived from the MEP pathway. This suggested that in this strain the primary isoprenoid metabolite is mainly biosynthesized via the MEP pathway, whereas the IPP for secondary products comes from the MVA pathway.

3.2.2 Cloning of MVA Pathway Gene Clusters

To eventually identify the complete MVA pathway in *Streptomyces* strain, an attempt to clone a first corresponding gene was performed. Takahashi et al. (1999) purified an HMGR from *Streptomyces* sp. CL190, and a gene encoding it was cloned by a reverse genetics. By searching flanking regions,

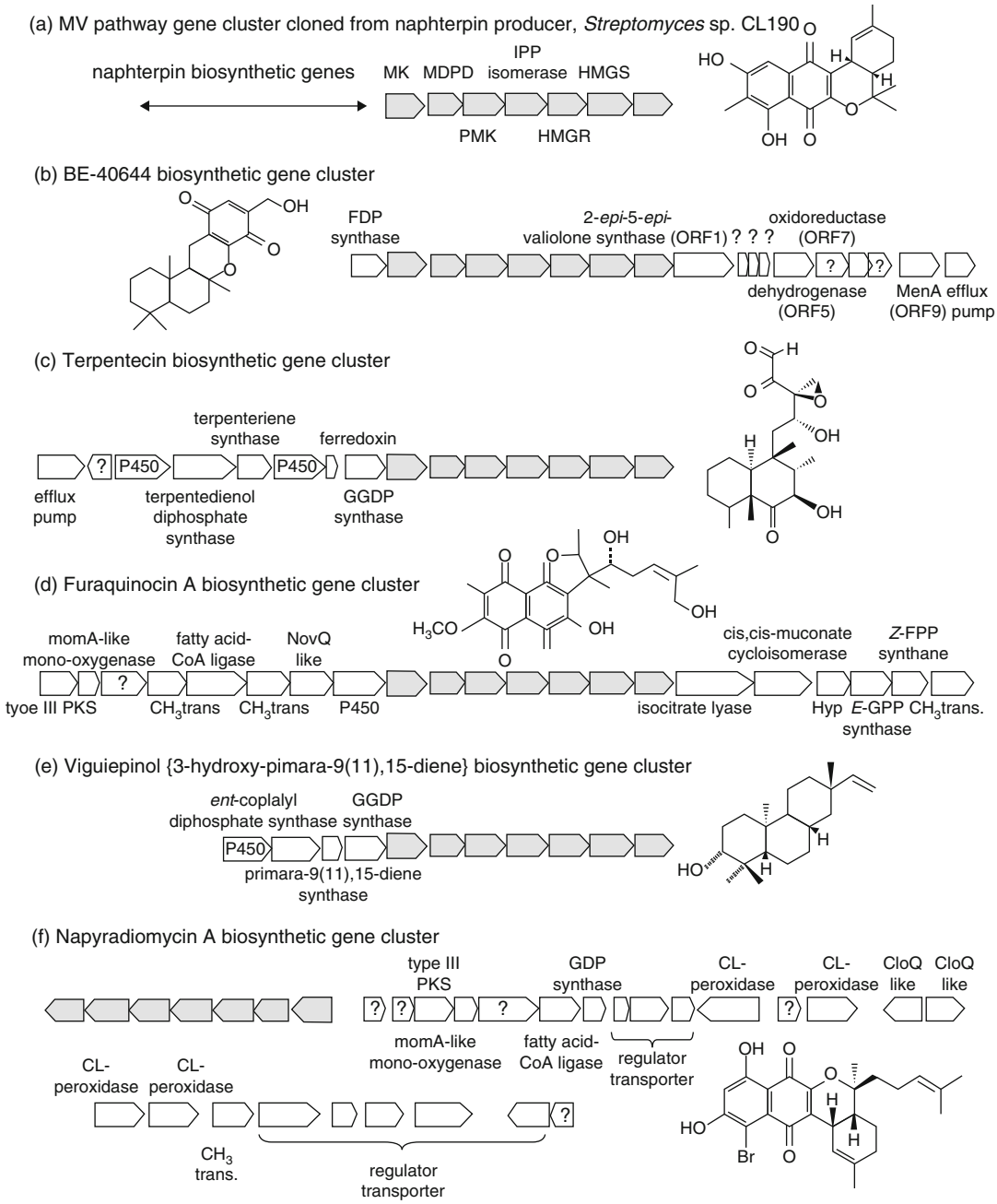

Fig. 3.1 MVA pathway gene cluster and its flanking regions cloned from naphterpin, BE-40644, terpentecin, furaquinocin A, viguiepinol, and napyradiomycin A producers

they found an MVA pathway gene cluster that consisted of MK, MDPD, PMK, type 2 IPP isomerase, HMGR, and HMGS in that order (Takagi et al. 2000) (Fig. 3.1). Very recently, a new type of acetoacetyl-CoA synthesizing enzyme was identified in MVA pathway gene clusters (Okamura et al. 2010; Dairi et al. 2011). *NphT7* of *Streptomyces* sp. strain CL190, a gene that is just located downstream of that coding for HMGS (Fig. 3.1), encodes an enzyme that catalyzes a single condensation of acetyl-CoA and malonyl-CoA to give acetoacetyl-CoA and CoA. An HMGR

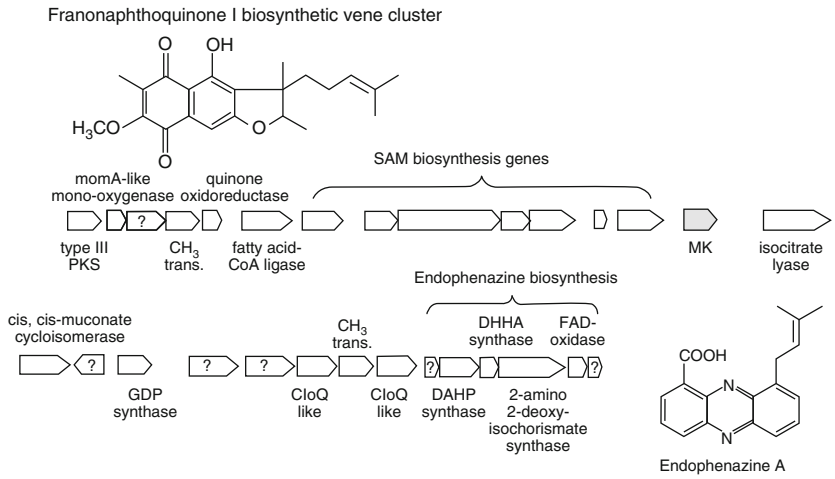

Fig. 3.2 Furanonaphthoquinone I and endophenazine A biosynthetic gene clusters

gene was also cloned from a terpentecin (diterpene compound) producer *Kitasatospora griseola* by a shotgun cloning experiment, using a mutant obtained by a mutagenesis (Dairi et al. 2000). The HMGR gene also made part of an operon with orthologs of other MV pathway genes in the same order as that in the strain CL190 (Hamano et al. 2001) (Fig. 3.1). In these two MVA pathway gene clusters, MK and PMK were similar to each other, and we could not identify which gene encodes the intrinsic MK (or PMK). To clarify this point, recombinant enzymes of these genes were prepared, and the former gene located at most upstream of the cluster was confirmed to encode the MK (Hamano et al. 2001). After that, a few MVA pathway gene clusters have been isolated from actinomycete strains such as BE-40644 (Kawasaki et al. 2003), furaquinocin (Kawasaki et al. 2004, 2006), and napyradiomycin A (Winter et al. 2007) producers. Moreover, an MVA pathway gene cluster was identified in *Nocardia farcinica* by genome sequencing (Ishikawa et al. 2004). All these clusters contained the same MVA pathway genes in the same order as those in the strain CL190 and *K. griseola* (Fig. 3.1). Interestingly, by Southern hybridization using the HMGR gene cloned from the terpentecin producer as a probe, two distinct HMGR genes were identified in furaquinocin A producer, *Streptomyces* sp. KO-3988. The nucleotide sequences of the entire MVA pathway clusters including each of the HMGR genes were determined, and six genes were identified in each of the clusters like in those found in naphterpin, terpentecin, and BE-40644 producers (Fig. 3.1). By a phylogenetic analysis, the two MVA pathway clusters were identified to be probably independently distributed in the strain KO-3988 (ortholog) rather than the hypothesis that one cluster was generated by the duplication of the other cluster (paralog) (Kawasaki et al. 2006). In contrast, only a MK gene was identified in furanonaphthoquinone I biosynthetic gene cluster (Haagen et al. 2006) (Fig. 3.2). Considering that furanonaphthoquinone I was confirmed to be mainly formed via the MVA pathway by a tracer experiment (Bringmann et al. 2007), the MVA pathway genes are located in at least two loci in furanonaphthoquinone I producer, *Streptomyces cinnamonensis* DSM 1042. This has been recently confirmed by Seeger et al. (2011).

3.2.3 Biological Significance of MVA Pathway in Actinomycetes

3.2.3.1 Temporal Expression of MVA Pathway Genes

As described in Sect. 3.2.2, naphterpin, a secondary metabolite, was shown to be synthesized via the MVA pathway by a tracer experiment, in spite of the fact that the producer possesses both the MEP and MVA pathways (Takagi et al. 2000).

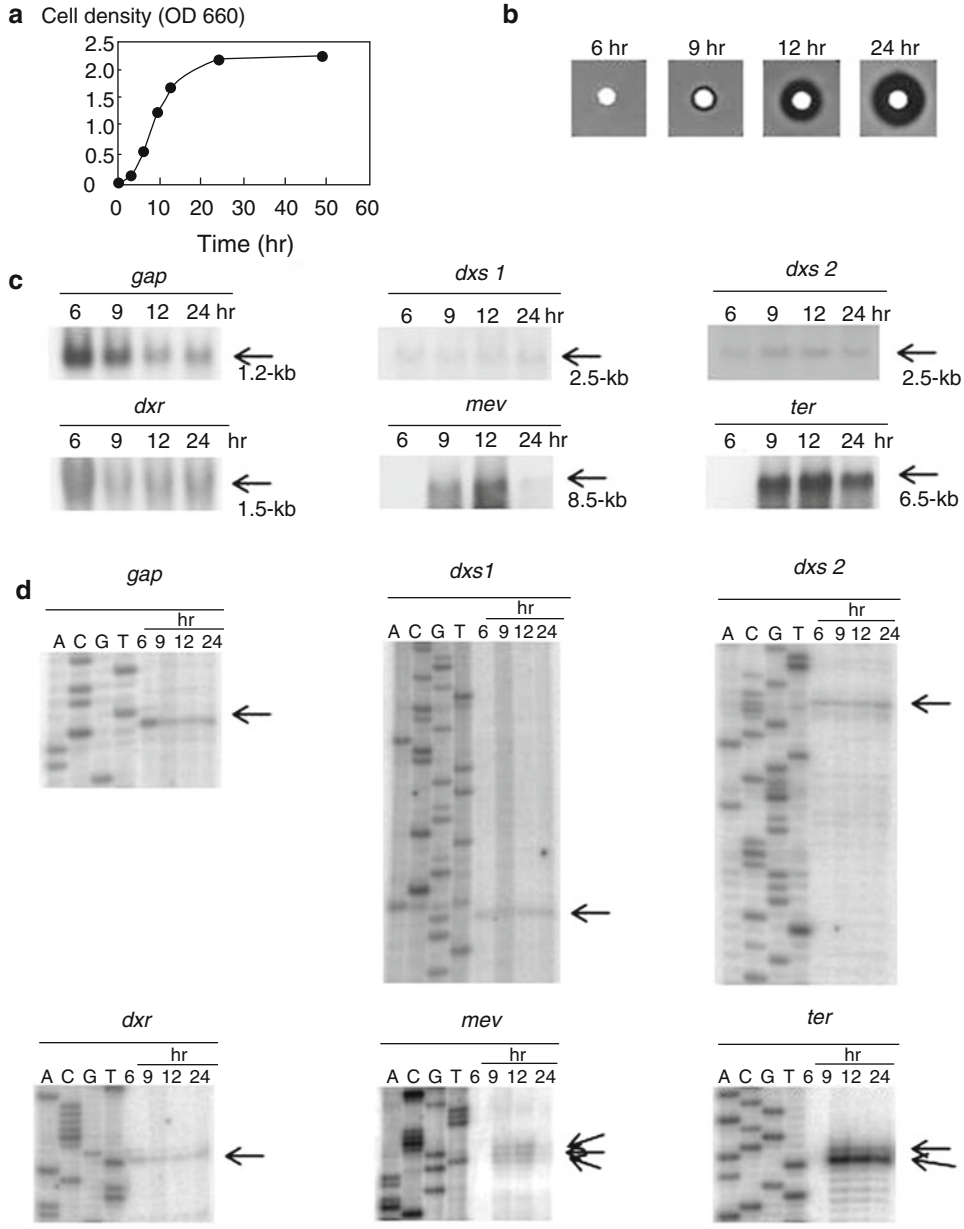

Fig. 3.3 Northern blot analysis (**c**) and primer extension analysis (**d**) of the genes responsible for biosyntheses of terpenoid in terpentecin producer. Total RNA was isolated from terpentecin producer grown at 30°C for 6, 9, 12, and 24 h, at which cell growth (**a**) and terpentecin productivity (**b**) were also measured and subjected to Northern blot analysis (**c**) and to primer extension analyses (**d**). *Arrows* in (**d**) indicate the transcriptional start sites

To examine if this is also the case in other actinomycete strains, Northern blot analysis was performed with a terpentecin producer. Although *dxs* and *dxr*, the first and the second genes in the MEP pathway, respectively, were transcribed throughout the cultivation, messages of the MVA pathway genes and terpentecin biosynthetic genes (see below) were not detected during the early growth phase but simultaneously appeared at late growth phase, which coincided with the beginning of terpentecin production (Hamano et al. 2002a) (Fig. 3.3). Taken these results together,

the MEP pathway operated throughout the cell growth and that the MVA pathway was transcriptionally regulated such as to operate only at late growth phase in the terpentecin producer.

3.2.3.2 Contribution of MVA Pathway for Production of Isoprenoid Compounds

As described in Sect. 3.2.3.1, the MVA pathway is operating during the late growth stage, suggesting that it contributes only to secondary metabolite production. To investigate in greater detail the relative contributions of the MVA and MEP pathways to terpentecin production, we constructed a mutant in which the HMG-CoA reductase gene (*hmgr*) was specifically disrupted by a double-crossing homologous recombination. Although the cell growth of the mutant strain was almost similar to that of the wild-type strain, the mutant strain produced approximately 60% less TP than the wild-type strain, thereby suggesting that the MVA pathway supplied some 60% of IPP for TP biosynthesis and the MEP pathway about 40% (Hamano et al. 2002a).

Recently, the group of Lutz Heide also examined the relative contribution of the MVA and MEP pathways for the production of furanonaphthoquinone I and endophenazine A (Fig. 3.2), both of which were produced by *Streptomyces cinnamonensis* DSM 1042, by measuring the incorporation ratio of [2-^{13}C]acetate and [2-^{13}C] glycerol into the compounds (Bringmann et al. 2007). They estimated that both compounds are predominantly formed via the MVA pathway (approximately 80%) (Bringmann et al. 2007).

3.2.4 Isoprenoid Biosynthetic Genes Identified in Flanking Regions of MVA Pathway Gene Cluster

3.2.4.1 Naphterpin Biosynthetic Gene Cluster

As described in Sect. 3.2.2, Kuzuyama et al. performed a pioneering study on the MVA pathway gene cluster in *Streptomyces* sp. CL190. After that, they found a naphterpin biosynthetic gene cluster in the upstream region of the MVA cluster. Of these, a gene encoding the prenylation enzyme (CloQ type) catalyzing a transfer of prenyl side chain to polyketide moiety was identified and excellent studies with recombinant enzymes have been carried out (Kuzuyama et al. 2006) (Fig. 3.1).

3.2.4.2 Terpentecin Biosynthetic Gene Cluster

As described in Sect. 3.2.2, we have been succeeded in isolation of the HMG-CoA reductase gene from the terpentecin producer by the shotgun cloning experiment. By analysis of adjacent region of the gene, the gene cluster of MVA pathway was also identified, and the geranylgeranyl diphosphate (GGDP) synthase gene was found located just upstream of the MVA pathway gene cluster (Hamano et al. 2001). Considering that antibiotic biosynthetic genes cloned from actinomycetes are usually clustered in the genomic DNA region and that GGDP synthase, which supplies a direct precursor of terpentecin biosynthesis, existed in the region just upstream of the MVA pathway cluster, a gene cluster for terpentecin biosynthesis was also expected to exist in the region further upstream of the GGDP synthase gene. To examine this possibility, the DNA sequence of that region was determined, and seven genes were identified in the same direction (Dairi et al. 2001) (Fig. 3.1).

In the cluster, two diterpene cyclase genes were identified by gene disruption and heterologous expression experiments as the first example of eubacterial diterpene cyclases. One is terpentedienol diphosphate (TDP) synthase, which has a significant sequence similarity with that of the *N*-terminal half of diterpene cyclases from eukaryotes (less than 30% identity), and the enzyme was shown to convert GGDP into TDP. The other is an enzyme that shares 25% sequence identity over 331 amino acid residues of the pentalenene synthase from *Streptomyces* sp. UC5319 and catalyzed the conversion of TDP into *ent*-clerod-3,13(16),14-triene (terpentetriene, TTE). Interestingly, the enzyme catalyzed the conversion of GGDP into 1,3(20),6,10,14-phytapentaene, α-springene, and 3,7,11,15-tetramethylhexadeca-1,3,6,10,14-pentaene (*E,E,E*). Furthermore, farnesyl diphosphate (FDP) was also converted to

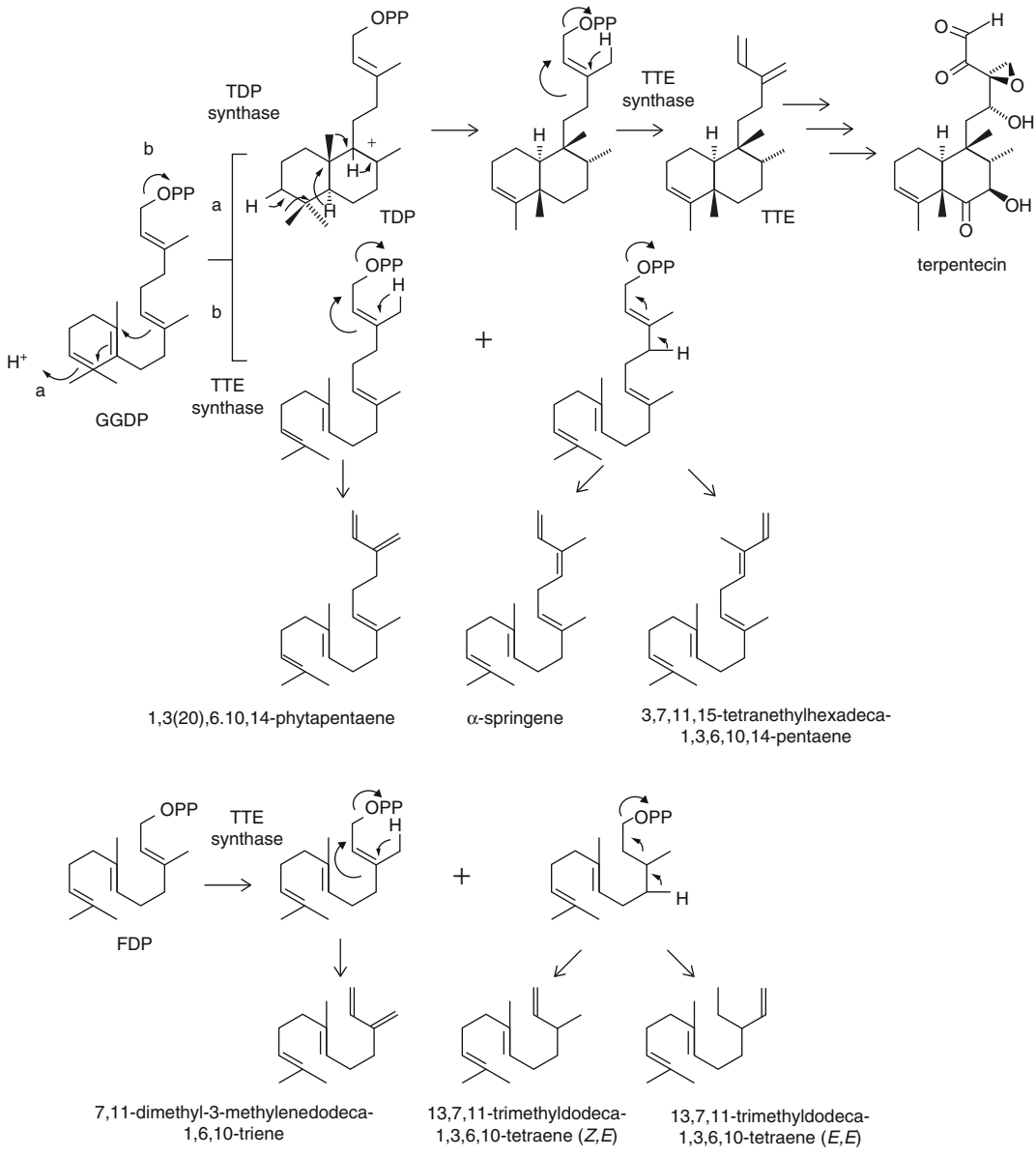

Fig. 3.4 Summary of the enzymatic reactions catalyzed by terpentedienol diphosphate synthase (TDP synthase) and terpentetriene synthase (TTE synthase)

7,11-dimethyl-3-methylenedodeca-1,6,10-triene (*E*); 3,7,11-trimethyldodeca-1,3,6,10-tetraene (*Z,E*); and 3,7,11-trimethyldodeca-1,3,6,10-tetraene (*E,E*) (Fig. 3.4). The kinetic properties of both recombinant enzymes were investigated and found to have almost the same as those of eukaryotic origin, such as requirement of Mg^{2+} and catalytic parameters (K_m and V_{max} values) (Hamano et al. 2002b).

3.2.4.3 BE-40644 Biosynthetic Gene Cluster

As described in Sects. 3.2.4.1 and 3.2.4.2, the MVA pathway gene cluster was located in the region adjacent to the terpentecin biosynthetic gene cluster, and its enzymes derived from supplied more than 60% of the IPP required for terpentecin biosynthesis. These facts led us to investigate whether MVA pathway genes and isoprenoid

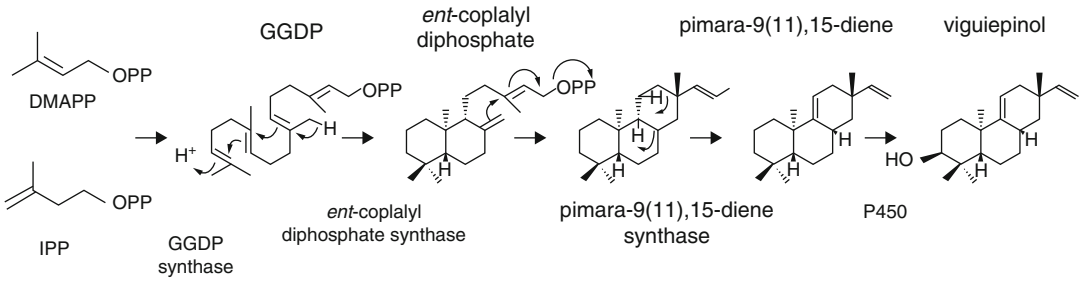

Fig. 3.5 Enzymatic reactions catalyzed by *ent*-copalyl diphosphate synthase and pimara-9(11),15-diene synthase found in a furaquinocin A producer, *Streptomyces* sp. strain KO-3988

biosynthetic genes are always clustered in strains possessing both the MVA and MEP pathways. Therefore, we cloned an MVA pathway gene cluster from *Actinoplanes* sp. strain A40644, a producer of the antibiotic BE-40644 that contains a sesquiterpenoid moiety as a partial structure, expecting that a BE-40644 biosynthetic gene cluster would be present in the region adjacent to the MVA pathway genes (Kawasaki et al. 2003) (Fig. 3.1).

We were able to clone an MVA pathway gene cluster that contained the same genes as those found in naphterpin and terpentecin producers. Moreover, a FDP synthase gene, which supplies a sesquiterpenoid moiety, was located at the region just upstream of the mevalonate kinase gene. Therefore, we expected the presence of the BE-40644 biosynthetic genes in the further upstream region of the MVA pathway gene cluster. However, by sequencing analysis of the region, we did not find any genes related to BE-40644 biosynthesis, but in the downstream region, we detected 11 genes that would possibly participate in the biosynthesis of BE-40644. By heterologous expression, the genes were confirmed to be responsible for biosynthesis of BE-40644. This result again proved that MVA pathway genes and isoprenoid biosynthetic genes were clustered in an actinomycete strain possessing both the MVA and MEP pathways.

3.2.4.4 Furaquinocin and Viguiepinol Biosynthetic Gene Clusters

As described in Sects. 3.2.4.1 to 3.2.4.3, we identified the two distinct MVA pathway gene clusters in *Streptomyces* sp. strain KO-3988, a producer of furaquinocin A, which is a polyketide-isoprenoid hybrid compound composed of naphthoquinone and monoterpene moieties (Kawasaki et al. 2006). Then, we analyzed the adjacent region of each of the cluster.

By sequencing the flanking region of one of the MVA clusters (MV1), we found 4 genes that could encode a putative cytochrome P450 (ORF1), a diterpene cyclase (ORF2), an unknown protein (ORF3), and a GGDP (C_{20}) synthase gene (ORF4) in the upstream region of the MV1 cluster (Kawasaki et al. 2004) (Fig. 3.1). Considering that the ORF2 product is similar to isoprenoid cyclases, it was assumed to convert GGDP into a cyclized intermediate. To examine this possibility, the ORF2 product was overproduced as a His-tagged recombinant protein and confirmed to catalyze the formation of *ent*-copalyl diphosphate (Ikeda et al. 2007). And the ORF3 was also shown to catalyze the conversion of *ent*-copalyl diphosphate into viguiepinol {pimara-9(11),15-diene} (Fig. 3.5). Since ORF2 and ORF3 are the first examples of enzymes with these biosynthetic functions from prokaryotes, enzymatic properties of both enzymes were investigated more in detail. ORF2 is likely to be a dimer and requires a divalent cation such as Mg^{2+} and Zn^{2+} for its activity. The optimum pH and temperature were 5.5 and 35°C, respectively. The K_m value was calculated to be 13.7 ± 1.0 μM for GGDP, and the *k*cat value was 3.3×10^{-2}/s. ORF3 is likely to be a monomer and also requires a divalent cation. The optimum pH and temperature were 7.0 and 30°C, respectively. The K_m value for *ent*-CDP was estimated to be 2.6 ± 0.2 μM, and the *k*cat value was 1.4×10^{-3}/s.

We next analyzed the flanking regions of the MV2 cluster. Consequently, we were able to localize a 25-kb DNA region that harbored furaquinocin biosynthetic genes both in the upstream and downstream regions of the MV2 cluster. This cluster included putative genes coding for THN synthase (type III polyketide synthase), P450, methyl transferase, prenyl transferase (similar to CloQ), etc. By a heterologous expression experiment, these genes were shown to participate in furaquinocin biosynthesis (Kawasaki et al. 2006) (Fig. 3.1). This was the first example of a gene cluster responsible for the biosynthesis of polyketide-isoprenoid hybrid compound.

3.2.4.5 Napyradiomycin A Biosynthetic Gene Cluster

An MVA pathway gene cluster was also identified in the napyradiomycin A biosynthetic gene cluster, which was found in two distinct strains, *S. aculeolatus* NRRL 18422 and the marine sediment-derived *Streptomyces* sp. CNQ-525 (Winter et al. 2007). The former and the latter were identified by a genome screening approach and PCR-amplified THN synthase and prenyltransferase as probes, respectively. The two clusters are similarly organized and 97% identical at nucleotide level. The cluster was heterologously expressed in *Streptomyces albus,* and the production of napyradiomycin A-related compounds was confirmed. The cluster contained 33 ORFs including two transposases (Fig. 3.1). Other 31 ORFs were categorized into five groups as follows: *nap*B1–B5, naphthoquinone polyketide synthesis; *nap*T1–T9, biosynthesis and attachment of isoprenoid; *nap*H1–H4, haloperoxidases; napR1–R9, putative regulators and transporters; and *nap*U1–U4, function unknown. Of these, the *nap*T6 to *nap*T1, which encode the MVA pathway enzymes, have high identities to those described above.

3.2.4.6 Furanonaphthoquinone I Biosynthetic Gene Cluster

As decribed in Sects. 3.2.4.1 to 3.2.4.5, the furanonaphthoquinone I biosynthetic gene cluster was cloned from *Streptomyces cinnamonensis* DSM 1042 (Bringmann et al. 2007). The cluster was identified at just flanking region of endophenazine A, a prenylated phenazine, biosynthetic genes (Fig. 3.2). Of 28 genes identified in the cluster, 13 showed high similarity to those in the furaquinocin A biosynthetic gene cluster. Considering the structural similarity between the two compounds, the existence of common genes is quite reasonable. Quite interestingly, in this cluster a complete set of genes is present which encode enzymes for recycling of *S*-adenosylhomocysteine to *S*-adenosylmethionine, being used as substrate for methylation reactions. To our knowledge, this is the first example for a complete set of SAM biosynthetic genes to make part of a secondary metabolic gene cluster.

3.3 Isoprenoid Biosynthetic Genes Cloned from Actinomycetes Possessing Only the MEP Pathway

Most of actinomycetes possess only the MEP pathway for the formation of IPP, and such strains are also known to produce various isoprenoid compounds. Biosynthetic genes of these compounds were identified by specific strategies and/or genome sequencing.

3.3.1 Isoprenoid Biosynthetic Genes Cloned by Specific Strategies

3.3.1.1 Pentalenene Synthase

A pioneering study on pentalenene synthase, a sesquiterpene synthase from an actinomycete strain, was performed by David Cane's laboratory. In 1994, the pentalenene synthase was purified, and a DNA fragment coding for was cloned by PCR using primers based on *N*-terminal and internal peptide sequences, thus for the first time of a prokaryotic isoprenoid cyclase (Cane et al. 1994). A recombinant enzyme was successfully produced in *E. coli,* and kinetic parameters of the enzyme were calculated. By site-directed mutagenesis, active-site residues of the enzyme were also analyzed (Seemann et al. 1999, 2002).

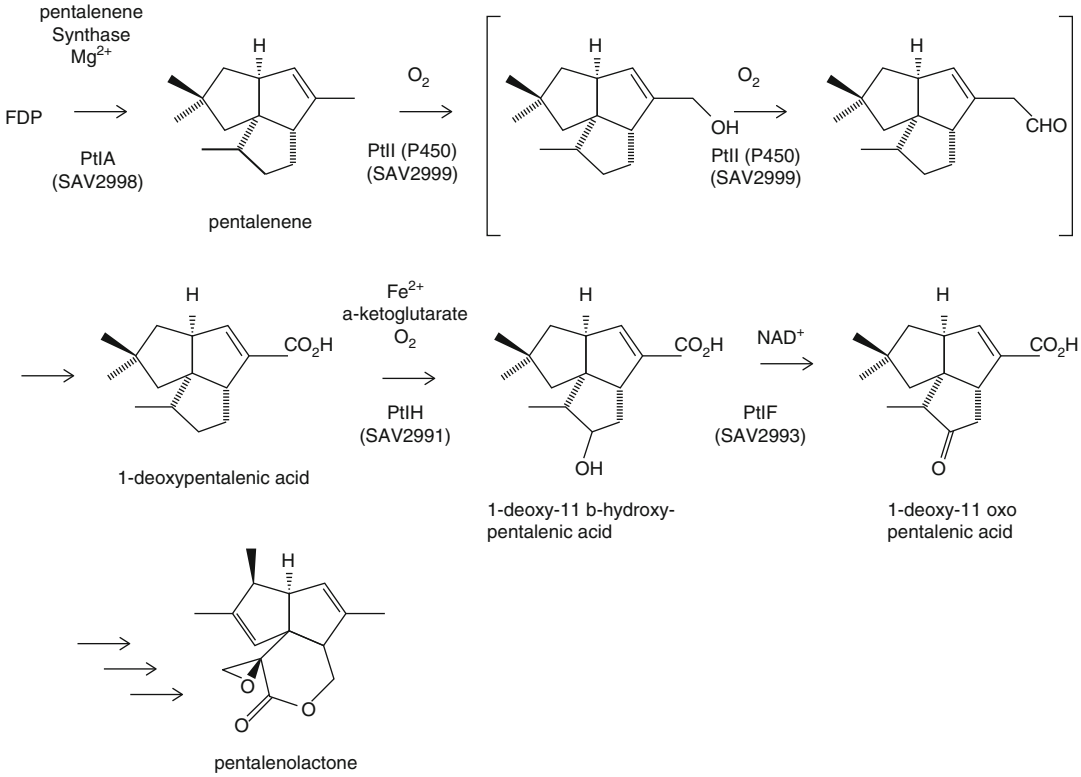

Fig. 3.6 Pentalenolactone biosynthetic pathway

Very recently, biosynthetic route from pentalenene into pentalenolactone has been proposed based on *in vitro* analyses of enzymes, the genes encoding which were identified by genome sequencing of *Streptomyces avermitilis* (Tetzlaff et al. 2006; Quaderer et al. 2006; You et al. 2006, 2007; Jiang et al. 2009; Seo et al. 2010; Zhu et al. 2011) (Fig. 3.6).

3.3.1.2 The Brasilicardin A Biosynthetic Gene Cluster

Brasilicardin A produced by *Nocardia brasiliensis* IFM 0406 (currently referred to as *N. terpenica*), has a structure consisting of a cyclic diterpene skeleton with L-rhamnose, *N*-acetylglucosamine, amino acid, and 3-hydroxybenzoate moieties. The gene cluster for brasilicardin A biosynthesis was identified by searching flanking regions of GGDP synthase and found to contain 11 genes though any genes related to L-rhamnose and *N*-acetylglucosamine biosyntheses were not integrated into the cluster (Hayashi et al. 2008) (Fig. 3.7). Among them, *bra3*, *bra4,* and *bra5* products present high amino acid identities to *plaT3* (phenalinolactone biosynthetic gene, see below, 47% identity), *plaT2* (43% identity), and *plaT1* (48% identity) products, respectively. Since the early step of the proposed biosynthetic pathway of brasilicardin A was thought to be identical to those of phenalinolactone (Fig. 3.8), high identities of amino acid sequences between the Bra3-5 and the PlaT3-1 make sense.

3.3.1.3 The Phenalinolactone Biosynthetic Gene Cluster

Phenalinolactone produced by *Streptomyces* sp. Tü6071 has a cyclic diterpene skeleton, to which L-amicetose, 5-methylpyrrole-2-carboxylic acid, and γ-butyrolactone moieties are attached. The phenalinolactone biosynthetic gene cluster was cloned with an L-amicetose biosynthetic gene as a probe (Dürr et al. 2006). The cluster contained

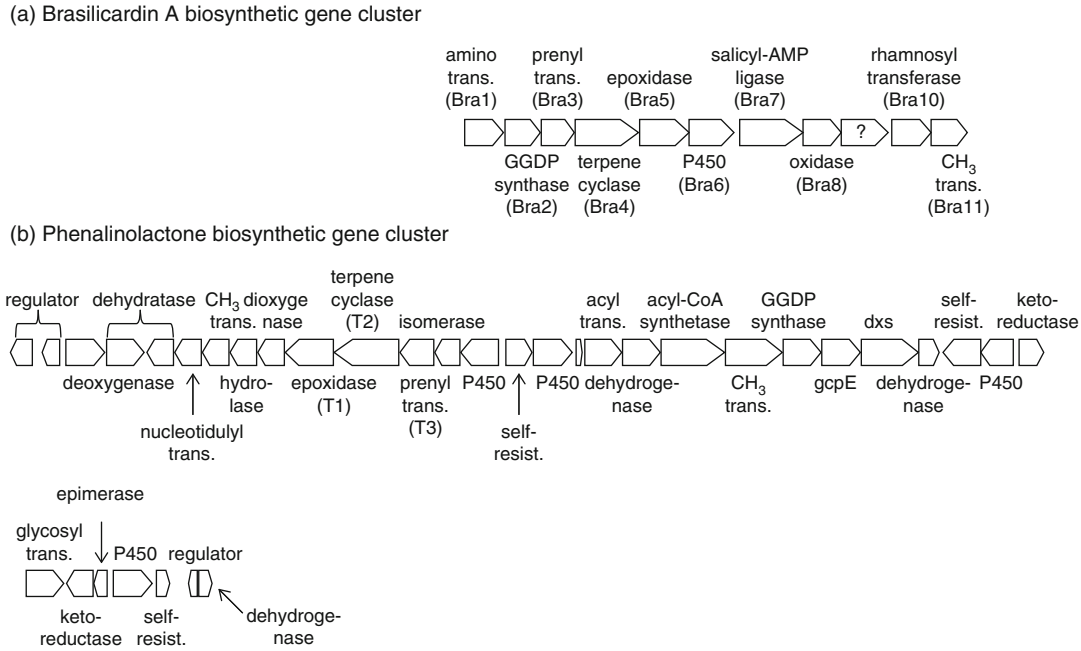

Fig. 3.7 Brasilicardin A and phenalinolactone biosynthetic gene clusters

35 genes (Fig. 3.7), and one of the genes (*plaT2*), which has a significant similarity to isoprenoid cyclases, was confirmed to be essential for the biosynthesis of phenalinolactone by a gene disruption experiment. Based on bioinformatic analyses and structures of intermediates accumulated in culture broth of the disruptants, a biosynthetic pathway to phenalinolactone was proposed (Fig. 3.8).

Interestingly, two MEP pathway genes, 1-deoxy-D-xylulose 5-phosphate synthase gene (*dxs*) and 4-hydroxy-3-methylbut-2-en-1-yl diphosphate synthase (*ispG*/*gcpE*/*HDS*) gene, made part of the phenalinolactone biosynthetic gene cluster though no such MEP genes were identified in the brasilicardin A biosynthetic gene cluster (Fig. 3.7). In the terpentecin producer that possesses both the MVA and the MEP pathway, we have already seen that some 60% of the IPP needed for the biosynthesis of terpentecin is supplied via the MVA pathway, while the MEP pathway contributes 40%. Considering that DXS was previously shown to be a rate-limiting enzyme in the MEP pathway, at least in plants (Estéves et al. 2001; see also elsewhere in this volume), the existence of the residual MEP genes might be reasonable for full production of isoprenoids in producers possessing only the MEP pathway.

3.3.1.4 The KS-505a (Longestin) Biosynthetic Gene Cluster

KS-505a (longestin) produced by *Streptomyces argenteolus* is a sole tetraterpene compound biosynthesized from octaprenyl diphosphate (OPD). It has a unique structure that consists of a tetraterpene (C40) skeleton, to which a 2-*O*-methylglucuronic acid and an *o*-succinylbenzoate moieties are attached. A KS505a biosynthetic gene cluster was cloned by using the OPD synthase gene as a probe, which yielded a C40 precursor (Hayashi et al. 2007). A gene disruption experiment was employed to confirm that the cluster indeed participates in KS-505a biosynthesis. The gene cluster consists of 24 ORFs though no genes related to glucuronic acid biosynthesis could be identified in the flanking regions (Fig. 3.9). The cluster contained an *o*-succinylbenzoate synthase gene and an isochorismate synthase gene for *o*-succinylbenzoate biosynthesis, a glycosyl transferase gene for the

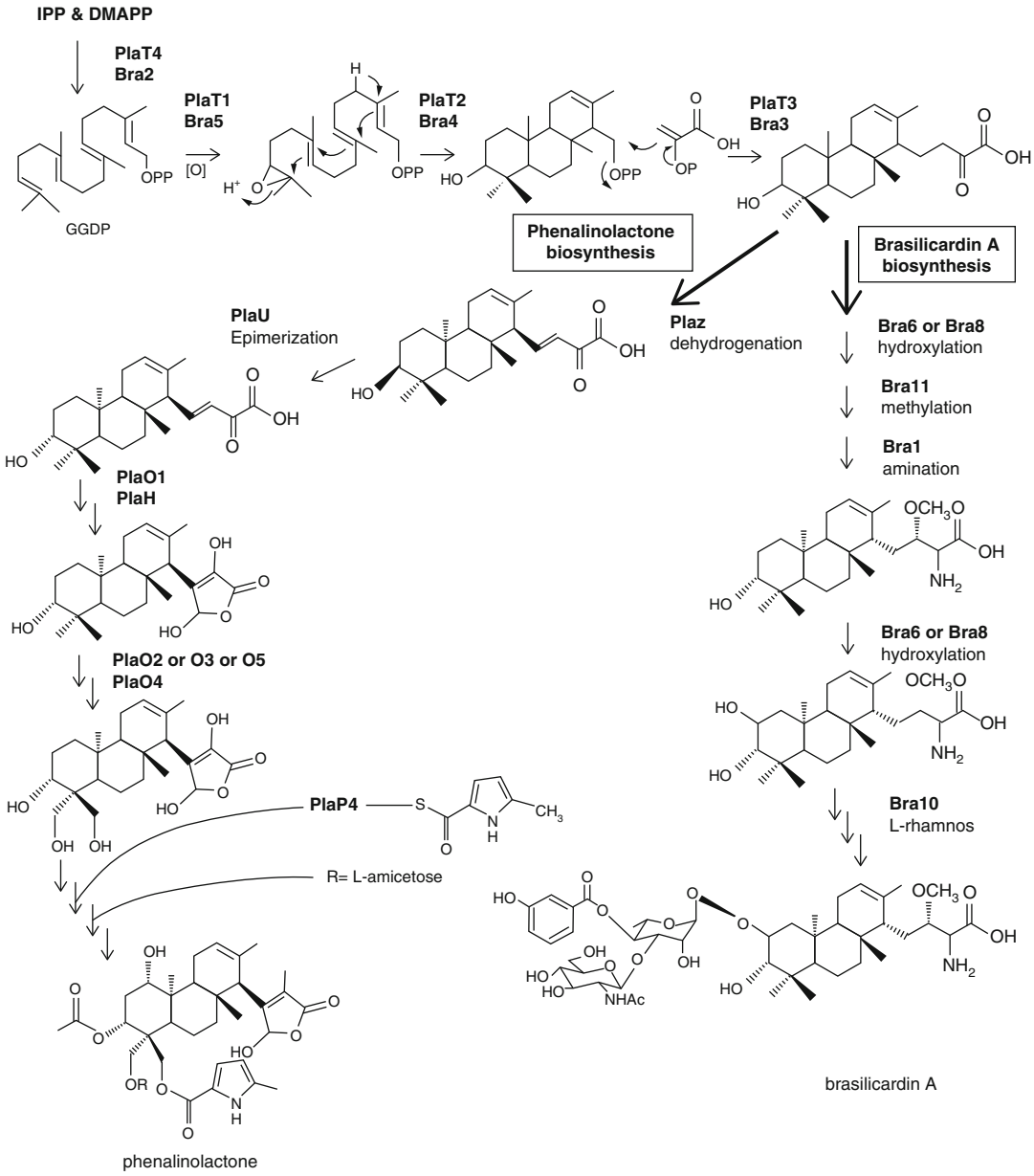

Fig. 3.8 Proposed biosynthetic pathways of brasilicardin A and phenalinolactone

attachment of glucuronic acid, two P450 genes for hydroxylation reactions, and three genes for methylation in addition to OPD synthase, prenyltransferase, and isoprenoid cyclase genes. In the cluster, two MEP pathway genes, *dxs* and *ispG*/*gcpE/HDS*, were also included in the same manner as in the phenalinolactone biosynthetic gene cluster.

3.3.1.5 Novobiocin and Clorobiocin Biosynthetic Gene Clusters

Novobiocin and clorobiocin produced by *Streptomyces roseochromogenes* and *Streptomyces spheroides*/*Streptomyces niveus*, respectively, are composed of three moieties, a noviose sugar, a substituted coumarin, and a prenylated 4-hydroxybenzoic acid, and these rings are linked by glycosidic

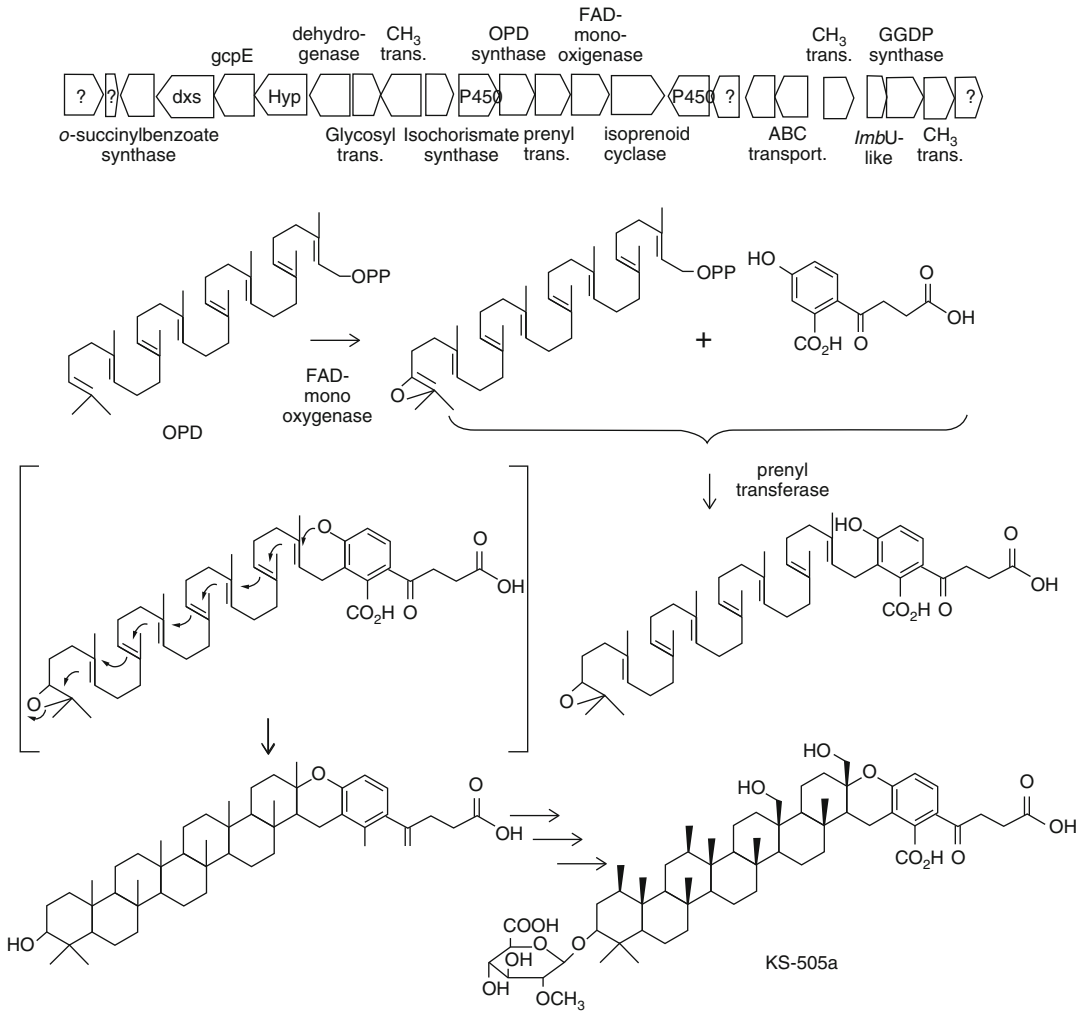

Fig. 3.9 Biosynthetic gene cluster of KS-505a and its proposed biosynthetic pathway

and amide bonds. The biosynthetic studies of these compounds were extensively studied by Lutz Heide's group. A novobiocin biosynthetic gene cluster was cloned with PCR-amplified (dNDP)-glucose 4,6-dehydratase gene as a probe (Steffensky et al. 2000). After that, a clorobiocin biosynthetic gene cluster was obtained with the novobiocin biosynthetic gene as a probe (Pojer et al. 2002) (Fig. 3.10). The authors noticed that there were no orthologs of *UbiA*-like gene, whose product catalyzes prenylation reactions in spite of the fact that both compounds possess 3-dimethylallyl-4-hydroxybenzoic acid as a structural component. Therefore, they searched a gene, which is present in these two clusters but absent in the biosynthetic gene cluster of A_1, which has the similar structure of those of novobiocin and clorobiocin, but without a prenylated moiety. Eventually, a candidate gene (*cloQ*) was selected and confirmed to represent the gene searched for by a gene disruption experiment. Prenylation activity *in vitro* was also detected with a recombinant CloQ and 4-hydroxyphenylpyruvate and DMAPP as substrates (Pojer et al. 2003).

3.3.1.6 The Moenomycin Biosynthetic Gene Cluster

Moenomycin is a phosphoglycolipid antibiotic with a unique C_{25} prenyl moiety. A biosynthetic gene cluster of moenomycin has been cloned

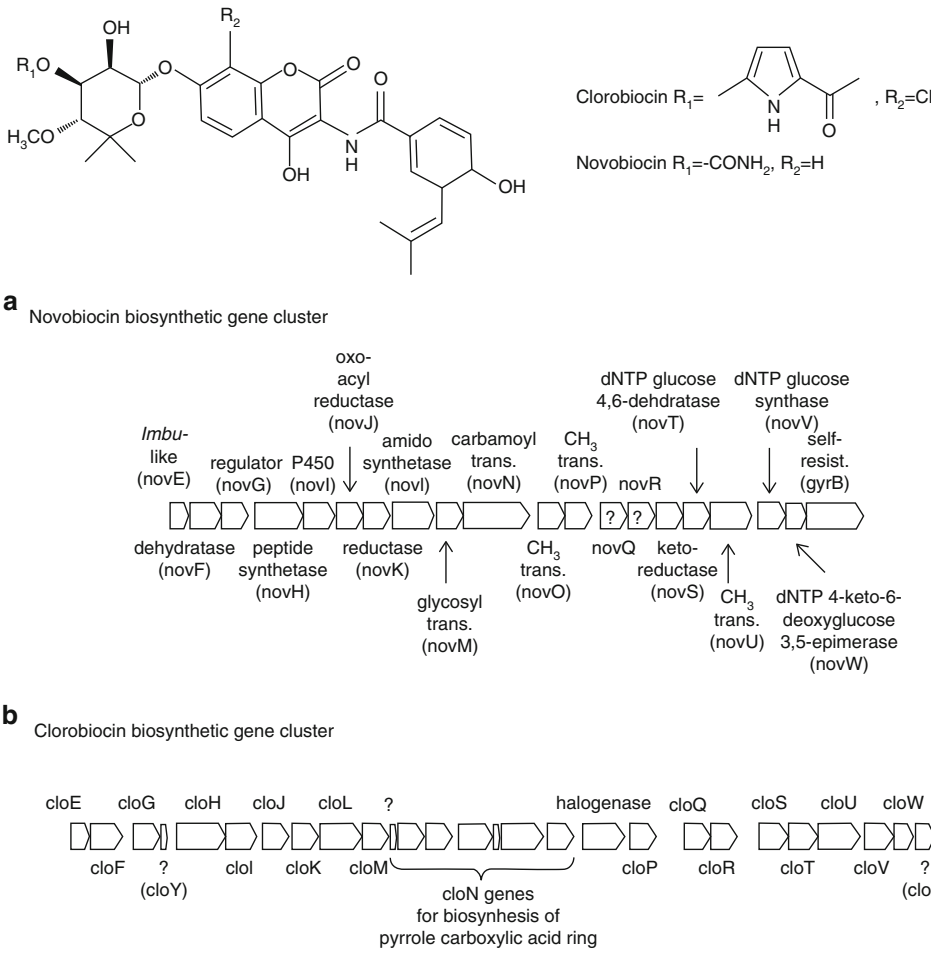

Fig. 3.10 Structures of clorobiocin and novobiocin and their biosynthetic gene clusters

from *Streptomyces ghanaensis* (ATCC14672) (Ostash et al. 2007). Three genes, *moe*A4, *moe*B4, and *moe*C4, which would encode acyl-CoA ligase, amide synthetase, and aminolevulinate synthase, respectively, and participate in biosynthesis of the C_5N subunit attached to the terminal glycoside, were cloned with PCR-amplified aminolevulinate synthase gene as a probe (cluster 2). Although these genes were confirmed to be essential for the biosynthesis of moenomycin by a gene disruption experiment, none of the other genes existed in flanking regions of these three genes. After that, another cluster (cluster 1) was identified by genome sequencing of the producer (Fig. 3.11). This cluster was also confirmed to be essential by a gene disruption experiment and by heterologous expression. The cluster contained two genes, *moe*N5 and *moe*O5, which would be related to biosynthesis of prenyl moiety. MoeN5 shows homology to other polyprenyl diphosphate synthases such as FDP synthase and GGDP synthase and was therefore suggested to be involved in the synthesis of the C_{25} lipid chain (Adachi et al. 2006). MoeO5 that shows weak similarity to the archaeal enzymes that form the first ether linkage between isoprenoid precursors and glycerol phosphate in the biosynthesis of the unusual membrane lipids is therefore predicted to catalyze the formation of the ether linkage between 3-*R*-phosphoglycerate and the isoprenyl residue (Fig. 3.12).

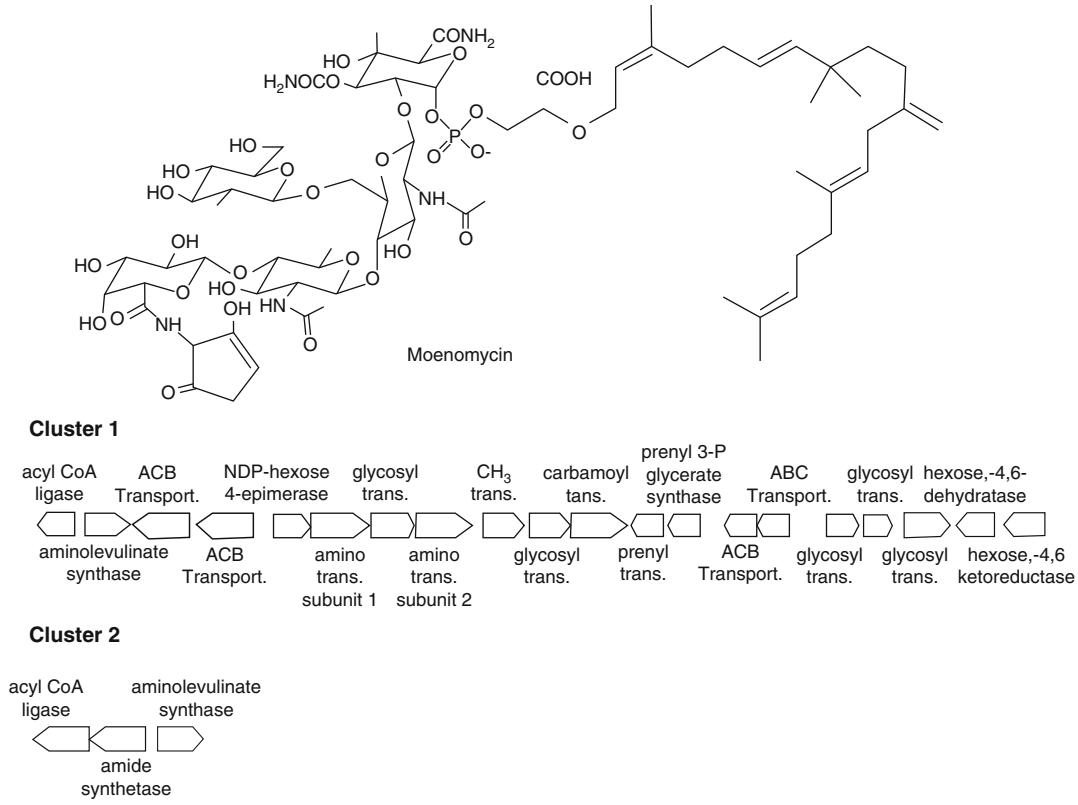

Fig. 3.11 Structure of moenomycin and its biosynthetic gene cluster

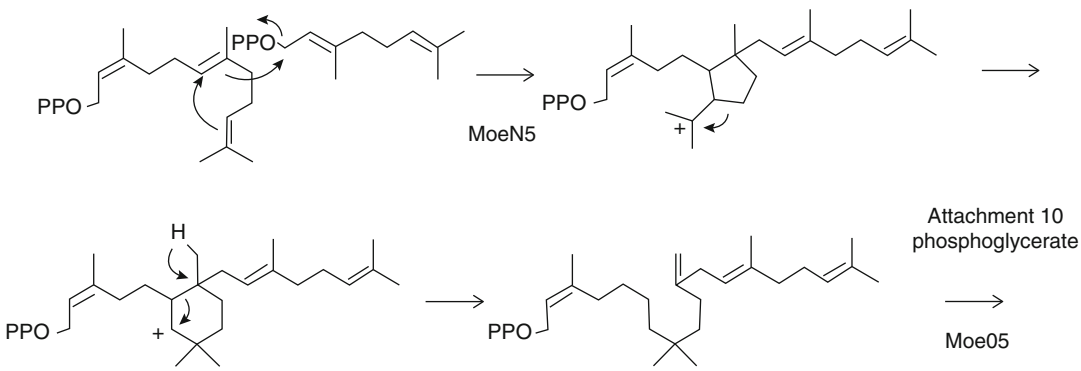

Fig. 3.12 Proposed mechanism of isoprenoid chain formation involved in moenomycin biosynthesis

3.3.2 Isoprenoid Biosynthetic Genes Identified by Genome Sequencing and Bioinformatics

3.3.2.1 2-Methylisoborneol Synthase

2-Methylisoborneol known as an odorous compound is a cyclic monoterpene found in actinomycetes. A monoterpene cyclase responsible for the formation of the compound from geranyl diphosphate (GDP) has been identified in *S. lasaliensis* (Komatsu et al. 2008) and *S. coelicolor* (Wang and Cane 2008). Moreover, it was shown that SAM-dependent methyltransferase first catalyzes methylation at the C2 position of GDP

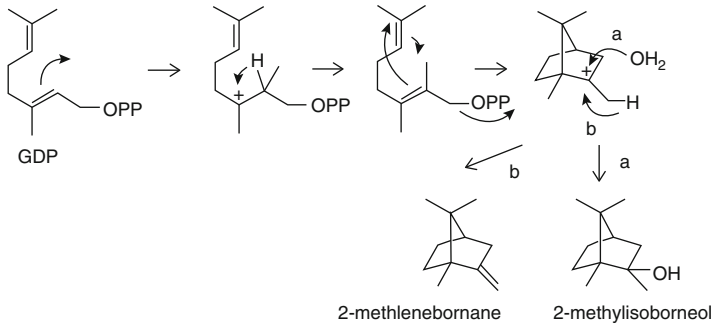

Fig. 3.13 Biosynthetic pathway to 2-methylenebornane and 2-methylisoborneol

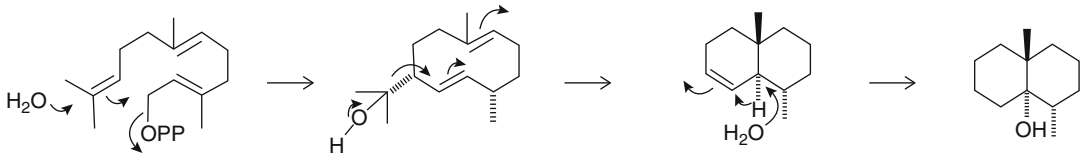

Fig. 3.14 Biosynthetic pathway of geosmin

and that the thus methylated GDP was successively cyclized by the monoterpene cyclase to form 2-methylisoborneol or 2-methylenebornane (Fig. 3.13).

3.3.2.2 Enzymes Responsible for the Biosynthesis of Geosmin

Geosmin, a sesquiterpenoid, is a well-known compound that causes an unpleasant "earthy" flavor. A recombinant SCO6073 and a recombinant SAV2163, which exist in *S. coelicolor* A3(2) and *S. avermitilis*, respectively, were shown to convert FDP into (4*S*,7*R*)-germacra-1(10)*E*,5*E*-diene-11-ol, concomitant with the formation of small amounts of geosmin in the presence of Mg^{2+} (Cane and Watt 2003; He and Cane 2004; Jiang et al. 2006; Cane et al. 2006). Recently, the detailed reaction mechanism has been reported: The *N*-terminal half of recombinant SCO6073 converts FDP into (4*S*,7*R*)-germacra-1(10)*E*,5*E*-diene-11-ol and germacrene D, and the C-terminal domain catalyzes the Mg^{2+}-dependent conversion of (4*S*,7*R*)-germacra-1(10)*E*,5*E*-diene-11-ol to geosmin by removing the C3 unit (Jiang et al. 2007; Nawrath et al. 2008; Jang and Cane 2008) (Fig. 3.14).

3.3.2.3 Enzymes Responsible for Biosynthesis of *Epi*-Isozizaene and Albaflavenone

Previously, *epi*-isozizaene was shown to be formed from FDP by SCO5222 (Lin et al. 2006). Recently, it has been reported that albaflavenone was synthesized from (−)-*epi*-isozizaene *via* (4*S*) or (4*R*)-albaflavenol, this by SCO5223 a P450 enzyme derived from *CYP170A1*) of *S. coelicolor* A3(2) by testing the recombinant enzyme (Zhao et al. 2008) (Fig. 3.15). The detailed reaction mechanism of cyclization was also studied with deuterated FDP (Lin and Cane 2009).

3.3.2.4 Tuberculosinol {(+)-5(6),13-halimadiene-15-ol} Synthase

By bioinformatic, screening the group of Hoshino identified a gene homologous to (oxido)

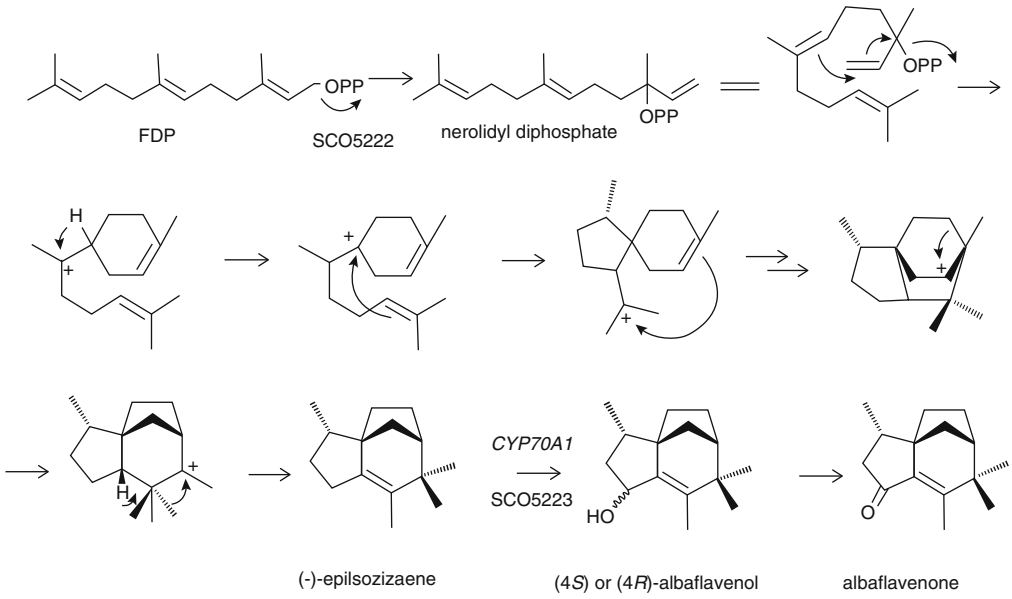

Fig. 3.15 Biosynthetic pathway of (−)-epi-isozizaene and albaflavenone

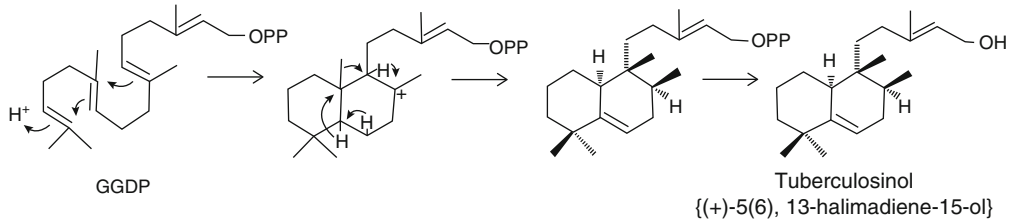

Rv3377c (*Mycobacteriumtuberculosis* H37Rv)

Fig. 3.16 Reaction catalyzed by Rv3377c of *Mycobacterium tuberculosis* H37Rv

squalene cyclases and some terpene cyclases in *Mycobacterium tuberculosis* H37Rv, after the whole-genome sequencing was completed. The gene product, Rv3377c, was cloned and expressed in *E. coli*. This gene product was shown to convert GGDP into tuberculosinol {(+)-5(6),13-halimadiene-15-ol}, which was probably an artificial product formed by elimination of the diphosphate group from tuberculosinol diphosphate due to the presence of a contaminating phosphatase in *E. coli* (Nakano et al. 2005) (Fig. 3.16).

3.3.2.5 Cyclomarazines Biosynthetic Gene Cluster

Prenylated cyclic dipeptides, cyclomarazines A/B, and heptapeptide, cyclomarin D, were isolated from the marine bacterium *Salinispora arenicola* CNS-205. By genome DNA sequencing of the strain, the biosynthetic gene cluster of these compounds was identified in a 47-kb region containing 23 genes (Schultz et al. 2008). This cluster was characterized by the presence of a large (23,358 bp) nonribosomal peptide synthetase

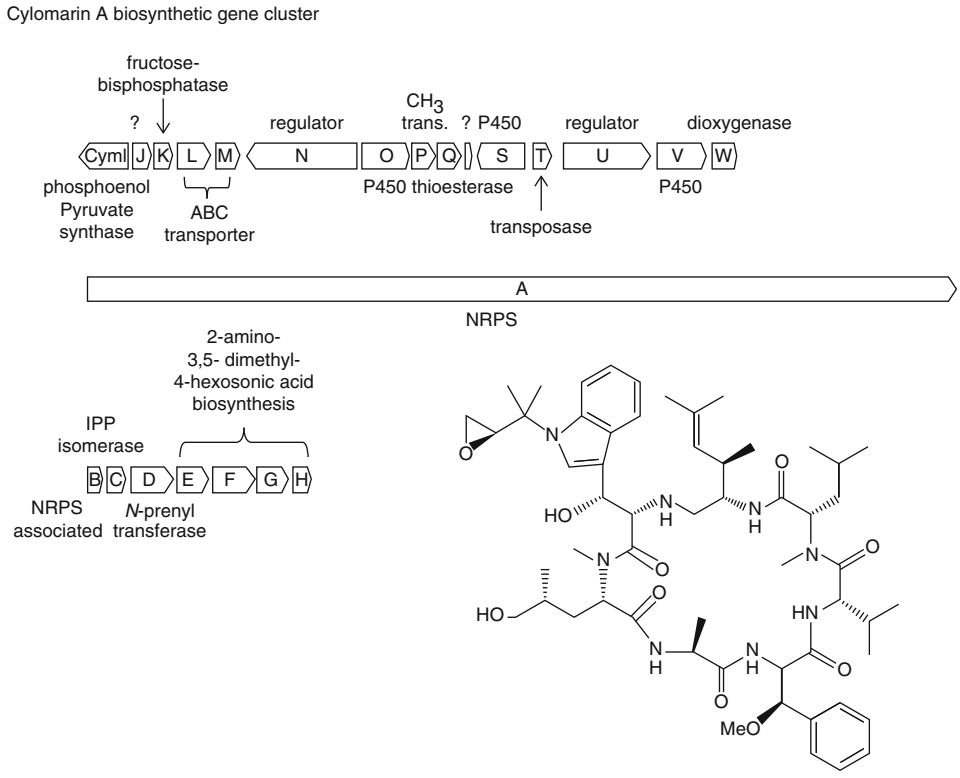

Fig. 3.17 Structure of cyclomarin A and its biosynthetic gene cluster

(NRPS) responsible for assembly of the full-length cyclomarin heptapeptides (Fig. 3.17). The NRPS therefore catalyzed the biosynthesis of differently sized peptides *in vivo*. The cluster further contained two isoprenoid-related genes, coding for a type I IPP isomerase (*cymC*) and for a prenyl transferase (*cymD*), which would catalyze a reverse prenylation of a tryptophan residue. The gene was disrupted by PCR-targeted gene replacement and the disruptant was confirmed to produce desprenyl cyclomarin and cyclomarazine analogs.

3.3.2.6 Enzymes Responsible for Biosynthesis of Avermitilol, (−)-δ-Cadinene, and (+)-T-Muurolol

Recently, some sesquiterpene cyclases, which were identified by genome mining, were investigated. Sav76 of *Streptomyces avermitilis* was confirmed to catalyze the formation of avermitilol, together with small amounts of germacrene A, germacrene B, and viridiflorol, this from FDP via a germacradienyl cation (Chou et al. 2010). Sscg_02150 and Sscg_03688 of *Streptomyces clavuligerus* were shown to catalyze the formation of (−)-δ-cadinene and (+)-T-muurolol, respectively (Hu et al. 2011).

3.3.2.7 An Alternative Menaquinone Biosynthetic Pathway

In some microorganisms including actinomycetes, menaquinone is an obligatory component of the electron-transfer pathway. Menaquinone is composed of naphthoquinone moiety and an isoprenoid side chain. The naphthoquinone moiety is derived from chorismate by action of seven consecutive enzymes (MenA–MenG in *Escherichia coli*). However, by tracer experiments, a novel pathway was demonstrated to be operational in a *Streptomyces* strain. Quite recently, the pathway has been shown to operate up to the formation of chorismate in a manner

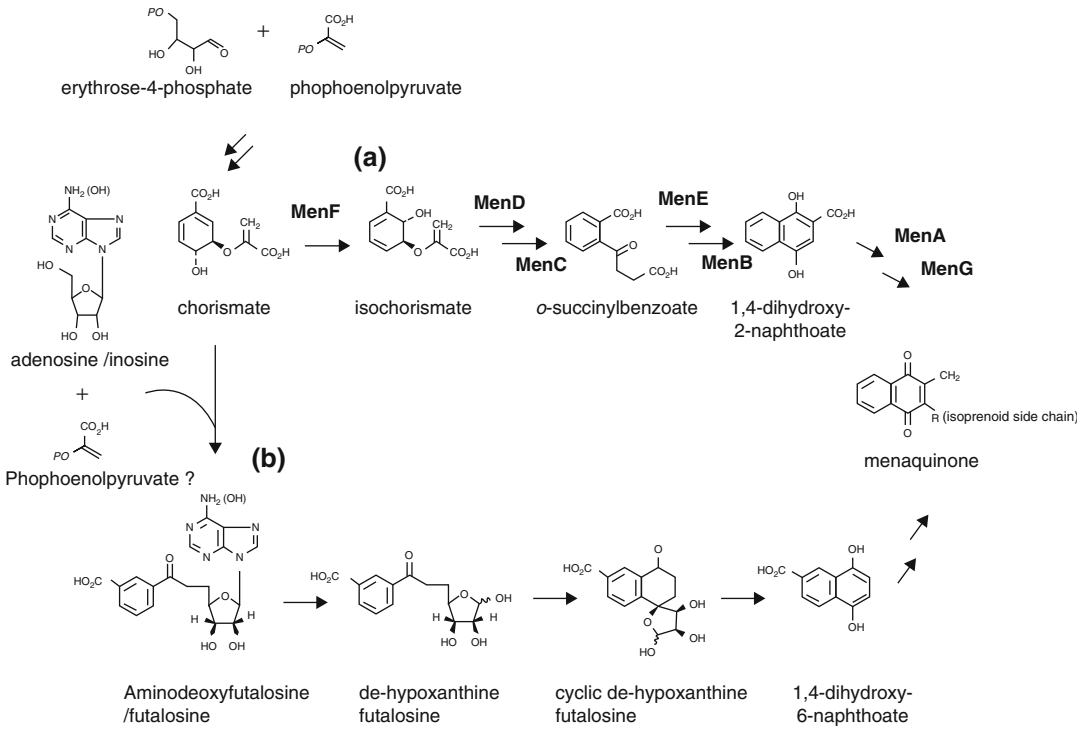

Fig. 3.18 Biosynthetic pathways of menaquinone. (**a**) Known pathway and (**b**) new pathway

similar to the known pathway but then follows a different route (Seto et al. 2008). MqnA (SCO4506 in *S. coelicolor*) would catalyze the condensation reaction of chorismate, inosine, and a C2 unit probably derived from phosphoenolpyruvate to form futalosine. Then, hypoxanthine is released to give de-hypoxanthine (dehypoxanthinyl) futalosine (DHFL) by MqnB (SCO4327). MqnC (SCO4550), a radical SAM enzyme, would cyclyze DHFL to form cyclic DHFL, followed by cleavage of the C3 unit to yield 1,4-dihydroxy-6-naphthoate by MqnD (SCO4326) (Hiratsuka et al. 2008) (Fig. 3.18). In the last two steps, orthologs of MenA (SCO4491) and MenG (SCO4556) probably catalyze the prenylation and the S-adenosylmethionine-dependent methylation. Very recently, three routes to the formation of menaquinone in the futalosine pathway were suggested. Futalosine may have been directly formed by MqnA in *T. thermophilus* and converted into DHFL. In *Acidothermus cellulolyticus*, *S. coelicolor*, and *H. pylori*, aminodeoxyfutalosine, which has an adenine moiety instead of hypoxanthine in futalosine, was formed by MqnA. In the case of the former two strains, aminodeoxyfutalosine was converted to futalosine by deaminases, then to DHFL. In contrast, aminodeoxyfutalosine was directly converted to DHFL in *H. pylori* (Arakawa et al. 2011).

References

Adachi M, Zhang Y, Leimkuhler C et al (2006) Degradation and reconstruction of moenomycin A and derivatives: dissecting the function of the isoprenoid chain. J Am Chem Soc 128:14012–14013

Arakawa C, Kuratsu M, Furihata K et al (2011) Diversity of the early step of the futalosine pathway. Antimicrob Agents Chemother 55:913–916

Bringmann G, Haagen Y, Gulder T et al (2007) Biosynthesis of the isoprenoid moieties of furanonaphthoquinone I and endophenazine A in *Streptomyces cinnamonensis* DSM 1042. J Org Chem 72: 4198–4204

Cane DE, Watt RM (2003) Expression and mechanistic analysis of a germacradienol synthase from *Streptomyces coelicolor* implicated in geosmin biosynthesis. Proc Natl Acad Sci USA 100:1547–1551

Cane DE, Sohng JK, Lamberson CR et al (1994) Pentalenene synthase: purification, molecular cloning, sequencing, and high-level expression in *Escherichia*

coli of a terpenoid cyclase from *Streptomyces* UC5319. Biochemistry 33:5846–5857

Cane DE, He X, Kobayashi S et al (2006) Geosmin biosynthesis in *Streptomyces avermitilis*. Molecular cloning, expression, and mechanistic study of the germacradienol/geosmin synthase. J Antibiot 59: 471–479

Chou WK, Fanizza I, Uchiyama T et al (2010) Genome mining in *Streptomyces avermitilis*: cloning and characterization of SAV_76, the synthase for a new sesquiterpene, avermitilol. J Am Chem Soc 132: 8850–8851

Connolly JD, Hill RA (1992) Dictionary of terpenoids. Chapman and Hall, New York

Dairi T (2005) Studies on biosynthetic genes and enzymes of isoprenoids produced by actinomycetes. J Antibiot 58:227–243

Dairi T, Motohira Y, Kuzuyama T et al (2000) Cloning of the gene encoding 3-hydroxy-3-methylglutaryl coenzyme A reductase from terpenoid antibiotic-producing *Streptomyces* strains. Mol Gen Genet 262:957–964

Dairi T, Hamano Y, Kuzuyama T et al (2001) Eubacterial diterpene cyclase genes essential for production of the isoprenoid antibiotic terpentecin. J Bacteriol 183: 6085–6094

Dairi T, Kuzuyama T, Nishiyama M et al (2011) Convergent strategies in biosynthesis. Nat Prod Rep 28:1054–1086

Dewick PM (2002) The biosynthesis of C5-C25 terpenoid compounds. Nat Prod Rep 19:181–222

Dürr C, Schnell H, Luzhetskyy A et al (2006) Biosynthesis of the terpene phenalinolactone in *Streptomyces* sp. Tü6071: analysis of the gene cluster and generation of derivatives. Chem Biol 13:365–377

Estéves JM, Cantero A, Reindl A et al (2001) 1-Deoxy-D-xylulose-5-phosphate synthase, a limiting enzyme for plastidic isoprenoid biosynthesis in plants. J Biol Chem 276:22901–22909

Haagen Y, Glück K, Fay K et al (2006) A gene cluster for prenylated naphthoquinone and prenylated phenazine biosynthesis in *Streptomyces cinnamonensis* DSM 1042. Chembiochem 7:2016–2027

Hamano Y, Dairi T, Yamamoto M et al (2001) Cloning of a gene cluster encoding enzymes responsible for the mevalonate pathway from a terpenoid-antibiotic-producing *Streptomyces* strain. Biosci Biotechnol Biochem 65:1627–1635

Hamano Y, Dairi T, Yamamoto M et al (2002a) Growth phase dependent expression of the mevalonate pathway in a terpenoid antibiotic-producing *Streptomyces* strain. Biosci Biotechnol Biochem 66:808–819

Hamano Y, Kuzuyama T, Itoh N et al (2002b) Functional analysis of eubacterial diterpene cyclases responsible for biosynthesis of a diterpene antibiotic, terpentecin. J Biol Chem 277:37098–37104

Hayashi Y, Onaka H, Itoh N et al (2007) Cloning of the gene cluster responsible for biosynthesis of KS-505a (longestin), a unique tetraterpenoid. Biosci Biotechnol Biochem 71:3072–3081

Hayashi Y, Matsuura N, Toshima H et al (2008) Cloning of the gene cluster responsible for the biosynthesis of brasilicardin A, a unique diterpenoid. J Antibiot 61:164–174

He X, Cane DE (2004) Mechanism and stereochemistry of the germacradienol/germacrene D synthase of *Streptomyces coelicolor* A3(2). J Am Chem Soc 126:2678–2679

Hiratsuka T, Furihata K, Ishikawa J et al (2008) An alternative menaquinone biosynthetic pathway operating in microorganisms. Science 321:1670–1673

Hu Y, Chou WK, Hopson R et al (2011) Genome mining in *Streptomyces clavuligerus*: expression and biochemical characterization of two new cryptic sesquiterpene synthases. Chem Biol 18:32–37

Ikeda C, Hayashi Y, Itoh N et al (2007) Functional analysis of eubacterial *ent*-copalyl diphosphate synthase and pimara-9(11),15-diene synthase with unique primary sequences. J Biochem 141:37–45

Ishikawa J, Yamashita A, Mikami Y et al (2004) The complete genomic sequence of *Nocardia farcinica* IFM 10152. Proc Natl Acad Sci USA 101:14925–14930

Jang J, Cane DE (2008) Geosmin biosynthesis. Mechanism of the fragmentation-rearrangement in the conversion of germacradienol to geosmin. J Am Chem Soc 130:428–429

Jiang J, He X, Cane DE (2006) Geosmin biosynthesis. *Streptomyces coelicolor* germacradienol/germacrene D synthase converts farnesyl diphosphate to geosmin. J Am Chem Soc 128:8128–8129

Jiang J, He X, Cane DE (2007) Biosynthesis of the earthy odorant geosmin by a bifunctional *Streptomyces coelicolor* enzyme. Nat Chem Biol 3:711–715

Jiang J, Tetzlaff CN, Takamatsu S et al (2009) Genome mining in *Streptomyces avermitilis*: a biochemical Baeyer-Villiger reaction and discovery of a new branch of the pentalenolactone family tree. Biochemistry 48:6431–6440

Kawasaki T, Kuzuyama T, Furihata K et al (2003) A relationship between the mevalonate pathway and isoprenoid production in actinomycetes. J Antibiot (Tokyo) 56:957–966

Kawasaki T, Kuzuyama T, Kuwamori Y et al (2004) Presence of copalyl diphosphate synthase gene in an actinomycete possessing the mevalonate pathway. J Antibiot (Tokyo) 57:739–747

Kawasaki T, Hayashi Y, Kuzuyama T et al (2006) Biosynthesis of a natural polyketide-isoprenoid hybrid compound, furaquinocin A: identification and heterologous expression of the gene cluster. J Bacteriol 188:1236–1244

Komatsu M, Tsuda M, Ômura S et al (2008) Identification and functional analysis of genes controlling biosynthesis of 2-methylisoborneol. Proc Natl Acad Sci USA 105:7422–7427

Kuzuyama T, Seto H (2003) Diversity of the biosynthesis of the isoprene units. Nat Prod Rep 20:171–183

Kuzuyama T, Takagi M, Takahasi S et al (2000) Cloning and characterization of 1-deoxy-D-xylulose 5-phosphate

synthase from *Streptomyces* sp. strain CL190, which uses both the mevalonate and nonmevalonate pathways for isopentenyl diphosphate biosynthesis. J Bacteriol 182:891–897

Kuzuyama T, Noel JP, Richard SB (2006) Structural basis for the promiscuous biosynthetic prenylation of aromatic natural products. Nature 435:983–987

Lin X, Cane DE (2009) Biosynthesis of the sesquiterpene antibiotic albaflavenone in *Streptomyces coelicolor*. Mechanism and stereochemistry of the enzymatic formation of epi-isozizaene. J Am Chem Soc 131: 6332–6333

Lin X, Hopson R, Cane DE (2006) Genome mining in *Streptomyces coelicolor*: molecular cloning and characterization of a new sesquiterpene synthase. J Am Chem Soc 128:6022–6023

Nakano C, Okamura T, Sato T et al (2005) *Mycobacterium tuberculosis* H37Rv3377c encodes the diterpene cyclase for producing the halimane skeleton. Chem Commun 28:1016–1018

Nawrath T, Dickschat JS, Müueller R et al (2008) Identification of (8*S*,9*S*,10*S*)-8,10-dimethyl-1-octalin, a key intermediate in the biosynthesis of geosmin in bacteria. J Am Chem Soc 130:430–431

Okamura E, Tomita T, Sawa R et al (2010) Unprecedented acetoacetyl-coenzyme A synthesizing enzyme of the thiolase superfamily involved in the mevalonate pathway. Proc Natl Acad Sci USA 107:11265–11270

Ostash B, Saghatelian A, Walker S (2007) A streamlined metabolic pathway for the biosynthesis of moenomycin A. Chem Biol 14:257–267

Pojer F, Li S-M, Heide L (2002) Molecular cloning and sequence analysis of the clorobiocin biosynthetic gene cluster: new insights into the biosynthesis of aminocoumarin antibiotics. Microbiology 148:3901–3911

Pojer F, Wemakor E, Kammerer B et al (2003) CloQ, a prenyltransferase involved in clorobiocin biosynthesis. Proc Natl Acad Sci USA 100:2316–2321

Quaderer R, Ômura S, Ikeda H et al (2006) Pentalenolactone biosynthesis. Molecular cloning and assignment of biochemical function to PtlI, a cytochrome P450 of *Streptomyces avermitilis*. J Am Chem Soc 128:13036–13067

Schultz AW, Oh D-C, Carney JR et al (2008) Biosynthesis and structures of cyclomarins and cyclomarazines, prenylated cyclic peptides of marine actinobacterial origin. J Am Chem Soc 130:4507–4516

Seeger K, Flinspach K, Haug-Schifferdecker E et al (2011) The biosynthetic genes for prenylated phenazines are located at two different chromosomal loci of *Streptomyces cinnamonensis* DSM 1042. Microb Biotechnol 4:252–262

Seemann M, Zhai G, Umezawa K et al (1999) Pentalenene synthase. Histidine-309 is not required for catalytic activity. J Am Chem Soc 121:591–592

Seemann M, Zhai G, Kraker J-W et al (2002) Pentalenene synthase. Analysis of active site residues by site-directed mutagenesis. J Am Chem Soc 124:7681–7689

Seo MJ, Zhu D, Endo S et al (2010) Genome mining in *Streptomyces*. Elucidation of the role of Baeyer-Villiger monooxygenases and non-heme iron-dependent dehydrogenase/oxygenases in the final steps of the biosynthesis of pentalenolactone and neopentalenolactone. Biochemistry 50:1739–1754

Seto H, Watanabe H, Furihata K (1996) Simultaneous operation of the mevalonate and non-mevalonate pathways in the biosynthesis of isopentenyl diphosphate in *Streptomyces aeriouvifer*. Tetrahedron Lett 37: 7979–7982

Seto H, Jinnai Y, Hiratsuka T et al (2008) Studies on a new biosynthetic pathway for menaquinone. J Am Chem Soc 130:5614–5615

Steffensky M, Mühlenweg A, Wang Z-X et al (2000) Identification of the novobiocin biosynthetic gene cluster of *Streptomyces spheroides* NCIB 11891. Antimicrob Agents Chemother 44:1214–1222

Takagi M, Kuzuyama T, Takahashi S et al (2000) A gene cluster for the mevalonate pathway from *Streptomyces* sp. strain CL190. J Bacteriol 182:4153–4157

Takahasi S, Kuzuyama T, Seto H (1999) Purification, characterization, and cloning of a eubacterial 3-hydroxy-3-methylglutaryl coenzyme A reductase, a key enzyme involved in biosynthesis of terpenoids. J Bacteriol 181:1256–1263

Tetzlaff CN, You Z, Cane DE et al (2006) A gene cluster for biosynthesis of the sesquiterpenoid antibiotic pentalenolactone in *Streptomyces avermitilis*. Biochemistry 45:6179–6186

Wang CM, Cane DE (2008) Biochemistry and molecular genetics of the biosynthesis of the earthy odorant methylisoborneol in *Streptomyces coelicolor*. J Am Chem Soc 130:8908–8909

Winter JM, Moffitt MC, Zazopoulos E et al (2007) Molecular basis for chloronium-mediated meroterpene cyclization: cloning, sequencing, and heterologous expression of the napyradiomycin biosynthetic gene cluster. J Biol Chem 282:16362–16368

You Z, Ômura S, Ikeda H et al (2006) Pentalenolactone biosynthesis. Molecular cloning and assignment of biochemical function to PtlH, a non-heme iron dioxygenase of *Streptomyces avermitilis*. J Am Chem Soc 128:6566–6567

You Z, Ômura S, Ikeda H et al (2007) Pentalenolactone biosynthesis: molecular cloning and assignment of biochemical function to PtlF, a short-chain dehydrogenase from *Streptomyces avermitilis*, and identification of a new biosynthetic intermediate. Arch Biochem Biophys 459:233–240

Zhao B, Lin X, Lei L et al (2008) Biosynthesis of the sesquiterpene antibiotic albaflavenone in *Streptomyces coelicolor* A3(2). J Biol Chem 283:8183–8189

Zhu D, Seo MJ, Ikeda H et al (2011) Genome mining in streptomyces. Discovery of an unprecedented P450-catalyzed oxidative rearrangement that is the final step in the biosynthesis of pentalenolactone. J Am Chem Soc 133:2128–2131

4 Interactions of Isoprenoid Pathway Enzymes and Indirect Stimulation of Isoprenoid Biosynthesis by Pentose Phosphate Cycle Substrates in *Synechocystis* PCC 6803

Kelly Poliquin, Francis X. Cunningham Jr., R. Raymond Gantt, and Elisabeth Gantt

Abstract

Interactions between enzymes of the 2-*C*-methyl-D-erythritol 4-phosphate (MEP) pathway of isoprenoid biosynthesis in the cyanobacterium *Synechocystis* PCC 6803 were examined using a bacterial two-hybrid genetic interaction assay. No protein-protein interactions other than self-interactions were detected, an observation at odds with the concept of a multienzyme complex and metabolic channeling for this pathway. A previously reported stimulation of isoprenoid synthesis by intermediates of the pentose phosphate cycle (PPC) *in vitro* was not affected by immunodepletion of IDS (LytB), the enzyme that catalyzes the terminal step of the MEP pathway. Addition of various PPC compounds supported a progression of *in vitro* isoprenoid synthesis, from C5 to C10 to C20, but the PPC compounds did not directly serve as substrates. It is concluded that the *in vitro* stimulation by PPC compounds is indirect and does not occur via the MEP pathway.

Keywords

Cyanobacteria • Epitope tagging • Farnesol • Isoprenoid pathway • LytB • 2-*C*-methyl-D-erythritol 4-phosphate (MEP) • Pentose phosphate cycle stimulation • Protein-protein interaction • *Synechocystis* PCC 6803

K. Poliquin • F.X. Cunningham Jr.
R.R. Gantt • E. Gantt (✉)
Department of Cell Biology and Molecular Genetics,
University of Maryland, College Park, MD 20742, USA
e-mail: EGantt@umd.edu

T.J. Bach and M. Rohmer (eds.), *Isoprenoid Synthesis in Plants and Microorganisms: New Concepts and Experimental Approaches*, DOI 10.1007/978-1-4614-4063-5_4,

Abbreviations

CMK	4-diphosphocytidyl methylerythritol kinase
CMS	4-diphosphocytidyl methylerythritol synthase
DMAPP	Dimethylallyl diphosphate
DMAOH	3-methyl-2-buten-1-ol
DTT	Dithiothreitol
DXR	Deoxyxylulose 5-phosphate reductoisomerase
DXS	Deoxyxylulose 5-phosphate synthase
FOH	Farnesol
FPP	Farnesyl diphosphate
FPS	Farnesyl diphosphate synthase
FR6P	Fructose 6-phosphate
G3P	Glyceraldehyde 3-phosphate
GGOH	Geranylgeraniol
GGPP	Geranylgeranyl diphosphate
GGPS	Geranylgeranyl diphosphate synthase
GOH	Geraniol
GPP	Geranyl diphosphate
HDS	Hydroxymethylbutenyl 4-diphosphate synthase
IDI	Isopentenyl diphosphate isomerase
IPP	Isopentenyl diphosphate
IDS	IPP/DMAPP synthase
MCS	Methylerythritol 2,4-cyclodiphosphate synthase
MEP	2-*C*-methyl-D-erythritol 4-phosphate
PPC	Pentose phosphate cycle

4.1 Introduction

Isoprenoids constitute a diverse class of natural compounds found in all organisms. In plant chloroplasts, in cyanobacteria, and in many eubacteria, isoprenoids are synthesized via the 2-*C*-methyl-D-erythritol 4-phosphate (MEP) pathway (cf. Rohmer 1999; Eisenreich et al. 2004; Bouvier et al. 2005). In cyanobacteria and plastids, which have only the MEP pathway, isoprenoids such as carotenoids are required for assembly and functioning of photosynthetic reaction centers (Cunningham and Gantt 1998; Masamoto et al. 2004; Pogson et al. 2005), as well as for electron transport and membrane structural stability (Lichtenthaler 1999). The MEP pathway that resides in a reduced plastid in the malarial blood parasite *Plasmodium falciparum* has been found to be essential for survival of the organism and has therefore been targeted as a site for antimalarial control (Jomaa et al. 1999; Röhrich et al. 2005). Although quite varied in their functions and structures, all isoprenoids are derived from one or a combination of two five-carbon compounds (C_5), isopentenyl diphosphate (IPP) and dimethylallyl diphosphate (DMAPP). Chain elongation generally occurs through a head to tail condensation of IPP with DMAPP or longer allylic diphosphates, as is the case for C_{10}, C_{15}, and C_{20} production, the formation of which is catalyzed by various prenyltransferase enzymes (Wang and Ohnuma 2000; Bouvier et al. 2005).

Much of the MEP pathway has been elucidated using the bacterium *Escherichia coli* as a model organism. The pathway in *E. coli* has come to be viewed as a linear sequence of reactions (Fig. 4.1), as is also assumed for the MEP pathway in plant plastids (Rodríguez-Concepción and Boronat 2002). The pathway begins with the condensation of pyruvate and glyceraldehyde 3-phosphate (G3P) to form 1-deoxy-D-xylulose 5-phosphate (DXP), a reaction catalyzed by deoxyxylulose-5-phosphate synthase (DXS). Six additional enzymes catalyze a stepwise series of reactions, with the enzyme IDS (IPP/DMAPP synthase) catalyzing a terminal step that leads to both IPP and DMAPP. With a single, largely unbranched pathway comprised of soluble enzymes and pathway intermediates, it is reasonable to consider that some form of metabolic channeling, facilitated perhaps by a multienzyme complex, might be necessary to ensure an adequate efficiency of the MEP pathway. Although there are a few reports indicative of specific enzyme interactions (Gabrielsen et al. 2004; Okada and Hase 2005), the concept of a metabolon of MEP pathway enzymes has received little attention in published work to date.

Synechocystis strain PCC 6803 is a photosynthetic cyanobacterium that possesses homologs of all of the genes of the MEP pathway (Kaneko et al. 1996). Previous work from our laboratory has yielded results contrary to the canonical concept

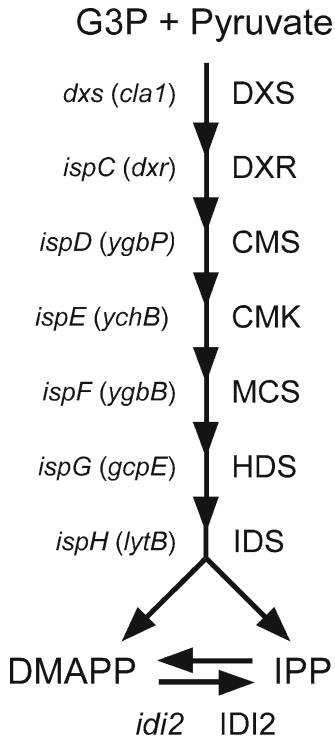

Fig. 4.1 The MEP isoprenoid pathway is illustrated schematically with the names of the enzymes catalyzing each step indicated at *right* and the genes encoding these enzymes listed at *left* (with some alternative gene designations given in *parentheses*). Enzyme abbreviations: *DXS*, deoxyxylulose 5-phosphate synthase*; DXR*, deoxyxylulose 5-phosphate reductoisomerase*; CMS*, 4-diphosphocytidyl methylerythritol synthase*; CMK*, 4-diphosphocytidyl methylerythritol kinase*; MCS*, methylerythritol 2,4-cyclodiphosphate synthase*; HDS*, hydroxymethylbutenyl 4-diphosphate synthase; *IDS*, IPP/DMAPP synthase*; IDI2*, type II isopentenyl diphosphate isomerase. Other abbreviations: *DMAPP*, dimethylallyl diphosphate*; G3P*, glyceraldehyde 3-phosphate*; IPP*, isopentenyl diphosphate

of a simple linear pathway leading to IPP and DMAPP. For example, fosmidomycin (1 mM), a potent inhibitor of DXR, the second enzyme of the MEP pathway, had no effect on the viability or growth rate of *Synechocystis* cells grown photoautotrophically, and it did not affect isoprenoid synthesis *in vitro* (Ershov et al. 2002). Also, additions of pathway substrates and intermediates such as pyruvate and DXP did not yield any stimulation of isoprenoid synthesis *in vitro* (Ershov et al. 2002). In contrast, phosphorylated photosynthetic metabolites of the pentose phosphate cycle (PPC) greatly stimulated isoprenoid biosynthesis in extracts of *Synechocystis in vitro* (Ershov et al. 2002; Poliquin et al. 2004), a phenomenon difficult to reconcile with a simple linear MEP pathway. Earlier results had led us to hypothesize that the PPC stimulation might occur via the MEP pathway (Ershov et al. 2002), with these compounds somehow feeding into the pathway after DXR (Poliquin et al. 2004) because fosmidomycin otherwise would have been expected to inhibit PPC-stimulated isoprenoid synthesis. In fact, the isolated DXR from *Synechocystis* is subject to inhibition by fosmidomycin and its analogs as was recently demonstrated by Woo et al. (2006).

In an effort to better understand isoprenoid biosynthesis in *Synechocystis*, we examined the interaction of MEP pathway enzymes using a bacterial two-hybrid genetic interaction assay system. To determine if the PPC compounds feed into the MEP pathway, we depleted the terminal MEP pathway enzyme, IDS (also known as LytB), from the *in vitro* system, and furthermore followed the progressive elongation of isoprenoids formed with stimulation by PPC compounds. It is concluded that stimulation of isoprenoid synthesis by PPC compounds is indirect and not via the MEP pathway.

4.2 Materials and Methods

4.2.1 Cell Culture and Fractionation

Synechocystis strain PCC 6803 (obtained from Wim Vermaas, Arizona State University) was grown in BG11 medium (Rippka et al. 1979) under continuous light (20–25 μE m^{-2} s^{-1}) with gentle shaking and slow bubbling of 5% CO_2 in air at 30°C. Concentrated aliquots of cells that had been harvested in the log phase of growth and stored at −80°C were thawed on ice; diluted with 100 mM HEPES/KOH (pH 7.7), 1 mM dithiothreitol (DTT); and broken (4 × 30 s with intermittent cooling) using a Mini-Beadbeater (Biospec Products Inc., Bartlesville, Okla.). The breakate was diluted with additional buffer, and after 1 h centrifugation (60,000 × g) at 4°C, the supernatant fluid (3–5 mg protein/mL) was collected for

immediate use. All chemicals were from Sigma Chemical Co. unless otherwise noted.

4.2.2 Incorporation of Radiolabeled IPP

[^{14}C]IPP incorporation into compounds extractable with petroleum ether after acid hydrolysis (i.e., allylic diphosphates) was used as an indirect assay of DMAPP synthesis in cell-free extracts of *Synechocystis* PCC 6803 (as in Poliquin et al. 2004). The reaction mixture contained supernatant fluid from broken cells (1.25–1.8 mg protein/mL final concentration) with 100 mM HEPES/KOH (pH 7.7), 1 mM DTT, 5 mM $MgCl_2$, 2.5 mM $MnCl_2$, 5 mM glutathione, 1 mM FAD, 1 mM NADPH, 500 μM NADP, 500 μM ATP, 250 μM CTP, 100 μM thiamine-PP, and 10 μM coenzyme B_{12}. Each reaction, in a final volume of 1 mL, was preincubated with 3 μM IPP for 20 min at 37 °C in order to deplete any endogenous DMAPP. Following this preincubation, 8.5 μM [1-^{14}C]IPP (American Radiolabeled Chemicals Inc., 8.25×10^5 dpm/mL) was added together with 500 μM fructose 6-phosphate (FR6P) when indicated. Aliquots of 0.2 mL were removed at various times after addition of [^{14}C]IPP. The incorporation of [^{14}C]IPP into the allylic isoprenoid fraction was measured after acid hydrolysis (0.5 N HCl, 20 min, 37°C) and extraction into petroleum ether (boiling point, 35–60°C).

Reverse-phase column chromatography was used to analyze the petroleum ether fraction. An aliquot of 0.8 mL of a 3 mL petroleum ether extract was applied to a column (Pharmacia, 1.8×26 cm) of silica gel 60, RP-18 (EM Industries), pre-equilibrated and eluted with either 100% acetonitrile or acetonitrile:H_2O, 4:1, at a flow rate of 7.8 mL/h. Fractions of 1.3 mL were collected and counted in 10 mL of ScintiSafe Econo 2 cocktail (Fisher Scientific). The column was calibrated using the following standards: dimethylallyl alcohol (C_5), geraniol (C_{10}), farnesol (C_{15}), and geranylgeraniol (C_{20}). Elution profiles of the standard compounds were monitored by the absorbance at 196 nm. Alternatively, thin layer chromatography was used after concentrating the petroleum ether extracts by partial evaporation under a stream of nitrogen gas, with samples spotted onto silica gel RP-18 glass plates (5×20 cm; EM Industries). Standards, as above, were spotted onto the same plate, and the plates were developed with acetonitrile:H_2O, 25:2. The adsorbent was scraped from sections of the plate and analyzed for radioactivity, the location of which was compared to positions of the standards, as ascertained by staining with iodine vapor.

4.2.3 Tandem Affinity Tagging of LytB

The *slr0348* gene (also known as *lytB* or *ispH*) encoding IPP/DMAPP synthase (IDS) in *Synechocystis* PCC 6803 was modified so as to produce a polypeptide with an epitope tag appended to the C terminus. Plasmid pBS1539 (Rigaut et al. 1999), containing the *t*andem *a*ffinity *p*urification (TAP) tag, was modified so as to replace the *URA3* selectable marker with a kanamycin resistance gene excised from plasmid pBR329K (Chamovitz et al. 1990), with the resulting plasmid referred to as p1539Kan. Construction of the tagged gene was achieved by overlapping PCR, essentially as in Murphy et al. (2000), using the primers listed in Table 4.1 together with a high-fidelity DNA polymerase (HF-2 from BD Biosciences Clontech) and genomic DNA prepared from *Synechocystis* as previously described (Williams 1988). A PCR product of the expected size (3.1 kB) was precipitated with ethanol to concentrate and sterilize it and then used to transform *Synechocystis* as earlier described (Williams 1988). Gene replacement by homologous recombination (Fig. 4.2) was confirmed by PCR using the "outer" primer pair (6803lytBNdn and 6803lytBCup).

4.2.4 LytB Immunodepletion

The LytB protein is readily soluble and hence present in the supernatant fluid obtained after pelleting of broken cells of *Synechocystis*. Detection of TAP-tagged LytB in *Synechocystis* extracts was according to a previously published

Table 4.1 Oligonucleotide primers for epitope tagging of LytB and cloning of *Synechocystis* PCC 6803 isoprenoid pathway genes

Oligonucleotide	Sequence[a]
For tagging LytB:	
TAP-KanN	tccatggaaaagagaagatggaa
Tap-KanC	agcgtaatgctctgccagtgtta
6803lytBNdn	GGAAATGCAGCTACTCAACGAC
6803lytBNup	ttccatcttctcttttccatggaTCCCGCAATTTCTAGGACGGGTT
6803lytBCdn	taacactggcagagcattacgctaGGCCTGGCTGTTGAGCATGAG
6803lytBCup	CGCTCTTAAACATCGCCATAAC
For cloning in the two-hybrid bait plasmid:	
6803dxsNBgl	cacagatct**ATG**CACATCAGCGAACTGAC
6803dxsC	TTAAAACCACTATGCCCCTCGAC
6803dxrNXho	gagagagactcgagcACGGCGGTA**ATG**GTGAAAC
6803dxrCHind	gagagagaagcttGACATAGAGCAATGGGTGATCC
6803ygbPNXho	gagagagactcgagTTTACTAATTCCAGCGGCGGGTTC
6803ygbPCHind	gagagagaagCTTGGATTGCTAGGCTCAAAGTC
6803ychBNBgl	cacaagatct**ATG**CATTCCTACACCCTCCA
6803ychBC	GCTGATGTAGGGGGAATTTCTG
6803ygbBNXho	gagagactcgagT**ATG**ACTGCTCTACGCATCG
6803ygbBCHind	gagagaaagCTTTACCAGTGGCATGGATAGGAC
6803gcpENXho	gagagagactcgagcCCC**ATG**GTAACCGCTTC
6803gcpEC	TTCCTTTGCTCCTGAAAACCAC
6803yfgBNXho	gagagagactcgagTATCGCC**ATG**GCCCCTTC
6803yfgBCHind	gagagaggaagcttCTCACTAAAAATCGGCCAAGC
6803sll1556NBam	gagaggatcc**ATG**GATAGCACCCCCCACCGTAAG
6803sll1556C	TCGTCAACCAGAGCAAAATGTC
6803ggpsNXho	gagagagactcgagcGTTGCCCAACAAACACGAAC
6803ggpsC	TTCCCAGCATGGTGAGTAGTGAG

[a]Underlined bases for primers 6803lytBNup and 6803lytBCdn introduce overhangs complementary to the product of the PCR reaction produced using the primers TAP-KanN and TAP-KanC. Residues in capital letters are complementary to *Synechocystis* genomic DNA. Underlined residues for the cloning primers indicate an introduced restriction site. Initiation codons are in boldface type.

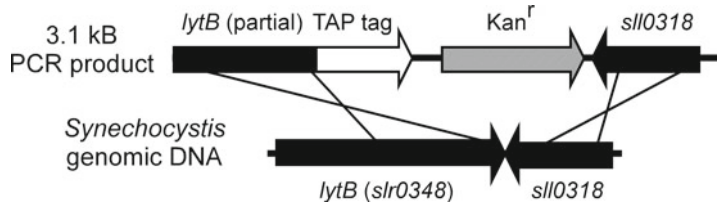

Fig. 4.2 Epitope tagging of the *lytB* gene (*ispH*) encoding the IPP/DMAPP synthase (*IDS*) of *Synechocystis* PCC 6803. The open reading frame of the *lytB* gene (*slr0348*) was fused, in frame, to the TAP tag of Rigaut et al. (1999), followed by a kanamycin resistance gene (Kan^r) and then a genomic DNA fragment that lies immediately downstream of *lytB* in the genome of *Synechocystis*. This construct was used to replace the *lytB* in the genome of *Synechocystis* by homologous recombination, with selection and segregation carried out on solid media containing kanamycin (see "Methods")

method (Walke et al. 2001). Depletion of TAP-tagged LytB from the *Synechocystis* supernatant fluid was accomplished essentially as described by Rigaut et al. (1999), with incubation with IgG Sepharose™ 6 Fast Flow resin (Amersham Pharmacia Biotech AB) for 2 h at 4°C in 100 mM HEPES/KOH (pH 7.7). The presence or absence of TAP-tagged LytB was verified by electrophoresis of samples on an SDS gel, transfer to an Immobilon membrane (Millipore) (according to Peluso and Rosenberg 1987), reaction with peroxidase anti-peroxidase (PAP, Sigma), detection with SuperSignal West Pico Chemiluminescent Substrate (Pierce Biotechnology Co.), and exposure to film (X-OMAT LS, Kodak).

4.2.5 Analysis of MEP Pathway Enzyme Interactions

A bacterial two-hybrid assay (BacterioMatch Two-Hybrid System, Stratagene Cloning Systems) was used, according to the manufacturer's instructions, to analyze interactions of *Synechocystis* MEP pathway enzymes. Genes encoding enzymes of the pathway were amplified by high-fidelity PCR (using the primers listed in Table 4.1) with the introduction of an *Xho* I, *Bgl* II, or *BamH* I site at the N terminus for cloning in the "bait" vector (pBT). The previously cloned *lytB* gene (*ispH*, *slr0348*) was excised from plasmid p6803lytB-TrcA (Cunningham et al. 2000) with *Hind* III and *Sma* I, cloned in the *Hind* III and *Xmn* I sites of pTrcHis A (Invitrogen), and then excised from this plasmid with *Xho* I and *Ssp* I for cloning in pBT. Reading frames of the cloned PCR products were verified by sequencing. Cloned PCR products included the complete open reading frame for each enzyme except that the first codon of *ggps* (*slr0739*), the first two codons of *ygbP* (*ispD*, *slr0951*), and the first four codons of *lytB* (*ispH*, *slr0348*) were lacking. Inserts were moved from the bait to the "target" vector (pTRG), with retention of the appropriate reading frame, by using the *Not* I site present in the multiple cloning sites of each vector. Transformants containing bait and target plasmids expressing *Synechocystis* isoprenoid pathway genes were spotted on Luria-Bertani agar plates containing the requisite antibiotics for maintenance of the bait plasmid, target plasmid, and reporter gene construct, together with either carbenicillin (at concentrations ranging from 250 to 1,000 μg/mL) or 5-bromo-4-chloro-3-indolyl-*beta*-D-galactopyranoside (X-gal, at 80 mg/L) and phenylethyl *beta*-D-thiogalactoside (200 μM). Growth on plates containing carbenicillin (enabled by transcription of a reporter gene encoding for ampicillin/carbenicillin resistance) was taken as presumptive evidence of a protein-protein interaction. Appearance of a blue color for colonies on plates containing X-gal (as a result of transcription of a "secondary" reporter gene encoding *beta*-galactosidase) provided validation for the interactions and a visual indication of their strength.

Presumptive interactions for MEP pathway enzymes of *E. coli*, *Synechocystis* PCC 6803, and other organisms were found by searching the Database of Interacting Proteins (http://dip.doe-mbi.ucla.edu/dip/; Salwinski et al. 2004) and IntAct (http://www.ebi.ac.uk/intact/site/index.jsf; Kerrien et al. 2007).

4.3 Results and Discussion

4.3.1 Interactions of MEP Pathway Enzymes of *Synechocystis*

For the most efficient production of IPP and DMAPP via a linear pathway comprised of numerous soluble enzymes and intermediates, it is reasonable to consider that a transient or stable assembly of some or all of the various enzymes might be necessary to provide for an adequate flux. There is abundant and increasing evidence for enzyme complexes and metabolic channeling for many pathways in a variety of organisms including photosynthetic ones (Winkel 2004; Jørgensen et al. 2005). We undertook a systematic analysis of interactions between and among the seven enzymes of the MEP pathway and some other gene products with known or suggested roles in isoprenoid biosynthesis in the cyanobacterium *Synechocystis* PCC 6803. A bacterial

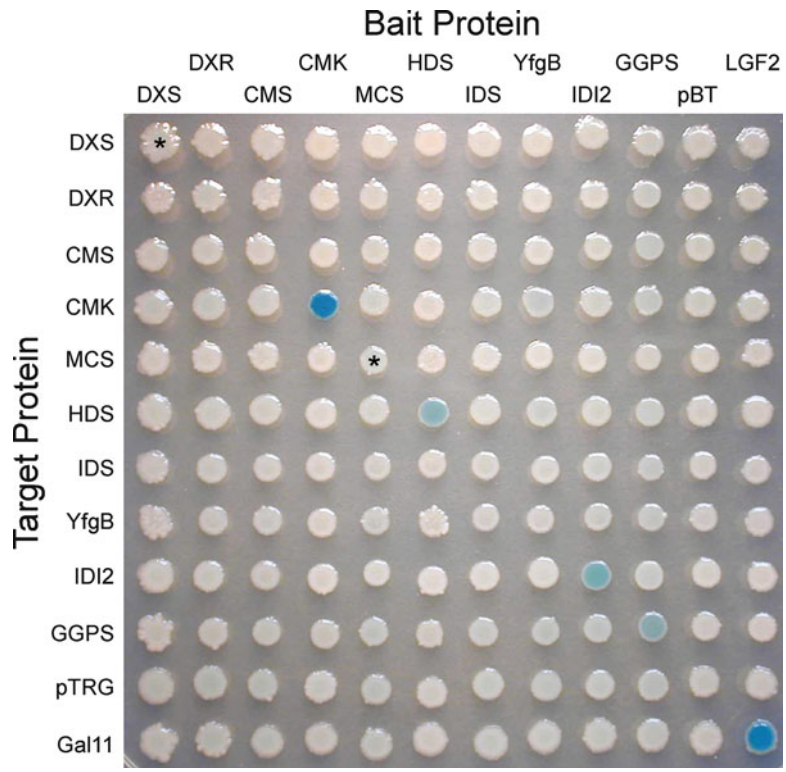

Fig. 4.3 Analysis of interactions of isoprenoid pathway enzymes of *Synechocystis* PCC 6803. A *blue color* for an *E. coli* colony on the agar plate is indicative of an interaction between proteins encoded by genes cloned in the target (indicated at *left*) and bait (indicated *above*) plasmids within its cells. *Asterisks mark colonies with a pale blue color* that was reproducibly darker than those of negative controls. The interaction of LGF2 and Gal11A (*lower right colony*) provided a positive control. The empty bait and target vectors (pBT and pTRG) served as negative controls. Enzyme abbreviations (with *Synechocystis* gene designations in *parentheses*): *DXS*, deoxyxylulose 5-phosphate synthase (*sll1945*); *DXR*, deoxyxylulose 5-phosphate reductoisomerase (*sll0019*); *CMS*, 4-diphosphocytidyl methylerythritol synthase (*slr0951*); *CMK*, 4-diphosphocytidyl methylerythritol kinase (*sll0711*); *MCS*, methylerythritol 2,4-cyclodiphosphate synthase (*slr1542*); *HDS*, hydroxymethylbutenyl 4-diphosphate synthase (*slr2136*); *IDS*, IPP/DMAPP synthase (*slr0348*); *YfgB*, product of the *yfgB* gene (*sll0098*), an iron-sulfur protein suggested to be an activator of HDS; *IDI2*, type II isopentenyl diphosphate isomerase (*sll1556*); *GGPS*, geranylgeranyl diphosphate synthase (*slr0739*)

two-hybrid assay system, recently used to good effect by others (Lahiri et al. 2005; Slepenkin et al. 2005), was employed for this purpose. As can be seen in Fig. 4.3, quite strong self-interactions were observed for two of the MEP pathway enzymes (CMK and HDS) and for two other gene products with roles in isoprenoid biosynthesis in *Synechocystis* (IDI2 and GGPS). Weaker self-interactions were found for two other MEP pathway enzymes (DXS and MCS).

The self-interactions found for certain of the *Synechocystis* MEP pathway enzymes were not unexpected. Except for HDS (the purified *E. coli* HDS was found to be a monomer in solution; Zepeck et al. 2005), all enzymes of the MEP pathway in *E. coli* have been reported to form homodimers (DXS, Xiang et al. 2007; DXR, Reuter et al. 2002; CMS, Richard et al. 2001; CMK, Miallau et al. 2003; IDS, Wolff et al. 2003; Seemann et al. 2009) or homotrimers (MCS; Steinbacher et al. 2002). The IDI2 of *Synechocystis* has been found to form homotetramers (Barkley et al. 2004), and prenyltransferases such as GGPS are known to form dimers (see Wang and Ohnuma 2000). In addition, two-hybrid studies of gene products of *Synechocystis* PCC 6803 (Sato et al. 2007)

and *Campylobacter jejuni* (Parrish et al. 2007) have shown DXS self-interactions, and pull-down assays of *E. coli* gene products have revealed self-interactions of DXS, CMK, MCS, HDS, YfgB, and IDS (Butland et al. 2005).

We found no evidence to indicate protein-protein interactions between any two different enzymes of the MEP pathway in *Synechocystis*. This observation contrasts with a recent study that reported an association of the *E. coli* CMS with CMK and CMK with MCS (Gabrielsen et al. 2004), albeit *in vitro* and with high concentrations of the purified enzymes. This same study also found associations of the *Campylobacter jejuni* and *Agrobacterium tumefaciens* CMS/MCS enzymes (a single polypeptide provides both enzyme activities in these bacteria as a result of a gene fusion) with their respective CMK enzymes. However, despite such interactions, Lherbet et al. (2006) were unable to find any evidence of metabolic channeling for the sequential reactions catalyzed by CMS, CMK, and MCS in *Agrobacterium tumefaciens*.

Global two-hybrid and/or "pull-down" assays have been conducted for polypeptides of several organisms that employ the MEP pathway for isoprenoid biosynthesis (Butland et al. 2005; Arifuzzaman et al. 2006; Parrish et al. 2007; Sato et al. 2007). A number of putative associations were found for MEP pathway enzymes, but very few involved interactions between two different MEP pathway enzymes or between an MEP pathway enzyme and a polypeptide with a function of any obvious relevance to isoprenoid biosynthesis. Among those interactions that appear meaningful, the HDS enzyme of *Thermosynechococcus elongatus* BP-1 has been shown to interact with ferredoxin (*petF1* gene; Okada and Hase 2005), and a pull-down assay of *E. coli* gene products showed an interaction of HDS with flavodoxin (Butland et al. 2005). Another *E. coli* pull-down study (Arifuzzaman et al. 2006) showed DXR to interact with undecaprenyl pyrophosphate synthase (encoded by the *uppS* gene), and the *E. coli* DXS was found to interact with the *aceE* gene product (a polypeptide of the pyruvate dehydrogenase complex) on the basis of a pull-down assay (Butland et al. 2005).

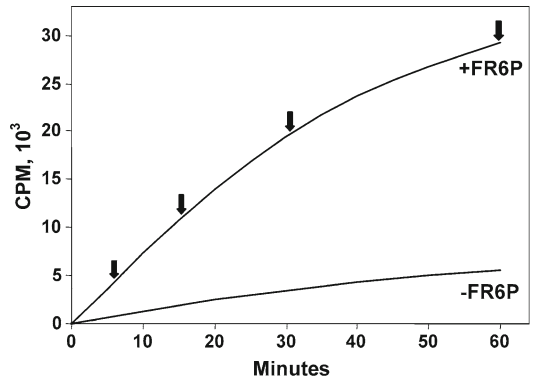

Fig. 4.4 Incorporation of [^{14}C]IPP into allylic isoprenoids in a cell-free extract of *Synechocystis* with (+FR6P) versus without (-FR6P) the addition of fructose 6-phosphate. *Arrows* indicate times when samples were taken for analysis

4.3.2 FR6P Stimulation of Isoprenoid Biosynthesis In Vitro

In our previous studies using cell-free extracts of *Synechocystis*, we found that the incorporation of [^{14}C]IPP into allylic isoprenoids was greatly enhanced by the addition of various phosphorylated pentose phosphate cycle (PPC) compounds but not by non-phosphorylated compounds, with glucose 6-phosphate and fructose 6-phosphate (FR6P) giving the highest stimulation (Ershov et al. 2002). In order to identify the progression of isoprenoids synthesized as a result of PPC stimulation, [^{14}C]IPP incorporation was performed in the presence of FR6P, and the radioactive products present in petroleum ether extracts of acid-hydrolyzed reaction mixtures were analyzed after 5, 15, 30, and 60 min of incubation (arrows, Fig. 4.4) by reverse-phase C_{18} column chromatography.

Figure 4.5 shows typical elution profiles for samples taken after incubation with [^{14}C]IPP for 5 min and 60 min. DMAOH (3-methyl-2-buten-1-ol), the C_5 alcohol of DMAPP, was the major product detected at the earliest time point (fractions 24 and 30). The first peak corresponded with the co-elution of a DMAOH standard (non-acid-hydrolyzed). The second peak, here referred to as DMAOH*, routinely appeared upon acid hydrolysis of DMAPP or of [^{3}H]DMAPP.

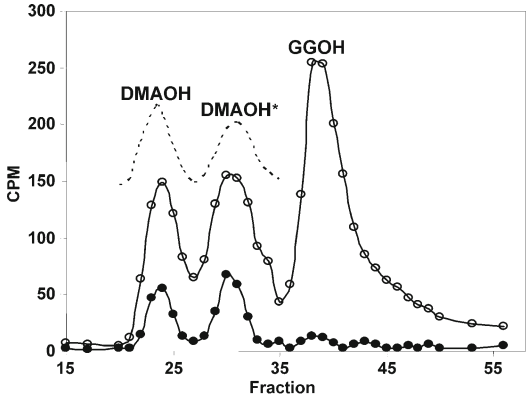

Fig. 4.5 Elution profile for the [^{14}C]-allylic isoprenoid fraction obtained after [^{14}C]IPP incorporation in a cell-free extract of *Synechocystis* with F6P added (as in Fig. 4.4). The allylic isoprenoids were separated on a reverse-phase silica gel column with samples taken 5 min (●) and 60 min (○) after the addition of [^{14}C]IPP. The elution profiles indicate an increase in isoprenoid chain length over time. Superimposed is an elution profile for products obtained after acid hydrolysis of [^{3}H]DMAOH (·····). The column was eluted with 100% acetonitrile

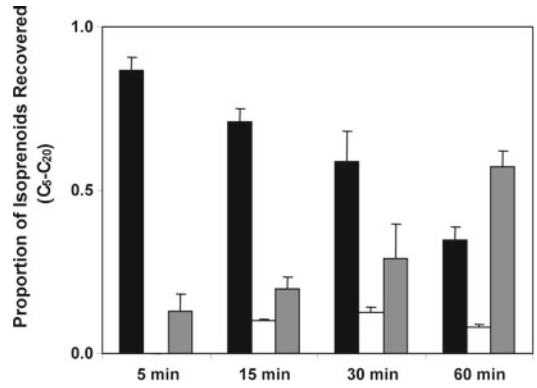

Fig. 4.6 Incorporation of [^{14}C]IPP into longer-chain isoprenoids over time, with F6P addition and incubation conditions as in Fig. 4.5. C_5 (*black*), C_{10} (*white*), and C_{20} (*gray*) isoprenoids are indicated

In attempts to identify DMAOH*, we compared its retention time with 2-methyl-3-buten-2-ol, reported by others to be a product of DMAPP acid hydrolysis (Fisher et al. 2001). In our system, however, the elution time for 2-methyl-3-buten-2-ol did not correspond with that of DMAOH*. We combined the counts of radioactivity in the peaks corresponding to DMAOH and DMAOH* and consider this combination to represent the DMAPP formed from [^{14}C]IPP in the cell-free reaction mixture (Fig. 4.5). The amount of DMAOH produced was likely much greater than what was actually observed since DMAOH is highly volatile and the loss of this compound could not be well controlled during column fractionation and TLC separation.

After 60 min of incubation, the predominant radioactivity was found in fractions 38–39, with elution time corresponding to the C_{20} isoprenoid alcohol geranylgeraniol (GGOH). Similar elution profiles were obtained using PPC compounds other than FR6P, including glucose 6-phosphate, ribulose 5-phosphate, and erythrose 4-phosphate (data not shown). In reaction mixtures that lacked PPC compounds, the recoverable radioactivity was too low for reliable analysis (Fig. 4.4). It should be noted that with PPC stimulation, as much as 50% of the radiolabel was in the C_5-C_{20} fractions by 60 min.

To ascertain if intermediate-size isoprenoids (C_{10}, C_{15}) were being produced, a weaker mobile phase of acetonitrile:H_2O (4:1) was used to elute the reverse-phase column. The increased resolution revealed a small peak that corresponded with the C_{10} geraniol (GOH, data not shown), but no label was observed in fractions coinciding with the C_{15} compound farnesol. The proportion of label in fractions coincident with GOH remained relatively small over the course of 5–60 min. Analysis of the proportion of label in C_5, C_{10}, and C_{20} compounds after a 5-, 15-, 30-, and 60-min incubation with FR6P supports the notion of a progression of synthesis (Fig. 4.6). The proportion of C_5 isoprenoids gradually decreased over time, and the amount of C_{20} isoprenoids steadily increased. While our analysis focused on isoprenoids of up to C_{20} in length, radioactivity was also found in less polar and, presumably, longer unidentified isoprenoid compounds, including carotenoids (C_{40}), which were recovered in a butanol:acetonitrile (1:1) wash of the column after the C_5-C_{20} compounds had been eluted. These less polar compounds were not further analyzed.

It was surprising that we could not reliably detect the C_{15} isoprenoid alcohol farnesol (FOH)

at any point in the time course because it is generally assumed that FOH is within the C_5 linear progression to longer-chained isoprenoids. This observation suggests that the C_{20} isoprenoid GGPP might be synthesized by a direct fusion of two C_{10} units rather than by the sequential addition of C5 units. In seeking further verification by thin layer chromatography, only a trace of radioactivity was found to co-migrate with the C_{15} FOH standard (not shown). The increase of GGOH labeling over time is congruent with prenyltransferase activity leading primarily to C_{20} compounds. Considering C_{20} compounds serving as substrates for the synthesis of phytol, carotenoids, and plastoquinone in photosynthetic organisms (for review, see Rohmer 1999; Bouvier et al. 2005), it is not surprising that the preponderance of the label would accumulate in this compound in the first 60 min. Interestingly, in examining the genome of *Synechocystis* (Kaneko et al. 1996), no homologs to C_{10} or C_{15} prenyltransferases have been identified, whereas two genes were predicted to encode GGPP synthases (*slr0611* and *slr0739*). The product of one of these two (*slr0611*) was later shown to have activity as a nonaprenyl diphosphate (C_{45}) synthase (Okada et al. 1997), whereas the product of the other one (*slr0739*) does indeed function as a GGPP synthase (Ershov Y, Cunningham FX Jr, Gantt E, unpublished; enzymatic activity was confirmed by functional complementation in *Escherichia coli*, as described in Cunningham and Gantt 2007).

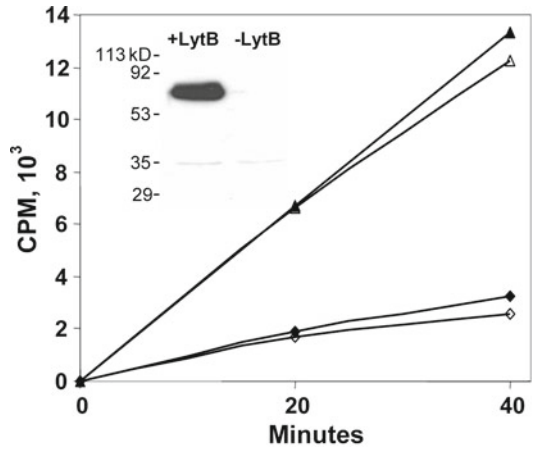

Fig. 4.7 Incorporation of [^{14}C]IPP into allylic isoprenoids in cell-free extracts of *Synechocystis*. The extract was depleted of LytB (Δ and ◊) or not (▲ and ♦), and was supplemented with F6P (Δ and ▲) or not (◊ and ♦). *Inset*: Immunoblot of cell-free extracts of *Synechocystis* with TAP-tagged LytB before (+) and after (−) immunodepletion. With the TAP tag appended, the predicted molecular weight for LytB is 66,188 Da

4.3.3 LytB Is Not Required for FR6P-Stimulated Isoprenoid Biosynthesis In Vitro

How exactly does FR6P contribute to the synthesis of isoprenoids in cell-free extracts of *Synechocystis*? Is the MEP pathway involved in this process? To answer these questions, we investigated whether FR6P stimulation of isoprenoid synthesis required the presence of LytB, the terminal enzyme of the MEP pathway.

LytB was first identified by Cunningham et al. (2000) in *Synechocystis* as an essential enzyme involved in the MEP pathway that was later shown to catalyze the conversion of hydroxy-2-methyl-2-butenyl 4-diphosphate into both IPP and DMAPP in a *ca.* 5:1 ratio, respectively (Rohdich et al. 2002). Subsequent studies with purified recombinant LytB demonstrated a requirement for reducing agents for activity, as well as for the reconstitution of a dioxygen-sensitive [4Fe-4S] cluster within the enzyme (Rohdich et al. 2004; Seemann et al. 2009). Notwithstanding the recognized susceptibility to O_2 of the 4Fe-4S cluster of LytB, we considered that in an oxygen-producing photosynthetic cyanobacterium, LytB might remain active in a cell-free supernatant. To determine whether LytB is required for FR6P-stimulated isoprenoid synthesis, we epitope-tagged LytB of *Synechocystis* and examined isoprenoid synthesis in cell-free extracts replete with LytB versus in extracts with LytB depleted.

Epitope-tagged LytB was quite effectively removed from cell-free extracts as ascertained by SDS-PAGE and immunoblotting (Fig. 4.7, inset). Growth of the epitope-tagged LytB mutant was unimpaired (data not shown), indicating that LytB retained enzymatic function *in vivo* despite the C-terminal epitope tag. Regardless of whether the LytB protein was present or absent in cell-free

extracts of *Synechocystis*, FR6P was found to stimulate the incorporation of [^{14}C]IPP into allylic isoprenoids (Fig. 4.7). These results indicate that the MEP pathway is not involved in the FR6P stimulation of isoprenoid synthesis in cell-free extracts of *Synechocystis*.

4.3.4 FR6P Is Not a Substrate for Isoprenoid Biosynthesis In Vitro

The question remains as to how compounds of the PPC affect the synthesis of isoprenoids in cell-free extracts of *Synechocystis*. Do they somehow provide substrates for the synthesis of DMAPP or is their salutary effect on the incorporation of [^{14}C]IPP into isoprenoids mediated less directly? Three radiolabeled compounds were separately added to the *Synechocystis* cell-free extract: [2-^{14}C]- and [6-^{14}C]glucose, [U-^{14}C]glyceraldehyde 3-phosphate, and [U-^{14}C]FR6P. For each of these compounds, after 60 min of incubations under our standard assay conditions, considerable amounts of radioactivity were recovered in the petroleum ether fraction after acid hydrolysis. However, when aliquots of these samples were analyzed by reverse-phase liquid chromatography (as in Fig. 4.5), no significant labeling was found in the fractions corresponding to C_5-C_{20} isoprenoids, nor was radioactivity detected in the less polar, later-eluting isoprenoid fractions. These observations lead us to conclude that the stimulation of [^{14}C]IPP incorporation by FR6P and other PPC compounds is indirect. These compounds do not enter into the MEP pathway, as previously hypothesized (Ershov et al. 2002; Poliquin et al. 2004), nor provide substrates for DMAPP synthesis by some other route. We speculate that the energy derived from metabolism of FR6P and other PPC compounds positively affects downstream reactions of the isoprenoid pathway or activates an otherwise cryptic IPP/DMAPP isomerase activity.

Acknowledgments This study was supported in part by grants from the Department of Energy (DE-FG02-98ER2032) and the National Science Foundation (MCB0316448).

References

Arifuzzaman M, Maeda M, Itoh A et al (2006) Large-scale identification of protein-protein interaction of *Escherichia coli* K-12. Genome Res 16:686–691

Barkley SJ, Desai SB, Poulter CD (2004) Type II isopentenyl diphosphate isomerase from *Synechocystis* sp. strain PCC 6803. J Bacteriol 186:8156–8158

Bouvier F, Rahier A, Camara B (2005) Biogenesis, molecular regulation, and function of plant isoprenoids. Prog Lipid Res 44:357–429

Butland G, Peregrín-Alvarez JM, Li J et al (2005) Interaction network containing conserved and essential protein complexes in *Escherichia coli*. Nature 433:531–537

Chamovitz D, Pecker I, Sandmann G et al (1990) Cloning a gene coding for norflurazon resistance in cyanobacteria. Z Naturforsch C 45:482–486

Cunningham FX Jr, Gantt E (1998) Genes and enzymes of carotenoid biosynthesis in plants. Annu Rev Plant Physiol Plant Mol Biol 49:557–583

Cunningham FX Jr, Gantt E (2007) A portfolio of plasmids for identification and analysis of carotenoid pathway enzymes: *Adonis aestivalis* as a case study. Photosynth Res 92:245–259

Cunningham FX Jr, Lafond TP, Gantt E (2000) Evidence of a role for LytB in the nonmevalonate pathway of isoprenoid biosynthesis. J Bacteriol 182:5814–5848

Eisenreich W, Bacher A, Arigoni D, Rohdich F (2004) Biosynthesis of isoprenoids via the non-mevalonate pathway. Cell Mol Life Sci 61:1401–1426

Ershov YV, Gantt RR, Cunningham FX Jr, Gantt E (2002) Isoprenoid biosynthesis in *Synechocystis* sp. strain PCC6803 is stimulated by compounds of the pentose phosphate cycle but not by pyruvate or deoxyxylulose 5-phosphate. J Bacteriol 184:5045–5051

Fisher AJ, Rosenstiel TN, Shirk MC, Fall R (2001) Nonradioactive assay for cellular dimethylallyl diphosphate. Anal Biochem 292:272–279

Gabrielsen M, Bond CS, Hallyburton I et al (2004) Hexameric assembly of the bifunctional methylerythritol 2,4-cyclodiphosphate synthase and protein-protein associations in the deoxy-xylulose-dependent pathway of isoprenoid precursor biosynthesis. J Biol Chem 279:52753–52761

Jomaa H, Wiesner J, Sanderbrand S et al (1999) Inhibitors of the nonmevalonate pathway of isoprenoid biosynthesis as antimalarial drugs. Science 285:1573–1576

Jørgensen K, Rasmussen AV, Morant M et al (2005) Metabolon formation and metabolic channeling in the biosynthesis of plant natural products. Curr Opin Plant Biol 8:280–291

Kaneko T, Sato S, Kotani H et al (1996) Sequence analysis of the genome of the unicellular cyanobacterium *Synechocystis* sp. strain PCC6803. II. Sequence determination of the entire genome and assignment of potential protein-coding regions. DNA Res 3: 109–136

Kerrien S, Alam-Faruque Y, Aranda B et al (2007) IntAct—open source resource for molecular interaction data. Nucleic Acids Res 35:D561–D565

Lahiri S, Pulakat L, Gavini N (2005) Functional NifD-K fusion protein in *Azotobacter vinelandii* is a homodimeric complex equivalent to the native heterotetrameric MoFe protein. Biochem Biophys Res Commun 337:677–684

Lherbet C, Pojer F, Richard SB et al (2006) Absence of substrate channeling between active sites in the *Agrobacterium tumefaciens* IspDF and IspE enzymes of the methyl erythritol phosphate pathway. Biochemistry 45:3548–3553

Lichtenthaler HK (1999) The 1-deoxy-D-xylulose 5-phosphate pathway of isoprenoid biosynthesis in plants. Annu Rev Plant Physiol Plant Mol Biol 50: 47–65

Masamoto K, Hisatomi S, Sakurai I et al (2004) Requirement of carotene isomerization for the assembly of photosystem II in *Synechocystis* sp. PCC6803. Plant Cell Physiol 45:1325–1329

Miallau L, Alphey MS, Kemp LE et al (2003) Biosynthesis of isoprenoids: crystal structure of 4-diphosphocytidyl-2*C*-methyl-D-erythritol kinase. Proc Natl Acad Sci USA 100:9173–9178

Murphy KC, Campellone KG, Poteete AR (2000) PCR-mediated gene replacement in *Escherichia coli*. Gene 246:321–330

Okada K, Hase T (2005) Cyanobacterial non-mevalonate pathway: (*E*)-4-hydroxy-3-methylbut-2-enyl diphosphate synthase interacts with ferredoxin in *Thermosynechococcus elongatus* BP-1. J Biol Chem 280:20672–20679

Okada K, Minehira M, Zhu X et al (1997) The *ispB* gene encoding octaprenyl diphosphate synthase is essential for growth of *Escherichia coli*. J Bacteriol 179:3058–3060

Parrish JR, Yu J, Liu G et al (2007) A proteome-wide protein interaction map for *Campylobacter jejuni*. Genome Biol 8:R130

Peluso RW, Rosenberg GH (1987) Quantitative electrotransfer of proteins from sodium dodecyl sulfate-polyacrylamide gels onto positively charged nylon membranes. Anal Biochem 162:389–398

Pogson BJ, Rissler HM, Frank HA (2005) The roles of carotenoids in energy quenching. In: Wydryzinski TJ, Satoh K (eds) Photosystem II: the light-driven water:plastoquinone oxidoreductase in photosynthesis. Springer, Dordrecht

Poliquin K, Ershov YV, Cunningham FX Jr et al (2004) Inactivation of *sll1556* in *Synechocystis* strain PCC 6803 impairs isoprenoid biosynthesis from pentose phosphate cycle substrates in vitro. J Bacteriol 186:4685–4693

Reuter K, Sanderbrand S, Jomaa H et al (2002) Crystal structure of 1-deoxy-D-xylulose-5-phosphate reductoisomerase, a crucial enzyme in the non-mevalonate pathway of isoprenoid biosynthesis. J Biol Chem 277:5378–5384

Richard SB, Bowman ME, Kwiatkowski W et al (2001) Structure of 4-diphosphocytidyl-2-*C*-methylerythritol synthetase involved in mevalonate-independent isoprenoid biosynthesis. Nat Struct Biol 8:641–647

Rigaut G, Shevchenko A, Rutz B et al (1999) A generic protein purification method for protein complex characterization and proteome exploration. Nat Biotechnol 17:1030–1032

Rippka R, Deruelles J, Waterbury JB et al (1979) Generic assignments, strains histories and properties of pure cultures of cyanobacteria. J Gen Microbiol 111:1–61

Rodríguez-Concepción M, Boronat A (2002) Elucidation of the methylerythritol phosphate pathway for isoprenoid biosynthesis in bacteria and plastids. A metabolic milestone achieved through genomics. Plant Physiol 130:1079–1089

Rohdich F, Hecht S, Gärtner K et al (2002) Studies on the nonmevalonate terpene biosynthetic pathway: metabolic role of IspH (LytB) protein. Proc Natl Acad Sci USA 99:1158–1163

Rohdich F, Bacher A, Eisenreich W (2004) Perspectives in anti-infective drug design. The late steps in the biosynthesis of the universal terpenoid precursors, isopentenyl diphosphate and dimethylallyl diphosphate. Bioorg Chem 32:292–308

Rohmer M (1999) The discovery of a mevalonate-independent pathway for isoprenoid biosynthesis in bacteria, algae and higher plants. Nat Prod Rep 16: 565–574

Röhrich RC, Englert N, Troschke K et al (2005) Reconstitution of an apicoplast localised electron transfer pathway involved in the isoprenoid biosynthesis of *Plasmodium falciparum*. FEBS Lett 579: 6433–6438

Salwinski L, Miller CS, Smith AJ et al (2004) The database of interacting proteins: 2004 update. Nucleic Acids Res 32:D449–D451

Sato S, Shimoda Y, Muraki A et al (2007) A large-scale protein-protein interaction analysis in *Synechocystis* sp. PCC6803. DNA Res 14:207–216

Seemann M, Janthawornpong K, Schweizer J et al (2009) Isoprenoid biosynthesis via the MEP pathway: in vivo Mössbauer spectroscopy identifies a $[4Fe\text{-}4S]^{2+}$ center with unusual coordination sphere in the LytB protein. J Am Chem Soc 131:13184–13185

Slepenkin A, de la Maza LM, Peterson EM (2005) Interaction between components of the type III secretion system of *Chlamydiaceae*. J Bacteriol 187: 473–479

Steinbacher S, Kaiser J, Wungsintaweekul J et al (2002) Structure of 2*C*-methyl-D-erythritol-2,4-cyclodiphosphate synthase involved in mevalonate-independent biosynthesis of isoprenoids. J Mol Biol 316:79–88

Walke S, Bragado-Nilsson E, Séraphin B, Nagai K (2001) Stoichiometry of the Sm proteins in yeast spliceosomal snRNPs supports the heptamer ring model of the core domain. J Mol Biol 308:49–58

Wang KC, Ohnuma S (2000) Isoprenyl diphosphate synthases. Biochim Biophys Acta 1529:33–48

Williams JGK (1988) Construction of specific mutations in photosystem II photosynthetic reaction center by

genetic engineering methods in *Synechocystis* 6803. Methods Enzymol 167:766–778

Winkel BSJ (2004) Metabolic channeling in plants. Annu Rev Plant Biol 55:85–107

Wolff M, Seemann M, Tse Sum Bui B et al (2003) Isoprenoid biosynthesis via the methylerythritol phosphate pathway: the (*E*)-4-hydroxy-3-methylbut-2-enyl diphosphate reductase (LytB/IspH) from *Escherichia coli* is a [4Fe-4S] protein. FEBS Lett 541:115–120

Woo Y-H, Fernandes RPM, Proteau PJ (2006) Evaluation of fosmidomycin analogs as inhibitors of the *Synechocystis* sp. PCC6803 1-deoxy-D-xylulose 5-phosphate reductoisomerase. Bioorg Med Chem 14:2375–2385

Xiang S, Usunow G, Lange G et al (2007) Crystal structure of 1-deoxy-D-xylulose 5-phosphate synthase, a crucial enzyme for isoprenoids biosynthesis. J Biol Chem 282:2676–2682

Zepeck F, Gräwert T, Kaiser J et al (2005) Biosynthesis of isoprenoids. Purification and properties of IspG protein from *Escherichia coli*. J Org Chem 70: 9168–9174

Metabolic Engineering of Monoterpenoid Production in Yeast

5

Marc Fischer, Sophie Meyer, Maryline Oswald, Patricia Claudel, and Francis Karst

Abstract

Plants generally produce only small amounts of the desired molecules, which prompted alternative strategies to increase productivity. The most popular organisms for fermentation strategies are *Escherichia coli* and the yeast *Saccharomyces cerevisiae*. Heterologous expression of geraniol synthase (GES) from *Ocimum basilicum* in yeast enabled geraniol production during fermentation. A strong increase in geraniol production was obtained by engineering the yeast FPP synthase to release GPP, which becomes then available in large amounts for monoterpenoid production in yeast. Moreover, GES integration in an industrial wine yeast bearing a wild-type FPPS also allowed a strong geraniol production, showing that additional metabolic features are able to trigger GPP availability.

Keywords

Monoterpenoids • Metabolic engineering • Yeast • Farnesyl diphosphate synthase • Site-directed mutagenesis • Heterologous expression • Geraniol synthase • Terpene synthase

5.1 Introduction

Natural compounds such as terpenoids are generally obtained by extraction from specific plant organs such as roots, flowers, or leaves. However, the natural sources generally produce only small amounts of the desired molecules, which prompted alternative strategies to increase productivity. Due to the multiple chiral centers, the chemical synthesis and/or product purification is generally difficult and economically nonviable. On the other hand, the production of terpenoids in heterologous host plants bears considerable advantages over extraction from low-productive native hosts. For this reason, alternative methods based on genetically modified plants have been developed.

The most basic approach is to increase the desired compound level in the natural host by overexpression of the limiting step of the pathway.

M. Fischer (✉) • S. Meyer • M. Oswald
P. Claudel • F. Karst
UMR SVQV, University of Strasbourg, INRA,
28 rue de Herrlisheim, Colmar 68000, France
e-mail: marc.fischer@colmar.inra.fr

T.J. Bach and M. Rohmer (eds.), *Isoprenoid Synthesis in Plants and Microorganisms: New Concepts and Experimental Approaches*, DOI 10.1007/978-1-4614-4063-5_5,

It was shown, for example, that overexpression of DXR (deoxyxylulose 5-phosphate reductoisomerase) in *Mentha* × *piperita* led to a 50% increase in mint oil production (Mahmoud and Croteau 2001). Plants such as *Nicotiana tabacum* or *Arabidopsis thaliana* for which known genetic tools exist are of special interest. Tobacco was among the first plants, for instance, engineered to produce trichodiene (Hohn and Ohlrogge 1991), amorpha-4,11-diene (Wallaart et al. 2001), or *trans*-isoperitenol (Lücker et al. 2004b). *Arabidopsis thaliana* is not an aromatic plant and was thus believed to have only little capacity for terpenoid production. However, its genomic sequence revealed the presence of about 40 terpene synthase-encoding genes (Aubourg et al. 2002). The overexpression of a maize sesquiterpene synthase in *Arabidopsis thaliana* resulted in a strong emission of sesquiterpenes (Schnee et al. 2006).

Plant cell cultures are also a possible tool for the production of secondary metabolites. Indeed, production levels up to 479 mg/L for shikonin has been achieved (Singh et al. 2010), and efforts for the production of vinblastine in *Catharanthus roseus* cell cultures have been undertaken (Collu et al. 2001; Costa et al. 2008; for literature and further details, see also Courdavault et al. 2012, this volume).

Although techniques of cell biology and genetics for plants are in continuous progress, the production of proteins or metabolites at an industrial level is better achieved in microorganisms.

For heterologous expression, the most popular organism is *E. coli*. Martin et al. (2001) were able to produce plant sesquiterpenes in *E. coli* but at very low level. To improve the level of the precursor farnesyl diphosphate (FPP), it was necessary to introduce in *E. coli* the complete yeast mevalonate pathway, comprising acetoacetyl-CoA thiolase, HMG-CoA synthase, and HMG-CoA reductase on a first operon and mevalonate kinase, phosphomevalonate kinase, and mevalonate diphosphate decarboxylase on a second operon. Additional expression of amorpha-4,11-diene synthase in the engineered host led to a strong increase of amorphadiene production (Martin et al. 2003). Another example is the work of Reiling et al. (2004) who were able to produce in *E. coli* the diterpenes casbene and *ent*-kaurene, as well as the monoterpene δ-3-carene.

The yeast *Saccharomyces cerevisiae* is another microorganism well known for heterologous protein production or for metabolic engineering, which is facilitated by a number of plasmids and promotors available, in addition to the possibility of chromosomal gene integration at nonessential loci. As to the isoprenoid pathway, yeast has, for instance, been engineered to produce hydrocortisone. This was achieved by the consecutive engineering of 13 genes in a single yeast strain. These genes included the animal cDNAs coding for enzymes that are involved in the metabolization of cholesterol into hydrocortisone, the deletion of yeast genes coding for enzymes that catalyze "unwanted reactions," and the expression of *Arabidopsis thaliana* Δ^7-sterol reductase required to produce a compatible sterol substrate. The engineered yeast strain was shown to produce the anti-inflammatory steroid from a single carbon source (Ménard Szczebara et al. 2003).

The feasibility of sesquiterpene production in yeast was evaluated by Jackson et al. (2003), who choose the heterologous expression of *Artemisia annua* epi-cedrol synthase; the best yield was obtained by synergic overexpression of a truncated form of HMG-CoA reductase in the presence of the *upc2-1* mutation conferring sterol uptake (for further details, see Paddon et al., this volume). FPP synthase overexpression did not improve sesquiterpene accumulation.

To achieve a higher level of FPP, the substrate of sesquiterpene synthases, several groups focused on the expression of the *ERG9* gene, encoding squalene synthase. Takahashi et al. (2007) used a yeast strain disrupted for *ERG9* and bearing an *upc2-1* mutation allowing sterol uptake and viability. Ro et al. (2006) and Asadollahi et al. (2008) used a more controlled strategy to enhance the FPP pool. The *ERG9* gene was placed under the control of the inducible *MET13* promoter, which allowed decreasing *ERG9* gene expression to such an extent that ergosterol formation was diminished but not blocked (see Maury et al., this volume). All these strategies permitted to produce several types of

sesquiterpenes in yeast transformed with plant sesquiterpene synthases, and several yeast genes of the isoprenoid pathway were checked to improve production.

5.2 Expression of Plant Monoterpene Synthases in Wild-Type Yeast

The production of monoterpenes has also been assessed through using plant, bacterial, and yeast heterologous expression systems. Plants contain a chloroplastidial GPP pool, and expression of monoterpene synthase genes in tobacco has been shown successful by using various possible combinations: one monoterpene synthase gene (Lewinsohn et al. 2001), several monoterpene synthase genes being co-expressed (Lücker et al. 2004a), or a monoterpene synthase gene being coupled to a P450 gene (Lücker et al. 2004b).

However, expression in *E. coli* results in low-level production; the work done so far has not concentrated on bulk production but rather on function identification for one (Colby et al. 1993) or a family (Martin et al. 2010) of candidate genes.

In this study here we wanted to evaluate yeast as a possible host for the production of aromatic plant monoterpenes. The precursor of all these C10 compounds is geranyl diphosphate (GPP), also considered as a reaction intermediate of farnesyl diphosphate (FPP) synthesis. Generally, only plants have the capacity to produce monoterpenes or the corresponding alcohols. One explanation could be that GPP as the putative intermediate of FPP synthesis would have a strong affinity for FPP synthase, and therefore it might not be released from the active site of the enzyme. In plants, GPP is synthesized via the MEP pathway in chloroplasts, and specific GPP synthase genes have been identified (Burke et al. 1999; Bouvier et al. 2000).

Already several years ago we searched for mutant yeast strains being defective in FPP synthase. These strains were isolated as temperature-sensitive mutants, with the hope of obtaining mutations that affect the affinity of GPP towards the enzyme. Some of the strains presented a specific feature, *viz.*, to excrete geraniol and linalool into the growth medium (Chambon et al. 1990). Genetic analysis indicated that these mutants carried, in addition to the *erg20-1* mutation affecting FPP synthase (Blanchard and Karst 1993), either an *erg12-2* mutation affecting mevalonate kinase or an *erg9-2* mutation affecting squalene synthase and that either one of the two is absolutely necessary for viability. Conversely, strains carrying both *erg12-1* and *erg9-1* mutations with *erg20-1* are viable but do not excrete monoterpenols (Chambon et al. 1991). We assumed that at least one of these leaky mutations was required to diminish the geraniol formation that could be toxic in yeast. Several attempts were thus made to increase the geraniol level in the culture medium: by crossing the original mutant with a wine yeast, some of the offsprings produced about 10 mg/L (geraniol, linalool and citronellol) monoterpenes in pilot-scale grape must fermentations (Javelot et al. 1991).

However, the identification of an enzyme activity being really involved in GPP dephosphorylation was unsuccessful, and we could not distinguish between the possibility that GPP could be present in the yeast cytoplasm where it would be dephosphorylated or that geraniol would be directly released from the catalytic site of FPP synthase.

The isolation of plant monoterpene synthases, limonene synthase (*Mentha spicata;* Colby et al. 1993), *S*-linalool synthase (*Clarkia breweri*; Dudareva et al. 1996), and geraniol synthase (*Ocimum basilicum*; Iijima et al. 2004) allowed to examine the availability of GPP in yeast. The three cDNAs, truncated as such to loosen the putative plastidial target sequence, were expressed in yeast, under the control of the strong *PMA1* promoter (Sauer and Stoltz 1994), without or with a GFP tag at the N-terminus. For the two first cDNAs, no monoterpene production was obtained whatsoever the yeast strain or growth conditions tested. Confocal microscopy revealed that limonene synthase and linalool synthase are present in yeast under the form of aggregated structures that could represent misfolded proteins (Fig. 5.1).

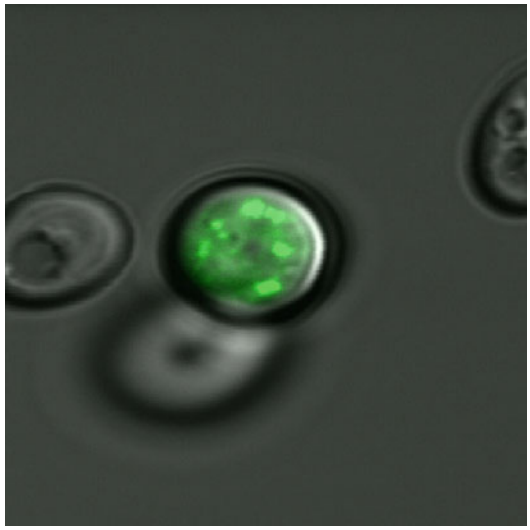

Fig. 5.1 Confocal microscopy of wild-type cells expressing LIS of *Clarkia breweri*. Yeast GFP fusion is at the C-terminal

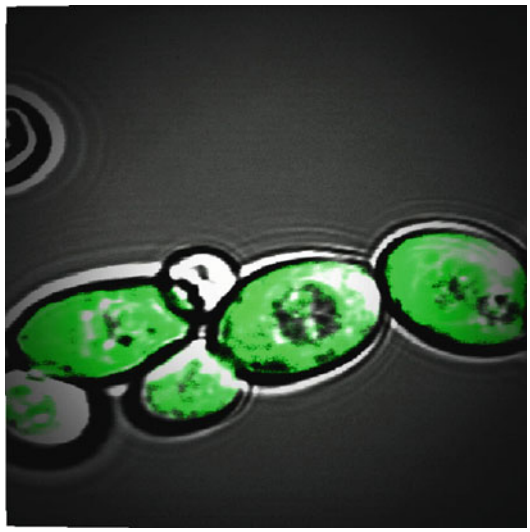

Fig. 5.2 Confocal microscopy of wild-type yeast cells expressing GES of *Ocimum basilicum*. Yeast GFP fusion is at the C-terminal

In contrast, the expression of geraniol synthase (GES) in a wild-type strain (Fig. 5.2) allowed the excretion of about 600 µg/L monoterpenes in minimal YNB medium (Oswald et al. 2007). Since these compounds are volatile, we verified that there is no terpenoid loss during cultivation by trapping the culture medium effluents on a hydrophobic resin. We also verified that cell pellets do not retain a significant amount of monoterpenoids. We later subjected the *ERG20* gene product to a set of amino acid mutations in the catalytic site at position K197 (Fischer et al. 2011). The K197G mutated strains expressing GES were able to produce up to 5 mg/L geraniol, suggesting a major improvement compared to other models.

These results showed clearly that yeast cells contain free GPP in significant amounts being accessible to GES for catalyzing geraniol formation. The lack of monoterpene formation in yeast is therefore very likely related to the lack of corresponding terpene synthase activity.

5.3 Effect of Wild-Type and Mutated *ERG20* Gene on Geraniol Formation

In contrast to plants, the yeast (*S. cerevisiae*) genome does apparently not contain a gene related to GPP synthase. As outlined above, it is reasonable to assume that in yeast GPP is produced by release from the catalytic site of FPP synthase and is a by-product of FPP synthase. Therefore, in order to increase geraniol formation in wild-type yeast, the first approach was the overexpression of FPP synthase. It has been described that overexpression of FPP synthase under the control of its own promoter on a replicative plasmid directs a sixfold increase of FPP synthase specific activity in cell-free extracts. This increase in FPP synthase activity is associated with an increase of 30% and 80% of ergosterol and dolichol levels, respectively. This result suggested that FPP synthase could indeed catalyze a limiting step in the biosynthesis of isoprenoids (Szkopinska et al. 2000).

Overexpression of either wild-type or mutated (*erg20-1*) FPP synthases had no effect on the geraniol level in wild-type yeast carrying GES. In contrast, overexpression of the FPP synthases in a strain deleted for chromosomal FPP synthase gene led to a 1.6- and 2.2-fold increase in the geraniol level. However, the level of about 1 mg/L

Table 5.1 Monoterpenoids produced in growth medium (μg/L)

	YNB medium			Auxerrois must fermentation		
Strain	Linalool	Citronellol	Geraniol	Linalool	Citronellol	Geraniol
Control 5247	ND	ND	ND	NT	NT	NT
5247 [GES]	43	ND	559	NT	NT	NT
CC25	70	5	47	NT	NT	NT
Control 58W3D4	ND	ND	ND	13	27	86
n FL100 ho::GES Kan	24	23	293	NT	NT	NT
2n FL100 ho::GES Kan/ho	30	24	260	NT	NT	NT
n 58W3D4 ho::GES Kan	30	12	254	NT	NT	NT
2n 58W3D4 ho::GES Kan/ ho::GES Kan	NT	NT	NT	680	709	962
Control 58W3D4	ND	ND	ND	13	27	86

ND not detected, *NT* not tested
5247 is a wild-type haploid strain
CC25 is a 5247 derivative, bearing *erg20-1, erg12-2, ura3-1, and trp1-1*
58W3D4 is a wine strain derivative
YNB medium, 200 mL yeasts were cultivated for 72 h at 28° with shaking. Inoculum: 5 × 105 cells/ml
Auxerrois must (20 L) fermentation was done at 20° until total sugar consumption (31 days); inoculum: 10^6 cells/mL

obtained is very close to that obtained with the haploid mutant CC25, bearing the *erg20-1* mutation and GES. These results show that FPP synthase activity is not a really limiting factor for geraniol formation. Instead, one could assume that IPP and/or DMAPP availability would be limiting. It is also thinkable that the activity of geraniol synthase is limiting, and this is in spite of the large amount of protein observed by confocal microscopy.

Further attempts to increase geraniol formation will be done by engineering enzymes upstream in the pathway, such as HMG-CoA reductase.

5.4 Chromosomal Integration of GES in Industrial Yeast

Experiments with plasmids need selection to avoid plasmid loss or variations in copy numbers. In addition, for metabolic engineering, the laboratory strains carry multiple auxotrophies that are quite useful for foreign gene expression or for gene deletions. These auxotrophies, however, limit the growth of the strains and require well-defined growth media.

For these reasons, we decided to construct a wild-type strain carrying a chromosomal integration of GES and without any additional mutation. As a suitable strain, we chose a wine yeast. In fact, wine yeasts are robust since they have to ferment acidic musts (pH 3.2) with a high osmotic pressure (about 200 g/L sugars) and under limiting oxygen supply. These strains usually present a high sterol level but are generally diploid or aneuploid or even hybrids. For this reason, we have attempted the integration of GES by transformation. GES cDNA was cloned under control of the *PMA1* promoter at the HO locus using the integrative vector M4297 provided by Dr. Davis Stillman (University of Utah, USA). Vector M4297 carries HO 5′ and 3′ sequences and a KanMX4 selection marker. We succeeded in the integration of GES into FL100 (our laboratory strain as control) and the 58W3D4 homozygote strain, derived from commercial wine yeast 58W3.

The results presented in Table 5.1 show that in minimal medium (YNB), a single integration gives about half of monoterpene levels compared to replicative plasmids, which strongly suggests that GES activity is limiting in GPP transformation into geraniol. However, the Auxerrois wine obtained with 58WD4, bearing a double GES integration, contained a very high level of terpenoids; the elevated citronellol level found is due to the reducing conditions in wine fermentation.

Additionally, it should be noted that the wine obtained had a strong "floral" taste, which was not the case with the control that contained a monoterpene level under the perception threshold.

5.5 Endogenous Geranyl Diphosphate Phosphatase in Yeast

Wild-type yeasts excrete geraniol only when they express GES. It has been shown that terpene synthases, including GES, catalyze the loss of the pyrophosphate group through a carbocation high-energy intermediate (Iijima et al. 2004). Blast search shows that yeast genomes do not contain similar sequences. However, yeast strains carrying the *erg20-1* mutation in farnesyl diphosphate synthase excrete geraniol, and at high levels this is quite toxic to some of them (Javelot et al. 1991). In addition, it has been reported that mutants defective in squalene synthase excrete farnesol. It is therefore temping to suppose that yeast contains either an isoprenoid diphosphate phosphatase, which means an enzyme activity similar to terpene synthases but with a different primary protein structure. However, it is also noteworthy that allylic isoprenoid diphosphates are unstable at acidic pH (Rittersdorf and Cramer 1967). Hence, it is therefore possible that GPP is transported into the acidic vacuole compartment in which degradation will produce the isomers geraniol and linalool. To this end, it can be observed that *erg20-1* mutants release geraniol and linalool in a ratio of about 3:2. In contrast, for strains expressing GES, this ratio is about 12:1, which is in good agreement with the above hypothesis.

5.6 Conclusion

The main finding of this work is that GPP is not simply an intermediate metabolite of FPP synthesis that remains tightly bound to the active site of the enzyme. Our data indicate the presence of an intracellular pool of free GPP, which opens an avenue towards using yeast as an efficient and flexible engineering tool for the production of monoterpene-derived compounds.

Acknowledgements We thank Dr. J. Mutterer (IBMP-CNRS Strasbourg) for help in confocal microscopy analysis.

References

Asadollahi MA, Maury J, Møller K et al (2008) Production of plant sesquiterpenes in *Saccharomyces cerevisiae*: effect of *ERG9* repression on sesquiterpene biosynthesis. Biotechnol Bioeng 99:666–677

Aubourg S, Lecharny A, Bohlmann J (2002) Genomic analysis of the terpenoid synthase (AtTPS) gene family of *Arabidopsis thaliana*. Mol Genet Genomics 267:730–745

Blanchard L, Karst F (1993) Characterization of a lysine-to-glutamic acid mutation in a conservative sequence of farnesyl diphosphate synthase from *Saccharomyces cerevisiae*. Gene 125:185–189

Bouvier F, Suire C, d'Harlingue A, Backhaus RA, Camara B (2000) Molecular cloning of geranyl diphosphate synthase and compartmentation of monoterpene synthesis in plant cells. Plant J 24:241–252

Burke CC, Wildung MR, Croteau R (1999) Geranyl diphosphate synthase: cloning, expression, and characterization of this prenyltransferase as a heterodimer. Proc Natl Acad Sci USA 96:13062–13067

Chambon C, Ladeveze V, Oulmouden A, Servouse M, Karst F (1990) Isolation and properties of yeast mutants affected in farnesyl diphosphate synthetase. Curr Genet 18:41–46

Chambon C, Ladeveze V, Servouse M et al (1991) Sterol pathway in yeast. Identification and properties of mutant strains defective in mevalonate diphosphate decarboxylase and farnesyl diphosphate synthetase. Lipids 26:633–636

Colby SM, Alonso WR, Katahira EJ, McGarvey DJ, Croteau R (1993) 4*S*-limonene synthase from the oil glands of spearmint (*Mentha spicata*). cDNA isolation, characterization, and bacterial expression of the catalytically active monoterpene cyclase. J Biol Chem 268:23016–23024

Collu G, Unver N, Peltenburg-Looman AM et al (2001) Geraniol 10-hydroxylase, a cytochrome P450 enzyme involved in terpenoid indole alkaloid biosynthesis. FEBS Lett 508:215–220

Costa MM, Hilliou F, Duarte P et al (2008) Molecular cloning and characterization of a vacuolar class III peroxidase involved in the metabolism of anticancer alkaloids in *Catharanthus roseus*. Plant Physiol 146:403–417

Dudareva N, Cseke L, Blanc VM, Pichersky E (1996) Evolution of floral scent in Clarkia: novel patterns of

S-linalool synthase gene expression in the *C. breweri* flower. Plant Cell 8:1137–1148

Fischer MJC, Meyer S, Claudel P, Bergdoll M, Karst F (2011) Metabolic engineering of monoterpene synthesis in yeast. Biotechnol Bioeng 108:1883–1892

Hohn TM, Ohlrogge JB (1991) Expression of a fungal sesquiterpene cyclase gene in transgenic tobacco. Plant Physiol 97:460–462

Iijima Y, Davidovich-Rikanati R, Fridman E et al (2004) The biochemical and molecular basis for the divergent patterns in the biosynthesis of terpenes and phenylpropenes in the peltate glands of three cultivars of basil. Plant Physiol 136:3724–3736

Jackson BE, Hart-Wells EA, Matsuda SP (2003) Metabolic engineering to produce sesquiterpenes in yeast. Org Lett 5:1629–1632

Javelot C, Girard P, Colonna-Ceccaldi B, Vladescu B (1991) Introduction of terpene-producing ability in a wine strain of *Saccharomyces cerevisiae*. J Biotechnol 21:239–252

Lewinsohn E, Schalechet F, Wilkinson J et al (2001) Enhanced levels of the aroma and flavor compound *S*-linalool by metabolic engineering of the terpenoid pathway in tomato fruits. Plant Physiol 127:1256–1265

Lücker J, Schwab W, van Hautum B et al (2004a) Increased and altered fragrance of tobacco plants after metabolic engineering using three monoterpene synthases from lemon. Plant Physiol 134:510–519

Lücker J, Schwab W, Franssen MCR et al (2004b) Metabolic engineering of monoterpene biosynthesis: two-step production of (+)-*trans*-isopiperitenol by tobacco. Plant J 39:140–145

Mahmoud SS, Croteau RB (2001) Metabolic engineering of essential oil yield and composition in mint by altering expression of deoxyxylulose phosphate reductoisomerase and menthofuran synthase. Proc Natl Acad Sci USA 98:2915–2920

Martin VJ, Yoshikuni Y, Keasling JD (2001) The in vivo synthesis of plant sesquiterpenes by *Escherichia coli*. Biotechnol Bioeng 75:497–503

Martin VJ, Pitera DJ, Withers ST et al (2003) Engineering a mevalonate pathway in *Escherichia coli* for production of terpenoids. Nat Biotechnol 21:796–802

Martin DM, Aubourg S, Schouwey MB et al (2010) Functional annotation, genome organization and phylogeny of the grapevine (*Vitis vinifera*) terpene synthase gene family based on genome assembly, FLcDNA cloning, and enzyme assays. BMC Plant Biol 10:226. doi:10.1186/1471-2229-10-226

Ménard Szczebara F, Chandelier C, Villeret C et al (2003) Total biosynthesis of hydrocortisone from a simple carbon source in yeast. Nat Biotechnol 21:143–149

Oswald M, Fischer M, Dirninger N, Karst F (2007) Monoterpenoid biosynthesis in *Saccharomyces cerevisiae*. FEMS Yeast Res 7:413–421

Reiling KK, Yoshikuni Y, Martin VJ et al (2004) Mono and diterpene production in *Escherichia coli*. Biotechnol Bioeng 87:200–212

Rittersdorf W, Cramer F (1967) Die hydrolyse von 2,3-dihydroterpenylphosphaten und -pyrophosphaten. Tetrahedon 23:3023–3038

Ro DK, Paradise EM, Ouellet M et al (2006) Production of the antimalarial drug precursor artemisinic acid in engineered yeast. Nature 440:940–943

Sauer N, Stolz J (1994) SUC1 and SUC2: two sucrose transporters from *Arabidopsis thaliana*; expression and characterization in baker's yeast and identification of the histidine-tagged protein. Plant J 6:66–77

Schnee C, Köllner TG, Held M, Turlings TCJ, Gershenzon J, Degenhardt J (2006) The products of a single maize sesquiterpene synthase form a volatile defense signal that attracts natural enemies of maize herbivores. Proc Natl Acad Sci USA 103:1129–1134

Singh RS, Gara RK, Bhardwaj PK et al (2010) Expression of *3-hydroxy-3-methylglutaryl-CoA reductase*, *p-hydroxybenzoate-m-geranyltransferase* and genes of phenylpropanoid pathway exhibits positive correlation with shikonins content in arnebia [*Arnebia euchroma* (Royle) Johnston]. BMC Mol Biol 11:88. doi:10.1186/1471-2199-11-88

Szkopińska A, Swiezewska E, Karst F (2000) The regulation of activity of main mevalonic acid pathway enzymes: farnesyl diphosphate synthase, *3-hydroxy-3-methylglutaryl-CoA reductase*, and squalene synthase in yeast *Saccharomyces cerevisiae*. Biochem Biophys Res Commun 267:473–477

Takahashi S, Yeo Y, Greenhagen BT et al (2007) Metabolic engineering of sesquiterpene metabolism in yeast. Biotechnol Bioeng 97:170–180

Wallaart TE, Bouwmeester HJ, Hille J, Poppinga L, Maijers NC (2001) Amorpha-4,11-diene synthase: cloning and functional expression of a key enzyme in the biosynthetic pathway of the novel antimalarial drug artemisinin. Planta 212:460–465

Metabolic Engineering of Isoprenoid Production: Reconstruction of Multistep Heterologous Pathways in Tractable Hosts

6

Jérôme Maury, Mohammad A. Asadollahi,
Luca R. Formenti, Michel Schalk, and Jens Nielsen

Abstract

Isoprenoids represent a wide group of chemically active compounds that can find a wide range of applications as flavors, perfumes, vitamins, nutraceuticals, and pharmaceuticals. Many isoprenoids are naturally produced in very low quantities by plants, which make their use in broader perspectives difficult. Microbial production of plant-originating isoprenoids quickly appeared as an alternative of choice. Metabolic engineering methods were applied and proved successful to improve the supply of precursors to derive toward isoprenoid compounds of interest. Combinations between metabolic engineering and the flourishing field of synthetic biology have also been observed with researchers attempting to reconstruct and optimize complex biosynthetic pathways in well-characterized and tractable microbial hosts. In this chapter, we review recent metabolic engineering studies for isoprenoid production in yeast and try to show, through key examples, that the fields of synthetic biology and metabolic engineering can go hand in hand to establish microbial cell factories for isoprenoid production.

Keywords

Metabolic engineering • Synthetic biology • Yeast • *Saccharomyces cerevisiae* • Heterologous gene • Mevalonate pathway • MEP pathway

J. Maury (✉) • M.A. Asadollahi
Novo Nordisk Foundation Center for Biosustainability - Technical University of Denmark, Fremtidsvej 3, 2970 Hørsholm, Denmark
e-mail: jrm.maury@gmail.com

L.R. Formenti
National Food Institute, Kgs Lyngby, Denmark

M. Schalk
Biotechnology Department, Firmenich SA, Geneva, Switzerland

J. Nielsen
Department of Chemical and Biological Engineering, Chalmers University of Technology, Gothenburg, Sweden

T.J. Bach and M. Rohmer (eds.), *Isoprenoid Synthesis in Plants and Microorganisms: New Concepts and Experimental Approaches*, DOI 10.1007/978-1-4614-4063-5_6,

6.1 Introduction

The yeast *Saccharomyces cerevisiae* is the most studied eukaryotic microorganism and has been used for thousands of years by human beings for the production of alcoholic beverages and leavened breads. In addition to its role as a model organism for understanding the biology of eukaryotic cells and human diseases, *S. cerevisiae* is currently used in various industrial processes for the production of ethanol, of baker's yeast, or recently for the production of pharmaceuticals.

Development of biotech processes has been traditionally based on the initial selection of an appropriate microorganism with a certain phenotype, which would undergo several rounds of strain improvement using mainly classical approaches involving random mutagenesis. However, in recent years, there has been a paradigm shift toward using a small number of selected cell factories (Maury et al. 2005). In many cases, however, development of so few cell factories for the production of a broad range of compounds requires the expression of heterologous genes for the biosynthesis of desired compounds and the deregulation of pathways supplying the precursors for those compounds. This can be achieved through a metabolic engineering approach which, systematically and rationally, aims at improving cellular phenotypes using directed application of recombinant DNA technology tools for strain improvement (Stephanopoulos et al. 1998). Metabolic engineering is a continuous and iterative process in which the phenotype of interest is improved in several rounds of modifications until the desired phenotype is obtained. Therefore, metabolic engineering can be considered as a cycle including three main steps, synthesis, analysis, and design, as illustrated in Fig. 6.1.

6.2 Metabolic Engineering for the Production of Isoprenoid Compounds

So far *E. coli* and the yeasts *S. cerevisiae* and *Candida utilis* have been the most studied cell factories for the production of isoprenoids, and numerous reports have been written on the heterologous production of various isoprenoids using these microorganisms. *S. cerevisiae* is generally a

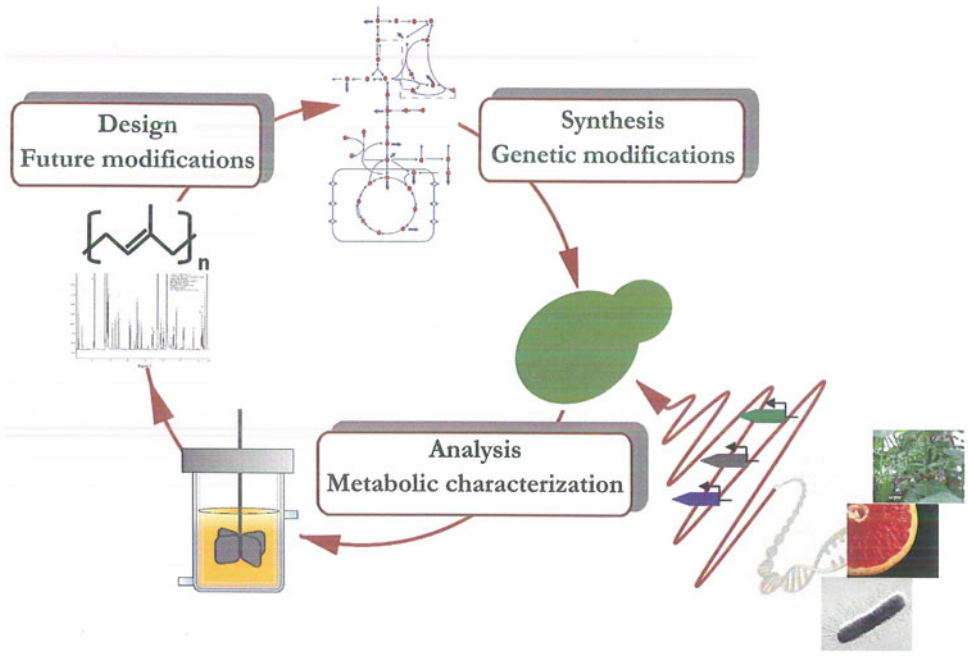

Fig. 6.1 The metabolic engineering cycle for the development of a cell factory for isoprenoid production

well-accepted cell factory for the development of new biotech processes due to its long historical use in making ethanol and baker's yeast, its public acceptance as a GRAS (Generally Regarded As Safe) microorganism, the availability of its complete genome sequence, the well-established fermentation processes for this organism, and its susceptibility for genetic modifications through recombinant DNA technology approaches (Ostergaard et al. 2000). The mevalonate pathway in yeast is responsible for the biosynthesis of isoprenoid precursors and leads to the formation of ergosterol as the major end product of the pathway; the content of which in *S. cerevisiae* can reach 5% of the cell dry weight (Lamacka and Sajbidor 1997). Therefore, yeast has a relatively high inherent capacity for the biosynthesis of isoprenoid precursors that may be directed to the production of heterologous compounds. Additionally, *S. cerevisiae* is considered a suitable host for the biosynthesis of plant isoprenoids, as it provides the biosynthetic machinery for the proper functioning of the downstream modifying enzymes and has less natural codon bias than *E. coli* (Chang and Keasling 2006; Takahashi et al. 2007).

One of the first attempts for heterologous production of isoprenoids in *S. cerevisiae* was carried out by Yamano et al. (1994). Expression of the required genes for the biosynthesis of lycopene (*crtE*, *crtB*, and *crtI*) and β-carotene (*crtE*, *crtB*, *crtI*, and *crtY*) from *Erwinia uredovora* in *S. cerevisiae* enabled the production of lycopene and β-carotene in yeast, though only at very low amounts. However, *S. cerevisiae* transformed with the carotenogenic genes from *Xanthophyllomyces dendrorhous* (formerly known as *Phaffia rhodozyma*) produced higher levels of carotenoids (Verwaal et al. 2007). Conversion of HMG-CoA to mevalonate catalyzed by HMG-CoA reductase is generally considered to represent the main flux-controlling step in the mevalonate pathway. Thus, overexpression of a truncated version of *HMG1*, named *tHMG1*, which is responsible for the synthesis of the catalytic domain of HMG-CoA reductase, resulted in an enhancement of carotenoid production by sevenfold. However, a bottleneck at the level of the phytoene desaturation step was highlighted, as phytoene was the main carotenoid formed. Overexpression of *crtI*, encoding phytoene desaturase, changed the composition of carotenoids in favor of β-carotene and led to a reduced accumulation of phytoene (Verwaal et al. 2007).

Heterologous production of several sesquiterpenes including epi-cedrol (Jackson et al. 2003), 5-epi-aristolochene, premnaspirodiene, valencene, capsidiol (Takahashi et al. 2007), amorphadiene (Lindahl et al. 2006; Ro et al. 2006), artemisinic acid (Ro et al. 2006), valencene, cubebol, and patchoulol (Asadollahi et al. 2008) in *S. cerevisiae* have been successfully reported (see Table 6.1). In one study (Ro et al. 2006), *S. cerevisiae* was exploited as a platform for the biosynthesis of artemisinic acid, which can be readily converted to the antimalarial drug artemisinin by semisynthetic routes (Ro et al. 2006). To this end, first the mevalonate pathway was deregulated by several modifications including overexpression of a truncated HMG-CoA reductase, downregulation of *ERG9*, overexpression of *upc2-1* (*UPC2* is a global transcription factor regulating sterol biosynthesis in yeast; see Leak et al. 1999 for more information about *upc2-1*), and overexpression of *ERG20*, encoding FPP synthase. The resulting strain was able to produce 153 mg/L amorphadiene. This engineered strain was subsequently transformed with a novel cytochrome P450 monooxygenase (*CYP71AV1*) from *Artemisia annua*, which converts amorphadiene to artemisinic acid through a three-step oxidation and produces up to 100 mg/L of artemisinic acid (Ro et al. 2006). Engineering of a pyruvate dehydrogenase bypass by overproduction of acetaldehyde dehydrogenase (encoded by *ALD6*) and a variant of acetyl-CoA synthetase from *Salmonella enterica* enhanced amorphadiene biosynthesis in *S. cerevisiae* (Shiba et al. 2007).

In a study by Asadollahi et al. (2008), *S. cerevisiae* was enabled to produce the plant sesquiterpenes valencene, cubebol, and patchoulol after transforming the yeast strains with the corresponding sesquiterpene synthase genes. Valencene was the major product of valencene synthase, whereas patchoulol and cubebol synthases were multiproduct enzymes and led to the production of a mixture of several sesquiterpenes in addition to their main products, i.e., patchoulol and cubebol, respectively (Asadollahi et al. 2008).

Table 6.1 Examples of heterologous production of isoprenoids by metabolically engineered yeast strains

Class	Isoprenoid	Host microorganism	Yield or concentration	References
Monoterpenes	Geraniol	*S. cerevisiae*	989 μg/L/OD_{600}	Oswald et al. (2007)
Diterpenes	Taxadiene	*S. cerevisiae*	1,000 μg/L	DeJong et al. (2006)
	Taxadien-5α-ol	*S. cerevisiae*	25 μg/L	DeJong et al. (2006)
	Taxadiene	*S. cerevisiae*	8,700 μg/L	Engels et al. (2008)
Sesquiterpenes	Amorphadiene	*S. cerevisiae*	153,000 μg/L	Ro et al. (2006)
	Amorphadiene	*S. cerevisiae*	120,000 μg/L	Shiba et al. (2007)
	Amorphadiene	*S. cerevisiae*	600 μg/L	Lindahl et al. (2006)
	Artemisinic acid	*S. cerevisiae*	100,000 μg/L	Ro et al. (2006)
	Epi-cedrol	*S. cerevisiae*	370 μg/L	Jackson et al. (2003)
	5-*Epi*-aristolochene	*S. cerevisiae*	90,000 μg/L	Takahashi et al. (2007)
	Premnaspirodiene	*S. cerevisiae*	90,000 μg/L	Takahashi et al. (2007)
	Capsidiol	*S. cerevisiae*	50,000 μg/L	Takahashi et al. (2007)
	Valencene	*S. cerevisiae*	20,000 μg/L	Takahashi et al. (2007)
	Valencene	*S. cerevisiae*	3,000 μg/L	Asadollahi et al. (2008)
	Cubebol	*S. cerevisiae*	2,000 μg/L	Asadollahi et al. (2008)
	Patchoulol	*S. cerevisiae*	16,900 μg/L	Asadollahi et al. (2008)
Triterpenes	β-Amyrin	*S. cerevisiae*	~6,000 μg/L	Kirby et al. (2008)
Carotenoids	Lycopene	*S. cerevisiae*	113 μg/g DW	Yamano et al. 1994
	Lycopene	*C. utilis*	758 μg/g DW	Miura et al. (1998a)
	Lycopene	*C. utilis*	1,100 μg/g DW	Miura et al. (1998b)
	Lycopene	*C. utilis*	7,800 μg/g DW	Shimada et al. (1998)
	β-Carotene	*S. cerevisiae*	103 μg/g DW	Yamano et al. (1994)
	β-Carotene	*S. cerevisiae*	5,918 μg/g DW	Verwaal et al. (2007)
	β-Carotene	*C. utilis*	400 μg/g DW	Miura et al. (1998b)
	Astaxanthin	*C. utilis*	400 μg/g DW	Miura et al. (1998b)

The ability of sesquiterpene synthases to make multiple products has been well documented and is probably a consequence of premature quenching of the highly unstable carbocationic intermediates generated from farnesyl diphosphate (FPP) (Davis and Croteau 2000). Downregulation of *ERG9*, achieved by replacing its native promoter with the repressible *MET3* promoter, led to a reduction in ergosterol content of yeast cells when cultivated in the presence of methionine and to an accumulation of FPP-derived compounds. Nevertheless, with the exception of patchoulol synthase, this strategy did not appreciably improve the production of the target sesquiterpenes but rather resulted in further production of farnesol as an FPP-derived by-product (Asadollahi et al. 2008). Unexpectedly, when cubebol was the heterologous sesquiterpene produced, a significant accumulation of squalene and restoration of ergosterol biosynthesis was observed. This could be explained by a toxicity effect of cubebol, possible resulting in a higher expression of the genes under the control of the promoter of *MET3*, which could lead to the accumulation of squalene and ergosterol (Asadollahi et al. 2010). In another study, a genome-scale metabolic model was used to seek genetic targets susceptible to enhance sesquiterpene production. Deletion of NADPH-dependent glutamate dehydrogenase encoded by *GDH1* was identified as the best target gene for the improvement of sesquiterpene biosynthesis (Asadollahi et al. 2009). Indeed the deletion of *GDH1* led to an 85% increase in cubebol production but significantly affected the maximum specific growth rate of the strain. The specific growth rate of the strain was significantly improved by concomitantly overexpressing *GDH2*, encoding a

NADH-dependent glutamate dehydrogenase (Asadollahi et al. 2009).

Taxol, known to be the most important anticancer drug introduced in the last fifteen years (Kingston 2001), was originally extracted from the bark of the Pacific yew (*Taxus brevifolia*) through an extensive isolation and purification process. However, extraction of enough Taxol to treat a single cancer patient requires six 100-year-old Pacific yew trees (Horwitz 1994). *S. cerevisiae* has been examined as a microbial host for the biosynthesis of Taxol intermediates. Total biosynthesis of Taxol from geranylgeranyl diphosphate (GGPP) occurs through 19 steps. Eight genes of the pathway were functionally expressed in yeast. Coexpression of GGPP synthase and taxadiene synthase resulted in a yeast strain producing 1 mg/L taxadiene. Further modification of this terpene backbone was limited by the first cytochrome P450 hydroxylation step and produced only 25 μg/L of taxadien-5α-ol (DeJong et al. 2006). In another attempt at the biosynthesis of the diterpene taxadiene in *S. cerevisiae* (Engels et al. 2008), coexpression of taxadiene synthase and GGPP synthase both from *Taxus chinensis* in yeast resulted in only 204 μg/L taxadiene. Overexpression of *tHMG1* enhanced taxadiene production by 50% whereas overexpression of *upc2-1* did not further increase taxadiene titer. Expression of a GGPP synthase from *Sulfolobus acidocaldarius*, which is able to synthesize GGPP through sequential combination of dimethylallyl diphosphate (DMAPP) building blocks rather than combination of FPP and isopentenyl diphosphate (IPP), prevented competition with squalene synthase for FPP as substrate and resulted in a slight increase in taxadiene production but in almost 100-fold improvement of geranylgeraniol titer. Codon optimization of taxadiene synthase for expression in *S. cerevisiae* combined with overexpression of *tHMG1*, *upc2-1*, and GGPP synthase from *S. acidocaldarius* enhanced taxadiene production 40-fold and also accumulated substantial amounts of geranylgeraniol (Engels et al. 2008).

Geranyl diphosphate (GPP) serves as the sole precursor for the biosynthesis of regular monoterpenes. The level of GPP in yeast seems to be very low due to its tight binding to the FPP synthase catalytic site. The cellular function of GPP in yeast has not been described. However, expression of geraniol synthase of *Ocimum basilicum* in yeast gave rise to the biosynthesis of geraniol and linalool in yeast. A tenfold increase in geraniol production was observed upon expression of geraniol synthase in a yeast mutant bearing an *erg20-2* mutation (Oswald et al. 2007; Fischer et al., this volume, chapter 5).

β-Amyrin is a pentacyclic plant triterpene with various potential applications in human health due to its antimicrobial, antidepressant, anti-inflammatory, antinociceptive, antiallergic, and gastroprotective activities (Holanda Pinto et al. 2008; Soldi et al. 2008). Isolation of β-amyrin synthase from *A. annua* and its introduction into the yeast *S. cerevisiae* led to production of β-amyrin. Overexpression of *tHMG1* combined with downregulation of lanosterol synthase encoded by *ERG7* was concomitant with a 50% increase in β-amyrin titer and a 12-fold increase in squalene accumulation compared to the control strain (Kirby et al. 2008).

The yeast *C. utilis* is also considered as a relevant microorganism for the production of isoprenoids based on its general acceptance by the food and feed industries as a safe organism, the successful development of large-scale cultivation processes, the use of *C. utilis* as foodstuff during the World War I, and its relatively high ergosterol content (Shimada et al. 1998). Transformation of *C. utilis* with *crtE*, *crtB*, and *crtI* genes from *E. uredovora* resulted in accumulation of 0.76 mg/g CDW lycopene and 0.41 mg/g CDW phytoene (Miura et al. 1998a). Modification of the codon usage of the genes responsible for lycopene biosynthesis according to the codon usage of the *C. utilis* glyceraldehyde 3-phosphate dehydrogenase improved the lycopene and phytoene contents of the strains 1.5- and 4-fold, respectively (Miura et al. 1998b). Overexpression of either full length or truncated version of the gene encoding HMG-CoA reductase further improved lycopene production two- and fourfold, respectively (Shimada et al. 1998). Subsequent disruption of *ERG9* encoding squalene synthase enabled a production of up to 7.8 mg/g CDW lycopene in *C. utilis* (Shimada et al. 1998).

Table 6.1 summarizes the metabolic engineering studies for heterologous production of isoprenoids in the yeasts *S. cerevisiae* and *C. utilis*

6.3 Bridging Between Metabolic Engineering and Synthetic Biology

Usually, metabolic engineering approaches begin with the introduction of one or more genes encoding enzymes, which will catalyze the transformation of readily available intracellular intermediates into the desired product. Then optimization will target both the aforementioned freshly introduced genes and enzymatic steps of the microbial host in order to improve metabolic fluxes toward the biosynthesis of the compound of interest. The key to success is to finely balance the expression of the transformational genes so that the enzymes are produced in catalytic amounts only sufficient to adequately transform metabolic intermediates into desired products at a sufficient rate. Imbalanced or too high expression levels of certain enzymatic steps of the pathway may lead to accumulation of intermediates in concentrations toxic to the cells or literally to the metabolic burden routing important building blocks away from biomass formation. This would indeed negatively impact the production process.

Metabolic engineers therefore need an adequate toolset to precisely control the expression of native and foreign genes in the chosen microbial host. A vast number of molecular biology tools are already available, usually appropriate to control the expression of single or few genes, but often not adequate for more complicated engineering tasks, e.g., control of large, heterologous metabolic pathways or signal transduction systems (Keasling 2008). Metabolic engineers may therefore significantly benefit from the emerging field of synthetic biology which aims at designing and constructing core components (parts of enzymes, genetic circuits, or metabolic pathways) that can be modeled, understood, and tuned to meet specific performance criteria and assembled into larger integrated systems that solve specific problems (Keasling 2008). Despite the obvious benefits synthetic biology could bring to yeast metabolic engineering, efforts in this field primarily focused on prokaryotic systems (Krivoruchko et al. 2011). Krivoruchko et al. discuss further how the recent advances in synthetic biology could be applied to metabolic engineering of *S. cerevisiae* (Krivoruchko et al. 2011).

In the field of terpene biotechnology, bridges between synthetic biology and metabolic engineering are already observable with attempts from researchers to create organisms with new properties of interest by transferring metabolic pathways from one organism to another. One particularly probing example is provided by the successful reconstruction in *S. cerevisiae* of an artificial and self-sufficient pathway for the biosynthesis of hydrocortisone, the major steroid in mammals (Szczebara et al. 2003). To achieve the transfer and bring to function in a single yeast cell this highly complex and mainly membrane-bound mammalian metabolic pathway, Szczebara et al. (2003) assembled, expressed, and engineered 13 different genes and rerouted the yeast endogenous sterol biosynthetic pathway toward the production of hydrocortisone, which became the major steroid produced. Some of the metabolic engineering challenges faced and solved in this work include the self-production of a suitable substrate for CYP11A1 (the first step of hydrocortisone synthesis), targeting of mitochondrial P450s and associated carriers, balancing the flux within the artificial pathway, and identifying side reactions diverting intermediates away from the desired product (Szczebara et al. 2003; Dumas et al. 2006). This work represented a major breakthrough in that it enabled a highly complex heterologous pathway constituted of differently localized enzymes (some being membrane-bound). It was also the first report of the total biosynthesis of hydrocortisone by a recombinant microorganism from a simple carbon source and stands as a solid basis for the development of an environmentally friendly and low-cost industrial process for the production of corticoid drugs (Szczebara et al. 2003).

Another example of bridging between synthetic biology and metabolic engineering is the

pioneering work described by Martin et al. (2003). In this study, aimed at achieving high production levels of artemisinin, an antimalarial drug usually isolated from plant material, Martin et al. (2003) elegantly transferred and engineered a eukaryotic isoprenoid biosynthetic pathway in the Gram-negative bacterium *Escherichia coli*. Considering that the overexpression of three flux-controlling enzymes of the endogenous *E. coli* pathway, the MEP pathway, only resulted in a 3.6-fold increase in amorphadiene concentration, the manipulation of the native pathway to increase isoprenoid precursor supply seemed limited by some additional native control mechanisms in *E. coli*. Martin et al. (2003) attempted to overcome these limiting intracellular regulations of the endogenous isoprenoid biosynthetic pathway by expressing an entire heterologous pathway for the supply of isoprenoid precursors, the *S. cerevisiae* mevalonate pathway. Introduction of the mevalonate pathway from *S. cerevisiae* into *E. coli* would potentially circumvent the as yet unidentified regulations of the native MEP pathway while minimizing the complicated regulatory network of the mevalonate pathway observed in yeast (Maury et al. 2005). Initial expression of the yeast pathway in *E. coli* led to such an abundance of isoprenoid precursors that cells either ceased to grow or mutated to overcome the toxicity (Martin et al. 2003). When combined with the expression of a synthetic codon-optimized amorphadiene synthase, growth inhibition was alleviated and amorphadiene production was boosted 11-fold compared to previously engineered MEP pathway (Martin et al. 2003). Following initial studies of amorphadiene production with precursors supplied by the heterologous mevalonate pathway, optimization of a number of parameters (e.g., amorphadiene volatility, fermentation process, balancing metabolic flux by fine-tuning of gene expression) was achieved. After optimization of the fermentation process, the engineered strain produced 480 mg/L amorphadiene in a fed-batch bioreactor supplemented with increased carbon and complex nutrients (Newman et al. 2006; Paddon et al. 2011). Cultivating the above-mentioned strain, harboring only the first three genes of the mevalonate pathway coded for by the MevT operon (Martin et al. 2003) in a medium supplemented with exogenous mevalonate, indicated a limited supply of mevalonate by the MevT operon. However, increasing expression of the MevT genes inhibited cell growth. Gene titration and metabolite profiling studies attributed the growth inhibition phenotype to the accumulation of HMG-CoA, an intermediate of the mevalonate pathway (Pitera et al. 2007). Recently, combined DNA microarray analysis and targeted metabolite profiling indicated that HMG-CoA cytotoxicity is mediated via the inhibition of fatty acid biosynthesis in the microbial host (Kizer et al. 2008). Introduction of an additional copy of *tHMG1* for conversion of the toxic HMG-CoA to nontoxic mevalonate restored the cell growth, reduced the accumulation of intracellular HMG-CoA, and improved mevalonate production twofold (Pitera et al. 2007). To remedy the imbalanced gene expression in the MevT genes, expression of the three genes in the operon was tuned by generating libraries of tunable intergenic regions (TIGRs), which resulted in a sevenfold increase in mevalonate production (Pfleger et al. 2006). All this work finally led to an improvement in amorphadiene production by over one-million-fold (Keasling 2008). The optimized amorphadiene *E. coli* producing strain was further engineered to produce artemisinic acid which can then be converted into artemisinin in two chemical steps. Finally, the use of the most appropriate promoters and expression vectors allowed *in vivo* production of fully oxidized artemisinic acid at levels exceeding 300 $mg.L^{-1}$ (Keasling 2008). Tsuruta et al. (2009) reported, after further improvements of the heterologous pathway, commercially relevant titers of amorphadiene after an optimized fed-batch fermentation process (Tsuruta et al. 2009).

Following the pioneering and successful strategy described by Martin et al. (2003), mevalonate pathways from other sources (e.g., *Streptomyces* sp., *Streptococcus pneumoniae*), either entire or truncated, have been introduced into *E. coli* and applied to the production of compounds like lycopene, β-carotene, or coenzyme Q10 (Vadali et al. 2005; Yoon et al. 2006, 2007; Zahiri et al. 2006; Rodríguez-Villalón et al. 2008).

Finally, as mentioned earlier, the metabolic pathway for paclitaxel (taxol) biosynthesis, a mitotic inhibitor used in cancer chemotherapy, has also been partly transferred from *Taxus* species to *E. coli* or *S. cerevisiae* (Huang et al. 2001; Dejong et al. 2006) in order to establish a microbial production process. Ten enzymatic steps from the paclitaxel biosynthesis of *Taxus* species were successfully and independently expressed in yeast (Dejong et al. 2006). Five sequential steps catalyzing the synthesis of the intermediate taxadien-5-α-acetoxy-10-β-ol were installed in a single yeast strain (Dejong et al. 2006). However, the complete pathway from the precursor geranylgeranyl diphosphate to paclitaxel includes nineteen steps in *Taxus* species (Dejong et al. 2006). An impressive effort for the production of taxadiene in *E. coli* was also recently described by Ajikumar et al. (2010). The authors describe a multivariate-modular approach which succeeded in balancing the fluxes between the native MEP pathway and the heterologous two-step pathway toward taxadiene, which was produced at the gram per liter level (Ajikumar et al. 2010). Ajikumar et al. also engineered the next step in taxol biosynthesis, a P450-mediated oxidation of taxadiene into taxadien-5α-ol (Ajikumar et al. 2010).

6.4 Reconstruction and Expression of a Heterologous Nonmevalonate Pathway in *S. cerevisiae*

This section mainly deals with the activities, carried out between 2004 and 2009, by the research group "Isoprenoid production in S. cerevisiae" based at the Center for Microbial Biotechnology-Denmark Technical University (Lyngby).

The aim of our research group at the Center for Microbial Biotechnology – Danish Technical University, Lyngby, Denmark was to engineer a tractable and well-characterized microbial host and turn it into a biological platform for the production of various types of isoprenoids, especially sesquiterpenes, having potent anticancer, antitumor, cytotoxic, antiviral, and antibiotic properties or with characteristic flavors and aromas, which are thus very attractive compounds for the industry. More general considerations led us to use the eukaryotic model organism *S. cerevisiae* as microbial host, namely its high inherent capacity for the synthesis and storage of isoprenoid compounds like ergosterol as a major end product (Lamacka and Sajbidor 1997), and because *S. cerevisiae* was shown suitable for the functional expression of proteins originating from higher eukaryotic organisms, even when associated to membrane structures like cytochrome P450 enzymes, which participate in the biosynthesis of many plant-derived natural compounds.

Largely inspired by the pioneering studies described further above, which demonstrated that transferring entire metabolic pathways into a new biological host and making them functional in a nonnative environment can result in tremendous improvements of the production of desired compounds, we embarked into the cloning and expression of the seven enzymatic steps of the MEP pathway from *E. coli* into *S. cerevisiae* (Fig. 6.2). The same rationale as Martin et al. (2003) was followed, i.e., that the expression of the nonnative MEP pathway may help overcome the complex regulation network occurring on the yeast mevalonate pathway and lead to a greater supply of isoprenoid building blocks IPP and DMAPP that can be further derived to desired products. The seven genes encoding the MEP pathway, i.e., *dxs*, *dxr*, *ispD (mct)*, *ispE (cmk)*, *ispF (mds)*, *gcpE (hds)*, and *lytB (hdr)*, were PCR-amplified using specific primers from *E. coli* genome. The specific primers were designed for the amplification of each open reading frame with 5′ and 3′overhangs allowing for the transfer into the expression plasmid either by restriction digestion-ligation or by *in vivo* homologous recombination in *S. cerevisiae* (Erdeniz et al. 1997). To choose a suitable yeast expression vector, it was important to take into account the fact that seven nonnative genes were to be expressed, their expression was to be strong, in the first place at least, and furthermore tightly controlled to avoid the accumulation of toxic intermediates during the cloning process. pESC yeast epitope-tagging vectors (Stratagene®) characterized by potent expression of two genes

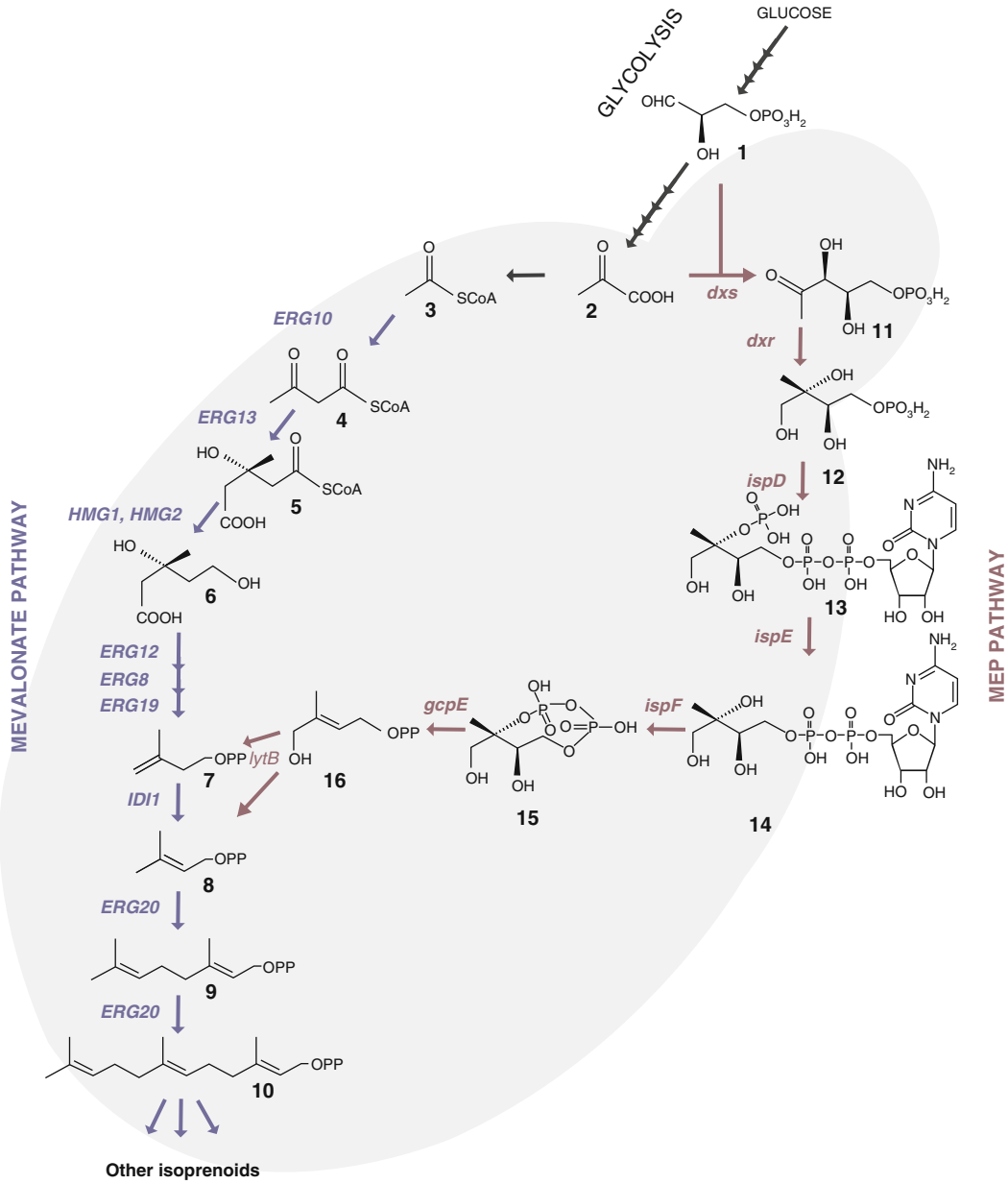

Fig. 6.2 The *E. coli* MEP pathway expressed in *S. cerevisiae* (Adapted from Maury et al. 2008). The origin of the isoprenoid biosynthetic pathway precursors in central metabolic pathways is schematically represented. The two types of isoprenoid biosynthetic pathways, the mevalonate pathway from *S. cerevisiae* (*blue*) and the MEP pathway from *E. coli* (*dark red*), are represented. Intermediates: **1** D-glyceraldehyde 3-phosphate, **2** pyruvate, **3** acetyl-CoA, **4** acetoacetyl-CoA, **5** 3-hydroxy-3-methylglutaryl-CoA, **6** mevalonate, **7** isopentenyl diphosphate, **8** dimethyl allyl diphosphate, **9** geranyl diphosphate, **10** farnesyl diphosphate, **11** 1-deoxy-D-xylulose 5-phosphate, **12** 2-*C*-methyl-D-erythritol 4-phosphate, **13** 4-diphosphocytidyl-2-*C*-methyl-D-erythritol, **14** 2- phospho-4-diphosphocytidyl-2-*C*-methyl-D-erythritol, **15** 2-*C*-methyl-D-erythritol 2,4-cyclodiphosphate, **16** 1-hydroxy-2-methyl-2-(*E*)-butenyl 4-diphosphate

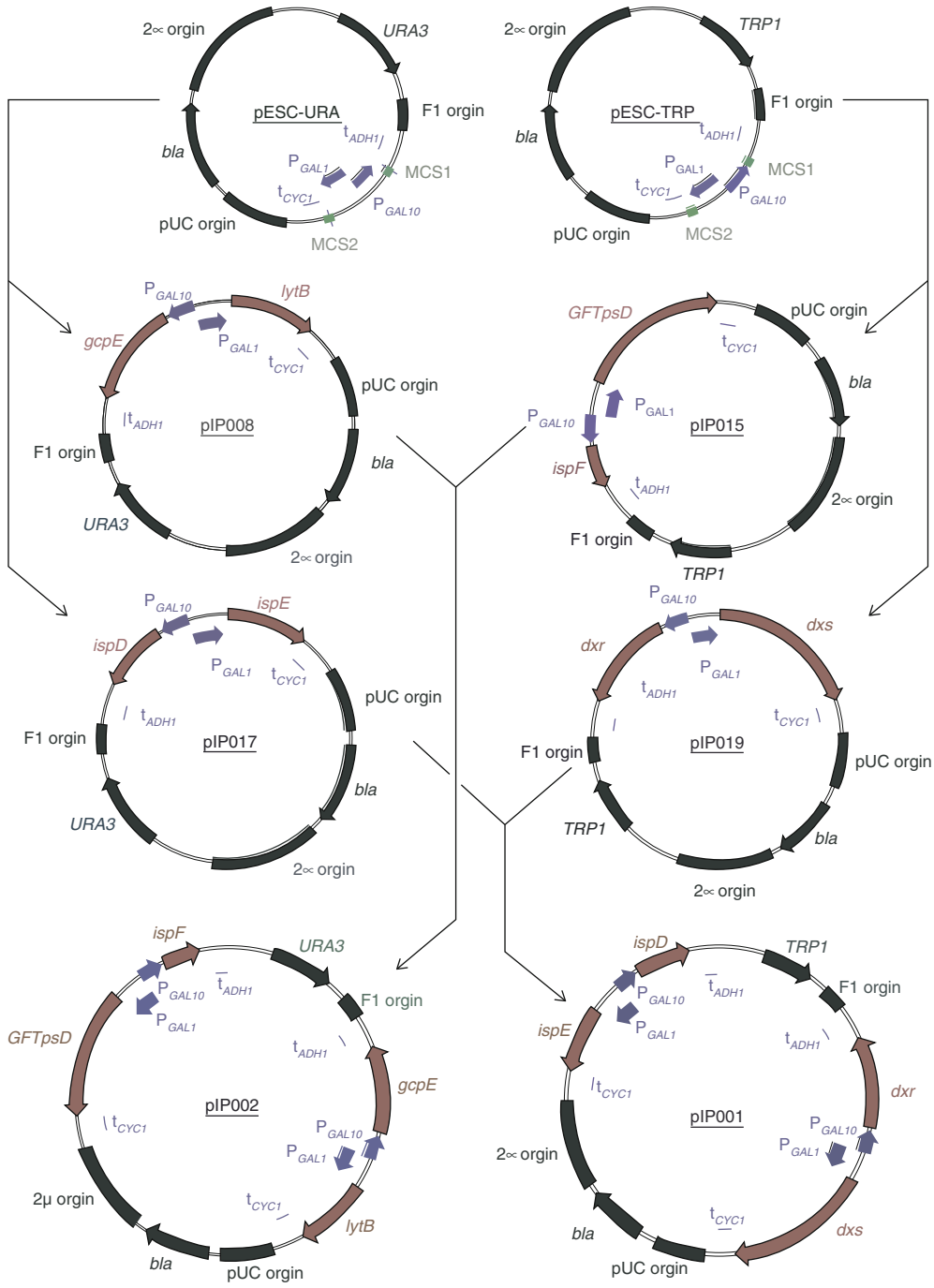

Fig. 6.3 Overall strategy for the cloning and expression of the seven MEP pathway encoding genes in *S. cerevisiae*

per vector, tight control of gene expression thanks to *GAL1* and *GAL10* promoters, strong expression levels achieved, and high plasmid copy number were finally chosen (Fig. 6.3). A terpene synthase encoding gene, valencene synthase, was also cloned as a biological reporter. The different

steps of the cloning process are summarized in Fig. 6.3. From a first cloning phase, four vectors were obtained: pIP019 (*dxs* and *dxr*), pIP017 (*ispD* and *ispE*), pIP015 (*ispF* and GFTpsD), and pIP008 (*gcpE* and *lytB*). Each of these vectors can trigger the expression of two genes specified in brackets. To assemble a whole functional MEP pathway through, a total of four different pESC vectors would be required. In order to reduce the number of plasmids to maintain in the final yeast strain and to minimize the number of genetic markers to be used, pESC-URA and pESC-TRP vectors were further modified to trigger the expression of four genes each instead of two initially (Fig. 6.3). To realize this, plasmids were fused in pairs using *in vivo* homologous recombination in *S. cerevisiae*. First, an insertion site placing the selective marker (*URA3* or *TRP1*) in between the two potential P_{GAL1}/P_{GAL10} expression cassettes was sought and found: *Xcm*I for pESC-TRP and *Mfe*I for pESC-URA. Positioning the genetic marker in between the two P_{GAL1}/P_{GAL10} expression cassettes allows the use of the constructed plasmids as templates for subsequent genomic integration of the MEP pathway encoding genes. Then, the homologous regions for insertion of the second P_{GAL1}/P_{GAL10} expression cassette were designed such that the two P_{GAL1} and the two P_{GAL10} situated on both sides of the genetic marker are inverted one to the other, thereby avoiding potential loss of genetic elements from the plasmid that can occur by homologous recombination between directly repeated regions (Fig. 6.3). Finally, two main multicopy plasmids, pIP001 and pIP002, were obtained. These two plasmids trigger the expression of the seven MEP pathway encoding genes from *S. cerevisiae GAL1* and *GAL10* promoters (Fig. 6.3). Purified pIP001 and pIP002 were transformed into *S. cerevisiae* strain YIP-00-02 to obtain strain YIP-DV-02, characterized by the presence of the seven MEP pathway genes and *GFTpsD* (the valencene synthase encoding gene). Expression levels of the MEP pathway genes in *S. cerevisiae* were assessed using a qualitative experiment based on RT-PCR and aiming at detecting specific mRNA for the seven bacterial genes. This experiment showed that all the seven *E. coli* genes are eventually transcribed in *S. cerevisiae* (Maury et al. 2008).

The *S. cerevisiae* strain expressing the MEP pathway, YIP-DV-02, was also shown to produce valencene, as analyzed by GC-MS, in batch cultivation using galactose as carbon source (data not shown). To try to demonstrate that a metabolic flux is indeed driven through the *E. coli* MEP pathway, growth of YIP-DV-02 in the presence of a potent and well-known mevalonate pathway inhibitor – mevinolin or lovastatin – was characterized (Maury et al. 2008). This experiment suggested that the *E. coli* MEP pathway is able to sustain growth of yeast cells under conditions where the native mevalonate pathway is inhibited. (Lovastatin acts as a specific inhibitor of HMG-CoA reductase, a major flux-controlling step of the mevalonate pathway.) However, this result should be further validated with the expression of the heterologous MEP pathway into *S. cerevisiae* strains deleted of genes encoding essential enzymatic steps of the native mevalonate pathway, like, e.g., *ERG13* or *HMG1 HMG2*.

To further stabilize the expression of the MEP pathway genes, the pathway was moved away from the initial proof-of-concept multicopy plasmids and integrated into *S. cerevisiae* genome using a bipartite gene targeting method (Fig. 6.4). The seven genes were divided into two gene clusters and integrated in two different chromosomal loci. The strategy for integration is as follows (Fig. 6.4).

The main issue to deal with was the presence of repeated DNA sequences, i.e., *GAL1* and *GAL10* promoters, *CYC1* and *ADH1* transcription terminators, which could lead to the loss of parts of integrated DNA material by homologous recombination. The seven genes were therefore divided into two gene clusters and integrated in two different genomic loci, on two different chromosomes. Furthermore, within the two gene clusters, caution was taken to avoid direct repeats of DNA sequences (Fig. 6.4). The procedure for integration of the two gene clusters was as follows (Fig. 6.4): For each gene cluster (*dxs*/*dxr*/*ispD*/*ispE* or *gcpE*/*lytB*/*ispF*), six PCR products were generated first (Fig. 6.4). These PCR products were then fused together during

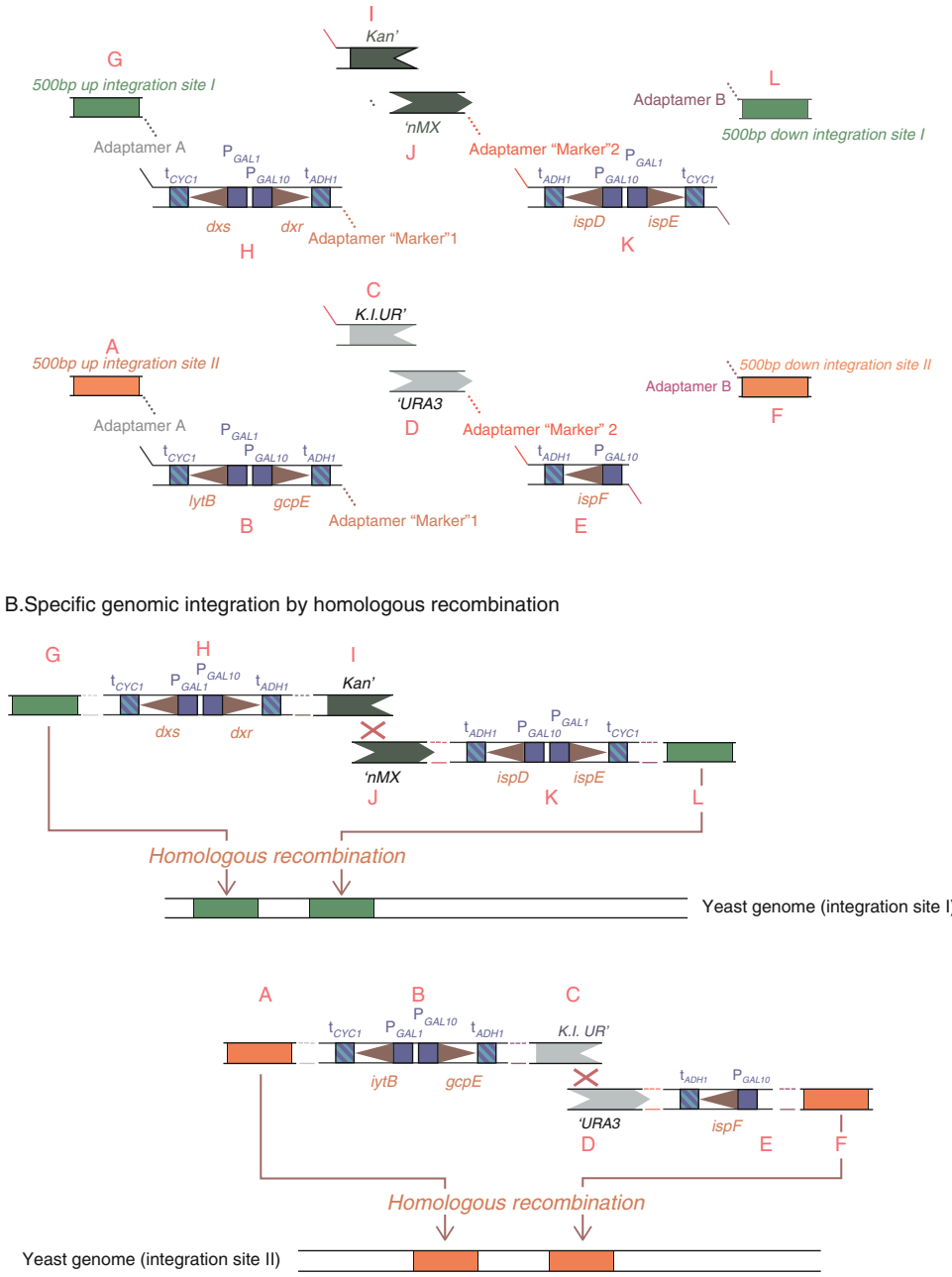

Fig. 6.4 Targeted integration of the MEP pathway encoding genes in *S. cerevisiae* genome. The different fragments, i.e., the fragments A to L, are amplified by PCR (**a**). Subsequently, specific fragments are fused together by fusion PCR using four different sets of adaptamers (**a**) to finally obtain fragments A/B/C, D/E/F, G/H/I, and J/K/L (**b**). Fragments A and F provide the required homologous regions for genomic integration of cluster *lytB/gcpE/ispF* while fragments G and L provide the necessary homologous regions for genomic integration of cluster *dxs/dxr/ispD/ispE*. Fragments A/B/C and D/E/F are cotransformed into *S. cerevisiae* to obtain a specific insertion of cluster *lytB/gcpE/ispF* at the integration site II (**b**). Fragments G/H/I and J/K/L are cotransformed into *S. cerevisiae* to obtain a specific integration of cluster *dxs/dxr/ispD/ispE* at the integration site I by *in vivo* homologous recombination (**b**)

two subsequent fusion PCR, using predefined sets of adaptamers. For example, fragments A, B, and C were first amplified separately. Then they were fused during two fusion PCR, resulting in a long linear A/B/C fragment (Fig. 6.4). The resulting fused PCR fragments were characterized by overlapping regions at the level of the selective marker (*Kluyveromyces lactis URA3* or *KanMX*) and by extremities sharing homology with the two defined integration sites on the genome. These features allowed for the targeted insertion of the two gene clusters in *S. cerevisiae* genome. A yeast strain expressing the MEP pathway genes from *S. cerevisiae* genome was obtained and is being further analyzed.

6.4.1 Pathway Flux Optimization: From Identification of Regulatory Points to Engineering

Reconstructing and expressing a heterologous isoprenoid biosynthetic pathway in *S. cerevisiae* was a first determining step, and further improvements are necessary to enhance the flux toward precursors of interesting products. In order to optimize the flux in the pathway and balance intermediate concentrations, two major approaches can be foreseen:

First, a "targeted" approach that would aim at identifying potential bottlenecks in the pathway using various modern metabolic engineering methods largely developed in the field of systems biology like, e.g., metabolic flux analysis, metabolite profiling, genome-wide transcription analysis, or metabolic network modeling could definitely help to define the next series of genetic targets to modify. Molecular biology tools available for the budding yeast can then be used to act and balance gene expression, enzyme activities, and metabolite concentrations and eventually increase the flux through the MEP pathway. In addition to these experimental methods, a close look into the literature can be very informative and help identify potential flux-controlling steps.

In contrast to the deep knowledge of the regulatory mechanisms controlling the mevalonate pathway, relatively little is known about the regulation of the MEP pathway. The enzyme that received the greatest interest so far is DXS, the first enzyme of the pathway. It is not the first specific step of the MEP pathway as it can be involved, in different organisms, in other pathways leading to vitamin biosyntheses. In *E. coli*, 1-deoxyxylulose 5-phosphate (DXP) is a precursor for the biosynthesis of thiamine (vitamin B1) and pyridoxal (vitamin B6) (Lois et al. 1998; see also elsewhere in this volume). In several higher plants, at least two classes of DXS enzyme have been identified, and their expression has been associated with different localizations and developmental phases of the plant (Walter et al. 2002, 2011; Seetang-Nun et al. 2008; Paetzold et al. 2010. Wolfertz et al. (2004) studied the properties of isoprene synthase in leaves and the ability to supply a regulated amount of DMAPP for isoprene synthesis during and after heatflecks. Supplying leaves with deuterated deoxyxylulose (DOX-d_2), which is incorporated into the MEP pathway at the level of its first intermediate, yielding deuterated 1-deoxyxylulose 5-phosphate (DXP-d_2), suggested a possible feedback inhibition over DXS by DMAPP, DXP, or other intermediates of the pathway, in order to keep constant the supply of DMAPP. The regulation over DXS seems effective as long as the supplemented amount of DOX-d_2 is not reduced to a very little percentage of the endogenous DXP, suggesting the regulation to be very effective. Guevara-García et al. (2005) showed that a differential regulation at the transcriptional and the translational level of DXS, in addition to a feedback regulation of DXS in response to the interruption of the flow of metabolites through the pathway occur in plants. By using a mutant of *LYTB*, they could observe a significant difference in the accumulation of *DXS* transcript and DXS protein. They also showed that DXS, DXR, and LYTB protein levels exhibit significant fluctuations during plant development. Posttranscriptional events seem to regulate the activity of DXS during early plant development.

Carretero-Paulet et al. (2002) elucidated some of the control mechanisms of the first committed step of the pathway, encoded by *DXR*. They proved a common regulation of the gene expression profile between *DXS* and *DXR*, but with a different regulation at the protein level, as inhibition

of the MEP pathway with fosmidomycin (that inhibits specifically DXR) shows accumulation of DXR but no further accumulation of DXS. DXR was then suggested to represent a major control point of regulation of the pathway: in fact, DXS could also be regulated by mechanisms that play a role in cofactor biosynthesis, independently from isoprenoid metabolism (Carretero-Paulet et al. 2002). In a more recent article, the same authors provided more evidence for DXR as being a flux-controlling step of the MEP pathway (Carretero-Paulet et al. 2006). They demonstrated that changes in DXR levels in *DXR*-overexpressing plants did not cause accumulation of DXS, while changing the isoprenoid levels in chloroplasts. Other points of regulation downstream of DXR are also suggested, as different levels of transcript, protein, and enzyme activity lead only to very similar levels of chlorophylls and carotenoids (Carretero-Paulet et al. 2006).

Very often optimal solutions for pathway engineering require the simultaneous deregulation of multiple genes to unravel complex regulatory networks or fine-tune multienzyme pathway activities. Furthermore, negative effects from expressing a heterologous isoprenoid biosynthetic pathway may originate from multiple causes that are difficult to anticipate, e.g., accumulation of toxic intermediates, accumulation of the final building blocks IPP and/or DMAPP, negative interaction with another pathway, and diversion of glyceraldehyde 3-phosphate and pyruvate away from central metabolic pathways. Taking this into consideration, a second and different approach to optimize the MEP pathway flux which would rely on the "nontargeted" and progressive adaptation of the flux through the MEP pathway may be more appropriate. Indeed, these two approaches, "targeted" and "nontargeted," are certainly complementary. Evolutionary engineering (Sauer 2001; Sonderegger and Sauer 2003; Kuyper et al. 2005; Wisselink et al. 2007), the use of genome-wide libraries (genomic DNA libraries, cDNA libraries, transposon libraries), and global transcription machinery engineering ("gTME" Alper et al. 2006) are methods that were proved suitable for the selection of improved strains with a specific phenotype or for the identification of potentially beneficial genetic targets. These methods combined with a specific, selective, and easy-to-assess screening system for the detection of improved MEP pathway flux may be applied here.

6.4.2 Perspectives

Many isoprenoids of pharmaceutical and economic interest are produced in very low quantities by plants, and this makes it difficult to use these chemicals more widely. Through the development of a general cell factory production platform, it will be possible not only to produce already existing isoprenoids but through combinatorial biochemistry it will further be possible to produce new chemical entities that may find interesting applications. A fundamental problem with the development of a general cell factory is, however, that endogenous pathways leading to isoprenoids, like the mevalonate pathway that leads to the production of ergosterol in yeast, are submitted to an extensive regulation at both the transcriptional and posttranscriptional level. These different types of regulation make it difficult to increase and redirect the flux toward the isoprenoid of interest, and this may hinder implementation of industrial processes. It is therefore interesting to engineer new pathways that circumvent endogenous regulation, and expression of the MEP pathway in yeast is an illustration of this concept.

Here, we have described initial work to reconstruct the MEP pathway in yeast. However, in order to obtain a high flux through the MEP pathway, it will be necessary to further optimize the expression of the different enzymes and ensure that there is a coordinated activity of all the steps in the pathway. Here, the large molecular biology toolset available for *S. cerevisiae*, like, e.g., well-defined promoters of different strength (Partow et al. 2010), large promoter libraries (Tochigi et al. 2010), specific single (Flagfeldt et al. 2009) or multicopy chromosomal integration sites (Parekh et al. 1996), or the creation of chimeric enzymes of host and heterologous origin (Albertsen et al. 2011), can prove useful. Furthermore, it may be necessary to optimize the complete metabolic

network to ensure efficient supply of the different precursors needed for isoprenoid production. This may require use of different traditional biochemical methods like enzyme activity measurements and elucidation of their kinetic properties, but it may also involve use of methods developed in the field of systems biology, e.g., metabolic flux analysis, genome-wide transcription analysis, and metabolic network modeling. This kind of analysis may lead to the identification of new metabolic engineering targets, and based on several rounds of optimization, eventually it will be possible to obtain an efficient cell factory for the production of isoprenoids.

Acknowledgements The authors gratefully acknowledge Firmenich SA for funding the research.

References

Ajikumar PK, Xia WH, Tyo KE et al (2010) Isoprenoid pathway optimization for taxol precursor overproduction in *Escherichia coli*. Science 330:70–74

Albertsen L, Chen Y, Bach LS et al (2011) Diversion of flux toward sesquiterpene production in *Saccharomyces cerevisiae* by fusion of host and heterologous enzymes. Appl Environ Microbiol 77:1033–1040

Alper H, Moxley J, Nevoigt E et al (2006) Engineering yeast transcription machinery for improved ethanol tolerance and production. Science 314:1565–1568

Asadollahi MA, Maury J, Møller K et al (2008) Production of plant sesquiterpenes in *Saccharomyces cerevisiae*: effect of *ERG9* repression on sesquiterpene biosynthesis. Biotechnol Bioeng 99:666–677

Asadollahi MA, Maury J, Patil KR et al (2009) Enhancing sesquiterpene production in *Saccharomyces cerevisiae* through in silico driven metabolic engineering. Metab Eng 11:328–334

Asadollahi MA, Maury J, Schalk M et al (2010) Enhancement of farnesyl diphosphate pool as direct precursor of sesquiterpenes through metabolic engineering of the mevalonate pathway in *Saccaromyces cerevisiae*. Biotechnol Bioeng 106:86–96

Carretero-Paulet L, Ahumada I, Cunillera N et al (2002) Expression and molecular analysis of the Arabidopsis *DXR* gene encoding 1-deoxy-D-xylulose 5-phosphate reductoisomerase, the first committed enzyme of the 2-C-methyl-D-erythritol 4-phosphate pathway. Plant Physiol 129:1581–1591

Carretero-Paulet L, Cairó A, Botella-Pavía P et al (2006) Enhanced flux through the methylerythritol 4-phosphate pathway in Arabidopsis plants overexpressing deoxyxylulose 5-phosphate reductoisomerase. Plant Mol Biol 62:683–695

Chang MCY, Keasling JD (2006) Production of isoprenoid pharmaceuticals by engineered microbes. Nat Chem Biol 2:674–681

Davis EM, Croteau R (2000) Cyclization enzymes in the biosynthesis of monoterpenes, sesquiterpenes and diterpenes. In: Leeper F, Vederas JC (eds) Topics in current chemistry: biosynthesis- aromatic polyketides, isoprenoids, alkaloids, vol 209. Springer, Heidelberg, pp 53–95

DeJong JM, Liu Y, Bollon AP et al (2006) Genetic engineering of taxol biosynthetic genes in *Saccharomyces cerevisiae*. Biotechnol Bioeng 93:212–224

Dumas B, Brocard-Masson C, Assemat-Lebrun K et al (2006) Hydrocortisone made in yeast: metabolic engineering turns a unicellular microorganism into a drug-synthesizing factory. Biotechnol J 1:299–307

Engels B, Dahm P, Jennewein S (2008) Metabolic engineering of taxadiene biosynthesis in yeast as a first step towards Taxol (Paclitaxel) production. Metab Eng 10:201–206

Erdeniz N, Mortensen UH, Rothstein R (1997) Cloning-free PCR-based allele replacement methods. Genome Res 7:1174–1183

Flagfeldt DB, Siewers V, Huang L et al (2009) Characterization of chromosomal integration sites for heterologous gene expression in *Saccharomyces cerevisiae*. Yeast 26:545–551

Guevara-García A, San Román C, Arroyo A et al (2005) Characterization of the Arabidopsis *clb6* mutant illustrates the importance of posttranscriptional regulation of the methyl-D-erythritol 4-phosphate pathway. Plant Cell 17:628–643

Holanda Pinto SA, Pinto LMS, Cunha GMA et al (2008) Anti-inflammatory effect of α, β-amyrin, a pentacyclic triterpene from *Protium heptaphyllum* in rat model of acute periodontitis. Inflammopharmacology 16:48–52

Horwitz SB (1994) How to make Taxol from scratch. Nature 367:593–594

Huang Q, Roessner CA, Croteau R et al (2001) Engineering *Escherichia coli* for the synthesis of taxadiene, a key intermediate in the biosynthesis of taxol. Bioorg Med Chem 9:2237–2242

Jackson BE, Hart-Wells EA, Matsuda SPT (2003) Metabolic engineering to produce sesquiterpenes in yeast. Org Lett 5:1629–1632

Keasling JD (2008) Synthetic biology for synthetic chemistry. ACS Chem Biol 3:64–76

Kingston DGI (2001) Taxol, a molecule for all seasons. Chem Commun 1:867–880

Kirby J, Romanini DW, Paradise EM et al (2008) Engineering triterpene production in *Saccharomyces cerevisiae*- β-amyrin synthase from *Artemisia annua*. FEBS J 275:1852–1859

Kizer L, Pitera DJ, Pfleger BF et al (2008) Application of functional genomics to pathway optimization for increased isoprenoid production. Appl Environ Microbiol 74:3229–3241

Krivoruchko A, Siewers V, Nielsen J (2011) Opportunities for yeast metabolic engineering: Lessons from synthetic biology. Biotechnol J 6:262–276

Kuyper M, Toirkens MJ, Diderich JA et al (2005) Evolutionary engineering of mixed sugar utilization by a xylose-fermenting *Saccharomyces cerevisiae* strain. FEMS Yeast Res 5:925–934

Lamacka M, Sajbidor J (1997) Ergosterol determination in *Saccharomyces cerevisiae*. Comparison of different methods. Biotechnol Tech 11:723–725

Leak FW Jr, Tove S, Parks LW (1999) In yeast, upc2-1 confers a decrease in tolerance to LiCl and NaCl, which can be suppressed by the P-type ATPase encoded by ENA2. DNA Cell Biol 18:133–139

Lindahl A-L, Olsson ME, Mercke P et al (2006) Production of the artemisinin precursor amorpha-4,11-diene by engineered *Saccharomyces cerevisiae*. Biotechnol Lett 28:571–580

Lois LM, Campos N, Putra SR et al (1998) Cloning and characterization of a gene from *Escherichia coli* encoding a transketolase-like enzyme that catalyzes the synthesis of D-1-deoxyxylulose 5-phosphate, a common precursor for isoprenoid, thiamin, and pyridoxol biosynthesis. Proc Natl Acad Sci USA 95:2105–2110

Martin VJ, Pitera DJ, Withers ST et al (2003) Engineering a mevalonate pathway in *Escherichia coli* for production of terpenoids. Nat Biotechnol 7:796–802

Maury J, Asadollahi MA, Møller K et al (2005) Microbial isoprenoid production: an example of green chemistry through metabolic engineering. Adv Biochem Eng Biotechnol 100:19–51

Maury J, Asadollahi MA, Formenti LR et al (2008) Reconstruction of a bacterial isoprenoid biosynthetic pathway in *Saccharomyces cerevisiae*. FEBS Lett 582:4032–4038

Meyer S, Oswald M, Fischer M et al (2011) Metabolic engineering of monoterpenoids production in yeast (this volume)

Miura Y, Kondo K, Shimada H et al (1998a) Production of lycopene by the food yeast, *Candida utilis* that does not naturally synthesize carotenoid. Biotechnol Bioeng 58:306–308

Miura Y, Kondo K, Saito T et al (1998b) Production of carotenoids lycopene, ß-carotene, and astaxanthin in the food yeast *Candida utilis*. Appl Environ Microbiol 64:1226–1229

Newman JD, Marshall J, Chang M et al (2006) High-level production of amorpha-4,11-diene in a two-phase partitioning bioreactor of metabolically engineered *Escherichia coli*. Biotechnol Bioeng 95:684–691

Ostergaard S, Olsson L, Nielsen J (2000) Metabolic engineering of *Saccharomyces cerevisiae*. Microbiol Mol Biol Rev 64:34–50

Oswald M, Fischer M, Dirninger N et al (2007) Monoterpenoid biosynthesis in *Saccharomyces cerevisiae*. FEMS Yeast Res 7:413–421

Paddon CJ, McPhee D, Westfall PJ et al (2011) Microbially-derived semi-synthetic artemisinin (this volume)

Paetzold H, Garms S, Bartram S et al (2010) The isogene 1-deoxy-D-xylulose 5-phosphate synthase 2 controls isoprenoid profiles, precursor pathway allocation, and density of tomato trichomes. Mol Plant 3:904–916

Parekh RN, Shaw MR, Wittrup KD (1996) An integrating vector for tunable, high copy, stable integration into the dispersed Ty delta sites of *Saccharomyces cerevisiae*. Biotechnol Prog 12:16–21

Partow S, Siewers V, Bjorn S et al (2010) Characterization of different promoters for designing a new expression vector in *Saccharomyces cerevisiae*. Yeast 27:955–964

Pfleger BF, Pitera DJ, Smolke CD et al (2006) Combinatorial engineering of intergenic regions in operons tunes expression of multiple genes. Nat Biotechnol 24:1027–1032

Pitera DJ, Paddon CJ, Newman JD et al (2007) Balancing a heterologous mevalonate pathway for improved isoprenoid production in *Escherichia coli*. Metab Eng 9:193–207

Ro D-K, Paradise EM, Ouellet M et al (2006) Production of the antimalarial drug precursor artemisinic acid in engineered yeast. Nature 440:940–943

Rodríguez-Villalón A, Pérez-Gil J, Rodríguez-Concepción M (2008) Carotenoid accumulation in bacteria with enhanced supply of isoprenoid precursors by upregulation of exogenous or endogenous pathways. J Biotechnol 135:78–84

Sauer U (2001) Evolutionary engineering of important microbial phenotypes. Adv Biochem Eng Biotechnol 73:129–169

Seetang-Nun Y, Sharkey TD, Suvachittanont W (2008) Isolation and characterization of two distinct classes of *DXS* genes in *Hevea brasiliensis*. DNA Seq 19:291–300

Shiba Y, Paradise EM, Kirby J et al (2007) Engineering of the pyruvate dehydrogenase bypass in *Saccharomyces cerevisiae* for high-level production of isoprenoids. Metab Eng 9:160–168

Shimada H, Kondo K, Fraser PD et al (1998) Increased carotenoid production by the food yeast *Candida utilis* through metabolic engineering of the isoprenoid pathway. Appl Environ Microbiol 64:2676–2680

Soldi C, Pizzolatti MG, Luiz AP et al (2008) Synthetic derivatives of the α- and β-amyrin triterpenes and their antinociceptive properties. Bioorg Med Chem 16:3377–3386

Sonderegger M, Sauer U (2003) Evolutionary engineering of *Saccharomyces cerevisiae* for anaerobis growth on xylose. Appl Environ Microbiol 69:1990–1998

Stephanopoulos G, Aristidou A, Nielsen J (1998) Metabolic engineering: principles and methodologies. Academic, San Diego

Szczebara FM, Chandelier C, Villeret C et al (2003) Total biosynthesis of hydrocortisone from a simple carbon source in yeast. Nat Biotechnol 2:143–149

Takahashi S, Yeo Y, Greenhagen BT et al (2007) Metabolic engineering of sesquiterpene metabolism in yeast. Biotechnol Bioeng 97:170–181

Tochigi Y, Sato N, Sahara T et al (2010) Sensitive and convenient yeast reporter assay for high-throughput analysis by using a secretory luciferase from *Cypridina noctiluca*. Anal Chem 82:5768–5776

Tsuruta H, Paddon CJ, Eng D et al (2009) High level production of amorpha-4,11-diene, a precursor of the antimalarial agent artemisinin, in Escherichia coli. PLoS One 4(2):e4489

Vadali RV, Fu Y, Bennett GN et al (2005) Enhanced lycopene productivity by manipulation of carbon flow to isopentenyl diphosphate in *Escherichia coli*. Biotechnol Prog 21:1558–1561

Verwaal R, Wang J, Meijnen J-P et al (2007) High-level production of beta-carotene in *Saccharomyces cerevisiae* by successive transformation with carotenogenic genes from *Xanthophyllomyces dendrorhous*. Appl Environ Microbiol 73:4342–4350

Walter MH, Hans J, Strack D (2002) Two distantly related genes encoding 1-deoxy-D-xylulose 5-phosphate synthases: differential regulation in shoots and apocarotenoid-accumulating mycorrhizal roots. Plant J 31: 243–254

Walter MH, Floß DS, Paetzold H et al (2011) Control of plastidial isoprenoid precursor supply: divergent 1-deoxy-D-xylulose 5 phosphate synthase (DXS) isogenes regulate the allocation to primary or secondary metabolism (this volume)

Wisselink HW, Toirkens MJ, del Rosario Franco Berriel M et al (2007) Engineering of *Saccharomyces cerevisiae* for efficient anaerobic alcoholic fermentation of L-arabinose. Appl Environ Microbiol 73:4881–4891

Wolfertz M, Sharkey TD, Boland W et al (2004) Rapid regulation of the methylerythritol 4-phosphate pathway during isoprene synthesis. Plant Physiol 135: 1939–1945

Yamano S, Ishii T, Nakagawa M et al (1994) Metabolic engineering for production of ß-carotene and lycopene in *Saccharomyces cerevisiae*. Biosci Biotechnol Biochem 58:1112–1114

Yoon SH, Lee YM, Kim JE et al (2006) Enhanced lycopene production in *Escherichia coli* engineered to synthesize isopentenyl diphosphate and dimethylallyl diphosphate from mevalonate. Biotechnol Bioeng 94:1025–1032

Yoon SH, Park HM, Kim JE et al (2007) Increased beta-carotene production in recombinant *Escherichia coli* harboring an engineered isoprenoid precursor pathway with mevalonate addition. Biotechnol Prog 23: 599–605

Zahiri HS, Yoon SH, Keasling JD et al (2006) Coenzyme Q10 production in recombinant *Escherichia coli* strains engineered with a heterologous decaprenyl diphosphate synthase gene and foreign mevalonate pathway. Metab Eng 8:406–416

Microbially Derived Semisynthetic Artemisinin

7

Christopher J. Paddon, Derek McPhee, Patrick J. Westfall, Kirsten R. Benjamin, Douglas J. Pitera, Rika Regentin, Karl Fisher, Scott Fickes, Michael D. Leavell, and Jack D. Newman

Abstract

Artemisinin is a sesquiterpene lactone endoperoxide with potent antimalarial properties, recommended by the World Health Organization for the treatment of malaria in artemisinin combination therapies (ACTs). It is extracted from the plant *Artemisia annua*, but its supplies are limited and its price is volatile. In order to increase supply and stabilize the price of artemisinin, a semisynthesis has been developed, whereby an artemisinin precursor (amorpha-4,11-diene) is produced in microbes and the isolated precursor converted chemically to artemisinin. *Escherichia coli* has been engineered to produce amorpha-4,11-diene by the expression of a heterologous mevalonate pathway along with amorpha-4,11-diene synthase (ADS) from *A. annua*. Development of the *E. coli* platform to increase production of amorpha-4,11-diene from 24 mg/L to >25 g/L is described. ADS has also been expressed in the yeast model system *Saccharomyces cerevisiae* which, following manipulation of the mevalonate pathway, produced 150 mg/L of amorpha-4,11-diene. The cDNAs encoding the cytochrome P450 that oxidizes amorpha-4,11-diene to artemisinic acid, *CYP71AV1*, and its cognate reductase were isolated from *A. annua* and expressed in amorpha-4,11-diene-producing *E. coli* and yeast, leading to the production of >1 g/L artemisinic acid from both organisms. A route for the chemical conversion of artemisinic acid to artemisinin is described. Production of semisynthetic artemisinin may lead to the development of a second source of the drug for incorporation into ACTs.

Keywords

Artemisinin • Malaria • Semisynthetic • *Escherichia coli* • *Saccharomyces cerevisiae* • Amorphadiene • Artemisinic acid

C.J. Paddon (✉) • D. McPhee • P.J. Westfall
K.R. Benjamin • D.J. Pitera • R. Regentin
K. Fisher • S. Fickes • M.D. Leavell • J.D. Newman
Amyris, Inc., 5885 Hollis Street, Suite 100,
Emeryville, CA 94608, USA
e-mail: paddon@amyris.com

T.J. Bach and M. Rohmer (eds.), *Isoprenoid Synthesis in Plants and Microorganisms: New Concepts and Experimental Approaches*, DOI 10.1007/978-1-4614-4063-5_7,

7.1 Introduction

7.1.1 Malaria and Its Treatment

Malaria is a disease predominantly affecting areas of poverty in the developing world. Sixty percent of malaria cases worldwide, and 80% of the deaths caused by malaria, occur in sub-Saharan Africa (Korenromp et al. 2005). The majority of clinical malaria episodes, of which there are estimated to be 350–500 million annually, are caused by the parasites *Plasmodium falciparum* and *P. vivax*. The most virulent form of malaria, caused by *P. falciparum*, has become resistant to almost all currently used drug therapies (Bloland 2001; Olumese 2006). Resistance by *P. falciparum* to both chloroquine and sulfadoxine-pyrimethamine originated in Southeast Asia and subsequently spread to Africa (Olumese 2006). While a degree of resistance to artemisinin has been reported in Southeast Asia (White 2008), isolates in Africa remain sensitive, and artemisinin combination therapy has a high efficacy rate.

Artemisinin is a sesquiterpene lactone endoperoxide extracted from the shrub *Artemisia annua* (sweet wormwood). Extracts of *A. annua* have long been used in traditional Chinese medicine, having first been described as the medicinal plant *quinghao* almost 1,800 years ago (Hsu 2006). The antimalarial properties of extracts of *quinghao* were discovered in 1971 following screening of the Chinese *materia medica*. The active compound, artemisinin, was subsequently isolated, and its chemical structure was elucidated in the late 1970s (Hsu 2006; Klayman 1985; White 2008). A derivative of artemisinin, dihydroartemisinin, generated by reduction of the lactone, was found to have more potent antimalarial activity than artemisinin itself. The effectiveness of artemisinin derivatives against all forms of human malaria was demonstrated by clinical studies during the 1980s and 1990s. Artemisinin and its derivatives act very rapidly and have a short half-life in the body. Low concentrations of artemisinin can lead to stasis but survival of the parasite (van Agtmael et al. 1999). In order to obtain effective antimalarial treatment with a low rate of recrudescence, a 5–7-day course of treatment with monotherapies of artemisinin is required. This long, required treatment period is often not completed, raising concern for selection of parasitic resistant to the drug. The incidence of recrudescence with unfinished artemisinin monotherapy and the possibility of selection for resistance led to the development of artemisinin combination therapies (ACTs) in which an artemisinin derivative is combined with other antimalarials such as mefloquine or amodiaquine. Artemisinin combination therapy is predicated on the concept that two or more simultaneously administered schizontocidal drugs possessing different modes of action will improve therapeutic effectiveness and delay the development of resistance to each individual drug in the combination. The World Health Organization (WHO) endorsed ACTs for the treatment of malaria in 2004 and in 2005 recommended a switch to ACTs for first-line malaria treatment (Olumese 2006).

A recent estimate of the annual cost of introducing ACTs into Tanzania calculated that a six-fold increase in the national budget for malaria treatment would be required (Njau et al. 2008). Unfortunately, as a consequence of their high cost, ACTs are often inaccessible to the people who need them most. Many patients use artemisinin monotherapies or inexpensive, but now ineffective, drugs such as chloroquine (Hale et al. 2007).

This chapter describes progress on the Semisynthetic Artemisinin Project which aims to develop an alternative process for the production of artemisinin so as to increase its supply and stabilize its price. This will be achieved by the development of microbes that produce amorpha-4,11-diene or artemisinic acid in a fermentation process, followed by chemical conversion to artemisinin. The project is rooted in the new discipline of synthetic biology, which aims to bring the modularity of the electronic and software industries to the construction of biological entities (Henkel and Maurer 2007). Either whole biosynthetic pathways have been transplanted into a microbial host (*Escherichia coli*), or the natural microbial pathway has been manipulated (*S. cerevisiae*) and supplemented with expression

of enzymes specific to the plant biosynthetic pathway for artemisinin production. The products of microbial biosynthesis, amorpha-4,11-diene or artemisinic acid, are extracted then chemically modified to produce artemisinin. Artemisinin can be derivatized to other compounds with superior pharmacological properties (e.g., artesunate or artemether) for incorporation into ACTs. The availability of an alternative supply, in addition to plant-derived artemisinin, will enable ACT manufacturers to avoid shortages and stabilize the price of the drug. It should be emphasized that it is not envisaged that microbially derived semisynthetic artemisinin will displace the product extracted from *A .annua*, but rather provide a supplementary supply of artemisinin that is consistently available, pure, and inexpensive (Hale et al. 2007).

7.1.2 Production of Artemisinin by *A. annua*

The biosynthesis of artemisinin, common to all isoprenoids, can be divided into four stages: (1) production of the C_5 monomer isopentenyl diphosphate (IPP) and dimethylallyl diphosphate (DMAPP), (2) polymerization of IPP and DMAPP to form farnesyl diphosphate (FPP), (3) cyclization to form the terpene backbone, and (4) modification of the terpene skeleton (McCaskill and Croteau 1997), in this case oxidation of amorpha-4,11-diene to form artemisinic acid. Two distinct pathways have evolved for the production of IPP and DMAPP. The mevalonate pathway is found primarily in eukaryotes and in some Gram-positive bacteria (see Sect. 7.1.3 below). The 1-deoxyxylulose 5-phosphate (DXP) pathway occurs in prokaryotes and the plastids of photosynthetic organisms (Chang and Keasling (2006) and the literature cited therein). Evidence supporting the involvement of both pathways in the production of artemisinin in *A. annua* has recently been summarized (Zeng et al 2007). In *A. annua,* artemisinin, along with other mono- and sesquiterpenes, is produced in ten-celled biseriate trichomes on the leaves (Covello et al 2007). Cyclization of farnesyl diphosphate (FPP) to form amorpha-4,11-diene, catalyzed by amorpha-4,11-diene synthase (ADS), is the first committed step in artemisinin biosynthesis (Bouwmeester et al 1999). The complementary DNA (cDNA) for ADS has been cloned by three different groups (Covello et al 2007).

7.1.3 Conversion of Amorpha-4, 11-diene to Artemisinic Acid

The pathway for the conversion of amorpha-4,11-diene to artemisinin in *A. annua* is somewhat unclear, and the evidence for the various possible alternatives is presented in a recent review (Covello et al. 2007). The cDNA encoding CYP71AV1, a cytochrome P450 enzyme capable of oxidizing amorpha-4,11-diene to artemisinic acid, was independently isolated by two groups. Ro et al. (2006) retrieved P450-expressed sequence tags (ESTs) from two Asteraceae family members, sunflower and lettuce, then used degenerate primers specific to the most abundant subfamilies in the Asteraceae, CYP71 and CYP82, to isolate unique P450 fragments from an *A. annua* trichome-enriched cDNA pool. Comparison of these P450 gene fragments against sunflower- and lettuce-expressed sequence tags (ESTs) using BLAST (Altschul et al. 1990) identified a single *A. annua* cDNA that had very high sequence identity to ESTs of unknown function from both plants while having much lower identity to sequences outside the Asteraceae family. The corresponding full-length cDNA encoding CYP71AV1 was recovered from *A. annua*. The native CYP71AV1 redox partner, cytochrome P450 reductase (CPR), was also isolated from *A. annua* (Ro et al. 2006). Teoh et al. (2006) also isolated the cDNA of CYP71AV1 from glandular trichomes of *A. annua*. *In vitro* enzyme assays conducted by Ro et al. (2006) ascertained that CYP71AV1 catalyzed all three oxidation steps from amorpha-4,11-diene to artemisinic acid (Fig. 7.1). Microsomes were prepared from a yeast strain expressing either CYP71AV1 and CPR or CPR alone. Addition of amorpha-4,11-diene, artemisinic alcohol, or artemisinic aldehyde to control microsomes expressing CPR

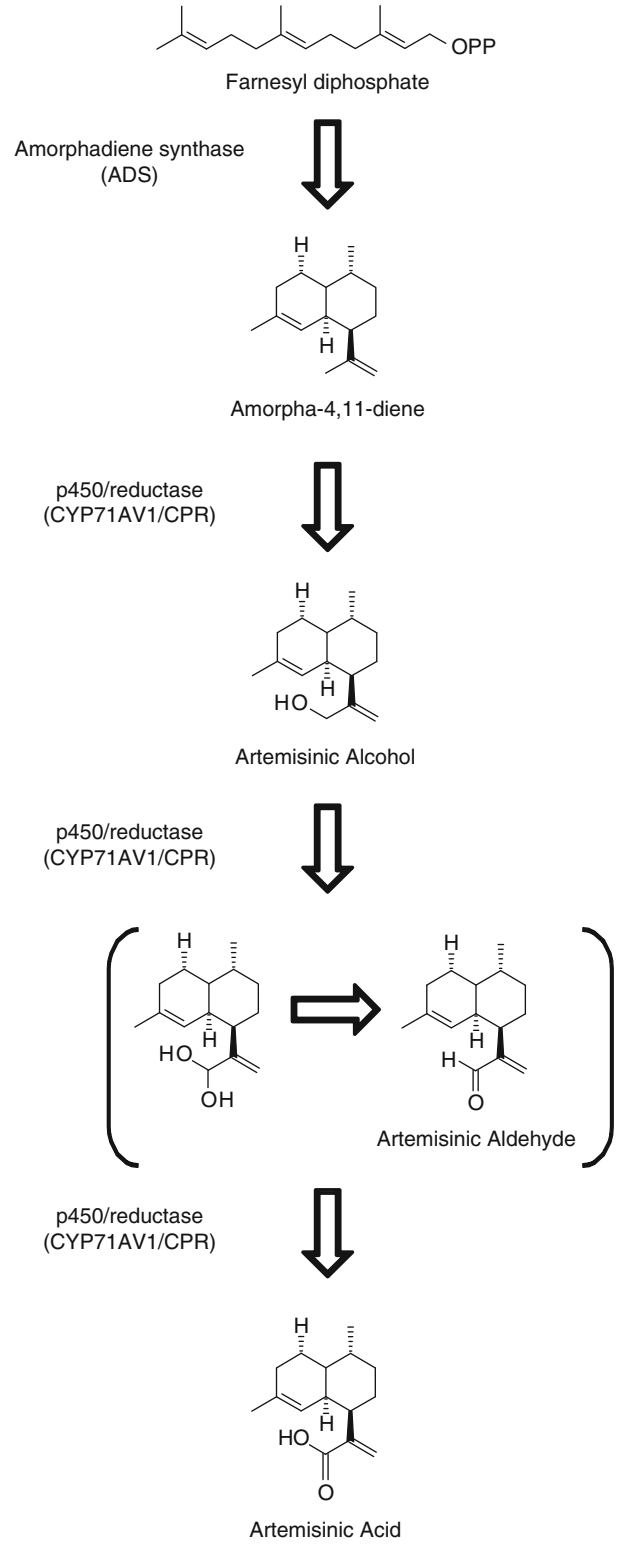

Fig. 7.1 Pathway from FPP to artemisinic acid showing chemical structures of FPP, amorpha-4, 11-diene, artemisinic alcohol, artemisinic aldehyde, and artemisinic acid. The enzyme catalyzing each reaction is shown

alone did not catalyze the oxidation of any pathway intermediate, whereas microsomes expressing both CYP71AV1 and CPR resulted in conversion to the final product, artemisinic acid. The efficient conversion of amorpha-4,11-diene to artemisinic acid by recombinant CYP71AV1 *in vivo* suggested that this membrane-bound, multifunctional cytochrome P450 is responsible for this conversion in *A. annua*. A similar conclusion was reached by Teoh et al. (2006) who also expressed CYP71AV1 in yeast microsomes, although they used CPR from *Arabidopsis thaliana* and only observed oxidation to artemisinic alcohol.

Bertea et al. (2005) analyzed the terpenoids from *A. annua* leaves and glandular trichomes and noted the presence of dihydroartemisinic aldehyde and dihydroartemisinic acid. They also demonstrated the presence of dehydrogenase activities that acted on artemisinic alcohol and dihydroartemisinic aldehyde. This led them to hypothesize that artemisinin biosynthesis involves amorpha-4,11-diene hydroxylation to artemisinic alcohol, followed by oxidation to artemisinic aldehyde. The C11-C13 double bond is then reduced to produce dihydroartemisinic aldehyde, followed by oxidation to dihydroartemisinic acid. The presence of an artemisinic aldehyde-11,13-double bond reductase was recently demonstrated in *A. annua* flower buds using a partially purified enzyme to isolate the corresponding cDNA, named *Dbr2* (Zhang et al. 2008). This gene was found to be highly expressed in glandular trichomes, and recombinant Dbr2 was found to be relatively specific for artemisinic aldehyde. Expression of Dbr2 in yeast, along with four other enzymes in the artemisinin pathway, resulted in the production of dihydroartemisinic acid. Thus, the identification and isolation of *Dbr2* cDNA supported the contention by Bertea et al. (2005) that dihydroartemisinic acid rather than artemisinic acid is the precursor for artemisinin synthesis in *A. annua*. The processes described below produce artemisinic acid, rather than dihydroartemisinic acid, and thus apparently differ from the artemisinin biosynthesis pathway native to *A. annua*.

7.2 Development of *E. coli* to Produce Amorpha-4,11-diene

Martin et al. (2003) described the expression of a heterologous mevalonate pathway in *Escherichia coli* for the production of amorpha-4,11-diene. Two synthetic operons were constructed to express the eight enzymes of the mevalonate pathway. These were referred to as the top pathway (MevT), expressing the three enzymes that convert acetyl-CoA to mevalonate, and the bottom pathway (MBIS), expressing the five enzymes that convert mevalonate to farnesyl diphosphate. Expression of the mevalonate pathway in *E. coli* resulted in severe growth inhibition, attributed to the buildup of the prenyl diphosphates IPP, DMAPP, and/or FPP. The expression of *A. annua* ADS, optimized for *E. coli* codon usage, prevented buildup of prenyl diphosphates and alleviated growth inhibition caused by mevalonate pathway expression (Fig. 7.2). Thus, the amorpha-4,11-diene-producing strain contained three plasmids, expressing the MevT operon, the MBIS operon, and ADS. In the absence of commercial amorpha-4,11-diene standards, production was measured as "caryophyllene equivalents," and total production of amorpha-4,11-diene was estimated to be 24 mg/L following growth on rich medium. It was subsequently demonstrated that *E. coli* strains expressing a heterologous mevalonate pathway accumulate pathway intermediates which limit flux and that high-level expression of mevalonate pathway enzymes inhibited cell growth (Pitera et al. 2007). Metabolite profiling and gene titration studies showed that accumulation of 3-hydroxy-3-methylglutaryl-coenzyme A (HMG-CoA) was responsible for the growth inhibition. The implication of this observation was that HMG-CoA reductase activity was limiting, allowing a buildup of HMG-CoA. Modulation of HMG-CoA reductase expression eliminated the pathway bottleneck and mevalonate production increased, demonstrating that balancing the carbon flux through the heterologous mevalonate pathway was important for optimal growth and

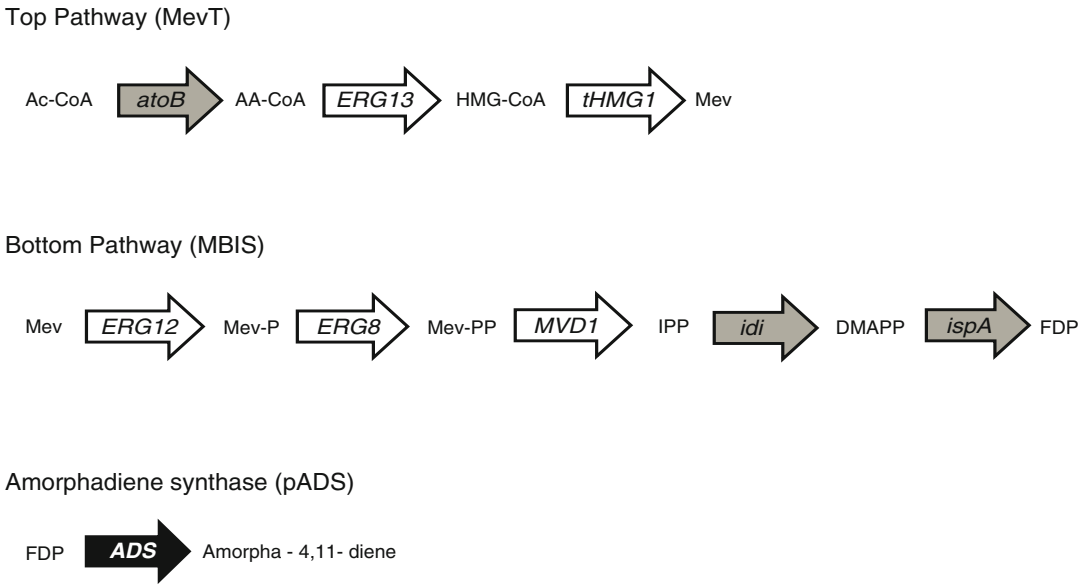

Fig. 7.2 Depiction of the heterologous mevalonate pathway expressed in *E. coli* to produce amorpha-4,11-diene. Genes in *grey arrows* are derived from *E. coli*, those in *white arrows* from yeast, and ADS (*black arrow*) from *A. annua*. MevT, MBIS, and pADS indicate the arrangement of genes on expression plasmids, corresponding with "top" and "bottom" mevalonate pathway designations. Gene names and the enzymes they encode the following: *atoB* acetoacetyl-CoA thiolase, *ERG13* HMG-CoA synthase, *tHMG1* truncated HMG-CoA reductase, *ERG12* mevalonate kinase, *ERG8* phosphomevalonate kinase, *MVD1* mevalonate pyrophosphate decarboxylase, *idi* IPP isomerase, *ispA* FPP synthase, *ADS* amorphadiene synthase. Pathway intermediates: *Ac-CoA* acetyl-CoA, *AA-CoA* acetoacetyl-CoA, *HMG-CoA* hydroxymethylglutaryl-CoA, *Mev-P* mevalonate 5-phosphate, *Mev-PP* mevalonate pyrophosphate, *IPP* isopentenyl pyrophosphate, *DMAPP* dimethylallyl pyrophosphate, *FPP* farnesyl pyrophosphate, *ADS* amorpha-4,11-diene synthase

production of amorpha-4,11-diene by *E. coli*. Additional work using a combination of DNA microarray analysis and metabolite profiling showed that the cytotoxicity caused by accumulation of HMG-CoA is due to inhibition of one or more enzymes involved in fatty acid biosynthesis (Kizer et al. 2008). The growth inhibition caused by HMG-CoA accumulation could be alleviated by supplementation of the growth medium with specific fatty acids. Supplementation of the medium with fatty acids is not a viable approach for large-scale industrial production of amorpha-4,11-diene or artemisinic acid; thus, alternative methods of balancing flux through the heterologous mevalonate pathway have been investigated. Modulation of individual genes in the MevT operon by library-based engineering of operon intergenic regions led to a sevenfold increase in mevalonate titers (Pfleger et al. 2006). In addition, the development of a biosensor assay has enabled screening of large numbers of pathway mutants that resulted from a library-based approach for enhanced production of mevalonate (Pfleger et al. 2007).

Anthony et al. (2009) adopted a different approach to balancing expression of genes in the heterologous mevalonate pathway. They first developed a simplified modular cloning system which enabled identification of two rate-limiting enzymes, mevalonate kinase and amorpha-4,11-diene synthase. Optimization of promoter strength alleviated the pathway bottleneck and improved amorpha-4,11-diene production fivefold. When expression of these genes was further increased by modifying plasmid copy numbers, a sevenfold increase in amorph-4,11-diene production compared to the original strain was observed. Thus, at least two different approaches to increase amorpha-4,11-diene production in *E. coli* based solely on manipulation of the heterologous mevalonate

pathway exist. In neither case were these strains tested in high cell density fed-batch fermentations.

An engineering approach to increase production of amorpha-4,11-diene from *E. coli* was also developed (Martin et al. 2003). It had been noted that amorpha-4,11-diene initially accumulated in the culture, but the concentration subsequently decreased. Newman et al. (2006) showed that while amorpha-4,11-diene has a high boiling point (~270°C), it is also volatile when added to aqueous solutions. The addition of dodecane, a long-chain water-immiscible hydrocarbon, led to the capture of amorpha-4,11-diene produced by the culture. The amorpha-4,11-diene was then extracted from the dodecane. Addition of dodecane to a bioreactor permitted production of 0.5 g/L amorpha-4,11-diene from rich undefined medium. As an additional benefit, the volatility of amorpha-4,11-diene allowed it to be prepared in high purity for use as a standard. The use of "caryophyllene equivalents" was found to have overestimated amorpha-4,11-diene concentrations by about 30%.

Tsuruta et al. (2009) continued development of the *E. coli* fermentation process for the production of amorpha-4,11-diene. While Newman et al. (2006) used an undefined excess carbon bioprocess, Tsuruta et al. (2009) developed a carbon-restricted chemically defined process, combining this fermentation approach with modification of the heterologous mevalonate pathway. The initial strain used was analogous to that used by Martin et al. (2003); the heterologous mevalonate pathway was identical, but the host strain of *E. coli* had been changed to the more robust DH1 background (Tsuruta et al. 2009). The advanced bioprocess involved the use of a defined medium in glucose-limited fed-batch fermentation with ammonia maintained between 30 and 60 mM until 100 h (process A). Production of amorpha-4,11-diene was initiated by the addition of IPTG to induce expression of the heterologous mevalonate pathway shortly after glucose exhaustion from the initial batch culture and commencement of the feeding phase. Maximum cell density (OD_{600} of 260) was attained after 100 h with a titer of 6.5 g/L amorpha-4,11-diene. After 100 h, the levels of glucose, acetate, and ammonia became elevated, most likely due to depletion of a medium component. Process A was modified to incorporate nitrogen limitation (process B) by eliminating ammonium sulfate from the feed. The ammonia in the medium was allowed to fall to zero, although nitrogen flow into the bioreactor still occurred due to base (ammonium hydroxide) addition. Thus, process B was doubly limited in both carbon and nitrogen. Process B supported a maximum cell density (OD_{600}) of 235. However, the amorpha-4,11-diene production profile between process A and process B diverged at the time when the measured level of nitrogen became zero in process B (~50 h). Process B achieved a peak amorpha-4,11-diene titer of 16.7 g/L at 120 h, a 2.5-fold improvement in titer compared to process A (Fig. 7.3).

Concomitant with the development of the fermentation processes described above, strain engineering was also undertaken. The genes in the heterologous mevalonate pathway expressed in the *E. coli* strains developed by Martin et al. (2003) were derived from *S. cerevisiae*. While most bacteria produce isoprenoids via the MEP pathway, some low-GC Gram-positive cocci express a mevalonate pathway analogous to the eukaryotic mevalonate pathway (Boucher and Doolittle 2000). Two classes of HMG-CoA reductases based on sequence comparison were identified. Human and yeast HMG-CoA reductases belong to class I, while many bacterial HMG-CoA reductases belong to class II (Bochar et al. 1999). Subsequent studies showed significant differences in the enzymology of the two classes of HMG-CoA reductase (Hedl et al. 2004). In view of the observation that the activity of HMG-CoA reductase could limit flux through the heterologous mevalonate pathway in *E. coli*, the effect of substituting the yeast HMG-CoA reductase with either of two different class II HMG-CoA reductase genes was tested (Pitera et al. 2007). The chosen class II HMG-CoA reductase genes were from *Enterococcus faecalis* and *Staphylococcus aureus*. An earlier report described a process for producing mevalonate using *E. coli* expressing a heterologous mevalonate pathway from *E. faecalis* that

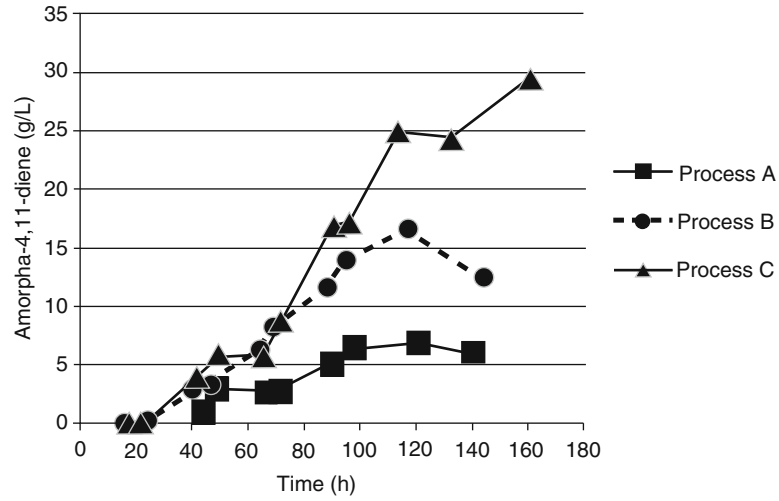

Fig. 7.3 Production of amorpha-4,11-diene in glucose-limited fed-batch fermentations by *E. coli* DH1 expressing the heterologous mevalonate pathway with yeast-derived top pathway (*atoB-ERG13-tHMG1*) in processes A and B and *S. aureus*-derived top pathway (*atoB-mvaS-mvaA*) in process C (see text for descriptions of fermentation processes)

Table 7.1 Construction of mevalonate top pathway plasmids. Enzyme activities capitalized with gene names in parentheses. *THI* acetoacetyl-CoA thiolase, *HMGS* HMG-CoA synthase, *HMGR* HMG-CoA reductase (See text for further description)

Plasmid name	Promoter	Gene 1	Codon opt?	Gene 2	Codon opt?	Gene 3	Codon opt?
pMevT	P*lac*	THI (*atoB*)	No	HMGS (*ERG13*)	No	tHMGR *(HMG1)*	No
pAM25	P*lacUV5*	THI (*atoB*)	Yes	HMGS (*ERG13*)	Yes	tHMGR *(HMG1)*	Yes
pAM34	P*lacUV5*	HMGS (*E.f. mvaS*)	No	THI/HMGR (*E.f. mvaE*)	No	n/a	n/a
pAM41	P*lacUV5*	THI (*atoB*)	Yes	HMGS (*ERG13*)	Yes	HMGR (*S.a. mvaA)*	No
pAM52	P*lacUV5*	THI (*atoB*)	Yes	HMGS *S.a. mvaS*	No	HMGR (*S.a. mvaA*)	No

produced 47 g/L of mevalonate (Tabata and Hashimoto 2004). The HMG-CoA reductase from *E. faecalis* is a class II enzyme, but is unusual in that it is fused to acetoacetyl-CoA thiolase (Hedl et al. 2002). HMG-CoA reductase from *E. faecalis* has a significantly lower V_{max} than that of other class II enzymes (including *S. aureus*) and is the only enzyme of the class that uses NADP(H) exclusively (Hedl et al. 2004). For these reasons, it was believed that the *S. aureus* HMG-CoA reductase had advantageous properties compared to the *E. faecalis* enzyme. The construction of the mevalonate "top pathway" operons is summarized in Table 7.1.

Strains expressing the heterologous mevalonate pathway containing the *S. aureus* HMG-CoA reductase produced more amorpha-4,11-diene in shake flasks than the earlier strains expressing the *S. cerevisiae* reductase. Both *S. cerevisiae* and *S. aureus* HMG-CoA reductase-expressing strains produced higher concentrations of amorpha-4,11-diene than the strain expressing the *E. faecalis* HMG-CoA reductase. Measurements of HMG-CoA reductase activity from strains expressing either *S. cerevisiae* or *E. faecalis* HMG-CoA reductases showed that the *E. faecalis* enzyme possessed significantly higher activity and was more stable in *E. coli* than the *S.*

cerevisiae enzyme. This may be due to the fact that the *S. cerevisiae* HMG-CoA reductase is a truncated enzyme containing only the catalytic domain, whereas the class II enzymes are naturally soluble. Thus, the decreased production of amorpha-4,11-diene by the strain expressing *E. faecalis* HMG-CoA cannot be explained by lower reductase activity and may reflect a limitation in acetoacetyl-CoA thiolase activity of the fused *E. faecalis* thiolase/ HMG-CoA reductase enzyme (note that this strain did not overexpress *atoB*, the *E. coli* acetoacetyl-CoA thiolase).

The strain expressing *S. aureus* HMG-CoA reductase was modified to express *S. aureus* HMG-CoA synthase in place of the *S. cerevisiae* HMG-CoA synthase (Fig. 7.4), and a further increase in production of amorpha-4,11-diene was obtained in shake flasks. Production of amorpha-4,11-diene by the strain expressing the *S. aureus* HMG-CoA synthase and reductase in process A (no ammonia limitation) surpassed that of the strain expressing exclusively *S. cerevisiae* enzymes by 2.5-fold, achieving 16.5 g/L. However, there was no further improvement of this strain by implementing process B (ammonia limitation). The *S. aureus* enzyme expressing strain was then grown in a modified ammonia-limited process (process C), whereby the amount of ammonium hydroxide in the base titrant was reduced. This process achieved production of 29.7 g/L amorpha-4,11-diene. Production of amorpha-4,11-diene was found to be reproducibly in excess of 25 g/L in additional runs (Fig. 7.3).

7.3 Development of *S. cerevisiae* to Produce Amorpha-4,11-diene

The principal product of the mevalonate pathway in *S. cerevisiae* is ergosterol, which is an essential component of membranes, although isoprenoids are also required for the biosynthesis of a number of other essential products such as ubiquinone, dolichol, heme, and farnesylated proteins. Ro et al. (2006) described manipulation of the *S. cerevisiae* mevalonate pathway to channel flux into production of amorpha-4,11-diene (Fig. 7.4).

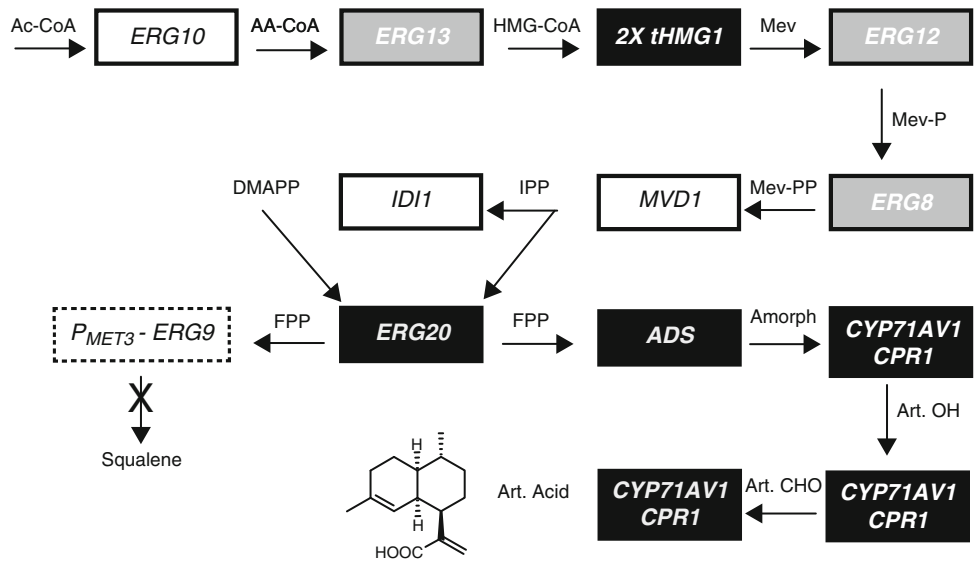

Fig. 7.4 Depiction of the mevalonate pathway in *S. cerevisiae* engineered for the production of amorpha-4,11-diene (final enzyme ADS) or artemisinic acid (final enzymes CYP71AV1 and CPR). Gene names and the enzymes they encode as Fig. 7.1 except the following: *ERG10* acetoacetyl-CoA thiolase, *IDI1* IPP isomerase, *ERG20* FPP synthase, *ERG9* squalene synthase. Genes in *black boxes* are overexpressed from the *GAL1* promoter; those in *grey boxes* are indirectly upregulated by *upc2-1* expression and *ERG9* downregulated by repression of the *MET3* promoter

Initial expression of ADS produced only low concentrations of amorpha-4,11-diene (4.4 mg/L), but a series of sequential manipulations to the mevalonate pathway resulted in substantial increases in production. Noteworthy alterations included overexpression of the catalytic domain of HMG-CoA reductase (*HMG1*: the soluble catalytic domain lacks the membrane anchor of the native enzyme, which is known to confer regulation of activity (Donald et al. 1997; Hampton et al. 1996)), overexpression of FPP synthase, and overexpression of a hyperactive allele (*UPC2-1*) of the UPC2 transcription factor known to regulate expression of many mevalonate pathway genes (Vik and Rine 2001). Another important modification was the creation of a "choke point" to limit flux into sterol production by regulation of *ERG9* (squalene synthase). This was accomplished by replacing the native promoter of *ERG9* with the methionine-regulated *MET3* promoter. The addition of methionine to the culture led to reduced *ERG9* transcription, squalene synthase production, and consequently decreased flux into sterols and increased flux into amorpha-4,11-diene (Paradise et al. 2008). The combined effects of these modifications led to the production of over 150 mg/L amorpha-4,11-diene. This concentration was almost 500-fold higher than had been previously reported for production of sesquiterpenes in *S. cerevisiae* (Jackson et al. 2003).

7.4 Conversion of Amorpha-4, 11-diene to Artemisinic Acid by *E. coli* and *S. cerevisiae*

Biological oxidations by cytochrome P450s have the advantages of regioselectivity, stereospecificity, and environmental friendliness of the reaction when compared to chemical oxidations. The simplest, cheapest semisynthetic route for the production of artemisinin requires biological production of artemisinic acid followed by chemical conversion to artemisinin. It is of considerable importance to select the production organism with the highest capacity for expression of functional CYP71AV1 and conversion of amorpha-4,11-diene to artemisinic acid. CYP71AV1 is a eukaryotic, membrane-anchored P450; this class of P450 enzymes is normally localized to the endoplasmic reticulum (Werck-Reichhart and Feyereisen 2000). *E. coli* is a prokaryote, lacking an endoplasmic reticulum, while *S. cerevisiae* is a eukaryotic model organism containing an endoplasmic reticulum that is frequently used for expression of P450 enzymes (Hamann and Møller 2007).

Chang et al. (2007) described the expression of CYP71AV1 and its cognate CPR from *A. annua* in *E. coli*. Expression of CYP71AV1 and CPR that had been codon-optimized for expression in *E. coli* led to production of low amounts of artemisinic alcohol. Additional engineering of expression levels along with changes in expression vectors, the N-terminal transmembrane sequence of AMO, the host strain, and the culture conditions, resulted in the production of 105 mg/L of artemisinic acid following 4 days of incubation at 20°C in shake flasks.

Further, strain engineering focused on developing a more robust version of the high artemisinic acid producing *E. coli* strain by moving parts of the heterologous pathway to a more stable plasmid. The stabilized strain was tested in high cell density, glucose-limited fed-batch fermentation using a chemically defined medium. Through optimization of temperature, feed profile, and induction timing, a maximum titer of 1.4 g/L artemisinic acid was achieved. Both artemisinic acid production and cell growth were temperature dependent. The optimal temperature of the production phase was determined to be 20°C. Fermentation at higher temperatures resulted in reduced artemisinic acid production, growth inhibition, and the accumulation of less oxidized intermediates.

When CYP71AV1 and CPR were expressed in *S. cerevisiae*, 115 mg/L of artemisinic acid was produced, whereas insignificant amounts of artemisinic alcohol or artemisinic aldehyde were detected (Ro et al. 2006). Artemisinic acid was found to be cell-associated, which enabled the development of a facile purification procedure yielding >95% pure artemisinic acid. The purified artemisinic acid was shown to be identical to

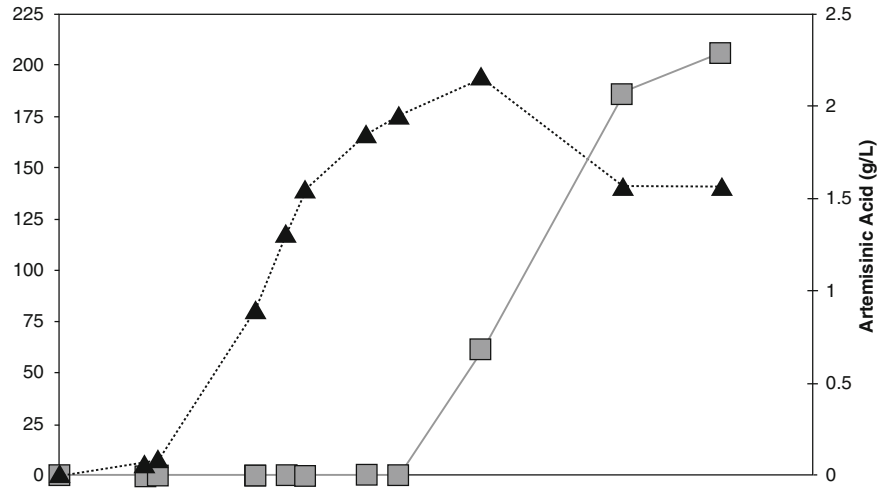

Fig. 7.5 Cell growth and artemisinic acid production by yeast in a fed-batch fermentation. OD_{600} (■), artemisinic acid (▲)

artemisinic acid isolated from the leaves of *A. annua* by nuclear magnetic resonance. Development of a defined-medium fed-batch fermentation process for the production of artemisinic acid from the *S. cerevisiae* strain described above resulted in reproducible production of 2.3 g/L of artemisinic acid after 6 days growth at 30°C (Lenihan et al. 2008; Ro et al. 2006) (Fig. 7.5).

7.5 Chemical Conversion of Artemisinic Acid or Amorpha-4,11-diene to Artemisinin

Given its unique chemical structure and biological properties, artemisinin has been a target of interest to the scientific community since its identification as the component responsible for the antimalarial activity of *A. annua* extracts (Hsu 2006; Klayman 1985; White 2008). Numerous total syntheses and semisyntheses of this target have been described in the literature (recently Haynes 2006; Kim and Sasaki 2006; Li et al. 2006). One possible synthesis, starting from artemisinic acid, is shown in Fig. 7.6 (Reiling et al. 2006). For this route to be both scalable and economical, several modifications of the previously published syntheses are required. The first step is the reduction of the 11,12 double bond to give dihydroartemisinic acid. Dihydroartemisinic acid has two stereoisomeric forms, only one of which (the *R,R* isomer) has the correct stereochemistry found in artemisinin. This reduction has typically been carried out with "nickel boride" ($NaBH_4$ + $NiCl_2$), which gives a ~3:1 ratio of dihydroartemisinic acid isomers, favoring the desired one. However, the need for a stoichiometric excess of the reducing agent and the poor isomer ratios make this reduction unacceptable from a cost perspective. We have found that catalytic hydrogenation in the presence of a variety of noble metal catalysts affords nearly quantitative amounts of the desired reduced acid in *R/S* isomer ratios >95:5 and without any overreduction to tetrahydroartemisinic acid.

The next step is the esterification of the carboxylic acid functionality. The subsequent reactions can be performed using dihydroartemisinic acid, but the presence of an ester avoids significant yield losses later in the sequence due to the formation of dihydroepideoxyarteannuin B, a five-membered lactone-containing compound.

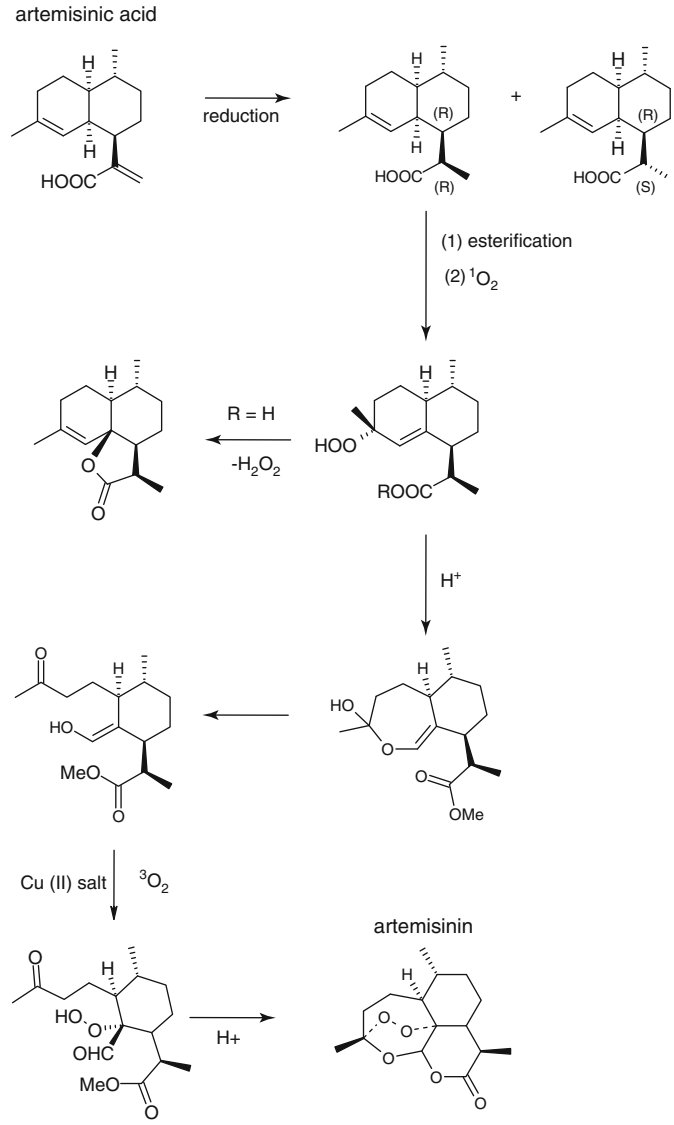

Fig. 7.6 Semisynthesis of artemisinin from artemisinic acid

Since esterification is a simple reaction to perform on an industrial scale, the focus of our research shifted to the remaining steps.

The third step is an "ene-type" reaction of the C4-C5 double bond of dihydroartemisinic acid ester with singlet oxygen ($^1O_2$, a metastable form of molecular oxygen with ~95 kJ/mol higher energy than ground state triplet oxygen $^3O_2$) to give an allylic 3-hydroperoxide. In prior syntheses, the $^1O_2$ was invariably generated by photosensitized energy transfer from dye molecules (rose bengal, methylene blue, porphyrins, etc.), but since there are very few photosynthetic processes in use at the industrial scale this project required, we sought another source of $^1O_2$. A practical alternative was found in the group VI metal salt-induced disproportionation reaction of concentrated H_2O_2 (Bohme and Brauer 1992). With this technique, the desired hydroperoxide could be formed in essentially quantitative yield in a solvent capable of conferring a reasonable lifetime to the $^1O_2$ species generated, with no evidence of possible isomeric hydroperoxides or other rearrangement products.

In the last step, the allylic hydroperoxide undergoes an acid-catalyzed Hock fragmentation and rearrangement to afford a ring-opened keto-aldehyde enol. Trapping of this enol with $^3O_2$ in the presence of a Cu(II) salt (to stabilize the desired enol form of the aldehyde) produces a vicinal hydroperoxide-aldehyde, which in a succession of acid-catalyzed rearrangements and cyclizations forms the endoperoxide bridge, the seven-membered cyclic ether and finally, a six-membered lactone, thus producing artemisinin with the correct stereochemistry (Sy and Brown 2002). Modification of this step involved substitution of expensive Cu triflate ($Cu(OSO_2CF_3)_2$, the preferred salt in published syntheses) with a less expensive alternative, replacement of pure $^3O_2$ by air, and modulation of the acidity of the medium to maximize the yield of artemisinin. These combined changes produced a four-step synthesis which can form the basis of an industrial production process.

7.6 Prospects for Development of a Commercial Process to Produce Semisynthetic Artemisinin

The work described in this chapter may form a basis for developing a commercial process for the production of semisynthetic artemisinin. The availability of a consistent additional source of artemisinin will increase the general supply and stabilize the price of artemisinin. The developments described are based on studies of the physiology of *A. annua* and advancements in the tools of synthetic biology. *E. coli* is able to produce high titers of amorpha-4,11-diene (25 g/L) following expression of a heterologous mevalonate pathway, but its ability to express functional eukaryotic P450 enzymes may present difficulties. CYP71AV1/CPR expressed in *E. coli* containing the heterologous mevalonate pathway only produced 1.5 g/L of artemisinic acid. Of particular significance, this strain was only able to produce artemisinic acid at 20°C, an unsustainably low temperature for industrial fermentation. *S. cerevisiae* was initially used solely as a platform for the functional expression and characterization of CYP71AV1 and only produced 150 mg/L of amorpha-4,11-diene. However, its ability to functionally express CYP71AV1 surpasses that of *E. coli*. A fermentation process was developed that produced 2.3 g/L artemisinic acid at 30°C, which is a realistic temperature for an industrial production process.

It appears that *S. cerevisiae* has more promise for the development of an industrial process to produce artemisinic acid. Important characteristics to be addressed in *S. cerevisiae* include not only the titer achieved, but the time taken to achieve this titer. Work so far has involved manipulation of a laboratory *S. cerevisiae* strain (S288C) primarily used for genetics research. It may be that an industrially characterized, related strain of *Saccharomyces cerevisiae* will be better suited to the development of a commercial process. The use of a heterologous, nonplant, host that does not produce significant quantities of other terpene molecules may allow the opportunity to produce a product of exceptional purity. Initial comparisons show that laboratory scale semisynthetic *S. cerevisiae*-derived artemisinin can be prepared to a purity that is comparable with plant-derived artemisinin obtained from various suppliers (Fig. 7.7). Semisynthetic artemisinin could be used as a starting material for the active pharmaceutical ingredients (artemisinin derivatives) in ACTs. Perhaps most importantly, semisynthetic artemisinin can simplify planning in the production supply chain of ACTs because a scalable, fermentation-based process does not rely on an annual plant harvest season. A sustainable, second source of artemisinin should stabilize the price and availability of ACTs and may be able to minimize the impact of market forces that have led to the drastic price spikes seen in recent years. If the work outlined in this chapter can be translated into the large-scale production and distribution of artemisinin as a starting material for ACTs, semisynthetic artemisinin will also demonstrate the potential global impact of synthetic biology.

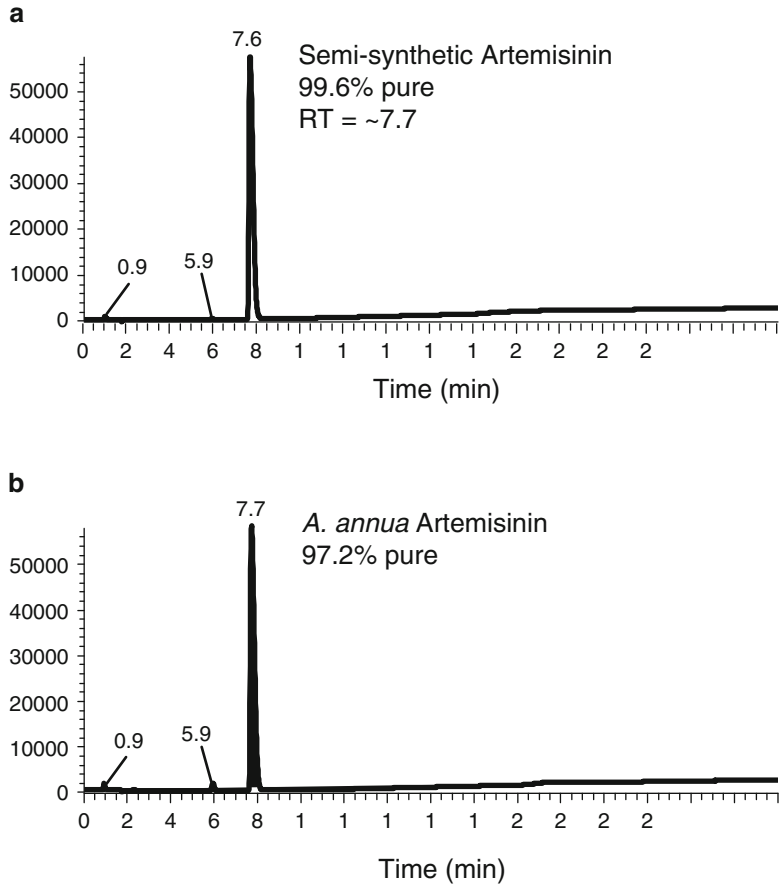

Fig. 7.7 HPLC assays of semisynthetic yeast-derived (*top*) and typical commercially available plant-derived artemisinin (*bottom*). Conditions: RP-HPLC column, C18, 100×4.6 mm, 3.5 μm; mobile-phase gradient, acetonitrile-water (50:50 to 0:100); flow rate, 1.0 mL/min; column temperature, 30°C; detection, UV at 216 nm

Acknowledgements We thank Jay Keasling and his lab members for many productive conversations. This research was conducted under the sponsorship of the Institute for OneWorld Health through the generous support of the Bill & Melinda Gates Foundation.

References

Altschul SF, Gish W, Miller W, Myers EW, Lipman DJ (1990) Basic local alignment search tool. J Mol Biol 215(3):403–410

Anthony JR, Anthony LC, Nowroozi F et al (2009) Optimization of the mevalonate-based isoprenoid biosynthetic pathway in *Escherichia coli* for production of the anti-malarial drug precursor amorpha-4,11-diene. Metab Eng 11(1):13–19

Bertea CM, Freije JR, van der Woude H et al (2005) Identification of intermediates and enzymes involved in the early steps of artemisinin biosynthesis in *Artemisia annua*. Planta Med 71(1):40–47

Bloland P (2001) Drug resistance in malaria. World Health Organization, Geneva

Bohme K, Brauer H-D (1992) Generation of singlet oxygen from hydrogen peroxide disproportionation catalyzed by molybdate ions. Inorg Chem 31:3468–3471

Bochar DA, Stauffacher CV, Rodwell VW. (1999) Sequence comparisons reveal two classes of 3-hydroxy-3-methylglutaryl coenzyme A reductase. Mol Genet Metab 66:122–127

Boucher Y, Doolittle WF (2000) The role of lateral gene transfer in the evolution of isoprenoid biosynthesis pathways. Mol Microbiol 37(4):703–716

Bouwmeester HJ, Wallaart TE, Janssen MH et al (1999) Amorpha-4,11-diene synthase catalyses the first

probable step in artemisinin biosynthesis. Phytochemistry 52(5):843–854
Chang MC, Keasling JD (2006) Production of isoprenoid pharmaceuticals by engineered microbes. Nat Chem Biol 2(12):674–681
Chang MC, Eachus RA, Trieu W, Ro DK, Keasling JD (2007) Engineering *Escherichia coli* for production of functionalized terpenoids using plant P450s. Nat Chem Biol 3:274–277
Covello PS, Teoh KH, Polichuk DR, Reed DW, Nowak G (2007) Functional genomics and the biosynthesis of artemisinin. Phytochemistry 68(14):1864–1871
Donald KA, Hampton RY, Fritz IB (1997) Effects of overproduction of the catalytic domain of 3-hydroxy-3-methylglutaryl coenzyme A reductase on squalene synthesis in *Saccharomyces cerevisiae*. Appl Environ Microbiol 63(9):3341–3344
Hale V, Keasling JD, Renninger N, Diagana TT (2007) Microbially derived artemisinin: a biotechnology solution to the global problem of access to affordable antimalarial drugs. Am J Trop Med Hyg 77(6_Suppl):198–202
Hamann T, Møller BL (2007) Improved cloning and expression of cytochrome P450s and cytochrome P450 reductase in yeast. Protein Expr Purif 56(1): 121–127
Hampton R, Dimster-Denk D, Rine J (1996) The biology of HMG-CoA reductase: the pros of contra-regulation. Trends Biochem Sci 21(4):140–145
Haynes RK (2006) From artemisinin to new artemisinin antimalarials: biosynthesis, extraction, old and new derivatives, stereochemistry and medicinal chemistry requirements. Curr Top Med Chem 6(5):509–537
Hedl M, Sutherlin A, Wilding EI et al (2002) *Enterococcus faecalis* acetoacetyl-coenzyme A thiolase/3-hydroxy-3-methylglutaryl-coenzyme A reductase, a dual-function protein of isopentenyl diphosphate biosynthesis. J Bacteriol 184(8):2116–2122
Hedl M, Tabernero L, Stauffacher CV, Rodwell VW (2004) Class II 3-hydroxy-3-methylglutaryl coenzyme A reductases. J Bacteriol 186(7):1927–1932
Henkel J, Maurer SM (2007) The economics of synthetic biology. Mol Syst Biol 3:117
Hsu E (2006) Reflections on the 'discovery' of the antimalarial qinghao. Br J Clin Pharmacol 61(6): 666–670
Jackson BE, Hart-Wells EA, Matsuda SP (2003) Metabolic engineering to produce sesquiterpenes in yeast. Org Lett 5(10):1629–1632
Kim BJ, Sasaki T (2006) Recent progress in the synthesis of artemisinin and its derivatives. Org Prep Proced Int 38(1):1–80
Kizer L, Pitera DJ, Pfleger BF, Keasling JD (2008) Application of functional genomics to pathway optimization for increased isoprenoid production. Appl Environ Microbiol 74:3229–3241.
Klayman DL (1985) Qinghaosu (artemisinin): an antimalarial drug from China. Science 228(4703):1049–1055
Korenromp E, Miller J, Nahlen B, Wardlaw T, Young M (2005) World malaria report 2005. Roll Back Malaria/ World Health Organization/UNICEF, Geneva
Lenihan JR, Tsuruta H, Diola D, Renninger NS, Regentin R (2008) Developing an industrial artemisinic acid fermentation process to support the cost-effective production of anti-malarial artemisinin-based combination therapies (ACTs). Biotechnol Prog 24(5): 1025–1032
Li Y, Huang HW, Wu Y-L (2006) Qinghaosu (artemisinin) – a fantastic antimalarial drug from a traditional Chinese medicine. In: Liang X-T, Fang W-S (eds) Medicinal chemistry of bioactive natural products. Wiley, New York, pp 183–256
Martin VJ, Pitera DJ, Withers ST, Newman JD, Keasling JD (2003) Engineering a mevalonate pathway in *Escherichia coli* for production of terpenoids. Nat Biotechnol 21(7):796–802
McCaskill D, Croteau R (1997) Prospects for the bioengineering of isoprenoid biosynthesis. Adv Biochem Eng Biotechnol 55:107–146
Newman JD, Marshall J, Chang M et al (2006) High-level production of amorpha-4,11-diene in a two-phase partitioning bioreactor of metabolically engineered *Escherichia coli*. Biotechnol Bioeng 95(4):684–691
Njau JD, Goodman CA, Kachur SP et al (2008) The costs of introducing artemisinin-based combination therapy: evidence from district-wide implementation in rural Tanzania. Malar J 7(1):4
Olumese P (2006) Guidelines for the treatment of malaria, 2nd edn. World Health Organization, Geneva
Paradise EM, Kirby J, Chan R, Keasling JD (2008) Redirection of flux through the FPP branch-point in *Saccharomyces cerevisiae* by downregulating squalene synthase. Biotechnol Bioeng 100(2):371–378
Pfleger BF, Pitera DJ, Smolke CD, Keasling JD (2006) Combinatorial engineering of intergenic regions in operons tunes expression of multiple genes. Nat Biotechnol 24:1027–1032
Pfleger BF, Pitera DJ, Newman JD, Martin VJ, Keasling JD (2007) Microbial sensors for small molecules: development of a mevalonate biosensor. Metab Eng 9:30–38
Pitera DJ, Paddon CJ, Newman JD, Keasling JD (2007) Balancing a heterologous mevalonate pathway for improved isoprenoid production in *Escherichia coli*. Metab Eng 9(2):193–207
Reiling KK, Renninger NS, McPhee DJ, Fisher KJ, Ockey DA (2006) Conversion of amorpha-4,11-diene to artemisinin and artemisinin precursors. WIPO (http://www.wipo.int/patentscope/en/) WO/2006/128126. Amyris Biotechnologies, Inc., New York
Ro DK, Paradise EM, Ouellet M et al (2006) Production of the antimalarial drug precursor artemisinic acid in engineered yeast. Nature 440(7086):940–943
Sy L-K, Brown GD (2002) The role of the 12-carboxylic group in the spontaneous autoxidation of dihydroartemisinic acid. Tetrahedron 58(5):909–923

Tabata K, Hashimoto S (2004) Production of mevalonate by a metabolically-engineered *Escherichia coli*. Biotechnol Lett 26(19):1487–1491

Teoh KH, Polichuk DR, Reed DW, Nowak G, Covello PS (2006) *Artemisia annua* L. (Asteraceae) trichome-specific cDNAs reveal CYP71AV1, a cytochrome P450 with a key role in the biosynthesis of the antimalarial sesquiterpene lactone artemisinin. FEBS Lett 580(5):1411–1416

Tsuruta H, Paddon CJ, Eng D, Lenihan JR et al (2009) High-level production of amorpha-4,11-diene, a precursor of the antimalarial agent artemisinin, in *Escherichia coli*. PLoS One 4:e4489

van Agtmael MA, Eggelte TA, van Boxtel CJ (1999) Artemisinin drugs in the treatment of malaria: from medicinal herb to registered medication. Trends Pharmacol Sci 20(5):199–205

Vik A, Rine J (2001) Upc2p and Ecm22p, dual regulators of sterol biosynthesis in *Saccharomyces cerevisiae*. Mol Cell Biol 21(19):6395–6405

Werck-Reichhart D, Feyereisen R (2000) Cytochromes P450: a success story. Genome Biol 1(6): REVIEWS3003

White NJ (2008) Qinghaosu (artemisinin): the price of success. Science 320(5874):330–334

Zhang Y, Teoh KH, Reed DW, Maes L, Goossens A, Olson DJ, Ross AR, Covello PS. (2008) The molecular cloning of artemisinic aldehyde Delta11(13) reductase and its role in glandular trichome-dependent biosynthesis of artemisinin in Artemisia annua. J Biol Chem 283: 21501–21508

Zeng Q, Qiu F, Yuan L (2007) Production of artemisinin by genetically-modified microbes. Biotechnol Lett 30(4):581–592

Artemisinin: Controlling Its Production in *Artemisia annua*

8

Pamela Weathers, Melissa Towler, Yi Wang, and Kristin K. Wobbe

Abstract

Artemisinin, a potent antimalarial sesquiterpene lactone, is produced in low quantities by the plant *Artemisia annua* L. We used inhibitors of both the mevalonate and nonmevalonate terpenoid pathways to study in both seedlings and hairy root cultures the source of isopentenyl diphosphate (IPP), the channeling of carbon from sterols to sesquiterpenes, and the role that sugars may play in controlling artemisinin biosynthesis. Together, our results indicated that artemisinin is likely biosynthesized from IPP pools originating in both the plastid and the cytosol and that channeling of carbon can be directed away from competing sterol pathways and toward sesquiterpenes. Although glucose stimulated artemisinin production, the response is very complex with ratios of glucose to fructose involved; artemisinin levels increased proportionate to increasing amounts of glucose. Disaccharides mainly inhibited artemisinin production, but the response was less definitive. Glucose also increased expression of some of the genes in the artemisinin biosynthetic pathway, thereby suggesting that this sugar is acting not only as a carbon source but also as a signal. As we develop a better understanding of the regulation of the artemisinin biosynthetic pathway, results suggest that many factors can possibly be harnessed to increase artemisinin production in *A. annua*.

Keywords

Amorphadiene synthase • CYP71AV1 • DMSO • Elicitation • Sugar signals

P. Weathers (✉) • M. Towler • Y. Wang
Biology and Biotechnology Department, Worcester Polytechnic Institute, Worcester, MA 01609, USA
e-mail: weathers@wpi.edu

K.K. Wobbe
Chemistry and Biochemistry Department, Worcester Polytechnic Institute, Worcester, MA 01609, USA

8.1 Introduction

Artemisinin (Fig. 8.1) and its derivatives are the most important drugs for treatment of malaria and, as part of a multidrug cocktail, *a*rtemisinin *c*ombination *t*herapy (ACT), minimize the

T.J. Bach and M. Rohmer (eds.), *Isoprenoid Synthesis in Plants and Microorganisms: New Concepts and Experimental Approaches*, DOI 10.1007/978-1-4614-4063-5_8,

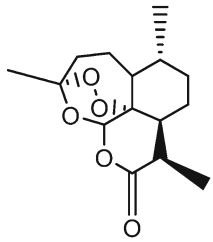

Fig. 8.1 Structure of artemisinin

development of resistant forms of the infecting parasite. Besides malaria, artemisinin also has been shown to be effective against other infectious agents including human cytomegaloviruses, herpes simplex, hepatitis B and C (Efferth et al. 2002; Romero et al. 2005), *Toxoplasma gondii* (Jones-Brando et al. 2006; D'Angelo et al. 2009), *Schistosoma* (Utzinger et al. 2001), and *Pneumocystis carinii* (Merali and Meshnick 1991). Artemisinin derivatives have also shown efficacy against numerous cancers (Singh and Lai 2004; Nam et al. 2007; de Vries and Dien 1996). Thus, there is an urgent need for considerable quantities of the drug. Unfortunately, there is currently not even enough artemisinin produced to treat malaria, let alone any of these other diseases.

Field-grown plants of *Artemisia annua* L. still remain the main source of the drug. After 4–6 months of growth, the plant produces ≤1.8% artemisinin of its total shoot dry weight, and this amount varies depending on environmental conditions. Much is still not known about the control of its biosynthesis *in planta*, and not all of the biosynthetic steps are confirmed. Here, we describe some of our recent efforts to enhance our general understanding of artemisinin biosynthesis and its regulation.

8.2 Where Does Artemisinin IPP Originate?

Terpenes in plants are produced by the successive condensation of multiple subunits of isopentenyl diphosphate (IPP), which can originate from one of two sources: either from the cytosolic mevalonic acid pathway (MVA) or from the plastidic nonmevalonic acid independent pathway (MEP) (Fig. 8.2a). IPP can shuttle between these two cellular compartments depending on the plant species and the product being synthesized (Laule et al. 2003; Hampel et al. 2005; Dudareva et al. 2005). For example, in monocots (Maier et al. 1998) and bryophytes (Adam et al. 1998), all the IPP for sesquiterpenes derives from the MEP pathway. In contrast, dicots from the Compositae, plants closely related to *A. annua*, derive their IPP in sesquiterpenes from both the MEP and the MVA pathways (Adam and Zapp 1998; Steliopoulos et al. 2002). Until recently (Towler and Weathers 2007), the source of IPP leading to artemisinin biosynthesis in *A. annua* was not known.

We used inhibitors specific to either the MVA or the MEP pathway to determine the effect of each on the routing of IPP for artemisinin production in 14-day axenic seedlings of *A. annua* (YU strain) (Towler and Weathers 2007). Fosmidomycin (FOS) inhibits the first enzyme, DXR (1-deoxy-D-xylulose 5-phosphate reductoisomerase), in the MEP pathway (Rodríguez-Concepción et al. 2004), while mevinolin (MEV) inhibits the enzyme HMG-CoA reductase in the MVA pathway (Bach and Lichtenthaler 1983). After 14 days of incubation and growth in the inhibitors, shoots were harvested, weighed, and extracted for artemisinin analysis by HPLC. Growth was inhibited from 30% to 40% when seedlings were grown in either FOS or MEV, but when both inhibitors were added, growth inhibition was effectively doubled, indicating an additive effect (Table 8.1). Inhibition of growth was about the same for roots and shoots; however, in FOS shoots also became chlorotic, probably because of the inhibition of chlorophyll synthesis (Towler and Weathers 2007). Each inhibitor also significantly inhibited artemisinin production about 70–80%; in the presence of both FOS and MEV, no artemisinin was detected in the seedlings (Table 8.1). Together, these data show that artemisinin is likely synthesized using IPP originating from both the MEP and the MVA pathways.

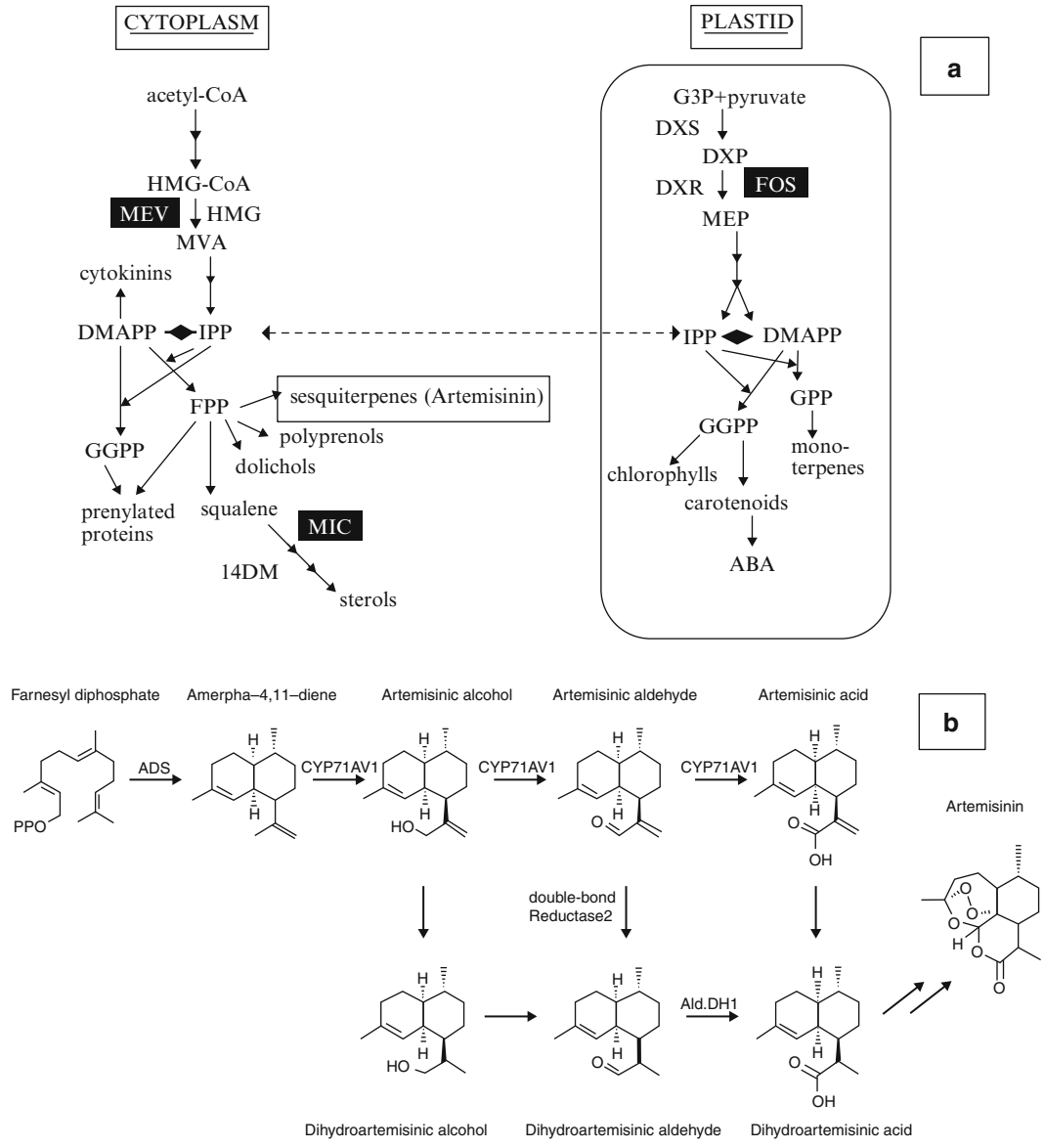

Fig. 8.2 Terpene and artemisinin metabolism showing (**a**) IPP compartmentalization and points of inhibition for metabolic studies. (**b**) Artemisinin biosynthesis post FPP (latter adapted from a graphic courtesy of KH Teoh). *HMG-CoA* hydroxymethylglutaryl CoA, *MEV* mevinolin, *HMGR* HMG-CoA reductase, *MVA* mevalonic acid, *DMAPP* dimethylallyl diphosphate, *IPP* isopentenyl diphosphate, *FPP* farnesyl diphosphate, *GGPP* geranylgeranyl diphosphate, *MIC* miconazole, *14DM* 14α-demethylase, *G3P* glyceraldehyde 3-phosphate, *DXP* deoxyxylulose 5-phosphate, *DXR* DXP reductoisomerase, *FOS* fosmidomycin, *DXS* DXP synthase, *MEP* methyl-erythritol 4-phosphate, *GPP* geranyl diphosphate, *ABA* abscisic acid, *ADS* amorphadiene synthase, *CYP71AV1* p450 catalyst specific to artemisinin biosynthesis

Table 8.1 Both FOS and MEV inhibit growth and artemisinin production in 14-day seedlings of *A. annua*

Organ	CON	FOS	MEV	FOS + MEV
Growth after 14 days (mg FW/plantlet)				
Roots	61.1a	42.0b	40.6b	16.7b
Shoots	56.0a	43.0b	35.7b	17.7c
Total	117.1a	85.0b	76.3b	34.4c
Artemisinin levels in shoots (relative %)				
	100	20	32	Nd

Letters after numbers indicate statistical difference at $p \leq 0.05$
Nd not detectable, *CON* control, *FOS* fosmidomycin, *MEV* mevinolin

8.3 Channeling Carbon Toward Artemisinin Biosynthesis

The complex terpenoid pathway offers several points whereby carbon can be rerouted, and for artemisinin, one especially attractive point is at farnesyl diphosphate (FDP) where sesquiterpenes and sterols diverge into separate branches (Fig. 8.2a). Shunting carbon from sterol biosynthesis to sesquiterpenes has been demonstrated in both yeast and plants through either genetic engineering or inhibition of specific enzymes (Asadollahi et al. 2008; Ro et al. 2006). These two pathways have shown evidence of coordinate control; conditions that stimulate sesquiterpene production also cause a decrease in sterols (Vögeli and Chappell 1988). Using similar reasoning, miconazole (MIC), an inhibitor of sterol 14α-demethylases (Zarn et al. 2003), was fed to *A. annua* shoot cultures (Woerdenbag et al. 1993; Kudakasseril et al. 1987) to inhibit sterol biosynthesis and to shunt carbon instead toward sesquiterpenes, and artemisinin increased. We further showed in *A. annua* seedlings that in the presence of MIC, artemisinin concentrations rose significantly (Table 8.2) compared to uninhibited controls, demonstrating that indeed carbon flux was likely rerouted from sterol biosynthesis toward sesquiterpenes and artemisinin production (Towler and Weathers 2007). Together, these results show that inducible shunting of carbon is a reasonable strategy for engineering increased levels of artemisinin *in planta*.

Table 8.2 Artemisinin production is stimulated by both inhibition of sterol biosynthesis and addition of DMSO in *A. annua* seedlings

Tissue	No treatment	Miconazole in DMSO	DMSO
Growth after 14 days (mg DW/seedling)			
Shoots	5.45a	5.23a	4.70a
Roots	6.34a	5.87a	7.81a
Total	11.80a	11.10a	12.51a
Artemisinin levels in shoots (relative %)			
	100	575	1,160

Letters after numbers indicate statistical difference at $p \leq 0.05$

8.4 Elicitation Effects on Artemisinin Production

More traditional approaches for increasing artemisinin production in culture have focused on use of nutrients (Wang and Tan 2002) and other cues including phytohormones (Weathers et al. 2005; Woerdenbag et al. 1993), chitosan (Putalun et al. 2007), light (Wang et al. 2001; Souret et al. 2003), or other abiotic elicitors (Ferreira et al. 1995; Baldi and Dixit 2008). Success, however, has been limited. For example, although Putalun et al. (2007) showed that chitosan increased artemisinin yields in *A. annua* hairy roots sixfold to a final concentration of about 1.8 mg/g DW, we could not confirm their work and also did not see any significant stimulation of artemisinin production in the presence of abiotic elicitors or methyl jasmonate in hairy roots (Ryan 1996) or seedlings (Fig. 8.3). Early experiments appeared to show that methyl jasmonate had some effect (Fig. 8.3). That experiment, however, required dissolving methyl jasmonate in DMSO, and when compared to the DMSO-only controls, the artemisinin production in the presence of methyl jasmonate was not statistically significant (Fig. 8.3).

Although none of the standard elicitors seemed to have increased production of artemisinin, we observed on numerous occasions that DMSO did. Indeed, both our studies with miconazole (Table 8.2; Towler and Weathers 2007) and with methyl jasmonate (Fig. 8.3) showed that the DMSO controls produced significant increases in artemisinin beyond the untreated control.

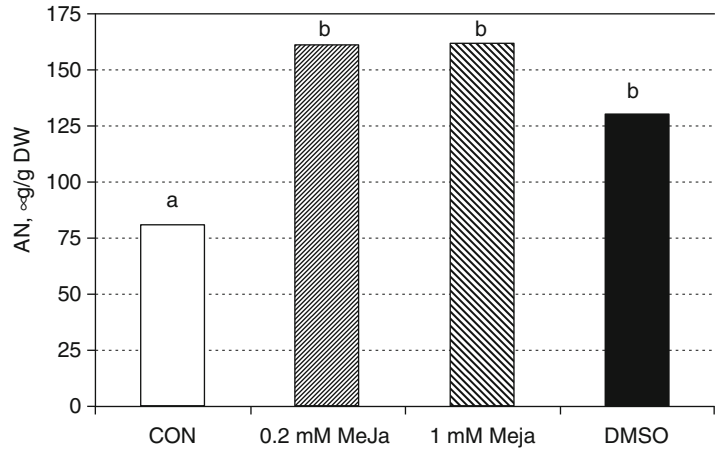

Fig. 8.3 Artemisinin is not elicited by methyl jasmonate in *A. annua* seedlings. *CON* untreated control, *MeJa* methyl jasmonate, *DMSO* dimethyl sulfoxide. Both the MeJa and the DMSO treated seedlings were provided DMSO at 0.5% (v/v). Different letters indicate statistical difference at $p \leq 0.5$

This stimulatory effect on artemisinin or any other secondary metabolite production has not to our knowledge been previously reported. In *A. annua*, DMSO is detected only by the roots, not the shoots, and was shown to increase peroxide levels in the plant resulting in enhanced dihydroartemisinic acid and artemisinin production in the leaves (Mannan et al. 2010).

8.5 Sugars Affect Artemisinin Production

A number of years ago, we serendipitously observed that when filter-sterilized medium was used to culture hairy roots of *A. annua*, the yield of artemisinin was more consistent. During autoclaving, sucrose is partially hydrolyzed to glucose and fructose (Schenk et al. 1991) as well as to small amounts of toxic products including furfurals (Rédei 1974), so autoclaving of sucrose produces an undefined medium with differing ratios of glucose, fructose, and sucrose (Weathers et al. 2004). We observed that both growth and artemisinin levels of *A. annua* hairy roots were further affected by the type of sugar provided in the culture medium. Glucose inhibited root growth, while sucrose and fructose stimulated it (Weathers et al. 2004). Production of artemisinin, however, was increased 300% and 200% by glucose and fructose, respectively, when compared to sucrose (Weathers et al. 2004). Sugars have been known for some time to play key regulatory roles in plant growth and development (Jang and Sheen 1994; Rolland et al. 2006), but our results suggested they may also be affecting the production of the secondary metabolite, artemisinin.

Others had reported that sugars had some effects on secondary metabolites, including in *Vitis vinifera*, where Larronde et al. (1998) showed that sucrose dramatically stimulated the production of anthocyanins. In an effort to provide clues to the mechanism of this sugar effect, they also used several glucose analogs. Mannose, which can be transported into plants and phosphorylated by hexokinase, mimicked the effect of sucrose in the production of anthocyanins, while another glucose analog, 3-*O*-methylglucose (3OMG), which can be taken up into plant cells but only slowly phosphorylated by hexokinase (HXK), did not. Mannoheptulose is a specific inhibitor of HXK, and when it was added, anthocyanin production by sucrose was inhibited. It was later suggested that HXK appeared to be involved in a sugar signal transduction pathway related to anthocyanin production (Vitrac et al. 2000).

8.5.1 Monosaccharide Effects on *A. annua* and Artemisinin

Considering these results, we subsequently used sugars alone, in combination, or with their

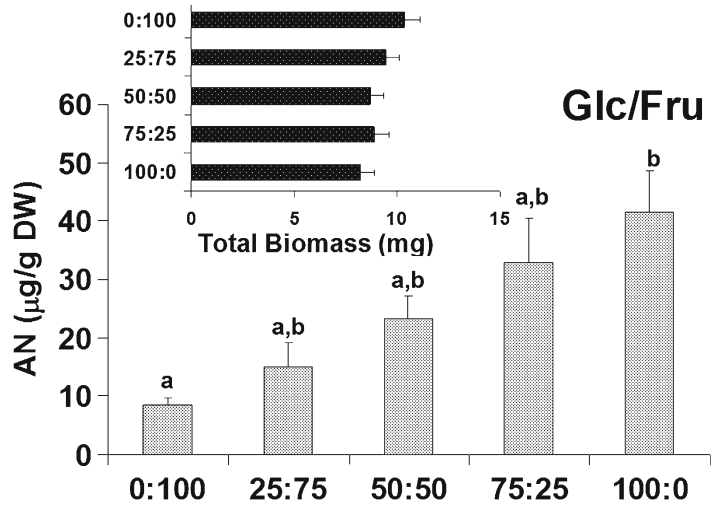

Fig. 8.4 Effect of increasing glucose concentrations relative to fructose on biomass and artemisinin production in *A. annua* 14-day seedlings. *AN* artemisinin (µg), *glc* glucose, *fru* fructose. Different letters indicate statistical difference at $p \leq 0.5$

respective analogs to investigate their role in the production of artemisinin in *A. annua* seedlings. When compared to sucrose, glucose increased artemisinin in seedling shoots by >200%; in contrast, fructose decreased artemisinin production by about 50% (Wang and Weathers 2007). Because it appeared in our earlier work that the plant was sensitive to varying ratios of glucose, fructose, and sucrose, we fed seedlings differing ratios of glucose to sucrose, but saw no significant differences in artemisinin production. When fed different ratios of glucose to fructose, however, specific artemisinin levels increased in direct proportion to increases in the relative glucose concentration (Fig. 8.4; Wang and Weathers 2007). These results suggested that artemisinin production was indeed responding to changing amounts of glucose in the seedling culture media. This stimulation by glucose was also observed in *A. annua* hairy root cultures, but the response was not as dramatic (Weathers et al. 2004).

We then used three glucose analogs, 3-*O*-methylglucose (3OMG), mannose, and mannitol, to obtain some clues on the possible mechanism of glucose control of artemisinin production. Although the 3OMG analog can be transported into the cell and phosphorylated to 3-*O*-methyl glucose-6-phosphate by HXK, the rate of phosphorylation is about 5 orders of magnitude slower than for mannose or glucose (Cortès et al. 2003), and thus this analog is useful to determine if HXK is involved in glucose sensing. Mannose can also be transported into the cell and phosphorylated to mannose-6-phosphate, but is thereafter very slowly metabolized (Pego et al. 1999; Baskin et al. 2001). Mannitol alters osmotic pressure; it does not enter and is not metabolized by most plant cells (Gibson 2000). Inhibition of a specific process by 3OMG would suggest involvement of HXK (Gonzali et al. 2002; Cortès et al. 2003), while inhibition by mannose might suggest that a step downstream of HXK is involved (Pego et al. 1999; Baskin et al. 2001). Any effect by mannitol suggests an osmotic effect or possible involvement of a monosaccharide transporter (Gibson 2000).

Each analog at 3 g/L along with glucose at 27 g/L was fed to seedlings for 14 days. Shoots were then harvested, weighed, and extracted for assay of artemisinin by HPLC. The analog 3OMG decreased artemisinin production >90%. Mannitol, on the other hand, seemed to stimulate artemisinin production by 50%, while mannose showed no significant effect on artemisinin yield compared to glucose (Fig. 8.5; Wang and Weathers 2007). Mannitol and 3OMG both decreased overall growth by about 30% (Fig. 8.5). Although the stimulation of artemisinin production by mannitol is interesting, there is no apparent explanation for this response and, thus, requires more study. Together, these results suggest that glucose plays some key role in regulating

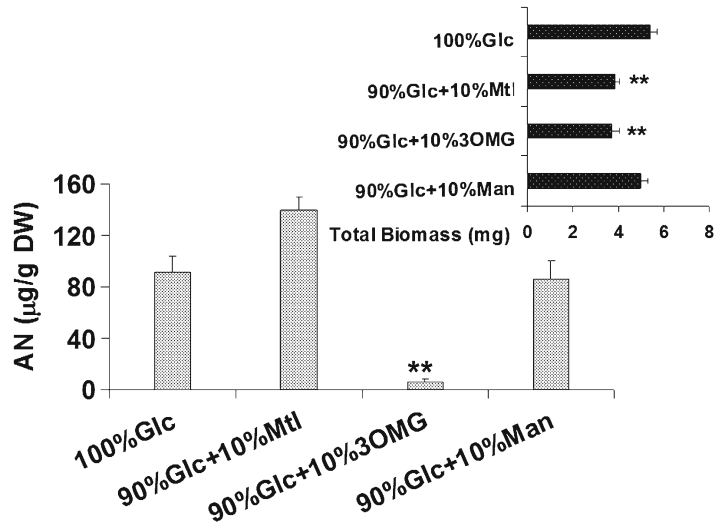

Fig. 8.5 Effect of glucose and its analogs on growth and artemisinin production in 14-day seedlings of *A. annua*. *Glc* glucose, *Mtl* mannitol, *Man* mannose, *3OMG* 3-*O*-methyl glucose, *AN* artemisinin(µg); **, $p \leq 0.01$

artemisinin production possibly through one of the glucose signaling pathways involving HXK because of the strong inhibition by 3OMG.

We also used tagatose, a stereoisomer of D-fructose, and found that when added in small amounts to fructose, it inhibited both growth and artemisinin production ~50% compared to fructose. Tagatose is not metabolized by plant cells, and its mechanism of inhibition is not yet understood; however, it has been hypothesized that if the analog were transported into cells, it would be phosphorylated by HXK to yield tagatose-6-phosphate (Kim 2004). Together, the results using tagatose support the results showing that increasing amounts of fructose relative to glucose are inhibitory to artemisinin production and that fructose clearly plays a role in regulating this sesquiterpene.

8.5.2 Disaccharide Effects on *A. annua* and Artemisinin

Disaccharides also seemed to interfere with artemisinin biosynthesis. We added palatinose, trehalose, maltose, cellobiose, or lactose as 10% of total sugars with the remaining 90% as sucrose. Compared to 100% sucrose, seedlings fed either palatinose or trehalose in conjunction with sucrose showed decreased biomass (Fig. 8.6). Palatinose and cellobiose, however, significantly inhibited artemisinin production up to 75% compared to plantlets grown in 100% sucrose. Palatinose is a sucrose analog that cannot be transported into cells through the sucrose transporter and is not made by plants. It is used to identify signals that may be detected external to the plant or by the sucrose transporter. As an example, extracellular invertases are induced by palatinose (Sinha et al. 2002). Although the role of cellobiose, the smallest subunit of cellulose, is not well understood, it is likely produced during cell wall degradation by pathogenic fungi and may, thus, play a role in pathogen defense. For example, cellobiose inhibits cellulase (Mandels and Reese 1965) and when added in conjunction with a fungal extract, stimulates lignin production in peach bark wounds (Biggs 1990). In *A. annua*, however, cellobiose inhibition of artemisinin production does not seem connected to pathogen defense.

8.5.3 Sugars Affect Artemisinin Gene Regulation

To determine if glucose, fructose, and sucrose affect mRNA transcription of the genes in the artemisinin biosynthetic pathway, young seedlings of *A. annua* were fed one of those

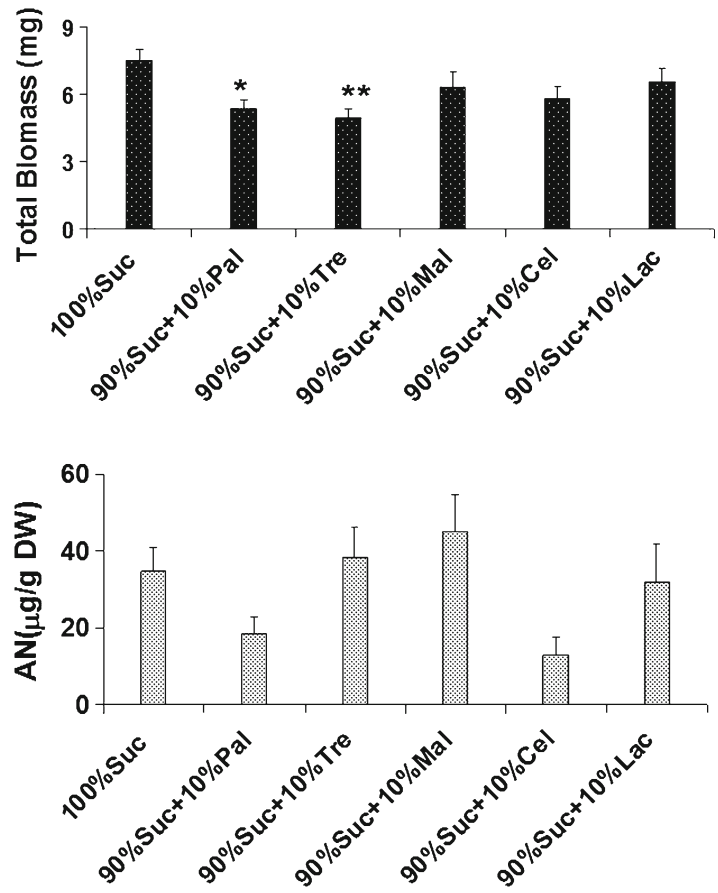

Fig. 8.6 Effect of sucrose and its analogs on growth and artemisinin production in 14-day seedlings of *A. annua*. *AN* artemisinin, *Suc* sucrose, *Pal* palatinose, *Tre* trehalose, *Mal* maltose, *Cel* cellobiose, *Lac* lactose; ** $p \leq 0.01$; * $p \leq 0.05$

three sugars for 14 days and then harvested. RNA was extracted from the shoots and real-time PCR was used to measure mRNA transcription using probes generated from the highly conserved regions of genes encoding enzymes that are associated with artemisinin biosynthesis including HMGR, FPS, DXS, DXR, SQS, ADS, and CYP71AV1. Results showed that compared to sucrose, glucose significantly upregulated and fructose downregulated transcription of both *ADS* and *CYP71AV1* in young seedlings (Fig. 8.7), providing further evidence that sugars, in particular glucose and fructose, are acting as signals to regulate artemisinin production (Arsenault et al. 2010a).

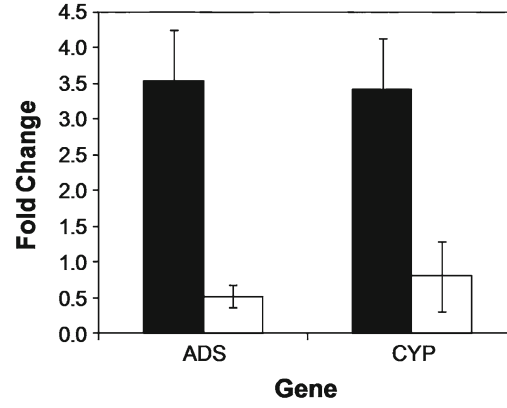

Fig. 8.7 Transcriptional response of *ADS* and C*YP71AV1* genes to glucose and fructose relative to sucrose in 7-day seedlings of *A. annua*. *Black* glucose, *white* fructose

Overall, these results suggest that both monosaccharide and disaccharide sugars may play a role well beyond that of a carbon source in downstream regulation of secondary metabolites like artemisinin and that the mechanism of these responses is complex.

8.6 Conclusions and Future Directions

In our efforts to provide a better understating of how artemisinin production is regulated in *A. annua* plants, we were the first to have shown that this sesquiterpene lactone is produced from IPP produced both in the cytosol via the MVA pathway and also from IPP stemming from the MEP pathway in the plastid. Additional inhibitor studies confirm earlier work with shoot cultures that indicated carbon can be rerouted from sterol production toward sesquiterpenes resulting in increased artemisinin. Although we have not observed any significant increase in artemisinin using typical elicitation molecules like methyl jasmonate or chitosan, we were the first to show that DMSO increases artemisinin production significantly, probably by increasing the ROS peroxide. Furthermore, compared to sucrose, artemisinin production is enhanced by glucose, inhibited by fructose, and particularly sensitive to the ratio of these two monosaccharides. Disaccharides also affect artemisinin production, but the response is not well understood. The increase in artemisinin production by glucose appears to be the result of the perception by the plant of glucose as a sugar signal, and this is further supported by results showing that at least two of the enzymes, ADS and CYP71AV1, in the artemisinin biosynthetic pathway are upregulated after seedlings are grown 14 days in glucose.

The mechanisms of action of both the DMSO and sugar stimuli have been further studied to show modulation of gene expression and metabolite levels during reproductive development of *A. annua* (Arsenault et al. 2010b), including at the level of leaf trichome formation. Although some progress has been made, as summarized in the review by Nguyen et al. (2011), the mechanisms of overall regulation of artemisinin synthesis require more study, as holds true with optimizing and upscaling the culture conditions of artemisinin-producing hairy root cultures (Sivakumar et al. 2010).

Acknowledgments The authors are indebted to Worcester Polytechnic Institute, the Arkansas Bioscience Institute, and NIH 2R15GM069562-03 for partial financial support of this work. Special thanks to Dan Vail (WPI) for Fig. 8.7.

References

Adam K, Zapp J (1998) Biosynthesis of the isoprene units of chamomile sesquiterpenes. Phytochemistry 48:953–959

Adam K, Thiel R, Zapp J, Becker H (1998) Involvement of the mevalonic acid pathway and the glyceraldehyde-pyruvate pathway in terpenoid biosynthesis of the liverworts *Ricciocarpos natans* and *Conocephalum conicum*. Arch Biochem Biophys 354:181–187

Arsenault PR, Vail D, Wobbe KK, Weathers PJ (2010a) Effect of sugars on artemisinin production in *Artemisia annua* L.: transcription and metabolite measurements. Molecules 15:2302–2318

Arsenault PR, Vail D, Wobbe KK, Erickson K, Weathers PJ (2010b) Reproductive development modulates gene expression and metabolite levels with possible feedback inhibition of artemisinin in *Artemisia annua*. Plant Physiol 154:958–968

Asadollahi MA, Maury J, Møller K, Nielsen KF, Schalk M, Clark A, Nielsen J (2008) Production of plant sesquiterpenes in *Saccharomyces cerevisiae*: effect of *ERG9* repression on sesquiterpene biosynthesis. Biotechnol Bioeng 99:666–677

Bach TJ, Lichtenthaler HK (1983) Inhibition by mevinolin of plant growth, sterol formation and pigment accumulation. Physiol Plant 59:50–60

Baldi A, Dixit VK (2008) Yield enhancement strategies for artemisinin production by suspension cultures of *Artemisia annua*. Bioresour Technol 99:4609–4614

Baskin TI, Remillong EL, Wilson JE (2001) The impact of mannose and other carbon sources on the elongation and diameter of the primary root of *Arabidopsis thaliana*. Aust J Plant Physiol 28:481–488

Biggs AR (1990) Managing wound-associated disease by understanding wound healing in the bark of woody plants. J Arboric 16:108–112

Cortès S, Gromova M, Evrard A, Roby C, Heyraud A, Rolin DB, Raymond P, Brouquisse RM (2003) In plants, 3-*O*-methylglucose is phosphorylated by hexokinase but not perceived as a sugar. Plant Physiol 131:824–837

D'Angelo JG, Bordón C, Posner GH, Yolken R, Jones-Brando L (2009) Artemisinin derivatives inhibit

Toxoplasma gondii in vitro at multiple steps in the lytic cycle. J Antimicrob Chemother 63:146–150

de Vries PJ, Dien TK (1996) Clinical pharmacology and therapeutic potential of artemisinin and its derivatives in the treatment of malaria. Drugs 52:818–836

Dudareva N, Andersson S, Orlova I, Gatto N, Reichelt M, Rhodes D, Boland W, Gershenzon J (2005) The non-mevalonate pathway supports both monoterpene and sesquiterpene formation in snapdragon flowers. Proc Natl Acad Sci USA 102:933–938

Efferth T, Marschall M, Wang X, Huong SM, Hauber I, Olbrich A, Kronschnabl M, Stamminger T, Huang ES (2002) Activity of artesunate towards wild-type, recombinant GFP-expressing sensitive and ganciclovir-resistant human cytomegaloviruses. J Mol Med 80:233–242

Ferreira JF, Simon JE, Janick J (1995) Relationship of artemisinin content of tissue-cultured, greenhouse-grown, and field-grown plants of *Artemisia annua*. Planta Med 61:351–355

Gibson SI (2000) Plant sugar-response pathways: part of a complex regulatory web. Plant Physiol 124:1532–1539

Gonzali S, Alpi A, Blando F, Bellis LD (2002) *Arabiodopsis* (HXK1 and HXK2) and yeast (HXK2) hexokinases over expressed in transgenic lines are characterized by different catalytic properties. Plant Sci 163:943–954

Hampel D, Mosandl A, Wust M (2005) Biosynthesis of mono- and sesquiterpenes in carrot roots and leaves (*Daucus carota* L.): metabolic cross talk of cytosolic mevalonate and plastidial methylerythritol phosphate pathways. Phytochemistry 66:305–311

Jang JC, Sheen J (1994) Sugar sensing in higher plants. Plant Cell 6:1665–1679

Jones-Brando L, D'Angelo J, Posner GH, Yolken R (2006) In vitro inhibition of *Toxoplasma gondii* by four new derivatives of artemisinin. Antimicrob Agents Chemother 50:4206–4208

Kim P (2004) Current studies on biological tagatose production using L-arabinose isomerase: a review and future perspective. Appl Microbiol Biotechnol 65:243–249

Kudakasseril GJ, Lam L, Staba EJ (1987) Effect of sterol inhibitors on the incorporation of ^{14}C-isopentenyl pyrophosphate into artemisinin by a cell-free system from *Artemisia annua* tissue cultures and plants. Planta Med 53:280–284

Larronde F, Krisa S, Decendit A, Chèze C, Deffieux G, Mérillon JM (1998) Regulation of polyphenol production in *Vitis vinifera* cell suspension cultures by sugars. Plant Cell Rep 17:946–950

Laule O, Fürholz A, Chang HS, Zhu T, Wang X, Heifetz PB, Gruissem W, Lange BM (2003) Crosstalk between cytosolic and plastidial pathways of isoprenoid biosynthesis in *Arabidopsis thaliana*. Proc Natl Acad Sci USA 100:6866–6871

Maier W, Schneider B, Strack D (1998) Biosynthesis of sesquiterpenoid cyclohexenone derivatives in mycorrhizal barley roots proceeds via the glyceraldehyde 3-phosphate/pyruvate pathway. Tetrahedron Lett 39:521–524

Mandels M, Reese ET (1965) Inhibition of cellulases. Annu Rev Phytopathol 3:85–102

Mannan A, Liu CZ, Arsenault PR, Towler MJ, Vail DR, Lorence A, Weathers PJ (2010) DMSO triggers the generation of ROS leading to an increase in artemisinin and dihydroartemisinic acid in *Artemisia annua* shoot cultures. Plant Cell Rep 29:143–152

Merali S, Meshnick SR (1991) Susceptibility of *Pneumocystis carinii* to artemisinin in vitro. Antimicrob Agents Chemother 35:1225–1227

Nam W, Tak J, Ryu JK, Jung M, Yook JI, Kim HJ, Cha IH (2007) Effects of artemisinin and its derivatives on growth inhibition and apoptosis of oral cancer cells. Head Neck 29:335–340

Nguyen KT, Arsenault PR, Weathers PJ (2011) Trichomes + roots + ROS = artemisinin: regulating artemisinin biosynthesis in *Artemisia annua* L. In Vitro Cell Dev Biol Plant 47:329–338

Pego JV, Weisbeek PJ, Smeekens SCM (1999) Mannose inhibits *Arabidopsis* germination via a hexokinase-mediated step. Plant Physiol 119:1017–1023

Putalun W, Luealon W, De-Eknamkul W, Tanaka H, Shoyama Y (2007) Improvement of artemisinin production by chitosan in hairy root cultures of *Artemisia annua* L. Biotechnol Lett 29:1143–1146

Rédei GP (1974) 'Fructose effect' in higher plants. Ann Bot 38:287–297

Ro DK, Paradise EM, Ouellet M, Fisher KJ, Newman KL, Ndungu JM, Ho KA, Eachus RA, Ham TS, Kirby J, Chang MC, Withers ST, Shiba Y, Sarpong R, Keasling JD (2006) Production of the antimalarial drug precursor artemisinic acid in engineered yeast. Nature 440:940–943

Rodríguez-Concepción M, Forés O, Martínez-García JF, González V, Phillips MA, Ferrer A, Boronat A (2004) Distinct light-mediated pathways regulate the biosynthesis and exchange of isoprenoid precursors during *Arabidopsis* seedling development. Plant Cell 16: 144–156

Rolland F, Baena-Gonzalez E, Sheen J (2006) Sugar sensing and signaling in plants: conserved and novel mechanisms. Annu Rev Plant Biol 57:675–709

Romero MR, Efferth T, Serrano MA, Castaño B, Macias RIR, Briz O, Marin JJG (2005) Effect of artemisinin/artesunate as inhibitors of hepatitis B virus production in an "in vitro" replicative system. Antiviral Res 68:75–83

Ryan JF (1996) The examination of culture conditions, biomass optimization, and terpene elicitation with chitosan, heavy metals, and light exposure of transformed roots cultures of Artemisia annua. M.S. thesis (Biotechnology), Worcester Polytechnic Institute, Worcester

Schenk N, Hsiao K-C, Bornman CH (1991) Avoidance of precipitation and carbohydrate breakdown in autoclaved plant tissue culture medium. Plant Cell Rep 10:115–119

Singh NP, Lai HC (2004) Artemisinin induces apoptosis in human cancer cells. Anticancer Res 24: 2277–2280

Sinha AK, Hofmann MG, Römer U, Köckenberger W, Elling L, Roitsch T (2002) Metabolizable and non-metabolizable sugars activate different signal transduction pathways in tomato. Plant Physiol 128: 1480–1489

Sivakumar G, Liu C, Towler MJ, Weathers PJ (2010) Biomass production of hairy roots of Artemisia annua and Arachis hypogaea in a scaled-up mist bioreactor. Biotechnol Bioeng 107:802–813

Souret FF, Kim Y, Wyslouzil BE, Wobbe KK, Weathers PJ (2003) Scale-up of *Artemisia annua* L. hairy root cultures produces complex patterns of terpenoid gene expression. Biotechnol Bioeng 83:653–667

Steliopoulos P, Wüst M, Adam K-P, Mosandl A (2002) Biosynthesis of the sesquiterpene germacrene D in *Solidago canadensis*: ^{13}C and ^{2}H labeling studies. Phytochemistry 60:13–20

Towler MJ, Weathers PJ (2007) Evidence of artemisinin production from IPP stemming from both the mevalonate and the nonmevalonate pathways. Plant Cell Rep 26:2129–2136

Utzinger J, Xiao S, N'Goran EK, Bergquist R, Tanner M (2001) The potential of artemether for the control of schistosomiasis. Int J Parasitol 31:1549–1562

Vitrac X, Larronde F, Krisa S, Decendit A, Deffieux G, Mérillon JM (2000) Sugar sensing and Ca^{2+}-calmodulin requirement in *Vitis vinifera* cells producing anthocyanins. Phytochemistry 53:659–665

Vögeli U, Chappell J (1988) Induction of sesquiterpene cyclase and suppression of squalene synthetase activities in plant cell cultures treated with fungal elicitor. Plant Physiol 88:1291–1296

Wang JW, Tan RX (2002) Artemisinin production in *Artemisia annua* hairy root cultures with improved growth by altering the nitrogen source in the medium. Biotechnol Lett 24:1153–1156

Wang Y, Weathers PJ (2007) Sugars proportionately affect artemisinin production. Plant Cell Rep 26:1073–1081

Wang Y, Zhang H, Zhao B, Yuan X (2001) Improved growth of *Artemisia annua* L. roots and artemisinin production under red light conditions. Biotechnol Lett 23:1971–1973

Weathers PJ, DeJesus-Gonzalez L, Kim YJ, Souret FF, Towler MJ (2004) Alteration of biomass and artemisinin production in *Artemisia annua* hairy roots by media sterilization method and sugars. Plant Cell Rep 23:414–418

Weathers PJ, Bunk G, McCoy MC (2005) The effect of phytohormones on growth and artemisinin production in *Artemisia annua* hairy roots. In Vitro Cell Dev Biol Plant 41:47–53

Woerdenbag HJ, Lüers JFJ, Uden W, Pras N, Malingré T, Alfermann AW (1993) Production of the new antimalarial drug artemisinin in shoot cultures of *Artemisia annua* L. Plant Cell Tissue Cult 32:247–257

Zarn JA, Brüschweiler BJ, Schlatter JR (2003) Azole fungicides affect mammalian steroidogenesis by inhibiting sterol 14α-demethylase and aromatase. Environ Health Perspect 111:255–261

Fosmidomycin as an Antimalarial Agent

9

Jochen Wiesner, Armin Reichenberg, Martin Hintz, Regina Ortmann, Martin Schlitzer, Serge Van Calenbergh, Steffen Borrmann, Bertrand Lell, Peter G. Kremsner, David Hutchinson, and Hassan Jomaa

Abstract

The isoprenoid biosynthesis of *Plasmodium falciparum*, the causative agent of malignant tertiana malaria, solely depends on the mevalonate-independent 2-*C*-methyl-D-erythritol 4-phosphate (MEP) pathway [also known as the 1-deoxy-D-xylulose 5-phosphate (DXP) pathway]. The enzymes of the MEP pathway of *P. falciparum* are located in a plastid-like organelle called the apicoplast. The growth of *P. falciparum* parasites is rapidly inhibited by fosmidomycin, an inhibitor of DXP reductoisomerase. The antimalarial activity of fosmidomycin has been substantiated in several clinical phase II studies. Most thoroughly, the treatment of malaria patients with a drug combination consisting of fosmidomycin and clindamycin has been investigated. With this combination, cure rates of approximately 90% were achieved after 3 days of treatment. *In vitro* studies revealed improved antimalarial activity of several fosmidomycin derivatives. At present, the compound FR-900098 represents the most promising derivative with respect to its low toxicity and proven activity in the *P. vinckei* mouse model.

Keywords

Apicoplast • Apicomplexa • Clinical studies • Drug development • DXP reductoisomerase • Fosmidomycin • Malaria • MEP pathway • *Plasmodium falciparum*

J. Wiesner
Fraunhofer Institute for Molecular Biology and Applied Ecology IME, Bioresources,Winchesterstrasse 2, Giessen, Germany
e-mail: jochen.wiesner@biochemie.med.uni-giessen.de

A. Reichenberg • M. Hintz • R. Ortmann • M. Schlitzer
S. Van Calenbergh • S. Borrmann • B. Lell
P.G. Kremsner • D. Hutchinson • H. Jomaa (✉)
Institut für Klinische Immunologie und Transfusionsmedizin, Justus-Liebig-Universität Gießen, Langhansstraße 7, Gießen D-35392, Germany
e-mail: hassan.jomaa@uniklinikum-giessen.de

T.J. Bach and M. Rohmer (eds.), *Isoprenoid Synthesis in Plants and Microorganisms: New Concepts and Experimental Approaches*, DOI 10.1007/978-1-4614-4063-5_9,

9.1 Introduction

Malaria is caused by parasitic protozoa of the genus *Plasmodium* with the four species *P. falciparum*, *P. vivax*, *P. ovale* and *P. malariae* being infectious to humans. Among these, *P. falciparum*, the causative agent of malignant tertiana malaria (malaria tropica), is the most dangerous being responsible for most of the fatal cases. The parasites are transmitted through the bite of mosquitoes of the genus *Anopheles*. When injected in the blood stream, the parasites first lead to an asymptomatic infection of liver cells. Finally, massive replication of the parasites inside the red blood cells occurs, associated with the typical clinical symptoms. A small number of parasites differentiate into sexual stages which can be taken up again by a mosquito.

Malaria ranges among the world's leading causes of morbidity and mortality, together with malnutrition, respiratory tract infections, AIDS, diarrhoea and tuberculosis. Over 40% of the world's population are at risk of malaria, with over 500 million symptomatic infections and one million fatal cases annually (Guerra et al. 2008). Children aged under 5 years and pregnant women are most vulnerable to dying of malaria or suffering serious consequences of the disease. Most cases and deaths occur in the countries south of the Sahara. Significant improvement of the global malaria situation is not foreseeable in the near future, one reason being that parasites resistant to affordable and previously highly effective drugs have emerged in virtually all endemic areas. This is particularly the case for chloroquine (Resorchin), the antifolate combination sulphadoxine-pyrimethamine (Fansidar) and to some extent for mefloquine (Lariam). The comparatively new drug combination atovaquone-proguanil (Malarone) is still highly effective, but unaffordable for most patients in developing countries. Several artemisinin derivatives, used increasingly for antimalarial therapy, are exceptionally fast-acting, leading to a reduction in parasitaemia within only 1 day. However, a treatment regimen of at least 5 days is needed to fully eliminate the parasites. In addition, the safety of these drugs is still insufficiently established (Clark et al. 2004). For this reason, the use of artemisinins in the first trimester of pregnancy is not recommended (Dellicour et al. 2007). Nevertheless, the use of drug combinations consisting of an artemisinin derivative and another established antimalarial drug resulting in shorter treatment courses is widely accepted to represent the best treatment available at present (Nosten and White 2007).

Recent efforts to develop new standardised combinations of existing therapies in order to come up with cost-effective treatments, such as chlorproguanil-dapsone (Lapdap) and chlorproguanil-dapsone-artesunate (Dacart), were terminated due to poor tolerability (Medicines for Malaria Venture 2008). The two other drug combinations dihydroartemisinin-piperaquine (Euartekin) and pyronaridine-artesunate (Pyramax) currently undergoing clinical development rely on compounds used in China for the treatment of malaria since the 1960s and 1980s, respectively (Davis et al. 2005; Looareesuwan et al. 1996). Projects at transition to clinical development exploiting new classes of compounds and addressing new targets are scarce.

Results obtained quite early after the elucidation of the first steps of the MEP pathway of isoprenoid biosynthesis in plants and bacteria indicated that this pathway is also used by malaria parasites and provided the basis for a new strategy in the development of antimalarial drugs (Jomaa et al. 1999). At the same time, fosmidomycin was identified as an inhibitor of DXP reductoisomerase, the second enzyme of the MEP pathway (Kuzuyama et al. 1998; Zeidler et al. 1998). Thereafter, demonstrating the inhibition of the growth of cultured malaria parasites by fosmidomycin was straightforward. Originally, fosmidomycin was isolated as an antibacterial compound produced by *Streptomyces lavendulae*. Early clinical studies on the tolerability and efficacy of fosmidomycin for the treatment of urinary tract infections conducted by Fujisawa Pharmaceutical Co. Ltd. in the 1980s without any knowledge of the mechanism of action revealed that this compound is impressively well tolerated in humans (Kuemmerle et al. 1985b). These findings encouraged several clinical trials on the treatment of malaria with fosmidomycin.

9.2 The Discovery of Fosmidomycin

In the late 1970s, four closely related phosphonic acid derivatives were identified as natural antibacterial products of *Streptomyces* spp. (Okuhara et al. 1980a, b; Iguchi et al. 1980; Kuroda et al. 1980). Fosmidomycin (FR-31564) **1** and FR-32863 **2** were isolated from the fermentation broth of *S. lavendulae*. FR-900098 **3** and FR-33289 **4** were isolated from *S. rubellomurinus* (Fig. 9.1). Two additional close derivatives (**5**,**6**; Fig. 9.1) were prepared by chemical synthesis (Hemmi et al. 1982). Among these compounds, fosmidomycin proved to be most active against most bacterial isolates. Fosmidomycin was reported to be more active than fosfomycin, cephalexin, carbenicillin and trimethoprim-sulfamethoxazole against *E. coli*, *Klebsiella pneumoniae*, *Proteus vulgaris*, *Enterobacter cloacae*, *Enterobacter aerogenes* and *Citrobacter* spp. (Mine et al. 1980; Neu and Kamimura 1981). Considerable activity was also reported against *Serratia marcescens*, *Proteus mirabilis* and some *Pseudomonas aeruginosa* strains. No activity was found against Gram-positive cocci and anaerobic species. The interaction of fosmidomycin with established antibacterial compounds was studied in several species of Enterobacteriaceae (Neu and Kamimura 1982). In about half of the isolates, tested synergy between fosmidomycin and the penicillins, cephalosporins and trimethoprim was observed. It was demonstrated that the entry of fosmidomycin into the cells of *P. aeruginosa* and *E. coli* depended on the glycerol 3-phosphate transporter and that the absence of this transporter confers resistance to fosmidomycin (Kojo et al. 1980; Sakamoto et al. 2003). Resistance of *E. coli* cells against fosmidomycin was also achieved by overexpression of a gene encoding a protein homologous to known bacterial drug export proteins, thereafter named fosmidomycin resistance gene (Fujisaki et al. 1996). In addition to its antibacterial activity, fosmidomycin was shown to exert herbicidal activity (Patterson 1987; Kamuro et al. 1991). In an early clinical phase II study conducted by Fujisawa Pharmaceutical Co. Ltd., 70 patients with urinary tract infections caused by Gram-negative bacteria were treated with fosmidomycin (Kuemmerle et al. 1985b). Although no detailed results were published, it was concluded that fosmidomycin should be used as a second choice antibiotic or in combination with a β-lactam antibiotic for this indication. Why the clinical development of fosmidomycin was discontinued at that time remains speculative, reduced efficacy compared to other antibiotics in development, the lack of activity against Streptococci and Staphylococci and development of resistance being among a number of probable reasons.

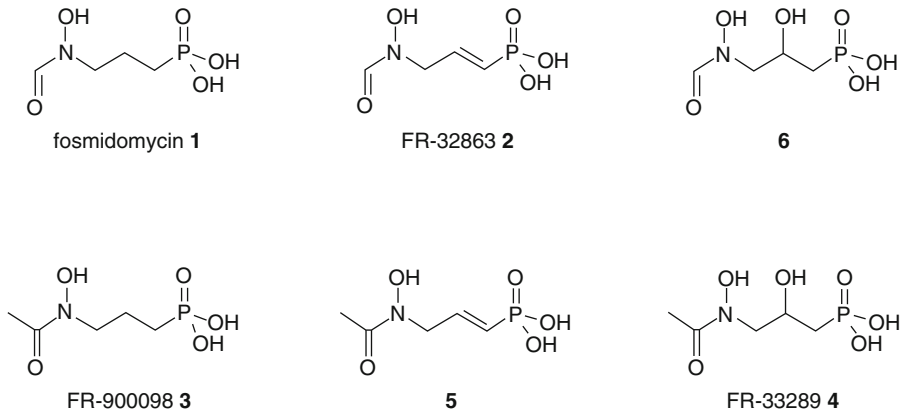

Fig. 9.1 Fosmidomycin and related compounds originally assessed as antibacterial agents. Fosmidomycin **1** and FR-32863 **2** were isolated from *S. lavendulae*. FR-900098 **3** and FR-33289 **4** were isolated from *S. rubellomurinus*. Compound **5** and **6** were prepared by chemical synthesis. No data on the stereochemistry of **4** and **6** are reported

9.3 Inhibition of DXP Reductoisomerase by Fosmidomycin

Until the discovery of the MEP pathway, the molecular target for fosmidomycin was unknown. Initial evidence for fosmidomycin inhibiting isoprenoid biosynthesis was provided by a study indicating that the antibiotic leads to decreased production of menaquinones, ubiquinones and carotenoids in *E. coli* and *Micrococcus luteus*, respectively (Shigi 1989). In 1998, Zeidler et al. found that in several plants, the production of chlorophylls and carotenoids as well as the emission of isoprene was diminished after treatment with fosmidomycin. Since it was already known that these isoprenoids are derived from the MEP pathway, it appeared likely that fosmidomycin inhibits one of the involved enzymes. With respect to the structural similarity between fosmidomycin and *N*-hydroxy-*N*-isopropyloxamate (IpOHA), a known inhibitor of plant and bacteria ketol acid reductoisomerase (also known as acetohydroxy acid isomeroreductase; Aulabaugh and Schloss 1990), it was concluded that DXP reductoisomerase is the probable target for fosmidomycin. Independently, Kuzuyama et al. (1998) demonstrated that the activity of recombinant DXP reductoisomerase of *E. coli* is inhibited by fosmidomycin. In subsequent studies, the inhibition of DXP reductoisomerase of various bacteria and plant species was shown (Wiesner and Jomaa 2007). Fosmidomycin was characterised as a slow, tight-binding competitive inhibitor of *E. coli* DXP reductoisomerase (Koppisch et al. 2002). The K_i values against DXP were 215 and 21 nM when determined for initial and final velocity, respectively. The existence of two distinguishable K_i values was interpreted to reflect an initial binding step, followed by conformational changes of the enzyme leading to a state which binds the inhibitor more tightly. Evidence for such an induced fit mechanism came also from crystallographic studies revealing an open and a closed conformation in the absence and presence of fosmidomycin, respectively (Reuter et al. 2002; Mac Sweeney et al. 2005; Yajima et al. 2007; Henriksson et al. 2007). Fosmidomycin was further shown to bind in a substrate-like manner to a divalent metal cation, either magnesium or manganese, at the active site (Steinbacher et al. 2003) (Fig. 9.2).

9.4 The Algal Trait and the Plastid-Like Organelle of Malaria Parasites

Plasmodium spp., together with various other parasites of both vertebrates and invertebrates, belong to the phylum Apicomplexa. The common feature of all the members of this phylum is the presence of a structure known as the apical complex in one or more stages of the life cycle.

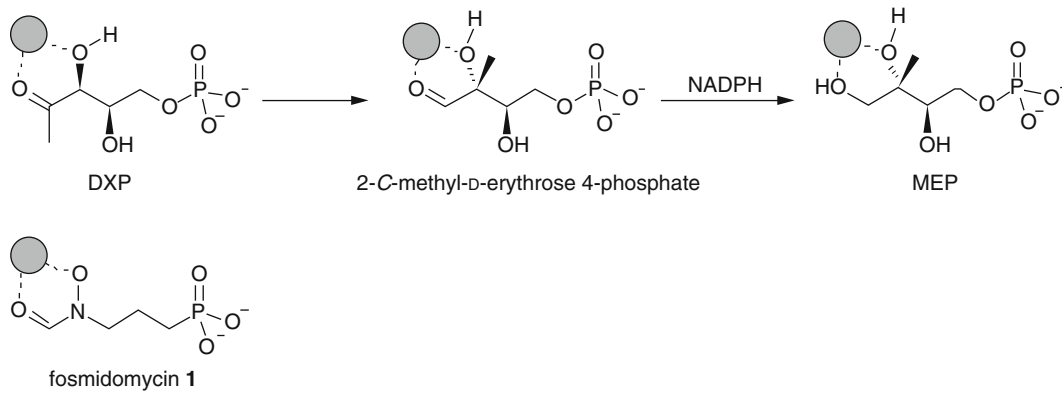

Fig. 9.2 Reaction mechanism of DXP reductoisomerase and binding mode of fosmidomycin **1**. DXP binds to either a Mg^{2+} or Mn^{2+} ion (*grey cycle*) in the active site. After an initial rearrangement step leading to the putative intermediate 2-*C*-methyl-D-erythrose 4-phosphate, NADPH-dependent reduction yields the product MEP. Fosmidomycin **1** binds in a substrate-like manner to the divalent cation

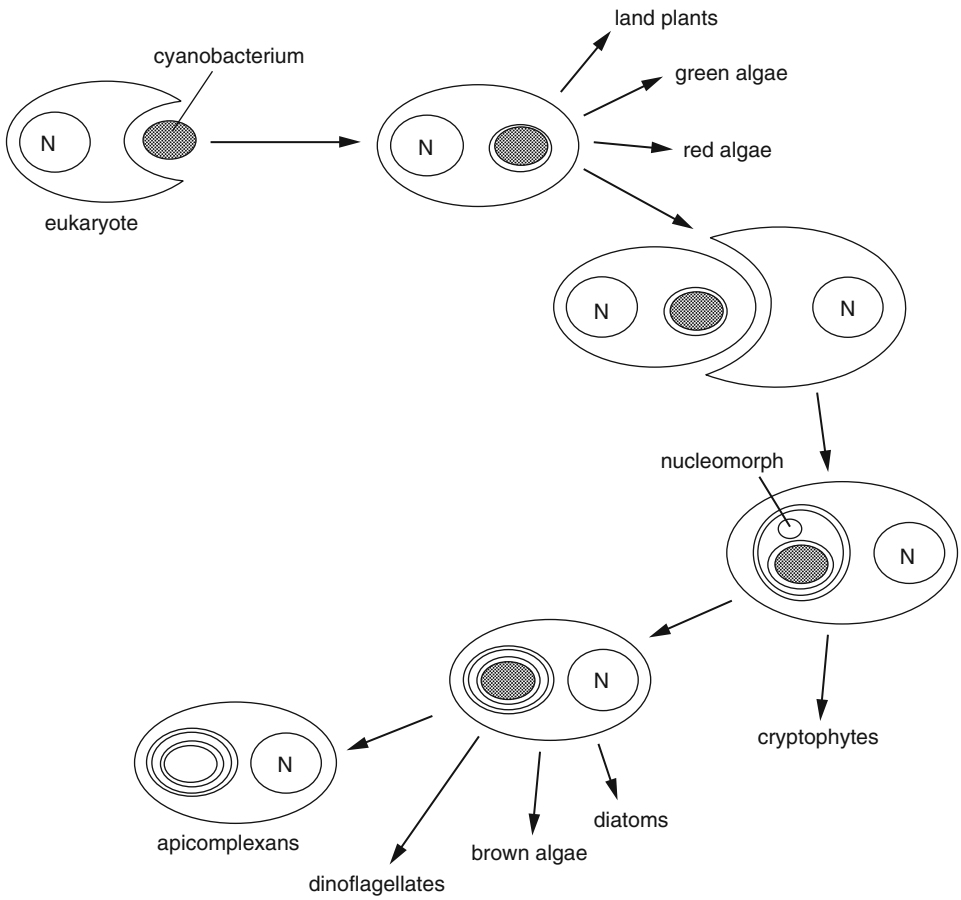

Fig. 9.3 Evolution of the Apicomplexa. In a primary endosymbiontic event, a cyanobacterium-like organism was engulfed by an ancient eukaryote giving rise to an algal cell with a chloroplast reminiscent to the modern red algae, green algae and land plants. In a secondary endosymbiontic event, presumably a red alga was engulfed by a further eukaryote. The cytoplasmatic compartment of this alga was then successively reduced. This evolutionary stage is represented by the recent cryptophytes which still maintain a remnant functional nucleus termed nucleomorph between the inner and the outer two membranes of their plastid. Further reduction led to several groups of algae with plastids surrounded by four (or secondarily three) membranes, including for example the diatoms, brown algae and dinoflagellates. In the apicomplexan lineage, the photosynthetic activity was fully lost. *N*, nucleus

The apical complex is an arrangement of vesicles and cytoskeletal fibres that are used to enter the host cell. Other apicomplexans in addition to *Plasmodium* spp. infectious to humans are found among the genera *Babesia*, *Toxoplasma*, *Cryptosporidium*, *Isospora* and *Cyclospora* (Wiesner et al. 2008). These parasites commonly cause less severe, self-limited diseases in immunocompetent individuals, but potentially lead to life-threatening illness in immunocompromised patients, including those with HIV infection. Apicomplexan parasites of considerable veterinary importance are represented by *Eimeria* spp. causing coccidiosis in poultry and *Theileria* spp. infecting cattle.

Phylogenetic analysis revealed that the dinoflagellates, a group of free-living unicellular marine and freshwater algae, are the closest relatives of the Apicomplexa (Cavalier-Smith 2002). It is assumed that a common eukaryotic ancestor of the dinoflagellates and the apicomplexans engulfed a red alga, which successively transferred parts of its genome to the nucleus of the host cell and finally fully lost its cytoplasmatic compartment, giving rise to a plastidial organelle surrounded by four membranes (Fig. 9.3). In the

apicomplexan clade, the photosynthetic activity of the endosymbiont's plastid was lost. The resulting non-photosynthetic plastid is commonly called the apicoplast. The apicoplast has been shown to be essential for the survival of *P. falciparum* and *Toxoplasma gondii* (Kohler et al. 1997; Fichera and Roos 1997; He et al. 2001). *Cryptosporidium parvum*, however, lacks an apicoplast (Zhu et al. 2000; Abrahamsen et al. 2004). It is believed that this parasite lost the apicoplast rather than never gained it with respect to its phylogenetic position at the base of the apicomplexan linage (Fast et al. 2001).

In accordance with the theory that all plastids are ultimately derived from a cyanobacterium-like organism, the apicoplast contains a relict circular genome consisting of bacteria-type genes almost exclusively involved in expression of that organellar genome. The 35 kb plastidial genome of *P. falciparum* encodes three subunits of an RNA polymerase, 17 ribosomal proteins, the elongation factor Tu (EF-Tu), large and small subunit ribosomal RNAs, and 25 tRNAs (Wilson et al. 1996). Only two apicoplast-encoded proteins appear to play a direct role in distinct metabolic functions. These are a homologue of the ClpC (Hsp93) chaperone presumably involved in the import of proteins and a SufB homologue essential for the assembly of iron-sulphur clusters (Wilson et al. 2003). The other apicoplast-located proteins are encoded by the nucleus. Their import into the organelle is mediated by a characteristic bipartite pre-sequence composed of an ER-signal peptide followed by a plastid transit domain (Tonkin et al. 2008). In *P. falciparum*, roughly 10% of the 5,282 proteins encoded by the nuclear genome are predicted to be apicoplast-targeted (Ralph et al. 2004).

While the function of about 70% of the apicoplast-targeted proteins is unknown, it appears that the synthesis of isoprenoid precursors by the MEP pathway and the synthesis of fatty acids by the bacteria-type FASII system are the dominant metabolic functions of this organelle (Mazumdar and Striepen 2007; Goodman and McFadden 2008). In addition, some reactions of haem biosynthesis, which is mainly located in the mitochondrion, take place inside the apicoplast (van Dooren et al. 2006). Other biochemical reactions characterised so far include the formation of iron–sulphur clusters (Wilson et al. 2003), the transfer of electrons via ferredoxin (Vollmer et al. 2001), lipoate synthesis (Crawford et al. 2006) and the cotranslational removal of the formyl group of formyl methionine typically present at the amino terminus of nascent prokaryotic proteins (Meinnel 2000; Bracchi-Ricard et al. 2001).

9.5 Studies on the Isoprenoid Biosynthesis in Malaria Parasites

Early studies on isoprenoid biosynthesis in malaria parasites were already performed before the discovery of the MEP pathway. Rietz et al. (1967) reported the occurrence of ubiquinones with 8 and 9 isoprene units (ubiquinone-8 and ubiquinone-9) in duck blood infected with the avian parasite *P. lophurae*, in contrast to only ubiquinone-10 in normal duck blood. In a subsequent study, the incorporation of [^{14}C]*p*-hydroxybenzoic acid, as precursor of the benzoquinone ring, into ubiquinone-8 and ubiquinone-9 by the simian parasite *P. knowlesi* was demonstrated (Skelton et al. 1969). On the assumption that the mevalonate pathway is the only existent route leading to IPP and DMAPP, cell-free extracts of *P. falciparum* and *P. knowlesi* were assayed for HMG-CoA reductase activity (Vial et al. 1984). As a result, no significant activity was detected. Nevertheless, Grellier et al. (1994) observed that the growth of *P. falciparum* parasites is inhibited *in vitro* by the HMG-CoA reductase inhibitors lovastatin and simvastatin and discussed the possibility to use such compounds as antimalarial drugs. However, growth inhibition occurred at high concentrations which are of no pharmacological relevance. In metabolic labelling experiments with cultured *P. falciparum* parasites, the incorporation of [^{3}H]farnesyl diphosphate and [^{3}H]geranylgeranyl diphosphate into dolichols of 11 and 12 isoprene units was found (Couto et al. 1999). Only very inefficient labelling of these compounds was achieved with acetate or mevalonate. The weak labelling with

acetate could be inhibited by mevastatin, which also was used at a comparably high concentration in this study. Another early study claimed the incorporation of radioactive mevalonate into isoprenoids, mainly farnesyl diphosphate, by cell-free *P. falciparum* extracts (Mbaya et al. 1990). However, thin-layer chromatography was used as the only technique for the characterisation of the reaction products.

Shortly after cloning the gene for DXP reductoisomerase of *E. coli* by Takahashi et al. (1998), the homologous gene of *P. falciparum* was identified in the emergent *P. falciparum* genome database (Jomaa et al. 1999). After initial experiments to express the gene for the DXP reductoisomerase of *P. falciparum* in *E. coli* failed, the deduced amino acid sequence was back-translated in the codon usage of *E. coli* and produced as a synthetic gene. With this construct, the enzyme was obtained in recombinant form and demonstrated to be catalytically active (Jomaa et al. 1999). However, the yield of soluble *P. falciparum* DXP reductoisomerase was quite low, and the enzyme turned out to be very unstable. Thus, the use of recombinant *P. falciparum* DXP reductoisomerase for biochemical and pharmaceutical characterisation is limited.

Applying a sensitive radioactive assay, DXP reductoisomerase activity could be detected in crude and partially purified protein extracts from *P. falciparum* (Wiesner et al. 2000). Another enzyme of the MEP pathway, the IspF (YgbB) protein of *P. falciparum* was produced in recombinant form (Rohdich et al. 2001). With the completion of the *P. falciparum* genome database, genes encoding all enzymes of the MEP pathway could be detected, all possessing a typical apicoplast-targeting sequence. In addition, most intermediates of the MEP pathway could be detected by electrospray mass spectrometry (ESI-MS) in extracts from *P. falciparum* parasites (Cassera et al. 2004). With respect to the fact that no homologies to any genes for enzymes of the mevalonate pathway are detectable in the fully sequenced *P. falciparum* genome, it appears very likely that the isoprene biosynthesis in malaria parasites solely relies on the MEP pathway.

The last enzyme of the MEP pathway, IspH (LytB), of *P. falciparum* has been characterised in some detail (Röhrich et al. 2005). The enzyme contains a Fe/S cluster (most likely a [4Fe–4S] cluster in the active form) and is denatured upon contact with oxygen. The conversion of (*E*)-4-hydroxy-3-methyl-but-2-enyl diphosphate (HMBPP) into IPP and DMAPP by the *P. falciparum* IspH protein yielded the two products in a ratio of approximately 5:1, as it was reported for the homologous enzymes of *E. coli* and *Aquifex aeolicus* (Rohdich et al. 2002, 2003; Altincicek et al. 2002; Wolff et al. 2003; Gräwert et al. 2004). For the kinetic characterisation of the *P. falciparum* IspH protein, an assay using dithionite-reduced methyl viologen as artificial one-electron donor was applied. Furthermore, catalytic activity was demonstrated in the presence of *P. falciparum*-derived ferredoxin, ferredoxin-$NADP^+$ reductase and NADPH, suggesting that ferredoxin represents the physiological redox partner of *P. falciparum* IspH. Ferredoxin and ferredoxin-$NADP^+$ reductase had already been previously identified in *P. falciparum* and demonstrated to be apicoplast-located (Vollmer et al. 2001). So far, the interaction with IspH is the only experimentally proven function of ferredoxin in *P. falciparum*.

Studies in *P. falciparum* on the isoprenoid metabolism downstream of IPP and DMAPP are limited. Genes encoding several prenyl diphosphate synthases responsible for the assembly of higher isoprenoids from IPP and DMAPP have been found in the *P. falciparum* genome (Ralph et al. 2004). Since these enzymes are apparently cytosolically located, there must exist a not as yet characterised mechanism for the export of IPP and DMAPP out of the apicoplast. Ubiquinones and dolichols probably represent the most dominant extraplastidic end products (Skelton et al. 1969; Couto et al. 1999; de Macedo et al. 2002; Cassera et al. 2004). While ubiquinones are involved in the mitochondrial electron transport, dolichols are essential for protein glycosylation. The dolichol-dependent transfer of glycosylphosphatidylinositol (GPI) anchors on to membrane-bound proteins is essential for most, if

not all, *P. falciparum* surface proteins and apparently represents the only glycoconjugate formation present in this organism (de Macedo et al. 2003; Kimmel et al. 2003). Prenylation of proteins, that is, the attachment of a farnesyl or geranylgeranyl residue, was identified as another essential role of isoprene chains in the cytosol of *P. falciparum* (Chakrabarti et al. 1998; Chakrabarti et al. 2002; Wiesner et al. 2004). In addition to the synthesis of cytosolic isoprenoids, the MEP pathway has also been predicted to play a role in the synthesis of isopentenylated tRNAs inside the apicoplast. Four tRNAs encoded by the apicoplast genome are likely to require an isopentenyladenosine residue in the anticodon loop (Preiser et al. 1995), and an apicoplast-targeted homologue of tRNA isopentenyltransferase, which probably uses DMAPP as substrate, has been identified in the *P. falciparum* genome (Ralph et al. 2004). Evidence for malaria parasites being able to synthesise steroids is lacking (Wunderlich et al. 1991).

9.6 Antimalarial Activity of Fosmidomycin In Vitro and in Mice

Among the human malaria parasites, only the intraerythrocytic stages of *P. falciparum* can be routinely maintained in culture by using human erythrocytes as host cells suspended in a cell culture medium (Trager and Jensen 1976). The determination of *in vitro* antimalarial activity of a potential drug is accomplished by observing the growth inhibition of cultured parasites either microscopically or by incorporation of [^{3}H] hypoxanthine into nucleic acids (Desjardins et al. 1979). Drugs addressing targets inside the apicoplast of *P. falciparum* and other apicomplexan parasites are in part well established (Wiesner and Seeber 2005). These comprise several antibiotics commonly used for the treatment of bacterial infections such as tetracyclines, lincosamides and macrolides, which inhibit the prokaryotic-like translation machinery of the apicoplast. In addition, rifampicin and several quinolones are known to inhibit the apicoplast-located RNA polymerase and gyrase, respectively. The clinical use of antibiotics in antimalarial therapy however is limited due to a phenomenon known as delayed kill effect, a term used to describe the observation that there is virtually no effect on parasite growth during the first intracellular replication cycle after drug exposure, whereas the parasites die during the second cycle after reinvasion of new host cells. Since the resulting delay in parasite clearance may be life-threatening, antibiotics are only used in combination with fast-acting drugs for the treatment of acute malaria. In clinical practice, doxycycline, tetracycline and increasingly clindamycin are used for this indication. Due to its comparably long plasma half-life, doxycycline is frequently recommended for malaria prophylaxis. More recently, efforts at establishing azithromycin as an antimalarial drug have been initiated (Schlitzer 2008).

In contrast to those antibiotics, exposure to fosmidomycin led to inhibition of the growth of *P. falciparum* parasites within the first cycle, thus being similarly fast-acting as most established antimalarials. This result demonstrated for the first time that inhibition of a target inside the apicoplast is not necessarily associated with delayed killing. In unrelated studies, fast parasite killing was also observed with inhibitors of fatty acid synthesis, which also takes place inside the apicoplast (Surolia and Surolia 2001; Ramya et al. 2007). The mechanism of the delayed kill effect still remains hypothetical. It appears that inhibition of the expression of the apicoplast-encoded genes by antibiotics does not immediately prevent the organelle from exerting its metabolic functions, which are almost exclusively catalysed by nuclear-encoded apicoplast-targeted proteins, whereas the apicoplasts of the progenies of the drug-treated parasites may be unable to import and process sufficient amounts of nuclear-encoded proteins (Dahl et al. 2006). Compounds directly inhibiting enzymes of apicoplast-located metabolic pathways such as isoprenoid or fatty acid synthesis, however, are fast-acting.

The *in vitro* growth of different laboratory-adapted *P. falciparum* strains was reported to be inhibited by fosmidomycin with IC_{50} values (the concentration at which parasite growth is inhibited by 50%) in the range of 300–1,200 nM

(Jomaa et al. 1999; Wiesner et al. 2002). Comparable results were obtained with 103 fresh clinical isolates from Cameroon (Tahar and Basco 2007). There was no evidence for cross-resistance with other antimalarial drugs. The *in vivo* antimalarial activity of fosmidomycin has been established in mice infected with the rodent-specific parasite *P. vinckei* (Jomaa et al. 1999). This parasite replicates with a 24-h cycle instead of the 48-h cycle of *P. falciparum* and reaches parasitaemias (percentage of infected erythrocytes) of over 80% before being lethal to the animals. After treatment for 4 days with three doses per day, fosmidomycin was effective with ED_{90} values (the dose at which the parasitaemia is reduced by 90%) of 5 mg/kg and 20 mg/kg after intraperitoneal (i.p.) and oral (p.o.) administration, respectively. Treatment was also effective when started at high parasitaemia of approximately 40%.

Fosmidomycin was only very moderately active against *Toxoplasma gondii* and *Eimeria tenella* despite the genes of the MEP pathway being unambiguously identified (Clastre et al. 2007). Among several possible explanations for this is the poor penetration of the membranes of the host cells and/or of the parasites by the drug. Indeed, fosmidomycin and its *N*-acetyl derivative FR-900098 can apparently only penetrate into erythrocytes that are infected by *P. falciparum* or *Babesia divergens* (a related parasite of cattle which occasionally infects immunocompromised humans), but not by *Toxoplasma gondii*. There is evidence for parasite-induced modification of membrane permeability by some, but not all Apicomplexa (Baumeister et al. 2011).

9.7 Pharmacokinetics and Toxicology of Fosmidomycin

The pharmacokinetics and metabolism of fosmidomycin have been studied in rats and dogs using [^{14}C]fosmidomycin (Tsuchiya et al. 1982). After intravenous administration, approximately 90% of the dose was excreted in the urine within 72 h, and less than 1% was excreted in the expired air (determined as $^{14}CO_2$) and bile of rats, which suggests the absence of enterohepatic circulation. After oral administration to rats, 34% and 61% of the dose were excreted in the urine and faeces, respectively, suggesting about 30% gastrointestinal absorption. Fosmidomycin was rapidly distributed in the tissues of rats and was maintained in high concentrations in the liver, kidney and bones. The serum protein binding in mice, rats and dogs was maximal at 4%. No metabolites were detected in the urine.

Human pharmacokinetic studies have been conducted in healthy male volunteers through single and repeated dose regimens using oral and parenteral routes of administration (Kuemmerle et al. 1985b). The gastrointestinal absorption rate after an oral dose of 500 mg was between 20% and 40%. The recovery rate in urine was 85.5%, 66.4% and 26% after intravenous (30 mg/kg), intramuscular (7.5 mg/kg) and oral (500 mg) doses, respectively. After oral administration of 500 mg of fosmidomycin, a peak serum concentration of 2.33 mg/l was reached after 2.36 h. The plasma half-life was 1.87 h. Significantly higher peak levels were reached after i.m. and i.v. administration. In repeated dose studies, no accumulation could be observed. The serum protein binding was less than 1%. Unmetabolised fosmidomycin was the only bioactive substance found in the urine.

For the previous pharmacokinetic studies in humans, a microbiological assay was used for the determination of fosmidomycin in blood and urine, relying on measuring the diameter of the inhibition zone obtained on an agar plate inoculated with the bacterium *Enterobacter cloacae* as the test organism (Murakawa et al. 1982). This assay has been re-established in recent work conducted in conjunction with a clinical trial to establish the antimalarial activity of fosmidomycin (Cheoymang et al. 2007; Na-Bangchang et al. 2007). In addition, a method for the determination of fosmidomycin in biological samples based on capillary electrophoresis has been published (Bronner et al. 2004). Work on the development of a more sensitive method using anion exchange chromatography with mass spectrometry detection is currently ongoing (Jomaa et al. unpublished).

The acute half-lethal dose (LD_{50}) of fosmidomycin in mice and rats was approximately

8,000 mg/kg after subcutaneous injection and higher than 11,000 mg/kg after oral administration (Kamiya et al. 1980). Diarrhoea was observed as a mean toxic effect at 2,500 and 12,500 mg/kg after oral administration. Piloerection was only observed at the 12,500 mg/kg dose level in both mice and rats.

A phase I study in 127 healthy male volunteers on the safety of fosmidomycin was conducted by Fujisawa Pharmaceutical Co. Ltd. (Kuemmerle et al. 1985a). Fosmidomycin was administered at doses of 2 g i.v. every 6 h for 7 days, 1 g i.m. every 6 h for 5 days and 1 g p.o. every 6 h for 7 days. No adverse events were reported, except for mild to moderate irritation at the site of injection. No side effects were reported in the group receiving the drug orally. No changes in the haematological and biochemical parameters were observed. A total of 70 patients with acute urinary tract infection were treated with fosmidomycin in a pilot phase II trial (Kuemmerle et al. 1985b). Only minor side effects occurred with some cases of nausea, vomiting and loose stools. Alteration of the intestinal flora may have been a causative factor for the observed gastrointestinal effects.

9.8 Clinical Efficacy of Fosmidomycin Monotherapy Against *P. falciparum* Malaria

The efficacy and safety of fosmidomycin for the treatment of acute *P. falciparum* malaria has been evaluated in adult patients in Gabon and Thailand (Lell et al. 2003). Ten subjects at each study site received 1,200 mg fosmidomycin orally three times daily for 7 days. All subjects were clinically and parasitologically cured on day 7. The mean parasite clearance time (PCT) was 46 h in Gabon and 48 h in Thailand. The mean fever clearance time (FCT) was 24 h in Gabon and 47 h in Thailand. On day 28, two subjects in Gabon and eight subjects in Thailand had developed recrudescent infections following the reappearance of parasitaemia. The higher recrudescence rate observed in Thailand may reflect differences in immunity between populations living in a hyperendemic area in Central Africa and a hypoendemic area in South East Asia.

In an additional study, adult Gabonese patients were treated with the same dosing regimen, and the treatment time was sequentially shortened from 5 days (Missinou et al. 2002).

Employing day 14 as the primary end point, cure rates of 89% (8/9), 88% (7/8) and 60% (6/10) were achieved for treatment durations of 5, 4 and 3 days, respectively. This study demonstrated that in Gabon, the minimum effective treatment duration, as defined by a cure rate >80% on day 14, is 4 days. However, on account of the complicated dosing regimen and the comparably high recrudescence rate, it was concluded that fosmidomycin monotherapy is not a realistic treatment option for malaria.

9.9 Clinical Efficacy of Fosmidomycin Combination Therapy Against *P. falciparum* Malaria

The principle of combination therapy is widely accepted for the treatment of malaria in order to increase the efficacy of the available drugs and to delay the development of resistance (Greenwood 2008). The interaction of fosmidomycin with a number of commonly used anti-infective drugs has been investigated in an *in vitro* study (Wiesner et al. 2002). Synergy was observed with the lincosamide antibiotics lincomycin and clindamycin, of which only clindamycin is of practical relevance in view of its preferential use in combination with quinine (Lell and Kremsner 2002; Griffith et al. 2007). Combining fosmidomycin with all other drugs tested resulted in additive or indifferent interaction; no antagonism was observed.

The first study to evaluate the combination of fosmidomycin-clindamycin was conducted in Gabonese children aged 7–14 years, with asymptomatic *P. falciparum* infection (Borrmann et al. 2004a). Fosmidomycin (30 mg/kg) plus clindamycin (5 mg/kg) was administered every 12 h for 5 days and compared to the two drugs alone in groups of 12 subjects. Subjects with asymptomatic infection were selected in order to avoid inadequate treatment in the clindamycin-alone group due to the slow onset of action of this antibiotic. It had been shown in a previous study

Table 9.1 Efficacy of fosmidomycin-clindamycin in the treatment of paediatric patients aged 7–14 years with uncomplicated *P. falciparum* malaria

	Parasite clearance time		Day 14 cure				Day 28 cure			
Treatment duration	Geometric mean	95% CI	n	No. (%) positive	Cure rate (%)	95% CI	n	No. (%) positive	Cure rate (%)	95% CI
5 days	41	33–49	10	0	100	69–100	10	0	100	69–100
4 days	38	32–49	10	0	100	69–100	10	0	100	69–100
3 days	39	28–42	10	0	100	69–100	10	1	90	55–100
2 days	35	25–58	10	0	100	69–100	10	3	70	35–93
1 day	63	43–88	10	5	50	19–81	10	9	10	0–45

conducted at the same study site by Missinou et al. (2003) that children with asymptomatic *P. falciparum* infection commonly develop clinical symptoms and, thus, benefit from early treatment. As expected, the parasite clearance time (PCT) in the fosmidomycin-clindamycin (PCT = 18 h) and the fosmidomycin (PCT = 25 h) group was significantly shorter than in the clindamycin group (PCT = 71 h). Treatment with fosmidomycin-clindamycin and clindamycin-alone led to a 100% cure rate on day 28 while parasites reappeared in 5 out of the 12 subjects treated with fosmidomycin alone. No difference was seen in the incidence of gastrointestinal adverse reactions between the fosmidomycin-clindamycin group and the clindamycin-alone group, whereas treatment with fosmidomycin-clindamycin compared to fosmidomycin alone led to a non-significant increase in the incidence rate of gastrointestinal adverse effects. This study demonstrated that the combination of fosmidomycin and clindamycin is well tolerated and superior to either drug alone with respect to the rapid and radical parasite clearance.

The efficacy of fosmidomycin-clindamycin for the treatment of children aged 7–14 years with acute uncomplicated *P. falciparum* malaria was evaluated in a further study conducted in Gabon (Borrmann et al. 2004b). Fosmidomycin (30 mg/kg) and clindamycin (10 mg/kg) were administered twice daily. Starting with 5 days of treatment, the duration of therapy was incrementally shortened by intervals of 1 day if >85% of the patients in the cohort were cured by day 14. The cure ratio on day 14 was 100% with treatment durations of 5, 4, 3 and 2 days (Table 9.1). The cure ratios on day 28 were 10/10, 10/10, 9/10 and 7/10 with treatment durations of 5, 4, 3 and 2 days, respectively. One day of treatment led to a cure ratio of 5/10 on day 14 and 1/10 on day 28. The mean parasite clearance times were 41, 38, 39, 35 and 63 h, respectively, in the five cohorts.

A study of similar design was performed to determine the efficacy of fosmidomycin (30 mg/kg) in combination with artesunate (1–2 mg/kg) (Borrmann et al. 2005). Despite the lack of evidence for a direct pharmacodynamic interaction between fosmidomycin and artesunate, artesunate was chosen as the combination drug due to its exceptionally fast parasite clearance. Similar to the fosmidomycin-clindamycin combination, the cure ratio with fosmidomycin-artesunate on day 14 was 100% with treatment durations of 5, 4, 3 and 2 days (Table 9.2). The cure ratios on day 28 were 10/10, 9/10, 10/10 and 6/10 with treatment durations of 5, 4, 3 and 2 days, respectively. One day of treatment led to a cure ratio of 7/10 on day 14 and 4/10 on day 28. The mean parasite clearance time was 22, 35, 17, 31 and 19 h, respectively.

In a further study, the efficacy of fosmidomycin (30 mg/kg) and clindamycin (10 mg/kg), administered twice daily for 3 days, was investigated in 51 paediatric patients aged 1–14 years with uncomplicated *P. falciparum* malaria (Borrmann et al. 2006). The treatment was generally well tolerated, but relatively high rates of neutropenia (8/51 [16%]) and falls of haemoglobin concentrations of 2 g/dl or more (7/51 [14%]) were of concern. Gastrointestinal side effects were very moderate. The median parasite and fever clearance times were 42 and 38 h, respectively. All evaluable patients were parasitologically and

Table 9.2 Efficacy of fosmidomycin-artesunate in the treatment of paediatric patients aged 7–14 years with *P. falciparum* malaria

	Parasite clearance time		Day 14 cure				Day 28 cure			
Treatment duration	Geometric mean	95% CI	n	No. (%) positive	Cure rate (%)	95% CI	n	No. (%) positive	Cure rate (%)	95% CI
5 days	22	18–29	9	0	100	66–100	9	0	100	66–100
4 days	35	27–45	10	0	100	69–100	10	1	90	55–100
3 days	17	13–22	10	0	100	69–100	10	0	100	69–100
2 days	31	22–43	10	0	100	69–100	10	4	60	26–88
1 day	19	14–25	10	3	70	35–93	10	6	40	12–74

clinically cured by day 14 (49/49; 95% confidence interval [CI], 93–100%). The day 28 cure rate appeared to be significantly age-dependent, being 37/39 (95%, CI 83–99%) in patients aged 3–14 years but only 5/8 (62%, CI 24–91%) in patients aged 1–2 years. The low efficacy in very young children may be due to low levels of parasite-specific immunity in this age group. However, inadequate drug administration may be an alternative explanation, since for these young children, fosmidomycin was given as a slurry with milk, possibly resulting in decreased gastrointestinal absorption.

In a randomised controlled trial, fosmidomycin-clindamycin was evaluated versus sulphadoxine-pyrimethamine in 105 Gabonese children aged 3–14 years with uncomplicated *P. falciparum* malaria (Oyakhirome et al. 2007). Fosmidomycin (30 mg/kg) and clindamycin (10 mg/kg) were administered twice daily for 3 days. Sulphadoxine-pyrimethamine was administered as a single dose. Although one patient in the fosmidomycin-clindamycin group had a serious adverse event (convulsion) on day 1, there were more adverse events in the sulphadoxine-pyrimethamine group, and all adverse events resolved spontaneously. The total number of adverse events was 64 in the fosmidomycin-clindamycin group and 100 in the sulphadoxine-pyrimethamine group. There was no evidence of increased gastrointestinal side effects in the fosmidomycin-clindamycin group. Vomiting occurred at a significantly higher rate in the sulfadoxine-pyrimethamine group (13/51 [26%]) as in the fosmidomycin-clindamycin group (1/54 [2%]). Both treatments resulted in identical efficacy of 94% on day 28. Notable in this study was the comparably high efficacy of sulfadoxine-pyrimethamine which had already been limited in its use due to the prevalence of resistant parasites.

The most recent study was conducted in an area of multidrug resistance in Thailand. Fosmidomycin and clindamycin were administered in total daily doses of 3,600 and 1,200 mg, respectively, either 6-hourly or 12-hourly over 3 days, to adult patients with acute uncomplicated *P. falciparum* malaria. Overall cure rates of approximately 90% were achieved in both treatment groups as confirmed by PCR analyses in recrudescent cases. Acceptable safety profiles based on a range of clinical and laboratory parameters were also established (Jomaa Pharma. Internal report).

9.10 Antimalarial Activity of Fosmidomycin Derivatives

A variety of fosmidomycin derivatives have been evaluated for inhibition of DXP reductoisomerase and antimicrobial activity. At present, there is no report on any derivative which inhibits the growth of bacteria more efficiently than fosmidomycin. However, a few analogues display improved antimalarial activity, possibly reflecting distinct structural features of the *P. falciparum* DXP reductoisomerase or a different cellular uptake mechanism (Fig. 9.4, Table 9.3). FR-900098 **3** represents the most thoroughly studied derivative. This compound differs from fosmidomycin only by an additional methyl group and was originally identified at the same time as fosmidomycin in

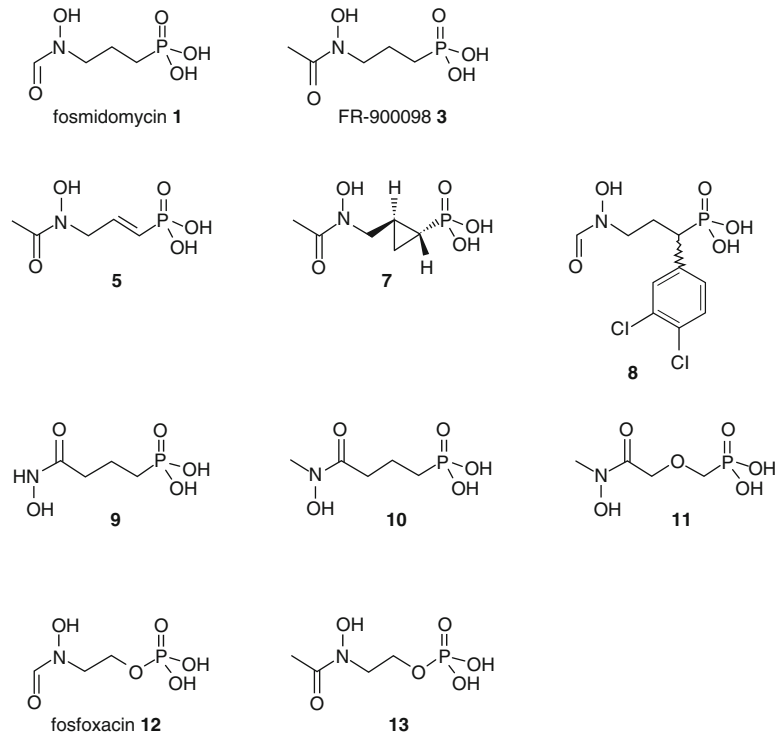

Fig. 9.4 Fosmidomycin derivatives with significant *in vitro* antimalarial activity and/or activity in the DXP reductoisomerase inhibition assay

Table 9.3 Biological activity of fosmidomycin derivatives

Compound	Inhibition of DXP reductoisomerase[a]	Inhibition of *P. falciparum* growth	Reference
	Relative potency		
Fosmidomycin **1**	1.0	1.0	
FR-900098 **3**	1.0	2.6	Giessmann et al. 2008
			Tahar and Basco 2007
5	0.31	–	Silber et al. 2005
7	1.0	1.0	Devreux et al. 2006
8	0.51	12	Haemers et al. 2006
9	0.19	–	Kuntz et al. 2005
10	0.67	1.2	Kuntz et al. 2005
			Haemers et al. 2008
11	0.75	5.0	Haemers et al. 2008
Fosfoxacin **12**	3.0	–	Woo et al. 2006
13	29	–	Woo et al. 2006

[a]The reported values for compounds **1**–**11** were obtained with recombinant DXP reductoisomerase of *E. coli*. The values for **12** and **13** were obtained with DXP reductoisomerase of *Synechocystis* sp. PCC6803. The relative potency of FR-900098 **3** compared to fosmidomycin **1** against recombinant DXP reductoisomerase of *P. falciparum* was 1.8 (Giessmann et al. 2008)

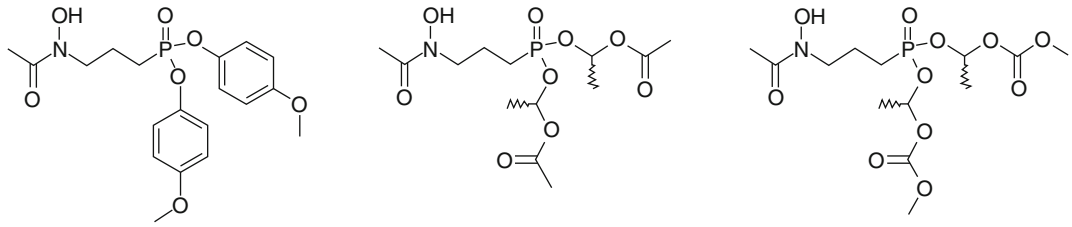

Fig. 9.5 Prodrugs of FR-900098 **3** with improved oral antimalarial activity in the *P. vinckei* mouse model

the culture broth of *S. rubellomurinus* (Okuhara et al. 1980a). FR-900098 inhibits the growth of cultured *P. falciparum* parasites at least two times more efficiently than fosmidomycin (Jomaa et al. 1999). In the study by Tahar and Basco (2007), the activity of fosmidomycin and FR-900098 was compared against 34 fresh clinical Cameroonian *P. falciparum* isolates. The geometric mean IC_{50} values (95% confidence interval) were 301 nM (245–370 nM) and 118 (93.3–149 nM) for fosmidomycin and FR-900098, respectively. The relative potency of FR-900098 versus fosmidomycin was 2.6. Approximately twofold improved activity of FR-900098 compared to fosmidomycin was also found in the murine *P. vinckei* and *P. berghei* models (Jomaa et al. 1999; Jomaa unpublished). The improved antimalarial activity of FR-900098 appears to result from a higher sensitivity of the target enzyme. The IC_{50} value of FR-900098 for the recombinant *P. falciparum* DXP reductoisomerase was 18 nM compared to 32 nM for fosmidomycin (Jomaa et al. 1999; Giessmann et al. 2008). Against the *E. coli* DXP reductoisomerase, both compounds are equally active with reported IC_{50} values of 50 and 51 nM for fosmidomycin and FR-900098, respectively (Giessmann et al. 2008). Preliminary toxicological data on FR-900098 indicate that this compound is similarly non-toxic as fosmidomycin (Kamiya et al. 1980; Jomaa unpublished).

In several studies, prodrug strategies were applied in order to further improve the antimalarial efficacy of FR-900098 (Reichenberg et al. 2001; Kurz et al. 2006). Temporarily masking the polar phosphonate group as aryl or double esters (Fig. 9.5) resulted in significantly improved suppression of parasitaemia in the *P. vinckei* mouse model after oral administration (Reichenberg et al. 2001; Ortmann et al. 2003, 2005). Roughly twofold higher activity was achieved with the most successful prodrugs when compared to the parent FR-900098 molecule. Although it was anticipated that the improved *in vivo* activity is mainly achieved by improved gastrointestinal absorption, two of the double esters were also shown to possess up to fivefold enhanced *in vitro* activity, probably related to increased drug uptake by the *P. falciparum*-infected erythrocytes and/or the parasites themselves (Wiesner et al. 2007). As expected, no inhibition of DXP reductoisomerase was observed with the unmetabolised prodrugs.

Among several fosmidomycin analogues featuring restricted conformational mobility, the *trans*-α,β-unsaturated analogue **5** (Figs. 9.1 and 9.4) was found to be approximately threefold less active than fosmidomycin against recombinant DXP reductoisomerase of *E. coli* (Silber et al. 2005). In addition, the enantiomerically pure *trans*-cyclopropyl *N*-acetyl analogue **7** (Fig. 9.4) displayed activity against *E. coli* DXP reductoisomerase and cultured *P. falciparum* parasites equal to fosmidomycin (Devreux et al. 2006). In a series of α-aryl-substituted fosmidomycin derivatives, several compounds were found to inhibit the *in vitro* growth of *P. falciparum* parasites more efficiently than fosmidomycin or FR-900098 (Haemers et al. 2006; Devreux et al. 2007). As the most potent compound, the dichlorophenyl derivative **8** (Fig. 9.4) displayed approximately 12-fold increased activity compared to fosmidomycin. The activity against recombinant *E. coli* DXP reductoisomerase was twofold lower compared to fosmidomycin. No data are available with recombinant *P. falciparum* DXP reductoisomerase and on potential *in vivo* activity.

Two phosphonohydroxamic acid derivatives **9** and **10** (Fig. 9.4) formally representing fosmidomycin and FR-900098 with a hydroxamate

instead of the retrohydroxamate moiety have been characterised (Kuntz et al. 2005). The non-methylated compound **9** displayed comparably low activity, inhibiting *E. coli* DXP reductoisomerase with an IC_{50} value five times higher than fosmidomycin. In contrast, the *N*-methyl hydroxamic acid derivative **10** was only 1.5 times less active than fosmidomycin. Remarkably, this compound inhibited the growth of *E. coli* bacteria which had been selected for fosmidomycin resistance, suggesting differences in uptake and/or detoxification (Kuntz et al. 2005). In the *P. falciparum* growth inhibition assay, the *N*-methyl hydroxamic acid derivative **10** was slightly more active than fosmidomycin, but significantly less active than FR-900098 (Haemers et al. 2008). Introduction of a β-oxa modification into this molecule yielded compound **11** (Fig. 9.4) with fivefold improved *in vitro* antimalarial activity compared to fosmidomycin (Haemers et al. 2008).

Fosfoxacin **12** (Fig. 9.4) represents a potentially highly potent DXP reductoisomerase inhibitor on which only very limited data are available at present. This compound, resembling the phosphate analogue of fosmidomycin, was isolated in 1990 from *Pseudomonas fluorescens* PK-54 as a new antibacterial compound (Katayama et al. 1990). Later, it was shown by Woo et al. (2006) that fosfoxacin **12** and its synthetic *N*-acetyl analogue **13** (Fig. 9.4) inhibit DXP reductoisomerase of the cyanobacterium *Synechocystis* sp. PCC6803 with 3-fold and 29-fold lower K_i values, respectively, compared to fosmidomycin. Data on growth inhibition of different bacteria by fosfoxacin **12** are published; however, fosmidomycin was not included for comparison (Katayama et al. 1990). Possibly, these phosphoric acid derivatives **12** and **13** are susceptible to degradation by nonspecific phosphatases and therefore less useful as potential drugs.

9.11 Conclusion

Despite some conflicting early studies, there is now compelling evidence that the isoprenoid biosynthesis of malaria parasites fully depends on the MEP pathway. The enzymes of the MEP pathway are located inside a non-photosynthetic plastid-like organelle called the apicoplast. Fosmidomycin, a known inhibitor of DXP reductoisomerase, leads to parasite growth inhibition within one intraerythrocytic cycle similar to most established antimalarial drugs. This rapid activity is in sharp contrast to some classical antibiotics known to inhibit the parasite growth with a delayed kinetic effect. In clinical studies, oral administration of fosmidomycin led to rapid resolution of symptoms and clearance of parasites below the microscopic detection threshold in the blood of patients with acute uncomplicated *P. falciparum* malaria. However, parasite clearance was incomplete, resulting in recrudescence in a comparably high number of patients. The development of recrudescent infections could be largely avoided by the administration of drug combinations consisting of fosmidomycin plus clindamycin or fosmidomycin plus artesunate. While there is only one clinical study on fosmidomycin-artesunate, the efficacy and safety of fosmidomycin-clindamycin has been substantiated in five phase II trials. It has been found that the minimum treatment regimen leading to >90% cure rate on day 28 in Gabon is two doses per day for 3 days. Therefore, fosmidomycin-clindamycin principally meets the criteria for a first-line treatment in Africa, notwithstanding that less frequent dosing would result in improved compliance. In addition to its potential use as an effective treatment for uncomplicated malaria, fosmidomycin-clindamycin may be of particular value for the treatment of severe malaria when patients are not able to tolerate oral medication. Antimalarial drugs which can be administered parenterally are very limited. At present, intravenous quinine, which is associated with considerable side effects, is used as standard therapy for severe malaria. In addition, efforts to establish artesunate as an intravenous formulation for this indication are ongoing (Jones et al. 2007). The development of an intravenous formulation of fosmidomycin-clindamycin should be technically feasible. In a phase I volunteer study, fosmidomycin administered intravenously at high doses was tolerated without significant side effects (Kuemmerle et al. 1985a). Clindamycin for intravenous administration is already available in the form of its phosphoric acid ester.

Only very few fosmidomycin derivatives are known to possess improved antiparasitic activity. Although not the most active *in vitro*, the close derivative FR-900098 **3** is considered the most attractive development candidate with respect to its proven *in vivo* activity and low toxicity.

References

Abrahamsen MS, Templeton TJ, Enomoto S et al (2004) Complete genome sequence of the apicomplexan, *Cryptosporidium parvum*. Science 304:441–445

Altincicek B, Duin EC, Reichenberg A et al (2002) LytB protein catalyzes the terminal step of the 2-*C*-methyl-D-erythritol 4-phosphate pathway of isoprenoid biosynthesis. FEBS Lett 532:437–440

Aulabaugh A, Schloss JV (1990) Oxalyl hydroxamates as reaction-intermediate analogues for ketol-acid reductoisomerase. Biochemistry 29:2824–2830

Baumeister S, Wiesner J, Reichenberg A et al (2011) Fosmidomycin uptake into *Plasmodium* and *Babesia*-infected erythrocytes is facilitated by parasite-induced new permeability pathways. PLoS One 6(5):e19334

Borrmann S, Adegnika AA, Matsiegui PB et al (2004a) Fosmidomycin-clindamycin for *Plasmodium falciparum* infections in African children. J Infect Dis 189:901–908

Borrmann S, Issifou S, Esser G et al (2004b) Fosmidomycin-clindamycin for the treatment of *Plasmodium falciparum* malaria. J Infect Dis 190: 1534–1540

Borrmann S, Adegnika AA, Moussavou F et al (2005) Short-course regimens of artesunate-fosmidomycin in treatment of uncomplicated *Plasmodium falciparum* malaria. Antimicrob Agents Chemother 49:3749–3754

Borrmann S, Lundgren I, Oyakhirome S et al (2006) Fosmidomycin plus clindamycin for treatment of pediatric patients aged 1 to 14 years with *Plasmodium falciparum* malaria. Antimicrob Agents Chemother 50:2713–2718

Bracchi-Ricard V, Nguyen KT, Zhou Y et al (2001) Characterization of an eukaryotic peptide deformylase from *Plasmodium falciparum*. Arch Biochem Biophys 396:162–170

Bronner S, Renault C, Hintz M et al (2004) Determination of fosmidomycin in human serum and urine by capillary electrophoresis. J Chromatogr B Analyt Technol Biomed Life Sci 806:255–261

Cassera MB, Gozzo FC, D'Alexandri FL et al (2004) The methylerythritol phosphate pathway is functionally active in all intraerythrocytic stages of *Plasmodium falciparum*. J Biol Chem 279:51749–51759

Cavalier-Smith T (2002) Nucleomorphs: enslaved algal nuclei. Curr Opin Microbiol 5:612–619

Chakrabarti D, Azam T, DelVecchio C et al (1998) Protein prenyl transferase activities of *Plasmodium falciparum*. Mol Biochem Parasitol 94:175–184

Chakrabarti D, Da Silva T, Barger J et al (2002) Protein farnesyltransferase and protein prenylation in *Plasmodium falciparum*. J Biol Chem 277:42066–42073

Cheoymang A, Hudchinton D, Kioy D et al (2007) Bioassay for determination of fosmidomycin in plasma and urine: application for pharmacokinetic dose optimisation. J Microbiol Methods 69:65–69

Clark RL, White TE, Clode SA et al (2004) Developmental toxicity of artesunate and an artesunate combination in the rat and rabbit. Birth Defects Res B Dev Reprod Toxicol 71:380–394

Clastre M, Goubard A, Prel A et al (2007) The methylerythritol phosphate pathway for isoprenoid biosynthesis in coccidia: presence and sensitivity to fosmidomycin. Exp Parasitol 116:375–384

Couto AS, Kimura EA, Peres VJ et al (1999) Active isoprenoid pathway in the intra-erythrocytic stages of *Plasmodium falciparum*: presence of dolichols of 11 and 12 isoprene units. Biochem J 341:629–637

Crawford MJ, Thomsen-Zieger N, Ray M et al (2006) *Toxoplasma gondii* scavenges host-derived lipoic acid despite its de novo synthesis in the apicoplast. EMBO J 25:3214–3222

Dahl EL, Shock JL, Shenai BR et al (2006) Tetracyclines specifically target the apicoplast of the malaria parasite *Plasmodium falciparum*. Antimicrob Agents Chemother 50:3124–3131

Davis TM, Hung TY, Sim IK et al (2005) Piperaquine: a resurgent antimalarial drug. Drugs 65:75–87

de Macedo CS, Uhrig ML, Kimura EA et al (2002) Characterization of the isoprenoid chain of coenzyme Q in *Plasmodium falciparum*. FEMS Microbiol Lett 207:13–20

de Macedo CS, Shams-Eldin H, Smith TK et al (2003) Inhibitors of glycosylphosphatidylinositol anchor biosynthesis. Biochimie 85:465–472

Dellicour S, Hall S, Chandramohan D et al (2007) The safety of artemisinins during pregnancy: a pressing question. Malar J. doi:10.1186/1475-2875-6-15

Desjardins RE, Canfield CJ, Haynes JD et al (1979) Quantitative assessment of antimalarial activity in vitro by a semiautomated microdilution technique. Antimicrob Agents Chemother 16:710–718

Devreux V, Wiesner J, Goeman JL et al (2006) Synthesis and biological evaluation of cyclopropyl analogues of fosmidomycin as potent *Plasmodium falciparum* growth inhibitors. J Med Chem 49:2656–2660

Devreux V, Wiesner J, Jomaa H et al (2007) Divergent strategy for the synthesis of α-aryl-substituted fosmidomycin analogues. J Org Chem 72:3783–3789

Fast NM, Kissinger JC, Roos DS et al (2001) Nuclear-encoded, plastid-targeted genes suggest a single common origin for apicomplexan and dinoflagellate plastids. Mol Biol Evol 18:418–426

Fichera ME, Roos DS (1997) A plastid organelle as a drug target in apicomplexan parasites. Nature 390:407–409

Fujisaki S, Ohnuma S, Horiuchi T et al (1996) Cloning of a gene from *Escherichia coli* that confers resistance to fosmidomycin as a consequence of amplification. Gene 175:83–87

Giessmann D, Heidler P, Haemers T et al (2008) Towards new antimalarial drugs: synthesis of non-hydrolyzable phosphate mimics as feed for a predictive QSAR study on 1-deoxy-D-xylulose-5-phosphate reductoisomerase inhibitors. Chem Biodivers 5:643–656

Goodman CD, McFadden GI (2008) Fatty acid synthesis in protozoan parasites: unusual pathways and novel drug targets. Curr Pharm Des 14:901–916

Gräwert T, Kaiser J, Zepeck F et al (2004) IspH protein of *Escherichia coli*: studies on iron-sulfur cluster implementation and catalysis. J Am Chem Soc 126:12847–12855

Greenwood B (2008) Progress in malaria control in endemic areas. Travel Med Infect Dis 6:173–176

Grellier P, Valentin A, Millerioux V et al (1994) 3-Hydroxy-3-methylglutaryl coenzyme A reductase inhibitors lovastatin and simvastatin inhibit in vitro development of *Plasmodium falciparum* and *Babesia divergens* in human erythrocytes. Antimicrob Agents Chemother 38:1144–1148

Griffith KS, Lewis LS, Mali S et al (2007) Treatment of malaria in the United States: a systematic review. JAMA 297:2264–2277

Guerra CA, Gikandi PW, Tatem AJ et al (2008) The limits and intensity of *Plasmodium falciparum* transmission: implications for malaria control and elimination worldwide. PLoS Med 5:e38

Haemers T, Wiesner J, Van Poecke S et al (2006) Synthesis of α-substituted fosmidomycin analogues as highly potent *Plasmodium falciparum* growth inhibitors. Bioorg Med Chem Lett 16:1888–1891

Haemers T, Wiesner J, Giessmann D et al (2008) Synthesis of β- and γ-oxa isosteres of fosmidomycin and FR900098 as antimalarial candidates. Bioorg Med Chem 16:3361–3371

He CY, Shaw MK, Pletcher CH et al (2001) A plastid segregation defect in the protozoan parasite *Toxoplasma gondii*. EMBO J 20:330–339

Hemmi K, Takeno H, Hashimoto M et al (1982) Studies on phosphonic acid antibiotics. IV. Synthesis and antibacterial activity of analogs of 3-(N-acetyl-N-hydroxyamino)-propylphosphonic acid (FR-900098). Chem Pharm Bull(Tokyo) 30:111–118

Henriksson LM, Unge T, Carlsson J et al (2007) Structures of *Mycobacterium tuberculosis* 1-deoxy-D-xylulose 5-phosphate reductoisomerase provide new insights into catalysis. J Biol Chem 282:19905–19916

Iguchi E, Okuhara M, Kohsaka M (1980) Studies on new phosphonic acid antibiotics. II. Taxonomic studies on producing organisms of the phosphonic acid and related compounds. J Antibiot (Tokyo) 33:19–23

Jomaa H, Wiesner J, Sanderbrand S et al (1999) Inhibitors of the nonmevalonate pathway of isoprenoid biosynthesis as antimalarial drugs. Science 285:1573–1576

Jones KL, Donegan S, Lalloo DG (2007) Artesunate versus quinine for treating severe malaria. Cochrane Database Syst Rev 4:CD005967

Kamiya T, Hashimoto M, Hemmi K, Takeno H (1980) Hydroxyaminohydrocarbon-phosphonic acids. Fujisawa Pharmaceutical Co. Ltd. U.S. Patent Application No. 4,206,156, 3 June 1980

Kamuro Y, Kawai T, Kakiuchi T (1991) Herbicidal methods and compositions comprising fosmidomycin. Fujisawa Pharmaceutical Co. Ltd. U.S. Patent Application No. 5,002,602, 26 March 1991

Katayama N, Tsubotani S, Nozaki Y et al (1990) Fosfadecin and fosfocytocin, new nucleotide antibiotics produced by bacteria. J Antibiot (Tokyo) 43: 238–246

Kimmel J, Ogun SA, de Macedo CS et al (2003) Glycosylphosphatidyl-inositols in murine malaria: *Plasmodium yoelii yoelii*. Biochimie 85:473–481

Kohler S, Delwiche CF, Denny PW et al (1997) A plastid of probable green algal origin in Apicomplexan parasites. Science 275:1485–1489

Kojo H, Shigi Y, Nishida M (1980) FR-31564, a new phosphonic acid antibiotic: bacterial resistance and membrane permeability. J Antibiot (Tokyo) 33:44–48

Koppisch AT, Fox DT, Blagg BS et al (2002) *E. coli* MEP synthase: steady-state kinetic analysis and substrate binding. Biochemistry 41:236–243

Kuemmerle HP, Murakawa T, Soneoka K et al (1985a) Fosmidomycin: a new phosphonic acid antibiotic. Part I: Phase I tolerance studies. Int J Clin Pharmacol Ther Toxicol 23:515–520

Kuemmerle HP, Murakawa T, Sakamoto H et al (1985b) Fosmidomycin, a new phosphonic acid antibiotic. Part II: 1. Human pharmacokinetics. 2. Preliminary early phase IIa clinical studies. Int J Clin Pharmacol Ther Toxicol 23:521–528

Kuntz L, Tritsch D, Grosdemange-Billiard C et al (2005) Isoprenoid biosynthesis as a target for antibacterial and antiparasitic drugs: phosphonohydroxamic acids as inhibitors of deoxyxylulose phosphate reductoisomerase. Biochem J 386:127–135

Kuroda Y, Okuhara M, Goto T et al (1980) Studies on new phosphonic acid antibiotics. IV. Structure determination of FR-33289, FR-31564 and FR-32863. J Antibiot (Tokyo) 33:29–35

Kurz T, Schlüter K, Kaula U et al (2006) Synthesis and antimalarial activity of chain substituted pivaloyloxymethyl ester analogues of Fosmidomycin and FR900098. Bioorg Med Chem 14:5121–5135

Kuzuyama T, Shizimu T, Takahashi S et al (1998) Fosmidomycin, a specific inhibitor of 1-deoxy-D-xylulose 5-phosphate reductoisomerase in the nonmevalonate pathway of isoprenoid biosynthesis. Tetrahedron Lett 39:7913–7916

Lell B, Kremsner PG (2002) Clindamycin as an antimalarial drug: review of clinical trials. Antimicrob Agents Chemother 46:2315–2320

Lell B, Ruangweerayut R, Wiesner J et al (2003) Fosmidomycin, a novel chemotherapeutic agent for malaria. Antimicrob Agents Chemother 47:735–738

Looareesuwan S, Kyle DE, Viravan C et al (1996) Clinical study of pyronaridine for the treatment of acute uncomplicated falciparum malaria in Thailand. Am J Trop Med Hyg 54:205–209

Mac Sweeney A, Lange R, Fernandes RP et al (2005) The crystal structure of *E.coli* 1-deoxy-D-xylulose 5-phosphate reductoisomerase in a ternary complex with the

antimalarial compound fosmidomycin and NADPH reveals a tight-binding closed enzyme conformation. J Mol Biol 345:115–127

Mazumdar J, Striepen B (2007) Make it or take it: fatty acid metabolism of apicomplexan parasites. Eukaryot Cell 6:1727–1735

Mbaya B, Rigomier D, Edorh GG et al (1990) Isoprenoid metabolism in *Plasmodium falciparum* during the intraerythrocytic phase of malaria. Biochem Biophys Res Commun 173:849–854

Medicines for Malaria Venture (2008) http://www.mmv.org/article.php3?id_article=459. Accessed 18 July 2008

Meinnel T (2000) Peptide deformylase of eukaryotic protists: a target for new antiparasitic agents? Parasitol Today 16:165–168

Mine Y, Kamimura T, Nonoyama S et al (1980) *In vitro* and *in vivo* antibacterial activities of FR-31564, a new phosphonic acid antibiotic. J Antibiot (Tokyo) 33:36–43

Missinou MA, Borrmann S, Schindler A et al (2002) Fosmidomycin for malaria. Lancet 360:1941–1942

Missinou MA, Lell B, Kremsner PG (2003) Uncommon asymptomatic *Plasmodium falciparum* infections in Gabonese children. Clin Infect Dis 36:1198–1202

Murakawa T, Sakamoto H, Fukada S et al (1982) Pharmacokinetics of fosmidomycin, a new phosphonic acid antibiotic. Antimicrob Agents Chemother 21:224–230

Na-Bangchang K, Ruengweerayut R, Karbwang J et al (2007) Pharmacokinetics and pharmacodynamics of fosmidomycin monotherapy and combination therapy with clindamycin in the treatment of multidrug resistant falciparum malaria. Malaria J. doi:10.1186/1475-2875-6-70

Neu HC, Kamimura T (1981) *In vitro* and *in vivo* antibacterial activity of FR-31564, a phosphonic acid antimicrobial agent. Antimicrob Agents Chemother 19:1013–1023

Neu HC, Kamimura T (1982) Synergy of fosmidomycin (FR-31564) and other antimicrobial agents. Antimicrob Agents Chemother 22:560–563

Nosten F, White NJ (2007) Artemisinin-based combination treatment of falciparum malaria. Am J Trop Med Hyg 77(6 Suppl):181–192

Okuhara M, Kuroda Y, Goto T et al (1980a) Studies on new phosphonic acid antibiotics. I. FR-900098, isolation and characterization. J Antibiot (Tokyo) 33: 13–17

Okuhara M, Kuroda Y, Goto T et al (1980b) Studies on new phosphonic acid antibiotics. III. Isolation and characterization of FR-31564, FR-32863 and FR-33289. J Antibiot (Tokyo) 33(24)

Ortmann R, Wiesner J, Reichenberg A et al (2003) Acyloxyalkyl ester prodrugs of FR900098 with improved *in vivo* anti-malarial activity. Bioorg Med Chem Lett 13:2163–2166

Ortmann R, Wiesner J, Reichenberg A et al (2005) Alkoxycarbonyloxyethyl ester prodrugs of FR900098 with improved *in vivo* antimalarial activity. Arch Pharm (Weinheim) 338:305–314

Oyakhirome S, Issifou S, Pongratz P et al (2007) Randomized controlled trial of fosmidomycin-clindamycin versus sulfadoxine-pyrimethamine in the treatment of *Plasmodium falciparum* malaria. Antimicrob Agents Chemother 51:1869–1871

Patterson DR (1987) Herbicidal hydroxyamino phosphonic acids and derivatives. Rohm and Haas Corp. U.S. Patent Application No. 4,693,742, 15 Sept 1987

Preiser P, Williamson DH, Wilson RJ (1995) tRNA genes transcribed from the plastid-like DNA of *Plasmodium falciparum*. Nucleic Acids Res 23:4329–4336

Ralph SA, van Dooren GG, Waller RF et al (2004) Tropical infectious diseases: metabolic maps and functions of the *Plasmodium falciparum* apicoplast. Nat Rev Microbiol 2:203–216

Ramya TN, Mishra S, Karmodiya K et al (2007) Inhibitors of nonhousekeeping functions of the apicoplast defy delayed death in *Plasmodium falciparum*. Antimicrob Agents Chemother 51:307–316

Reichenberg A, Wiesner J, Weidemeyer C et al (2001) Diaryl ester prodrugs of FR900098 with improved *in vivo* antimalarial activity. Bioorg Med Chem Lett 11:833–835

Reuter K, Sanderbrand S, Jomaa H et al (2002) Crystal structure of 1-deoxy-D-xylulose-5-phosphate reductoisomerase, a crucial enzyme in the non-mevalonate pathway of isoprenoid biosynthesis. J Biol Chem 277:5378–5384

Rietz PJ, Skelton FS, Folkers K (1967) Occurrence of ubiquinones-8 and -9 in *Plasmodium lophurae*. Int Z Vitaminforsch 37:405–411

Rohdich F, Eisenreich W, Wungsintaweekul J et al (2001) Biosynthesis of terpenoids. 2*C*-Methyl-D-erythritol 2,4-cyclodiphosphate synthase (IspF) from *Plasmodium falciparum*. Eur J Biochem 268: 3190–3197

Rohdich F, Hecht S, Gärtner K et al (2002) Studies on the nonmevalonate terpene biosynthetic pathway: metabolic role of IspH (LytB) protein. Proc Natl Acad Sci USA 99:1158–1163

Rohdich F, Zepeck F, Adam P et al (2003) The deoxyxylulose phosphate pathway of isoprenoid biosynthesis: studies on the mechanisms of the reactions catalyzed by IspG and IspH protein. Proc Natl Acad Sci USA 100:1586–1591

Röhrich RC, Englert N, Troschke K et al (2005) Reconstitution of an apicoplast-localised electron transfer pathway involved in the isoprenoid biosynthesis of *Plasmodium falciparum*. FEBS Lett 579:6433–6438

Sakamoto Y, Furukawa S, Ogihara H et al (2003) Fosmidomycin resistance in adenylate cyclase deficient (cya) mutants of *Escherichia coli*. Biosci Biotechnol Biochem 67:2030–2033

Schlitzer M (2008) Antimalarial drugs – what is in use and what is in the pipeline. Arch Pharm (Weinheim) 341:149–163

Shigi Y (1989) Inhibition of bacterial isoprenoid synthesis by fosmidomycin, a phosphonic acid-containing antibiotic. J Antimicrob Chemother 24:131–145

Silber K, Heidler P, Kurz T et al (2005) AFMoC enhances predictivity of 3D QSAR: a case study with DXP-reductoisomerase. J Med Chem 48:3547–3563

Skelton FS, Lunan KD, Folkers K et al (1969) Biosynthesis of ubiquinones by malarial parasites. I. Isolation of [14C]ubiquinones from cultures of rhesus monkey blood infected with *Plasmodium knowlesi*. Biochemistry 8:1284–1287

Steinbacher S, Kaiser J, Eisenreich W et al (2003) Structural basis of fosmidomycin action revealed by the complex with 2-*C*-methyl-D-erythritol 4-phosphate synthase (IspC). Implications for the catalytic mechanism and anti-malaria drug development. J Biol Chem 278:18401–18407

Surolia N, Surolia A (2001) Triclosan offers protection against blood stages of malaria by inhibiting enoyl-ACP reductase of *Plasmodium falciparum*. Nat Med 7:167–173

Tahar R, Basco LK (2007) Molecular epidemiology of malaria in Cameroon. XXV. *In vitro* activity of fosmidomycin and its derivatives against fresh clinical isolates of *Plasmodium falciparum* and sequence analysis of 1-deoxy-D-xylulose 5-phosphate reductoisomerase. Am J Trop Med Hyg 77:214–220

Takahashi S, Kuzuyama T, Watanabe H et al (1998) A 1-deoxy-D-xylulose 5-phosphate reductoisomerase catalyzing the formation of 2-*C*-methyl-D-erythritol 4-phosphate in an alternative nonmevalonate pathway for terpenoid biosynthesis. Proc Natl Acad Sci USA 95:9879–9884

Tonkin CJ, Foth BJ, Ralph SA et al (2008) Evolution of malaria parasite plastid targeting sequences. Proc Natl Acad Sci USA 105:4781–4785

Trager W, Jensen JB (1976) Human malaria parasites in continuous culture. Science 193:673–675

Tsuchiya T, Ishibashi K, Terakawa M et al (1982) Pharmacokinetics and metabolism of fosmidomycin, a new phosphonic acid, in rats and dogs. Eur J Drug Metab Pharmacokinet 7:59–64

van Dooren GG, Stimmler LM, McFadden GI (2006) Metabolic maps and functions of the Plasmodium mitochondrion. FEMS Microbiol Rev 30:596–630

Vial HJ, Philippot JR, Wallach DF (1984) A reevaluation of the status of cholesterol in erythrocytes infected by *Plasmodium knowlesi* and *P. falciparum*. Mol Biochem Parasitol 13:53–65

Vollmer M, Thomsen N, Wiek S et al (2001) Apicomplexan parasites possess distinct nuclear-encoded, but apicoplast-localized, plant-type ferredoxin-NADP$^+$ reductase and ferredoxin. J Biol Chem 276:5483–5490

Wiesner J, Jomaa H (2007) Isoprenoid biosynthesis of the apicoplast as drug target. Curr Drug Targets 8:3–13

Wiesner J, Seeber F (2005) The plastid-derived organelle of protozoan human parasites as a target of established and emerging drugs. Expert Opin Ther Targets 9:23–44

Wiesner J, Hintz M, Altincicek B et al (2000) *Plasmodium falciparum*: detection of the deoxyxylulose 5-phosphate reductoisomerase activity. Exp Parasitol 96:182–186

Wiesner J, Henschker D, Hutchinson DB et al (2002) *In vitro* and *in vivo* synergy of fosmidomycin, a novel antimalarial drug, with clindamycin. Antimicrob Agents Chemother 46:2889–2894

Wiesner J, Kettler K, Sakowski J et al (2004) Farnesyltransferase inhibitors inhibit the growth of malaria parasites *in vitro* and *in vivo*. Angew Chem Int Ed Engl 43:251–254

Wiesner J, Ortmann R, Jomaa H et al (2007) Double ester prodrugs of FR900098 display enhanced in-vitro antimalarial activity. Arch Pharm (Weinheim) 340:667–669

Wiesner J, Reichenberg A, Heinrich S et al (2008) The plastid-like organelle of apicomplexan parasites as drug target. Curr Pharm Des 14:855–871

Wilson RJ, Denny PW, Preiser PR et al (1996) Complete gene map of the plastid-like DNA of the malaria parasite *Plasmodium falciparum*. J Mol Biol 261:155–172

Wilson RJ, Rangachari K, Saldanha JW et al (2003) Parasite plastids: maintenance and functions. Philos Trans R Soc Lond B Biol Sci 358:155–162

Wolff M, Seemann M, Tse Sum Bui B et al (2003) Isoprenoid biosynthesis via the methylerythritol phosphate pathway: the (*E*)-4-hydroxy-3-methylbut-2-enyl diphosphate reductase (LytB/IspH) from *Escherichia coli* is a [4Fe-4S] protein. FEBS Lett 541:115–120

Woo YH, Fernandes RP, Proteau PJ (2006) Evaluation of fosmidomycin analogs as inhibitors of the *Synechocystis* sp. PCC6803 1-deoxy-D-xylulose 5-phosphate reductoisomerase. Bioorg Med Chem 14:2375–2385

Wunderlich F, Fiebig S, Vial H et al (1991) Distinct lipid compositions of parasite and host cell plasma membranes from *Plasmodium chabaudi*-infected erythrocytes. Mol Biochem Parasitol 44:271–277

Yajima S, Hara K, Iino D et al (2007) Structure of 1-deoxy-D-xylulose 5-phosphate reductoisomerase in a quaternary complex with a magnesium ion, NADPH and the antimalarial drug fosmidomycin. Acta Crystallogr Sect F Struct Biol Cryst Commun 63:466–470

Zeidler J, Schwender J, Müller C et al (1998) Inhibition of the non-mevalonate 1-deoxy-D-xylulose-5-phosphate pathway of plant isoprenoid biosynthesis by fosmidomycin. Z Naturforsch C 53:980–986

Zhu G, Marchewka MJ, Keithly JS (2000) *Cryptosporidium parvum* appears to lack a plastid genome. Microbiology 146:315–321

Regulation of Isoprene and Monoterpene Emission

10

Isabel Nogués and Francesco Loreto

Abstract

Isoprene and monoterpenes are synthesized and emitted into the atmosphere by many plant species, constitutively and/or after induction by environmental changes. Volatile isoprenoids are involved in defence against biotic and abiotic stresses. It is known that changes of the emission of volatile isoprenoids can be explained by the regulation of the activity of the corresponding synthases (isoprene or monoterpene synthases) or by substrate availability, but there are still gaps in the understanding of regulatory mechanisms controlling the emissions. Short-term variations in isoprene and monoterpene emissions depend basically on light and temperature, but control of monoterpene emission from plants that do not store terpenes is different from that of plants having specialized structures for their storage. Long-term and seasonal variations, however, are explained by developmental processes and by environmental factors, such as temperature and water stress.

Keywords

Isoprene • Monoterpenes • Photosynthesis • Dimethylallyl diphosphate • Geranyl diphosphate • Isoprene synthase • Monoterpene synthases • Light • Temperature

10.1 Introduction: The Biogenic Emission of Isoprene and Monoterpenes

Leaves of many plant species emit volatile organic compounds (VOCs) into the atmosphere. Among the biogenic VOCs, isoprene and monoterpenes are among the most abundant and reactive volatiles (Guenther et al. 1995; Hoffmann et al. 1997). The discovery that plants can emit

I. Nogués (✉)
CNR – Istituto di Biologia Agroambientale e Forestale,
Via Salaria km. 29,300, 00016
Monterotondo Scalo (Roma), Italy
e-mail: isabel.nogues@ibaf.cnr.it

F. Loreto
CNR – Istituto per la Protezione delle Piante,
Via Madonna del Piano 10, 50019
Sesto Fiorentino (Firenze), Italy

T.J. Bach and M. Rohmer (eds.), *Isoprenoid Synthesis in Plants and Microorganisms: New Concepts and Experimental Approaches*, DOI 10.1007/978-1-4614-4063-5_10,

isoprene is relatively recent (Rasmussen and Went 1965), and the functional role of isoprene is still not clear. It has been suggested that isoprene stabilizes thylakoid membranes, increasing tolerance of photosynthesis to high temperatures (Sharkey and Yeh 2001). Recently, Velikova et al. (2011) provided biophysical evidence that isoprene improves the integrity and functionality of the thylakoid membranes at high temperature. Isoprene also reduces ozone damage in leaves by quenching reactive oxygen species (ROS) (Loreto and Velikova 2001; Loreto et al. 2001a) and by decreasing intercellular NO and H_2O_2 concentrations (Velikova et al. 2005). Isoprene is not stored inside the leaves; that means that the emission of isoprene is controlled by its synthesis, which depends mainly on photosynthetic photon flux densities (PPDF) (Sharkey and Loreto 1993) and leaf temperature (Monson et al. 1992).

The functions of monoterpenes have been much more clearly identified. Monoterpenes are frequent constituents of oils and resins, and their accumulation is often associated with complex secretory structures such as glandular trichomes, secretory cavities or resin ducts (Fahn 1979). Monoterpene biosynthesis is generally restricted to certain developmental stages (Bernard-Dagan et al. 1982; Dudareva et al. 1996). Monoterpenes are involved in defence against herbivores and pathogens, allelopathic interactions and entomophilous pollination (Langenheim 1994). Much alike isoprene, monoterpenes were also demonstrated to protect against abiotic (thermal or oxidative) stresses (Delfine et al. 2000; Loreto et al. 2004) and to react with ROS (Hoffmann et al. 1997). Monoterpenes are also among the most important constituents of flavourings and fragrances for human consumption (Mulder-Krieger et al. 1988) and can serve as therapeutic agents in human medicine (Gould 1997).

Monoterpenes are emitted by both storing and non-storing plant species, but the emission is regulated differently in these two groups of plants. For storing species, it has been assumed that monoterpene emission is controlled only by total monoterpene content (Lerdau et al. 1995), volatility and foliar temperatures that determine the vapour pressure of specific monoterpenes (Tingey et al. 1991; Guenther et al. 1994; Monson et al. 1995). Whereas for non-storing species, light intensity plays an important role as a regulatory factor of monoterpene synthesis. Núñez et al. (2002), however indicated that part of monoterpene emission from storing species is also linked to recent biosynthesis and therefore regulated by ambient solar radiation and air temperature.

Both isoprene and monoterpenes are key molecules in atmospheric chemistry. Because of their high reactivity with anthropogenic pollutants and compounds ubiquitously resident in the troposphere following light reactions, volatile isoprenoids can be involved in the formation of pollutants such as photochemical ozone (Chameides et al. 1988), aerosol and particles (Di Carlo et al. 2004).

10.2 General Remarks on the Biosynthesis of Volatile Isoprenoids

The biosynthesis of isoprene and monoterpenes starts with the synthesis of a fundamental and common precursor, isopentenyl diphosphate (IDP=IPP). The formation of this basic C_5 unit and of its isomer dimethylallyl diphosphate (DMADP=DMAPP) can proceed via two pathways: the long known cytosolic mevalonate (MVA) pathway stepping from acetyl-CoA formation (cf. Bochar et al. 1999) and the essentially chloroplastic methylerythritol phosphate (MEP) pathway, which synthesizes isoprenoid precursors from pyruvate and glyceraldehyde 3-phosphate (Rohmer et al. 1993; Eisenreich et al. 2001). The two pathways are supposed to cross talk to some extent, but little or not at all when VOCs like isoprene (Schwender et al. 1997) or 2-methyl-3-buten-2-ol are concerned (Zeidler and Lichtenthaler 2001). The exchange of metabolites seems to occur prevalently from the plastids to the cytosol (Bick and Lange 2003), while no significantly enhanced incorporation of cytosolic carbon into VOCs has been observed, even when the chloroplastic pathway was completely blocked by the MEP pathway inhibitor fosmidomycin (Loreto et al. 2004). However, stressed

leaves seem to emit isoprene that incorporates an increasing percentage of unlabelled carbon that, therefore, is not derived from photosynthetic intermediates (Funk et al. 2004; Brilli et al. 2007). As a rule of thumb, isoprene and monoterpenes are quickly and almost completely labelled by ^{13}C from $^{13}CO_2$ (Delwiche and Sharkey 1993; Loreto et al. 1996b), which suggests that their biosynthesis is predominantly dependent on the availability of photosynthetic intermediates that are shunted from the carbon fixation cycle.

The synthesis of both isoprene and monoterpenes is under enzymatic control. Isoprene synthase (IS) catalyses the formation of isoprene from DMADP (Silver and Fall 1991) in the chloroplast (Mgaloblishvili et al. 1979). Soluble forms of this enzyme have been isolated and characterized from different plant species (Kuzma and Fall 1993; Silver and Fall 1995; Schnitzler et al. 1996), though IS activity bound to thylakoid membranes has also been reported (Wildermuth and Fall 1996; Fall and Wildermuth 1998). On the other hand, geranyl diphosphate synthase (GPPS), also localized in the chloroplasts (Bouvier et al. 2000), is the prenyltransferase that catalyses the condensation reaction between DMADP and an IDP unit to generate geranyl diphosphate (GDP=GPP) (C_{10}), the precursor of monoterpenes and hence the substrate of monoterpene synthases. Whereas the K_m of IS for DMADP is in the millimolar range (Silver and Fall 1995), the K_m of GPPS for DMADP is in the micromolar range (Tholl et al. 2001). This difference is important for the distribution of the DMADP between IS and GDPS and constitutes a regulatory point in the synthesis of isoprene and monoterpenes. Some monoterpene synthases have also been isolated from plants (Croteau 1987), and it has been observed that all those enzymes are very similar in their physical and chemical properties (Trapp and Croteau 2001). Also interesting is the fact that monoterpene synthases are reported to have a higher affinity for GDP than isoprene synthase for DMADP (Wolfertz et al. 2004). This might cause differences in the regulation and pattern of emission of isoprene and monoterpenes.

10.3 Environmental Regulation of Isoprene and Monoterpene Emission

10.3.1 Short-Term Environmental Regulation of Isoprene Emission and Its Biochemical Basis

Early studies firmly established that the instantaneous emission of isoprene largely depends on photosynthetic photon flux densities (PPDF) (Sharkey and Loreto 1993) and leaf temperature (Monson et al. 1992), while other environmental factors, such as soil moisture, air humidity and CO_2 concentration, play a minor role in controlling short-term variations (Guenther et al. 1991).

The light dependence of isoprene emission was first described by Sanadze (1969); this was the cornerstone finding that allowed to link isoprenoid metabolism with primary carbon fixation (Monson and Fall 1989; Evans et al. 1985; von Caemmerer and Farquhar 1981). Isoprene pools have never been detected inside leaves, and its internal concentration has been estimated small, as its emission is sustained only for a very limited time (Singsaas et al. 1997; Loreto et al. 1998). This explains why isoprene emission drops to zero within few minutes after darkening leaves (Loreto and Sharkey 1990). Light controls the production of photosynthetic metabolites and the supply of ATP plus NADPH to the chloroplastic isoprenoid pathway (Eisenreich et al. 2001; Sharkey and Yeh 2001). Thus, the fast inhibition of isoprene emission in the dark is due to the limited availability of both these cofactors. The *in vivo* IS kinetic properties from aspen leaves suggested that the enzyme mainly operates under substrate limitation and that short-term light, CO_2 and O_2 dependencies of isoprene emission result from variation in DMADP pool size rather than from modifications in isoprene synthase activity (Rasulov et al. 2009).

The light dependency of isoprene emission and of photosynthesis are very similar (Fig. 10.1a). As for photosynthesis, isoprene emission increases linearly at low to moderate

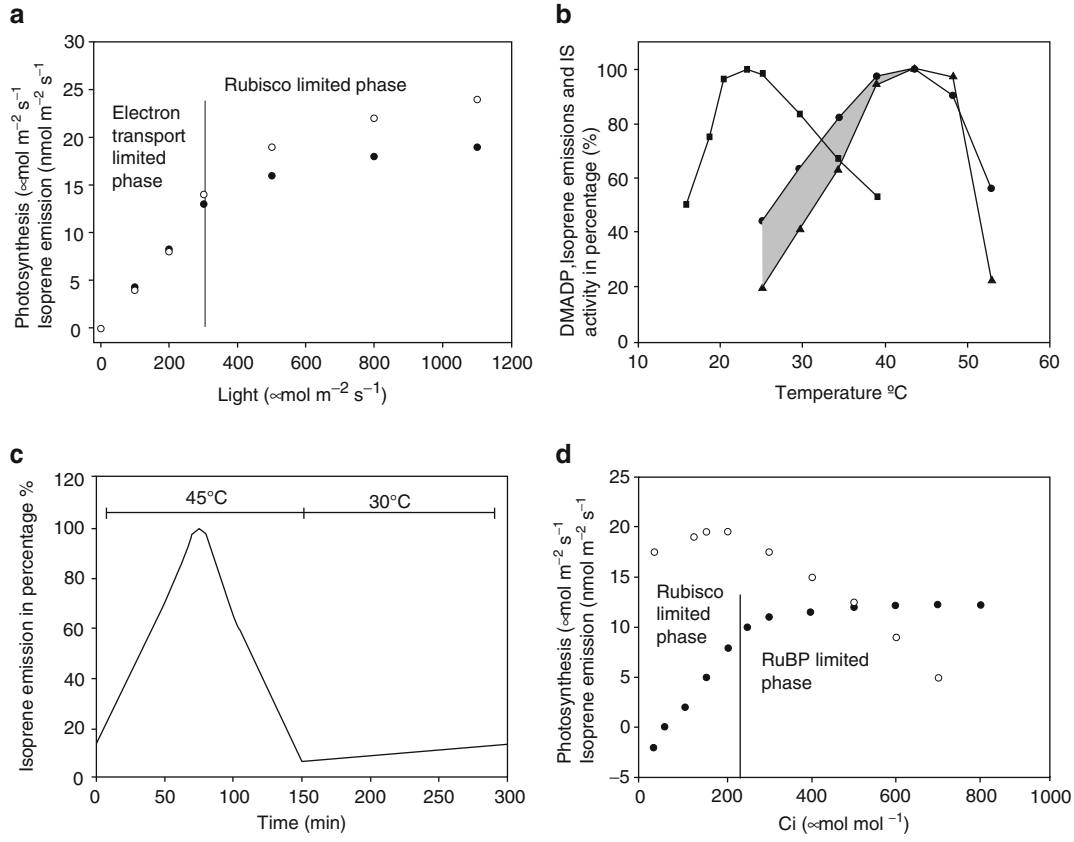

Fig. 10.1 (**a**) Response of photosynthesis (*black symbols*) and isoprene emission rates (*white symbols*) to light intensity in *E. globulus* leaves under ambient air conditions (Data taken from Loreto and Delfine 2000). The text inside the graph is referred to the photosynthesis curve. (**b**) DMADP (*black rectangles*) isoprene emission (*black circles*) and IS activity (*black triangles*) at different temperatures expressed in percentage of the maximum (Data taken from Monson et al. 1992). (**c**) Time course of the emission of isoprene following exposure to high temperature of *Phragmites* leaves. The sequence of temperature exposure (30–45°C and 45–30°C) is shown in the top part of the figure. Emission is expressed as percentage of the maximum emission at 45°C (Data taken from Loreto et al. 2006). (**d**) Effects of Ci on photosynthesis (*black symbols*) and isoprene emission rates (*white symbols*) from branches of *M. communis* measured at 26°C and light intensity of 1,000 μmol m^{-2} s^{-1} (Data taken from Affek and Yakir (2002))

PPFD, indicating that emission is limited by a light-dependent factor under these conditions (Fig. 10.1a). At PPFDs slightly below to far above growth light intensities, the emission of isoprene increases less than proportionally with PPFDs, as it happens with photosynthesis. In some cases, isoprene emission saturates at the same light intensity as photosynthesis (at PPFDs ranging from 1,000 to 2,000 μmol m^{-2} s^{-1}, with photosynthesis being generally saturated already at the growth light intensity), but in most cases, isoprene emission continues to increase with light intensity above those where photosynthesis gets saturated (Sharkey et al. 1991; Sharkey and Loreto 1993; Harley et al. 1996; Lerdau and Keller 1997). For instance, isoprene emission from kudzu leaves responds to light intensities up to 3,000 μmol m^{-2} s^{-1} (Sharkey and Loreto 1993). This unexpected increase in the rate of isoprene emission, which uncouples the emission from photosynthetic activity, may be caused by an excess of photosynthetic electron transport, leading to low NADP concentrations as final electron acceptors. The excess of light energy may not be efficiently utilized by the Calvin cycle (which is also the main cause of photosynthesis saturation

at high light) and may become available for alternative uses, which also helps to reconstitute the pools of ADP and NADP. A greater fractional investment of electrons in isoprene production, at higher photon flux, has been indeed postulated (Niinemets et al. 1999). On the other hand, an increase of available substrate from other sources may also be invoked to explain why isoprene emission increases even when photosynthesis is light saturated. It has been proposed that, under conditions of limited photosynthesis, transitory starch (Schnitzler et al. 2004) or xylem-derived sugars (Mayrhofer et al. 2004) might constitute alternative carbon sources for isoprene emission. Whether the same activation on alternative sources also occurs under light-saturated photosynthesis, when large amounts of sugars accumulate (Delaney et al. 1977), is not known.

Isoprene emission is also strongly dependent on instantaneous changes of temperature, increasing exponentially when temperature increases from 15°C to 35°C (Fig. 10.1b) (Tingey et al. 1979; Monson and Fall 1989; Loreto and Sharkey 1990; Hansted et al. 1994). Optimal temperatures for both isoprene emission and IS activity range between 40°C and 44°C (Monson et al. 1992). The exponential increase of isoprene emission occurs with a Q_{10} variable between 2 and 4, which is typical of enzyme-driven reactions. Indeed, Monson et al. (1992) showed that IS activity has the same temperature dependence of isoprene emission, as shown by the similar slope below 40°C (Fig. 10.1b). Thus, while the light dependency of isoprene emission is explained by some substrate limitation, the response to temperature can be mainly attributed to changes of IS activity. However, Niinemets et al. (1999) found that isoprene emission increases faster than IS activity with temperature and peaks at temperatures lower than those being optimal for IS activity. This observation suggests that the shape of the temperature response curve of isoprene emission not only depends on isoprene synthase features but is also influenced by the temperature stability of photosynthetic electron transport. The electron transport rate driving photosynthesis operates at a temperature optimum lower than that for isoprene synthase activity, but a substantial rate of electron transport can already drive isoprene synthesis when isoprene emission is highly stimulated by temperature whereas IS activity still remains low, as shown by the shaded area of Fig. 10.1b (Niinemets et al. 1999).

Isoprene emission is reduced at temperatures above a certain optimum. This was attributed to the adverse effect of heat on enzyme structure (Monson et al. 1992). However, even maintaining for several hours, the temperature at 40°C (the optimal temperature for isoprene emission and IS activity) causes isoprene emission to drop (Fig. 10.1c and Singsaas and Sharkey 2000). A reversible control on isoprene synthesis, rather than enzyme denaturation, might cause isoprene to drop at high temperatures (Singsaas and Sharkey 2000). Indeed, isoprene emission rapidly returns to the levels attained before exposure to high temperatures, once the temperature is reduced again (Fig. 10.1c), which would not be possible if IS were denatured (Loreto et al. 2006). In agreement with this, Magel et al. (2006) have shown that DMADP concentration begins to drop at temperatures above 25°C. Thus, the availability of DMADP may be responsible for the down-regulation of isoprene emission in response to continued exposure to high temperatures.

The very high rates of isoprene emission at high temperatures are interpreted as an indirect evidence for isoprene to protect leaves from high-temperature damage (Singsaas et al. 1997). Singsaas and Sharkey (1998) showed that isoprene emission changes are fast enough to follow the large and very rapid temperature changes observed in an oak canopy. Thus, isoprene may in particular protect leaves from very rapid heat flecks, when other, slower, protective mechanisms are still not activated. The study by Singsaas and Sharkey (1998) also indicated that there may be two processes, characterized by their different kinetics, which cause isoprene emission to increase with leaf temperature. The fastest process likely reflects the influence of temperature on the maximum velocity of enzymes, while the slower process may be the one reflecting IS activation.

Isoprene emission is also influenced by CO_2 (Fig. 10.1d). The inhibitory effect of elevated

CO_2 on isoprene emission has been often described (Sharkey et al. 1991; Rosenstiel et al. 2003; Centritto et al. 2004). This is a rather surprising effect since neither substrate availability (i.e. photosynthates) nor enzyme (IS) properties could explain why isoprene drops, while photosynthesis is stimulated by rising CO_2 levels. Velikova et al. (2009) investigated the interactive effects of increasing CO_2 (380 and 800 μmol mol^{-1}, respectively) and heat wave (39°C) occurrence on isoprene emission in leaves of *Platanus orientalis* L. and concluded that high temperature might to some extent outweigh the inhibitory effects of elevated atmospheric CO_2 on isoprene emission. Rosenstiel et al. (2002) hypothesized that isoprene biosynthesis may compete with several cytosolic processes depending on PEP, particularly respiration and nitrate reduction (Rosenstiel et al. 2004). As PEP is the source of pyruvate for DMADP production, a lower import of PEP into chloroplasts may result in a decline in isoprene emission when plants are grown at elevated CO_2 (Rosenstiel et al. 2003). Loreto et al. (2007) recently offered support for this hypothesis, with the observation that isoprene emission is inversely related to PEP carboxylase activity. However, a direct relationship between isoprene emission and respiration was also found (Loreto et al. 2007), which implies a more subtle regulation of isoprene emission. Perhaps only one of the anaplerotic pathways driving respiration (the one requiring PEP) is competing with isoprene for the same substrate (Loreto et al. 2007).

Isoprene emission is also sensitive to low CO_2, increasing at CO_2 concentrations rising from zero to sub-ambient (Fig. 10.1d). Since this increase in isoprene emission is associated with a linear increase of photosynthesis, which represents the activation of RuBisCO (Farquhar et al. 1980), isoprene emission may also be limited by RuBisCO activity in this range of CO_2 concentration. On the other hand, Niinemets et al. (1999) indicated that the decline in isoprene emission at low Ci (the intracellular CO_2 concentration) might be related not only to reduced electron or carbon availability at low Ci but also to a greater electron cost of isoprene synthesis at low Ci.

10.3.2 Short-Term Environmental Regulation of Monoterpene Emission and Its Biochemical Basis

Monoterpene emission has also been shown to depend on light and temperature (Bertin et al. 1997; Ciccioli et al. 1997; Staudt and Bertin 1998; Kesselmeier and Staudt 1999). However, as outlined before, the pattern of terpene emission from plants that do not store terpenes in specialized structures is definitely different from that of plants having specialized structures for their storage (Lerdau 1991; Lerdau et al. 1995; Seufert et al. 1995; Loreto et al. 1996a). Based on this difference, it can be expected that the short-term response of monoterpene emission rates to PPFD will be stronger and faster in non-storing species than in storing ones (Staudt and Seufert 1995). In fact, monoterpenes from plants lacking specialized structures are rapidly labelled by $^{13}CO_2$ (Loreto et al. 1996b), following the same pattern of isoprene labelling, which indicates that the carbon supply comes almost exclusively from the photosynthetic carbon metabolism. Thus, monoterpene emission that changes with light intensity for non-storing species is likely limited by substrate availability as it is true for isoprene emission.

Several studies have reported light dependency for monoterpene emissions from leaves of *Quercus ilex* (Staudt and Seufert 1995; Loreto et al. 1996a), *Helianthus annuus* and *Fagus sylvatica* (Schuh et al. 1997) and other *Quercus* sp. (Bertin et al. 1997; Street et al. 1997). Owen et al. (2002) examined the effects of light and temperature on monoterpene emission from some Mediterranean plant species. Their results showed that all species studied emitted one or more compounds with some degree of light dependency.

Also, several conifers, all of which are listed as species storing monoterpenes in resin ducts, have been reported to present light-dependent monoterpene emission, e.g. *Pinus sylvestris* (Janson 1993; Shao et al. 2001), *Pinus pinea* (Staudt et al. 1997; Loreto et al. 2000) and *Picea abies* (Steinbrecher 1989; Schürmann et al. 1993; Steinbrecher and Ziegler 1997). Therefore, in addition to the emission from extensive storage

pools, which may be limited by large diffusive resistances due to the tightness of storage cells (Tingey et al. 1991), monoterpenes immediately synthesized in chloroplasts of mesophyll cells in the light also contribute significantly to total emission of conifers (Schürmann et al. 1993).

Temperature also affects monoterpene emission (Loreto and Sharkey 1990; Loreto et al. 1996a). Temperature dependence is exponential, with maximal monoterpene emission set at 40°C in *P. abies* and *Q. ilex* (Fischbach et al. 2000). As for isoprene, this probably also reflects the temperature dependence of the specific enzymes, mostly likely monoterpene synthases (Fischbach et al. 2000). In fact, it has been shown that leaf temperature exerts a strong control over monoterpene synthase activity of most monoterpene species (Melle et al. 1996; Fischbach et al. 2000).

Furthermore, it has been suggested that monoterpene synthase activity is influenced by the chloroplastic (stromal) pH (Niinemets et al. 2002). As a decrease in photosynthetic activity at temperatures above the optimum of photosynthesis leads to some acidification of the stromal pH, a decrease in photosynthesis should favour monoterpene emission since pH optima of monoterpene synthases are slightly shifted to the acidic range (Bohlmann et al. 1998; Fischbach et al. 2000; Niinemets et al. 2002).

In conclusion, light and temperature dependencies of monoterpene emissions are variable and may depend on different properties of the synthase enzymes or on substrate requirements and availability as well. In monoterpene-storing species, the most important factor driving light dependency is the pool size of monoterpenes that are stored in reservoir organs from where they are slowly released. In species that do not store monoterpenes, as holds true with isoprene, it seems that the light dependency of the monoterpene emissions is rather controlled by substrate availability, whereas temperature dependency reflects more or less the kinetic properties of various monoterpene synthases.

As to the CO_2 dependency of short-term monoterpene emissions, there exist some contrasting results: Whereas Loreto et al. (1996a) and Staudt et al. (2001) demonstrated that monoterpene emissions are not affected by short-term changes in CO_2 concentrations, other authors have indicated that CO_2 rising within a short period may become inhibitory (Rapparini et al. 2001). The same effect was observed when whole plants were exposed long term to elevated CO_2 (Monson and Fall 1989; Loreto and Sharkey 1990; Sharkey et al. 1991; Loreto et al. 2001b; Scholefield et al. 2004; Rosenstiel et al. 2003), but there are also some exceptions (Tognetti et al. 1998; Constable et al. 1999; Buckley 2001; Staudt et al. 2001).

Loreto et al. (2001b) proposed that, in the Mediterranean region, multiple stresses, such as high temperature and irradiance combined with limited water availability, could have strong effects on isoprenoid emission, especially in summer. Accordingly, in their long-term study on field-grown *Q. ilex* plants under elevated CO_2 conditions, the inhibitory effect of high CO_2 on monoterpene emission was not observed when plants experienced a very severe summer drought, suggesting that the effect of these environmental stresses can counteract and overcome the negative effect of elevated CO_2.

10.3.3 Long-Term Environmental Regulation of Isoprene Emission (Diurnal to Seasonal) and Its Biochemical Basis

Diurnal variations of isoprene emission are also almost entirely due to variations of light intensity and leaf temperature. Highest isoprene emission rates are observed at noon under maximum temperatures and light intensities, and a decline of the emission rate occurs when light and temperature drop. However, a circadian mechanism of control of isoprene emission cannot be excluded and indeed has been postulated recently (Wilkinson et al. 2006; Loivamäki et al. 2007). IS transcript levels have also been observed to change during the day (Arimura et al. 2004: Mayrhofer et al. 2005), with a daily pattern similar to isoprene emission. However, changes in IS transcript level and protein quantity do not correspond to changes in IS activity, as the latter

does not seem to vary during the course of the day (Mayrhofer et al. 2005). On the other hand, DMADP pools also have been shown to fluctuate diurnally in different species (Fisher et al. 2001; Brüggemann and Schnitzler 2002; Magel et al. 2006). The daily variations in DMADP concentration have been shown to be similar to that of isoprene emission, with maximum values at noon (Mayrhofer et al. 2005). Therefore, it seems that daily variations of isoprene emission are controlled by both isoprene synthase transcript level and DMADP availability.

Several studies (Monson et al. 1994; Kempf et al. 1996; Funk et al. 2005; Mayrhofer et al. 2005) have observed a strong seasonal variation of isoprene emission rates, with an increase in springtime and a rapid decline in autumn. Seasonal variations in isoprene emission correlate with the inherent capacity of the leaves to synthesize isoprene (Monson et al. 1994). This capacity depends on the developmental stage of the leaves (Kuzma and Fall 1993). Leaves undergo physiological and developmental changes over the course of the growing season, and isoprenoid basal emission rates (normalized at 30°C and 1,000 μmol m^{-2} s^{-1} of PPFD (Guenther et al. 1991)) vary accordingly (Kuhn et al. 2004). It is long known that photosynthetic competence develops several days before significant isoprene emission (Loreto and Sharkey 1993; Wiberley et al. 2005). Both young and senescent leaves emit low rates of isoprene, whereas the highest emissions are measured for fully developed mature leaves during the main growing season (Kuhn et al. 2004). It has been reported that isoprene emission rate of velvet bean (*Mucuna* sp.) leaves increases as much as 125-fold as leaves develop and then declines with increasing age (Grinspoon et al. 1991). This pattern again corresponds to that of extractable isoprene synthase activity in leaves (Kuzma and Fall 1993). However, it is also known that young leaves contain lower amounts of DMADP than mature ones with high rates of isoprene emission (Loreto et al. 2004).

Changes of IS activity over the growing season have been reported for different species: European oaks (Lehning et al. 1999; Brüggemann and Schnitzler 2001), *Mucuna* sp. (Kuzma and Fall 1993), *Phragmites australis* (Scholefield et al. 2004) and *Pueraria montana* (Wiberley et al. 2005). Whereas there is agreement about the role played by IS activity on the seasonal variation of isoprene emission, the opinions on whether the DMADP pool size also regulates long-term patterns of emissions diverge. For some authors, DMADP may also be responsible for the seasonal and developmental variation of isoprene emission (Geron et al. 2000; Brüggemann and Schnitzler 2002), and there is a positive correlation between the metabolic flux through the plastidic pathway and the IS activity present in the leaves (Eisenreich et al. 2001). However, we have recently shown that the DMADP pool size is inversely related to isoprene emission when pool and emission were measured over a vegetative season (Nogués et al. 2006).

Other factors can influence seasonal isoprene emission such temperature (Monson et al. 1994), light intensity, water stress (Fang et al. 1996) and the availability of nutrients, such as nitrogen (Litvak et al. 1996). The light growth environment clearly affects leaf isoprene emissions. Sunlight-exposed leaves emit by far more isoprene than leaves of the same tree grown in the shade, both when sampled at the growth light environment and under standard conditions (30°C and 1,000 μmol m^{-2} s^{-1} of PPFD) (Harley et al. 1996; Owen et al. 2002). As it is known that sun leaves present photosynthetic rates higher than shade leaves (Litvak et al. 1996), leaves grown in the sun may simply possess more chloroplastic DMADP than shade leaves, leading to enhanced isoprene synthesis, at least when calculated on an surface area basis, as sun leaves are thicker than shade leaves.

The temperature during plant development also influences the delay between the leaves becoming photosynthetically competent and when they begin to emit isoprene (Monson et al. 1994; Wiberley et al. 2005). As expected, leaves grown at low temperature begin to emit isoprene later than those grown at higher temperatures (Sharkey et al. 2007). A possible explanation might consist in a different IS activity between the two conditions. Even after leaves are fully

developed, air temperature of the previous few hours and even up to weeks affects the basal rate of isoprene emission (Goldstein et al. 1998; Fuentes and Wang 1999; Fuentes et al. 1999; Sharkey et al. 1999; Pétron et al. 2001). Changes in the activity of IS can be observed in response to the temperature of the previous few days (Lehning et al. 2001).

Environmental stresses may also exert a long-term control on isoprene emission. While isoprene biosynthesis is definitely resistant to mild water stress (Brilli et al. 2007; Fortunati et al. 2008), severe water stress is known to reduce the rate of isoprene emission, but isoprene emission is still present when photosynthesis is completely inhibited by drought stress. Under these conditions, carbon for isoprene emission must come from alternative sources (Karl et al. 2002; Kreuzwieser et al. 2002; Affek and Yakir 2003; Schnitzler et al. 2004; Brilli et al. 2007).

Also interesting is that under mild water stress that inhibits photosynthesis, a slight isoprene emission increase has been observed in leaves of different plant species (Sharkey and Loreto 1993; Pegoraro et al. 2004, 2005). The activation of alternative routes of isoprene synthesis already under mild water stress conditions has been disproved (Brilli et al. 2007). Perhaps isoprene emission is stimulated, both under mild water stress and under high vapour pressure deficit as a result of stomatal closure and of the resulting decrease in intercellular CO_2 concentration (Ci) (Pegoraro et al. 2004). This also leads to a rather evident increase in the proportion of assimilated carbon lost as isoprene in water-stressed leaves (Pegoraro et al. 2004).

10.3.4 Long-Term Environmental Regulation of Monoterpene Emission and Its Biochemical Basis

Diurnal monoterpene emissions are quite heterogenous. In species that do not store monoterpenes, large emissions have been observed only during the day (Staudt et al. 1997) though a small release of monoterpenes has been observed also at night (Loreto et al. 2000). In the latter report, a burst of emission upon illumination of pre-darkened leaves was also found, which was interpreted as indicating the release of a small pool of monoterpenes consequent to stomatal opening.

Monoterpene emissions do not show a marked seasonality as isoprene emission, and emission patterns differ among species. However Llusià and Peñuelas (2000) have shown that Mediterranean woody plants normally present maximum values of emission in the spring-summer period. Leaf development is an important factor influencing monoterpene emission. In *Q. ilex*, the monoterpene emission rate increases tenfold during leaf growth, with slight changes in the composition of the monoterpene blend (Staudt and Bertin 1998). It has been shown that monoterpene emission by the evergreen leaves of *Q. ilex* leaves peaks in summer for two consecutive years (Ciccioli et al. 2002). On the other hand, plants may produce individual monoterpenes with different seasonal cycles. Downy birch (*Betula pubescens*) has been shown to emit large amounts of linalool and sesquiterpenes early in the growing season, while later in the season emissions consist mainly of sabinene and trans-β-ocimene (Hakola et al. 2001). Norway spruce (*Picea abies*) emits monoterpenes in May (Schürmann et al. 1993), whereas its emission mainly consists of isoprene in June and of sesquiterpenes in July (Hakola et al. 2003). Loreto et al. (2000) reported a large seasonal (summer) emission of trans-β-ocimene by needles of the Mediterranean pine *Pinus pinea*. This emission was light-dependent, indicating the activation of the formation of monoterpenes that are not stored in resin ducts. Even species that normally emit isoprene may seasonally emit monoterpenes. At early stage of leaf growth, during late spring, leaves of poplars (*Populus* sp., a family of plants that emit large amounts of isoprene only (cf. Centritto et al. 2011; Guidolotti et al. 2011)) were shown to emit several monoterpenes (Hakola et al. 1998; Brilli et al. 2009). Interestingly, the emission of monoterpenes seems to be inversely related to the emission of isoprene, being progressively reduced when isoprene starts to be emitted and eventually becoming undetectable when isoprene is largely

emitted (unpublished results). This observation reveals that the same pool of carbon probably produces monoterpenes or isoprene. The chain of events that seasonally cause the switch between emitted compounds is currently unknown.

It has been shown that monoterpene synthases activities control long-term monoterpene emission. Activities of these enzymes strongly change with leaf development, leaf age and temperature. Enzyme activities have been shown to change during the season in *Q. ilex* leaves, increasing rapidly in spring, reaching maximum values in summer and then declining during the following winter period (Fischbach et al. 2002).

Environmental stresses may also concur to set seasonal emission rates of monoterpenes. Drought also limits emissions of non-stored monoterpenes, possibly by decreasing carbon substrate and/or ATP (Bertin and Staudt 1996). Rewatering of drought-stressed plants brings emissions to a level slightly lower than the pre-stress one, which indicates an incomplete recovery of functionality of the pathway, much alike what has been recently described for isoprene (Fortunati et al. 2008). Drought also likely reduced monoterpene synthase activities, thus causing a summer reduction of the emissions of non-stored monoterpenes, especially in the Mediterranean area (Loreto et al. 2001b).

Some studies show that monoterpene emission is affected by the concentration of atmospheric CO_2 during growth, though results are sometimes contradictory in this respect. Emission of some monoterpenes seems to be enhanced by high CO_2 concentrations, whereas emission of other monoterpenes seems to be inhibited or not affected when CO_2 is raised (Constable et al. 1999; Loreto et al. 2001b; Staudt et al. 2001; Rapparini et al. 2004).

10.4 Conclusions

Although the regulatory mechanisms controlling isoprene and monoterpene emissions are not completely understood, it seems clear that control of short- and long-term emissions of isoprene and non-stored monoterpenes by temperature, water stress and CO_2 can be explained by the regulation of IS transcript levels and activity and/or by regulation of key substrates, predominantly the supply of DMADP or GDP. There are, however, some gaps in complete understanding of the effects of temperature and CO_2 on emissions.

The long-term control of volatile isoprenoid emissions is more complex. Diurnal variations of isoprene release are again set by light and temperature, the two factors that control emission by regulating isoprene synthase transcript levels and activity and substrate availability. Although monoterpene emissions at a daily scale are also known to be controlled by temperature and light (at least in non-stored monoterpenes), it has still to be elucidated if these environmental factors influence substrate availability, synthases activities or both.

Seasonal emissions seem to be associated to leaf development as IS and monoterpene synthases are under strong developmental control. This, and the impact of seasonal stresses, namely drought, can strongly modify emission rates and profiles over the season (cf. Velikova et al. 2009; cf. Vickers et al. 2009; Fares et al. 2010; Centritto et al. 2011).

References

Affek HP, Yakir D (2002) Protection by isoprene against singlet oxygen in leaves. Plant Physiol 129:269–277

Affek HP, Yakir D (2003) Natural abundance carbon isotope composition of isoprene reflects incomplete coupling between isoprene synthesis and photosynthetic carbon flow. Plant Physiol 131:1727–1736

Arimura G, Huber DPW, Bohlmann J (2004) Forest tent caterpillars (*Malacosoma disstria*) induce local and systemic diurnal emissions of terpenoid volatiles in hybrid poplar (*Populus trichocarpa* x *deltoides*): cDNA cloning, functional characterisation, and patterns of gene expression of (−)- germacrene D synthase, PtdTPS1. Plant J 37:603–616

Bernard-Dagan C, Pauly G, Marpeau A, Gleizes M, Carde JP, Baradat P (1982) Control and compartmentation of terpene biosynthesis in leaves of *Pinus pinaster*. Physiol Vég 20:775–795

Bertin N, Staudt M (1996) Effect of water stress on monoterpene emissions from young potted holm oak (*Quercus ilex* L.) trees. Oecologia 107:456–462

Bertin N, Staudt M, Hansen U et al (1997) The BEMA-project: diurnal and seasonal course of monoterpene

emissions by *Quercus ilex* L. under natural conditions – application of light and temperature algorithms. Atmos Environ 31:135–144

Bick JA, Lange BM (2003) Metabolic cross talk between cytosolic and plastidial pathways of isoprenoid biosynthesis: unidirectional transport of intermediates across the chloroplast envelope membrane. Arch Biochem Biophys 415:146–154

Bochar DA, Friesen JA, Stauffacher CV, Rodwell VW (1999) Biosynthesis of mevalonic acid from acetyl-CoA. In: Cane DE (ed) Comprehensive natural product chemistry, isoprenoids including steroids and carotenoids, vol 2. Pergamon Press Inc., Tarrytown

Bohlmann J, Meyer-Gauen G, Croteau R (1998) Plant terpenoid synthases: molecular biology and phylogenetic analysis. Proc Natl Acad Sci USA 95:4126–4133

Bouvier F, Suire C, d'Harlingue A, Backhaus RA, Camara B (2000) Molecular cloning of geranyl diphosphate synthase and compartmentation of monoterpene synthesis in plant cells. Plant J 24:241–252

Brilli F, Barta C, Fortunati A, Lerdau M, Loreto F, Centritto M (2007) Response of isoprene emission and carbon metabolism to drought in white poplar (*Populus alba*) saplings. New Phytol 175:244–254

Brilli F, Ciccioli P, Frattoni M, Prestininzi M, Spanedda AF, Loreto F (2009) Constitutive and herbivore-induced monoterpenes emitted by *Populus x euroamericana* leaves are key volatiles that orient *Chrysomela populi* beetles. Plant Cell Environ 32:542–552

Brüggemann N, Schnitzler JP (2001) Influence of powdery mildew (*Microsphaera alphitoides*) on isoprene biosynthesis and emission of pedunculate oak (*Quercus robur* L.) leaves. J Appl Bot 75:91–96

Brüggemann N, Schnitzler JP (2002) Comparison of isoprene emission, intercellular isoprene concentration and photosynthetic performance in water-limited oak (*Quercus pubescens* Willd. *and Quercus robur* L.) saplings. Plant Biol 4:456–463

Buckley PT (2001) Isoprene emissions from a Florida scrub oak species grown in ambient and elevated carbon dioxide. Atmos Environ 35:631–634

Centritto M, Nascetti P, Petrilli L, Raschi A, Loreto F (2004) Profiles of isoprene emission and photosynthetic parameters in hybrid poplars exposed to free-air CO_2 enrichment. Plant Cell Environ 27:403–412

Centritto M, Brilli F, Fodale R, Loreto F (2011) Different sensitivity of isoprene emission, respiration and photosynthesis to high growth temperature coupled with drought stress in black poplar (*Populus nigra*) saplings. Tree Physiol 31:275–286

Chameides WL, Lindsay RW, Richardson J, Kiang CS (1988) The role of biogenic hydrocarbons in urban photochemical smog: Atlanta as a case study. Science 241:1473–1475

Ciccioli P, Fabozzi C, Brancaleoni E et al (1997) Use of isoprene algorithm for predicting the monoterpene emission from the Mediterranean holm oak *Quercus ilex* L.: performance and limits of this approach. J Geophys Res 102:23319–23328

Ciccioli P, Brancaleoni E, Frattoni M, Brachetti A, Marta S (2002) Daily and seasonal variations of monoterpene emissions from an evergreen oak (Quercus ilex L.) forest of southern Europe. In: Raes F, Angeletti G, Hjorth J (eds) A changing atmosphere: Proceedings of the 8th European symposium on the physico-chemical behaviour of atmospheric pollutants. European Commission, DG Research and Joint Research Center, Ispra, 5 pp

Constable JVH, Litvak ME, Greenberg JP, Monson RK (1999) Monoterpene emission from coniferous trees in response to elevated CO2 concentration and climate warming. Global Change Biol 5:255–267

Croteau R (1987) Biosynthesis and catabolism of monoterpenoids. Chem Rev 87:929–954

Delaney ME, Owen WJ, Rogers LJ (1977) Accumulation of sugars and polysaccharide accompanying an inhibition of the light reaction in photosynthesis. J Exp Bot 28:1153–1162

Delfine S, Csiky O, Seufert G, Loreto F (2000) Fumigation with exogenous monoterpenes of a non-isoprenoid-emitting oak (*Quercus suber*): monoterpene acquisition, translocation, and effect on the photosynthetic properties at high temperatures. New Phytol 146: 27–36

Delwiche CF, Sharkey TD (1993) Rapid appearance of 13C in biogenic isoprene when 13CO2 is fed to intact leaves. Plant Cell Environ 16:587–591

Di Carlo P, Brune WH, Martinez M et al (2004) Missing OH reactivity in a forest: evidence for unknown reactive biogenic VOCs. Science 304:722–725

Dudareva N, Cseke L, Blanc VM, Pichersky E (1996) Evolution of floral scent in *Clarkia*: novel patterns of *S*-linalool synthase gene expression in the *C. breweri* flower. Plant Cell 8:1137–1148

Eisenreich W, Rohdich F, Bacher A (2001) Deoxyxylulose phosphate pathway to terpenoids. Trends Plant Sci 6:78–84

Evans RC, Tingey DT, Gumpertz ML (1985) Interspecies variation in terpenoid emissions from engelmann and sitka spruce seedlings. For Sci 31:132–142

Fahn A (1979) Secretory tissues in plants. Academic, London

Fall R, Wildermuth MC (1998) Isoprene synthase: from biochemical mechanism to emission algorithm. J Geophys Res 103:25599–25609

Fang CW, Monson RK, Cowling EB (1996) Isoprene emission, photosynthesis, and growth in sweetgum (*Liquidambar styraciflua* L.) seedlings exposed to repeated cycles of water stress. Tree Physiol 16: 441–446

Fares S, Oksanen E, Lännenpää M, Julkunen-Tiito R, Loreto F (2010) Volatile emissions and phenolic compound concentrations along a vertical profile of *Populus nigra* leaves exposed to realistic ozone concentrations. Photosynth Res 104:61–74

Farquhar GD, von Caemmerer S, Berry JA (1980) A biochemical model of photosynthetic CO2 assimilation in leaves of C3 species. Planta 149:78–90

Fischbach RJ, Zimmer I, Steinbrecher R, Pfichner A, Schnitzler JP (2000) Monoterpene synthase activities in leaves of *Picea abies* (L.) Karst. and *Quercus ilex* L. Phytochemistry 54:257–265

Fischbach R, Staudt M, Zimmer I, Rambal S, Schnitzler JP (2002) Seasonal pattern of monoterpene synthase activities in leaves of the evergreen tree *Quercus ilex* L. Physiol Plant 114:354–360

Fisher AJ, Rosenstiel TN, Shirk MC, Fall R (2001) Nonradioactive assay for cellular dimethylallyl diphosphate. Anal Biochem 292:272–279

Fortunati A, Barta C, Brilli F, Centritto M, Zimmer I, Schnitzler J-P, Loreto F (2008) Isoprene emission is not temperature-dependent during and after severe drought-stress: a physiological and biochemical analysis. Plant J 55:687–697. doi:10.1111/j.1365-313X.2008.03538.x

Fuentes JD, Wang D (1999) On the seasonality of isoprene emission from a mixed temperate forest. Ecol Appl 9:1118–1131

Fuentes JD, Wang D, Gu L (1999) Seasonal variations in isoprene emissions from a boreal aspen forest. J Appl Meteorol 38:855–869

Funk JL, Mak JE, Lerdau MT (2004) Stress-induced changes in carbon sources for isoprene production in *Populus deltoides*. Plant Cell Environ 27:747–755

Funk JL, Jones CG, Gray DW, Throop HL, Hyatt LA, Lerdau MT (2005) Variation in isoprene emission from *Quercus rubra*: sources, causes, and consequences for estimating fluxes. J Geophys Res 110: D04301. doi:10.1029/2004JD005229

Geron C, Guenther A, Sharkey TD, Arnts RR (2000) Temporal variability in the basal isoprene emission factor. Tree Physiol 20:799–805

Goldstein AH, Goulden ML, Munger JW, Wofsy SC, Geron CD (1998) Seasonal course of isoprene emissions from a midlatitude deciduous forest. J Geophys Res 103:31045–31056

Gould MN (1997) Cancer chemoprevention and therapy by monoterpenes. Environ Health Perspect 105:977–979

Grinspoon J, Bowman WD, Fall R (1991) Delayed onset of isoprene emission in developing velvet bean (*Mucuna* sp.) leaves. Plant Physiol 97:170–174

Guenther AB, Monson RK, Fall R (1991) Isoprene and monoterpene emission rate variability: observations with eucalyptus and emission rate algorithm development. J Geophys Res 96:10799–10808

Guenther A, Zimmerman P, Wildermuth M (1994) Natural volatile organic compound emission rate estimates for U.S. woodland landscapes. Atmos Environ 28:1197–1210

Guenther A, Hewitt CN, Erickson D, Fall R, Geron C (1995) A global model of natural volatile organic compound emissions. J Geophys Res 100:8873–8892

Guidolotti G, Calfapietra C, Loreto F (2011) The relationship between isoprene emission, CO_2 assimilation and water use efficiency across a range of poplar genotypes. Physiol Plant. doi:10.1111/j.1399-3054.2011.01463.x

Hakola H, Rinne J, Laurila T (1998) The hydrocarbon emission rates of tea-leafed willow (*Salix phylicifolia*), silver birch (*Betula pendula*) and European aspen (*Populus tremula*). Atmos Environ 32:1825–1833

Hakola H, Laurila T, Lindfors V, Hellén H, Gaman A, Rinne J (2001) Variation of the VOC emission rates of birch species during the growing season. Boreal Environ Res 6:237–249

Hakola H, Tarvainen V, Laurila T, Hiltunen V, Hellen H, Keronen P (2003) Seasonal variation of VOC concentrations above a boreal coniferous forest. Atmos Environ 37:1623–1634

Hansted L, Jakobsen HB, Olsen CE (1994) Influence of temperature on the rhythmic emission of volatiles from *Ribes nigrum* flowers in situ. Plant Cell Environ 17:1069–1072

Harley PC, Guenther AB, Zimmerman PR (1996) Effects of light, temperature and canopy position on net photosynthesis and isoprene emission from sweetgum (*Liquidambar styraciflua*) leaves. Tree Physiol 16: 25–32

Hoffmann T, Odum JR, Bowman F et al (1997) Formation of organic aerosols from the oxidation of biogenic hydrocarbons. J Atmos Chem 26:189–222

Janson R (1993) Monoterpene emission of Scots pine and Norwegian spruce. J Geophys Res 98:2839–2850

Karl T, Fall R, Rosenstiel TN et al (2002) On-line analysis of the $13CO_2$ labeling of leaf isoprene suggests multiple subcellular origins of isoprene precursors. Planta 215:894–905

Kempf K, Allwine E, Westberg H, Claiborn C, Lamb B (1996) Hydrocarbon emissions from spruce species using environmental chamber and branch enclosure methods. Atmos Environ 30:381–1389

Kesselmeier J, Staudt M (1999) Biogenic volatile organic compounds (VOC): an overview on emission, physiology and ecology. J Atmos Chem 33:23–88

Kreuzwieser J, Graus M, Wisthaler A et al (2002) Xylem-transported glucose as additional carbon source for leaf isoprene formation in *Quercus robur*. New Phytol 156:171–178

Kuhn U, Rottenberger S, Biesenthal T et al (2004) Strong correlation between isoprene emission and gross photosynthetic capacity during leaf phenology of the tropical tree species *Hymenaea courbaril* with fundamental changes in volatile organic compounds emission composition during early leaf development. Plant Cell Environ 27:1469–1485

Kuzma J, Fall R (1993) Leaf isoprene emission rate is dependent on leaf development and the level of isoprene synthase. Plant Physiol 101:435–440

Langenheim JH (1994) Higher plant terpenoids: a phytocentric overview of their ecological roles. J Chem Ecol 20:1223–1280

Lehning A, Zimmer I, Steinbrecher R, Brüggemann N, Schnitzler JP (1999) Isoprene synthase activity and its relation to isoprene emission in *Quercus robur* L. leaves. Plant Cell Environ 22:495–504

Lehning A, Zimmer W, Zimmer I, Schnitzler JP (2001) Modeling of annual variations of oak (*Quercus robur* L.)

isoprene synthase activity to predict isoprene emission rates. J Geophys Res 106:3157–3166

Lerdau M (1991) Plant function and biogenic emission. In: Sharkey TD, Holland EA, Mooney HA (eds) Trace gas emission by plants. Academic, San Diego

Lerdau M, Keller M (1997) Controls on isoprene emission from trees in a subtropical dry forest. Plant Cell Environ 20:569–578

Lerdau M, Matson P, Fall R, Monson R (1995) Ecological controls over monoterpene emissions from Douglas-Fir (*Pseudotsuga menziesii*). Ecology 76:2640–2647

Litvak ME, Loreto F, Harley PC, Sharkey TD, Monson RK (1996) The response of isoprene emission rate and photosynthetic rate to photon flux and nitrogen supply in aspen and white oak trees. Plant Cell Environ 19: 549–559

Llusià J, Peñuelas J (2000) Seasonal patterns of terpene content and emission from seven Mediterranean woody species in field conditions. Am J Bot 87: 133–140

Loivamäki M, Louis S, Cinege G, Zimmer I, Fischbach RJ, Schnitzler JP (2007) Circadian rhythms of isoprene biosynthesis in grey poplar leaves. Plant Physiol 143:540–551

Loreto F, Barta C, Brilli F, Nogues I (2006) On the induction of volatile organic compound emissions by plants as consequence of wounding or fluctuations of light and temperature. Plant Cell Environ 29: 1820–1828

Loreto F, Centritto M, Barta C, Calfapietra C, Fares S, Monson RK (2007) The relationship between isoprene emission rate and dark respiration rate in white poplar (*Populus alba* L.) leaves. Plant Cell Environ 30: 662–669

Loreto F, Delfine S (2000) Emission of isoprene from salt-stressed *Eucalyptus globulus* leaves. Plant Physiol 123:1605–1610

Loreto F, Sharkey TD (1990) A gas exchange study of photosynthesis and isoprene emission in red oak (*Quercus rubra* L.). Planta 182:523–531

Loreto F, Sharkey TD (1993) On the relationship between isoprene emission and photosynthetic metabolites under different environmental conditions. Planta 189: 420–424

Loreto F, Velikova V (2001) Isoprene produced by leaves protects the photosynthetic apparatus against ozone damage, quenches ozone products, and reduces lipid peroxidation of cellular membranes. Plant Physiol 127:1781–1787

Loreto F, Ciccioli P, Cecinato A, Brancaleoni E, Frattoni M, Tricoli D (1996a) Influence of environmental-factors and air composition on the emission of α-pinene from *Quercus ilex* leaves. Plant Physiol 110: 267–275

Loreto F, Ciccioli P, Cecinato A, Brancaleoni E, Frattoni M, Tricoli D (1996b) Evidence of the photosynthetic origin of monoterpenes emitted by *Quercus ilex* leaves by 13C labeling. Plant Physiol 110:1317–1322

Loreto F, Ciccioli P, Brancaleoni E, Cucinato A, Frattoni M (1998) Measurement of isoprenoid content in leaves of Mediterranean *Quercus* spp. by a novel and sensitive method and estimation of the isoprenoid partition between liquid and gas phase inside the leaves. Plant Sci 136:25–30

Loreto F, Nascetti P, Graverini A, Manozzi M (2000) Emission and content of monoterpenes in intact and wounded needles of the Mediterranean Pine *Pinus pinea*. Funct Ecol 14:589–596

Loreto F, Mannozzi M, Maris C, Nascetti P, Ferranti F, Pasqualini S (2001a) Ozone quenching properties of isoprene and its antioxidant role in leaves. Plant Physiol 126:993–1000

Loreto F, Fischbach RJ, Schnitzler JP et al (2001b) Monoterpene emission and monoterpene synthase activities in the Mediterranean evergreen oak *Quercus ilex* L. grown at elevated CO2 concentrations. Global Change Biol 7:709–717

Loreto F, Pinelli P, Manes F, Kollist H (2004) Impact of ozone on monoterpene emissions and evidence for an isoprene-like antioxidant action of monoterpenes emitted by *Quercus ilex* leaves. Tree Physiol 24: 361–367

Magel E, Mayrhofer S, Müller A, Zimmer I, Hampp R, Schnitzler JP (2006) Photosynthesis and substrate supply for isoprene biosynthesis in poplar leaves. Atmos Environ 40:S138–S151

Mayrhofer S, Heizmann U, Magel E et al (2004) Carbon balance in the leaves of young poplar trees. Plant Biol 6:730–745

Mayrhofer S, Teuber M, Zimmer I, Louis S, Fischbach RJ, Schnitzler JP (2005) Diurnal and seasonal variation of isoprene biosynthesis-related genes in grey poplar leaves. Plant Physiol 139:474–484

Melle C, Steinbrecher R, Hauff K, Schnitzler P (1996) Characterisation of monoterpene cyclase activities in needles of Norway spruce seedlings. In: Borrell PM, Borrell P, Cvitsh T, Kelly K, Seiler W (eds) Proceedings of EUROTRAC symposium '96. Computational Mechanics Publications, Southampton

Mgaloblishvili MP, Khetsuriana ND, Kalandaze AN, Sanadze GA (1979) Localization of isoprene biosynthesis in poplar leaf chloroplasts. Sov Plant Physiol 26:837–842

Monson RK, Fall R (1989) Isoprene emission from aspen leaves: the influence of environment and relation to photosynthesis and photorespiration. Plant Physiol 90:267–274

Monson RK, Jaeger CH, Adams WW, Driggers EM, Silver GM, Fall R (1992) Relationships among isoprene emission rate, photosynthesis, and isoprene synthase activity as influenced by temperature. Plant Physiol 98:1175–1180

Monson RK, Harley PC, Litvak ME et al (1994) Environmental and developmental controls over the seasonal pattern of isoprene emission from aspen leaves. Oecologia 99:260–270

Monson R, Lerdau M, Sharkey T, Schimel D, Fall R (1995) Biological aspects of constructing biological hydrocarbon emission inventories. Atmos Environ 29:2989–3002

Mulder-Krieger T, Verpoorte R, Svendse A, Scheffer J (1988) Production of essential oils and flavours in

plant cell and tissue cultures. A review. Plant Cell Tissue Organ Cult 13:85–114

Niinemets U, Tenhunen JD, Harley PC, Steinbrecher R (1999) A model of isoprene emission based on energetic requirements for isoprene synthesis and leaf photosynthetic properties for *Liquidambar* and *Quercus*. Plant Cell Environ 22:1319–1335

Niinemets U, Seufert G, Steinbrecher R, Tenhunen JD (2002) A model coupling foliar monoterpene emissions to leaf photosynthetic characteristics in Mediterranean evergreen 25 *Quercus* species. New Phytol 153: 257–275

Nogués I, Brilli F, Loreto F (2006) Dimethylallyl diphosphate (DMADP) and geranyl-diphosphate (GDP) pools of plant species characterized by different isoprenoid emissions. Plant Physiol 141:721–730

Núñez L, Plaza J, Pérez-Pastor R et al (2002) Corrigendum to "high water vapour pressure deficit influence on *Quercus ilex* and *Pinus pinea* field monoterpene emission in the central Iberian Peninsula (Spain)". Atmos Environ 36:4441–4452

Owen SM, Harley P, Guenther AB, Hewitt CN (2002) Light dependency of VOC emissions from selected Mediterranean plant species. Atmos Environ 36: 3147–3159

Pegoraro E, Rey A, Bobich EG et al (2004) Effect of elevated CO_2 concentration and vapour pressure deficit on isoprene emission from leaves of *Populus deltoides* during drought. Funct Plant Biol 31:1137–1147

Pegoraro E, Abrell L, Van Haren J et al (2005) The effect of elevated atmospheric CO_2 and drought on sources and sinks of isoprene in a temperate and tropical rainforest mesocosm. Glob Chang Biol 11: 1234–1246

Pétron G, Harley P, Greenberg J, Guenther A (2001) Seasonal temperature variations influence isoprene emission. Atmos Environ 28:1707–1710

Rapparini F, Baraldi R, Facini O (2001) Seasonal variation of monoterpene emission from *Malus domestica* and *Prunus avium*. Phytochemistry 57:681–687

Rapparini F, Baraldi R, Miglietta F, Loreto F (2004) Isoprenoid emission in trees of *Quercus pubescens* and *Quercus ilex* with lifetime exposure to naturally high CO_2 environment. Plant Cell Environ 27: 381–392

Rasmussen RA, Went FW (1965) Volatile organic material of plant origin in the atmosphere. Proc Natl Acad Sci USA 53:215–220

Rasulov B, Copolovici L, Laisk A, Niinemets U (2009) Postillumination isoprene emission: in vivo measurements of dimethylallyldiphosphate pool size and isoprene synthase kinetics in aspen leaves. Plant Physiol 149:1609–1618

Rohmer M, Knani M, Simonin P, Sutter B, Sahm H (1993) Isoprenoid biosynthesis in bacteria: a novel pathway for the early steps leading to isopentenyl diphosphate. Biochem J 295:517–524

Rosenstiel TN, Fisher AJ, Fall R, Monson RK (2002) Differential accumulation of dimethyallyl diphosphate in leaves and needles of isoprene and methylbuthenol-emitting and non-emitting species. Plant Physiol 129:1276–1284

Rosenstiel TN, Potosnak MJ, Griffin KL, Fall R, Monson RK (2003) Increased CO_2 uncouples growth from isoprene emission in an agriforest ecosystem. Nature 421:256–259

Rosenstiel TN, Ebbets AL, Khatri WC, Fall R, Monson RK (2004) Induction of poplar leaf nitrate reductase: a test of extrachloroplastic control of isoprene emission rate. Plant Biol 6:12–21

Sanadze GA (1969) Light-dependent excretion of molecular isoprene. Prog Photosynth Res 2:701–706

Schnitzler JP, Arenz R, Steinbrecher R, Lehning A (1996) Characterization of an isoprene synthase from leaves of *Quercus petraea* (Mattuschka) Liebl. Bot Acta 109:216–221

Schnitzler JP, Graus M, Kreuzwieser J et al (2004) Contribution of different carbon sources for isoprene emitted from poplar leaves. Plant Physiol 135:152–160

Scholefield PA, Kieron J, Doick KJ et al (2004) Impact of rising CO_2 on VOC emissions: isoprene emission from *Phragmites australis* growing at elevated CO_2 in a natural carbon dioxide spring. Plant Cell Environ 27:381–392

Schuh G, Heiden AC, Hoffman T et al (1997) Emissions of volatile organic compounds from sunflower and beech: dependence on temperature and light intensity. J Atmos Chem 27:291–318

Schürmann W, Ziegler H, Kotzias D, Schönwitz R, Steinbrecher R (1993) Emission of biosynthesized monoterpenes from needles of Norway spruce. Naturwissenschaften 80:276–278

Schwender J, Zeidler J, Gröner R et al (1997) Incorporation of 1-deoxy-D-xylulose into isoprene and phytol by higher plants and algae. FEBS Lett 414:129–134

Seufert G, Kotzias D, Spartà C, Versino B (1995) Volatile organics in Mediterranean shrubs and their potential role in a changing environment. Ecol Stud 177: 343–365

Shao M, Czapiewski KV, Heiden AC et al (2001) Volatile organic compound emissions from Scots Pine: mechanisms and description by algorithms. J Geophys Res 106:20483–20491

Sharkey TD, Loreto F (1993) Water stress, temperature, and light effects on the capacity for isoprene emission and photosynthesis of kudzu leaves. Oecologia 95:328–333

Sharkey TD, Yeh S (2001) Isoprene emission from plants. Annu Rev Plant Physiol Plant Mol Biol 52:407–436

Sharkey TD, Loreto F, Delwiche CF (1991) High carbon dioxide and sun/shade effects on isoprene emission from oak and aspen tree leaves. Plant Cell Environ 14:333–338

Sharkey TD, Singsaas EL, Lerdau MT, Geron CD (1999) Weather effects on isoprene emission capacity and applications in emissions algorithms. Ecol Appl 9:1132–1137

Sharkey TD, Bernacchi CJ, Farquhar GD, Singsaas EL (2007) Fitting photosynthetic carbon dioxide response curves for C3 leaves. Plant Cell Environ 30:1035–1040

Silver GM, Fall R (1991) Enzymatic synthesis of isoprene from dimethylallyl diphosphate in Aspen leaf extracts. Plant Physiol 97:1588–1591

Silver GM, Fall R (1995) Characterization of aspen isoprene synthase, an enzyme responsible for leaf isoprene emission to the atmosphere. J Biol Chem 270:13010–13016

Singsaas EL, Sharkey TD (1998) The regulation of isoprene emission responses to rapid leaf temperature fluctuations. Plant Cell Environ 21:1181–1188

Singsaas EL, Sharkey TD (2000) The effects of high temperature on isoprene synthesis in oak leaves. Plant Cell Environ 23:751–757

Singsaas EL, Lerdau M, Winter K, Sharkey TD (1997) Isoprene increases thermotolerance of isoprene-emitting species. Plant Physiol 115:1413–1420

Staudt M, Bertin N (1998) Light and temperature dependency of the emission of cyclic and acyclic monoterpenes from holm oak (*Quercus ilex* L.) leaves. Plant Cell Environ 21:385–395

Staudt M, Seufert G (1995) Light-dependent emissions of monoterpenes by Holm oak (*Quercus ilex* L.). Naturwissenschaften 82:89–92

Staudt M, Bertin N, Hansen U et al (1997) Seasonal and diurnal patterns of monoterpene emissions from *Pinus pinea* (L.) under field conditions. Atmos Environ 31:145–156

Staudt M, Joffre R, Rambal S, Kesselmeier J (2001) Effect of elevated CO_2 on monoterpene emission of young *Quercus ilex* trees and its relation to structural and ecophysiological parameters. Tree Physiol 21:437–445

Steinbrecher R (1989) Gehalt und Emission von Monoterpenen in oberirdischen Organen von *Picea abies* (L.) Karst., Ph.D. thesis, Universität München

Steinbrecher R, Ziegler H (1997) Monoterpene production by plants. In: Rennenberg H, Eschrich W, Ziegler H (eds) Trees—contributions to modern tree physiology. Backhuys Publishers, Leiden

Street R, Owen S, Duckam S, Boissard C, Hewitt C (1997) The BEMA project: effect of habitat and age on variations in emissions from *Quercus ilex* and *Pinus pinea*. Atmos Environ 31:89–100

Tholl D, Croteau R, Gershenzon J (2001) Partial purification and characterization of the short-chain prenyltransferases, geranyl diphosphate synthase and farnesyl diphosphate synthase, from *Abies grandis* (grand fir). Arch Biochem Biophys 386:233–242

Tingey DT, Manning M, Grothaus LC, Burns WF (1979) The influence of light and temperature on isoprene emission rates from live oak. Physiol Plant 47: 112–118

Tingey DT, Turner DP, Weber JA (1991) Factors controlling the emission of monoterpenes and other volatiles compounds. In: Sharkey TD, Holland EA, Mooney HA (eds) Trace gas emission by plants. Academic, San Diego

Tognetti R, Johnson JD, Michelozzi M, Raschi A (1998) Response of foliar metabolism in mature trees of *Quercus pubescens* and *Quercus ile*x to long-term elevated CO_2. Environ Exp Bot 39:233–245

Trapp SC, Croteau RB (2001) Genomic organization of plant terpene synthases and molecular evolutionary implications. Genetics 158:811–832

Velikova V, Tsonev T, Pinelli P, Alessio GA, Loreto F (2005) Localized ozone fumigation system for studying ozone effects on photosynthesis, respiration, electron transport rate and isoprene emission in field-grown Mediterranean oak species. Tree Physiol 25:1523–1532

Velikova V, Tsonev T, Barta C et al (2009) BVOC emissions, photosynthetic characteristics and changes in chloroplast ultrastructure of *Platanus orientalis* L. exposed to elevated CO_2 and high temperature. Environ Pollut 157:2629–2637

Velikova V, Várkonyi Z, Szabó M, Maslenkova L, Nogues I, Kovács L, Peeva V, Busheva M, Garab G, Sharkey TD, Loreto L (2011) Increased thermostability of thylakoid membranes in isoprene-emitting leaves probed with three biophysical techniques. Plant Physiol 157: 905–916

Vickers CE, Gershenzon J, Lerdau MT, Loreto F (2009) A unified mechanism of action for isoprenoids in plant abiotic stress. Nature Chem Biol 5:283–291

von Caemmerer S, Farquhar GD (1981) Some relationships between the biochemistry of photosynthesis and the gas-exchange of leaves. Planta 153:376–387

Wiberley AE, Linskey AR, Falbel TG, Sharkey TD (2005) Development of the capacity for isoprene emission in kudzu. Plant Cell Environ 28:898–905

Wildermuth MC, Fall R (1996) Light-dependent isoprene emission – characterization of a thylakoid-bound isoprene synthase in *Salix discolor* chloroplasts. Plant Physiol 112:171–182

Wilkinson MJ, Owen SM, Possell M et al (2006) Circadian control of isoprene emissions from oil palm (*Elaeis guineensis*). Plant J 47:960–968

Wolfertz M, Sharkey TD, Boland W, Kunhnemann F (2004) Rapid regulation of the methylerythritol 4-phosphate pathway during isoprene synthesis. Plant Physiol 135:1939–1945

Zeidler J, Lichtenthaler HK (2001) Biosynthesis of 2-methyl-3-buten-2-ol emitted from needles of *Pinus ponderosa* via the non-mevalonate DOXP/MEP pathway of isoprenoid formation. Planta 213:323–326

11 Involvement of Compartmentalization in Monoterpene and Sesquiterpene Biosynthesis in Plants

Michael Gutensohn, Dinesh A. Nagegowda, and Natalia Dudareva

Abstract

Terpenoids play numerous vital roles in basic plant processes with volatile monoterpenes and sesquiterpenes contributing to plant defense and reproduction. The biosynthesis of terpenoids in plants occurs in different subcellular compartments, which until recently were believed to include the cytosol, plastids, and mitochondria. The plastidic MEP pathway and the cytosolic MVA pathway give rise to IPP and DMAPP, which are subsequently utilized by prenyltransferases to produce prenyl diphosphates. It has been accepted that GPP and monoterpenes are synthesized in plastids, whereas FPP and sesquiterpenes are produced in the cytosol. Here we discuss how compartmentalization contributes to the formation of terpenoid diversity in plants in light of recent reports on new subcellular localizations for some enzymatic steps as well as on bifunctional terpene synthases capable of producing both mono- and sesquiterpenes.

Keywords

Monoterpenes • Sesquiterpenes • Mevalonic acid pathway • Methylerythritol-phosphate pathway • Prenyltransferases • Terpene synthases • Subcellular compartmentalization

11.1 Introduction

Terpenoids represent the largest and most diverse class among plant secondary metabolites. They are involved in various basic plant processes, such as photosynthesis, respiration, growth, development, and adaptation to environmental conditions (Gershenzon and Kreis 1999; Rodríguez-Concepción and Boronat 2002). Volatile terpenoids, monoterpenes (C10), sesquiterpenes (C15), and some diterpenes (C20) play

M. Gutensohn • N. Dudareva (✉)
Department of Horticulture and Landscape Architecture, Purdue University, West Lafayette, IN 47907, USA
e-mail: dudareva@purdue.edu

D.A. Nagegowda
CSIR - Central Institute of Medicinal and Aromatic Plants, Bengaluru, India

T.J. Bach and M. Rohmer (eds.), *Isoprenoid Synthesis in Plants and Microorganisms: New Concepts and Experimental Approaches*, DOI 10.1007/978-1-4614-4063-5_11,

important roles in direct and indirect plant defense against herbivores and pathogens, as well as in reproduction by attracting pollinators and seed disseminators (Dudareva et al. 2006). Biosynthesis of terpenoids in plants occurs in different subcellular compartments including the cytosol, plastids, and mitochondria, which is consistent with their various functions.

All terpenoids originate from the universal five-carbon precursors, isopentenyl diphosphate (IPP) and its allylic isomer dimethylallyl diphosphate (DMAPP), which are derived from two alternative biosynthetic pathways localized in different subcellular compartments. The classical mevalonic acid (MVA) pathway, which until recently has been believed to operate in the cytosol, gives rise to IPP from three molecules of acetyl-CoA (McCaskill and Croteau 1995; Newman and Chappell 1999). In contrast, the methylerythritol-phosphate (MEP) pathway takes place in plastids and produces IPP from pyruvate and glyceraldehyde 3-phosphate (cf. Eisenreich et al. 1998; Lichtenthaler 1999; Rohmer 1999; and elsewhere in this volume). Although the subcellular compartmentalization allows the MVA and MEP pathways to operate independently, metabolic "crosstalk" between them has been reported (Schuhr et al. 2003), particularly in the direction from plastids to the cytosol (Hemmerlin et al. 2003a; Laule et al. 2003; Dudareva et al. 2005).

In both subcellular compartments, IPP and DMAPP are subsequently utilized by prenyltransferases to produce prenyl diphosphates. In the cytosol, farnesyl diphosphate synthase (FPPS) catalyzes the condensation of one DMAPP molecule and two IPP molecules to produce FPP (C15), the precursor of sesquiterpenes (McGarvey and Croteau 1995). In plastids, a head-to-tail condensation of one IPP and one DMAPP molecule catalyzed by geranyl diphosphate synthase (GPPS) forms GPP (C10), the universal precursor of monoterpenes (cf. Ogura and Koyama 1998; Poulter and Rilling 1981), whereas condensation of one DMAPP molecule with three IPP molecules by the action of geranylgeranyl diphosphate synthase (GGPPS) yields GGPP (C20), the precursor of diterpenes (Koyama and Ogura 1999). Upon the formation of the prenyl diphosphate precursors GPP, FPP, and GGPP, a wide range of structurally diverse cyclic and acyclic monoterpenes, sesquiterpenes, and diterpenes are generated through the action of a large family of terpene synthases/cyclases (TPSs) (Cane 1999; Wise and Croteau 1999; and literature cited therein).

It has generally been accepted that GPP and monoterpenes are synthesized in plastids, whereas FPP and sesquiterpenes are produced in the cytosol. Here we will discuss how the subcellular compartmentalization contributes to the formation of terpenoid diversity in plants in light of recent reports on bifunctional terpene synthases capable of producing both mono- and sesquiterpenes as well as on metabolic engineering of the terpenoid profile by switching the subcellular localization of terpene synthases.

11.2 IPP and DMAPP Are Formed in Various Subcellular Compartments

11.2.1 The Mevalonic Acid Pathway

The MVA pathway consists of six enzymatic steps, which lead to the formation of IPP (Fig. 11.1) and provide the precursors for sesquiterpenes, sterols, and ubiquinone in plants (Newman and Chappell 1999; Disch et al. 1998). Generally, the MVA pathway in plants (in contrast to mammals, see Kovacs et al. 2002, 2007) is considered to operate in the cytosol; however, only fragmented experimental data existed until recently regarding the subcellular compartmentalization of the enzymes involved. The initial step of the pathway, the condensation of two molecules of acetyl-CoA, is catalyzed by acetoacetyl-CoA thiolase (AACT). The first plant AACT was cloned from radish, by functional complementation of a yeast mutation (Vollack and Bach 1996). Biochemical characterization of two *Arabidopsis* homologs, AACT1 and AACT2, and the analysis of T-DNA insertion mutants for both genes revealed that only AACT2 is involved in the MVA pathway, while the metabolic role of AACT1 still remains to be determined (Jin and Nikolau 2007; Ahumada et al. 2008). Transient

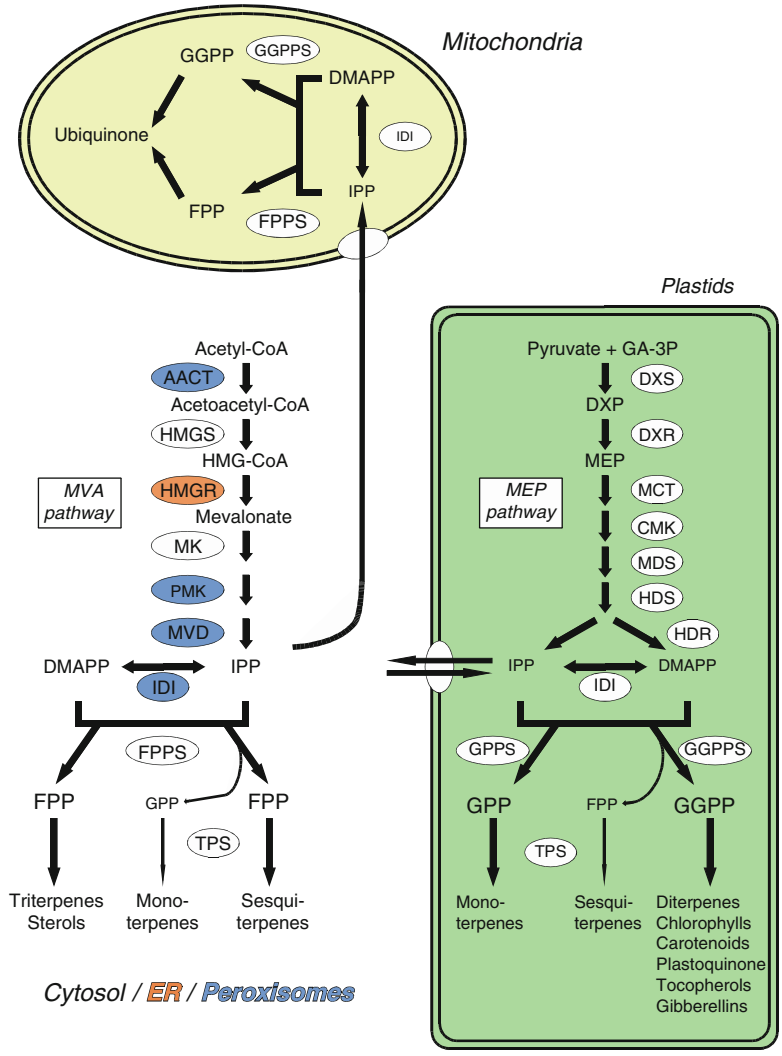

Fig. 11.1 Compartmentalization of metabolic pathways involved in the terpenoid biosynthesis in plants. Plastids and mitochondria are highlighted in green and yellow, respectively. Enzymes of the MVA pathway localized in peroxisomes and at ER/ER-derived membranes are labeled in blue and orange, respectively. The enzymatic steps are indicated by *arrows* and the enzymes involved are depicted as *circles* with the abbreviation of their names. Abbreviations: *AACT* acetoacetyl-CoA thiolase, *CMK* 4-(Cytidine 5′-diphospho)-2-*C*-methyl-D-erythritol kinase, *DMAPP* dimethylallyl diphosphate, *DXP* 1-deoxy-D-xylulose 5-phosphate, *DXR* 1-deoxy-D-xylulose 5-phosphate reductoisomerase, *DXS* 1-deoxy-D-xylulose 5-phosphate synthase, *FPP* farnesyl diphosphate, *FPPS* farnesyl diphosphate synthase, *GA-3P* D-glyceraldehyde 3-phosphate, *GGPP* geranylgeranyl diphosphate, *GGPPS* geranylgeranyl diphosphate synthase, *GPP* geranyl diphosphate, *GPPS* geranyl diphosphate synthase, *HDR* (*E*)-4-hydroxy-3-methylbut-2-enyl diphosphate reductase, *HDS* (*E*)-4-hydroxy-3-methylbut-2-enyl diphosphate synthase, *HMG-CoA* 3-hydroxy-3-methylglutaryl-CoA, *HMGR* 3-hydroxy-3-methylglutaryl-CoA reductase, *HMGS* 3-hydroxy-3-methylglutaryl-CoA synthase, *IDI* isopentenyl diphosphate isomerase, *IPP* isopentenyl diphosphate, *MCT* 2-*C*-methyl-D-erythritol 4-phosphate cytidylyltransferase, *MDS* 2-*C*-methyl-D-erythritol 2,4-cyclodiphosphate synthase, *MEP* 2-*C*-methyl-D-erythritol 4-phosphate, *MK* mevalonate kinase, *MVA* mevalonate, *MVD* mevalonate diphosphate decarboxylase, *PMK* phosphomevalonate kinase, *TPS* terpene synthases (including monoterpene synthases, sesquiterpene synthases, and bifunctional terpene synthases)

expression of AACT1 and AACT2 fused in frame to the C-terminus of a green fluorescent protein (GFP) showed that *Arabidopsis* AACT2 is localized in the cytosol, whereas AACT1 is located in the peroxisomes (Carrie et al. 2007; Ahumada et al. 2008). A peroxisomal/glyoxysomal localization suggests the potential involvement of AACT1 in fatty acid degradation (Hartmann et al., this volume). However, recent proteomic analyses identified AACT2 in *Arabidopsis* leaf peroxisomes (Reumann et al. 2007, 2009), which could be due to the existence of a yet unidentified splicing variant of AACT2 being targeted to this organelle. The second step of the MVA pathway is catalyzed by HMG-CoA synthase (HMGS) and includes the condensation of one molecule of acetyl-CoA with acetoacetyl-CoA to form 3-hydroxy-3-methylglutaryl-CoA (HMG-CoA). Subcellular localization of HMGS has been studied only in *Brassica juncea*, which contains four HMGS isoforms with 97% amino acid identity (Nagegowda et al. 2005). Despite the presence of putative peroxisome targeting PTS2-like signals in all *Brassica juncea* HMGS isoforms, GFP localization studies showed that at least BjHMGS1 is a cytosolic enzyme (Nagegowda et al. 2005).

In the next step, 3-hydroxy-3-methylglutaryl-CoA reductase (HMGR) catalyzes the formation of mevalonic acid from 3-hydroxy-3-methylglutaryl-CoA, which is considered to represent the rate-limiting step in the MVA pathway leading to phytosterols (cf. Bach 1986; Chappell et al. 1995). Plant HMGRs have two hydrophobic transmembrane regions at their N-terminus, while the highly conserved catalytic domain is exposed to the cytosol (Campos and Boronat 1995). Earlier *in vitro* studies using isolated microsomal membranes suggested that *Arabidopsis* and tomato HMGRs are capable of integrating into the endoplasmic reticulum (ER) membrane (Campos and Boronat 1995; Denbow et al. 1996). Heterologous expression of two isoforms of radish HMGR in a yeast *hmgr*$^-$ mutant led to microsome-bound enzyme (Vollack et al. 1994). However, more recent extensive investigation of subcellular localization of HMGR in *Arabidopsis* revealed its dual localization: in the ER where it is synthesized and inserted into the membrane as well as within spherical vesicular structures derived from subdomains of the ER and located in the cytosol and the central vacuole (Leivar et al. 2005). Membrane domains of two tobacco HMGR isozymes fused to GFP were also targeted differentially: The domain belonging to one HMGR isoform was targeted to ER, while that of the second isoform was found in globular structures and seemed to be directed by the actin skeleton (Merret et al. 2007).

The downstream steps from mevalonate to IPP involve two phosphorylation reactions and a single decarboxylation reaction that are catalyzed by mevalonate kinase (MK), phosphomevalonate kinase (PMK), and mevalonate diphosphate decarboxylase (MVD), respectively. While these enzymes are well studied in other eukaryotic systems (Kovacs et al. 2007), very little is known about their subcellular localization in plants. Recently, cDNAs encoding these three MVA pathway enzymes were cloned from *Catharanthus roseus*, and their activities were confirmed by functional complementation of yeast *erg12*, *erg8*, and *mvd1* mutants defective in MK, PMK, and MVD, respectively (Simkin et al. 2011). Since these *C. roseus* enzymes and their respective *Arabidopsis* homologs contain N-terminal PTS2 consensus or PTS2-related sequences, their subcellular localization was analyzed by transient expression of fusion constructs with yellow fluorescent protein (YFP). While the MK-YFP was exclusively localized in the cytosol, the PMK-YFP and MVD-YFP were co-localized to a large extent with a peroxisomal marker and only a small portion remained in the cytosol (Simkin et al. 2011). These results suggest that in plants PMK and MVD are potentially peroxisomal enzymes; however, additional analyses using different techniques will be necessary to further confirm this subcellular localization.

11.2.2 The MEP Pathway

The mevalonate-independent pathway known as the MEP pathway involves seven enzymes to form IPP and DMAPP from pyruvate and

D-glyceraldehyde 3-phosphate and provides the precursors for monoterpenes, diterpenes, carotenoids, tocopherols, and the prenyl moiety of chlorophyll (Fig. 11.1). In plants, the MEP pathway has been fully elucidated using a combination of biochemical and genomic approaches (see Rodríguez-Concepción and Boronat 2002; Rodríguez-Concepción et al., this volume). The following unified nomenclature has been proposed recently for the MEP pathway enzymes (Phillips et al. 2008b): 1-deoxy-D-xylulose 5-phosphate synthase (DXS), 1-deoxy-D-xylulose 5-phosphate reductoisomerase (DXR), 2-*C*-methyl-D-erythritol 4-phosphate cytidylyltransferase (MCT), 4-(Cytidine 5′-diphospho)-2-*C*-methyl-D-erythritol kinase (CMK), 2-*C*-methyl-D-erythritol 2,4-cyclodiphosphate synthase (MDS), (*E*)-4-hydroxy-3-methylbut-2-enyl diphosphate synthase (HDS), and (*E*)-4-hydroxy-3-methylbut-2-enyl diphosphate reductase (HDR). In contrast to questions concerning subcellular localization of enzymes involved in the MVA pathway, all enzymes of the plant MEP pathway are known to possess transit peptides for plastid targeting and their plastidic localization has been demonstrated experimentally in numerous reports (Bouvier et al. 2000; Carretero-Paulet et al. 2002; Querol et al. 2002; Hsieh and Goodman 2005; Hsieh et al. 2008).

11.2.3 Isopentenyl Diphosphate Isomerases

While the cytosolic MVA pathway produces IPP and requires its subsequent isomerization to DMAPP, the plastidic MEP pathway results in the synthesis of both IPP and DMAPP. However, HDR, catalyzing the last step in the MEP pathway and responsible for the so-called pathway "branching" (Hoeffler et al. 2002; Tritsch et al. 2010), produces IPP and DMAPP in a ratio of approximately 6:1 (Rohdich et al. 2003; Eisenreich et al. 2004), suggesting that isomerization of IPP is also required in plastids to optimize the substrate formation for the subsequent steps. Thus, both cytosolic and plastidic formation of terpenoid compounds relies on isopentenyl diphosphate isomerase (IDI) activity (Fig. 11.1). IDI is a divalent metal ion-requiring enzyme interconverting IPP and DMAPP found in all living organisms (cf. Gershenzon and Kreis 1999). The *Arabidopsis* genome contains two genes, *IDI1* and *IDI2* (Campbell et al. 1997), both encoding proteins with N-terminal sequences that were shown to target a fused GFP to the plastids in the case of IDI1 and to the mitochondria in the case of IDI2 (Okada et al. 2008; Phillips et al. 2008a; Sapir-Mir et al. 2008). While these IDIs provide DMAPP for plastid- and mitochondria-derived isoprenoids (Fig. 11.1), it has remained unclear until recently how the MVA-derived cytosolic IPP undergoes isomerization to DMAPP. Remarkably, shorter transcripts for both *Arabidopsis IDI* genes have been identified that code for IPP isomerase proteins lacking the N-terminal extensions (Okada et al. 2008; Phillips et al. 2008a). Both short versions of IDIs were shown to be localized to peroxisomes, suggesting that this particular step downstream of the MVA pathway takes place in this organelle (Sapir-Mir et al. 2008). However, more studies in different plant systems are needed to confirm this.

11.3 Prenyl Diphosphate Synthases/Prenyltransferases Function in Different Subcellular Compartments

The steps following the synthesis of the basic isoprene units IPP and DMAPP involve head-to-tail condensation of DMAPP with one or more IPP residues, catalyzed by short-chain prenyl diphosphate synthases/prenyltransferases, leading to the formation of the prenyl diphosphate precursors GPP, FPP, and GGPP (Fig. 11.1) for the various terpenoid families (Koyama and Ogura 1999; Liang et al. 2002).

11.3.1 Geranyl Diphosphate Synthase

A head-to-tail condensation of one molecule of IPP and DMAPP in a reaction catalyzed by gera-

nyl diphosphate synthase (GPPS) leads to the formation of GPP, the precursor of monoterpenes (Poulter and Rilling 1981; Ogura and Koyama 1998). GPPSs were isolated from a diverse range of plant species and found to exist in two fundamentally different dimeric structures. Heterodimeric GPPSs were found in peppermint (*Mentha piperita*), snapdragon (*Antirrhinum majus*), Clarkia (*Clarkia breweri*), and hop (*Humulus lupulus*) (Burke et al. 1999; Tholl et al. 2004; Wang and Dixon 2009), while in grand fir (*Abies grandis*), Norway spruce (*Picea abies*), and the orchid *Phalaenopsis bellina* (Burke and Croteau 2002a; Schmidt and Gershenzon 2008; Schmidt et al. 2010; Hsiao et al. 2008) GPPS is a homodimeric enzyme.

In the heterodimeric GPPS, a small subunit alone is catalytically inactive, while the large subunit alone could be inactive as well, as was found in peppermint (Burke et al. 1999), or represent a functional geranylgeranyl diphosphate synthase (GGPPS) on its own, as was shown in snapdragon and hop (Tholl et al. 2004; Wang and Dixon 2009). Only the formation of a heterodimer between these two subunits leads to an active enzyme producing GPP. A prenyltransferase from *Arabidopsis thaliana* as well as its tomato homolog were originally proposed to represent homodimeric GPPSs (Bouvier et al. 2000; van Schie et al. 2007a). However, further detailed characterization of this *Arabidopsis* enzyme revealed that it rather is a polyprenyl pyrophosphate synthase (AtPPPS) catalyzing the formation of C_{25} to C_{45} medium-/long-chain products (Hsieh et al. 2011). Likewise, two AtPPPS homologs from *P. abies* and *Quercus robur* were shown to catalyze the synthesis of larger prenyl diphosphate products (Schmidt and Gershenzon 2008). Remarkably, a new subtype of GPPS small subunit (SSU-II) was identified recently in *Arabidopsis,* which is capable of interacting with endogenous GGPPS, and the resulting heterodimer catalyzes the synthesis of GPP (Wang and Dixon 2009). Biochemical studies also showed that GPPS small subunits can interact with GGPPS from phylogenetically distant plant species, thus changing their GGPPS activity to efficient GPP production *in vitro* (Burke and Croteau 2002b; Tholl et al. 2004; Wang and Dixon 2009). The formation of such chimeric enzyme *in planta* was recently demonstrated by overexpression of snapdragon small subunit of GPPS in tobacco plants (*Nicotiana tabacum*) (Orlova et al. 2009). The total GPPS activity and monoterpene emission from leaves and flowers was increased in these transgenic plants, indicating the formation of functional heterodimers with the endogenous large subunit partners. The formation of chimeric GPPS in transgenic plants led to leaf chlorosis, increased light sensitivity, and dwarfism, most likely due to a diminished synthesis of geranylgeranyl diphosphate (GGPP) needed for formation of photosynthetic pigments and gibberellic acid (Orlova et al. 2009). The observed decrease in sesquiterpene emission suggested that an increase in flux toward GPP formation in plastids reduced the IPP pool and its transport to the cytosol (Orlova et al. 2009).

The GPPS subunits are known to contain transit peptides required for their plastid targeting, and numerous reports support their plastidic localization (Fig. 11.1). The first evidence came from biochemical studies in *Vitis vinifera* which demonstrated the presence of GPPS activity in isolated intact plastids after tryptic digestion (Soler et al. 1992). Thereafter, an *in situ* localization study using antibodies generated against GPPS confirmed plastidic localization of GPPS in *Marchantia polymorpha* (Suire et al. 2000). Moreover, immunogold localization studies using antibodies generated against the small subunit of GPPS showed that it is localized exclusively within the leucoplasts of epidermal cells of snapdragon petals (Tholl et al. 2004). Transient expression of the large (LSU) and small subunits (SSU) of hop GPPS fused in frame to the N-terminus of GFP demonstrated that LSU is plastid localized, whereas the SSU-GFP fusion protein aggregated around the plastids (Wang and Dixon 2009). In contrast to all other characterized plant GPPS, a cytosolic localization was demonstrated for GPPS in *Lithospermum erythrorhizon* cell cultures, using cell fractionation, marker enzyme assays, and immunoblotting with antibodies against GPPS (Sommer et al. 1995). These results were in agreement with *in vivo*

feeding experiments with ^{13}C-labeled glucose and the MVA pathway inhibitor mevinolin showing that the GPP-derived hemiterpenoid shikonin is formed via the cytosolic MVA pathway in *L. erythrorhizon* cells (Li et al. 1998).

11.3.2 Farnesyl Diphosphate Synthase

The sequential condensation of two molecules of IPP with one DMAPP molecule in a reaction catalyzed by farnesyl diphosphate synthase (FPPS) leads to the formation of FPP, the precursor of sesquiterpenes (cf. McGarvey and Croteau 1995). Genes encoding FPPS, a homodimeric enzyme, have been isolated and characterized from various plant species, and it has been shown that some plants contain at least two genes encoding different FPPS isoforms (Delourme et al. 1994; Attucci et al. 1995; Adiwilaga and Kush 1996; Cunillera et al. 1996; Li and Larkins 1996; Matsushita et al. 1996; Pan et al. 1996; Hemmerlin et al. 2003b). Two FPPS genes, *FPS1* and *FPS2,* were identified in *Arabidopsis* (Cunillera et al. 1996; Cunillera et al. 1997). *FPS1* alone produces two different isoforms of the enzyme, FPPS1S and FPPS1L, derived from two *FPS1* transcripts with alternative transcription start sites. The corresponding FPPS1L protein contains an additional 41 aa at its N-terminus, missing in a shorter FPPS1S version, which target this isoform into the mitochondria (Fig. 11.1), where it provides FPP for the mitochondrial isoprenoid compounds such as ubiquinone (Campbell et al. 1997). In contrast, FPPS1S and FPPS2 are localized in the cytosol (Fig. 11.1) with FPPS1S providing FPP for general plant cell functions and FPPS2 being involved in the isoprenoid synthesis for more specialized functions (Cunillera et al. 2000). In addition to the above-mentioned subcellular localizations of FPPSs, immunocytochemical studies suggested that FPPS is localized in the chloroplasts of rice mesophyll cells (Sanmiya et al. 1999). Immunoblot analysis of subcellular fractions as well as trypsin-treated chloroplasts also detected FPPS in chloroplasts of tobacco and wheat leaves (Sanmiya et al. 1999). However, the reaction of those antibodies exclusively with FPPS, and not with other prenyltransferases, needs to be confirmed.

All plant FPPSs characterized to date catalyze the head-to-tail condensation of one DMAPP molecule and two IPP molecules in the trans (*E*) configuration; however, an FPP synthase (zFPPS) recently identified from the wild tomato *Solanum habrochaites* was shown to catalyze the condensation of IPP and DMAPP in the *cis* (*Z*) configuration resulting in *Z,Z*-FPP (Sallaud et al. 2009; Tissier et al. 2013, this volume). This enzyme carries a 45-aa N-terminal transit peptide which mediates the transport of a fused GFP into chloroplasts, suggesting that zFPPS is localized in plastids and uses IPP and DMAPP provided by the plastidic MEP pathway.

11.4 Compartmentalization of Mono- and Sesquiterpene Biosynthesis

Following the formation of prenyl diphosphate precursors, low-molecular-weight terpene metabolites are formed by the action of a large family of enzymes known as terpene synthases (TPS) (cf. Cane 1999; Wise and Croteau 1999; Nagegowda 2010; Chen et al. 2011). The large diversity of TPSs seems to have originated from repeated duplications and subsequent divergence of an ancestral TPS involved in primary metabolism (Bohlmann et al. 1998b; Trapp and Croteau 2001). One of the most outstanding properties of TPSs is their proclivity for making multiple products from a single prenyl diphosphate substrate (Tholl 2006). These enzymes can be classified into three functional classes, monoterpene synthases, sesquiterpene synthases, and diterpene synthases, the first two being the subject of our discussion.

11.4.1 Monoterpene Synthases

The biosynthesis of monoterpenes, C10 compounds, is catalyzed by specialized monoterpene synthases, which utilize GPP as a substrate. In the last decade, a number of monoterpene

synthases have been isolated and characterized from various plant species (see for references: Nagegowda and Dudareva 2007; Dudareva and Pichersky 2008; Nagegowda 2010). Many of the monoterpene synthases catalyze the formation of a single product; however, several multiproduct monoterpene synthases have also been identified. For example, *Arabidopsis* myrcene/ocimene synthase converts GPP into myrcene, *(E)*-β-ocimene and small amounts of cyclic monoterpenes (Bohlmann et al. 2000), while LtMTS2, a monoterpene synthase from tomato (*Solanum lycopersicum*), produces β-phellandrene, β-myrcene, and sabinene from GPP (van Schie et al. 2007b). Another tomato monoterpene synthase, phellandrene synthase (PHS1), is unique in its use of neryl diphosphate (NPP) as preferred substrate to form primarily β-phellandrene as well as other monoterpenes, δ-2-carene, α-phellandrene, and limonene. It can also use GPP to form myrcene, ocimene, and linalool (Schilmiller et al. 2009). To date, it is believed that monoterpene biosynthesis takes place in plastids. Indeed, all isolated monoterpene synthases have a typical transit peptide at their N-terminus responsible for chloroplast targeting and therefore are 50–70 aa longer than sesquiterpene synthases (Bohlmann et al. 1998b; Williams et al. 1998). Despite the large number of isolated monoterpene synthases, their subcellular localization was investigated for only a few enzymes, among which (4*S*)-limonene synthase (LS) represents the most widely studied. Immunogold labeling studies using antibodies generated against LS combined with *in vitro* protein import experiments with isolated pea chloroplasts provided direct evidence that LS is localized to the leucoplasts of the secretory cells of peppermint (*Mentha* x *piperita*) oil glands (Turner et al. 1999). LS was also found in plastids of *Arabidopsis*, tobacco, and *Citrofortunella mitis* by *in situ* localization studies with antibodies generated against LS (Bouvier et al. 2000; Ohara et al. 2003). Moreover, GFP localization experiments showed that the N-terminal part of a lemon LS synthase directs the GFP protein to tobacco plastids (Aharoni et al. 2004). In contrast to the general agreement that all monoterpenes are synthesized in plastids, recent reports indicate that monoterpene biosynthesis might occur in the cytosol (Aharoni et al. 2004) or can have a dual, plastidic and mitochondrial, localization (Aharoni et al. 2004; Lee and Chappell 2008).

11.4.2 Sesquiterpene Synthases

Sesquiterpene synthases are responsible for the biosynthesis of C15 sesquiterpenoid compounds from FPP. Several sesquiterpene synthases have been cloned and biochemically characterized from various plant species and are believed to be located in the cytosol, consistent with the sesquiterpene biosynthesis in this cellular compartment (Chappell 1995; Bohlmann et al. 1998a). As in the case of monoterpene synthases, only a few studies were devoted to the subcellular localization of sesquiterpene synthases. *In vitro* protein import experiments with two putative *Medicago truncatula* sesquiterpene synthases, MtTps1 and MtTps2, demonstrated that these two proteins were not imported into the isolated chloroplasts, suggesting their cytosolic localization (Gomez et al. 2005). Recently, it was also shown in GFP fusion experiments that two sesquiterpene synthases, (+)-germacrene D synthase and (*E,E*)-α-farnesene synthase, responsible for the volatile profile of kiwifruit (*Actinidia deliciosa*) flowers are localized in the cytoplasm (Nieuwenhuizen et al. 2009).

Although sesquiterpene synthases are expected to be cytosolically localized, the presence of a putative plastid targeting sequence at the N-terminus, similar to monoterpene synthases, was recently reported for some sesquiterpene synthases. *Pinus sylvestris* PsTPS2, responsible for the formation of 1(10),5-germacradiene-4-ol and other products with a germacrene skeleton, contains a putative N-terminal transit peptide of 37 aa in size (Köpke et al. 2008). However, to date, there is no experimental evidence for its plastidic localization. Also, an atypical terpene synthase, santalene and bergamotene synthase (SBS), was isolated from the wild tomato *Solanum habrochaites* that is responsible for the synthesis of type II sesquiterpenes from *Z,Z*-FPP (Sallaud et al. 2009). Like the zFPPS described earlier, the SBS contains an N-terminal transit

peptide that mediates transport of a fused GFP into the plastids.

11.5 Bifunctional Terpene Synthases Involved in Mono- and Sesquiterpene Synthesis

It is generally accepted that GPP and FPP, the precursors for monoterpenes and sesquiterpenes, respectively, are compartmentally separated and that monoterpene biosynthesis takes place in plastids, where GPP is synthesized, whereas sesquiterpene formation occurs in the cytosol, where FPP is formed (Aharoni et al. 2005). However, it has been well documented that sesquiterpene synthases from various plant species are able to accept both GPP and FPP (Pechous and Whitaker 2004; Tholl et al. 2005; Green et al. 2007), with sesquiterpene synthase activities significantly exceeding their monoterpene synthase activities. Recently, bifunctional enzymes capable of efficient formation of both monoterpenes and sesquiterpenes depending on substrate availability were discovered. It has been shown that such bifunctional enzymes could be directed to different subcellular compartments, thus extending the range of available substrates for enzyme utilization and increasing the diversity of the metabolites produced. We have recently isolated two nerolidol/linalool synthases (AmNES/LIS-1/-2) from snapdragon (*A. majus*) (Nagegowda et al. 2008). Further examples include two nerolidol synthase genes, *FaNES1* and *FaNES2,* from strawberry (*Fragaria ananassa*) (Aharoni et al. 2004) and *terpene synthase 1* from maize (*Zea mays*) (Schnee et al. 2002).

In snapdragon, AmNES/LIS-1 and AmNES/LIS-2 enzymes share 95% identity and are both capable of producing linalool and nerolidol from GPP and FPP, respectively, with very similar catalytic efficiencies (Nagegowda et al. 2008). However, AmNES/LIS-1 is localized in the cytosol and is responsible for nerolidol biosynthesis, whereas AmNES/LIS-2 has a 30 aa transit peptide in its N-terminus and was shown to be located in plastids and accounts for linalool formation. The presence of both monoterpene/sesquiterpene synthase activities in plastids was further confirmed using purified leucoplasts, which produced nerolidol from FPP and linalool from GPP (Nagegowda et al. 2008). The coexistence of AmNES/LIS-1 and AmNES/LIS-2 enzymes with dual monoterpene/sesquiterpene activities in the cytoplasm and leucoplasts does not rule out that minute quantities of linalool and nerolidol can be made in the cytosol and plastids, respectively, as a result of the possible presence of GPP and FPP in trace amounts in the corresponding cellular compartments. However, feeding of cut snapdragon flowers with exogenously supplied [$^2H_2$] mevalolactone efficiently labeled nerolidol and showed no detectable incorporation into linalool (Dudareva et al. 2005), suggesting that if a GPP pool exists in the cytosol, it is small and does not contribute significantly to linalool formation.

Similar to snapdragon, the cultivated strawberry *Fragaria ananassa* contains two nerolidol synthases, FaNES1 and FaNES2, which efficiently convert GPP and FPP into the monoterpene and sesquiterpene alcohols linalool and nerolidol, respectively (Aharoni et al. 2004). As in snapdragon, one of the two enzymes, FaNES1, is localized in the cytosol and the other, FaNES2, has an N-terminal extension, which can target GFP to mitochondria and plastids upon transient expression in tobacco protoplasts. In contrast to snapdragon flowers, only one of these two genes, *FaNES1* encoding the cytosolic enzyme, is highly expressed in ripe strawberry, while *FaNES2* expression was barely detectable. This observation implies that both linalool and nerolidol in strawberry fruits are exclusively formed by FaNES1 in the cytosol and that sufficient levels of both substrates exist in the cytoplasm to support the biosynthesis of roughly similar quantities of linalool and nerolidol produced by fruits (Aharoni et al. 2004). Although FaNES1 might be involved in the synthesis of linalool in the cytosol due to its dual enzymatic activity, these data do not exclude the simultaneous presence of a yet unknown linalool synthase localized in plastids and being predominantly responsible for linalool synthesis in strawberry fruits.

Bifunctional terpene synthases like those found in the dicotyledons snapdragon (Nagegowda et al. 2008) and strawberry (Aharoni et al. 2004) have also been identified in monocotyledons.

The TPS1 enzyme, encoded by the maize *terpene synthase 1* gene, is capable of producing (*E*)-nerolidol, (*E*)-β-farnesene, and (*E*,*E*)-farnesol from FPP, as well as linalool from GPP *in vitro* (Schnee et al. 2002). After herbivore damage of maize plants, *tps1* expression was increased by almost eightfold leading to the emission of a volatile blend with (*E*)-β-farnesene, linalool, and the (*E*)-nerolidol metabolite (3*E*)-4,8-dimethyl-1,3,7-nonatriene (DMNT) as the prominent compounds. Initially, no transit peptide was detected in the TPS1 protein, suggesting its cytosolic localization and involvement in sesquiterpene formation (Schnee et al. 2002). However, more recent bioinformatic analysis of TPS1 using various algorithms predicted its plastidic targeting (Nagegowda et al. 2008). Thus, compartmentalization of TPS1 remains to be determined experimentally, which should show the sites of linalool, (*E*)-β-farnesene, and DMNT biosynthesis within the cells, as well as the contribution of TPS1 to their formation.

11.6 Metabolic Engineering of Mono- and Sesquiterpene Synthesis Reveals Small GPP and FPP Pools in Cytosol and Plastids, Respectively

In the case of bifunctional enzymes localized in one subcellular compartment, the level of available substrates will play a crucial role in determining the type and relative amounts (monoterpenes versus sesquiterpenes) of products formed. To date, little is known about the endogenous pools of GPP and FPP in different subcellular compartments including the cytosol and plastids. However, recent metabolic engineering of the terpenoid spectrum (cf. Dudareva and Pichersky 2008) has greatly contributed to the evaluation of precursor pool sizes in different compartments of plant cells. When N-terminally truncated monoterpene synthases, limonene synthases from *Perilla frutescens* and *Citrus limon*, were ectopically expressed in tobacco, transgenic plants produced low but measurable levels of limonene, indicating the presence of a small GPP pool in the cytosol (Ohara et al. 2003; Wu et al. 2006). Similarly, the overexpression of basil sesquiterpene synthase, α-zingiberene synthase (ZIS) (which can also utilize GPP and produce a number of monoterpenes *in vitro*), in tomato fruits under the control of a fruit ripening-specific promoter led to the accumulation of a number of monoterpenes including α-thujene, α-pinene, β-phellandrene, and γ-terpinene in addition to expected high levels of α-zingiberene and several other sesquiterpenes (Davidovich-Rikanati et al. 2008), indicating that a small pool of GPP is available in the cytosol of tomato fruits as well. On the other hand, the direction of patchoulol synthase (PTS), a sesquiterpene synthase from *Pogostemon cablin*, to the plastids of transgenic tobacco using an N-terminal transit peptide of the RubisCO small subunit yielded plants that accumulated low levels of patchoulol and several other sesquiterpenes, showing the presence of a small FPP pool in tobacco plastids (Wu et al. 2006). These results were consistent with the previously reported detection of FPPS in tobacco chloroplasts (Sanmiya et al. 1999)

In many cases, FPP, which is expected to be produced in relatively large amounts in the cytosol, needed for sterol biosynthesis, is not readily available for catalysis by introduced sesquiterpene synthases (Aharoni et al. 2005). Only very low levels of the respective sesquiterpenes were obtained in *Arabidopsis* plants overexpressing a chicory germacrene A synthase (Aharoni et al. 2003) and in tobacco plants expressing the amorpha-4,11-diene synthase from *Artemisia annua* or a fungal trichodiene synthase (Hohn and Ohlrogge 1991; Wallaart et al. 2001). To date, the constitutive overexpression of the cytosolically localized maize TPS10 and PTS in *Arabidopsis* and tobacco, respectively, represent the two most successful attempts at producing high levels of volatile sesquiterpenes by enzymes targeted to the cytosol (Schnee et al. 2006; Wu et al. 2006), suggesting a sufficient supply of FPP for cytosolic sesquiterpene synthesis in these cases.

The ectopic expression of bifunctional terpene synthases in transgenic plants is of particular interest since these enzymes can efficiently use both GPP and FPP substrates and may allow for

the estimation of the relative ratio of these two substrate pools in a distinct subcellular compartment. Recently, cytosolically localized bifunctional linalool/nerolidol synthase FaNES1 from strawberry was targeted to *Arabidopsis* and potato plastids (Aharoni et al. 2003; Aharoni et al. 2006) as well as to *Arabidopsis* mitochondria (Kappers et al. 2005) by the addition of the respective targeting signals. Both transgenic *Arabidopsis* and potato plants expressing the plastid-targeted version of FaNES1 produced high levels of linalool and its glycosylated and hydroxylated derivatives (Aharoni et al. 2003; Aharoni et al. 2006). Surprisingly, these *Arabidopsis* plants also produced some nerolidol, although at levels 100- to 300-fold lower than those of linalool, thus once again suggesting that a small pool of FPP is present in plastids (Aharoni et al. 2003). Targeting of FaNES1 to mitochondria resulted in transgenic *Arabidopsis* plants emitting nerolidol at levels that were 20- to 30-fold higher than those from transgenic plants with the plastid-targeted FaNES1 in addition to the nerolidol derivative (*E*)-DMNT (Kappers et al. 2005). Thus, these results show that plant mitochondria indeed have a readily available FPP pool, which is generated by the mitochondria-localized FPPS isoform (Cunillera et al. 1997) or alternatively imported from the cytosol (Hartmann and Bach 2001) and is normally used for ubiquinone biosynthesis. Overall, the above-described metabolic engineering studies suggest the presence of substrates for mono- and sesquiterpene biosynthesis in both plastids and cytosol, although at different levels: high GPP/trace FPP in plastids versus high FPP/trace GPP in cytosol. These substrate pools allow endogenous (bifunctional) enzymes to produce their respective products in both subcellular compartments, however, at a level representative of that of the precursors.

11.7 Summary and Future Perspectives

The past decade has witnessed significant progress in the identification of genes and enzymes involved in terpenoid biosynthesis in plants. However, to date, only limited knowledge exists about the subcellular localization of enzymes involved in the terpenoid network and the contribution of different cellular compartments to terpenoid formation. While only plastids are believed to be involved in IPP and DMAPP biosynthesis via the MEP pathway, at least four different compartments, cytosol, peroxisomes, ER, and spherical vesicular structures, contribute to the formation of IPP and DAMPP via the MVA pathway (Fig. 11.1). Further analysis of subcellular localization of the enzymes involved in the MVA pathway and in reactions downstream of IPP will provide new insights on the role of compartmentalization in the regulation of the flux toward terpenoid precursors and allow us to understand the FPP allocation for sterol and sesquiterpene biosynthesis. Given the involvement of various subcellular compartments in the biosynthesis of terpenoid precursors, it seems obvious that numerous transport processes across the organellar membranes are required (Fig. 11.1). This might include the transport of intermediates of the MVA pathway between the cytosol and peroxisomes, IPP as well as other up- and downstream metabolites between plastids and cytosol, and IPP from the cytosol to mitochondria. However, to date, very little is known about these transport processes, the transporters involved, and their substrate specificities.

The existence of small pools of GPP and FPP in the cytosol and plastids, respectively, also raises the question about their origin. They might originate from incomplete reactions catalyzed by the cytosolic FPPS and the plastidic GGPPS, releasing small quantities of the reaction intermediates GPP and FPP, respectively (Fig. 11.1). Alternatively, they can be the products of cytosolic GPPS and plastidic FPPS, which have been identified in limited plant species. Future functional genomic, transcriptomic, and proteomic analysis will show whether one of these two scenarios is prevalent in the plant kingdom. Moreover, such analysis will also lead to the identification of putative transporters involved in the transport of terpenoid precursors across the organellar membranes described above. Knowledge about the endogenous pools of GPP

and FPP in different subcellular compartments will be even more crucial for rational metabolic engineering in the light of the ability of many sesquiterpene synthases as well as bifunctional terpene synthases to produce both mono- and sesquiterpene compounds. This knowledge will provide a foundation for future successful metabolic engineering of plant terpenoid profiles to boost plant defense, increase pollinator attraction, and heighten the production of biologically valuable compounds (Aharoni et al. 2005, 2006; Dudareva and Pichersky 2008).

References

Adiwilaga K, Kush A (1996) Cloning and characterization of cDNA encoding farnesyl diphosphate synthase from rubber tree (*Hevea brasiliensis*). Plant Mol Biol 30:935–946

Aharoni A, Giri AP, Deuerlein S et al (2003) Terpenoid metabolism in wild-type and transgenic *Arabidopsis* plants. Plant Cell 15:2866–2884

Aharoni A, Giri P, Verstappen FWA et al (2004) Gain and loss of fruit flavor compounds produced by wild and cultivated strawberry species. Plant Cell 16: 3110–3131

Aharoni A, Jongsma MA, Bouwmeester HJ (2005) Volatile science? Metabolic engineering of terpenoids in plants. Trends Plant Sci 10:594–602

Aharoni A, Jongsma MA, Kim TY et al (2006) Metabolic engineering of terpenoid biosynthesis in plants. Phytochem Rev 5:49–58

Ahumada I, Cairo A, Hemmerlin A et al (2008) Characterisation of the gene family encoding acetoacetyl-CoA thiolase in *Arabidopsis*. Funct Plant Biol 35:1100–1111

Attucci S, Aitken SM, Gulick PJ et al (1995) Farnesyl pyrophosphate synthase from white lupin: molecular cloning, expression, and purification of the expressed protein. Arch Biochem Biophys 321:493–500

Bach TJ (1986) Hydroxymethylglutaryl-CoA reductase, a key enzyme in phytosterol synthesis? Lipids 21:82–88

Bohlmann J, Crock J, Jetter R et al (1998a) Terpenoid-based defenses in conifers: cDNA cloning, characterization, and functional expression of wound-inducible (*E*)-α-bisabolene synthase from grand fir (*Abies grandis*). Proc Natl Acad Sci USA 95:6756–6761

Bohlmann J, Meyer-Gauen G, Croteau R (1998b) Plant terpenoid synthases: molecular biology and phylogenetic analysis. Proc Natl Acad Sci USA 95:4126–4133

Bohlmann J, Martin D, Oldham NJ et al (2000) Terpenoid secondary metabolism in *Arabidopsis thaliana*: cDNA cloning, characterization, and functional expression of a myrcene/(*E*)-β-ocimene synthase. Arch Biochem Biophys 375:261–269

Bouvier F, Suire C, d'Harlingue A et al (2000) Molecular cloning of geranyl diphosphate synthase and compartmentation of monoterpene synthesis in plant cells. Plant J 24:241–252

Burke CC, Croteau R (2002a) Geranyl diphosphate synthase from Abies grandis: cDNA isolation, functional expression, and characterization. Arch Biochem Biophys 405:130–136

Burke CC, Croteau R (2002b) Interaction with the small subunit of geranyl diphosphate synthase modifies the chain length specificity of geranylgeranyl diphosphate synthase to produce geranyl diphosphate. J Biol Chem 277:3141–3149

Burke CC, Wildung MR, Croteau R (1999) Geranyl diphosphate synthase: cloning, expression, and characterization of this prenyltransferase as a heterodimer. Proc Natl Acad Sci USA 96:13062–13067

Campbell M, Hahn FM, Poulter CD et al (1997) Analysis of the isopentenyl diphosphate isomerase gene family from *Arabidopsis thaliana*. Plant Mol Biol 36:323–328

Campos N, Boronat A (1995) Targeting and topology in the membrane of plant 3-hydroxy-3-methylglutaryl coenzyme A reductase. Plant Cell 7:2163–2174

Cane DE (1999) Sesquiterpene biosynthesis: cyclization mechanisms. In: Cane DD (ed) Comprehensive natural products chemistry, vol 2. Elsevier, Amsterdam

Carretero-Paulet L, Ahumada I, Cunillera N et al (2002) Expression and molecular analysis of the Arabidopsis *DXR* gene encoding 1-deoxy-D-xylulose 5-phosphate reductoisomerase, the first committed enzyme of the 2-*C*-methyl-D-erythritol 4-phosphate pathway. Plant Physiol 129:1581–1591

Carrie C, Murcha MW, Millar AH et al (2007) Nine 3-ketoacyl-CoA thiolases (KATs) and acetoacetyl-CoA thiolases (ACATs) encoded by five genes in *Arabidopsis thaliana* are targeted either to peroxisomes or cytosol but not to mitochondria. Plant Mol Biol 63:97–108

Chappell J (1995) The biochemistry and molecular biology of isoprenoid metabolism. Plant Physiol 107:1–6

Chappell J, Wolf F, Proulx J et al (1995) Is the reaction catalyzed by 3-hydroxy-3-methylglutaryl coenzyme A reductase a rate-limiting step for isoprenoid biosynthesis in plants? Plant Physiol 109:1337–1343

Chen F, Tholl D, Bohlmann J et al (2011) The family of the terpene synthases in plants: a mid-size family of genes for specialized metabolism that is highly diversified throughout the kingdom. Plant J 66: 212–229

Cunillera N, Arró M, Delourme D et al (1996) *Arabidopsis thaliana* contains two differentially expressed farnesyl-diphosphate synthase genes. J Biol Chem 271: 7774–7780

Cunillera N, Boronat A, Ferrer A (1997) The *Arabidopsis thaliana FPS1* gene generates a novel mRNA that encodes a mitochondrial farnesyl-diphosphate synthase isoform. J Biol Chem 272:15381–15388

Cunillera N, Boronat A, Ferrer A (2000) Spatial and temporal patterns of GUS expression directed by 5′ regions

of the *Arabidopsis thaliana* farnesyl diphosphate synthase genes *FPS1* and *FPS2*. Plant Mol Biol 44: 747–758

Davidovich-Rikanati R, Lewinsohn E, Bar E et al (2008) Overexpression of the lemon basil α-zingiberene synthase gene increases both mono- and sesquiterpene contents in tomato fruit. Plant J 56:228–238

Delourme D, Lacroute F, Karst F (1994) Cloning of an *Arabidopsis thaliana* cDNA coding for farnesyl diphosphate synthase by functional complementation in yeast. Plant Mol Biol 26:1867–1873

Denbow CJ, Lång S, Cramer CL (1996) The N-terminal domain of tomato 3-hydroxy-3-methylglutaryl-CoA reductases: sequence, microsomal targeting and glycosylation. J Biol Chem 271:9710–9715

Disch A, Hemmerlin A, Bach TJ, Rohmer M (1998) Mevalonate-derived isopentenyl diphosphate is the biosynthetic precursor of ubiquinone prenyl side chain in tobacco BY-2 cells. Biochem J 331:615–621

Dudareva N, Pichersky E (2008) Metabolic engineering of plant volatiles. Curr Opin Biotechnol 19:181–189

Dudareva N, Andersson S, Orlova I et al (2005) The nonmevalonate pathway supports both monoterpene and sesquiterpene formation in snapdragon flowers. Proc Natl Acad Sci USA 102:933–938

Dudareva N, Negre F, Nagegowda DA et al (2006) Plant volatiles: recent advances and future perspectives. Crit Rev Plant Sci 25:417–440

Eisenreich W, Schwarz M, Cartayrade A et al (1998) The deoxyxylulose phosphate pathway of terpenoid biosynthesis in plants and microorganisms. Chem Biol 5:R221–R233

Eisenreich W, Bacher A, Arigoni D et al (2004) Biosynthesis of isoprenoids via the non-mevalonate pathway. Cell Mol Life Sci 61:1401–1426

Gershenzon J, Kreis W (1999) Biochemistry of terpenoids: monoterpenes, sesquiterpenes, diterpenes, sterols, cardiac glycosides and steroid saponins. In: Wink M (ed) Biochemistry of plant secondary metabolism. Ann Plant Rev 3:222–299, CRC Press, Boca Raton

Gomez SK, Cox MM, Bede JC et al (2005) Lepidopteran herbivory and oral factors induce transcripts encoding novel terpene synthases in *Medicago truncatula*. Arch Insect Biochem Physiol 58:114–127

Green S, Friel EN, Matich A et al (2007) Unusual features of a recombinant apple α-farnesene synthase. Phytochemistry 68:176–188

Hartmann M-A, Bach TJ (2001) Incorporation of all-*trans*-farnesol into sterols and ubiquinone in *Nicotiana tabacum* L. cv bright yellow cell cultures. Tetrahedron Lett 42:655–657

Hemmerlin A, Hoeffer JF, Meyer O et al (2003a) Crosstalk between the cytosolic mevalonate and the plastidial methylerythritol phosphate pathways in tobacco bright yellow-2 cells. J Biol Chem 278:26666–26676

Hemmerlin A, Rivera SB, Erickson HK et al (2003b) Enzymes encoded by the farnesyl diphosphate synthase gene family in the big sagebrush *Artemisia tridentata* ssp. Spiciformis. J Biol Chem 278: 32132–32140

Hoeffler JF, Hemmerlin A, Grosdemange-Billiard C et al (2002) Isoprenoid biosynthesis in higher plants and in *Escherichia coli*: on the branching in the methylerythritol phosphate pathway and the independent biosynthesis of isopentenyl diphosphate and dimethylallyl diphosphate. Biochem J 366:573–583

Hohn TM, Ohlrogge JB (1991) Expression of a fungal sesquiterpene cyclase gene in transgenic tobacco. Plant Physiol 97:460–462

Hsiao YY, Jeng MF, Tsai WC et al (2008) A novel homodimeric geranyl diphosphate synthase from the orchid *Phalaenopsis bellina* lacking a DD(*X*)2-4D motif. Plant J 55:719–733

Hsieh MH, Goodman HM (2005) The Arabidopsis IspH homolog is involved in the plastid nonmevalonate pathway of isoprenoid biosynthesis. Plant Physiol 138:641–653

Hsieh MH, Chang CY, Hsu SJ et al (2008) Chloroplast localization of methylerythritol 4-phosphte pathway enzymes and regulation of mitochondrial genes in *ispD* and *ispE* albino mutants in Arabidopsis. Plant Mol Biol 66:663–673

Hsieh F-L, Chang T-H, Ko T-P et al (2011) Structure and mechanism of an Arabidopsis medium/long-chain-length prenyl pyrophosphate synthase. Plant Physiol 155:1079–1090

Jin H, Nikolau BJ (2007) Genetic, biochemical and physiological studies of acetyl-CoA metabolism via condensation. In: Benning C, Ohlrogge J (eds) Current advances in the biochemistry and cell biology of plant lipids. Aardvark Global Publishing, Salt Lake City

Kappers I, Aharoni A, van Herpen TWJM et al (2005) Genetic engineering of terpenoid metabolism attracts bodyguards to *Arabidopsis*. Science 309:2070–2072

Köpke D, Schröder R, Fischer HM et al (2008) Does egg deposition by herbivorous pine sawflies affect transcription of sesquiterpene synthases in pine? Planta 228:427–438

Kovacs WJ, Olivier LM, Krisans SK (2002) Central role of peroxisomes in isoprenoid biosynthesis. Prog Lipid Res 41:369–391

Kovacs WJ, Tape KN, Shackelford JE et al (2007) Localization of the pre-squalene segment of the isoprenoid biosynthetic pathway in mammalian peroxisomes. Histochem Cell Biol 127:273–290

Koyama T, Ogura K (1999) Isopentenyl diphosphate isomerase and prenyltransferases. In: Barton D, Nakanishi K (eds) Comprehensive natural products chemistry, vol 2. Elsevier, Oxford

Laule O, Fürholz A, Chang HS et al (2003) Crosstalk between cytosolic and plastidial pathways of isoprenoid biosynthesis in *Arabidopsis thaliana*. Proc Natl Acad Sci USA 100:6866–6871

Lee S, Chappell J (2008) Biochemical and genomic characterization of terpene synthases in *Magnolia grandiflora*. Plant Physiol 147:1017–1033

Leivar P, González VM, Castel S et al (2005) Subcellular localization of Arabidopsis 3-hydroxy-3-methylglutaryl-coenzyme A reductase. Plant Physiol 137:57–69

Li CP, Larkins BA (1996) Identification of a maize endosperm-specific cDNA encoding farnesyl pyrophosphate synthetase. Gene 171:193–196

Li SM, Hennig S, Heide L (1998) Shikonin: a geranyl diphosphate-derived plant hemiterpenoid formed via the mevalonate pathway. Tetrahedron Lett 39:2721–2724

Liang PH, Ko TP, Wang AHJ (2002) Structure, mechanism and function of prenyltransferases. Eur J Biochem 269:3339–3354

Lichtenthaler HK (1999) The 1-deoxy-D-xylulose-5-phosphate pathway of isoprenoid biosynthesis in plants. Annu Rev Plant Physiol Plant Mol Biol 50:47–65

Matsushita Y, Kang WY, Charlwood BV (1996) Cloning and analysis of a cDNA encoding farnesyl diphosphate synthase from *Artemisia annua*. Gene 172:207–209

McCaskill D, Croteau R (1995) Monoterpene and sesquiterpene biosynthesis in glandular trichomes of peppermint (*Mentha x piperita*) rely exclusively on plastid-derived isopentenyl diphosphate. Planta 197:49–56

McGarvey DJ, Croteau R (1995) Terpenoid metabolism. Plant Cell 7:1015–1026

Merret R, Cirioni J, Bach TJ, Hemmerlin A (2007) A serine involved in actin-dependent subcellular localization of a stress-induced tobacco BY-2 hydroxymethylglutaryl-CoA reductase isoform. FEBS Lett 581:5295–5299

Nagegowda DA (2010) Plant volatile terpenoid metabolism: biosynthetic genes, transcriptional regulation and subcellular compartmentation. FEBS Lett 584:2965–2973

Nagegowda DA, Dudareva N (2007) Plant biochemistry and biotechnology of flavor compounds and essential oils. In: Kayser O, Quax W (eds) Medicinal plant biotechnology. From basic research to industrial applications. Wiley-VCH, Weinheim

Nagegowda DA, Ramalingam S, Hemmerlin A et al (2005) *Brassica juncea* HMG-CoA synthase: localization of mRNA and protein. Planta 221:844–856

Nagegowda DA, Gutensohn M, Wilkerson CG et al (2008) Two nearly identical terpene synthases catalyze the formation of nerolidol and linalool in snapdragon flowers. Plant J 55:224–239

Newman JD, Chappell J (1999) Isoprenoid biosynthesis in plants: carbon partitioning within the cytoplasmic pathway. Crit Rev Biochem Mol Biol 34:95–106

Nieuwenhuizen NJ, Wang MY, Matich AJ et al (2009) Two terpene synthases are responsible for the major terpenes emitted from the flowers of kiwifruit (*Actinidia deliciosa*). J Exp Bot 60:3203–3219

Ogura K, Koyama T (1998) Enzymatic aspects of isoprenoid chain elongation. Chem Rev 98:1263–1276

Ohara K, Ujihara T, Endo T et al (2003) Limonene production in tobacco with *Perilla* limonene synthase cDNA. J Exp Bot 54:2635–2642

Okada K, Kasahara H, Yamaguchi S et al (2008) Genetic evidence for the role of isopentenyl diphosphate isomerases in the mevalonate pathway and plant development in Arabidopsis. Plant Cell Physiol 49:604–616

Orlova I, Nagegowda DA, Kish CM et al (2009) The small subunit of snapdragon geranyl diphosphate synthase modifies the chain length specificity of tobacco geranylgeranyl diphosphate synthase *in planta*. Plant Cell 21:4002–4017

Pan Z, Herickhoff L, Backhaus RA (1996) Cloning, characterization, and heterologous expression of cDNAs for farnesyl diphosphate synthase from the guayule rubber plant reveals that this prenyltransferase occurs in rubber particles. Arch Biochem Biophys 332:196–204

Pechous SW, Whitaker BD (2004) Cloning and functional expression of an (E, E)-α-farnesene synthase cDNA from peel tissue of apple fruit. Planta 219:84–94

Phillips MA, D'Auria JC, Gershenzon J et al (2008a) The *Arabidopsis thaliana* type I isopentenyl diphosphate isomerases are targeted to multiple subcellular compartments and have overlapping functions in isoprenoid biosynthesis. Plant Cell 20:677–696

Phillips MA, León P, Boronat A et al (2008b) The plastidial MEP pathway: unified nomenclature and resources. Trends Plant Sci 13:619–623

Poulter CD, Rilling HC (1981) Prenyl transferases and isomerase. In: Porter JW, Spurgeon SL (eds) Biosynthesis of isoprenoid compounds, vol 1. Wiley, New York

Querol J, Campos N, Imperial S et al (2002) Functional analysis of the *Arabidopsis thaliana* GCPE protein involved in plastid isoprenoid biosynthesis. FEBS Lett 514:343–346

Reumann S, Babujee L, Ma C et al (2007) Proteome analysis of *Arabidopsis* leaf peroxisomes reveals novel targeting peptides, metabolic pathways, and defense mechanisms. Plant Cell 19:3170–3193

Reumann S, Quan S, Aung K et al (2009) In-depth proteome analysis of Arabidopsis leaf peroxisomes combined with in vivo subcellular targeting verification indicates novel metabolic and regulatory functions of peroxisomes. Plant Physiol 150:125–143

Rodríguez-Concepción M, Boronat A (2002) Elucidation of the methylerythritol phosphate pathway for isoprenoid biosynthesis in bacteria and plastids. A metabolic milestone achieved through genomics. Plant Physiol 130:1079–1089

Rohdich F, Zepeck F, Adam P et al (2003) The deoxyxylulose phosphate pathway of isoprenoid biosynthesis: studies on the mechanisms of the reactions catalyzed by IspG and IspH protein. Proc Natl Acad Sci USA 100:1586–1591

Rohmer M (1999) The discovery of a mevalonate-independent pathway for isoprenoid biosynthesis in bacteria, algae and higher plants. Nat Prod Rep 16:565–574

Sallaud C, Rontein D, Onillon S et al (2009) A novel pathway for sesquiterpene biosynthesis from Z, Z-farnesyl pyrophosphate in the wild tomato *Solanum habrochaites*. Plant Cell 21:301–317

Sanmiya K, Ueno O, Matsuoka M et al (1999) Localization of farnesyl diphosphate synthase in chloroplasts. Plant Cell Physiol 40:348–354

Sapir-Mir M, Mett A, Belausov E et al (2008) Peroxisomal localization of Arabidopsis isopentenyl diphosphate isomerases suggests that part of the plant isoprenoid mevalonic acid pathway is compartmentalized to peroxisomes. Plant Physiol 148:1219–1228

Schilmiller AL, Schauvinhold I, Larson M et al (2009) Monoterpenes in the glandular trichomes of tomato are synthesized from a neryl diphosphate precursor rather than geranyl diphosphate. Proc Natl Acad Sci USA 106:10865–10870

Schmidt A, Gershenzon J (2008) Cloning and characterization of two different types of geranyl diphosphate synthases from Norway spruce (*Picea abies*). Phytochemistry 69:49–57

Schmidt A, Wächtler B, Temp U et al (2010) A bifunctional geranyl and geranylgeranyl diphosphate synthase is involved in terpene oleoresin formation in *Picea abies*. Plant Physiol 152:639–655

Schnee C, Köllner TG, Gershenzon J et al (2002) The maize gene terpene synthase 1 encodes a sesquiterpene synthase catalyzing the formation of (E)-β-farnesene, (E)-nerolidol, and (E, E)-farnesol after herbivore damage. Plant Physiol 130:2049–2060

Schnee C, Köllner TG, Held M et al (2006) The products of a single maize sesquiterpene synthase form a volatile defense signal that attracts natural enemies of maize herbivores. Proc Natl Acad Sci USA 103:1129–1134

Schuhr CA, Radykewicz T, Sagner S et al (2003) Quantitative assessment of crosstalk between the two isoprenoid biosynthesis pathways in plants by NMR spectroscopy. Phytochem Rev 2:3–16

Simkin AJ, Guirimand G, Papon N et al (2011) Peroxisomal localisation of the final steps of the mevalonic acid pathway *in planta*. Planta 234:903–914

Soler E, Feron G, Clastre M et al (1992) Evidence for a geranyl diphosphate synthase located within the plastids of *Vitis vinifera* L. cultivated *in vitro*. Planta 187:171–175

Sommer S, Severin K, Camara B et al (1995) Intracellular localization of geranylpyrophosphate synthase from cell cultures of *Lithospermum erythrorhizon*. Phytochemistry 38:623–627

Suire C, Bouvier F, Backhaus RA et al (2000) Cellular localization of isoprenoid biosynthetic enzymes in *Marchantia polymorpha.* Uncovering a new role of oil bodies. Plant Physiol 124:971–978

Tholl D (2006) Terpene synthases and the regulation, diversity and biological roles of terpene metabolism. Curr Opin Plant Biol 9:297–304

Tholl D, Kish CM, Orlova I et al (2004) Formation of monoterpenes in *Antirrhinum majus* and *Clarkia breweri* flowers involves heterodimeric geranyl diphosphate synthases. Plant Cell 16:977–992

Tholl D, Chen F, Petri J et al (2005) Two sesquiterpene synthases are responsible for the complex mixture of sesquiterpenes emitted from Arabidopsis flowers. Plant J 42:757–771

Tissier A, Sallaud C, Rontein D (2013) Tobacco trichomes as a platform for terpenoid biosynthesis engineering. In: Bach TJ, Rohmer M (eds) Isoprenoid synthesis in plants and microorganisms: New concepts and experimental approaches. Springer, New York

Trapp SC, Croteau RB (2001) Genomic organisation of plant terpene synthases and molecular evolutionary implications. Genetics 158:811–832

Tritsch D, Hemmerlin A, Bach TJ, Rohmer M (2010) Plant isoprenoid biosynthesis *via* the MEP pathway: *in vivo* IPP/DMAPP ratio produced by (*E*)-4-hydroxy-3-methylbut-2-enyl diphosphate reductase in tobacco BY-2 cell cultures. FEBS Lett 584:129–134

Turner G, Gershenzon J, Nielson EE et al (1999) Limonene synthase, the enzyme responsible for monoterpene biosynthesis in peppermint, is localized to leucoplasts of oil gland secretory cells. Plant Physiol 120:879–886

van Schie CCN, Ament K, Schmidt A et al (2007a) Geranyl diphosphate synthase is required for biosynthesis of gibberellins. Plant J 52:752–762

van Schie CCN, Haring MA, Schuurink RC (2007b) Tomato linalool synthase is induced in trichomes by jasmonic acid. Plant Mol Biol 64:251–263

Vollack K-U, Bach TJ (1996) Cloning of a cDNA encoding cytosolic acetoacetyl-coenzyme A thiolase from radish by functional expression in *Saccharomyces cerevisiae*. Plant Physiol 111:1097–1107

Vollack K-U, Dittrich B, Ferrer A et al (1994) Two radish genes for 3-hydroxy-3-methylglutaryl-CoA reductase isozymes complement mevalonate auxotrophy in a yeast mutant and yield membrane-bound active enzyme. J Plant Physiol 143:479–487

Wallaart TE, Bouwmeester HJ, Hille J et al (2001) Amorpha-4,11-diene synthase: cloning and functional expression of a key enzyme in the biosynthetic pathway of the novel antimalarial drug artemisinin. Planta 212:460–465

Wang G, Dixon RA (2009) Heterodimeric geranyl(geranyl) diphosphate synthase from hop (*Humulus lupulus*) and the evolution of monoterpene biosynthesis. Proc Natl Acad Sci USA 106:9914–9919

Williams DC, McGarvey DJ, Katahira EJ et al (1998) Truncation of limonene synthase preprotein provides a fully active 'pseudomature' form of this monoterpene cyclase and reveals the function of the amino-terminal arginine pair. Biochemistry 37:12213–12220

Wise ML, Croteau R (1999) Monoterpene biosynthesis. In: Cane DD (ed) Comprehensive natural products chemistry, vol 2. Elsevier, Amsterdam

Wu S, Schalk M, Clark A et al (2006) Redirection of cytosolic or plastidic isoprenoid precursors elevates terpene production in plants. Nat Biotech 24:1441–1447

Strategies for the Manipulation of Carbocations by Aristolochene Synthase

12

David J. Miller and Rudolf K. Allemann

Abstract

Aristolochene synthase is a sesquiterpene cyclase that catalyses the high-precision conversion of farnesyl diphosphate to the sesquiterpene (+)-aristolochene via a tightly chaperoned carbocationic reaction cascade. This article examines recent work focussed on understanding the role this and other related enzymes play in controlling this chemistry. Through the use of X-ray crystallography, site-directed mutagenesis and substrate analogues, a better picture of how such proteins manipulate carbocations to arrive at specific hydrocarbon products is emerging.

Keywords

Terpenes • Aristolochene synthase • Farnesyl diphosphate • Inhibition • Carbocation • Template

12.1 Introduction

In spite of the enormous complexity and magnitude of the chemical library represented by terpenoid natural products, these compounds ultimately derive from just two simple stereoisomers, namely, dimethylallyl diphosphate (**1**) and isopentenyl diphosphate (**2**) (Fig. 12.1) (Glasby 1982). These two molecules can be linked together by enzymes that catalyse cyclopropanoation, cyclobutanoation or branching reactions (routes a–c in Fig. 12.1). Alternatively, head-to-tail elongation (route d, Fig. 12.1) catalysed by terpene synthases leads to the generation of geranyl diphosphate (**3a**), farnesyl diphosphate (**3b**) and geranylgeranyl diphosphate (**3c**). Interestingly, the enzymes that catalyse these four metal ion-dependent reaction types appear to have evolved from a common ancestor (Thulasiram et al. 2007; Thulasiram et al. 2008).

These linear prenyl diphosphates are then converted to a large number of terpenoid products by terpene synthases. All known ionisation-dependent terpene synthases rely on the shared three-dimensional class I terpene synthase fold (Christianson 2006) (Fig. 12.2) to catalyse what is arguably the most complex chemical reaction

D.J. Miller • R.K. Allemann (✉)
School of Chemistry & Cardiff Catalysis Institute, Cardiff University, Main Building, Park Place, Cardiff CF10 3AT, United Kingdom
e-mail: allemannrk@cardiff.ac.uk

T.J. Bach and M. Rohmer (eds.), *Isoprenoid Synthesis in Plants and Microorganisms: New Concepts and Experimental Approaches*, DOI 10.1007/978-1-4614-4063-5_12,

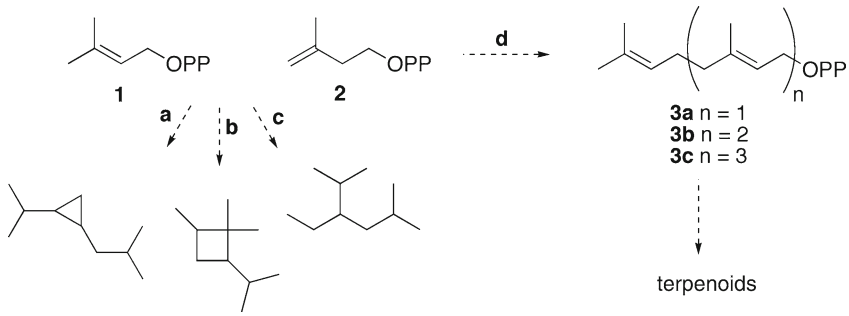

Fig. 12.1 Terpene precursors dimethylallyl diphosphate (**1**) and isopentenyl diphosphate (**2**) can be linked in several different ways within organisms. Geranyl diphosphate (**3a**), farnesyl diphosphate (**3b**) and geranylgeranyl diphosphate (**3c**) are the parent compounds of the mono-, sesqui- and di-terpenoids, respectively

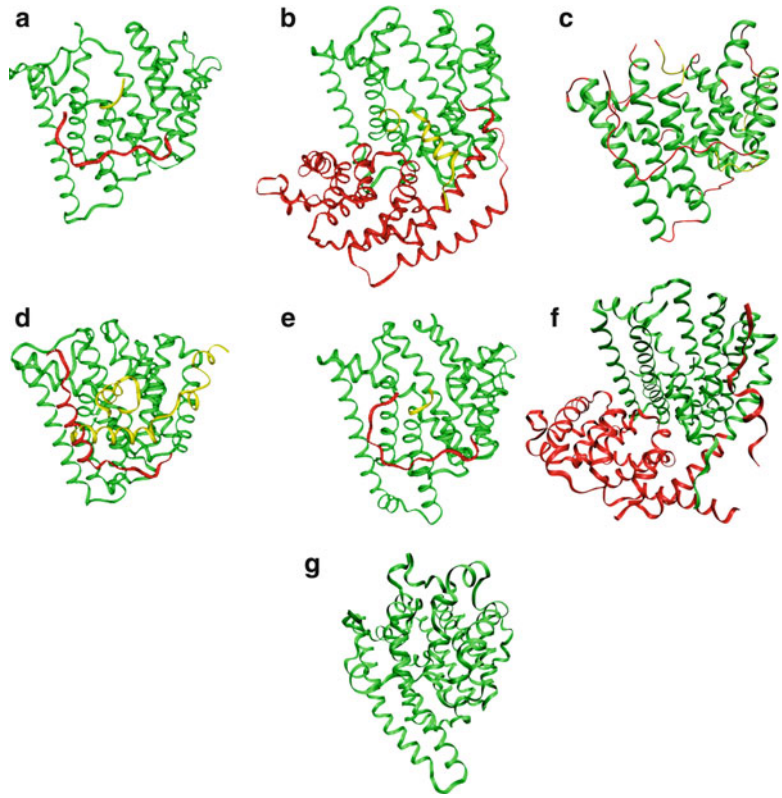

Fig. 12.2 Structural analysis of terpene synthases has revealed a shared fold – the class I terpene synthase fold represented here in green for the sesquiterpene synthases; (**a**) aristolochene synthase from *Penicillium roqueforti* (PR-AS) (Caruthers et al. 2000), (**b**) tobacco 5-*epi*-aristolochene synthase (EAS) (Starks et al. 1997), (**c**) aristolochene synthase from *Aspergillus terreus (*Shishova et al. 2007), (**d**) trichodiene synthase from *Fusarium sporotrichioides* (Rynkiewicz et al. 2001), (**e**) pentalenene synthase from *Streptomyces* UC5319 (Lesburg et al. 1997), (**f**) δ-cadinene synthase from *Gossypium arboreum* (DCS) (Gennadios et al. 2009) and (**g**) *epi*-isozizaene synthase from *Streptomyces coelicolor* A3(2) (Aaron et al. 2010). EAS and DCS also contain an α-helical N-terminal domain (*red*) comparable to that observed in class II terpenoid synthases. This domain is thought to be to be catalytically silent in both enzymes

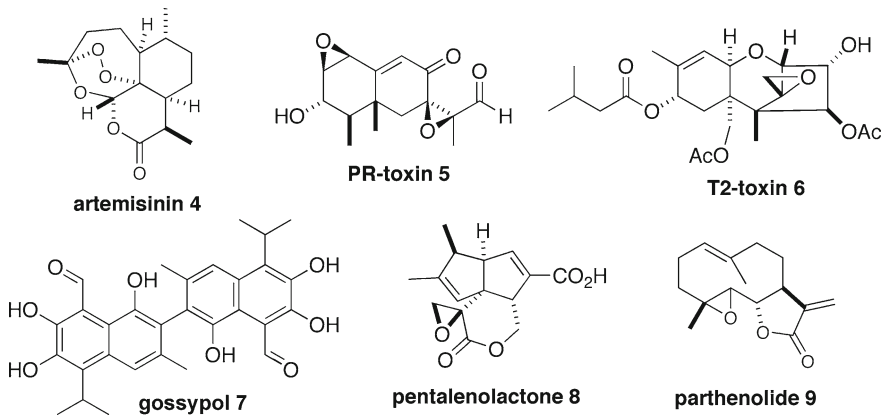

Fig. 12.3 Representative sesquiterpene natural products

found in nature; on average, two thirds of the carbon atoms of the linear prenyl diphosphates undergo changes in bonding, hybridisation and configuration during a cyclisation cascade that is initiated by the breakage of a carbon-oxygen bond leading to the formation of an enzyme-bound diphosphate and a highly reactive carbocationic intermediate. Most terpene synthases generate a unique hydrocarbon product with exquisite regio- and stereochemical specificity and are hence responsible to a large extent for the immense chemical complexity observed for this class of natural products. For the 15-carbon sesquiterpenes alone, more than 300 different hydrocarbon scaffolds are generated in plants, bacteria and fungi from farnesyl diphosphate (FPP, **3b**), the substrate of all sesquiterpene synthases. These hydrocarbon products are further derivatised to lead to many thousand sesquiterpene products such as the antimalarial compound artemisinin (**4**), PR- and T-2 toxins (**5** and **6**), the male natural contraceptive gossypol (**7**), antibiotics such as pentalenolactone (**8**) or parthenolide (**9**), which has an anti-migraine effect (Fig. 12.3).

Unlike most biological reaction mechanisms, which go through neutral and anionic intermediates, terpene biosynthesis is essentially carbocationic in nature. The key question in all these reactions is how the high-energy carbocations are generated and stabilised within the "mild" environment provided by the active sites of enzymes. Extrapolating from our own results obtained from the study of the sesquiterpene synthase aristolochene synthase, we describe here the picture that begins to emerge on how these fascinating catalysts facilitate the generation of high-energy prenyl-cations and subtly channel the reaction in an often highly regio- and stereoselective fashion along a complex reaction coordinate relying on efficient cation stabilisation within an active site that prevents free water access and rigorous control of the conformation of substrate and reaction intermediates.

12.2 Reaction Mechanism of Aristolochene Synthase

12.2.1 Early Work

The monomeric enzyme aristolochene synthase from *Penicillium roqueforti* (PR-AS) catalyses the bivalent metal-dependent cyclisation of FPP to (+)-aristolochene (**15**) (Scheme 12.1), the precursor of several fungal toxins including the potentially lethal PR-toxin (Fig. 12.3) (Cane 1990; Wei et al. 1975). Studies with labelled FPP (Cane et al. 1990a), the mechanism-based inhibitors 12-methylidenefarnesyl diphosphate (Cane and Bryant 1994) and (7*R*)-6,7-dihydrofarnesyl diphosphate (Cane and Tsantrizos 1996), led to the proposal that the cyclisation of FPP to aristolochene proceeds through at least two discrete intermediates, (-)-germacrene A (**11**) and eudesmane cation (**12**)

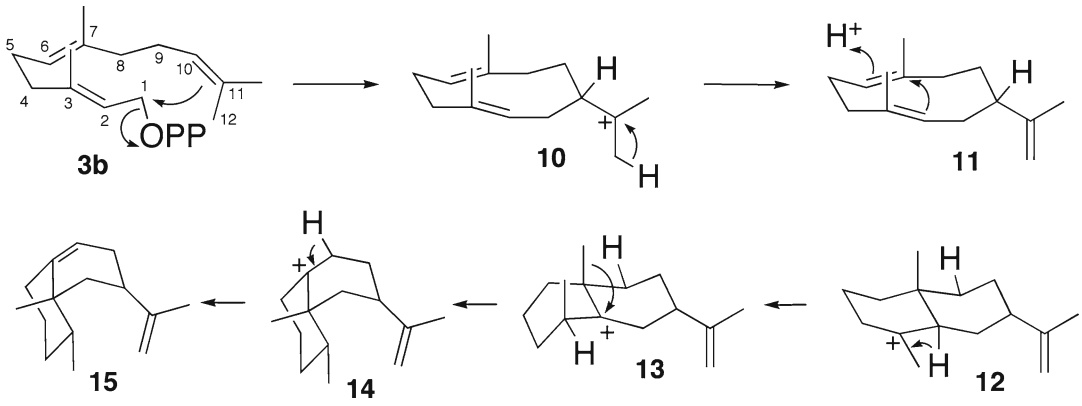

Scheme 12.1

(Scheme 12.1). Germacrene A has never been observed as a substrate of PR-AS; however, this may be due to its lack of availability to the enzyme in such experiments as a consequence of its poor water solubility. A careful analysis of the reaction products generated on incubation of FPP with PR-AS revealed that in addition to aristolochene, significant amounts of germacrene A (7.5% of the total amount of products) and a small amount of valencene (~1%) were also present (Calvert et al. 2002a). These results supported the intermediacy of germacrene A.

Based on the above results, a reaction sequence was proposed where the C10-C11 double bond of FPP attacks C1 subsequent to (or concurrent with) Mg^{2+}-triggered diphosphate departure (Scheme 12.1). Deprotonation from C12 results in the formation of the cyclic sesquiterpene (-)-germacrene A (**11**). Protonation of germacrene A at C6 and cyclisation through electron flow from the double bond at C2-C3 yields the bicyclic eudesmane cation (**12**). A hydride shift from C2 followed by a methyl shift from C7 to C2 and deprotonation at C8 then result in the formation of aristolochene (**15**).

12.2.2 Substrate Conformation and Enzyme Templating

The solution of the X-ray crystal structures of seven sesquiterpene synthases (Caruthers et al. 2000; Starks et al. 1997; Shishova et al. 2007; Rynkiewicz et al. 2001; Lesburg et al. 1997; Gennadios et al. 2009; Aaron et al. 2010), two monoterpene synthases (Whittington et al. 2002; Hyatt et al. 2007) and most recently two diterpene synthases (Köksal et al. 2011a; Köksal et al. 2011b) and one hemiterpene synthase (Köksal et al. 2010) indicated that their active sites were lined with largely inert, often bulky amino acids and free of solvent. Many terpene synthases act as high-fidelity templates that chaperone reactive substrates and intermediates to generate predominantly (or exclusively) single products, while others generate many different products and reflect therefore significant evolutionary potential (Yoshikuni et al. 2006a). It is interesting to note in this context that a high-resolution analysis of the "high-fidelity" enzyme 5-*epi*-aristolochene synthase (EAS) revealed the production of an additional 24 alternative (minor) products, suggesting synthetic evolutionary potential for all terpene synthases (O'Maille et al. 2006). Because these enzymes rely on shared, closely related protein folds for catalysis, only small changes to their active-site geometries can alter their templating character and change the resulting reatction product(s); often, the change of only one or a few amino acid residues appears sufficient to alter product distribution (Yoshikuni et al. 2006a; Deligeorgopoulou and Allemann 2003; Yoshikuni et al. 2006b; Greenhagen et al. 2006). Because these enzymes display such plasticity, even non-conservative changes to the chemical structures of the substrates can often be tolerated. For

instance, FPP analogues in which the methyl groups were replaced with phenyl-substituents acted as potent competitive inhibitors of aristolochene synthase, suggesting that changes to the active site of the enzyme should allow the turnover of these unnatural substrates and open the way to the production of unnatural terpenoid-like products (Miller et al. 2007a).

Over the last few years, it has become increasingly clear that the templating effect of terpene synthases is critical for their catalytic specificity. The enzymes serve as templates that bind their substrate in a reactive conformation that facilitates the breaking of the ester bond to generate diphosphate and a reactive carbocation that is poised to undergo further reactions. Efficient templating of the reaction sequence is crucial since the enzyme must discriminate the desired cationic species from possible isomeric cations that in the absence of a good complementary template would be of similar energy and lead to different products. Site-directed mutagenesis experiments with PR-AS revealed that Tyr 92 is critical in facilitating cyclisation (Deligeorgopoulou and Allemann 2003; Calvert et al. 2002b); when the size of the active-site residue was reduced, increasing amounts of linear farnesenes were formed, which are simple diphosphate elimination products. Interestingly, an almost linear relationship was found between the size of residue 92 and the amount of linear products. Analysis of the products generated by mutants of aristolochene synthase from *P. roqueforti* (PR-AS) revealed the prominent structural role played by the aliphatic residue Leu 108 in maintaining the productive conformation of farnesyl diphosphate, which ensures C1-C10 (σ-bond) ring-closure and hence (+)-aristolochene production (Faraldos et al. 2011a). Experiments with the substrate analogue 12,13-difluoro-FPP, which acts as a competitive inhibitor of PR-AS rather than (*vide infra*), revealed that this initial reaction occurs in a concerted fashion under the stereoelectronic control exerted by bulky amino acid residues that ensure optimal overlap between the breaking C-O bond and the π-system of the C10-C11 double bond (Yu et al. 2007). When this alignment is relaxed through amino acid substitutions, the reaction occurs in an S_N1-like fashion and produces significant amounts of α- and β-farnesenes. Clearly, Tyr 92 together with other active-site residues such as Phe 112 (Forcat and Allemann 2006), Leu 108 (Faraldos et al. 2011a) and Trp 334 (Deligeorgopoulou et al. 2003) directs FPP into the reactive conformation.

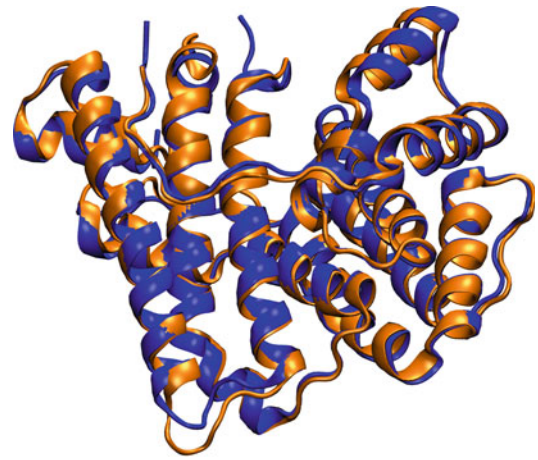

Fig. 12.4 AT-AS (*gold*) and PR-AS (*blue*) share the common class I terpenoid synthase fold

12.2.3 The Physical Steps That Lead to the Michaelis Complex: Tight Control of Conformation of FPP in AS

The results described above indicated that substrate conformation in the Michaelis complex is a crucial determinant of the biosynthetic outcome of the terpenoid synthase reaction. The active site of aristolochene synthase serves as a high-fidelity template that fixes FPP in a single, productive conformation in the Michaelis complex – otherwise, aberrant cyclisation products will result.

To study the conformational control of FPP in the active site of aristolochene synthase, we have employed X-ray crystallography to determine the structural details of complexes of the intact substrates FPP and 2-fluorofarnesyl diphosphate (2F-FPP) and the inhibitor 12,13-difluorofarnesyl diphosphate (DF-FPP) (*vide infra*) with AS from *Aspergillus terreus* (AT-AS) (Shishova et al. 2008). AT-AS and PR-AS display 61% sequence identity and nearly identical catalytic properties. The three-dimensional folds of the two enzymes are similar (Fig. 12.4), but crystals of AT-AS are

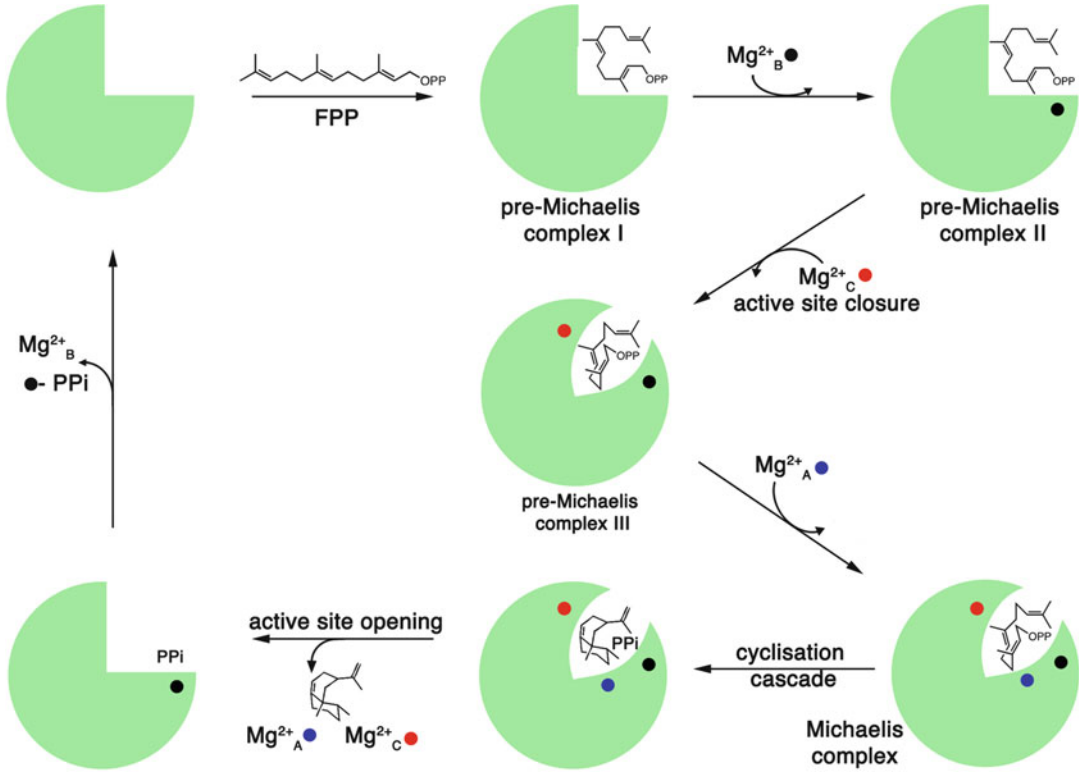

Fig. 12.5 Cartoon of the metal-dependent physical steps leading to the formation of the Michaelis complex, AT-AS-FPP-Mg_3^{2+} (Adapted from Shishova et al. (2008))

more readily obtainable. In addition, AT-AS crystallised as a tetramer (Shishova et al. 2007), while PR-AS was monomeric (Caruthers et al. 2000). Subtle differences in active site and substrate conformations were observed in the crystal structures of the complexes of FPP, 2F-FPP and DF-FPP with AT-AS that could be linked to differences in metal binding and catalysis (Shishova et al. 2008). Due to the tetrameric nature of AT-AS in the crystal, this work provided 12 independent "snapshots" of FPP binding to the enzyme that suggest a specific metal ion binding sequence for catalysis (Fig. 12.5); first, the isoprenoid tail is sequestered to the hydrophobic interior of the active site followed by Mg_B^{2+} binding. Subsequent binding of Mg_C^{2+} appears to trigger a conformational change of a loop that lies above the active site from its open to the closed form, thereby removing bulk solvent from the active site.

Crystallographic evidence with AT-AS (Shishova et al. 2007; Shishova et al. 2008) and with a monoterpene synthase (Hyatt et al. 2007) suggests that this conformational change (Fig. 12.6) from an open to a closed active-site conformation is a prerequisite for catalysis and leads to binding of the third ion, Mg_A^{2+}, to generate the active Michaelis complex. The observed conformations of intact FPP, 2F-FPP and DF-FPP are all non-productive and likely result from binding to the open active-site conformation, which in turn is a consequence of incomplete metal binding. The observation of non-productive isoprenoid binding modes suggests that the productive binding of substrates, and at least some intermediates, is under kinetic control in the active sites of AT-AS and other class I terpenoid synthases. The complex reaction sequence that leads to the formation of the reactive Michaelis complex underlines the careful choreography

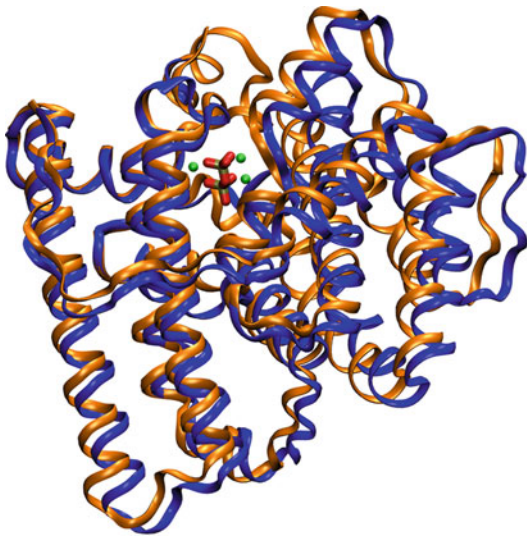

Fig. 12.6 Overlay of ribbon diagrams of the closed (*gold*) and open (*blue*) loop conformations of AT-AS. Bound diphosphate is indicated in a ball and stick model

employed by these enzymes to fold their substrates into reactive conformations that undergo cyclisations with high specificities.

12.2.4 Cation-π Interactions

Unlike most biological reaction mechanisms, which go through neutral and anionic intermediates, terpene biosynthesis is essentially carbocationic in nature. The key question in all these reactions is how the high-energy carbocations are generated and stabilised within the "mild" environment provided by the active sites of enzymes. Negatively charged amino acids are largely ruled out since their interaction with the carbocationic intermediates might easily lead to alkylation and hence suicide inhibition. Since the generation of carbocations normally requires strong acid, it had been suggested, based on results from density functional theory (DFT), semi-empirical and high-level molecular orbital theory calculations in the gas phase, to study the cyclisation of FPP along with molecular docking and modelling studies in the active site of PR-AS, employing combined quantum mechanical and molecular mechanical (QM/MM) methods that germacrene A might not be an intermediate of the conversion of FPP to aristolochene (Allemann et al. 2007). Rather, protonation of the C6-C7 double bond might be accomplished by intramolecular proton transfer from C12 of **10** rather than through the involvement of a general acid thereby bypassing the neutral intermediate germacrene A (**11**). In this mechanism, the direct intramolecular proton transfer had a computed barrier of about 22 kcal/mol, which was further lowered to 16–20 kcal/mol by PR-AS. However, when the stereochemistry of the elimination/protonation reactions was investigated, a direct intramolecular proton transfer was firmly excluded (Miller et al. 2008). Several candidates have been proposed for the acid that reprotonates germacrene A (**11**), including Lys 206 (Miller et al. 2008), a proton shuttle from the solvent to Tyr 92 in the active site by way of Arg 200, Asp 203 and Lys 206 (Calvert et al. 2002a), an unprecedented active-site oxonium ion (Miller et al. 2008), or the diphosphate itself (Shishova et al. 2007), but it has so far proved difficult to find conclusive experimental support for any of these proposals. Nevertheless, the intermediacy of germacrene A, which results from the quenching of a positive charge, suggests that carbocations are formed with relative ease within the active site of AS by a combination of general acid catalysis, tight control of the conformation of substrate and intermediates and efficient stabilisation of carbocations.

The X-ray crystal structures of terpene synthases reveal that their active sites are lined with many aromatic amino acids thereby providing unreactive hydrophobic environments that mimic aprotic organic solvents. It has been proposed that the interaction between intermediate carbocations and π-electrons of aromatic amino acid side chains such as phenylalanine, tyrosine and tryptophan could provide significant stabilisation (Ma and Dougherty 1997; Dougherty 1996). Results from site-directed mutagenesis experiments with PR-AS have provided evidence that such cation-π interactions are key to the polycyclisation reaction. Inspection of the X-ray structure of PR-AS suggested that the π-system of Trp 334 could interact favourably with the positive charge at C3 of eudesmane cation. In agreement

with this proposal, replacement of Trp 334 with Phe did not significantly change the distribution of terpenoids produced in incubations with FPP. However, the enzymes PR-ASW334V produced predominantly germacrene A in addition to ~5% aristolochene, while PR-ASW334L produced exclusively germacrene A (Deligeorgopoulou et al. 2003). It is worthy of note that the catalytic activity of PR-ASW334L and PR-ASW334V was dramatically reduced, indicating that Trp 334 also plays a role in the catalytic steps before the formation of eudesmane cation. These experiments suggest a quantitative influence of the π-electron density of aromatic amino acid side chains on the turnover in PR-AS. The conversion of germacrene A to eudesmane cation during PR-AS catalysis appears to depend on the π-electron density of residue 334. To test this hypothesis, experiments have been performed to introduce non-canonical amino acids into PR-AS. Initial experiments have involved replacing Trp 334 with *para*-substituted phenylalanines of increasing electron-withdrawing properties. This led to a progressive accumulation of germacrene A with a good correlation with the interaction energies of simple cations such as Na^+ with substituted benzenes (Faraldos et al. 2011b). These results provide direct evidence that Trp 334 plays a cation stabilising role for the energetically demanding transformation of germacrene A to eudesmane cation in aristolochene synthase catalysis. Further experiments replacing Trp 334 with groups such as naphthyl- and amino-naphthyl alanine are currently underway. The conversion of germacryl cation to aristolochene is also facilitated by the bulky aromatic side chain of Phe 178, a residue that is ideally placed to stabilise the developing positive charge on C2/C3 of eudesmane cation. However, it appears that it is the large size of Phe 178 that promotes the 1,2 hydride shift from C2 in eudesmane cation rather than its aromaticity that promotes the formation of aristolochene during AS catalysis (Forcat and Allemann 2006). The aromaticity of Phe 178 on the other hand is involved in the efficient formation of germacryl cation from FPP (Forcat and Allemann 2004).

One of the other key residues for the efficient formation of germacryl cation is Phe 112. Its replacement with alanine or cysteine led to reduced catalytic activity and the production of small amounts of germacrene A (and in the case of PR-ASF112C, 5% aristolochene) in addition to the linear (*E*)-α- and (*E*)-β-farnesene, indicating that residue 112 contributes significant stabilisation to the transition state leading to germacryl cation (**10**) (Forcat and Allemann 2006).

These results suggest that carbocations are stabilised in the active sites of terpene synthases through the interaction with aromatic active-site residues. In addition, the fact that diphosphate release appeared to be often the final step in this complex reaction cascade indicated that additional stabilisation is provided by the negatively charged diphosphate. Hence, it may be that during the reaction, an ion pair is maintained, thereby preventing the build up of significant overall charge within the active sites. These enzymes have developed a subtle strategy for the manipulation of cationic chemistry that is based on a combination of minimising charge separation, stabilisation of the cationic intermediates by the π-systems of suitably placed active-site residues and the enhancement of the reactivity of intermediates through templating effects.

12.2.5 Fluorinated Substrate Analogues

The examples described above show that site-directed mutagenesis experiments can be pivotal in deciphering reaction mechanisms of FPP cyclisations and the modes of catalysis employed by terpene synthases. However, the interpretation of results from site-specific mutants of terpene synthases requires some caution since the change of only a single amino acid in their active site can alter their templating potential. Such local geometrical changes can be inherently difficult to detect since they may not affect the global fold of the proteins but nevertheless lead to the synthesis of novel products through subtle alterations of the reaction pathway.

An alternative strategy that has been employed to explore the mechanism of the enzyme-catalysed cyclisations to terpenoid products relies on the

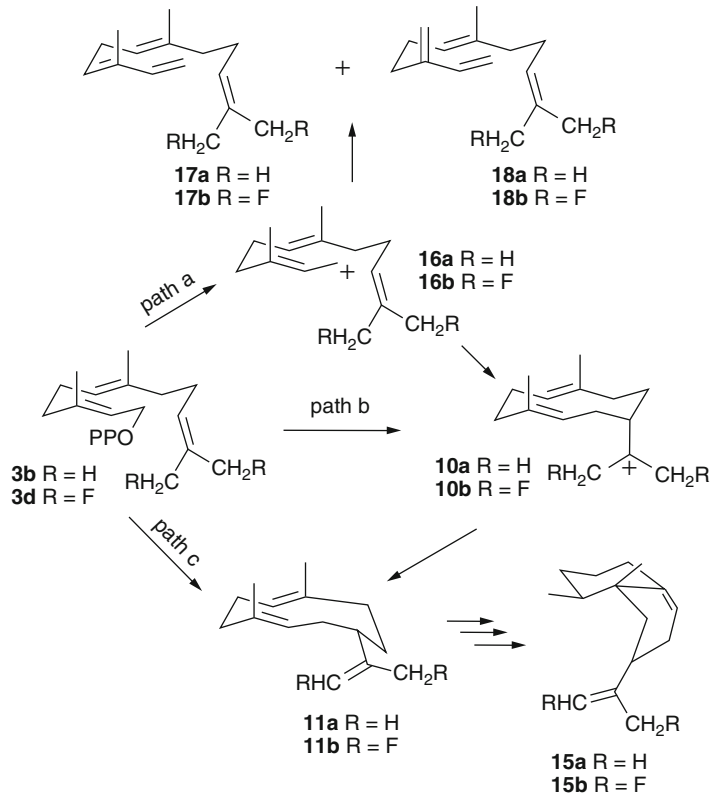

Fig. 12.7 Possible pathways for the cyclisation of FPP to germacrene A catalysed by PR-AS

use of substrate analogues such as fluoro-prenyl diphosphates as probes (Jin et al. 2005). Fluoride substituents do not greatly affect the binding affinities as a consequence of size and shape but at the same time exert a strong influence on the electronic environment at the site of replacement in that they stabilise cations on the α-carbon by π-donation but exert a destabilising inductive effect on cations located on the β-carbon (Banks and Tatlow 1986). It is important to stress here, however, that a combination of experimental approaches is needed to reveal the intricate details of terpene synthase chemistry.

The utility of fluorinated FPP analogues in elucidating such detail in reaction mechanism is nicely illustrated by experiments involving the substrate analogue 12, 13-difluorofarnesyl diphosphate (**FF-FPP**). The results obtained with site-specific mutants of AS suggested that diphosphate ionisation leads to the formation of farnesyl cation which is subsequently attacked by the C10-C11 π-bond to generate germacryl cation (Fig. 12.7, path a) (Forcat and Allemann 2006). Alternatively, the formation of germacryl cation could take place in a concerted reaction in which farnesyl diphosphate ionisation is accompanied by electrophilic attack of C1 of FPP by the C10, C11 π-system (Fig. 12.7, path b) (Shishova et al. 2007). This mechanism is in agreement with the observation that the reaction of stereospecifically deuterated FPP occurred with inversion of configuration at C1 (Cane et al. 1989). Yet another possible cyclisation pathway to germacrene A is initiated by deprotonation from C12 (Cane et al. 1990b) and concurrent bond formation between C10 and C1 (Fig. 12.7, path c).

Due to the electronic effects of fluoro substituents on carbocations described above, incubation of 12, 13-difluorofarnesyl diphosphate with AS would be expected to generate different outcomes for the three cyclisation pathways illustrated in Fig. 12.7. For path a, the destabilising effect of the two fluoro substituents on the putative carbocation on C11 should lead to the accumulation of the 12,13-difluorofarnesyl cation (**16b**) and the formation of 12,13-difluoro-(*E*)-α-farnesene

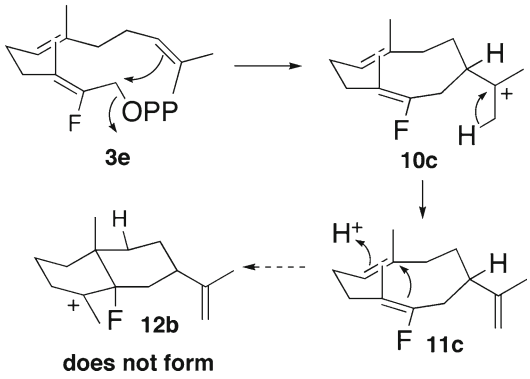

Fig. 12.8 Cyclisation of 2F-FPP by PR-AS stops at 2F-germacrene A (**11c**) since cation **12b** is destabilised by the presence of the fluoride

(**17b**) and 12,13-difluoro-(E)-β-farnesene (**18b**) through deprotonation from C4 or C15. For a reaction where phosphate departure occurs simultaneously with electron flow from the C10-C11 double bond, **3d** would be expected to act as a competitive inhibitor. In pathway c, the acidifying effect of the fluoro substituents on the protons on C12 and C13 should allow the reaction to proceed, ultimately generating 12,13-difluoro-aristolochene (**15b**). For PR-AS, it was found that 12,13-difluorofarnesyl diphosphate, prepared using Suzuki-Miyaura chemistry in a key synthetic step, was a potent competitive inhibitor of PR-AS (K_I=0.8 μM±0.2 comparable to the Michaelis constant for PR-AS catalysis; K_M=2.3 μM), thereby indicating that the initial cyclisation during PR-AS catalysis generates germacryl cation in a concerted reaction (Yu et al. 2007).

In a similar example, synthesis and incubation with PR-AS of 2F-FPP (**3e**) provided a strong indication that germacrene A is indeed an on-pathway product of catalysis by aristolochene synthase (Miller et al. 2007b). 2F-FPP was converted by PR-AS to 2-fluorogermacrene A (**11c**), suggesting that after an initial concerted cyclisation of FPP to germacryl cation, deprotonation leads to the formation of germacrene A (Miller et al. 2007b). Further, reaction towards a fluorinated aristolochene product is prevented by the fluoride substituent in this case since it is located β to the developing positive charge on C3 upon cyclisation of protonated germacrene A (Fig. 12.8).

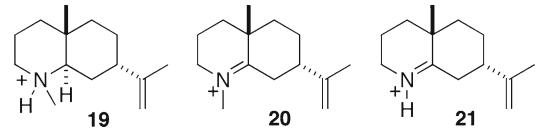

Fig. 12.9 Aza analogues of putative intermediates during catalysis by PR-AS

12.2.6 Aza Analogues

The intermediacy of cations such as **10** or **12** can only be inferred indirectly from experimentation, and a useful approach for their study is the use of structural analogues. Nitrogen-containing "aza analogues" of putative carbocations involved in terpene biosynthesis effectively mimic both the structure and electrostatics of their carbocation analogues, and there are many examples of their use in the study of mono- (McGeady et al. 1992), sesqui- (Aaron et al. 2010; Vedula et al. 2007; Vedula et al. 2005) and diterpene synthase chemistry (Mann et al. 2009; Ravn et al. 2002; Roy et al. 2007; Peters et al. 2001). In contrast to the extensive evidence supporting the formation and intermediacy of germacrene A (**11**), the lack of evidence for later steps in the catalytic cycle of PR-AS led us to synthesise a variety of aza analogues designed to mimic eudesmane cation and to test these analogues for their potential to act as inhibitors of PR-AS (Fig. 12.9).

The tertiary ammonium ion **19**, designed to be a mimic of the eudesmane cation itself, is a potent competitive inhibitor of PR-AS (K_I=0.35±0.12 μM), implying that eudesmane cation is a genuine intermediate species in this catalytic cycle and that this compound is an effective mimic. Interestingly, this compound was equally potent as an inhibitor of PR-AS in the presence or absence of inorganic diphosphate (PPi). The iminium ions **20** and **21**, designed to mimic the transition state *en route* to the formation of eudesmane cation from germacrene A, were potent competitive inhibitors of PR-AS in the presence of 250 μM PPi only (K_I=5.9±1.2 μM and K_I=0.41±0.19 μM, respectively) (Faraldos and Allemann 2011). In the absence of diphosphate, **20** and **21** acted as much weaker inhibitors

($K_I = 219 \pm 17$ μM and 28.4 ± 3 μM, respectively) (Faraldos and Allemann 2011). These observations suggest that the presence of inorganic diphosphate is not required for the stabilisation of eudesmane cation itself but that it plays a role in its generation from neutral germacrene A, suggesting that diphosphate may act as the general acid in the reprotonation of germacrene A (and potentially in the deprotonation of the final cation **14** *en route* to aristolochene; Scheme 12.1) (Shishova et al. 2007). Strong evidence for the participation of diphosphate in protonation changes during terpene synthase chemistry was recently found from an X-ray crystallographic analysis of isoprene synthase where the generation of isoprene from dimethylallyl diphosphate appears to occur in a *syn*-periplanar elimination, in which the diphosphate-leaving group acts as the general base (Köksal et al. 2010).

12.3 Conclusions

Extensive studies of the aristolochene synthase-catalysed conversion of FPP to aristolochene have illuminated many aspects of the catalytic strategy used by this enzyme and related terpene synthases. Clearly, nature combines several well-known chemical strategies to control the specificity of prenyl diphosphate cyclisation through a cascade of mostly carbocationic reaction intermediates within a shared three-dimensional enzyme fold in what represents the masterpiece in combinatorial chemistry and directed organic synthesis. Deciphering the terpene specificity code developed by nature should enable further evolution of terpene synthases and the enzymes that are further downstream in terpene biosynthesis both *in vitro* and *in vivo* to generate novel "unnatural" terpenoids in a truly cross-disciplinary approach with contributions from synthetic organic and mechanistic chemistry, molecular biology and metabolic engineering with enormous potential for chemistry, biology and medicine.

Acknowledgements The authors would like to acknowledge the many contributions made by the members of the Allemann group. This work was supported by the UK's Biotechnology and Biological Sciences Research Council through research grants 6/B17177, BBS/Q/Q/2004/05499 and BB/G003572/1, the Engineering and Physical Sciences Research Council through grant EP/D06958/1, the Royal Society (grant 2007R2) and Cardiff University. We are grateful to Neil Young for preparing Figs. 12.4 and 12.6.

References

Aaron JA, Lin X, Cane DE, Christianson DW (2010) Structure of epi-isozizaene synthase from *Streptomyces coelicolor* A3(2), a platform for new terpenoid cyclization templates. Biochemistry 49:1787–1797

Allemann RK, Young NJ, Ma S, Truhlar DG, Gao J (2007) Synthetic efficiency in enzyme mechanisms involving carbocations: aristolochene synthase. J Am Chem Soc 129:13008–13013

Banks RE, Tatlow JC (1986) A guide to modern organofluorine chemistry. J Fluor Chem 33:227–284

Calvert MJ, Ashton PR, Allemann RK (2002a) Germacrene A is a product of the aristolochene synthase-mediated conversion of farnesylpyrophosphate to aristolochene. J Am Chem Soc 124:11636–11641

Calvert MJ, Taylor SE, Allemann RK (2002) Tyrosine 92 of aristolochene synthase directs cyclisation of farnesyl pyrophosphate. Chem Commun 2384–2385

Cane DE (1990) The enzymatic formation of sesquiterpenes. Chem Rev 90:1089–1093

Cane DE, Bryant C (1994) Aristolochene synthase. Mechanism-based inhibition of a terpenoid cyclase. J Am Chem Soc 116:12063–12064

Cane DE, Tsantrizos YS (1996) Aristolochene synthase. Elucidation of the cryptic Germacrene A synthase activity using the anomalous substrate dihydrofarnesyl diphosphate. J Am Chem Soc 118:10037–10040

Cane DE, Prabhakaran PC, Salaski EJ, Harrison PHM, Noguchi H, Rawlings BJ (1989) Aristolochene biosynthesis and enzymatic cyclization of farnesyl pyrophosphate. J Am Chem Soc 111:8914–8916

Cane DE, Prabhakaran PC, Oliver JS, McIlwaine DB (1990a) Aristolochene biosynthesis. Stereochemistry of the deprotonation steps in the enzymatic cyclization of farnesyl pyrophosphate. J Am Chem Soc 112: 3209–3210

Cane DE, Prabhakaran PC, Oliver JS, McIlwaine DB (1990b) Aristolochene biosynthesis. Stereochemistry of the deprotonation steps in the enzymatic cyclization of farnesyl pyrophosphate. J Am Chem Soc 112: 3209–3210

Caruthers JM, Kang I, Rynkiewicz MJ, Cane DE, Christianson DW (2000) Crystal structure determination of aristolochene synthase from the blue cheese mold, *Penicillium roqueforti*. J Biol Chem 275: 25533–25539

Christianson DW (2006) Structural biology and chemistry of the terpenoid cyclases. Chem Rev 106:3412–3442

Deligeorgopoulou A, Allemann RK (2003) Evidence for differential folding of farnesyl pyrophosphate in the active site of aristolochene synthase: a single-point mutation converts aristolochene synthase into an (*E*)-β-farnesene synthase. Biochemistry 42:7741–7747

Deligeorgopoulou A, Taylor SE, Forcat S, Allemann RK (2003) Stabilisation of eudesmane cation by tryptophan 334 during aristolochene synthase catalysis. Chem Commun 2162–2163

Dougherty DA (1996) Cation-π interactions in chemistry and biology: a new view of benzene, Phe, Tyr, and Trp. Science 271:163–168

Faraldos JA, Allemann RK (2011) Inhibition of (+)-aristolochene synthase with iminium salts resembling eudesmane cation. Org Lett 13:1202–1205

Faraldos JA, Gonzalez V, Senske M, Allemann RK (2011) Templating effects in aristolochene synthase catalysis: elimination versus cyclisation. Org Biomol Chem 9. 6920–9623

Faraldos JA, Antonczak AK, González VG, Fullerton R, Tippmann EM, Allemann RK (2011) Probing eudesmane cation–π Interactions in catalysis by aristolochene synthase with non-canonical amino acids. J Am Chem Soc 133:13906–13909

Forcat S, Allemann RK (2004) Dual role for phenylalanine 178 during catalysis by aristolochene synthase. Chem Commun 2094–2095

Forcat S, Allemann RK (2006) Stabilisation of transition states prior to and following eudesmane cation in aristolochene synthase. Org Biomol Chem 4:2563–2567

Gennadios HA, Gonzalez V, Di Costanzo L, Li AA, Yu FL, Miller DJ, Allemann RK, Christianson DW (2009) Crystal structure of (+)-δ-cadinene synthase from *Gossypium arboreum* and evolutionary divergence of metal binding motifs for catalysis. Biochemistry 48:6175–6183

Glasby JS (1982) Encyclopedia of Terpenoids. Wiley, Chichester

Greenhagen BT, O'Maille PE, Noel JP, Chappell J (2006) Identifying and manipulating structural determinates linking catalytic specificities in terpene synthases. Proc Natl Acad Sci USA 103:9826–9831

Hyatt DC, Youn B, Zhao Y, Santhamma B, Coates RM, Croteau RB, Kang C (2007) Structure of limonene synthase, a simple model for terpenoid cyclase catalysis. Proc Natl Acad Sci USA 104:5360–5365

Jin Y, Williams DC, Croteau R, Coates RM (2005) Taxadiene synthase-catalyzed cyclization of 6-fluorogeranylgeranyl diphosphate to 7-fluoroverticillenes. J Am Chem Soc 127:7834–7842

Köksal M, Zimmer I, Schnitzler JP, Christianson DW (2010) Structure of isoprene synthase illuminates the chemical mechanism of teragram atmospheric carbon emission. J Mol Biol 402:363–373

Köksal M, Hu HY, Coates RM, Peters RJ, Christianson DW (2011a) Structure and mechanism of the diterpene cyclase *ent*-copalyl diphosphate synthase. Nat Chem Biol 7:431–433

Köksal M, Jin YH, Coates RM, Croteau R, Christianson DW (2011b) Taxadiene synthase structure and evolution of modular architecture in terpene biosynthesis. Nature 469:116–120

Lesburg CA, Zhai G, Cane DE, Christianson DW (1997) Crystal structure of pentalenene synthase: mechanistic insights on terpenoid cyclization reactions in biology. Science 277:1820–1824

Ma JC, Dougherty DA (1997) The cation-π interaction. Chem Rev 97:1303–1324

Mann FM, Prisic S, Hu HY, Xu MM, Coates RM, Peters RJ (2009) Characterization and inhibition of a class II diterpene cyclase from *Mycobacterium tuberculosis*: implications for tuberculosis. J Biol Chem 284:23574–23579

McGeady P, Pyun HJ, Coates RM, Croteau R (1992) Biosynthesis of monoterpenes: Inhibition of (+)-pinene and (-)-pinene cyclases by thia and aza analogs of the 4*R*- and 4*S*-α-terpinyl carbocation. Arch Biochem Biophys 299:63–72

Miller DJ, Yu F, Young NJ, Allemann RK (2007a) Competitive inhibition of aristolochene synthase by phenyl-substituted farnesyl diphosphates: evidence of active site plasticity. Org Biomol Chem 5:3287–3298

Miller DJ, Yu F, Allemann RK (2007b) Aristolochene synthase-catalyzed cyclization of 2-fluorofarnesyldiphosphate to 2-fluorogermacrene A. ChemBioChem 8:1819–1825

Miller DJ, Gao J, Truhlar DG, Young NJ, Gonzalez V, Allemann RK (2008) Stereochemistry of eudesmane cation formation during catalysis by aristolochene synthase from *Penicillium roqueforti*. Org Biomol Chem 6:2346–2354

O'Maille PE, Chappell J, Noel JP (2006) Biosynthetic potential of sesquiterpene synthases: alternative products of tobacco 5-epi-aristolochene synthase. Arch Biochem Biophys 448:73–82

Peters RJ, Ravn MM, Coates RM, Croteau RB (2001) Bifunctional abietadiene synthase: free diffusive transfer of the (+)-copalyl diphosphate intermediate between two distinct active sites. J Am Chem Soc 123: 8974–8978

Ravn MM, Peters RJ, Coates RM, Croteau R (2002) Mechanism of abietadiene synthase catalysis: stereochemistry and stabilization of the cryptic pimarenyl carbocation intermediates. J Am Chem Soc 124:6998–7006

Roy A, Roberts FG, Wilderman PR, Zhou K, Peters RJ, Coates RM (2007) 16-Aza-*ent*-beyerane and 16-Aza-*ent*-trachylobane: potent mechanism-based inhibitors of recombinant ent-kaurene synthase from *Arabidopsis thaliana*. J Am Chem Soc 129:12453–12460

Rynkiewicz MJ, Cane DE, Christianson DW (2001) Structure of trichodiene synthase from *Fusarium sporotrichioides* provides mechanistic inferences on the terpene cyclization cascade. Proc Natl Acad Sci USA 98:13543–13548

Shishova EY, Di Costanzo L, Cane DE, Christianson DW (2007) X-ray crystal structure of aristolochene synthase from *Aspergillus terreus* and evolution of templates for the cyclization of farnesyl diphosphate. Biochemistry 46:1941–1951

Shishova EY, Yu F, Miller DJ, Faraldos JA, Zhao YX, Coates RM, Allemann RK, Cane DE, Christianson DW

(2008) X-ray crystallographic studies of substrate binding to aristolochene synthase suggest a metal ion binding sequence for catalysis. J Biol Chem 283:15431–15439

Starks CM, Back K, Chappell J, Noel JP (1997) Structural basis for cyclic terpene biosynthesis by tobacco 5-*epi*-aristolochene synthase. Science 277:1815–1820

Thulasiram HV, Erickson HK, Poulter CD (2007) Chimeras of two isoprenoid synthases catalyze all four coupling reactions in isoprenoid biosynthesis. Science 316:73–76

Thulasiram HV, Erickson HK, Poulter CD (2008) A common mechanism for branching, cyclopropanation, and cyclobutanation reactions in the isoprenoid biosynthetic pathway. J Am Chem Soc 130:1966–1971

Vedula LS, Cane DE, Christianson DW (2005) Role of arginine-304 in the diphosphate-triggered active site closure mechanism of trichodiene synthase. Biochemistry 44:12719–12727

Vedula LS, Zhao YX, Coates RM, Koyama T, Cane DE, Christianson DW (2007) Exploring biosynthetic diversity with trichodiene synthase. Arch Biochem Biophys 466:260–266

Wei RD, Schnoes HK, Hart PA, Strong FM (1975) The structure of PR toxin, a mycotoxin from *Penicillium roqueforti*. Tetrahedron 31:109–114

Whittington DA, Wise ML, Urbansky M, Coates RM, Croteau RB, Christianson DW (2002) Bornyl diphosphate synthase: structure and strategy for carbocation manipulation by a terpenoid cyclase. Proc Natl Acad Sci USA 99:15375–15380

Yoshikuni Y, Ferrin TE, Keasling JD (2006a) Designed divergent evolution of enzyme function. Nature 440:1078–1082

Yoshikuni Y, Martin VJJ, Ferrin TE, Keasling JD (2006b) Engineering cotton (+)-δ-cadinene synthase to an altered function: germacrene D-4-ol synthase. Chem Biol 13:91–98

Yu F, Miller DJ, Allemann RK (2007) Probing the reaction mechanism of aristolochene synthase with 12,13-difluorofarnesyl diphosphate. Chem Commun 4155–4157

13

Elucidating the Formation of Geranyllinalool, the Precursor of the Volatile C_{16}-Homoterpene TMTT Involved in Indirect Plant Defense

Marco Herde, Katrin Gärtner, Tobias Köllner, Benjamin Fode, Wilhelm Boland, Jonathan Gershenzon, Christiane Gatz, and Dorothea Tholl

Abstract

Plants produce volatile compounds as communication signals for the interaction with other organisms. The volatile C16-homoterpene TMTT (4,8,12-trimethyltrideca-1,3,7,11-tetraene) is released from the foliage of many plants including *Arabidopsis thaliana* upon herbivore attack and is assumed to play a role in attracting parasitoids or predators of herbivores. Despite the widespread occurrence of TMTT, its biosynthesis is not well understood. We have identified *Arabidopsis* TPS04 (At1g61120) as the terpene synthase catalyzing the first dedicated step in TMTT formation. TPS04 functions as a geranyllinalool synthase (GES) by converting the C20 diterpene precursor all-*trans*-geranylgeranyl diphosphate (GGPP)

M. Herde
Albrecht-von Haller-Institute for Plant Sciences, Georg-August-University Göttingen, Göttingen D-37073, Germany

Department of Biochemistry and Molecular Biology, Michigan State University, East Lansing, MI 48824, USA

K. Gärtner • B. Fode • C. Gatz
Albrecht-von Haller-Institute for Plant Sciences, Georg-August-University Göttingen, Göttingen D-37073, Germany

T. Köllner • J. Gershenzon
Department of Biochemistry, Max-Planck-Institute for Chemical Ecology, Jena D-07745, Germany

W. Boland
Department of Bioorganic Chemistry, Max-Planck-Institute for Chemical Ecology, Jena D-07745, Germany

D. Tholl (✉)
Department of Biological Sciences, Virginia Tech, 408 Latham Hall, Agquad Lane, Blacksburg, VA 24061, USA
e-mail: tholl@vt.edu

T.J. Bach and M. Rohmer (eds.), *Isoprenoid Synthesis in Plants and Microorganisms: New Concepts and Experimental Approaches*, DOI 10.1007/978-1-4614-4063-5_13,

into the C20 tertiary alcohol (*E*,*E*)-geranyllinalool (GL). GL is further converted into TMTT by enzymatic oxidative degradation. *Arabidopsis TPS04* gene knockout lines are deficient in the formation of GL and TMTT. This phenotype is complemented by expression of *GES* under control of an alcohol-inducible or constitutive promoter. Constitutive formation of GL and TMTT causes the appearance of lesions on cotyledons and leads to reduced growth. Transcription of *GES* and the synthesis of GL and TMTT are induced by feeding of the crucifer-specialist *Plutella xylostella* and by treatment with the fungal elicitor alamethicin or the jasmonate mimic coronalon. Regulation of *GES* transcription is dependent on the octadecanoid-dependent signaling pathway and is not modified by salicylic acid or ethylene. In contrast to other diterpene synthases, GES is not located in plastids but resides instead in the cytosol or the endoplasmic reticulum. The identification of *GES* provides a useful tool to further investigate the specific role of TMTT in plant–organism interactions and to elucidate the TMTT biosynthetic pathway and its regulation.

Keywords
Norterpene • Geranyllinalool • Terpene synthase • Arabidopsis • Plant volatile • Plant defense • Herbivory

13.1 Introduction

Volatile organic compounds are important tools in the interaction of plants with their environment. Volatiles released from vegetative tissue have a significant function in defense, since they either directly ward off herbivorous insects or attract natural enemies of herbivores, a response that is also known as indirect defense or the "plant's call for help." Homoterpenes, such as the C_{11}-homoterpene DMNT (4,8-dimethylnona-1,3,7-triene) and the C_{16}-homoterpene TMTT (4,8,12-trimethyltrideca-1,3,7,11-tetraene), represent an important group of volatile compounds emitted upon insect attack and are involved in indirect defense (Hopke et al. 1994; Dicke 1994; Ament et al. 2006). Several studies support the role of DMNT and TMTT in the attraction of herbivore predators. For example, de Boer et al. (2004) demonstrated that TMTT emitted from spider mite-infested lima bean leaves influenced the foraging behavior of predatory mites. A similar response by predatory mites was observed on tomato plants that released increased amounts of TMTT upon spider mite attack (Kant et al. 2004).

Another intriguing function of homoterpene volatiles is their ability to elicit defense responses in plants. Arimura et al. (2000) demonstrated that TMTT induces the expression of defense genes in lima bean. Therefore, this volatile might also play a role in plant–plant interactions by priming neighboring noninfested plants for defense responses. In addition to emission from foliage, TMTT is a common constituent of floral fragrances and contributes to the so-called white floral image of night-scented flowers such as orchids or lilies (Donath and Boland 1994). Because of the widespread occurrence of TMTT in plants and its ecological significance in plant–environment interactions, there is a strong interest in investigating the biosynthesis and regulation of this volatile in detail.

A putative biosynthetic pathway for the formation of TMTT was suggested by Boland and coworkers. Their studies using stable isotope precursors indicated that TMTT is derived from the tertiary diterpene alcohol (*E*,*E*)-geranyllinalool

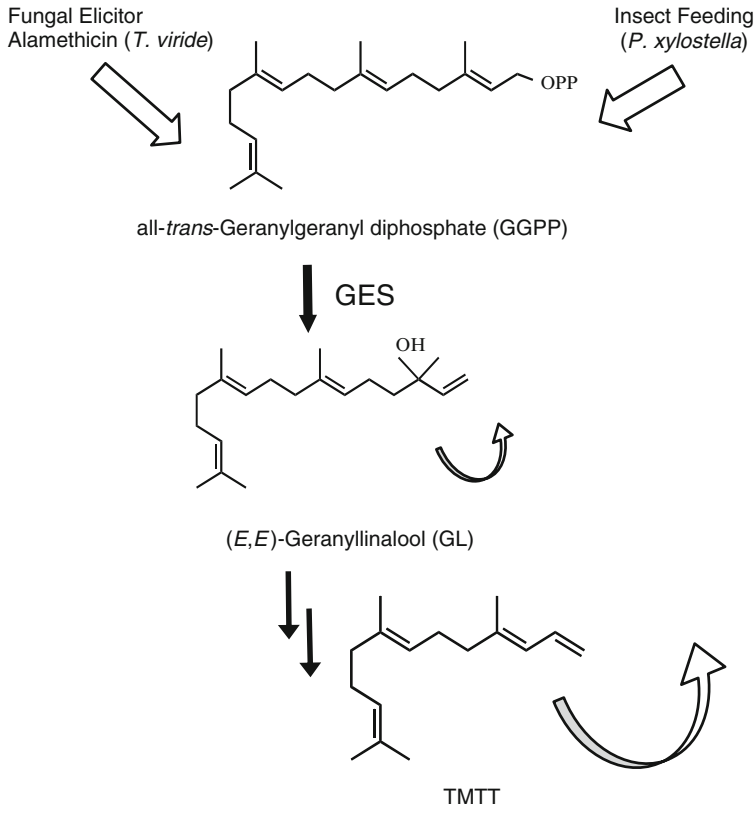

Fig. 13.1 Proposed biosynthetic pathway for the formation of the volatile C_{16}-homoterpene TMTT. Formation and emission of TMTT and its precursor (*E,E*)-geranyllinalool (GL) are induced in *Arabidopsis* leaves by treatment with the fungal elicitor alamethicin and in response to insect feeding. GL is synthesized from the substrate all-*trans*-GGPP by activity of a GL synthase (GES). Conversion of GL into TMTT occurs by steps of oxidative degradation

(GL), which is converted into TMTT by subsequent oxidative degradation catalyzed by cytochrome P450-type enzymes (Boland and Gabler 1989; Gabler et al. 1991; Boland et al. 1998). A GL synthase (GES) activity was reported by Ament et al. (2006) that showed a stringent correlation with the formation of TMTT in tomato leaves in response to treatment with jasmonic acid (JA). Based on these findings, we hypothesized that the formation of GL, the first committed step in TMTT biosynthesis, is catalyzed by a diterpene synthase that converts the C_{20}-prenyl diphosphate intermediate all-*trans*-geranylgeranyl diphosphate (GGPP) into the tertiary alcohol GL by hydrolysis of the diphosphate moiety and allylic rearrangement (Fig. 13.1). The reaction is analogous to those catalyzed by linalool synthases and nerolidol synthases for the conversion of geranyl diphosphate (GPP, C_{10}) and (*E*,*E*)-farnesyl diphosphate (FPP, C_{15}) to linalool and (*E*)-nerolidol, respectively (Pichersky et al. 1994; Pichersky et al. 1995; Bouwmeester et al. 1999; Degenhardt and Gershenzon 2000). Despite the characterization of linalool and nerolidol synthase genes from several plants such as *Clarkia breweri*, maize, strawberry, and spruce (Dudareva et al. 1996; Schnee et al. 2002; Martin et al. 2004; Aharoni et al. 2004), no sequence of a *GES* had been identified at the time of our investigations. Here, we report the identification of a terpene synthase that is required for the synthesis of the TMTT precursor GL in the model plant *Arabidopsis thaliana*.

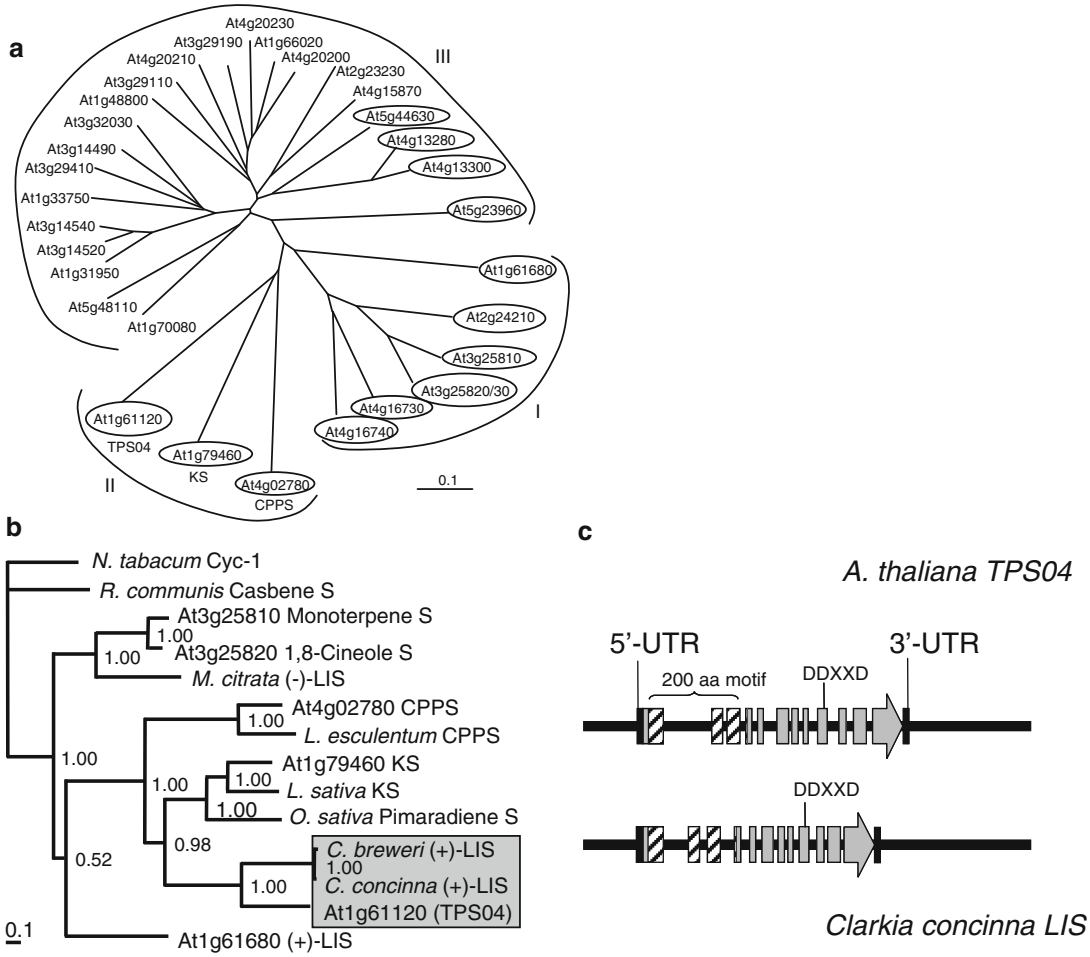

Fig. 13.2 Gene structure and phylogenetic relationship of *Arabidopsis* terpene synthase *TPS04*. (**a**) A neighbor-joining tree based on degree of amino acid sequence similarity between the enzymes of the *Arabidopsis* terpene synthase (TPS) family. Functionally characterized TPSs are circled. Clade I contains monoterpene synthases of the TPS-b subfamily (Aubourg et al. 2002). Clade II contains TPS04 and the diterpene synthases copalyl diphosphate synthase (subfamily TPS-c) and *ent*-kaurene synthase (subfamily TPS-e). Clade III comprises sesquiterpene synthases and uncharacterized putative monoterpene or diterpene synthases. (**b**) Phylogenetic relationship of *Arabidopsis* TPS04 with selected *Arabidopsis* and other angiosperm monoterpene and diterpene synthases. A Bayesian tree was generated from an alignment of the presented TPS proteins. TPS04 and closely related linalool synthases (LIS) from *Clarkia breweri* and *Clarkia concinna* are marked in *gray*. S, synthase; CPPS, copalyl diphosphate synthase; KS, kaurene synthase. (**c**) Closely related gene structures of *Arabidopsis TPS04* and *LIS* of *C. concinna* (Cseke et al. 1998). *Gray boxes* represent exons separated by introns. *Striped boxes* indicate exons encoding an ancestral 200 amino acid motif. Vertical black bars indicate 5′- and 3′ untranslated regions (UTRs). Both genes contain the highly conserved amino acid sequence motif DDXXD that is required for the ionization-initiated reaction mechanism of class-I TPSs (Davis and Croteau 2000; Tholl 2006) (Fig. 13.2b, Reproduced from Herde et al. (2008), Copyright American Society of Plant Biologists, www.plantcell.org)

13.2 *Arabidopsis:* A Model for Volatile Terpene Biosynthesis

Arabidopsis is a suitable model for investigating terpene secondary metabolite biosynthesis and function (Chen et al. 2003; Fäldt et al. 2003; Aharoni et al. 2003). The *Arabidopsis* genome contains a gene family of 32 predicted terpene synthases (*TPS*) that are expressed in aerial tissues and roots (Fig. 13.2a) (Chen et al. 2003; Ro et al. 2006). Several monoterpene and sesquiterpene synthases show constitutive expression in floral organs and are responsible for the release of a blend of monoterpene and sesquiterpene volatiles (Tholl et al. 2005). In addition to emission from flowers, terpene volatiles including the monoterpene (*E*)-β-ocimene, the sesquiterpene (*E,E*)-α-farnesene, and the C_{16}-homoterpene TMTT are synthesized de novo in *Arabidopsis* leaves as an induced response to herbivore-feeding damage (Van Poecke et al. 2001). The emitted volatiles, especially the common homoterpene TMTT, are most likely acting as indirect defense signals by attracting herbivore-parasitizing wasps such as *Cotesia rubecula*. Consequently, the parasitization of *P. rapae* caterpillars by *C. rubecula* resulted in an increase in plant fitness in terms of seed production (van Loon et al. 2000), underscoring the significance of herbivore-induced TMTT emission in plant defense.

13.3 Identification of a *GES* Gene Candidate in *Arabidopsis* by Phylogenetic Comparison and Gene Transcript Analysis

Arabidopsis terpene synthases can be clustered in three main clades (Fig. 13.2a): (I) seven monoterpene synthases, all of which have been biochemically characterized (Bohlmann et al. 2000; Chen et al. 2003; Fäldt et al. 2003; Chen et al. 2004; Huang et al. 2010); (II) 22 terpene synthases, of which 18 enzymes carry putative plastidial or mitochondrial targeting sequences and four that lack a transit peptide (all sesquiterpene synthases) (Tholl et al. 2005; Ro et al. 2006); and (III) a clade of three enzymes containing the previously annotated terpene synthase TPS04 (At1g61120) and the two characterized diterpene synthases, copalyl diphosphate synthase (CPPS) and ent-kaurene synthase (KS) involved in gibberellin (GA) biosynthesis (Sun and Kamiya 1994; Yamaguchi et al. 1998). *TPS04* represented a likely candidate for encoding a GES since it clusters with other *Arabidopsis* diterpene synthases but is also closely related (43% similarity) to linalool synthases (LISs) from *Clarkia breweri* and *Clarkia concinna* (Cseke et al. 1998; Aubourg et al. 2002) when compared to known terpene synthases from other species (Fig. 13.2b). Both LISs enzymes catalyze a similar reaction to GES but convert the 10-carbon substrate GPP rather than the 20-carbon all-*trans*-GGPP into linalool. *TPS04* and *Clarkia LISs* share almost identical gene structures, having 12 exons and code for a conserved N-terminal 200 amino acid domain of unknown function similar to the structure found in all plant TPSs encoded by the presumed progenitor gene (Fig. 13.2c) (Bohlmann et al. 1998; Trapp and Croteau 2001; Aubourg et al. 2002). All the other known monoterpene synthase genes of angiosperm origin, for instance, the *Arabidopsis* LIS, consist of only seven exons and code for enzymes that lack the conserved 200 amino acid domain. Hence, *Clarkia* LISs have an interesting phylogenetic position in the TPS superfamily and may have evolved from a diterpene synthase precursor such as GES.

To further determine *TPS04* as a putative *GES* gene, we investigated its expression in *Arabidopsis* rosette leaves after treatment with alamethicin, a peptaibol elicitor from the phytoparasitic fungus *Trichoderma viride*. Alamethicin is known to induce the emission of volatile terpenes including TMTT in lima bean (Engelberth et al. 2001). Alamethicin treatment of detached rosette leaves as well as intact hydroponically grown plants of the *Arabidopsis* ecotype Columbia caused the release of a volatile blend similar to that observed

upon feeding by *Pieris rapae* (Van Poecke et al. 2001). The major induced volatile compounds were methyl salicylate (MeSA), the sesquiterpene (*E,E*)-α–farnesene, and the C_{16}-homoterpene TMTT, which showed highest emission rates during 20–30 h of incubation with alamethicin (Fig. 13.3a). Minor amounts of the presumed TMTT precursor GL were detected, as confirmed by mass spectrometry using a synthetic GL standard.

By analyzing the expression of all *TPS* genes from RNA of rosette leaves exposed to 30 h of alamethicin treatment, we observed induced transcripts of three genes of the monoterpene synthase clade I, *At2g24210*, *At4g16740*, and *At4g16730*. Of these genes, *At2g24210* encodes a myrcene/ocimene synthase, and At4g16730 and At4g16740 have been characterized as ocimene/farnesene synthases (Bohlmann et al. 2000; Fäldt et al. 2003; Huang et al. 2010). The only other gene with induced expression, as demonstrated by RT-PCR and Northern blot analysis, was *TPS04* (Fig. 13.3b), corroborating an enzymatic function of TPS04 in GL and TMTT biosynthesis. Transcription of *TPS04* was also induced in leaves that were treated with the jasmonate mimic coronalon and upon feeding damage by larvae of the crucifer-specialist *Plutella xylostella* (diamond back moth) (Fig. 13.3b). Both coronalon and insect treatments caused the release of a volatile mixture similar to that induced with alamethicin (Fig. 13.3a). No emission of any of the four volatiles and no *TPS04* mRNA were observed upon mechanical wounding.

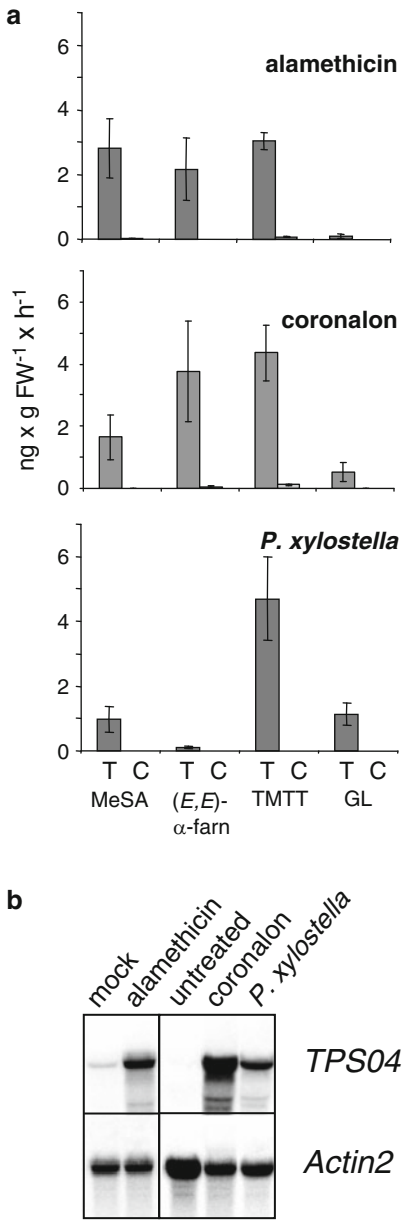

Fig. 13.3 Volatile emission and expression of *TPS04* in *Arabidopsis* rosette leaves in response to elicitor treatment and insect feeding (Reproduced from Herde et al. (2008), Copyright American Society of Plant Biologists, www.plantcell.org). (**a**) Comparative quantitative analysis of the volatiles methyl salicylate (MeSA), (*E,E*)-β-farnesene, 4,8,12-trimethyltrideca-1,3,7,11-tetraene (TMTT), and GL collected during 21–30 h of treatment. Elicitors were applied to detached leaves (alamethicin, 5 μg/mL) or through the roots of intact hydroponically grown plants (coronalon, 100 μM). For the insect-feeding experiment, two *P. xylostella* larvae were applied on each medium size and fully expanded rosette leaf. Volatiles Vwere collected by a closed-loop stripping procedure (Tholl et al. 2005) and analyzed by gas chromatography–mass spectrometry (GC–MS) analysis (Herde et al. 2008). The results represent the means ± SE of three replicates. *T* treatment, *C* control. (**b**) Northern blot analysis of *TPS04* transcripts in *Arabidopsis* leaves 31 h after the different treatments. Control samples were extracted from detached leaves treated with 0.1% ethanol (mock) or from leaves of intact hydroponically grown plants. *Actin2* was used as a transcriptional control

13.4 *Arabidopsis TPS04* Encodes a Functional GL Synthase

We analyzed the biochemical function of *TPS04* as a *GES* by heterologous expression in *Escherichia coli* (Herde et al. 2008). Expression of a stable GES enzyme required several steps of experimental optimization and could only be achieved by incubation of *E. coli* cultures at a constant temperature of 18 °C prior and post-induction with isopropyl-β-D-thiogalactopyranoside (IPTG). In a TPS enzyme assay with all-*trans*-GGPP as the substrate, the affinity-purified, recombinant TPS04 enzyme produced a single product, which was identified as (*E,E*)-geranyllinalool by comparison of its retention time and mass spectrum with those of an authentic standard (Fig. 13.4a, b). Similar to other plant terpene synthases (Davis and Croteau 2000), GES activity requires the presence of the divalent metal ions Mg^{2+} or Mn^{2+} (Herde et al. 2008). Highest activity was observed in the presence of 10 mM Mg^{2+}. The enzyme shows high substrate specificity towards all-*trans*-GGPP since GPP and (*E*,*E*)-FPP were not converted to their corresponding tertiary alcohols (Herde et al. 2008).

13.5 *In Planta* Activity of the *Arabidopsis GES* Gene

We further investigated the GES activity of *TPS04* *in planta* by analyzing *TPS04* gene knockout lines and by complementation of these mutants with *TPS04* under control of a constitutive and inducible promoter. As expected, no GL or TMTT were detected in the headspace of the two *TPS04* T-DNA insertion lines *salk_039864* and *salk_078187* upon treatment with coronalon, while the two other induced volatiles, MeSA and (*E,E*)-α-farnesene, were present (Herde et al. 2008). In agreement with the results of the volatile analysis, no *TPS04* mRNA was detected after coronalon treatment of these lines.

For complementation of the observed phenotype, line *salk_039864* was transformed with the *TPS04* gene under the control of two different heterologous promoters. An alcohol-inducible promoter (*AlcA*) was selected to avoid possible secondary effects by the constitutive formation of GL and TMTT. Treatment of the rosette leaves of these lines with 5% ethanol induced the emission of GL and TMTT, while both compounds were not released in the absence of

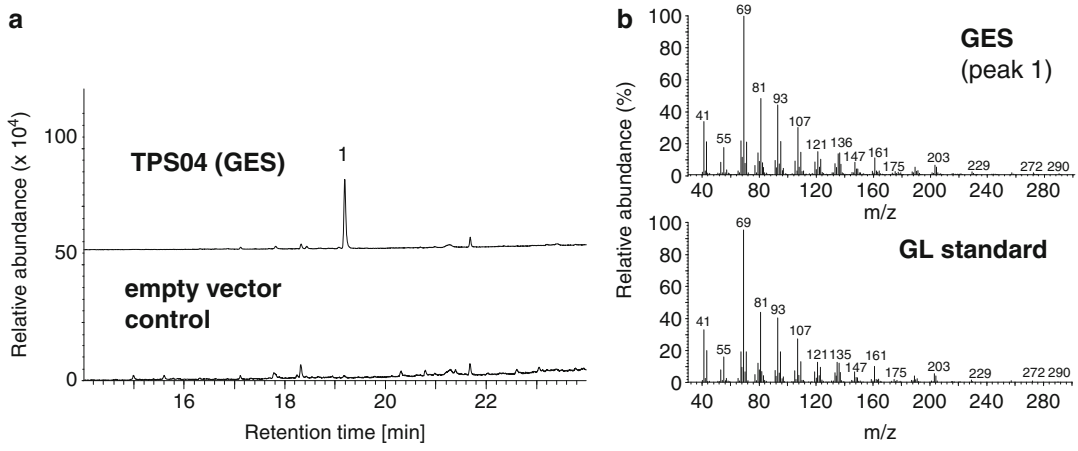

Fig. 13.4 Arabidopsis recombinant TPS04 functions as a GL synthase (GES). (**a**) Terpene synthase assay with recombinant TPS04 protein and all-*trans*-GGPP (88 μM) as the substrate. The enzymatic product (*1*) was extracted with hexane and analyzed by GC–MS (Herde et al. 2008). Retention time and mass spectrum of (*1*) are identical with those of an authentic GL standard. (**b**) *TPS04* was expressed in *E. coli*, extracted, and affinity-purified using the pASK-IBA7 expression vector (IBA GmbH, Göttingen, Germany). An extract of *E. coli* carrying the empty expression vector was used as a negative control

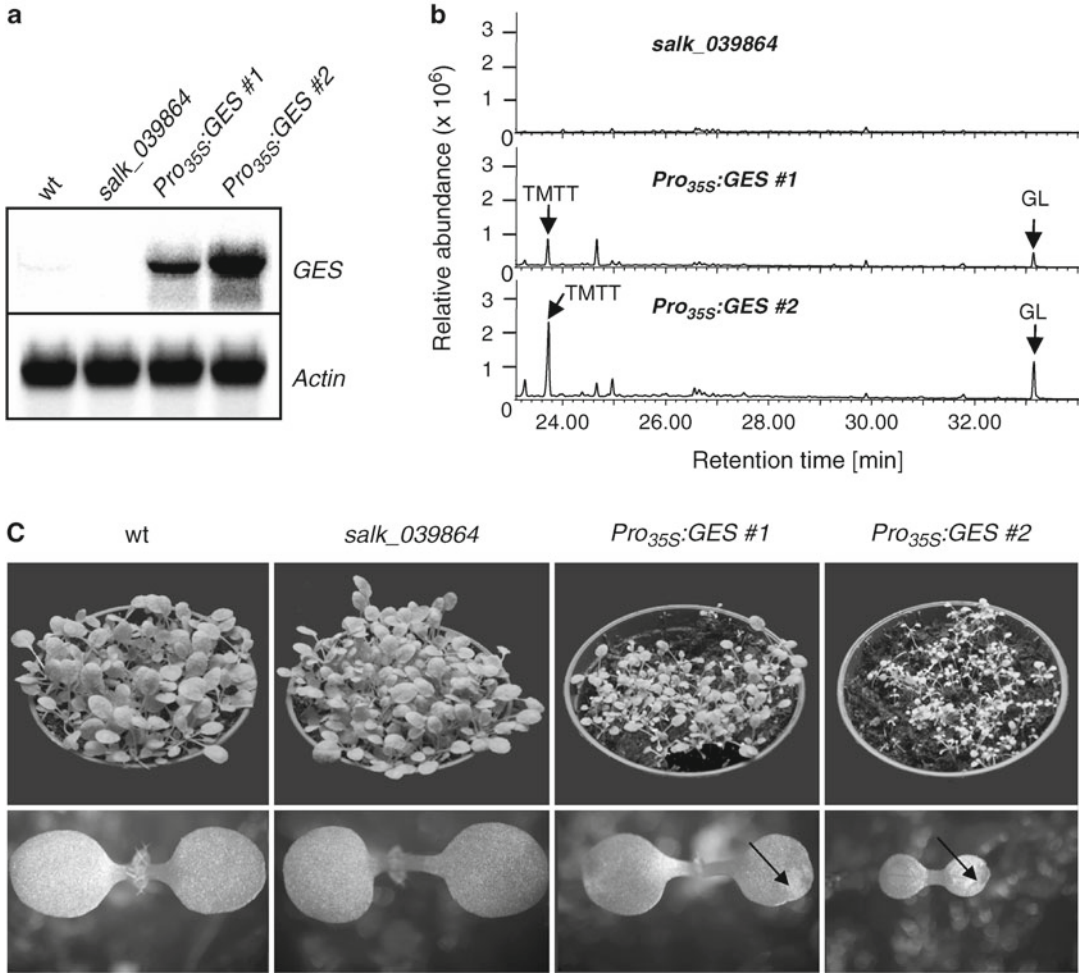

Fig. 13.5 Constitutive expression of *Arabidopsis GES* causes formation of lesions and growth retardation (Reproduced from Herde et al. (2008), Copyright American Society of Plant Biologists, www.plantcell.org). (**a**) Northern blot analysis of *GES* transcripts in leaves of 3-week-old transgenic lines (#1 and #2) expressing *GES* under control of the *CaMV 35S* promoter in comparison to wild-type and the *GES* knockout line *salk_039864*. (**b**) Constitutive emission of GL and TMTT from leaves of the two *GES*-expressing lines analyzed by GC–MS. Both volatiles were not emitted from line *salk_039864*. (**c**) Phenotype of the *GES*-expressing plant lines. Three-week-old transgenic plants grown under long day conditions show reduced growth in comparison to wild-type and *GES* knockout plants (*upper row*). *GES* expression lines form lesions on cotyledons as indicated by arrows (*lower row*)

ethanol or from ethanol-treated wild-type plants (Herde et al. 2008). Induced GL and TMTT formation correlated with the accumulation of the *TPS04* transcript.

In addition, transgenic lines were generated that constitutively expressed *TPS04* under the control of the *Cauliflower Mosaic Virus* (*CaMV*) *35S* promoter (Pro_{35S}). These plants constitutively produced GL and TMTT (Fig. 13.5a, b). The emission of both compounds was accompanied by growth retardation and the formation of lesions on cotyledons at the seedling stage (Fig. 13.5c). The lesion phenotype might be elicited by GL and/or TMTT acting as signals that induce defense-type responses. However, this phenotype vanishes when the plant matures. Reduced growth of mature plants may be caused by toxic or inhibitory effects of both compounds.

Quantitative analysis of volatiles from detached leaves of Pro_{35S}:*GES* plants revealed that TMTT is emitted at levels comparable to those of wild-type plants after alamethicin treatment, whereas emission rates of GL were similar to those of wild-type plants induced with coronalon or by *P. xylostella* (Herde et al. 2008). The formation of TMTT in both ethanol-inducible and constitutive transgenic lines indicated the presence of converting enzymes responsible for oxidative degradation of GL and suggested these activities to be constitutively expressed or induced upon accumulation of GL. The overall ratio of TMTT to GL in the transgenic lines ranged from 1 to 1.5, which was lower than that observed in wild-type plants treated with alamethicin, the jasmonate mimic coronalon, or *P. xylostella*, indicating less efficient oxidative degradation of GL in the transgenic lines.

13.6 Subcellular Localization and Tissue-Specific Regulation of GES

The formation of diterpenes is believed to occur predominantly in plastids, based on previous characterizations of diterpene synthases containing plastidial transit peptide sequences (Davis and Croteau 2000). Interestingly, no obvious plastidial transit peptide could be identified for the GES by using different algorithms such as TargetP and ChloroP. To further determine the compartment of GES activity, *GES* knockout plants were transformed with a GES–yellow fluorescent protein (YFP) fusion under the control of the *CaMV 35S* promoter. Although the transgenic lines emitted GL indicating a functionally active expressed GES protein, no YFP was observed in plastids. Instead, YFP appeared to reside in the cytosol or the endoplasmic reticulum suggesting GES localization in these compartments (Fig. 13.6a). It is likely that a pool of the substrate all-*trans*-GGPP for conversion into GL is present in the cytosol or ER since two *Arabidopsis* GGPP synthases were identified with a localization pattern similar to that observed for GES (Okada et al. 2000). Hence, constitutive expression of GES may interfere with GGPP pools in the cytosol but does not seem to significantly deplete GGPP pools for the biosynthesis of carotenoids and chlorophyll in plastids. This notion is supported by the occurrence of lesions instead of a bleaching phenotype in transgenic seedlings.

To assess the tissue-specific regulation of GES, we determined the activity of the *GES* promoter by generating stably transformed *Arabidopsis* plants carrying a 1.6-kb *GES* promoter fragment fused to the β-*glucuronidase* (*GUS*) reporter gene. GUS activity was detected in developing and mature flowers, specifically in the stigma, anthers, filaments, and sepals, but not in petals (Fig. 13.6c). GUS activity also occurred in the abscission zone of floral organs. Despite an active *GES* promoter and the presence of *GES* mRNA in flowers (Zimmermann et al. 2004), only small amounts of TMTT have been observed in this organ (Tholl et al. 2005). Possible reasons for reduced formation of TMTT in flowers could be low GL-converting enzyme activity or reduced GGPP substrate availability. The expression pattern of *GES* in the flower resembles those of the recently characterized *Arabidopsis* floral terpene synthases. However, in contrast to *GES*, these genes are expressed exclusively in flowers (Tholl et al. 2005) and not induced in leaves by treatment with alamethicin.

In leaves, GUS activity was detected at wound sites (Fig. 13.6c). This finding is in contrast to the absence of *GES* mRNA and TMTT emission in leaves 30 h after mechanical wounding (Herde et al. 2008). However, it could be demonstrated by real-time PCR analysis that *GES* mRNA accumulates only transiently around the wound zone in the first 2 h after leaf damage. This transient mRNA level causes accumulation of the stable GUS protein but is not sufficient to provide enough GES enzyme for detectable formation of TMTT (Herde et al. 2008).

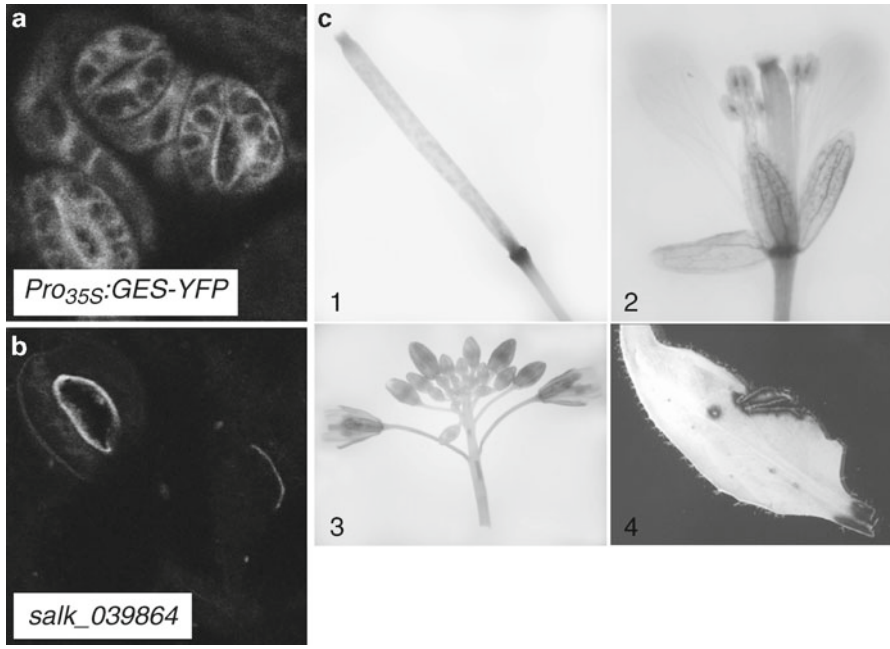

Fig. 13.6 *Arabidopsis* GES is expressed in specific tissues and not located in plastids. (**a**) Subcellular localization of GES fused to YFP by fluorescence microscopy of leaf epidermal cells. For transformation, a 6-kb genomic *GES* fragment starting with the presumed transcriptional start site was used. Fusion with YFP was established at the C-terminus of GES. Bright areas indicate the presence of YFP. GES–YFP is not located in plastids. (**b**) Fluorescence background analysis in leaves of the *GES* knockout line *salk_039864*. (**c**) *GES-promoter*-GUS activity in a silique (*1*), a flower (*2*), an inflorescence (*3*), and a mechanically wounded leaf (*4*) from Pro_{GES}:*GUS* plants. Dark zones indicate formation of the GUS enzymatic product

13.7 Hormonal Regulation of *GES* and TMTT Synthesis

The composition of induced volatile blends usually depends on the signaling network elicited by the specific type of biotic stressor. To determine which major stress-related signaling pathways contribute to *GES* transcription and TMTT synthesis, different *Arabidopsis* signaling mutants were treated with alamethicin (Fig. 13.7a). No induced *GES* expression was observed in the jasmonate biosynthesis mutant *dde2-2*, which is defective in the biosynthesis of the major octadecanoid phytohormones 12-oxo-phytodienoic acid (OPDA) and JA (Park et al. 2002) as well as in the *acx1/5* double mutant, which does not convert OPDA into JA (Schilmiller et al. 2007). A similar response was found in the *coi1* mutant indicating that the F-box protein COI1, which is a central regulator of most JA-mediated responses (Xie et al. 1998; Devoto et al. 2005), is required for *GES* transcription. Many JA-dependent responses are modulated by other phytohormones like SA and ethylene. However, alamethicin-induced transcription of *GES* was neither affected in the ethylene-insensitive mutant *ein2* (Guzman and Ecker 1990) nor in the SA-degrading *nahG* (Gaffney et al. 1993) and SA synthesis-deficient *sid2* plants (Nawrath and Metraux 1999; Wildermuth et al. 2001). In addition, the *npr1* mutant, compromised in a major branch of the SA signal transduction network (Cao et al. 1994), also did not show an altered response with regard to *GES* induction.

Volatile collections from alamethicin-treated signaling mutants demonstrated that the emission of all volatiles including TMTT and GL was absent in the *coi1* mutant and is, therefore, dependent on

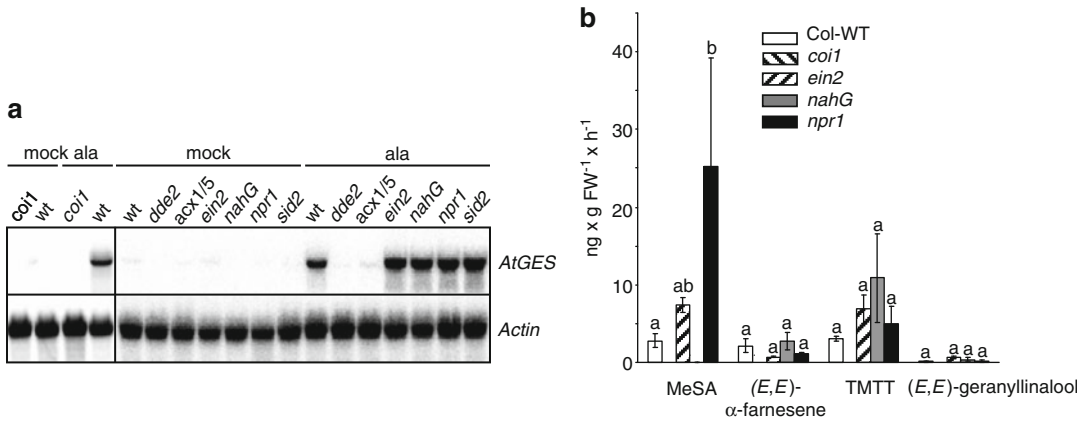

Fig. 13.7 Transcription of *GES* is dependent on the octadecanoid pathway and is not affected by salicylic acid and ethylene (Reproduced from Herde et al. (2008), Copyright American Society of Plant Biologists, www.plantcell.org). (**a**) Northern blot analysis of *GES* transcript levels in alamethicin-treated leaves of wild-type plants and mutants deficient in SA, JA and ethylene synthesis or signal transduction. Alamethicin was applied 24 h prior to the extraction of RNA. A 0.1% ethanol solution was used as a control. (**b**) Volatile analysis of alamethicin-treated wild-type and mutant lines. Volatiles were collected with the closed-loop stripping procedure during 21–30 h of alamethicin treatment. The results represent the means ± SE of three replicates. Letters above each bar indicate significant differences for each set of volatiles after Tukey test ($p < 0.05$). MeSA was absent in the SA-converting *nahG* plants. In contrast, approximately tenfold higher emission of MeSA was observed in the *npr1* mutant in comparison to wild type, since *npr1* lacks the autoregulatory negative feedback loop for SA synthesis (Cao et al. 1994)

COI1 (Fig. 13.7b). Both the SA- and ethylene-deficient/insensitive mutants showed consistent results at the *GES* transcript level with no significant differences in the amount of emitted GL and TMTT in comparison to wild-type plants (Fig. 13.7b).

Our finding that SA and ethylene do not modify *GES* expression and TMTT emission is in contrast to the interplay of signals controlling the volatile emission of other plants. For example, in lima bean, SA interferes with JA biosynthesis by blocking the conversion of OPDA to JA. Depending on the internal SA levels, differences in the concentration of the phytohormones OPDA and JA affect the volatile blend emitted from lima bean leaves (Koch et al. 1999). In *Arabidopsis*, JA-dependent genes such as *PDF1.2* are subject to antagonistic effects by SA (Spoel et al. 2003) or synergistic interaction with ethylene (Penninckx et al. 1998). However, expression of *GES* does not seem to follow these regulatory patterns. In summary, transcription of *GES* and the formation of GL and TMTT are primarily regulated by the octadecanoid pathway and are independent of SA and ethylene. Consistent with this finding, *GES* transcription and emission of GL and TMTT were induced by coronalon, which mimics the jasmonic acid–isoleucine conjugate that has been shown to interact with COI1 (Thines et al. 2007). Therefore, JA–Ile, or a structurally related conjugate, may represent the signal that induces *GL synthase* transcription.

13.8 Conclusion and Outlook

Homoterpenes represent one of the most common classes of volatiles emitted from plants. Their release from flowers and their function in attracting natural enemies of herbivores emphasize their importance in the evolution of volatile communication between plants and other organisms. We have identified the enzyme that catalyzes the first committed step in the biosynthesis of the C_{16}-homoterpene TMTT in *Arabidopsis*. Because of the widespread occurrence of TMTT, it is expected that genes encoding GESs are present in many other plant species. Recently, a wound-inducible bifunctional terpene synthase, MtTPS3, was characterized in *Medicago truncatula*, which converts

FPP and GGPP into nerolidol and geranyllinalool, respectively (Arimura et al. 2008). However, the MtTPS3 protein (Gomez et al. 2005) shows closer homology to monoterpene synthases of the TPS-b subfamily (Aubourg et al. 2002) such as the *Arabidopsis* linalool synthase than to *Clarkia* LISs and *Arabidopsis* GES. These sequence differences indicate that GESs, as with many other terpene synthases, can evolve independently as a product of convergent gene evolution. This notion is further supported by the characterization of a GES activity in tomato (Ament et al. 2006) and the apparent absence of an *Arabidopsis*-type *GES* gene in the tomato genome.

The identification of a GES in *Arabidopsis* and the available *GES* expression and mutant lines have supported recent research on revealing the cytochrome P450 monooxygenase, CYP82G1, which is induced by insect feeding and responsible for the terminal step in TMTT formation (Lee et al. 2010). CYP82G1 also converts (*E*)-nerolidol to the C_{11}-homoterpene DMNT in vitro; however, DMNT is generally not detected or found only in small amounts in wild-type *Arabidopsis* leaves because of the absence or low activity of a (*E*)-nerolidol synthase in this tissue. *Arabidopsis* plants that ectopically express a nerolidol synthase from strawberry targeted to the mitochondria produce DMNT (Kappers et al. 2005) presumably by transport of nerolidol into the cytosol and degradation by CYP82G1 at the endoplasmic reticulum. Together, these studies have elucidated the entire homoterpene biosynthetic pathway in *Arabidopsis* aerial tissues and will help in identifying regulatory factors in homoterpene formation and addressing the contribution of homoterpenes in ecological interactions.

Acknowledgments We thank Bettina Raguschke, Katrin Heisse, Anna Hermann, Annette Gunkel, and Roland Scholz for technical assistance. We are grateful to Shuangchun (Jemery) Yan and Dr. Boris Vinatzer for support with the molecular phylogenetic analysis. The work was supported by the Max Planck Society (D.T.; J.G.; W.B.) and by grants from the Alfried Krupp von Bohlen und Halbach Foundation (M.H.) and the Deutsche Forschungsgemeinschaft (GA330-16; K.G.).

References

Aharoni A, Giri AP, Deuerlein S, Griepink F et al (2003) Terpenoid metabolism in wild-type and transgenic *Arabidopsis* plants. Plant Cell 15:2866–2884

Aharoni A, Giri AP, Verstappen FWA et al (2004) Gain and loss of fruit flavor compounds produced by wild and cultivated strawberry species. Plant Cell 16:3110–3131

Ament K, Van Schie CC, Bouwmeester HJ, Haring MA, Schuurink RC (2006) Induction of a leaf specific geranylgeranyl pyrophosphate synthase and emission of (*E*, *E*)-4,8,12-trimethyltrideca-1,3,7,11-tetraene in tomato are dependent on both jasmonic acid and salicylic acid signaling pathways. Planta 224:1197–1208

Arimura G, Ozawa R, Shimoda T, Nishioka T, Boland W, Takabyashi J (2000) Herbivory-induced volatiles elicit defence genes in lima bean leaves. Nature 406:512–515

Arimura GI, Garms S, Maffei M, Bossi S et al (2008) Herbivore-induced terpenoid emission in *Medicago truncatula*: concerted action of jasmonate, ethylene and calcium signaling. Planta 227:453–464

Aubourg S, Lecharny A, Bohlmann J (2002) Genomic analysis of the terpenoid synthase (*AtTPS*) gene family of *Arabidopsis thaliana*. Mol Genet Genomics 267:730–745

Bohlmann J, Meyer-Gauen G, Croteau R (1998) Plant terpenoid synthases: molecular biology and phylogenetic analysis. Proc Natl Acad Sci USA 95:4126–4133

Bohlmann J, Martin D, Oldham NJ, Gershenzon J (2000) Terpenoid secondary metabolism in *Arabidopsis thaliana*: cDNA cloning, characterization, and functional expression of a myrcene/(*E*)-β-ocimene synthase. Arch Biochem Biophys 375:261–269

Boland W, Gabler A (1989) Biosynthesis of homoterpenes in higher plants. Helv Chim Acta 72:247–253

Boland W, Gabler A, Gilbert M, Feng ZF (1998) Biosynthesis of C-11 and C-16 homoterpenes in higher plants - stereochemistry of the C-C-bond cleavage reaction. Tetrahedron 54:14725–14736

Bouwmeester HJ, Verstappen FWA, Posthumus MA, Dicke M (1999) Spider mite-induced (3*S*)-(*E*)-nerolidol synthase activity in cucumber and lima bean. The first dedicated step in acyclic C11-homoterpene biosynthesis. Plant Physiol 121:173–180

Cao H, Bowling SA, Gordon AS, Dong XN (1994) Characterization of an *Arabidopsis* mutant that is nonresponsive to inducers of systemic acquired-resistance. Plant Cell 6:1583–1592

Chen F, Tholl D, D'Auria JC, Farooq A, Pichersky E, Gershenzon J (2003) Biosynthesis and emission of terpenoid volatiles from *Arabidopsis* flowers. Plant Cell 15:481–494

Chen F, Ro DK, Petri J, Gershenzon J, Bohlmann J, Pichersky E, Tholl D (2004) Characterization of a root-specific *Arabidopsis* terpene synthase responsible for the formation of the volatile monoterpene 1,8-cineole. Plant Physiol 135:1956–1966

Cseke L, Dudareva N, Pichersky E (1998) Structure and evolution of linalool synthase. Mol Biol Evol 15:1491–1498

Davis EM, Croteau R (2000) Cyclization enzymes in the biosynthesis of monoterpenes, sesquiterpenes, and diterpenes. In: Leeper FJ, Vederas JC (eds) Topics in current chemistry: biosynthesis-aromatic polyketides, isoprenoids, alkaloids. Springer, Heidelberg, pp 53–95

de Boer JG, Posthumus MA, Dicke M (2004) Identification of volatiles that are used in discrimination between plants infested with prey or nonprey herbivores by a predatory mite. J Chem Ecol 30:2215–2230

Degenhardt J, Gershenzon J (2000) Demonstration and characterization of (*E*)-nerolidol synthase from maize: a herbivore-inducible terpene synthase participating in (3*E*)-4,8-dimethyl-1,3,7-nonatriene biosynthesis. Planta 210:815–822

Devoto A, Ellis C, Magusin A, Chang HS, Chilcott C, Zhu T, Turner JG (2005) Expression profiling reveals *COI1* to be a key regulator of genes involved in wound- and methyl jasmonate-induced secondary metabolism, defence, and hormone interactions. Plant Mol Biol 58:497–513

Dicke M (1994) Local and systemic production of volatile herbivore-induced terpenoids: their role in plant-carnivore mutualism. J Plant Physiol 143:465–472

Donath J, Boland W (1994) Biosynthesis of acyclic homoterpenes in higher plants parallels steroid hormone metabolism. J Plant Physiol 143:473–478

Dudareva N, Cseke L, Blanc VM, Pichersky E (1996) Evolution of floral scent in *Clarkia*: novel patterns of S-linalool synthase gene expression in the *C. breweri* flower. Plant Cell 8:1137–1148

Engelberth J, Koch T, Schuler G, Bachmann N, Rechtenbach J, Boland W (2001) Ion channel-forming alamethicin is a potent elicitor of volatile biosynthesis and tendril coiling. Cross talk between jasmonate and salicylate signaling in lima bean. Plant Physiol 125:369–377

Fäldt J, Arimura G, Gershenzon J, Takabayashi J, Bohlmann J (2003) Functional identification of AtTPS03 as (*E*)-β-ocimene synthase: a monoterpene synthase catalyzing jasmonate- and wound-induced volatile formation in *Arabidopsis thaliana*. Planta 216:745–751

Gabler A, Boland W, Preiss U, Simon H (1991) Stereochemical studies on homoterpene biosynthesis in higher plants – mechanistic, phylogenetic, and ecological aspects. Helv Chim Acta 74:1773–1789

Gaffney T, Friedrich L, Vernooij B, Negrotto D, Nye G, Uknes S, Ward E, Kessmann H, Ryals J (1993) Requirement of salicylic-acid for the induction of systemic acquired-resistance. Science 261:754–756

Gomez SK, Cox MM, Bede JC, Inoue K, Alborn HT, Tumlinson JH, Korth KL (2005) Lepidopteran herbivory and oral factors induce transcripts encoding novel terpene synthases in *Medicago truncatula*. Arch Insect Biochem Physiol 58:114–127

Guzman P, Ecker JR (1990) Exploiting the triple response of *Arabidopsis* to identify ethylene-related mutants. Plant Cell 2:513–523

Herde M, Gärtner K, Köllner TG, Fode B, Boland W, Gershenzon J, Gatz C, Tholl D (2008) Identification and regulation of TPS04/GES, an *Arabidopsis* geranyllinalool synthase catalyzing the first step in the formation of the insect-induced volatile C-16-homoterpene TMTT. Plant Cell 20:1152–1168

Hopke J, Donath J, Blechert S, Boland W (1994) Herbivore-induced volatiles – the emission of acyclic homoterpenes from leaves of *Phaseolus lunatus* and *Zea mays* can be triggered by a β-glucosidase and jasmonic acid. FEBS Lett 352:146–150

Huang M, Abel C, Sohrabi R, Petri J, Haupt I, Cosimano J, Gershenzon J, Tholl D (2010) Variation of herbivore-induced volatile terpenes among *Arabidopsis* ecotypes depends on allelic differences and subcellular targeting of two terpene synthases, TPS02 and TPS03. Plant Physiol 153:1293–1310

Kant MR, Ament K, Sabelis MW, Haring MA, Schuurink RC (2004) Differential timing of spider mite-induced direct and indirect defenses in tomato plants. Plant Physiol 135:483–495

Kappers IF, Aharoni A, van Herpen TWJM, Luckerhoff LLP, Dicke M, Bouwmeester HJ (2005) Genetic engineering of terpenoid metabolism attracts bodyguards to *Arabidopsis*. Science 309:2070–2072

Koch T, Krumm T, Jung V, Engelberth J, Boland W (1999) Differential induction of plant volatile biosynthesis in the lima bean by early and late intermediates of the octadecanoid-signaling pathway. Plant Physiol 121:153–162

Lee S, Badieyan S, Bevan DR, Herde M, Gatz C, Tholl D (2010) Herbivore-induced and floral homoterpene volatiles are biosynthesized by a single P450 enzyme (CYP82G1) in *Arabidopsis*. Proc Natl Acad Sci USA 107:21205–21210

Martin DM, Fäldt J, Bohlmann J (2004) Functional characterization of nine Norway spruce *TPS* genes and evolution of gymnosperm terpene synthases of the TPS-d subfamily. Plant Physiol 135:1908–1927

Nawrath C, Metraux JP (1999) Salicylic acid induction-deficient mutants of *Arabidopsis* express PR-2 and PR-5 and accumulate high levels of camalexin after pathogen inoculation. Plant Cell 11:1393–1404

Okada K, Saito T, Nakagawa T, Kawamukai M, Kamiya Y (2000) Five geranylgeranyl diphosphate synthases expressed in different organs are localized into three subcellular compartments in *Arabidopsis*. Plant Physiol 122:1045–1056

Park JH, Halitschke R, Kim HB, Baldwin IT, Feldmann KA, Feyereisen R (2002) A knock-out mutation in allene oxide synthase results in male sterility and defective wound signal transduction in *Arabidopsis* due to a block in jasmonic acid biosynthesis. Plant J 31:1–12

Penninckx IAMA, Thomma BPHJ, Buchala A, Metraux JP, Broekaert WF (1998) Concomitant activation of jasmonate and ethylene response pathways is required for induction of a plant defensin gene in *Arabidopsis*. Plant Cell 10:2103–2113

Pichersky E, Raguso RA, Lewinsohn E, Croteau R (1994) Floral scent production in *Clarkia* (Onagraceae).1.

Localization and developmental modulation of monoterpene emission and linalool synthase activity. Plant Physiol 106:1533–1540

Pichersky E, Lewinsohn E, Croteau R (1995) Purification and characterization of *S*-linalool synthase, an enzyme involved in the production of floral scent in *Clarkia breweri*. Arch Biochem Biophys 316:803–807

Ro DK, Ehlting J, Keeling CI, Lin R, Mattheus N, Bohlmann J (2006) Microarray expression profiling and functional characterization of *AtTPS* genes: duplicated *Arabidopsis thaliana* sesquiterpene synthase genes At4g13280 and At4g13300 encode root-specific and wound-inducible (*Z*)-γ-bisabolene synthases. Arch Biochem Biophys 448:104–116

Schilmiller AL, Koo AJK, Howe GA (2007) Functional diversification of acyl-coenzyme A oxidases in jasmonic acid biosynthesis and action. Plant Physiol 143:812–824

Schnee C, Köllner TG, Gershenzon J, Degenhardt J (2002) The maize gene terpene synthase 1 encodes a sesquiterpene synthase catalyzing the formation of (*E*)-β-farnesene, (*E*)-nerolidol, and (*E*,*E*)-farnesol after herbivore damage. Plant Physiol 130:2049–2060

Spoel SH, Koornneef A, Claessens SMC et al (2003) NPR1 modulates cross-talk between salicylate- and jasmonate-dependent defense pathways through a novel function in the cytosol. Plant Cell 15:760–770

Sun TP, Kamiya Y (1994) The *Arabidopsis* GA1 locus encodes the cyclase *ent*-kaurene synthetase a of gibberellin biosynthesis. Plant Cell 6:1509–1518

Thines B, Katsir L, Melotto M, Niu Y et al (2007) JAZ repressor proteins are targets of the SCFCO11 complex during jasmonate signalling. Nature 448:661–665

Tholl D (2006) Terpene synthases and the regulation, diversity and biological roles of terpene metabolism. Curr Opin Plant Biol 9:297–304

Tholl D, Chen F, Petri J, Gershenzon J, Pichersky E (2005) Two sesquiterpene synthases are responsible for the complex mixture of sesquiterpenes emitted from *Arabidopsis* flowers. Plant J 42:757–771

Trapp SC, Croteau RB (2001) Genomic organization of plant terpene synthases and molecular evolutionary implications. Genetics 158:811–832

van Loon JJA, de Boer JG, Dicke M (2000) Parasitoid-plant mutualism: parasitoid attack of herbivore increases plant reproduction. Entomol Exp Appl 97:219–227

Van Poecke RMP, Posthumus MA, Dicke M (2001) Herbivore-induced volatile production by *Arabidopsis thaliana* leads to attraction of the parasitoid *Cotesia rubecula*: Chemical, behavioral, and gene-expression analysis. J Chem Ecol 27:1911–1928

Wildermuth MC, Dewdney J, Wu G, Ausubel FM (2001) Isochorismate synthase is required to synthesize salicylic acid for plant defence. Nature 414:562–565

Xie DX, Feys BF, James S, Nieto-Rostro M, Turner JG (1998) COI1: an *Arabidopsis* gene required for jasmonate-regulated defense and fertility. Science 280: 1091–1094

Yamaguchi S, Sun TP, Kawaide H, Kamiya Y (1998) The GA2 locus of *Arabidopsis thaliana* encodes ent-kaurene synthase of gibberellin biosynthesis. Plant Physiol 116:1271–1278

Zimmermann P, Hirsch-Hoffmann M, Hennig L, Gruissem W (2004) GENEVESTIGATOR. *Arabidopsis* microarray database and analysis toolbox. Plant Physiol 136:2621–2632

Strigolactones: A Cry for Help Results in Fatal Attraction. Is Escape Possible?

14

Carolien Ruyter-Spira, Juan Antonio López-Ráez, Catarina Cardoso, Tatsiana Charnikhova, Radoslava Matusova, Wouter Kohlen, Muhammad Jamil, Ralph Bours, Francel Verstappen, and Harro Bouwmeester

Abstract

During evolution, plants have adapted an ecological balance with their associates, competitors, predators, and pests. Keeping this balance intact is an active process during which the plant needs to respond to many different stimuli in order to survive.

For example, plants have developed an array of physiological and biochemical responses to phosphate deprivation. One of these responses is the production of isoprenoid-derived molecules called strigolactones. Strigolactones are used to stimulate the formation of symbiotic associations

C. Ruyter-Spira (✉) • T. Charnikhova • W. Kohlen • M. Jamil • R. Bours • F. Verstappen • H. Bouwmeester
Laboratory for Plant Physiology, Arboretumlaan 4, Wageningen, BD 6703, The Netherlands
e-mail: carolien.ruyter@wur.nl

J.A. López-Ráez
Laboratory for Plant Physiology, Arboretumlaan 4, Wageningen, BD 6703, The Netherlands

Soil Microbiology and Symbiotic Systems, Estacion Experimental del Zaidin (CSIC), Granada, Spain

C. Cardoso
Laboratory for Plant Physiology, Arboretumlaan 4, Wageningen, BD 6703, The Netherlands

Cropdesign - BASF Plant Sciences, Zwijnaarde, Belgium

R. Matusova
Laboratory for Plant Physiology, Arboretumlaan 4, Wageningen, BD 6703, The Netherlands

Institute of Plant Genetics and Biotechnology, Slovak Academy of Sciences, Nitra, Slovakia

T.J. Bach and M. Rohmer (eds.), *Isoprenoid Synthesis in Plants and Microorganisms: New Concepts and Experimental Approaches*, DOI 10.1007/978-1-4614-4063-5_14,

of plant roots with arbuscular mycorrhizal (AM) fungi. AM fungi colonize the root cortex to obtain carbon from their host while assisting the plant in phosphate acquisition. However, strigolactones also stimulate the germination of root parasitic plant seeds. Only upon perception of the presence of a host through its strigolactone production, seeds of the parasites germinate and attach to the roots of many plant species. In contrast to a mutual symbiotic relationship, where both partners benefit from the affiliation through an exchange of resources, the host is heavily exploited by a parasitic plant and suffers strongly from the interaction because it is robbed from its assimilates, water, and nutrients.

In this chapter, we focus on the knowledge about the biosynthetic origin of the strigolactones, their ecological significance, and physiological and biochemical regulation. We finally point at recent scientific developments which may explain why a nonmycorrhized plant like Arabidopsis is still producing strigolactones.

Keywords

Strigolactones • Germination stimulants • Parasitic plants • Arbuscular mycorrhiza • Phosphate starvation • Hormones • Shoot branching

14.1 Introduction

Plants produce a large variety of chemicals for which no role has yet been found in growth, photosynthesis, reproduction, or other "primary" functions. These chemicals are generally called secondary metabolites. It has been estimated that 15–25% of plant genes are dedicated to plant secondary metabolism (Pichersky and Gang 2000). The chemical structures of secondary metabolites are extremely diverse; many thousands have been identified and can be subdivided in several major classes. One of those classes is represented by the terpenoids, an abundant and structurally diverse group consisting of more than 40,000 different chemical structures. They are of great importance to plants because of their multitude of functions in signaling and defense, and they enable plants to communicate with their environment.

Terpenoid secondary metabolites occur across a wide range of plant tissue types and are often emitted at particular times or under specific conditions related to their function. In the rhizosphere, plants secrete terpenoid-derived molecules, the so-called strigolactones, from their roots to establish a symbiotic relationship with the arbuscular mycorrhizal fungi such as *Gigaspora* and *Glomus* spp. However, unfortunately for the host plant, these molecules are also recognized by the seeds of root parasitic plants. In this case, strigolactone perception triggers germination of the parasitic plant seeds hereby ensuring the close vicinity of a host plant which is a prerequisite for survival of the parasitic plant seedlings.

14.2 Parasitic Plants

Root parasitic plants such as *Orobanche* and *Striga* spp. derive all or most of their sustenance from the host plant. They are geographically widespread, occupying all major ecosystems on the planet (Press and Graves 1995). In some species of parasitic plants, the ability to obtain sugars from a host is believed to have led to decreased selection pressure on retaining a functional photosynthetic apparatus. This is reflected in reduced ability to photosynthesize, alterations to

the structure of the plastid genome (Revill et al. 2005), or even complete disappearance of chlorophyll, for example, in the *Orobanchaceae*. Although the evolution of parasitism seems to require complex metabolic, developmental, and anatomical adaptations, parasitism has evolved independently at least ten times within the angiosperms and is found in approximately 4,000 plant species among 22 families (Nickrent et al. 1998).

Some parasitic plants, particularly those in the Scrophulariaceae, are economically important weeds, causing dramatic losses in crop yield (Stewart and Press 1990; Parker and Riches 1993). The hemiparasitic *Striga* spp. infects important crops such as maize, sorghum, pearl millet, finger millet, and upland rice, causing devastating losses in cereal yields in sub-Saharan Africa and, therefore, obstructing food supply in many developing countries (Joel 2000; Scholes and Press 2008). Several of the holoparasitic *Orobanche* spp. are the most damaging parasitic weeds in Mediterranean areas and Central Asia, parasitizing important agricultural crops such as legumes, crucifers, tomato, sunflower, hemp, and tobacco (Joel 2000; Press et al. 2001; Shen et al. 2006; Yoneyama et al. 2010).

All parasitic plants penetrate the tissue of their host, subsequently develop feeding structures known as haustoria that allow rapid removal of solutes (Hibberd and Jeschke 2001; Seel and Jeschke 1999). However, species differ in the type and amount of solutes that they remove. Some, such as *Striga,* feed on the host xylem (Dörr 1996), while others, for example, members of *Cuscuta* and *Orobanche*, are highly specialized phloem feeders (Jeschke et al. 1994; Hibberd et al. 1999). Upon vascular connection, the parasitic plants continue to develop, emerge from the soil, flower, and finally set seed. The seeds of the parasitic plants are tiny and contain few nutrient reserves. After germination, they must attach to a host root within days or they will die. To prevent the seeds from germinating too far from the host, these parasites have evolved a mechanism by which parasitic plant seeds only germinate upon perception of a specific germination stimulatory signal produced by the root of the host plant.

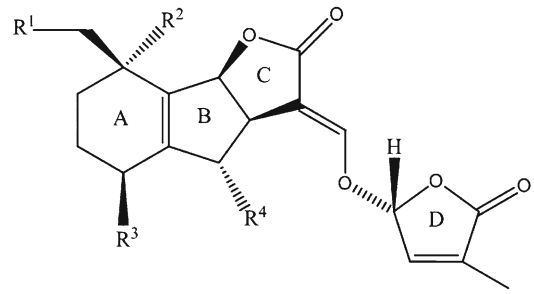

$R^1 = R^3 = R^4 = H$, $R^2 = CH_3$: 5-Deoxystrigol;
$R^1 = R^4 = H$, $R^2 = CH_3$, $R^3 = OH$: Strigol;
$R^1 = R^3 = H$, $R^2 = CH_3$, $R^4 = OH$: Orobanchol;
$R^1 = R^3 = H$, $R^2 = CH_3$, $R^4 = OAc$: Orobanchyl acetate;
$R^1 = R^2 = R^3 = R^4 = H$: Sorgolactone;
$R^3 = R^4 = H$, $R^2 = CH_3$, $R^1 = OH$: Sorgomol;

Fig. 14.1 Common structure of strigolactones. The strigolactone backbone is decorated with various side groups (R) that are characteristic for the different strigolactones

14.3 Strigolactones Are Germination Stimulants for Parasitic Plants

Germination stimulants are secreted by the roots of the host plant in very low amounts. Several different strigolactones have been detected in the root exudates of a wide range of plant species, including mono- and dicotyledonous plants. Even different cultivars of one crop species may produce different strigolactones and/or mixtures (Bouwmeester et al. 2007; Yoneyama et al. 2008). It has been proposed that 5-deoxystrigol, which does not have any hydroxyl substituent, could be the precursor of all the different strigolactones (Rani et al. 2008; Matusova et al. 2005).

The structural core of the strigolactone molecules consists of a tricyclic lactone (ABC part) which connects via an enol ether bridge to a butyrolactone group (the D-ring) (Fig. 14.1). All known strigolactones have one or two methyl substituents on the cyclohexyl A-ring and various combinations of hydroxyl or acetate substituents around the A- and B-rings. The C- and D-rings remain constant, except for the enol ether bridge for which also an *epi* orientation has been reported. It has been suggested that the biological

activity of the strigolactones resides in this enol ether bridge (Magnus and Zwanenburg 1992). According to the putative modifications that could take place in the A- and B-rings, over a hundred strigolactone derivatives can be predicted to exist in the plant kingdom (Rani et al. 2008; Matusova et al. 2005; Yoneyama et al. 2010; Xie et al. 2010).

An interesting question is whether these small changes have an effect on putative receptor binding in the parasitic plant seeds and hence on host-parasite specificity. The recognition of the germination stimulant is a crucial moment in the life cycle of the parasitic plants. Here, a strong selection pressure is present that should ensure that the seeds of the parasites only germinate in the presence of a true host and enabling them to complete their life cycle. Germination experiments with seed batches collected from *S. hermonthica* and *O. ramosa* plants parasitizing several different host species show that the parasites develop a preference for the exudate of the host species they were growing on (Matusova and Bouwmeester 2006).

14.4 Biosynthetic Origin of Strigolactones

The strigolactones were originally identified to be sesquiterpene lactones (Butler 1995; Yokota et al. 1998), but there is also some structural similarity to higher-order terpenoids/isoprenoids such as abscisic acid and other compounds, which are derived from the carotenoid pathway (Parry and Horgan 1992; Tan et al. 1997; Bouwmeester et al. 2003; Matusova et al. 2005; Matusova and Bouwmeester 2006).

To verify the biosynthetic origin of the strigolactones, Matusova et al. (2005) studied the effect of chemicals that affect several different isoprenoid biosynthetic pathways on the production of germination stimulants by the roots of host plants. In parallel to this biochemical approach, several mutants in the predicted biosynthetic pathways were examined for germination stimulant production. The isoprenoid-pathway inhibitors mevastatin (inhibitor of the cytosolic MVA pathway) and fosmidomycin (inhibitor of the plastidic MEP pathway) only had a minor effect on germination stimulant formation, possibly because of the exchange of IPP that has been shown to occur between the two pathways, particularly upon the use of these inhibitors (Hemmerlin et al. 2003). However, the carotenoid pathway inhibitor fluridone reduced maize root-exudate-induced germination by about 80% compared with untreated seedlings, suggesting that the germination stimulants produced by maize are derived from the carotenoid pathway (Matusova et al. 2005). Subsequently, the root exudates of several maize carotenoid mutants *y10, al1, al1y3, vp5,* and *y9* (Fig. 14.2)

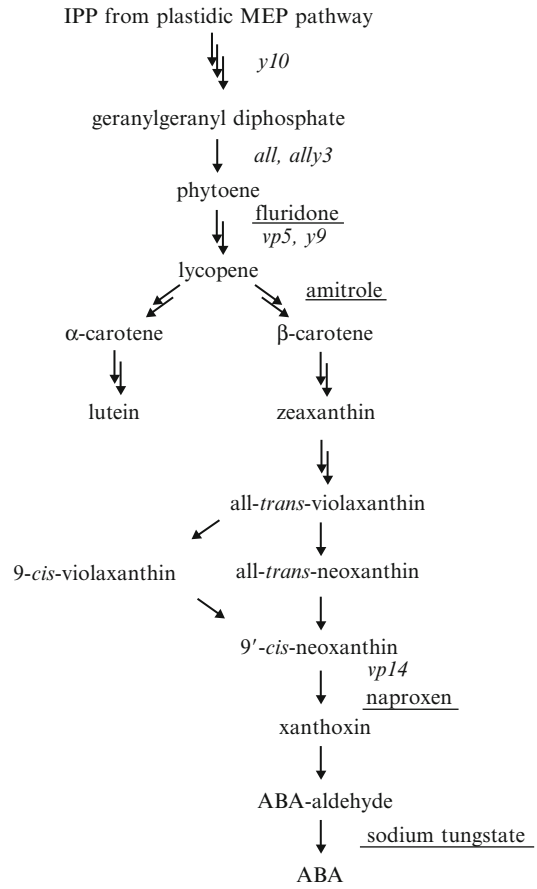

Fig. 14.2 Schematic representation of the carotenoid and abscisic acid biosynthetic pathway. Carotenoids maize mutants (*italics*) and inhibitors (*underlined*) at different steps in the pathway are indicated (From Matusova and Bouwmeester 2006)

were tested for induction of *S. hermonthica* seed germination. The carotenoid biosynthesis inhibitor fluridone blocks the activity of phytoene desaturase, which corresponds to the maize *vp5* locus (Li et al. 1996; Hable et al. 1998). Both fluridone-treated maize and *vp5* mutant root exudates induced significantly lower germination of *S. hermonthica.* In addition to this, also treatment with the herbicide amitrole that blocks lycopene cyclase in maize seedlings (Dalla Vecchia et al. 2001) resulted in lower germination of *S. hermonthica* seeds than induced by control seedlings. The results in germination bioassays with root exudates of amitrole-treated plants suggest that the germination stimulants are derived from the carotenoid pathway below lycopene (Fig. 14.2) (Matusova et al. 2005). Also, the seedlings of all other mutants that were tested induced lower germination of *S. hermonthica* seeds in comparison to their corresponding wild-type siblings (Matusova et al. 2005). The branching point from the carotenoid pathway for strigolactone biosynthesis could not be identified.

Matusova et al. (2005) postulated a hypothetical biosynthetic pathway leading to the formation of all known strigolactones suggesting that they are produced by oxidative cleavage of a carotenoid substrate through the action of a 9-*cis* epoxycarotenoid dioxygenase (NCED) or carotenoid cleavage dioxygenase enzyme (CCD) (Fig. 14.3). The NCED/CCD family is composed of nine different members in Arabidopsis and 12 in rice, and they can be grouped into six different clusters (Bouwmeester et al. 2007). NCEDs are involved in the production of the plant hormone abscisic acid (ABA), which is derived from *cis*-neoxanthin (Taylor et al. 2005). Matusova et al. (2005) and López-Ráez et al. (2008) have shown that the ABA-deficient mutants *viviparous14* (*vp14*) in maize and *notabilis* in tomato, with a null mutation in the genes *ZmNCED* and *LeNCED1,* respectively, induce less germination of parasitic plant seeds of *S. hermonthica* and *O. ramosa*, respectively. Moreover, for tomato it was demonstrated using LC-MS analysis that this reduction in germination stimulatory activity correlates closely with a reduction in the exudation of strigolactones. This shows that either NCED1 is directly involved in strigolactone biosynthesis or exerts a regulatory role on strigolactone production through ABA. In the latter case, the reduced production of strigolactones in the mutants *notabilis* and *vp14* is due to the reduced ABA content observed in these mutant lines. Hence, it is clear that NCED(s) is involved in the biosynthesis of strigolactones, although further research is required to determine whether their involvement in this biosynthetic pathway is direct or indirect (López-Ráez et al. 2008; López-Ráez et al. 2010).

14.5 Strigolactones Are Branching Factors for AM Fungi

A puzzling question that was asked when the strigolactone germination stimulants were first discovered was: why do plants produce these signaling molecules while they induce germination of one of their worst enemies?

The work of Akiyama and coworkers (2005, 2006) shed some light on this aspect when they demonstrated that these secondary metabolites are involved in signaling between plants and the symbiotic arbuscular mycorrhizal (AM) fungi. AM fungi are obligate symbionts that need to grow in association with a host plant to survive and complete their life cycle (Harrison 2005; Paszkowski 2006). Their spores can germinate spontaneously and undergo an initial asymbiotic stage of hyphal growth. If these fungal hyphae do not encounter a symbiotic partner, they will stop growth and retract. When there is a host plant root in the vicinity of the germinating spore, signaling molecules released by the roots into the rhizosphere – shown by Akiyama et al. (2005) to be strigolactones – reach the hyphae, and the fungus responds to this with increased growth and intensive hyphal branching. This intensive branching is expected to increase the probability of the root and fungi to find each other and to establish a symbiosis (Paszkowski 2006; Besserer et al. 2006). Despite this apparently important

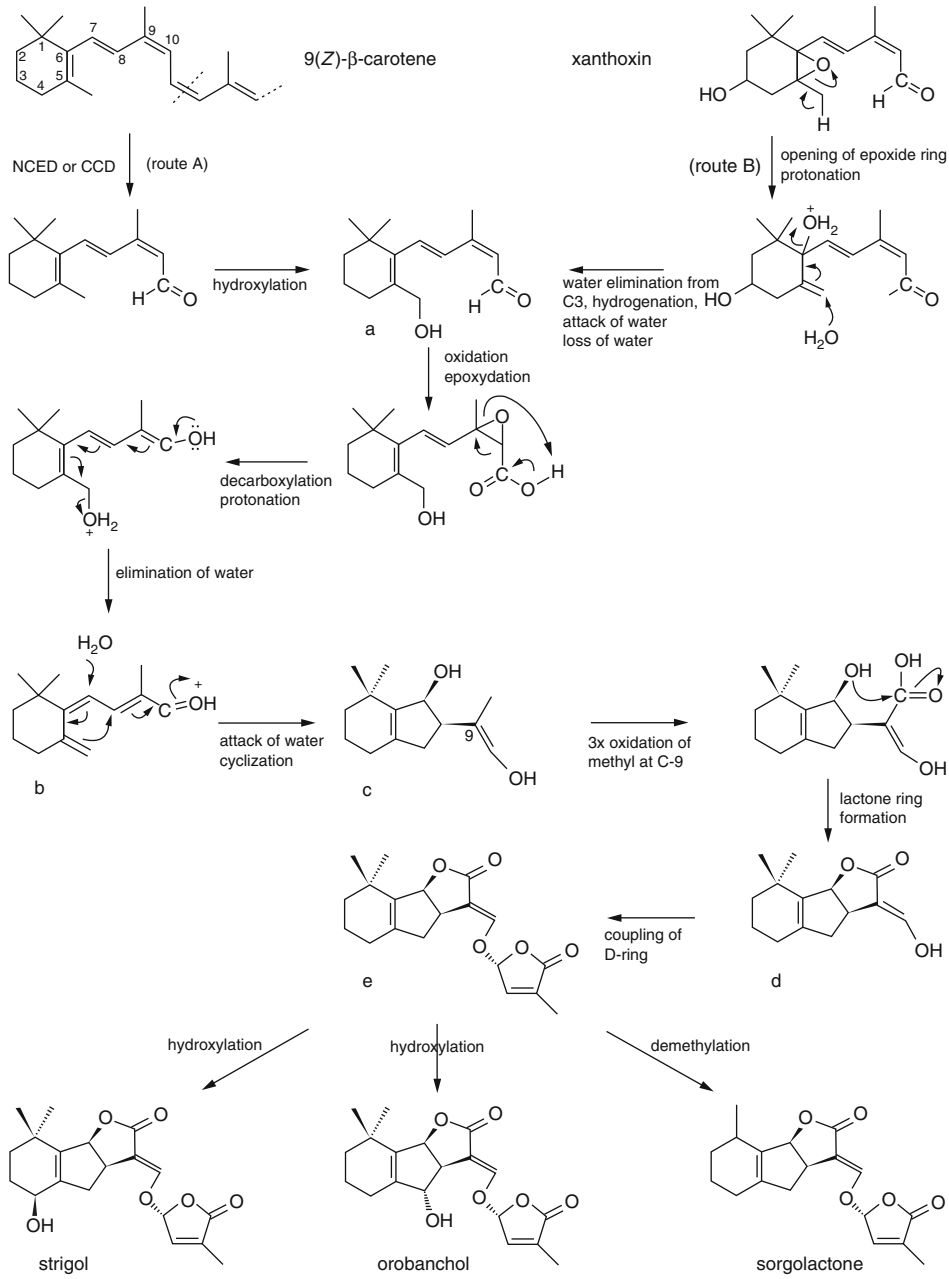

Fig. 14.3 Putative biogenetic scheme for the formation of strigol, orobanchol, and sorgolactone. *CCD* carotenoid cleavage dioxygenase (From Matusova et al. 2005)

function, it is not yet fully understood how essential strigolactones are for the establishment of the symbiosis and/or whether they also play a role in subsequent steps of the interaction (López-Ráez et al. 2009).

14.6 Regulation of Strigolactone Production

One of the primary roles of AM fungi in the symbiotic relationship with plants is the delivery of

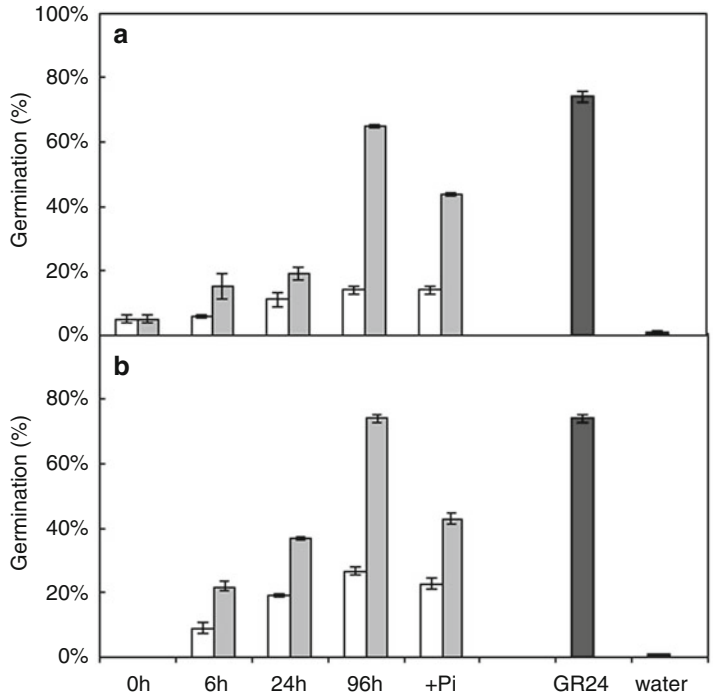

Fig. 14.4 Effect of inorganic phosphate (Pi) availability on the production of germination stimulants by tomato roots. Plants were grown for 3 weeks on half-strength Hoagland's nutrient solution and then transferred to the same solution with 0.2 mM Pi (*open bars*) or without Pi (*gray bars*) and grown for an additional 0, 6, 24, or 96 h. After 96 h, Pi was added back to the remaining plants of the Pi starvation treatment (+Pi). Germination bioassays with *O. ramosa* seeds were carried out using (**a**) root exudates or (**b**) root extracts. GR24 (10^{-9} M), and demineralized water were used as positive and negative controls, respectively. Within each experiment, the concentrations of root exudates were equalized by dilution to the same ratio of volume of exudates to root fresh weight. Bars represent the average of three independent replicates ± SE (**a**) or the average of three replicate disks ± SE (**b**) (From López-Ráez et al. (2008). Reprinted with permission of New Phytologist copyright 2008)

mineral nutrients and particularly phosphate (Karandashov and Bucher 2005). The availability of phosphate is limiting plant growth in many areas of the world, not the least in the African continent. AM fungi can help to improve the uptake of phosphate and hence improve agricultural production in these areas (Johansson et al. 2004; Bagayoko et al. 2000; López-Ráez et al. 2011).

In agreement with their role in the uptake of phosphate, it was shown that root exudates produced by phosphate-limited plants are more stimulatory to AM fungi (Nagahashi and Douds 2004). Indeed, low phosphate conditions also stimulate the exudation of the strigolactone orobanchol by red clover (Yoneyama et al. 2007a).

López-Ráez et al. (2008) investigated whether the increase in the germination stimulant activity under Pi starvation observed in tomato was caused by an increase in the exudation by the roots or by de novo production of germination stimulants. A germination bioassay was performed with either root extracts or root exudates (Fig. 14.4). The increase in germination stimulation by Pi starvation, as observed in root exudates, was also found with root extracts, suggesting that the increase in germination stimulant activity is mainly caused by de novo biosynthesis of strigolactones rather than by an increase in the exudation only.

Yoneyama and coworkers recently described that not only phosphorous but also nitrogen deficiency promotes the production and exudation of 5-deoxystrigol in sorghum. They suggest that the response in strigolactone production and

exudation to nutrient availability varies between groups of plant species. Legumes that can establish symbiosis with *Rhizobia* and acquire nitrogen from root nodules only respond to phosphate deficiency with enhanced strigolactone production to attract AM fungi, whereas in nonleguminous plant species, both phosphate and nitrogen starvation enhance the production of strigolactones (Yoneyama et al. 2007b).

14.7 Interaction Between Parasitic Plants and AM Fungi

In a number of studies with the parasitic plant *S. hermonthica*, it was demonstrated that maize and sorghum have a 30–50% reduction in the number of *S. hermonthica* shoots after inoculation with AM fungi (Gworgwor and Weber 2003; Lendzemo et al. 2007). AM fungi may confer resistance to other biotic stresses as well. For example, there are a number of reports showing that plants colonized by AM fungi are protected against subsequent infection with nematodes and plant pathogenic fungi (Borowicz 2001; Johansson et al. 2004). This protection has been suggested to be due to improved nutritional status of the host, but there is ample evidence that this cannot be the (only) explanation (Johansson et al. 2004; Harrison 2005). Several studies have shown that during mycorrhizal symbiosis, the expression of defense-related genes is induced (Pozo et al. 2002; Kuster et al. 2004). However, improved defense is not likely to be the only possible explanation for the lower infection of mycorrhizal sorghum and maize by Striga. Sun et al. (2008) have shown that the exudates of maize roots, colonized by AM fungi, induce less germination of Striga seeds than control root exudates (Fig. 14.5). Control experiments, in which the synthetic strigolactone analog GR24 was mixed with exudates of AM colonized maize, showed that this effect was not due to the presence of inhibitors. Similar results were obtained with root exudates of mycorrhized sorghum plants and Striga seeds (Lendzemo et al. 2007). These results suggest that the reduction of Striga infection of sorghum and maize, when colonized by AM

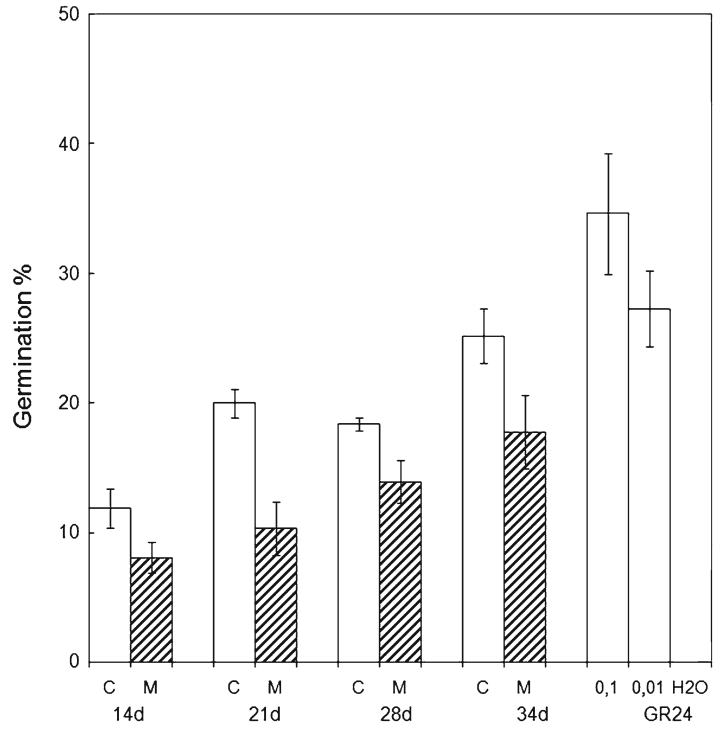

Fig. 14.5 Effect of colonization by *Glomus intraradices* of maize roots on the induction of *Striga hermonthica* seed germination. Root exudates from four plants per treatment (C, noncolonized control plants; M, plants colonized by *G. intraradices*) were collected separately for 24 h in demineralized water at 14, 21, 28, and 34 days after inoculation. The exudate of each plant was diluted to the same concentration of g root fresh weight per mL of root exudate, and induction of *S. hermonthica* germination was assessed. GR24 was used as positive control and demineralized water as negative control. Error bars indicate standard error (n = 4) (From Sun et al. 2008)

fungi, is caused at least partly by a decrease in the formation or secretion of strigolactone germination stimulants. It will be of special interest to find out if the downregulation of strigolactone production could be explained by a regulatory mechanism other than improved plant fitness and/or nutritional status.

14.8 Strigolactones and the Inhibition of Shoot Branching

If the persistence of strigolactones through evolution would be explained solely by their role in the process of mycorrhization, it is hard to explain their presence in nonmycorrhized plants like Arabidopsis as was found by (Goldwasser et al. 2008; Machiguchi et al. 2009).

Therefore, strigolactones may have additional functions. Two recent publications shed some new light on this aspect (Gomez-Roldan et al. 2008; Umehara et al. 2008). In their hunt for the identification of the CCD/NCED genes responsible for the cleavage of the apocarotenoid carbon backbone in the strigolactone biosynthetic pathway, both research groups discovered that mutations in the CCD7 and CCD8 genes of garden pea and rice are involved in this pathway.

In these studies, it was shown that root exudates of *P. sativum* carrying *ccd7* or *ccd8* mutations had significantly reduced activity in promoting fungal hyphae branching and that this could be restored with exogenous strigolactone (Gomez-Roldan et al. 2008). Furthermore, root exudates of mutant plants promoted less germination of parasitic plant seeds when compared with wild-type exudates. In accordance with this finding, *ccd8* mutant pea plants were infected by fewer parasitic *Striga* plants (Matusova et al. unpublished results) (Fig. 14.6).

While two different strigolactones were detected in wild-type root exudates, root exudates of *ccd8* mutant plants did not contain any detectable strigolactones.

The latter was also shown for rice *ccd7* and *ccd8* mutants (Umehara et al. 2008). In line with such observations, strigolactone deficiency in the fast-neutron-mutagenized tomato mutant

Fig. 14.6 Two garden pea plants (*Pisum sativum*) both initially infected with an equal amount of seeds from the parasitic plant *Orobanche crenata*. (*left*) Wild-type pea and (*right*) *ccd8* pea mutant showing its branched phenotype. *Arrows* indicate early development of the parasitic plants on the root system of the wild-type pea plant (Matusova et al. unpublished results)

SL-ORT1 led to resistance to the parasitic weeds *Phelipanche* and *Orobanche* spp. (Dor et al. 2011), but plants were again parasitized after application of the synthetic germination stimulant GR24.

CCD7 and CCD8 are also known to be involved in the production of an as yet unidentified signal controlling the outgrowth of axillary buds (Foo et al. 2001; Morris et al. 2001; Sorefan et al. 2003; Booker et al. 2004; Zou et al. 2006; Arite et al. 2007; Mouchel and Leyser 2007).

Mutations in those genes result in enhanced shoot branching (Fig. 14.6). Other genes playing a role in the biosynthesis of this signal include a cytochrome P450 monooxygenase (Booker et al. 2005) and an F-box leucine-rich repeat family protein (Stirnberg et al. 2002). The latter is presumably involved in recognition and signal transduction and not in the actual production

of the signal itself. Umehara et al. (2008) and Gomez-Roldan et al. (2008) tested whether mutants in this F-box protein in rice, respectively pea, that also displayed the branched phenotype were capable of producing strigolactones, and indeed, substantial levels were detected. This is an extra indication that the reduced strigolactone levels seen in the *ccd7* and *ccd8* mutants are not a result from the aberrant phenotype and hormonal abnormalities observed in shoot-branching mutants.

Knowing that *ccd7* and *ccd8* mutants lack a branching inhibiting signal leading to excessive shoot branching and at the same time appear to be deficient in strigolactones raises, an intriguing question arises. Could it be that both carotenoid-derived compounds are related? Therefore, Gomez-Roldan et al. (2008) applied the synthetic strigolactone GR24 to the axillary buds of *ccd8* and F-box mutant plants in pea and Arabidopsis. Umehara et al. (2008) performed a similar complementation assay for *ccd8* and F-box shoot-branching mutants both in rice and Arabidopsis; however, in this study, GR24 was applied to the growth medium of the plants. In both studies, GR24 was found to contain shoot-branching inhibitory capacity, specifically in the *ccd8* mutant plants, but not in the F-box (receptor) mutant.

Therefore, it is proposed that either strigolactones themselves or closely related molecules produced from the administered strigolactones are the branching inhibiting signal which seems to be transported in the xylem (Kohlen et al. 2011).

Altogether, this puts the class of strigolactones in an entirely new perspective as this all points to the discovery of a new phytohormone. Evidence for additional roles in establishing root system architecture (Kapulnik et al. 2011; Koltai et al. 2010; Ruyter-Spira et al. 2011), seed germination (Tsuchiya et al. 2010), and light signaling (Shen et al. 2007; Tsuchiya et al. 2010) is accumulating at a fast pace.

14.9 Future Research

This also opens up a new era for strigolactone research.

A major challenge lies in the biochemical characterization of the bioactive form of the branch-inhibiting hormone and its link with the strigolactones. Although different strigolactones are all composed of the same building blocks as reflected by the A-, B-, C-, and D-rings, the diversity seen in the decorations of the ABC part is immense. It is far from clear what their functional biological significance is, how they are determined, and if there are any regulatory factors in this decoration process. And if strigolactones are closely related to the branch-inhibiting hormone, does this hormone itself also allow a great structural diversity to be functional?

When looking at the chemical structures of strigolactones, it is obvious that not all biosynthetic enzymes have been identified so far. Especially, the putative coupling of the D-ring to the ABC part is likely to be an enzymatic step calling for a corresponding responsible enzyme. So far, genetic loci of branching mutants in Arabidopsis did not result in a candidate, maybe as a result of redundancy.

It is now clear that strigolactones not only have a role underground in the establishment of a symbiosis with arbuscular mycorrhiza upon phosphate starvation but also have a role inside the plant in the regulation of plant development upon different environmental stimuli. Indeed, the decrease in bud outgrowth observed during phosphate starvation is indeed mediated through an increase in strigolactone production (Kohlen et al. 2011). In this respect, research aimed at the elucidation of the underlying regulatory processes and the interplay with (other) phytohormones will be of great interest, for instance, with the auxin status of the plant (Ruyter-Spira et al. 2011).

References

Akiyama K, Hayashi H (2006) Strigolactones: chemical signals for fungal symbionts and parasitic weeds in plant roots. Ann Bot 97:925–931

Akiyama K, Matsuzaki K, Hayashi H (2005) Plant sesquiterpenes induce hyphal branching in arbuscular mycorrhizal fungi. Nature 435(7043):750–751

Arite T, Iwata H, Ohshima K, Maekawa M et al (2007) DWARF10, an RMS1/MAX4/DAD1 ortholog, controls lateral bud outgrowth in rice. Plant J 51:1019–1029

Bagayoko M, George E, Römheld V, Buerkert A (2000) Effects of mycorrhizae and phosphorus on growth and nutrient uptake of millet, cowpea and sorghum on a West African soil. J Agric Sci 135:399–407

Besserer A, Puech-Pages V, Kiefer P et al (2006) Strigolactones stimulate arbuscular mycorrhizal fungi by activating mitochondria. PLoS Biol 4:1239–1247

Booker J, Auldridge M, Wills S, McCarty D, Klee H, Leyser O (2004) MAX3/CCD7 is a carotenoid cleavage dioxygenase required for the synthesis of a novel plant signaling molecule. Curr Biol 14:1232–1238

Booker J, Sieberer T, Wright W et al (2005) *MAX1* encodes a cytochrome P450 family member that acts downstream of MAX3/4 to produce a carotenoid-derived branch-inhibiting hormone. Dev Cell 8:443–449

Borowicz VA (2001) Do arbuscular mycorrhizal fungi alter plant-pathogen relations? Ecology 82:3057–3068

Bouwmeester HJ, Matusova R, Zhongkui S, Beale MH (2003) Secondary metabolite signalling in host-parasitic plant interactions. Curr Opin Plant Biol 6:358–364

Bouwmeester HJ, Roux C, López-Ráez JA, Bécard G (2007) Rhizosphere communication of plants, parasitic plants and AM fungi. Trends Plant Sci 12:224–230

Butler LG (1995) Chemical communication between the parasitic weed *Striga* and its crop host a new dimension of allelochemistry. In: Dakshini KMM, Einhellig FA (eds) Allelopathy: organisms, processes and applications, vol 582, ACS Symposium Series. American Chemical Society, Washington, DC, pp 158–168

Dalla Vecchia F, Barbato R, La Rocca N, Moro I, Rascio N (2001) Responses to bleaching herbicides by leaf chloroplasts of maize plants grown at different temperatures. J Exp Bot 52:811–820

Dor E, Yoneyama K, Wininger S, Kapulnik Y et al (2011) Strigolactone deficiency confers resistance in tomato line SL-ORT1 to the parasitic weeds *Phelipanche* and *Orobanche* spp. Phytopathology 101:213–222

Dörr I (1996) New results on interspecific bridges between parasites and their hosts. In: Moreno MT, Cubero JI, Berner D, Joel D, Musselman JL, Parker CR (eds) Advances in parasitic plant research. Junta de Andalucia, Spain, pp 196–201

Foo E, Turnbull CG, Beveridge C (2001) Long-distance signalling and the control of branching in the *rms1* mutant of pea. Plant Physiol 126:203–209

Goldwasser Y, Yoneyama K, Xie X, Yoneyama K (2008) Production of strigolactones by *Arabidopsis thaliana* responsible for *Orobanche aegyptiaca* seed germination. Plant Growth Regul 55:21–28

Gomez-Roldan V, Fermas S, Brewer P et al (2008) Strigolactone inhibition of shoot branching. Nature 455:189–194

Gworgwor NA, Weber HC (2003) Arbuscular mycorrhizal fungi-parasite-host interaction for the control of *Striga hermonthica* (Del.) Benth. in sorghum [*Sorghum bicolor* (L.) Moench]. Mycorrhiza 13:277–281

Hable WE, Oishi KK, Schumaker KS (1998) *Viviparous-5* encodes phytoene desaturase, an enzyme essential for abscisic acid (ABA) accumulation and seed development in maize. Mol Gen Genet 257:167–176

Harrison MJ (2005) Signaling in the arbuscular mycorrhizal symbiosis. Annu Rev Microbiol 59:19–42

Hemmerlin A, Hoeffler JF, Meyer O et al (2003) Cross-talk between the cytosolic mevalonate and the plastidial methylerythritol phosphate pathways in tobacco bright yellow-2 cells. J Biol Chem 278:26666–26676

Hibberd JM, Jeschke WD (2001) Solute transfer into parasitic plants. J Exp Bot 52:2043–2049

Hibberd JM, Quick WP, Press MC, Scholes JD, Jeschke WD (1999) Solute fluxes from tobacco to the parasitic angiosperm *Orobanche cernua* and the influence of infection on host carbon and nitrogen relations. Plant Cell Environ 22:937–947

Jeschke WD, Räth N, Bäumel P, Czygan FC, Proksch P (1994) Modelling of the flows and partitioning of carbon and nitrogen in the holoparasite *Cuscuta reflexa* Roxb. and its host *Lupinus albus* L. II. Flows between host and parasite within the parasitized host. J Exp Bot 45:801–812

Joel DM (2000) The long-term approach to parasitic weeds control: 1 manipulation of specific developmental mechanisms of the parasite. Crop Prot 19:753–758

Johansson JF, Paul LR, Finlay RD (2004) Microbial interactions in the mycorrhizosphere and their significance for sustainable agriculture. FEMS Microbiol Ecol 48:1–13

Kapulnik Y, Delaux P-M, Resnick N, Mayzlish-Gati E, Wininger S, Bhattacharya C, Séjalon-Delmas N, Combier J-P, Bécard G, Belausov E, Beeckman T, Dor E, Hershenhorn J, Koltai H (2011) Strigolactones affect lateral root formation and root-hair elongation in *Arabidopsis*. Planta 233:209–216

Karandashov V, Bucher M (2005) Symbiotic phosphate transport in arbuscular mycorrhizas. Trends Plant Sci 10:22–29

Kohlen W, Charnikova T, Liu Q et al (2011) Strigolactones are transported through the xylem and play a key role in shoot architectural response to phosphate deficiency in nonarbuscular mycorrhizal host *Arabidopsis*. Plant Physiol 155:974–987

Koltai H, Dor E, Hershenhorn J, Joel D, Weininger S, Lekalla S, Shealtiel H, Bahattacharya C, Eliahu E, Resnick N, Barg R, Kapulnik Y (2010) Strigolactones' effect on root growth and root-hair elongation may be mediated by auxin-efflux carriers. J Plant Growth Regul 29:129–136

Kuster H, Hohnjec N, Krajinski F et al (2004) Construction and validation of cDNA-based Mt6k-RIT macro- and microarrays to explore root endosymbioses in the model legume *Medicago truncatula*. J Biotechnol 108:95–113

Lendzemo VW, Kuyper TW, Matusova R et al (2007) Colonization by arbuscular mycorrhizal fungi of sorghum leads to reduced germination and subsequent attachment and emergence of *Striga hermonthica*. Plant Signal Behav 2:58–62

Li ZH, Matthews PD, Burr B, Wurtzel ET (1996) Cloning and characterization of a maize cDNA encoding phytoene desaturase, an enzyme of the carotenoid biosynthetic pathway. Plant Mol Biol 30:269–279

López-Ráez JA, Charnikhova T, Gómez-Roldán V et al (2008) Tomato strigolactones are derived from carotenoids and their biosynthesis is promoted by phosphate starvation. New Phytol 178:863–874

López-Ráez JA, Matusova R, Cardoso C et al (2009) Strigolactones: ecological significance and use a target for parasitic plant control. Pest Manag Sci 65:963–965

López-Ráez JA, Kohlen W, Charnikhova T et al (2010) Does abscisic acid affect strigolactone biosynthesis? New Phytol 187:343–354

López-Ráez JA, Charnikhova T, Fernández I, Bouwmeester H, Pozo MJ (2011) Arbuscular mycorrhizal symbiosis decreases strigolactone production in tomato. J Plant Physiol 168:294–297

Magnus EM, Zwanenburg B (1992) Tentative molecular mechanisms for germination stimulation of *Striga* and *Orobanche* seeds by strigol and its synthetic analogues. J Agric Food Chem 40:1066–1070

Mashiguchi K, Sasaki E, Shimada Y et al (2009) Feedback regulation of strigolactone biosynthetic genes and strigolactone-regulated genes in *Arabidopsis*. Biosci Biotechnol Biochem 73:2460–2465

Matusova R, Bouwmeester HJ (2006) The effect of host-root-derived chemical signals on the germination of parasitic plants. In: Dicke M, Takken W (eds) Chemical ecology: from gene to ecosystem. Springer, Netherlands, pp 39–54

Matusova R, Rani K, Verstappen FWA, Franssen MCR, Beale MH, Bouwmeester HJ (2005) The strigolactone germination stimulants of the plant-parasitic *Striga* and *Orobanche* spp. are derived from the carotenoid pathway. Plant Physiol 139:920–934

Morris SE, Turnbull CG, Murfet IC, Beveridge CA (2001) Mutational analysis of branching in pea. Evidence that *Rms1* and *Rms5* regulate the same novel signal. Plant Physiol 126:1205–1213

Mouchel CF, Leyser O (2007) Novel phytohormones involved in long-range signaling. Curr Opin Plant Biol 10:473–476

Nagahashi G, Douds DD (2004) Isolated root caps, border cells, and mucilage from host roots stimulate hyphal branching of the arbuscular mycorrhizal fungus, *Gigaspora gigantea*. Mycol Res 108:1079–1088

Nickrent DL, Duff RJ, Colwell AE et al (1998) Molecular phylogenetic and evolutionary studies of parasitic plants. In: Soltis DE, Soltis PS, Doyle JJ (eds) Molecular systematics of plants, II. Kluwer, Boston, pp 211–241

Parker C, Riches CR (1993) Parasitic plants of the world. CAB International, UK

Parry AD, Horgan R (1992) Abscisic-acid biosynthesis in roots. 1. The identification of potential abscisic-acid precursors, and other carotenoids. Planta 187:185–191

Paszkowski U (2006) Mutualism and parasitism: the yin and yang of plant symbioses. Curr Opin Plant Biol 9:364–370

Pichersky D, Gang DR (2000) Genetics and biochemistry of secondary metabolites in plants: an evolutionary perspective. Trends Plant Sci 5:439–445

Pozo MJ, Cordier C, Dumas-Gaudot E, Gianinazzi S, Barea JM, Azcón Aguilar C (2002) Localized versus systemic effect of arbuscular mycorrhizal fungi on defence responses to Phytophthora infection in tomato plants. J Exp Bot 53:525–534

Press MC, Graves JD (1995) Parasitic plants. Chapman and Hall, London, pp 103–124

Press MC, Scholes JD, Riches CR (2001) Current status and future prospects for management of parasitic weeds (*Striga* and *Orobanche*). In: Riches CR (ed) The world's worst weeds. British Crop Protection Council, Brighton/Farnham, pp 71–90

Rani K, Zwanenburg B, Sugimoto Y, Yoneyama K, Bouwmeester HJ (2008) Biosynthetic considerations could assist the structure elucidation of host plant produced rhizosphere signalling compounds (strigolactones) for arbuscular mycorrhizal fungi and parasitic plants. Plant Physiol Biochem 46:617–626

Revill MJW, Stanley S, Hibberd JM (2005) Plastid genome structure and loss of photosynthetic ability in the parasitic genus *Cuscuta*. J Exp Bot 56:2477–2486

Ruyter-Spira C, Kohlen W, Charnikova T et al (2011) Physiological effects of the synthetic strigolactone analog GR24 on root system architecture in *Arabidopsis*: another belowground role for strigolactones? Plant Physiol 155:721–734

Scholes JD, Press MC (2008) *Striga* infestation of cereal crops - an unsolved problem in resource limited agriculture. Curr Opin Plant Biol 11:180–186

Seel WE, Jeschke WD (1999) Simultaneous collection of xylem sap from *Rhinanthus minor* and the hosts *Hordeum* and *Trifolium*: hydraulic properties, xylem sap composition and effect of attachment. New Phytol 143:281–298

Shen H, Ye W, Hong L, Huang H, Wang Z, Deng X, Yang Q, Xu Z (2006) Progress in parasitic plant biology: host selection and nutrient transfer. Plant Biol 8: 175–185

Shen H, Luong P, Huq E (2007) The F-box protein MAX2 functions as a positive regulator of photomorphogenesis in *Arabidopsis*. Plant Physiol 145:1471–1483

Sorefan K, Booker J, Haurogné K et al (2003) *MAX4* and *RMS1* are orthologous dioxygenase-like genes that regulate shoot branching in *Arabidopsis* and pea. Genes Dev 17:1469–1474

Stewart GR, Press MC (1990) The physiology and biochemistry of parasitic angiosperms. Ann Rev Plant Physiol Plant Mol Biol 41:127–151

Stirnberg P, van De Sande K, Leyser O (2002) *MAX1* and *MAX2* control shoot lateral branching in *Arabidopsis*. Development 129:1131–1141

Sun Z, Has J, Walter MH, Matusova R, Beekwilder J, Verstappen FWA, Ming Z, van Echtelt E, Strack D, Bisseling T, Bouwmeester HJ (2008) Cloning and characterisation of a maize carotenoid cleavage dioxygenase (*ZmCCD1*) and its involvement in the biosynthesis of apocarotenoids with various roles in mutualistic and parasitic interactions. Planta 228:789–801

Tan BC, Schwartz SH, Zeevaart JAD, McCarty DR (1997) Genetic control of abscisic acid biosynthesis in maize. Proc Natl Acad Sci USA 94:12235–12240

Taylor IB, Sonneveld T, Bugg TDH, Thompson AJ (2005) Regulation and manipulation of the biosynthesis of abscisic acid, including the supply of xanthophyll precursors. J Plant Growth Regul 24:253–273

Tsuchiya Y, Vidaurre D, Toh S, Hanada A, Nambara E, Kamiya Y, Yamaguchi S, McCourt P (2010) A small-molecule screen identifies new functions for the plant hormone strigolactone. Nat Chem Biol 6:741–749

Umehara M, Hanada A, Yoshida S et al (2008) Inhibition of shoot branching by new terpenoid plant hormones. Nature 455:195–200

Xie X, Yoneyama K, Yoneyama K (2010) The strigolactone story. Annu Rev Phytopathol 48:93–117

Yokota T, Sakai H, Okuno K, Yoneyama K, Takeuchi Y (1998) Alectrol and orobanchol, germination stimulants for *Orobanche minor*, from its host red clover. Phytochemistry 49:1967–1973

Yoneyama K, Xie X, Kusumoto D et al (2007a) Nitrogen deficiency as well as phosphorous deficiency in sorghum promotes the production and exudation of 5-deoxystrigol, the host recognition signal for arbuscular mycorrhizal fungi and root parasites. Planta 227:125–132

Yoneyama K, Yoneyama K, Takeuchi Y, Sekimoto H (2007b) Phosphorus deficiency in red clover promotes exudation of orobanchol, the signal for mycorrhizal symbionts and germination stimulant for root parasites. Planta 225:1031–1038

Yoneyama K, Xie X, Sekimoto H et al (2008) Strigolactones, host recognition signals for root parasitic plants and arbuscular mycorrhizal fungi, from Fabaceae plants. New Phytol 179:484–494

Yoneyama K, Awad AA, Xie X, Yoneyama K, Takeuchi Y (2010) Strigolactones as germination stimulants for root parasitic plants. Plant Cell Physiol 51:1095–1103

Zou J, Zhang S, Zhang W et al (2006) The rice *HIGH-TILLERING DWARF1* encoding an ortholog of *Arabidopsis MAX3* is required for negative regulation of the outgrowth of axillary buds. Plant J 48: 687–698

Prenyldiphosphate Synthases and Gibberellin Biosynthesis

15

Chris C.N. van Schie, Michel A. Haring, and Robert C. Schuurink

Abstract

Gibberellins are derived from the diterpene precursor geranylgeranyl diphophosphate (GGPP). GGPP is converted to ent-kaurene, which contains the basic structure of gibberellins, in the plastids by the combined actions of copalyl diphosphate synthase (CPS) and ent-kaurene synthase (KS). Generally, geranylgeranyl diphosphate synthase (GGPS) is suggested to use isopentenyl diphosphate (IPP) and dimethylallyl diphosphate (DMAPP) as substrates to generate the GGPP that is used by CPS.

In this chapter we will provide data to show that actually the activity of geranyl diphosphate synthase (GPS) is required in both tomato (*Solanum lycopersicum*) and *Arabidopsis thaliana* for the biosynthesis of gibberellins. This finding indicates that GGPS uses GPP and IPP as substrates to produce the GGPP precursor for gibberellin biosynthesis. We will also argue that the pool of GGPP that is used for the biosynthesis of gibberellins is different from those GGPP pools that are used for other terpenoid-based molecules. Through analysis of Arabidopsis microarray data we attempt to predict which member of the GGPS gene family is actually involved in gibberellin precursor biosynthesis.

Keywords

Terpene • Gibberellin • Tomato • Arabidopsis • Terpenoid precursors

C.C.N. van Schie (✉)
University of California, San Diego,
Division of Biological Sciences,
Natural Sciences Building 1, Rm. 6322, 9500 Gilman Dr., #0380, La Jolla, CA 92093-0380, USA
e-mail: cvanschie@ucsd.edu

M.A. Haring • R.C. Schuurink
Department of Plant Physiology, Swammerdam Institute for Life Sciences, Science Park 904, Amsterdam, XH 1098, The Netherlands

15.1 Introduction

The isoprene units IPP and DMAPP are the substrates for enzymes often referred to as prenyltransferases. However, to prevent confusion with protein prenyltransferases, we prefer calling them prenyldiphosphate synthases. Prenyldiphosphates are the basic backbones of terpenes,

T.J. Bach and M. Rohmer (eds.), *Isoprenoid Synthesis in Plants and Microorganisms: New Concepts and Experimental Approaches*, DOI 10.1007/978-1-4614-4063-5_15,

ranging from IPP, geranyl diphosphate (GPP, C10), farnesyl diphosphate (FPP, C15) and geranylgeranyl diphosphate (GGPP, C20), etc., to polyprenyldiphosphates containing several hundreds to thousands of isoprene units (e.g. natural rubber).

Prenyldiphosphate synthases can generate chains with double bonds in either *cis* or *trans* configuration and in addition, product chain length can vary greatly (Wang and Ohnuma 2000; Liang et al. 2002). In this chapter, only the short chain, *trans*-type enzymes geranyl diphosphate synthase (GPS), farnesyl diphosphate synthase (FPS) and geranylgeranyl diphosphate synthase (GGPS) will be discussed. X-ray crystallography, sequence comparisons and mutational analyses showed that these enzymes have a large central cavity containing two DDxxD motifs for binding of IPP and GPP or FPP, with one exception in orchids (Hsiao et al. 2008). Furthermore, the size of this pocket influences chain length specificity and this is mainly determined by the position of two large aromatic amino acids that form the bottom of the pocket (Wang and Ohnuma 2000; Liang et al. 2002). Next to these biochemical properties, GPS, FPS and GGPS also have different subcellular locations and some occur in gene families. In *Arabidopsis thaliana*, *GPS* is a single-copy gene (Lange and Ghassemian 2003), and the protein is targeted to plastids, although an alternative initiation site for a protein with a cytosolic localization has been proposed (Bouvier et al. 2000). There are two *FPS* copies in the Arabidopsis genome, of which one gene (*FPS2*) encodes a cytosolic protein and the other (*FPS1*) a cytosolic or mitochondrial protein, if an upstream start codon is used (Cunillera et al. 1997). Finally, the *GGPS* gene family consists of 12 members, of whom nine encode proteins that are plastid-localized, two encode cytosolic/ER-localized proteins and one a mitochondrial protein. Below we will give more details about different functions and properties of these family members.

Not surprisingly, there are some exceptions to the basic "rules" of short-chain plant prenyldiphosphate synthases. While it has been shown that GPSs function as homomers (Croteau and Purkett 1989; Heide and Berger 1989; Clastre et al. 1993), the GPS of mint, hop, snapdragon and *Clarkia* were found to be heterodimeric, consisting of a small subunit (ssu) with no apparent homology to prenyldiphosphate synthases and a large subunit (lsu) closely resembling GGPS (Burke et al. 1999; Tholl et al. 2004; Wang and Dixon 2009) (see Figs. 15.1 and 15.2). Apparently in Arabidopsis ssu homologs are also present that can alter the activity of GPPS partners *in vitro* (Wang and Dixon 2009). In addition, in grand fir (*Abies grandis*, a gymnosperm), three GPSs were identified that all share high homology to GGPSs instead of to other GPSs (Burke and Croteau 2002b). Finally, two maize FPSs were identified that also display minor GGPS activity *in vitro* (Cervantes-Cervantes et al. 2006); the orchid GPS has significant FPS activity (Hsiao et al. 2008); and in spruce, a GPS showed some FPS and GGPS activity (Schmidt and Gershenzon 2008), while another bifunctional GPS/GGPS was detected as well (Schmidt et al. 2010). Although the *in planta* functional significance is unknown, the latter indicates that chain length specificity of prenyldiphosphate synthases is not always strict.

15.2 GPP, FPP and GGPP Precursors

It is largely unknown how GPP, FPP and GGPP precursor pools (required for the vast majority of terpenes) are monitored and regulated. Regulation of prenyldiphosphate synthases can be deduced from Arabidopsis micro-array data (www.genevestigator.ethz.ch; Figs. 15.3 and 15.4) that indicate that *GPS* is constitutively and ubiquitously expressed, whereas six monoterpene synthases are expressed in an organ-specific manner and upregulated by various stresses, pathogens

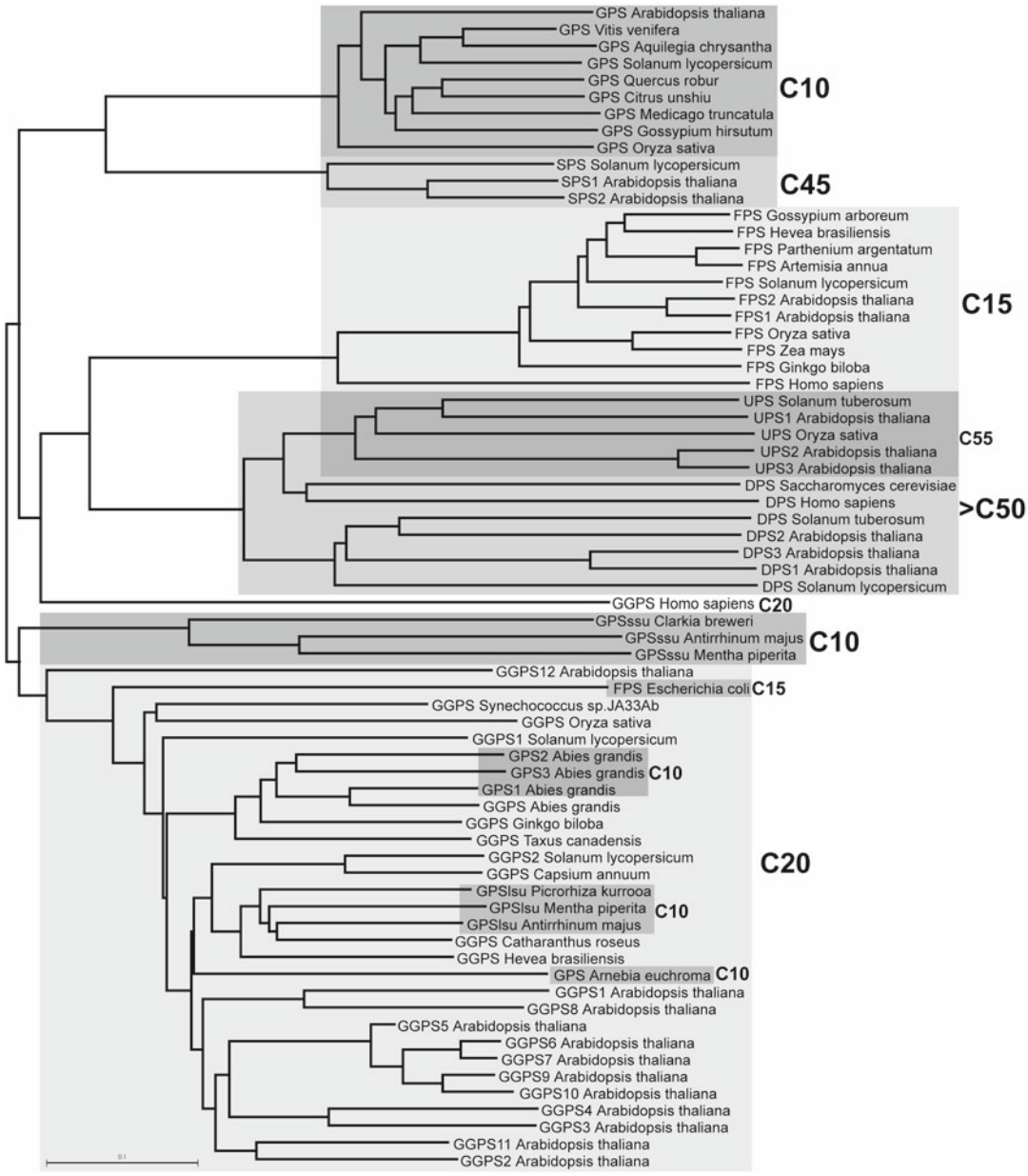

Fig. 15.1 *Sequence homology of prenyldiphosphate synthases*. A neighbor-joining tree is shown (uncorrected distances) derived from an amino acid sequence alignment made with ClustalW software using the PAM350 matrix. The used full-length sequences include all Arabidopsis prenyldiphosphate synthases (with the exception of two polyprenyldiphosphate synthases). For each class of prenyldiphosphate synthases, a representative subset of sequences from other plant species has been included. Abbreviations: *GPS* geranyl diphosphate synthase, *SPS* solanesyldiphosphate synthase, *FPS* farnesyl diphosphate synthase, *UPS* undecaprenyldiphosphate synthase, *DPS* dehydrodolicholdiphosphate synthase, *GGPS* geranylgeranyl diphosphate synthase, *ssu* small subunit, *lsu* large subunit. *Shaded boxes* indicate separate branches or sub-groups with distinct activities

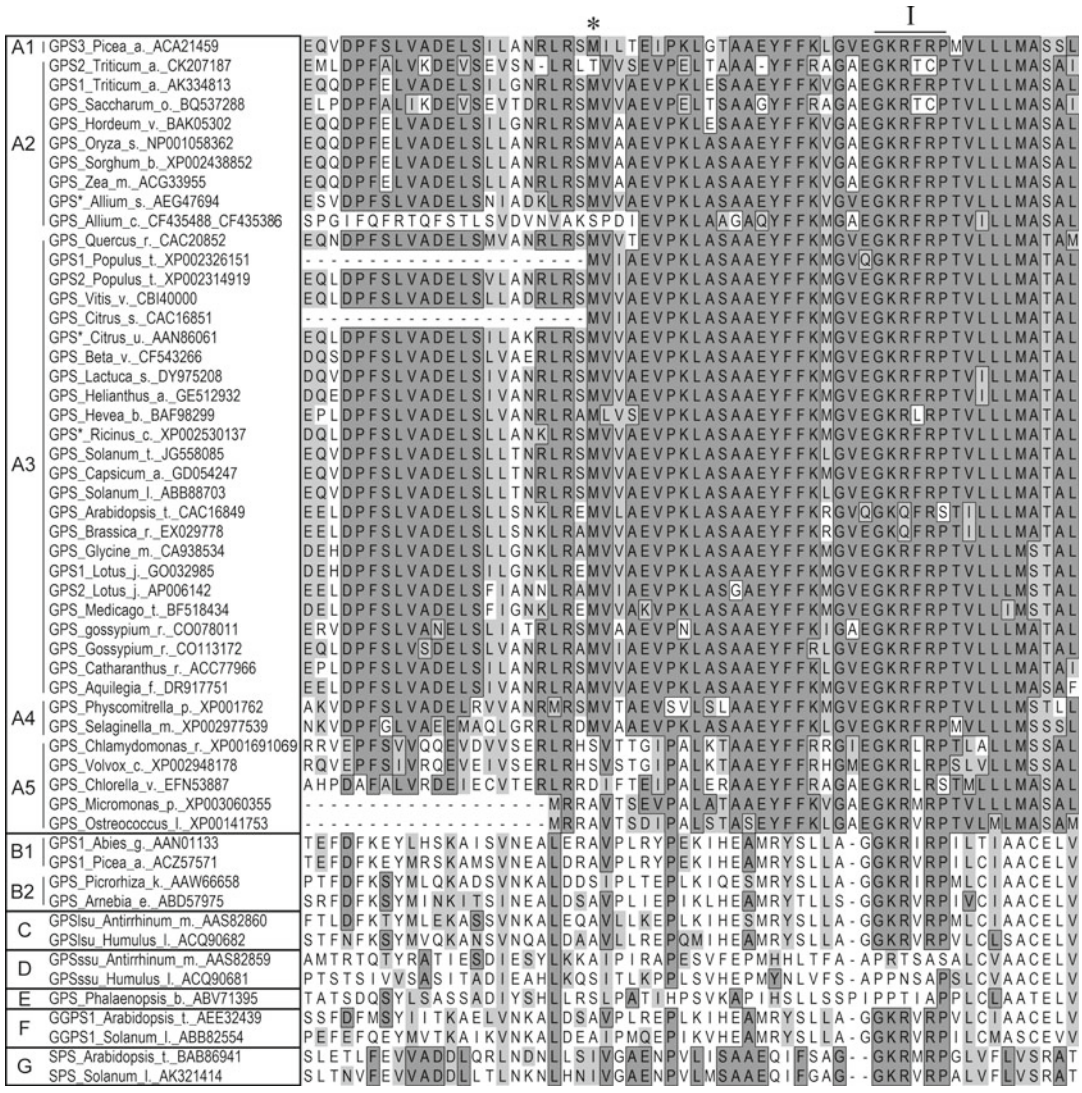

Fig. 15.2 *Alignment of GPS amino acid sequences.* Sequence databases GenBank (www.ncbi.nlm.nih.gov/genbank/) and plantGDB (www.plantgdb.org/) were searched for geranyl diphosphate synthase sequences using keywords and/or the BLAST function. A 60 amino acid section of the final alignment is shown, corresponding to amino acid 72–132 of LeGPS. The asterisk indicates the second methionine putatively used in Arabidopsis GPS. A conserved prenyldiphosphate synthase motif is indicated by a Roman I. The alignment includes Homomeric GPSs (type *A*) (*A1*: gymnosperm, *A2*: angiosperm monocot, *A3*: angiosperm dicot, *A4*: mosses, *A5*: green algae), Homomeric GPSs (type *B*, "GGPS-like") (*B1*: gymnosperm, *B2*: angiosperm), Heteromeric GPSs (*C*: "GGPS-like" large subunit, *D*: small subunit), Homomeric GPS (type *E*) (*E*: orchids), GGPSs (*F*), and solanesyl diphosphate synthases SPSs (*G*). All protein and translated nucleotide sequences shown include the GenBank ID. *Annotated as GGPS. Sequences were aligned using ClustalX2

and elicitors, resulting in highly fluctuating GPP requirements. Similarly, the two *FPS* genes are expressed constitutively and in most organs, but relatively high in flowers and roots (Cunillera et al. 1996; Cunillera et al. 2000). The sesquiterpene synthases are expressed mostly in flowers and roots and several root-specific genes are upregulated by pathogens and stresses. In addition, sq ualene synthase (sterols), ubiquinone synthesis and protein farnesyltransferase also require FPP

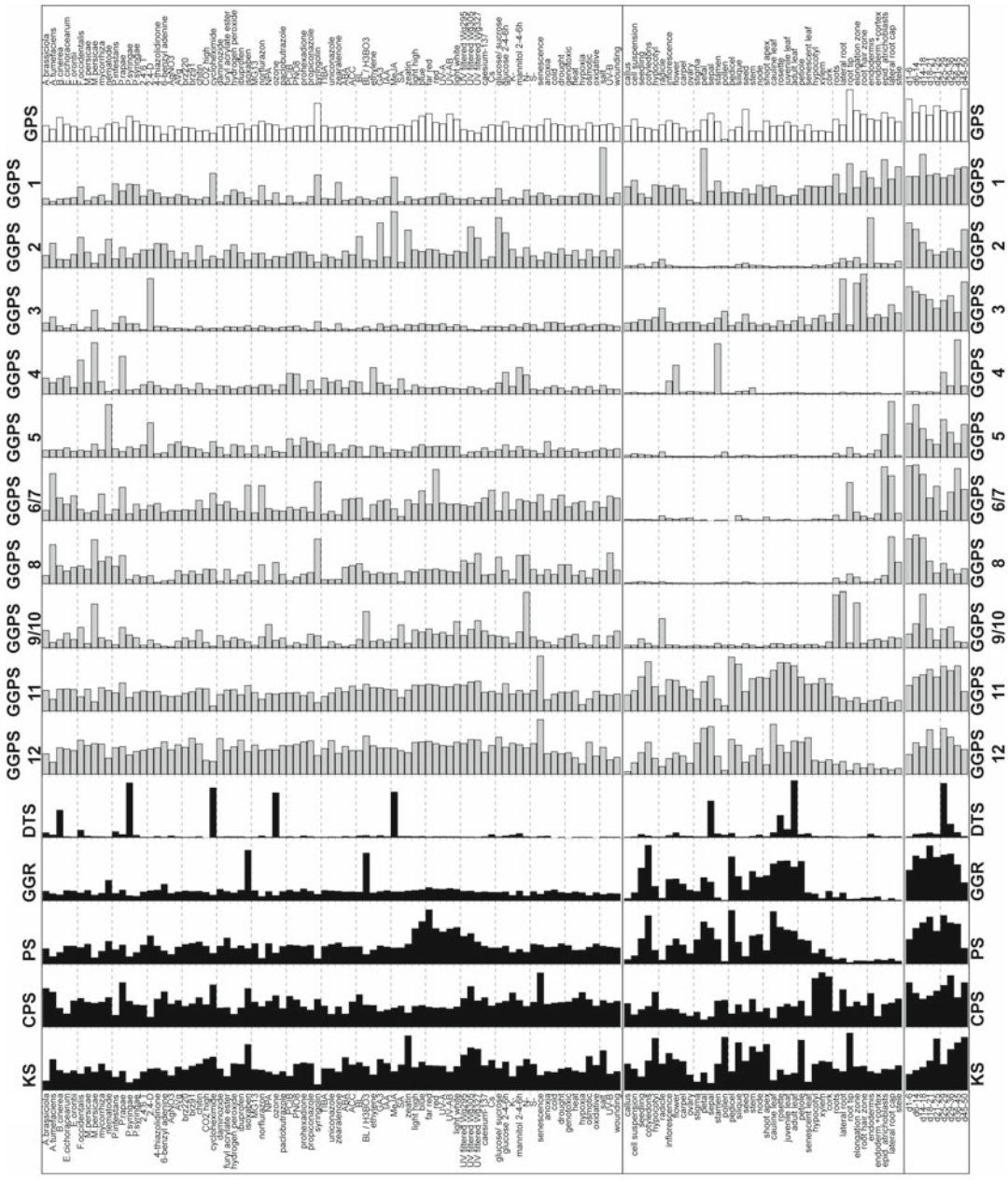

Fig. 15.3 (**a**) *Relative expression levels in response to various treatments, in different organs and during developmental stages.* Expression data were retrieved from Genevestigator of the Arabidopsis genes kaurene synthase (*KS*), copalyldiphosphate synthase (*CPS*), phytoene synthase (*PS*), geranylgeranyl reductase (*GGR*), diterpene synthase (*DTS*), geranylgeranyl diphosphate synthase 1–12 (GGPS) and geranyl diphosphate synthase (*GPS*). Gene numbers are indicated in Fig. 15.4. Subcellular localizations (putative) are indicated by p (plastid), c (cytosol/ER) and m (mitochondria). Average signals are indicated for each gene. Asterisks (*) indicate bars with low reliability (few replicates or very low signals of control-treatments before calculating fold-increase).

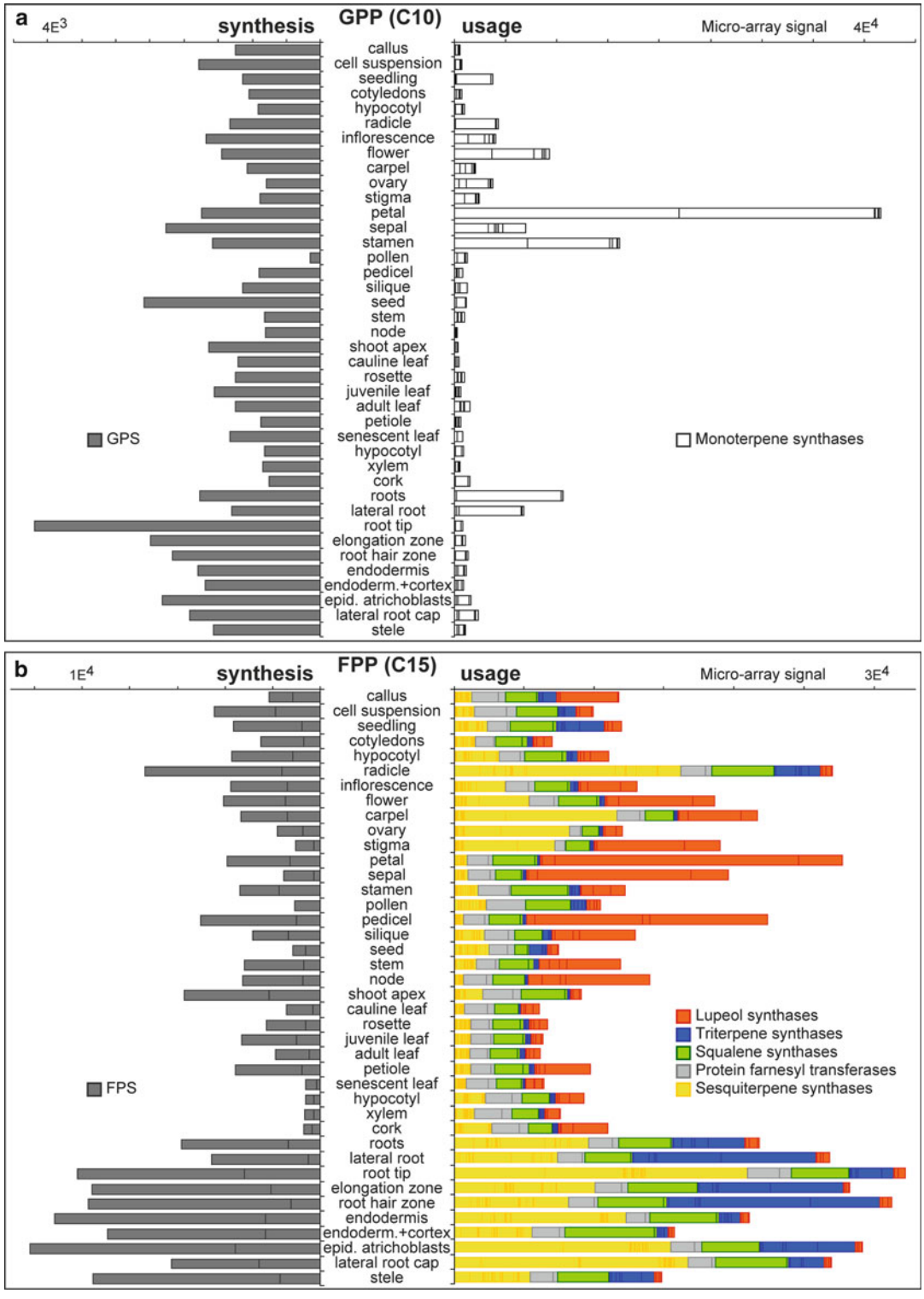

Fig. 15.4 *Expression of genes related to terpene biosynthesis in various Arabidopsis organs.* (**a**), (**b**). Prenyldiphosphate synthesis and usage in different organs are visualized by side-by-side plotting of (cumulative) microarray signals of the genes encoding prenyldiphosphate synthase(s) and the enzymes that use their products.

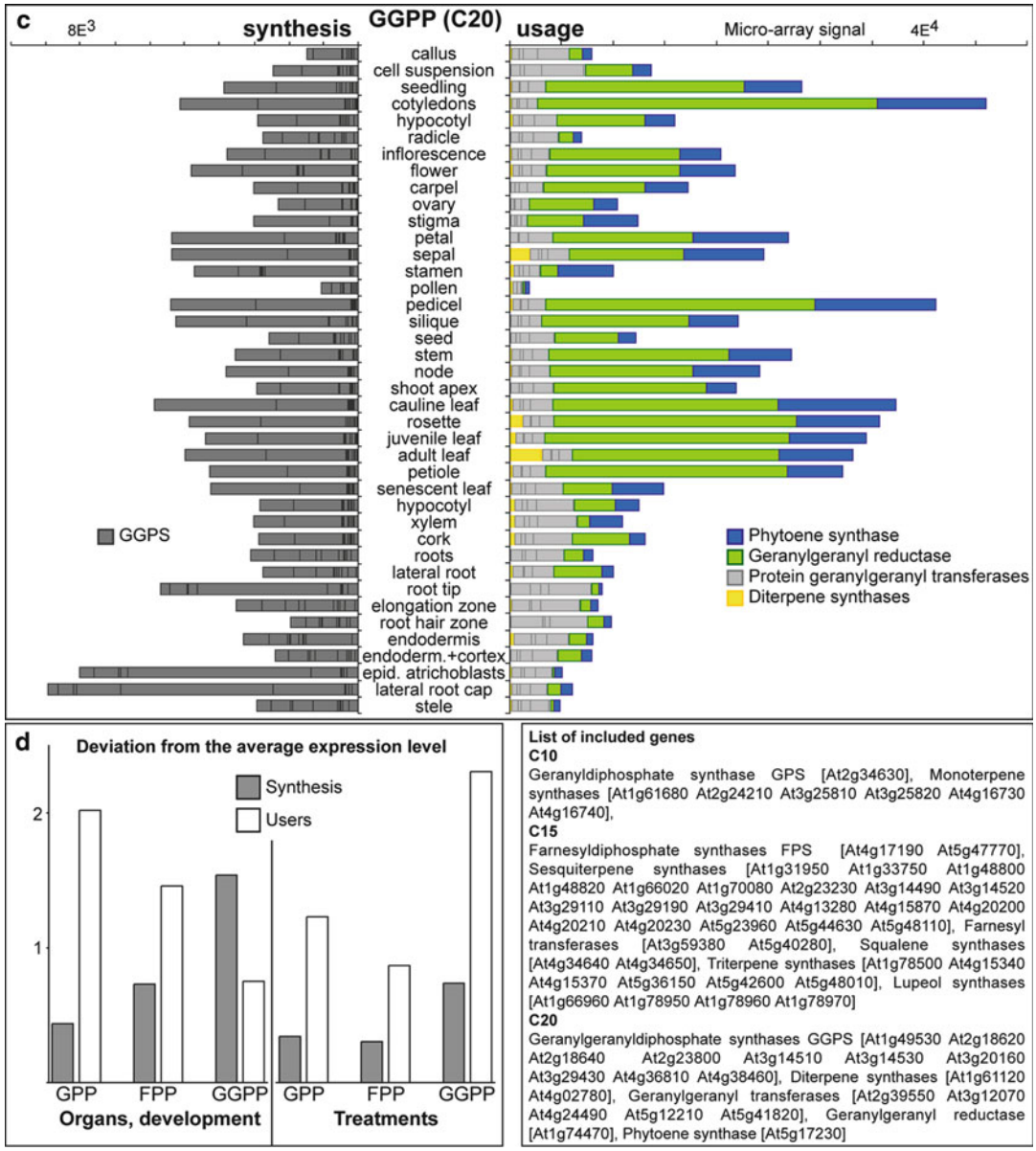

Fig. 15.4 (continued) Thus, this allows comparison of synthesis versus usage of GPP (**a**), FPP (**b**) and GGPP (**c**) in all plant parts. (**d**) The extent of gene-regulation with regard to organ-specificity, development and responses to treatments for enzymes synthesizing or using prenyldiphosphates was analyzed. Organ expression data were normalized for each gene to obtain a relative expression level compared to the average value that was set to 1.0. Treatment expression data for each gene were taken as fold increase compared to control. The magnitude of the standard deviation of gene expression was used as a measure for the arbitrary 'regulation level' for a gene or group of genes in the different organs or by different treatments

Table 15.1 *Arabidopsis prenyldiphosphate synthase genes*. Expression data of Arabidopsis genes were obtained mainly from Genevestigator (www.genevestigator.org). Putative subcellular localization is indicated with *p* plastid, *c* cytosol/ER, *m* mitochondria

Table 1. GPs, FPS and GGPs genes from Arabidopsis

	Gene	localization	sequence	additional reference	most prominent expression
Arabidopsis thaliana	GPS	p	At2g34630	Bouvier et al., 2000	ubiquitous
		c	alt. translation	"	
	FPS1	c	At4g17190	Cunillera et al., 1996	ubiquitous, roots, inflorescences
	FPS2	c	At5g47770	"	ubiquitous, roots, inflorescences
		m	alt. translation	Cunillera et al., 1997	
	GGPS1	m	At1g49530	Zhu et al., 1997b; Okada et al., 2000	ubiquitous; induction by salt
	GGPS2	p	At2g18620		roots; induction by MeJA, GA3, zeatin, sugar
	GGPS3	c	At2g18640	Okada et al., 2000	roots; induction by 2,4-D
	GGPS4	c	At2g23800	Zhu et al., 1997a; Okada et al., 2000	flowers; induction by herbivory
	GGPS5	p	At3g14510		roots; induction by nematodes
	GGPS6/7	p	At3g14530/50	Okada et al., 2000	roots
	GGPS8	p	At3g20160		roots
	GGPS9/10	p	At3g29430/32040		roots; induction by N-shortage
	GGPS11	p	At4g36810	Okada et al., 2000	ubiquitous
	GGPS12	p	At4g38460		ubiquitous

and are expressed ubiquitously and hardly regulated by stimuli. It is currently not clear whether prenyldiphosphate synthases are subject to feedback-regulation by their products. However, it can be hypothesized that GPP and FPP pools are constitutively maintained at a sufficiently high level to feed (induced) mono- and sesquiterpene synthases (and other FPP requiring enzymes).

In contrast to the readily available and "non-regulated" GPP and FPP pools, GGPP pools seem more specifically controlled. GGPP is used for a greater variety of terpene products of which most are primary metabolites for which one might assume that GGPP demand is probably quite constant. However, synthesis of some GGPP-dependent terpenes like diterpene phytoalexins and the volatile C16-norterpene TMTT (for 4,8,12-trimethyltrideca-1,3,7,11-tetraene) (Lee et al. 2010; Ament et al. 2006; Herde et al. 2008; Lee et al.) are highly regulated. In addition, expression of genes encoding GGPP requiring enzymes is very variable in Arabidopsis (Fig. 15.3). Interestingly, the Arabidopsis genome contains 12 putative *GGPS*s, and therefore, it can be hypothesized that individual GGPSs are involved in generating GGPP for specific terpene biosynthesis pathways. This is supported by the highly variable *GGPS* expression patterns in Arabidopsis, both in organ- and treatment-specific manners (see Table 15.1, www.genevestigator.ethz.ch and Fig. 15.3). Furthermore, a fruit- and flower-specific GGPS involved in carotenoid synthesis has been identified in tomato (Ament et al. 2006; Galpaz et al. 2006) and is regulated differently from a leaf-specific GGPS involved in herbivory-induced TMTT synthesis (Ament et al. 2006).

A question that remains is whether competition for common precursors will occur. This would be possible if precursor requirement exceeds precursor synthesis capacity. It is known that when challenged with high light, pathogens or elicitors, plants show growth retardation. It is not clear what causes the reduction of growth and whether terpene biosynthesis pathways are involved. Nevertheless, such mechanism suggests substrate allocation to preferred metabolites. An example that points in this direction is the downregulation of gibberellin synthesis upon induction of phytoalexin synthesis in rice (two pathways both requiring GGPP) (Chang et al. 2005). This suggests an active regulation of substrate allocation rather than a simple depletion by a dominant pathway. Other examples of competition for terpene precursors were found after artificially redirecting precursor fluxes. For instance, ectopic overexpression of phytoene synthase (carotenoid biosynthesis) in tomato resulted in dwarfed plants, with lower gibberellin levels caused by a depletion of the GGPP pool (Fray et al. 1995), whereas overexpression of a linalool synthase in Arabidopsis also led to growth-reduction (Aharoni et al. 2003), probably by depleting IPP or GPP pools that might be required for gibberellins.

15.3 GPS, FPS and GGPS

Based on information in sequence databases (www.ncbi.nlm.nih.gov and www.plantGDB.org) and literature, *GPS* seems a single-copy gene in most plants, also in tomato with the genome recently been sequenced (http://solgenomics.net/). However, in the gymnosperms *Abies grandis* and *Picea abies*, three *GPS* genes were identified (Burke and Croteau 2002a; Schmidt and Gershenzon 2008; Schmidt et al. 2010) and for lotus, cotton and wheat, two different ESTs putatively encoding GPSs have been found (Fig. 15.2). Here, we describe the details for the Arabidopsis *GPS* gene as an example. It has been proposed that this *GPS* gene can be transcribed into two possible messengers, the long one resulting in a plastid-targeted protein, while the shorter one would be translated from a downstream methionine and therefore localize to the cytosol (Bouvier et al. 2000). Other evidence for cytosolic GPP or monoterpene synthesis is limited (Sommer et al. 1995). The role of cytosolic GPS remains unclear, but one could speculate that cytosolic GPP might be incorporated in FPP or cytosolic GGPP. Unpublished data show that Arabidopsis GPS is also targeted to the mitochondria (Ducluzeau et al. 2011).

This observation indicates that roles of a single copy gene might be diversified by variations in subcellular targeting of the encoded protein. Similarly, one of the two FPSs also has a dual subcellular localization, the longer messenger (FPS1L) results in a protein with mitochondrial targeting, while the shorter one (FPS1S) and FPS2 are predicted to be cytosolic (Cunillera et al. 1997). Again, although FPSs are ubiquitously expressed (see below), their contributions to FPP-dependent terpenes might be rather specific, which is supported by differential subcellular targeting. In fact they act redundantly and only double knockouts cause early developmental arrest (Ferrer et al. 2010).

Finally, the GGPS family is not only the largest prenyldiphosphate synthase family, but also the most diverse. Expression patterns of individual members vary greatly as do their predicted subcellular localizations (Table 15.1). Nine GGPSs are (predicted) to be plastid targeted, two are cytosolic or ER-localized, probably involved in GGPP supply for geranylgeranylation of proteins since all five geranylgeranyl transferases are cytosolic, and one is mitochondrial (Okada et al. 2000; Lange and Ghassemian 2003). These observations support the statement that individual GGPSs are required for different GGPP pools. However, besides organ-specific, developmentally regulated, treatment-induced expression patterns and specific subcellular localizations, the other property that very likely differs between GGPS family members is their biochemical activity. One of the difficulties of supporting this statement is that there are only few examples where different enzymes were tested within one experiment. In the case of the three highly homologous GPSs of *Abies grandis*, it can clearly be observed that one enzyme has significant FPS activity (Burke and Croteau 2002a). For the Arabidopsis GGPSs, five enzymes have been characterized and it is clear that the GGPP solanesyldiphosphate (by-)products can differ at least an estimated 50-fold. Unfortunately, the enzyme-assays were all done with IPP and FPP (Zhu et al. 1997; Okada et al. 2000). First, FPP is a very unlikely substrate for plastidial GGPSs and second, the ability to use DMAPP or GPP as allylic substrate remains unknown, leaving us with very little information about substrate preference.

Feeding GGPS with IPP and DMAPP or GPP would provide us with indications of which substrates are used by GGPSs *in planta*, which is not clear to date. Comparing results from researchers that do test different allylic substrates in their GGPS characterizations reveals large differences. Looking at plant GGPSs, (Dogbo and Camara 1987; Laferrière and Beyer 1991; Laskaris et al. 2000; Takaya et al. 2003) K_m values (in μM) for DMAPP as allylic substrate with IPP vary from 0.95 to 127, those for GPP vary from 2.3 to 9 and those for FPP vary from 0.5 to 26 (Burke and Croteau 2002a), indicating different substrate preferences *in vitro*. In general, K_ms for GPP and FPP are lower than for DMAPP and K_{cat}s higher, indicating that if present, GPS or FPS might supply GGPP precursors to GGPS. We hypothesize

that individual GGPSs use different substrates, depending on the tissue, their subcellular localization, their biochemical preference and the availability of substrates. We have clear indications that GGPS required for gibberellin synthesis uses GPP as substrate, whereas GGPS required for carotenoids and chlorophyll synthesis does not use GPP and is localized to a different tissue (van Schie et al. 2007b). These observations suggest that, although the highly diversified terpene biosynthesis pathways are fed by a limited number of prenyldiphosphate precursors, prenyldiphosphate synthases contribute to this highly regulated precursor pool by functioning as differentially regulated and targeted gene family members and even isoforms with varying enzymatic properties.

15.4 GPS Is Required for the Biosynthesis of Gibberellins

Manipulation of *GPS*, *FPS* and *GGPPS* has, to the best of our knowledge, been limited to *FPS*-overexpression and knock-outs in Arabidopsis plants. Overexpression of both the mitochondrial and the cytosolic isoform lead to strong pleiotropic effects (chlorosis and cell death), which is probably due to IPP depletion from the cytosol and decreasing cytokinin levels (Masferrer et al. 2002; Manzano et al. 2006). Only double knockouts caused early developmental arrest (Ferrer et al. 2010).

We took a silencing approach to investigate the role of GPS in terpene biosynthesis in tomato (*Solanum lycopersicum*) and Arabidopsis. Much too our surprise, this revealed that GPS is required for the biosynthesis of the diterpene-derived gibberellins (van Schie et al. 2007a). The two different silencing approaches: virus-induced gene silencing (VIGS) in tomato and RNAi (through inverted repeats) in Arabidopsis both resulted in dwarfed plants (Fig. 15.5). The amount of gibberellins was significantly reduced in the GPS-silenced, dwarfed tomato plants (van Schie et al. 2007a), which could be rescued by application of external gibberellins (Fig. 15.5). Interestingly, silencing of *GPS* had no effect on carotenoid and chlorophyll levels.

These results suggest that GPP feeds into the GGPP biosynthesis pathway that leads to gibberellins. GGPSs involved in gibberellin synthesis would thus use GPP as substrate for condensation of two additional IPP units. Interestingly, the precursor pool for carotenoid and chlorophyll synthesis is not dependent on *GPS* expression. Therefore, pigments and gibberellins originate from separate GGPP pools and GGPSs involved in pigment synthesis are probably not dependent on GPP. A schematic representation of how the role of different GGPP pools in gibberellin and carotenoid/chlorophyll biosynthesis can be envisioned is depicted in Fig. 15.6.

Various studies had already indicated that, in the aerial parts, gibberellins and pigments are made in different tissues. Localization of the first dedicated step in gibberellin synthesis (conversion of GGPP to *ent*-copalyl diphosphate, *ent*-CPP) was studied using *ent*-CPP synthase promoter-GUS fusions in Arabidopsis. This revealed that CPS is mostly expressed in provasculature or vasculature tissue of developing embryos, seedlings, and young as well as mature leaves (Sun and Kamiya 1997; Yamaguchi et al. 2001). In contrast, chlorophyll and carotenoid synthesis occurs mainly in chloroplasts of mesophyll cells (chlorenchym) (Reiter et al. 1994; Cookson et al. 2003). However, some data published earlier suggested precursor sharing. Firstly, depletion of the plastidial terpene precursor pool upstream of GGPP by antisense or chemical suppression of IPP synthesis in Arabidopsis lead to both a pigment-deficient and a dwarfed phenotype (Okada et al. 2002). IPP is indeed required for both metabolites. However, in these experiments the IPP pool is lowered in both cell types (vascular and mesophyll tissue), and thus does not provide evidence for the sharing of a GGPP pool. Secondly, ectopic overexpression of a carotenoid biosynthesis gene, phytoene synthase, in tomato plants or Arabidopsis seeds causes precursor depletion, and leads to lower gibberellin levels and dwarfed plants or delayed germination, respectively (Fray et al. 1995; Lindgren et al. 2003). In these cases, the ectopic and therefore ‘mislocalized’ carotenoid

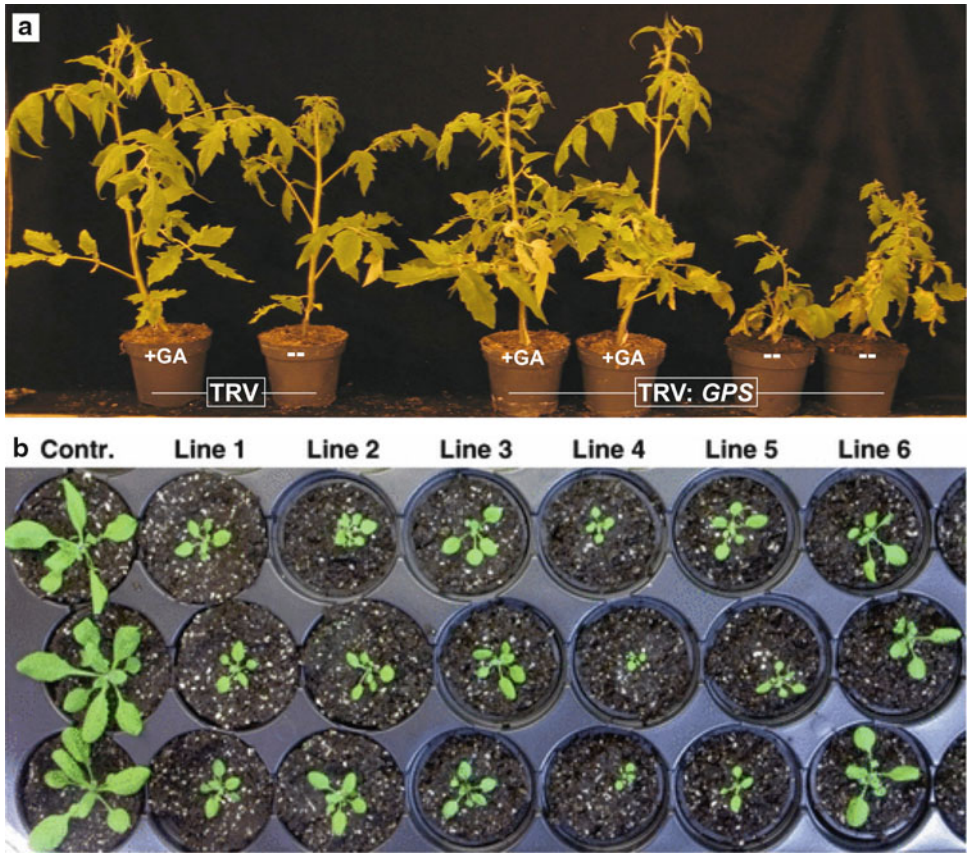

Fig. 15.5 *Phenotype of GPS-silenced tomato plants using virus-induced gene silencing and the effect of GPS silencing in Arabidopsis.* (**a**) Pictures were taken 35 days after inoculation. The dwarf phenotype was rescued by spraying gibberellic acid (GA3) biweekly. (**b**) Phenotype of Arabidopsis plants transformed with an AtGPS-RNAi(1) construct. Three T2 plants of six independent lines are shown

biosynthesis apparently depleted the GGPP pool normally used for gibberellin biosynthesis. Lastly, GGPP sharing between GA and pigment biosynthesis has been assumed earlier, based on the observations that GA production is repressed and photosynthetic pigment production increased during deetiolation via inhibition of CPS activity by light through increased Mg^{2+} levels (Prisic and Peters 2007). However, there is no direct indication that GGPP pools are shared during de-etiolation. Rather than explaining these interactions by regulation of the GGPP flux between "competing" metabolites, it may well be that strict regulation of gibberellin levels and synthesis of photosynthetic pigments is required to control the integrated regulatory effects of light and gibberellins on plant development, mediated by DELLA proteins (Achard et al. 2007; Feng et al. 2008). Therefore, the cell type-specific biosynthesis of gibberellin precursors, as we propose (Fig. 15.6), does not contradict previously published data.

15.5 Effect of *GPS* Silencing on Volatile Terpene Synthesis

A question we originally wanted to address in the *GPS* silencing experiments described above was whether *GPS1* silencing in tomato would result in decreased production of monoterpenes. Both in the headspace of intact *GPS*-silenced plants and in their leaf extracts, monoterpene

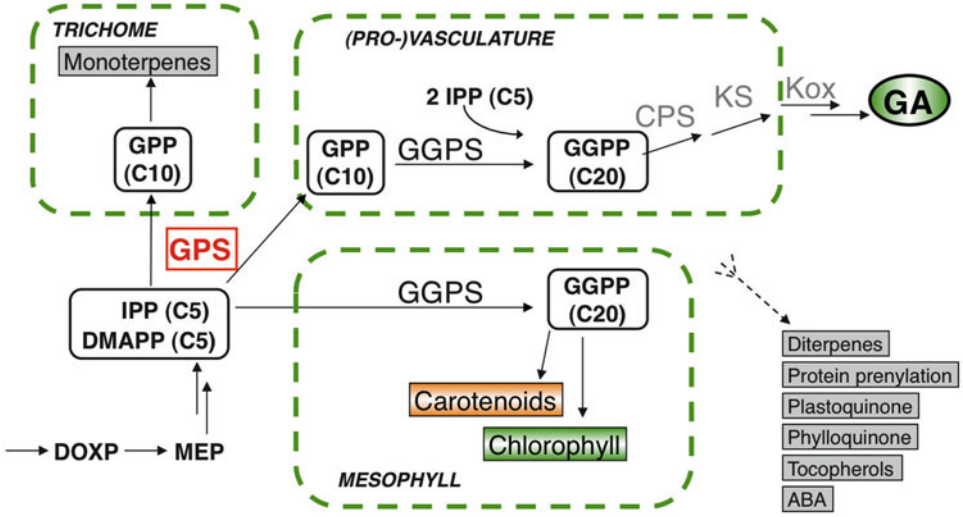

Fig. 15.6 *Schematic representation of terpene biosynthesis, focused on synthesis of the prenyl diphosphates isopentenyl diphosphate (IPP), dimethylallyl diphosphate (DMAPP), geranyl diphosphate (GPP) and geranylgeranyl diphosphate (GGPP) in plastids of the aerial parts of a plant.* Three different cell types are schematically indicated whereas the synthesis of IPP and DMAPP is a common pathway to all cells. Prenyldiphosphates are indicated by rounded boxes and terpene endproducts are indicated by filled boxes. Dotted arrows indicate the possible requirement of other prenyldiphosphate synthases or uncertain substrate origins and intermediate steps. *CPS* *ent*-copalyldiphosphate synthase, DOXP 1-deoxy-D-xylulose 5-phosphate, Kox *ent*-kaurene oxidase, KS *ent*-kaurene synthase, MEP methyl-D-erythritol phosphate. C5–C20 refers to carbon chain length

contents were unaltered (data not shown). A first explanation for this could be that monoterpenes are predominantly synthesized in the glandular trichomes of tomato (Van Schie et al. 2007a) and therefore, it is possible that VIGS does not reach these symplastically isolated organs, although spreading of viruses or silencing signals into trichomes has been reported (Besser et al. 2009). It is also possible that monoterpenes are stored very early in leaf development when VIGS does not affect the leaf yet, or that GPP levels are not limiting in trichomes when GPS expression is partially silenced. Another explanation is the recent identification of a trichome-specific *cis*-prenyltransferase, catalyzing the formation of neryl diphosphate (NPP) from DMAPP and IPP and consequently named NPP synthase (Schilmiller et al. 2009). NPP is a substrate for a monoterpene synthase (phellandrene synthase 1), which besides α- and β-phellandrene produces several other monoterpenes, including α- and γ-terpinene, 2-carene and limonene (Schilmiller et al. 2009).

15.6 What Other Functions May GPS Have?

The *in vitro* activity of the recombinant protein shows that tomato SlGPS1 is a bona fide GPS but suggests that SlGPS1 can also generate FPP and minute amounts of GGPP (van Schie et al. 2007a). It is unclear to what extent the additional activity of this recombinant protein occurs *in planta*. The homologous AtGPS did not have clear FPS activity (Bouvier et al. 2000) although later reports show that it can have polyprenyl diphosphate synthase activity (Hsieh et al. 2011) or solanesyl diphosphate synthase activity (Ducluzea et al. 2011). Chain length specificity of prenyltransferases is not always highly stringent. Still, it should be kept in mind that *in vitro* assay products do not necessarily reflect the *in planta* situation because of for instance unknown K_ms, specific assay conditions (buffer composition, pH), enzyme truncation and addition of purification tags. Especially the ratio DMAPP-IPP

used in the reaction, (varying from 2:1 to 1:15) can determine the outcome, i.e. the length of the product (Hsieh et al.; Bouvier et al. 2000; Hsieh et al. 2011). It will be interesting to investigate to what extent possible prenyltransferase by-products contribute to the sometimes hypothesized, but unexpected presence of GPP in the cytosol or FPP in plastids (Aharoni et al. 2003; Wu et al. 2006). However, in a systematic study of Arabidopsis ecotypes that were challenged by coronatin, a jasmonate mimic eliciting responses similar to those caused by insect feeding, quantitative variation was for instance found for the emission of the monoterpene (*E*)-β-ocimene and the sesquiterpene (*E,E*)-α farnesene (Huang et al. 2010). Differential subcellular compartmentalization of two terpene synthases (encoded by allecic *TPS02* and *TPS03*) appear to control the variation and plasticity of volatile emissions in Arabidopsis ecotypes (Huang et al. 2010).

Thus far, the exact role of GPS in di-, tri-, tetra-, and/or polyterpene synthesis received little attention and is still unclear. It remains to be investigated whether GPS-silenced plants have other phenotypes. We analyzed only gibberellin-, carotenoid- and chlorophyll- levels and therefore, it is unknown whether GPS is involved in synthesis of other large terpenes (+derivatives) like plastoquinone, phylloquinone, tocopherols or GGPP for protein prenylation. Taking into account that GPS could also be localized to the cytosol (Bouvier et al. 2000), although its function there is unknown, it is tempting to speculate that GPS is even involved in synthesis of cytosolic terpenes like sesquiterpenes, steroids and dolichols. Some recent data show that Arabidopsis GPS is also targeted to the mitochondria (Ducluzeau et al. 2012).

What still remains to be investigated is, if and how the GGPP precursor pools are shared among different terpene metabolites, and how this is regulated. Furthermore, we should take into account that GPS functions might differ between plant species. Firstly, it is not clear yet whether cytosolic localization of GPS or FPP formation in plastids is common in plants. Secondly, the existence of homomeric as well as heteromeric GPSs suggests independent origins of this protein activity, which makes it likely that GPS functions can differ. Finally, existence of single copy GPSs or multiple GPSs adds an extra layer of complexity to this possible variability.

15.6.1 EST Database Analysis Supports Conservation of the Second Start Codon in GPSs

The Arabidopsis *GPS* gene contains two possible transcriptional and translational start sites leading to mRNAs with two different start codons (Bouvier et al. 2000). Northern blot analysis showed two hybridizing GPS transcripts of which the short one was truncated at the 5′ side. Moreover, *in vitro* transcription-translation with the full length GPS cDNA yielded two proteins. When we take a look at the (putative) homomeric angiosperm GPSs, nearly all contain these two translation start sites (the second one is referred to as ‘alternative methionine’) (Fig. 15.2). Some GPS sequences are posted/annotated in the database as short, cytosolic forms: *Citrus sinensis* CAC16851, *Populus trichocarpa* XP002326151 and *Vitis vinifera* AAR08151 (not shown). However, in all cases, there is evidence from longer cDNA clones or gDNA that suggests these GPSs also have a longer form (Fig. 15.2). The *C. sinensis* GPS amino acid sequence is 99% identical to *C. unshiu* GPS that was annotated as a GGPS. However, there is no experimental support for GGPS activity and based on its sequence, it can be predicted that the encoded *C. unshiu* protein will have GPS activity. Other putative GPS proteins probably mis-annotated include *Allium sativum* and *Ricinus communis* “GGPSs” (AEG47694 and XP_002530137) and *Zea mays* “decaprenyl-diphosphate synthase” (ACG33955) (Fig. 15.2). Sequence searches, focusing only on the N-terminal half of the protein, yielded several *GPS* sequences deviating from the consensus (Fig. 15.2). First, the *Triticum aestivum* GPS1 (CK207187) probably does not contain the second, alternative, methionine. However, it should be kept in mind that this is a single EST sequence. Second, the *Allium cepa GPS* sequence (CF435488/CF435386) also does not contain the

alternative methionine and, moreover, does not share homology with the upstream N-terminal region. It is an open question whether this is a functional GPS or perhaps the result of a rearrangement event leading to a hybrid messenger. In conclusion: there are many GPS ESTs that contain a highly conserved region, including the alternative ATG. This suggests that more plant species could contain multiple forms of GPS targeted to different organelles.

Additionally, after characterization of three GPSs from *Abies grandis* (Burke and Croteau 2002a), it was concluded that gymnosperm GPSs are closer related to GGPSs than angiosperm GPSs (Fig. 15.1). However, Norway spruce (*Picea abies*) was recently shown to contain two GPSs, one similar to angiosperm GPSs, and one similar to gymnosperm GPSs (Schmidt and Gershenzon 2008). Furthermore, angiosperm GPSs from *Picrorhiza kurroa* and *Arnebia euchroma* resemble gymnosperm GPSs and GGPSs (Fig. 15.2). Many GPS cDNAs await characterization, which hopefully offers us insight in functions and localizations of GPSs *in planta.*

We have indicated earlier that angiosperm *GPSs* are probably single copy. That assumption is based on the characterization of the unique *GPS* gene in the Arabidopsis genome sequence. However, by searching EST databases for (partial) GPSs, it appears that some plant species probably possess a second GPS. Figure 15.2 shows two GPSs for Lotus, cotton (*Gossypium*) and wheat (*Triticum*), which are not the result of recent duplications since their sequences have diverged even more than, for instance, GPSs from different Solanaceae family members.

15.6.2 Evolution of "Green" GPS Activity

It is intriguing to see that GPS activity is encoded by such diverse groups of genes. There is no straightforward hypothesis that can explain this enzyme diversity using phylogeny and evolution of plant species. First, there seemed to be a consensus that angiosperms have "typical" homomeric GPS and gymnosperms have GGPS-like GPS. However, the gymnosperm *Picea abies*, was shown to also contain a "typical" angiosperm-like GPS (Fig. 15.2, A1) and the angiosperm *Arnebia euchroma* appeared to have a GGPS-like GPS (Fig. 15.2 B2, Singh et al. 2006 unpublished). Heteromeric GPSs were discovered in 2004 in mint and snapdragon, consisting of a large subunit very similar to GGPSs, and a small subunit only weakly similar to GGPSs. Therefore, angiosperms proved to have either homomeric or heteromeric GPSs encoded by very divergent genes. Here, we present evidence that these two classes of GPS coexist in several angiosperms. Using the GPS small subunit (GPSssu) as query, BLAST results identified GPSssu's in six genera (*H. brasiliensis* BAF98300, *R. communis* XP002532570, *P. trichocarpa* XP0022322072, *V. vinifera* XP002278023, *G. max* ABY90133, *M. truncatula* CU179894, *M. sativa* AEL29573) that also contain a homomeric GPS. Questions that come to mind are whether these GPS activities are the result of convergent evolution, and which GPS-type is the most ancient. Interestingly, we found sequences in Algae with high homology to the "typical" angiosperm GPS (Fig. 15.2 A5). However, these Algae GPSs are either short and/or do not seem to have the second methionine discussed earlier, raising the possibility that these are for instance localized to only one organelle. The primitive mosses (Fig. 15.2 A4) do have the "typical" angiosperm GPS with second methionine. Therefore, we can hypothesize that this GPS class could be the first, "ancient" GPS. Homomeric gymnosperm GPS and heteromeric angiosperm GPS probably evolved later, and independent of each other, from GGPSs.

These hypotheses postulated above suggest that all plant species have the "ancient", GPS. In some species, this GPS might have become obsolete when a new GPS-type evolved and potentially disappeared. However, the coexistence of different GPS types in various combinations described above suggests there is a possibility that these enzymes function in distinct terpene biosynthesis pathways, most likely in different tissues. As genome sequence information rapidly expands, we will be able to see whether coexistence of ancient GPS with other GPS types is indeed

common. In addition, characterization of enzyme activities of tentatively annotated prenyldiphosphate synthases will help our understanding GPS evolution.

15.7 Linking Precursors to End-Products: Using Expression Databases to form Hypotheses

The availability of microarray data from all Arabidopsis genes allows investigation of linkage between expression of precursor and end-product genes. Therefore, we have retrieved all expression data of *AtGGPS* genes as well as diterpene synthases required for synthesis of gibberellins (copalyldiphosphate synthase, CPS, and kaurene synthase, KS), carotenoids (phytoene synthase, PS), chlorophyll (geranylgeranyl reductase, GGR), and geranyllinalool synthase (DTS in Fig. 15.3 or GES) (Herde et al. 2008) in order to search for correlations that might indicate which GGPS is involved in synthesis of either of these GGPP-requiring products (Fig. 15.3)(Genevestigator.ethz.ch)(Zimmermann et al. 2004). These data showed that individual GGPS genes had highly variable expression patterns, in contrast to for instance *GPS*.

If one aims at linking genes to specific terpene synthesis pathways, subcellular localization should also be taken into account. For instance, while most GGPSs are plastid localized, GGPS1 is targeted to mitochondria and GGPS3 and 4 localize to ER or cytosol (Okada et al. 2000; Lange and Ghassemian 2003). Therefore, regardless of their expression patterns, these GGPSs are probably not involved in synthesis of gibberellin precursors, which is plastid localized (Sun and Kamiya 1997). Rather, GGPS1 might be involved in ubiquinone side chain synthesis, whereas GGPS3 and 4 might be required for protein prenylation in the cytosol. The first dedicated steps in gibberellin synthesis are catalyzed by CPS and KS, which convert GGPP via CPP to the diterpene *ent*-kaurene, respectively. KS expression is higher than CPS expression and CPS is the rate-limiting step in ent-kaurene synthesis (Silverstone et al. 1997; Fleet et al. 2003). CPS is widely expressed throughout the plant and only moderately increased in GA-requiring organs and tissues like elongating roots, hypocotyls and inflorescence. Higher expression in xylem, cork and root endodermis correlate with earlier findings on CPS localization in (pro-)vasculature (Sun and Kamiya 1997; Yamaguchi et al. 2001). Looking at expression patterns of the plastidial *GGPS11* and *GGPS12* suggests an involvement in synthesis of the photosynthetic pigments chlorophyll and carotenoids as it correlates with those of GGR and PS, being relatively high in green tissues and low in roots (Fig. 15.3, Pearson correlation coefficient, r = 0.44–0.7).

From the other plastidial GGPSs, GGPS5, 6/7 and 8 are strongest expressed in root-tips (Fig. 15.3), whereas GGPS2 and 9/10 expression occurs more in the elongating parts of roots and seedlings and vasculature, making it plausible that GGPS2 and 9/10 supply GGPP for gibberellin synthesis. An abstract (ICAR1114) presented during the 2008 Arabidopsis meeting (Arabidopsis.org) indicates that one (unspecified) GGPS is specifically involved in chlorophyll and carotenoid biosynthesis and not in gibberellin biosynthesis, thus supporting this model.

For a more thorough analysis, the expression data from Genevestigator were used for clustering expression patterns of prenyldiphosphate synthases and the first dedicated steps to gibberellin (CPS and KS) and pigment biosynthesis (GGR and PS(Y)), using Gene Cluster 3.0 (Eisen et al. 1998) or the Genevestigator cluster tool. Either the Correlation- or Euclidean- similarity metric was used for arrays from treatments as well as tissues. The results are somewhat variable, but a consistent observation is that, as indicated before, GGR, PSY, GGPS11 and GGPS12 cluster together (green). In addition, CPS and KS cluster together (blue), close to GPS, FPS1 and FPS2, also relatively close to the "pigment-cluster" (Fig. 15.7b). However, CPS and KS do not consistently cluster with another specific GGPS. The closest plastidial GGPS is GGPS2 (treatments) or GGPS9/10 or GGPS2 (tissues), also confirming our hypothesis that GGPS2 or GGPS9/10 could be involved in gibberellin biosynthesis. It is interesting to note that geranyllinalool synthase (GES), recently

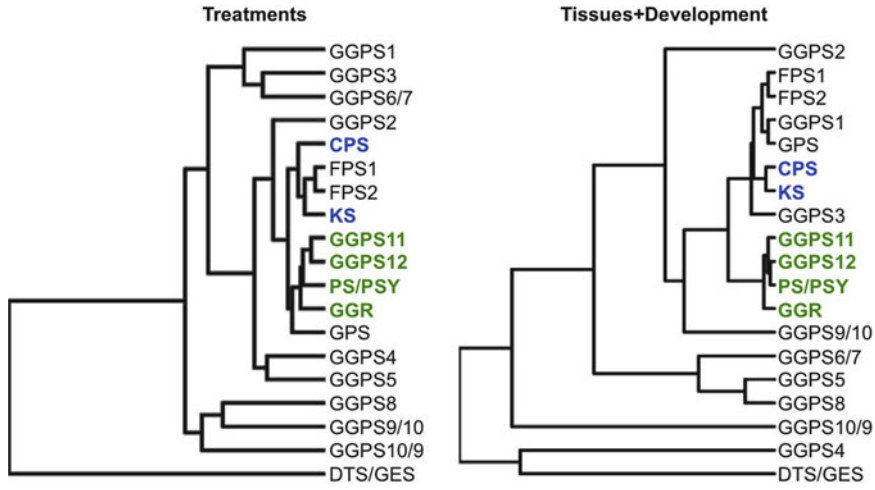

Fig. 15.7 (**b**) *Cluster analysis of gene expression profiles in the Genevestigator database for prenyldiphosphate synthases and the genes encoding the first dedicated steps to gibberellin (blue) and pigment (green) biosynthesis*. Euclidean clustering with complete linkage was used. Expression data from treatments (*left*) was log2 transformed, and data from tissues and developmental stages (*right*) was normalized to the average expression level for each gene. GGPS6/7 indicates that one probe recognizes both GGPS6 and 7 on the arrays, whereas for GGPS9 and GGPS10, two probes recognize both genes

shown to be likely cytosolic (Herde et al. 2008), clusters most closely with the cytosolic GGPS4 in tissue expression data (Fig. 15.7b) and pooled data from all treatments, tissues and developmental stages (not shown). GGPS4 might thus supply GGPP for GES.

In a broader perspective, we attempted to correlate the input and the output of the pools of GPP, FPP and GGPP using cumulative tissue-specific gene expression data from *GPS*, *FPSs* and *GGPSs* and from genes encoding enzymes that utilize prenyldiphosphates from this pool. This might give an idea whether prenyldiphosphate synthesis is adjusted to the variable requirements throughout different organs. We observed for instance that expression of *FPSs* is closely correlated with expression of genes encoding enzymes that require FPP (Fig. 15.4) ($r = 0.7$). In contrast, GPP synthesis and GPP usage by monoterpene synthases (MTS) are not correlated (Fig. 15.4) ($r = 0.1$). *GPS* expression is relatively high in organs that hardly produce monoterpenes, indicating that GPP might be synthesized for other terpene products than only monoterpenes, which we have indeed confirmed for gibberellins. Figure 15.4a shows that cumulative expression of MTSs is highly variable between organs.

Moreover, contribution of individual MTSs also differs. In seedlings, radicle and roots, the 1,8-cineole synthase gene (At3g25820/30) is the highest expressed MTS (Chen et al. 2004), whereas in flowers, inflorescence, petals and stamen, the *S*-linalool synthase gene (At1g61680) and the myrcene/ocimene synthase gene (At2g24210) are highly expressed (Bohlmann et al. 2000; Chen et al. 2003). Interestingly, the MTS gene (At3g25810) expressed most abundantly in carpel and ovary is specifically expressed in these organs and generates many different products (e.g. (*E*)-β-ocimene, β-myrcene, α-pinene, sabinene, β-pinene) that might serve as antimicrobials (Chen et al. 2003). In addition, sepals specifically express the ocimene synthase gene (At4g16740) (Faldt et al. 2003) next to the *S*-linalool synthase gene. Remember that these data concern untreated plants. Upon for instance insect herbivory or jasmonate treatment, expression of some monoterpene synthases is induced (Van Poecke et al. 2001; Faldt et al. 2003), but also upon pathogen infection (www.genevestigator.ethz.ch, data not shown).

Figure 15.4 shows that *FPS* expression is correlated to expression of genes encoding FPP-using enzymes. The two *FPS* genes are not specifically regulated and probably both contribute

to synthesis of all FPP requiring metabolites. Interestingly, expression of protein farnesyl transferases and squalene synthases required for primary steroid synthesis (growth and developmental hormones, membrane components) is ubiquitous, whereas expression of genes involved in secondary metabolism is organ-specific (Fig. 15.4). Lupeol synthases are predominantly expressed in floral tissues, pedicel and stem and are putatively involved in synthesis of antimicrobial triterpenes in the waxy cuticle (Guhling et al. 2006). A group of uncharacterized oxidosqualene-dependent triterpene synthase genes is highly expressed in roots but also in radicle, seed and pollen, where they might provide components with antimicrobial activity (Haralampidis et al. 2001; Haralampidis et al. 2002). Expression of sesquiterpene synthases (20 genes) is abundant in flowers and roots. At5g23960 and At5g44630 are expressed in carpel, ovary, stigma and nectaries, where they produce volatile terpenes ((−)-*E*-β-caryophyllene and α-humulene or (+)-thujopsene, (+)-β-chamigrene, β-acoradiene, *E*-β-farnesene and (+)-α-barbatene, respectively), which probably serve as antimicrobials (Chen et al. 2003; Tholl et al. 2005). Interestingly, At3g14520 is specifically expressed in siliques. In roots, sesquiterpene synthase genes At1g31950, At1g33750, At1g70080 and At5g48110 are mainly expressed in the root tips, whereas in the endoderm, vasculature, radicle and hypocotyl, At3g29410, At5g48110 and to a lesser extent At4g20210, At4g20230, At1g66020 and At4g13280 are most abundant. The latter generates (−)-β-bisabolene and is also induced in leaves upon wounding (Ro et al. 2006).

Figure 15.4 shows that cumulative *GGPS* expression moderately correlates with expression of genes encoding GGPP-requiring enzymes ($r = 0.35$). Only in the root tip, root cap and atrichoblast (non-hair epidermal cells), *GGPS* expression seemed relatively high and could be attributed to GGPS5, 6/7 and 8, whose expression was specific for these tissues (see also Fig. 15.3). It is not clear what role GGPSs could play in root tips and epidermis but they might provide precursors for strigolactone synthesis (Gomez-Roldan et al. 2008). In root endodermis and vasculature, carotenoids as well as gibberellins might be synthesized but no diterpene phytoalexins since, in contrast to rice (Otomo et al. 2004), Arabidopsis does not possess such a diterpene synthase. It is apparent that protein geranylgeranyl transferases are constitutively present and that GGR and PS are the predominant GGPP using enzymes in aerial parts of the plant. Above, we have already indicated that the highly expressed GGPS11 and 12 probably supply this GGPP. However, in stamen (flower), GGPS4 is the major GGPS and likely involved in synthesis of yellow-colored carotenoids. Obviously, the diterpene synthases DTS and CPS are relatively low in all tissues; only DTS expression can be seen in Fig. 15.3 in leaves and sepals. KS was not included since this enzyme does not directly use GGPP.

To summarize the level of gene regulation for enzymes synthesizing or using prenyl diphosphates, with regard to organ-specificity and responses to treatments, we determined the deviation of the gene expression level from the average (arbitrarily set to 1). This calculation was performed for the different organs or treatments and it was used as a measure for the differential regulation of a gene or group of genes (Fig. 15.4d). These calculations indicated that *GPS* expression is constant, while expression of GPP requiring monoterpene synthases greatly varies between organs and upon treatments. Furthermore, *FPS* expression differs moderately among organs and is not clearly regulated by treatments, whereas expression of genes encoding FPP utilizing enzymes is again more variable. In contrast, the variation in expression of GGPS genes between plant organs is much larger than would be expected from the relatively ubiquitous requirement of GGPP. In the expression analyses described above, we have not included nine polyprenyl transferases (At1g17050, At1g78510, At2g23410, At5g58770, At5g58780, At2g17570, At5g60500, At4g23660, At3g11950) of which five are cytosolic, three mitochondrial and one plastidial (Lange and Ghassemian 2003). It is unknown which substrates they use (GPP, FPP or GGPP).

The above mentioned data surveys support most of the earlier research results found in literature, but also allowed formation or confirmation of hypotheses about terpene precursor fluxes.

First, *GPS* is probably used for other terpenes than only monoterpenes and, second, *GGPS* genes are subject to specific regulation, more than *GPS* or *FPS*, suggesting that they contribute to multiple GGPP pools for various products. These data are very useful but should only be used as tools to formulate hypotheses that should be verified and repeated in experimental systems. In addition, one should take into account that expression data of treatments might be collected from whole plants or other organs than the ones of interest. A general remark about expression analysis is that even in isolated organs, expression can vary greatly between different cell-types that are pooled upon analysis. Finally, gene expression might not always be a correct representation of protein levels or activity due to post-transcriptional regulation mechanisms.

15.8 Conclusion

If only one thing from our studies has to be emphasized, it would be the fact that we need more manipulation of prenyldiphosphate synthases *in planta*. *In vitro* studies and bioinformatics can give hints leading to useful hypotheses, but up- or downregulation of prenyldiphosphate synthases (if possible combined with localisation studies) will lead to direct (and sometimes surprising) insight in their real function.

Acknowledgements We thank Dr. Petra Bleeker for critically reading the manuscript.

References

Achard P, Liao L, Jiang C, Desnos T, Bartlett J, Fu X, Harberd NP (2007) DELLAs contribute to plant photomorphogenesis. Plant Physiol 143:1163–1172

Aharoni A, Giri AP, Deuerlein S et al (2003) Terpenoid metabolism in wild-type and transgenic *Arabidopsis* plants. Plant Cell 15:2866–2884

Ament K, Van Schie CC, Bouwmeester HJ, Haring MA, Schuurink RC (2006) Induction of a leaf specific geranylgeranyl pyrophosphate synthase and emission of (E, E)-4,8,12-trimethyltrideca-1,3,7,11-tetraene in tomato are dependent on both jasmonic acid and salicylic acid signaling pathways. Planta 224:1197–1208

Besser K, Harper A, Welsby N et al (2009) Divergent regulation of terpenoid metabolism in the trichomes of wild and cultivated tomato species. Plant Physiol 149:499–514

Bohlmann J, Martin D, Oldham NJ, Gershenzon J (2000) Terpenoid secondary metabolism in *Arabidopsis thaliana*: cDNA cloning, characterization, and functional expression of a myrcene/(*E*)-β-ocimene synthase. Arch Biochem Biophys 375:261–269

Bouvier F, Suire C, D'Harlingue A, Backhaus RA, Camara B (2000) Molecular cloning of geranyl diphosphate synthase and compartmentation of monoterpene synthesis in plant cells. Plant J 24:241–252

Burke C, Croteau R (2002a) Geranyl diphosphate synthase from *Abies grandis*: cDNA isolation, functional expression, and characterization. Arch Biochem Biophys 405:130–136

Burke C, Croteau R (2002b) Interaction with the small subunit of geranyl diphosphate synthase modifies the chain length specificity of geranylgeranyl diphosphate synthase to produce geranyl diphosphate. J Biol Chem 277:3141–3149

Burke CC, Wildung MR, Croteau R (1999) Geranyl diphosphate synthase: cloning, expression, and characterization of this prenyltransferase as a heterodimer. Proc Natl Acad Sci USA 96:13062–13067

Cervantes-Cervantes M, Gallagher CE, Zhu CF, Wurtzel ET (2006) Maize cDNAs expressed in endosperm encode functional farnesyl diphosphate synthase with geranylgeranyl diphosphate synthase activity. Plant Physiol 141:220–231

Chang YJ, Kim BR, Kim SU (2005) Metabolic flux analysis of diterpene biosynthesis pathway in rice. Biotechnol Lett 27:1375–1380

Chen F, Tholl D, D'Auria JC, Farooq A, Pichersky E, Gershenzon J (2003) Biosynthesis and emission of terpenoid volatiles from *Arabidopsis* flowers. Plant Cell 15:481–494

Chen F, Ro DK, Petri J, Gershenzon J, Bohlmann J, Pichersky E, Tholl D (2004) Characterization of a root-specific *Arabidopsis* terpene synthase responsible for the formation of the volatile monoterpene 1,8-cineole. Plant Physiol 135:1956–1966

Clastre M, Bantignies B, Feron G, Soler E, Ambid C (1993) Purification and characterization of geranyl diphosphate synthase from *Vitis vinifera* L. cv Muscat de Frontignan cell cultures. Plant Physiol 102:205–211

Cookson PJ, Kiano JW, Shipton CA et al (2003) Increases in cell elongation, plastid compartment size and phytoene synthase activity underlie the phenotype of the *high pigment-1* mutant of tomato. Planta 217:896–903

Croteau R, Purkett PT (1989) Geranyl pyrophosphate synthase: characterization of the enzyme and evidence that this chain-length specific prenyltransferase is associated with monoterpene biosynthesis in sage (*Salvia officinalis*). Arch Biochem Biophys 271:524–535

Cunillera N, Arró M, Delourme D, Karst F, Boronat A, Ferrer A (1996) *Arabidopsis thaliana* contains two

differentially expressed farnesyl-diphosphate synthase genes. J Biol Chem 271:7774–7780

Cunillera N, Boronat A, Ferrer A (1997) The *Arabidopsis thaliana FPS1* gene generates a novel mRNA that encodes a mitochondrial farnesyl-diphosphate synthase isoform. J Biol Chem 272:15381–15388

Cunillera N, Boronat A, Ferrer A (2000) Spatial and temporal patterns of GUS expression directed by 5' regions of the *Arabidopsis thaliana* farnesyl diphosphate synthase genes *FPS1* and *FPS2*. Plant Mol Biol 44:747–758

Dogbo O, Camara B (1987) Purification of isopentenyl pyrophosphate isomerase and geranylgeranyl pyrophosphate synthase from *Capsicum* chromoplasts by affinity chromatography. Biochim Biophys Acta 920:140–148

Ducluzeau A-L, Wamboldt Y, Elowsky CG, Mackenzie SA, Schuurink RC, Basset GJC (2012) Gene network reconstruction identifies the authentic trans-prenyl diphosphate synthase that makes the solanesyl moiety of ubiquinone-9 in Arabidopsis. Plant J 69:366–375

Eisen MB, Spellman PT, Brown PO, Botstein D (1998) Cluster analysis and display of genome-wide expression patterns. Proc Natl Acad Sci USA 95:14863–14868

Faldt J, Arimura G, Gershenzon J, Takabayashi J, Bohlmann J (2003) Functional identification of AtTPS03 as (*E*)-β-ocimene synthase: a monoterpene synthase catalyzing jasmonate- and wound-induced volatile formation in *Arabidopsis thaliana*. Planta 216:745–751

Feng S, Martinez C, Gusmaroli G et al (2008) Coordinated regulation of *Arabidopsis thaliana* development by light and gibberellins. Nature 451:475–479

Ferrer A, Closa M, Vranova E, Bortolotti C, Bigler L, Arró M, Gruissem W (2010) The *Arabidopsis thaliana* FPP synthase isozymes have overlapping and specific functions in isoprenoid biosynthesis, and complete loss of FPP synthase activity causes early developmental arrest. Plant J 63:512–525

Fleet CM, Yamaguchi S, Hanada A, Kawaide H, David CJ, Kamiya Y, Sun TP (2003) Overexpression of *AtCPS* and *AtKS* in *Arabidopsis* confers increased *ent*-kaurene production but no increase in bioactive gibberellins. Plant Physiol 132:830–839

Fray RG, Wallace A, Fraser PD, Valero D, Hedden P, Bramley PM, Grierson D (1995) Constitutive expression of a fruit phytoene synthase gene in transgenic tomatoes causes dwarfism by redirecting metabolites from the gibberellin pathway. Plant J 8:693–701

Galpaz N, Ronen G, Khalfa Z, Zamir D, Hirschberg J (2006) A chromoplast-specific carotenoid biosynthesis pathway is revealed by cloning of the tomato white-flower locus. Plant Cell 18:1947–1960

Gomez-Roldan V, Fermas S, Brewer PB et al (2008) Strigolactone inhibition of shoot branching. Nature 455:189–194

Guhling O, Hobl B, Yeats T, Jetter R (2006) Cloning and characterization of a lupeol synthase involved in the synthesis of epicuticular wax crystals on stem and hypocotyl surfaces of *Ricinus communis*. Arch Biochem Biophys 448:60–72

Haralampidis K, Bryan G, Qi X, Papadopoulou K, Bakht S, Melton R, Osbourn A (2001) A new class of oxidosqualene cyclases directs synthesis of antimicrobial phytoprotectants in monocots. Proc Natl Acad Sci USA 98:13431–13436

Haralampidis K, Trojanowska M, Osbourn AE (2002) Biosynthesis of triterpenoid saponins in plants. Adv Biochem Eng Biotechnol 75:31–49

Heide L, Berger U (1989) Partial purification and properties of geranyl pyrophosphate synthase from *Lithospermum erythrorhizon* cell cultures. Arch Biochem Biophys 273:331–338

Herde M, Gärtner K, Köllner TG et al (2008) Identification and regulation of TPS04/GES, an Arabidopsis geranyllinalool synthase catalyzing the first step in the formation of the insect-induced volatile C16-homoterpene TMTT. Plant Cell 20:1152–1168

Hsiao YY, Jeng MF, Tsai WC et al (2008) A novel homodimeric geranyl diphosphate synthase from the orchid *Phalaenopsis bellina* lacking a DD(X)2-4D motif. Plant J 55:719–733

Hsieh FL, Chang TH, Ko TP, Wang AH (2011) Structure and mechanism of an Arabidopsis medium/long-chain-length prenyl pyrophosphate synthase. Plant Physiol 155:1079–1090

Huang M, Abel C, Sohrabi R, Petri J, Haupt I, Cosimano J, Gershenzon J, Tholl D (2010) Variation of herbivore-induced volatile terpenes among Arabidopsis ecotypes depends on allelic differences and subcellular targeting of two terpene synthases, TPS02 and TPS03. Plant Physiol 153:1293–1310

Laferrière A, Beyer P (1991) Purification of geranylgeranyl diphosphate synthase from *Sinapis alba* etioplasts. Biochim Biophys Acta 1077:167–172

Lange BM, Ghassemian M (2003) Genome organization in *Arabidopsis thaliana*: a survey for genes involved in isoprenoid and chlorophyll metabolism. Plant Mol Biol 51:925–948

Laskaris G, van der Heijden R, Verpoorte R (2000) Purification and partial characterisation of geranylgeranyl diphosphate synthase, from *Taxus baccata* cell cultures – An enzyme that regulates taxane biosynthesis. Plant Sci 153:97–105

Lee S, Badieyan S, Bevan DR, Herde M, Gatz C, Tholl D (2010) Herbivore-induced and floral homoterpene volatiles are biosynthesized by a single P450 enzyme (CYP82G1) in *Arabidopsis*. Proc Natl Acad Sci USA 107:21205–21210

Liang PH, Ko TP, Wang AH (2002) Structure, mechanism and function of prenyltransferases. Eur J Biochem 269:3339–3354

Lindgren LO, Stålberg KG, Höglund AS (2003) Seed-specific overexpression of an endogenous *Arabidopsis* phytoene synthase gene results in delayed germination and increased levels of carotenoids, chlorophyll, and abscisic acid. Plant Physiol 132:779–785

Manzano D, Busquets A, Closa M et al (2006) Overexpression of farnesyl diphosphate synthase in *Arabidopsis* mitochondria triggers light-dependent

lesion formation and alters cytokinin homeostasis. Plant Mol Biol 61:195–213

Masferrer A, Arró M, Manzano D et al (2002) Overexpression of *Arabidopsis thaliana* farnesyl diphosphate synthase (FPS1S) in transgenic *Arabidopsis* induces a cell death/senescence-like response and reduced cytokinin levels. Plant J 30:123–132

Okada K, Saito T, Nakagawa T, Kawamukai M, Kamiya Y (2000) Five geranylgeranyl diphosphate synthases expressed in different organs are localized into three subcellular compartments in *Arabidopsis*. Plant Physiol 122:1045–1056

Okada K, Kawaide H, Kuzuyama T, Seto H, Curtis IS, Kamiya Y (2002) Antisense and chemical suppression of the nonmevalonate pathway affects *ent*-kaurene biosynthesis in *Arabidopsis*. Planta 215:339–344

Otomo K, Kanno Y, Motegi A et al (2004) Diterpene cyclases responsible for the biosynthesis of phytoalexins, momilactones A, B, and oryzalexins A-F in rice. Biosci Biotechnol Biochem 68:2001–2006

Prisic S, Peters RJ (2007) Synergistic substrate inhibition of *ent*-copalyl diphosphate synthase: a potential feed-forward inhibition mechanism limiting gibberellin metabolism. Plant Physiol 144:445–454

Reiter RS, Coomber SA, Bourett TM, Bartley GE, Scolnik PA (1994) Control of leaf and chloroplast development by the *Arabidopsis* gene *pale cress*. Plant Cell 6:1253–1264

Ro DK, Ehlting J, Keeling CI, Lin R, Mattheus N, Bohlmann J (2006) Microarray expression profiling and functional characterization of *AtTPS* genes: duplicated *Arabidopsis thaliana* sesquiterpene synthase genes At4g13280 and At4g13300 encode root-specific and wound-inducible (*Z*)-γ-bisabolene synthases. Arch Biochem Biophys 448:104–116

Schilmiller AL, Schauvinhold I, Larson M, Xu R, Charbonneau AL, Schmidt A, Wilkerson C, Last RL, Pichersky E (2009) Monoterpenes in the glandular trichomes of tomato are synthesized from a neryl diphosphate precursor rather than geranyl diphosphate. Proc Natl Acad Sci USA 106(26):10865–10870

Schmidt A, Gershenzon J (2008) Cloning and characterization of two different types of geranyl diphosphate synthases from Norway spruce (*Picea abies*). Phytochemistry 69:49–57

Schmidt A, Wächtler B, Temp U, Krekling T, Séguin A, Gershenzon J (2010) A bifunctional geranyl and geranylgeranyl diphosphate synthase is involved in terpene oleoresin formation in *Picea abies*. Plant Physiol 152:639–655

Silverstone AL, Chang C, Krol E, Sun TP (1997) Developmental regulation of the gibberellin biosynthetic gene *GA1* in *Arabidopsis thaliana*. Plant J 12:9–19

Singh RS, Gara RK, Bhardwaj PK, Kaachra A, Malik S, Kumar R, Sharma M, Ahuja PS, Kumar S (2010) Expression of 3-hydroxy-3-methylglutaryl-CoA reductase, p-hydroxybenzoate-mgeranyltransferase and genes of phenylpropanoid pathway exhibits positive correlation with shikonins content in arnebia [Arnebia euchroma (Royle) Johnston]. BMC Mol Biol 2010, 11:88 (http://www.biomedcentral.com/1471-2199/11/88)

Sommer A, Severin K, Camara B, Heide L (1995) Intracellular localization of geranyl pyrophosphate synthase from cell cultures of *Lithospermum erythrorhizon*. Phytochemistry 38:623–627

Sun TP, Kamiya Y (1997) Regulation and cellular localization of *ent*-kaurene synthesis. Physiol Plant 101: 701–708

Takaya A, Zhang YW, Asawatreratanakul K et al (2003) Cloning, expression and characterization of a functional cDNA clone encoding geranylgeranyl diphosphate synthase of *Hevea brasiliensis*. Biochim Biophys Acta 1625:214–220

Tholl D, Kish CM, Orlova I, Sherman D, Gershenzon J, Pichersky E, Dudareva N (2004) Formation of monoterpenes in *Antirrhinum majus* and *Clarkia breweri* flowers involves heterodimeric geranyl diphosphate synthases. Plant Cell 16:977–992

Tholl D, Chen F, Petri J, Gershenzon J, Pichersky E (2005) Two sesquiterpene synthases are responsible for the complex mixture of sesquiterpenes emitted from *Arabidopsis* flowers. Plant J 42:757–771

Van Poecke RM, Posthumus MA, Dicke M (2001) Herbivore-induced volatile production by *Arabidopsis thaliana* leads to attraction of the parasitoid *Cotesia rubecula*: chemical, behavioral, and gene-expression analysis. J Chem Ecol 27:1911–1928

van Schie CCN, Haring MA, Schuurink RC (2007a) Tomato linalool synthase is induced in trichomes by jasmonic acid. Plant Mol Biol 64:251–263

van Schie CCN, Ament K, Schmidt A, Lange T, Haring MA, Schuurink RC (2007b) Geranyl diphosphate synthase is required for biosynthesis of gibberellins. Plant J 52:752–762

Wang G, Dixon RA (2009) Heterodimeric geranyl(geranyl) diphosphate synthase from hop (*Humulus lupulus*) and the evolution of monoterpene biosynthesis. Proc Natl Acad Sci USA 106:9914–9919

Wang KC, Ohnuma S (2000) Isoprenyl diphosphate synthases. Biochim Biophys Acta 1529:33–48

Wu S, Schalk M, Clark A, Miles RB, Coates R, Chappell J (2006) Redirection of cytosolic or plastidic isoprenoid precursors elevates terpene production in plants. Nat Biotechnol 24:1441–1447

Yamaguchi S, Kamiya Y, Sun TP (2001) Distinct cell-specific expression patterns of early and late gibberellin biosynthetic genes during *Arabidopsis* seed germination. Plant J 28:443–453

Zhu XF, Suzuki K, Saito T et al (1997) Geranylgeranyl pyrophosphate synthase encoded by the newly isolated gene *GGPS6* from *Arabidopsis thaliana* is localized in mitochondria. Plant Mol Biol 35:331–341

Zimmermann P, Hirsch-Hoffmann M, Hennig L, Gruissem W (2004) GENEVESTIGATOR. *Arabidopsis* microarray database and analysis toolbox. Plant Physiol 136:2621–2632

Gibberellin Phytohormone Metabolism

16

Reuben J. Peters

Abstract

Gibberellin (GA) phytohormones are potent and complex diterpenoids biosynthesized by a phylogenetically diverse group of organisms. Originally discovered in the phytopathogen *Fusarium fujikuroi*, it is now appreciated that analogous metabolism exists in plants, fungi, and bacteria. Intriguingly, each of these broad groups of organisms appears to have independently evolved biosynthetic pathways leading to the production of these complex natural products. Our current understanding of the diverse GA metabolism in each group is presented here, with an emphasis on the characteristics, particularly relevant enzymatic type, that differentiate their GA biosynthetic pathways from each other. Furthermore, in plants GA biosynthesis shares steps in common with other isoprenoid and related diterpenoid natural products, and an overview is provided of the necessary metabolic integration as well as various catabolic process involved in breaking down bioactive GAs *in planta*.

Keywords

Gibberellins • Phytohormones • Diterpenoid natural products • Labdane-related • Terpene synthases • Cytochromes P450 • Dioxygenases • Metabolism • Biosynthesis

16.1 Introduction

Gibberellins, originally known as gibberellin A and gibberellic acid (hence the commonly observed GA abbreviation), are a group of diterpenoid natural products that include important phytohormones involved in many aspects of higher plant growth and development (MacMillan 1997). The well-understood nature of the

R.J. Peters (✉)
Department of Biochemistry, Biophysics, and Molecular Biology, Iowa State University,
4216 Mol. Biol. Bldg., Ames, IA 50011, USA
e-mail: rjpeters@iastate.edu

T.J. Bach and M. Rohmer (eds.), *Isoprenoid Synthesis in Plants and Microorganisms: New Concepts and Experimental Approaches*, DOI 10.1007/978-1-4614-4063-5_16,

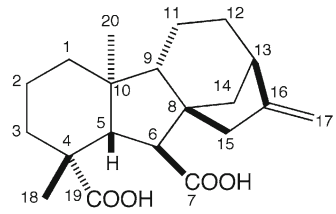

Fig. 16.1 Basic gibberellane structure, with numbering of constituent carbon atoms as indicated

bioactive GA phytohormones is owed, at least to some extent, to the fortuitous production of analogous natural products by *Fusarium fujikuroi* (previously called *Gibberella fujikuroi*). This fungus is the causative agent of bakanae, the "foolish seedling" disease of rice. Indeed, the production of bioactive GAs by *F. fujikuroi* is directly responsible for the observed excessive stem elongation disease symptoms, immediately suggesting a physiological role for similar compounds in promoting stem elongation during normal plant development.

Cultures of *F. fujikuroi* provided a ready source of GAs for early investigations, beginning with isolation of bioactive components; first in Japan (Yabuta and Hayashi 1939a, b) (Yabuta and Sumiki 1938), while later follow-up work in England and the USA led to isolation of a similar, but not identical, metabolite (Cross 1955; Stodola et al. 1955). In each case, these were closely followed by reports that the purified compounds restored normal growth to dwarf varieties while having relatively little effect on wild-type, in several higher plant species, consistent with the hypothesis that similar compounds might operate in normal plant development (Brian and Hemming 1955; Phinney 1956; Tudzynski and Hölter 1998). Evidence for the occurrence of endogenous, similar compounds in higher plants soon followed (Radley 1956; Phinney et al. 1957).

The initially isolated GAs were suggested to have a tetracyclic lactone structure, which was confirmed by crystallographic structural determination (Hartsuck and Lipscomb 1963; Mende et al. 1997). Radio-tracer studies further demonstrated that these natural products were isoprenoid, specifically diterpenoid, in nature (Rojas et al. 2001). All diterpenoid natural products since identified as containing the corresponding tetracyclic 6-5-6-5 *ent*-gibberellane ring structure have been grouped together and termed gibberellins (GAs), although most do not exhibit the originally observed growth-promoting effects in plants (Fig. 16.1). Note that the bioactive GAs are all 19-carbon (C_{19}) norditerpenoids, wherein carbon 20 (C20) has been replaced by a γ-lactone ring connecting C10,19. The GAs are distinguished by subscripted number, gibberellin A_1–A_n (GA_1–GA_n), which has been assigned essentially on the basis of their order of discovery (MacMillan and Takahashi 1968), with *n* currently at 136 (www.plant-hormones.info/gibberellins.htm).

16.2 Physiological Roles

As suggested by the observed biological activity of the originally isolated gibberellins from *F. fujikuroi*, the bioactive GAs have a clear role in promoting vegetative growth (e.g., shoot/stem and root elongation, as well as leaf expansion), with mutants in GA metabolism typically exhibiting significantly reduced shoot/stem size as their most obvious phenotype (Fig. 16.2). Strikingly, the semidwarf strains of rice and wheat that provided the physical basis (i.e., shorter stronger stalks) for much of the increased cereal grain yield of the "Green Revolution" were eventually found to arise from alterations in GA metabolism (Hedden 2003). This emphasizes the important role that phytohormones can play in agriculture.

In addition to excessive shoot elongation, another dominant characteristic of the bakanae disease is the pale yellow color of infected seedlings, with some resemblance to etiolated (dark-grown) seedlings. Perhaps not surprisingly then, the bioactive GAs also suppress chlorophyll maturation, playing an antagonistic role in photomorphogenesis (e.g., the process of de-etiolation) in normal plant development (Garcia-Martinez and Gil 2001).

Bioactive GAs also play a role in seed germination, and their ability to promote cereal germination has been extensively studied. Indeed, the bioactive GA_3 metabolite produced in large

Fig. 16.2 Effect on bioactive GA deficiency on plant growth and development in *Arabidopsis thaliana* (wild-type plant on *right*, GA-deficient plant on *left*)

quantities by *F. fujikuroi*, with wild isolates yielding up to 1 g/L of culture and optimized industrial strains over fivefold more, has been put to practical use in accelerating the barley grain malting process in beer brewing (Bruckner and Blechschmidt 1991). Other uses for GA_3 are more directly agricultural in nature, primarily related to the role of bioactive GAs in governing reproductive development, with the primary commercial application of GA_3 being in the grape sector where it increases berry set and size, particularly in seedless varieties. Secondary uses include application to citrus crops for similar purposes (i.e., increased yield and synchronized development, along with delayed maturation and abscission) as well as to sugarcane to increase both yield and sugar content (Bruckner and Blechschmidt 1991). Consistent with these effects, bioactive GAs play a role in the morphological initiation of both leaves and flowers (Fleet and Sun 2005).

The production of bioactive GAs by *F. fujikuroi* has been suggested to aid the pathogenic lifestyle of this fungus. However, there are examples of other, non-plant pathogenic fungi that also produce GAs. In addition, certain bacteria have been shown to produce bioactive GAs, including plant growth-promoting bacteria such as the *Bradyrhizobium japonicum* commonly applied to commercially grown soybean, and it is speculated that such phytohormone production contributes to the observed resulting increase in plant biomass. Intriguingly, despite the common complex "end product," the biosynthetic pathways leading to bioactive GAs in plant and fungi provide an example of convergent evolution (Hedden et al. 2001), with that in bacteria potentially representing a third, independently evolved pathway for production of this phylogenetically widespread metabolite (Fischbach and Clardy 2007). This presumably reflects the profound effects of the highly bioactive GAs on plant physiology, with the application of nanogram quantities to individual plants being sufficient to observe readily detectable effects (Phinney 1956), providing strong selective pressure for the evolution of such biosynthesis in these diverse organisms.

16.3 Biosynthesis and Regulation

16.3.1 Isoprenoid Precursor Production

Like all isoprenoids, GAs are formed from dimethylallyl diphosphate (DMAPP) and isopentenyl diphosphate (IPP) precursors, which are derived from the mevalonate (MEV) or methylerythritol

phosphate (MEP) pathway, depending on the producing organism and subcellular compartment (Rohmer 2008). For example, in plants GA biosynthesis is initiated in the plastids predominantly using DMAPP/IPP from the MEP pathway (Kasahara et al. 2002). In all cases, DMAPP and IPP are shared with many other important isoprenoid-dependent physiological processes, including electron transport and photosynthesis. A relevant example arises from the geranylgeranyl diphosphate (GGPP) formed by coupling of one molecule of DMAPP with three of IPP. This C_{20} isoprenoid precursor can be used to initiate gibberellin (or other diterpenoid) biosynthesis, but its primary metabolic fate in plants is incorporation into photosynthetic pigments, as GGPP is a direct precursor of both carotenoids and the phytol side chain of chlorophyll (Fig. 16.3). Accordingly, control exerted at the level of the relevant MEP pathway is presumably targeted at regulation of isoprenoid metabolism more generally, with any effect on GA metabolism being largely tangential.

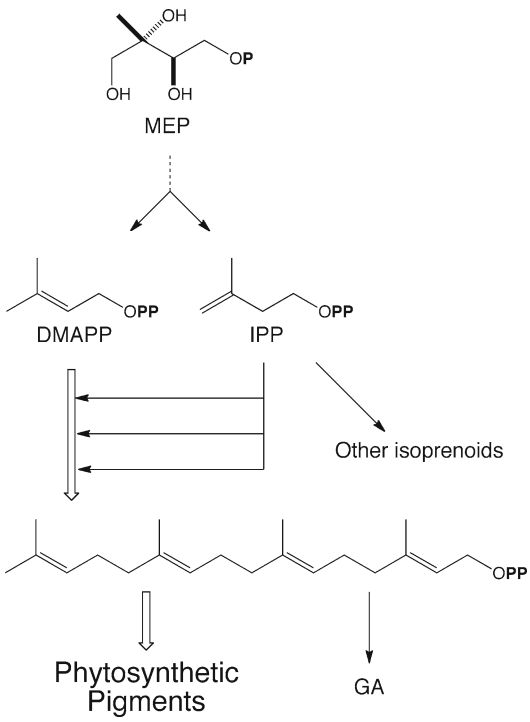

Fig. 16.3 Plant plastid isoprenoid biosynthesis (major flux to photosynthetic pigments indicated by *open arrows*)

16.3.2 Pre-GA: The Early Steps

GA biosynthesis is generally considered as being initiated by the cyclization of GGPP to *ent*-labdadienyl/copalyl diphosphate (*ent*-CPP) catalyzed by a stereospecific CPP synthase (CPS). However, it should be noted that there are many secondary (i.e., more specialized) metabolites that are derived from *ent*-CPP besides GA. These are members of the labdane-related diterpenoid superfamily of natural products, which boasts ~7,000 known members (Peters 2010), with many plant-specialized metabolites being derived from *ent*-CPP. Nevertheless, CPS is considered the "gatekeeper" to GA metabolism, as transcription of the corresponding gene, at least in *Arabidopsis thaliana*, is tightly controlled (Silverstone et al. 1997). In addition, it appears that the activity of plant CPS involved in GA metabolism is limited by a feedforward regulatory mechanism via synergistic substrate inhibition exerted by both GGPP and, particularly, the requisite divalent magnesium ion enzymatic cofactor, whose concentration varies in plastids (e.g., in response to light) (Prisic and Peters 2007). By contrast, CPS involved in more specialized metabolism do not exhibit the same sensitivity to such substrate/cofactor inhibition (Prisic and Peters 2007; Hayashi et al. 2008), and the basis for this has been traced to a single amino acid switch whose identity is tightly coupled to this inhibitiory effect (Mann et al. 2010). Thus, this mechanism seems to represent a further layer of regulation acting to limit production of the highly active phytohormone forms of GA.

Production of the relevant diterpene olefin intermediate *ent*-kaur-16-ene from *ent*-CPP is mediated by *ent*-kaurene synthases (KS). Notably, while CPS and KS both mediate carbocation-driven cyclization and, in the case of KS, rearrangement reactions their mechanisms for formation of the initial carbocation are clearly distinct (Fig. 16.4). CPS are prototypical class II

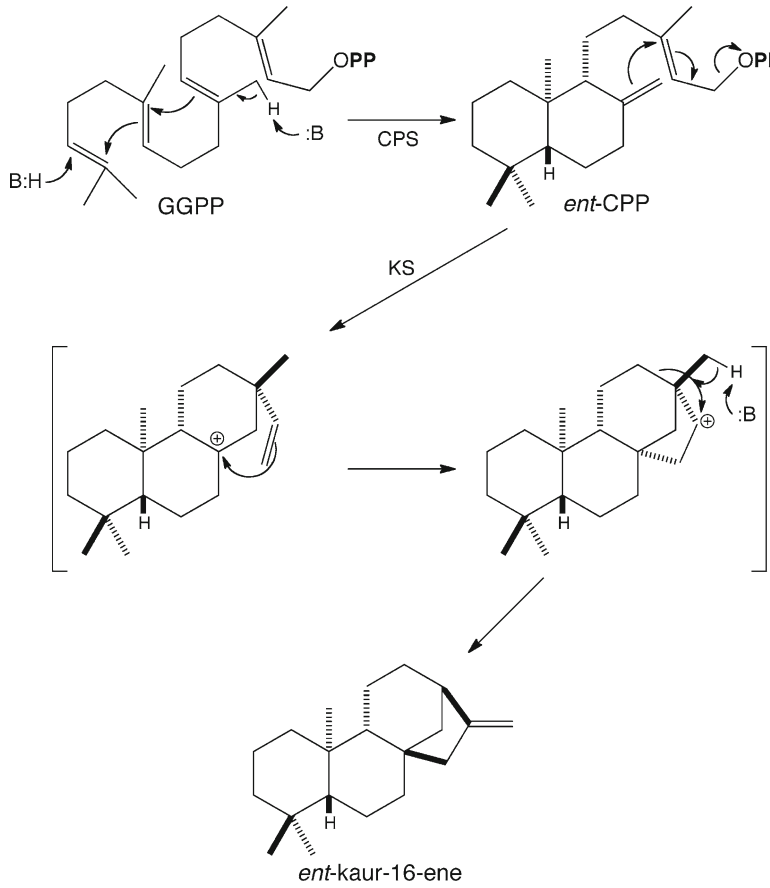

Fig. 16.4 Cyclization of GGPP to *ent*-CPP and then *ent*-kaurene mediated by the class II diterpene cyclase CPS and the class I terpene synthase KS, respectively

diterpene cyclases, carrying out protonation of the terminal C14,15 double bond in GGPP to produce the initial carbocation using a conserved DXDD motif (Prisic et al. 2007). On the other hand, KS mediates ionization of the allylic diphosphate ester bond in a reaction mechanism that critically depends on divalent magnesium ions bound by conserved DDXXD and NDX_2TX_3E motifs (Zhou and Peters 2009). However, there is a clear phylogenetic relationship between these two mechanistically distinct enzymes (Bohlmann et al. 1998). Examples are known of plant diterpene synthases that mediate both types of reactions, which are carried out in separate active sites (Peters et al. 2001), including a bifunctional diterpene synthase from the bryophyte (moss) *Physcomitrella patens* that produces, at least in part, *ent*-kaurene (Hayashi et al. 2006). Further, GA-producing fungi contain similarly bifunctional diterpene synthases responsible for both CPS and KS activities (Kawaide et al. 1997; Tudzynski et al. 1998), wherein the CPS and KS activities are partially separable into different regions of the enzyme that contain the conserved motifs associated with each (Kawaide et al. 2000). In all these cases, the enzymes are of similar length. Intriguingly, it has been demonstrated that GA-producing bacteria such as *B. japonicum* contain separate CPS and KS, again with the motifs associated with the activity of each (Morrone et al. 2009). The size of the bacterial CPS and KS is correlated with the putative

separate domains containing the distinct CPS and KS active sites in plant and fungal diterpene synthases (Fig. 16.5), which suggests the possibility of homology between the diterpene synthases from these phylogenetically diverse organisms. Indeed, very recently reported crystal structures have demonstrated the expected domain structure, consistent with fusion of an ancestral CPS and KS to form the precursor to all plant (di)terpene synthases (Köksal et al. 2011a, b).

The *ent*-kaur-16-ene diterpene olefin intermediate undergoes a series of oxidative reactions that transform its C19-methyl group into a carboxylic acid, forming *ent*-kaur-16-en-19-oic acid (Fig. 16.6). This reaction sequence is mediated by a single multifunctional cytochrome P450 monooxygenase in both plants and fungi (Helliwell et al. 1999; Tudzynski et al. 2001). However, the corresponding P450s, despite their common designation as *ent*-kaurene oxidases, do not exhibit significant homology, other than both being members of the widely disparate cytochromes P450 (CYP) clan. The *ent*-kaurene oxidases from plants are members of the CYP701 family (Helliwell et al. 1998; Davidson et al. 2004; Itoh et al. 2004; Sawada et al. 2008; Miyazaki et al. 2011), while those from fungi fall within the CYP503 family (Tudzynski et al. 2001). By definition, no P450s from separate CYP families share more than 40% identity at the amino acid sequence level (Schuler and Werck-Reichhart 2003), with that between CYP701 and CYP503 being <15%. Notably, while the integral membrane "microsomal" P450s of eukaryotes are typically associated with the outer face of the endoplasmic reticulum (ER), the CYP701A P450s responsible for these initial oxidation reactions in plant GA metabolism have been localized to the outer face of the plastid envelope (Helliwell et al. 2001b). Such localization suggests that the hydrophobic *ent*-kaurene diterpene olefin intermediate is further transformed in the plastid into *ent*-kaurenoic acid, a much more polar metabolite, which may then be more amendable to transfer, either diffusion or assisted, to the ER for further processing. Most notably, ring contraction from the 6-6-6-5 ring structure of kauranes to the 6-5-6-5 giberrellane backbone represents the committed step in GA-specific biosynthesis. This is perhaps best understood by placing it in context relative to other kaurene-derived natural products, of which there are over 1,000 known (Buckingham 2002). One caveat to the hypothesis that plant kaurene oxidases (KO) provide a direct means by which metabolite transfer is mediated are reports that KO may be found on the ER in at least some species (Humphrey et al. 2006) as well as findings from promoter-based expression analysis indicating

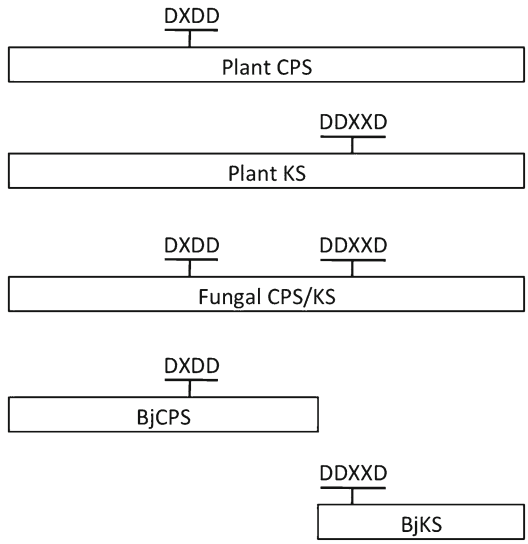

Fig. 16.5 Comparison of plant, fungal, and bacterial CPS and KS enzymes, with conservation of aspartate-rich motifs as indicated

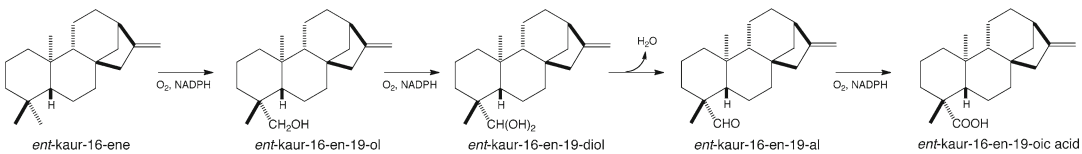

Fig. 16.6 Reaction sequence catalyzed the P450 KO, with requisite cosubstrates as indicated

that CPS is expressed in different tissues than KO (Yamaguchi et al. 2001). Either of these would preclude a coupled metabolic mechanism, and the latter would further require intercellular transport of the *ent*-kaurene diterpene olefin intermediate.

16.3.3 Production of Bioactive GA

16.3.3.1 Convergent Evolution in Action

As noted above, the production of *ent*-kaurene in plants, fungi, and bacteria results from the action of diterpene synthases that may share homology. However, the production of bioactive GAs in plants, fungi, and bacteria represents a clear example of convergent evolutionary solutions for production of these potent phytohormones. This is particularly true for plant and fungal biosynthesis (Hedden et al. 2001), for which essentially complete pathways are known (Fig. 16.7) (Tudzynski 2005; Pimenta Lange and Lange 2006), while more recent evidence indicates that bacterial GA production represents a third independently evolved pathway (Morrone et al. 2009). Thus, the pathway leading to production of bioactive GAs will be presented for each type of organism separately below. In the case of plants and fungi, this proceeds from their common *ent*-kaurenoic acid intermediate, while the little known in bacteria limits discussion as to how bioactive GAs might be produced from *ent*-kaurene in prokaryotes. The key differences that demonstrate the convergent evolutionary origin for bioactive GA production in each type of organism also will be presented.

16.3.3.2 Plants

Following transport of the plastid-derived *ent*-kaurenoic acid to the ER, the subsequently acting P450 carries out multiple oxidation reactions (Helliwell et al. 2001a; Davidson et al. 2003). These multifunctional P450s are members of the CYP88 family and termed *ent*-kaurenoic acid oxidases (KAO). It is in this reaction sequence that the "B" ring of the kaurane backbone undergoes contraction to produce the 6-5-6-5 skeletal structure characteristic of gibberellanes. Specifically, during oxidation of the initially formed *ent*-7α-hydroxykaur-16-en-19-oic acid, the reaction resulting in the production of GA_{12}-aldehyde (Fig. 16.8). Thus, KAO catalyzes the committed step in GA-specific biosynthesis (i.e., relative to other kaurenoic acid-derived natural products that are made by some, although not all, plants). While KAO is capable of further oxidation of GA_{12}-aldehyde to produce the (second) carboxylic acid of GA_{12}, in some plant species, it has been suggested that this later reaction is catalyzed by a specific 2-oxoglutarate-dependent dioxygenase termed GA7-oxidase (GA7ox) (Lange 1997). Interestingly, overexpression of CPS in *A. thaliana* leads to >1,000-fold increases in *ent*-kaurene and *ent*-kaurenoic acid but only tenfold increases in GA_{12} levels, with no increase in downstream metabolites nor change in KAO mRNA levels (Fleet et al. 2003). This indicates that GA metabolism is limited by either transport of *ent*-kaurene or *ent*-kaurenoic acid from the plastid to ER, biochemical regulation of KAO activity, or an increase in direct catabolism of GA_{12} (see Sect. 16.4 below).

In most plant species, GA_{12} is partially, but not entirely, hydroxylated at C13, forming GA_{53}. The early occurrence of C13-hydroxylation in plants contrasts with fungal GA biosynthesis (Fig. 16.7), where the analogous step occurs late (see Sect. 16.3.3.3 below). Intriguingly, while it has been suggested that C13-hydroxylation is mediated by a P450 (Hedden and Phillips 2000), the relevant enzyme has not been identified from any plant species to date. Both GA_{12} and GA_{53} can undergo further transformations in parallel pathways that each result in bioactive GAs, either with (e.g., GA_1) or without (e.g., GA_4) a C13-hydroxyl group (Fig. 16.9). These downstream reactions are analogous and typically assumed to be carried out by the same enzymes. However, there appear to be multiple isozymes of all the subsequently acting enzymes, each of which may exhibit differing catalytic efficiencies with C13-hydroxylated or nonhydroxylated metabolites. Notably, it remains an open question as to why so

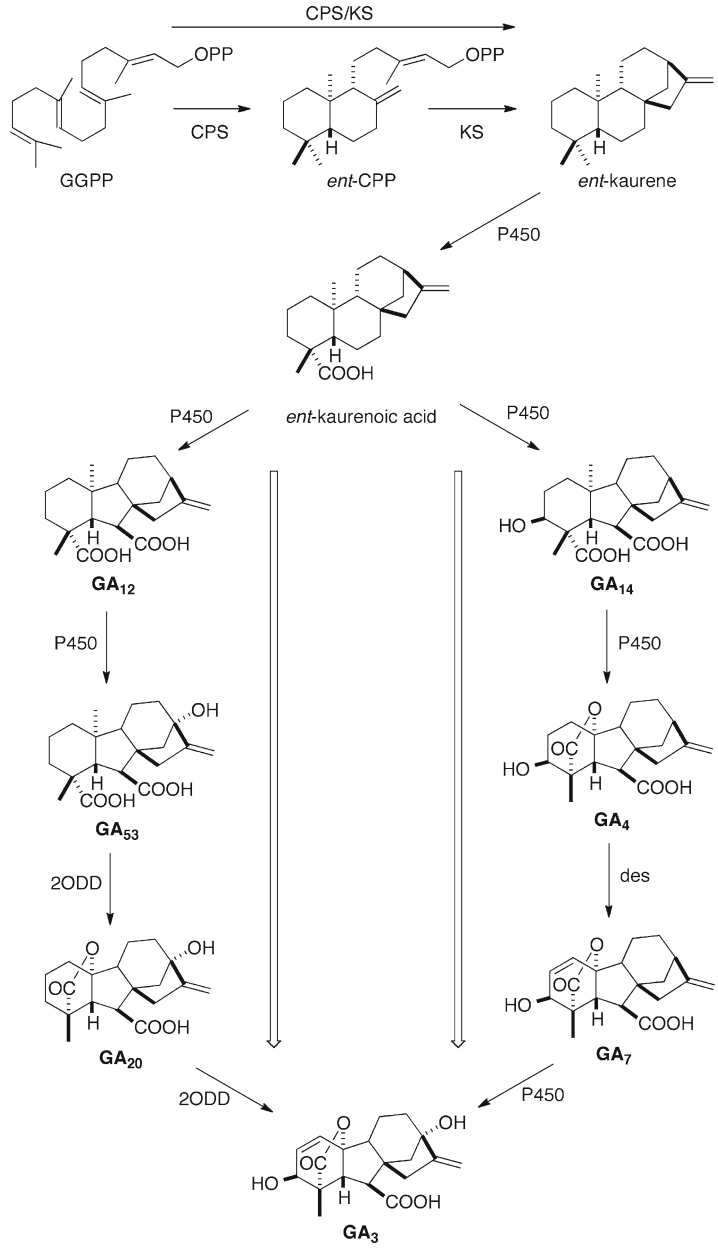

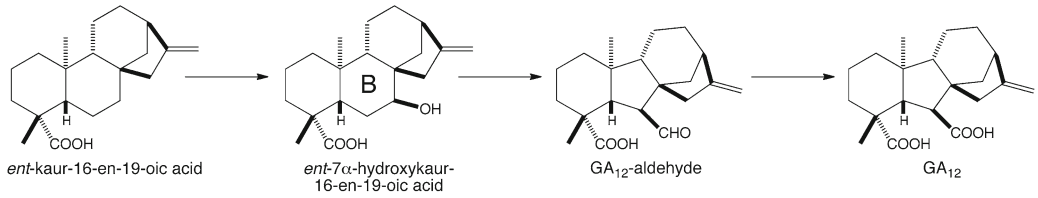

Fig. 16.7 Comparison of plant versus fungal GA_3 biosynthesis, with indicated enzymatic type as indicated

Fig. 16.8 Reaction sequence catalyzed by the P450 KAO

many plants produce C13-hydroxylated GAs, as phytohormone activity is exhibited by GAs both with and without this modification, although presumably there are differences in their relative activity.

The remaining reactions required for bioactive GA production in plants are mediated by 2-oxoglutarate-dependent dioxygenases (2ODD) (Hedden and Phillips 2000). These are soluble cytosolic enzymes, representing a third location for GA biosynthesis in plants (plastid, ER membrane, and now cytosol). However, this may not require an active transport mechanism, as GA_{12} and GA_{53} are expected to be sufficiently polar/soluble to be readily released from the active site of the relevant P450, located on the outer face of the ER membrane, to the cytosol. The use of 2ODDs for these later oxidative steps is the clearest difference between GA metabolism in plants relative to fungi and bacteria, which do not use 2ODDs (see Sects. 16.3.3.3 and 16.3.3.4 below).

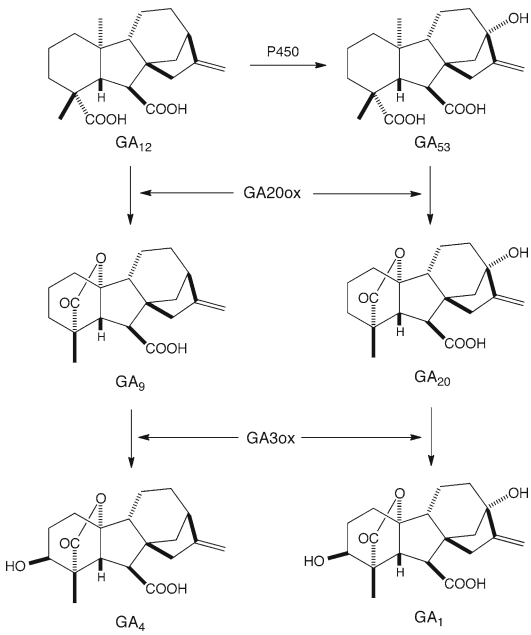

Fig. 16.9 C13-hydroxylated and nonhydroxylated bioactive GA pathways

The first 2ODD acting in GA biosynthesis catalyzes sequential oxidations of the C_{20}-methyl group that lead to its removal (released as CO_2) and formation of a γ-lactone ring connecting C10,19 (Fig. 16.10) (Lange et al. 1994). Reflecting its site of action, these multifunctional 2ODDs are termed GA20 oxidases (GA20ox). Production of bioactive GAs is then completed by a second 2ODD, which carries out C3β-hydroxylation (Chiang et al. 1995). Thus, these have been termed GA3 oxidases (GA3ox). Such late C3-hydroxylation in plants further contrasts with fungal GA biosynthesis (Fig. 16.7), where the analogous step occurs early (see Sect. 16.3.3.3 below). In addition, it is thought that GA3ox also mediates the C1,2-dehydrogenation necessary for formation of the corresponding bioactive GAs in plants, possibly as a side reaction (Hedden and Phillips 2000).

Notably, the transcription of GA20ox and GA3ox seems to be under feedback regulation, with reductions in mRNA levels observed upon the application of bioactive GAs (Chiang et al. 1995; Xu et al. 1995). This appears to be particularly important, as overexpression of these genes can lead to increases in bioactive GA concentrations and aberrant phenotypes (Hedden and Phillips 2000). There are multiple GA20ox and GA3ox in all plant species examined to date, often with different expression patterns and response to feedback suppression, providing the means by which the level of bioactive GAs can be varied throughout plant growth and development (e.g., at different times and in different tissues).

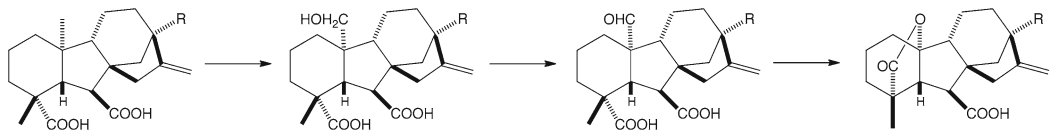

Fig. 16.10 Reaction sequence catalyzed by the 2ODD GA20ox

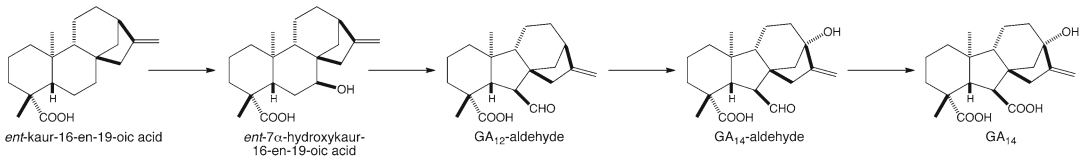

Fig. 16.11 Reaction sequence catalyzed by the *F. fujikuroi* P450-1 (CYP68A1)

16.3.3.3 Fungi

The biosynthetic pathway leading to production of bioactive GAs in the fungus *F. fujikuroi* is known (Tudzynski 2005) and is assumed to be representative of fungal GA metabolism more generally. Identification of the corresponding enzymes, and subsequent realization that these represented a convergent evolutionary solution to bioactive GA production (Hedden et al. 2001), was enabled by the discovery that the genes for this biosynthetic pathway were clustered together in the *F. fujikuroi* genome (Tudzynski and Hölter 1998). Prior to this breakthrough, only the enzymatic gene encoding the bifunctional CPS/KS (Tudzynski et al. 1998) had been cloned in homology-based efforts dependent on previously identified fungal genes (i.e., the CPS/KS from a *Phaeosphaeria* fungal species [Kawaide et al. 1997]). Identification of a differentially expressed P450 whose expression was upregulated under GA-inducing growth conditions led to a genomic fragment containing two neighboring P450s. Chromosome walking found an additional P450, the previously identified CPS/KS, and a putative GGPP synthase as immediate neighbors of the two originally discovered P450s (Tudzynski and Hölter 1998). Later work determined that a fourth P450 and novel desaturase (des) that also function in GA biosynthesis were part of this biosynthetic gene cluster (Tudzynski et al. 2001, 2003). Thus, the oxygenation/oxidation steps in fungal bioactive GA production were subsequently determined to rely on four P450s (originally simply termed P450-1 to 4) and a desaturase, rather than the mixture of P450s and 2ODDs found in plant GA metabolism (Tudzynski 2005). These seven coclustered genes, which are sufficient to product GA from central metabolism, provided an early example of nonessential metabolic pathway clustering in fungi, which is now a more generally appreciated feature of such specialized metabolism in fungi (i.e., while a primary metabolite required for normal growth and development in plants, bioactive GAs do not play an essential role in fungal metabolism). As a more specialized metabolite, GA biosynthesis in fungi does not appear to be heavily regulated, with only repression by high nitrogen levels noted (Tudzynski 2005).

Following the production of *ent*-kaurenoic acid mediated by CYP503/P450-4 (Tudzynski et al. 2001), CYP68A1/P450-1 carries out multiple reactions to form GA_{14} (Rojas et al. 2001). These entail not only the contraction of the kaurane "B" ring to form the characteristic 6-5-6-5 gibberellane ring structure via C7β-hydroxylation and subsequent oxidative rearrangement to GA_{12}-aldehyde,but also C3β-hydroxylation and further oxidation of the aldehyde to a (second) carboxylic acid (Fig. 16.11), reflecting the preferred reaction sequence. While this reaction sequence has obvious parallels to that mediated by the plant KAO P450, there is <15% identity between these (i.e., CYP88 and CYP68A) at the amino acid sequence level (Hedden et al. 2001). The early C3-hydroxylation mediated by the multifunctional CYP68A1 also contrasts with plant GA biosynthesis, where this modification occurs late (Fig. 16.7), and is mediated by the 2ODD GA3ox rather than a P450 in any case.

A similar contrast in enzymatic type can be seen in the subsequent production of a C10,19-lactone norditerpenoid, which is mediated by CYP68B1/P450-2 in *F. fujikuroi*, but the 2ODD GA20ox in plants (Fig. 16.7). Very little enzymatic analysis has been carried out on this multifunctional P450, although it is known that C20 is released as CO_2 (Dockerill and Hanson

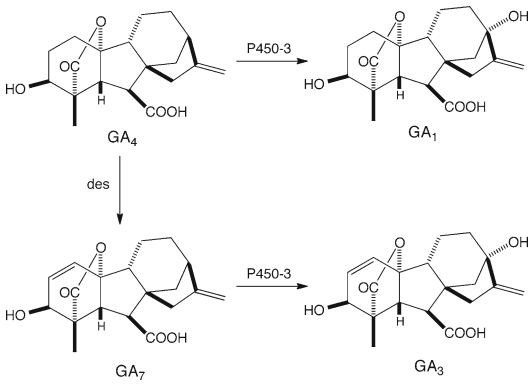

Fig. 16.12 Last two steps in *F. fujikuroi* GA biosynthesis

1978), just as found with plant 2ODD GA20ox. Intriguingly, the resulting GA_4 is generally considered to be bioactive, yet in *F. fujikuroi* two additional enzymes have been recruited for further elaboration, including C13-hydroxylation. It is tempting to speculate that it was development of such bioactive GA_4 production by pathogens that led to C13-hydroxlation in plants and subsequently in fungi, providing an example of escalating chemical elaboration gamesmanship/warfare between these groups of organisms.

Regardless of such speculation, the GA biosynthetic gene cluster in *F. fujikuroi* does include a subsequently acting desaturase that carries out C1,2-dehydrogenation of GA_4 to produce GA_7. Both GA_4 and GA_7 can be hydroxylated at C13 to produce GA_1 or GA_3, respectively, with GA_3 being the predominant "end product" from *F. fujikuroi*. This C13-hydroxylation is mediated by CYP69A1/P450-3, and the late occurrence of this modification in fungi provides additional contrast with plant GA biosynthesis.

Notably, between these later two enzymatic activities (Fig. 16.12), *F. fujikuroi* produces all four of the GAs most commonly found to exhibit phytohormone activity [i.e., GA_1, GA_3, GA_4, and GA_7 (Hedden and Phillips 2000)]. Such "combinatorial" biosynthesis of bioactive GAs provides an additional or alternative rationale for inclusion of these enzymatic genes in pathogenic fungal GA biosynthesis and the corresponding gene cluster. Specifically, this makes it more difficult for host plants to develop resistance (e.g., by alteration in receptor specificity). In addition, it is important to note that bioactive GA production by plant-associated microbes is not always pathogenic in nature (e.g., such biosynthesis may be a mechanism by which rhizobacteria promote the growth of their plant hosts – see Sect. 16.3.3.4 below), providing counterpressure against further elaboration.

16.3.3.4 Bacteria

How bacteria produce bioactive GAs is uncertain at this time, although it has been suggested that this may result from the enzymatic activities of the gene products encoded by an operon found in GA-producing rhizobacteria. In particular, previous investigation of *B. japonicum* identified an operon containing three P450s, an associated ferredoxin (presumably to supply electrons to these bacterial P450s), a short-chain alcohol dehydrogenase (SDR), and putative GGPP and (di)terpene synthases. It was further determined that transcription of this operon was induced by anaerobic conditions, potentially so that GA production occurs in the oxygen-deprived environment of root nodules where the production of such plant growth-promoting substances is presumably advantageous (Tully et al. 1998). Note that the associated P450s show no obvious homology to those involved in either plant or fungal GA biosynthesis, exhibiting ≤15% identity at the amino acid sequence level. Nevertheless, analysis of the subsequently determined genome sequence (Kaneko et al. 2002) suggests that this is the only (di)terpenoid biosynthetic operon in *B. japonicum*.

Very recent biochemical characterization of the two putative diterpene synthases from this operon demonstrated that these are separate CPS and KS, whose size and sequence (particularly conservation and relative location of motifs associated with catalytic activity – Fig. 16.5) suggests potential homology between the diterpene synthases found in the phylogenetically diverse GA-producing organisms (Morrone et al. 2009). By contrast, the composition of this operon indicates that bacteria have independently evolved a third biosynthetic route to bioactive GAs. Notably, this pathway appears to be common to at least all GA-producing rhizobacteria, as those with known genome sequences contain a homologous operon

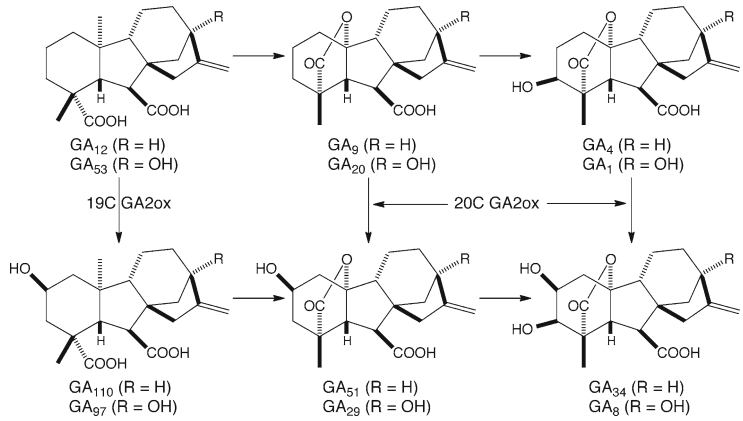

Fig. 16.13 Catabolic C2β-hydroxylations catalyzed by 2ODD GA2ox

with the same enzymatic gene content. Given that *B. japonicum* has been suggested to produce GA_3 (Boiero et al. 2007), the corresponding three P450s and SDR are presumably capable of carrying out the many oxygenation/oxidative reactions necessary to transform the *ent*-kaur-16-ene product of the associated diterpene synthases. This requires at least several, if not all, of these enzymes to be multifunctional, and elucidation of the relevant activities will be interesting from evolutionary, biochemical, and biosynthetic perspectives. However, even in the absence of such detailed understanding, the lack of homology and reduction in number of P450s, along with the use of an alcohol dehydrogenase rather than hydrocarbon desaturase, clearly indicate that production of bioactive GAs by rhizobacteria differs from that of fungi, with even more obvious differences relative to plant GA metabolism (i.e., no use of 2ODD). Thus, assuming that this operon is responsible for bioactive GA production, bacterial biosynthesis represents yet another convergent evolutionary solution to the production of these complex molecules (Morrone et al. 2009).

16.4 Catabolism of Bioactive GA

Production of bioactive GAs by microbes represents "end product-" specialized metabolites that affect host plants, with no rationale for further modification. At least in *F. fujikuroi*, this is consistent with the known accumulation of the GA_3 "end product" of the associated gene cluster, with natural isolates able to produce up to 1 g/L in liquid culture (Tudzynski 1999). However, in plants themselves, bioactive GAs undergo catabolism, presumably as part of the physiological response (i.e., degradation of these potent phytohormones to end the signaling process). The discussion here focuses on those catabolic reactions for which the relevant enzymes have been identified.

The most widely appreciated catabolic reaction is simple C2β-hydroxylation, carried out by dedicated 2ODD termed GA2ox (Fig. 16.13) (Thomas et al. 1999). Such modification is sufficient to significantly reduce the biological activity exerted by that particular GA (e.g., the C2β-hydroxyl derivative of GA_1 is GA_8, which is considered to be biologically inactive). The GA2ox will react with not only bioactive GAs but their precursors as well (e.g., the GA_{20} precursor to GA_1 can be converted to its C2β-hydroxylated derivative GA_{29}). This reaction "siphons off" metabolites, reducing the formation of bioactive GAs. Not surprisingly then, the GA2ox are regulated by bioactive GA levels, with increases in GA2ox mRNA levels observed upon such phytohormone application (Rieu et al. 2008). In addition, while the originally identified GA2ox is selective for the norditerpenoid C_{19} GAs, recent results demonstrate that there is a separate class of 2ODDs that catalyze C2β-hydroxylation of C_{20} GA precursors (Fig. 16.13), representing another "siphon" that can reduce metabolic flux towards bioactive GAs (Schomburg

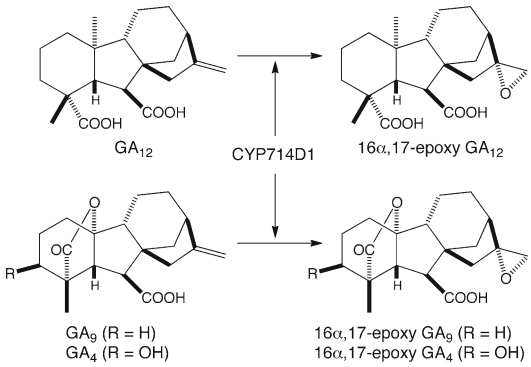

Fig. 16.14 Catabolic epoxidation catalyzed by CYP714D1

et al. 2003; Lee and Zeevaart 2005; Lo et al. 2008). These dioxygenases also are called GA2ox, although they are not closely related to the C_{19}-specific enzymes (i.e., these two type of 2ODD share less than 40% identity at the amino acid sequence level) and do not react with C_{19} GAs. Note that the 2Cβ-hydroxylated C_{20} GA_{97} is the major form of GA observed in spinach (Lee and Zeevaart 2005), suggesting that such modification is not followed by further elaboration (e.g., by GA20ox and GA3ox to form GA_8), and is a major sink for GA metabolism in this plant species. By contrast, it has been suggested that C2β-hydroxylation of the C_{19} norditerpenoids is a major GA inactivation pathway in *A. thaliana* (Rieu et al. 2008).

Enzymes carrying out two previously unappreciated GA catabolic reactions have been identified recently. One of these is the P450 CYP714D1 from rice, which carries out α-epoxidation of the C16,17 double bond in non-C13-hydroxylated versions of both C_{19} and C_{20} forms of GA (Fig. 16.14), with several of the resulting 16α,17-epoxy GAs present in wild-type rice. These GA metabolites were discovered recently enough that it appears they have not yet been assigned a designated number in the common GA nomenclature scheme. CYP714D1 was identified as the gene inactivated in the elongated uppermost internode mutant used in hybrid rice breeding and appears to play a role in specific stages of rice plant development (Zhu et al. 2006). Interestingly, functional homologs are found in *A. thaliana*, suggesting that

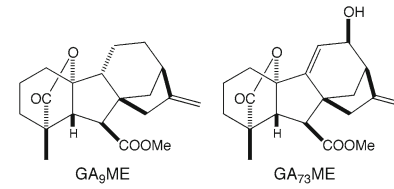

Fig. 16.15 GA methyl esters with antheridiogen activity

this catabolic mechanism may be widespread among higher plants (i.e., found in both mono- and dicots), although the *A. thaliana* homologs are from the differing CYP714A subfamily (i.e., these share only between 40% and 55% identity at the amino acid sequence level with CYP714D1) (Zhang et al. 2011).

The other recently identified GA catabolic enzymes are *S*-adenosine-*L*-methionine-dependent methyltransferases that carry out carboxylic acid methylation of many common GAs, albeit with differing levels of efficiency, as found with the only characterized pair of such enzymes from *A. thaliana*. Plants with inactivating mutations in these genes (GAMTs) exhibit high GA levels in developing seeds, while their overexpression results in dwarfed plants, consistent with a role in GA catabolism for the encoded enzymes. However, the expected GA methyl esters (GA_xMEs) are not readily apparent, even in plants overexpressing GAMT, which presumably reflects further metabolic transformation of these GA_xMEs (Varbanova et al. 2007). However, it should be noted that no GAMT homologs are apparent in the rice genome, suggesting that such inactivating methylation may be more limited in its distribution as a GA catabolic mechanism among higher plants.

16.5 Antheridiogens: GA-Derived Fern Hormones

Beyond the identified roles for GAs in plant growth and development discussed above (Sect 1.2), GA derivatives play a role in fern antheridial formation. These have been termed antheridiogens, a major form of which are GA_xMEs (Fig. 16.15), such as those produced by the GAMT identified in *A. thaliana* (i.e., GA_9ME).

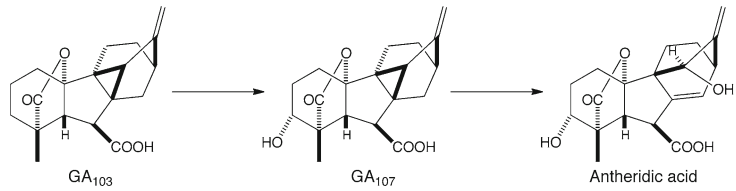

Fig. 16.16 Antheridic acid biosynthesis

While the *A. thaliana* GAMT seems to be involved in GA catabolism (Varbanova et al. 2007), it is possible that related enzymes are involved in fern antheridiogen biosynthesis. Another major form of antheridiogens is represented by antheridic acid, which has been shown to be derived from GA_{103} via GA_{107} (Fig. 16.16) (Yamauchi et al. 1991). Intriguingly, the antheridiogens may presage discovery of alternative biological roles for other such modified forms of GA.

16.6 Conclusions

The review of GA phytohormone metabolism presented here has emphasized the variation in GA biosynthesis by the phylogenetically diverse producing organisms. The observed fundamental differences between the biosynthetic pathways for bioactive GA biosynthesis in plants, fungi, and bacteria indicate that three evolutionarily independent solutions have been found for production of these complex molecules. This highlights the potent biological activity exhibited by these phytohormones, which presumably provided the driving force (i.e., selective pressure) for assembly of these convergent biosynthetic pathways. In this regard, it will be of interest to investigate the evolution of GA metabolism in plants themselves. It has been reported that the lycophyte *Selaginella moellendorffii*, but not the bryophyte *P. patens*, produces and responds to GA, suggesting that GA metabolism evolved in vascular plants (Hirano et al. 2007). These species further provide a comparative system through which the evolution of plant GA metabolism is being investigated (Hayashi et al. 2006; Miyazaki et al. 2011).

Also presented is a slight variation on the usual view of GA metabolism in plants, one that emphasizes GA specific relative to other diterpenoid metabolism. In particular, the role of the *ent*-kaurenoic acid oxidase P450 in initiating GA-specific metabolism relative to that of other labdane-related diterpenoids, of which there are ~7,000 known. Although not found in all plant species, in those that do produce other labdane-related diterpenoids, there may exit alternative regulatory mechanisms, as suggested by the finding that CPS involved in more specialized, (rather than GA) metabolism exhibits much less sensitivity to substrate/cofactor inhibition, thus enabling higher flux towards such specialized natural products. Thus, it will be of interest to investigate the potential regulation of KAO activity discussed above (Sect. 16.3.3.2).

In conclusion, study of GA phytohormone metabolism has provided fertile ground for scientific studies for many decades and seems set to continue being an active area of investigation through the foreseeable future. Work in the author's laboratory on GA metabolism is supported by the National Science Foundation, which is gratefully acknowledged here.

References

Bohlmann J, Meyer-Gauen G, Croteau R (1998) Plant terpenoid synthases: molecular biology and phylogenetic analysis. Proc Natl Acad Sci USA 95:4126–4133

Boiero L, Perrig D, Masciarelli O et al (2007) Phytohormone production by three strains of *Bradyrhizobium japonicum* and possible physiological and technological implications. Appl Microbiol Biotechnol 74:874–880

Brian PW, Hemming HG (1955) The effect of gibberellic acid on shoot growth of pea seedlings. Physiol Plantarum 8:669–681

Bruckner B, Blechschmidt D (1991) The gibberellin fermentation. Crit Rev Biotech 11:163–192
Buckingham J (2002) Dictionary of natural products (online web edition). Chapman & Hall/CRC Press, UK
Chiang H-H, Hwang I, Goodman HM (1995) Isolation of the Arabidopsis *GA4* locus. Plant Cell 7:195–201
Cross BE (1955) Gibberellic acid. Part I. J Chem Soc 1954:4670–4676
Davidson SE, Elliot RC, Helliwell CA et al (2003) The pea gene *NA* encodes *ent*-kaurenoic acid oxidase. Plant Physiol 131:335–344
Davidson SE, Smith JJ, Helliwell CA et al (2004) The pea gene *LH* encodes *ent*-kaurene oxidase. Plant Physiol 134:1123–1134
Dockerill B, Hanson JR (1978) The fate of C-20 in C19 gibberellin biosynthesis. Phytochemistry 17:701–704
Fischbach MA, Clardy J (2007) One pathway, many products. Nat Chem Biol 3:353–355
Fleet CM, Sun T-P (2005) A DELLAcate balance: the role of gibberellin in plant morphogenesis. Curr Opin Plant Biol 8:77–85
Fleet CM, Yamaguchi S, Hanada A et al (2003) Overexpression of *AtCPS* and *AtKS* in Arabidopsis confers increased *ent*-kaurene production but no increase in bioactive gibberellins. Plant Physiol 132:830–839
Garcia-Martinez JL, Gil J (2001) Light regulation of gibberellin biosynthesis and mode of action. J Plant Growth Regul 20:354–368
Hartsuck JA, Lipscomb WN (1963) Molecular and crystal structure of the di-p-bromobenzoate of the methylester of gibberellic acid. J Am Chem Soc 85:3414–3419
Hayashi K, Kawaide H, Notomi M et al (2006) Identification and functional analysis of bifunctional *ent*-kaurene synthase from the moss *Physcomitrella patens*. FEBS Lett 580:6175–6181
Hayashi Y, Toyomasu T, Hirose Y et al (2008) Comparison of the enzymatic properties of *ent*-copalyl diphosphate synthases in the biosynthesis of phytoalexins and gibberellins in rice. Biosci Biotechnol Biochem 72:523–530
Hedden P (2003) The genes of the green revolution. Trends Genet 19:5–9
Hedden P, Phillips AL (2000) Gibberellin metabolism: new insights revealed by the genes. Trends Plant Sci 5:523–530
Hedden P, Phillips AL, Rojas MC et al (2001) Gibberellin biosynthesis in plants and fungi: a case of convergent evolution? J Plant Growth Regul 20:319–331
Helliwell CA, Sheldon CC, Olive MR et al (1998) Cloning of the *Arabidopsis ent*-kaurene oxidase gene GA3. Proc Natl Acad Sci USA 95:9019–9024
Helliwell CA, Poole A, Peacock WJ et al (1999) *Arabidopsis ent*-kaurene oxidase catalyzes three steps of gibberellin biosynthesis. Plant Physiol 119:507–510
Helliwell CA, Chandler PM, Poole A et al (2001a) The CYP88A cytochrome P450, *ent*-kaurenoic acid oxidase, catalyzes three steps of the gibberellin biosynthesis pathway. Proc Natl Acad Sci USA 98:2065–2070
Helliwell CA, Sullivan JA, Mould RM et al (2001b) A plastid envelope location of *Arabidopsis ent*-kaurene oxidase links the plastid and endoplasmic reticulum steps of the gibberellin biosynthesis pathway. Plant J 28:201–208
Hirano K, Nakajima M, Asano K et al (2007) The GID1-mediated gibberellin perception mechanism is conserved in the Lycophyte *Selaginella moellendorffii* but not in the Bryophyte *Physcomitrella patens*. Plant Cell 19:3058–3079
Humphrey TV, Richman AS, Menassa R et al (2006) Spatial organisation of four enzymes from *Stevia rebaudiana* that are involved in steviol glycoside synthesis. Plant Mol Biol 61:47–62
Itoh H, Tatsumi T, Sakamoto T et al (2004) A rice semidwarf gene, *Tan-Ginbozu* (*D35*), encodes the gibberellin biosynthesis enzyme, *ent*-kaurene oxidase. Plant Mol Biol 54:533–547
Kaneko T, Nakamura Y, Sato S et al (2002) Complete genomic sequence of nitrogen-fixing symbiotic bacterium *Bradyrhizobium japonicum* USDA110. DNA Res 9:189–197
Kasahara H, Hanada A, Kuzuyama T et al (2002) Contribution of the mevalonate and methylerythritol phosphate pathways to the biosynthesis of gibberellins in Arabidopsis. J Biol Chem 277:45188–45194
Kawaide H, Imai R, Sassa T et al (1997) *Ent*-kaurene synthase from the fungus *Phaeosphaeria* sp. L487. cDNA isolation, characterization, and bacterial expression of a bifunctional diterpene cyclase in fungal gibberellin biosynthesis. J Biol Chem 272:21706–21712
Kawaide H, Sassa T, Kamiya Y (2000) Functional analysis of the two interacting cyclase domains in *ent*-kaurene synthase from the fungus *Phaeosphaeria* sp. L487 and a comparison with cyclases from higher plants. J Biol Chem 275:2276–2280
Köksal M, Hu H, Coates RM et al (2011a) Structure of copalyl diphosphate synthase from *Arabidopsis thaliana*, a protonation-dependent diterpene cyclase. Nat Chem Biol 7:431–433
Köksal M, Jin Y, Coates RM et al (2011b) Taxadiene synthase structure and evolution of modular architecture in terpene biosynthesis. Nature 469:116–120
Lange T (1997) Cloning gibberellin dioxygenase genes from pumpkin endosperm by heterologous expression of enzyme activities in *Escherichia coli*. Proc Natl Acad Sci USA 94:6553–6558
Lange T, Hedden P, Graebe JE (1994) Expression cloning of a gibberellin 20-oxidase, a multifunctional enzyme involved in gibberellin biosynthesis. Proc Natl Acad Sci USA 91:8552–8556
Lee DJ, Zeevaart JAD (2005) Molecular cloning of GA 2-oxidase 3 from spinach and its ectopic expression in *Nicotiana sylvestris*. Plant Physiol 138:243–254
Lo S-F, Yang S-Y, Chen K-T et al (2008) A novel class of gibberellin 2-oxidases control semidwarfism, tillering, and root development in rice. Plant Cell 20: 2603–2618
MacMillan J (1997) Biosynthesis of the gibberellin plant hormones. Nat Prod Rep 14:221–243

MacMillan J, Takahashi N (1968) Proposed procedure for the allocation of trivial names to the gibberellins. Nature 217:170–171

Mann FM, Prisic S, Davenport EK et al (2010) A single residue switch for Mg^{2+}-dependent inhibition characterizes plant class II diterpene cyclases from primary and secondary metabolism. J Biol Chem 285: 20558–20563

Mende K, Homann V, Tudzynski B (1997) The geranylgeranyl diphosphate synthase gene of *Gibberella fujikuroi*: isolation and expression. Mol Gen Genet 255:96–105

Miyazaki S, Katsumata T, Natsume M et al (2011) The CYP701B1 of *Physcomitrella patens* is an *ent*-kaurene oxidase that resists inhibition by uniconazole-P. FEBS Lett 585:1879–1883

Morrone D, Chambers J, Lowry L et al (2009) Gibberellin biosynthesis in bacteria: separate *ent*-copalyl diphosphate and *ent*-kaurene synthases in *Bradyrhizobium japonicum*. FEBS Lett 583:475–480

Peters RJ (2010) Two rings in them all: the labdane-related diterpenoids. Nat Prod Rep 27:1521–1530

Peters RJ, Ravn MM, Coates RM et al (2001) Bifunctional abietadiene synthase: free diffusive transfer of the (+)-copalyl diphosphate intermediate between two distinct active sites. J Am Chem Soc 123:8974–8978

Phinney BO (1956) Growth response of single-gene dwarf mutants in maize to gibberellic acid. Proc Natl Acad Sci USA 42:185–189

Phinney BO, West CA, Ritzel M et al (1957) Evidence for gibberellin-like substances from flowering plants. Proc Natl Acad Sci USA 43:398–403

Pimenta Lange PM, Lange T (2006) Gibberellin biosynthesis and the regulation of plant development. Plant Biol 8:281–290

Prisic S, Peters RJ (2007) Synergistic substrate inhibition of *ent*-copalyl diphosphate synthase: a potential feed-forward inhibition mechanism limiting gibberellin metabolism. Plant Physiol 144:445–454

Prisic S, Xu J, Coates RM et al (2007) Probing the role of the DXDD motif in class II diterpene cyclases. Chembiochem 8:869–874

Radley M (1956) Occurrence of substances similar to gibberellic acid in higher plants. Nature 178:1070–1071

Rieu I, Eriksson S, Powers SJ et al (2008) Genetic analysis reveals that C19-GA 2-oxidation is a major gibberellin inactivation pathway in Arabidopsis. Plant Cell 20:2420–2436

Rohmer M (2008) From molecular fossils of bacterial hopanoids to the formation of isoprene units: discovery and elucidation of the methylerythritol phosphate pathway. Lipids 43:1095–1107

Rojas MC, Hedden P, Gaskin P et al (2001) The P450-1 gene of *Gibberella fujikuroi* encodes a multifunctional enzyme in gibberellin biosynthesis. Proc Natl Acad Sci USA 98:5838–5843

Sawada Y, Katsumata T, Kitamura J et al (2008) Germination of photoblastic lettuce seeds is regulated via the control of endogenous physiologically active gibberellin content, rather than of gibberellin responsiveness. J Exp Bot 59:3383–3393

Schomburg FM, Bizzell CM, Lee DJ et al (2003) Overexpression of a novel class of gibberellin 2-oxidases decreases gibberellin levels and creates dwarf plants. Plant Cell 15:151–163

Schuler MA, Werck-Reichhart D (2003) Functional genomics of P450s. Annu Rev Plant Biol 54:629–667

Silverstone AL, Chang C-W, Krol E et al (1997) Developmental regulation of the gibberellin biosynthetic gene GA1 in *Arabidopsis thaliana*. Plant J 12:9–19

Stodola FH, Raper KB, Fennell DI et al (1955) The microbiological production of gibberellins A and X. Arch Biochem Biophys 54:240–245

Thomas SG, Phillips AL, Hedden P (1999) Molecular cloning and functional expression of gibberellin 2-oxidases, multifunctional enzymes involved in gibberellin deactivation. Proc Natl Acad Sci USA 96: 4698–4703

Tudzynski B (1999) Biosynthesis of gibberellins in *Gibberella fujikuroi*: biomolecular aspects. Appl Microbiol Biotechnol 52:298–310

Tudzynski B (2005) Gibberellin biosynthesis in fungi: genes, enzymes, evolution, and impact on biotechnology. Appl Microbiol Biotechnol 66:597–611

Tudzynski B, Hölter K (1998) Gibberellin biosynthetic pathway in *Gibberella fujikuroi*: evidence for a gene cluster. Fungal Genet Biol 25:157–170

Tudzynski B, Kawaide H, Kamiya Y (1998) Gibberellin biosynthesis in *Gibberella fujikuroi*: cloning and characterization of the copalyl diphosphate synthase gene. Curr Genet 34:234–240

Tudzynski B, Hedden P, Carrera E et al (2001) The *P450-4* gene of *Gibberella fujikuroi* encodes *ent*-kaurene oxidase in the gibberellin biosynthesis pathway. Appl Environ Microbiol 67:3514–3522

Tudzynski B, Mihlan M, Rojas MC et al (2003) Characterization of the final two genes of the gibberellin biosynthetic gene cluster of *Gibberella fujikuroi*. J Biol Chem 278:28635–28643

Tully RE, van Berkum P, Lovins KW et al (1998) Identification and sequencing of a cytochrome P450 gene cluster from *Bradyrhizobium japonicum*. Biochim Biophys Acta 1398:243–255

Varbanova M, Yamaguchi S, Yang Y et al (2007) Methylation of gibberellins by Arabidopsis GAMT1 and GAMT2. Plant Cell 19:32–45

Xu Y-L, Li L, Wu K et al (1995) The *GA5* locus of *Arabidopsis thaliana* encodes a multifunctional gibberellin 20-oxidase: molecular cloning and functional expression. Proc Natl Acad Sci USA 92:6640–6644

Yabuta T, Sumiki Y (1938) On the crystal of gibberellin, a substance to promote plant growth. J Agric Chem Soc Japan 14:1526

Yabuta T, Hayashi T (1939a) Biochemical studies on "bakane" fungus of rice. II: Isolation of gibberellin, the active principle which produces slender rice seedlings. J Agr Chem Soc Japan 15:257–266

Yabuta T, Hayashi T (1939b) Biochemical studies of the "bakane" fungus. III. Physiological action of gibberellin on the plant. J Agr Chem Soc Japan 15:403–413

Yamaguchi S, Kamiya Y, Sun T-P (2001) Distinct cell-specific expression patterns of early and late gibberellin biosynthetic genes during Arabidopsis seed germination. Plant J 28:443–453

Yamauchi T, Oyama N, Yamane H et al (1991) Biosynthesis of antheridic acid, the principal antheridiogen in *Anemia phyllitidis*. Phytochemistry 30:3247–3250

Zhang Y, Zhang B, Yan D et al (2011) Two Arabidopsis cytochrome P450 monooxygenases, CYP714A1 and CYP714A2, function redundantly in plant development through gibberellin deactivation. Plant J 67: 342–353

Zhou K, Peters RJ (2009) Investigating the conservation pattern of a putative second terpene synthase divalent metal binding motif in plants. Phytochemistry 70:366–369

Zhu Y, Nomura T, Xu Y et al (2006) ELONGATED UPPERMOST INTERNODE encodes a cytochrome P450 monooxygenase that epoxidizes gibberellins in a novel deactivation reaction in rice. Plant Cell 18:442–456

17 Control of Plastidial Isoprenoid Precursor Supply: Divergent *1-Deoxy-D-Xylulose 5-Phosphate Synthase* (*DXS*) Isogenes Regulate the Allocation to Primary or Secondary Metabolism

Michael H. Walter, Daniela S. Floss, Heike Paetzold, Kerstin Manke, Jessica Vollrath, Wolfgang Brandt, and Dieter Strack

Abstract

Following the description of two separate pathways for isoprenoid precursor biosynthesis in plants, a new level of complexity has been introduced by the discovery of two divergent gene classes encoding the first enzyme of the plastidial methylerythritol phosphate (MEP) pathway. These nonredundant *1-deoxy-D-xylulose 5-phosphate synthase* (*DXS*) isogenes are differentially expressed in such a way that DXS1 appears to serve housekeeping functions, whereas DXS2 is associated with the production of specialized (secondary) isoprenoids involved in ecological functions. Examples of the

M.H. Walter (✉)
Abteilung Sekundärstoffwechsel, Leibniz-Institut für Pflanzenbiochemie, Weinberg 3, Halle (Saale) 06120, Germany
e-mail: mhwalter@ipb-halle.de

D.S. Floss
Abteilung Sekundärstoffwechsel, Leibniz-Institut für Pflanzenbiochemie, Weinberg 3, Halle (Saale) 06120, Germany

Boyce Thompson Institute for Plant Research, Ithaca, NY, USA

H. Paetzold • K. Manke • J. Vollrath • D. Strack
Abteilung Sekundärstoffwechsel, Leibniz-Institut für Pflanzenbiochemie, Weinberg 3, Halle (Saale) 06120, Germany

W. Brandt
Abteilung Natur- und Wirkstoffchemie, Leibniz-Institut für Pflanzenbiochemie, Weinberg 3, Halle (Saale) 06120, Germany

T.J. Bach and M. Rohmer (eds.), *Isoprenoid Synthesis in Plants and Microorganisms: New Concepts and Experimental Approaches*, DOI 10.1007/978-1-4614-4063-5_17,

latter are apocarotenoid formation in roots colonized by arbuscular mycorrhizal fungi and mono- or diterpenoid biosynthesis in trichomes. Knockdown of *DXS2* genes can specifically suppress secondary isoprenoid formation without affecting basic plant functions. Analyzing *DXS* isogenes along the progression of land plant evolution shows separation in structure and complementary expression already at the level of gymnosperms, which is maintained in all angiosperms except Arabidopsis.

Keywords
Methylerythritol phosphate (MEP) pathway • 1-Deoxy-D-xylulose 5-phosphate synthase (DXS) • Gene duplication • Evolution • Arbuscular mycorrhiza • Trichomes • Carotenoids • Apocarotenoids • RNAi

17.1 Introduction

Plant cells accumulate a plethora of different isoprenoid end products involved in primary or secondary metabolism, which are all assembled from the common precursors isopentenyl diphosphate (IPP) and dimethylallyl diphosphate (DMAPP). For decades it was thought that IPP and DMAPP are solely produced in the cytosol by the mevalonate pathway and then imported into organelles for subsequent biogenesis of specific organellar end products. Such a mechanism was assumed even for the abundant isoprenoid end products accumulating in plastids despite contradictions to results from labeling studies. This early view on plastidial isoprenoid precursor supply organization was fundamentally changed by the discovery of a novel, independent pathway for IPP/DMAPP formation operating inside plastids. This new route is known as the methylerythritol phosphate (MEP) pathway. The tale of its discovery has been nicely narrated by Rodríguez-Concepción and Boronat (2002) and updated recently (Cordoba et al. 2009). The MEP pathway is also addressed several times elsewhere in this volume. Studies on isoprenoid precursor exchange between plastids and the cytosol have revealed only limited cross talk under normal conditions indicating that plastids largely synthesize their isoprenoid precursors themselves (Hemmerlin et al. 2003; Laule et al. 2003). The dependence of fundamental plant functions on MEP pathway genes and plastidial isoprenoid precursor supply is underscored by albino phenotypes of MEP pathway mutants (Mandel et al. 1996; Budziszewski et al. 2001; cf. León and Cordoba, this volume chapter 31).

17.2 Inducible Apocarotenoid Biosynthesis in Roots Colonized by Arbuscular Mycorrhizal Fungi: A System for Discovery of *1-Deoxy-D-Xylulose 5-Phosphate Synthase* (*DXS*) Isogenes and More

Abundant carotenoid accumulation related to fruit ripening has been shown to be fed by IPP precursors provided by the MEP pathway (Lois et al. 2000). Similarly, massive accumulation of apocarotenoids in roots colonized by mycorrhizal fungi has been reported to correlate with strong upregulation of transcript levels of MEP pathway genes (Walter et al. 2000). Results from analyses of mycorrhizal roots also provided the basis for another change of paradigm concerning plastidial isoprenoid precursor supply: A new level of complexity was reached by the discovery of at least two distantly related *1-deoxy-D-xylulose 5-phosphate synthase (DXS)* isogenes, whose encoded proteins apparently fulfill complementary functions in plant primary or secondary

metabolism, respectively (Walter et al. 2002). DXS catalyzes the first out of seven steps of the MEP pathway by converting glyceraldehyde 3-phosphate and pyruvate into 1-deoxy-D-xylulose 5-phosphate (DXP) in a transketolase-like reaction releasing CO_2 (Sprenger et al. 1997; Lois et al. 1998; Xiang et al. 2007). The enzyme requires thiamine diphosphate (TPP) as cofactor. The DXS-catalyzed step appears to be a bottleneck in plastidial IPP/DMAPP biosynthesis. It has been suggested to be rate limiting on the basis of studies on tomato fruit carotenoid accumulation. Increases in *DXS* transcript levels were correlated with the strong rise in carotenoids during fruit ripening, but transcript levels of 1-deoxy-D-xylulose 5-phosphate reductoisomerase (DXR) catalyzing the second step were not (Lois et al. 2000). Upregulation of *DXS* expression has also been reported by a number of other developmental or environmental cues, yet little or no consideration of potential DXS isoforms or *DXS* isogenes has been given (Mandel et al. 1996; Bouvier et al. 1998; Lange et al. 1998; Chahed et al. 2000; Estévez et al. 2000; Dudareva et al. 2005; Sharkey et al. 2005; Kishimoto and Ohmiya 2006). Limitation of precursor flux by DXS activity is also suggested by results from introduction of *DXS* transgenes into Arabidopsis and tomato. Upregulation or downregulation of *DXS* expression by these approaches correlated with correspondingly altered levels of various isoprenoid end products (Estévez et al. 2001; Enfissi et al. 2005). Constitutive expression of the Arabidopsis *DXS (CLA1)* gene in spike lavender led to elevated levels of isoprenoid essential oils (Muñoz-Bertomeu et al. 2006).

The discovery of *DXS* isogenes was first described following an analysis of roots from the model legume *Medicago truncatula* colonized by the arbuscular mycorrhizal fungi *Glomus intraradices* and *G. mosseae*. The same phenomenon of duplicate, differentially regulated *DXS* genes was observed in mycorrhizal roots of tobacco, tomato, and maize (Walter et al. 2002). The strongly elevated transcript levels of a second gene for DXS (*DXS2*) were shown to be correlated with the massive accumulation of two types of apocarotenoids in fungus-colonized roots. The accumulation of these apocarotenoids—one of them being yellow—is often strong enough to recognize a yellowish coloration of colonized roots by the naked eye. The apocarotenoid biosynthetic pathway in this experimental system as shown in Fig. 17.1 has been extensively studied for more than a decade, and its molecular analysis has provided a number of interesting findings for isoprenoid research (reviewed in Walter et al. 2007, 2010; Walter and Strack 2011). One recent example is the validation of a distinct function of the *DXS2* isogene by a selective knockdown approach in *M. truncatula* (Floss et al. 2008a), which will be described more in depth at the end of this chapter together with some general implications. Since this useful experimental system of inducible isoprenoid biosynthesis is still largely unknown in the isoprenoid community, it will be elucidated here in some more detail.

The arbuscular mycorrhizal (AM) symbiosis is a mutualistic plant-microbe interaction between a small number of obligately biotrophic fungal species from the recently defined phylum Glomeromycota and the roots of most terrestrial plants (Smith and Read 2008). The AM symbiosis can determine plant biodiversity and productivity and is thus an important component of sustainable agroecosystems. Its most salient feature for the plant is the improved acquisition of mineral nutrients, especially phosphate, *via* fungal hyphae pervading the soil and collecting nutrients in a much more effective way than root hairs. In turn, the fungi receive carbohydrates from roots to sustain their life cycle. Moreover, water supply and resistance to biotic and abiotic stresses are also typically improved in mycorrhizal plants. The main symbiotic organs are haustoria-like fungal arbuscules developing inside root cortex cells from hyphae. They are regarded as the predominant sites for nutrient uptake from the fungal partner. Arbuscules are transient structures, which are constantly degraded and newly formed with an average generation time of 7–10 days (Alexander et al. 1988). Root metabolism is markedly altered by the interaction with these fungi as indicated by extensive

alterations in gene expression (Hohnjec et al. 2005) but also by observation of altered plastid and mitochondria biogenesis and function (Lohse et al. 2005).

Particularly, plastids undergo extensive proliferation, and their reorganization even exhibits differences in two phases of arbuscule development inside root cells (Lohse et al. 2006). The second phase, when arbuscules start to degrade, is accompanied by proliferation of structurally distinct plastids, which are large and tubular, suggesting specific metabolic activities in this phase. Indeed, arbuscule-specific accumulation of an isoprenoid biosynthetic enzyme from the MEP pathway, DXR, is preferentially associated with this late phase of arbuscule development (Hans et al. 2004; Lohse et al. 2006). In agreement with this result obtained by immunolocalization, the apocarotenoid products, assumed to be related to this biosynthetic activity, are also preferentially found in the vicinity of degrading "second-phase" arbuscules (Fester et al. 2002). The chemical structures of these abundant apocarotenoids of mycorrhizal roots have been extensively characterized (Fig. 17.1, reviewed by Strack and Fester 2006). Two types of AM-induced apocarotenoids accumulate within roots. These are derivatives of (1) C_{13} cyclohexenones, which are usually glycosylated (Maier et al. 1995), and of (2) linear polyenic C_{14} carotenoic acids called mycorradicins (Klingner et al. 1995). It is thought that both originate from a common but still unknown C_{40} carotenoid precursor (Fig. 17.1, Walter et al. 2000). Mycorradicins and part of the cyclohexenone derivatives are integrated in a highly complex mixture of various compounds linked by ester bonds. Alkaline hydrolysis of root extracts can liberate mycorradicin and cyclohexenones from this complex (Fester et al. 2002).

This experimental system of inducible apocarotenoid formation has recently been proven useful again, this time for elucidation of the mechanisms of carotenoid cleavage (Floss et al. 2008b). In mycorrhizal roots, the C_{14} central linear dialdehyde product of carotenoid cleavage (see Fig. 17.1) is oxidized to the dicarboxylic acid mycorradicin, which appears to be esterified and integrated into a high-molecular-weight complex, thereby possibly preventing further metabolization and degradation. In other systems, the C_{14} dialdehyde can be reduced to the unstable alcohol (rosafluene) or is otherwise modified and often degraded to nontraceable products. Owing in part to this unique metabolic fate of the C_{14} apocarotenoids in the mycorrhizal root system, it was possible to follow up differential modifications of C_{13} and C_{14} apocarotenoids upon strong knockdown of the expression of a *carotenoid cleavage dioxygenase 1* (*CCD1*) gene in mycorrhizal hairy roots of composite *M. truncatula* plants. It could be shown that C_{13} cyclohexenone derivatives were reduced to only about 50% of empty-vector controls, whereas C_{14} derivatives were strongly reduced almost to the limits of detection (Floss et al. 2008b). Together with strong accumulation of C_{27} apocarotenoids in *CCD1*-suppressed mycorrhizal roots, this result led us to propose a novel scheme for carotenoid cleavage *in planta* in which C_{40} carotenoid cleavage is organized in two consecutive steps (Fig. 17.1). Contrary to earlier belief based on *in vitro* analyses, only the second step appears to be catalyzed by CCD1 in a compartmentalized plant cell. A prime candidate for the missing first player en route from C_{40} carotenoids to C_{13} and C_{14} cleavage products in mycorrhizal roots was CCD7, which catalyzes C_{27} synthesis upon expression of *AtCCD7* in carotenoid-producing *Escherichia coli* strains (Schwartz et al. 2004). The CCD7 is also known to be involved in the formation of carotenoid-derived branching inhibitor hormones, which have been identified as strigolactones (Gomez-Roldan et al. 2008; Umehara et al. 2008). Current projects are targeting *CCD7*-silenced transgenics and *ccd7* mutants. This work has now confirmed the proposed role of CCD7 and the scheme shown in Fig. 17.1 (Vogel et al. 2010). CCD7 thus provides a third case of loss-of-function mutation in an apocarotenoid biosynthetic step in mycorrhizal roots, which can now be used to further investigate the biological function of these compounds. An updated general account on isogene organization and function in both early and late steps of carotenoid and apocarotenoid biosynthesis has recently been published (Walter and Strack 2011).

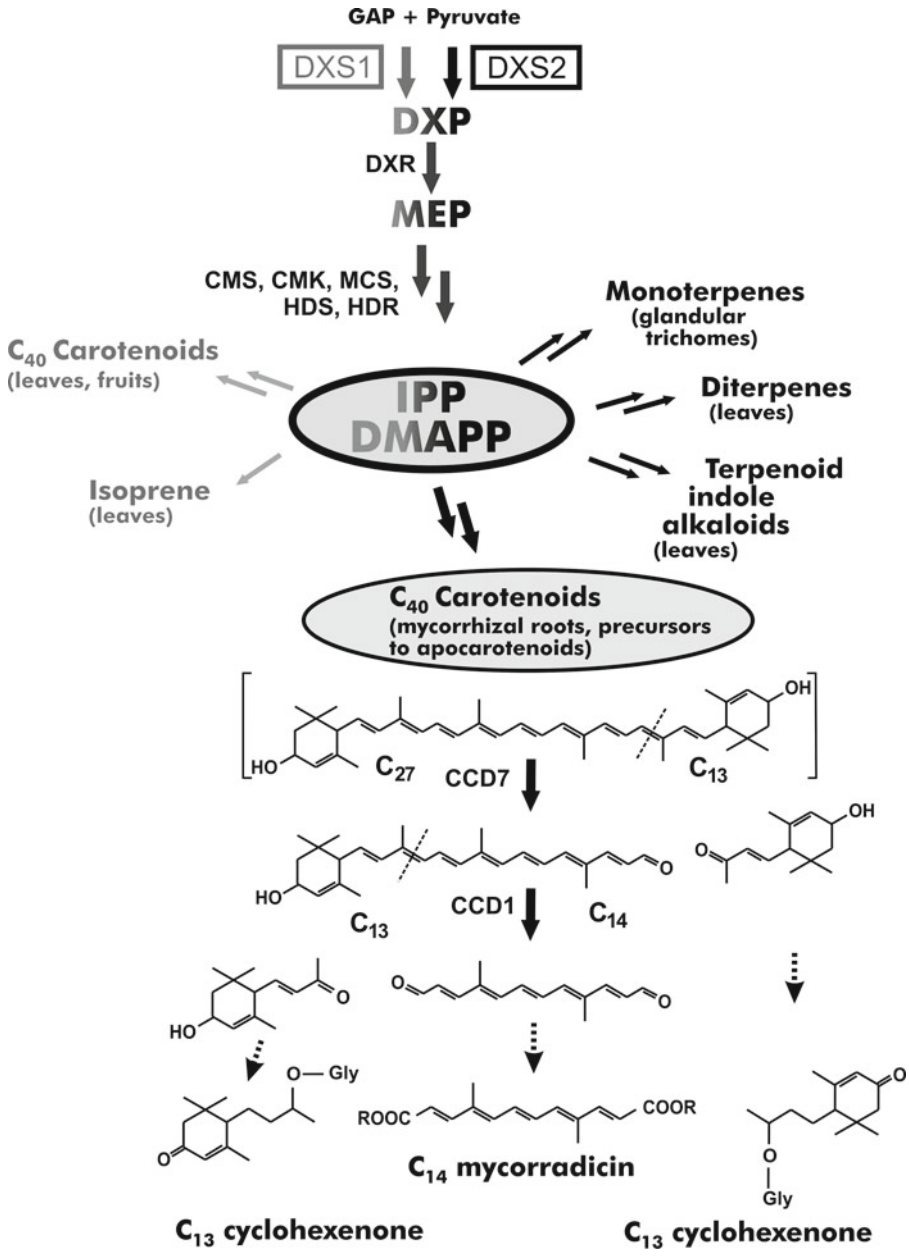

Fig. 17.1 Dedicated roles of DXS isoforms in MEP pathway-based supply of IPP/DMAPP to isoprenoid end product biogenesis. *DXS2* genes are specifically regulated in the biosynthesis of secondary isoprenoids (*black arrows*), whereas *DXS1* genes are involved in housekeeping (primary) metabolism (*gray arrows*). Increased expression of *DXS2* in mycorrhizal roots of *Medicago truncatula* is a prerequisite for massive accumulation of two types of apocarotenoids (C_{13} cyclohexenone and C_{14} mycorradicin derivatives) derived from a common C_{40} carotenoid precursor, which has not yet been identified (*square brackets*). Carotenoid cleavage has recently been shown to occur via two consecutive cleavage steps, in which CCD1 catalyzes only the second step, whereas CCD7 performs the first step (Floss et al. 2008b; Vogel et al. 2010). Enzyme designations are *DXS* 1-deoxy-D-xylulose 5-phosphate synthase, *DXR* 1-deoxy-D-xylulose 5-phosphate reductoisomerase, *CMS* 4-(cytidine 5′-diphospho)-2-*C*-methyl-D-erythritol (CDP-ME) synthase, *CMK* 4-(cytidine 5′-diphospho)-2-*C*-methyl-D-erythritol CDP-ME) kinase, *MCS* 2-*C*-methyl-D-erythritol 2,4-cyclodiphosphate (ME-cPP) synthase, *HDS* 4-hydroxy-3-methylbut-2-enyl diphosphate (HMBPP) synthase), *HDR* HMBPP reductase, *CCD7* carotenoid cleavage dioxygenase 7, and *CCD1* carotenoid cleavage dioxygenase 1

17.3 Complex Organization of *DXS* Isogenes and Their Complementary Expression in Angiosperms

Following the discovery of two *DXS* genes in the mycorrhizal root system of *M. truncatula* (*MtDXS1* and *MtDXS2*), initial database searches using the two amino acid sequences have uncovered that the occurrence of two *DXS* genes is a widespread phenomenon among plant genomes and that existing DXS amino acid sequences could be classified into one of the two classes of DXS newly defined by Walter and coworkers (2002). Moreover, a third class of DXS-like proteins and genes was identified in this work on mycorrhizal roots of *M. truncatula* from clone 92, which exhibits a rather distant relationship to DXS1 and DXS2 (Walter et al. 2002). This "DXS3" of *M. truncatula* is highly similar to a deduced protein tentatively named DXS3 from Arabidopsis *thaliana* (Rodríguez-Concepción and Boronat 2002; cf. León and Cordoba, this volume chapter 31). Recently, a maize gene belonging to the DXS3 class has been shown to complement an *E. coli dxs* mutant arguing for its functionality as a true DXS (Cordoba et al. 2011). However, demonstration of its catalytic activity or the description of the phenotypical outcome of a loss-of-function mutation is still missing. Many more sequences of *DXS* and *DXS*-like genes and deduced proteins including gene expression data have become available allowing a much more comprehensive view on *DXS* isogene organization in angiosperms. The current status on DXS and DXS-like isozymes deduced from published sequences or database entries is summarized in an amino acid sequence similarity tree of deduced DXS proteins (Fig. 17.2). However, for the sake of clarity, this presentation cannot be fully exhaustive, and apologies are expressed to those colleagues whose work could not be mentioned here.

Some of the sequences specified in Fig. 17.2 have been renamed to adapt them into a current classification of three main classes of DXS and DXS-like isozymes, which is suggested by aligning all available angiosperm sequences. A first renaming is appropriate for AtDXS2 previously reported in an alignment together with AtDXS1 (CLA1) and AtDXS3, which was published at the same time as our report on class 2-DXS (Rodríguez-Concepción and Boronat 2002). Current alignments and positioning of the sequence into the similarity tree (Fig. 17.2) suggest this "AtDXS2" to be a second copy of a class 1-DXS next to the well-known CLA1 protein (AtDXS1A; Mandel et al. 1996; Estévez et al. 2000). It will therefore be termed AtDXS1B in this contribution. Interestingly, the Arabidopsis genome lacks a genuine class 2-*DXS* gene, which has been found to represent the only known case of a confirmed absence of a *DXS2*-type gene in a plant genome (Walter et al. 2002; Paetzold et al. 2010), and this statement is still valid today. Another renaming is advisable for two *DXS* isogenes described from the oil palm *Elaeis guineensis* Jacq. (Khemvong and Suvachittanont 2005). The first cDNA-encoding DXS from this system (*EgDXS1*) was cloned from leaves, and the deduced full-length protein clearly falls into class 1 (named here EgDXS1A, Fig. 17.2). However, the second DXS isozyme (deduced from a cDNA called "*dxs2*") reported from oil palm, of which only partial sequences are available, can also be classified as a member of class 1 (84% amino acid sequence similarity to EgDXS1A) and exhibits no signatures of the class 2-DXS. The deduced protein is therefore renamed EgDXS1B (Fig. 17.2). Interestingly, this "*dxs2*"*/EgDXS1B* gene is strongly expressed in oil palm fruits correlated with the massive accumulation of β-carotene during fruit ripening (Khemvong and Suvachittanont 2005). Unfortunately, no expression profiles of *EgDXS1A* and also no information of "*dxs2*"*/EgDXS1B* expression apart from fruit ripening is as yet available. It is therefore possible but not proven that *EgDXS1B* is a specific isogene committed to carotenoid biosynthesis during fruit ripening. Another case of gene duplication within class 1 concerns the *M. truncatula* genome. From the ongoing genome sequencing project, a second *DXS1* genomic sequence became available, and the MtDXS1B protein deduced from it exhibits only 80% identity to the previously described

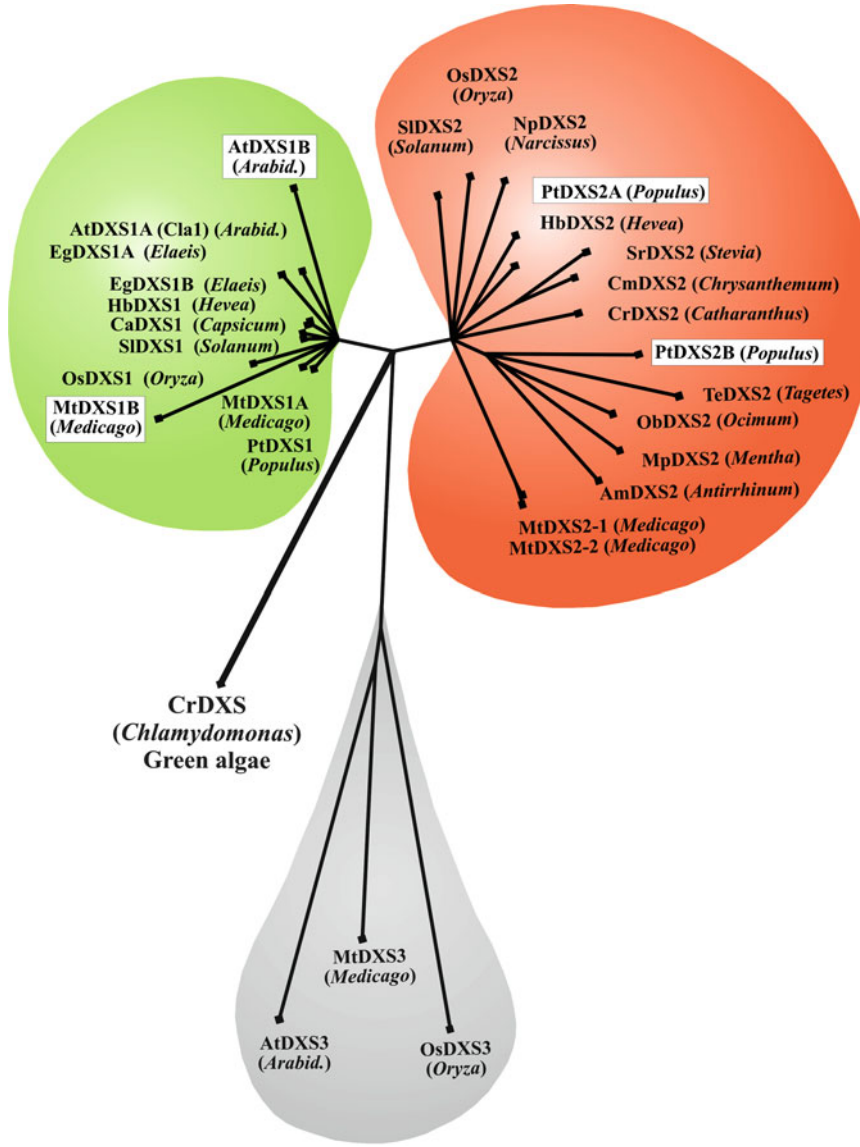

Fig. 17.2 Amino acid sequence similarity tree of DXS and DXS-like proteins of angiosperm plants displaying the divergence of two prevalent classes of plant DXS isoforms (DXS1 and DXS2) and of a less prominent third class of DXS-like proteins. A single DXS sequence from the green algae *Chlamydomonas rheinhardtii* is used as an out-group. N-terminal plastidial targeting peptides were excluded from the analysis. The color code of branches indicates the expression pattern of corresponding genes specifying housekeeping functions (*green*), biotic interactions/secondary metabolism (*red*), and unknown expression profiles (*white* or *gray*). References for biotic interaction-related expression of *DXS2* genes are listed starting from upper left corner of the DXS2 branch: SlDXS2 (*Solanum lycopersicum*), methyl jasmonate induction, Sánchez-Hernández et al. 2006; OsDXS2 (*Oryza sativa*), chitin elicitor induction, Okada et al. 2007; NpDXS2 (*Narcissus pseudonarcissus*) accession AJ279019, petal origin of mRNA; PtDXS2A (*Populus trichocarpa*) derived from genomic sequence, http://jgi-psf.org; HbDXS2 (*Hevea brasiliensis*) latex expression, Seetang-Nun et al. 2008a; SrDXS2 (*Stevia rebaudiana*) steviol-accumulating leaves, Totté et al. 2003; CmDXS2 (*Chrysanthemum morifolium*) petal expression, Kishimoto and Ohmiya 2006; CrDXS2 (*Catharanthus roseus*) terpenoid indole alkaloid accumulating cell cultures, Veau et al. 2000; PtDXS2B (*Populus trichocarpa*) derived from genomic sequence, http://jgi-psf.org; TeDXS2 (*Tagetes erecta*) elevated transcript levels in petals, Moehs et al. 2001; ObDXS2 (*Ocimum basilicum*) peltate glandular trichomes, Iijima et al. 2004; MpDXS2 (*Mentha x piperita*) glandular trichomes, Lange et al. 1998; AmDXS2 (*Antirrhinum majus*) flower volatiles, Dudareva et al. 2005; and MtDXS2-1 apocarotenoid-accumulating mycorrhizal roots, Walter et al. 2002; Floss et al. 2008a. The tree was constructed from a Clustal alignment using the programs "distances" and "splits" of the HUSAR program package using default values

MtDXS1 (Walter et al. 2002) yet still clearly falls into class 1 (Fig. 17.2). However, its relationship to the MtDXS1 (now tentatively renamed to MtDXS1A) is surprisingly distant, similar to the comparably distant relationship of AtDXS1B to AtDXS1A (CLA1) as visualized by extended displacement from the core *DXS1* genes in the phylogenetic tree (Fig. 17.2). The commonality of these two class 1-*DXS* variant genes is their very low expression. Only a single EST could be identified in the EST databases of *M. truncatula* or *A. thaliana*, respectively, whereas both genes for MtDXS1A and AtDXS1A (CLA1) are abundantly expressed in all kinds of tissues and are represented by >20 ESTs each. The functionality of these two "B" variants is not known, although there is no interruption of the open reading frame. Their low expression appears to indicate a low importance but it cannot be excluded that these genes are expressed in specific developmental situations or induced states not yet discovered. They may be descendants of the "A"-type *DXS1* in the two species, and reduced selection pressure might explain the rather large deviation from the consensus *DXS1*. Single *DXS1* genes from other species are abundantly expressed in all kinds of tissues, indicating their involvement in essential housekeeping functions (Bouvier et al. 1998; Walter et al. 2002; Estévez et al. 2000). Taken together, all DXS1 isozymes with known functionality (excluding the Arabidopsis and *M. truncatula* "B"-type variants) and reported strong constitutive expression have highly conserved amino acid sequences as indicated by the short connecting lines in the tree to their assumed common ancestor within the DXS1 branch (Fig. 17.2). This suggests strong constraint and selection of a specific primary structure of a single-copy DXS1 protein in plant species acting in housekeeping functions.

The DXS2 branch of amino acid sequences in the similarity tree is more expanded, that is, the similarity scores between DXS2 sequences of different species are generally lower than among the DXS1 proteins. In other words, the constraint on a specific primary sequence and the selection pressure imposed on it seem to be less strong than in the case of DXS1. Within the DXS2 branch, one subgroup appears to be somewhat separated from the rest of DXS2 sequences comprising *Tagetes*, *Ocimum*, *Mentha*, and *Antirrhinum* species as well as a poplar DXS2 sequence. The poplar sequence is particularly remarkable, since it is one out of two poplar DXS2 sequences which are only rather distantly related to each other (75% sequence identity between PtDXS2A and PtDXS2B), yet both belong to the DXS2 class. As judged from EST databases, both poplar *DXS2* genes are expressed (*PtDXS2A*: 8 ESTs and *PtDXS2B*: 3 ESTs). The existence of the two poplar DXS2 sequences (and also of dual gymnosperm DXS2, see below) argues for subgroups within the DXS2 branch with potentially different subfunctions. However, the available information for PtDXS2A and PtDXS2B is still too limited to confirm their expression in relation to environmental stimuli. They have therefore been excluded from the coloration in the DXS2 branch in Fig. 17.2, indicating a particular expression profile. In *M. truncatula*, a second *DXS2* gene was identified also, yet in this case it is almost identical to the previously described *MtDXS2* gene (98% identity of nucleotide sequence in exons, 76–95% in introns). It has been termed *MtDXS2-2* altering the original sequence to *MtDXS2-1* (Floss et al. 2008a). The very close relationship suggested it to be an allele (which is the justification for the different nomenclature used compared to other DXS isoforms). However, genomic analysis has defined this gene pair as a tandem repeat in the *M. truncatula* genome (Floss et al. 2008a). *MtDXS2-2* is most likely a daughter gene of *MtDXS2-1* since amino acid exchanges in the corresponding enzyme compared to the protein deduced from *MtDXS2-1* deviate from the consensus among legume DXS2 proteins. The deviant nomenclature is still retained to indicate that this is a *DXS* paralog, whereas in other cases orthology or paralogy of isogenes still need to be established. The possible significance of this and other tandem repeats in the evolution of *DXS* gene duplicates will further be discussed below. Various *Tagetes* species and cultivars (including *T. patula* and *T. tenuifolia*) were analyzed for variants of *DXS2* genes with a similarly close

relationship as the two *M. truncatula DXS2* paralogs. Two such variants could be identified from *T. patula* (Manke and Walter, unpublished results). However, since *T. patula* is known as an allotetraploid plant, it cannot be decided whether these genes are representatives of different genomes, alleles, or tandem duplicates.

The most striking feature of *DXS2*-type genes across all plant families is their expression pattern, which is distinct from *DXS1* genes, as marked by the red coloring of the DXS2 branch *versus* the green color for constitutively expressed DXS1 enzymes and genes (Fig. 17.2). For most of the *DXS2*-type genes described to date, there is information on expression related to adaptation processes to environmental conditions but not in plant development. This was first established for *MtDXS2-1* in the AM symbiosis as already discussed above, which, together with available literature data, led to the initial proposal of distinct functions of DXS1 and DXS2 in primary or secondary metabolism, respectively (Walter et al. 2002). More recently, herbivory-related and wound-induced inductions of *MtDXS2-1* transcript levels were reported (Arimura et al. 2008; Tretner et al. 2008). A *DXS2*-type gene was activated by methyl jasmonate treatment in the *spr2* mutant of tomato (Sánchez-Hernández et al. 2006). Pathogenic fungus-related expression has been shown for a rice *DXS2* ortholog (alignments suggest this gene to be a *DXS2* ortholog, although it was termed *OsDXS3* by the authors, Okada et al. 2007). The rise in transcript levels of this gene in chitin elicitor-treated cell cultures correlated with rice diterpene phytoalexin formation. *OsDXS2* transcript levels but not those of *OsDXS1* were also induced upon UV irradiation of seedlings (Kim et al. 2005). *Hevea brasiliensis DXS2* gene expression was elevated by etephone treatment in latex, differing from regulation of a *DXS1*-type isogene (Seetang-Nun et al. 2008a). A *DXS* regulated in leaf steviol diterpene biosynthesis of *Stevia rebaudiana* is of a *DXS2* type (*SrDXS2*, Totté et al. 2003). Terpenoid indole alkaloid production in periwinkle (*Catharanthus roseus*) requires MEP pathway activity and is correlated with upregulation of a *DXS2*-type *DXS* isogene (Chahed et al. 2000). A *DXS* gene regulated in monoterpene and sesquiterpene volatile emission from snapdragon flowers also turns out to be of the *DXS2*-type (Fig. 17.2; Dudareva et al. 2005). Finally, the *Mentha piperita DXS* involved in monoterpene biosynthesis of peppermint trichomes belongs to the *DXS2* class (Lange et al. 1998). A few other cases of *DXS2* involvement in responses to ecological cues are listed in the legend of Fig. 17.2. The reports on trichome-related *DXS2* expression have prompted additional work in a new project on the role of the *DXS2* isogene in glandular trichomes of tomato. Enrichment of *DXS2* transcripts in isolated tomato trichomes has been observed (Paetzold et al. 2010). On the contrary, *DXS2* transcripts were not elevated during the later stages of tomato fruit ripening when carotenoids accumulate abundantly, while *DXS1* transcripts were strongly elevated. This confirms earlier reports on strong upregulation of expression of a *DXS* gene during tomato fruit ripening (Lois et al. 2000), which can now be classified as a *DXS1* gene (Paetzold et al. 2010). It is also in agreement with upregulation of a *DXS1*-type isogene in oil palm fruit ripening as already discussed above (Khemvong and Suvachittanont 2005). The commonality and basis of all the *DXS2* upregulations appear to be the requirement for rapid, strong, and/or often local supply of IPP/DMAPP precursors for the formation of various end products involved in ecological functions.

The biochemical function and biological role of a third class of *DXS*-related genes and proteins are still a mystery despite the above-mentioned complementation of an *E. coli dxs* mutant by a maize *DXS3* sequence (Cordoba et al. 2011). This class has been called DXS-like and class 3 by us (Walter et al. 2002, Fig. 17.2) and is usually annotated as DXS-like in databases. As briefly addressed above, an ortholog of this class has also been described as AtDXS3 from Arabidopsis (Rodríguez-Concepción and Boronat 2002, Fig. 17.2). There are also orthologs in rice (Fig. 17.2) and ESTs of this class can frequently be found in other plant databases. Preliminary expression analyses of *MtDXS3* in *M. truncatula* have indicated a constitutive expression profile distinct from both *MtDXS1* and *MtDXS2* (Manke and Walter, unpublished results). Current *in silico*

data on expression obtained from the *M. truncatula* gene expression atlas (http://mtgea.noble.org/v2/) indicate rather constitutive expression at low level but moderately elevated transcript levels in cell cultures regardless of treatment with yeast elicitor or MeJA (data not shown). *DXS3* orthologs are only distantly related to class 1 and class 2 (Fig. 17.2). The deduced MtDXS3 protein is 62% identical to MtDXS1 and 58% identical to MtDXS2 (see also alignment in Fig. 17.3). Its position in the similarity tree (Fig. 17.2) suggests that it is unlikely to be a descendant of any of two other classes, but has probably evolved independently. Attempts to predict targeting signals from N-terminal amino acid sequences leads to conflicting results when using DXS3 sequences from different plants, yet there is an N-terminal extension compared to bacterial DXS sequences. Alignment of MtDXS3 sequences with MtDXS1, MtDXS2-1, and a bacterial DXS sequence from *Deinococcus radiodurans* (Xiang et al. 2007; Xiang et al. this volume) highlights a potentially important modification of DXS3-sequences: Many of the amino acids predicted to be involved in binding of the TPP coenzyme are modified in DXS3 (Fig. 17.3). This appears to preclude TPP binding at least at the known—and across all taxa highly conserved—sites and leaves the "DXS3" as a presently rather unlikely candidate for a TPP-dependent DXS protein.

While the division of labor between DXS1 and DXS2 in primary and secondary metabolism has now become more obvious owing to many data on the strictly differential expression of their genes, the importance and function of the differences in their primary structures are still elusive. The biochemical reaction condensing glyceraldehyde 3-phosphate and pyruvate to yield DXP should be identical, and these two substrates should not be variable. Both isoforms from *M. truncatula* exhibited enzyme activity without recognizable differences (Walter et al. 2002). In other systems, each of the isoform has been shown to be functional, again without obvious differences in activity (Lange et al. 1998; Bouvier et al. 1998).

Exchanges of single amino acids between class 1 and class 2 DXS of one species (e. g., *M. truncatula*) are not particularly meaningful. Only those exchanges which are consistently found in most or all members of one class suggest a significant impact on a conserved 3D structure or a particular functional feature of one isozyme class. Therefore, only those amino acid exchanges between MtDXS1 and MtDXS2-1 (a total of 70) are marked by asterisks in Fig. 17.3, which have been found to constitute conserved exchanges. This was done from an alignment of 18 DXS sequences from angiosperms (8 from class 1 and 10 from class 2, alignment not shown). None of these differences, conserved between class 1 and class 2, concerns residues involved in binding of the TPP coenzyme or binding of GAP, which have recently been defined (Xiang et al. 2007; Xiang et al. this volume, chapter 2). Moreover, specific residues leading to loss of activity upon site-directed mutagenesis are also invariable between class 1 and class 2 DXS (Fig. 17.3). This indicates that the biochemical differences, if any, may be linked to differences in enzyme kinetics or other features but do not alter the basic catalytic features of the isoforms.

Fig. 17.3 (continued) Fully conserved amino acids are indicated in white letters on blue background, red and yellow shadings indicate strong or less strong conservation, respectively. The start of the predicted mature protein excluding the signal peptide is indicated by an *arrowhead* (▲) The markings on top of the alignment specify the following features: *asterisks* (*), amino acids highly conserved in either class 1 or class 2 DXS as deduced from an alignment of 8 DXS1 sequences and 10 DXS2 sequences (not shown); *rhombs* (♦), residues predicted to be involved in TPP binding; *slashes* (/), separate the three domains as defined by Xiang et al. (2007); *squares* (■), residues involved in catalysis and shown to be essential for activity by site-directed mutagenesis; *white arrow* on black background (➘), intron position (not all introns are indicated); and gray background, regions or special importance as indicated. The alignment was performed with Clustal using default parameters

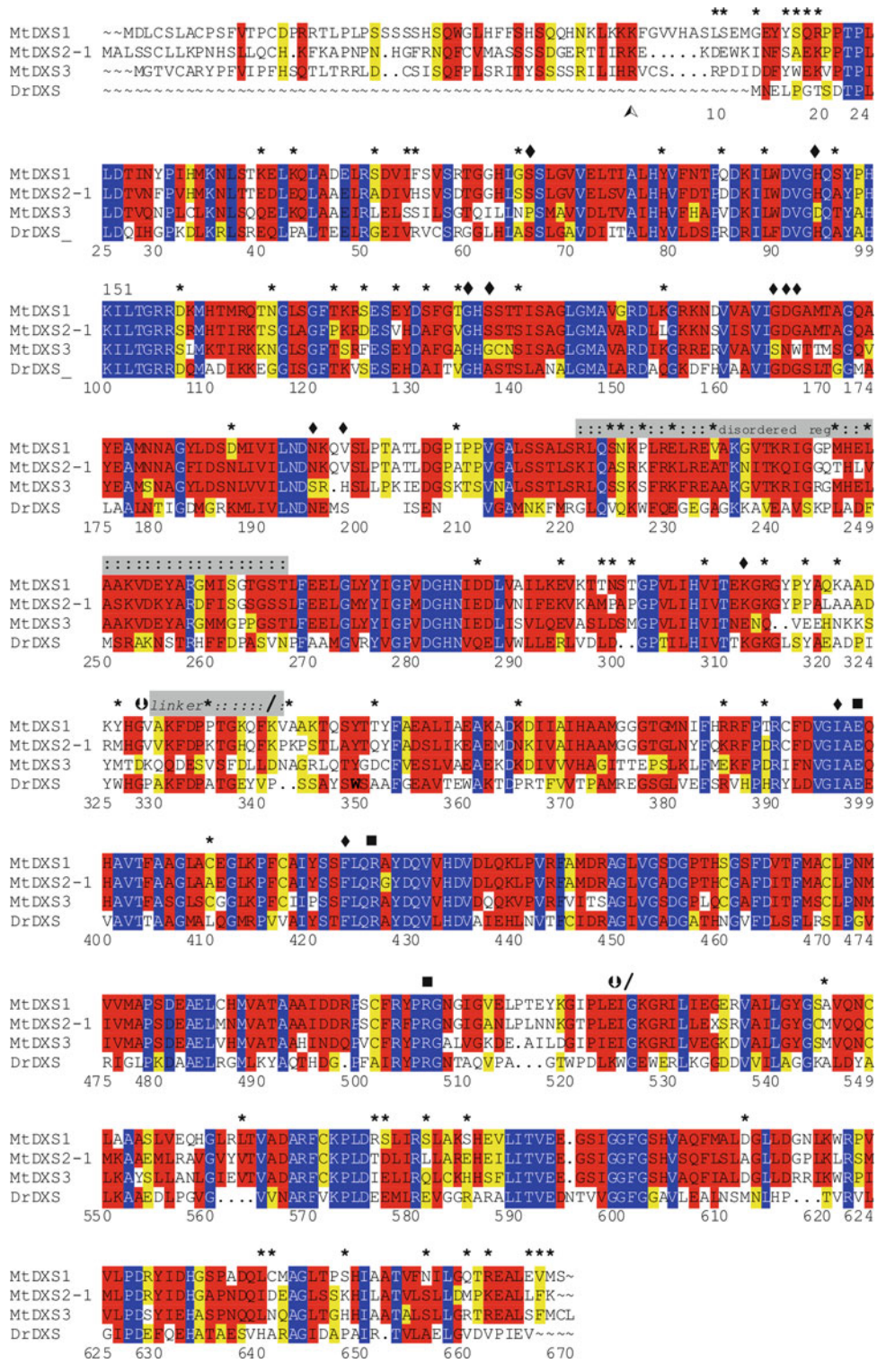

Fig. 17.3 Alignment of amino acid sequences of MtDXS1, MtDXS2-1, and MtDXS3 from *Medicago truncatula* with a bacterial DXS sequence from *Deinococcus radiodurans* (DrDXS; Xiang et al. 2007). MtDXS1 and MtDXS2-1 are confirmed functional DXS isozymes, whereas MtDXS3 is a DXS-like sequence and its functionality is unknown.

The 3D structure of the *D. radiodurans* DXS monomer has been elucidated (Xiang et al. 2007). It has been divided into three domains (I, II, and III, borders highlighted by slashes in the alignment of Fig. 17.3). All three domains have a central, mostly parallel β-sheet that is enclosed by α-helices. Domain I is the largest (corresponding to residues 1–341 in Fig. 17.3). Differences between DXS1 and DXS2 of plants occur preferentially at the outer ends of domain I (residues 1–140 including N-terminus and 286–341). The region between amino acid (aa) 328 (Gly) and aa 349 (Lys) has been described as a linker between domain I and II in the bacterial structure (Xiang et al. 2007). At the upstream end of this linker, there is an intron in both plant *DXS* isogenes from *M. truncatula*. (Floss et al. 2008a) corroborating the notion that the two domains may constitute entities of different functional significance. Domain II extends from residue 342 to 524, and an intron is located right at its border to domain III again in both the *MtDXS1* and the *MtDXS2-1* genes (Fig. 17.3, Floss et al. 2008a). There are only few conserved differences between DXS1 and DXS2 in domain II. Domain III reaches from residue 525 to 669 and harbors a number of amino acid exchanges conserved within class 1 and class 2 DXS. The most prominent ones locate to the C-terminus. The three domains form the DXS monomer, and two monomers are arranged side by side in the DXS dimer of *D. radiodurans* (Xiang et al. 2007). Homodimer formation is also likely for the plant DXS monomers, and there is no hint for a difference in monomer arrangement between the two types of plant DXS discussed here. However, it is conceivable that dimer formation and/or dimer stability is different. Preliminary analysis of structural models of tomato DXS1 and DXS2 isoforms using the *D. radiodurans* structure as a template has indicated that many of the residues discriminating the two isoforms are surface exposed (Brandt, Paetzold and Walter, unpublished results). Another possibility for different properties of the isoforms is therefore differential interaction with other proteins or with other plastidial regulatory components. These differences might contribute to differential turnover of the two isoforms. A shorter half-life of an inducible isoform needed only transiently (DXS2) as compared to the housekeeping isoform (DXS1) would make sense. DXS1 isoforms have been shown to be posttranscriptionally regulated depending on MEP pathway flux (Guevara-García et al. 2005; Rodríguez-Concepción 2006; Flores-Perez et al. 2008). Nothing is known about post-transcriptional regulation of *DXS2* genes or proteins. In summary, the combined evidence for a role of the structural differences and the potential importance of conserved discriminating residues is still weak and does not allow safe conclusions at this point.

17.4 The Duplication and Subfunctionalization of *DXS* Genes Has a Long and Still Ongoing Evolutionary History

The gymnosperms being evolutionarily older than angiosperms provide a number of pharmacologically important MEP-pathway-dependent isoprenoid compounds, which are likely to be the results of constitutive or induced adaptation strategies against environmental stresses. Among those are the diterpenes taxol of pacific yew (*Taxus brevifolia)* and the ginkgolides of the maiden hair tree (*Ginkgo biloba*), which are valuable compounds in cancer treatment or in treating cerebrovascular insufficiencies associated with cognitive decline and neurosensory impairments, respectively. This raises the question whether gymnosperms also use a specific second *DXS* gene for regulating isoprenoid precursor supply to their plastidial secondary isoprenoids. Systematic sequencing of a *Taxus cuspidata* cell suspension culture induced for taxoid production resulted in identification of four DXS-like sequences but these were not further classified (Jennewein et al. 2004). However, one full-length cDNA clone from the EMBL database (accession AY505129) encoding *Taxus* DXS clearly falls into class 2-DXS defined for angiosperms (Fig. 17.4a).

Mining of spruce EST databases provided additional indications for the existence of *DXS2*-related genes in gymnosperm genomes. Closer

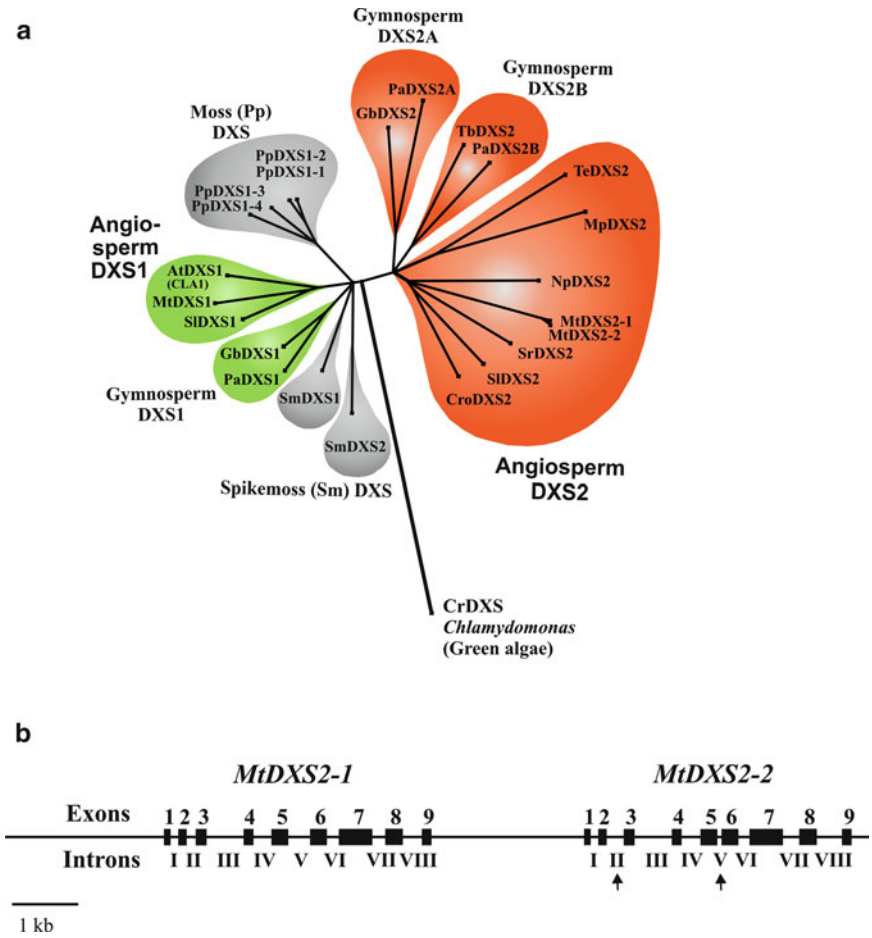

Fig. 17.4 Indications for *DXS* gene duplication events during land plant evolution. (**a**) Proposed evolutionary relationships of DXS from lower plants, gymnosperms, and angiosperms as deduced from an amino acid sequence similarity tree. The evolutionarily oldest plant (the moss *Physcomitrella patens* (Pp)) exhibits four closely related genes clustering close to the DXS1 branch of higher plants. *Selaginella moellendorfii* (Sm), a spikemoss, contains two more diverged *DXS* genes, which still cluster close to the DXS1 branch. Gymnosperm genomes harbor at least two considerably more diverged *DXS* genes, which cluster separately close to DXS1 and DXS2 branches of angiosperms. Spruce (*Picea abies* (Pa)) contains two DXS2 isoforms and genes (*PaDXS2A*, *PaDXS2B*). A selection of divergent angiosperm DXS1 and DXS2 sequences has been introduced into the dendrogram for comparison (see Fig. 17.2). Parameters for tree construction were as in Fig. 17.2. (**b**) Recent duplication event of a *DXS2* gene in the *M. truncatula* angiosperm genome as evidenced by two almost identical genes organized as a tandem repeat with only about 3 kb physical distance. Coding sequences are 98% identical in nucleotide sequence, and introns exhibit 72–98 % sequence identity. Exons are shown as *black boxes* and introns are *spaces in between*. Only introns II and V (marked by *arrows*) are somewhat different in size

analysis of genes involved in the early biosynthetic steps of induced oleoresins, a viscous mixture of mono-, sesqui-, and diterpenes involved in defense to herbivores and pathogens, revealed the existence of both class 1 and class 2 *DXS* genes in *Picea abies* (Phillips et al. 2007). Moreover, two distinct class 2 genes for DXS were characterized from this system, exhibiting only 80% amino acid sequence identity to each other and being both about 75% identical to a single class 1 DXS. Interestingly, while both class 2 *DXS* genes were regulated by pathogens, pathogen elicitors, or other environmental cues, they showed distinct responses to individual environmental cues.

PaDXS2A responded to treatment with chitosan, methyl salicylate, and infection by the pathogen *Ceratocystis polonica*, while *PaDXS2B* was responsive to methyl jasmonate and chitosan but not to methyl salicylate. The *DXS1* gene of *P. abies* did not respond to either of these treatments (Phillips et al. 2007). These results indicate differential regulation of three *DXS* genes in primary and defensive isoprenoid metabolism of spruce trees. Searching the extensive pine TGI database at DFCI (http://compbio.dfci.harvard.edu/tgi/) indicates orthologs of the three spruce *DXS* genes in this conifer as well. As described above, two distantly related genes of class 2 have also been found in the angiosperm poplar tree genome, and it will be interesting to find out whether trees in general allow themselves the luxury of maintaining two distinct *DXS2* genes with defense-related expression.

Next to the spruce system, more detailed analyses of *DXS* genes are available from the gymnosperm *G. biloba* in the context of ginkgolide biosynthesis. A class 2-*DXS* gene of *G. biloba* appears to be exclusively transcribed in embryonic roots, which is the site of ginkgolide biosynthesis, suggesting a specific role in the accumulation of these secondary defensive compounds. A *GbDXS1* gene showed elevated transcript levels in leaves consistent with its distinct role in housekeeping functions (Kim et al. 2006). Placing the GbDXS2 amino acid sequence in a similarity tree indicates its close relationship with the DXS2A class of spruce and pine. Whether *G. biloba* might also contain a gene of the gymnosperm DXS2B class, whose transcripts have not yet been identified, is a matter of speculation at this time. Taken together, there is ample evidence that *DXS* isogenes have evolved in gymnosperms to a similar or even larger level of complexity and division of labor as in angiosperms. Moreover, extensive studies in the group of Soo-Un Kim of Seoul National University on the complexity of subsequent MEP pathway steps in *G. biloba* in the context of ginkgolide biosynthesis have revealed isoforms in two other steps as well. The fourth step catalyzed by 4-(cytidine 5-diphospho)-2-*C*-methyl-D-erythritol kinase (CMK) occurs in two isoforms, and CMK2 is preferentially expressed in ginkgolide-accumulating embryonic roots and radicles (Kim et al. 2008a). 1-Hydroxy-2-methyl-2-(*E*)-butenyl 4-diphosphate reductase (called IDS for IPP/DMAPP synthase in this chapter) performing the seventh and last step of plastidial IPP biosynthesis is organized in at least two differentially expressed isogenes as well. *GbIDS2* transcript levels again correlate with ginkgolide biosynthesis in roots (Kim et al. 2008b). *GbIDS2* clusters close to a pine (*Pinus taeda*) *PtIDS2* sequence in a sequence similarity tree suggesting the existence of orthologs for *IDS2* isogenes among gymnosperms. Moreover, an additional apparently paralogous copy of *IDS2* (*GbIDS2*-1) has been reported from the *G. biloba* system (Kim et al. 2008b). As for angiosperms, two *DXR* gene copies have been described from the rubber tree *Hevea brasiliensis* exhibiting differential expression (Seetang-Nun et al. 2008b). However, the two deduced DXR proteins were highly similar (94% identity in amino acid sequence) indicating that these are likely to be paralogous genes of this species. Other steps appear to be catalyzed by single isoforms (Rodríguez-Concepción 2006).

In continuing on the story of *DXS* isogene evolution, the next step is to go to evolutionary even older plants by investigating *DXS* gene complexity in the moss *Physcomitrella patens*. Mining databases and the sequenced genome (http://www.phytozome.net/physcomitrella), we have identified four different *DXS* genes from this species (Manke, Leuchte, Walter, unpublished results). They are all very closely related to each other (93–98% amino acid sequence identity of proteins) and are most closely related to class 1 DXS of gymnosperms and angiosperms (Fig. 17.4a). A closer view, however, appears to reveal the separation of two classes (Fig. 17.4a). Unfortunately, the differences are too few to reliably decide whether this might indicate an early separation of primary structures of *DXS* isogenes towards the two differentially regulated classes found in angiosperms and gymnosperms. The existence of an even higher complexity in the moss with four genes is surprising but might be explained by a whole genome duplication of *P. patens* recently discovered (Rensing et al. 2007).

This latter process could have partitioned a single *DXS* gene duplication into the four *DXS* genes in today's moss genome. Initial analyses for potential differential regulation of these genes including wounding or methyl jasmonate treatments have not indicated differential regulation, but these results are too preliminary to come to final conclusions.

A logic extension of this approach is to now enter into steps of land plant evolution intermediate to mosses and gymnosperms. The spikemoss *Selaginella moellendorfii* nicely fulfills this condition, and its sequence is available. As one might have tentatively expected, this system indeed contains two *DXS* genes related to class 1 of higher plants which are diverged from each other further than the moss *DXS* genes are. However, the few differences between SmDXS1 and SmDXS2 are not sufficient to presently establish, whether they are descendants of the moss *DXS* isogenes and ancestors of the gymnosperm *DXS* isogene classes. Analyses of further clubmosses and ferns will be required to define a potentially continuous evolution of *DXS* isogenes during land plant evolution.

Returning to modern angiosperm times, one can also witness still ongoing or at least fairly recent *DXS* gene duplications. Screening phage libraries for genomic sequences of the *MtDXS2* cDNA, we have encountered by accident genomic sequences of a minor variant of this gene together with the corresponding gene itself. After assembly of all genomic fragments, it turned out that the two genes are linked and are separated by only about 3 kb in the *M. truncatula* genome, the duplicate copy being downstream of its parent gene (Fig. 17.4b). In the meantime, this tandem repeat of two *DXS2* genes has been confirmed by the *M. truncatula* genome sequencing project. Tandem duplication and close linkage is a hallmark of a recent single gene duplication, releasing a new gene copy into the genome to acquire a novel (sub)function or, if unsuccessful, perish as a nonfunctional pseudogene. The *MtDXS2-2* paralog of *MtDXS2-1* must be a very recent descendant since it has only 47 nucleotide exchanges in its 2,133 nts of coding sequence and even its intron sequences are closely related (70–98%) to its parent gene. It seems to be expressed in a similar AM-inducible fashion as *MtDXS2-1* yet at a much lower level. The promoter sequences of *MtDXS2-2* proximal to the transcription start site are also related to *MtDXS2-1*, but deviation increases in regions further upstream.

17.5 Knockdown of *DXS2* Expression by RNAi: A Novel Tool to Selectively Manipulate the Levels of Secondary Isoprenoids by Targeting Their Precursor Supply

Correlation of spatiotemporal expression of *DXS2* genes with accumulation of secondary isoprenoids is on its own not a sufficient proof for a distinct and essential function of the DXS2 isoform in nonhousekeeping biotic interactions. Such a proof can only be obtained from analyses of mutants or transgenic plants with a loss of function of the DXS2 isoform. Since no such mutant was available, an RNAi knockdown approach on *MtDXS2* isogene expression in transgenic mycorrhizal hairy roots of composite *M. truncatula* plants with a wild-type shoot was initiated. As discussed above, *MtDXS2* genes are organized as a tandem repeat of two highly similar paralogous isogenes (*MtDXS2-1* and *MtDXS2-2*), but since these two copies are almost identical in coding and noncoding regions, any silencing construct should repress both of these genes. On the other hand, the silencing construct has to be specific for the two *MtDXS2* genes and must not repress *MtDXS1*. Loss of function of MtDXS1 would be a lethal mutation as can be seen from the albino *CLA1* mutant phenotype (Mandel et al. 1996; Estévez et al. 2000). The latter requirement of missing out *MtDXS1* in the silencing approach appeared to be accomplishable by targeting regions of low nucleotide sequence similarity between *MtDXS2* and *MtDXS1* isogenes. These regions at the enzyme level are located at the N-terminus in the region coding for the signal peptide for plastid import and at the C-terminus. Independent RNAi constructs from these two regions were both shown to be capable of selectively downregulating

expression of *MtDXS2* genes by RNAi in transgenic hairy roots of *M. truncatula*, while not negatively affecting *MtDXS1* expression (Floss et al. 2008a).

Reduced levels of *MtDXS2* transcripts in mycorrhizal hairy roots of *M. truncatula* correlated with reduced levels of both C_{13} cyclohexenone and C_{14} mycorradicin derivatives, proving for the first time that these two apocarotenoids are formed via a DXS2-dependent part of the MEP pathway (Floss et al. 2008a). Very strong suppression of *MtDXS2* resulted in correspondingly strongly reduced levels of C_{13} and C_{14} apocarotenoids almost to the limits of detection, and such a strong reduction correlated with a severe alteration in the transcription profile of AM-induced plant marker genes (Floss et al. 2008a). This result validates a distinct function of DXS2 in the biosynthesis of secondary isoprenoid products exemplified with the apocarotenoid compounds of the AM plant-microbe interaction. *MtDXS1* transcript levels were not affected or even showed a slightly elevated level in some cases. Although there were thus reasonable overall levels of *MtDXS1* transcripts detectable in mycorrhizal RNAi roots, they obviously cannot compensate for the loss of *MtDXS2* transcripts. This might indicate that MtDXS1 and MtDXS2 are not interchangeable in catalyzing conversion of glyceraldehyde and pyruvate to DXP and ultimately supporting apocarotenoid biosynthesis in mycorrhizal roots. However, one needs to be cautious with such a conclusion. Biosynthesis and accumulation of AM-induced apocarotenoids has been shown to be a local event in root cells containing fungal arbuscules (Fester et al. 2002; Hans et al. 2004). The need for rapid and strong cell-specific upregulation of isoprenoid precursor supply may thus be the decisive factor for DXS action in this case. The question, whether DXS2 is replaceable by an appropriately expressed DXS1 isoform could be answered by simultaneously silencing *DXS2* and introducing a *DXS1* gene driven by a *DXS2* promoter. The *MtDXS2*-RNAi plants did not show any phenotypic alteration compared to empty-vector controls except for their mycorrhizal performance (Floss et al. 2008a). This result supports the proposed view that DXS2 is not essential for housekeeping functions. Again, a cautionary note is required here since with our approach we have silenced *MtDXS2* expression only in the roots and since *A. rhizogenes* induces hairy roots, which are transgenic, but gene-silencing effects do not spread to the shoot (Limpens et al. 2004). It remains to be shown that nonroot housekeeping functions are also independent of *DXS2* expression in *M. truncatula*.

Another RNAi approach targeted selectively on *DXS2* genes has been performed by us in tomato (*Solanum lycopersicum*) in the project briefly addressed above. This time the RNAi construct driven by the 35S promoter was constitutively expressed in all plant organs after *A. tumefaciens*-mediated gene transfer. Significant phenotypic alterations or changes in isoprenoid profiles were found in trichomes (Paetzold et al. 2010). Use of specific peptide antibodies indicated localization of DXS2 in the head cells of trichomes known to abundantly produce monoterpenes but also sesquiterpenes. The DXS2-RNAi lines exhibited a decreased ratio of mono- to sesquiterpenes compared to wild-type plants presumably as a result of suppression of MEP pathway function, which is mainly required for mono- but not sesquiterpenes. The observation of an increase in trichome density in these lines might be interpreted as a compensating response to a reduced biosynthetic capacity in individual trichomes leading to upregulation of trichome numbers (Paetzold et al. 2010). Overall, the results corroborate the view that DXS2 but not DXS1 is required for cell-specific upregulation of isoprenoid precursor supply in trichomes as well.

As for the general role of DXS2 in plant isoprenoid precursor supply, the single known case of nonoccurrence of *DXS2*-type genes in plant genomes is to be discussed further. As shown in Fig. 17.2 and mentioned above, there are two rather distantly related copies of *DXS1* and one copy of a "*DXS3*"-*DXS*-like gene, but no *DXS2*-type copy in the Arabidopsis genome. *A. thaliana* is perfectly viable but has also been called an ecologically poor species (Harvey et al. 2007). Arabidopsis does not enter into root symbioses and is one of the few species which are a nonhost to AM fungi. It also does not produce appreciable flower scent or petal color. Some of these deficiencies might be linked to a lack or poor

production of secondary isoprenoids, and it is tempting to speculate that at least some of these deficiencies of Arabidopsis might be related to the lack of a DXS2-dependent inducible precursor supply to secondary isoprenoid formation. The question, whether the lack of a *DXS2* gene copy extends to other members of the Brassicaceae, which are generally believed to be nonmycorrhizal, is still unresolved until further Brassicaceae genomes have been fully sequenced. Current rapeseed EST databases do not provide evidence for *DXS2*-type transcripts from this species. Given the fact that the presence of a *DXS2*-type gene copy in the genome of all higher plants seems to be the rule rather than the exception, one could speculate that Arabidopsis and perhaps other members of the Brassicaceae have lost their *DXS2* gene copy and are therefore compromised in particular adaptation strategies to biotic interactions.

Unraveling the role of specific secondary isoprenoids for a given interaction of plants with their environment is usually a challenging task. The biosynthetic routes of such compounds are often unknown or some of the enzymes and genes are involved in housekeeping or other unrelated functions. The role of precursor supply in these instances is unknown in most cases, but the widespread occurrence and manifold expression of *DXS2* genes dedicated to secondary metabolism in angiosperms (Fig. 17.2) and gymnosperms (Fig. 17.4a) suggests its importance. A well-organized IPP/DMAPP precursor supply may be an important asset in the arms race between plant and pathogen or in the control of a symbiont, at least when it comes to producing real weapons (abundant toxic phytoalexins, etc.) and not only doing intelligence (receptors and signaling). *DXS2* appears to be of key importance in precursor supply for the massive accumulation of secondary isoprenoids, and its manipulation may be a valuable tool to get initial insights into the importance of secondary isoprenoids of plastidial origin in a given interaction. This includes, next to apocarotenoid biosynthesis in mycorrhizal roots, diterpene phytoalexin biosynthesis in rice, mono- and diterpene biosynthesis in trichomes of mint and solanaceous species, as well as many aroma, scent, and spice compounds accumulating in specialized organs and tissues. However, as we currently experience in our ongoing quest for the function of the C_{13} and C_{14} apocarotenoids in the mycorrhizal symbiosis, this approach may not always give a clear answer as to the function of certain end products (Floss et al. 2008a). A phenotype correlated with reduced levels of the end products in question can theoretically also be brought about by the lack of another unknown DXS2-dependent compound or an intermediate. Normalizing the phenotype of the transgenics by supplementing with the compounds in question may be complicated or made impractible by very local and cell-specific accumulation of the respective compounds in the wild-type plant. While the information gained from the precursor-supply-downregulation approach may still be valuable, additional experimental strategies may be needed to arrive at more definitive conclusions. In case of reduced product levels and no alteration of phenotype or outcome of the interaction, the interpretation may be easier and allow excluding the participation of the respective compounds.

In conclusion, we have shown that a highly regulated IPP/DMAPP precursor supply to downstream isoprenoids is important for plant ecology and that differential silencing of *DXS2* genes is a feasible approach to selectively suppress plastidial isoprenoid precursor allocation to secondary isoprenoid end products. This result opens up new perspectives for manipulating other secondary isoprenoid end product levels and investigating their ecological roles without prior knowledge on downstream biosynthetic steps and without negatively affecting basic plant functions.

Acknowledgments This work was financially supported in part by grants to M.H.W. from the Deutsche Forschungsgemeinschaft within the priority programs SPP1084 and SPP1152 as well as by grant Wa536/5-1.

References

Alexander T, Meier R, Toth R, Weber HC (1988) Dynamics of arbuscule development and degeneration in mycorrhizas of *Triticum aestivum* L. and *Avena sativa* L. with reference to *Zea mays* L. New Phytol 110:363–370

Arimura GI, Garms S, Maffei M et al (2008) Herbivore-induced terpenoid emission in *Medicago truncatula*: concerted action of jasmonate, ethylene and calcium signaling. Planta 227:453–464

Bouvier F, D'Harlingue A, Suire C, Backhaus RA, Camara B (1998) Dedicated roles of plastid transketolases during the early onset of isoprenoid biogenesis in pepper fruits. Plant Physiol 117:1423–1431

Budziszewski G, Lewis SP, Glover LW et al (2001) Arabidopsis genes essential for seedlings viability: isolation of insertional mutants and molecular cloning. Genetics 159:1765–1778

Chahed K, Oudin A, Guivarc'h N, Hamdi S, Chénieux J-C, Rideau M, Clastre M (2000) 1-Deoxy-D-xylulose 5-phosphate synthase from periwinkle: cDNA identification and induced gene expression in terpenoid indole alkaloid-producing cells. Plant Physiol Biochem 38:559–566

Cordoba E, Salmi M, León P (2009) Unravelling the regulatory mechanisms that modulate the MEP pathway in higher plants. J Exp Bot 60:2933–2943

Cordoba E, Porta H, Arroyo A et al (2011) Functional characterization of the three genes encoding 1-deoxy-D-xylulose 5-phosphate synthase in maize. J Exp Bot 62:2023–2038

Dudareva N, Andersson S, Orlova I et al (2005) The nonmevalonate pathway supports both monoterpene and sesquiterpene formation in snapdragon flowers. Proc Natl Acad Sci USA 102:933–938

Enfissi EMA, Fraser PD, Lois L-M, Boronat A, Schuch W, Bramley P (2005) Metabolic engineering of the mevalonate and non-mevalonate isopentenyl diphosphate-forming pathways for the production of health-promoting isoprenoids in tomato. Plant Biotech J 3:17–27

Estévez JM, Cantero A, Romero C et al (2000) Analysis of the expression of *CLA1* a gene that encodes the 1-deoxy-D-xylulose 5-phosphate synthase of the 2-*C*-methyl-D-erythritol-4-phosphate pathway in Arabidopsis. Plant Physiol 124:95–103

Estévez JM, Cantero A, Reindl A, Reichler S, León P (2001) 1-deoxy-D-xylulose-5-phosphate synthase, a limiting enzyme for plastidic isoprenoid biosynthesis in plants. J Biol Chem 276:22901–22909

Fester T, Hause B, Schmidt D et al (2002) Occurrence and localization of apocarotenoids in arbuscular mycorrhizal plant roots. Plant Cell Physiol 43:256–265

Flores-Perez U, Sauret-Güeto S, Gas E, Jarvis P, Rodríguez-Concepción M (2008) A mutant impaired in the production of plastome-encoded proteins uncovers a mechanism for the homeostasis of isoprenoid biosynthetic enzymes in Arabidopsis plastids. Plant Cell 20:1303–1315

Floss DS, Hause B, Lange PR, Küster H, Strack D, Walter MH (2008a) Knock-down of the MEP pathway isogene *1-deoxy*-D-*xylulose 5-phosphate synthase 2* inhibits formation of arbuscular mycorrhiza-induced apocarotenoids and abolishes normal expression of mycorrhiza-specific plant marker genes. Plant J 56:86–100

Floss DS, Schliemann W, Schmidt J, Strack D, Walter MH (2008b) RNAi-mediated repression of *MtCCD1 carotenoid cleavage dioxygenase* in mycorrhizal roots of *Medicago truncatula* causes accumulation of C27 apocarotenoids shedding light on the functional role of CCD1. Plant Physiol 148:1267–1282

Gomez-Roldan V, Fermas S, Brewer PB et al (2008) Strigolactone inhibition of shoot branching. Nature 455(7210):189–194

Guevara-García A, San Román C, Arroyo A et al (2005) Characterization of the Arabidopsis *clb6* mutant illustrates the importance of posttranscriptional regulation of the methyl-D-erythritol 4-phosphate pathway. Plant Cell 17:628–643

Hans J, Hause B, Fester T, Strack D, Walter MH (2004) Cloning, characterization and immunolocalization of a mycorrhizal-inducible 1-deoxy-D-xylulose 5-phosphate reductoisomerase in arbuscule-containing cells of maize. Plant Physiol 134:614–624

Harvey JA, Witjes LMA, Benkirane M, Duyts H, Wagenaar R (2007) Nutritional suitability and ecological relevance of *Arabidopsis thaliana* and *Brassica oleracea* as food plants for the cabbage butterfly, *Pieris rapae*. Plant Ecol 189:117–126

Hemmerlin A, Hoeffler J-F, Meyer O et al (2003) Cross-talk between the cytosolic mevalonate and the plastidial methylerythritol phosphate pathway in tobacco bright yellow-2 cells. J Biol Chem 278:26666–26676

Hohnjec N, Vieweg MF, Pühler A, Becker A, Küster H (2005) Overlaps in the transcriptional profiles of *Medicago truncatula* roots inoculated with two different *Glomus* fungi provide insights into the genetic program activated during arbuscular mycorrhiza. Plant Physiol 137:1283–1301

Iijima Y, Davidovich-Rikanati R, Fridman E et al (2004) The biochemical and molecular basis for the divergent patterns in the biosynthesis of terpenes and phenylpropenes in the peltate glands of three cultivars of basil. Plant Physiol 136:3724–3736

Jennewein S, Wildung MR, Chau M, Walker K, Croteau R (2004) Random sequencing of an induced *Taxus* cell cDNA library for identification of clones involved in Taxol biosynthesis. Proc Natl Acad Sci USA 101:9149–9154

Khemvong S, Suvachittanont W (2005) Molecular cloning and expression of a cDNA encoding 1-deoxy-D-xylulose-5-phosphate synthase from oil palm *Elaeis guineensis* Jacq. Plant Sci 169:571–578

Kim B-R, Kim SU, Chang YJ (2005) Differential expression of three 1-deoxy-D:-xylulose-5-phosphate synthase genes in rice. Biotechnol Lett 27:997–1001

Kim S-M, Kuzuyama T, Chang Y-J, Song K-S, Kim S-U (2006) Identification of class 2 1-deoxy-D-xylulose 5-phosphate synthase and 1-deoxy-D-xylulose 5-phosphate reductoisomerase genes from *Ginkgo biloba* and their transcription in embryo culture with respect to ginkgolide biosynthesis. Planta Med 72:234–240

Kim S-M, Kim Y-B, Kuzuyama T, Kim S-U (2008a) Two copies of 4-(cytidine 5-diphospho)-2-*C*-methyl-D-erythritolkinase (CMK) gene in *Ginkgo biloba*: molecular cloning and functional characterization. Planta 228:941–950

Kim S-M, Kuzuyama T, Kobayashi A, Sando T, Chang Y-J, Kim S-U (2008b) 1-Hydroxy-2-methyl-2-(*E*)-butenyl

4-diphosphate reductase (IDS) is encoded by multicopy genes in gymnosperms *Ginkgo biloba* and *Pinus taeda*. Planta 227:287–298

Kishimoto S, Ohmiya A (2006) Regulation of carotenoid biosynthesis in petals and leaves of chrysanthemum (*Chrysanthemum morifolium*). Physiol Plant 128: 436–447

Klingner A, Bothe H, Wray V, Marner FJ (1995) Identification of a yellow pigment formed in maize roots upon mycorrhizal colonization. Phytochemistry 38:53–55

Lange BM, Wildung MR, McCaskill D, Croteau R (1998) A family of transketolases that directs isoprenoid biosynthesis via a mevalonate-independent pathway. Proc Natl Acad Sci USA 95:2100–2104

Laule O, Fürholz A, Chang H-S et al (2003) Crosstalk between cytosolic and plastidial pathways of isoprenoid biosynthesis in *Arabidopsis thaliana*. Proc Natl Acad Sci USA 100:6866–6871

Limpens E, Ramos J, Franken C et al (2004) RNA interference in *Agrobacterium rhizogenes*-transformed roots of *Arabidopsis* and *Medicago truncatula*. J Exp Bot 55:983–992

Lohse S, Schliemann W, Ammer C, Kopka J, Strack D, Fester T (2005) Organization and metabolism of plastids and mitochondria in arbuscular mycorrhizal roots of *Medicago truncatula*. Plant Physiol 139:329–340

Lohse S, Hause B, Hause G, Fester T (2006) Ftsz characterization and immunolocalization in the two phases of plastid reorganization in arbuscular mycorrhizal roots of *Medicago truncatula*. Plant Cell Physiol 47:1124–1134

Lois LM, Campos N, Rosa Putra S, Danielsen K, Rohmer M, Boronat A (1998) Cloning and characterization of a gene from *Escherichia coli* encoding a transketolase-like enzyme that catalyzes the synthesis of 1-deoxy-D-xylulose 5-phosphate, a common precursor for isoprenoid, thiamin and pyridoxol biosynthesis. Proc Natl Acad Sci USA 95:2105–2110

Lois LM, Rodríguez-Concepción M, Gallego F, Campos N, Boronat A (2000) Carotenoid biosynthesis during tomato fruit development: regulatory role of 1-deoxy-D-xylulose 5-phosphate synthase. Plant J 22:503–513

Maier W, Peipp H, Schmidt J, Wray V, Strack D (1995) Levels of a terpenoid glycoside (blumenin) and cell wall-bound phenolics in some cereal mycorrhizas. Plant Physiol 109:465–470

Mandel MA, Feldmann KA, Herrerra-Estrella L, Rocha-Soasa M, León P (1996) *CLA1*, a novel gene required for chloroplast development, is highly conserved in evolution. Plant J 9:649–658

Moehs CP, Tian L, Osteryoung KW, DellaPenna D (2001) Analysis of carotenoid biosynthetic gene expression during marigold petal development. Plant Mol Biol 45:281–293

Muñoz-Bertomeu J, Arrillaga I, Ros R, Segura J (2006) Up-regulation of 1-deoxy-D-xylulose 5-phosphate synthase enhances production of essential oils in transgenic *Lavandula latifolia* (spike lavender). Plant Physiol 142:890–900

Okada A, Shimizu T, Okada K et al (2007) Elicitor induced activation of the methylerythritol phosphate pathway toward phytoalexins biosynthesis in rice. Plant Mol Biol 65:177–187

Paetzold H, Garms S, Bartram S, Wieczorek J et al (2010) The isogene *1-deoxy-D-xylulose 5-phosphate synthase 2* controls isoprenoid profiles, precursor pathway allocation, and density of tomato trichomes. Mol Plant 3:904–916

Phillips MA, Walter MH, Ralph SG et al (2007) Functional identification and differential expression of 1-deoxy-D-xylulose 5-phosphate synthase in induced terpenoid resin formation of Norway spruce (*Picea abies*). Plant Mol Biol 65:243–257

Rensing SA, Ick J, Fawcett JA, Lang D, Zimmer A, Van de Peer Y, Reski R (2007) An ancient genome duplication contributed to the abundance of metabolic genes in the moss *Physcomitrella patens*. BMC Evol Biol 7:130. doi:10.1186/1471-2148-7-13

Rodríguez-Concepción M (2006) Early steps in isoprenoid biosynthesis: multilevel regulation of the supply of common precursors in plant cells. Phytochem Rev 5:1–15

Rodríguez-Concepción M, Boronat A (2002) Elucidation of the methylerythritol phosphate pathway for isoprenoid biosynthesis in bacteria and plastids: a metabolic milestone achieved through genomics. Plant Physiol 130:1079–1089

Sánchez-Hernández C, López MG, Délano-Frier JP (2006) Reduced levels of volatile emissions in jasmonate-deficient *spr2* tomato mutants favour oviposition by insect herbivores. Plant Cell Environ 29:546–557

Schwartz SH, Qin X, Loewen MC (2004) The biochemical characterization of two carotenoid cleavage enzymes from Arabidopsis indicates that a carotenoid-derived compound inhibits lateral branching. J Biol Chem 279:46940–46945

Seetang-Nun Y, Sharkey TD, Suvachittanont W (2008a) Isolation and characterization of two distinct classes of DXS genes in *Hevea brasiliensis*. DNA Seq 19:291–300

Seetang-Nun Y, Sharkey TD, Suvachittanont W (2008b) Molecular cloning and characterization of two cDNAs encoding 1-deoxy-D-xylulose 5-phosphate reductoisomerase from *Hevea brasiliensis*. J Plant Physiol 165:991–1002

Sharkey TD, Yeh S, Wiberley AE, Falbel TG, Gong D, Fernandez DE (2005) Evolution of the isoprene biosynthetic pathway in Kudzu. Plant Physiol 137:700–712

Smith SE, Read DJ (2008) Mycorrhizal symbiosis, 3rd edn. Academic, New York/London

Sprenger GA, Schörken U, Wiegert T et al (1997) Identification of a thiamin-dependent synthase in *Escherichia coli* required for the formation of the 1-deoxy-D-xylulose 5-phosphate precursor to isoprenoids, thiamin and pyridoxol. Proc Natl Acad Sci USA 94:12857–12862

Strack D, Fester T (2006) Isoprenoid metabolism and plastid reorganization in arbuscular mycorrhizal roots. New Phytol 172:22–34

Totté N, van den Ende W, Van Damme EJM, Compernolle F, Baboeuf I, Geuns JMC (2003) Cloning and heterologous expression of early genes in gibberellin and steviol biosynthesis via the methylerythritol phosphate pathway in *Stevia rebaudiana*. Can J Bot 81:517–522

Tretner C, Huth U, Hause B (2008) Mechanostimulation of *Medicago truncatula* leads to enhanced levels of jasmonic acid. J Exp Bot 59:2847–2856

Umehara M, Hanada A, Yoshida S et al (2008) Inhibition of shoot branching by new terpenoid plant hormones. Nature 455(7210):195–200

Veau B, Courtois M, Oudin A, Chénieux JC, Rideau M, Clastre M (2000) Cloning and expression of cDNAs encoding two enzymes of the MEP pathway in *Catharanthus roseus*. Biochim Biophys Acta 1517:159–163

Vogel JT, Walter MH, Giavalisco P et al (2010) SlCCD7 controls strigolactone biosynthesis, shoot branching and mycorrhiza-induced apocarotenoid formation in tomato. Plant J 61:300–311

Walter MH, Strack D (2011) Carotenoids and their cleavage products: biosynthesis and functions. Nat Prod Rep 28:663–692

Walter MH, Fester T, Strack D (2000) Arbuscular mycorrhizal fungi induce the non-mevalonate methylerythritol phosphate pathway of isoprenoid biosynthesis correlated with the accumulation of the 'yellow pigment' and other apocarotenoids. Plant J 21:571–578

Walter MH, Hans J, Strack D (2002) Two distantly related genes encoding 1-deoxy-D-xylulose 5-phosphate synthases: differential regulation in shoots and apocarotenoid-accumulating mycorrhizal roots. Plant J 31: 243–254

Walter MH, Floss DS, Hans J, Fester T, Strack D (2007) Apocarotenoid biosynthesis in arbuscular mycorrhizal roots: contributions from methylerythritol phosphate pathway isogenes and tools for its manipulation. Phytochemistry 68:130–138

Walter MH, Floss DS, Strack D (2010) Apocarotenoids: hormones, mycorrhizal metabolites and aroma volatiles. Planta 232:1–17

Xiang S, Usunow G, Lange G, Busch M, Tong L (2007) Crystal structure of 1-deoxy-D-xylulose 5-phosphate synthase, a crucial enzyme for isoprenoid biosynthesis. J Biol Chem 282:2676–2682

Tobacco Trichomes as a Platform for Terpenoid Biosynthesis Engineering

18

Alain Tissier, Christophe Sallaud, and Denis Rontein

Abstract

Many plant species have evolved specialized organs dedicated to the production of a restricted number of secondary metabolites. These organs have secretory tissues which can lead to very significant accumulations of products, in the range of mg per g of fresh weight. These natural cell factories are therefore interesting targets for metabolic engineering. Plant glandular trichomes in particular have attracted interest because of the relative ease to isolate them and to analyse the compounds they produce because they are secreted onto the leaf surface. Depending on the species, trichomes can produce a variety of metabolites. Terpenoids however are particularly well represented and have been used by humans in a variety of industries, including as aroma, fragrance and pharmaceutical ingredients. Tobacco trichomes produce diterpenoids in large amounts and were therefore chosen as a model system for engineering the biosynthesis of this important class of compounds. We present here our strategy and first results, which bode well for the future of glandular trichomes as engineered natural cellular factories.

A. Tissier (✉)
Leibniz Institute of Plant Biochemistry,
Weinberg 3, Halle (Saale) 06120, Germany
e-mail: alain.tissier@ipb-halle.de

C. Sallaud
Functional and Applied Cereal Group (FAC), Biogemma,
ZI du Brezet, 8 rue des Frères Lumière, Clermont-Ferrand Cedex 2 63028, France

D. Rontein
AnaScan, 17 rue du chemin Neuf, Gréoux les Bains
04800, France

T.J. Bach and M. Rohmer (eds.), *Isoprenoid Synthesis in Plants and Microorganisms: New Concepts and Experimental Approaches*, DOI 10.1007/978-1-4614-4063-5_18,

Keywords
Glandular trichomes • Tobacco trichomes • Sandalwood • "Nature identical" products • Laticifers • Secretory ducts • Cembratrien-diol (α- and β-CBT-diol) • *Nicotiana* species • Tobacco trichome exudate • CYP71D16 • Casbene synthase • Taxadiene synthase • Metabolic profile • Transcription promoters • Gene silencing • Diterpene secretion • Oxidized terpenes • 5(12)-oxa-3(11)-cyclotaxane

18.1 Introduction

The use of plant secondary metabolites by humans probably dates back to the early days of our history, and they still find many applications as ingredients in the flavour and fragrance, fine chemicals and pharmaceutical industries, to cite the most important. Compared to food crops, most plant species which are grown for their secondary metabolite production have been the object of little improvement, whether qualitative or quantitative, over their long history of human usage. This is understandable as the priority has been, and still is, to be able to feed humanity in the most efficient and durable way. However, the growing pressure on arable land calls for an improvement of all plant species which are used in agriculture. Increasing the productivity is one objective, as it will allow a reduction in the surfaces grown for a given product. Another reason for improvement is the reduction of undesirable compounds, as those which are cited as allergens in the seventh amendment of the European Commission directive n°76/768 (available online at http://ec.europa.eu/enterprise/cosmetics/html/cosm_legal_intro.htm). Yet another issue is species conservation. Some products are extracted from wild species whose survival is threatened due to overexploitation. This is the case for sandalwood (*Santalum album*), a semi-parasitic tree prized for its fragrant essential oil. Transferring the production of the critical ingredients of sandalwood oil in an easily cultivable plant would allow a long-term management of this threatened species. Finally, an important concern is the sustainability of the current fine chemicals production system which relies for the most part on fossil carbon sources. Since the advent of the petrochemical industry, many natural products have been replaced by synthetic analogues or "nature identical" products of synthetic origin, and a whole range of new chemicals and products have been developed, such as plastics, and are now part of our everyday life. However, the current rising costs of fossil carbon sources coupled to the eventual disappearance of such resources will undoubtedly call for a return to plant feedstock. Nonetheless, there will be stiff competition for arable land between food, energy, medicinal, flavour and fragrance crops, and there is no doubt that improvement in productivity, robustness and quality will be paramount to the successful management of this competition.

Plants synthesize a wide range of metabolites and macromolecules, and often these productions take place in specialized structures. These can be broadly classified in two main classes: external or internal. Within each class, there is considerable diversity, but these organs share common features which are relevant to metabolic engineering. The internal class of secretory structures comprises laticifers and secretory ducts. Secretory ducts such as the resin canals of conifers are composed of an epithelium of secretory cells forming a cylinder in the middle of which the compounds are secreted. Laticifers on the other hand, whether fused or not, are at the same time the site of production and of accumulation of the compounds. External structures involved in the secretion of secondary metabolites are mainly represented by glandular trichomes, which are leaf hairs more or less protruding from the surface of the aerial parts of the plant. In the rest of this chapter, we will focus on glandular trichomes, but the principles of metabolic engineering which we will present for glandular trichomes should be applicable to other specialized secretory structures as well.

There are two main types of glandular trichomes. Peltate trichomes, typically found in the *Lamiaceae* (mint family), are adapted for the production and storage of volatile compounds in a subcuticular space located between the plate of secretory cells and their apical cuticle. On the other hand, trichomes involved in the secretion of resinous, non-volatile material, like those of the *Solanaceae*, are devoid of such subcuticular storage space, and the secretory cells are often stacked on top of each other with the secretion exuding at the tip of the trichome head.

The types of compounds produced by glandular trichomes are very diverse and include terpenoids, phenylpropanoids, flavonoids, alkaloids, fatty acid derivatives and acylated sugars. The purpose of this chapter is not to review the diversity of the plant trichome structures. These have been covered in excellent reviews which the reader is referred to (Pickard 2008; Schilmiller et al. 2008; Wagner 1991). We will rather focus on the requirements and rationale for metabolic engineering in these secretory organs and introduce our model platform, the tobacco glandular trichomes.

18.2 Complexity of the Endogenous Metabolic Profile

Depending on the species or even the chemotypes within a species, the productions of plant secretory structures can be fairly complex or on the contrary contain a limited number of compounds. For example, the resin ducts of conifers such as pine are able to produce a mixture of terpenoids, principally monoterpenes such as pinenes, and diterpenoid resin acids (Steele et al. 1998). Glandular trichomes of basil (*Ocimum basilicum*) leaves also produce close to 30 different compounds belonging to different classes, mainly monoterpenoids, sesquiterpenoids and phenylpropanoids (Iijima et al. 2004). On the other hand, glandular trichomes of certain species accumulate a single or a restricted set of related compounds. For example, peppermint produces mostly monoterpenes derived from (−)-limonene, with menthol and menthone being the major compounds (Maffei et al. 1989). Similarly, glandular trichomes of the wild tobacco *Nicotiana sylvestris* produce two stereoisomers of the macrocyclic diterpenoid cembratrien-diol (α- and β-CBT-diol) which, combined, represent around 95% of the leaf exudate (our unpublished results). Other species may have fairly complex profiles, but this may be due to the expression of a multi-product terpene synthase. For example, patchouli (*Pogostemon cablin*) produces a mixture of sesquiterpenes, including patchoulol, which is largely accounted for by the expression of a single sesquiterpene synthase (Deguerry et al. 2006).

According to the purpose of metabolic engineering, several issues should be taken into consideration. If the aim is to modify or improve the profile of a given extract, for example, by increasing the concentration of a particular compound or removing an undesirable one, it seems more reasonable to directly modify the concerned plant species, either by transgenesis or by mutagenesis. On the other hand, the use of metabolic engineering to develop the production of novel compounds or the production of single isolated compounds rather than a mixture requires the use of carefully chosen host species. In the previous paragraph, we pointed the fact that certain species have a complex secondary metabolite profile resulting from the activation of multiple and distantly connected pathways, for example, basil which produces terpenoids and phenylpropanoids, while others have a much simpler profile with a single major pathway. A low-complexity profile offers a more favourable situation for engineering the biosynthesis of compounds which are of the same class as that of the compounds produced by the host plant. This is particularly true of terpenoids, because terpenoids are all derived from the same precursors, namely isopentenylpyrophospahte (IPP) and dimethylallylpyrophosphate (DMAPP).

18.3 Reasons for Choosing Tobacco as a Host for Engineering Terpenoid Biosynthesis

The wild tobacco, *Nicotiana sylvestris*, presents a number of features which make it an attractive model for terpenoid engineering. Many *Nicotiana* species produce a sticky resin covering the leaves which is composed mainly of diterpenoids and

sucrose esters. *N. sylvestris*, together with *N. tomentosiformis*, is a presumed progenitor of cultivated tobacco, the allotetraploid *N. tabacum*, and has thus a diploid genome. From a genetics standpoint, diploid species are more convenient to work with, especially with regard to gene redundancy and the ability to inactivate specific genes, by induced mutagenesis or gene silencing. Like its cultivated relative, *N. sylvestris* is easily transformed by *Agrobacterium tumefaciens*, and regenerated plants can be recovered within 3–4 months. The metabolic profile of *N. sylvestris* trichome exudate is also much simpler than those of *N. tomentosiformis* and *N. tabacum*. As mentioned above, *N. sylvestris* leaf exudate consists of a mixture of α- and β-cembratrien-diols representing around 95% of the exudate. *N. tomentosiformis* produces an array of labdanoid compounds, most of them derived from the labdanoid diterpene *cis*-abienol, and a complex mixture of sucrose esters with short-chain straight and branched carboxylic acids. *N. tabacum* cultivars exhibit a wide spectrum of diversity in the composition of the trichome exudate, but most of the isolates produce sucrose esters, labdanoids and cembranoids, in varying quantities. Thus, *N. sylvestris* presents both the advantage of a diploid genome and a simpler metabolic profile. Additionally, *N. sylvestris* does not spontaneously cross with *N. tabacum*, neither with any major food crop—important criteria to consider if one is to use this plant as a vehicle for the production of biologically active compounds. Finally, due to the close phylogenetic relationship between them, *N. sylvestris* benefits from the large-scale sequencing programmes (EST and genomic) of *N. tabacum*, thus providing access to useful sequence information.

18.4 Advantages of Using Secretory Trichomes as Engineering Targets

Although trichomes represent a small part of the plant's volume, the actual output of these organs in terms of biomass can be considerable. For example, menthol mint (*Mentha arvensis*) can produce up to 150–200 kg of essential oil per ha, for an estimated total dry biomass of around 2,500 kg. Thus, although trichomes represent less than 1% of the total volume of the plant, their production may reach close to 10% of the total dry biomass. Similarly, the exudate of *N. sylvestris* leaves, like that of *N. tabacum* (Wang and Wagner 2003), may reach up to 10% of the total leaf biomass. These high yields are favoured when relatively moderate to high stress conditions (drought and high temperatures) occur during the growth of the plant. Under these conditions, an adult *N. sylvestris* plant typically produces 100–150 g of fresh biomass. With a density of 50,000 plants per ha, this leads to 50–75 kg of leaf exudate/ha. In addition, there may be up to three harvests per year, bringing the total amount of exudate per ha to 150–225 kg/ha. An interesting feature of the tobacco trichome exudate is that it is precisely located on the outside of the trichome and can be recovered by simply washing the leaf in an appropriate solvent, without grinding. The complexity of the extract produced this way is therefore limited to the trichome secretions in addition to other compounds soluble in the solvent, usually waxes from the cuticle. Another advantage of glandular trichomes is that the whole pathway takes place within the secretory cells meaning that the pathway may be diverted at any step. In Fig. 18.1, the tobacco CBT-diol pathway is shown with potential branching points to other classes of terpenoids.

18.5 General Strategy for the Engineering of Terpenoid Metabolism in Tobacco Trichomes

The rationale is to divert the massive metabolic flux in tobacco glandular trichomes towards terpenoids of interest. For example, if the objective is to have tobacco trichomes produce novel diterpenes, this can be done by expressing diterpene synthases in the trichome secretory cells and at the same time down-regulating or inactivating the endogenous tobacco diterpene synthases

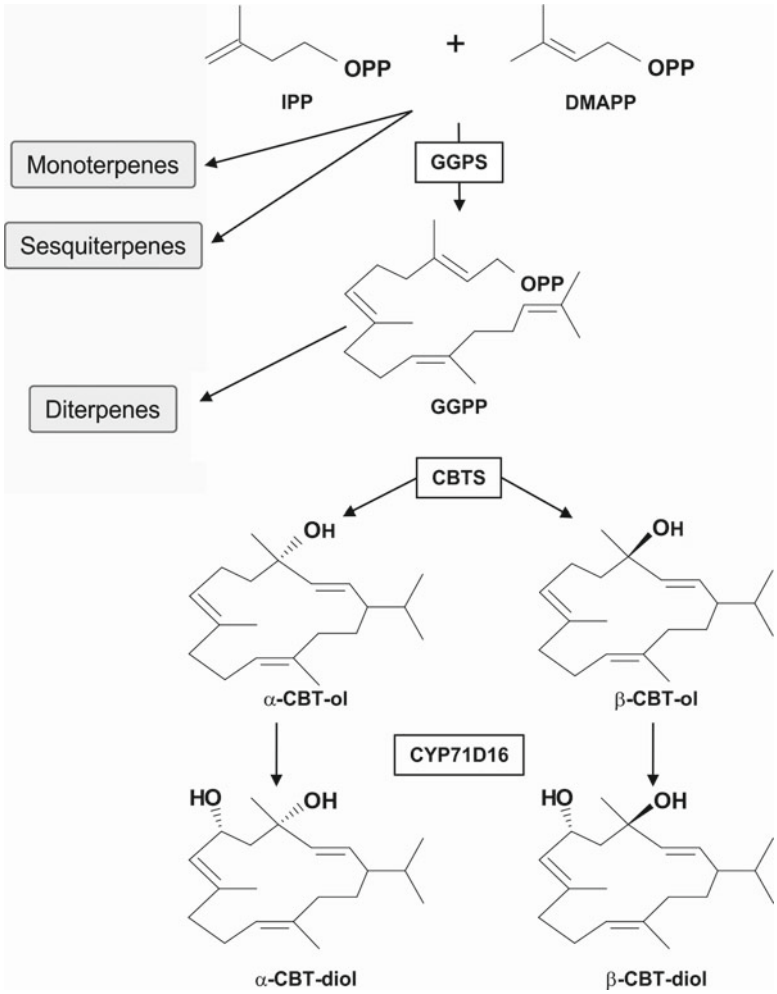

Fig. 18.1 *Biosynthesis pathway of cembratrien-diols in tobacco trichomes.* The precursors isopentenyldiphosphate (*IPP*) and dimethylallyldiphosphate (*DMAPP*) are the substrates of the geranylgeranyl diphosphate synthase (*GGPS*) to give geranylgeranyl diphosphate (*GGPP*). The cembratrien-ol synthases (*CBTS*) then convert GGPP to a mixture of α- and β-cembratrien-ol (CBT-ol). α-CBT-ol and β-CBT-ol are then hydroxylated to α- and β-CBT-diol, respectively, by CYP71D16, a cytochrome P450 oxygenase. IPP and DMAPP may be used to produce mono- or sesquiterpenes, and GGPP to produce diterpenes

(Fig. 18.2). One would expect that inhibiting the endogenous terpene synthases should make the precursor, in this case GGPP, available for the heterologous terpene synthases, while eliminating the endogenous products to facilitate the identification and purification of the novel compounds produced. Ideally, to take advantage of the separation of the glandular trichome from the rest of the plant, expression of the heterologous terpene synthases will be under the control of a trichome-specific promoter, in particular to avoid potentially toxic effects of the production of novel diterpenes in the main body of the plant. This has been observed previously when production of taxadiene was attempted in Arabidopsis under the control of the ubiquitous cauliflower mosaic virus 35S (CaMV 35S) promoter (Besumbes et al. 2004), which resulted in growth retardation and decreased content of carotenoid pigments. This was interpreted not as a direct toxic effect of taxadiene but as a perturbation of the GGPP pool in the whole plant resulting in

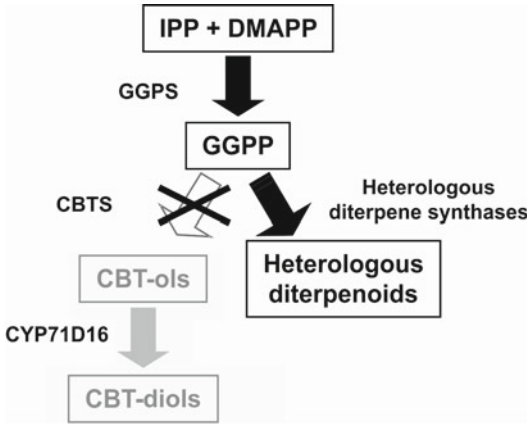

Fig. 18.2 *Strategy for the engineering of diterpene biosynthesis in tobacco trichomes.* The CBT-diol pathway will be blocked at the CBTS, for example, by gene silencing, and heterologously expressed under the control of a trichome-specific promoter

interference with gibberellin and carotenoid metabolisms. We also have observed that even low levels of expression of certain diterpene synthases outside the trichome cells can lead to deleterious effects (see below), underpinning the need of highly specific expression in trichome cells.

18.6 Identification of Transcription Promoters Specific of Trichome Glandular Cells

Trichome-specific promoters have been identified and characterized from several species, notably *Arabidopsis thaliana* and cotton (*Gossypium hirsutum*). The promoter of the trichome regulatory Myb gene *GLABROUS 1* (*GL1*) of Arabidopsis was the first of the series. Interestingly, it was found that the upstream region of the gene was sufficient for trichome-specific expression only when a 3′-non-coding enhancer was present in the reporter construct (Larkin et al. 1993; Oppenheimer et al. 1991). Trichome-specific promoters from other genes were isolated from *Arabidopsis*, but most of these, like *GL1*, encode regulatory proteins whose expression is either transient during the development of the trichomes or is not exclusively specific to the trichomes because they are also involved in the developmental control of other organs, frequently root hairs, whose epidermal fate bears similarities to that of leaf trichomes. Thus, for the purpose of metabolic engineering, where high specificity together with persistent expression during the life of the trichome is desirable, these promoters cannot be considered ideal candidates. In addition, there is evidence that the ontology of trichome development differs between plants like *Arabidopsis* and cotton on one hand and *Antirrhinum* and Solanaceae species on the other (for review see Serna and Martin 2006), indicating that promoters driving the expression in trichome from one species may not do the same in another species. This suggests that searching for promoters of genes which are expressed in the species that is targeted for metabolic engineering is probably the best approach. As mentioned earlier, the biosynthetic pathways of isoprenoid compounds secreted by glandular trichomes take place entirely in these cells (Keene and Wagner 1985; Gershenzon et al. 1989, 1992; Guo et al. 1994). The corresponding genes are therefore likely to be the best providers of trichome-specific promoters. Using this approach, Wagner and co-workers cloned the promoter of the gene encoding CYP71D16, a cytochrome P450 monooxygenase involved in the hydroxylation of cembratrien-ol (CBT-ol) to cembratrien-diol (CBT-diol) (Wang et al. 2002). Following the same approach, we set out to isolate other tobacco trichome-specific promoters. Our model plant is *Nicotiana sylvestris*, which is one of the presumptive parents of cultivated tobacco. Its genes thus often show sequence identity levels of 99% with those of *Nicotiana tabacum*. In addition, CBT-diol biosynthesis in tobacco is inherited from *N. sylvestris*; thus, the genes of the CBT-diol pathway are likely to be highly conserved between the two species. We reasoned that the gene encoding the cembratrien-ol synthase (CBTS) would provide a suitable candidate for a trichome-specific promoter with a high level of expression given

the generally low catalytic turnover of terpene synthases. Previous work leads to the identification of a candidate gene for CBTS (Wang and Wagner 2003). We found that CBTS activity in the trichome is in fact encoded by a multigene family of at least four members and that the genomic copy identified previously (Genbank number AY049090) was not expressed in the glandular trichomes. We named those four genes *CBTS-2a*, *CBTS-2b*, *CBTS-3* and *CBTS-4*. All four genes are expressed in the trichomes, and the upstream region of all four was cloned by anchored PCR on genomic DNA. 1.1 kb was sequenced for all promoters and up to 3.4 kb for the promoter of the *CBTS-2b* gene (Ennajdaoui et al. 2010). The sequences are highly similar, which is consistent with the comparable levels of expression of these genes in the trichome. Given the level of sequence identity between those genes, it can be assumed that they are the result of fairly recent gene duplications and are likely to be localized at the same chromosomal locus. However, no data currently corroborates this hypothesis.

18.7 Trichome-Specific Expression Driven by the *CBTS-2b* Promoter

Several constructs with fragments of varying lengths (1.0–3.4 kb) from the *CBTS-2b* promoter were cloned upstream of a GUS reporter gene. In particular, a construct with 1.0 kb of *CBTS-2b* promoter sequence gave a specific expression in the glandular cells, albeit at a low and highly variable level. To increase the level of expression of this construct, the transcription enhancer from the CaMV 35S promoter was cloned 5′ to the promoter. This led to increased levels of expression in the trichome cells but was accompanied by expression in other parts of the plant, notably conductive tissues and roots, and upon wounding. This is not desirable as it could lead to deleterious effects on growth when the produced compounds are toxic for the plant. On the other hand, a 1.7-kb fragment conferred a fairly strong and stable trichome-specific expression (Fig. 18.3).

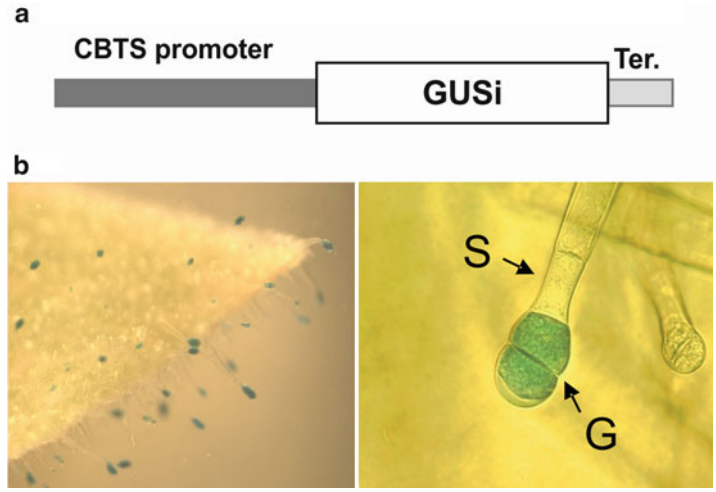

Fig. 18.3 *The CBTS promoter is specific of the trichome secretory cells.* (**a**) Schematic drawing of the construct used to assay the CBTS promoter. A 1.7-kb fragment of the CBTS-2b promoter was fused to the GUS reporter gene with an intron (GUSi) and to the 3′ region of the CBTS-2b gene to serve as transcription terminator (Ter.). (**b**) GUS staining of *N. sylvestris* plants expressing the construct described in (a) The picture on the *left* shows a portion of a leaf with the secretory trichomes staining blue. The picture on the *right* shows a detailed view of secretory trichome. The glandular cells (*G*) are stained in blue, while cells of the stem of the trichome do not stain

18.8 Silencing the Endogenous Tobacco Diterpenoid Pathway

As part of our strategy outlined earlier, the next step was the down-regulation of the endogenous CBT-diol pathway. For diterpenoid engineering, the step to knock down was the CBT-ol synthase (CBTS). Inactivating this enzyme should lead to two effects: elimination of endogenous *N. sylvestris* diterpenoids and availability of the diterpenoid precursor, geranylgeranyl diphosphate (GGPP), for the biosynthesis of other diterpenoids. To rapidly generate plants with a CBTS-deficient phenotype, we adopted a gene silencing strategy. Gene inactivation by targeted gene mutation is a possibility, but the presence of several very closely related CBTS genes most likely clustered together makes the success of this approach uncertain, as it would require selecting for recombinants between very closely linked genes. Intron hairpin (ihp) gene silencing has been described as an efficient technique to knock down the expression of genes in plants (Smith et al. 2000; Wesley et al. 2001), and it was applied to the CBTS gene of *N. sylvestris*. The second exon of the *CBTS-2a* gene was chosen as the target region because it is the most highly conserved sequence fragment between the *CBTS* genes. The second exon together with the second intron was thus cloned upstream of the second exon in antisense orientation. The splice donor and acceptor sites of the intron 2 were preserved to ensure correct splicing and maximal silencing efficiency. This ihp*CBTS* construct was cloned 3′ of the 1.7-kb fragment of the *CBTS-2a* promoter and upstream of the *CBTS*-2a terminator region. The construct is shown in Fig. 18.2. Cloning of this construct in a T-DNA vector allowed transformation of *N. sylvestris* plants via *Agrobacterium tumefaciens*. Over 15 independent transformants were recovered. Extracts of exudate were prepared by washing leaves of the transformants with hexane and analysed by GC-MS. Representative profiles of exudates from ihp-*CBTS* transgenics and wild-type plants are presented in Fig. 18.4. CBT-diol levels in ihpCBTS plants are strongly reduced, and no additional compounds could be observed in the leaf exudate. Transformants with a single copy of the T-DNA were selected for further analysis by quantitative real-time PCR. Upon self-fertilization of the mono-copy transformants, T1 seeds were recovered and put to germinate. T1 plants with the ihpCBTS in the homozygous state were selected for further analysis. Examination of the exudate content of these plants confirmed the observations made on the T0 plants. On average, CBT-diol levels were down to around 1% of the wild-type levels.

18.9 Expression of Casbene Synthase in Tobacco Trichomes

Casbene is a diterpene produced by castor bean (*Ricinus communis*) seedlings upon elicitation by fungal pathogens (Dueber et al. 1978; Stekoll and West 1978). Casbene synthase (CS) was the first diterpene synthase cloned from an angiosperm (Mau and West 1994). The CS cDNA was cloned either downstream of the 1.7-kb *CBTS* promoter (*CBTS*1.7) or downstream of the 1.0-kb *CBTS* promoter fragment coupled to the CaMV 35S enhancer (enh35S-*CBTS*1.0). Both constructs were cloned into a T-DNA vector, and transgenic plants were produced via *Agrobacterium tumefaciens* transformation. Interestingly, plants expressing CS under the enh35S-*CBTS*1.0 promoter showed extensive necrotic patches on leaves and retarded growth. This indicated that casbene elicited a HR-like response in tobacco plants. On the other hand, CBTS1.7:CS plants showed no sign of necrosis and behaved like wild-type plants with regard to growth. Leaf exudate from these plants was analysed by GC-MS as described previously. Casbene could be detected in the exudate of both classes of transformants, and typical chromatograms are shown in Fig. 18.5. enh35S-*CBTS*1.0 plants showed a consistently higher level of casbene (in the range of 50–100 μg/g FW) than *CBTS*1.7:CS plants (around 10 μg/g FW). This could be explained by a somewhat higher level of expression in the trichome glandular cells but also by the contribution of leaf cells to the output of casbene due to the contribution of the 35S enhancer to ectopic expression.

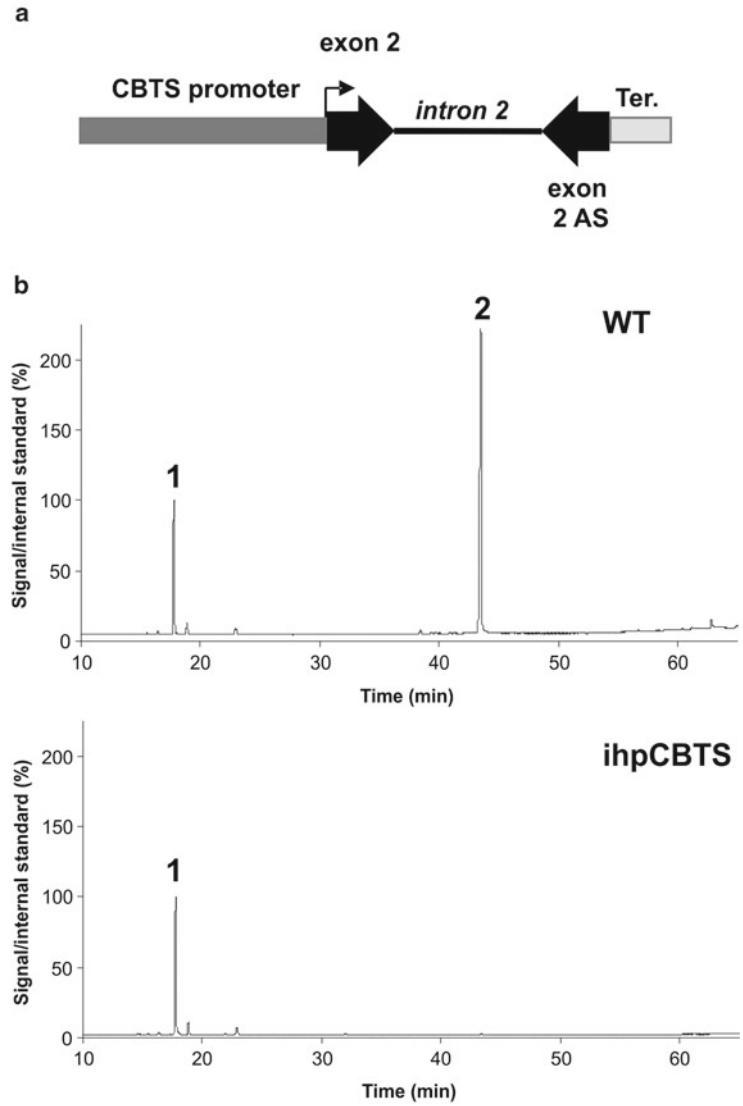

Fig. 18.4 *Gene silencing of the CBTS genes strongly reduces the production of CBT-diols by tobacco trichomes.* (**a**) Schematic drawing of the intron hairpin construct used to silence the CBTS genes. The second exon (exon 2) of the CBTS-2b gene was cloned in antisense orientation (exon 2 AS) downstream of the exon 2 and the second intron (intron 2). This ihpCBTS cassette was cloned between the CBTS promoter and the CBTS terminator (see Fig. 18.3). (**b**) Gas chromatography profiles of a *N. sylvestris* wild-type plant (WT) and a *N. sylvestris* plant expressing the ihpCBTS construct (ihpCBTS). *Peak 1* corresponds to an added internal standard (caryophyllene), and *peak 2* corresponds to the CBT-diols (α and β) which cannot be separated under these conditions

18.10 Secretion of Engineered Diterpenes

In wild-type plants, over 90% of the CBT-diols is secreted, and less than 10% remains in the trichome or is reabsorbed by the leaf. This has been determined by washing leaves in an extraction solvent twice and then completely extracting the leaf after grinding. This ratio of secreted versus non-secreted indicates that there is an active transport of CBT-diol from the glandular cells unto the leaf surface. In the case of casbene

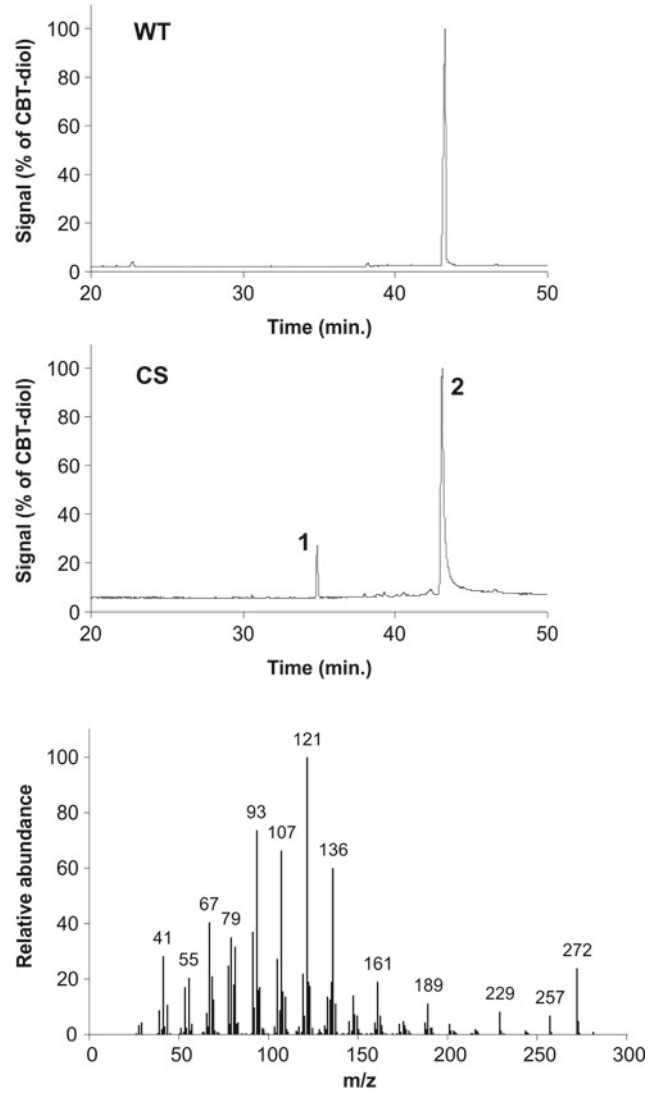

Fig. 18.5 *Production of casbene in tobacco glandular trichomes.* The casbene synthase gene was cloned downstream of the CBTS promoter in a T-DNA vector and integrated in the genome of *N. sylvestris* plants. A typical gas chromatogram of exudate from wild-type plants (WT) and plants expressing casbene synthase (CS) is shown. *Peak 1* corresponds to the CBT-diols and *peak 2* to casbene. The mass spectrum and the structure of casbene are presented in the *lower panel*

produced by transgenic *N. sylvestris*, we found that this ratio is reversed with around 90% of casbene inside the leaf and 10% secreted. Thus, plants with 100 μg/g FW of casbene in the exudate do in fact produce a total of 1 mg/g FW, which is the highest level of heterologous terpenoid ever reported in transgenic plants. This is partial evidence for the transport of the diterpenoids from the trichome secretory cells to be an active and selective process.

18.11 Impact of Down-Regulation of CBT-Diol Production on Casbene Production

The purpose of down-regulating CBT-diol production was twofold. The first is a simplification of the exudate by eliminating or strongly reducing the presence of CBT-diols in the extract, leading to an easier characterization of the novel molecules produced. The second was to increase

the level of diterpene precursor, GGPP, available in the trichome cells, which could lead to higher levels of heterologous diterpene, in our case casbene. To test these hypotheses, plants expressing CS were crossed with ihp*CBTS* plants. F1 plants were allowed to self-fertilize, and F2 plants with both transgenes in the homozygous conditions were selected. These were compared to plants homozygous for the CS transgene in a wild-type background. The exudate analysis revealed no significant difference between the two sets of plants, indicating that, at least in the case of casbene, there was no appreciable impact of eliminating CBT-diol production on the production levels of casbene.

18.12 Expression of Other Diterpene Synthases

Taxa-4(5),11(12)-diene is the diterpene precursor of taxanes which include anticancer ingredients like Taxol® (Hezari et al. 1995). Much progress in understanding the biosynthesis of taxanes has been achieved by the Croteau and collaborators (Jennewein and Croteau 2001). A gene encoding a taxadiene synthase (TS) was identified (Wildung and Croteau 1996). The TS cDNA was cloned downstream of the *CBTS* promoter, and as for casbene, taxadiene could be recovered in the exudate of plants expressing TS at levels averaging 5–10 μg/g FW. Again, no significant increase was found in plants expressing TS and with a down-regulated *CBTS* gene, and the secreted taxadiene represented around 10% of the total taxadiene.

18.13 Production of Oxidized Terpenes

En route to their chemical functionalization, terpenes are frequently oxidized, typically by cytochrome P450 oxygenases. Thus, one further step to demonstrate the relevance and adequacy of tobacco trichomes for terpenoid engineering was to express P450 oxidases. The Taxol pathway has been extensively studied, and several P450 enzymes were shown to hydroxylate a taxane backbone (for review see Jennewein et al. 2004a). Taxadien-5-α-hydroxylase (CYP725A4) in particular was shown to be the likely first step in this complex pathway (Jennewein et al. 2004b). We therefore cloned the *CYP725A4* gene under the control of a trichome-specific promoter and transformed tobacco plants expressing taxadiene synthase with this construct. Taxadiene was no longer detected in plants expressing both genes, indicating that it was metabolized to another product. However, no 5-α-hydroxytaxadiene could be found, suggesting that either it was further modified by endogenous tobacco enzymes or that the product of CYP725A4 was not 5-α-hydroxytaxadiene. The identification, purification and characterization of a product found exclusively in plants expressing TS and CYP725A4, confirmed by expression of CYP725A4 in yeast cells, demonstrated that the CYP725A4 is not a taxadien-5-α-hydroxylase. Instead, the major product of CYP725A4 on taxadiene was shown to be a novel taxane, 5(12)-oxa-3(11)-cyclotaxane, which is in fact the result of a complex rearrangement of the taxadiene molecule (Rontein et al. 2008).

18.14 Conclusion

The tools for engineering terpenoid pathways in tobacco trichomes have been established. First, we have shown that the endogenous pathway can be silenced, thus providing a convenient background for the detection and isolation of novel terpenoids. We have used a tobacco trichome-specific promoter to drive the expression of casbene and taxadiene synthase and showed that these can be produced at fairly high levels (up to 100 μg/g FW) without compromising the growth of the plant. We also showed that downstream steps catalysed by P450s can be successfully added, thus confirming the general utility of this system. Our work also raises several issues. The first is the level of production which, despite being among the highest ever reported for transgenic plants, still remains below the level of endogenous tobacco diterpenoids. One aspect to

be resolved is the expression levels. A better understanding of the regulation of gene expression in trichome cells should certainly lead to significant improvements in this area. Two *cis*-acting regions in the *N. sylvestris CBTS*-2a promoter have been identified, one of which located between positions −589 and 479 from the transcription initiation site conferring a broad transcriptional activation, not only in glandular cells but also in cells of the trichome stalk and in the leaf epidermis and the root, whereas a second region located between positions −279 and −119 had a broad repressor activity, except in glandular cells (Ennajdaoui et al. 2010). Those observations pave the way for the identification of trans-regulators required for the expression of the CBTS genes restricted to the secretory cells of glandular trichomes. Another important issue is the export of terpenoids from the glandular cells onto the leaf surface. This could play a critical role in the overall production levels. The implication of transporters of the ABC family in the export of sclareol, a tobacco diterpenoid induced by elicitors, was shown earlier (Jasinski et al. 2001), but further investigation will be required to see if this type of transporters is also involved in the secretion of diterpenoids by tobacco glandular trichomes. Advances in these areas should help increase the production levels of engineered terpenoids by tobacco trichomes and create opportunities to move beyond the laboratory phase.

Bibliography

Besumbes O, Sauret-Güeto S, Phillips MA, Imperial S, Rodríguez-Concepción M, Boronat A (2004) Metabolic engineering of isoprenoid biosynthesis in Arabidopsis for the production of taxadiene, the first committed precursor of Taxol. Biotechnol Bioeng 88:168–175

Deguerry F, Pastore L, Wu S, Clark A, Chappell J, Schalk M (2006) The diverse sesquiterpene profile of patchouli, *Pogostemon cablin*, is correlated with a limited number of sesquiterpene synthases. Arch Biochem Biophys 454:123–136

Dueber MT, Adolf W, West CA (1978) Biosynthesis of the diterpene phytoalexin casbene: partial purification and characterization of casbene synthetase *from Ricinus communis*. Plant Physiol 62:598–603

Ennajdaoui H, Vachon G, Giacalone C, Besse I, Sallaud C, Herzog M, Tissier A (2010) Trichome specific expression of the tobacco (*Nicotiana sylvestris*) cembratrien-ol synthase genes is controlled by both activating and repressing *cis*-regions. Plant Mol Biol 73:673–685

Gershenzon J, Maffei M, Croteau R (1989) Biochemical and histochemical localization of monoterpene biosynthesis in the glandular trichomes of spearmint (*Mentha spicata*). Plant Physiol 89:1351–1357

Gershenzon J, McCaskill D, Rajaonarivony JI, Mihaliak C, Karp F, Croteau R (1992) Isolation of secretory cells from plant glandular trichomes and their use in biosynthetic studies of monoterpenes and other gland products. Anal Biochem 200:130–138

Guo Z, Severson RF, Wagner GJ (1994) Biosynthesis of the diterpene *cis*-abienol in cell-free extracts of tobacco trichomes. Arch Biochem Biophys 308:103–108

Hezari M, Lewis NG, Croteau R (1995) Purification and characterization of taxa-4(5),11(12)-diene synthase from Pacific yew (*Taxus brevifolia*) that catalyzes the first committed step of Taxol biosynthesis. Arch Biochem Biophys 322:437–444

Iijima Y, Gang DR, Fridman E, Lewinsohn E, Pichersky E (2004) Characterization of geraniol synthase from the peltate glands of sweet basil. Plant Physiol 134:370–379

Jasinski M, Stukkens Y, Degand H, Purnelle B, Marchand-Brynaert J, Boutry M (2001) A plant plasma membrane ATP binding cassette-type transporter is involved in antifungal terpenoid secretion. Plant Cell 13: 1095–1107

Jennewein S, Croteau R (2001) Taxol: biosynthesis, molecular genetics, and biotechnological applications. Appl Microbiol Biotechnol 57:13–19

Jennewein S, Long RM, Williams RM, Croteau R (2004a) Cytochrome p450 taxadiene 5alpha-hydroxylase, a mechanistically unusual monooxygenase catalyzing the first oxygenation step of Taxol biosynthesis. Chem Biol 11:379–387

Jennewein S, Wildung MR, Chau M, Walker K, Croteau R (2004b) Random sequencing of an induced Taxus cell cDNA library for identification of clones involved in Taxol biosynthesis. Proc Natl Acad Sci USA 101:9149–9154

Keene CK, Wagner GJ (1985) Direct demonstration of duvatrienediol biosynthesis in glandular heads of tobacco trichomes. Plant Physiol 79:1026–1032

Larkin JC, Oppenheimer DG, Pollock S, Marks MD (1993) Arabidopsis *GLABROUS1* gene requires downstream sequences for function. Plant Cell 5: 1739–1748

Maffei M, Chialva F, Sacco T (1989) Glandular trichomes and essential oils in developing peppermint leaves. I. Variation of peltate trichome number and terpene distribution within leaves. New Phytol 111:707–716

Mau CJ, West CA (1994) Cloning of casbene synthase cDNA: evidence for conserved structural features among terpenoid cyclases in plants. Proc Natl Acad Sci USA 91:8497–8501

Oppenheimer DG, Herman PL, Sivakumaran S, Esch J, Marks MD (1991) A *myb* gene required for leaf

trichome differentiation in Arabidopsis is expressed in stipules. Cell 67:483–493

Pickard WF (2008) Laticifers and secretory ducts: two other tube systems in plants. New Phytol 177:877–888

Rontein D, OnillonS HG, Lesot A, Werck-Reichhart D, Sallaud C, Tissier A (2008) CYP725A4 from yew catalyzes complex structural rearrangement of taxa-4(5),11(12)-diene into the cyclic ether 5(12)-oxa-3(11)-cyclotaxane. J Biol Chem 283:6067–6075

Schilmiller AL, Last RL, Pichersky E (2008) Harnessing plant trichome biochemistry for the production of useful compounds. Plant J 54:702–711

Serna L, Martin C (2006) Trichomes: different regulatory networks lead to convergent structures. Trends Plant Sci 11:274–280

Smith NA, Singh SP, Wang MB, Stoutjesdijk PA, Green AG, Waterhouse PM (2000) Total silencing by intron-spliced hairpin RNAs. Nature 407:319–320

Steele C, Katoh S, Bohlmann J, Croteau R (1998) Regulation of oleoresinosis in grand fir (*Abies grandis*). Differential transcriptional control of monoterpene, sesquiterpene, and diterpene synthase genes in response to wounding. Plant Physiol 116:1497–1504

Stekoll M, West CA (1978) Purification and properties of an elicitor of castor bean phytoalexin from culture filtrates of the fungus *Rhizopus stolonifer*. Plant Physiol 61:38–45

Wagner GJ (1991) Secreting glandular trichomes: more than just hairs. Plant Physiol 96:675–679

Wang E, Wagner GJ (2003) Elucidation of the functions of genes central to diterpene metabolism in tobacco trichomes using posttranscriptional gene silencing. Planta 216:686–691

Wang E, Gan S, Wagner GJ (2002) Isolation and characterization of the *CYP71D16* trichome-specific promoter from *Nicotiana tabacum* L. J Exp Bot 53:1891–1897

Wesley SV, Helliwell CA, Smith NA, Wang MB, Rouse DT, Liu Q, Gooding PS, Singh SP, Abbott D, Stoutjesdijk PA, Robinson SP, Gleave AP, Green AG, Waterhouse PM (2001) Construct design for efficient, effective and high-throughput gene silencing in plants. Plant J 27:581–590

Wildung MR, Croteau R (1996) A cDNA clone for taxadiene synthase, the diterpene cyclase that catalyzes the committed step of taxol biosynthesis. J Biol Chem 271:9201–9204

19 Prenylated Proteins Are Required for Methyl-Jasmonate-Induced Monoterpenoid Indole Alkaloids Biosynthesis in *Catharanthus roseus*

Vincent Courdavault, Marc Clastre, Andrew John Simkin, and Nathalie Giglioli-Guivarc'h

Abstract

In *Catharanthus roseus*, monoterpenoid indole alkaloids (MIA) result from the condensation of the indole precursor tryptamine with the terpenoid precursor secologanin, which is derived from the plastidial methyl-D-erythritol 4-phosphate (MEP) pathway. Nevertheless, inhibition of the classical so-called mevalonate pathway leads to inhibition of MIA biosynthesis, suggesting that there is some cross regulation between these two pathways. The purpose of this chapter is to outline a new function for protein prenylation. Our results suggest that prenylated proteins, apparently mevalonate pathway end products, act as part of the regulatory mechanism coordinating the exchange of metabolites between compartmentalized metabolic pathways and that this process is governed by methyl jasmonate. Methyl jasmonate is a major inducer of alkaloid biosynthesis through enhancing MEP pathway gene expression. In *C. roseus* cells, inhibition of protein prenylation leads to the down-regulation of methyl-jasmonate-induced expression of MEP pathway genes and thus abolishes MIA biosynthesis. Jointly, failure of protein prenylation also inhibits the methyl-jasmonate-induced expression of the transcription factor ORCA3 which acts as a central regulator of MIA biosynthesis. Furthermore, the specific silencing of protein prenyltransferases in *C. roseus* cells mediated by RNA interference shows that inhibition of type I protein geranylgeranyltransferase down-regulates the expression of ORCA3. These data point to a specific role of protein geranylgeranylation in jasmonate signalling leading to MIA formation.

V. Courdavault • M. Clastre • A.J. Simkin • N. Giglioli-Guivarc'h (✉)
Université François-Rabelais de Tours, EA 2106 Biomolécules et Biotechnologies végétales, 31 avenue Monge, 37200 Tours, France
e-mail: vincent.courdavault@univ-tours.fr; marc.clastre@univ-tours.fr; asimkin@essex.ac.uk; nathalie.guivarch@univ-tours.fr;

T.J. Bach and M. Rohmer (eds.), *Isoprenoid Synthesis in Plants and Microorganisms: New Concepts and Experimental Approaches*, DOI 10.1007/978-1-4614-4063-5_19,

Keywords
Terpenoids • Protein isoprenylation • Jasmonate • *Catharanthus roseus* • Alkaloid • Type I protein geranylgeranyltransferase

19.1 Introduction

Terpenoids are the most numerous and structurally diverse group of natural compounds. The common building block in terpenoid biosynthesis is a C_5-diphosphate precursor, isopentenyl diphosphate (IPP), but also its chemically active isomer dimethylallyl diphosphate (DMAPP). These building blocks are either synthesized via the mevalonic acid (MVA) pathway or via the 2-*C*-methyl-D-erythritol 4-phosphate (MEP) pathway. The MVA pathway was first elucidated in yeast and animals as early as in the middle of last century (Bloch 1965). Thus, it became widely accepted that in all organisms IPP is synthesized from acetyl-CoA via MVA (Chappell 1995; McGarvey and Croteau 1995). However, several observations had already suggested that things might be more complex. The alternative MVA-independent MEP pathway, discovered at the end of the 1980s in bacteria (Flesch and Rohmer 1988; Rohmer et al. 1993) and in plants (Rohmer 1999, and literature cited therein), raised considerable new interest in isoprenoid biosynthesis and regulation studies. It is now well established that higher plants host both metabolic pathways, which operate in different subcellular compartments. The MVA pathway, which provides C_5 precursors for the synthesis of some sesquiterpenes, sterols and the side chain of ubiquinone, is partially localized in the cytoplasm and partially in the peroxisome (Simkin et al. 2011), while the plastid-localized MEP pathway provides the substrate for the synthesis of monoterpenes, some sesqui- and diterpenes, chlorophylls and carotenoids, the major classes of photosynthetic pigments as well as other plastid-related terpenoid metabolites.

The vast majority of these terpenoid compounds synthesized by plants is defined as belonging to 'natural products' or 'secondary metabolites'. These include not only hemi-, mono-, sesqui-, di-, tri- and tetraterpenes but also other families of products, such as anthraquinones, apocarotenoids, terpenoid indole alkaloids, prenylated flavonoids and isoflavonoids, which are often species specific. In addition, they are frequently involved in ecological processes by acting in communications between species as well as in defence mechanisms (e.g. essential oils, flower pigmentation, insect attractants, phytoalexins, antimicrobial agents, anti-feedants and protection from various predators). Many terpenoids also have essential functions in plant development. Among those we can cite hormones (abscisic acid, cytokinins, gibberellins, brassinosteroids and the newly discovered strigolactones, see Ruyter-Spira et al. this volume), photosynthetic pigments (chlorophylls and carotenoids), electron carriers (cytochrome *a*, quinones), membrane components (steroids) or those being involved in signalling events (isoprenylated proteins). Seen from a more applied view, several of these compounds have important therapeutic and commercial values. A great deal of effort has been made to produce pharmaceuticals like artemisinin (a potent antimalarial drug—see elsewhere in this volume), taxol, vinblastine and vincristine that are used in the treatment against cancer, or β-carotene (provitamin A) and α-tocopherol (vitamin E), which represent important nutrients for human health. However, the production of high concentrations of such valuable terpene compounds is challenging. For instance, extractions from producing organisms are inefficient due to relatively low yields, and chemical synthesis is costly due to the structural complexity of the compounds. Therefore, metabolic engineering provides a promising approach to achieve a higher production of isoprenoids in plants. For this purpose, a complete understanding of their biosynthetic pathways as well as their regulation remains an essential prerequisite.

The Madagascar periwinkle (*Catharanthus roseus*) is a pantropical *Apocynaceae* that synthesizes a wide range of monoterpenoid indole alkaloids (MIA). Among the 130 MIA characterized so far in the whole plant, several valuable therapeutic MIA have been identified, including monomers such as ajmalicine and serpentine used in the treatment of circulatory diseases and anxiety and heterodimers such as vinblastine and vincristine, known as powerful anticancer drugs (Levêque et al. 1996; Levêque and Jehl 2007). All MIA result from the condensation of the indole precursor tryptamine with the terpenoid precursor secologanin. This condensation is catalysed by strictosidine synthase (STR; de Waal et al. 1995) and leads to the formation of strictosidine, the precursor of all MIA (Fig. 19.1).

Tryptamine is derived from the decarboxylation of tryptophan, catalysed by tryptophan decarboxylase (TDC; De Luca et al. 1989), whereas secologanin biosynthesis requires two successive biosynthetic pathways, the plastidial MEP pathway and the monoterpene secoiridoid pathway. The MEP pathway provides isopentenyl diphosphate and its isomer dimethylallyl diphosphate that are condensed to form geranyl diphosphate and then geraniol through two enzymatic steps (Contin et al. 1998). The secoiridoid pathway is initiated by the hydroxylation of geraniol catalysed by geraniol 10-hydroxylase (G10H; Collu et al. 2001) and ends with the biosynthesis of secologanin catalysed by secologanin synthase (SLS; Irmler et al. 2000). Different studies based on precursor feeding experiments with suspension cells showed that the major rate-limiting step in MIA biosynthesis is the ability to produce the terpenoid precursor secologanin (Mérillon et al. 1986; Arvy et al. 1994) through the MEP pathway (Contin et al. 1998).

C. roseus is the unique source of the powerful antitumour drugs vinblastine and vincristine. These two MIA became lead compounds for new hemisynthetic drugs such as vinorelbine and vinflunine (Aapro et al. 2001; Okouneva et al. 2003). Due to the economical value of *C. roseus* MIA, physiological, cellular, biochemical and molecular aspects of their biosynthesis have been extensively studied over the past 30 years. Consequently, this medicinal plant was chosen to develop a model system for biotechnology studies on plant secondary metabolism.

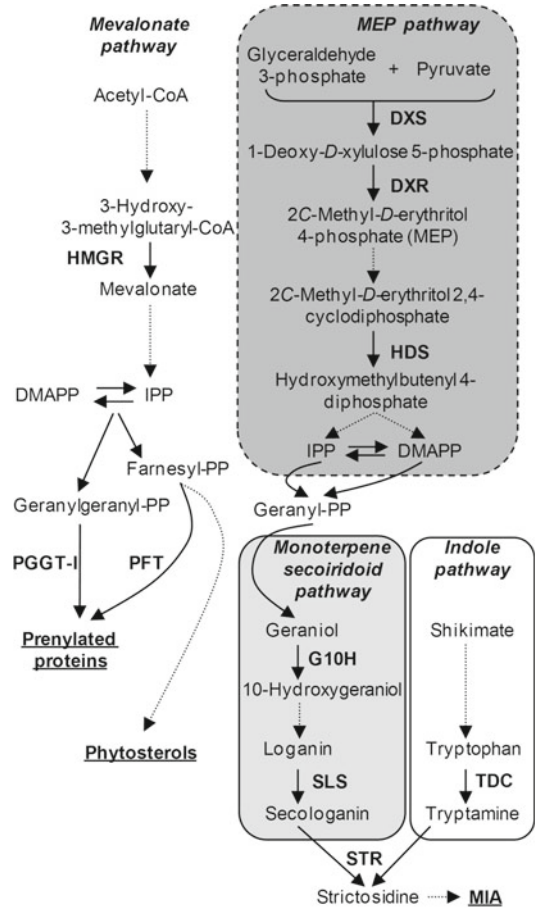

Fig. 19.1 Monoterpenoid indole alkaloids and mevalonate-derived metabolite pathways in *C. roseus*. *C. roseus* monoterpenoid indole alkaloids (*MIA*) result from the condensation of tryptamine and secologanin. The terpenoid moiety of MIA is derived from two successive pathways: the 2-*C*-methyl-D-erythritol 4-phosphate (*MEP*) pathway and the monoterpene secoiridoid pathways. *Solid lines* represent a single enzymatic conversion, whereas *dashed lines* indicate multiple enzymatic steps. *DXS* 1-deoxy-D-xylulose 5-phosphate synthase, *DXR* 1-deoxy-D-xylulose 5-phosphate reductoisomerase, *DMAPP* dimethylallyl diphosphate, *G10H* geraniol 10-hydroxylase, *HDS* hydroxymethylbutenyl 4-diphosphate synthase, *HMGR* 3-hydroxy-3-methylglutaryl-CoA reductase, *IPP* isopentenyl diphosphate, *PFT* protein farnesyltransferase, *PGGT-I*, type I protein geranylgeranyltransferase, *SLS* secologanin synthase, *STR* strictosidine synthase, *TDC* tryptophan decarboxylase

It is believed that plants gain advantage from the coexistence of MVA and MEP pathways in different cell compartments. This ability to produce isoprenoids via these two pathways prompted us to address the question of how they might interact and what mechanisms might be involved in coarse control and even fine-tuning of one or both pathways, depending on the structure and functional destination of terpenoid derivatives. The periwinkle C20D cell line was selected due to its ability to produce some MIA under phytohormonal control. Thus, C20D *C. roseus* cells provide an original inducible plant cell system to investigate the regulation of terpenoid pathways gene expression, alkaloid accumulation and the cross-talk between the two terpenoid biosynthesis pathways.

19.2 Hormonal Regulation of Monoterpenoid Indole Alkaloid Biosynthesis in *C. roseus* Cell Suspensions

Due to the complexity of the MIA biosynthetic pathway and considering the large number of enzymatic steps and their low biosynthetic rates *in planta* (Mahroug et al. 2007; Oudin et al. 2007a), simplified models of *C. roseus* such as cell suspension have emerged as powerful tools to study the regulation of MIA biosynthesis, including the role of hormonal signalling (Giglioli-Guivarc'h et al. 2006; Hedhili et al. 2007). For example, in the *C. roseus* C20D cell line, auxin provided as 2,4-dichlorophenoxyacetic acid (2,4-D) inhibits MIA production (Arvy et al. 1994) as a consequence of the down-regulation of the first two MEP pathway genes (Chahed et al. 2000; Veau et al. 2000), coding for 1-deoxy-D-xylulose 5-phosphate synthase (DXS) and 1-deoxy-D-xylulose 5-phosphate reductoisomerase (DXR), and the down-regulation of the secoiridoid pathway gene encoding G10H (Papon et al. 2005). In contrast, cytokinins increase MIA biosynthesis (Décendit et al. 1992) and enhance at least *DXS*, *DXR* and *G10H* expression (Oudin et al. 2007b). Furthermore, synergistic interaction between cytokinin and ethylene transduction pathways has been reported, since the addition of these two hormones further enhances G10H expression (Papon et al. 2005).

Jasmonate (JA) was also reported to be a general inducer of plant secondary metabolite biosynthesis (Memelink et al. 2001). JA or its methyl ester, methyl jasmonate (MeJA), also appears to function as a central regulator of MIA biosynthesis in *C. roseus* (Gantet et al. 1998). Additionally, both plants and seedlings of *C. roseus* respond to JA with an increased production of MIA (Aerts et al. 1994; El-Sayed and Verpoorte 2005), whereas inhibition of JA biosynthesis in suspension cell lines blocks MIA production (Gantet et al. 1998). In C20D *C. roseus* cell suspension, application of exogenous MeJA leads to a coordinate up-regulation of all characterized genes associated with the biosynthesis of the terpenoid precursor of MIA (van der Fits and Memelink 2000; Oudin et al. 2007b) and to the subsequent increase in MIA biosynthesis. The way by which jasmonate regulates MIA gene expression has been partially elucidated by the isolation of two specific AP2/ERF-domain transcription factors, ORCA2 and ORCA3 (Menke et al. 1999; van der Fits and Memelink 2000; Memelink et al. 2001). ORCA3 exhibits the most pleiotropic effects by enhancing the expression of genes involved in many steps of MIA biosynthesis, such as terpenoid and indole precursor biosynthesis, strictosidine synthesis and modification (van der Fits and Memelink 2000). Recently, it has been shown that the bHLH protein CrMYC2 regulates ORCA gene expression (Zhang et al. 2011).

19.3 Involvement of Protein Prenylation Events in MIA Biosynthesis Regulation

Previous work designed to study the role of the MVA pathway in MIA biosynthesis showed, unexpectedly, that MIA biosynthesis in *C. roseus* cell line was completely inhibited when the MVA pathway was blocked with an inhibitor of HMG-CoA reductase (Imbault et al. 1996). Since mevalonate is not a precursor for the biosynthesis of the isoprenoid moiety of MIA (Contin et al. 1998),

the HMG-CoA reductase inhibitor was expected to have an indirect effect on MIA biosynthesis. However, this class of inhibitors is also known to interfere with protein prenylation by depleting the endogenous pool of prenyl precursors. Considering that isoprenylated proteins may constitute one of the end products of the MVA pathway and that MIA result from the MEP pathway, such covalently modified proteins may represent the coordinating factor that is implicated in the co-regulation of these two terpenoid biosynthetic pathways. The aim of the following study was to test this hypothesis.

Protein isoprenylation in animals has received considerable attention because several oncogenic forms of isoprenylated proteins depend on prenyl modifications for their runaway cellular multiplication effects and for tumour development (Gelb et al. 2006). Protein isoprenylation consists of a post-translational modification by the formation of cysteine thioether bonds with a farnesyl (C_{15}) or geranylgeranyl (C_{20}) moiety at the carboxy terminus (see elsewhere in this volume). The corresponding terpenoid substrates of protein prenyltransferase are farnesyl diphosphate and/or geranylgeranyl diphosphate, which are commonly considered to originate from the MVA pathway. In the plant system, the situation is not quite so clear. It has recently been demonstrated that the geranylgeranylation of a green fluorescent protein (GFP), N-terminally fused to the carboxyterminal polybasic domain of rice calmodulin CaM61 bearing a geranylgeranylation motif, is clearly dependent on the MEP pathway when stably expressed in tobacco BY-2 cells (Gerber et al. 2009). Two different protein geranylgeranyl transferases (PGGT-I and Rab PGGT-II) and a single protein farnesyl transferase (PFT) catalyse the prenylation reactions in animal, yeast and plant cells (Schafer and Rine 1992; Zhang and Casey 1996; Rodríguez-Concepción et al. 1999; see also Crowell and Huizinga, this volume). These enzymes use two substrates, a protein and a prenyl diphosphate group. PFT and PGGT-I are classified in a common CaaX-prenyltransferase (CaaX-PTase) family. They are heterodimeric enzymes that share a common α-subunit but have distinct β-subunits. Both enzymes recognize a conserved C-terminal amino acid sequence motif known as CaaX box, in which 'C' represents a conserved cysteine, 'a' aliphatic amino acids and 'X' is usually serine, methionine, cysteine, alanine, glutamine or leucine. If 'X' is leucine, the protein is a substrate for PGGT-I, while other residues are recognized preferentially by PFT (Moores et al. 1991; Schafer and Rine 1992; Crowell and Huizinga, this volume).

Protein isoprenylation events in the regulation of MIA biosynthesis have been elucidated by applying a CaaX-PTase inhibitor-based strategy. The prenyltransferase inhibitor *S*-perillyl alcohol (Tamanoi 1993; Gelb et al. 1995; Ren et al. 1997) has been used with *C. roseus* C20D cells to reduce endogenous isoprenylation. This is confirmed by the loss of the incorporation of [^{14}C]-mevalonate-derived prenyl moieties with known prenylated proteins (Courdavault et al. 2009). The inhibition of protein isoprenylation is correlated with a large reduction, up to 98%, in MIA and a specific down-regulation of MEP pathway genes (such as *DXR, DXS* and *G10H*). Interestingly, exogenous supply of *C. roseus S*-perillyl alcohol-treated cells with various terpenoid precursors, such as loganin or secologanin, restored MIA biosynthesis. This suggests that the initial rate-limiting MEP biosynthesis pathway steps requiring CaaX-PTase activity are localized between 1-deoxy-D-xylulose 5-phosphate and loganic acid biosynthesis (Courdavault et al. 2005a, b). The *C. roseus* genes encoding the β-subunits of each CaaX-PTase have been cloned (Courdavault et al. 2005b). Using this data, we generated *C. roseus* cell lines for RNA interference: RNAi PFT and RNAi PGGT-I cell lines. In these cell lines, the transcripts encoding the specific β-subunit of each CaaX-PTase α,β-heterodimer have been targeted by siRNA in order to down-regulate the corresponding CaaX-PTase activity (Courdavault et al. 2005a, b). In order to show more precisely how CaaX-PTase acts on MIA biosynthesis, two sets of genes have been chosen according to their position in the MIA biosynthetic pathway. The first set corresponds to genes involved in the early steps of MIA biosynthesis, and the second set to steps of the central part of MIA biosynthesis. As shown in Fig. 19.2, both CaaX-PTase

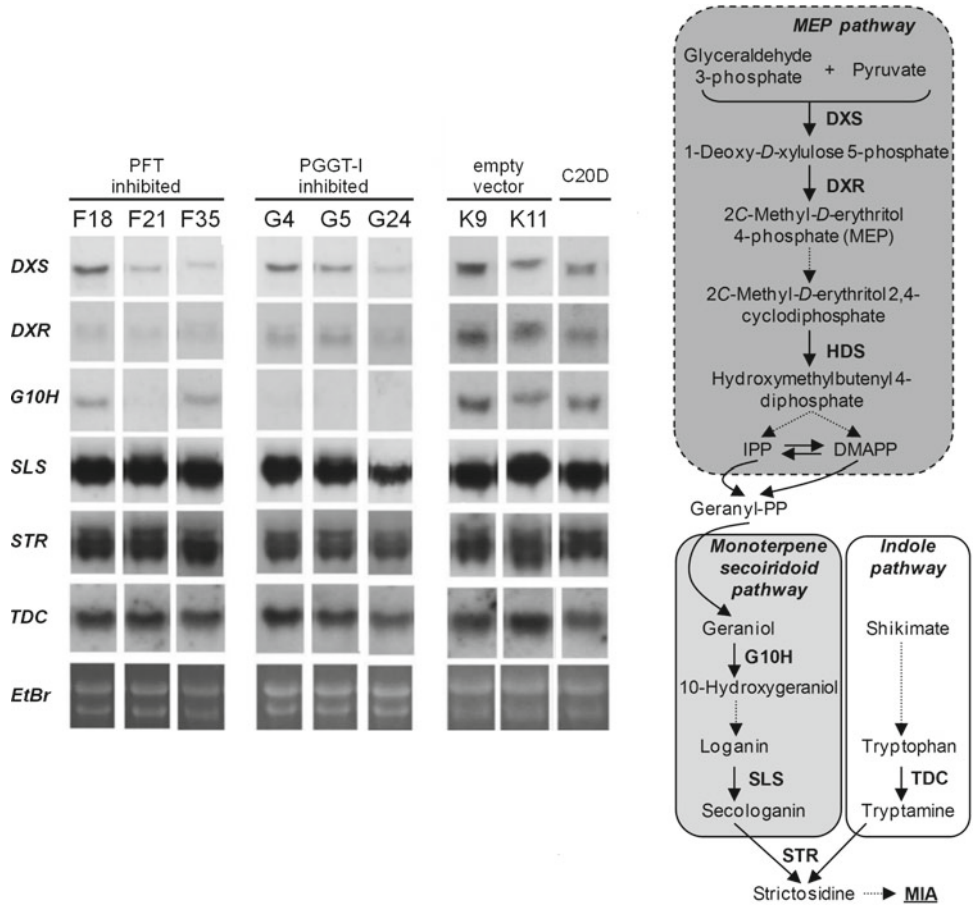

Fig. 19.2 Expression of MIA biosynthetic pathway genes in CaaX-PTase interference cell lines. Total RNA was extracted from 5-day-old transformed C20D cell lines cultured in auxin-free medium. Three PFT silenced cell lines (F18, F21 and F35, PFT inhibited) and three PGGT-I silenced cell lines (G4, G5 and G24, PGGT-I inhibited) were selected for this study. Two empty vector-transformed cell lines (K9 and K11) were used as a control. Equal loading of total RNA samples in each lane was confirmed by ethidium bromide (EtBr) staining. Northern blots were performed with nucleotide probes corresponding to *DXS*, *DXR*, *G10H*, *SLS*, *STR* and *TDC* cDNA

activities are required for the expression of *DXS*, *DXR* and *G10H*, while no decrease in *SLS*, *STR* and *TDC* transcript levels is observed. These results are consistent with the role of PFT- and PGGT-I-dependent protein isoprenylation in the cascade of events leading to an efficient transcriptional activation of early steps in monoterpenoid biosynthesis, following auxin depletion. Interestingly, in the aerial organs of young *C. roseus* plants, the prenylated protein-dependent genes, *DXS, DXR* and *G10H*, were found to be expressed specifically in internal phloem parenchyma cells (Burlat et al. 2004), whereas secologanin synthase (*SLS*), tryptophan decarboxylase (*TDC*) and strictosidine synthase (*STR*) expression was restricted to epidermal cells (St-Pierre et al. 1999; Irmler et al. 2000). Such tissue-specific expression in phloem parenchyma potentially involves a coordinated regulatory process, which may require CaaX-PTase activity. Gene expression and enzymatic activity studies of CaaX-PTases, compared to DXS, provided evidence for the requirement of CaaX-PTases in the regulation of MEP pathway genes expression not only in the C20D cell line but also in differentiated plant tissues and organs (Courdavault et al.

2005a and b). Furthermore, a comparison of the cell-specific expression pattern of DXS and the β-subunit of PFT showed that these two transcripts were found in the same vascular bundles but in distinct consecutive tissues (Courdavault et al. 2005a). Nevertheless, the particular anatomy of *C. roseus* vascular bundles is compatible with the regulation of MIA biosynthesis pathway by farnesylated proteins, which may be translocated to internal phloem parenchyma cells.

19.4 Inhibition of Endogenous Protein Isoprenylation Disrupts the Positive Effect of MeJA on MIA Biosynthesis and MEP Pathway Gene Expression

In an attempt to better understand the involvement of CaaX-PTases in MIA biosynthesis, the potential role of protein isoprenylation in the JA signalling cascade was investigated. Recently, isoprenylated proteins have been shown to be involved in part of the JA signalling pathway (Trusov et al. 2006, 2007) through the characterization of *Arabidopsis* αβγ heterotrimeric G protein mutants. The two G protein γ-subunits (Gγ) of *Arabidopsis* are small proteins that bear a PGGT-I-specific CaaX motif (Mason and Botella 2000, 2001). The activity of heterotrimeric G proteins depends on the isoprenylation status of Gγ since *Arabidopsis* mutants, bearing a CaaX-truncated γ-subunit, present altered responses to the physiological process involving heterotrimeric G proteins (Chakravorty and Botella 2007). This is directly related to the ability of the geranylgeranyl moiety of Gγ to drive the anchoring of the βγ dimer to the plasma membrane or its interaction with receptors and effectors (Adjobo-Hermans et al. 2006). The use of the CaaX-PTase inhibitor, *S*-perillyl alcohol, provided the first piece of evidence for the involvement of isoprenylated proteins in the MeJA signalling pathway leading to MIA biosynthesis in *C. roseus*. *S*-perillyl alcohol-mediated inhibition of protein isoprenylation led to a dramatic decrease of MIA biosynthesis, which was not restored by addition of exogenous MeJA (Courdavault et al. 2009). Furthermore, the inhibition of protein isoprenylation abolished the MeJA-induced up-regulation of DXS, HDS and G10H, resulting in overall lower levels of MIA biosynthesis. Thus, isoprenylated proteins could positively act on early steps of JA signalling, leading to regulation of MIA biosynthetic gene expression. Such isoprenylated proteins still await to be identified; however, αβγ heterotrimeric G proteins would be good candidates as they act generally in the very early steps of transduction cascades.

19.5 PGGT-I Is Specifically Required for the JA Signalling Triggering ORCA3 Expression

To gain insight into the involvement of isoprenylated proteins in the JA signalling cascade, we studied the regulation of the expression of the transcriptional factor *ORCA3*. *ORCA3* was shown to be specifically involved in the early steps of JA signalling cascade that prompt MIA biosynthesis. In the absence of MeJA, *ORCA3* is not expressed in C20D cells, whereas the addition of exogenous MeJA leads to an induction in *ORCA3* expression with peak transcript levels being reached half an hour after treatment. This increase is followed by a decrease in transcript levels over the next 6 h (Fig. 19.3a). Under these conditions, when endogenous protein isoprenylation is inhibited by *S*-perillyl alcohol treatment, *ORCA3* transcripts were barely detectable 1/2 and 6 h after MeJA supply (Fig. 19.3a). This data points to a specific role of protein isoprenylation in JA signalling.

As *S*-perillyl alcohol is a general inhibitor of protein isoprenylation according to Gelb et al. (1995), it cannot be determined which kind of CaaX-PTase activity is involved in JA signalling. To circumvent this problem, we took advantage of the specific RNAi PFT- or RNAi PGGT-I-inhibited *C. roseus* cell lines. In parallel, *C. roseus* cell lines transformed with a non-interfering construct were used as a control. In these control cell lines, the abundance of *ORCA3* transcripts half an hour after MeJA treatment is similar to those

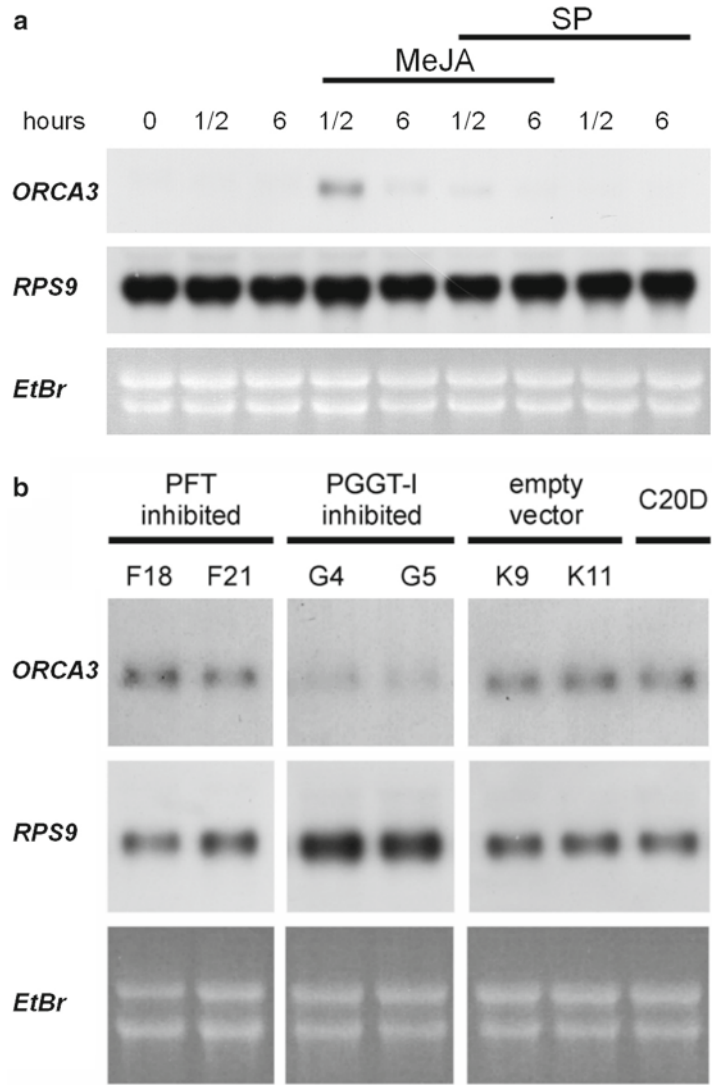

Fig. 19.3 Inhibition of protein prenylation blocks the MeJA-induced expression of *ORCA3* gene. (**a**) The accumulation of *ORCA3* transcripts was monitored in C20D cells by northern blot analysis using *RPS9* expression as a control. Three-day-old C20D cells were treated with 1 mM *S*-perillyl alcohol (*SP*) or not and supplemented 24 h thereafter with 100 μM MeJA when indicated. Total RNA was extracted from cells harvested at the indicated time points following treatments. (**b**) Northern blot analysis of *ORCA3* transcripts in PFT-inhibited cell lines (F18 and F21) and PGGT-I-inhibited cell lines (G4 and G5). Cells transformed by a non-silencing vector (K9 and K11) and C20D cells were used as controls. Total RNA was extracted from cells harvested 1/2 h after MeJA treatment. Equal loading of total RNA samples in each lane was confirmed by ethidium bromide (EtBr) staining

observed in wild-type C20D cells (Fig. 19.3b). Abolishment of PFT activity does not alter *ORCA3* expression, indicating that farnesylated proteins are not likely to play a part in JA signalling. In contrast, the depletion of PGGT-I activity leads to a down-regulation of *ORCA3* expression to a similar extent as previously observed in *S*-perillyl alcohol-treated cells. This partial inhibition of *ORCA3* expression points to a positive and specific action in JA signalling of proteins that are isoprenylated by PGGT-I. Furthermore, it is likely that PGGT-I-dependent isoprenylated proteins act positively in the JA signal transduction cascade and that it is not PGGT-I activity alone that affects JA signalling since MeJa stimulation of C20D cells does not modify PGGT-I activities when compared to non-stimulated cells (Courdavault et al. 2009). Thus, the MeJA-induced expression of *ORCA3* could be a consequence of the PGGT-I protein substrate production and/or mobilization.

Interestingly, *DXS* down-regulation correlates with the inhibition of *ORCA3* expression in *S*-perillyl alcohol-treated cells, which is consistent with the enhancement of *DXS* expression in *ORCA3* over-expressing *C. roseus* cells lines (van

der Fits and Memelink 2000). However, these authors have shown that cycloheximide-mediated inhibition of de novo *ORCA3* translation did not affect the MeJA-induced expression of MIA biosynthetic genes, which suggests that this process could depend on the activation of pre-existing ORCA3 protein (van der Fits and Memelink 2001). This could reflect the involvement of PGGT-I isoprenylated proteins in the early steps of JA signalling prior to ORCA3 activation and the induction of *ORCA3* expression. Additionally, ORCA3 has been shown not to be sufficient for the JA signalling pathway that induced G10H expression, suggesting that other mechanisms regulate the expression of MIA genes under the control of MeJA. Thus, PGGT-I isoprenylated proteins could act positively on the early steps of JA signalling, thereby initiating an ORCA3-dependent and an ORCA3-independent regulation of MIA biosynthetic gene expression.

19.6 Discussion

In the *C. roseus* C20D cell line, CaaX-PTases appear to constitute an essential component for the regulation of MIA biosynthesis by triggering the up-regulation of some of the genes implicated in the early steps of plastidial terpenoid biosynthesis. In *Arabidopsis thaliana*, CaaX-PTases mutational analysis has allowed numerous physiological functions to be associated with each CaaX-PTase. Thus, PFT has been implicated in several regulation mechanisms such as cell division (Morehead et al. 1995; Qian et al. 1996; Galichet and Gruissem 2006), meristem cellular differentiation (Yalovsky et al. 2000a, b; Running et al. 2004) and flower development (Ziegelhoffer et al. 2000). PFT has also been shown to be involved in the ABA signalling pathway that controls stomatal closure, drought tolerance (Cutler et al. 1996; Pei et al. 1998; Allen et al. 2002; Wang et al. 2005) and leaf senescence (Barth et al. 2004). Furthermore, it has been suggested that PFT acts in the auxin signalling pathway since it negatively regulates the expression of the transcription factor ABI3 which is stimulated by auxin (Brady et al. 2003). In contrast, the physiological functions of PGGT-I remain less understood. Following an elegant biochemical characterization of PGGT-I (Caldelari et al. 2001), Johnson and co-workers (2005) have shown that PGGT-I negatively regulates ABA signalling in guard cells and auxin signalling leading to lateral root initiation without affecting other ABA or auxin responses. Regarding the effect of a lack of CaaX-PTase on the regulation of the MEP pathway, one may be surprised to learn that the *Arabidopsis* PFT mutant *era1* or the double CaaX-PTase mutant *plp* has not been studied at this level. However, the green colour of these mutants indicates that the lack of CaaX-PTase activities does not affect chlorophyll synthesis, which reflects that the MEP pathway-derived phytol chain is still synthesized. This addresses the question of whether the requirement of CaaX-PTases for MEP pathway expression in *C. roseus* has a broader signification. In contrast, in tobacco or *C. roseus* etiolated leaves, chemical inhibition of CaaX-PTases inhibits chlorophyll synthesis under light condition (Courdavault and Giglioli-Guivarc'h, personal data). This is consistent with the previously described relationship between CaaX-PTases and MEP pathway regulation. The reasons for such species-to-species differences is unclear, but since regulation of terpenoid biosynthesis is likely controlled by several regulatory mechanisms, it is reasonable to assume that some of these mechanisms are prevalent over others in some plants, or under different growth conditions. Such a model for terpenoid metabolism has previously been proposed for the regulation of the carotenoid biosynthetic pathway (Simkin et al. 2003).

Biosynthesis of *C. roseus* MIA is a highly regulated mechanism, depending on various hormonal stimuli including auxin as a repressor and cytokinin and MeJA as enhancers. To date, isoprenylated proteins have only been linked to the MeJA signalling pathway leading to MIA biosynthesis, while no involvement in auxin or cytokinin signalling mechanisms has been described (Courdavault et al. 2009). The sensitivity of MeJA signalling pathway to CaaX-PTase inhibitors may explain both their inhibitory effect on the basal

level of MIA biosynthesis pathway gene expression and on the MeJA-induced biosynthesis of MIA. Furthermore, the MeJA-induced expression of *ORCA3* is strongly down-regulated by the inhibition of protein prenylation, while the induction of the expression of *CrRR3*, a gene encoding a type A response regulator in *C. roseus* cells cultures (Papon et al. 2003), following cytokinin treatment is not affected (Courdavault et al. 2009). Taken together, these results strongly suggest a specific involvement of prenylated proteins in the JA signalling pathway and marginally or not in the cytokinin signalling pathway that regulate the biosynthesis of MIA in *C. roseus*. Nevertheless, it was recently shown that cytokinin biosynthesis is dependent on the farnesylated status of AtIPT3, the adenoside phosphate-isopentenyl transferase being involved in the cytokinin biosynthesis pathway (Galichet et al. 2008). A similar mechanism could also exist in *C. roseus* that may explain the involvement of PFT in MIA biosynthesis.

Finally, using the PFT or PGGT-I silenced *C. roseus* cell lines, we also reported that the up-regulation of *ORCA3* induced by MeJA is specifically dependent upon isoprenylation events catalysed by PGGT-I. This provides evidence for a new physiological role of PGGT-I in JA signalling. As previously described for the involvement of PFT in abscisic acid signalling (Cutler et al. 1996; Pei et al. 1998; Allen et al. 2002), PGGT-I may act indirectly in the signalling pathway through its specific protein targets, which remain to be identified.

Acknowledgements This work was financially supported by the 'Ministère de l'Education Nationale, de l'Enseignement Supérieur et de la Recherche' (France) and the 'Ligue Nationale contre le Cancer'. We thank the 'Le STUDIUM' (Agency for Research and Hosting Foreign Associated Researchers in the Centre Region (France)) for the financial support of A. J. Simkin.

References

Aapro MS, Harper P, Johnson SA, Vermorken JB (2001) Developments in cytotoxic chemotherapy: advances in treatment utilising vinorelbine. Crit Rev Oncol Hematol 40:250–263

Adjobo-Hermans MJ, Goedhart J, Gadella TWJ Jr (2006) Plant G protein heterotrimers require dual lipidation motifs of Gα and Gγ and do not dissociate upon activation. J Cell Sci 119:5087–5097

Aerts R, Gisi D, De Carolis E, De Luca V, Baumann TW (1994) Methyl jasmonate vapor increases the developmentally controlled synthesis of alkaloids in *Catharanthus* and *Cinchona* seedlings. Plant J 5:635–643

Allen GJ, Murata Y, Chu SP, Nafisi M, Schoeder JI (2002) Hypersensitivity of abscisic acid-induced cytosolic calcium increases in the *Arabidopsis* farnesyltransferase mutant *era1-2*. Plant Cell 14:1649–1662

Arvy M-P, Imbault N, Naudascher F, Thiersault DP (1994) 2,4-D and alkaloid accumulation in periwinkle cell suspensions. Biochimie 76:410–416

Barth O, Zschiesche W, Siersleben S, Humbeck K (2004) Isolation of a novel cDNA encoding a nuclear protein involved in stress response and leaf senescence. Physiol Plant 121:282–293

Bloch K (1965) The biological synthesis of cholesterol. Science 150:19–28

Brady SM, Sarkar SF, Bonetta D, McCourt P (2003) The *ABSCISIC ACID INSENSITIVE 3 (ABI3)* gene is modulated by farnesylation and is involved in auxin signaling and lateral root development in *Arabidopsis*. Plant J 34:67–75

Burlat V, Oudin A, Courtois M, Rideau M, St-Pierre B (2004) Co-expression of three MEP pathway genes and geraniol 10-hydroxylase in internal phloem parenchyma of *Catharanthus roseus* implicates multicellular translocation of intermediates during the biosynthesis of monoterpene indole alkaloids and isoprenoid-derived primary metabolites. Plant J 38: 131–141

Caldelari D, Sternberg H, Rodríguez-Concepción M, Gruissem W, Yalovsky S (2001) Efficient prenylation by a plant geranylgeranyltransferase-I requires a functional CaaL box motif and a proximal polybasic domain. Plant Physiol 126:1416–1429

Chahed K, Oudin A, Guivarc'h N, Hamdi S, Chénieux JC, Rideau M, Clastre M (2000) 1-Deoxy-D-xylulose 5-phosphate synthase from periwinkle: cDNA identification and induced gene expression in terpenoid indole alkaloid-producing cells. Plant Physiol Biochem 38:559–566

Chakravorty D, Botella JR (2007) Over-expression of a truncated *Arabidopsis thaliana* heterotrimeric G protein γ subunit results in a phenotype similar to α and β subunit knockouts. Gene 393:163–170

Chappell J (1995) The biochemistry and molecular biology of isoprenoid metabolism. Plant Physiol 107:1–6

Collu G, Unver N, Peltenburg-Looman AM, van der Heijden R, Verpoort R, Memelink J (2001) Geraniol 10-hydroxylase, a cytochrome P450 enzyme involved in terpenoid indole alkaloid biosynthesis. FEBS Lett 508:215–220

Contin A, van der Heijden R, Lefebre AW, Verpoorte R (1998) The iridoid glucoside secologanin is derived from the novel triose phosphate/pyruvate pathway in a *Catharanthus roseus* cell culture. FEBS Lett 4: 413–416

Courdavault V, Burlat V, St-Pierre B, Giglioli-Guivarc'h N (2005a) Characterisation of CaaX-prenyltransferases in *Catharanthus roseus*: relationships with the expression of genes involved in the early stages of monoterpenoid biosynthetic pathway. Plant Sci 168: 1097–1107

Courdavault V, Thiersault M, Courtois M, Gantet P, Oudin A, Doireau P, St-Pierre B, Giglioli-Guivarc'h N (2005b) CaaX-prenyltransferases are essential for expression of genes involved in the early stages of monoterpenoid biosynthetic pathway in *Catharanthus roseus* cells. Plant Mol Biol 57:855–870

Courdavault V, Burlat V, St-Pierre B, Giglioli-Guivarc'h N (2009) Proteins prenylated by type I protein geranylgeranyltransferase act positively on the jasmonate signalling pathway triggering the biosynthesis of monoterpene indole alkaloids in *Catharanthus roseus*. Plant Cell Rep 28:83–93

Cutler S, Ghassemian M, Bonetta D, Cooney S, McCourt P (1996) A protein farnesyltransferase involved in abscisic acid signal transduction in *Arabidopsis*. Science 273:1239–1241

De Luca V, Marineau C, Brisson N (1989) Molecular cloning and analysis of cDNA encoding a plant tryptophan decarboxylase: comparison with animal dopa decarboxylases. Proc Natl Acad Sci USA 86: 2582–2586

de Waal A, Meijer AH, Verpoorte R (1995) Strictosidine synthase from *Catharanthus roseus*: purification and characterization of multiple forms. Biochem J 306:571–580

Décendit A, Liu D, Ouelhazi L, Doireau P, Mérillon JM, Rideau M (1992) Cytokinin-enhanced accumulation of indole alkaloids in *Catharanthus roseus* cell cultures. The factors affecting the cytokinin response. Plant Cell Rep 11:400–403

El-Sayed M, Verpoorte R (2005) Methyljasmonate accelerates catabolism of monoterpenoid indole alkaloids in *Catharanthus roseus* during leaf processing. Fitoterapia 76:83–90

Flesch G, Rohmer M (1988) Prokaryotic hopanoids: the biosynthesis of the bacteriohopane skeleton. Formation of isoprenic units from two distinct acetate pools and a novel type of carbon/carbon linkage between a triterpene and D-ribose. Eur J Biochem 175:405–411

Galichet A, Gruissem W (2006) Developmentally controlled farnesylation modulates AtNAP1;1 function in cell proliferation and cell expansion during *Arabidopsis* leaf development. Plant Physiol 142:1412–1426

Galichet A, Hoyerová K, Kamínek M, Gruissem W (2008) Farnesylation directs AtIPT3 subcellular localization and modulates cytokinin biosynthesis in *Arabidopsis*. Plant Physiol 146:1155–1164

Gantet P, Imbault N, Thiersault M, Doireau P (1998) Necessity of a functional octadecanoic pathway for indole alkaloid synthesis by *Catharanthus roseus* cell suspensions cultured in an auxin-starved medium. Plant Cell Physiol 39:220–225

Gelb MH, Tamanoi F, Yokoyama K, Ghomashchi F, Esson K, Gould MN (1995) The inhibition of protein prenyltransferases by oxygenated metabolites of limonene and perillyl alcohol. Cancer Lett 91:169–175

Gelb MH, Brunsveld L, Hrycyna CA et al (2006) Therapeutic intervention based on protein prenylation and associated modifications. Nat Chem Biol 2:518–528

Gerber E, Hemmerlin A, Hartmann M et al (2009) The plastidial 2-*C*-methyl-D-erythritol 4-phosphate pathway provides the isoprenyl moiety for protein geranylgeranylation in tobacco BY-2 cells. Plant Cell 21:285–300

Giglioli-Guivarc'h N, Courdavault V, Oudin A, Crèche J, St-Pierre B (2006) Madagascar periwinkle, an attractive model for studying the control of the biosynthesis of terpenoid derivative compounds. In: Texeira da Silva JA (ed) Floriculture, ornamental and plant biotechnology: advances and topical issues, vol 2, 1st edn. Global Science Books™, Isleworth, Middlesex, UK

Hedhili S, Courdavault V, Giglioli-Guivarc'h N, Gantet P (2007) Regulation of the terpene moiety biosynthesis of *Catharanthus roseus* terpene indole alkaloids. Phytochem Rev 6:341–351

Imbault N, Thiersault M, Dupéron P, Benabdelmouna A, Doireau P (1996) Pravastatin: a tool for investigating the availability of mevalonate metabolites for primary and secondary metabolism in *Catharanthus roseus* cell suspension. Physiol Plant 98:803–809

Irmler S, Schröder G, St-Pierre B, Crouch NP, Hotze M, Schmidt J, Strack D, Matern U, Schröder J (2000) Indole alkaloid biosynthesis in *Catharanthus roseus*: new enzyme activities and identification of cytochrome P450 CYP72A1 as secologanin synthase. Plant J 24:797–804

Johnson CD, Chary SN, Chernoff EA, Zeng Q, Running MP, Crowell DN (2005) Protein geranylgeranyltransferase is involved in specific aspects of abscisic acid and auxin signaling in *Arabidopsis*. Plant Physiol 139:722–723

Levêque D, Jehl F (2007) Molecular pharmacokinetics of *Catharanthus* (vinca) alkaloids. J Clin Pharmacol 47:579–588

Levêque D, Wihlm J, Jehl F (1996) Pharmacology of *Catharanthus* alkaloids. Bull Cancer 83:176–186

Mahroug S, Burlat V, St-Pierre B (2007) Cellular and subcellular organisation of the monoterpenoid indole alkaloid pathway in *Catharanthus roseus*. Phytochem Rev 6:363–381

Mason MG, Botella JR (2000) Completing the heterotrimer: isolation and characterization of an *Arabidopsis thaliana* G protein γ-subunit cDNA. Proc Natl Acad Sci USA 97:14784–14788

Mason MG, Botella JR (2001) Isolation of a novel G-protein γ-subunit from *Arabidopsis thaliana* and its interaction with G β. Biochim Biophys Acta 1520:147–153

McGarvey DJ, Croteau R (1995) Terpenoid metabolism. Plant Cell 7:1015–1026

Memelink J, Verpoorte R, Kijne JW (2001) ORCAnization of jasmonate-responsive gene expression in alkaloid metabolism. Trends Plant Sci 6:212–219

Menke FL, Champion A, Kjine JW, Memelink J (1999) A novel jasmonate- and elicitor-responsive element in the periwinkle secondary metabolite biosynthetic gene *Str* interacts with a jasmonate- and elicitor-inducible AP2-domain transcription factor ORCA2. EMBO J 18:4455–4463

Mérillon JM, Doireau P, Guillot A, Chénieux JC, Rideau M (1986) Indole alkaloid accumulation and tryptophan decarboxylase activity in *Catharanthus roseus* cells cultured in three media. Plant Cell Rep 5:23–26

Moores SL, Schaber MD, Mosser SD et al (1991) Sequence dependence of protein isoprenylation. J Biol Chem 266:14603–14610

Morehead TA, Biermann BJ, Crowell DN, Randall SK (1995) Changes in protein isoprenylation during the growth of suspension-cultured tobacco cells. Plant Physiol 109:277–284

Okouneva T, Hill BT, Wilson L, Jordan MA (2003) The effects of vinflunine, vinorelbine, and vinblastine on centromere dynamics. Mol Cancer Ther 2:427–436

Oudin A, Courtois M, Rideau M, Clastre M (2007a) The iridoid pathway in *Catharanthus roseus* alkaloid biosynthesis. Phytochem Rev 6:259–276

Oudin A, Mahroug S, Courdavault V et al (2007b) Spatial distribution and hormonal regulation of gene products from methyl erythritol phosphate and monoterpene-secoiridoid pathways in *Catharanthus roseus*. Plant Mol Biol 65:13–30

Papon N, Oudin A, Vansiri A, Rideau M, Chénieux JC, Crèche J (2003) Differential expression of two type-A response regulators in plants and cell cultures of *Catharanthus roseus* (L.) G. Don. J Exp Bot 54: 1793–1795

Papon N, Bremer J, Vansiri A, Andreu F, Rideau M, Crèche J (2005) Cytokinin and ethylene control indole alkaloid production at the level of the MEP/terpenoid pathway in *Catharanthus roseus* suspension cells. Planta Med 71:572–574

Pei ZM, Ghassemian M, Kwak CM, McCourt P, Schroeder JI (1998) Role of farnesyltransferase in ABA regulation of guard cell anion channels and plant water loss. Science 282:287–290

Qian D, Zhou D, Ju R, Cramer CL, Yang Z (1996) Protein farnesyltransferase in plants: molecular characterization and involvement in cell cycle control. Plant Cell 8:2381–2394

Ren Z, Elson CE, Gould MN (1997) Inhibition of type I and type II geranylgeranyl-protein transferases by the monoterpene perillyl alcohol in NIH3T3 cells. Biochem Pharmacol 54:113–120

Rodríguez-Concepción M, Yalovsky S, Gruissem W (1999) Protein prenylation in plants: old friends and new targets. Plant Mol Biol 39:865–870

Rohmer M (1999) The discovery of a mevalonate-independent pathway for isoprenoid biosynthesis in bacteria, algae and higher plants. Nat Prod Rep 16:565–574

Rohmer M, Knani M, Simonin P, Sutter B, Sahm H (1993) Isoprenoid biosynthesis in bacteria: a novel pathway for the early steps leading to isopentenyl diphosphate. Biochem J 295:517–524

Running MP, Lavy M, Sternberg H et al (2004) Enlarged meristems and delayed growth in *plp* mutants results from lack of CaaX-prenyltransferase. Proc Natl Acad Sci USA 101:7815–7820

Schafer WR, Rine J (1992) Protein prenylation: genes, enzymes, targets and functions. Annu Rev Genet 26:209–237

Simkin AJ, Labouré AM, Kuntz M, Sandmann G (2003) Comparison of carotenoid content, gene expression and enzyme levels in tomato (*Lycopersicon esculentum*) leaves. Z Naturforsch C 58c: 371–380

Simkin AJ, Guirimand G, Papon N et al (2011) Peroxisomal localisation of the final steps of the mevalonic acid pathway in *planta*. Planta 234:903–914

St-Pierre B, Vázquez-Flota FA, De Luca V (1999) Multicellular compartmentation of *Catharanthus roseus* alkaloid biosynthesis predicts intercellular translocation of a pathway intermediate. Plant Cell 11:887–900

Tamanoi F (1993) Inhibitors of Ras farnesyltransferases. Trends Biochem Sci 18:349–353

Trusov Y, Rookes JE, Chakravorty D, Armour D, Schenk PM, Botella JR (2006) Heterotrimeric G proteins facilitate *Arabidopsis* resistance to necrotrophic pathogens and are involved in jasmonate signaling. Plant Physiol 140:210–220

Trusov Y, Rookes JE, Tilbrook K et al (2007) Heterotrimeric G protein γ subunits provide functional selectivity in Gβγ dimer signaling in *Arabidopsis*. Plant Cell 19:1235–1250

van der Fits L, Memelink J (2000) ORCA3, a jasmonate-responsive transcriptional regulator of plant primary and secondary metabolism. Science 289: 295–297

van der Fits L, Memelink J (2001) The jasmonate-inducible AP2/ERF-domain transcrition factor ORCA3 activates gene expression via interaction with a jasmonate-responsive promoter element. Plant J 25: 43–53

Veau B, Courtois M, Oudin A, Chenieux JC, Rideau M, Clastre M (2000) Cloning and expression of cDNAs encoding two enzymes of the MEP pathway in *Catharanthus roseus*. Biochim Biophys Acta 1517: 159–163

Wang Y, Ying J, Kuzma M et al (2005) Molecular tailoring of farnesylation for plant drought tolerance and yield protection. Plant J 43:413–424

Yalovsky S, Kulukian A, Rodríguez-Concepción M, Young CA, Gruissem W (2000a) Functional requirement of plant farnesyltransferase during development in *Arabidospsis*. Plant Cell 12:1267–1278

Yalovsky S, Rodríguez-Concepción M, Bracha K, Toledo-Ortiz G, Gruissem W (2000b) Prenylation of the floral transcription factor APETALA1 modulates its function. Plant Cell 12:1257–1266

Zhang FL, Casey PJ (1996) Protein prenylation: molecular mechanisms and functional consequences. Annu Rev Biochem 65:241–269

Zhang H, Hedhili S, Montiel G, Zhang Y, Chatel G, Pré M, Gantet P, Memelink J (2011) The basic helix-loop-helix transcription factor CrMYC2 controls the jasmonate-responsive expression of the ORCA genes that regulate alkaloid biosynthesis in *Catharanthus roseus*. Plant J 67:61–71

Ziegelhoffer EC, Medrano LJ, Meyerowitz EM (2000) Cloning of the *Arabidopsis WIGGUM* gene identifies a role for farnesylation in meristem development. Proc Natl Acad Sci USA 97:7633–7638

The Role of Prenylcysteine Methylation and Metabolism in Abscisic Acid Signaling in *Arabidopsis thaliana*

20

Dring N. Crowell* and David H. Huizinga

Abstract

Protein prenylation is a posttranslational modification resulting in thioether linkage of a 15-carbon farnesyl, or 20-carbon geranylgeranyl, moiety to a cysteine residue at or near the carboxyl terminus of a protein. Most prenylated proteins are further modified by carboxyl terminal proteolysis and/or methylation, the latter being the only reversible step in this series of modifications. In *Arabidopsis thaliana*, protein prenylation has been shown to be necessary for negative regulation of abscisic acid (ABA) signaling. This chapter summarizes recent literature on the role of methylation and demethylation of prenylated proteins in negative regulation of ABA signaling. Degradation of prenylated proteins generates farnesylcysteine (FC) and geranylgeranylcysteine (GGC), which are potent competitive inhibitors of isoprenylcysteine methyltransferase (ICMT), the enzyme that methylates the carboxyl terminus of prenylated proteins. Thus, FC and GGC metabolism also affects ABA signaling, and this chapter summarizes recent literature on prenylcysteine metabolism and its role in negative regulation of ABA signaling.

Keywords

Abscisic acid signaling • *Arabidopsis thaliana* • Farnesol dehydrogenase • Farnesol kinase • Farnesylcysteine lyase • Prenylcysteine demethylation • Prenylcysteine methylation

* Passed away on June 30, 2012.

D.H. Huizinga (✉)
Dow AgroSciences LLC, 9330 Zionsville Rd,
Indianapolis, IN 46268, USA
e-mail: dhhuizinga@dow.com

T.J. Bach and M. Rohmer (eds.), *Isoprenoid Synthesis in Plants and Microorganisms: New Concepts and Experimental Approaches*, DOI 10.1007/978-1-4614-4063-5_20,

20.1 Introduction

Prenylated proteins are posttranslationally modified by thioether linkage of an isoprenoid lipid (e.g., farnesyl or geranylgeranyl) to a cysteine residue at or near the carboxyl terminus (Clarke 1992; Zhang and Casey 1996; Crowell 2000; Crowell and Huizinga 2009). Proteins with a carboxyl terminal CaaX motif (C = cys, a = aliphatic, X = ala, cys, gln, met, ser) are modified by protein farnesyltransferase (PFT) (Reid et al. 2004; Andrews et al. 2010), a heterodimeric metalloenzyme that requires zinc and magnesium for activity (Clarke 1992; Zhang and Casey 1996; Crowell 2000; Crowell and Huizinga 2009). Proteins with a similar carboxyl terminal CaaX motif (X = leu) are modified by protein geranylgeranyltransferase type I (PGGT I) (Reid et al. 2004; Andrews et al. 2010), a heterodimeric metalloenzyme with an α-subunit identical to that of PFT and a distinct β-subunit. Unlike PFT, PGGT I requires zinc, but not magnesium, for activity (Clarke 1992; Zhang and Casey 1996; Crowell 2000; Crowell and Huizinga 2009). RAB GTPases with an XXCC, CCXX, XCXC, or XCCX carboxyl terminal motif are bound by the RAB ESCORT PROTEIN (REP) and then modified by RAB geranylgeranyltransferase (also called protein geranylgeranyltransferase type II), a heterodimeric enzyme with unique α- and β-subunits (Leung et al. 2006, 2007). Prenylation facilitates the association of these proteins with membranes and/or other proteins and has been shown in many cases to be essential for proper intracellular targeting and function (Clarke 1992; Zhang and Casey 1996; Crowell 2000; Crowell and Huizinga 2009).

CaaX proteins that are modified by either PFT or PGGT I are further modified (Clarke 1992; Zhang and Casey 1996; Crowell 2000; Crowell and Huizinga 2009). Following cysteinyl prenylation, CaaX proteins undergo carboxyl terminal proteolysis, which removes the three amino acids downstream of the prenylated cysteine residue (aaX) (Gutierrez et al. 1989; Hrycyna and Clarke 1992; Boyartchuk et al. 1997; Schmidt et al. 1998; Tam et al. 1998). Two CaaX proteases, encoded by the *STE24* and *RCE1* genes in *Saccharomyces cerevisiae* and by the *AtSTE24* (At4g01320) and *AtFACE-2* (At2g36305) genes in *Arabidopsis thaliana*, have been identified (Hrycyna and Clarke 1992; Boyartchuk et al. 1997; Schmidt et al. 1998; Tam et al. 1998; Bracha et al. 2002; Cadiñanos et al. 2003). The prenylcysteine residue at the newly formed carboxyl terminus is then carboxyl methylated by a specific isoprenylcysteine methyltransferase (ICMT), which is encoded by the *STE14* gene in Saccharomyces and by the *AtSTE14A* (At5g23320) and *AtSTE14B* (At5g08335) genes in Arabidopsis (Clarke et al. 1988; Gutierrez et al. 1989; Ong et al. 1989; Hrycyna and Clarke 1990; Kawata et al. 1990; Yamane et al. 1990; Fujiyama et al. 1991; Hrycyna et al. 1991; Sapperstein et al. 1994; Fukada 1995; Crowell et al. 1998; Crowell and Kennedy 2001; Narasimha Chary et al. 2002). Because carboxyl methylation is the only potentially reversible step in this series of posttranslational modifications (Fig. 20.1), the subcellular localization and function of many prenylated proteins may be governed by methylation status.

In Arabidopsis, protein farnesylation is necessary for negative regulation of abscisic acid (ABA) signaling. Indeed, knockout mutations in the *ERA1* (*ENHANCED RESPONSE TO ABA1*, At5g40280) gene, which encodes the β-subunit of PFT, cause an enhanced response to ABA in seeds and guard cells, resulting in delayed germination and reduced water loss under drought conditions, respectively (Cutler et al. 1996; Pei et al. 1998). *era1* mutants were subsequently shown to exhibit enlarged meristems and supernumerary floral organs (Running et al. 1998; Bonetta et al. 2000; Yalovsky et al. 2000; Ziegelhoffer et al. 2000). Thus, protein farnesylation is also required for normal meristem development (i.e., negative regulation of meristem size). The *era1* phenotype is greatly exaggerated in Arabidopsis plants with knockout mutations in the *PLP* (*PLURIPETALA*, At3g59380) gene, which encodes the shared α-subunit of PFT and PGGT I (Running et al. 2004). The relatively severe phenotype of *plp* mutant plants suggests that PGGT I partially compensates for loss of PFT in *era1* plants.

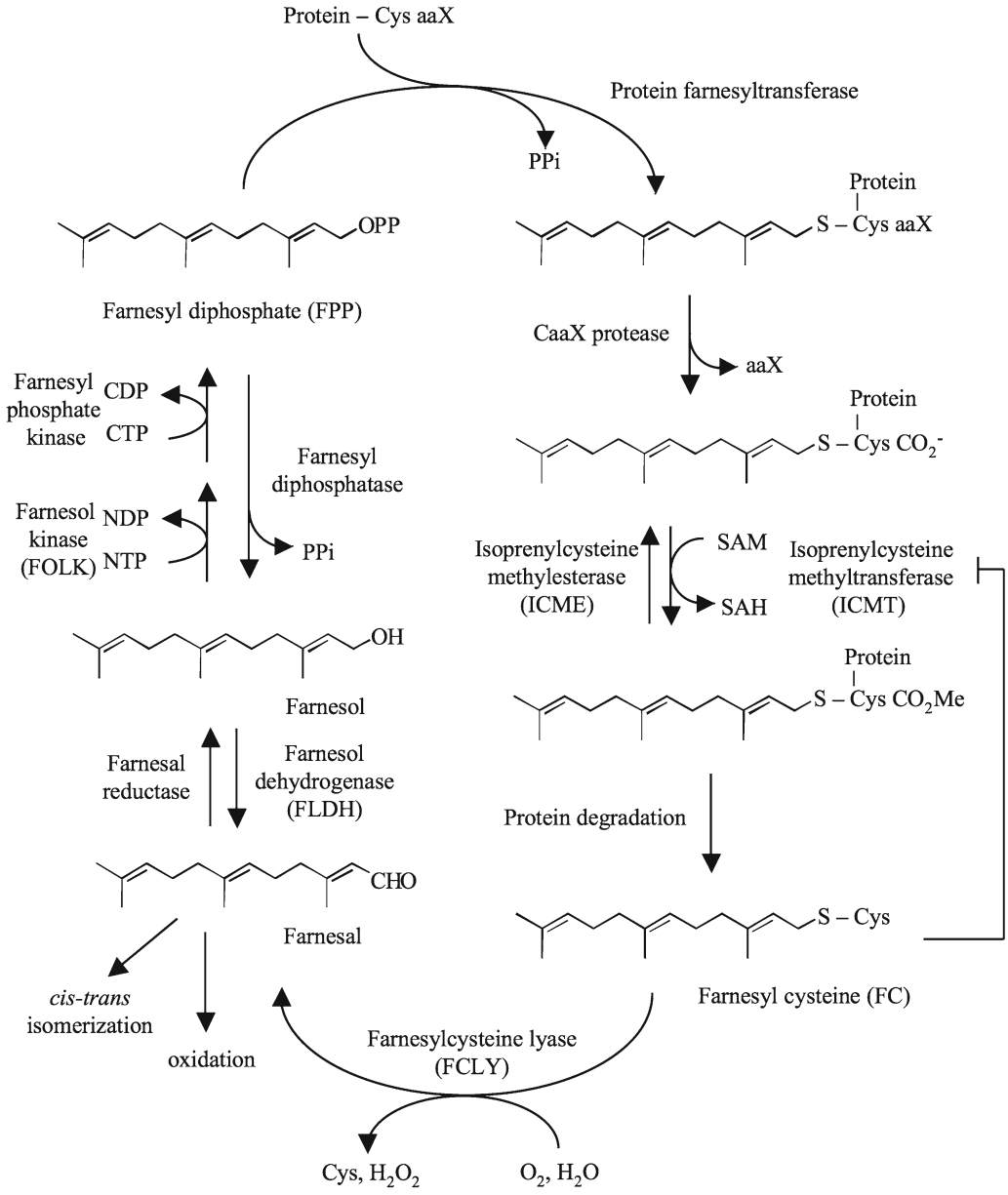

Fig. 20.1 *Utilization and salvage cycle for farnesyl diphosphate in plants*. The transfer of a farnesyl group from farnesyl diphosphate to a CaaX protein is followed by postprenylation processing (proteolysis and carboxyl methylation). Degradation of the farnesylated protein generates FC, which is oxidized by FC lyase to farnesal. Farnesal is then reduced to farnesol, and farnesol is phosphorylated to farnesyl diphosphate to complete the cycle (Crowell et al. 2007)

Knockout mutations in the *GGB* (*GERANYLGERANYLTRANSFERASE BETA*, At2g39550) gene, which encodes the β-subunit of PGGT I, cause no obvious developmental phenotypes (Johnson et al. 2005). Nevertheless, *ggb* mutant plants exhibit an enhanced response to ABA in guard cells, but not seeds, and an enhanced response to auxin-induced lateral root formation, but not

auxin inhibition of primary root growth. Thus, PGGT I appears to be involved in specific aspects of ABA and auxin signaling. Furthermore, overexpression of *GGB* in *era1-4* plants suppresses the *era1* phenotype, confirming the suggestion that PGGT I partially compensates for loss of PFT in *era1* mutant plants (Johnson et al. 2005).

20.2 Prenylcysteine Methyltransferase in Arabidopsis

As described above, prenylcysteine methylation is potentially reversible and, thus, may regulate the targeting and function of prenylated proteins, at least one of which is a negative regulator of ABA signaling. Two ICMT enzymes, encoded by the *AtSTE14A* and *AtSTE14B* genes, have been described in Arabidopsis (Narasimha Chary et al. 2002). The enzyme encoded by the *AtSTE14B* gene exhibits lower apparent K_m values for biologically relevant prenylcysteine substrates and higher specific activities than the enzyme encoded by the *AtSTE14A* gene (Table 20.1). Moreover, *AtSTE14B* gene expression is higher and more ubiquitous in Arabidopsis tissues and organs than *AtSTE14A* gene expression. It follows that if protein farnesylation is required for negative regulation of ABA signaling, prenylcysteine methylation may also be required for negative regulation of ABA signaling. Consistent with this hypothesis, competitive inhibitors of ICMT cause an enhanced response to ABA in Arabidopsis seeds (Fig. 20.2)

Table 20.1 Kinetic properties of Arabidopsis isoprenylcysteine methyltransferase isozymes

	Apparent Km (μM)		Specific activity (pmol/min/mg)	
	AFC	AGGC	AFC	AGGC
AtSTE14A	22.7 +/− 3.7	13.7 +/− 4.1	5.0 +/− 1.1	3.7 +/− 0.6
AtSTE14B	5.0 +/ −0.0	3.0 +/− 1.0	220 +/− 56	296 +/− 100

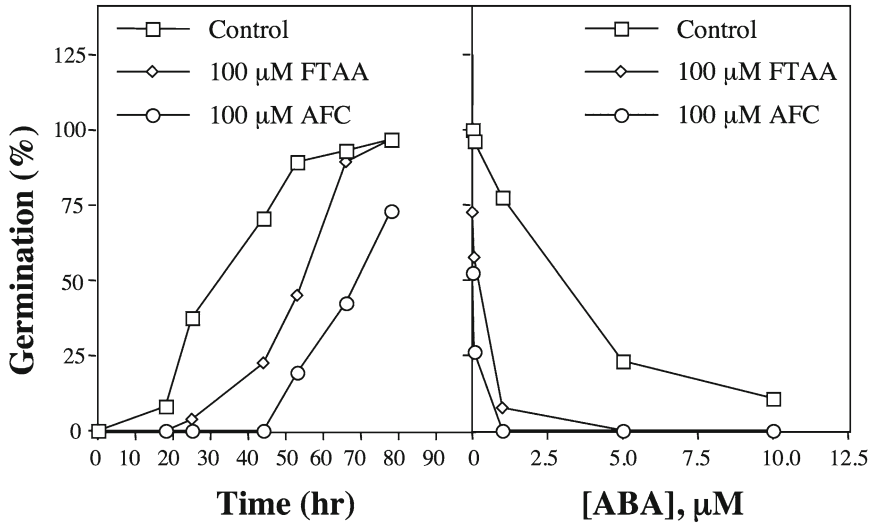

Fig. 20.2 *Inhibitors of ICMT activity cause an enhanced response to ABA in seed germination assays. Arabidopsis thaliana* ecotype Columbia seeds were germinated in the presence of 100 μM AFC (*N*-acetyl-*S*-*trans*,*trans*-farnesyl-L-cysteine), 100 μM FTAA (*S*-farnesylthioacetic acid), or 100 μM AGC (*N*-acetyl-*S*-*trans*-geranyl-L-cysteine, a biologically irrelevant prenylcysteine control). Germination was recorded as a function of time or as a function of ABA concentration after 66 h and recorded as percent germination (n = 20–30) (Narasimha Chary et al. 2002)

(Narasimha Chary et al. 2002). Furthermore, overexpression of *AtSTE14B* in transgenic Arabidopsis plants results in an ABA-insensitive phenotype (Huizinga et al. 2008). This result strongly suggests that prenylated negative regulators of ABA signaling are incompletely methylated in wild-type Arabidopsis plants (i.e., if they were completely methylated, overproduction of ICMT would have no effect). Thus, ICMT is a *bona fide* negative regulator of ABA signaling.

20.3 Prenylcysteine Methylesterase in Arabidopsis

If prenylcysteine methylation is a reversible process, an esterase exists to catalyze the demethylation of carboxyl terminal prenylcysteine methyl esters (Fig. 20.1). Recently, a specific prenylcysteine methylesterase activity was identified in Arabidopsis membranes that specifically demethylates biologically relevant prenylcysteine methyl ester substrates (Fig. 20.3) (Deem et al. 2006). A gene encoding this activity was also identified. Arabidopsis prenylcysteine methylesterase, which is encoded by the *AtPCME* (*PRENYLCYSTEINE METHYLESTERASE*, *ICME*, At5g15860) gene, exhibits relatedness to sterol esterases, insect juvenile hormone esterases, and carboxyl ester lipases and possesses a carboxylesterase type-B serine active site and a predicted transmembrane domain. Interestingly, when the *AtPCME* gene was expressed in Saccharomyces, the resulting activity exhibited greater specificity for biologically relevant prenylcysteine methyl ester substrates than the activity detected in Arabidopsis membrane preparations (Fig. 20.3) (Deem et al. 2006). This finding suggests that both specific and nonspecific esterases may catalyze the demethylation of carboxyl terminal prenylcysteine methyl esters in Arabidopsis. Because the *AtSTE14A* and *AtSTE14B* genes are negative regulators of ABA signaling, it follows that the *AtPCME* gene is a positive regulator of ABA signaling. Indeed, overexpression of *AtPCME* results in an enhanced response to ABA (Huizinga et al. 2008).

20.4 Farnesylcysteine Lyase in *Arabidopsis*

The degradation of prenylated proteins poses a metabolic problem for eukaryotic cells. This process generates farnesylcysteine (FC) and geranylgeranylcysteine (GGC), which must be metabolized to recycle the amino acid and isoprenoid moieties and to prevent the accumulation of prenylcysteine inhibitors of ICMT. In mammals, a peroxisomal prenylcysteine lyase has been described that catalyzes the oxidation of both FC and GGC. This unusual thioether oxidase utilizes molecular oxygen, water, and FAD to oxidize prenylcysteine substrates to cysteine, a prenyl aldehyde (farnesal or geranylgeranial), and hydrogen peroxide (Zhang et al. 1997; Tschantz et al. 1999, 2001; Digits et al. 2002). Recently, a prenylcysteine lyase activity was also detected in Arabidopsis membranes (Fig. 20.4) (Crowell et al. 2007). Interestingly, the farnesal product of FC oxidation was subsequently reduced to farnesol by an NAD(P)H-dependent reductase. The latter conclusion was based on the observation that preincubation of Arabidopsis membranes with NADase, which destroys NADH and NADPH, abolished the conversion of farnesal to farnesol (Fig. 20.4). Moreover, the kinetics of farnesal and farnesol formation were consistent with the hypothesis that FC is oxidized to farnesal, which is subsequently reduced to farnesol (all products were identified by TLC and HPLC comigration with authentic standards) (Crowell et al. 2007). Interestingly, the Arabidopsis prenylcysteine lyase, which was present in all tissues and organs of mature Arabidopsis plants, seedlings, and cell cultures, was specific for FC. Even a 50-fold molar excess of unlabeled GGC failed to significantly inhibit the conversion of [^{3}H]FC to [^{3}H]farnesal, whereas unlabeled FC at this concentration was an effective competitor (Crowell et al. 2007). The Arabidopsis gene encoding FC lyase, designated *FCLY* (*FARNESYLCYSTEINE LYASE*, At5g63910), was identified by sequence relatedness to the human prenylcysteine lyase

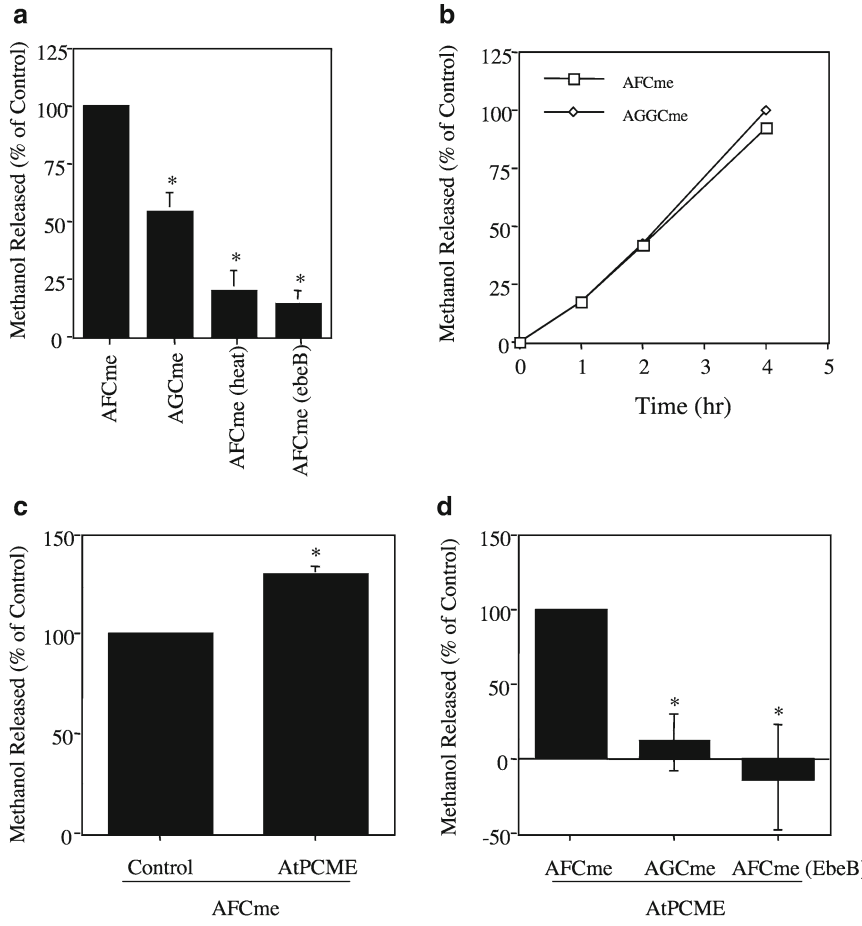

Fig. 20.3 *PCME activity in Arabidopsis cell membranes and recombinant AtPCME activity expressed in Saccharomyces*. (**a**) Reactions were performed for 2 h at 30°C in the presence of 70 μg of Arabidopsis membrane protein and 30,000 cpm of the indicated [^{3}H]methyl-ester substrate, and radioactivity released in the form of [^{3}H] methanol was quantified by liquid scintillation. Heated samples were incubated at 95°C for 5 min. Ebelactone B was used at 0.4 mM. The standard error of the mean is shown for all data points. *Asterisks* indicate significant differences ($P<0.01$ by Student's t test). The data shown are representative of six independent experiments. (**b**) Reactions were done as (a) in the presence of 70 μg of Arabidopsis membrane protein and the methyl-ester of [^{3}H]AFC or [^{3}H]AGGC (*N*-acetyl-*S*-all-*trans*-geranylgeranyl-L-cysteine) for varying times. The experiment shown is representative of three independent experiments. (**c**) Membranes from control and *AtPCME*-expressing yeast cells were analyzed for PCME activity in the presence of [^{3}H]AFC methylester. (**d**) PCME activity in the presence of [^{3}H]AFC methylester, [^{3}H]AGC methyl-ester, and [^{3}H]AFC methylester plus 0.4 mM ebelactone B is shown for membranes of *AtPCME*-expressing yeast cells. The PCME activity of control yeast cells in the pres-ence of [^{3}H]AFC methylester, [^{3}H]AGC methylester, and [^{3}H]AFC methylester plus 0.4 mM ebelactone B was subtracted from the values shown. The standard error of the mean is shown for all data. *Asterisks* indicate significant differences ($P<0.05$ by Student's t test) (Deem et al. 2006)

gene, and two *fcly* mutants, with T-DNA insertions in the *FCLY* gene, were identified. Neither insertion ablated *FCLY* expression (one was an intron insertion, and one was a 5′-flanking insertion). Nevertheless, both insertion mutants exhibited reduced *FCLY* expression and a dramatically enhanced response to ABA in seed germination assays (Fig. 20.5) (Crowell et al. 2007). Thus, like ICMT, FC lyase is a *bona fide* negative regulator of ABA signaling. The enhanced response to ABA was likely caused by FC accumulation and inhibition of ICMT because both *fcly* mutants

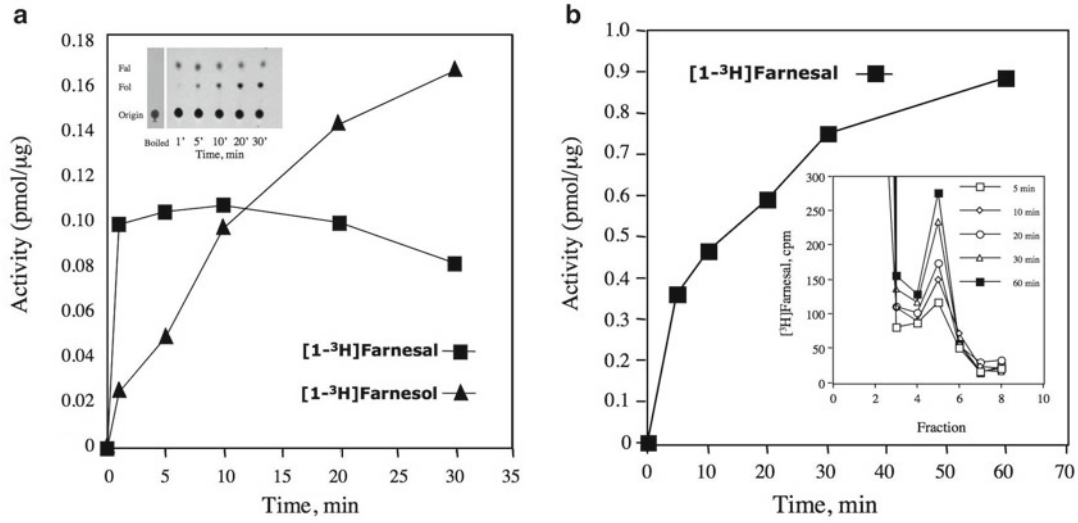

Fig. 20.4 *Metabolism of [1-³H]FC to [1-³H]farnesal and [1-H]farnesol in the presence of Arabidopsis membranes*. (**a**) [1-³H]FC was incubated with Arabidopsis membranes at 30 °C for 30 min, and reaction products were analyzed by silica gel thin layer chromatography. Radioactive products were identified by comigration with authentic chemical standards and quantified by liquid scintillation of excised TLC spots. The dependence of product formation on time is shown. (**b**) Reactions were performed as in (**a**) with NADase pretreatment. The *inset* shows the radioactivity corresponding to farnesal in TLC fraction five (no farnesol was detected). These data are representative of three independent experiments. *Fol* farnesol, *Fal* farnesal (Crowell et al. 2007)

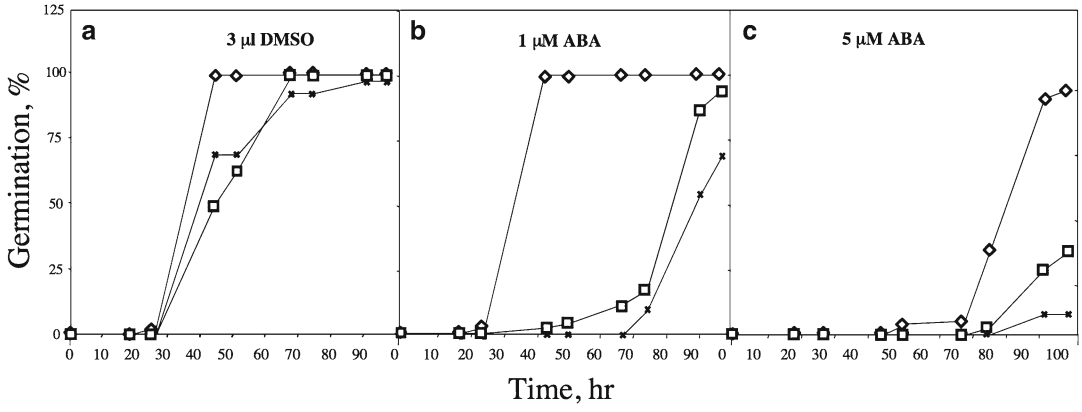

Fig. 20.5 *The effect of ABA on germination of wild-type (Col-0) and mutant (fcly-1 and fcly-2) seeds*. (**a**–**c**) Germination in the presence or absence of the indicated concentration of ABA was analyzed as a function of time under a dissecting microscope. DMSO was used as a solvent control (Crowell et al. 2007). *Diamonds* represent wild-type seeds, *squares* represent *fcly-1* seeds, and *asterisks* represent *fcly-2* seeds

accumulated 10–30% more FC than wild type and ICMT overproduction suppressed the ABA hypersensitivity of both mutants (Huizinga et al. 2010). Consistent with the observation that the protein product of the *FCLY* gene is specific for FC and that GGC metabolism involves an alternative pathway, incubation of [³H]GGC in the presence of Arabidopsis membranes did not result in the formation of geranylgeranial (Huizinga et al. 2010).

20.5 Conclusions

The results shown in Figs. 20.2 and 20.5 demonstrate that ABA signaling in Arabidopsis is strongly influenced by reversible methylation of carboxyl terminal prenylcysteine residues and metabolism of prenylcysteine compounds generated during the degradation of prenylated proteins, respectively. Carboxyl methylation of prenylated proteins is necessary for negative regulation of ABA signaling. This conclusion is supported by the data in Fig. 20.2, which shows that specific competitive inhibitors of ICMT cause an enhanced response to ABA (i.e., loss of negative regulation of ABA signaling). This conclusion is also supported by the observation that overproduction of ICMT causes an ABA-insensitive phenotype (Huizinga et al. 2008). Thus, ICMT is a negative regulator of ABA signaling. By inference, demethylation of prenylated proteins is necessary for positive regulation of ABA signaling. This inference is supported by the observation that overproduction of prenylcysteine methylesterase causes an enhanced response to ABA (Huizinga et al. 2008). Interestingly, ABA induces the expression of the *AtPCME* gene (Huizinga et al. 2008). Together, these observations demonstrate that ABA signaling is under positive feedback control via induction of *AtPCME* gene expression and demethylation (i.e., inactivation) of prenylated negative regulators of ABA signaling. Because mutants with decreased FC lyase activity exhibit an enhanced response to ABA, FC lyase, like ICMT, is a negative regulator of ABA signaling. Interestingly, FC accumulation and concomitant inhibition of ICMT are the likely cause of the *fcly* phenotype (Huizinga et al. 2010).

Other genes involved in FC metabolism have been identified and shown to be involved in ABA signaling. The *FLDH* (*FARNESOL DEHYDROGENASE*, At4g33360) gene encodes an NAD^+-dependent dehydrogenase that oxidizes farnesol to farnesal (Bhandari et al. 2010), and the *FOLK* (*FARNESOL KINASE*, At5g58560) gene encodes a kinase that phosphorylates farnesol to farnesyl phosphate (Fitzpatrick et al. 2011). Both genes encode negative regulators of ABA signaling, and both are repressed by ABA. These observations, along with those discussed above, suggest a complex relationship between prenylcysteine methylation and metabolism and ABA signal transduction.

References

Andrews M, Huizinga DH, Crowell DN (2010) The CaaX specificities of Arabidopsis protein prenyltransferases explain *era1* and *ggb* phenotypes. BMC Plant Biol 10:118

Bhandari J, Fitzpatrick AH, Crowell DN (2010) Identification of a novel abscisic acid-regulated farnesol dehydrogenase from Arabidopsis. Plant Physiol 154:1116–1127

Bonetta D, Bayliss P, Sun S, Sage T, McCourt P (2000) Farnesylation is involved in meristem organization in Arabidopsis. Planta 211:182–190

Boyartchuk VL, Ashby MN, Rine J (1997) Modulation of Ras and a-factor function by carboxyl-terminal proteolysis. Science 275:1796–1800

Bracha K, Lavy M, Yalovsky S (2002) The Arabidopsis AtSTE24 is a CAAX protease with broad substrate specificity. J Biol Chem 277:29856–29864

Cadiñanos J, Varela I, Mandel DA, Schmidt WK, Díaz-Perales A, López-Otín C, Freije JM (2003) AtFACE-2, a functional prenylated protein protease from *Arabidopsis thaliana* related to mammalian Ras-converting enzymes. J Biol Chem 278:42091–42097

Clarke S (1992) Protein isoprenylation and methylation at carboxyl-terminal cysteine residues. Annu Rev Biochem 61:355–386

Clarke S, Vogel JP, Deschenes RJ, Stock J (1988) Posttranslational modification of the Ha-ras oncogene protein: evidence for a third class of protein carboxyl methyltransferases. Proc Natl Acad Sci USA 85:4643–4647

Crowell DN (2000) Functional implications of protein isoprenylation in plants. Prog Lipid Res 39:393–408

Crowell DN, Huizinga DH (2009) Protein isoprenylation: the fat of the matter. Trends Plant Sci 14:163–170

Crowell DN, Kennedy M (2001) Identification and functional expression in yeast of a prenylcysteine α-carboxyl methyltransferase gene from *Arabidopsis thaliana*. Plant Mol Biol 45:469–476

Crowell DN, Randall SK, Sen SE (1998) Prenycysteine α-carboxyl methyltransferase in suspension-cultured tobacco cells. Plant Physiol 118:115–123

Crowell DN, Huizinga DH, Deem AK, Trobaugh C, Denton R, Sen SE (2007) *Arabidopsis thaliana* plants possess a specific farnesylcysteine lyase that is involved in detoxification and recycling of farnesylcysteine. Plant J 50:839–847

Cutler S, Ghassemian M, Bonetta D, Cooney S, McCourt P (1996) A protein farnesyl transferase involved in abscisic acid signal transduction in Arabidopsis. Science 273:1239–1241

Deem AK, Bultema RL, Crowell DN (2006) Prenylcysteine methylesterase in *Arabidopsis thaliana*. Gene 380: 159–166

Digits JA, Pyun HJ, Coates RM, Casey PJ (2002) Stereospecificity and kinetic mechanism of human prenylcysteine lyase, an unusual thioether oxidase. J Biol Chem 277:41086–41093

Fitzpatrick AH, Bhandari J, Crowell DN (2011) Farnesol kinase is involved in farnesol metabolism, ABA signaling and flower development in Arabidopsis. Plant J 66:1078–1088

Fujiyama A, Tsunasawa S, Tamanoi F, Sakiyama F (1991) *S*-farnesylation and methyl esterification of C-terminal domain of yeast RAS2 protein prior to fatty acid acylation. J Biol Chem 266:17926–17931

Fukada Y (1995) Prenylation and carboxylmethylation of G-protein γ subunit. Methods Enzymol 250:91–105

Gutierrez L, Magee AI, Marshall CJ, Hancock JF (1989) Post-translational processing of p21ras is two-step and involves carboxyl-methylation and carboxy-terminal proteolysis. EMBO J 8:1093–1098

Hrycyna CA, Clarke S (1990) Farnesyl cysteine C-terminal methyltransferase activity is dependent upon the *STE14* gene product in *Saccharomyces cerevisiae*. Mol Cell Biol 10:5071–5076

Hrycyna CA, Clarke S (1992) Maturation of isoprenylated proteins in *Saccharomyces cerevisiae*. Multiple activities catalyze the cleavage of the three carboxyl-terminal amino acids from farnesylated substrates in vitro. J Biol Chem 267:10457–10464

Hrycyna CA, Sapperstein SK, Clarke S, Michaelis S (1991) The *Saccharomyces cerevisiae STE14* gene encodes a methyltransferase that mediates C-terminal methylation of a-factor and RAS proteins. EMBO J 10:1699–1709

Huizinga DH, Omosegbon O, Omery B, Crowell DN (2008) Isoprenylcysteine methylation and demethylation regulate abscisic acid signaling in *Arabidopsis*. Plant Cell 20:2714–2728

Huizinga DH, Denton R, Koehler KG, Tomasello A, Wood L, Sen SE, Crowell DN (2010) Farnesylcysteine lyase is involved in negative regulation of abscisic acid signaling in *Arabidopsis*. Mol Plant 3:143–155

Johnson CD, Chary SN, Chernoff EA, Zeng Q, Running MP, Crowell DN (2005) Protein geranylgeranyltransferase I is involved in specific aspects of abscisic acid and auxin signaling in Arabidopsis. Plant Physiol 139:722–733

Kawata M, Farnsworth CC, Yoshida Y, Gelb MH, Glomset JA, Takai Y (1990) Posttranslationally processed structure of the human platelet protein smg p21B: evidence for geranylgeranylation and carboxyl methylation of the C-terminal cysteine. Proc Natl Acad Sci USA 87:8960–8964

Leung KF, Baron R, Seabra MC (2006) Thematic review series: lipid posttranslational modifications. geranylgeranylation of Rab GTPases. J Lipid Res 47:467–475

Leung KF, Baron R, Ali BR, Magee AI, Seabra MC (2007) Rab GTPases containing a CAAX motif are processed post-geranylgeranylation by proteolysis and methylation. J Biol Chem 282:1487–1497

Narasimha Chary S, Bultema RL, Packard CE, Crowell DN (2002) Prenylcysteine alpha-carboxyl methyltransferase expression and function in *Arabidopsis thaliana*. Plant J 32:735–747

Ong OC, Ota IM, Clarke S, Fung BK (1989) The membrane binding domain of rod cGMP phosphodiesterase is posttranslationally modified by methyl esterification at a C-terminal cysteine. Proc Natl Acad Sci USA 86:9238–9242

Pei ZM, Ghassemian M, Kwak CM, McCourt P, Schroeder JI (1998) Role of farnesyltransferase in ABA regulation of guard cell anion channels and plant water loss. Science 282:287–290

Reid TS, Terry KL, Casey PJ, Beese LS (2004) Crystallographic analysis of CaaX prenyltransferases complexed with substrates defines rules of protein substrate selectivity. J Mol Biol 343:417–433

Running MP, Fletcher JC, Meyerowitz EM (1998) The WIGGUM gene is required for proper regulation of floral meristem size in Arabidopsis. Development 125:2545–2553

Running MP, Lavy M, Sternberg H, Galichet A, Gruissem W, Hake S, Ori N, Yalovsky S (2004) Enlarged meristems and delayed growth in *plp* mutants result from lack of CaaX prenyltransferases. Proc Natl Acad Sci USA 101:7815–7820

Sapperstein S, Berkower C, Michaelis S (1994) Nucleotide sequence of the yeast *STE14* gene, which encodes farnesylcysteine carboxyl methyltransferase, and demonstration of its essential role in a-factor export. Mol Cell Biol 14:1438–1449

Schmidt WK, Tam A, Fujimura-Kamada K, Michaelis S (1998) Endoplasmic reticulum membrane localization of Rce1p and Ste24p, yeast proteases involved in carboxyl-terminal CAAX protein processing and amino-terminal a-factor cleavage. Proc Natl Acad Sci USA 95:11175–11180

Tam A, Nouvet FJ, Fujimura-Kamada K, Slunt H, Sisodia SS, Michaelis S (1998) Dual roles for Ste24p in yeast a-factor maturation: NH2-terminal proteolysis and COOH-terminal CAAX processing. J Cell Biol 142:635–649

Tschantz WR, Zhang L, Casey PJ (1999) Cloning, expression, and cellular localization of a human prenylcysteine lyase. J Biol Chem 274:35802–35808

Tschantz WR, Digits JA, Pyun HJ, Coates RM, Casey PJ (2001) Lysosomal prenylcysteine lyase is a FAD-dependent thioether oxidase. J Biol Chem 276: 2321–2324

Yalovsky S, Kulukian A, Rodríguez-Concepción M, Young CA, Gruissem W (2000) Functional requirement of plant farnesyltransferase during development in *Arabidopsis*. Plant Cell 12:1267–1278

Yamane HK, Farnsworth CC, Xie HY, Howald W, Fung BK, Clarke S, Gelb MH, Glomset JA (1990) Brain G protein γ subunits contain an all-*trans*-geranylgeranylcysteine methyl ester at their carboxyl termini. Proc Natl Acad Sci USA 87:5868–5872

Zhang FL, Casey PJ (1996) Protein prenylation: molecular mechanisms and functional consequences. Annu Rev Biochem 65:241–269

Zhang L, Tschantz WR, Casey PJ (1997) Isolation and characterization of a prenylcysteine lyase from bovine brain. J Biol Chem 272:23354–23359

Ziegelhoffer EC, Medrano LJ, Meyerowitz EM (2000) Cloning of the Arabidopsis WIGGUM gene identifies a role for farnesylation in meristem development. Proc Natl Acad Sci USA 97:7633–7638

What We Do and Do Not Know About the Cellular Functions of Polyisoprenoids

21

Liliana Surmacz and Ewa Swiezewska

Abstract

Natural compounds classified as products of secondary metabolism are widely studied as to their potential biological role. Identification of possible cellular functions of polyisoprenoids, generally considered as secondary products, has been our focus for some 30 years already. The results of these studies for instance in the context of membrane permeability and protein modification are briefly described and discussed in this chapter.

Keywords

Polyisoprenoid alcohols • *cis*-/*trans*-polyprenols, dolichols • *cis*-prenyltransferases • Solanesol (all-*trans* prenol-9) • Bactoprenol (prenol-11) • Membrane fluidity • Protein glycosylation • Polyisoprenylated proteins • [^{3}H]farnesol • [^{3}H]geranylgeraniol

21.1 Structural Aspects of Polyisoprenoids

The term polyisoprenoids is used here to designate linear polymers of several up to more than 100 isoprene units (Fig. 21.1). Neither short-chain oligoterpenes ($n<5$) nor higher isoprene polymers ($n>300$) such as natural rubber or gutta-percha will be discussed (but see elsewhere in this volume). Although the simple and modest polymeric structure of polyisoprenoids does not leave too much room for diversification, still some structural variants are known, and their structures together with newly described compounds have been summarized recently (Skorupinska-Tudek et al. 2008b; Surmacz and Swiezewska 2011).

Two main types of polyisoprenoid alcohols have been described so far differing in the hydrogenation status of their OH-terminal (α-) isoprene unit; these are polyprenols (α-unsaturated) and dolichols (α-saturated) compounds. Further diversity of natural polyisoprenoid alcohols concerns the *cis*/*trans* (*Z*/*E*) configuration of double bonds and the chain-length of molecules (Hemming 1985). Typical polyprenols and dolichols are of "mainly *cis*-" configuration; thus,

L. Surmacz (✉) • E. Swiezewska
Institute of Biochemistry and Biophysics,
Polish Academy of Sciences, Pawinskiego 5a,
Warsaw 02-106, Poland
e-mail: surmacz@ibb.waw.pl

T.J. Bach and M. Rohmer (eds.), *Isoprenoid Synthesis in Plants and Microorganisms: New Concepts and Experimental Approaches*, DOI 10.1007/978-1-4614-4063-5_21,

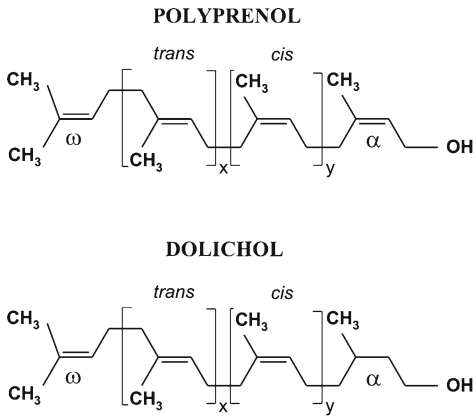

Fig. 21.1 Structure of polyprenol and dolichol. The isoprenoid units in *trans* and *cis* configuration are indicated, *x* and *y* stand for the number of internal *trans* and *cis* units, respectively, while ω and α represent the terminal ones

their molecules consist of a few (two or three for some polyprenols) *trans* isoprene units adjacent to the α-unit. Solanesol (all-*trans*-Prenol-9) is almost the unique representative of the all-*trans* polyisoprenoids. Polyprenols are found in plant photosynthetic tissues and bacterial cells, while dolichols are typical animal and yeast lipids. Recently, dolichols have also been identified in plant roots (Skorupinska-Tudek et al. 2003).

A unique feature of polyisoprenoids is their occurrence in the tissues as mixtures of homologues. Prenol-11, bactoprenol typical for bacteria, and all-*trans*-Prenol-9 are the best known exceptions accumulated as single homologues. Dolichol families are quite "small" (6–8 dolichols accumulated in the tissue). Dolichol chain-lengths are rather homogenous in nature – the dominant Dol consists of 16 isoprene units (i.e., in the yeast *Saccharomyces cerevisiae* and in plant roots), 18 i.u. (mice and rat tissues), 19 i.u. (human), and 21 i.u. (second less abundant yeast family). In contrast, plant polyprenol families found in green tissues are really diverse (from 5 to more than 130 polyprenols, with dominant polyprenols from Pren-7 to Pren-28), and their composition can be considered as a species-specific chemotaxonomic marker (Swiezewska and Danikiewicz 2005).

21.2 Biosynthesis of Polyprenols and Dolichols in Plants

Recently, the origin of isopentenyl diphosphate used for construction of polyisoprenoid alcohols in plants has been studied in detail. Incorporation experiments performed with plant roots (where dolichols are the dominant form) revealed that both the MVA and the MEP pathways served as the source of IPP molecules, integrated into the polyisoprenoid hydrocarbon skeleton. According to the model derived from this study, the biosynthesis of dolichols starts in plastids with IPP of mixed origin (MEP and MVA), and oligoprenyl diphosphates thus formed are exported to the cytoplasm where a few α-terminal isoprene units of solely MVA origin are used for the last steps of elongation and termination of the dolichol molecule (Skorupinska-Tudek et al. 2008a). Consequently, this model predicts a constitutive exchange of intermediates between cellular compartments – a more or less unidirectional flow of IPP from cytoplasm to plastids and of oligoprenyl diphosphates from plastids to the cytoplasm. Whether the biosynthesis of α-unsaturated polyisoprenoid alcohols in photosynthetic tissue is also spatially organized in a similar manner requires further experiments.

Several steps of this model remain elusive, e.g., the mechanism of the intracellular transport of intermediates and the identity of the prenyltransferases involved. Enzymes responsible for the head-to-tail condensations of successive IPPs leading to the formation of polyisoprenoid chains in plants, i.e., the putative plastidial farnesyl diphosphate synthase and *cis*-prenyltransferases (CPT), await their characterization. A few genes encoding CTP have been cloned in plants. The Arabidopsis genome contains a family of nine putative genes with homology to yeast CPTs (*RER2* and *SRT1*) (GenBank); however, only one of them, *ACTP1*, was characterized at the molecular level (Cunillera et al. 2000; Oh et al. 2000). Two cDNAs encoding CPT from *Hevea brasiliensis* (HRT1 and HRT2) have also been reported (Asawatreratanakul et al. 2003). Very recently,

the Nogo-B receptor has been described as an essential component of the CPT machinery necessary for dolichol biosynthesis and protein *N*-glycosylation in mammalian and yeast (NUS1) cells (Harrison et al. 2011). A plant orthologue of Nogo-BR has not been identified so far.

21.3 Function of Polyprenols and Dolichols

All eukaryotic cells studied so far contain polyisoprenoid alcohols. Polyisoprenoids are accumulated as free alcohols and/or esters with carboxylic acids, while a fraction (usually a small portion) is also found in the form of phosphates; for dolichols, conjugates with sugars were also reported (Hemming 1985). The content of polyisoprenoid alcohols is highly increased in the tissues during the life span: in senescing plant leaves, a 20-fold increase has been noted, and in the richest plant sources (photosynthetic tissue), the concentration of polyprenols is up to 5% of dry mass (Swiezewska et al. 1994). In mammalian tissues, a 100-fold increase in human brain has been observed, and the highest content reaching mg quantities per g of wet weight was found in endocrine tissues (in pituitary glands, the amount of dolichols is equal to that of phospholipids) (Chojnacki and Dallner 1988).

Besides the increased content of polyisoprenoids related to aging, several external factors have been shown to further increase free polyisoprenoid concentration in plant tissue. Significant light-stimulated accumulation of polyisoprenoid alcohols in the leaves has been reported (Bajda et al. 2005). Recently, viral infection (tobacco mosaic virus) has been shown to considerably induce the accumulation of solanesol (all-*trans*-Pren-9) and polyprenols in tobacco leaves; virus-inoculated leaves contained a 2.5- and 7-fold higher concentration of polyprenols and solanesol, respectively, and a similarly increased concentration of both types of polyisoprenoids was measured in leaves located above the site of infection (systemic leaves) (Bajda et al. 2009). This observation indicates the possible role of polyisoprenoids in plant defense against pathogens, both locally and at a systemic level; however, the underlying mechanism remains elusive. Two possibilities are currently taken into consideration. Firstly, polyisoprenoid alcohols modulate the biophysical properties of biological membranes. This statement is based on the results of *in vitro* experiments where polyisoprenoids were shown to increase the fluidity and permeability of model membranes and to modulate the surface curvature of membranes by formation of fluid microdomains (Valtersson et al. 1985; Janas et al. 2000; Ciepichal et al. 2011). Increased stress tolerance in plants has been correlated with increased membrane fluidity, and this property is most often attributed to increased unsaturation of fatty acids (Wallis and Browse 2002). It seems plausible to assume that polyisoprenoids work in concert with polyunsaturated fatty acids and also exert their bilayer-fluidizing effect *in vivo*. The influence of α-*cis*- and α-*trans*-polyprenols on the structure and properties of model membranes was investigated, from which it was inferred that the *cis*/*trans* isomerization of the α-residue of polyisoprenoid molecules might constitute some mechanism responsible for modulation of cellular membrane permeability (Ciepichal et al. 2011). The concomitant occurrence of alloprenols and ficaprenols in plant tissues is a strong argument into this direction (Ciepichal et al. 2011). Secondly, the putative role of polyisoprenoids as scavengers of reactive oxygen spices in the membranes should also be discussed. Several reports suggest that in plants, volatile isoprenoids confer additional protection in cooperation with carotenes and tocopherols or serve as an alternative defensive mechanism when other well-conserved mechanisms are not efficient enough against oxidative stress (Peñuelas and Munné-Bosch 2005). Moreover, direct antioxidant properties of isoprene and other monoterpenes have been suggested (Loreto et al. 2004). Similarly, a role of dolichol in the antioxidant defense in mammalian cells has been proposed (Bergamini et al. 2004).

Worth noting are the results that were obtained by phenotypical analysis of yeast mutants devoid

of one of the two CPT encoding genes. The involvement of polyisoprenoids in intracellular traffic of proteins was suggested (Sato et al. 1999). Later, dolichols were considered as being essential for anterograde vesicle trafficking (Belgareh-Touze et al. 2003). Very recently, an impairment of dolichol phosphorylation has been recognized as a cause of a new inherited human disorder, and severely diminished protein glycosylation was considered as a major reason of metabolic dysfunctions, whereas protein prenylation had not been analyzed (Kranz et al. 2007). Most recently, the new type of the congenital disorder of glycosylation (CDG) has been attributed to the mutation in a human gene *SRD5A3* identified as necessary for the reduction of the α-isoprene unit of polyprenols to form dolichols (Cantagrel et al. 2010). This CDG type 1 severely disrupts infant eye and brain development; supplementation of the diet with dolichol has been suggested as a potential treatment for this syndrome (editorial comment in American Journal of Medical Genetics A 2010 Oct;152A).

In human brain, dolichol is increased in lysosomal storage disorders, including mucopolysaccharidosis and neuronal ceroid lipofuscinosis (Sakakihara et al. 1994), in liver cancer and preneoplastic noduli (Olsson et al. 1991, 1995), and in regenerating liver (Trentalance 1994). Several xenobiotics are known to induce dolichol accumulation in mammalian liver (Chojnacki and Dallner 1988), but somehow contradictory in this context was the observation of a decrease of dolichol content in rat hepatocytes upon carbon tetrachloride treatment (Parentini et al. 2003).

21.4 Functions of Polyprenyl and Dolichyl Phosphates

The well-documented function of polyisoprenoid diphosphates is their role as cofactors of protein glycosylation in eukaryotic and prokaryotic cells. In mammalian and yeast systems, dolichyl phosphates function as cofactors in the biosynthesis of *N*- and *O*-glycoproteins and GPI-anchor (Burda and Aebi 1999; Samuelson et al. 2005). Also in the plant system, dolichyl rather than polyprenyl phosphates are thought to serve as lipid carriers in this process (Lehle and Tanner 1983; Kaushal and Elbein 1989; Wilson 2002). In prokaryote, prenyl (bactoprenyl) phosphate has been proved to also act as a cofactor of peptidoglycan biosynthesis (Shibaev 1986).

Since the discovery of polyisoprenylated proteins, the putative role of polyisoprenoid phosphates as donors of the polyprenyl group has been discussed. This phenomenon was observed for the first time in rat kidney (Bruenger and Rilling 1986), and later was characterized in rat liver (Thelin et al. 1991). Further evidence for protein dolichylation in rat was the mass spectrometry identification of dolichol (Hjertman et al. 1997) or short-chain (5 and 6 isoprenoid units) polyprenols (Parmryd and Dallner 1999) cleaved from covalently linked protein–lipid adducts. Studies on prenylation of proteins in plants were initiated by identification of farnesylated and geranylgeranylated proteins in tobacco suspension cells and *Atriplex nummularia* (Randall et al. 1993; Zhu et al. 1993) and in parallel in spinach (Swiezewska et al. 1993; Shipton et al. 1995). In the latter case, analysis of isoprenoid groups cleaved from lipid-modified proteins showed that phytol and a family of polyprenols were covalently linked to the proteins besides farnesol and geranylgeraniol. Initially, identification of these isoprenoids was based on chromatographic co-elution of standards with tritiated hydrophobic products released by hydrolytic cleavage from proteins obtained after metabolic labeling with [^{3}H]mevalonate. Since different mixtures of isoprenoid products were cleaved from [^{3}H]-labeled proteins by methyl iodide (mainly farnesol and geranylgeraniol) and alkali (mainly phytol and long-chain polyisoprenoids); a different nature of the chemical linkages between isoprenoids and peptides was postulated in these cases (thioether and ester for the former and latter compounds, respectively). In line with the ester type of the chemical bond linking proteins and polyprenols was the recovery of a fraction of polyprenols in a polar lipid fraction. Later, the structure of the bound phytol was confirmed by GC–MS (Parmryd et al. 1999). Structural analysis of polyisoprenoids covalently linked to proteins in Arabidopsis using

HPLC/MS was performed later (Gutkowska et al. 2004). A family of polyprenols (Pren-9 and Pren-11 with Pren-10 dominating) together with dolichols (Dol-15–17 with Dol-16 dominating) were identified by mass spectrometry analysis of polyprenols released from native polyprenylated proteins, while the same spectrum of [^{3}H]isoprenoids released from metabolically ([^{3}H]mevalonate) labeled proteins was recorded by HPLC/radiometric detection. Use of other metabolic precursors ([^{3}H]farnesol and [^{3}H]geranylgeraniol) confirmed the occurrence of several proteins metabolically labeled with these precursors. A brief fractionation procedure revealed that a significant portion of these proteins was recovered from the light vesicles/cytoplasmic fraction.

The role of plant proteins modified by farnesyl or geranylgeranyl groups has been summarized in several reviews (Nambara and McCourt 1999; Rodríguez-Concepción et al. 1999; Yalovsky et al. 1999; Crowell 2000; Galichet and Gruissem 2003). Some recent studies describing the functions of farnesylated and geranylgeranylated proteins are mentioned below. Farnesylated and geranylgeranylated proteins were shown to be involved in regulation of meristem growth since mutants identified in PLURIPETALA (encodes the α-subunit shared between protein farnesyltransferase and protein geranylgeranyltransferase I) were found to have a spectacularly increased meristem and increased floral organ number (Running et al. 2004). Downregulation of protein farnesylation in Arabidopsis, through downregulation of either the α- or β-subunit of farnesyltransferase, enhances the plant's response to ABA and drought tolerance (Wang et al. 2005). Farnesylation status of a nucleosome assembly protein 1 (AtNAP1;1) regulates leaf cell proliferation vs. cell expansion during Arabidopsis leaf development (Galichet and Gruissem 2006). Geranylgeranylated AtRab7 protein was shown to control the plant response to salt and osmotic stress through regulation of intracellular vesicle trafficking (Mazel et al. 2004). The γ subunits of heterotrimeric G proteins, AGG1 and AGG2, required prenylation for their activity, and both proteins can be prenylated by either geranylgeranyltransferase I or farnesyl protein transferase (Zeng et al. 2007).

So far, the peptide moiety of any endogenous polyprenyl- or dolichyl-modified proteins has not been identified. It could be only speculated that the long hydrophobic tail of polyisoprenylated proteins is required for tight association of proteins with membranes.

Interestingly, the MEP-derived IPPs were shown to be built into the isoprenoid groups utilized for covalent modification of proteins by application of [^{14}C]deoxyxylulose. According to the mobility of [^{14}C]proteins labeled from this precursor on SDS-PAGE, prenyl groups of small G proteins were derived from the MEP pathway. This observation was independent of the inhibition of the MVA pathway by mevinolin; however, the precise structure of isoprenoid moiety has not been confirmed yet (Hemmerlin et al. 2003). This problem was somewhat overcome when tobacco BY-2 cells were stably transformed with a dexamethasone-inducible gene coding for a GFP fused with a carboxy-terminal polybasic domain from rice calmodulin CaM61, bearing a geranylgeranylation motif. Re-isolation of the plasma membrane-bound, covalently modified protein, followed by digestion by a specific protease and HPLC-MS/MS analysis of peptides, led to the identification of a geranylgeranylated peptide of the predicted mass and sequence (Gerber et al. 2009). In the same study, it was demonstrated that nearly exclusively the plastidial MEP pathway provided the substrate for cytoplasmic protein geranylgeranylation under the conditions applied, i.e., in the presence of pathway-specific inhibitors like mevinolin or fosmidomycin (Gerber et al. 2009).

In conclusion, it should be underlined that the biological role of polyisoprenoids is still far from being clear. The general conclusion based on recent data suggests that polyprenols and dolichols, so far known as markers of aging, might be perhaps also considered as markers of stress. The elucidation of the putative role of polyisoprenylated proteins, be it those that form chemically stable thioether bonds with isoprenyl residues or those that form easily hydrolyzable thioester bonds, still requires more experimental effort and awaits explanation. The same holds true as to the identification and intracellular localization of putative protein isoprenyl

transferases that catalyze the thioesterification of target proteins and the peptide motives being involved in recognition.

Acknowledgments We are deeply grateful to Professor Thomas Bach for his stimulation and inestimable help during the preparation of this chapter. Studies performed in our laboratory described here were partially financed by the Ministry of Science and Higher Education grants No PBZ/MEiN/01/2006/45 and MNiSW NN303 311837 and by the grant funded by the Polish National Cohesion Strategy Innovative Economy UDA-POIG 01.03.01-14-036/09.

References

Asawatreratanakul K, Zhang YW, Wititsuwannakul D et al (2003) Molecular cloning, expression and characterization of cDNA encoding *cis*-prenyltransferases from *Hevea brasiliensis*. A key factor participating in natural rubber biosynthesis. Eur J Biochem 270: 4671–4680

Bajda A, Chojnacki T, Hertel J et al (2005) Light conditions alter accumulation of long chain polyprenols in leaves of trees and shrubs throughout the vegetation season. Acta Biochim Pol 52:233–241

Bajda A, Konopka-Postupolska D, Krzymowska M et al (2009) Role of polyisoprenoids in tobacco resistance against biotic stresses. Physiol Plant 135:351–364

Belgareh-Touze N, Corral-Debrinski M, Launhardt H et al (2003) Yeast functional analysis: identification of two essential genes involved in ER to Golgi trafficking. Traffic 4:607–617

Bergamini E, Bizzarri R, Cavallini G et al (2004) Ageing and oxidative stress: a role for dolichol in the antioxidant machinery of cell membranes? J Alzheimers Dis 6:129–135

Bruenger E, Rilling HC (1986) Prenylated protein from kidney. Biochem Biophys Res Commun 139:209–214

Burda P, Aebi M (1999) The dolichol pathway of *N*-linked glycosylation. Biochim Biophys Acta 1426:239–257

Cantagrel V, Lefeber DJ, Ng BG et al (2010) SRD5A3 is required for converting polyprenol to dolichol and is mutated in congenital glycosylation disorders. Cell 142:203–217

Chojnacki T, Dallner G (1988) The biological role of dolichol. Biochem J 251:1–7

Ciepichal E, Jemiola-Rzeminska M, Hertel J, Swiezewska E, Strzalka K (2011) Configuration of polyisoprenoids affects the permeability and thermotropic properties of phospholipids/polyisoprenoid model membranes. Chem Phys Lipids 164:300–306

Crowell DN (2000) Functional implications of protein isoprenylation in plants. Prog Lipid Res 39:393–408

Cunillera N, Arró M, Fores O, Manzano D, Ferrer A (2000) Characterization of dehydrodolichyl diphosphate synthase of *Arabidopsis thaliana*, a key enzyme in dolichol biosynthesis. FEBS Lett 477:170–174

Galichet A, Gruissem W (2003) Protein farnesylation in plants – conserved mechanisms but different targets. Curr Opin Plant Biol 6:530–535

Galichet A, Gruissem W (2006) Developmentally controlled farnesylation modulates AtNAP1;1 function in cell proliferation and cell expansion during Arabidopsis leaf development. Plant Physiol 142:1412–1426

Gerber E, Hemmerlin A, Hartmann M et al (2009) The plastidial 2-*C*-methyl-D-erythritol 4-phosphate pathway provides the isoprenyl moiety for protein geranylgeranylation in tobacco BY-2 cells. Plant Cell 21:285–300

Gutkowska M, Bienkowski T, Hung VS et al (2004) Proteins are polyisoprenylated in *A. thaliana*. Biochem Biophys Res Commun 322:998–1004

Harrison KD, Park EJ, Gao N et al (2011) Nogo-B receptor is necessary for cellular dolichol biosynthesis and protein *N*-glycosylation. EMBO J 30:2490–2500

Hemmerlin A, Hoeffler JF, Meyer O et al (2003) Cross-talk between the cytosolic mevalonate and the plastidial methylerythritol phosphate pathways in tobacco bright yellow-2 cells. J Biol Chem 278:26666–26676

Hemming FW (1985) Glycosyl phosphopolyprenols. In: Wiegandt L (ed) Glycolipids. Elsevier Science, Amsterdam

Hjertman M, Wejde J, Dricu A et al (1997) Evidence for protein dolichylation. FEBS Lett 416:235–238

Janas T, Walinska K, Chojnacki T et al (2000) Modulation of properties of phospholipid membranes by the long-chain polyprenol (C(160)). Chem Phys Lipids 106:31–40

Kaushal GP, Elbein AD (1989) Glycoprotein processing enzymes of plants. Methods Enzymol 179:452–475

Kranz C, Jungeblut C, Denecke J et al (2007) A defect in dolichol phosphate biosynthesis causes a new inherited disorder with death in early infancy. Am J Hum Genet 80:433–440

Lehle L, Tanner W (1983) Polyprenol-linked sugars and glycoprotein synthesis in plants. Biochem Soc Trans 11:568–574

Loreto F, Pinelli P, Manes F, Kollist H (2004) Impact of ozone on monoterpene emissions and evidence for an isoprene-like antioxidant action of monoterpenes emitted by *Quercus ilex* leaves. Tree Physiol 24:361–367

Mazel A, Leshem Y, Tiwari BS, Levine A (2004) Induction of salt and osmotic stress tolerance by overexpression of an intracellular vesicle trafficking protein AtRab7 (AtRabG3e). Plant Physiol 134:118–128

Nambara E, McCourt P (1999) Protein farnesylation in plants: a greasy tale. Curr Opin Plant Biol 2:388–392

Oh SK, Han KH, Ryu SB, Kang H (2000) Molecular cloning, expression, and functional analysis of a *cis*-prenyltransferase from *Arabidopsis thaliana*. Implications in rubber biosynthesis. J Biol Chem 275: 18482–18488

Olsson JM, Eriksson LC, Dallner G (1991) Lipid compositions of intracellular membranes isolated from rat liver nodules in Wistar rats. Cancer Res 51: 3774–3780

Olsson JM, Schedin S, Teclebrhan H et al (1995) Enzymes of the mevalonate pathway in rat liver nodules induced

by 2-acetylaminofluorene treatment. Carcinogenesis 16:599–605

Parentini I, Bergamini E, Cecchi L et al (2003) The effect of carbon tetrachloride and ultraviolet radiation on dolichol levels in liver cells isolated from 3- and 24-month-old male Sprague–Dawley rats. Biogerontology 4:365–370

Parmryd I, Dallner G (1999) In vivo prenylation of rat proteins: modification of proteins with penta- and hexaprenyl groups. Arch Biochem Biophys 364: 153–160

Parmryd I, Andersson B, Dallner G (1999) Protein prenylation in spinach chloroplasts. Proc Natl Acad Sci USA 96:10074–10079

Peñuelas J, Munné-Bosch S (2005) Isoprenoids: an evolutionary pool for photoprotection. Trends Plant Sci 10:166–169

Randall SK, Marshall MS, Crowell DN (1993) Protein isoprenylation in suspension-cultured tobacco cells. Plant Cell 5:433–442

Rodríguez-Concepción M, Yalovsky S, Gruissem W (1999) Protein prenylation in plants: old friends and new targets. Plant Mol Biol 39:865–870

Running MP, Lavy M, Sternberg H et al (2004) Enlarged meristems and delayed growth in plp mutants result from lack of CaaX prenyltransferases. Proc Natl Acad Sci USA 101:7815–7820

Sakakihara Y, Imabayashi T, Suzuki Y, Kamoshita S (1994) Elevated levels of dolichol in the brains of mucopolysaccharidosis and related disorders. Mol Chem Neuropathol 22:97–102

Samuelson J, Banerjee S, Magnelli P et al (2005) The diversity of dolichol-linked precursors to Asn-linked glycans likely results from secondary loss of sets of glycosyltransferases. Proc Natl Acad Sci USA 102:1548–1553

Sato M, Sato K, Nishikawa S, Hirata A et al (1999) The yeast *RER2* gene, identified by endoplasmic reticulum protein localization mutations, encodes *cis*-prenyltransferase, a key enzyme in dolichol synthesis. Mol Cell Biol 19:471–483

Shibaev VN (1986) Biosynthesis of bacterial polysaccharide chains composed of repeating units. Adv Carbohydr Chem Biochem 44:277–339

Shipton CA, Parmryd I, Swiezewska E, Andersson B, Dallner G (1995) Isoprenylation of plant proteins in vivo. J Biol Chem 270:566–572

Skorupinska-Tudek K, Bienkowski T, Olszowska O et al (2003) Divergent pattern of polyprenols and dolichols in different organs in *Coluria geoides*. Lipids 38: 981–991

Skorupinska-Tudek K, Poznanski J, Wojcik J et al (2008a) Contribution of the mevalonate and methylerythritol phosphate pathways to the biosynthesis of dolichols in plants. J Biol Chem 283:21024–21035

Skorupinska-Tudek K, Wojcik J, Swiezewska E (2008b) Polyisoprenoid alcohols – recent results of structural studies. Chem Rec 8:33–45

Surmacz L, Swiezewska E (2011) Polyisoprenoids – secondary metabolites or physiologically important superlipids? Biochem Biophys Res Commun 407: 627–632

Swiezewska E, Danikiewicz W (2005) Polyisoprenoids: structure, biosynthesis and function. Prog Lipid Res 44:235–258

Swiezewska E, Thelin A, Dallner G, Andersson B, Ernster L (1993) Occurrence of prenylated proteins in plant cells. Biochem Biophys Res Commun 192:161–166

Swiezewska E, Sasak W, Mankowski T, Jankowski WJ, Vogtman T, Krajewska I, Hertel J, Skoczylas E, Chojnacki T (1994) The search for plant polyprenols. Acta Biochim Pol 41:221–260

Thelin A, Low P, Chojnacki T, Dallner G (1991) Covalent binding of dolichyl phosphate to proteins in rat liver. Eur J Biochem 195:755–761

Trentalance A (1994) Dolichols and proliferating systems. Acta Biochim Pol 41:339–344

Valtersson C, van Duijn G, Verkleij AJ et al (1985) The influence of dolichol, dolichyl esters, and dolichyl phosphate on phospholipid polymorphism and fluidity in model membranes. J Biol Chem 260:2742–2751

Wallis JG, Browse J (2002) Mutants of Arabidopsis reveal many roles for membrane lipids. Prog Lipid Res 41:254–278

Wang Y, Ying J, Kuzma M et al (2005) Molecular tailoring of farnesylation for plant drought tolerance and yield protection. Plant J 43:413–424

Wilson IB (2002) Glycosylation of proteins in plants and invertebrates. Curr Opin Struct Biol 12:569–577

Yalovsky S, Rodriguez-Concepción M, Gruissem W (1999) Lipid modifications of proteins – slipping in and out of membranes. Trends Plant Sci 4:439–445

Zeng Q, Wang X, Running MP (2007) Dual lipid modification of Arabidopsis G γ-subunits is required for efficient plasma membrane targeting. Plant Physiol 143:1119–1131

Zhu JK, Bressan RA, Hasegawa PM (1993) Isoprenylation of the plant molecular chaperone ANJ1 facilitates membrane association and function at high temperature. Proc Natl Acad Sci USA 90:8557–8561

22

Regulation of 3-Hydroxy-3-Methylglutaryl-CoA Synthase and 3-Hydroxy-3-Methylglutaryl-CoA Reductase and Rubber Biosynthesis of *Hevea brasiliensis* (B.H.K.) Mull. Arg

Pluang Suwanmanee, Nualpun Sirinupong, and Wallie Suvachittanont

Abstract

It is rather well established that rubber biosynthesis in rubber trees (*Hevea brasiliensis*) takes place in laticifers and is dependent on mevalonate (MVA). 3-Hydroxy-3-methylglutaryl coenzyme A reductase (HMGR, EC 1.1.1.34) has been shown to catalyze a rate-limiting step in this pathway. However, our studies demonstrated that both 3-hydroxy-3-methylglutaryl coenzyme A synthase (HMGS, EC 2.3.3.10) and HMGR are essential enzymes involved in rubber biosynthesis. In this chapter, we report on the current information as to the regulation of both HMGS and HMGR and their effect on rubber biosynthesis in *H. brasiliensis*. *Hevea* HMGS is encoded by a small gene family consisting of *hmgs*-1 and *hmgs*-2. The available information concerning the nature of the gene(s) encoding HMGS is also summarized. Enzyme activity and mRNA transcripts were mainly found in tissues with more laticifers, the sites of rubber biosynthesis. In latex of the high-yielding rubber clone, *hmgs* mRNA levels and enzyme activity were significantly higher than in the latex of the low-yield variety. Furthermore, the mRNA transcripts and enzyme activity in latex

P. Suwanmanee (✉)
Biology Department, Thaksin University,
140, Moo 4, Tambon Khoa-Roob-Chang,
Muang District, Songkhla 90000, Thailand
e-mail: pluang@tsu.ac.th

N. Sirinupong
Biochemistry and Molecular Biology,
Wayne State University School of Medicine,
540 E. Canfield Avenue, Detroit, MI 48201, USA

W. Suvachittanont
Biochemistry Department, Prince of Songkla University,
Hat Yai, Songkhla 90112, Thailand

T.J. Bach and M. Rohmer (eds.), *Isoprenoid Synthesis in Plants and Microorganisms: New Concepts and Experimental Approaches*, DOI 10.1007/978-1-4614-4063-5_22,

were higher at night than daytime, which is reflected by the dry rubber content. Ethephon treatment, which is known to increase the latex yield, had a direct effect on both *hmgs* mRNA transcripts and enzyme activity. The *hmgs* mRNA levels and dried rubber content per tapping from intraclone rubber trees were also shown to be highly correlated. HMG-CoA acts as a substrate for HMGR to form mevalonate, which is further converted to isoprenoid compounds as well as natural rubber. Three genes are known to encode HMGR in *H. brasiliensis*, namely, *hmgr-1*, *hmgr-2,* and *hmgr-3*, and *hmgr-1* is likely to be involved in rubber biosynthesis. The *hmgr-1* mRNA level was well correlated with dried rubber content, similar to those observed in the case of *hmgs* gene expression.

These findings clearly indicated that both HMGS and HMGR enzyme activities are involved in early steps of rubber biosynthesis in *H. brasiliensis* at the level of their gene expression. The two enzymes possibly function in concert in response to the supply of substrate for rubber biosynthesis, similar to the synthesis of cholesterol in animals.

Keywords

HMG-CoA reductase • HMC-CoA synthase • Acetoacetyl-CoA • Bacterial ACP synthase III (family) • Rubber biosynthesis • *Hevea brasiliensis* • *cis*-1,4-Polyisoprene • Laticifers • Latex C-serum • High rubber yield clones

22.1 Introduction

H. brasiliensis, a perennial tropical tree originating from South America, is now mostly cultivated in Southeast Asia, especially in Thailand, for the production of natural rubber. The rubber plantation is shown in Fig. 22.1a. The unique isoprenoid compound "*cis*-1,4 polyisoprene" present in latex is the raw material for the world's rubber. Natural rubber is highly valued because no synthetic substitute has comparable elasticity, resilience, and resistance to high temperature. The economic importance of natural rubber has led to intensive investigations on the biochemical aspects of rubber biosynthesis. From that, it is well established that *cis*-1,4-polyisoprene is synthesized on particles that are suspended in the cytosol of specialized cells called laticifers (Hepper and Audley 1969). After tapping, the severed laticifers expel latex (Fig. 22.1b), which contains 30–50% (w/w) of *cis*-1,4-polyisoprene; usual cell organelles; two characteristic bodies, namely, the lutoid particle and the Frey-Wyssling complex; and C-serum as shown in Fig. 22.1c. The pathway leading to natural rubber biosynthesis can be divided into two parts: first, the synthesis of isopentenyl diphosphate (IPP) and dimethylallyl diphosphate (DMAPP) and, second, the polymerization of IPP into allylic diphosphate substrates such as farnesyl diphosphate, geranylgeranyl diphosphate, etc. to form a high molecular weight *cis*-1,4-polyisoprene (Fig. 22.2) (for review, see Steinbüchel 2003). The pathway for synthesis of IPP and DMAPP proceeds by two independent synthetic pathways, the well-known "classical" mevalonic acid (MVA) and the newly discovered 2-*C*-methyl-D-erythritol 4-phosphate (MEP) pathways using pyruvate and glyceraldehyde-3-phosphate to form 1-deoxy-D-xylulose 5-phosphate which is further converted to MEP (Lichtenthaler et al. 1997a, b see also elsewhere in this volume). The MVA pathway is localized in the cytoplasm and is mainly responsible for the synthesis of sesquiterpenes, steroids, and ubiquinones, while the MEP pathway, occurring in the plastids, is mainly involved in the formation of isoprene, diterpenes, carotenoids, chlorophylls,

Fig. 22.1 A plantation of rubber trees (**a**), latex collection (**b**), and four fractions of fresh latex after centrifugal fractionation in a prechilled rotor at 30,000 × g (average) for 45 min (**c**)

phylloquinone, tocopherols, and plastoquinones. In *H. brasiliensis*, genes encoding the enzymes involved in early steps of isoprenoid biosynthesis via MEP exist (Seetang-Nun et al. 2008). There is strong compartmental separation between the MVA and MEP pathways in higher plants: plants lacking the first enzyme of the MEP pathway do not survive (Mandel et al. 1996), but under specific conditions, some cross-talk between the pathways seems to exist (cf. Kasahara et al. 2002; Hemmerlin et al. 2003; Laule et al. 2003) The precursor to rubber biosynthesis, IPP, is believed to be mainly formed via the MVA pathway, similar to cholesterol biosynthesis in animals. In mammals, cholesterol synthesis has been shown to be coordinately regulated by HMGS and HMGR activity, and the two enzymes are under feedback regulation by cholesterol (Goldstein and Brown 1990). Both HMGS and HMGR activities are also present in rubber latex (Lynen 1969). Hepper and Audley (1969) demonstrated that HMG-CoA was efficiently incorporated into rubber upon incubation with *H. brasiliensis* latex. The conversion of HMG-CoA into mevalonate by HMGR is apparently a rate-limiting step in rubber synthesis (Lynen 1969; Hepper and Audley 1969). Later, more detailed studies have been focused on the further characterization of

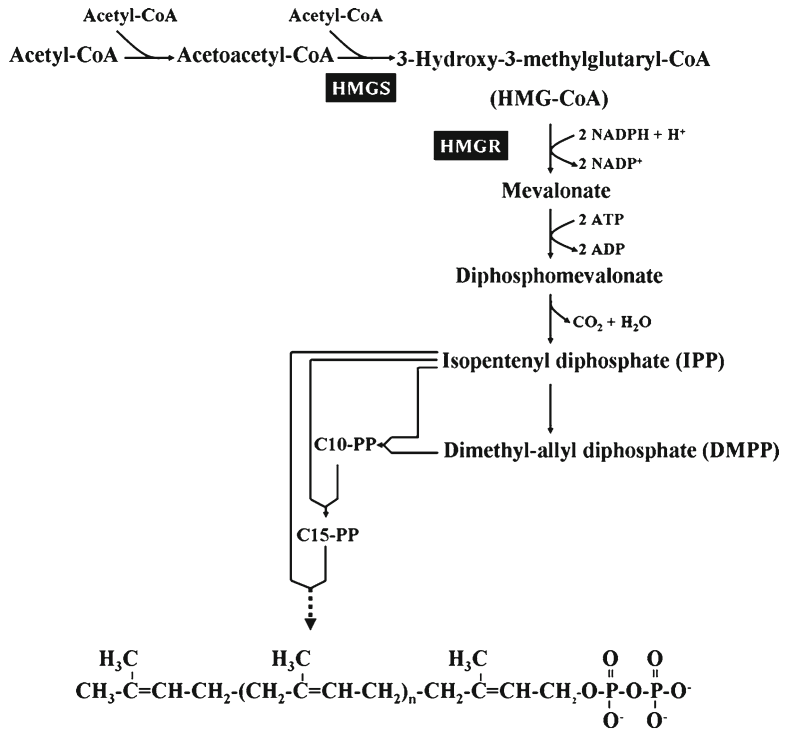

Fig. 22.2 Natural rubber biosynthesis pathway in *Hevea brasiliensis* (Adapted from Lynen 1969)

HMGR in *H. brasiliensis*, which for instance led to the determination of some kinetic properties (Sipat 1982), the discovery of a diurnal cycle in the activity of HMGR in latex (Wititsuwannakul 1986), and purification of HMGR from the latex of *H. brasiliensis* (Wititsuwannakul et al. 1990), closely following a protocol that had been used for membrane-bound radish HMGR (Bach et al. 1986). From the beginning, in analogy to the situation in yeast and animal cells, the enzyme was thought as catalyzing a bottleneck step and thus, controlling the synthesis of rubber in *H. brasiliensis*. It followed the characterization of genes encoding HMGR in *H. brasiliensis* (Chye et al. 1991, 1992) and heterologous expression of the *H. brasiliensis hmgr-1* gene in tobacco (Schaller et al. 1995). However, at that time, only few attempts had been directed so far to increase the biosynthesis of HMG-CoA via the activity of HMGS in rubber latex. Therefore, it became interesting to study HMGS- and HMGR-encoding genes and enzymes in parallel and their involvement in rubber biosynthesis in *H. brasiliensis*. This chapter summarizes current information on the regulation of HMGS and HMGR and the expression of the two genes in rubber biosynthesis from *H. brasiliensis*.

22.2 Properties of *H. brasiliensis* HMGS and HMGR Enzymes

3-Hydroxy-3-methylglutaryl coenzyme A synthase (HMGS, formerly EC 4.1.3.5, now EC 2.3.3.10) catalyzes the condensation of acetyl-CoA and acetoacetyl-CoA to form 3-hydroxy-3-methylglutaryl coenzyme A (HMG-CoA). Two forms of HMGS have been reported to exist in mammals, one in the mitochondria and one in the cytoplasm (Clinkenbeard et al. 1975a, b). In rats and humans, these isoenzymes are encoded by two different genes (Ayté et al. 1990a, b). This enzyme is also present in bacteria (Sutherlin et al. 2002) and in plants (Lynen 1969; Alam et al.

1991; Bach et al. 1994; Van der Heijden et al. 1994b; Alex et al. 2000). The HMG-CoA produced acts as a substrate for HMGR to form mevalonate, which is further converted to cytoplasmic isoprenoid compounds, such as growth regulators like cytokinins and brassinosteroids, to phytoalexins, and to natural rubber. HMG-CoA is also an intermediate in the degradation of the branched-chain amino acid leucine. HMGS activity has been first demonstrated to be present in *H. brasiliensis* latex by Lynen (1969). In the latex, the HMGS catalyzes the utilization of acetyl-CoA to form isoprene units in a similar way like cholesterol synthesis in mammalian systems or ergosterol in yeast. HMGS activity was found mainly in C-serum, which represents the cytosolic fraction of laticiferous cells (Suvachittanont and Wititsuwannakul 1995). It is most likely that the HMGS in C-serum is involved in isoprenoid synthesis (in this case, largely rubber formation). The optimum pH of HMGS in C-serum was found around 8.2 (Suvachittanont and Wititsuwannakul 1995) similar to that of the enzyme from the cytosolic fraction of rat brain (Shah 1982). The Michaelis–Menten kinetics, and apparent K_m, for acetyl-CoA was calculated with 9 mM; it is much higher than the K_m of cytosolic synthase purified from chicken liver (Clinkenbeard et al. 1975b). The addition of 0.1 mM EDTA increased the activity of the enzyme, suggesting that the presence of endogenous cations in the C-serum such as Mg^{2+}, Cd^{2+}, Pb^{2+}, and Fe^{2+} had some inhibitory effect (Suvachittanont and Wititsuwannakul 1995). In respect of these observations, the enzyme in C-serum is similar to the cytosolic synthase in rat brain (Shah 1982) but differs from that in rat liver cytosol, which is activated by Mg^{2+} (Miziorko et al. 1982). When such above-mentioned K_m values are compared to those determined with HMGS1 from *Brassica juncea* (Nagegowda et al. 2004), it becomes evident that enzyme properties seem to be quite species-specific.

That HMGS plays a regulatory role in rubber biosynthesis is evident since the total activity of HMGS and dried rubber content correlated reasonably well (Suvachittanont and Wititsuwannakul 1995). This finding is similar to that observed in the case of HMGR activity and rubber content (Wititsuwannakul 1986). It seems reasonable to assume that the rubber biosynthetic pathway is coordinately regulated by both the activities of HMGS and HMGR. In the case of HMGR, its activity is mostly found in the bottom fraction, which represents the lutoid particles of laticiferous cells. HMGR enzyme from the latex of *H. brasiliensis* was successfully purified by Wititsuwannakul and Suwanmanee (1990). The denatured form of the purified enzyme (HbHMGR) showed a molecular weight of 44,000 and 176,000 Da for the nature form. These values are close to that found for the radish enzyme (Bach et al. 1986). The optimum pH is 7.0 similar to all HMGRs previously examined thus far ranging from 6.5 to 7.7 (Brown and Rodwell 1980). The K_m value of 13 μM with respect to (*S*)-HMG-CoA is higher than that of the enzymes purified from yeast, rat and chicken livers (Rogers et al. 1983), and even from radish (Bach et al. 1986). It is, however, lower than the K_m reported for the HMGR of the crude membrane fraction from the bottom fraction of *Hevea* latex (Sipat 1982) and the cytosolic HMGR of *Parthenium argentatum* leaves (Reddy and Das 1986). The purified HbHMGR activity was shown to be activated by dithiothreitol with the maximum reached at 15 mM, which is similar to the maximum dithiothreitol concentration for the purified HMGR from *P. argentatum* (Reddy and Das 1986).

22.3 Molecular Biology of HMGS

The regulation and expression of the *hmgs* gene(s) involved in the biosynthesis of natural rubber have also been studied. We cloned and characterized a *hmgs* cDNA from latex of *H. brasiliensis*. HbHMGS is encoded by a small gene family comprised of two members, *Hbhmgs-1* (Suwanmanee et al. 2002) and *Hbhmgs-2* (Sirinupong et al. 2005). The full-length *Hbhmgs-1* and *Hbhmgs-2* consist of 1,804 bp and 1,916 bp, respectively. The nucleotide sequence of *Hbhmgs-2* differs from *Hbhmgs-1* at 77 positions. Of all the changes, 44 nucleotides were

silent changes and 33 were missense. As a consequence, HbHMGS-2 differs in 28 amino acids from HbHMGS-1. Like *Hbhmgs-1*, the isolated *Hbhmgs-2* cDNA encodes a cytosolic HMGS because it lacks the N-terminal mitochondrial leader peptide sequence that makes up the first 37 amino acids of the human mitochondrial sequence. The fact that *H. brasiliensis* HMGS is encoded by two *hmgs* genes is also supported by other workers as there are two HMGS in mammals, the mitochondrial and cytosolic isoforms reported by Ayte et al. (1990a). In other plants, up to four *hmgs* cDNAs have been found, for example, in *Brassica juncea*: BjHMGS1 has an amino acid identity of 97%, 96%, and 95% with BjHMGS2, BjHMGS3, and BjHMGS4, respectively. *Bjhmgs1* displays a nucleotide identity with *Bjhmgs2*, *Bjhmgs3*, and *Bjhmgs4* of 85–92% (Alex et al. 2000). Moreover, Montamat et al. (1995) suggested the possibility of a second gene encoding HMGS on the basis of Southern blot analysis of *A. thaliana* DNA. Wegener et al. (1997) detected two putative *Pinus hmgs* mRNAs. Therefore, it appears that there are gene families encoding HMGS in plants, as is often the case for HMGR. This is in line with the fact that *H. brasiliensis* has at least two genes encoding for HMGS as found by Suwanmanee, Suvachittanont, and Fincher (2002).

By a search for all known *hmgs* sequences in the GenBank database by using *Hbhmgs* as query, among others, the amino acid sequences of bacterial ACP synthase III were obtained. Proper multiple alignments obtained after careful "cropping" of the sequences to approximately the same lengths identified all the conserved residues existing in *hmgs* and ACP synthase III (Sirinupong et al. 2005). The plant amino acid sequences reveal the expected high identity to *H. brasiliensis* HMGS. Lower identity occurs with and between animal and bacterial HMGS species and ACP synthase III. A phylogenetic tree shows that *Hbhmgs-1* and *Hbhmgs-2* recently diverged by gene duplication in terms of amino acid replacement. Likewise, the two "condensing enzymes," HMGS and ACP synthase III, have emerged from a common ancestor gene. In the evolutionary lineage, *hmgs* was duplicated to a new gene first in bacteria as is the case for ACP synthase III genes. The *hmgs* sequences remain constant among eukaryotes, *C. elegans* and yeast, and diverged to plants and higher animals. The phylogenetic analysis shows that some of ACP synthases III were localized in the HMGS cluster (Fig. 22.3 and Table 22.1). This finding supports that HMGS belongs to a large protein family comprising other acetyl-CoA condensing enzymes, such as ACP synthase III (Lange et al. 2000). It is surprising that the absolutely conserved residues, Cys117, His247, and Asn326 (the numbers are referred to *H. brasiliensis* HMGS), existing in both enzymes are important amino acids in the catalytic reaction of ACP synthase III. In the case of HMGS, it is suggested that Cys117 and His247 play a role in the catalytic site whereas such a role has not yet been implicated for Asn326. The three conserved residues, Cys117, His247, and Asn326, of several HMGS and the other species of ACP synthase III sequences have recently been demonstrated as the active residues for condensing enzymes (Price et al. 2001). In particular, ACP synthase III, the most divergent member of the condensing enzymes family, has been extensively studied for drug targets at catalytic residues in *M. tuberculosis* ACP synthase III, Cys122, His244, and Asn274 (Scarsdale et al. 2001). Moreover, the acetylation of Cys112 proves that it is clearly defined in the primer binding pocket. Modeling based on a bound CoA molecule suggests a catalytic role for His244 and Asn274 in *Escherichia coli* ACP synthase III (Qiu et al. 1999). The catalytic role of Asn326 in HMGS was firstly demonstrated by our group (Sirinupong et al. 2005). When *H. brasiliensis* HMGS Cys117 and Asn326 were substituted with alanine by site-directed mutagenesis, it was found that the Asn326Ala mutation had a clear negative effect on the catalytic cycle, supporting that an invariant Asn326 is a significant residue for HMGS in the same way as Cys117. Early studies on HMGS present in yeast and chicken mitochondria have established that the catalysis mechanism of the enzyme involves a three-step process: acetylation,

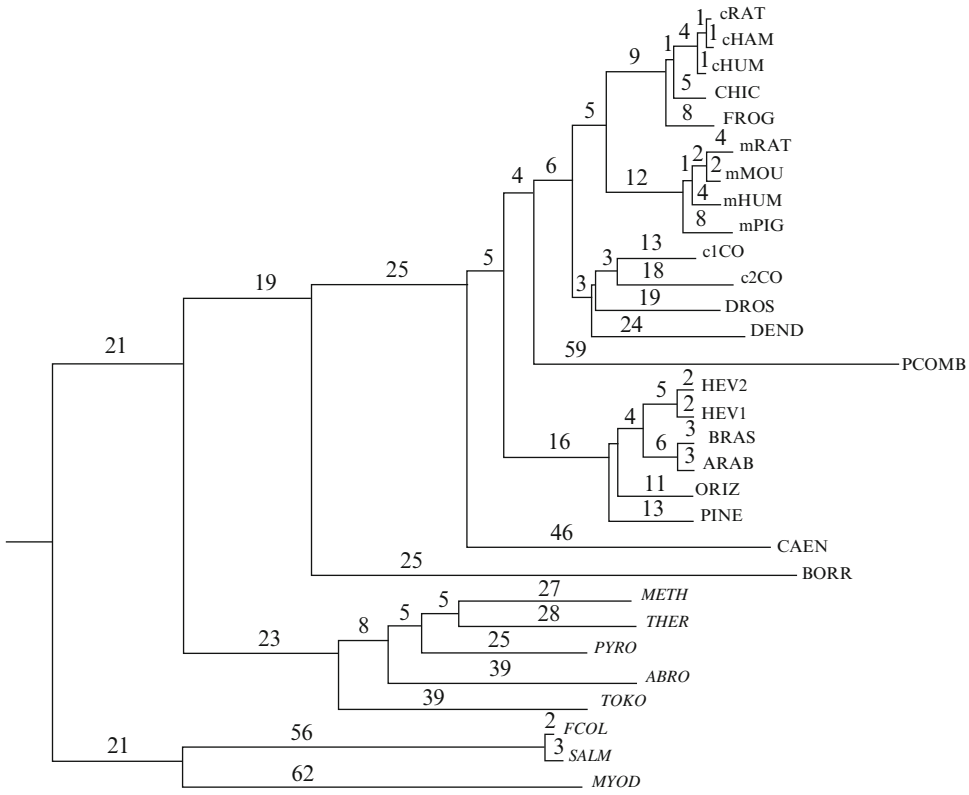

Fig. 22.3 Phylogenetic relationship of ACP synthase III sequences from bacteria (*italics*) and HMGS sequences from mammals, avian, amphibian, insects, yeast, plants, worm, and bacteria. The tree was constructed based on growing methodologies and corresponds to the progressive alignment to determine the branching order of the sequences. *Numbers* indicate branch lengths. Full name species and GenBank accession numbers of the sequences are provided in Table 22.1

condensation, and hydrolysis (Miziorko et al. 1975). Cys129 is required to form the acetyl-S-enzyme intermediate (Misra et al. 1993; Vollmer et al. 1988); this was confirmed by mutagenesis studies on the recombinant avian enzyme. His264 has been implicated in binding the second substrate, acetoacetyl-CoA, by the kinetic characterization of mutants (Misra and Miziorko 1996). Glu95 was proposed to have an additional role in the C–C bond formation upon condensation with the second substrate and also to play a role in the acid/base catalysis (Chun et al. 2000). Recent work in chicken HMGS on the influence of several conserved aromatic residues near the active site indicated that Tyr130, Phe204, or Tyr376 have an effect on the conformation of the covalent acetyl-S-enzyme intermediate (Misra et al. 2003). In addition, an enzyme assay of crude extracts with higher protein concentrations leveled off after peaking on a linear relationship between protein and specific activity similar to the recombinant *B. juncea* HMGS (Alex et al. 2000). This is most likely because of the presence of negatively interfering activities acting on the acetyl-CoA and acetoacetyl-CoA, probably thioesterase that attacks the CoA moiety and thus render the substrate inactive for HMGS (Van der Heijden et al. 1994a, b). The detailed study on heterologously expressed BjHMGS1, also after mutation of other seemingly conserved residues than those mentioned above, led to the discovery of profound variations in the kinetic properties of the enzyme, such as loss of inhibition by its second substrate acetoacetyl-CoA and to a lesser

Table 22.1 Details of the sequences used for phylogenetic tree (accession numbers for the sequence databases accessible through the National Center for Biotechnology Information)

Organism name	Abbreviation	Kingdom	Accession number
Rattus norvegicus (rat)	cRAT	Eukaryote	NP_058964
Cricetulus griseus (Chinese hamster)	cHAM	Eukaryote	P13704
Homo sapiens (human)	cHUM	Eukaryote	NP_002121
Gallus gallus (chicken)	CHIC	Eukaryote	P23228
Xenopus laevis (African clawed frog)	FROG	Eukaryote	AAH42929
Rattus norvegicus (Norway rat)	mRAT	Eukaryote	NP_775117
Mus musculus (house mouse)	mMOU	Eukaryote	NP_032282
Homo sapiens (human)	mHUM	Eukaryote	NP_005509
Sus scrofa (pig)	mPIG	Eukaryote	U90884
Blattella germanica (German cockroach)	c1CO	Eukaryote	P54961
Blattella germanica (German cockroach)	c2CO	Eukaryote	P54870
Drosophila melanogaster (fruit fly)	DROS	Eukaryote	NM_079972
Dendroctonus jeffreyi (Jeffrey pine beetle)	DEND	Eukaryote	AF166002
Schizosaccharomyces pombe (fission yeast)	POMB	Eukaryote	NP_593859
Hevea brasiliensis	HEV2	Eukaryote	AY534617
Hevea brasiliensis	HEV1	Eukaryote	AF396829
Brassica juncea	BRAS	Eukaryote	AAG32924
Arabidopsis thaliana (thale cress)	ARAB	Eukaryote	NM_117251
Oryza sativa (japonica cultivar-group)	ORIZ	Eukaryote	NP_912446
Pinus sylvestris (Scots pine)	PINE	Eukaryote	X96386
Caenorhabditis elegans	CAEN	Eukaryote	NP_504496
Borrelia burgdorferi B31	BORR	Eubacteria	NP_212817
Methanocaldococcus jannaschii DSM 2661	METH	Archaea	NP_248554
Thermoplasma volcanium GSS1	THER	Archaea	BAB59274
Pyrococcus furiosus DSM 3638	PYRO	Archaea	NP_578701
Sulfolobus tokodaii str. 7	TOKO	Archaea	NP_377303
Aeropyrum pernix K1	AERO	Archaea	NP_148228
Escherichia coli O157:H7 str. Sakai	ECOL	Eubacteria	BAB34892
Salmonella typhimurium LT2	SALM	Eubacteria	NP_460163
Mycobacterium tuberculosis H37Rv	MYCO	Eubacteria	CAB08984

extent by its reaction product HMG-CoA (Nagegowda et al. 2004) but even to a higher catalytic efficiency, apparently at the expense of affinity to acetoacetyl-CoA. The crystallization and elucidation of its structure by X-ray analysis confirmed the dimeric nature of BjHMGS1 and showed that all those essential residues that reside quite distantly in the primary sequence of the protein, group around the active site (Pojer et al. 2006).

22.4 Role of HMGS and HMGR in Rubber Biosynthesis

A variety of factors has been demonstrated to affect rubber yield in *H. brasiliensis,* such as variation of clones, tapping time, ethylene stimulation, and latex vessel density. These parameters led us to further investigate the regulation of the *Hbhmgs-1* regarding the point of control of the rubber biosynthesis. When the expression level

of *hmgs-1* mRNA was determined by Northern blot analysis of several tissues of *H. brasiliensis* (clone RRIM 600), it was found that *Hbhmgs-1* mRNA is more abundant in the latex, stem, and petiole than in leaves of rubber seedlings and mature trees. The expression of the *hmgs-1* gene was shown to correlate with the presence of more laticiferous cells in the corresponding tissues. This finding correlates with *hmgr* gene expression: *Hbhmgr-1*, *Hbhmg-2*, and *Hbhmgr-3* are clearly differentially expressed. *Hbhmgr-1,* which predominantly expresses in laticifers and hardly in leaves, is thus believed to be involved in natural rubber (*cis* 1–4 polyisoprene) biosynthesis, as laticifers are the sites for rubber biosynthesis. Therefore, it is likely that the isoenzyme derived from the *Hbhmgs-1* transcript detected in laticiferous cells is involved in forming HMG-CoA as an intermediate in the biosynthesis of rubber. By comparison of clone RRIM 600 (with higher rubber yield) and the wild type from which all clones originate, it was evident that RRIM 600 also shows higher expression of the *Hbhmgs-1* gene, and consequently the enzyme activity in latex from RRIM 600 is also higher than that in latex from wild type. Rubber latex from the two clones was collected at the same time of the day, and the two rubber clones display a similar diurnal rhythm. HMGS activity varied during a 24-h cycle occurred in the latex of rubber clone RRIM 600 (Suvachittanont and Wititsuwannakul 1995) as reported for HMGR (Wititsuwannakul 1986). The diurnal variation of *Hbhmgs* mRNA coincides with the apparent activity of HMGS and so does the dried rubber content in the latex. These observations support the finding that the expression of *Hbhmgs* is likely related to the total activity of the enzyme and to the total synthesis of rubber in the rubber trees. This finding is similar to rat liver cytosolic and adrenal gland HMGS which exhibit the diurnal rhythm of the activity of the enzyme; however, not unexpectedly, the appearance of *hmgs-1* mRNA was slightly ahead of the enzyme activity (Balasubramaniam et al. 1977; Royo et al. 1991). The activity of both HMGS and HMGR was highest after dark and lowest during the daylight period in rats (Balasubramaniam et al. 1977), similar to what is found for HMGS in rubber latex. As rodents are night-active and feeding, this would be more or less logical, less in the case of rubber tree, where a correlation with photosynthetic activity would be expected. The peak of the HMGS activity in C-serum occurs at 2:00 A.M.; this is different from the 10:00 P.M. that had been previously reported (Suvachittanont and Wititsuwannakul 1995). The discrepancy observed in the previous study suggests that the highest enzyme activity in the first 24-h cycle and the following cycle might not be the same (Suvachittanont and Wititsuwannakul 1995). At present, there is no clear explanation for this observation.

Ethylene is one of the extensively studied plant hormones in relation to rubber biosynthesis, and it is applied as ethephon (2-chloroethylphosphonic acid), which *in planta* is metabolized to ethylene. Bark treatment with ethephon is known to increase the latex yield between 1.5- and 2-fold in *Hevea* (Coupé and Chrestin 1989; Pujade-Renaud et al. 1997). During the past several years, a number of investigations have been done to study the expression pattern of various rubber biosynthesis-related genes. It was also found that ethephon dramatically increased the levels of *Hbhmgs* mRNA and enzyme activity as well. Thus, the transcription of the gene encoding HbHMGS was induced by ethephon, and this gene and the enzyme derived from it can be truly considered as being implied in rubber biosynthesis. The result agrees well with the report that ethephon increases latex production in rubber trees, and the expression of some enzymes has been induced, for example, the mRNA levels of *hmgr-1*, glutamine synthase, and rubber elongation factor (REF) increase as a result of ethephon treatment (Chye et al. 1992; Pujade-Renaud et al. 1994; Priya et al. 2007). Nevertheless, no detailed report on the direct correlation between gene expression and rubber content in *Hevea* latex had been published yet. Therefore, we studied more closely the putative relationship between the expression of *Hbhmgs-1* and *Hbhmgr-1*genes in latex and rubber content in another *Hevea* rubber clone (PB235). The *Hevea* clone PB235 has also been promoted for rubber plantations in Thailand. High rubber yield can be obtained from this

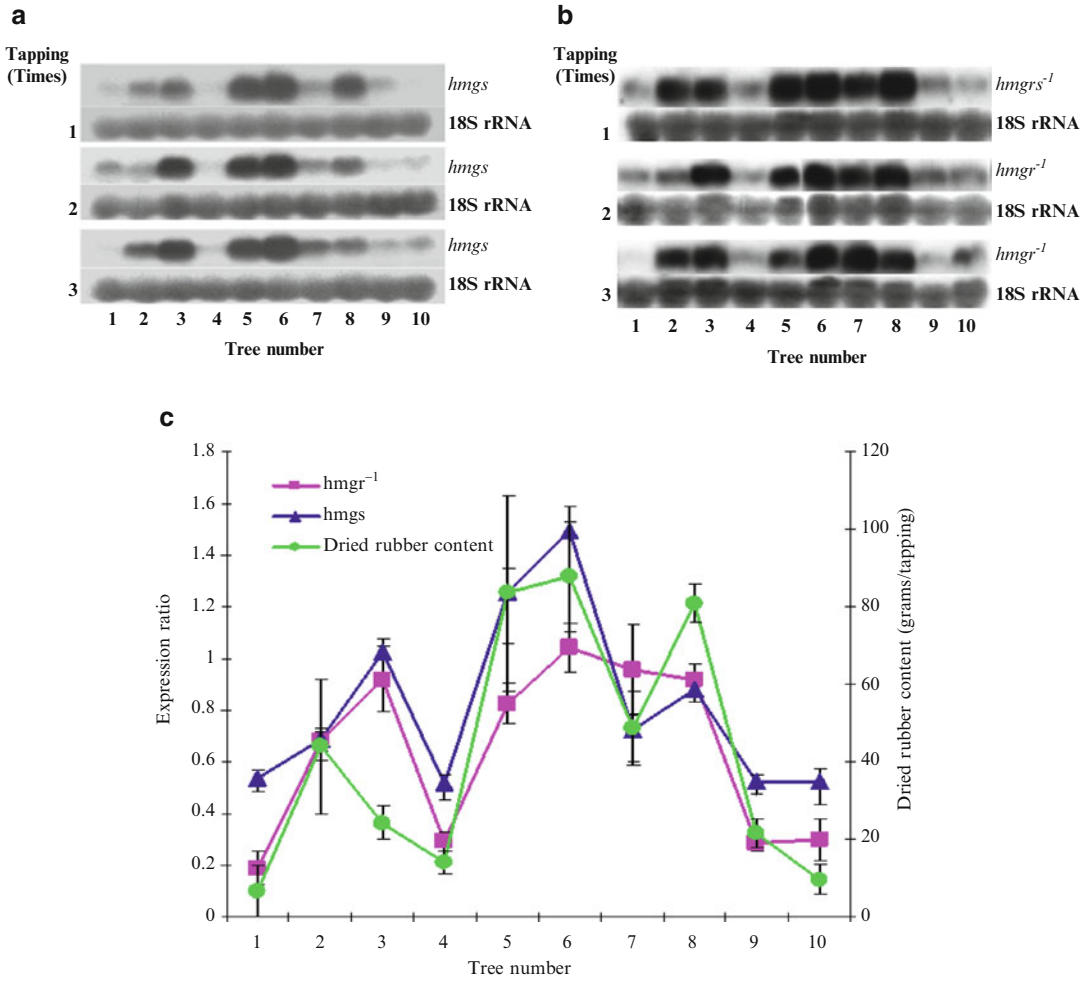

Fig. 22.4 Northern blot analysis of *hmgs-1* (**a**) and *hmgr-1*(**b**) and comparison of the average dried rubber content per tapping with *hmgs-1* mRNA and *hmgr-1* mRNA from three tappings of each trees (**c**)

Hevea clone, but the yields show high variations among different trees within the same plantation. Therefore, rubber yields from 30 samples from 10 different trees were determined. The average dried rubber content per tapping from these trees was significantly different. The cDNAs *Hbhmgs-1* and *Hbhmgr-1* were used as probes to determine the mRNA levels of *Hbhmgs-1* and *Hbhmgr-1* in total RNA from rubber latex by Northern blot analysis (Fig. 22.4a, b). The relative intensity of *Hbhmgs-1* mRNA levels from three tappings of each tree was significantly different. The average dried rubber content per tapping of each tree coincides with *Hbhmgs-1* and *Hbhmgr-1* mRNA levels (Fig. 22.4c). The relationship between *Hbhmgs-1* mRNA level and dried rubber content exhibited a positive correlation with a coefficient of 0.77 ($p < 0.001$) (Fig. 22.5a), while the correlation coefficient between *Hbhmgr-1* mRNA level and dried rubber content was calculated to be 0.71 ($p < 0.001$) (Fig. 22.5b). This result indicated that the expression level of both *Hbhmgs-1* and *Hbhmgr-1* genes is involved in the regulation of rubber biosynthesis in the *Hevea* PB235 clone.

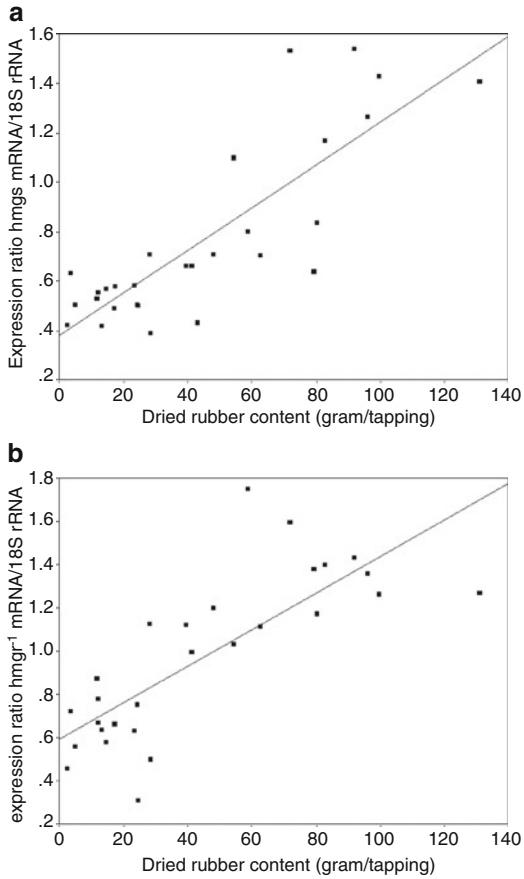

Fig. 22.5 Correlation of dried rubber content with *hmgs-1* mRNA (**a**) and *hmgr-1*(**b**) from 30 tappings of 10 rubber trees

22.5 Conclusion

To date, HMGS and HMGR were generally accepted to coordinately regulate cholesterol synthesis in mammal. Both HMGS and HMGR were also suggested to be equally important for isoprenoid biosynthetic pathway in plants. Our observations clearly show that rubber biosynthesis in *H. brasiliensis* is coordinately regulated by HMGS and HMGR via production of IPP, comparable to mammalian cholesterol biosynthesis. Presently, our group is investigating the co-regulation of both HMGS and HMGR in rubber biosynthesis in more detail. But we take also into account that the MEP pathway might contribute to rubber production in *H. brasiliensis* (cf. Seetang-Nun et al. 2008). For instance, only one of two identified *H. brasiliensis* genes coding for 1-deoxy-D-xylulose 5-phosphate reductoisomerase (DXR, EC 1.1.1.267, also known as MEP synthase) was shown to be more expressed after ethephon treatment, with a higher expression already in the clone RRIM 600 than in the wild type. However, the transcriptome analysis of *H. brasiliensis* latex through generation of 10.040 expressed sequence tags (ESTs) did not really argue for the contribution of MEP-derived IPP to rubber biosynthesis, presumably synthesized in Frey-Wyssling particles, which represent specialized latex plastids (Chow et al. 2007). And even transcripts of genes coding for mevalonate kinase, phosphomevalonate kinase, FPP synthase, and IPP isomerase were only detected by using QRT-PCR analysis (Chow et al. 2007). This knowledge is important for a possible application of biotechnology to improve rubber yield in rubber tree plantation.

Acknowledgments The authors would like to thank the Thailand Research Fund (MRG4680164 and PHD/00124/2541) and the National Science and Technology and Development Agency, Thailand (GREC40-01-002), for their support, and the support from Biology Department, Taksin University, for the research facility, and also Professor Thomas J. Bach for arranging some financial support for Suwannmanee P. to participate in the 8th TERPNET 2007, April 30–May 4, 2007 Strasbourg, France.

References

Alam A, Britton G, Powls R et al (1991) Aspects related to 3-hydroxy-3-methylglutaryl-CoA synthesis in higher plants. Biochem Soc Trans 19:164–168

Alex D, Bach TJ, Chye ML (2000) Expression of *Brassica juncea* 3-hydroxy-3-methylglutaryl-CoA synthase is developmentally regulated and stress-repressive. Plant J 22:414–426

Ayté J, Gil-Gómez G, Haro D et al (1990a) Rat mitochondrial and cytosolic 3-hydroxy-3-methylglutaryl-CoA synthase are encoded by two different genes. Proc Natl Acad Sci USA 87:3874–3878

Ayté J, Gil-Gómez G, Hegardt FG (1990b) Nucleotide sequence of a rat liver cDNA encoding the cytosolic 3-hydroxy-3-methylglutaryl coenzyme A synthase. Nucleic Acids Res 18:3642–3642

Bach TJ, Rogers DH, Rudney H (1986) Detergent-solubilization, purification, and characterization of membrane-bound 3-hydroxy-3-methylglutaryl coenzyme A reductase from radish seedlings. Eur J Biochem 154:103–111

Bach TJ, Raudot V, Vollack K-U et al (1994) Further studies on the enzymatic conversion of acetyl-coenzyme A into 3-hydroxy-3-methylglutaryl-coenzyme A in radish. Plant Physiol Biochem 32:775–783

Balasubramaniam S, Goldstein JL, Brown MS (1977) Regulation of cholesterol synthesis in rat adrenal gland through coordinate control of 3-hydroxy-3-methylglutaryl-CoA synthase and reductase activity. Proc Natl Acad Sci USA 74:1421–1425

Brown WE, Rodwell VW (1980) Hydroxymethylglutaryl CoA reductase. In: Jeffery J (ed) Dehydrogenases requiring nicotinamide coenzymes. Birkhäuser Verlag, Berlin

Chow K-S, Wan K-L, Isa MNM, Bahari A, Tan S-H, Harikrishna K, Yeang H-Y (2007) Insights into rubber biosynthesis from transcriptome analysis of *Hevea brasiliensis* latex. J Exp Bot 58:2429–2440

Chun KY, Vinarov DA, Zajicek J et al (2000) 3-Hydroxy-3-methylglutaryl-CoA synthase: a role for glutamate-95 in general acid/base catalysis of C–C bond formation. J Biol Chem 275:17946–17953

Chye ML, Kush A, Tan CT et al (1991) Characterization of cDNA and genomic clones encoding 3-hydroxy-3-methylglutaryl coenzyme A reductase from *Hevea brasiliensis*. Plant Mol Biol 19:562–577

Chye ML, Tan CT, Chua NH (1992) Three genes encode 3-hydroxy-3-methylglutaryl coenzyme A reductase in *Hevea brasiliensis*: *hmg1* and *hmg2* are differentially expressed. Plant Mol Biol 19:473–484

Clinkenbeard KD, Reed WD, Mooney RD et al (1975a) Intracellular localization of the 3-hydroxy-3-methylglutaryl coenzyme A cycle enzymes in liver. J Biol Chem 250:3108–3116

Clinkenbeard KD, Sugiyama T, Reed WD et al (1975b) Cytoplasmic 3-hydroxy-3-methylglutaryl coenzyme A synthase from liver: purification, properties and role in cholesterol synthesis. J Biol Chem 250:3124–3135

Coupé M, Chrestin H (1989) Physiochemical and biochemical mechanisms of hormonal (ethylene) stimulation. In: Auzac JD, Jacob JL, Chrestin H (eds) Physiology of rubber tree latex. CRC Press, Boca Raton

Goldstein JL, Brown MS (1990) Regulation of the mevalonate pathway. Nature 343:425–430

Hemmerlin A, Hoeffler JF, Meyer O et al (2003) Cross-talk between the cytosolic mevalonate and the plastidial methylerythritol phosphate pathways in tobacco bright yellow-2 cells. J Biol Chem 278:26666–26676

Hepper CM, Audley BG (1969) The biosynthesis of rubber from β-Hydroxy-β- methylglutaryl coenzyme A in *Hevea brasiliensis* latex. Biochem J 114:379–386

Kasahara H, Hanada A, Kuzuyama T, Takagi M, Kamiya Y, Yamaguchi S (2002) Contribution of the mevalonate and methylerythritol phosphate pathways to the biosynthesis of gibberellins in Arabidopsis. J Biol Chem 277:45188–45194

Lange BM, Rujan T, Martin W et al (2000) Isoprenoid biosynthesis: the evolution of two ancient and distinct pathways across genomes. Proc Natl Acad Sci USA 97:13172–13177

Laule O, Fürholz A, Chang HS, Zhu T, Wang X, Heifetz PB, Gruissem W, Lange M (2003) Crosstalk between cytosolic and plastidial pathways of isoprenoid biosynthesis in *Arabidopsis thaliana*. Proc Natl Acad Sci USA 100:6866–6871

Lichtenthaler HK, Rohmer M, Schwender J (1997a) Two independent biochemical pathways for isopentenyl diphosphate and isoprenoid biosynthesis in higher plants. Physiol Plant 101:643–652

Lichtenthaler HK, Schwender J, Disch A et al (1997b) Biosynthesis of isoprenoids in higher plant chloroplasts proceeds via a mevalonate-independent pathway. FEBS Lett 400:271–274

Lynen F (1969) Biochemical problems of rubber synthesis. J Rubb Res Inst Malaya 21:389–406

Mandel MA, Feldmann KA, Herrera-Estrella L et al (1996) A novel gene required for chloroplast development, is highly conserved in evolution. Plant J 9:649–658

Misra I, Miziorko HM (1996) Evidence for the interaction of avian 3-hydroxy-3 methylglutaryl-CoA synthase histidine-246 with acetoacetyl-CoA. Biochemistry 35:9610–9616

Misra I, Narasimhan C, Miziorko HM (1993) Avian 3-hydroxy-3-methylglutaryl-CoA synthase, characterization of a recombinant cholesterogenic isozymes and demonstration of the requirement for a sulfhydryl functionality in formation of the acetyl-S-enzyme reaction intermediate. J Biol Chem 268:12129–12135

Misra I, Wang CZ, Miziorko HM (2003) The influence of conserved aromatic residue in 3-hydroxy-3-methylglutaryl-CoA synthase. J Biol Chem 278:26443–26449

Miziorko HM, Clinkenbeard KD, Reed WD et al (1975) 3-Hydroxy-3-methylglutaryl-CoA synthase. J Biol Chem 250:5768–5773

Miziorko HM, Kramer PR, Kulkoski JA (1982) *S*-(3-Oxobutyl)coenzymeA. Interaction with acetoacetyl coenzyme A utilizing enzymes. J Biol Chem 257: 2842–2847

Montamat F, Guilloton M, Karst F et al (1995) Isolation and characterization of a cDNA encoding *Arabidopsis thaliana* 3-hydroxy-3-methylglutaryl-CoA synthase. Gene 167:197–201

Nagegowda DA, Bach TJ, Chye ML (2004) *Brassica juncea* 3-hydroxy-3-methylglutaryl (HMG)-CoA synthase 1: expression and characterization of recombinant wild-type and mutant enzymes. Biochem J 383: 517–527

Pojer F, Ferrer JL, Richard SB, Nagegowda DA, Chye ML, Bach TJ, Noel JP (2006) Structural basis for the design of potent and species-specific inhibitors of 3-hydroxy-3-methylglutaryl CoA synthases. Proc Natl Acad Sci USA 103:11491–11496

Price AC, Choi K-H, Health RJ et al (2001) Inhibition of β-ketoacyl-acyl carrier protein synthases by thiolactomycin and cerulenin. Structure and mechanism. J Biol Chem 276:6551–6559

Priya P, Venkatachalam P, Thulaseedharam A (2007) Differential expression pattern of rubber elongation factor (REF) mRNA transcripts from high and low yielding clones of rubber tree (*Hevea brasiliensis* Muell. Arg.). Plant Cell Rep 26:1833–1838

Pujade-Renaud V, Clement A, Perrot-Rechenmann C et al (1994) Ethylene-induced increase in glutamine synthetase activity and mRNA levels in *Hevea brasiliensis* latex cells. Plant Physiol 105:127–132

Pujade-Renaud V, Clement A, Perrot-Rechenmann C et al (1997) Ethylene-induced increase in glutamine synthetase activity and mRNA levels in *Hevea brasiliensis* latex cells. Plant Physiol 105:127–132

Qiu X, Janson CA, Konstantinidis AK et al (1999) Crystal structure of β-ketoacyl-acyl carrier protein synthase III: a key condensing enzyme in bacterial fatty acid biosynthesis. J Biol Chem 274: 36465–36471

Reddy AR, Das VSR (1986) Partial purification and characterization of 3-hydroxy-3-methylglutaryl coenzyme A reductase from the leaves of guayule (*Parthenium argentatum*). Phytochemistry 25:2471–2474

Rogers DH, Panini SR, Rudney H (1983) Properties of HMG CoA reductase and its mechanism of action. In: Sabine JR (ed) 3-Hydroxy-3-methylglutaryl coenzyme A reductase. CRC Press, Boca Raton

Royo T, Ayté J, Albericio FE et al (1991) Diurnal rhythm of rat liver cytosolic 3-hydroxy-3-methylglutaryl-CoA synthase. Biochem J 280:61–64

Scarsdale JN, Kazanina G, He X et al (2001) Crystal structure of the *Mycobacterium tuberculosis* β-ketoacylacyl carrier protein synthase III. J Biol Chem 276:20516–20522

Schaller H, Grausem B, Benveniste P et al (1995) Expression of the *Hevea brasiliensis* (H.B.K.) Muell. Arg. 3-methylglutaryl-CoA reductase1 in tobacco results in sterol overproduction. Plant Physiol 109: 761–770

Seetang-Nun Y, Sharkey TD, Suvachittanont W (2008) Molecular cloning and characterization of two cDNAs encoding 1-deoxy-D-xylulose 5-phosphate reductoisomerase from *Hevea brasiliensis*. Plant Physiol 165: 991–1002

Shah SN (1982) Cytosolic 3-hydroxy-3-methyglutaryl coenzyme A synthase in rat brain: properties and developmental change. Neurochem Res 7:1359–1366

Sipat AB (1982) Hydroxymethylglutaryl CoA reductase NADPH (EC 1.1.1.34) in the latex of *Hevea brasiliensis*. Phytochemistry 21:2613–2618

Sirinupong N, Suwanmanee P, Doolittle RR et al (2005) Molecular cloning of a new cDNA and expression of 3-hydroxy-3-methylglutaryl-CoA synthase gene from *Hevea brasiliensis*. Planta 221:502–512

Steinbüchel A (2003) Production of rubber-like polymers by microorganisms. Curr Opin Microbiol 6:261–270

Sutherlin A, Hedl M, Sanchez-Neri B et al (2002) *Enterococcus faecalis* 3-hydroxy-3-methylglutaryl-CoA synthase, an enzyme of isopentenyl diphosphate biosynthesis. J Bacteriol 184:4065–4070

Suvachittanont W, Wititsuwannakul R (1995) 3-Hydroxy-3-methylglutaryl coenzyme A synthase in *Hevea brasiliensis*. Phytochemistry 40:757–761

Suwanmanee P, Suvachittanon W, Fincher GB (2002) Molecular cloning and sequencing of a cDNA encoding 3-hydroxy-3-methylglutaryl-CoA synthase from *Hevea brasiliensis* (HBK) Muell Arg. Sci Asia 28:29–36

Van der Heijden R, de Boer-Hlupa V, Verpoorte R et al (1994a) Enzymes involved in the metabolism of 3-hydroxy-3-methylglutaryl-coenzyme A in *Catharanthus roseus*. Plant Cell Tiss Org Cult 38:345–349

Van der Heijden R, Verpoorte R, Duine JA (1994b) Biosynthesis of 3-hydroxy-3-methylglutaryl coenzyme A in *Catharanthus roseus*: acetoacetyl-Co A thiolase and HMG-Co A synthase show similar chromatographic behavior. Plant Physiol Biochem 32:807–812

Vollmer SH, Mende-Mueller LM, Miziorko HM (1988) Identification of the site of the acetyl-*S*-enzyme formation on avian liver mitochondrial 3-hydroxy-3-methylglutaryl-CoA synthase. Biochemistry 27:4288–4292

Wegener A, Gimbel W, Werner T et al (1997) Molecular cloning of ozone-inducible protein from *Pinus sylvestris* L. with high sequence similarity to vertebrate 3-hydroxy-3-methylglutaryl-CoA synthase. Biochem Biophys Acta 28:247–252

Wititsuwannakul R (1986) Diurnal variation of HMG-CoA reductase in latex of *Hevea brasiliensis*. Experientia 42:45–46

Wititsuwannakul R, Wititsuwannakul D, Suwanmanee P (1990) 3-Hydroxy-3-methylglutaryl coenzyme A reductase from the latex of *Hevea brasiliensis*. Phytochemistry 29:1401–1403

Development of Crops to Produce Industrially Useful Natural Rubber

23

Maureen Whalen, Colleen McMahan, and David Shintani

Abstract

Natural rubber, *cis*-1,4-polyisoprene, is an essential industrial commodity that most developed countries have to import. *Hevea brasiliensis* (Hevea), grown in tropical and subtropical areas, is the primary source of natural rubber. The high quality and quantity of the rubber cause us to focus on understanding rubber production in Hevea and two temperate plant species, guayule (*Parthenium argentatum*) and Russian dandelion (*Taraxacum kok-saghyz*). We review the cell biology, physiology, and biochemistry of rubber production in these three species. Rubber is synthesized on subcellular vesicles called rubber particles. Purified rubber particles alone contain all necessary factors for rubber production. We have used genomic approaches to identify expressed genes associated with rubber-producing tissues and proteomics to identify proteins associated with rubber particles. The protein and EST identifications guided our analysis of key proteins in rubber production, including *cis*-prenyltransferase, rubber elongation factor, small rubber particle protein, allene oxide synthase, HMG-CoA reductase, and allylic diphosphate synthases. We discuss biotechnological approaches to improve rubber production.

Keywords

Natural rubber • *Cis*-1,4-polyisoprene • *Hevea brasiliensis* • *Parthenium argentatum* • Guayule • *Taraxacum kok-saghyz* • Russian dandelion • Rubber particles • Biotechnology • Genomics • Proteomics

M. Whalen (✉) • C. McMahan
Crop Improvement and Utilization Unit,
Western Regional Research Center, ARS-USDA,
800 Buchanan Street, Albany, CA 94710, USA
e-mail: maureen.whalen@ars.usda.gov

D. Shintani
Department of Biochemistry, University of Nevada,
Reno, NV 89557, USA

T.J. Bach and M. Rohmer (eds.), *Isoprenoid Synthesis in Plants and Microorganisms: New Concepts and Experimental Approaches*, DOI 10.1007/978-1-4614-4063-5_23,

23.1 Introduction

Worldwide, natural rubber is the largest, single volume elastomer that is commercially used. It has outstanding performance properties, including elasticity, resilience, heat dispersion, and abrasion resistance, that cannot be reproduced by synthetically produced polymers. Around the globe, most developed countries are completely dependent on importing natural rubber for applications where synthetic rubber cannot substitute. In fact, the United States Congress declared natural rubber as "a commodity of vital importance to the economy, the defense, and the general well-being of the Nation" (Critical Agricultural Materials Act 7, Public Law 107–293, Nov. 12, 2002, Sec. 2 07 U.S.C 178). Prices for natural rubber and latex continue to rise as demand increases, and worldwide shortages are predicted. The almost complete dependence on rubber from the tropical tree *Hevea brasiliensis* is disquieting. The genetic base is extremely narrow, and the fact that the rubber industry in Brazil was almost destroyed from South American leaf blight disease in the early 1900s requires continuous containment measures that include intensive control of international air traffic and freight shipments from South America to other tropical areas (Lieberei 2007). The natural rubber supply is decidedly unstable.

In the introduction to US Public Laws 95–592 and 98–284 (7 USC Chapter 8A) passed by the US Congress, the state of dependence on Hevea imports was considered regrettable, and a research effort into the development of alternative rubber-producing crop plants was approved. In a parallel fashion, in the recent round of European Union scientific research funding, an international Framework 7 project (EU-PEARLS) to study alternative sources of natural rubber was funded (van Beilen and Poirier 2007).

More than 2,500 plants have been reported to produce rubber; most of them are tropical. A small subset have been shown to have sufficient rubber production to be commercially viable, and just a few of those grow in temperate regions (Bonner and Galston 1947). Overall, only three rubber-producing plants are well studied: *Hevea brasiliensis* (Hevea or Brazilian rubber tree), *Parthenium argentatum* (guayule), and *Taraxacum kok-saghyz* (Russian dandelion). Hevea is a tropical tree that is clonally propagated. Guayule is a perennial desert shrub, native to southwestern USA and northern Mexico. Russian dandelion is a perennial, rosette plant native to the Tien Shan mountains in Central Asia. All three of these plants produce high quality and high quantities of *cis*-1,4-polyisoprene rubber and will be the focus of this chapter.

23.2 Cell Biology of Rubber Production

Rubber is produced in plants and stored in small rubber particles that are suspended within the cytoplasm of specialized cells. This aqueous suspension is called latex. In Hevea trees, the rubber-containing latex is produced by laticifer cells, which develop from cells laid on by the vascular cambium and are closely associated with phloem parenchyma (Bobilioff 1925). Laticifers produced in one season fuse, when contiguous end walls dissolve. An extensive network of laticiferous vessels thereby forms within the bark tissue. When a Hevea tree is tapped, latex flow is initiated from the reduction in water potential caused by the release of turgor pressure in the incised cell (Bonner and Galston 1947). In this manner, over eight million metric tons annually of latex is manually harvested for commercial processing. Russian dandelion produces rubber in its roots. Networks of laticiferous vessels are found in the phloem parenchyma (Krotkov 1945). Similar to Hevea and Russian dandelion, guayule produces rubber in cells of the phloem parenchyma. In contrast, guayule does not have laticifer vessels or connected networks; therefore, latex harvest requires grinding of plant tissue to release rubber particles.

Rubber particles have a core of rubber and appear to be surrounded by an unconventional unit membrane (Siler et al. 1997; Cornish et al. 1999; Wood and Cornish 2000). The protein and lipid composition of the negatively charged rubber particle membrane varies from species to species (de Fay et al. 1989; Cornish et al. 1993; Siler et al. 1997). The proteins in the membrane

have access to substrates in the cytoplasm, and the hydrophobic rubber is compartmentalized within the particle.

Rubber particles range in size from 0.2 to 10 μm (Backhaus and Walsh 1983; Cornish et al. 1993; Singh et al. 2003a). Sizes vary from species to species and within the same plant. For example, Hevea rubber particles have two size classes, with mean diameters of 0.2 and 1.0 μm (Cornish et al. 1993; Wood and Cornish 2000). Interestingly, a correlation between rubber particle size and rubber molecular weight has been demonstrated in Hevea (Yeang et al. 1995; Tarachiwin et al. 2005a). Small rubber particles (0.15–0.25 μm) have both high and low molecular weight rubber, whereas large rubber particles (>0.25 μm) have mostly only low molecular weight rubber. In addition, the smaller particles have higher levels of protein overall (Tarachiwin et al. 2005b) as well as higher rubber transferase activity (Dennis and Light 1989; Dennis et al. 1989; Ohya et al. 2000). Moreover, the low molecular weight rubber in large rubber particles is associated with high levels of fatty acid ester groups suggesting the prevalence of terminated rubber molecules (Tarachiwin et al. 2005a, b). Tarachiwin et al. (2005b) further suggest a model of rubber synthesis actively taking place in the small rubber particles, but not in the larger ones. Overall, this work presents a dynamic picture of rubber particle structure and function.

In both Hevea and guayule, rubber particles appear to eventually coalesce with the central vacuole during the development of the rubber-producing cell (Popovici 1926; Cornish and Wood 2002). Hevea latex has vacuolar structures called lutoids, which are found in the bottom fraction after centrifugation and appear to be somewhat lysosomal in nature (Gidrol et al. 1988). Bursting of lutoids is associated with the coagulation response to latex tapping or wounding (Gidrol et al. 1994) by releasing the lectin-like protein hevein. The interaction of hevein with a glycosylated protein called small rubber particle protein (SRPP) in the rubber particle membrane is thought to mediate coagulation (Gidrol et al. 1994; Wititsuwannakul et al. 2008a, b). Coagulation staunches the flow of laticifer cell contents (latex), which clearly confers a selective advantage to Hevea physiology.

23.3 Physiology of Rubber Production

Rubber synthesis has seasonal cycles in all three plants. This is most pronounced in guayule. Low night temperatures (40–45 °F), coupled with relatively warm day temperatures (65 °F), result in accumulation of rubber (Bonner 1943). These temperatures induce dormancy in guayule, resulting in cessation of growth and flowering. The increased rubber in response to cold temperatures is correlated with increased activity of the rubber-synthesizing enzyme (Cornish and Backhaus 2003). In Russian dandelion, optimal rubber production appears to be associated with flowering, with induction of flowering most responsive to long days (Bonner and Galston 1947). In addition, cold treatment may also play a role, but that is less clearly delineated (Krotkov 1945). Hevea rubber production appears to depend upon a well-established leaf canopy. Leaf canopy loss during the dry season reduces latex production. Maximum rubber production in Hevea takes place when new leaves grow in the rainy season. The precise molecular basis of any of these seasonal responses is not known at present.

Rubber, once produced, does not undergo catabolic conversion *in planta*. Interesting relationships exist between rubber accumulation and storage forms of photosynthate. In guayule, inulin normally accumulates at the same time that rubber does (Hassid et al. 1944; Kelly and Van Staden 1991), suggesting that rubber is not made from breakdown products of this storage carbohydrate. Accumulation of inulin in Russian dandelion roots also appears to follow the same pattern as rubber accumulation, both continuously going up during the growing season (Krotkov 1945, 1950). On the other hand, accumulation of photosynthate as starch in Hevea phloem is the inverse of rubber accumulation (Bonner and Galston 1947), suggesting the possibility of a catabolic relationship between starch storage and rubber production. Labeling experiments would have to be performed for a definitive assessment of the relationship between storage carbohydrate and rubber metabolism. It is notable that in the two temperate plants, rubber increases

at the same time as the storage carbohydrate increases, suggesting that these plants experience an overload of fixed carbon molecules when they are not being used for growth or reproduction. Rubber is a metabolic dead end for the plant and seemingly harmless. Stored inulin is used by these plants when they emerge from cold-induced dormancy.

23.4 Biochemistry of Rubber Production

Rubber is a product of the isoprenoid pathway that starts with the metabolite acetyl-CoA (Fig. 23.1). Rubber is synthesized by a condensation reaction of two products of the mevalonate pathway, an allylic diphosphate (APP) initiator and the substrate isopentenyl diphosphate (IPP; C5), catalyzed by the enzyme rubber transferase (Archer and Audley 1987; Madhaven et al. 1989; Cornish and Siler 1995). After initiation, IPP is used by rubber transferase to elongate the polymer. A divalent cation such as Mg^{2+} or Mn^{2+} is also required as cofactor (da Costa et al. 2005, 2006; Scott et al. 2003). Rubber transferase (EC2.5.1.20) is a *cis*-prenyltransferase. It is intimately associated with rubber particles, in that isolated rubber particles are able to produce rubber (Archer et al. 1963; Audley and Archer 1988; Cornish and Backhaus 1990; Madhaven et al. 1989; Cornish and Siler 1996). When they are disrupted, rubber synthesis is also disrupted, indicating that rubber particle structure is an essential component of the activity of rubber transferase. Rubber transferase accepts a broad

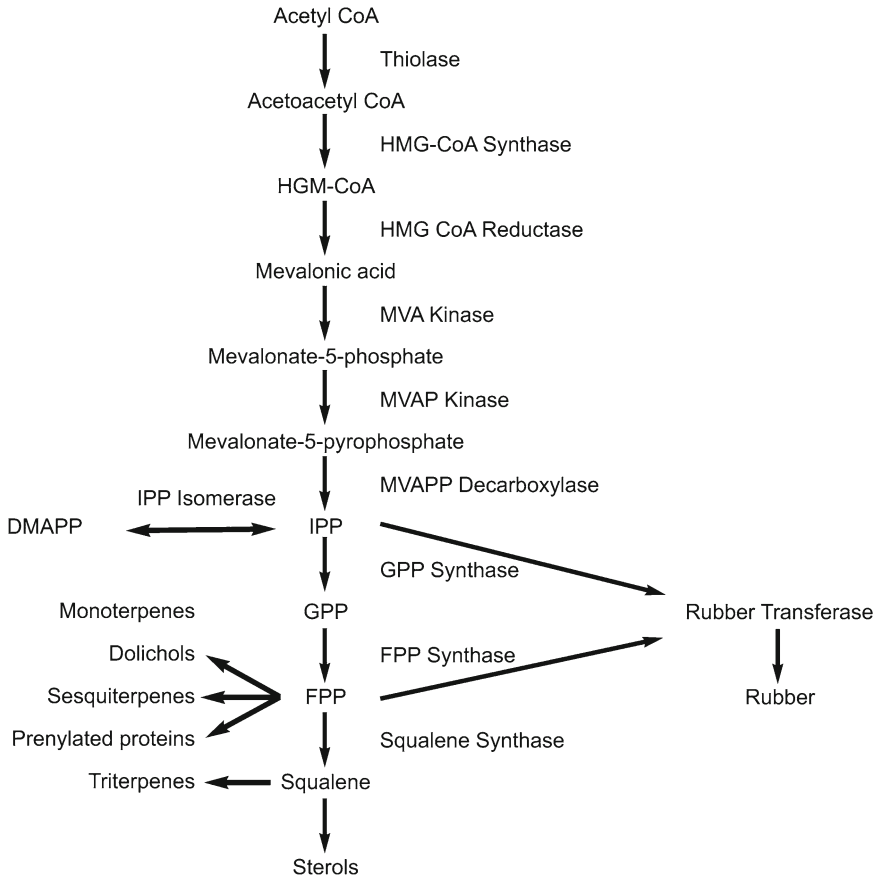

Fig. 23.1 Isoprenoid synthesis pathway in plants from acetyl-CoA to rubber, sterols, terpenes, and dolichols

range of initiator molecules, with farnesyl diphosphate (FPP) (C15) being preferred (Tanaka et al. 1996; Castillon and Cornish 1999; Mau et al. 2003). The length of the polymer produced depends on concentrations of the substrate IPP, the ratio of concentrations of IPP and initiator APP, the size of the initiator (Castillon and Cornish 1999), and probably other unknown factors. Some plants (e.g., *Ficus elastica*, *Helianthus annuus*) produce rubber but only of low molecular weight. The mechanism by which plants control the molecular weight of rubber is not well understood.

As mentioned earlier, protein quantity and protein composition of rubber particles vary from species to species. At present, nothing has been published on proteins in rubber particles from Russian dandelion. On the other hand, it is well known that Hevea rubber particles have a high number of proteins. Two of the dominant proteins in Hevea rubber particles are the 14-kDa rubber elongation factor (REF) and the 24-kDa SRPP (Czuppon et al. 1993; Oh et al. 1999). The species specificity of rubber particle protein composition was demonstrated by Singh et al. (2003a, b), who showed by immunoelectron microscopy that SRPP was found on Hevea rubber particles but not on rubber particles from various *Ficus* species examined. In Hevea, there is a correlation between the size of the rubber particle and the particular protein composition (Dennis and Light 1989; Bahri and Hamzah 1996). More SRPP and less REF were found on small rubber particles, compared to large rubber particles. Interestingly, small rubber particles have more rubber transferase activity than large particles (Ohya et al. 2000).

Guayule rubber particles possess few proteins (Cornish et al. 1993). In guayule, the dominant protein is a 53-kDa monooxygenase P450, an allene oxide synthase (AOS) (Backhaus et al. 1991; Pan et al. 1995). It comprises about 50% of the rubber particle protein. The extreme difference in protein composition and quantity between Hevea and guayule is the raison d'être for production of guayule latex for biomedical applications (Mooibroek and Cornish 2000). Hevea latex proteins trigger severe allergies in people with type I latex allergies. Guayule latex does not contain the same proteins, therefore making guayule latex an important product that circumvents the life-threatening allergenic reactions to Hevea latex.

23.5 Genomic Approach for Study of Rubber Production

We have chosen to use genomic and proteomic approaches to study rubber production. Genes that are expressed in rubber-producing tissues are likely to be important for rubber production. Our genomic efforts involved sequencing of populations of cDNAs from Russian dandelion roots and guayule bark. The cDNA sequences are called expressed sequence tags (ESTs). These EST populations (~10,000 each species) were compared with those from Hevea using the BLAST algorithm (Altschul et al. 1990), with a probability cutoff of $P < 10^{-30}$ in the Blast results (Table 23.1). Our results demonstrate that all of the biosynthetic genes are expressed in Russian dandelion roots, as well as the rubber particle proteins SRPP and AOS. In guayule, two of the biosynthetic genes are missing from our EST population (mevalonate kinase and IPP isomerase), suggesting that our guayule library may not be complete. Additional ESTs should be sequenced to remedy that problem. On average, the EST populations from Russian dandelion reflected the fact that mRNA was isolated from the entire root. When compared with the large EST population (~42,000) from common dandelion, *Taraxacum officinale*, Russian dandelion roots had more rubber-associated gene expression than *T. officinale*. It is clear that there is specialization for rubber production in Russian dandelion roots.

It is important to keep in mind that probability scores do not address function. The identification of homologous sequences suggests that a protein with a similar structure leading to similar function is produced, but until an assay of function is performed, it remains theoretical. Furthermore, the absence of a sequence does not necessarily mean that the transcript is not present in that tissue. Transcripts that are expressed at extremely

Table 23.1 Sequences present in EST libraries of guayule bark and Russian dandelion root. Hevea proteins were used as query sequence in tblastn similarity searches. Probability levels of the best match are given. The minimum cutoff to be considered significant is $P < 10^{-30}$, while identical sequences in this study have probabilities ranging from $<10^{-75}$ to $<10^{-149}$

Protein sequences		Probability of EST encoding a similar sequence[a]	
Function	Hevea genbank accession number	Guayule bark[b]	Russian dandelion root
Rubber-associated			
Small rubber particle protein	AAO66433	$<10^{-54}$	$<10^{-50}$
Rubber elongation factor	P15252	–	–
Allene oxide synthase	AAY27751	$<10^{-92}$	$<10^{-101}$
Biosynthesis			
Thiolase	AAL18924	$<10^{-69}$	$<10^{-102}$
HMG-CoA synthase	AAL18930	$<10^{-89}$	$<10^{-95}$
HMG-CoA reductase	P29057	$<10^{-90}$	$<10^{-113}$
MVA kinase	AAL18925	–	$<10^{-64}$
MVAP kinase	AAL18926	$<10^{-49}$	$<10^{-84}$
MVAPP decarboxylase	AAL18927	$<10^{-71}$	$<10^{-108}$
IPP isomerase	AAD41765	–	$<10^{-107}$
cis-Prenyltransferase	BAB83522	$<10^{-31}$	$<10^{-52}$
FPPS	AAM98379	$<10^{-104}$	$<10^{-82}$

[a]Means that at the cutoff value of $P < 10^{-30}$, no homologue was present
[b]Bark was cold-induced

low levels are technically difficult to isolate in any one population, and a sampling of 10,000 ESTs is not exhaustive. EST profiles do provide a snapshot of the rubber-producing tissues of guayule and Russian dandelion and allow identification of candidates for biotechnological manipulation.

The next step is to study the impact on rubber production of altering expression levels of rubber-associated genes. If manipulating gene expression by overexpression or silencing results in a change in rubber quantity or quality, then we have established a causal relationship. Because it is straightforward to genetically transform and grows relatively quickly, Russian dandelion presents an excellent model organism for these kinds of studies. Transgenic Russian dandelion plants take 4 months to mature, produce detectable amounts of rubber within the first 2 months after transplanting in soil, and do not take up large amounts of greenhouse space. Guayule, on the other hand, requires 2 years in the field for optimal rubber analysis. The slowest of all is Hevea, which is usually tapped after 7 years and is difficult to transform. For genes that are held in common, our strategy is to use Russian dandelion to test the impact of transgenes on rubber phenotypes before analogous studies on the other two species.

23.6 Proteomics Approach for Study of Rubber Production

In addition to a genomics approach, we have also used a proteomics approach. Because rubber particles contain all the machinery to synthesize rubber, we hypothesized that identification of proteins in rubber particles would lead us to all the essential and important proteins. Moreover, an intraspecific comparison would lend weight to determination of essentiality for rubber production. To identify proteins, rubber particles were isolated from Hevea latex, guayule bark, and Russian dandelion roots, and proteins fractionated using two-dimensional gel electrophoresis. As expected from standard SDS-PAGE separation, the overall protein profiles were quite different. Russian dandelion had about ten times more proteins overall than Hevea or guayule. Extensive washing of the Russian dandelion rubber particles did not change the profile. For identification, protein spots were excised from the gels, and

Table 23.2 Comparison of proteins present in rubber particles of Hevea latex, guayule bark, and Russian dandelion roots. Proteins were fractionated by two-dimensional gel electrophoresis, followed by mass spectrometric identification of tryptic fragments. Proteins with at least two peptides identified were considered valid matches

Protein sequences	Presence in rubber particles		
Function	Hevea	Guayule	Russian dandelion
Rubber-associated			
Small rubber particle protein	+	–	+
Rubber elongation factor	+	–	+
Allene oxide synthase	–	+	+
Defense- or stress-related			
Lipoxygenase, chitinase, PGase inhibitor	–	+	+
Proteases, protease inhibitors	–	+	+
Phospholipase C, lipases, peroxidase, acid phosphatase	+	–	+
Dehydration-, wound-, stress-inducible proteins	+	–	–
Annexin	+	–	+
Endomembrane-associated	+	+	+
Mitochondria-associated	–	+	+

mass spectrometry was used to identify tryptic fragments (Table 23.2).

Abundant proteins associated with Hevea and guayule rubber particles that had been previously identified were present, including SRPP and REF in Hevea and allene oxide synthase (AOS) in guayule rubber particles. Interestingly, an AOS was found to be associated with Russian dandelion rubber particles. AOS has been found in Hevea leaves (Norton et al. 2007), but we did not find it associated with Hevea rubber particles. Many proteins were not present in sufficient quantities for mass spectrometric identification.

A total of eight different proteins were identified in Hevea rubber particles. In addition to REF and SRPP, Hevea rubber particles also had phospholipase C, early dehydration-inducible protein, annexin, and vacuolar ATPase subunits. Both phospholipase C and early dehydration-inducible or LEA-like proteins have been shown to be associated with biotic and abiotic stress responses (Yamaguchi et al. 2005; Hundertmark and Hincha 2008). LEA-like proteins are thought to stabilize cells under stressful conditions. It has been known for a long time that Hevea latex has many defense- and stress-related proteins (Sussman et al. 2002), but our results are the first to show a direct association of these with rubber particles. Annexins are abundant proteins with a variety of different functions. The functions that may be relevant to rubber production are phospholipid binding in a calcium-dependent manner (Delmar and Potikha 1997), induction of aggregation of liposomes or plant secretory vesicles (Blackbourn and Battey 1993), anticoagulation (Tait et al. 1988), and association with vacuolar membranes (Seals et al. 1994). The latter possible function is consistent with the presence of vacuolar ATPase subunits in Hevea rubber particles. Hevea rubber particles are thought to coalesce with vacuoles (Popovici 1926), and perhaps, that process is mediated by annexin and ATP hydrolysis. Further studies are required to understand the role of these proteins, if any, in rubber particle function and cell biology in Hevea.

Guayule rubber particles also had stress- and defense-associated proteins including a lipoxygenase, proteinase, an LEA protein, and a stress-responsive protein. Determining the association of the lipoxygenase and AOS would be interesting to pursue because the hydroperoxide that is thought to be a natural substrate for guayule AOS is produced by the activity of a lipoxygenase (Song et al. 1993). Similar to Hevea rubber particles, the guayule rubber particle has vacuolar ATPase subunits associated with it. Several mitochondrial proteins were also found. Although some mitochondrial proteins have also been shown to localize in more than one subcellular compartment (Zhao et al. 2003), it is equally likely

that these proteins are persistent contaminants because of the large number of mitochondria per cell. Alternatively, if the rubber particle does in fact originate in the endoplasm reticulum, it is possible that its nascent site of origin is physically located adjacent to a mitochondrial attachment domain (Staehelin and Newcomb 2000), explaining the consistent copurification of mitochondrial proteins with rubber particles. Studies targeted to the nonmitochondrial proteins would be the first priority for further study in guayule.

Russian dandelion rubber particles had more than 50 different proteins associated with them. SRPP proteins were present in abundance. In addition to several stress-inducible proteins, there were ER- and vacuole-associated proteins, many different mitochondrial proteins, annexin, and more than 20 different cytoplasmic proteins. A lipoxygenase and a peroxidase were present, which is found in Hevea latex, but not associated with Hevea rubber particles. It will take time before the importance of all these proteins is sorted out. It is not clear why the Russian dandelion rubber particle, despite extensive washing, retains so many different proteins, in particular, so many mitochondrial proteins. Further analysis will involve manipulation of gene expression levels to determine the consequence on rubber phenotypes.

23.7 Key Proteins in Rubber Production

23.7.1 *cis*-Prenyltransferase (CPT)

Rubber transferase has CPT activity, catalyzing a condensation reaction of IPP units onto an APP initiator in the *cis* conformation to make long-chain rubber molecules (Fig. 23.1). In Hevea, rubber molecular weight varies from around 100,000 to 4,000,000 Da (Dennis and Light 1989), with an average of 1,000,000 Da. If rubber is a linear molecule, then the *cis*-prenyl transferase activity of rubber transferase, once initiated, would have to add on an average of 15,000 IPPs. If high molecular weight rubber is branched (Tarachiwin et al. 2005b, c), then the unit length would be considerably shortened, requiring about 400 IPPs. In either scenario, these are extremely long-chain products. CPTs are ubiquitous enzymes, found from microbes to mammals. They synthesize short-chain (C15), medium-chain (C50–55), and long-chain (C70–120) (Kharel et al. 2006), and presumably very long-chain (C2,000–300,000) products. None of the CPTs isolated so far have been shown to have the capacity for making very long-chain length polyisoprene. Remarkably, *cis*- and *trans*-prenyltransferase sequences and crystal structures are completely different (Fujihashi et al. 2001; Kharel and Koyama 2003).

Undecaprenyl diphosphate synthase is a CPT that catalyzes the synthesis of medium-chain length undecaprenyl diphosphate (C55), which serves as a glycosyl carrier lipid in bacteria (Koyama 1999). Yeast encodes an ER-localized CPT called dedol-PP synthase (RER2), which synthesizes dehydrodolichol diphosphate (dedol-PP) by condensation of IPP units onto FPP in a *cis* configuration (Sato et al. 1999). Dedol-PP is a long-chain polyprenol (C65–105) that is essential to protein glycosylation in the endoplasmic reticulum. Interestingly, another yeast dedol-PP synthase (SRT1) was identified and shown to target to lipid bodies (Sato et al. 2001). It is intriguing that in the yeast *Pichia pastoris*, the carbon and energy source supply impacted both the chain length of dolichol and its subcellular compartmentalization (Skoneczny et al. 2006). In addition, IPP substrate concentration has been shown to affect the final chain length of dolichols, similarly to rubber transferase (Ericsson et al. 1991). In plants, the first CPT cloned was from Arabidopsis (Oh et al. 2000). Arabidopsis CPT catalyzes the formation of long-chain dolichols (C120). It is predicted to be membrane associated and does not make very long-chain rubber.

The genes for two CPTs were cloned from Hevea, *HRT1* and *HRT2*; the predicted proteins are 92% identical (Asawatreatnakul et al. 2003). The two genes are predicted to encode hydrophilic proteins with a transmembrane domain in their N-termini. These two genes are expressed only in latex. Crude homogenates of HRT-overexpressing *Escherichia coli* cells were incubated with rubber particles to test if the recombinant

protein lysates have an impact on IPP incorporation. HRT1 had no effect. On the other hand, HRT2 with rubber particles stimulated IPP incorporation over rubber particles alone. Indeed IPP incorporation increased in an HRT2-dependent fashion. The rubber produced by HRT2 coincubated with rubber particles was of long-chain (10^3–10^4 Da) and very long-chain (10^5–10^6 Da). HRT2 alone produced only long-chain polyisoprene, similar to dolichols. The authors propose that HRT2 synthesizes dolichol length molecules, which are then further processed into long-chain rubber either by HRT2 in concert with rubber particle factors or rubber particle factors alone. Clearly more research is required to identify the rubber-synthesizing CPT.

23.7.2 Rubber Elongation Factor (REF)

The 14.6-kDa protein REF that is tightly associated with rubber particles in Hevea was first described by Dennis and Light (1989). It is also found as a noncovalent homotetramer of ~58 kDa (Czuppon et al. 1993; Goyvaerts et al. 1991). REF, also known as Hev b 1, is one of the major allergens in Hevea latex (Czuppon et al. 1993). Dennis and Light (1989) experimentally produced rubber particles with decreasing amounts of intact REF and showed a corresponding decrease in rubber biosynthetic activity. Unable to reconstitute rubber biosynthesis *in vitro* with REF, they showed that anti-REF antibodies inhibited rubber biosynthesis in rubber particles. This may be a direct or indirect effect. REF protein structure is predicted to have amphipathic alpha-helices (Dennis et al. 1989), which may be important for the overall structure of a rubber particle. There are at least two loci for *REF* in the Hevea genome (Sookmark et al. 2002). *REF* gene expression is higher in latex than in leaves (Han et al. 2000; Ko et al. 2003; Priya et al. 2007) and is markedly higher in higher latex yielding Hevea clones than in lower yielding ones (Priya et al. 2007). All these results point to an association of REF with rubber production.

The most definitive association of REF with rubber synthesis was made when we used a benzophenone-modified farnesyl diphosphate analogue to bind to the initiation site of a washed rubber particle (DeGraw et al. 2007; Xie et al. 2008). When rubber particles from Hevea were photoaffinity labeled with this analogue, REF was identified as a binding protein. Additional studies are required to determine REF's actual function. Any strategy to use REF to engineer for enhanced rubber production would have to take into account its highly allergenic nature.

23.7.3 Small Rubber Particle Protein (SRPP)

SRPP is a 22-kDa protein found tightly associated with rubber particles in Hevea and is a well-known latex allergen called Hev b 3 (Wagner et al. 1999). SRPP is predicted to be a hydrophobic protein (Oh et al. 1999) that appears to be posttranslationally glycosylated with *N*-acetylglucosamine (GlcNAc) residues (Gidrol et al. 1994). It has significant homology with REF overall (47%) (Lu et al. 1995), with local regions of greater homology (72%) (Oh et al. 1999). Wagner et al. (1999) demonstrated cross-reactivity of antibodies, but not all epitopes in REF and SRPP are the same. SRPP is involved in *in planta* latex coagulation by virtue of its GlcNAc binding to hevein, which is freed when lutoids burst (Gidrol et al. 1994; Wititsuwannakul et al. 2008a, b, c). The hevein acts as a multivalent bridge between rubber particles. Chitinase in the latex, by cleaving the GlcNAc moiety from SRPP, is an anticoagulation protein because its action prevents hevein binding and hence coagulation. Chitinase is also involved in defense against fungal invaders.

In Hevea, SRPP is more highly expressed in latex than leaves, and its expression is not stimulated by wounding or ethylene-releasing ethephon (Oh et al. 1999). Adding recombinant GST-SRPP to rubber particles increased IPP incorporation in a concentration-dependent manner, and poly- and monoclonal antibodies to SRPP inhibited incorporation. Furthermore, the recombinant protein present in a bacterial lysate produced polyisoprene. However, without molecular weight stan-

dards in their analysis, there is no certainty about the molecular weight, and there may have been other factors in the lysates as well. Considering SRPP as rubber transferase is problematic because not all rubber-producing species have SRPP (Singh et al. 2003b). Nonetheless, SRPP appears to be an important protein in rubber synthesis.

Although there are none in *Ficus* spp., there are SRPP homologues in guayule and Russian dandelion (Singh et al. 2003b; Kim et al. 2004). The guayule protein, called guayule homologue of SRPP (GHS), is 50% identical to Hevea SRPP and was shown to play a role in IPP incorporation (Kim et al. 2004). Although it is unclear if there is an effect on rubber molecular weight, recombinant GHS protein enhanced IPP incorporation in a concentration-dependent manner. From our proteomics analysis, there appear to be three SRPPs associated with the rubber particle in Russian dandelion. One protein that has distant similarity to SRPP is a chaperone protein from a protist, suggesting that SRPP may function as a chaperone, possibly for rubber transferase. Further characterization is forthcoming.

23.7.4 Allene Oxide Synthase (AOS)

AOS is the most abundant protein in guayule rubber particles. It comprises about 50% of the total protein in a particle. It was indirectly shown to be internal to the rubber particles and therefore inaccessible to proteases (Backhaus et al. 1991). Initially called rubber particle protein (RPP), and thought early on to be involved in rubber synthesis, guayule AOS is a P450 monooxygenase in the CYP74A family. As all P450s, it has a characteristic absorbance spectrum. Unlike most P450s, guayule AOS has unusual features. It does not require oxygen, NADPH, or a P450 reductase (Pan et al. 1995; Chapple 1998). In addition, guayule AOS is present at high levels (Pan et al. 1995), when normally P450s are not. Moreover, guayule AOS does not have a chloroplast or an obvious vacuole transit sequence (Pan et al. 1995; Song et al. 1993; Xu et al. 2006).

Lipid hydroperoxides produced by the action of lipoxygenases are converted by AOS into the unstable epoxide allene oxide (Fig. 23.2). AOS metabolizes hydroperoxides by intramolecular oxygen transfer. Both guayule and Russian dandelion rubber particles have associated lipoxygenases (Table 23.2), and rubber particles in all three species contain lipids (e.g., Siler et al. 1997), indicating that the associated machinery to produce AOS's substrate is colocated. The location of guayule AOS in parenchyma cells of the phloem is not a surprise, as the enzyme allene oxide cyclase, thought to be physically associated with AOS for metabolic channeling, is also found in phloem and parenchyma cells of vascular bundles in non-rubber-producing plants (Hause et al. 2000, 2003).

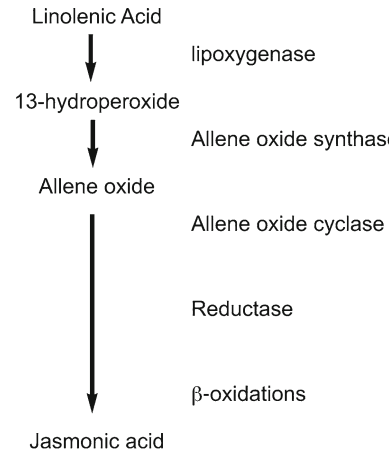

Fig. 23.2 Pathway of jasmonic acid synthesis starting from linolenic acid

It is of interest that one of the cyclopentyl metabolite products of AOS action is a precursor for jasmonic acid (JA). JA is a well-known and important signaling molecule in plant stress and defense responses and in normal development (Park et al. 2002; Balbi and Devoto 2008). The AOS enzymes in chloroplasts have been shown to catalyze the rate-limiting step in the synthesis of JA (Laudert et al. 1996). Recently, an AOS with a chloroplast transit sequence was isolated from Hevea leaves (Norton et al. 2007). It is most similar to the guayule AOS. It has been shown that treatment with JA stimulated laticifer formation (Hao and Wu 2000), which was inhibited by both a JA synthesis inhibitor and a lipoxygenase

inhibitor (Wu et al. 2002). Norton et al. (2007) showed that the normally JA-counteractive defense signaling molecule salicylic acid (SA) is a competitive inhibitor of the Hevea AOS. If AOS is in fact found in latex, this work suggests that there is a balancing act between SA signaling defense and simultaneously preventing laticifer differentiation, and JA stimulating differentiation. It would be interesting to see the effect of JA and SA on differentiation of guayule and Russian dandelion rubber-producing cells. Additionally, JA is involved in the redistribution of nutrients (Creelman and Mullet 1997), which may mean that it plays a positive role in recruiting fixed carbon to rubber-producing cells.

None of the possible reasons that JA would have a positive effect on rubber production explain why AOS would have evolved to be present at such high levels in guayule rubber particles, unless massive amounts of JA were required for the most beneficial effect. Guayule AOS did have the expected function *in vitro* (Pan et al. 1995), but what that function has to do directly with rubber synthesis remains cryptic. It is noteworthy that related AOSs in the CYP74 group have interesting activation parameters that depend on their state of aggregation (Hughes et al. 2006a, b), but with no direct connection apparent between AOS's activity and rubber production, the importance of this is not known. Although we know that guayule AOS has two predicted hydrophobic, transmembrane domains in the central region of the protein, with a third weakly predicted domain at the extreme C-terminus, we do not know if it aggregates in the rubber particle based on hydrophobic interactions. Studies of the role of AOS's function in rubber particles are necessary to solve its mysteries.

23.7.5 3-Hydroxy-3-Methylglutaryl-Coenzyme A Reductase (HMGR)

IPP is the precursor for all isoprenoids (Fig. 23.1). It is synthesized by two pathways in plants, the acetate/mevalonate (MEV) pathway in the cytoplasm and the methylerythritol 4-phosphate (MEP) pathway in plastids (cf. Lichtenthaler 1999). Exchange of isoprenoids, possibly IPP or FPP, is thought to occur between the two compartments (Nagata et al. 2002; Hemmerlin et al. 2003; Dudareva et al. 2005; Lichtenthaler 2007). HMGR is considered to be the key-regulatory step in IPP synthesis in the cytosol (Bach 1986). Our preliminary results demonstrate that it is crucially important for rubber quantity in Russian dandelion.

Hevea has three genes for HMGR, *hmg1*, *hmg2*, and *hmg3* (Chye et al. 1992). Only *hmg1* is expressed in latex, suggesting that it is associated with providing precursors for rubber synthesis. Overexpression of *hmg1* in tobacco resulted in increased production of sterols (Schaller et al. 1995), and overexpression of a truncated form of HMGR in tobacco likewise resulted in greater levels of total sterols (Chappell et al. 1995; Harker et al. 2003). Even though there is ample evidence that MEV and MEP pathway products move between the compartments (see above), Enfissi et al. (2005) showed that when genes for controlling enzymes were overexpressed in their respective compartments, no transcompartment enhancements in product levels were found. This suggests a complex control system. Although none of the HMGR overexpression transgenic lines had any apparent phenotypic aberrations, an Arabidopsis *hmg1*$^{-}$ mutant was dwarfed, senesced early, was male sterile, and had reduced sterol and triterpenoid levels (Suzuki et al. 2004). Our preliminary results suggest that overexpression of a truncated HMGR in Russian dandelion results in severalfold increase in rubber quantity. Overexpression of HMGR does not appear to have negative effects on plant growth and indeed may have a positive effect on rubber production, suggesting an attractive strategy for enhancing rubber through metabolic engineering.

Control of production of different classes of isoprenoids takes place when FPP is channeled into either the major end-product sterols or nonsterol isoprenoids, including sesquiterpenes, ubiquinone, heme, polyprenols, or prenylated proteins (Wentzinger et al. 2002). Feedback mechanisms regulate HMGR activity. Inhibition of squalene synthase (SQS), the first dedicated enzyme in the sterol biosynthesis pathway, stimulated HMGR activity (Wentzinger et al. 2002; Suzuki et al. 2004). Accordingly, transgenic lines

with two overexpressed genes, coding for truncated HMGR and a sterol methyltransferase (SMT1), had high levels of sterols (Holmberg et al. 2003). Downregulation of SQS or SMT1 in a rubber-producing plant may therefore achieve two purposes, decreasing carbon flow into a competing pathway and increasing carbon flow into rubber.

23.7.6 Allylic Diphosphate Synthases (APPS)

The first attempt to genetically engineer any industrial crop plant for improved rubber production was made with guayule. Because *in vitro* experiments on rubber particles showed that the rate of rubber biosynthesis depends on initiator concentration (Tanaka et al. 1995, 1996; Tangpakdee and Tanaka 1998; Castillon and Cornish 1999; Cornish 2001), the first target genes for our genetic engineering efforts encoded APPS enzymes. It was hypothesized that increasing the availability of APP initiators would increase the rate of rubber synthesis. Of course, as described above for FPP, APPs are used as starting materials for many other secondary compounds in plants, including growth regulators. Three different APPS genes were transformed into three different guayule lines and field trials performed to assess the impact of the transgenes on plant growth, resin and rubber (Veatch et al. 2005). Placed under constitutive promoters, the three genes encoded farnesyl diphosphate synthase (FPPS) (Koyama et al. 1993), geranylgeranyl diphosphate synthase (GGPPS) (Ohnuma et al. 1994), and a variant of GGPPS, hexa-heptaprenyl diphosphate synthase (HHPPS) (Ohnuma et al. 1996). No significant differences were found in dry weights at the end of 2 years of field growth between the transgenic and control lines, indicating that there was no massive disturbance of growth patterns resulting from the overexpression of APPSs. Otherwise, results are difficult to interpret because independent transgenic events were grouped, and there were insufficient replicates of each line, including controls. However, although there was more resin in the APPS overexpressing plants, apparently there was no effect on rubber amount. The enhanced APP was channeled into resins, which in guayule contain various terpenes. The impact on sterols was not assessed. The end result of this groundbreaking field trial was that enhancing initiator levels is insufficient for enhancement of rubber production, probably because IPP became limiting. At present, tissue from individual lines that had corresponding controls in the later field trial is being assessed for prenyltransferase activity and rubber quantity and quality to see if any correlations exist. Preliminary analysis suggests that when results from independent lines are dissected out, some lines contain a significant positive effect on prenyltransferase activity and on the rubber phenotype.

23.8 Biotechnological Approaches to Engineering Rubber Production

The need for increasing quantities of natural rubber, for use in critical applications for which synthetic elastomers are not suited, far outweighs the current supply. Recently, guayule latex has been commercialized in the southwestern US as an alternative to Hevea latex, especially for medical devices. Interest in development of Russian dandelion as a commercial rubber-producing crop is also increasing. While expanded plantings of Hevea and guayule are underway, genetic improvements of rubber-producing plants hold the most significant and efficient potential for dramatic increases in rubber yields.

Genetic improvements via metabolic engineering may prove advantageous in that transformation systems have been developed and efficiencies are improving (e.g., Dong et al. 2006). Natural rubber is a metabolic endpoint, i.e., not catabolized *in planta*, simplifying strategies. Finally, introduction of genetically modified industrial plants may be more broadly acceptable than plants consumed as food. Initial metabolic engineering of the IPP-associated pathways in plants has been accomplished, from which important lessons have been learned. One lesson is that the unpredictability inherent in engineering a complex pathway demands thorough phenotypic

and metabolomic analysis of each independent transgenic line (McCaskill and Croteau 1998; Enfissi et al. 2005; Fraser et al. 2007). Another is that coordinate expression of transgenes and native genes is crucial to success (Holmberg et al. 2003), perhaps pointing to the use of transcription factors for a "top-down" approach (McCaskill and Croteau 1999). Other improvements in agronomic characteristics may be realized as well with a biotech strategy, also based on the recent characterization of the plastome sequence of guayule (Kumar et al. 2009), which paves the way to transfer complete pathways into plastids.

Using marker-assisted breeding to improve rubber production is a complementary and equally important approach. These efforts have begun in Hevea (e.g., Lieberei 2007). The mapping of the genomes of guayule (2n = 36) and Russian dandelion (2n = 16) is at present hampered by a dearth of sexually reproducing, diploid germplasm. In addition, Russian dandelion and guayule are both self-incompatible. Nevertheless, while we acquire the germplasm required for genetic mapping, our EST collections can be used as the basis of finding sequence-specific markers associated with high and low yielding lines. Genetic maps with rubber-associated and agronomic traits are important goals.

The everlasting question is why plants make the metabolic dead-end product rubber? Understanding the role it plays in conferring a selective advantage, if any, would aid in design of strategies for improvement of rubber-producing crops. Considering the susceptibility of Hevea to disease (Lieberei 2007) and Russian dandelion to herbivory, insects, fungal pathogens, nematodes, aphids, and ants (Krotkov 1945), rubber is not providing a perfect defense system. Perhaps, it was evolutionarily good enough. Even though organisms in all kingdoms make a multitude of products from IPP, rubber production is found only in plants and only in the dicotyledons. In the dicotyledons, it appears to have arisen many times. Perhaps it is the relative harmlessness of rubber compared to other isoprenoid-derived products that is the key point. Why plants make rubber remains a mystery.

Acknowledgments We acknowledge Dr. Katrina Cornish for her pioneering work and getting most of us started in this research field. We thank the members of our research laboratories for the work we have reviewed above and Dr. Terry Coffelt of ARS-ALARC, Maricopa, AZ, USA, for graciously providing guayule shrubs. This work was supported by NSF Plant Genome Research Grant DBI 0321690, USDA-CSREES-IFAFS Grant, and USDA-ARS Research project, *Development of Domestic Natural Rubber-Producing Industrial Crops through Biotechnology* at WRRC, Albany, CA, USA.

References

Altschul SF, Gish W, Miller W et al (1990) Basic local alignment search tool. J Mol Biol 215:403–410

Archer BL, Audley BG (1987) New aspects of rubber biosynthesis. Bot J Linn Soc 94:181–196

Archer BL, Audley BG, Cockbain EG et al (1963) The biosynthesis of rubber. Incorporation of mevalonate and isopentenyl pyrophosphate into rubber by *Hevea brasiliensis*-latex fractions. Biochem J 89:565–574

Asawatreratanakul K, Zhang YW, Wititsuwannakul D et al (2003) Molecular cloning, expression and characterization of cDNA encoding *cis*-prenyltransferases from *Hevea brasiliensis*. A key factor participating in natural rubber biosynthesis. Eur J Biochem 270: 4671–4680

Audley BG, Archer BL (1988) Biosynthesis of rubber. In: Roberts AD (ed) Natural rubber science and technology. Oxford University Press, London, p 35

Bach TJ (1986) Hydroxymethylglutaryl-CoA reductase, a key enzyme in phytosterol synthesis? Lipids 21: 82–88

Backhaus RA, Cornish K, Chen SF et al (1991) Purification and characterization of an abundant rubber particle protein from guayule. Phytochemistry 30:2493–2497

Backhaus RA, Walsh S (1983) The ontogeny of rubber formation in guayule, *Parthenium argentatum* Gray. Bot Gaz 144:391–400

Bahri ARS, Hamzah S (1996) Immunocytochemical localisation of rubber membrane protein in *Hevea* latex. J Nat Rubb Res 11:88–95

Balbi V, Devoto A (2008) Jasmonate signalling network in *Arabidopsis thaliana*: crucial regulatory nodes and new physiological scenarios. New Phytol 177: 301–318

Blackbourn HD, Battey NH (1993) Annexin-mediated secretory vesicle aggregation in plants. Physiol Plant 89:27–32

Bobilioff W (1925) Observations on latex vessels in the living condition. Arch Rubbercultuur 9:313–342

Bonner J (1943) Effects of temperature on rubber accumulation by the guayule plant. Bot Gaz 105:233–243

Bonner J, Galston AW (1947) The physiology and biochemistry of rubber formation in plants. Bot Gaz 13:543–596

Castillon J, Cornish K (1999) Regulation of initiation and polymer molecular weight of *cis*-1,4-polyisoprene synthesized in vitro by particles isolated from *Parthenium argentatum* (Gray). Phytochemistry 51:43–51

Chappell J, Wolf F, Proulx J et al (1995) Is the reaction catalyzed by 3-hydroxy-3-methylglutaryl coenzyme a reductase a rate-limiting step for isoprenoid biosynthesis in plants? Plant Physiol 109:1337–1343

Chapple C (1998) Molecular genetic analysis of plant cytochrome P450-dependent monooxygenases. Annu Rev Plant Physiol Plant Mol Biol 49:311–343

Cornish K (2001) Similarities and differences in rubber biochemistry among plant species. Phytochemistry 57:1123–1134

Cornish K, Backhaus RA (1990) Rubber transferase activity in rubber particles of guayule. Phytochemistry 29:3809–3813

Cornish K, Backhaus RA (2003) Induction of rubber transferase activity in guayule (*Parthenium argentatum* Gray) by low temperatures. Industrial Crop Prod 17:83–92

Cornish K, Siler DJ (1995) Effect of different allylic diphosphates on the initiation of new rubber molecules and on *cis*-1,4-polyisoprene biosynthesis in Guayule (*Parthenium argentatum* Gray). J Plant Physiol 147:301–305

Cornish K, Siler DJ (1996) Characterization of *cis*-prenyl transferase activity localised in a buoyant fraction of rubber particles from *Ficus elastica* latex. Plant Physiol Biochem 34:377–384

Cornish K, Siler DJ, Grosjean OK et al (1993) Fundamental similarities in rubber particle architecture and function in three evolutionarily divergent species. J Nat Rubber Res 8:275–285

Cornish K, Wood DF (2002) Visualization of the malleability of the rubber core of rubber particles from *Parthenium argentatum* Gray and other rubber-producing species under extremely cold temperatures. J Polym Environ 10:155–162

Cornish K, Wood DF, Windle JJ (1999) Rubber particles from four different species, examined by transmission electron microscopy and electron-paramagnetic-resonance spin labeling, are found to consist of a homogeneous rubber core enclosed by a contiguous, monolayer biomembrane. Planta 210:85–96

Creelman RA, Mullet JE (1997) Biosynthesis and action of jasmonates in plants. Annu Rev Plant Physiol Plant Mol Biol 48:355–381

Chye ML, Tan CT, Chua HH (1992) Three genes encode 3-hydroxy-3-methylglutaryl-coenzyme A reductase in *Hevea brasiliensis*: *hmg1* and *hmg3* are differentially expressed. Plant Mol Biol 19:473–484

Czuppon AB, Chen Z, Rennert S et al (1993) The rubber elongation factor of rubber trees (*Hevea brasiliensis*) is the major allergen in latex. J Allergy Clin Immunol 92:690–697

da Costa BM, Keasling JD, Cornish K (2005) Regulation of rubber biosynthetic rate and molecular weight in *Hevea brasiliensis* by metal cofactor. Biomacromolecules 6:279–289

da Costa BM, Keasling JD, McMahan CM et al (2006) Magnesium ion regulation of *in vitro* rubber biosynthesis by *Parthenium argentatum* Gray. Phytochemistry 67:1621–1628

de Fay E, Hebant C, Jacob JL (1989) Cytology and cytochemistry of the laticifer system. In: d'Auzac J, Jacob JL, Chrestin H (eds) Physiology of rubber tree latex. CRC Press, Boca Raton, pp 15–29

DeGraw AJ, Zhao Z, Strickland CL et al (2007) A photoactive isoprenoid diphosphate analogue containing a stable phosphonate linkage: synthesis and biochemical studies with prenyltransferases. J Org Chem 72: 4587–4595

Delmar DP, Potikha TS (1997) Structures and functions of annexins in plants. Cell Mol Life Sci 53:546–553

Dennis MS, Henzel WJ, Bell J et al (1989) Amino acid sequence of rubber elongation factor protein associated with rubber particles in *Hevea* latex. J Biol Chem 264:18618–18626

Dennis MS, Light DR (1989) Rubber elongation factor from *Hevea brasiliensis*. Identification, characterization, and role in rubber biosynthesis. J Biol Chem 264:18608–18617

Dong N, Montanez B, Creelman RA et al (2006) Low light and low ammonium are key factors for guayule leaf tissue shoot organogenesis and transformation. Plant Cell Rep 25:26–34

Dudareva N, Andersson S, Orlova I et al (2005) The nonmevalonate pathway supports both monoterpene and sesquiterpene formation in snapdragon flowers. Proc Natl Acad Sci USA 102:933–938

Enfissi EM, Fraser PD, Lois LM et al (2005) Metabolic engineering of the mevalonate and non-mevalonate isopentenyl diphosphate-forming pathways for the production of health-promoting isoprenoids in tomato. Plant Biotechnol J 3:17–27

Ericsson J, Thelin A, Chojnacki T et al (1991) Characterization and distribution of *cis*-prenyl transferase participating in liver microsomal polyisoprenoid biosynthesis. Eur J Biochem 202:789–796

Fraser PD, Enfissi EM, Halket JM et al (2007) Manipulation of phytoene levels in tomato fruit: effects on isoprenoids, plastids, and intermediary metabolism. Plant Cell 19:3194–3211

Fujihashi M, Zhang YW, Higuchi Y et al (2001) Crystal structure of *cis*-prenyl chain elongating enzyme, undecaprenyl diphosphate synthase. Proc Natl Acad Sci USA 98:4337–4342

Gidrol X, Chrestin H, Mounoury G et al (1988) Early activation by ethylene of the tonoplast H-pumping ATPase in the latex from *Hevea brasiliensis*. Plant Physiol 86:899–903

Gidrol X, Chrestin H, Tan HL et al (1994) Hevein, a lectin-like protein from *Hevea brasiliensis* (rubber tree) is involved in the coagulation of latex. J Biol Chem 269:9278–9283

Goyvaerts E, Dennis M, Light D et al (1991) Cloning and sequencing of the cDNA encoding the rubber elongation factor of *Hevea brasiliensis*. Plant Physiol 97: 317–321

Han KH, Shin DH, Yang J et al (2000) Genes expressed in the latex of *Hevea brasiliensis*. Tree Physiol 20: 503–510

Hao BZ, Wu JL (2000) Laticifer differentiation in *Hevea brasiliensis*: induction by exogenous jasmonic acid and linolenic acid. Annals Bot 85:37–43

Harker M, Holmberg N, Clayton JC et al (2003) Enhancement of seed phytosterol levels by expression of an N-terminal truncated *Hevea brasiliensis* (rubber tree) 3-hydroxy-3-methylglutaryl-CoA reductase. Plant Biotechnol J 1:113–121

Hassid WZ, McRary WL, Dore WH et al (1944) Inulin in guayule, *Parthenium argentatum* Gray. J Am Chem Soc 66:1970–1972

Hause B, Hause G, Kutter C et al (2003) Enzymes of jasmonate biosynthesis occur in tomato sieve elements. Plant Cell Physiol 44:643–648

Hause B, Stenzel I, Miersch O et al (2000) Tissue-specific oxylipin signature of tomato flowers: allene oxide cyclase is highly expressed in distinct flower organs and vascular bundles. Plant J 24:113–126

Hemmerlin A, Hoeffler JF, Meyer O et al (2003) Cross-talk between the cytosolic mevalonate and the plastidial methylerythritol phosphate pathways in tobacco bright yellow-2 cells. J Biol Chem 278:26666–26676

Holmberg N, Harker M, Wallace AD et al (2003) Co-expression of N-terminal truncated 3-hydroxy-3-methylglutaryl CoA reductase and C24-sterol methyltransferase type 1 in transgenic tobacco enhances carbon flux towards end-product sterols. Plant J 36:12–20

Hughes RK, Belfield EJ, Ashton R et al (2006a) Allene oxide synthase from *Arabidopsis thaliana* (CYP74A1) exhibits dual specificity that is regulated by monomer-micelle association. FEBS Lett 580:4188–4194

Hughes RK, Belfield EJ, Muthusamay M et al (2006b) Characterization of *Medicago truncatula* (barrel medic) hydroperoxide lyase (CYP74C3), a water-soluble detergent-free cytochrome P450 monomer whose biological activity is defined by monomer-micelle association. Biochem J 395:641–652

Hundertmark M, Hincha DK (2008) LEA (Late Embryogenesis Abundant) proteins and their encoding genes in *Arabidopsis thaliana*. BMC Genomics 9:118. doi:10.1186/1471-2164-9-118

Kelly KM, Van Staden J (1991) A preliminary study of the carbohydrate metabolism in *Parthenium argentatum*. Bioresource Technol 35:127–132

Kharel Y, Koyama T (2003) Molecular analysis of *cis*-prenyl chain elongating enzymes. Nat Prod Rep 20: 111–118

Kharel Y, Takahashi S, Yamashita S et al (2006) Manipulation of prenyl chain length determination mechanism of *cis*-prenyltransferase. FEBS J 273: 647–656

Kim IJ, Ryu SB, Kwak YS et al (2004) A novel cDNA from *Parthenium argentatum* Gray enhances the rubber biosynthetic activity in vitro. J Exp Bot 55: 377–385

Ko JH, Chow KS, Han KH (2003) Transcriptome analysis reveals novel features of the molecular events occurring in the laticifers of *Hevea brasiliensis* (para rubber tree). Plant Mol Biol 53:479–492

Koyama T (1999) Molecular analysis of prenyl chain elongating enzymes. Biosci Biotechnol Biochem 63:1671–1676

Koyama T, Obata S, Osabe M et al (1993) Thermostable farnesyl diphosphate synthase of *Bacillus stearothermophilus*—molecular cloning, sequence determination, overproduction and purification. J Biochem 113:355–363

Krotkov G (1950) Changes in the carbohydrate metabolism of *Taraxacum kok-saghyz* during the first and second years of growth. Plant Physiol 25:169–180

Krotkov GA (1945) A review of literature on *Taraxacum kok-saghyz*. Bot Rev 11:417–461

Kumar S, Hahn FM, McMahan CM, Cornish K, Whalen MC (2009) Comparative analysis of the complete sequence of the plastid genome of *Parthenium argentatum* and identification of DNA barcodes to differentiate *Parthenium* species and lines. BMC Plant Biol 9:131. doi:10.1186/1471-2229-9-131

Laudert D, Pfannschmidt U, Lottspeich F et al (1996) Cloning, molecular and functional characterization of *Arabidopsis thaliana* allene oxide synthase (CYP 74), the first enzyme of the octadecanoid pathway to jasmonates. Plant Mol Biol 31:323–335

Lichtenthaler HK (1999) The 1-deoxy-D-xylulose-5-phosphate pathway of isoprenoid biosynthesis in plants. Annu Rev Plant Physiol Plant Mol Biol 50:47–65

Lichtenthaler HK (2007) Biosynthesis, accumulation and emission of carotenoids, alpha-tocopherol, plastoquinone, and isoprene in leaves under high photosynthetic irradiance. Photosynth Res 92:163–179

Lieberei R (2007) South American leaf blight of the rubber tree (*Hevea* spp.): new steps in plant domestication using physiological features and molecular markers. Annals Bot 100:1125–1142

Lu LJ, Kurup VP, Hoffman DR et al (1995) Characterization of a major latex allergen associated with hypersensitivity in spina bifida patients. J Immunol 155:2721–2728

Madhaven S, Greenblatt GA, Foster MA et al (1989) Stimulation of isopentenyl pyrophosphate incorporation into polyisoprene in extracts from guayule plants (*Parthenium argentatum* Gray) by low-temperature and 2-(3,4-dichlorophenoxy)triethylamine. Plant Physiol 89:506–511

Mau CJ, Garneau S, Scholte AA et al (2003) Protein farnesyltransferase inhibitors interfere with farnesyl diphosphate binding by rubber transferase. Eur J Biochem 270:3939–3945

McCaskill D, Croteau R (1998) Some caveats for bioengineering terpenoid metabolism in plants. Trends Biotechnol 16:349–355

McCaskill D, Croteau R (1999) Strategies for bioengineering the development and metabolism of glandular tissues in plants. Nat Biotechnol 17:31–36

Mooibroek H, Cornish K (2000) Alternative sources of natural rubber. Appl Microbiol Biotechnol 53: 355–365

Nagata N, Suzuki M, Yoshida S et al (2002) Mevalonic acid partially restores chloroplast and etioplast development in *Arabidopsis* lacking the non-mevalonate pathway. Planta 216:345–350

Norton G, Pappusamy A, Yusof F et al (2007) Characterisation of recombinant *Hevea brasiliensis* allene oxide synthase: effects of cycloxygenase inhibitors, lipoxygenase inhibitors and salicylates on enzyme activity. Plant Physiol Biochem 45:129–138

Oh SK, Han KH, Ryu SB et al (2000) Molecular cloning, expression, and functional analysis of a *cis*-prenyltransferase from *Arabidopsis thaliana.* Implications in rubber biosynthesis. J Biol Chem 275:18482–18488

Oh SK, Kang H, Shin DH et al (1999) Isolation, characterization, and functional analysis of a novel cDNA clone encoding a small rubber particle protein from *Hevea brasiliensis*. J Biol Chem 274:17132–17138

Ohnuma S, Hirooka K, Hemmi H et al (1996) Conversion of product specificity of archaebacterial geranylgeranyldiphosphate synthase. J Biol Chem 271:18831–18837

Ohnuma S, Suzuki M, Nishino T (1994) Archaebacterial ether-linked lipid biosynthetic gene—expression cloning, sequencing and characterization of geranylgeranyldiphosphate synthase. J Biol Chem 269:14792–14797

Ohya N, Tanaka Y, Wititsuwannakul D et al (2000) Activity of rubber transferase and rubber particle size in *Hevea* latex. J Rubber Res 3:214–221

Pan Z, Durst F, Werck-Reichhart D et al (1995) The major protein of guayule rubber particles is a cytochrome P450. Characterization based on cDNA cloning and spectroscopic analysis of the solubilized enzyme and its reaction products. J Biol Chem 270:8487–8494

Park JH, Halitschke R, Kim HB et al (2002) A knock-out mutation in allene oxide synthase results in male sterility and defective wound signal transduction in *Arabidopsis* due to a block in jasmonic acid biosynthesis. Plant J 31:1–12

Popovici H (1926) Contribution à l'etude cytologique des lacticifers. Comp Rend Acad Sci Paris 183:143–145

Priya P, Venkatachalam P, Thulaseedharan A (2007) Differential expression pattern of rubber elongation factor (REF) mRNA transcripts from high and low yielding clones of rubber tree (*Hevea brasiliensis* Muell. Arg.). Plant Cell Rep 26:1833–1838

Sato M, Fujisaki S, Sato K et al (2001) Yeast *Saccharomyces cerevisiae* has two *cis*-prenyltransferases with different properties and localizations. Implication for their distinct physiological roles in dolichol synthesis. Genes Cells 6:495–506

Sato M, Sato K, Nishikawa S et al (1999) The yeast *RER2* gene, identified by endoplasmic reticulum protein localization mutations, encodes *cis*-prenyltransferase, a key enzyme in dolichol synthesis. Mol Cell Biol 19:471–483

Schaller H, Grausem B, Benveniste P et al (1995) Expression of the *Hevea brasiliensis* (H.B.K.) Mull. Arg. 3-hydroxy-3-methylglutaryl-coenzyme A reductase 1 in tobacco results in sterol overproduction. Plant Physiol 109:761–770

Scott DJ, da Costa BM, Espy SC et al (2003) Activation and inhibition of rubber transferases by metal cofactors and pyrophosphate substrates. Phytochemistry 64:123–134

Seals DF, Parrish ML, Randall SK (1994) A 42-kilodalton annexin-like protein is associated with plant vacuoles. Plant Physiol 106:1403–1412

Siler DJ, Goodrich-Tanrikulu M, Cornish K, Stafford AE, McKeon TA (1997) Composition of rubber particles of *Hevea brasiliensis, Parthenium argentatum, Ficus elastica*, and *Euphorbia lactiflua* indicates unconventional surface structure. Plant Physiol Biochem 35:881–889

Singh AP, Wi SG, Chung GC et al (2003a) The micromorphology and protein characterization of rubber particles in *Ficus carica*, *Ficus benghalensis* and *Hevea brasiliensis*. J Exp Bot 54:985–992

Singh AP, Wi SG, Kang H et al (2003b) Simple and rapid methods for SEM observation and TEM immunolabeling of rubber particles. J Histochem Cytochem 51:1105–1108

Skoneczny M, Kludkiewicz B, Swiezewska E et al (2006) Activity of *Pichia pastoris* alternative *cis*-prenyltransferase is correlated with proliferation of peroxisomes. Cell Biol Int 30:122–126

Song WC, Funk CD, Brash AR (1993) Molecular cloning of an allene oxide synthase: a cytochrome P450 specialized for the metabolism of fatty acid hydroperoxides. Proc Natl Acad Sci USA 90:8519–8523

Sookmark U, Pujade-Renaud V, Chrestin H et al (2002) Characterization of polypeptides accumulated in the latex cytosol of rubber trees affected by the tapping panel dryness syndrome. Plant Cell Physiol 43:1323–1333

Staehelin LA, Newcomb EH (2000) Membrane structure and membraneous organelles. In: Buchanan BB, Gruissem W, Jones RL (eds) Biochemistry and molecular biology of plants. American Society of Plant Physiologists, Rockville, pp 2–50

Sussman GL, Beezhold DH, Kurup VP (2002) Allergens and natural rubber proteins. J Allergy Clin Immunol 110:S33–S39

Suzuki M, Kamide Y, Nagata N et al (2004) Loss of function of 3-hydroxy-3-methylglutaryl coenzyme A reductase 1 (HMG1) in Arabidopsis leads to dwarfing, early senescence and male sterility, and reduced sterol levels. Plant J 37:750–761

Tait JF, Sakata M, McMullen BA et al (1988) Placental anticoagulant proteins: isolation and comparative characterization four members of the lipocortin family. Biochemistry 27:6268–6276

Tanaka Y, Aikhwee E, Ohya N et al (1996) Initiation of rubber biosynthesis in *Hevea brasiliensis*: characterization of initiating species by structural analysis. Phytochemistry 41:1501–1505

Tanaka Y, Kawahara S, Aik-Hwee E et al (1995) Initiation of biosynthesis in *cis* polyisoprenes. Phytochemistry 39:779–784

Tangpakdee J, Tanaka Y (1998) Long-chain polyprenols and rubber in young leaves of *Hevea brasiliensis*. Phytochemistry 48:447–450

Tarachiwin L, Sakdapipanich JT, Tanaka Y (2005a) Relationship between particle size and molecular weight of rubber from *Hevea brasiliensis*. Rubber Chem Technol 78:694–704

Tarachiwin L, Sakdapipanich J, Ute K et al (2005b) Structural characterization of alpha-terminal group of natural rubber. 1. Decomposition of branch-points by lipase and phosphatase treatments. Biomacromolecules 6:1851–1857

Tarachiwin L, Sakdapipanich J, Ute K et al (2005c) Structural characterization of alpha-terminal group of natural rubber. 2. Decomposition of branch-points by phospholipase and chemical treatments. Biomacromolecules 6:1858–1863

van Beilen JB, Poirier Y (2007) Guayule and Russian dandelion as alternative sources of natural rubber. Crit Rev Biotechnol 27:217–231

Veatch ME, Ray DT, Mau CJD et al (2005) Growth, rubber and resin evaluation of two-year old transgenic guayule. Ind Crop Prod 22:65–74

Wagner B, Krebitz M, Buck D et al (1999) Cloning, expression, and characterization of recombinant Hev b 3, a *Hevea brasiliensis* protein associated with latex allergy in patients with spina bifida. J Allergy Clin Immunol 104:1084–1092

Wentzinger LF, Bach TJ, Hartmann MA (2002) Inhibition of squalene synthase and squalene epoxidase in tobacco cells triggers an up-regulation of 3-hydroxy-3-methylglutaryl coenzyme A reductase. Plant Physiol 130:334–346

Wititsuwannakul R, Pasitkul P, Jewtragoon P et al (2008a) *Hevea* latex lectin binding protein in C-serum as an anti-latex coagulating factor and its role in a proposed new model for latex coagulation. Phytochemistry 69:656–662

Wititsuwannakul R, Pasitkul P, Kanokwiroon K et al (2008b) A role for a *Hevea* latex lectin-like protein in mediating rubber particle aggregation and latex coagulation. Phytochemistry 69:339–347

Wititsuwannakul R, Rukseree K, Kanokwiroon K et al (2008c) A rubber particle protein specific for *Hevea* latex lectin binding involved in latex coagulation. Phytochemistry 69:1111–1118

Wood DF, Cornish K (2000) Microstructure of purified rubber particles. Int J Plant Sci 161:435–445

Wu JL, Hao BZ, Tan HY (2002) Wound-induced differentiation in *Hevea brasiliensis* shoots mediated by jasmonic acid. J Nat Rubber Res 5:53–63

Xie W, McMahan CM, Degraw AJ et al (2008) Initiation of rubber biosynthesis: in vitro comparisons of benzophenone-modified diphosphate analogues in three rubber-producing species. Phytochemistry 69: 2539–2545

Xu Y, Ishida H, Reisen D, Hanson MR (2006) Upregulation of a tonoplast-localized cytochrome P450 during petal senescence in *Petunia inflata*. BMC Plant Biol 6. doi:10.1186/1471-2229-6-8

Yamaguchi T, Minami E, Ueki J et al (2005) Elicitor-induced activation of phospholipases plays an important role for the induction of defense responses in suspension-cultured rice cells. Plant Cell Physiol 46:579–587

Yeang HY, Yip E, Hamzah S (1995) Characterization of zone 1 and zone 2 rubber particles in *Hevea brasiliensis* latex. J Nat Rubber Res 10:108–123

Zhao J, Onduka T, Kinoshita JY et al (2003) Dual subcellular distribution of cytochrome b5 in plant, cauliflower, cells. J Biochem 133:115–121

24

Occurrence of Two Acetoacetyl-Coenzyme A Thiolases with Distinct Expression Patterns and Subcellular Localization in Tobacco

Laurent Wentzinger, Esther Gerber, Thomas J. Bach, and Marie-Andrée Hartmann

Abstract

Acetoacetyl-coenzyme A thiolase (AACT, EC 2.3.1.9) catalyzes the condensation of two acetyl-CoA units into acetoacetyl-CoA. By screening a tobacco (*Nicotiana tabacum* L.) cDNA library using a radish probe, we isolated two genes encoding an AACT. The deduced protein sequences, referred to as *Nt*AACT1 and *Nt*AACT2, were found to be 77% identical and to share high homologies with other AACTs. Here, we report that both *NtAACTs* exhibited distinct expression patterns *in planta* and that the enzymes localize to separate cell compartments, suggesting different metabolic functions. At its C-terminus, *Nt*AACT1 bears an SSL motif corresponding to a peroxisomal targeting signal of type 1. We present evidence that *Nt*AACT1 is readily imported into glyoxysomes by demonstrating *in vivo* colocalization of the chimeric proteins, GFP-*Nt*AACT1 and RFP-SKL, in transiently transformed tobacco BY-2 cells. The importance of the SSL motif was stressed by the absence of glyoxysomal delivery of the fusion protein lacking the tripeptide. In contrast, *Nt*AACT2 is clearly a soluble enzyme, with no obvious targeting signal to a defined cell membrane compartment. Its participation in isoprenoid biosynthesis via the mevalonate pathway was attested by potato virus X-induced gene silencing

L. Wentzinger
Actelion Pharmaceuticals Ltd, Allschwil, Switzerland

E. Gerber
Department of Genetic Engineering,
Deinove Company, Paris, France

T.J. Bach (✉) • M.-A. Hartmann
Institut de Biologie Moléculaire des Plantes
(CNRS UPR 2357), Département "Réseaux
métaboliques", Université de Strasbourg,
28 Rue Goethe, Strasbourg F-67083, France
e-mail: bach@unistra.fr

T.J. Bach and M. Rohmer (eds.), *Isoprenoid Synthesis in Plants and Microorganisms: New Concepts and Experimental Approaches*, DOI 10.1007/978-1-4614-4063-5_24,

experiments in *Nicotiana benthamiana* plants. Silencing of endogenous *NbAACT2* was shown indeed to trigger a 50% reduction in the levels of sterol biosynthetic precursors. A spatiotemporal study of expression patterns of both genes *in planta* indicated that *NtAACT2* was expressed throughout the plant, but more effectively in young tissues. In contrast, *NtAACT1* displayed a significant expression only in senescent leaves and early stages of germination and appears to be functional in the glyoxysomal/peroxisomal β-oxidation of fatty acids, catalyzing the last step.

Keywords
Acetoacetyl-CoA thiolase (AACT) • *Nicotiana tabacum* • Tobacco BY-2 cells • Virus-induced gene silencing (VIGS) • Squalene synthase (SQS) • Peroxisomal/glyoxysomal localization • Colocalization • GFP and RFP fusion proteins • Confocal microscopy • qPCR

24.1 Introduction

Acetoacetyl-CoA thiolase (AACT) (or acetyl-CoA acetyltransferase, EC 2.3.1.9.) catalyzes a Claisen-type condensation of two acetyl-CoA units to form acetoacetyl-CoA (cf. Meriläinen et al. 2009). This reaction has been recognized as the first step in the classical acetate/mevalonate (MVA) pathway occurring in the cell cytoplasm and leading to the synthesis of a vast array of isoprenoid compounds and derivatives such as sterols, dolichols, the side chain of ubiquinone or farnesylated proteins. In this pathway, 3-hydroxy-3-methylglutaryl CoA reductase (HMGR) plays a key role. In mammalian cells, this enzyme constitutes the major limiting step in cholesterol biosynthesis (Goldstein and Brown 1990). In plants, HMGR is encoded by a multigene family (Enjuto et al. 1994, 1995; cf. Stermer et al. 1994; Bach 1995; see also elsewhere in this volume). It has been recently proposed that individual HMGR isoforms might be involved in the synthesis of specific classes of isoprenoids within distinct metabolic channels or metabolons (Chappell 1995; Weissenborn et al. 1995). Sterols, as a mixture of mainly sitosterol, stigmasterol, and 24-methylcholesterol, represent the major end-products of this multibranched pathway, but what controls the whole pathway is still far from being understood. In higher plant cells, HMGR also participates in regulating the carbon flux toward sterols (Gondet et al. 1994; Schaller et al. 1995; Chappell et al. 1995), but other enzymes might play a role. In contrast to HMGR, comparably little attention has been paid to AACT. In yeast (Servouse and Karst 1986; Dimster-Denk and Rine 1996) as well as in mammals (Honda et al. 1998), a sterol-mediated feedback control of AACT has been reported. Acetyl-CoA, the substrate of AACT, is also an important intermediate for fatty acid biosynthesis. Competition between sterols and fatty acids for common pools of acetyl-CoA implies a tight regulation of carbon flux through each pathway. To get more insights into the role played by AACT in controlling the plant sterol pathway in tobacco, a prerequisite was to isolate the corresponding gene. The first gene encoding a plant AACT was previously isolated from radish by functional complementation of the *Saccharomyces cerevisiae erg10A* mutant (Vollack and Bach 1996). By screening a tobacco cDNA library for homologous sequences with the radish AACT as a probe, we isolated two distinct genes, hereafter referred as *NtAACT1* and *NtAACT2*. Both genes were shown to encode thiolases, with many homologies to AACTs isolated from other organisms (cf. Peretó et al. 2005). Here, we show that *NtAACT1* and *NtAACT2* exhibit distinct expression patterns, in separate cell compartments, suggesting that they are involved in different metabolic pathways. In another study, started

independently, the corresponding AACT genes were cloned and characterized from *Arabidopsis thaliana* (Ahumada et al. 2008). In this chapter, we focus on studying the putatively regulatory role of AACT in the sterol pathway by using a virus-induced gene silencing (VIGS) approach in *Nicotiana benthamiana*, also in comparison with silencing of squalene synthase (SQS), catalyzing the first committed step in phytosterol and triterpene biosynthesis.

24.2 Results

24.2.1 Isolation and Sequence Analysis of Two Tobacco cDNA Encoding AACT

A radish cDNA sequence encoding a cytosolic AACT (Vollack and Bach 1996) was used as a probe to screen for homologous sequences from a *Nicotiana tabacum* L. cDNA library. Nine positive clones were isolated. Sequence analysis indicated two populations. The first one was represented by a full-length cDNA with an open reading frame of 1,212 bp (GenBank accession number AY748245), encoding a polypeptide of 404 amino acids with a calculated molecular mass of 41.3 kD. The second one contained a cDNA with a 1,242-bp open reading frame (GenBank accession number AY748246), encoding a protein of 414 amino acids with a molecular mass of 42.0 kD. The two deduced protein sequences, which were assigned to as *Nt*AACT2 and *Nt*AACT1, respectively, share 77% identity and 91% similarity.

Alignment and comparison of the predicted amino acid sequences of *Nt*AACT1 and *Nt*AACT2 with other available AACT sequences clearly show significant homologies, especially when they are compared with those of plant AACTs (Table 24.1, Fig. 24.1a). A partial alignment of both *Nt*AACT sequences and selected AACT sequences from human, yeast, and the prokaryote *Zooglea ramigera* indicates that several residues, which have been recognized as being important for enzyme activity, are present in all the sequences (Fig. 24.1b). This is the case for the ^{360}H and the two ^{98}C and ^{390}C (see Vollack and Bach 1996; Miziorko 2011 and references herein). The motif M-L/I-KDGL-T/W-D between residues 152 and 159 of both *Nt*AACTs, which is very conserved, has been reported to be involved in the substrate specificity of the *Z. ramigera* AACT, for which a crystalline structure was obtained (Modis and Wierenga 1999). As shown in Fig. 24.1a and c, plant AACT amino acid sequences are distributed into two distinct groups. AACTs from the first one, including *Nt*AACT2, have a shorter C-terminal. The *Nt*AACT2 sequence did not reveal any obvious targeting signal for a defined cell membrane compartment. It is closely related to the radish AACT (81% identity and 93% similarity), an enzyme reported to be cytosolic and whose activity has been demonstrated by functional complementation of the yeast *erg10* mutation and measuring the synthesis of HMG-CoA from acetyl-CoA together with endogenous HMG-CoA synthase (Vollack and Bach 1996). Thus, proteins of this group are likely involved in the MVA isoprenoid pathway. [The actual nomenclature in the numbering of thiolase enzymes comes from a systematic proteomic analysis of peroxisomes (Reumann et al. 2007) and some subcellular targeting observations (Carrie et al. 2007). But we avoid the abbreviation "ACAT," as this is established for acyl-CoA cholesterol acyltransferases. The AACT identified in peroxisomal preparations from *Arabidopsis thaliana* was then numbered "1," although its biological role might not be so important. In a more recent study of *Arabidopsis* AACTs (Ahumada et al. 2008), this nomenclature was adopted, too. In the data banks,

Table 24.1 Comparison of deduced amino acid sequences between available plant AACTs. At *Arabidopsis thaliana*, At1 (AY059736), At2 (NM_124146); Nt *Nicotiana tabacum*; Os *Oryza sativa* (BAB39872); Hb *Hevea brasiliensis* (AF429383); Rs *Raphanus sativus* (X78116)

	At2	At1	Nt2	Nt1	Os	Hb	Rs
At2	100	75/91	83/94	76/89	71/88	76/90	92/94
At1		100	77/93	78/94	73/90	81/93	73/85
Nt2			100	77/91	72/91	80/92	81/93
Nt1				100	75/90	82/93	74/88
Os					100	75/91	70/82
Hb						100	73/85

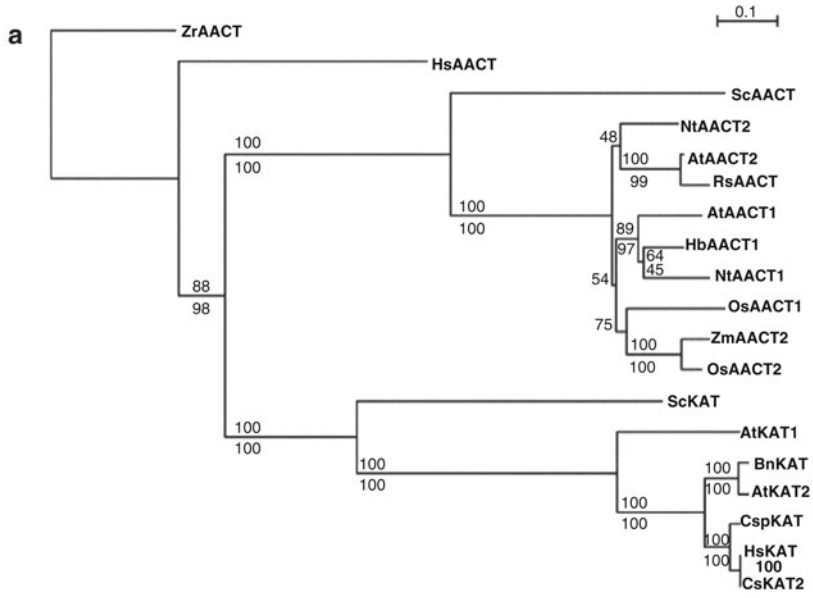

b

```
NtAACT2  94  VNKVCASGLKATMLAAQSIQLGINDVVVAGGMESMSNVPKYIAEARKGSRLGH  146
NtAACT1  94  INKVCSSGLKATMIAAQTIQSGSNDIVVTGGMESMSNVPKYLAQARKGSRLGH  146
HsmAACT 122  INKVCASGMKAIMMASQSLMCGHQDVMVAGGMESMSNVPYVMN--RGSTPYGG  172
ScAACT   87  VNKVCASAMKAIILGAQSIKCGNADVVVAGGDESMTNAPYYMPAARAGAKFGQ  139
ZrAACT   85  MNQLCGSGLRAVALGMQQIATGDASIIVAGGMESMSMAPHCAH-LRGGVKMGD  136
                         *

NtAACT2 147 DSLVDGMLKDGLTDVYKDCGMGVCAEICA 175
NtAACT1 147 DTIVDGMLKDGLWDAYNDFGMGVCAELCA 175
HsmAACT 173 VKLEDLIVKDGLTDVYNKIHMGSCAENTA 201
ScAACT  140 TVLVDGVERDGLNDAYDGLAMGVHAEKCA 168
ZrAACT  137 FKMIDTMIKDGLTDAFYGYHMGTTAENVA 165

NtAACT2 348  KVNVHGGAVSLGHPLGCSGARILVTLLGVLRQKNGKYGAAGVCNGGGG 395
NtAACT1 348  KLNAHGGAVSLGHPLGCSGARILVSLLGVLKHKNGKFGVAGICNGGGG 395
HsmAACT 373  KVNINGGSVSLGHPIGMSGARIVGHLTHALKQ--GEYGLASFCNGGGG 418
HscAACT 341  KVNIEGGAIALGHPLGASGCRILVTLLHTLERMGRSRGVAALCIGGGM 388
ScAACT  342  KVNVYGGAVALGHPLGCSGARVVVTLLSILQQEGGKIGVAAICNGGGG 389
ZrAACT  336  IVNVNGGAIAIGHPIGASGARILNTLLFEMKRRGARKGLATLCIGGGM 383
                         *                          *
```

c

```
NtAACT2  144  GHDSLVDGMLKDGLTDVYKDCGMGVCAEICA  175
BmAACT2  145  GHDSLVDGMLKDGLWDVYNDYGMGVCAEICA  176
CrAACT2  145  GHDTLVDGMMKDGLWDVYNDCGMGVCAEICA  176
VvAACT2  144  GHDSLVDGMLKDGLWDVYSDTGMGVCAELCA  175
CoAACT2  148  GHDSLVDGMLKDGLWDVYNDYGMGVCAELCA  179
PkAACT2  144  GHDSLVDGMLKDGLWDVYNDYGMGVCAELCA  175
HbAACT2-1 144 GHDSLVDGMLKDGLWDVYNDVGMGSCAEICA  175
HbAACT2-2 148 GHDSLVDGMLKDGLWDVYNDVGMGSCAEICA  179
GmAACT2  147  GHDSLVDGMLKDGLWDVYKDVGMGVCVELCA  178
PtAACT2  141  GHDSLVDGMLKDGLWDVYNDYGMGNCAELCA  172
AllAACT2 143  GHDSLVDGMLKDGLWDVYNDCGMGSCAELCA  174
AtAACT2  143  GHDSLVDGMLKDGLWDVYNDCGMGSCAELCA  174
MsAACT2  143  GHDSLVDGMLKDGLWDVYKDVGMGVCAELCA  174
MtAACT2  147  GHDSLVDGMLKDGLWDVYKDVGMGVCAELCA  178
AtAACT ? 138  GHDSLVDGMLKDGLWDVYNDCGMGSCAELCA  169
RsAACT   144  GHDSLVDGMLKDGLWDVYNDCGMGSCAELCA  175

ZrAACT   124  GDFKMIDTMIKDGLTDAFYGYHMGTTAENVA  165

NtAACT1  145  GHDTIVDGMLKDGLWDAYNDFGMGVCAELCA  176
HbAACT1  144  GHDTIIDGMLKDGLWDVYNDFGMGVCAEICA  175
PtAACT1  143  GHDTIVDGMMKDGLWDIYNDFGMGVCAEICA  174
AtAACT1  146  GHDTVVDGMMKDGLWDVYNDFGMGVCGEICA  177
HaAACT1  143  GHDAIIDGMIKDGLWDVYNDFGMGVCGELCA  174
AlAACT1  146  GHDSVVDGMMKDGLWDVYNDFGMGVCGEICA  177
VvAACT1  143  GHDTIVDGMIKDGLWDVYNDFGMGICAEICA  174
OsiAACT1 148  GHDVLIDGMLKDGLWDVYNDFPMGMCAELCA  179
OsjAACT1 148  GHDVLIDGMLKDGLWDVYNDFPMGMCAELCA  179
ZmAACT1  153  GHDVLVDGMLKDGLWDVYNDFPMGMCAELCS  184
```

d

```
                                              175
                                              176
NtAACT2  390  NGGGGASALVLELV  404
BmAACT2  391  NGGGGASALVVELV  405
CrAACT2  391  NGGGGASALVVELV  405
VvAACT2  390  NGGGGASALVVELV  404
CoAACT2  394  NGGGGASALVVELL  408
PkAACT2  390  NGGGGASAVVIELL  404
HbAACT2-1 390 NGGGGASALVVELL  404
HbAACT2-2 394 NGGGGASALVVELL  408
GmAACT2  393  NGGGGAFALVVELQ  407
PtAACT2  387  NGGGGASAVVVELL  401
AllAACT2 389  NGGGGASALVLELL  403
AtAACT2  389  NGGGGASALVLELL  403
MsAACT2  389  NGGGGASALVVELL  403
MtAACT2  393  NGGGGASALVVELL  407
AtAACT ? 384  NGGGGASALVLELL  398
RsAACT   392  NGGGGASALVLEVV  406

NtAACT1  391  NGGGGASALVVELMPIRMVARSSL  414
HbAACT1  388  NGGGGASALVLELMSVGRVGRSLL  411
PtAACT1  389  NGGGGASALVLELMQVARVGPSSL  412
AtAACT1  392  NGGGGASALVLEFMSEKTIGYSAL  415
HaAACT1  389  NGGGGASALVLELMPSA-GTLSKL  411
AlAACT1  392  NGGGGASAIVLEFMSEKTIGYSAL  415
VvAACT1  388  NGGGGASALVLELMPVARLGHSKL  411
OsiAACT1 393  NGGGGASALVVELMQPSLFTRSSL  416
OsjAACT1 393  NGGGGASALVVELMQPSLFTRSSL  416
ZmAACT1  398  NGGGGASALVLELMQPSSHIHSSL  421
```

a large number of hits under "thiolase" will distinguish between the much larger group of KAT-type enzymes, "thiolase I," and acetoacetyl-CoA thiolase, "thiolase II."]

AACTs, from the second group in which *Nt*AACT1 belongs , have ten additional amino acids at the C-terminal, ending with S-A/L/S-l corresponding to a peroxisomal targeting signal of type 1 or PTS1 (Gietl 1996; Reumann et al. 2007, 2009), suggesting that they are associated with peroxisomes and glyoxysomes. As shown in Fig. 24.1a, both groups of AACTs are clearly distinct from degradative thiolases, also known as 3-keto(oxo)acyl-CoA thiolases (KAT) (EC 2.3.1.16), which catalyze the cleavage of 3-ketoacyl-CoAs of different lengths during the fatty acid β-oxidation cycle to yield acetyl-CoA and shortened acyl-CoAs. Moreover, KATs are characterized by the presence of a leader peptide at the N-end of type PTS2 (Gietl 1996). Furthermore, the above-mentioned motif M-L/I-KDGL-T/W-D is not found in any KAT examined and thus represents a means to clearly distinguish both thiolase types.

Fig. 24.1 Alignment of AACT and KAT amino acid sequences and phylogenetic analysis. (**a**) Amino acid sequences of AACT and KAT were aligned using the Clustal X program (version 1.8) and phylogenetically analyzed with the software PHYLIP (http://bioweb.Pasteur.fr/sequanal/phylogeny/phylip-fr.htlm). Both the least squares method of Fitch-Margoliash and the parsimony method were used. In each case, a bootstrap of 100 replicates was made. The unrooted tree was obtained by the Fitch-Margoliash distance method and designed with NJplot (http://pbil.univ-lyon1.fr/software/njplot.htlm). Only bootstrap values close to or higher than 50 are indicated. Branch lengths are proportional to evolutionary distance (number of amino acid substitutions by site). *Numbers above* and *below horizontal lines* correspond to values obtained by the distance method of Fitch-Margoliash and the parsimony method, respectively. The first two letters correspond to the organism from which the sequence is derived: At *Arabidopsis thaliana*, Bn *Brassica napus*, Cs *Cucumis sativus*, Csp *Cucurbita sp*, Hb *Hevea brasiliensis*, Hs *Homo sapiens*, Nt *Nicotiana tabacum*, Os *Oryza sativa*, Rs *Raphanus sativus*, Sc *Saccharomyces cerevisiae*, Zm *Zea mays,* Zr *Zooglea ramigera*. The sequences are available at the NCBI database with the following accession numbers: *At*AACT2 (AAL24148), *At*AACT1 (NP_199583), *At*KAT1 (AAC17877), *At*KAT2 (BAA25248), *Bn*KAT (CAA63598), *Cs*KAT (CAA47926), *Csp*KAT (BAA11117), *Hb*AACT (AAL18924), *Hs*AACT (NP_005882), *Hs*KAT (CAA47926), *Nt*AACT2 (AAU95618), *Nt*AACT1 (AAU95619), *Rs*AACT (CAA55006), *Sc*AACT (AAA62378), *Sc*KAT (CAA37893), *Zr*AACT (AAA27706). Amino acid sequences of *Os*AACT1 and *Zm*AACT have been deduced from corresponding mRNA sequences, AK102536 and AY103699, respectively. (**b**) Comparison of central parts of *Nt*AACT1 and *Nt*AACT2 amino acid sequences with those of AACTs from yeast, human, and *Zooglea ramigera*. This region includes the consensus sequence corresponding to the acetyl-CoA binding site in the crystalline structure of *Z. ramigera* AACT (Modis and Wierenga 1999). Further, functionally important amino acid residues are labeled by the sign *. Note that human mitochondrial AACT (*Hs*mAACT), which contains a mitochondrial target sequence is displayed in the first two rows, while human cytosolic AACT (*Hs*cAACT) is shown in addition only in the third row (Kursula et al. 2005). (**c**) Extended alignment of plant AACT sequences in proximity of the AACT signature like in (**b**). *Fat print in red*: Aligned amino acid residues that are identical in all peptides. *Fat print in blue*: Only one AA residue is different; *Fat print in blue green*: two residues are different. In the *upper part*, AACT2 sequences are on display; in the *lower part*, only separated by the *Z. ramigera* partial sequence, the AACT1 sequences, which albeit being highly conserved in this region, too, show some more conservative AA exchanges. (**d**) Alignment of some C-end amino acid sequences of plant AACTs. Two groups of proteins can be distinguished: a first group, including *Nt*AACT2 (AAU95618) and a second one, including *Nt*AACT1 (AAU95619), with ten additional amino acid residues and a PTS1 signal S-S/A/L-L. Bm *Bacopa monnieri*, AACT2 (ACU87560); Cr *Catharanthus roseus*, AACT2 (AEC13714); Vv *Vitis vinifera*, AACT2 (XP_00226590.1); Co *Camellia oleifera*, AACT2 (ADD10719.1; Pk *Picrorhiza kurroa*, AACT2 (ABC74567.1); Hb *Hevea brasiliensis* AACT2-1 (BAF 98276), AACT2-2 (BAF98277); Gm *Glycine max*, AACT2 (ACU19591); Pt *Populus trichocarpa*, AACT2 (XP_002320528.1); All *Arabidopsis lyrata*, subspecies *lyrata*, AACT2 (XP_0028656.1); At *Arabidopsis thaliana*, AACT2 (NP_568694); Ms *Medicago sativa*, AACT2 (ACX47470); Mt *Medicago truncatula*, AACT2 (ACJ84564); AtAACT2 ? (NP_851154 = AED95639); Rs *Raphanus sativus*, AACT (CAA55006.1); Hb *H. brasiliensis*, AACT1 (AAL18842); Pt *P. trichocarpa*, AACT1 (XP_0023087551.1); At *A. thaliana*, AACT1 (NP_199583); Ha *Helianthus annuus*, AACT1 (ACX46381); All *Arabidopsis lyrata lyrata*, AACT1 (XP_002865105); VvAACT1 (CBI33249); Osi *Oryza sativa Indica* group), AACT1 (EEC69797); Osj *O. sativa Japonica* group, AACT1 (BAB39872); Zm *Zea mays*, AACT1 (ACF87213)

24.2.2 Structural Modeling

When the first part of this study was initiated, only one reliable X-ray structure of a biosynthetic thiolase from *Zoogloea ramigera* had been described (Modis and Wierenga 1999). The structure has been refined more recently (Meriläinen et al. 2009). It followed the structure of human cytosolic AACT (Kursula et al. 2005) and that of human mitochondrial AACT (Haapalainen et al. 2007). Recently, Pye et al. (2010) have solved the crystal structures of *A. thaliana* and *Helianthus annuus* KATs in their dimeric state to high resolution (1.5 and 1.8 Å, respectively). The authors presented also convincing evidence for redox regulation of those peroxisomal KATs and formation of complexes with a multifunctional protein, catalyzing the two preceding steps in β-oxidation (Pye et al. 2010).

Homology modeling of *Nt*AACt single-chain proteins was attempted on the basis of sequence comparisons and using first the template 1wl5 (A chain) of human cytosolic AACT (Kursula et al. 2005) and by the aid of the SWISS-MODEL server (Fig. 24.2a) (Guex and Peitsch 1997; Schwede et al. 2003; Arnold et al. 2006). The structure of peroxisomal KAT from Arabidopsis (2cy7y-A) (Pye et al. 2010) was also used, but as expected, the sequence identity was calculated as 35% in the latter case, against 4 (*Nt*AACT1) and 45% (*Nt*AACT2) on 1wl5, respectively. The best fit was achieved with human mitochondrial AACT (2f2s) as template, with sequence identity of 47% (*Nt*AACT1) and 49% (*Nt*AACT2), respectively (Fig. 24.2b). The pdb models on the basis of template 2iby D chain display the bound coenzyme A (Fig. 24.2b). The QMEAN Z-scores of −3.223 for *Nt*AACT1 and of −2.932 for the *Nt*AACT2 model (Benkert et al. 2011) look reasonable.

The limited accuracy of models did not allow constructing dimeric (plant KAT) or even tetrameric structures (human AACT). Despite their relative sequence similarity, the search of protein sequences by *Nt*AACT1 and *Nt*AACT2 did not detect the same collection of related sequences

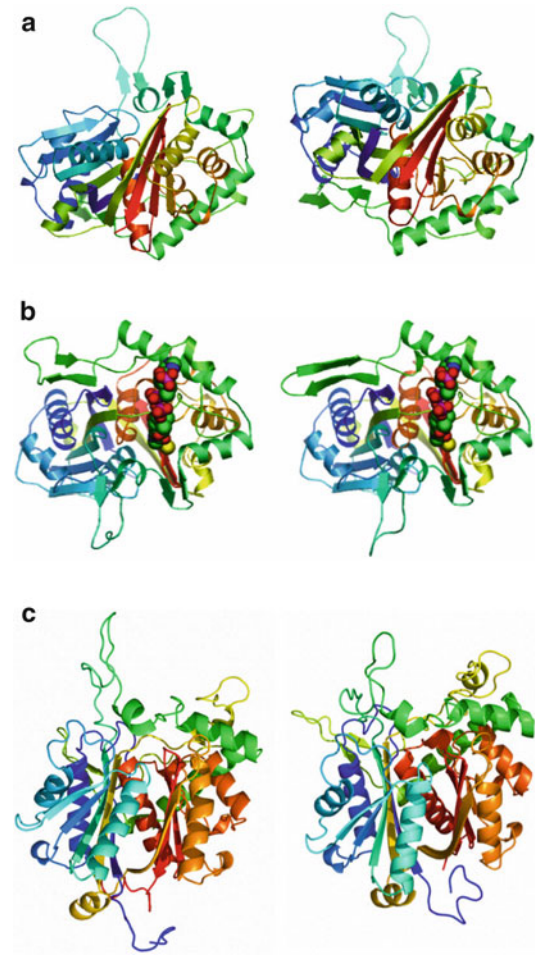

Fig. 24.2 Structural modeling of *Nt*AACT1 and *Nt*AACT2. (**a**) *Left* model of *Nt*AACT1 using the monomer structure of human cytosolic AACT2 as a template (pdb 1wl5A, at 2.26 Å; 41.12% sequence identity; QMEAN Z-score: −2.264). *Right* model of *Nt*AACT2 on the same template (sequence identity 44.81 %; QMEAN Z-score: −2.283). Models were generated by using the SWISS-MODEL Workspace. (**b**) *Left* model of *Nt*AACT1 versus human mitochondrial AACT (pdb 2f2A at 2.00 Å) with bound coenzyme A (sequence identity 46.58%, AA 10 to 404; QMEAN Z-score: −3.223). *Right* The same with *Nt*AACT2 (sequence identity 48.86%, AA 10 to 404; QMEAN Z-score: −2.932). Models were generated by using the SWISS-MODEL Workspace. (**c**) *Left* model of *Nt*AACT1 on the basis of templates 1wl5A, 2ibyD, 2vu2D, and 3ss6B. *Right* model of *Nt*AACT2 on the basis of templates 1wl5A, 2ibyD, and 2vu2D. The models, generated by using the Phyre[2] server, are displayed in similar orientation to better display similarities and slight differences. *Rainbow coloring*: N-terminal end starts with *blue*, C-terminal part is *red*

(>1,000). For modeling based on alignments, the results with the highest resolution and with 98% of residues modeled at >90% confidence were obtained with "Phyre2" at the Imperial College London (Kelley and Sternberg 2009). Binding site predictions were obtained by using "3DligantSite" on the same server (Wass et al. 2010). The putative structure of *Nt*AACT2, as displayed in Fig. 24.2c, was based on the combination of best fitting pdb files: 1wl5A, 2ibyD, and 2vu2D, without considering some amino acids at the N- and C-terminal ends, which were quite diverged. For *Nt*AACT1, the templates 1wl5A, 2ibyD, 2vu2D, and 3ss6B were used, all with slightly inferior sequence identity as compared to *Nt*AACT2. The relative accurateness of such models became clear through overlay of modeled structures (not shown). Interestingly, in a quite recent study, it was shown that CoA inhibits *Medicago sativa* AACT *in vitro* (Soto et al. 2011). As seen in Fig. 24.2b, this substrate neatly fits into the so-called thiolase fold of cytosolic and peroxisomal tobacco AACTs.

24.2.3 Transiently Expressed *Nt*AACT1 Is Targeted to BY-2 Glyoxysomes/Peroxisomes

In order to determine if the gene product of *NtAACT*1 is indeed a peroxisomal protein, we performed *in vivo* targeting experiments using GFP fusion proteins with *Nt*AACT1. Three types of constructs were generated as described in "Materials and Methods." The construct pGFP-MRC (Rodríguez-Concepción et al. 1999), containing only the GFP sequence, was used as a control. The entire coding sequence of *Nt*AACT1 or the same sequence lacking the three terminal codons corresponding to the SSL motif were fused with the 3′ end of GFP to generate pGFP-AACT1 and pGFP-AACT1ΔSSL. We also used a construct with the sequence of RFP, instead of GFP, fused at its C-end with the consensus peroxisome-targeting signal SKL. These constructs were introduced into tobacco BY-2 cells by ballistic bombardment and observed after 15 h by confocal laser scanning microscopy (CLSM).

Fusion of *Nt*AACT1 to the C-terminus of GFP targets the fluorescence to about 1-μm punctuate bodies in the cytoplasm of tobacco BY-2 cells (Fig. 24.3a). To obtain direct evidence that these structures were glyoxysomes, the specialized type of peroxisomes characteristic of tobacco BY-2 cells (Lee et al. 1997), we co-expressed GFP-AACT1 and RFP-SKL fusion proteins. The presence of SKL, or a closely related sequence, at the C-end of a protein has been indeed previously shown to target this protein to the matrix of plant peroxisomes (Hayashi et al. 1996; Lee et al. 1997). Both fluorescent markers exhibited the same distribution as evidenced by yellow structures obtained after merging both images (Fig. 24.3c). Expression of the GFP-truncated AACT1 fusion protein, which lacks the three terminal SSL residues, fails to produce fluorescent punctuate bodies (Fig. 24.3e). In this case, GFP fluorescence was uniformly distributed throughout the cytoplasm and nucleoplasm in a way similar to that of GFP alone (Fig. 24.3f). This result clearly indicates that the tripeptide SSL is both necessary and sufficient for sorting *Nt*AACT1 to BY-2 peroxisomes.

24.2.4 *In Planta* Functional Characterization of *Nt*AACT2

As outlined before, the amino acid sequence of *Nt*AACT2 appeared to be closely related to the cytosolic radish AACT, previously reported as being involved in the MVA isoprenoid metabolism (Vollack and Bach 1996). To analyze the function of *Nt*AACT2, we used a virus-induced gene silencing (VIGS) approach in *Nicotiana benthamiana*, which provides a means to down-regulate expression of host plant genes (Baulcombe 1999; Voinnet 2001). The rationale was that silencing of *NtAACT2* would block or at least reduce the carbon flux toward sterols. For VIGS experiments, we used the vector pPC2C2S, derived from the potato virus X (PVX), a well-characterized system to silence genes in *N. benthamiana* (Baulcombe et al. 1995). A 393-bp fragment of the *NtAACT2* gene was inserted in the vector pPC2C2S to generate the construct

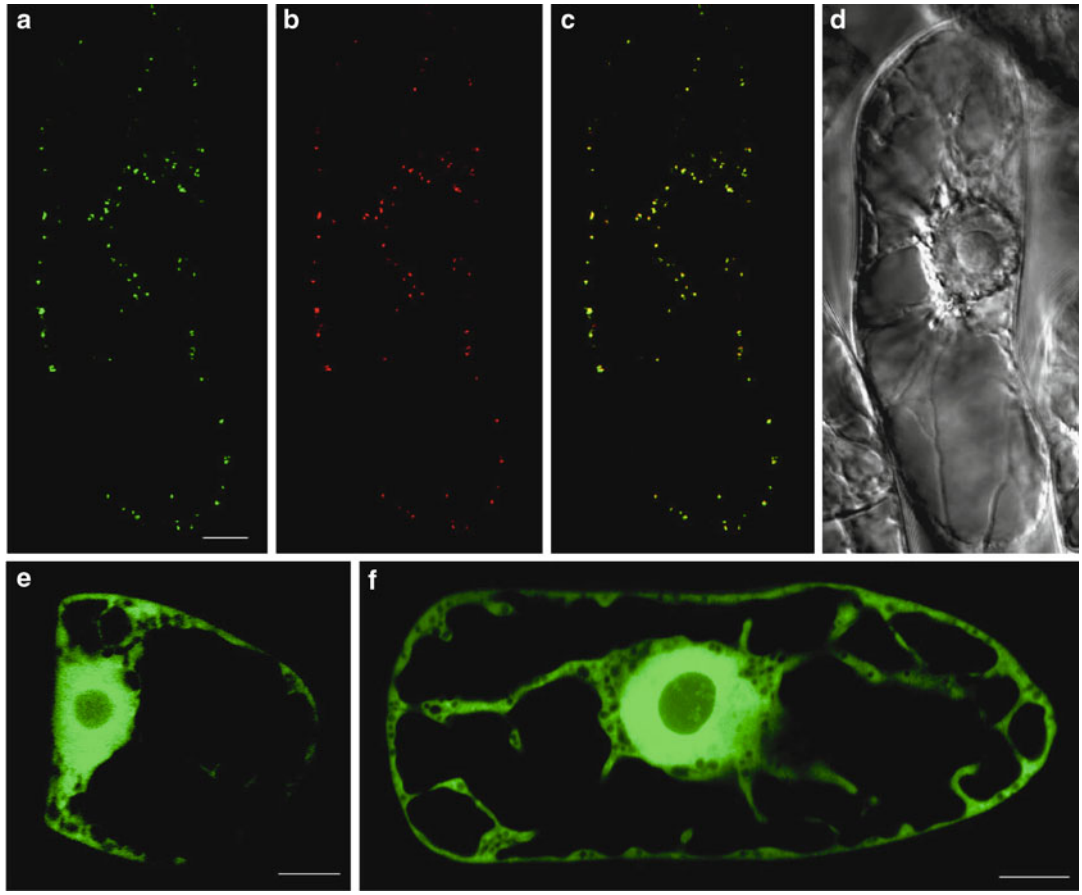

Fig. 24.3 GFP-*Nt*AACT1 is targeted to glyoxysomes/peroxisomes in tobacco BY-2 cells. BY-2 cells were transiently transformed by microprojectile bombardment with pGFP, pGFP-AACT1, pGFP-AACT1-SSL, or pRFP-SKL and analyzed by CLSM after 15 h. (**a**–**d**) Single confocal images of a BY-2 cell co-expressing GFP-AACT1 and RFP-SKL fusion proteins. (**a**) GFP-AACT1 staining (*green*). (**b**) RFP-SKL staining (*red*). (**c**) Merged image shows a complete colocalization of the two proteins (*yellow*), indicating that AACT1 is associated with BY-2 glyoxysomes. (**d**) Nomarski image of the same cell (**e**) BY-2 cell expressing a truncated GFP-AACT1 fusion protein. (**f**) Control: typical cytosolic and nuclear distribution of GFP in a cell transformed with pGFP-MRC. Scale bars=10 μm

PVX::AACT2, as described in "Materials and Methods." Because both *N. tabacum* and *N. benthamiana* genera share an almost identical codon usage (http://www.kazusa.or.jp/codon/), an efficient posttranslational silencing of *NbAACT2* was expected upon inoculation with the viral transcripts of *PVX::NtAACT2*. To check the efficiency of this VIGS approach, we performed parallel experiments to silence endogenous expression of the gene encoding squalene synthase (SQS), the first committed enzyme to the sterol branch. A *PVX::SQS* construct was generated by inserting a 618-bp fragment of the *NbSQS* open reading frame in the vector pPC2C2S. RNAs resulting from the *in vitro* transcription of both gene fragments as well as that of the empty vector (control) were inoculated to 3-week-old *N. benthamiana* plants. At least two plants were inoculated with each construct in three independent experiments. Plants were analyzed after 24 days.

The first signs resulting from the viral infection appeared between 7 and 10 days. After 24 days, plants inoculated with *PVX* transcripts exhibited the typical viral symptoms consisting in plant stunting and distorted leaves. As shown

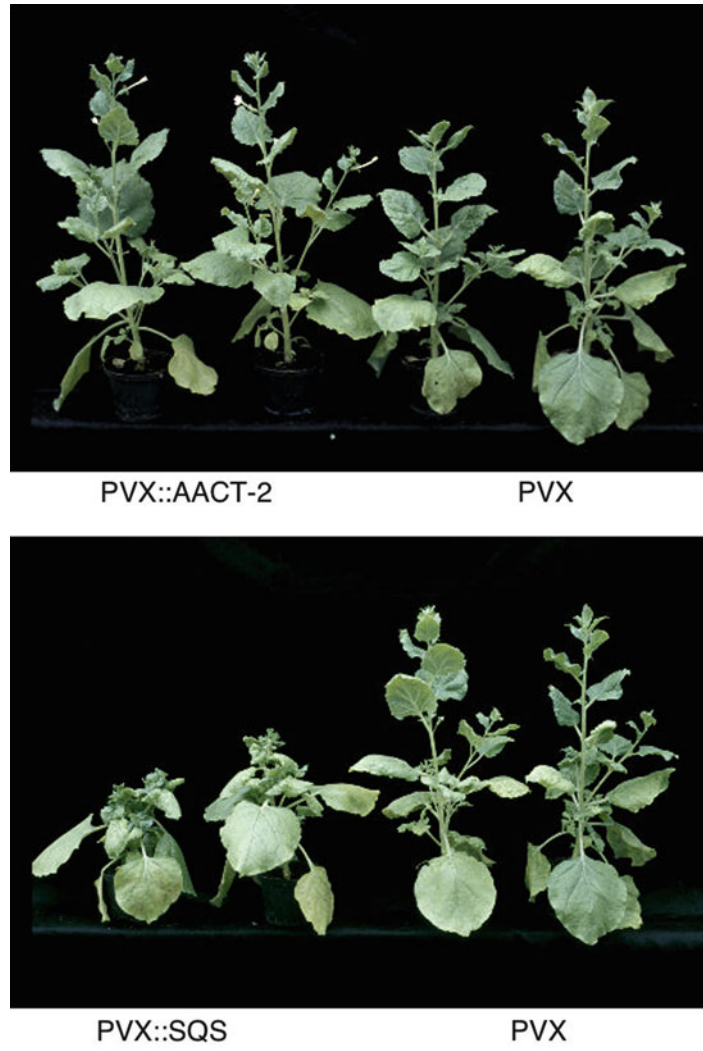

Fig. 24.4 VIGS experiments in *Nicotiana benthamiana*: morphological aspect of plants 24 days after inoculation with transcripts from *PVX*, *PVX::AACT2,* or *PVX::SQS*

in Fig. 24.4a, plants inoculated with *PVX::AACT2* transcripts were not altered in their morphology and were even in better shape compared to mock-inoculated plants. In contrast, growth of *SQS*-silenced plants was severely affected, resulting in a dwarf phenotype (Fig. 24.4b). The reduced stature was mainly due to reduction in stem length between internodes. Leaves above the site of inoculation were very small compared with other leaves.

The efficiency of posttranscriptional silencing of the endogenous *AACT2* and *SQS* was checked by measurements of corresponding mRNA levels by real-time PCR. Whereas the levels of *SQS* transcripts were dramatically reduced by 80–90%, a decrease by only 20–40% was found for *AACT2* transcripts (data not shown).

This study was completed by the determination of the sterol profile of the different populations of silenced plants, as described in the experimental section. Sterols, which were analyzed as the sum of the free and esterified forms, were separated into different classes. *N. benthamiana* end-products (sterols) were represented mainly by sitosterol (28%), stigmasterol (28%), 24-methylcholesterol (19%), and cholesterol

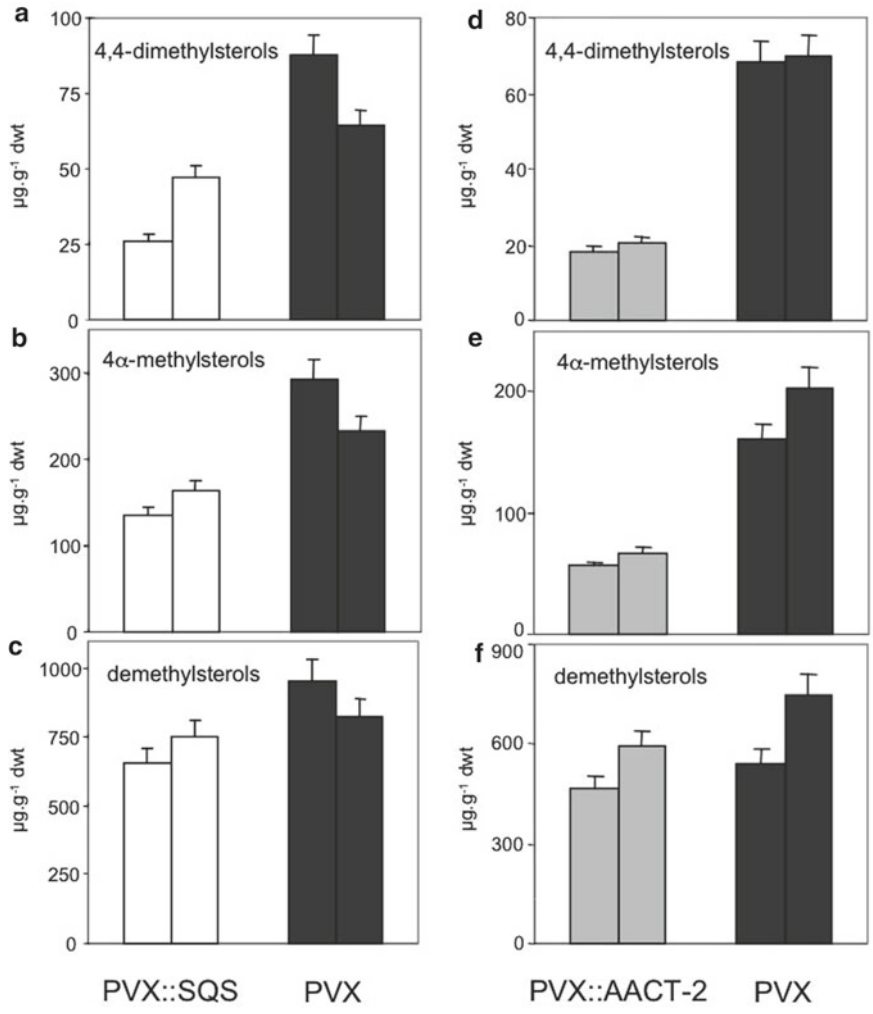

Fig. 24.5 Sterol composition of mature leaves from *N. benthamiana* plants inoculated with *PVX*, *PVX::AACT2*, or *PVX::SQS* transcripts and analyzed after 24 days. Results are representative of two series of independent experiments carried out with two plants for each construct. Sterols were extracted from lyophilized tobacco leaves, separated in different classes, and analyzed by gas chromatography as acetate derivatives. (**a**, **d**) 4,4-dimethylsterols (**b**, **e**) 4α-methylsterols (**c**, **f**) 4-demethylsterols

(10%). The major biosynthetic precursors were cycloartenol and 24-methylene cycloartanol (4,4-dimethylsterols) as well as obtusifoliol (4α-methylsterol) (data not shown). In Fig. 24.5, results representative of two separate experiments performed with two plants for each construct are shown. Compared to mock-inoculated plants, AACT2-silenced plants were found to contain twofold reduced amounts of 4,4-dimethyl- and 4α-methylsterols, but very similar levels of sterol end-products. In contrast, *SQS*-silenced plants displayed a net decrease in total sterols, as expressed in mg per g of fresh weight, but no change in the sterol profile. When expressed as mg/g of dry weight, the amounts of total sterols in control and *SQS*-silenced were identical, indicating that a near-complete block of *SQS* expression took place very fast after inoculation. This result is consistent with the previous observation that SQS inhibition by squalestatin rapidly blocks the cell cycle of tobacco BY-2 cells (Hemmerlin et al. 2000).

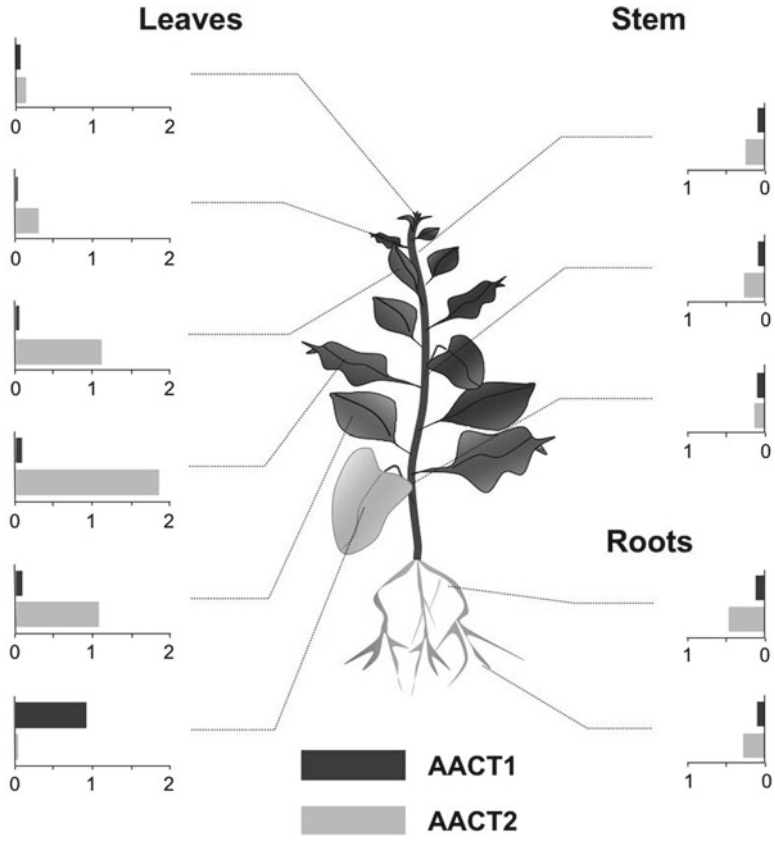

Fig. 24.6 *NtAACT1* and *NtAACT2* expression patterns in different parts of *N. tabacum* plants. Corresponding mRNA levels were determined by real-time PCR

24.2.5 Spatiotemporal Study of *NtAACT1* and *NtAACT2* Expression in Tobacco Plants

To get more insights into the biological functions of both *NtAACT* genes, we studied their expression patterns in different parts of 6-week-old tobacco plants (stage of 12 leaves). *NtAACT1* and *NtAACT2* mRNA levels were determined using real-time PCR, as described in "Materials and Methods." As shown in Fig. 24.6, *NtAACT2* is highly expressed in young and middle-aged leaves. The gene is also expressed in stems and roots. A constitutive expression of *NtAACT1* was detected in all parts of the plant, but with significantly lower levels compared to *NtAACT2*. However, a significant expression of *NtAACT1* was observed in senescent leaves where *NtAACT2* was simultaneously very low.

We investigated in more detail the *NtAACT1* expression pattern during the process of leaf senescence. Three distinct stages, related to the color of leaves, were taken into account: 100% green, 50% green, and 0% green (100% yellow). As shown in Fig. 24.7a, high levels of *NtAACT1* mRNA were observed in all the three stages, concomitantly with a decrease in the amount of *NtAACT2* transcripts. In the last stage, the level of *NtAACT1* transcripts was 16-fold the level of *NtAACT2* transcripts.

We also determined expression patterns of both *NtAACT* genes during seed germination. Tobacco seeds were allowed to grow in Petri dishes on a nutritive medium and in the dark. After 3 days, the seeds were placed in the light and analyzed after 3, 5, and 11 days for *NtAACT1* and *NtAACT2* mRNA levels. Whereas an active *NtAACT1* expression was observed at the onset

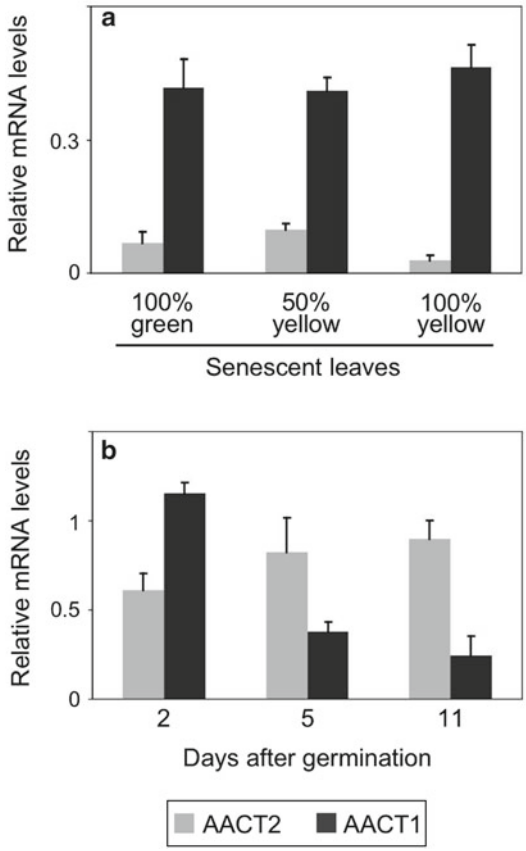

Fig. 24.7 *NtAACT1* and *NtAACT2* expression patterns at different stages of leaf senescence (**a**) and early germination growth (**b**) corresponding mRNA levels were determined by real-time PCR

of the germination, a significant decrease occurred after 6 and 11 days (Fig. 24.7b). Concomitantly, a high level of *NtAACT2* expression was found during all the processes.

24.3 Discussion

Here, we report the isolation of two *Nicotiana tabacum* genes encoding acetoacetyl-CoA thiolases. Alignment and comparison of the corresponding predicted amino acid sequences with available AACT sequences from other organisms clearly indicate that both *Nt*AACT1 and *Nt*AACT2 could belong to the class of biosynthetic thiolases, which are known to catalyze a Claisen-type condensation of two acetyl-CoA units to form acetoacetyl-CoA. The putative specificity of these enzymes for acetyl-CoA is attested by the presence of the highly conserved motif M-L/I-KDGL-T/W-D between residues 153 and 159, which is located within a highly conserved domain of all plant AACTs sequenced so far. Such a sequence has been shown to be involved in the active site of the *Zooglea ramigera* AACT, which functions in the poly-β-hydroxybutyrate biosynthesis (Modis and Wierenga 1999). This sequence is not present in KATs, a different class of thiolases, which mediate degradation of 3-ketoacyl-CoAs (Fig. 24.1a).

Several arguments are consistent with an involvement of *Nt*AACT2 in the MVA isoprenoid pathway: (1) The *Nt*AACT2 sequence did not reveal any leader peptide with resemblance to mitochondrial or chloroplastic targeting sequences or to any other cell membrane compartment, suggesting a cytosolic localization for this thiolase. *Nt*AACT2 is closely related to the radish AACT (*Rs*AACT, 81% identity/93% similarity; Table 24.1), which has been shown to exhibit a high activity in the cytosol, when expressed in the *S. cerevisiae erg10* mutant (Vollack and Bach 1996); (2) as demonstrated by VIGS experiments carried out in *N. benthamiana* plants, silencing of endogenous *NbAACT2* resulted in a 50% decrease in the levels of 4α-methyl- and 4,4-dimethylsterols, the biosynthetic intermediates of the sterol pathway (Fig. 24.5), suggesting a reduced carbon flux toward sterols. The relatively low efficiency of *AACT2* silencing, as revealed by the decrease by only 20–40% in endogenous *NbAACT2* mRNA, the absence of significant effect on levels of sterol end-products as well as the lack of phenotype might question the reliability of the overall approach. But it should be pointed out that AACT is the first enzyme of the acetate/mevalonate pathway, which is involved in the synthesis of a wide array of isoprenoid compounds, including sterols. Thus, silencing of *AACT2* might be not as efficient as silencing of genes encoding downstream enzymes of specific pathways (e.g., SQS). In that context, Burger-Probst (2003) tried to silence several *NtHMGR* isogenes, using the same VIGS approach, under similar conditions,

but did not succeed either to obtain a decrease in sterol end-products (Burger-Probst 2003). Alternatively, a large body of evidence has been given that an active exchange of precursors (metabolic cross-talk) can occur between both isoprenoid biosynthetic pathways occurring in plant cells (see for instance Hemmerlin et al. 2003). Thus, reduction of the carbon flux, due to *AACT2* silencing, might be partially overcome by metabolic intermediates provided by plastids. In contrast, very demonstrative results were obtained in the case of *SQS* silencing. The squalene synthesis constitutes the first committed step of the cytoplasmic sterol pathway. Silencing of endogenous *NbSQS* was found to be very efficient, as attested by the 80–90% decrease in the corresponding transcripts as well as by a severe growth reduction, which mainly affected the parts of the plant located above the site of inoculation (Fig. 24.4b), suggesting a blockade of cell division. This result is consistent with previous observations, which showed that inhibition of SQS by squalestatin 1 rapidly triggered an arrest of the cell cycle, in the early G1 phase of synchronized tobacco BY-2 cell cultures (Hemmerlin et al. 2000). It should be emphasized that efficiency of such a VIGS approach has been also demonstrated for silencing other enzymes of the sterol biosynthetic pathway: the obtusifoliol 14-demethylase (Burger et al. 2003), Δ^7-sterol-C5(6)-desaturase (Burger et al. 2003), and 4-sterol methyloxidases (Darnet and Rahier 2004); and (3) evidence is given for a constitutive expression pattern for the *NtAACT2* gene, with a higher level of transcripts in the rapidly growing parts (young leaves, early stages of germination) of tobacco plants.

Taken together, all these data suggest that *Nt*AACT2 is most likely involved in the acetate/mevalonate pathway, especially in controlling the carbon flux leading to sterols. Further experiments will be necessary to investigate whether or not *Nt*AACT2 is regulated by a sterol feedback mechanism as in animal (Honda et al. 1998) and yeast cells (Servouse and Karst 1986; Dimster-Denk et al. 1999). Quite recently, it has been suggested that the gene encoding biosynthetic AACT in alfalfa (*Medicago sativa*) is upregulated during abiotic stress adaptation (Soto et al. 2011), which seems to contribute to resistance to cold and salinity stress. When alfalfa seedlings were treated with an inhibitor of HMGR, thereby interrupting the flux from acetyl-CoA to HMG-CoA and further downstream in the sterol pathway, the stress-sensitive phenotype could be overcome by addition of ascorbate, which was interpreted to mean that the MVA pathway is involved in the production of some antioxidant molecules (Soto et al. 2011). AACT overexpressing alfalfa roots showed some resistance to salt stress, which might be the result of some increased accumulation of squalene. In this context, it is worthwhile to mention that overexpression of wild-type and mutated HMGS – the sequel enzyme of AACT in the MVA pathway – from *Brassica juncea* (BjHMGS1) in Arabidopsis was also accompanied by a higher stress resistance and increased phytosterol levels (Wang et al. 2012), which points to a new role of the cytosolic isoprenoid pathway under stress conditions. In this latter study, an upregulation of genes coding for enzymes in the sterol pathway, including HMGR, was observed (Wang et al. 2012). However, such correlations are difficult to generalize: For instance, RNAi-mediated disruption of SQS in rice improved drought tolerance and yield (Manavalan et al. 2012), due to reduced stomatal conductance, slightly increased root length, and an enhanced number of lateral roots. Such observations point to a hormonal effect, for instance, induced by abscisic acid, and it is tempting to assume that in some way, protein isoprenylation might be involved.

Amino acid sequence analysis of *Nt*AACT1 revealed the presence of a tripeptide SSL at the C-end of the protein, which is closely related to the consensus sequence PTS1, known to trigger the import of the protein into peroxisomes (Gietl 1996; Reumann et al. 2007, 2009). Experiments with transiently transformed tobacco BY-2 cells, in which GFP-AACT2 and RFP-SKL were co-expressed, clearly demonstrated the association of *Nt*AACT2 with punctuate structures assigned to be glyoxysomes (Lee et al. 1997). We also showed that the SSL of the C-end was required for appropriate targeting of the enzyme.

In higher plants, glyoxysomes/peroxisomes are known to play a major role in different metabolic pathways: lipid breakdown, photorespiration, and H_2O_2 degradation (cf. Reumann et al. 2007, 2009). Glyoxysomes contain enzymes of the fatty acid β-oxidation and the glyoxylate cycle, whereas leaf peroxisomes contain a different set of enzymes that mediate a photorespiratory glycolate metabolism. We found that *NtAACT1* was constitutively expressed in all parts of tobacco plants but displayed a far better level of expression in senescent leaves (Figs. 24.6 and 24.7a). A high level of transcripts was also observed during early post-germination growth (Fig. 24.7b). Interestingly, such an expression pattern is reminiscent of that displayed by the activity of the fatty acid β-oxidation cycle throughout plant development (Gerhardt 1992). Fatty acid β-oxidation is indeed strongly induced upon seed germination, then decreases during vegetative growth and establishment of photosynthesis, and finally is reactivated upon senescence. *KAT* genes, encoding 3-keto(oxo) acyl-CoA thiolases, also exhibit the same pattern of expression (Kato et al. 1996; Germain et al. 2001). KAT enzymes belong to a different class of thiolases (EC 2.3.1.16.), which mediate the cleavage of fatty acyl-CoAs of different chain lengths to generate acetyl-CoA and shortened acyl-CoAs, i.e., the last step of the fatty acid β-oxidation cycle (cf Peretó et al. 2005). Moreover, KATs are known for being imported into glyoxysomes by a PTS2 targeting way (Gietl 1996; Carrie et al. 2007). The presence of two distinct thiolases, a "biosynthetic" one and a degradative one, in the same cell compartment might appear surprising. However, the occurrence of an AACT in sunflower glyoxysomes (Oeljeklaus et al. 2002) as well as in peroxisomes from the yeast *Candida tropicalis* (Kurihara et al. 1988) or rat liver (Thompson and Krisans 1990) has been already reported. The question is now to determine the function of this glyoxysomal/peroxisomal AACT. In liver of mammalian cells, the identification of a PTS1 signal in several enzymes of the cholesterol pathway, including AACT, raised the question of a putative involvement of peroxisomes in MVA isoprenoid metabolism (Olivier et al. 2000). However, such a role has not been confirmed (Hogenboom et al. 2002). To our knowledge, no evidence has been given either for the presence of an isoprenoid biosynthetic pathway in plant peroxisomes/glyoxysomes. Similarly, attempts failed to demonstrate the translocation of the sequel enzyme in the MVA pathway, HMG-CoA synthase, into BY-2 cell glyoxysomes/peroxisomes (Nagegowda et al. 2005). If any presence of MVA pathway steps in plant peroxisomes should occur, then it must be downstream, as has recently found some experimental support for mevalonate phosphate kinase and mevalonate diphosphate decarboxylase in cells of Madagascar periwinkle (*Catharanthus roseus,* Simkin et al. 2011). The AACT enzyme assay alone, nearly always measured in the energetically favored cleavage direction (cf. Miziorko 2011), like with a heterologously expressed and partially purified enzyme from sunflower (*Helianthus annuus* L.) apparently carrying the PST2 signal (Dyer et al. 2009), cannot distinguish between putatively anabolic or catabolic functions.

The glyoxysomal enzyme was previously purified from sunflower cotyledons (Oeljeklaus et al. 2002). The sequel enzyme of cytosolic AACT, HMG-CoA synthase, which catalyzes an energetically favored aldol condensation of acetoacetyl-CoA with another unit of acetyl-CoA, has a high affinity towards acetoacetyl-CoA (Nagegowda et al. 2004), which ensures the flux from acetyl-CoA to (*S*)-HMG-CoA. This high affinity to acetoacetyl-CoA leads even to substrate inhibition *in vitro* (Nagegowda et al. 2004). Furthermore, separation of AACT from HMGS during purification from *C. roseus* cells proved very difficult (van der Heijden et al. 1994 a, b), suggesting some close (functional) interaction of both enzymes. If we consider the presence of different HMG-CoA reductase isozymes in plants (Enjuto et al. 1994, 1995), which in BY-2 cells are also differentially regulated (Hemmerlin et al. 2003) and localized (Merret et al. 2007), then the putative existence of metabolons directing the substrate flux to different MVA-dependent products (Chappell et al. 1995) looks even more attractive.

24.4 Materials and Methods

24.4.1 Plant Material

Tobacco (*Nicotiana tabacum* L. cv Bright Yellow-2 [BY-2]) cell suspension cultures were maintained as described by Nagata et al. (1992). Cells were grown in modified Murashige and Skoog medium, at 27°C, in the dark, under agitation (154 rpm), and subcultured weekly. *N benthamiana* and *N. tabacum* plants were grown in greenhouse at 24°C under a 16/8 h photoperiod.

24.4.2 GFP/RFP Constructs

The binary vector pGFP-MRC, which contains the GFP gene under the control of a double 35S promoter (Rodríguez-Concepción et al. 1999), was kindly provided by Dr. M. Rodríguez-Concepción (Barcelona, Spain). This vector was used as a control. The entire *NtAACT1* coding sequence was amplified and modified by overlap extension PCR in order to introduce the restriction sites *Sac*I and *Xba*I at the ends of *NtAACT1*. The PCR product was fused in-frame to the 3′ end of the GFP sequence by cloning into the *Sac*I and *Xba*I sites of pGFP-MRC to create pGFP-AACT1, encoding the fusion protein GFP-AACT1. A construct containing the sequence of the *NtAACT1* without the last three codons corresponding to the SSL motif was also generated (pGFP-AACT2ΔSSL). An optimized version of pDsRed2 (Clontech), containing the *Discosoma* red fluorescent protein (RFP), was provided by Dr. A. Hemmerlin (IBMP, Strasbourg). The DsRed2 sequence was amplified and modified by PCR in order to introduce a sequence encoding the tripeptide SKL between the last amino acid and the termination codon of the RFP cistron as well as the restriction sites *Sac*I and *Xba*I. The PCR product was inserted into pGFP-MRC vector in place of the GFP sequence to generate pRFP-SKL. The nucleotide sequences of all constructs were checked by sequencing analysis.

24.4.3 Microprojectile Bombardment of Tobacco BY-2 Cells

M-17 tungsten particles (Bio-Rad) (1 mg per plasmid) were sterilized in absolute ethanol (1 mL) during 20 min at room temperature. The beads were recovered by centrifugation and dried under vacuum. They were incubated in sterile 50% glycerol (16.5 µL), DNA (4 µL, 1 µg/µL of pGFP-MRC, pGFP-AACT1ΔSSL, pGFP-AACT1, or pRFP-SKL), $CaCl_2$ 2 M (16.5 µL), and spermidine 2 M (7.5 µL). After 20 min at room temperature, the mixture was centrifuged. The particles were rinsed successively in ethanol 70% and ethanol 100% (150 µL), dried for 5 min, and put in absolute ethanol (14 µL).

Two or three-day-old BY-2 cells (*ca* 5 mL) were spread over a sterile filter paper and placed on a 0.5% agar MS medium plate. The tobacco cells were bombarded two times with a particle inflow gun (Finer et al. 1992) with a freshly prepared suspension of particle (7 µL) under vacuum (0.8 bar). Cells were then left in the dark at 27°C for 15 h. Cells expressing GFP were selected by observation with a Leica MZ12 magnifying glass, equipped with a blue filter.

24.4.4 Confocal Laser Scanning Microscope (CLSM) Observations

Fluorescence of BY-2 cells was observed with a Zeiss (Jena, Germany) LSM 510 inverted laser scanning confocal microscope equipped with a C-Apochromat (×63, 1.2 W Korr) water immersion objective lens. GFP was excited at 488 nm with an argon laser, and the fluorescence emitted was detected with a 505–550 nm band-pass filter. RFP was excited at 543 nm (with a helium/neon laser), and fluorescence was detected with a long pass filter (585 nm). The images were coded green (GFP) and red (RFP), giving yellow colocalization in merged images. Differential interference contrast (DIC) images were recorded using the laser as transmission light source. Final images, which

were all derived from single optical sections, were obtained after processing with LSM Image Browser version 2.8 (Zeiss) and Photoshop 6.0 (Adobe Systems, San Jose, CA, USA).

24.4.5 Isolation of *Nt*AACT cDNAs

NtAACT cDNAs were isolated by screening 300,000 recombinants from a cDNA *Nicotiana tabacum* L. library prepared in λ-ZapII (Stratagene) using the whole radish AACT open reading frame as a probe (Vollack and Bach 1996). 300,000 pfu were screened with ^{32}P-random-labeled cDNA probe from radish (entire open reading frame). Hybridization was carried out at 55°C according to standard conditions. cDNAs were isolated as pBluescript SK (Stratagene) derivatives, which were sequenced on both strands with an automatic sequencer Perkin Elmer model 373 using T3, T7, and specific primers.

24.4.6 VIGS Experiments

We used the vector pP2C2S, derived from theyt potato virus X (PVX), a well-characterized VIGS system to silence genes in *Nicotiana benthamiana* (Baulcombe et al. 1995). The fragments of target genes were inserted between the restriction sites *Cla*I and *Sal*I of this vector. A 393-bp fragment of the 3′ end of the *NtAACT2* gene and a 618-bp fragment of the coding sequence of the *N. benthamiana SQS* were amplified by PCR using the following pairs of primers: AACT2ntF (5′-cc<u>atcgat</u>^{1062}gttaattgtacatg-gtggagctgta-3′) and AACT2ntR (5′tcgc<u>gtcgac</u>^{1455}at- gaggaatgcaattg-cattgct-3′), for *AACT2* and SQSnbF (5′-cc<u>atcgat</u>^{406}cgtagctttgctctcgtcattca-3′) and SQSnbR (5′-ttcgc<u>gtcgac</u>^{1025}aacatacggcacttgggtacttca-3′), for *SQS*. Underlined nucleotides correspond to engineered restriction sites. The *NtAACT2* cDNA fragment was chosen in the 3′ end of the gene because it is in this region that both *NtAACT* genes are the most divergent (less than 60% identity). The resulting fragments were cloned in the sense orientation into the vector pP2C2S to yield the constructs *PVX::AACT2* and *PVX::SQS*. The empty vector was used as a control. Identity of the inserts was checked by sequencing.

Infectious PVX RNA molecules were produced by *in vitro* transcription of the PVX derivatives. The constructs were first made linear using the site *Spe*I, and the transcripts were produced using the Ribomax™ Large Scale RNA production System T7 kit (Promega). The freshly prepared RNA was resuspended in 50 mM phosphate buffer containing macaloid (0.05%) and rubbed onto the top of two leaves of 5-week-old *N. benthamiana* plantlets in the presence of celite (Baulcombe et al. 1995). Plants were allowed to grow for a further 24 days. Two plants were used for each construct, and three individual VIGS experiments were carried out.

24.4.7 Sterol Analysis of *Nicotiana benthamiana* Plants

The lyophilized plant material was homogenized using an Ultra-Turrax in the presence of 6% (w/v) KOH in methanol and heated at 90°C under reflux for 2 h. After addition of 1 vol of water, total sterols (i.e., as the sum of free sterols and sterols from esterified forms) were extracted three times with three vol of *n*-hexane. The extract was dried on Na_2SO_4, evaporated under dryness, and layered on silica gel plates (60 F_{254}) developed in ethyl acetate-*n*-hexane (15:85, v/v). After chromatography, sterols were resolved in individual classes: 4-demethyl- (R_f 0.27), 4α-methyl- (R_f 0.38), and 4,4-dimethylsterols (R_f 0.44), which were analyzed by GC. Analysis was carried out with a Varian GC model 8300 equipped with a flame ionization detector and a fused capillary column (WCOT 30 m × 0.25 mm i.d.) coated with DB1 (flow rate of hydrogen: 2 mL/min). The temperature program included a 30°C/min increase from 60°C to 240°C, then a 2°C/min increase from 240°C to 280°C. Cholesterol was added as internal standard for quantification of 4α-methyl- and 4,4-dimethylsterols and coprostanol for quantification of 4-demethylsterols. All the compounds were identified by GC-MS (Rahier and Benveniste 1989) using an Agilent 5973N spectrometer coupled with a gas

chromatograph (Agilent 6890), equipped with an on-column injector and a capillary column (30 m×0.25 mm i.d.) coated with DB5.

24.4.8 Measurements of Transcript Levels

Transcript levels were determined by real-time PCR analysis. Total RNA from various parts (leaf, stem, root…) of *N. tabacum* or *N. benthamiana* plants were isolated with the TRIzol® reagent (Invitrogen Life Technologies) and treated with RNAse-free DNAse to remove any residual DNA. Subsequently, total RNAs (1 µg) were converted into cDNA using 200 units of reverse transcriptase M-MLV (Promega), random hexamers (200 ng, Boehringer Mannheim), and 500 µM dNTPs in a final volume of 20 µL. The reaction proceeded at 37°C for 60 min. Real-time PCR assays were performed with SYBR® green PCR master mix (10 µL) including 0.5 unit of Hot Start Ampli*Taq* Gold polymerase (Applied Biosystems), cDNA (5 µL, 25× diluted), and 0.18 µM of appropriate primer pairs in a final volume of 25 µL. Assays were run in duplicates on a GeneAmp® 5700 Sequence Detection System (Applied Biosystems) under the following conditions: initial denaturation step at 95°C for 10 min, 40 cycles of 95°C for 15 s, and 60°C for 1 min. PCR cycle number was optimized to ensure that amplification end points were in the logarithmic phase. To quantify *N. tabacum AACT1 and AACT2* mRNA levels, we used the primers: rtac1bF (5′-^{1256}tggtgcttgcggtggatta-3′) and rtac1bR (5′-^{1322}aaacagaggttgcacaatcatctc-3′) for *AACT2* and rtac2bF (5′-^{1127}caacaaaagactgctcaatctcaatt-3′) and rtac2bR (5′-^{1210}tgcaccccaagggatgtc-3′) for *AACT1*. As an internal standard, we measured transcript levels of *tob10 (*GeneBank accession number U60495), a gene encoding *N. tabacum* actin, with the primers rtact1F (5′-tgctgatcgtatgagcaaggaa-3′) and rtact1R (5′-ggtggagcaacaaccttaatcttc-3′).

The measurements of *N. benthamiana AACT2* and *SQS* mRNA levels were performed using the primers gsac14F (5′-^{666}gggaagaggaaaaccatccatt-3′) and gsac14R (5′-^{746}ggaggtttctcaattttg- caccat-3′) for *AACT2* and gssqs1F (5′-^{255}tcgtagctttgctctcgtcatt-3′) and gssqs2R (5′-^{1344}ccggat- agctgtgcgagaataat-3′) for *SQS*.

24.4.9 Sequence Comparisons and Homology Modeling

Newly deposited sequences with homology to *Nt*AACTs were searched on the NCBI protein data bank. The PRALINE web server was also used for sequence analyses and alignments (Pirovano et al. 2008). Structural modeling was performed by using the SWISS-MODEL workspace (Arnold et al. 2006; Benkert et al. 2011) and by the use of the "Phyre²" server at the Imperial College London (Kelley and Sternberg 2009; Wass et al. 2010).

Acknowledgments We thank Prof. P. Benveniste for providing us the *N. tabacum* cDNA library prepared with mRNAs isolated from 8-week-old SH6 tobacco calli. We are grateful to Dr. M. Rodríguez-Concepción (University of Barcelona, Spain) and Dr. A. Hemmerlin (IBMP, Strasbourg) for making available the pGFP-MRC and pRFP vectors, respectively.

We also thank Valérie Cognat (IBMP, Strasbourg) for her help in phylogenetic analyses.

The Confocal Microscopy Platform was cofinanced by the Centre National de la Recherche Scientifique, the Université de Strasbourg, the Région Alsace, the Association pour la Recherche sur le Cancer (ARC), and the Ligue Nationale contre le Cancer.

References

Ahumada I, Cairo A, Hemmerlin A et al (2008) Characterization of the gene family encoding acetoacetyl-CoA thiolase in *Arabidopsis*. Funct Plant Biol 35:1100–1111

Arnold K, Bordoli L, Kopp J, Schwede T (2006) The SWISS-MODEL workspace: a web-based environment for protein structure homology modelling. Bioinformatics 22:195–201

Bach TJ (1995) Some new aspects of isoprenoid biosynthesis in plants- a review. Lipids 30:191–202

Baulcombe DC (1999) Fast forward genetics based on virus-induced gene silencing. Curr Opin Plant Biol 2:109–113

Baulcombe DC, Chapman S, Santa Cruz S (1995) Jellyfish green fluorescent protein as a reporter for virus infections. Plant J 7:1045–1053

Benkert P, Biasini M, Schwede T (2011) Toward the estimation of the absolute quality of individual protein structure models. Bioinformatics 27:343–350

Burger C, Rondet S, Benveniste P, Schaller H (2003) Virus-induced silencing of sterol biosynthetic genes: identification of a *Nicotiana tabacum* L. obtusifoliol-14α-demethylase (CYP51) by genetic manipulation of the sterol biosynthetic pathway in *Nicotiana benthamiana* L. J Exp Bot 54:1675–1683

Burger-Probst C (2003) Rôle de la 3-hydroxy-3-méthylglutaryl Coenzyme A réductase dans la régulation de la biosynthèse des stérols chez les plantes. Ph.D. thesis, Université Louis Pasteur, Strasbourg

Carrie C, Murcha MW, Millar AH, Smith SM, Whelan J (2007) Nine 3-ketoacyl-CoA thiolases (KATs) and acetoacetyl-CoA thiolases (ACATs) encoded by five genes in *Arabidopsis thaliana* are targeted either to peroxisomes or cytosol but not to mitochondria. Plant Mol Biol 63:97–108

Chappell J (1995) The biochemistry and molecular biology of isoprenoid metabolism. Plant Physiol 107:1–6

Chappell J, Wolf F, Proulx J, Cuellar R, Saunders C (1995) Is the reaction catalyzed by 3-hydroxy-3-methylglutaryl coenzyme A reductase a rate-limiting step for isoprenoid biosynthesis in plants? Plant Physiol 109:1337–1343

Darnet S, Rahier A (2004) Plant sterol biosynthesis: identification of two distinct families of sterol 4alpha-methyl-oxidases. Biochem J 378:889–898

Dimster-Denk D, Rine J (1996) Transcriptional regulation of a sterol-biosynthetic enzyme by sterol levels in *Saccharomyces cerevisiae*. Mol Cell Biol 16: 3981–3989

Dimster-Denk D, Rine J, Phillips J et al (1999) Comprehensive evaluation of isoprenoid biosynthesis regulation in *Saccharomyces cerevisiae* utilizing the Genome Reporter Matrix™. J Lipid Res 40:850–860

Dyer JH, Maina A, Gomez ID, Cadet M, Oeljeklaus S, Schiedel AC (2009) Cloning, expression and purification of an acetoacetyl CoA thiolase from sunflower cotyledon. Int J Biol Sci 5:736–744

Enjuto M, Balcells L, Campos N, Caelles C, Arró M, Boronat A (1994) *Arabidopsis thaliana* contains two differentially expressed 3-hydroxy-3-methylglutaryl-CoA reductase genes, which encode microsomal forms of the enzyme. Proc Natl Acad Sci USA 9:927–931

Enjuto M, Lumbreras V, Marín C, Boronat A (1995) Expression of the *Arabidopsis HMG2* gene, encoding 3-hydroxy-3-methylglutaryl coenzyme A reductase, is restricted to meristematic and floral tissues. Plant Cell 7:517–527

Finer JJ, Vain P, Jones MW, McMullen MD (1992) Development of the particle inflow gun for DNA delivery to plant cells. Plant Cell Rep 11:323–328

Gerhardt B (1992) Fatty acid degradation in plants. Prog Lipid Res 31:417–446

Germain V, Rylott EL, Larson TR et al (2001) Requirement for 3-ketoacyl-CoA thiolase-2 in peroxisome development, fatty acid β-oxidation and breakdown of triacylglycerol in lipid bodies of *Arabidopsis* seedlings. Plant J 28:1–12

Gietl C (1996) Protein targeting and import into plant peroxisomes. Physiol Plant 97:599–608

Goldstein JL, Brown MS (1990) Regulation of the mevalonate pathway. Nature 343:425–430

Gondet L, Bronner R, Benveniste P (1994) Regulation of sterol content in membranes by subcellular compartmentation of steryl-esters accumulating in a sterol-overproducing tobacco mutant. Plant Physiol 105: 509–518

Guex N, Peitsch MC (1997) SWISS-MODEL and the Swiss-PdbViewer: an environment for comparative protein modelling. Electrophoresis 18:2714–2723

Haapalainen AM, Meriläinen G, Pirilä PL, Kondo N, Fukao T, Wierenga RK (2007) Crystallographic and kinetic studies of human mitochondrial acetoacetyl-CoA thiolase: the importance of potassium and chloride ions for its structure and function. Biochemistry 46:4305–4321

Hayashi M, Aoki M, Kato A, Kondo M, Nishimura M (1996) Transport of chimeric proteins that contain a carboxy-terminal targeting signal into plant microbodies. Plant J 10:225–234

Hemmerlin A, Fischt I, Bach TJ (2000) Differential interaction of branch-specific inhibitors of isoprenoid biosynthesis with cell cycle progression in tobacco BY-2 cells. Physiol Plant 110:342–349

Hemmerlin A, Hoeffler JF, Meyer O et al (2003) Cross-talk between the cytosolic mevalonate and the plastidial methylerythritol phosphate pathways in tobacco bright yellow-2 cells. J Biol Chem 278:26666–26676

Hogenboom S, Romeijn GJ, Houten SM, Baes M, Wanders RJ, Waterham HR (2002) Absence of functional peroxisomes does not lead to deficiency of enzymes involved in cholesterol biosynthesis. J Lipid Res 43:90–98

Honda A, Salen G, Nguyen LB, Xu G, Tint GS, Batta AK, Shefer S (1998) Regulation of early cholesterol biosynthesis in rat liver: effects of sterols, bile acids, lovastatin, and BM 15.766 on 3-hydroxy-3-methylglutaryl coenzyme A synthase and acetoacetyl coenzyme A thiolase activities. Hepatology 27:154–159

Kato A, Hayashi M, Takeuchi Y, Nishimura M (1996) cDNA cloning and expression of a gene for 3-ketoacyl-CoA thiolase in pumpkin cotyledons. Plant Mol Biol 31:843–852

Kelley LA, Sternberg MJE (2009) Protein structure prediction on the web: a case study using the Phyre server. Nat Protoc 4:363–371

Kurihara T, Ueda M, Tanaka A (1988) Occurrence and possible roles of acetoacetyl-CoA thiolase and 3-ketoacyl-CoA thiolase in peroxisomes of an *n*-alkane-grown yeast, *Candida tropicalis*. FEBS Lett 229:215–218

Kursula P, Sikkilä H, Fukao T, Kondo N, Wierenga RK (2005) High resolution crystal structures of human cytosolic thiolase (CT): a comparison of the active sites of human CT, bacterial thiolase, and bacterial KAS I. J Mol Biol 347:189–201

Lee MS, Mullen RT, Trelease RN (1997) Oilseed isocitrate lyases lacking their essential type 1 peroxisomal targeting signal are piggybacked to glyoxysomes. Plant Cell 9:185–197

Manavalan LP, Chen X, Clarke J, Salmeron J, Nguyen HT (2012) RNA-mediated disruption of squalene synthase

improves drought tolerance and yield in rice. J Exp Bot 63:163–175

Meriläinen G, Poikela V, Kursula P, Wierenga RK (2009) The thiolase reaction mechanism: the importance of Asn316 and His348 for stabilizing the enolate intermediate of the Claisen condensation. Biochemistry 48:11011–11025

Merret R, Cirioni J, Bach TJ, Hemmerlin A (2007) A serine involved in actin-dependent subcellular localization of a stress-induced tobacco BY-2 hydroxymethylglutaryl-CoA reductase isoform. FEBS Lett 581:5295–5299

Miziorko HM (2011) Enzymes of the mevalonate pathway of isoprenoid biosynthesis. Arch Biochem Biophys 505:131–143

Modis Y, Wierenga RK (1999) A biosynthetic thiolase in complex with a reaction intermediate: the crystal structure provides new insights into the catalytic mechanism. Structure 7:1279–1290

Nagata T, Nemoto Y, Hasezawa S (1992) Tobacco BY-2 cell line as the "HeLa" cell in the cell biology of higher plants. Int Rev Cytol 132:1–30

Nagegowda DA, Bach TJ, Chye ML (2004) *Brassica juncea* 3-hydroxy-3-methylglutaryl (HMG)-CoA synthase 1: expression and characterization of recombinant wild-type and mutant enzymes. Biochem J 383: 517–527

Nagegowda DA, Ramalingam S, Hemmerlin A, Bach TJ, Chye ML (2005) *Brassica juncea* HMG-CoA synthase: localization of mRNA and protein. Planta 221:844–856

Oeljeklaus S, Fischer K, Gerhardt B (2002) Glyoxysomal acetoacetyl-CoA thiolase and 3-oxoacyl-CoA thiolase from sunflower cotyledons. Planta 214:597–607

Olivier LM, Kovacs W, Masuda K, Keller GA, Krisans SK (2000) Identification of peroxisomal targeting signals in cholesterol biosynthetic enzymes. AA-CoA thiolase, HMG-CoA synthase, MPPD, and FPP synthase. J Lipid Res 41:1921–1935

Peretó J, López-García P, Moreira D (2005) Phylogenetic analysis of eukaryotic thiolases suggests multiple proteobacterial origins. J Mol Evol 61:65–74

Pirovano W, Feenstra KA, Heringa J (2008) PRALINE™: a strategy for improved multiple alignment of transmembrane proteins. Bioinformatics 24:492–497

Pye VE, Christensen CE, Dyer JH, Arent S, Henriksen A (2010) Peroxisomal plant 3-ketoacyl-CoA thiolase structure and activity are regulated by a sensitive redox switch. J Biol Chem 285:24078–24088

Rahier A, Benveniste P (1989) Mass spectral identification of phytosterols. In: Nes WD, Parish EJ (eds) Analysis of sterols and other significant steroids. Academic, New York, pp 223–250

Reumann S, Babujee L, Ma C et al (2007) Proteome analysis of *Arabidopsis* leaf peroxisomes reveals novel targeting peptides, metabolic pathways, and defense mechanisms. Plant Cell 19:3170–3193

Reumann S, Quan S, Aung K et al (2009) In-depth proteome analysis of *Arabidopsis* leaf peroxisomes combined with in vivo subcellular targeting verification indicates novel metabolic and regulatory functions of peroxisomes. Plant Physiol 150:125–143

Rodríguez-Concepción M, Yalovsky S, Zik M, Fromm H, Gruissem W (1999) The prenylation status of a novel plant calmodulin directs plasma membrane or nuclear localization of the protein. EMBO J 18:1996–2007

Schaller H, Grausem B, Benveniste P, Chye ML, Tan CT, Song YH, Chua NH (1995) Expression of the *Hevea brasiliensis* (H.B.K.) Mull. Arg. 3-hydroxy-3-methylglutaryl-coenzyme A reductase 1 in tobacco results in sterol overproduction. Plant Physiol 109:761–770

Schwede T, Kopp J, Guex N, Peitsch MC (2003) SWISS-MODEL: an automated protein homology-modeling server. Nucleic Acids Res 31:3381–3385

Servouse M, Karst F (1986) Regulation of early enzymes of ergosterol biosynthesis in *Saccharomyces cerevisiae*. Biochem J 240:541–547

Simkin AJ, Guirimand G, Papon N et al (2011) Peroxisomal localisation of the final steps of the mevalonic acid pathway *in planta*. Planta 234:903–914. doi: 10.1007/s00425-011-1444-6

Soto S, Stritzler M, Lisi C et al (2011) Acetoacetyl-CoA thiolase regulates the mevalonate pathway during abiotic stress adaptation. J Exp Bot 62:5699–5711. doi:10.1093/jxb/err287

Stermer BA, Bianchini GM, Korth KL (1994) Regulation of HMG-CoA reductase activity in plants. J Lipid Res 35:1133–1140

Thompson SL, Krisans SK (1990) Rat liver peroxisomes catalyze the initial step in cholesterol synthesis. The condensation of acetyl-CoA units into acetoacetyl-CoA. J Biol Chem 265:5731–5735

Van der Heijden R, Verpoorte R, Duine JA (1994a) Biosynthesis of 3*S*-hydroxy-3-methylglutaryl-coenzyme A in *Catharanthus roseus*: acetoacetyl-CoA thiolase and HMG-CoA synthase show similar chromatographic behaviour. Plant Physiol Biochem 32:807–812

Van der Heijden R, de Boer-Hlupá V, Verpoorte R, Duine JA (1994b) Enzymes involved in the metabolism of 3-hydroxy-3-methylglutaryl-coenzyme A in *Catharanthus roseus*. Plant Cell Tiss Org Cult 38:345–349

Voinnet O (2001) RNA silencing as a plant immune system against viruses. Trends Genet 17:449–459

Vollack K-U, Bach TJ (1996) Cloning of a cDNA encoding cytosolic acetoacetyl-coenzyme A thiolase from radish by functional expression in *Saccharomyces cerevisiae*. Plant Physiol 111:1097–1107

Wang H, Nagegowda DN, Rawat R et al (2012) Overexpression of *Brassica juncea* wild-type and mutant HMG-CoA synthase 1 in Arabidopsis up-regulates genes in sterol biosynthesis and enhances sterol production and stress tolerance. Plant Biotechnol J 10:31–42

Wass MN, Kelley LA, Sternberg MJE (2010) 3DligandSite: predicting ligand-binding sites using similar structures. Nucleic Acids Res 38:W469–W473

Weissenborn DL, Denbow CJ, Laine M, Lång SS, Yang Z, Yu X, Cramer CL (1995) HMG-CoA reductase and terpenoid phytoalexins: molecular specialization within a complex pathway. Physiol Plant 93:393–400

The Sterol C4-Demethylation in Higher Plants

25

Alain Rahier, Sylvain Darnet, Florence Bouvier, and Bilal Camara

Abstract

Sterols become functional only after removal of the two methyl groups at C4 by a membrane-bound multienzymatic complex. The process of C4-demethylation is complex and involves a sterol-C4 methyl oxidase (SMO), a 3βhydroxysteroid dehydrogenase/C4 decarboxylase (3βHSD/D) and a 3-oxosteroid reductase (SR). Two distinct families of *SMO* genes termed *SMO1* and *SMO2* and two *3βHSD/D* genes have been molecularly characterized from *Arabidopsis thaliana*. Arabidopsis 3βHSD/D was identified as a bifunctional short-chain dehydrogenase/reductase (SDR) protein. We report *in vivo* functional expression in the relevant yeast deletion mutants, *in vitro* enzymological characterization of the recombinant enzymes, and *in planta* down regulation by virus-induced gene silencing. Further, we made use of three-dimensional homology modeling and site-directed mutagenesis to identify key amino acids involved in 3βHSD/D substrate binding and catalysis. The present combination of molecular, biological, chemical, and structural approaches allowed a thorough identification and functional characterization of SMO*s* and 3βHSD/Ds as three further steps in the completion of the molecular inventory of sterol synthesis in higher plants.

Keywords

C4-demethylation • Non-heme iron oxygenase • Hydroxysteroid dehydrogenase • Oxidative decarboxylation • Homology modeling • Sterol biosynthesis • Catalytic mechanism

A. Rahier (✉) • S. Darnet • F. Bouvier • B. Camara
Institut de Biologie Moléculaire des Plantes,
CNRS, UPR2357, 28 rue Goethe,
Strasbourg cedex 67083, France
e-mail: alain.rahier@ibmp-cnrs.unistra.fr

T.J. Bach and M. Rohmer (eds.), *Isoprenoid Synthesis in Plants and Microorganisms: New Concepts and Experimental Approaches*, DOI 10.1007/978-1-4614-4063-5_25,

25.1 Introduction

In all organisms the sterol molecule becomes functional only after removal of the two methyl groups at C4 (Benveniste 2004; Bouvier et al. 2005; Lees et al. 1995). In animals and yeast, both methyl groups at C4 are removed successively early in the biosynthetic pathway. In contrast, in higher plants, biosynthetic studies have shown that the first C4-methyl group is removed early from a cyclopropylsterol precursor, while the second C4-methyl group is eliminated several steps later. Thus, demethylation occurs in the sequence C14, C4, C4 in animals and yeast and C4, C14, C4 in plants. The C4-demethylation process is central in sterol biosynthesis and involves 10 of the 20 enzymatic steps from oxidosqualene to end-pathway sterols. It is energetically costly since it requires 6 upon the 11 oxygen molecules and 8 upon the 18 NAD(P)H molecules consumed in the post-squalene segment of sterol biosynthesis. Moreover, since at least three crucial enzymes are involved, there are more opportunities for regulation and inhibition.

It has been first demonstrated in animals that C4-demethylation in rat liver requires the action three distinct enzymes, that is, a sterol C4-methyl oxidase (SMO), a 4αcarboxysterol-3βhydroxysteroid dehydrogenase/C4-decarboxylase (3β HSD/D), and a 3-oxosteroid reductase (SR) (Faust et al. 1988). In plants, we have first characterized the corresponding activities in order to define the steps involved in plant C4-demethylation (Fig. 25.1). The first step is initiated by the NADH- and cytochrome b_5-dependent SMO (Pascal et al. 1993; Rahier et al. 1997; Darnet and Rahier 2003), whereby this enzyme oxidizes through three successive monooxygenation steps the C4α methyl group to produce a 4α-carboxysterol derivative (Fig. 25.1). This is subsequently oxidatively decarboxylated by the NAD^+-dependent 3βHSD/D (Rondet et al. 1999) to produce a C4-monodemethylated 3-oxosteroid which is then stereospecifically reduced by the NADPH-dependent 3-oxosteroid reductase (Pascal et al. 1994).

Yeast mutants affected in the C4-demethylation process are lethal (Bard et al. 1996), and in animals, deficiency in C4-demethylation process

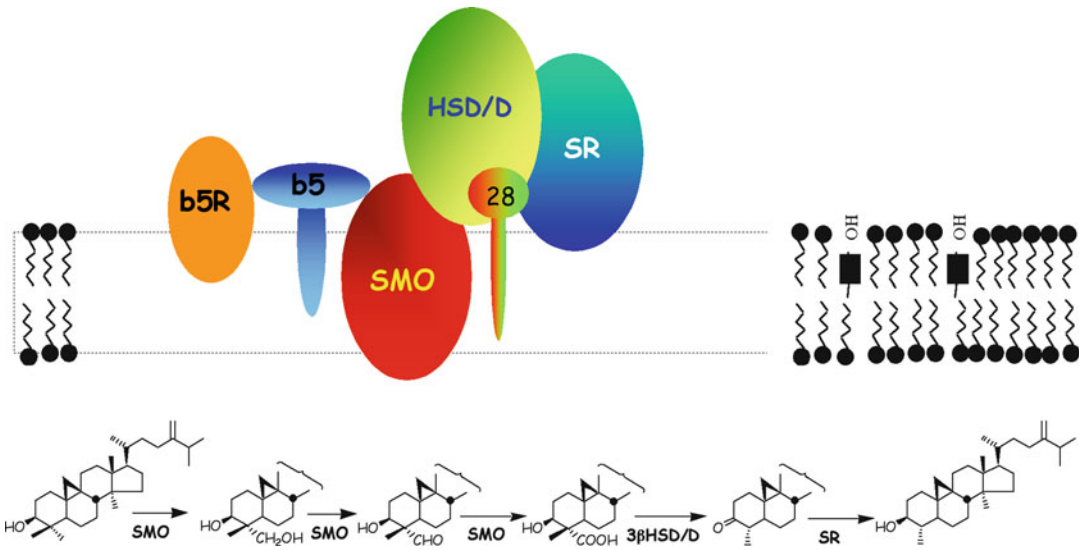

Fig. 25.1 Putative components of the ER-bound plant C4-demethylation enzymatic complex. *SMO* sterol methyl oxidase, a non-heme iron monooxygenase; *HSD/D* 3β-hydroxysteroid dehydrogenases/C4 decarboxylase, a member of the short-chain dehydrogenases/reductases (SDR) family; *SR* 3-oxosteroid reductase; *28* Erg28p, a transmembrane protein supposed to tether HSD/D and SR to the ER (Gachotte et al. 2001); *b5* cytochrome b_5; *b5R* NADH cytochrome b_5 reductase. Reactions pathway for removing of the first C4-methyl group of 24-methylenecycloartanol in plants

produces prenatal lethality (König et al. 2000). During the last years, mutants affected in several steps in the sterol biosynthetic pathway have been identified in Arabidopsis which help to shed new light on the essential role of sterols in plant development (cf. Clouse 2002). Mutants blocked in the late steps in the sterol biosynthetic pathway, that is, downstream from the second C4-demethylation step, such as the *dwarf7* mutant being defective in sterol-C5(6)-desaturase, share many phenotypic characteristics including dwarfism and can be rescued to wild-type morphology by brassinosteroid treatment. In contrast, mutants blocked more early, that is, before the second demethylation step, including the *fackel* mutant affected in the Δ14-reductase step, show a distinct phenotype. In addition to growth effects, they present severe disruption of embryogenesis, which cannot be rescued by brassinosteroid treatment. Thus, in plants, C4-methylated sterols may be implicated in the severe developmental effects observed in mutants where they accumulate. Moreover, mutants deficient in C4-demethylation have not been reported yet, probably reflecting that blockade of this step is lethal and suggesting regulatory functions for C4-methylated-sterol intermediates.

Furthermore, in plants, little is known about non-heme iron oxygenases as well as hydroxysteroid dehydrogenases from the short-chain dehydrogenases/reductases (SDR) (Oppermann et al. 2001, 2003; Kallberg et al. 2002) or aldo-keto-reductases (AKR) families (Hyndman et al. 2003) such as those involved in the C4-demethylation process, and identification and characterization of gene(s) encoding enzymes involved in the C4-demethylation process in plant has not been reported thus far.

During the past decade, the direct studies of plant sterol biosynthesis enzymes have been facilitated by the cloning of most of the corresponding genes. However, details of the 3D structure for membrane enzymes involved in the post oxidosqualene segment of sterol synthesis in plants, animals, and fungi are not available. In particular, the structure and the substrate-binding characteristics, and the detailed catalytic mechanism of membrane-bound enzymes of the C4-demethylation process are unknown. Due to the difficulty to crystallize membrane proteins, homology modeling provides a convenient means for understanding their functions.

To further our knowledge about non-heme iron oxygenases, hydroxysteroid dehydrogenases, and the sterol C4-demethylation multienzymatic complex in plants, we have identified and characterized at the molecular and enzymatic levels, novel SMO and 3βHSD/D isoforms from Arabidopsis. We performed identification and cloning of these *SMO* and *3βHSD/D* cDNAs, *in vivo* heterologous functional expression in yeast, *in vitro* enzymological characterization of the recombinant isoenzymes and *in planta* down-regulation by virus-induced gene silencing. We also constructed *in silico* a homology 3D-model of Arabidopsis 3βHSD/D, which provided novel information on substrate and cofactor three-dimensional interactions with the 3βHSD/D active site and allowed to propose a catalytic mechanism for this bifunctional HSD.

25.2 Molecular and Functional Characterizations of SMOs in Arabidopsis

By combining homology and sequence motif searches with knowledge relating to sterol biosynthetic genes across species, five SMO cDNAs from Arabidopsis (*At*SMO) belonging to two families have been cloned (Darnet et al. 2001; Darnet and Rahier 2004). All *At*SMOs amino-acid sequences were characterized by the presence of three histidine-rich motifs, $HX_3H\ X_{8or9}\ HX_2HH\ X_{73or75}\ HX_2HH$, which exhibit a topology and spacing of amino acids within the histidine motifs being typical of the *ERG3–ERG25* family, Pfam01598. Moreover, the spacing and topology of the histidine motifs are clearly distinct from those found in the extended family of membrane-bound fatty acid desaturases/hydroxylases (Shanklin and Cahoon 1998). One possible function for these tripartite motifs would be to provide the ligands for a presumed catalytic diiron center, as previously proposed for other enzymes possessing these motifs and catalyzing desaturation

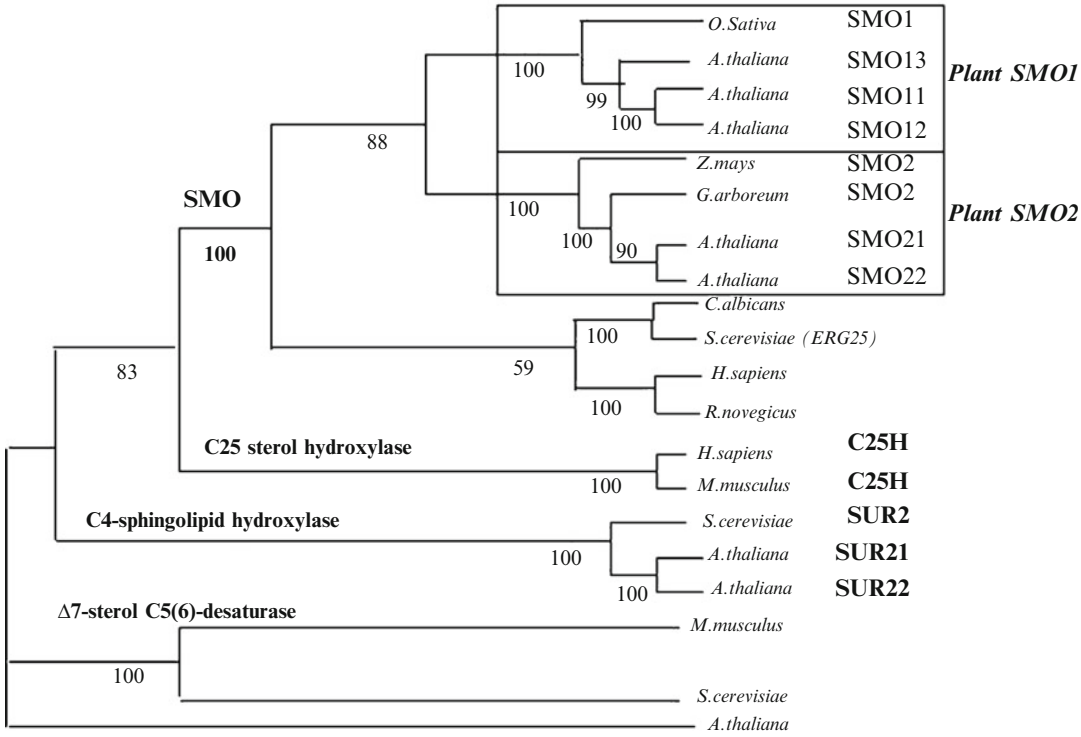

Fig. 25.2 Phylogram of putative or characterized (*boxed*) *SMO* proteins, of sterol C5-desaturases (C5-DES), and other membrane-bound non-heme iron oxygenases: *C25H* cholesterol-C25-hydroxylase, *SUR2* sphingolipide-C4-hydroxylase

or hydroxylation reactions (Shanklin and Cahoon 1998; Taton et al. 2000). From the multiple alignments of the full-length amino-acid sequences of *At*SMOs, and sterol-desaturase-like enzymes, we constructed a phylogenetic tree (Fig. 25.2). This tree clearly confirmed the existence of two families of putative plant SMOs isoenzymes, SMO1 and SMO2. AtSMO1 and AtSMO2 families contain three and two isoforms, respectively, and sequence comparison shows that the plant sequences are orthologous to the fungal and mammalian sequences.

25.2.1 Complementation of the Yeast Erg25 Ergosterol Auxotroph Lacking SMO Activity by SMOs from Arabidopsis

Two groups of complementation were obtained with plant *SMO* cDNAs: the *SMO2* group of complementation restored growth but only low levels of ergosterol biosynthesis. The *SMO1* group did not complement *erg25-25c* (Darnet et al. 2001; Darnet and Rahier 2004). This data suggest that only one family of SMOs is functional for the oxidation of 4,4-dimethylzymosterol, the physiological substrate of the yeast SMO accumulating in *erg25* (Bard et al. 1996; Darnet and Rahier 2003). It could reflect a strict and distinct substrate specificity of the plant SMO1 isoenzymes which are unable to oxidize 4,4-dimethylzymosterol, the physiological substrate of yeast SMO (Darnet and Rahier 2003) in contrast to the *Saccharomyces cerevisiae* SMO and to the plant SMO2 isozymes.

25.2.2 Functional Identification of Two Distinct Families of SMOs by VIGS in *Nicotiana benthamiana*

To elucidate the precise functions of *SMO1* and *SMO2* gene families, we have reduced their expression by using a virus-induced gene

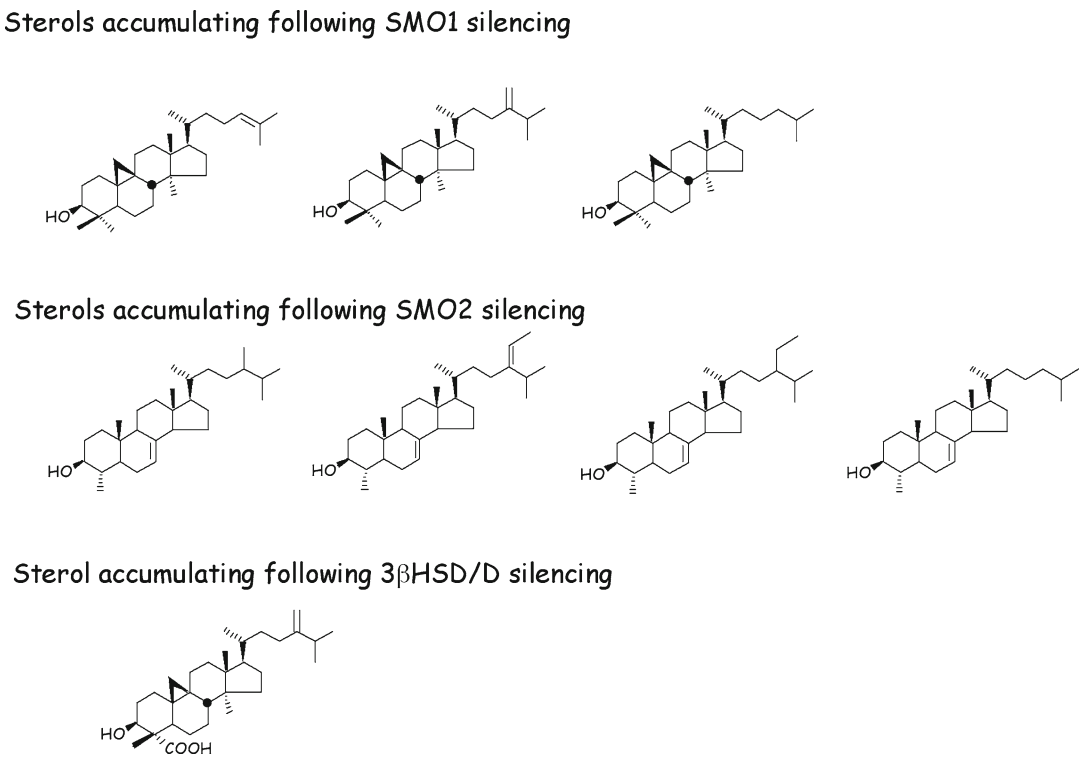

Fig. 25.3 Biochemical phenotypes of genetic inhibition of SMOs and 3βHSD/D by VIGS in *Nicotiana benthamiana*. Accumulation of sterol precursors induced by SMO1, SMO2, or 3βHSD/D silencing

silencing (VIGS) approach in *N. benthamiana* (Darnet and Rahier 2004). The genetic inhibition of the plant SMOs should result in the accumulation of the substrates of the targeted enzymes. Remarkably, following silencing of *SMO1*, a significant accumulation 4,4-dimethyl-9β19cyclopropyl-sterols was obtained (Fig. 25.3), while qualitative and quantitative levels of 4α-methylsterols were not affected. In the case of silencing of *SMO2*, a substantial accumulation of 4α-methyl-Δ^7-sterols was found, with no change in the levels of 4,4-dimethylsterols. The clear distinct biochemical phenotypes observed indicate that 4,4-dimethyl-9β,19-cyclopropyl-sterols were the preferred substrates of SMO1 and 4α-methyl-Δ^7-sterols that of SMO2. This specific accumulation of 4,4-dimethylsterols or 4α-methylsterols, respectively, is consistent with a poor overlapping in the substrate specificities of these two families of tobacco SMOs. The data are remarkably well in agreement with the clear distinct substrate specificities previously determined for the native microsomal maize SMOs (Pascal et al. 1993). Moreover, these substrate specificities are fully consistent with the abovementioned sequential events of the plant sterol biosynthetic pathway where removal of the two C4 methyl groups of sterol precursors does not occur consequently as it does in animals and fungi but is interrupted by several enzymatic steps. Remarkably, neither plant SMOs can accommodate a Δ^8-unsaturation which is present in the substrates of the mammalian and yeast SMOs (Fig. 25.4).

The data clearly ascribe the function of SMO1 as a 4,4-dimethyl-9β,19-cyclopropylsterol-4α-methyl oxidase and SMO2 as a 4α-methyl-Δ^7-sterol-4α-methyl oxidase, indicating that in photosynthetic eukaryotes, two distinct families of sterol C4-methyl oxidases control respectively the level of 4,4-dimethyl- and 4α-methylsterol precursors (Darnet and Rahier 2004).

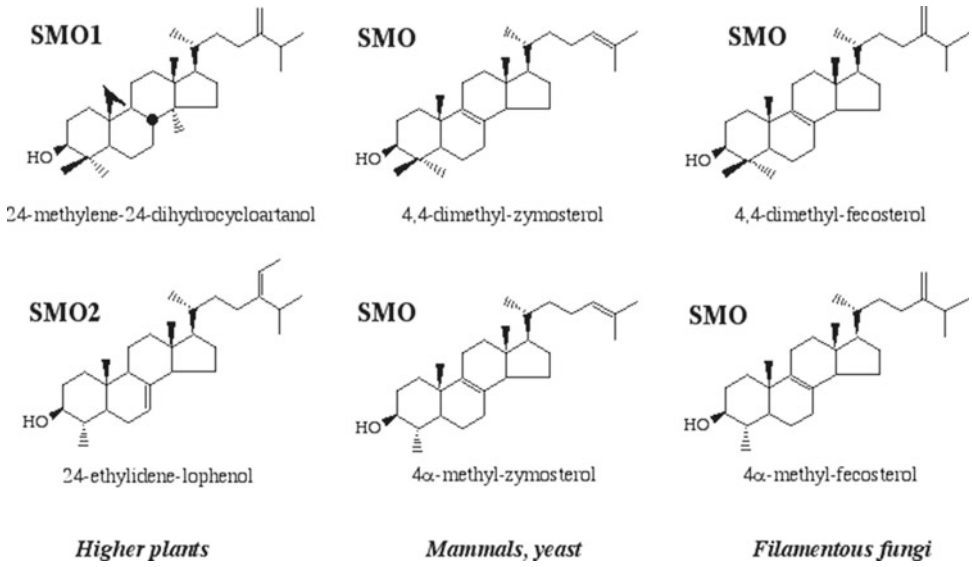

Fig. 25.4 Substrate preference of the sterol methyl oxidases in different organisms. In plants, the specificities of *SMO1* (4,4-dimethylsterol-4α-methyl oxidase) and *(SMO2)* 4α-methylsterol-4α-methyl oxidase were defined, *in vitro*, in microsomal extracts. The two plant SMOs show clear and distinct substrate specificities. In contrast, in animals and yeast, a single *SMO* is involved in the successive removal of the two methyl groups at C4

25.3 Molecular, Enzymatic, and Structural Characterizations of Novel Bifunctional 3β-Hydroxysteroid Dehydrogenases/ C4-Decarboxylases (3βHSD/D) from *A. thaliana*

By data mining for genes encoding putative orthologs of the yeast *ERG26* gene and also belonging to the hydroxysteroid dehydrogenase family, we isolated two cDNAs from *A. thaliana* encoding bifunctional 3β-hydroxysteroid dehydrogenase/C4-decarboxylases (3βHSD/D) involved in sterol synthesis, termed *At3βHSD/D1* (1,143 bp) and *At3βHSD/D2* (1,173 bp) (Rahier et al. 2006). They share 80% identity between each other and less than 40% identity with the corresponding yeast and animal orthologs. These clones show 25% identity with the human 3β-hydroxysteroid dehydrogenase/isomerase and 26% identity with the cholesterol dehydrogenase from *Nocardia*, with all enzymes catalyzing dehydrogenation of 3β-hydroxysteroids. The calculated molecular mass, 42 kDa for both, is in agreement with the apparent mass of 45 kDa found previously for the native maize 3βHSD/D (Rondet et al. 1999). The two Arabidopsis 3βHSD/Ds share the typical signatures of the SDR family (Fig. 25.6), including a nonclassical N-terminal glycine-rich motif TGGXGXXA, in which the third Gly residue is replaced by Ala. This nonclassical motif is generally found in the SDR group belonging to multifunctional enzyme complexes (Kallberg et al. 2002). In addition, the highly conserved YX_3K segment (residues 159–163 in 3βHSD/D1), assigned to the catalytic center (Jornvall et al. 1995), is found in both *At*3βHSD/D1 and -D2. The similarity of the two 3βHSD/Ds to erg26p and the NADPH steroid dehydrogenase-like protein (NSDHL) from animals is higher than with any other HSDs. Together with the present 3βHSD/Ds from plants, the yeast and animals orthologs form a differentiated cluster distinct from other HSDs, particularly those catalyzing dehydrogenations at positions other than 3β of the steroid nucleus or displaying an opposite stereochemistry for C3-hydride abstraction (Rahier et al. 2006). The formation of this distinct subfamily could reflect the remarkable bifunctionality of the 3βHSD/D proteins.

25.3.1 Complementation of the Yeast Erg26 Ergosterol Auxotroph Lacking 3βHSD/D Activity by 3βHSD/Ds from Arabidopsis

Complementation of the yeast *erg26* mutant by plant *3βHSD/D* cDNAs restored growth, high levels of ergosterol biosynthesis, and *in vitro*, high catalytically competent 3βHSD/Ds localized exclusively to the corresponding microsomal extracts, albeit a single hydrophobic portion was found in the Arabidopsis 3βHSD/D proteins which contained an ER retrieval signal (Rahier et al. 2006). In contrast to most SDR proteins including HSDs, biochemical studies performed in animals (Rahimtula and Gaylor 1972), yeast (Mo et al. 2002), and plants (Rondet et al. 1999) have shown that native 3βHSD/D is membrane-bound. This data indicates that *At*3βHSD/D is functionally inserted in the yeast C4-demethylation enzymatic complex and is able to channel endogenous 4αcarboxy-4β-methyl-cholest-8,24-dien-3β-ol through this complex and the sterol pathway.

25.3.2 Enzymatic and Kinetic Characterizations of 3βHSD/Ds

Our yeast system allowed the isolation of sufficient amount of recombinant 3βHSD/Ds to investigate their enzymological properties in the corresponding yeast microsomal preparations. The apparent kinetic parameters of 3βHSD/Ds with 4α-carboxysterol substrate revealed Km values in the same order of magnitude as those of a variety of post-squalene sterol biosynthetic enzymes from different sources. In contrast, the measured rates appear relatively high in comparison to the rates of other enzymes in the pathway, including other components of the C4-demethylation complex. The data suggest that the 3βHSD/D is not rate-limiting the overall process of C4-demethylation and that 4-carboxysterols are probably transient intermediates, which is consistent with the observation that they have not been isolated in plant or wild-type yeast thus far.

Deuterium isotopic effects have been used extensively to study the mechanism of numerous enzymes involving a hydrogen transfer step. However, no such study has been carried out with an HSD thus far. In noncompetitive assays, we compared the kinetics of carboxysterol substrate with its 3alpha-deuterated analog. The observed primary deuterium isotope effects for oxidation of the deuterated substrate were near unity. This lack of an isotope effect indicates that the 3α-hydrogen-carbon bond cleavage is not the rate-limiting step of the reaction (Rahier et al. 2006). One possibility to explain the lack of an isotope effect would be that one or several steps of the reaction pathway, including chemical steps and products release, might be slower than the hydride transfer step and thus completely masked the ^{D}V. Another possibility is that carboxysterol behaves as a sticky substrate that reacts to give products as fast or faster than it dissociates from the enzyme, that is, the enzyme-substrate complex has a high commitment to catalysis (Cleland 1982, 2003; Northrop 1999). However, measurement of a single isotope effect is not sufficient to elucidate the mechanism of the 3βHSD/Ds; this will need further studies, although it seems logical that 3C–H bond cleavage and decarboxylation are separate events. In line with such observations, in a number of enzymes catalyzing similar oxidative decarboxylation reaction, exemplified by the malic enzyme or the 6-phosphogluconate dehydrogenase, a stepwise mechanism was shown to exist.

25.3.3 Substrate Screening of the At3βHSD/Ds

To complete our catalytic analysis of this unique bifunctional HSD, we looked for the molecular determinants of the substrate essential for productive interaction with the enzyme (Fig. 25.5). For both 3βHSD/Ds, substrate specificity required a 3β-hydroxyl group and a free C4α-carboxyl group but was quite tolerant in terms of variation of the sterol nucleus and side-chain structure (Rahier et al. 2006). Remarkably, no preference between substrates with one or two substituents at C4 was observed, and specificity of the two 3βHSD/D isoenzymes was very similar.

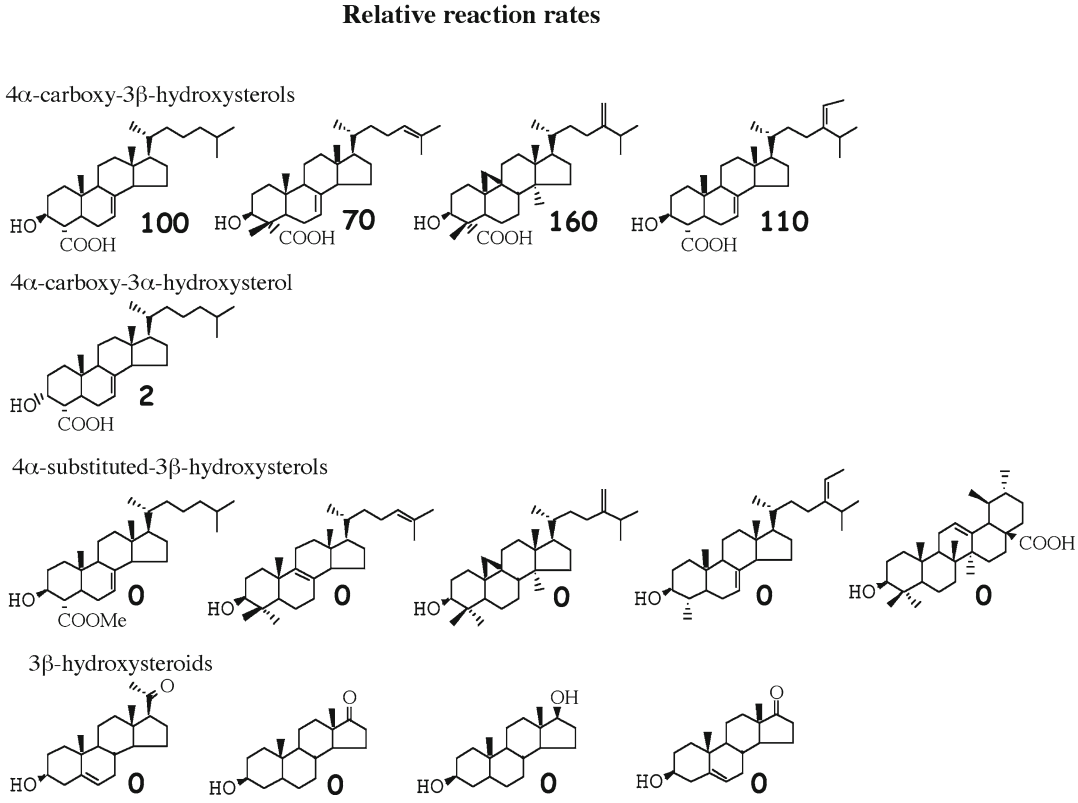

Fig. 25.5 Substrate preference of recombinant Arabidopsis 3βHSD/Ds. The specificity of 3βHSD/D was analyzed in the corresponding yeast microsomal extracts. The substrate preferences of the two 3βHSD/D isoenzymes were found to be very similar. The reaction rates of the various substrates at a 40 μM concentration were measured in the same enzymatic preparation and compared to the rate obtained with 4α-carboxy-cholest-7-en-3β-ol which was taken as 100%

This leads us to address the question of the strict and distinct structural requirements observed for the two SMO families.

25.3.4 Silencing of Endogenous *N. benthamiana* 3βHSD/D

To learn more about the function *in planta* of the cloned 3βHSD/Ds, we carried out VIGS experiments in *N. benthamiana*. A 500-bp cDNA fragment homologous to the N terminus of 3βHSD/Ds from *A. thaliana* was isolated and cloned into the viral TTO vector. This cDNA fragment shares 57–59% identity with the Arabidopsis 3βHSD/Ds and thus falls clearly within the family. Young *N. benthamiana* inoculated with infectious TTO mRNA constructs or noninfected plants were then grown for three additional weeks postinoculation. The VIGS experiments led to young *N. benthamiana* plants exhibiting a clear biochemical phenotype. These biochemical changes obtained after infection with *TTO-Nb3βHSD/D* correlating with the specific reductions in *Nb3βHSD/D* mRNA levels confirm the genetic silencing of the corresponding *Nb3βHSD/D* endogene. Silencing of *Nb3βHSD/D* resulted in a substantial accumulation of a novel 4α-carboxysterol, 4α-carboxy-4β14αdimethyl-9β,19-cyclo- ergost-24(24[1])-en-3β-ol (Fig. 25.3), involved in the pathway for removing the first methyl group at C4, thereby confirming the function of the present 3βHSD/Ds *in planta* (Rahier et al. 2006).

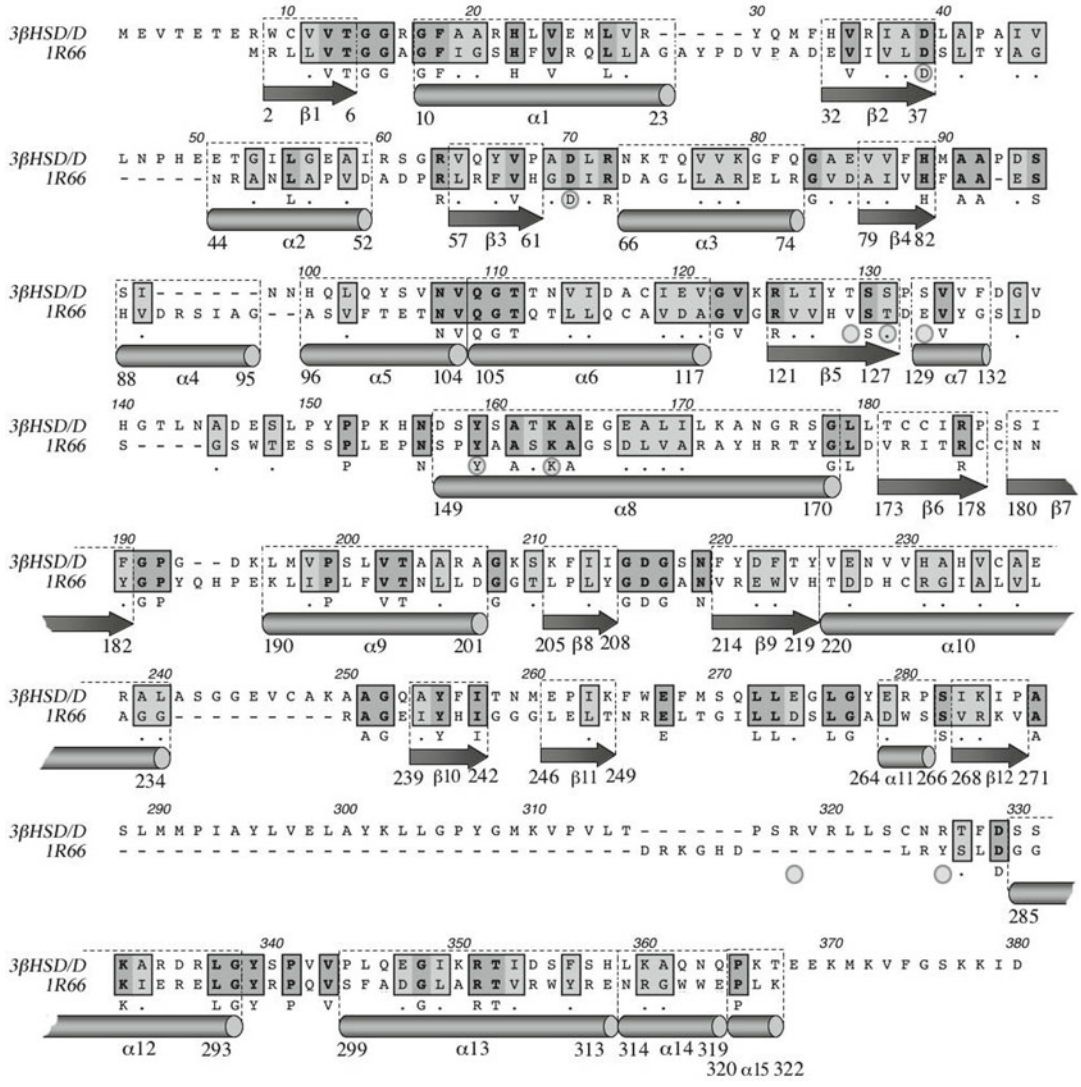

Fig. 25.6 Alignment and secondary structure comparison between 3β-hydroxysteroid dehydrogenase/C4-decarboxylase (3βHSD/D) from *Arabidopsis thaliana* and the template protein dTDP-glucose 4,6-dehydratase (1R66) from *Streptomyces venezuelae*. The secondary structure elements are indicated as *arrows* for β-strands and as cylinders for α-helices. Amino acid further analyzed by mutagenesis is shown with a *gray point*. The nomenclature used for helices and strands corresponds to that of the 1R66 pdb file

25.3.5 Determining Structure and Function of 3βHSD/D by Sequence Analysis, Homology Modeling, and Rational Mutational Analysis

Amino-acid sequence analysis suggests that 3βHSD/D is a member of the SDR family (Pfam 01073). When the sequence of 3βHSD/D was compared with those of all SDR enzymes for which crystal structures have been reported, the structure with the greatest percentage identity was that of dTDP-glucose-4,6-dehydratase (DesIV) from *Streptomyces venezuelae* (Allard et al. 2004) (Fig. 25.6). The peptide sequence of 3βHSD/D displayed 24% identity and 40% similarity when aligned with that of DesIV. Furthermore, 3βHSD/D (42 kDa) and DesIV

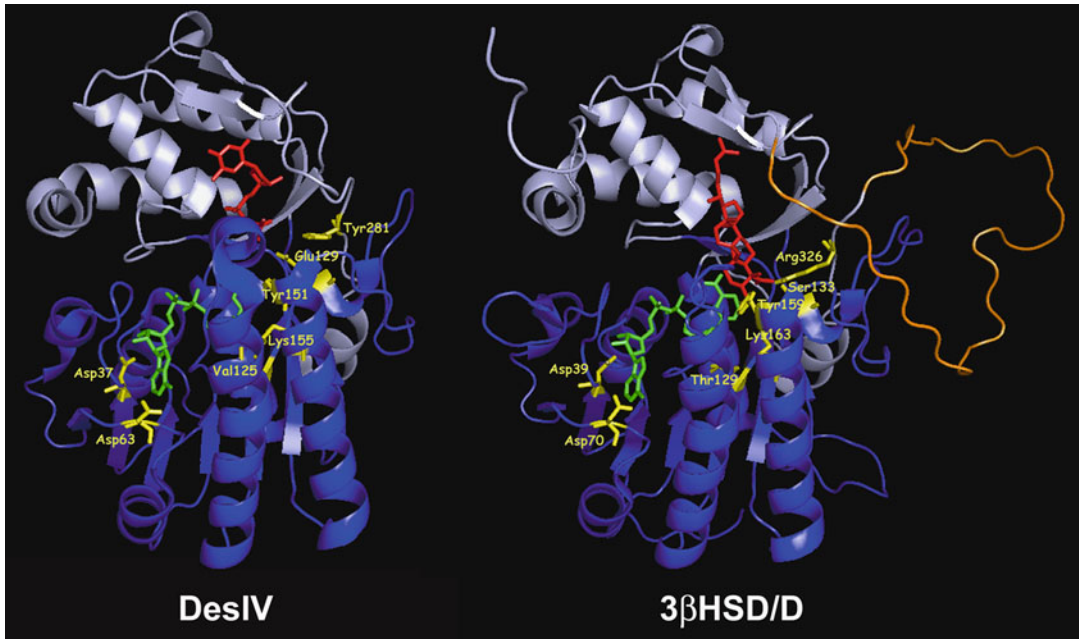

Fig. 25.7 Ribbon diagrams of *Arabidopsis thaliana* 3β-hydroxysteroid dehydrogenase/C4-decarboxylase (3βHSD/D) based on homology modeling and of dTDP-glucose 4,6-dehydratase (DesIV) used as a template, with key amino acids identified. The N-terminal domain, responsible for NAD docking (*dark blue*) and C-terminal domain responsible for carboxysterol or DAU positioning (*light blue*) are shown. The loop in *orange* including the putative hydrophobic membrane-interacting domain could not be reliably modeled. The NAD^+ (*green*) and carboxysterol and DAU structures (*red*) are included. For 3βHSD/D, the key catalytic Tyr159 and Lys163 residues for 3β-dehydrogenation, the carboxysterol-stabilizing residue Arg326, and the carboxysterol 4β-methyl proximal residue Ser133 are also shown (*yellow*). Asp39, Asp70, Ser95, and Thr129 residues are shown with hydrogen bonding to NAD^+. The homologous residues are shown for DesIV

(37 kDa) share a rather big size as compared to other hydroxysteroid dehydrogenases (381 for 3βHSD/D versus 250 amino acid residues for HSDs), and have strict NAD^+ cofactor specificity (Rondet et al. 1999). Thus, we used the three-dimensional structure of DesIV for homology modeling of 3βHSD/D (Fig. 25.7) (Rahier et al. 2009; Rahier 2011). There is no doubt about the fit (Oppermann et al. 2001, 2003; Jornvall et al. 1995), particularly because of (1) the conservation of the catalytic YxxxK motif, (2) the presence in the 3βHSD/D of the TGGxGxxA signature in the β1α1 turn, (3) the conservation of many of the conserved residues in the DesIV structural family that are in contact with the NAD cofactor, (4) the presence of an aspartate residue in the β2α2 turn of 3βHSD/D that predicts NAD preference in cofactor binding, and (5) all the secondary elements of DesIV could be preserved in 3βHSD/D except one α-helix (α4) (Figs. 25.6 and 25.7).

The validity of using the three-dimensional structure of DesIV as a model for 3βHSD/D was biochemically tested by mutation studies (Rahier et al. 2009). Key amino acids were subjected to site-directed mutagenesis and the mutated enzymes were expressed and assayed both *in vivo* and *in vitro* in an *erg26* yeast strain defective in 3βHSD/D. We show that Tyr159 and Lys163 which are oriented near the 3βhydroxyl group of the substrate in the model are essential for the 3βHSD/D activity, consistent with their involvement in the initial dehydrogenation step of the reaction (Figs. 25.8, 25.9, and 25.10). The essential Arg326 residue is predicted to form a salt bridge with the 4α-carboxyl group of the substrate, suggesting its involvement both in substrate binding and in the decarboxylation step.

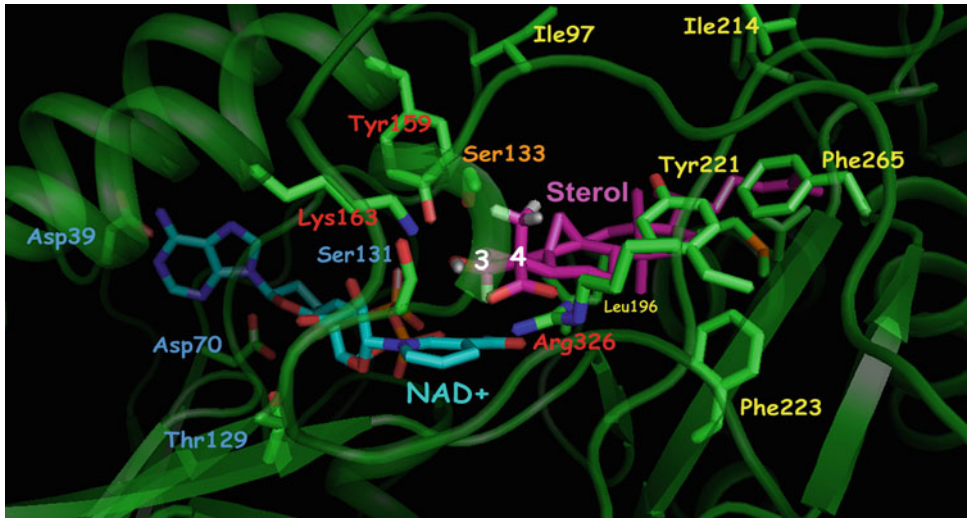

Fig. 25.8 Close-up view of active-site residues in 3βHSD/D determined by homology modeling in relation to modeled NAD⁺ and steroid substrate (4α-carboxy-4β14αdimethyl-cholesta-9β,19-cyclo-24-en-3βol) molecules. Residues analyzed in this study are mentioned. Tyr159 and Lys163 are in catalytic distance to the substrate and in distance to interact with each other. The substrate is further stabilized by a salt bridge with Arg326. Ser133 is in close proximity of the C4β-methyl group of the steroid substrate. Asp39, Asp70, Ser95, and Thr129 residues are interacting with NAD⁺. Hydrophobic residues that are in the immediate surroundings of the carboxysterol in its binding pocket are also shown as well as Glu147, possibly interacting with Arg326 in absence of substrate. The figure was created with PyMOL (DeLano 2002)

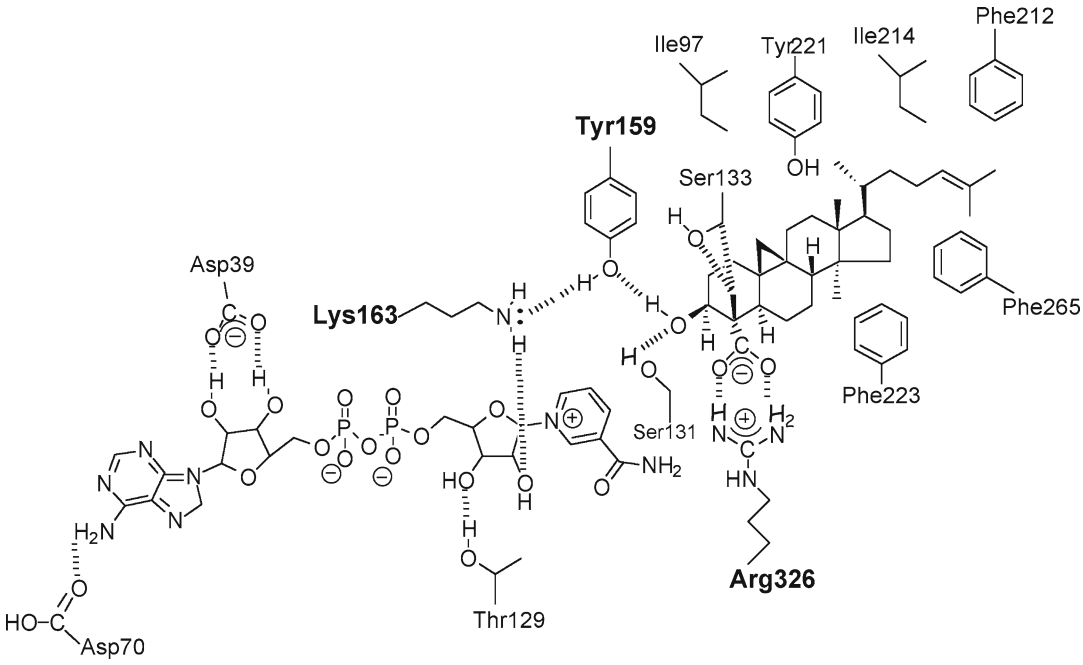

Fig. 25.9 Scheme of the predicted interactions in the catalytic pocket of 3βHSD/D with NAD⁺ and the carboxysterol. Hydrogen bonds, salt bridge and steric interactions between amino acids, NAD⁺ and carboxysterol substrate are indicated by *dashed lines*. Hydrophobic residues that are in the immediate surroundings of the carboxysterol in its docking pocket are also shown

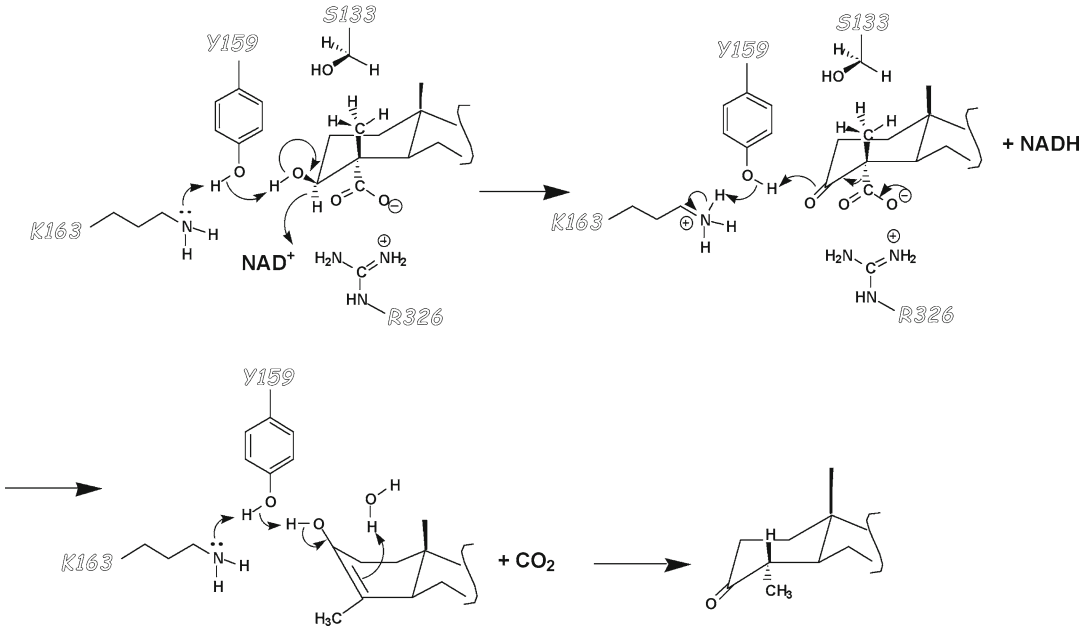

Fig. 25.10 Proposed reaction mechanism of 3β-hydroxysteroid dehydrogenase/C4-decarboxylase. Tyr159, Lys163, and Arg326 are proposed to be involved in the dehydrogenation and decarboxylation of 4α-carboxysterol with NAD^+. 4α-Carboxysterol binding is stabilized by Arg326. Tyr159 acts as the general base to abstract the proton of the hydroxyl group of steroid and facilitates the hydride transfer to NAD^+ and acts as the general acid to deliver a proton to the 3-keto group and together with Arg326 facilitates the decarboxylation of the carboxysteroid. Tyr159 and a water molecule probably help to the final tautomerization step

The essential Asp39 residue is in close contact with the hydroxyl groups of the adenosine-ribose ring of NAD^+ in good agreement with the strong preference of 3βHSD/D for NAD^+. Data obtained with Ser133 mutants suggest a close proximity between the Ser133 residue and the C4β-domain of the bound sterol. We suggest that the dual action of 3βHSD/D is associated with the 130 additional residues on the carbonyl end of the enzyme compared to the other members of the SDR family.

25.3.6 Catalytic Mechanism of 3βHSD/D

Based on the data, we propose a tentative mechanism for 3βHSD/D activity (Fig. 25.10) (Rahier et al. 2009). In the first step catalyzed by 3βHSD/D, Arg326 stabilizes the substrate, while Tyr159 functions as the catalytic base, and Lys163 lowers the pKa of the Tyr-OH to promote proton transfer during the dehydrogenation of the carboxysterol to produce the corresponding ketone. In the decarboxylation of the 3-oxo acid to produce the enol, Tyr159 donates a proton to the 3-keto group, while Arg326 maintains the carboxyl group in a deprotonated state. Tautomerization of the enol to produce the 3-keto-C4-decarboxylated product is possibly helped by extraction of the proton from the C3-hydroxyl by Tyr159 and addition of a proton on the β-face at C4 from a water molecule. During the course of C4-demethylation of 4,4-dimethysterols, the 4α-methyl group is first oxidized by the SMO to yield a carboxyl; this is then decarboxylated and the intermediate enol is protonated on the β-face, presenting to the oxygenase another 4α-methyl group for the same treatment.

25.4 Conclusion

The present combination of molecular, biological chemical, and structural approaches allowed a thorough identification and functional characterization of *SMOs* and *3βHSD/Ds* as three further

steps in the completion of the molecular inventory of sterols synthesis in higher plants. Genetic redundancy or lethality may account for the failure to isolate plant *SMOs* or *3βHSD/D* genes by screening of phenotypes by using a genetic approach. Given that plant mutants affected in *SMO* and *3βHSD/D* have thus far not been reported, the present studies provide important clues for the physiological roles of C4-substituted sterols in photosynthetic eukaryotes. The novel *3βHSD/Ds* constitute the first hydroxysteroid dehydrogenase genes of the SDR superfamily to be molecularly and enzymatically characterized in plants. The present study based on *Arabidopsis* 3βHSD/D provides the first data on the three-dimensional molecular interactions of a sterol biosynthetic enzyme with its substrate in the steps downstream oxidosqualene cyclase. The homology model can be used to target other key amino acids responsible for coenzyme and steroid binding, membrane interaction, and interactions with other components of the C4-demethylation complex. These informations could give clues for the design of novel and selective structure-based inhibitors. *In vivo*, such inhibitors should offer the possibility to phenocopy not yet identified plant 3βHSD/D mutants.

References

Allard ST, Cleland WW, Holden HM (2004) High resolution X-ray structure of dTDP-glucose 4,6-dehydratase from Streptomyces venezuelae. J Biol Chem 279: 2211–2220

Bard M, Bruner PA, Pierson CA et al (1996) Cloning and characterization of ERG25, the *Saccharomyces cerevisiae* gene encoding C-4 sterol methyl oxidase. Proc Natl Acad Sci USA 93:186–190

Benveniste P (2004) Biosynthesis and accumulation of sterols. Annu Rev Plant Phys 55:429–457

Bouvier F, Rahier A, Camara B (2005) Biogenesis, molecular regulation and function of plant isoprenoids. Prog Lipid Res 44:357–429

Cleland WW (1982) Use of isotope effects to elucidate enzyme mechanisms. CRC Crit Rev Biochem 13:385–428

Cleland WW (2003) The use of isotope effects to determine enzyme mechanisms. J Biol Chem 278: 51975–51984

Clouse SD (2002) Arabidopsis mutants reveal multiple roles for sterols in plant development. Plant Cell 14:1995–2000

Darnet S, Rahier A (2003) Enzymological properties of sterol-C4-methyl-oxidase of yeast sterol biosynthesis. Biochim Biophys Acta 1633:106–117

Darnet S, Rahier A (2004) Plant sterol biosynthesis: identification of two distinct families of sterol 4α-methyl oxidases. Biochem J 378:889–898

Darnet S, Bard M, Rahier A (2001) Functional identification of sterol-4α-methyl oxidase cDNAs from *Arabidopsis thaliana* by complementation of a yeast *erg25* mutant lacking sterol-4α-methyl oxidation. FEBS Lett 508:39–43

DeLano WL (2002) The PyMOL Molecular Graphic System. DeLano Scientific, Palo Alto, CA

Faust JR, Trzaskos JM, Gaylor JL (1988) Cholesterol biosynthesis. In: Yeagle PL (ed) Biology of cholesterol. CRC Press, Boca Raton, pp 19–38

Gachotte D, Eckstein J, Barbuch R, Hughes T, Roberts C, Bard M (2001) A novel gene conserved from yeast to humans is involved in sterol biosynthesis. J Lipid Res 42:150–154

Hyndman D, Bauman DR, Heredia VV, Penning M (2003) The aldo-keto reductase superfamily homepage. Chem Biol Interact 143–144:621–631

Jornvall H, Persson B, Krook M, Atrian S, Gonzales-Duarte R, Jeffery J, Ghosh D (1995) Short-chain dehydrogenases/reductases (SDR). Biochemistry 34: 6003–6013

Kallberg Y, Oppermann U, Jörnvall H, Persson B (2002) Short-chain dehydrogenase/reductase (SDR) relationships: a large family with eight clusters common to human, animal, and plant genomes. Protein Sci 11:636–641

König A, Happle R, Bornholdt D, Engel H, Grzeschik K-H (2000) Mutations in the NSDHL gene, encoding a 3β-hydroxysteroid dehydrogenase, cause CHILD syndrome. Am J Med Genet 90:339–346

Lees ND, Skaggs B, Kirsch DR, Bard M (1995) Cloning of the late genes in the ergosterol biosynthetic pathway of *Saccharomyces cerevisiae*. Lipids 30: 221–226

Mo C, Valachovic M, Randall SK, Nickels JT, Bard M (2002) Protein-protein interactions among C-4 demethylation enzymes involved in yeast sterol biosynthesis. Proc Natl Acad Sci USA 99:9739–9744

Northrop DB (1999) Rethinking fundamentals of enzyme action. Adv Enzymol Relat Areas Mol Biol 73: 25–54

Oppermann U, Filling C, Jörnvall H (2001) Forms and functions of human SDR enzymes. Chem Biol Interact 130–132:699–705

Oppermann U, Filling C, Hult M et al (2003) Short-chain dehydrogenases/reductases (SDR): the 2002 update. Chem Biol Interact 143–144:247–253

Pascal S, Taton M, Rahier A (1993) Plant sterol biosynthesis: identification and characterization of two dis-

tinct microsomal oxidative enzymatic systems involved in sterol C4-demethylation. J Biol Chem 268: 11639–11654

Pascal S, Taton M, Rahier A (1994) Plant sterol biosynthesis: identification of a NADPH dependent plant sterone reductase involved in the sterol-4-demethylation. Arch Biochem Biophys 312:260–271

Rahier A (2011) Dissecting the sterol C-4 demethylation process in higher plants. From structures and genes to catalytic mechanism. Steroids 76:340–352

Rahier A, Smith M, Taton M (1997) The role of cytochrome b5 in 4α-methyl-oxidation and C5(6) desaturation of plant sterol precursors. Biochem Biophys Res Commun 236:434–437

Rahier A, Darnet S, Bouvier F, Camara B, Bard M (2006) Molecular and enzymatic characterizations of novel bifunctional 3β-hydroxysteroid dehydrogenases/C4 decarboxylases from *Arabidopsis thaliana*. J Biol Chem 281:27264–27277

Rahier A, Bergdoll M, Génot G, Bouvier F, Camara B (2009) Homology modeling and site-directed mutagenesis reveal catalytic key amino acids of 3β-hydroxysteroid-dehydrogenase/C4-decarboxylase from Arabidopsis. Plant Physiol 149:1872–1886

Rahimtula AD, Gaylor JL (1972) Partial purification of a microsomal sterol 4 -carboxylic acid decarboxylase. J Biol Chem 247:9–15

Rondet S, Taton M, Rahier A (1999) Identification, characterization and partial purification of 4α-carboxysterol-C3-dehydrogenase-C4-decarboxylase from *Zea mays*. Arch Biochem Biophys 366:249–260

Shanklin J, Cahoon EB (1998) Desaturation and related modifications of fatty acids. Annu Rev Plant Phys 49:611–641

Taton M, Husselstein T, Benveniste P, Rahier A (2000) Role of highly conserved residues in the reaction catalyzed by recombinant Δ7-sterol C5(6)-desaturase studied by site-directed mutagenesis. Biochemistry 39:701–711

Sterol C22-Desaturase and Its Biological Roles

26

Daisaku Ohta and Masaharu Mizutani

Abstract

The C22-unsaturated sterols are primarily found in fungi and plants. The C22-desaturation reaction is catalyzed by independent cytochrome P450 family proteins, CYP61 in fungi, and CYP710 in plants. We describe our extensive characterization studies of plant CYP710 family proteins and discuss possible evolutional relationships of C22-desaturation reactions among eukaryotic organisms. We also discuss possible research directions toward understanding physiological implications of sterols in unidentified brassinosteroid-independent growth/developmental processes.

Keywords

Cytochrome P450 • Sterol • Side chain • Desaturase • Evolution • Diversification • Eukaryotes • Brassinosteroid-independent processes

26.1 Introduction

Sterols in eukaryotic cells are functioning as both the essential components of biological membranes and biosynthetic precursors of steroid hormones. Diversities in membrane sterol structures are ascribed to various steps of hydroxylation, alkylation, and double-bond formation in both the nucleus and the side chain. Different sterol profiles in microorganisms are repeatedly discussed as to species evolution processes (Volkman 2003), and inhibition of the sterol biosynthetic pathway constitutes a very important mode of action in antimicrobial drug development. On the other hand, major sterol end products are common to higher plants, which implicates an extensive conservation

D. Ohta (✉)
Graduate School of Life and Environmental Sciences, Osaka Prefecture University, 1-1 Gakuen-cho, Sakai, Osaka 599-8531, Japan
e-mail: ohtad2g30490@bioinfo.osakafu-u.ac.jp

M. Mizutani
Graduate School of Life and Environmental Sciences, Osaka Prefecture University, 1-1 Gakuen-cho, Sakai, Osaka 599-8531, Japan

Chemical Research Institute, Kyoto University, Uji 611-0011, Japan

T.J. Bach and M. Rohmer (eds.), *Isoprenoid Synthesis in Plants and Microorganisms: New Concepts and Experimental Approaches*, DOI 10.1007/978-1-4614-4063-5_26,

of the entire sterol biosynthetic pathway enzymes. A typical sterol profile is represented by a model plant species, *Arabidopsis thaliana* Col-0 containing sitosterol, 24-methyl cholesterol (a mixture of 24-*epi*-campesterol and campesterol, only different in the stereochemistry of the 24-methyl group), stigmasterol, and isofucosterol (Schaller 2004; Benveniste 2004 and literature cited therein). It has been known that *Brassicaceae* family plants contain 24-methyl-Δ^{22}-sterols as a mixture of brassicasterol (ergosta-5,22E-dien-3β-ol) or crinosterol (campesta-5,22E-dien-3β-ol), which are derived from 24-*epi*-campesterol (ergost-5-en-3β-ol) and campesterol (campest-5-en-3β-ol), respectively (Matsumoto et al. 1983; Benveniste 2004).

In eukaryotic organisms, a prominent structural difference of sterols between animals (cholesterol), fungi (ergosterol), and plants (stigmasterol) consists in the presence or absence of the C22-double bond. A fungal cytochrome P450 monooxygenase, CYP61, has been shown to act as sterol C22-desaturase and thereby to produce ergosta-5,7,22,24(28)-tetraenol from the immediate precursor, ergosta-5,7,24(28)-trienol, as the penultimate step in the ergosterol biosynthetic pathway (Skaggs et al. 1996; Kelly et al. 1997).

Here, we describe the identification and characterization of cytochrome P450 (P450s) belonging to the CYP710A subfamily, as the enzymes responsible for the C22-desaturation reaction that afford stigmasterol from β-sitosterol and brassicasterol/crinosterol from 24-*epi*-campesterol and campesterol. Also, we discuss possible future research areas aiming at elucidation of physiological roles of membrane sterols in plants.

26.2 Sterol C22-Desaturase in Plants

The fungal P450 CYP61 is the only enzyme so far identified as a sterol C22-desaturase (Skaggs et al. 1996; Kelly et al. 1997). Several lines of evidence, for instance, from sequence comparison suggested that CYP710 was a candidate for sterol C22-desaturase in plants as soon as Arabidopsis CYP710 EST sequences became available. CYP710A family proteins among plant P450s share the highest sequence identity with CYP61s (about 26%). Between CYP710 and CYP61, a specific conserved sequence motive [FLFA(A/S)QDAS(T/S)S] has been identified in the I helix distal to the heme group, constituting one of the putative substrate recognition sites (SRS4) of P450s (Gotoh 1992). The conserved sequence between CYP61 and CYP710 is characterized by the presence of two Ala residues (corresponding to Ala-295 and Ala-299 in Arabidopsis CYP710A1, and Ala-296 and Ala-340 in yeast CYP61). Most P450 monooxygenases catalyzing hydroxylation reactions contain a conserved Thr residue at the second of these two positions, participating in the oxygen activation and proton delivery in P450 monooxygenase reactions (Meunier et al. 2004). In addition, the CYP710A family is phylogenetically close to the 51 clan composed of CYP51 (the sterol C14-demethylase) and the 85 clan comprised of P450s including CYP85, CYP88, and CYP90, which are involved in a variety of activities in plants, there metabolizing terpenoid compounds such as sterols and brassinosteroids (Nelson 2006). These observations strongly indicated that CYP710A family proteins represent the functional C22-desaturase in plants. However, so far, the enzyme activities have not been characterized in greater detail.

Our first attempt in characterization of CYP710A was its heterologous expression in yeast. The four *CYP710A* coding sequences were amplified by PCR from the Arabidopsis genome (*CYP710A1*: At2g34500; *CYP710A2*: At2g34490; *CYP710A3*: At2g28850; *CYP710A4*: At2g28860). These coding sequences did not contain introns, and the predicted amino acid sequence of CYP710A1 is 81.9%, 77.7%, and 76.1% identical to those of CYP710A2, CYP710A3, and CYP710A4, respectively. The CYP710A3 protein sequence is 73.9% and 93.9% identical to those of CYP710A2 and CYP710A4, respectively. Using the amino acid sequence of CYP710A1 as the bait for a tblastn search at The TIGR Gene Indices (http://tigrblast.tigr.org/tgi/), we identified a tomato EST clone (gi: 7334215) containing a putative entire coding region for tomato CYP710A11 protein. The deduced primary structure consists of 501 amino acids with a calculated molecular mass of 57,511 Da, and the

Table 26.1 Sterol compositions in T87 transformed cells

Sample	Brassicasterol[a]	Campesterol[a]	Stigmasterol	β-Sitosterol
C	1.40 ± 0.44	17 ± 0.25	0.75 ± 0.050	47 ± 0.70
A1-1	1.60 ± 0.26	12 ± 0.63	44 ± 2.2	27 ± 3.9
A1-2	1.9 ± 0.51	5.1 ± 0.47	55 ± 11	17 ± 1.7
A2-1	12 ± 4.6	6.4 ± 2.9	4.3 ± 0.34	76 ± 5.5
A2-2	1.4 ± 0.57	7.6 ± 6.7	0.5 ± 0.05	76 ± 3.1
A3-1	0.85 ± 0.044	5.3 ± 0.35	7.6 ± 0.73	89 ± 10
A3-2	1.7 ± 0.44	9.3 ± 1.0	6.3 ± 0.50	74 ± 6.7
A4-1	21 ± 0.048	6.1 ± 0.70	4.4 ± 0.27	86 ± 3.0
A4-2	22 ± 0.028	6.6 ± 0.89	3.9 ± 0.080	71 ± 1.7
RNAi-1	0.19 ± 0.025	6.4 ± 0.035	0.092 ± 0.0012	180 ± 15
RNAi-2	0.26 ± 0.013	15 ± 0.018	0.19 ± 0.024	120 ± 18

[a] The C24-epimers were not separately analyzed

Sample C means nontransformed T87 cells. A1-1 and A1-2, A2-1 and A2-2, A2-1 and A2-2, and A4-1 and A4-2 were independent cell lines of *CYP710A1*, *CYP710A2*, *CYP710A3*, and *CYP710A4* overexpression, respectively. Two independent RNA interference lines generated using a pART27 binary vector (Wesley et al. 2001). Data are the means ± SD of triplicate determinations. Values are given in μg/g FW. The C24-epimers were not separately analyzed

amino acid sequence is 58.8% identical to that of CYP710A1 protein.

First, these Arabidopsis *CYP710A* coding sequences were used for the expression under the control of GAL1 promoter in an *erg5* mutant of a yeast strain, YPH 499 (*MAT*a *ura3-52 lys2-801_amber ade2-101_ochre trp1-Δ63 his3-Δ200 leu2-Δ1 erg5*; Sikorski and Hieter 1989). GC-MS analyses demonstrated that the transformed yeast cells did not produce Δ^{22}-sterols (Ohta et al., unpublished results), although genetic complementation studies with yeast mutants have been successfully applied to elucidate plant sterol biosynthetic pathway genes (Gachotte et al. 1996; Bach and Benveniste 1997; Darnet et al. 2001). In considering the possible substrate structures of plant C22-desaturase, it seems likely that plant C22-desaturase did not accept ergosta-5,7, 24(28)-trienol, the true substrate of CYP61. Furthermore, the microsomes from the transformed yeasts did not catalyze the C22-desaturation reaction to produce stigmasterol and brassicasterol from β-sitosterol and campesterol, respectively, and the recombinant enzymes of CYP710A1 from a baculovirus/insect cell expression system did not present a detectable level of C22-desaturase activity as well. On the other hand, in the same enzyme assay system as that used for recombinant CYP710A1, the recombinant tomato CYP710A11 expressed in the insect cells was sufficiently active to produce stigmasterol from β-sitosterol. Likewise, when *CYP710A* genes from the moss *Physcomitrella patens* encoding C22-desaturase were expressed in baculovirus/insect cells, activity that converted β-sitosterol into stigmasterol was found (Morikawa et al. 2009). Furthermore, in both *CYP710A1*- and *CYP710A11*-overexpression lines of *Arabidopsis*, stigmasterol levels were greatly enhanced, supporting *in planta* the C22-desaturation activity of the recombinant CYP710A proteins (Table 26.1, Morikawa et al. 2006). Enhanced accumulation of stigmasterol was also observed when *Arabidopsis CYP710A1, CYP710A2*, *CYP710A3*, and *CYP710A4* were overexpressed in the *Arabidopsis* suspension-cultured cells (T87), providing further evidence for the C22-desaturation activity of CYP710A proteins (Table 26.1). In addition, the T87 cells with the CYP710A2 overexpression contained elevated levels of 24-methyl-Δ^{22}-sterols (brassicasterol/crinosterol), suggesting that CYP710A2 was involved in the production of 24-methyl-Δ^{22}-sterols. Following these results *in planta*, we examined the recombinant CYP710A activities very carefully and demonstrated that the Arabidopsis CYP710A (Morikawa et al. 2006) and *P. patens* CYP710A proteins were the active C22-desaturases (Morikawa et al. 2009).

The sterol profiles from the T87 overexpression study indicated that CYP710A2 from

Arabidopsis is the only enzyme that accepts 24-methylsterols as the substrate for the C22-desaturase reaction. It is known that *Brassicaceae* family plants contain 24-methyl-Δ^{22}-sterols as a mixture of brassicasterol and crinosterol, which are derived from 24-*epi*-campesterol and campesterol, respectively (Matsumoto et al. 1983; Benveniste 2004). The four *Arabidopsis* CYP710A proteins and tomato CYP710A2 did not exhibit C22-desaturase activity with campesterol to produce the Δ^{22}-sterol (crinosterol) (Morikawa et al. 2006). The tomato CYP710A11 was also inactive with campesterol as the substrate. We then synthesized 24-*epi*-campesterol to clarify whether the stereoconfigurations of the 24-methyl group might be distinguished by the Arabidopsis CYP710A proteins. The Arabidopsis CYP710A2 indeed catalyzed the C22-desaturase reaction to produce brassicasterol with the synthesized 24-*epi*-campesterol, while no crinosterol production was detected with the Arabidopsis CYP710A1 (Morikawa et al. 2006). These results indicated that CYP710A2 was the desaturase responsible for the production of brassicasterol from 24-*epi*-campesterol in Arabidopsis (Fig. 26.1). Further evidence *in planta* was that the T-DNA insertion within the CYP710A2 gene did not contain detectable level of 24-methyl-Δ^{22}-sterols (Morikawa et al. 2006).

26.3 CYP710 Family

CYP710A is one of the oldest plant P450 genes including *CYP51*, *CYP97*, and *CYP746,* which predated the emergence of land plants, and the function seems to be conserved among diverse plant species from gymnosperms to monocots and dicots (Schuler and Werck-Reichhart 2003; Nelson 2006). A phylogenetic tree (Fig. 26.2) was obtained with CYP710A proteins from higher plants, CYP710A13 and CYP710A14 from the moss (*P. patens*), CYP710Bs from green algae (*Chlamydomonas reinhardtii*), red algae (*Cyanidioschyzon merolae*), and the multicellular green alga (*Volvox carteri*), and the CYP710 related sequences from *Trypanosomatidae*. It has been reported that *C. reinhardtii* produces ergosterol and 7-dehydroporiferasterol as the major end sterols (Salimova et al. 1999). In the *P. patens* tissues, stigmasterol was the major sterol (66% of total sterol) with β-sitosterol (7% of total sterol) as a minor component (Morikawa et al. 2009). The Arabidopsis T87 cells with the moss CYP710A14 overexpression contained elevated levels of stigmasterol (40 ~ 150-fold increase) but not brassicasterol/crinosterol (Morikawa et al. 2009), which proves that CYP710A in the moss is involved in the production of stigmasterol.

In the phylogenetic tree, the cluster of the higher plant CYP710s was distinct from the CYP61 cluster, and both CYP710s and CYP61s were distant from another P450 monooxygenase, CYP51, involved in the sterol biosynthetic pathway and catalyzing the sterol 14-demethylation (Benveniste 2004). A branch was comprised of the algal CYP710Bs and the CYP710-related sequences in *Trypanosoma cruzi* (XP_818982) and *Leishmania major* (XP_001684965). The primary structure deduced from the *T. cruzi* sequence was 48%, 36%, and 26% identical to those of *Chlamydomonas* CYP710B, *Arabidopsis* CYP710A1, and yeast CYP61, respectively. Note that *T. brucei* is lacking a *CYP710* sequence in the genome. It has been suggested that *Trypanosomatidae* descended from an ancestor other than photosynthetic organisms (El-Sayed et al. 2005); the genus *Leishmania* diverged first and the subgenus *Trypanosoon* (*T. brucei)* evolved later than *Schizotrypanum* (*T. cruzi*). The amastigotes of *T. cruzi* did not contain Δ^{22}-sterols, but epimastigotes produced Δ^{22}-sterols, and the bloodstream form of *T. brucei* contains predominantly cholesterol, apparently suppressing de novo synthesis of C28 sterols (Roberts et al. 2003). It is therefore possible that the sterol biosynthetic activities in *Trypanosomatidae* are downregulated during their life cycle, and the availability of host sterols might have affected the loss of a *CYP710* sequence in *T. brucei*.

A cellular slime mold (*Dictyostelium discoideum*) produces Δ^{22}-sterols such as dictyosterol, (24*R*)-24-ethylcholest-*trans*-22-en-3β-ol (Nes et al. 1990). *D. discoideum* contains a CYP524 with the particular sequence, [F(L/M)FA(A/S)QDA(S/T)

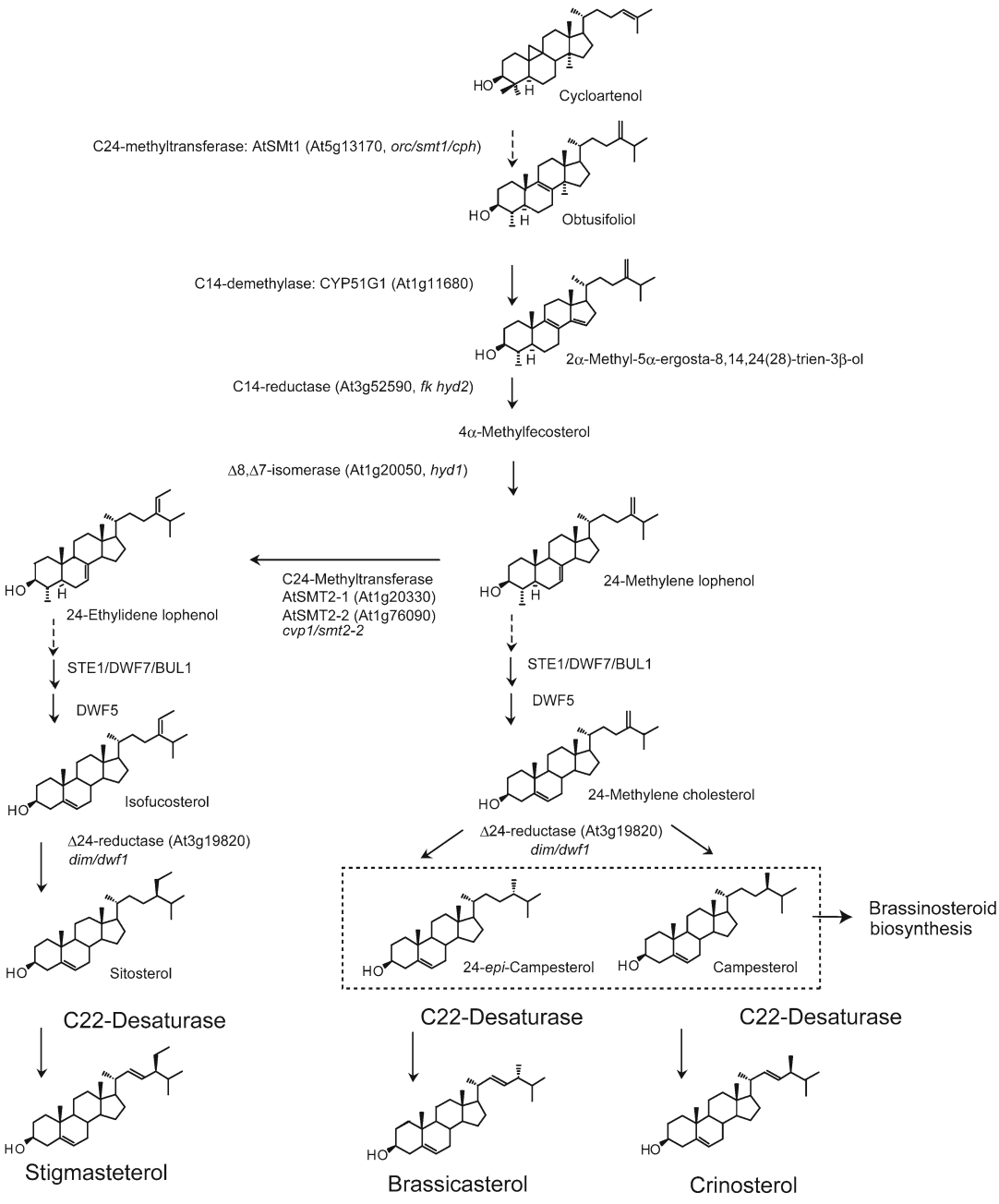

Fig. 26.1 Sterol biosynthetic pathway in Arabidopsis. The pathway from cycloartenol to the Δ^{22}-sterols is shown. 24-methylsterols are a mixture of (24*R*)- and (24*S*)-epimers of campesterol (Morikawa et al. 2006). The Δ^{22}-desaturases catalyze the C22-desaturation reaction to yield Stigmasterol and crinosterol/brassicasterol from their immediate precursors, respectively. *Dashed arrows* indicate several enzymatic steps not shown here. Campesterol and 24-*epi*-campesterol are the precursors for brassinosteroid (BR) biosynthesis

(S/T)S], which is conserved in the SRS4 site of both CYP61 and CYP710 proteins. Thus, CYP524 could be involved in the sterol C22-desaturation reaction in the slime mold. Sterol analysis suggested that the slime mold evolved from algal rather than fungal ancestors (Nes et al. 1990).

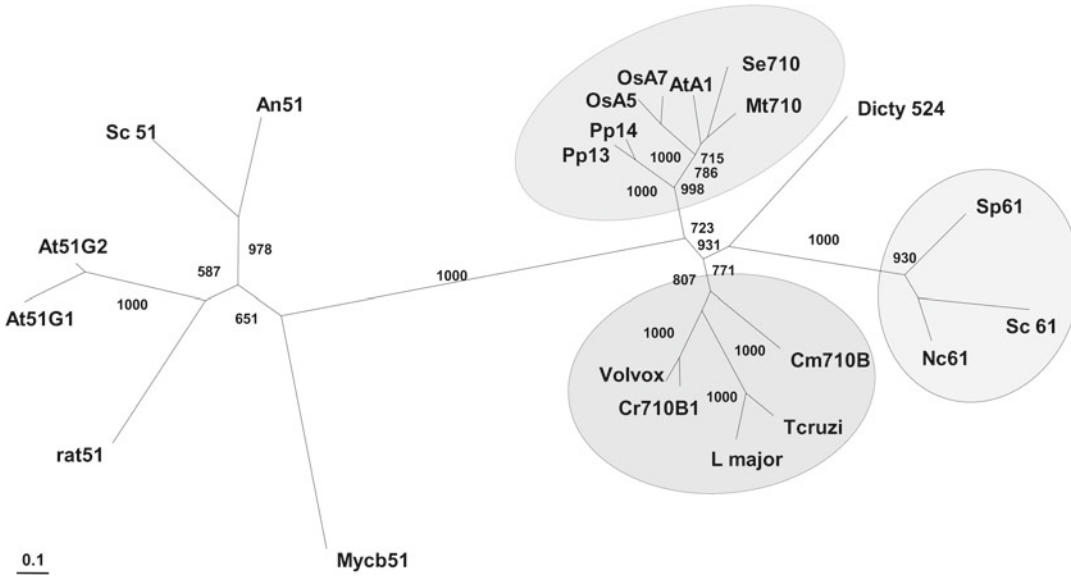

Fig. 26.2 Phylogenetic tree for CYP710 proteins and major Δ^{22}-sterols. Amino acid sequences were aligned at the DNA Data Bank of Japan (DDBJ http://www.ddbj.nig.ac.jp/search/clustalw-e.html) using the ClustalW program with bootstrap analysis ($n = 1{,}000$), and phylogenetic trees in phylip outputs were visualized using TreeView software (http://taxonomy.zoology.gla.ac.uk/rod/treeview.html). The phylogenetic tree of CYP710-related sequences was obtained with CYP710A1 (AtA1; At2g34500) from *Arabidopsis*, CYP710A11 (Se710) from tomato (gi: 7334215), CYP710A (Mt710) from *Medicago truncatula* (TC101450 at http://tigrblast.tigr.org/tgi/), CYP710A5 and CYP710A7 (Os01g0210900 and Os01g0211200) from *Oryza sativa*, CYP710A13 and CYP710A14 from *Physcomitrella patens* (PHYSCObase, http://moss.nibb.ac.jp/), CYP710B (Cm710B) from *Chlamydomonas reinhardtii* (ChlamyDB http://www.chlamy.org/chlamydb.html), CYP710B (Cr710B) from *Cyanidioschyzon merolae* (http://merolae.biol.s.u-tokyo.ac.jp/), CYP710 (Volvox) from *Volvox carteri* (http://genome.jgi-psf.org/Volca1/Volca1.home.html), CYP710 sequences from *Trypanosoma cruzi* (Tcruzi, XP_818982) and *Leishmania major* (Lmajor, XP_001684965), CYP524 (Dicty524) from *Dictyostelium discoideum* (dictyBase http://dictybase.org/), CYP61 (Sp61) from *Schizosaccharomyces pombe* (GenBank gi: 7007345), CYP61 (Nc61) from *Neurospora crassa* (GenBank gi: 28923500), CYP61 (Sc61) from *Saccharomyces cerevisiae* (GenBank gi: 798924), CYP51 (An51) from *Aspergillus nidulans* (GenBank gi: 66847777), CYP51F1 (Sc51) from *S. cerevisiae* (GenBank gi: 798924), CYP51G1 (At51G) and CYP51G2 (At51G2) from *Arabidopsis thaliana* (At1g16880 and At2g17330), CYP51 from rat (rat51, NP_037073), and CYP51B1 (Mycb51) from *Mycobacterium tuberculosis* (GenBank gi: 15607904)

There is an inconsistency about the coexistence of lanosterol synthase (fungi and animals)/cycloartenol synthase (plants) and CYP61 (fungi and animals)/CYP710 (plants). The fungal ergosterol pathways involve lanosterol synthase for the cyclization of 2,3-oxidosqualene and CYP61 for the C22-desaturation, while in plants, the first cyclization of 2,3-oxidosqualene is primarily catalyzed by cycloartenol synthase, and CYP710 is in charge of the C22-desaturation. It should be noted that higher plants also contain lanosterol synthase (e.g., AtLAS1 at3g45130 from Arabidopsis, Kolesnikova et al. 2006; Suzuki et al. 2006), but sequence comparison clearly indicates that such plant lanosterol synthase is closer to plant cycloartenol synthase rather than to fungal lanosterol synthase (Phillips et al. 2006). The cycloartenol pathway is conserved in some but not all protozoa, suggesting the coexistence of at least two nonphotosynthetic protozoan lineages, which are phylogenetically distinct; protozoan species comprising *Dictyostelium* might have formed one nonphotosynthetic group, while *Leishmania* formed another nonphotosynthetic group (Nes et al. 1990). *Leishmania* species synthesize lanosterol in their sterol biosynthetic pathway and contain the *CYP710* sequences (Lepesheva et al. 2006). On the other hand, *Dictyostelium* supposedly derived from photosynthetic organisms (Nes et al. 1990)

synthesizes cycloartenol and contains CYP524 as its C22-desaturase candidate. Nonetheless, *CYP710*-related sequences are conserved in both *Dictyostelium* and *Leishmania*, while *CYP61* sequences have so far been found only in fungi. Further information to clarify when and how the C22-desaturase genes have evolved may provide detailed evolutional relationships among protozoa, fungi, and plants.

26.4 Physiological Roles

In Arabidopsis, the gene clusters for a pair of *CYP710A1* and *CYP710A2* and a pair of *CYP710A3* and *CYP710A4* are located on chromosome 2. Among these four highly similar *CYP710* genes, only the enzyme derived from *CYP710A2* was responsible for the activity to produce brassicasterol from 24-*epi*-campesterol. It has been suggested that these *CYP710A* genes recently duplicated, maintaining the same function of the C22-desaturation in different tissues (Nelson 2006). In Arabidopsis, only CYP710A2 among the four CYP710As contains an insertion of four amino acids near the SRS4. It is possible that this insertion event in *CYP710A2* should be after the duplication of the *CYP710A1 and CYP710A2* on chromosome 2. A similar insertion was also seen in a *CYP710A* sequence from *Brassica napus* (Masaharu Mizutani, personal communication), and the C22-desaturation reaction with 24-methylsterols might be a new function acquired in *Brassicaceae* species. Each of *CYP710A1, A2, A3,* and *A4* genes displayed unique expression profiles, and the differential regulation of these genes covered every tissue and growth stage of Arabidopsis plants (Morikawa et al. 2006). Poplar has only one CYP710 gene, and physiological functions of CYP710 should not be diversified among different tissues in plants (Nelson 2006).

Phytosterols have been suggested to be involved in brassinosteroid (BR)-independent processes of embryonic and postembryonic development (Lindsey et al. 2003; Schaller 2004). Gene disruptions in the upstream part of the sterol biosynthetic pathway (Fig. 26.1) caused severe impairment in embryogenesis and development at specific stages, which cannot be rescued by exogenous BRs. The Arabidopsis mutants, *sterolmethyltransferase1* (*smt1/orc*), are defective in cycloartenol C24-methyltransferase (Diener et al. 2000; Willemsen et al. 2003), and *fackel* (*fk*) is due to the mutation of the C14-reductase gene (Jang et al. 2000; Schrick et al. 2000). The *hydra1* (*hyd1*) mutants are defective in the Δ^8 Δ^7-isomerase (Souter et al. 2002). Other embryonic mutants of *cephalopod (cph)* and *hydra2* (*hyd2*) have been found to be allelic to *smt1* and *fk*, respectively (Souter et al. 2002; Schrick et al. 2002). The mutants of *fk* and *hyd1*, and *smt1/cph* accumulated unique sterols and were characterized by incomplete cell walls and aberrant cell wall thickenings in embryonic and postembryonic tissues with an ectopic callose and lignin deposit (Schrick et al. 2004). However, specific roles of such unusually accumulated sterols have not been clarified in BR-independent developmental processes (He et al. 2003; Schrick et al. 2004). Lindsey et al. (2003) also reported developmental abnormalities with altered sterol compositions of *smt1/cph/orc* mutants with disturbed polar localizations of PIN proteins, suggesting abnormal membrane properties in these mutants (Willemsen et al. 2003). On the other hand, PIN protein trafficking was not affected in either the *hyd1* or *hyd2/fk* mutant (Souter et al. 2002). Nonetheless, these sterol biosynthetic mutants being defective in the upper part of the pathway display severely affected membrane sterol compositions, and the developmental abnormalities have been discussed in relation to altered sterol profiles, affecting the processes of plant pattern formation, morphogenesis, and cell polarity. Men et al. (2008) reported that the mutant defective in cyclopropylsterol isomerase gene displayed abnormal root gravitropism responses with alterations of PIN2 endocytosis and sterol composition.

The phenotypes associated with the mutations in the methyltransferase gene (*SMT2*) encoding the C24-methytransferase to produce 24-ethylidene lophenol from 24-methyl-lophenol (Fig. 26.1) were less severe compared with those of the upstream mutants such as *smt1/cph/orc*,

caused by the disruption of the first step methyltransferase. The mutations of *sterolmethyltransferase2* (*smt2*) and *cotyledon vascular pattern 1* (*cvp1*) are due to *SMT2* gene disruption (Schaeffer et al. 2001; Carland et al. 2002). *cvp1* plants displayed postembryonic vascular patterning defects (Carland et al. 2002), and *SMT2* cosuppression lines contained higher levels of campesterol and lower levels of β-sitosterol, exhibiting developmental abnormalities such as reduced apical dominance and reduced fertility that could not be restored by exogenous BRs (Schaeffer et al. 2001). Schaeffer et al. (2001) suggested that SMT2 is involved in the balancing of proper ratio of campesterol to β-sitosterol for normal growth and membrane integrity.

The mutations in the enzymatic steps after the reaction of the C4-demethylase, such as *ste1/dwf7/bul1*, *dwf5*, and *dim* (Fig. 26.1), result in BR deficiency due to the loss of campesterol, the BR biosynthetic precursor (Schaller 2004). Thus, the 24-ethylsterols including β-sitosterol and stigmasterol are not primarily involved in the phenotypes of *ste1/dwf7/bul1*, *dwf5*, and *dim* mutants. In other words, the *smt2*/*cvp1* phenotype such as postembryonic vascular patterning defects (Carland et al. 2002) may imply a specific role of 24-ethylsterols.

The phenotype of aberrant vascular development cannot be simply ascribed to altered sterol compositions and thereby affecting membrane properties. It should be noted that *cvp1* plants exhibiting the abnormal vascular development (Carland et al. 2002) still contained significant amounts of β-sitosterol (28–42% of wild-type) and stigmasterol (44–56% of wild-type). In an *Arabidopsis CYP710A1* overexpression line with no observable phenotypes (Ohta et al., unpublished results), the β-sitosterol level decreased to 33% of that in wild-type (81 μg/g fresh weight in the overexpression line and 246 μg/g fresh weight in wild-type) with the 32-fold increase in the stigmasterol level (107 μg/g fresh weight in the overexpression line and 3.4 μg/g fresh weight in wild type). Also, a T-DNA insertion event within the *CYP710A2* gene completely abolished the 24-methyl-Δ^{22}-sterol production activity without any observable phenotypic alterations in Arabidopsis (Morikawa et al. 2006). Interestingly, a similar phenotype in vascular patterning is seen in Arabidopsis double knockout lines with regard to xylogen genes encoding two nonspecific lipid transfer protein family proteins (Motose et al. 2004). Xylogen is an apoplastic proteoglycan-like factor required for local and inductive cell-cell interactions essential for xylem differentiation in *Zinnia* cultured cells. Xylogen protein has a selective binding activity to stigmasterol and also with a weaker affinity to brassicasterol, suggesting that xylem differentiation processes involve a sterol-xylogen complex formation (Motose et al. 2004). The Arabidopsis genome contains more than 20 xylogen-related genes with annotations as protease inhibitor/seed storage/lipid transfer protein, and detailed genome analyses of specific physiological roles of these genes could provide new insight into cellular sterol metabolism.

A number of experimental evidences have suggested that proper sterol compositions in the cell are crucial for normal developmental processes, and it is likely that there might be unidentified cellular processes depending on specific roles of sterols rather than general biophysical membrane properties. It should be noted that biophysical membrane properties in such mutant plants have not been reported (Schaller 2004). In the cells of yeasts and mammals, and in plant cells as well, specialized detergent-resistant membrane regions called lipid microdomains/rafts are enriched in sphingolipids and sterols, constituting a platform to accommodate proteins being involved in a variety of physiological processes such as signal transduction for cellular proliferation and differentiation, vesicular trafficking, and cytoskeleton organization. We obtained a 1% Triton-X-100-insoluble fraction as detergent-resistant membranes (DRMs) from microsomes of Arabidopsis T87 cells by discontinuous density gradient centrifugation. As those reported with other sources such as tobacco BY-2 cells (Mongrand et al. 2004), Arabidopsis root callus (Borner et al. 2005), and leek seedlings (Laloi et al. 2007), the relative sterol composition in the DRMs was not different from those of microsomes and total cellular sterols (Table 26.2). Borner et al. (2005) reported an approximately fourfold higher sterol-to-protein content in *Arabidopsis* DRMs, accumulating specific proteins such as

Table 26.2 Relative sterol compositions of detergent-resistant membranes (DRMs) from T87 transformed cells

Sterol	Non-TF	A1-2	A2-2	RNAi-1
	(% of total sterols)			
Cholesterol	0.81	0.62	0.75	0.43
Brassicasterol	0.83	1.3	13	0.12
Campesterol	13	15	4.4	16
Stigmasterol	1.5	80	8.1	0.23
β-Sitosterol	85	2.7	73	83

Microsomal fractions from T87 cells were treated with 1% (w/v) Triton-X-100, and DRMs were obtained by discontinuous density gradient (0%, 45%, 50%) centrifugation (200,000 × *g*) using OptiPrep™ (from SIGMA)

glycosylphosphatidylinositol-anchored proteins, several plasma membrane ATPases, and multidrug resistance proteins. In the DRMs from the T87 cells, we detected a variety of proteins classified into several functional categories including tubulin β-1 chain (At1g75780), tubulin β-9 chain, actin 7/actin 2 (At4g20890), glucuronosyl/UDP-glycosyltransferase family protein (At1g73880), S-adenosylmethionine synthetase (At3g17390), SPFH domain/ band 7 family protein (At2g03510), sporulation-related protein (at1g33290), shepherd protein (At4g24190), and heat shock protein (At5g56010) (Ohta et al. unpublished results). The vacuole localization of SPFH domain/band 7 family has been reported (Jaquinod et al. 2007), while SPFH domain proteins have been described as a lipid raft marker (Browman et al. 2007).

Exhaustive proteomic research targeting DRM-accumulated proteins is prerequisite to open new avenues to uncover physiological roles of lipid microdomains/rafts; however, a very strict quantitative proteomic analysis is not even close to clarify the physiological roles of sterols. One possible clue to understand the developmental roles of sterols may come from genome-wide gene expression network analyses. For example, an Arabidopsis *DIMINUTO/DWARF1* (sterol-C24-isomerase/reductase) orthologue (Q39085) in tobacco was suggested to localize to lipid rafts (Mongrand et al. 2004). The Arabidopsis gene coexpression analyses such as ATTEDII (http://www.atted.bio.titech.ac.jp/search.shtml) and Confetto (http://pmnedo.kazusa.or.jp/kagiana/index.html) revealed a gene expression network of Arabidopsis *DIMINUTO* with some sterol biosynthesis-related genes (farnesyl diphosphate synthase, At5g47770; cycloeucalenol cycloisomerase, At5g50375, and the Arabidopsis homolog of yeast *ERG28*, At1g10030). *HYD1* (sterol Δ^8-isomerase, At1g20050) had a high score of gene expression correlation with cycloeucalenol cycloisomerase. *DIMINUTO* expression was also correlated with the genes for tubulin-α chains (At1g04820, At4g14960, and At1g50010). It is therefore possible that at least a part of sterol biosynthesis may be associated with the lipid microdomains in plants and that alterations of the microdomain properties, such as the changes in the relative sterol composition, may affect associated metabolic processes. Collections of transgenic resources with altered sterol compositions, such as the Arabidopsis cultured cells with the modified levels of the Δ^{22}-sterols, are essential for such research purposes. We have obtained DRMs from Arabidopsis T87 cell lines overexpressing either *CYP710A1* or *CYP710A2* and an RNA interference line targeting all the *CYP710A1, A2, A3,* and *A4* genes. The sterol composition in the DRMs from these transformed cells reflected *CYP710A* gene expression levels: *CYP710A1* overexpression resulted in a 53-fold increase in stigmasterol and a 31-fold decrease in β-sitosterol, and *CYP710A2* overexpression resulted in a 16.5-fold increase in brassicasterol at the expense of campesterol (threefold decrease). The levels of the Δ^{22}-sterols were dramatically decreased in the RNAi line.

Integrated approaches of proteomics with sterol profiling using such transgenic lines is a straightforward option to provide molecular evidence to clarify the possible involvement of proper sterol composition in developmental regulation processes in plants.

References

Bach TJ, Benveniste P (1997) Cloning of cDNAs or genes encoding enzymes of sterol biosynthesis from plants and other eukaryotes: heterologous expression and

complementation analysis of mutations for functional characterization. Prog Lipid Res 36:197–226

Benveniste P (2004) Biosynthesis and accumulation of sterols. Annu Rev Plant Biol 55:429–457

Borner GH, Sherrier DJ, Weimar T et al (2005) Analysis of detergent-resistant membranes in Arabidopsis. Evidence for plasma membrane lipid rafts. Plant Physiol 137:104–116

Browman DT, Hoegg MB, Robbins SM (2007) The SPFH domain-containing proteins: more than lipid raft markers. Trends Cell Biol 17:394–402

Carland FM, Fujioka S, Takatsuto S, Yoshida S, Nelson T (2002) The identification of *CVP1* reveals a role for sterols in vascular patterning. Plant Cell 14: 2045–2058

Darnet S, Bard M, Rahier A (2001) Functional identification of sterol-4α-methyl oxidase cDNAs from *Arabidopsis thaliana* by complementation of a yeast *erg25* mutant lacking sterol-4α-methyl oxidation. FEBS Lett 508:39–43

Diener AC, Li H, Zhou W, Whoriskey WJ, Nes WD, Fink GR (2000) Sterol methyltransferase 1 controls the level of cholesterol in plants. Plant Cell 12:853–870

El-Sayed NM, Myler PJ, Bartholomeu DC et al (2005) The genome sequence of *Trypanosoma cruzi*, etiologic agent of Chagas disease. Science 309:409–415

Gachotte D, Husselstein T, Bard M, Lacroute F, Benveniste P (1996) Isolation and characterization of an *Arabidopsis thaliana* cDNA encoding a Δ7-sterol-C-5-desaturase by functional complementation of a defective yeast mutant. Plant J 9:391–398

Gotoh O (1992) Substrate recognition sites in cytochrome P450 family 2 (CYP2) proteins inferred from comparative analyses of amino acid and coding nucleotide sequences. J Biol Chem 267:83–90

He JX, Fujioka S, Li TC, Kang SG et al (2003) Sterols regulate development and gene expression in *Arabidopsis*. Plant Physiol 131:1258–1269

Jang JC, Fujioka S, Tasaka M, Seto H et al (2000) A critical role of sterols in embryonic patterning and meristem programming revealed by the *fackel* mutants of *Arabidopsis thaliana*. Genes Dev 14:1485–1497

Jaquinod M, Villiers F, Kieffer-Jaquinod S et al (2007) A proteomics dissection of *Arabidopsis thaliana* vacuoles isolated from cell culture. Mol Cell Proteomics 6:394–412

Kelly SL, Lamb DC, Baldwin BC, Corran AJ, Kelly DE (1997) Characterization of *Saccharomyces cerevisiae* CYP61, sterol Δ22-desaturase, and inhibition by azole antifungal agents. J Biol Chem 272:9986–9988

Kolesnikova MD, Xiong Q, Lodeiro S, Hua L, Matsuda SP (2006) Lanosterol biosynthesis in plants. Arch Biochem Biophys 447:87–95

Laloi M, Perret AM, Chatre L, Melser S et al (2007) Insights into the role of specific lipids in the formation and delivery of lipid microdomains to the plasma membrane of plant cells. Plant Physiol 143:461–472

Lepesheva GI, Hargrove TY, Ott RD, Nes WD, Waterman MR (2006) Biodiversity of CYP51 in trypanosomes. Biochem Soc Trans 34:1161–1164

Lindsey K, Pullen ML, Topping JF (2003) Importance of plant sterols in pattern formation and hormone signalling. Trends Plant Sci 8:521–525

Matsumoto T, Shimizu N, Shigemoto T, Itoh T, Iida T, Nishioka A (1983) Isolation of 22-dehydrocampesterol from the seeds of *Brassica juncea*. Phytochemistry 22:789–790

Men S, Boutté Y, Ikeda Y, Li X, Palme K et al (2008) Sterol-dependent endocytosis mediates post-cytokinetic acquisition of PIN2 efflux carrier polarity. Nat Cell Biol 10:237–244

Meunier B, de Visser SP, Shaik S (2004) Mechanism of oxidation reactions catalyzed by cytochrome P450 enzymes. Chem Rev 104:3947–3980

Mongrand S, Morel J, Laroche J et al (2004) Lipid rafts in higher plant cells: purification and characterization of Triton X-100-insoluble microdomains from tobacco plasma membrane. J Biol Chem 279:36277–36286

Morikawa T, Mizutani M, Aoki N et al (2006) Cytochrome P450 *CYP710A* encodes the sterol C22-desaturase in Arabidopsis and tomato. Plant Cell 18:1008–1022

Morikawa T, Saga H, Hashizume H, Ohta D (2009) *CYP710A* genes encoding sterol C22-desaturase in *Physcomitrella patens* as molecular evidence for the evolutionary conservation of a sterol biosynthetic pathway in plants. Planta 229:1311–1322

Motose H, Sugiyama M, Fukuda H (2004) A proteoglycan mediates inductive interaction during plant vascular development. Nature 429:873–878

Nelson DR (2006) Plant cytochrome P450s from moss to poplar. Phytochem Rev 5:193–204

Nes WD, Norton RA, Crumley FG, Madigan SJ, Katz ER (1990) Sterol phylogenesis and algal evolution. Proc Natl Acad Sci USA 87:7565–7569

Phillips DR, Rasbery JM, Bartel B, Matsuda SP (2006) Biosynthetic diversity in plant triterpene cyclization. Curr Opin Plant Biol 9:305–314

Roberts CW, McLeod R, Rice DW, Ginger M, Chance ML, Goad LJ (2003) Fatty acid and sterol metabolism: potential antimicrobial targets in apicomplexan and trypanosomatid parasitic protozoa. Mol Biochem Parasitol 126:129–142

Salimova E, Boschetti A, Eichenberger W, Lutova L (1999) Sterol mutants of *Chlamydomonas reinhardtii*: characterisation of three strains deficient in C24(28) reductase. Plant Physiol Biochem 37:241–249

Schaeffer A, Bronner R, Benveniste P, Schaller H (2001) The ratio of campesterol to sitosterol that modulates growth in Arabidopsis is controlled by *STEROL METHYLTRANSFERASE 2;1*. Plant J 25:605–615

Schaller H (2004) New aspects of sterol biosynthesis in growth and development of higher plants. Plant Physiol Biochem 42:465–476

Schrick K, Mayer U, Horrichs A, Kuhnt C et al (2000) *FACKEL* is a sterol C-14 reductase required for organized cell division and expansion in Arabidopsis embryogenesis. Genes Dev 14:1471–1484

Schrick K, Mayer U, Martin G et al (2002) Interactions between sterol biosynthesis genes in embryonic development of Arabidopsis. Plant J 31:61–73

Schrick K, Fujioka S, Takatsuto S et al (2004) A link between sterol biosynthesis, the cell wall, and cellulose in *Arabidopsis*. Plant J 38:227–243

Schuler MA, Werck-Reichhart D (2003) Functional genomics of P450s. Annu Rev Plant Biol 54: 629–667

Sikorski RS, Hieter P (1989) A system of shuttle vectors and yeast host strains designed for efficient manipulation of DNA in *Saccharomyces cerevisiae*. Genetics 122:19–27

Skaggs BA, Alexander JF, Pierson CA et al (1996) Cloning and characterization of the *Saccharomyces cerevisiae* C-22 sterol desaturase gene, encoding a second cytochrome P-450 involved in ergosterol biosynthesis. Gene 169:105–109

Souter M, Topping J, Pullen M, Friml J et al (2002) *hydra* mutants of *Arabidopsis* are defective in sterol profiles and auxin and ethylene signaling. Plant Cell 14:1017–1031

Suzuki M, Xiang T, Ohyama K, Seki H et al (2006) Lanosterol synthase in dicotyledonous plants. Plant Cell Physiol 47:565–571

Volkman JK (2003) Sterols in microorganisms. Appl Microbiol Biotechnol 60:495–506

Wesley SV, Helliwell CA, Smith NA et al (2001) Construct design for efficient, effective and high-throughput gene silencing in plants. Plant J 27:581–590

Willemsen V, Friml J, Grebe M, van den Toorn A, Palme K, Scheres B (2003) Cell polarity and PIN protein positioning in *Arabidopsis* require *STEROL METHYLTRANSFERASE1* function. Plant Cell 15:612–625

Enzymatic Synthesis of Unnatural Cyclic Triterpenes

27

Ikuro Abe

Abstract

The broad substrate tolerance and catalytic potential of bacterial squalene cyclases and plant oxidosqualene cyclases are remarkable; the enzymes accept a wide variety of nonphysiological substrate analogues and efficiently perform sequential ring-forming reactions to produce a series of unnatural cyclic triterpenes. By utilizing such properties of the enzymes, it is possible to generate unnatural novel cyclic polyprenoids by enzymatic conversion of chemically synthesized substrate analogues. Here we present recent examples including (a) enzymatic formation of a "supranatural" hexacyclic polyprenoid as well as heteroaromatic ring containing cyclic polyprenoids by bacterial squalene–hopene cyclase from *Alicyclobacillus acidocaldarius* and (b) enzymatic cyclization of 22,23-dihydro-2,3-oxidosqualene and 24,30-bisnor-2,3-oxidosqualene by plant oxidosqualene-β-amyrin cyclase from *Pisum sativum.*

Keywords

Cyclic triterpenes • Squalene epoxide cyclases • Squalene cyclases • *Pisum sativum* • Supranatural triterpenes • β-Amyrin • Oxidosqualene-lupeol cyclase • Intermediate carbocations • Cation-π interactions • Carbon-carbon bond formation • 3-(Geranylgeranyl)indole • 3-(Farnesyldimethylallyl) indole • Bisnoroxidosqualene • *Alicyclobacillus acidocaldarius* • Squalene–hopene cyclase

27.1 Introduction

The formation of tetracyclic and pentacyclic triterpenes by squalene cyclizing enzymes offers an impressive example of enzyme-templated sequential polyene cyclization reactions (Woodward and Bloch 1953; Eschenmoser et al. 1955; Ourisson

I. Abe (✉)
Graduate School of Pharmaceutical Sciences,
The University of Tokyo, 7-3-1 Hongo, Bunkyo-ku,
Tokyo 113-0033, Japan
e-mail: abei@mol.f.u-tokyo.ac.jp

T.J. Bach and M. Rohmer (eds.), *Isoprenoid Synthesis in Plants and Microorganisms: New Concepts and Experimental Approaches*, DOI 10.1007/978-1-4614-4063-5_27,

et al. 1987; Abe et al. 1993; Wendt et al. 2000; Hoshino and Sato 2002; Segura et al. 2003; Xu et al. 2004; Abe 2007). The cyclase enzymes catalyze formation and stabilization of polycyclic carbocations and direct the enzyme-templated formation of new carbon-carbon bonds in regio- and stereochemically defined manner. Squalene and oxidosqualene are thus converted to various skeletal types of triterpenes including sterols, this by different enzyme systems. The structure-function relationships of squalene cyclases (SCs) and 2,3-oxidosqualene cyclases (OSCs) are of great interest. In principle, only small modifications of the active-site structure of the enzyme lead to production of dramatically different cyclization products (Ourisson et al. 1987; Abe et al. 1993).

SCs and OSCs initiate the cyclization cascade by presenting a general acid to protonate the terminal double bond or oxirane ring. The enzymes provide a template that chaperone the flexible substrate and intermediate carbocations through a series of precise conformations leading to one unique cyclization product, by shielding the cationic intermediates from premature addition of water or elimination. The sequential carbon-carbon bond forming reactions are accelerated by stabilization of intermediate cations by electron-rich environment (Wendt et al. 2000). The hydrophobic active site is lined with conserved aromatic residues which are thought to stabilize the partially cyclized carbocationic intermediates through cation-π interactions (Dougherty 1996). Recent advances on crystallographic and structure-based mutagenesis studies as well as utilization of synthetic active-site-targeted probes have begun to reveal intimate structural details of the catalytic mechanism of the enzyme-templated sequential ring-forming reactions.

27.2 Bacterial Squalene Cyclase

27.2.1 Squalene–Hopene Cyclase

Bacterial squalene–hopene cyclase (SHC) binds squalene (**1**) in all-*chair* conformation and initiates the sequential ring-forming reaction by protonating the terminal double bond (Fig. 27.1a) (Poralla 1999). The cyclization first produces the 6.6.6.6.5-fused pentacyclic hopanyl C-22 carbocation (**2**), which then undergoes either regiospecific proton elimination of *Z*-methyl group or addition of water to produce hop-22(29)-ene (**3**) along with hopan-22-ol (**4**). During the cyclization reaction, no methyl or hydride migration takes place. The enzyme-controlled sequential carbon-carbon bond formation reactions are thought to proceed through a series of discrete, conformationally rigid, partially cyclized carbocationic intermediates (van Tamelen 1982). On the basis of computational model studies, it has been recently proposed that a bicyclic tertiary cation (**6**) is the only reaction intermediate with a significant lifetime, and then formation of rings C, D, and E follows via a single transition state to produce a 6.6.6.6.5 pentacyclic hopanyl C-22 cation (**2**) (99%) along with a 6.6.6.5 tetracyclic tertiary cation by-product (**8**) (1%) (Fig. 27.1b) (Rajamani and Gao 2003; Pale-Grosdemange et al. 1998).

The X-ray crystal structure of SHC from a thermoacidophilic bacterium *Alicyclobacillus acidocaldarius* has been solved at 2.0-Å resolution (Wendt et al. 1997, 1999). The crystal structures of the homodimeric monotopic membrane-bound 72-kDa protein revealed a dumbbell-shaped (α/α) barrel domains connected by long loops which together enclose a large central cavity of 1,200 $Å^3$. The active site is located in the large central cavity, consisting of an extended hydrophobic section lined with conserved aromatic residues. The π-electrons of aromatic residues in the cavity have been proposed to stabilize the partially cyclized cationic intermediates during the cyclization cascade through cation-π interactions (Dougherty 1996). Further, recently reported crystal structure complexed with the inhibitor 2-azasqualene clearly demonstrated that the substrate analogue binds with a conformation very close to that required for the all-*chair* conformations of hopene, suggesting that the bound squalene indeed undergoes only small conformational changes during the sequential carbon-carbon bond formation reaction (Reinert et al. 2004).

Interestingly, the bacterial SHC, catalyzing a stereochemically and mechanistically simpler

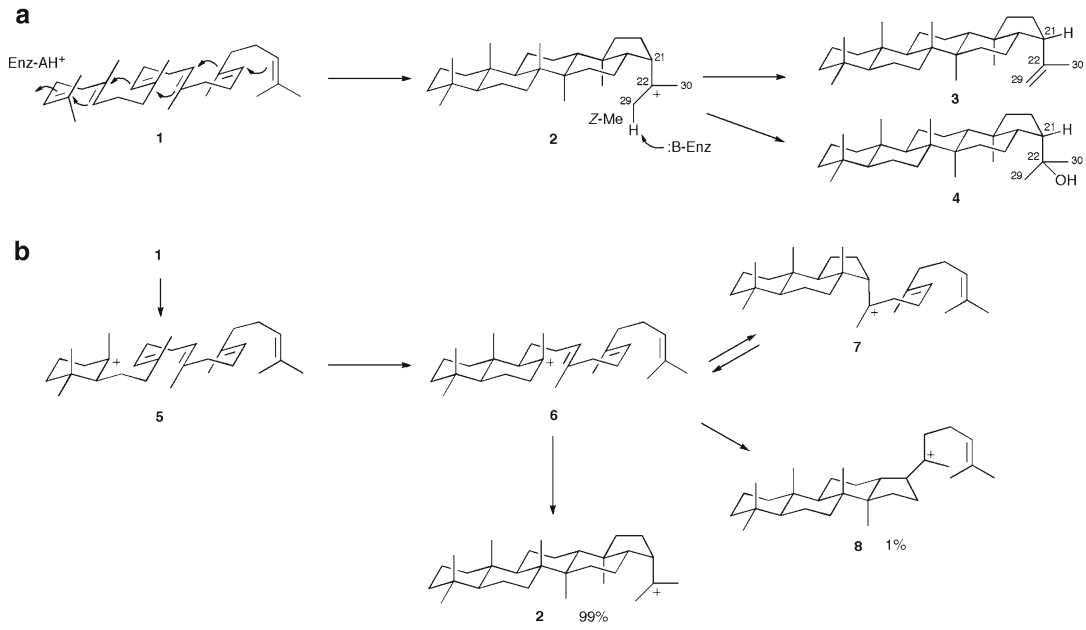

Fig. 27.1 (**a**) Enzymatic formation of hopene by bacterial SHC and (**b**) proposed mechanism for formation of hopene by Rajamani and Gao (2003)

process than eukaryotic OSCs, shows broad substrate tolerance and remarkable catalytic potential; the enzyme accepts a wide variety of squalene analogues and efficiently performs sequential ring-forming reactions to produce a series of unnatural cyclic polyprenoids (Ourisson et al. 1987; Abe et al. 1993; Hoshino and Sato 2002; Abe 2007). On the basis of the crystal structures of *A. acidocaldarius* SHC, the hydrophobic active-site cavity lined with aromatic residues appears to have enough space to accept bulky substrate analogues. By utilizing such properties of the enzyme, it is possible to generate unnatural novel cyclic polyprenoids by enzymatic conversion of chemically synthesized substrate analogues.

27.2.2 Enzymatic Synthesis of "Supranatural" Hexacyclic Polyprenoid

One of the most impressive examples is the enzymatic formation of a "supranatural" novel hexacyclic polyprenoid (**10**) from a synthetic C_{35} analogue (**9**) in which a farnesyl C_{15} unit is connected in a head-to-head fashion to a geranylgeranyl C_{20} unit (Fig. 27.2a) (Abe et al. 2002). Recombinant *A. acidocaldarius* SHC efficiently accepted the C_{35} analogue and catalyzed sequential ring-forming reactions to generate a novel hexacyclic polyprenoid with a 6.6.6.6.6.5-fused ring system. This is the first demonstration of the remarkable ability of the squalene (C_{30}) cyclizing enzyme to perform construction of the C_{35} "supranatural" hexacyclic skeleton.

Here the C_{35} analogue (**9**) was chemically synthesized by coupling of farnesyl phenylsulfone with geranylgeranyl bromide and followed by dephenylsulfonation by $LiHBEt_3$ in the presence of catalytic amount of $PdCl_2$[1,3-bis(diphenylphosphino)propane]. When incubated with purified recombinant *A. acidocaldarius* SHC, the hexacyclic polyprenoid (**10**) ($[\alpha]_D^{25} = -22.0°$) was obtained as a single product in 10% yield. The structure with the 6.6.6.6.6.5-fused hexacyclic ring system was uniquely consistent with both biogenetic reasoning and NMR spectroscopic data. Further, the ring junctions and the stereochemistry of ring substituents were unambiguously determined by NOE experiments.

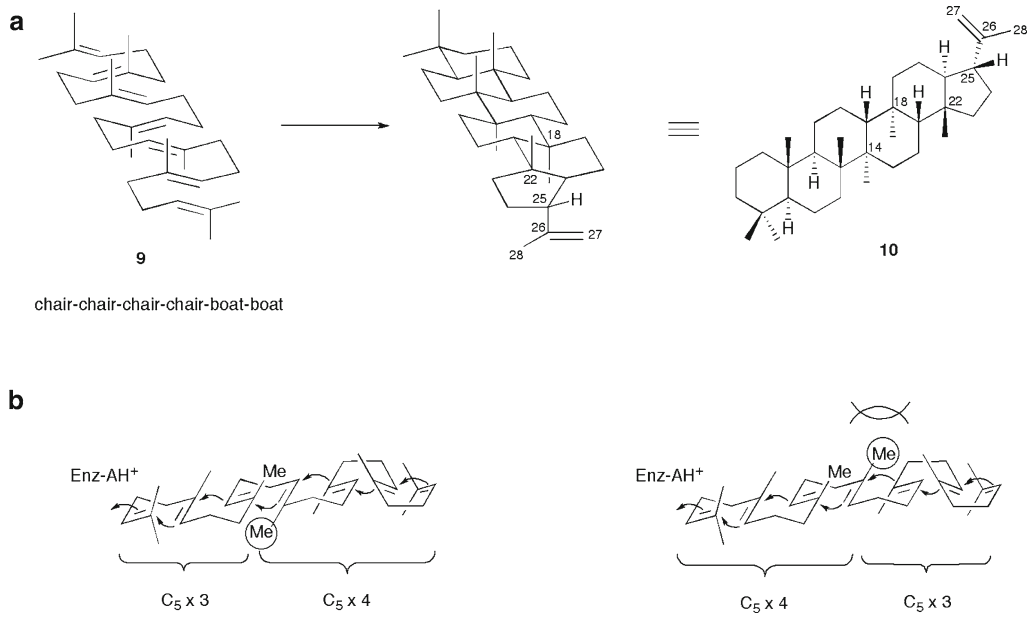

Fig. 27.2 Enzymatic formation of "supranatural" hexacyclic polyprenoid by *A. acidocaldarius* SHC

Interestingly, the cyclization of the C_{35} analogue (C_{15} unit + C_{20} unit) is initiated from the C_{15} farnesyl end and not by a proton attack on the terminal double bond of the C_{20} geranylgeranyl side (Fig. 27.2b). This suggests that α-orientation of the *pro*-C14 methyl group is crucial to the correct folding and binding of the substrate, as in the case of the cyclization of the physiological substrate squalene (C_{15} unit × 2). The alternative β-orientation of the *pro*-C14 methyl group may interact repulsively with the *pro*-C10 methyl or a nearest neighbor from the substrate binding pocket of the bacterial enzyme. Further, the substrate must be folded in *chair-chair-chair-chair-**boat-boat*** conformation to achieve the stereochemistry of the cyclization product; i.e., the α-axial orientation of the methyl group at C-18 and the isopropenyl group at C-25, as well as the β-axial orientation of the methyl group at C-22 (Fig. 27.2b). Moreover, as in the case of the formation of hop-22(29)-ene, the cyclization reaction proceeds without carbon rearrangement and is terminated by specific proton elimination at C-27. It should be noted that the stereochemistry of the sequential ring-forming reaction is rigidly controlled by the enzyme, even for the artificial substrate with an additional C_5 isoprene unit.

On the other hand, a C_{40} analogue in which two geranylgeranyl C_{20} units are connected in a head-to-head fashion (C_{20} unit + C_{20} unit) and an unnatural C_{30} analogue in which a geranylgeranyl C_{20} unit is connected to a geranyl C_{10} in a head-to-head fashion (C_{20} unit + C_{10} unit) did not afford polycyclic products but just yielded only bicyclic products, while a C_{25} analogue (C_{15} unit + C_{10} unit) produced an unnatural novel tetracyclic sesterterpene with a 6.6.6.5-fused ring system (Abe et al. 2003). This suggested again that α-orientation of the *pro*-C14 methyl group is crucial to the correct folding and binding of the substrate by the bacterial SHC. Interestingly, it has been reported that *A. acidocaldarius* SHC also accepts the truncated analogues having carbon-chain lengths of C_{15} and C_{20}, while geraniol (C_{10}) is not a substrate for the enzyme (Hoshino et al. 2004).

27.2.3 Enzymatic Synthesis of Polyprenoids with Heteroaromatic Ring

Indole-containing substrate analogues, 3-(geranylgeranyl)indole (**11**) and 3-(farnesyldimethylallyl)indole (**12**), in which a C_{20} isoprene unit is

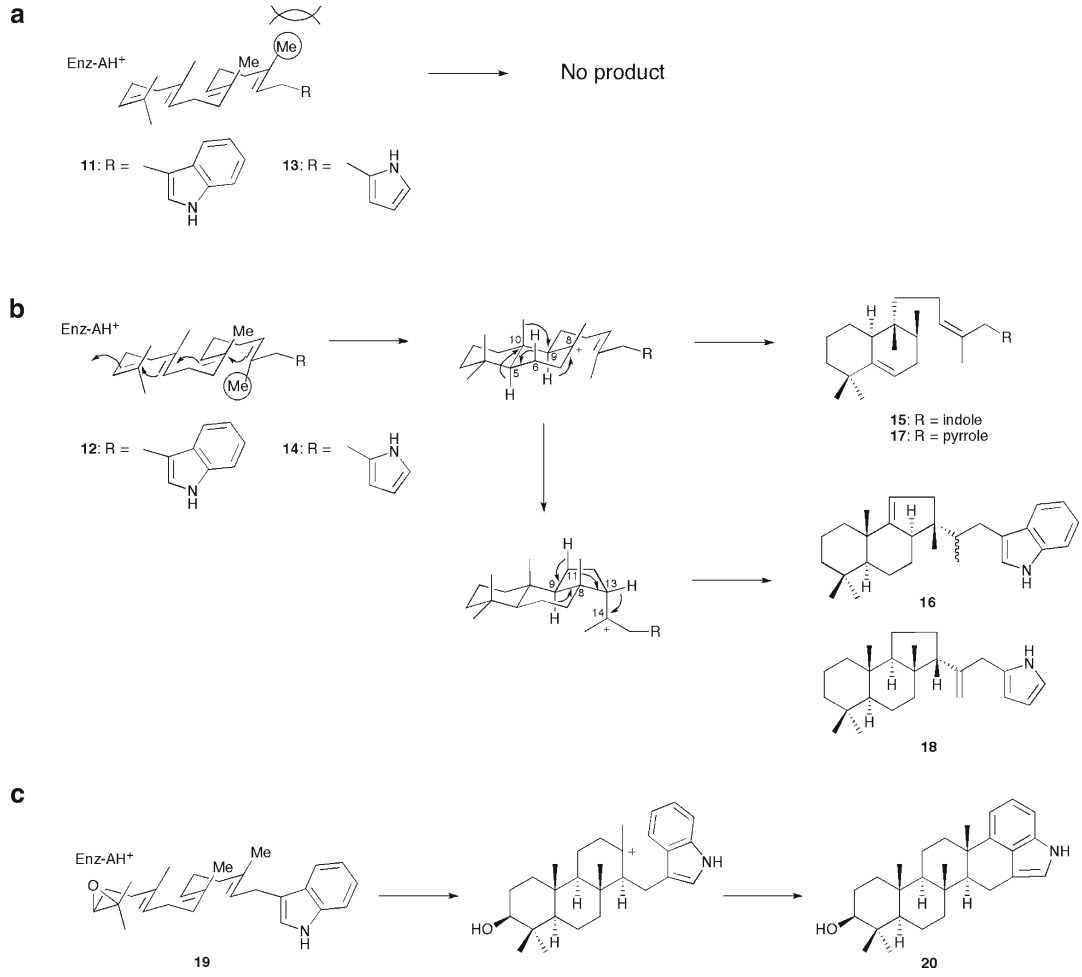

Fig. 27.3 (**a**) and (**b**) enzymatic cyclization of heteroaromatic ring containing substrates analogues by *A. acidocaldarius* SHC and (**c**) enzymatic formation of petromindole by *A. thaliana* OSLuC

connected to indole, were chemically synthesized and tested for the enzymatic cyclization by *A. acidocaldarius* SHC (Fig. 27.3) (Tanaka et al. 2005). Substrate **11** is a putative precursor for natural indole diterpenes; its epoxide, 3-(ω-oxidogeranylgeranyl)indole (**19**), has been previously shown to enzymatically convert into petromindole (**20**), a hexacyclic indole diterpene with 6.6.6.6.6.5-fused ring system, by plant oxidosqualene-lupeol cyclase (OSLuC) from *Arabidopsis thaliana* (Fig. 27.3c) (Xiong et al. 2003). On the other hand, substrate **12** contains a farnesyl C_{15} unit as in the case of the natural substrate squalene (C_{15} unit × 2). The π-π interactions between the indole ring and the active-site aromatic residues of the enzyme were anticipated for the both substrate analogues, which could significantly affect the stereoelectronical course of the enzyme reactions.

Interestingly, 3-(geranylgeranyl)indole (**11**) was found to be not a substrate for *A. acidocaldarius* SHC (Fig. 27.3a), which is in sharp contrast with the enzymatic cyclization of 3-(ω-oxidogeranylgeranyl)indole by the plant OSLuC. As described above, the bacterial SHC is indeed sensitive to the orientation of the *pro*-C14 methyl group and fails to bind the geranylgeranyl substrate (Abe et al. 2002). In contrast, 3-(farnesyldimethylallyl)indole (**12**) is converted to a 1:2 mixture (total yield 8%) of a bicyclic (**15**) and a tricyclic (**16**) unnatural novel polyprenoid (Fig. 27.3b). The cyclization reaction, initiated in

a *chair-chair-chair* conformation, was apparently interrupted at the bicyclic or tricyclic cationic stage probably due to the stereoelectronic effect of the bulky, electron-rich indole moiety. Presumably, the π-π interactions of the indole ring with the active-site aromatic residues (e.g., Trp169 and Phe605 on the basis of the crystal structure of *A. acidocaldarius* SHC) would cause perturbation in the folding conformation of the substrate and the intermediate carbocations, which resulted in the irregular rearrangement reaction and the proton abstraction. Thus, from the 6/6-fused bicyclic tertiary cation, a backbone rearrangement (H-9α → 8α, CH_3-10β → 9β, H-5α → 10α) with elimination of H-6β produced the minor product **15**, while from the tricyclic Markovnikov cation with a 6/6/5-fused ring system, a backbone rearrangement (H-13β → 14 , CH_3-8β → 13β, H-9α → 8α) with elimination of H-11β yielded the major product **16** (Fig. 27.3b). It is remarkable that the stereochemistry of the cyclization reactions of the unnatural substrate was strictly controlled by the enzyme in a regio- and stereospecific manner.

Similar results have been obtained with enzyme reactions with pyrrole-containing substrate analogues: 2-(geranylgeranyl)pyrrole (**13**) and 2-(farnesyldimethylallyl)pyrrole (**14**). When incubated with *A. acidocaldarius* SHC, 2-(geranylgeranyl)pyrrole (**13**) was not a substrate for the enzyme (Fig. 27.3a), while 2-(farnesyldimethylallyl)pyrrole (**14**) was enzymatically converted to a 1:10 mixture (total yield 1%) of a bicyclic (**17**) and a tricyclic (**18**) unnatural novel polyprenoids (Fig. 27.3b) (Tanaka et al. 2006). Here it should be noted that the less bulky pyrrole-containing analogue **14** was not a good substrate of *A. acidocaldarius* SHC as the indole-containing analogue **12**. The yield of the pyrrole product **18** was five times lower than that of the indole product **16**. Presumably, the bulky, π-electron-rich indole ring moiety may better fit into the active site of *A. acidocaldarius* SHC due to more efficient π-π interactions with the active-site aromatic residues.

27.3 Plant Oxidosqualene Cyclase

27.3.1 Oxidosqualene-β-Amyrin Cyclase

Since the Ruzicka school proposed the "biogenetic isoprene rule" (Eschenmoser et al. 1955; Eschenmoser and Arigoni 2005), the remarkable cyclization of (3*S*) 2,3-oxidosqualene (**21**) to β-amyrin (**27**) has fascinated organic chemists for over half a century. The complex cyclization and rearrangement reaction is initiated in the *chair-chair-chair-boat* conformation of (3*S*) 2,3-oxidosqualene, and the proton-initiated cyclization first produces the 6.6.6.5-fused tetracyclic dammarenyl *tertiary* cation (**22**). After D-ring expansion, an electrophilic addition of the tetracyclic baccharenyl *secondary* cation (**23**) on to the terminal double bond generates the 6.6.6.6.5-fused pentacyclic lupanyl *tertiary* cation (**24**), which is followed by E-ring expansion to yield the oleanyl *secondary* cation (**25**). Finally, the oleanyl C-19 carbocation undergoes sequential 1,2-hydride shifts (H-18α → 19 , H-13β → 18β) followed by elimination of H-12α to yield β-amyrin (**27**) with the 6.6.6.6.6-fused pentacyclic ring system (Fig. 27.4).

Oxidosqualene-β-amyrin cyclase (OSAC) from several plants including *Pisum sativum* has been cloned and functionally expressed in *Saccharomyces cerevisiae* (Kushiro et al. 1998; Morita et al. 2000). The plant OSAC and the bacterial *A. acidocaldarius* SHC share only ca. 20% overall amino acid sequence identity. On the basis of site-directed mutagenesis of OSAC from *Panax ginseng*, it has been proposed that the active-site aromatic residues Tyr261 and Trp259 of OSAC play a critical role for the D/E-ring formation of β-amyrin. Thus, Tyr261 is thought to stabilize one of the cationic intermediates generated after the dammarenyl C-20 cation, while Trp259 controls β-amyrin formation through stabilization of the oleanyl C-19 carbocation (Kushiro et al. 1999, 2000).

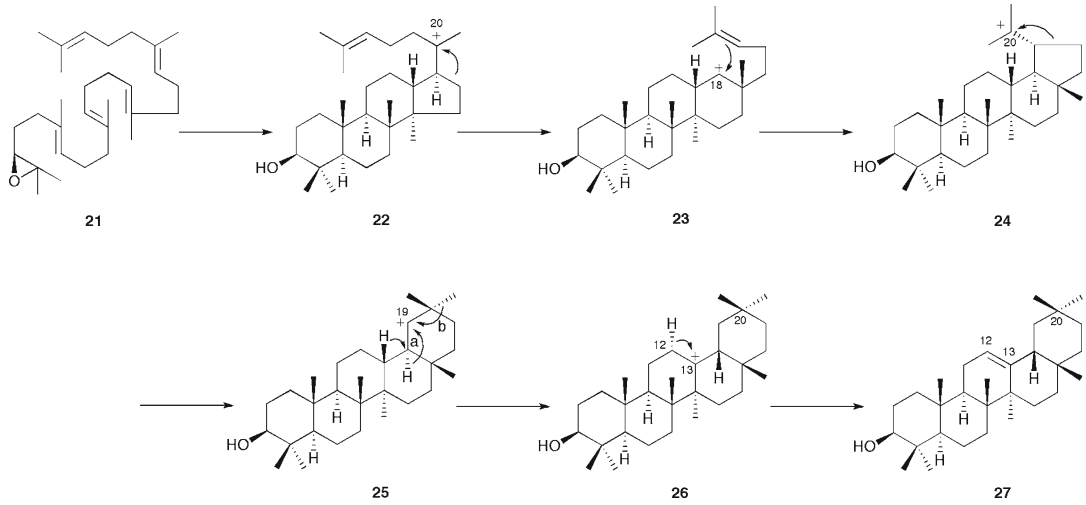

Fig. 27.4 Enzymatic formation of β-amyrin by plant OSAC

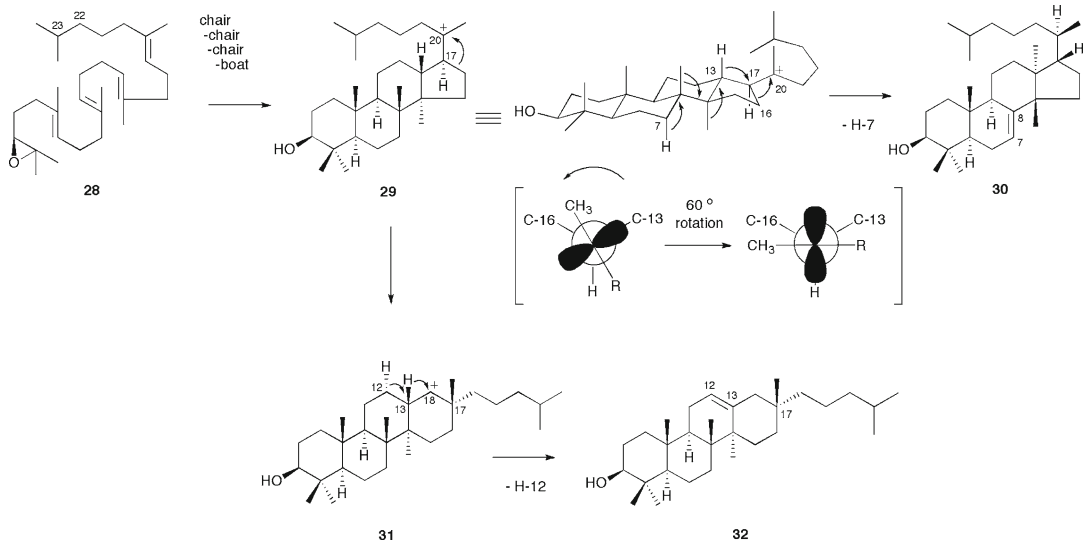

Fig. 27.5 Enzymatic cyclization of dihydrooxidosqualene by *P. sativum* OSAC

27.3.2 Enzymatic Cyclization of Dihydrooxidosqualene

During the biosynthesis of β-amyrin, D-ring formation is thought to proceed through a five-membered ring closure to generate a Markovnikov *tertiary* dammarenyl cation (**22**), which is followed by D-ring expansion to yield the 6.6.6.6-fused tetracyclic baccharenyl *secondary* cation (**23**) (Fig. 27.4). In order to understand the reaction mechanism, we carried out enzymatic conversion of 22,23-dihydro-2,3-oxidosqualene (**28**), a synthetic analogue lacking the terminal double bond of 2,3-oxidosqualene. It is accordingly no longer possible to generate the pentacyclic ring system (Fig. 27.5) (Abe et al. 2004a).

Enzyme reaction with recombinant *P. sativum* OSAC afforded a 4:1 mixture (total 5% yield) of unnatural tetracyclic products, euph-7-en-3β-ol (**30**) and bacchar-12-en-3β-ol (**32**), which were completely separated by reverse phase HPLC (Fig. 27.5). Thus, in the absence of the terminal double bond, the enzyme reaction was interrupted at a tetracyclic dammarenyl *tertiary* cation (**29**) with the 17β-side chain, which was followed by a backbone rearrangement (H-17α → 20α, H-13β → 17β, CH_3-14α → 13α, CH_3-8β → 14β) with elimination of H-7α to yield the major product euph-7-en-3β-ol (**30**), while D-ring expansion to the 6.6.6.6-fused baccharenyl C-18 *secondary* cation (**31**), and a subsequent hydride shift (H-13β → 18β) with loss of H-12α, as in the case of β-amyrin synthesis, produced the minor product bacchar-12-en-3β-ol (**32**).

This is the first demonstration of the enzymatic formation of the 6.6.6.6-fused baccharene skeleton with a six-membered D-ring. Here one of the most important points is that the D-ring expansion proceeds even in the absence of the terminal double bond. Thus, the enzymatic formation of the anti-Markovnikov six-membered D-ring does not depend on the participation of the terminal π-electrons. In contrast, it has been reported that the bacterial SCs, normally catalyzing formation of pentacyclic triterpenes, converted 2,3-dihydrosqualene into thermodynamically favored tetracyclic products with a Markovnikov five-membered D-ring; squalene:tetrahymanol cyclase (STC) from the ciliate protozoan *Tetrahymena pyriformis* yielded euph-7-ene, while *A. acidocaldarius* SHC produced a 1:1 mixture of (20*R*)-dammar-13(17)-ene and (20*R*)-dammar-12-ene (Abe and Rohmer 1991, 1994). It is possible that properly positioned electron-rich active-site aromatic residues of *P. sativum* OSAC may play a crucial role for the D-ring expansion reaction and the formation of the baccharene product. On the other hand, in OSAC, the active-site residues involved in the termination of the enzyme reaction by regiospecific proton abstraction at H-12α remain to be unidentified.

In the absence of the terminal double bond, however, most of the reactions are interrupted at the dammarenyl *tertiary* cation with the 6.6.6.5-fused tetracyclic ring system and followed by the backbone rearrangement to yield euph-7-en-3β-ol (Fig. 27.5). Here it should be noted that the stereochemistry of the cyclization reaction is strictly controlled by the enzyme to generate only the product with the C-20*R* configuration. The formation of the C-20*R* stereochemistry from the dammarenyl C-20 cation is thought to involve the least motion pathway; i.e., only 60° rotation around the C-17–C-20 bond prior to the proton migration from C-17 to C-20. Interestingly, as described above, *T. pyriformis* STC yielded euph-7-ene from 2,3-dihydrosqualene in the similar manner (Abe and Rohmer 1991, 1994). Finally, these results suggest a close relationship between OSAC and other plant OSCs that produce pentacyclic triterpenes such as eupha-7,24-dien-3β-ol and bacchara-12,21-dien-3β-ol. Indeed, only a small modification of the active-site structure would generate the diversity of the cyclization products.

27.3.3 Enzymatic Cyclization of Bisnoroxidosqualene

Recent advances in enzymology and molecular biology of OSAC prompted us to reinvestigate the still unanswered questions regarding the mechanism and stereochemistry of the remarkable cyclization and rearrangement reaction, which includes the enzymatic cyclization of 24,30-bisnor-2,3-oxidosqualene (**33**) (Abe et al. 2004b). As earlier described by Corey and Gross in 1968, the removal of the terminal methyl groups could significantly affect the stereoelectronical course of the D/E-ring formation reaction, which is the most complex and interesting process of the β-amyrin biosynthesis (Corey and Gross (1967) (Fig. 27.6).

We chemically synthesized 24,30-bisnor-2,3-oxidosqualene (**33**) in racemic form starting from 1,1′,2-trisnorsqualene-3-aldehyde (Abe et al. 2004b). Further, in order to elucidate the reaction mechanism, two isotopomers, [23-^{13}C]-**33** and [23,23-^{2}H]-**33**, were also prepared by Wittig condensation of the aldehyde with $^{13}CH_3PPh_3I$ (99 atom% ^{13}C) and $C^2H_3PPh_3I$ (95+ atom% ^{2}H),

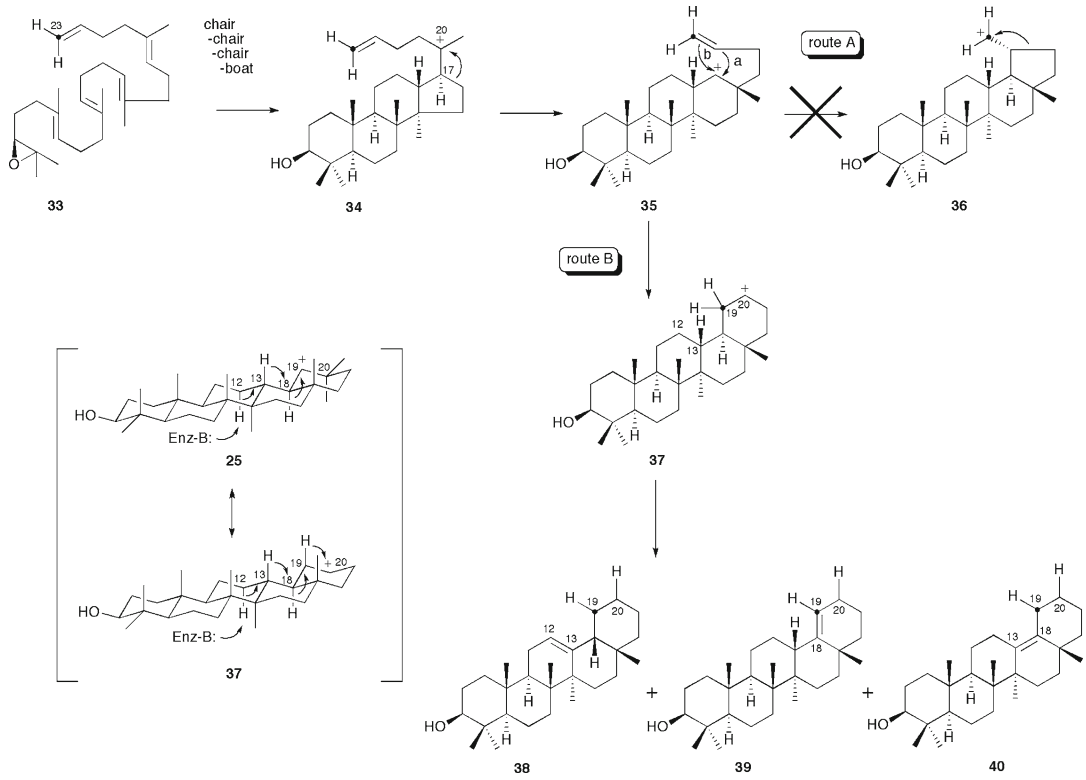

Fig. 27.6 Enzymatic cyclization of bisnoroxidosqualene by *P. sativum* OSAC

respectively. Enzyme reaction of **33** with the recombinant *P. sativum* OSAC yielded a 3:1:0.2 mixture (total 27% yield) of three regioisomers of the 6.6.6.6.6-fused pentacyclic products: 29,30-bisnor-β-amyrin (**38**), 29,30-bisnorgermanicol (**39**), and 29,30-bisnor-δ-amyrin (**40**) (Fig. 27.6) (Abe et al. 2004b). In addition, incubation with [23-^{13}C]-**33** and [23,23-^{2}H]-**3** afforded the corresponding ^{13}C- and ^{2}H-labeled products. No significant isotope effects were observed for the yields and patterns of the enzyme reaction products. The NMR spectra of the [^{13}C]-**38** clearly demonstrated that the [^{13}C]-label at C-19 (δ34.2), while C-18 (δ 51.8, d, $^{1}J_{CC}$ = 31 Hz) and C-20 (δ 27.4, d, $^{1}J_{CC}$ = 30 Hz), appeared as doublets. On the other hand, in the ^{1}H-decoupled ^{13}C NMR of the [^{2}H]-**38**, α-deuterium isotope effects were observed for C-19 ($\delta_{C(D)}$ 33.7, t, $^{1}J_{CD}$ = 21 Hz) and C-20 ($\delta_{C(D)}$ 26.8, t, $^{1}J_{CD}$ = 18 Hz), accompanied by β-deuterium shifted C-18 ($\delta_{C(D)}$ 51.7) and C-21 ($\delta_{C(D)}$ 22.2).

The labeling patterns of the [^{13}C]- and [^{2}H]-labeled isotopomers clearly indicated that the E-ring-forming reaction does not proceed through formation of a lupanyl *primary* cation (**36**) with a five-membered E-ring (route A) (the physiological β-amyrin biosynthesis involves formation of the lupanyl *tertiary* cation), but instead, an electrophilic addition of the tetracyclic baccharenyl C-18 cation (**35**) onto the terminal double bond directly generates a thermodynamically favored oleanyl *secondary* carbocation (**37**) with a less-strained six-membered E-ring (or its equivalent) (route B) (Fig. 27.6). The E-ring formation of the bisnor products is thus apparently under thermodynamic control.

On the other hand, the formation of three regioisomers with the Δ^{12}, $\Delta^{13(18)}$, and Δ^{18} double bond suggests lack of control on the stereochemistry of the final rearrangement reactions. It should be noted that formation of **38** from the oleanyl

C-20 cation (**37**) requires *three* 1,2-hydride shifts (H-19β → 20β, H-18α → 19α, H-13β → 18β) while that of β-amyrin from the oleanyl C-19 cation (**25**) involves only *two* 1,2-hydride shifts (H-18α → 19α, H-13β → 18β) followed by H-12α abstraction (Fig. 27.6). Presumably, the absence of the terminal methyl groups causes structural perturbation in the folding conformation of the E-ring moiety of the intermediate C-20 cation (**37**), which resulted in the interruption of the sequential 1,2-hydride shifts.

27.4 Conclusions

The broad substrate tolerance and catalytic potential of the bacterial SHC and the plant and fungal OSAC are remarkable; the enzymes accept a wide variety of nonphysiological substrate analogues and efficiently perform sequential ring-forming reactions to produce a series of unnatural novel cyclic triterpenes. Further analyses of the catalytic potential and plasticity of functionally divergent cyclase enzymes promise to reveal intimate structural details of the enzyme-templated sequential carbon-carbon bond forming reactions and suggest strategies for the structure-based rational engineering of the enzyme proteins. Manipulation of the enzyme reactions by newly designed substrate analogues along with the rationally engineered mutant enzymes would thus lead to further production of chemically and structurally disparate "supranatural" cyclic triterpenes, which is now in progress in our laboratories.

Acknowledgments The author expresses his appreciation to an excellent group of coworkers at Shizuoka, whose contributions are cited in the text. Financial support at Shizuoka has been provided by the PRESTO program from Japan Science and Technology Agency and Grants-in-Aid for Scientific Research from the Ministry of Education, Culture, Sports, Science and Technology, Japan.

References

Abe I (2007) Enzymatic synthesis of cyclic triterpenes. Nat Prod Rep 24:1311–1331

Abe I, Rohmer M (1991) Enzymatic cyclization of 2,3-dihydrosqualene into euph-7-ene by a cell-free system from the protozoon *Tetrahymena pyriformis*. J Chem Soc Chem Comm 902–903

Abe I, Rohmer M (1994) Enzymic cyclization of 2,3-dihydrosqualene and squalene 2,3-epoxide by squalene cyclases: from pentacyclic to tetracyclic triterpenes. J Chem Soc Perkin Trans I 783–791

Abe I, Rohmer M, Prestwich GD (1993) Enzymatic cyclization of squalene and oxidosqualene to sterols and triterpenes. Chem Rev 93:2189–2206

Abe I, Tanaka H, Noguchi H (2002) Enzymatic formation of an unnatural hexacyclic C35 polyprenoid by bacterial squalene cyclase. J Am Chem Soc 124: 14514–14515

Abe I, Tanaka H, Takahashi Y, Lou W, Noguchi H (2003) In: Proceedings of the 45th symposium on the chemistry of natural products, Kyoto

Abe I, Sakano Y, Tanaka H, Lou W, Noguchi H, Shibuya M, Ebizuka Y (2004a) Enzymatic cyclization of 22,23-dihydro-2,3-oxidosqualene into euph-7-en-3 β-ol and bacchar-12-en-3β-ol by recombinant β-amyrin synthase. J Am Chem Soc 126:3426–3427

Abe I, Sakano Y, Sodeyama M, Tanaka H, Noguchi H, Shibuya M, Ebizuka Y (2004b) Mechanism and stereochemistry of enzymatic cyclization of 24,30-bisnor-2,3-oxidosqualene by recombinant β-amyrin synthase. J Am Chem Soc 126:6880–6881

Corey EJ, Gross SK (1967) Formation of sterols by the action of 2,3-oxidosqualene-sterol cyclase on the factitious substrates 2,3:22,23-dioxidosqualene and 2,3-oxido-22,23-dihydrosqualene. J Am Chem Soc 89:4561–4562

Corey EJ, Gross SK (1968) Direct biosynthesis of the 29,30-bisnoramyrin system from 29,30-bisnor-2,3-oxidosqualene in pea seedlings. J Am Chem Soc 90: 5045–5046

Dougherty DA (1996) Cation-π interactions in chemistry and biology: a new view of benzene, phe, tyr, and trp. Science 271:163–168

Eschenmoser A, Arigoni D (2005) Revisited after 50 years: 'the stereochemical interpretation of the biogenetic isoprene rule for the triterpenes'. Helv Chim Acta 88:3011–3050

Eschenmoser A, Ruzicka L, Jeger O, Arigoni D (1955) Eine stereochemische Interpretation der biogenetischen Isoprenregel bei den Triterpenen. Helv Chim Acta 38:1890–1904

Hoshino T, Sato T (2002) Squalene–hopene cyclase: catalytic mechanism and substrate recognition. Chem Commun 291–301

Hoshino T, Kumai Y, Kudo I, Nakano S, Ohashi S (2004) Enzymatic cyclization reactions of geraniol, farnesol and geranylgeraniol, and those of truncated squalene analogs having C20 and C25 by recombinant squalene cyclase. Org Biomol Chem 2:2650–2657

Kushiro T, Shibuya M, Ebizuka Y (1998) β-Amyrin synthase - cloning of oxidosqualene cyclase that catalyzes the formation of the most popular triterpene among higher plants. Eur J Biochem 256:238–244

Kushiro T, Shibuya M, Ebizuka Y (1999) Chimeric triterpene synthase. A possible model for multifunc-

tional triterpene synthase. J Am Chem Soc 121: 1208–1216

Kushiro T, Shibuya M, Masuda K, Ebizuka Y (2000) Mutational studies on triterpene synthases: engineering lupeol synthase into β-amyrin synthase. J Am Chem Soc 122:6816–6824

Morita M, Shibuya M, Kushiro T, Masuda K, Ebizuka Y (2000) Molecular cloning and functional expression of triterpene synthases from pea (*Pisum sativum*). New α-amyrin-producing enzyme is a multifunctional triterpene synthase. Eur J Biochem 267:3453–3460

Ourisson G, Rohmer M, Poralla K (1987) Prokaryotic hopanoids and other polyprenoid sterol surrogates. Annu Rev Microbiol 41:301–333

Pale-Grosdemange C, Feil C, Rohmer M, Poralla K (1998) Occurrence of cationic intermediates and deficient control during the enzymatic cyclization of squalene to hopanoids. Angew Chem Int Ed 37:2237–2240

Poralla K (1999) Cycloartenol and other triterpene cyclases. In: Barton DHR, Nakanishi K (eds) Comprehensive natural products chemistry, vol 2. Pergamon, New York

Rajamani R, Gao J (2003) Balancing kinetic and thermodynamic control: the mechanism of carbocation cyclization by squalene cyclase. J Am Chem Soc 125:12768–12781

Reinert DJ, Balliano G, Schulz GE (2004) Conversion of squalene to the pentacarbocyclic hopene. Chem Biol 11:121–126

Segura MJR, Jackson BE, Matsuda SPT (2003) Mutagenesis approaches to deduce structure-function relationships in terpene synthases. Nat Prod Rep 20:304–317

Tanaka H, Noguchi H, Abe I (2005) Enzymatic formation of indole-containing unnatural cyclic polyprenoids by bacterial squalene–hopene cyclase. Org Lett 7: 5873–5876

Tanaka H, Noma H, Noguchi H, Abe I (2006) Enzymatic formation of pyrrole-containing novel cyclic polyprenoids by bacterial squalene–hopene cyclase. Tetrahedron Lett 47:3085–3089

van Tamelen EE (1982) Bioorganic characterization and mechanism of the 2,3-oxidosqualene-lanosterol conversion. J Am Chem Soc 104:6480–6481

Wendt KU, Poralla K, Schulz GE (1997) Structure and function of a squalene cyclase. Science 277: 1811–1815

Wendt KU, Lenhart A, Schulz GE (1999) The structure of the membrane protein squalene–hopene cyclase at 2.0 Å resolution. J Mol Biol 286:175–187

Wendt KU, Schulz GE, Corey EJ, Liu DR (2000) Enzyme mechanisms for polycyclic triterpene formation. Angew Chem Int Ed 39:2812–2833

Woodward RB, Bloch K (1953) The cyclization of squalene in cholesterol synthesis. J Am Chem Soc 75:2023–2024

Xiong Q, Zhu X, Wilson WK, Ganesan A, Matsuda SPT (2003) Enzymatic synthesis of an indole diterpene by an oxidosqualene cyclase: mechanistic, biosynthetic, and phylogenetic implications. J Am Chem Soc 125:9002–9003

Xu R, Fazio GC, Matsuda SPT (2004) On the origins of triterpenoid skeletal diversity. Phytochemistry 65: 261–291

Saponin Synthesis and Function

28

Sam T. Mugford and Anne Osbourn

Abstract

Saponins are one of the most numerous and diverse groups of plant natural products. They serve a range of ecological roles including plant defence against disease and herbivores and possibly as allelopathic agents in competitive interactions between plants. Some saponins are also important pharmaceuticals, and the underexplored biodiversity of plant saponins is likely to prove to be a vital resource for future drug discovery. The biological activity of saponins is normally attributed to the amphipathic properties of these molecules, which consist of a hydrophobic triterpene or sterol backbone and a hydrophilic carbohydrate chain, although some saponins are known to have potent biological activities that are dependent on other aspects of their structure. This chapter will focus on the biological activity and the synthesis of some of the best-studied examples of plant saponins and on recent developments in the identification of the genes and enzymes responsible for saponin synthesis.

Keywords

Triterpenes • Natural products • Plant defence • Pharmaceuticals • Biosynthesis • Oxidosqualene cyclase • Cytochrome p450 • Acyltransferase • Glycosyltransferase

28.1 Introduction

Saponins are glycosides of triterpenes and steroids (Fig. 28.1). Steroidal glycoalkaloids are sometimes also referred to as saponins. The triterpene and steroid backbones are both derived from the mevalonic acid pathway, the common precursor being 2,3-oxidosqualene (Fig. 28.2). The name "saponin" derives from the soap-like

S.T. Mugford • A. Osbourn (✉)
Department of Metabolic Biology, John Innes Centre, Norwich Research Park, Norwich NR4 7UH, UK
e-mail: anne.osbourn@bbsrc.ac.uk

T.J. Bach and M. Rohmer (eds.), *Isoprenoid Synthesis in Plants and Microorganisms: New Concepts and Experimental Approaches*, DOI 10.1007/978-1-4614-4063-5_28,

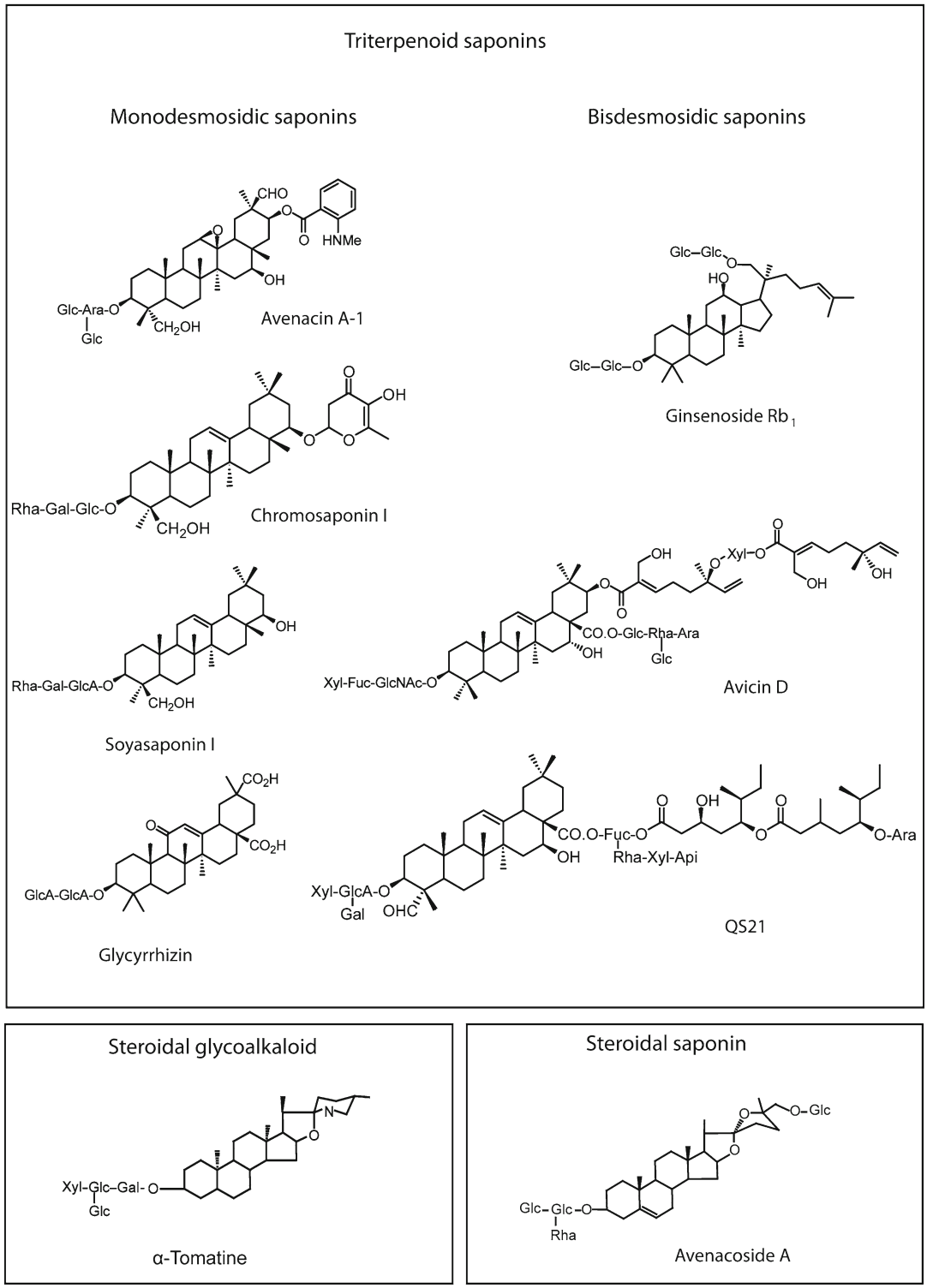

Fig. 28.1 Structures of plant saponins. Triterpenoid saponins (*top panel*): avenacin A-1 from oat roots (*Avena* spp.), chromosaponin I from pea seed (*Pisum sativum*), ginsenoside Rg_1 from ginseng roots (*Panax* spp.), soyasaponin I (also known as soyasaponin Bb) from soya (*Glycine max*), avicin D from *Acacia victoriae* seed pods, glycyrrhizin from liquorice roots (*Glycyrrhiza* spp.) and QS21 from *Quillaja saponaria* bark. Examples of both monodesmosidic (one sugar chain) and bisdesmosidic (two sugar chains) saponins are shown. *Bottom panels*: Steroidal glycoalkaloid α-tomatine from tomato leaves (*Solanum lycopersicum*); the steroidal saponin avenacoside A from oat leaves (*Avena* spp.)

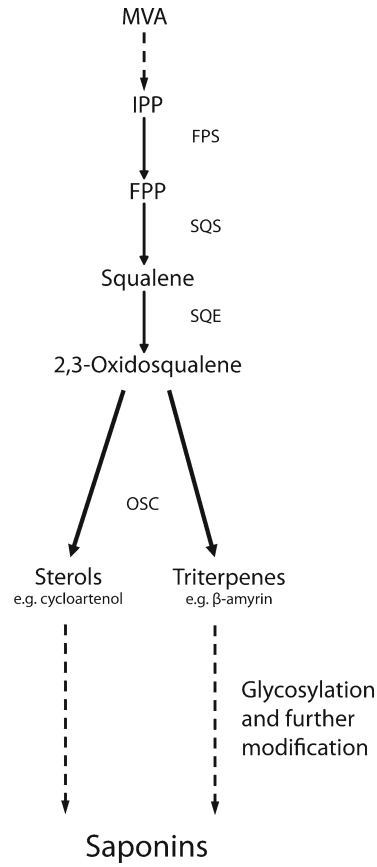

Fig. 28.2 Saponin biosynthesis in plants. Farnesyl diphosphate (FPP) is synthesised from isopentyl diphosphate (IPP) by farnesyl diphosphate synthase (FPS). Squalene synthase (SQS) converts FPP to squalene, and squalene epoxidase (SQE) then oxidises squalene to produce 2,3-oxidosqualene. 2,3-Oxidosqualene serves as the substrate for a range of oxidosqualene cyclase (OSC) enzymes, including cycloartenol synthase for primary sterol synthesis and β-amyrin synthase. These enzymes are responsible for the synthesis of the major sterol and triterpene precursors of saponin biosynthesis, respectively. Triterpenes and sterols derived from 2,3 oxidosqualene are further elaborated by oxidative and other modifications, and by glycosylation, leading to the synthesis of saponins

properties of these compounds. The highly polar sugar moieties together with the non-polar triterpene or sterol backbones result in a highly amphipathic compound. Hence, these compounds produce stable foams, a feature often associated with aqueous extracts from saponin-accumulating plants (Hostettmann and Marston 1995). Indeed, the names of some plants originate from this property, such as soapwort (*Saponaria officinalis*), which was historically used as a source of detergent.

Saponins represent a sizable proportion of the number of known plant natural products, which is in excess of 200,000 (Dixon 2001; Hartmann 2007; Osbourn et al. 2011). While plant natural products used to be regarded as waste products of a "luxurious metabolism", they are now accepted as the products of natural selection with diverse biological activities and important ecological roles (Dixon 2001; Hartmann 2007). The structural diversity of saponins is reflected in the array of different biological activities associated with these compounds, and these diverse compounds provide a significant resource for drug and agrochemical discovery. Indeed, many plant-derived saponins are currently used as important pharmaceuticals in the treatment of a range of diseases in conventional and traditional medicine (Arase et al. 1997; Cinatl et al. 2003; Jayatilake et al. 2003; Germonprez et al. 2004; Harada 2005). Research into the functions and synthesis of saponins has provided a wealth of information on the properties of this important group of compounds, both for human use and in plants.

The basis of the diversity of saponins lies in several aspects of their structure (Fig. 28.1) (Hostettmann and Marston 1995). Firstly, the aglycone triterpenes and sterols themselves encompass a wide range of structures, with variation in the degree and nature of cyclization and oxidation of the backbone. Secondly, the nature of glycosylation is widely variable with respect to the number and type of sugar molecules, the types of inter-sugar linkages and the presence of one or more sugar chains. *Monodesmosidic* saponins have a single sugar chain attached at the C-3 position, while *bidesmosidic* saponins have an additional sugar chain at the C-28 (for triterpenoid saponins) or C-26 (steroid saponins) position. Further modifications of the saponin backbone give rise to even greater structural diversity, such as the addition of acyl- or ether-linked groups derived from organic acids (e.g. avenacin A-1, chromosaponin I, avicin D and QS21; Fig. 28.1) (Begley et al. 1986; Kudou et al. 1993; Yoshikawa et al. 1994, 1997, 2000, 2005; Germonprez et al. 2004; Zou et al. 2005).

The function and synthesis of saponins in plants will be discussed in this chapter, with particular focus on triterpenoid saponins and on the oat root triterpenoid saponins known as avenacins.

28.2 Function

28.2.1 Biological Activity of Saponins

As might be expected from their chemical diversity, saponins collectively have a wide range of biological activities. Many of these compounds have antimicrobial and/or anti-herbivore activity and so may have roles in plant defence (Osbourn 1996; Morrissey and Osbourn 1999; Francis et al. 2002; Friedman 2002, 2006; Sparg et al. 2004). Saponins also have a range of important pharmaceutical properties, for example, anti-inflammatory, antifungal, antibacterial, anti-parasitic, anti-cancer and antiviral activities (reviewed by Sparg et al. 2004; Podolak et al. 2010). Saponins have further applications in a range of industries extending beyond pharmaceuticals. Their surfactant properties are important in the beverage and cosmetics industries, and saponins are used as foaming agents for a variety of purposes including in fire extinguishers (Hostettmann and Marston 1995). In addition, some saponins are used as flavourings due to their intense sweetness or bitterness (Price et al. 1987; Grenby 1991; Kitagawa 2002; Heng et al. 2006). For example, the sweetness of liquorice root is attributable to the presence of the triterpenoid saponin glycyrrhizin (Kitagawa 2002).

Saponins generally act by permeabilising plasma membranes. Their amphipathic properties enable them to penetrate membranes, where they complex with sterols and cause pore formation (Roddick 1979; Roddick and Drysdale 1984; Steel and Drysdale 1988; Fenwick et al. 1992; Armah et al. 1999). While membrane permeabilisation is a common feature of saponins, these compounds are also likely to have further effects on cells, for example, by interfering with cellular processes, such as enzyme activities, transport, organelle integrity, redox-related functions and other signal transduction processes and through triggering apoptosis (e.g. McManus et al. 1993; Ohana et al. 1998; Sparg et al. 2004; Haridas et al. 2001a; Lemeshko et al. 2006). For some saponins, it has been shown that biological activity does not depend on amphipathicity, making it unlikely that their mode of action is through membrane permeabilisation (Oda et al. 2003; Simons et al. 2006).

The biological properties of saponins in the context of their ecological functions and commercial applications are discussed below.

28.2.1.1 Ecological Roles

Oat Saponins

Avenacins are triterpenoid saponins that are found in the tips of oat roots (Crombie et al. 1984; Crombie and Crombie 1986; Hostettmann and Marston 1995). Oats appear to be unique amongst the cereals in being able to synthesise saponins (Ohmoto and Ikuse 1970; Osbourn et al. 2003). There are four forms of avenacin. The major form (avenacin A-1) is shown in Fig. 28.1. Avenacins are oleane-type triterpenoids derived from β-amyrin (Begley et al. 1986; Haralampidis et al. 2002). β-Amyrin is elaborated by addition of various functional groups including hydroxyls and an epoxide and by addition of a branched trisaccharide chain consisting of one L-arabinose and two D-glucose molecules. In addition, avenacins are acylated at the C-21 carbon of the triterpene with either *N*-methyl anthranilate (avenacins A-1 and B-1) or benzoate (avenacins A-2 and B-2). The *N*-methylanthraniloyl acyl group confers bright blue fluorescence under UV illumination, and this fluorescence can be readily seen in the root tip. Avenacins are potent antifungal compounds and are effective against the fungal pathogen *Gaeumannomyces graminis* var. *tritici*, which is the casual agent of take-all disease (Papadopoulou et al. 1999). Take-all causes major yield losses in wheat crops throughout the world, and there is currently no effective means of control. In contrast, oats are highly resistant to infection by *G. graminis*. Around half a century ago, it was suggested that the resistance of oats to this disease might be associated with the blue fluorescent material in the root tips of oat plants, which was shown to be antifungal (Goodwin and

Pollock 1954; Turner 1960). Isolation of the antifungal components of oat roots then led to the purification and structural identification of the avenacins (Burkhardt et al. 1964; Maizel et al. 1964). Osbourn et al. (1994) provided further evidence to highlight the importance of avenacins in resistance to take-all. Avenacins are only found in the *Avena* genus, and most oat species synthesise the compounds, suggesting that avenacins confer a selective advantage. One oat species, *Avena longiglumis*, was found to lack avenacins in its roots and was also shown to be susceptible to *G. graminis* var. *tritici*, while all other oat accessions investigated produced avenacins and were resistant to this pathogen. Further compelling evidence for a role for avenacins in plant defence came from the mutagenesis of a diploid avenacin-producing oat species (*Avena strigosa*), and the demonstration that avenacin-deficient mutants (isolated by screening for reduced root fluorescence) have enhanced susceptibility to a range of soil-borne fungal pathogens including *G. graminis* var. *tritici* (Papadopoulou et al. 1999).

Glycosylation of saponins is generally critical for antifungal activity (Sandrock and Van Etten 1998; Morrissey and Osbourn 1999). The loss of a single sugar from the oligosaccharide chain does not greatly reduce the amphipathicity of saponins but can impair the ability to complex with sterols (Arneson and Durbin 1967). Many fungi can hydrolyse sugars from saponins, thereby reducing antifungal activity (Sandrock and Van Etten 1998; Morrissey and Osbourn 1999). For example, the ability of an oat-attacking variant of the take-all fungus (*G. graminis* var. *avenae*) to infect oats is dependent on its ability to produce a saponin glycosyl hydrolase known as avenacinase (Bowyer et al. 1995). The various deglucosylated forms of avenacin have significantly reduced antifungal activity and reduced ability to complex membrane sterols. Examples of saponin glycosyl hydrolases have been reported from various other plant pathogenic fungi, including pathogens of oat leaves (which encounter the steroidal avenacosides) and of tomato (which encounter the steroidal glycoalkaloid α-tomatine) (Sandrock and Van Etten 1998; Morrissey and Osbourn 1999) (Fig. 28.1).

Like many plant secondary metabolites, avenacins are localised in the plant vacuole. An interesting insight into the role of saponin glycosylation in self-protection in plants was made recently during investigation of oat mutants that fail to fully glycosylate avenacins (Mylona et al. 2008). These mutants have stunted roots, a root hair-deficiency phenotype and membrane-trafficking defects. These defects were shown to be due to accumulation of the incompletely glucosylated avenacin intermediate. Thus, although this intermediate is less toxic to fungi (Turner 1961; Bowyer et al. 1995) and has a reduced capacity to cause permeabilisation of fungal membranes, it is toxic to plants cells. Glucosylation may be important for transport of avenacins to the vacuole. Consistent with this, the incompletely glucosylated avenacin intermediate has an atypical subcellular distribution and is not appropriately targeted to the vacuole. This suggests that vacuolar sequestration is an important self-protection mechanism (Mylona et al. 2008).

Avenacins are synthesised and accumulate in the epidermal cells of the root tip (Haralampidis et al. 2001). They are also released into the soil (Carter et al. 1999), although it is not clear whether this is an active process or a consequence of sloughing of the root epidermis. Carter et al. (1999) analysed fungi isolated from the roots of field-grown oat plants and found that many of these fungi were resistant to the toxic effects of avenacins and most were able to degrade these saponins. Thus, avenacins are likely to influence the growth of microorganisms in and around oat roots. The release of avenacins into the soil also has implications for competitive interactions between plants. Saponins from other plant species have been shown to have phytotoxic properties and as a consequence have been implicated in allelopathy (Oleszek and Jurzysta 1987; Waller et al. 1993; Hiradate et al. 1999; Li et al. 2004). Avenacins are phytotoxic and may therefore also have functions in suppression of the growth of neighbouring plants (Field et al. 2006). Oats are an important weed of other cereals, and understanding the basis of this competitive ability could lead to benefits for agriculture.

Triterpenoid Saponins from Legumes and Brassicaceae

Ecological roles for saponins have been identified in a range of other plant species. Soyasaponins, like avenacins, have a pentacyclic oleane triterpene skeleton. Members of the soyasaponin group of saponins are found in a variety of agriculturally important legumes (Hostettmann and Marston 1995; Yoshiki et al. 1998; Suzuki et al. 2002, 2005; Agrell et al. 2003), and several of these compounds have important pharmacological properties (Konoshima et al. 1992; Milgate and Roberts 1995; Dixon and Sumner 2003; Gurfinkel and Rao 2003). Soyasaponins are a diverse group of compounds that exist as mono- and bisdesmosidic forms (Hostettmann and Marston 1995). An example of a monodesmosidic soyasaponin is soyasaponin I (Fig. 28.1). In some bisdesmosidic legume saponins, the terminal monosaccharide of the C-22 sugar chain is modified by the addition of a γ-pyranoyl group (an ether-linked 2,3-dihydro-2,5-dihydroxy-6-methyl-4*H*-pyran-4-one (DDMP) group: Yoshiki et al. 1998; Tsurumi et al. 1992). One such γ-pyronyl saponin, chromosaponin I (Fig. 28.1), sometimes also referred to as soyasaponin VI (Hostettmann and Marston 1995), has been shown to have a growth-promoting effect on other plants (Tsurumi and Wada 1995; Tsurumi and Ishizawa 1997; Tsurumi et al. 2000) and is believed to exert its effects through regulation of auxin influx (Rahman et al. 2001). While chromosaponin I promotes plant growth, other legume saponins have been shown to suppress the growth of other plant species, an observation that is of particular relevance to organic farming methods in which these species are used as green fertiliser crops and that may explain why this practice can have a negative impact on subsequent crop yields (Oleszek and Jurzysta 1987; Waller et al. 1993; Hiradate et al. 1999; Li et al. 2004).

Accumulation of a variety of triterpenes including soyasaponin I (Fig. 28.1) (also known as soyasaponin B_b) and the related bidesmosidic saponin, medicagenic acid, occurs in response to fungal elicitors (Suzuki et al. 2002, 2005), wounding and herbivory in *Medicago sativa* (Agrell et al. 2003) and has been linked with plant defence. Similarly, soyasaponins have been shown to be major insecticidal and antifeedant components of pea seeds (Taylor et al. 2004) and are likely to protect these plants from herbivory by insects. Resistance to insect herbivores in the Brassicaceae is known to be mediated by glucosinolates (Bones and Rossiter 1996; Halkier and Gershenzon 2006). Some specialist herbivores are not affected by glucosinolate toxicity and use the compounds as a signal to stimulate oviposition on the plant (Huang et al. 1994). However, the ability of one brassicaceous species, *Barbarea vulgaris*, to resist attack by the specialist diamondback moth (*Plutella xylostella*) was found to be associated with the accumulation of a triterpenoid saponin in the plant (Shinoda et al. 2002). The saponin is associated with antifeedant effects towards the larva of *P. xylostella* and causes toxicity at high concentrations. Antifeedant activity and/or toxicity to insects have also been suggested for a number of other saponins (Hlywka et al. 1994; Agrell et al. 2003; Taylor et al. 2004) and may be an important component of plant defence. Saponins also impact on palatability for other animals including humans. For example, some saponins are used as sweeteners (Hayashi et al. 1999, 2001a). Conversely, other saponins have anti-sweet properties and are able to suppress the sweet taste of glucose (Yoshikawa et al. 1994, 1997, 2000). The flavour properties of soyasaponins have been investigated through the stimulation of the glossopharyngeal nerve of frogs by direct application of pure saponins (Yoshiki et al. 1998). Antiherbivore activity and bitterness can also have detrimental consequences for agriculture (Francis et al. 2002), and saponins from legumes can reduce the ability of ruminant mammals to digest plant material (Milgate and Roberts 1995; Dixon and Sumner 2003).

Steroidal Glycoalkaloids from the Solanaceae

Many solanaceous species produce antifungal steroidal glycoalkaloid saponins. Tomato plants produce α-tomatine, a monodesmosidic steroidal glycoalkaloid with a tetrasaccharide side chain that accumulates in the leaves and immature fruit

(Friedman 2002) (Fig. 28.1). α-Tomatine is fungitoxic and has been implicated in protection against fungal infection (Sandrock and Van Etten 1998; Morrissey and Osbourn 1999; Friedman 2002). As with other saponins, α-tomatine is toxic to a wide range of fungal species. Toxicity is generally ascribed to the ability of the saponin to complex with sterols and permeabilise fungal plasma membranes (Arneson and Durbin 1968a; Roddick 1979; Keukens et al. 1992, 1995). α-Tomatine has recently also been shown to induce reactive oxygen-mediated programmed cell death in fungi (Ito et al. 2007). Specialist pathogens of tomato generally have a higher level of resistance to α-tomatine when compared with fungi that do not infect tomato (Arneson and Durbin 1968b; Steel and Drysdale 1988; Suleman et al. 1996; Sandrock and Van Etten 1998; Morrissey and Osbourn 1999). The tomato leaf spot fungus, *Septoria lycopersici*, provides an interesting example of this plant-pathogen relationship. *S. lycopersici* is resistant to α-tomatine and is able to infect tomato plants. This fungus produces an α-tomatine-hydrolysing enzyme, tomatinase, which deglucosylates α-tomatine to the less toxic product β_2-tomatine (Arneson and Durbin 1967). Tomatinase-deficient mutants of *S. lycopersici* (generated by insertional inactivation of the tomatinase gene) are unable to degrade α-tomatine and have enhanced sensitivity to this saponin. Such mutants are not compromised in their ability to cause disease on tomato leaves. However, they do trigger enhanced cell death and elevated expression of defence genes during early infection (Martin-Hernandez et al. 2000). Heterologous expression of *S. lycopersici* tomatinase in the phytopathogenic fungi *Cladosporium fulvum* and *Nectria haematococca*, both of which are normally unable to degrade α-tomatine, resulted in enhanced sporulation on tomato plants (Melton et al. 1998; Sandrock and Van Etten 2001), providing further evidence for a role for tomatinase in virulence. Another fungal pathogen of tomato, *Fusarium oxysporum* f. sp. *lycopersici,* produces a tomatinase enzyme that has a different mode of action to that of *S. lycopersici* and that hydrolyses α-tomatine to give the tetrasaccharide lycotetraose and the aglycone tomatidine. Gene silencing and targeted gene disruption experiments indicate that *F. oxysporum* f. sp. *lycopersici* tomatinase is required for full virulence on tomato (Ito et al. 2002; Pareja-Jaime et al. 2008). Importantly, the α-tomatine hydrolysis products β_2-tomatine, tomatidine and lycotetraose have all been shown to suppress induced defence responses in tomato (Bourab et al. 2002; Ito et al. 2004, 2007), suggesting that hydrolysis of α-tomatine may serve a dual function during infection of tomato plants by fungi, namely, detoxification of a preformed toxin and subversion of the hydrolysis products for suppression of induced defences. Significantly, the α-tomatine aglycone, tomatidine, has been shown to inhibit sterol biosynthesis in yeast (Simons et al. 2006), although the mechanism by which tomatidine and other α-tomatine hydrolysis products interfere with induced plant defence responses is as yet unknown.

28.2.1.2 Roles in Human Health

Saponins are exploited as important pharmaceuticals and for a variety of other industrial uses. The triterpenoid ginsenoside saponins (e.g. ginsenoside Rb_1; Fig. 28.1) are the major bioactive components of ginseng, the roots of which are widely used in traditional Chinese medicine. Ginsenosides have multiple pharmacological properties, including anti-tumour, immunomodulatory and neurological activity (Attele et al. 1999). The triterpenoid saponin from liquorice, glycyrrhizin (Fig. 28.1), also has wide-ranging medical uses. This compound has antiviral activity and is used in the treatment of hepatitis (Arase et al. 1997). Glycyrrhizin is also active against the HIV and SARS viruses (Cinatl et al. 2003; Harada 2005) and in addition has anti-inflammatory (Matsui et al. 2004), immunomodulatory (Takahara et al. 1994) and anti-ulcer activity (He et al. 2001). The main use of glycyrrhizin globally is, however, as a sweetener in the food industry (Kitagawa 2002). Avicins (e.g. avicin D; Fig. 28.1) are triterpenoid saponins from the Australian desert tree *Acacia victoriae* that have anti-tumour activity (Jayatilake et al. 2003) and are used in the treatment of cancer. Avicins have a range of physiological effects in mammalian

cells including induction of apoptosis (Haridas et al. 2001a), suppression of inflammatory responses (Haridas et al. 2001b), inhibition of cell proliferation (Mujoo et al. 2001) and prevention of mutagenesis caused by environmental toxins (Hanausek et al. 2001), all of which may contribute to the anti-cancer properties of this compound. Two modes of action have been identified. Avicins permeabilise the mitochondrial outer membrane (Lemeshko et al. 2006; Haridas et al. 2007); they also covalently modify a transcription factor leading to modulation of responses to oxidative stress (Haridas et al. 2005). The main forms of avicin, such as avicin D, are acylated at the C-21 carbon with a group derived from two monoterpenes joined via a xylose (Fig. 28.1) (Jayatilake et al. 2003), and this group is essential for both modes of action (Haridas et al. 2005, 2007).

An important adjuvant used to improve the effectiveness of vaccines is a saponin derived from the bark of the South American tree *Quillaja saponaria*, known as QS21 (Kensil et al. 1991) (Fig. 28.1). A number of saponins have been shown to act as adjuvants (Barr et al. 1998; Oda et al. 2003). Interestingly, the most effective adjuvant saponins are bidesmosidic (Oda et al. 2003). This contrasts with other biological activities of saponins, which often depend on the amphipathic properties associated with monodesmosidic saponins. A comprehensive review of the pharmacological effects of saponins can be found in Sparg et al. (2004).

Saponins also have important dietary properties, and their presence in food crops has implications for human health. Saponins ingested as part of the human diet have been linked with a variety of effects on health, including reducing blood cholesterol levels (Milgate and Roberts 1995; Friedman 2002). The major steroidal glycoalkaloids found in potato are α-chaconine and α-solanine, which are monodesmosides of the steroidal alkaloid aglycone solanidine that differ only in the nature of the carbohydrate chain (Friedman 2006). Glycoalkaloids accumulate in potato tubers in response to insect damage (Hlywka et al. 1994) and also during post-harvest deterioration after exposure to light or as a result of physical damage (Mondy et al. 1987; Dao and Friedman 1994). α-Solanine and α-chaconine are inhibitors of acetylcholine esterase (Abbott et al. 1960; Roddick 1989), which is also the mode of action of many insecticides and can result in neurological symptoms in animals. Consumption of potatoes containing elevated levels of these glycoalkaloids can result in vomiting, diarrhoea, disorientation and death (Hansen 1925; McMillan and Thompson 1979; Korpan et al. 2004), and these symptoms are associated with reduced serum cholinesterase activity (McMillan and Thompson 1979).

The tomato steroidal glycoalkaloid α-tomatine accumulates to high levels in immature tomato fruits (up to 500 mg/kg of fresh fruit weight) (Friedman 2002). However, the consumption of immature tomatoes does not appear to cause symptoms, and likewise, tomato varieties that accumulate high levels of α-tomatine in the mature fruit do not appear to cause ill effects amongst the Peruvians who eat them (Rick et al. 1994), indicating that α-tomatine is not so toxic to humans as the potato glycoalkaloids. In fact, the steroidal glycoalkaloids from these solanaceous species have been found to have health-promoting effects. Both tomato and potato steroidal glycoalkaloids have antiproliferative effects against human cancer cell lines *in vitro* (Lee et al. 2004) and have also been shown to act as chemosensitisers, increasing the effectiveness of chemotherapeutic drugs by blocking their export through multi-drug resistance-type transport proteins (Lavie et al. 2001). In addition, α-tomatine has recently been shown to protect fish against tumours induced by an environmental toxin (Friedman et al. 2007).

28.3 Synthesis

28.3.1 Oxidosqualene Cyclization

Triterpenes and sterols are derived from a common precursor 2,3-oxidosqualene, which is synthesised from acetyl-CoA via mevalonic acid (MVA) and isopentyl diphosphate (IPP) (Haralampidis et al. 2002). Figure 28.2 shows an

outline of saponin biosynthesis. The enzymes that convert 2,3-oxidosqualene into the precursors of more elaborate sterols and triterpenes belong to the oxidosqualene cyclase (OSC) family. The products of OSC enzymes are diverse, varying principally in the degree of cyclization (Haralampidis et al. 2002; Phillips et al. 2006; Lodeiro et al. 2007; Vincken et al. 2007; Abe 2007). Collectively, OSCs are capable of cyclising 2,3-oxidosqualene into a diverse range of different products, highlighting the importance of this single enzymatic step. Triterpenoid skeletons alone account for more than 200 different structures that have been described (Segura et al. 2003; Connolly and Hill 2007). The genes encoding the cycloartenol synthase enzyme (CAS) are widely conserved across plant lineages, consistent with the role of this enzyme in the synthesis of essential membrane sterols (Phillips et al. 2006). However, the OSC gene family has expanded and diversified in many plants, providing a molecular basis for triterpene diversity (Suzuki et al. 2002; Ebizuka et al. 2003; Phillips et al. 2006; Field and Osbourn 2008).

Some OSC enzymes produce single cyclization products, while others are multifunctional and generate a variety of different products (Kushiro et al. 2000a; Segura et al. 2000; Basyuni et al. 2006; Phillips et al. 2006; Lodeiro et al. 2007.; Shibuya et al. 2007; Abe 2007). Indeed, a single OSC enzyme from *Arabidopsis thaliana* was found to be responsible for the synthesis of at least nine distinct triterpenes when heterologously expressed in yeast (Kushiro et al. 2000a). Amongst the best-characterised members of the plant OSC family are the sterol synthase, cycloartenol synthase and the triterpene synthase, β-amyrin synthase (Haralampidis et al. 2002; Abe 2007). Synthesis of β-amyrin is the first committed step in the triterpene pathways leading to avenacins in oat, glycyrrhizin in liquorice and soyasaponins in soy (Fig. 28.1), and β-amyrin synthases have been cloned and characterised from these plant species (Chung et al. 1994; Hayashi et al. 2001a; Haralampidis et al. 2001; Shibuya et al. 2006). Numerous other plant OSC enzymes have also been characterised by heterologous expression in yeast (e.g. Kushiro et al. 2000a; Hayashi et al. 2001a, b; Kawano et al. 2002; Ebizuka et al. 2003; Zhang et al. 2003; Suzuki et al. 2006; Tansakul et al. 2006; Xiang et al. 2006; Shinozaki et al. 2008a, b; Abe 2007). Although there is as yet no crystal structure for plant OSCs, the structures of the related bacterial enzyme, squalene cyclase (Lenhart et al. 2002) and the human OSC lanosterol synthase (Thoma et al. 2004) have been determined empirically. Extensive work has also been carried out on investigating the mode of action of OSCs through site-directed mutagenesis and directed evolution (Dang and Prestwich 2000; Kushiro et al. 2000b; Sato and Hoshino 2001; Meyer et al. 2002; Wu and Griffin 2002; Segura et al. 2002; 2003; Wu and Chang 2004; Wu et al. 2005, 2006). In some cases, this knowledge has enabled the rational engineering of OSC enzymes to give altered product profiles (e.g. Kushiro et al. 2000b; Meyer et al. 2002; Lodeiro et al. 2004; Wu and Chang 2004).

28.3.2 Oxidative Modification of the Saponin Backbone

The diversity of triterpene and sterol saponin skeletons is not solely due to the variety of cyclization reactions but also to the further elaboration of the structure by oxidative modifications. All triterpenes and sterols have in common a C-3 hydroxyl group originating from the epoxide of 2,3 oxidosqualene, although some OSC enzymes can utilise the unusual dioxidosqualene substrate resulting in the synthesis of a product bearing two hydroxyl groups (Shan et al. 2005) (e.g. arabidiol, which is produced by the *Arabidopsis thaliana* arabidiol synthase enzyme (Xiang et al. 2006)). Also, some OSC enzymes can accept a range of artificial substrates leading to the synthesis of unusual compounds bearing multiple functional groups (Noma et al. 2004; Abe, this volume). Many saponin skeletons include multiple oxidative modifications that are introduced after cyclization, including further hydroxylation, desaturation and epoxidation (Begley et al. 1986; Yoshiki et al. 1998; Jayatilake 2003; Qi et al. 2006; Seki et al. 2008). Oxidation of sterols

and triterpenes can influence their biological activity (Ji et al. 1990), although the functional significance of these types of modification for the action of saponins is apparent in only a few examples. The relevance of saponin skeleton modifications has been studied through the chemical modification of these compounds. Chemical modification of glycyrrhizin to alter the number of hydroxyl groups and positions of desaturations had significant impact on the inhibition of interleukins in human cell culture (Matsui et al. 2004). Also, in some cases, the comparison of the biological activities of naturally occurring compounds that differ specifically in these types of modification can reveal the importance of the modifications for activity. For example, the legume saponins avicins D and G differ only by one hydroxyl group, but this difference is sufficient to affect their respective abilities to inactivate caspase (Haridas et al. 2001b), although the hydroxyl group in question is associated with the acyl group and not with the triterpene skeleton. In some instances, this type of approach may also reveal that certain modifications have little impact on biological activity (Yoshikawa et al. 2005).

The avenacin pathway downstream of β-amyrin synthase involves a number of steps, including extensive oxidative modification of the triterpene ring structure. While plant OCS enzymes are relatively well characterised, the enzymes that catalyse the subsequent functionalisation of the triterpene backbone are only poorly understood (Haralampidis et al. 2002). A cytochrome P450 from oat (SAD2) has been shown to be required for avenacin synthesis and is likely to mediate oxygenation of β-amyrin at an as yet undetermined position (Qi et al. 2006). SAD2 belongs to the ancient and highly conserved CYP51 family of cytochrome P450s. Prior to the characterisation of SAD2, CYP51 enzymes were only known to function in the sterol pathway as sterol demethylases. SAD2 is the first CYP51 enzyme to be identified that has a different function – in the synthesis of defence-related triterpene glycosides (avenacins). This unusual CYP450 is the founder member of a monocot-specific divergent subfamily of CYP51 enzymes (defined as the CYP51H subfamily; Nelson et al. 2004). The functions of CYP51H enzymes in other cereals and grasses await investigation. It is possible that these enzymes may also have roles in plant defence.

Two other CYP450s that mediate modification of the triterpene backbones of saponins in other plant species have been identified through bioinformatics-based approaches. The soya CYP93E1 enzyme was identified using a combination of large-scale expressed sequence tag (EST) analysis and gene expression analysis to identify candidate genes involved in soyasaponin biosynthesis. This approach was facilitated by the fact that synthesis of soyasaponins can be induced by elicitor treatment (Shibuya et al. 2006). Candidate CYP450 enzymes identified in these experiments were functionally characterised by heterologous expression in yeast. The CYP93E1 enzyme was shown to catalyse the 24-hydroxylation of β-amyrin and also the formation of the 21-hydroxylated derivative, sophoradiol (Shibuya et al. 2006). A similar approach was used to characterise the triterpene-modifying CYP450 CYP88D6 from liquorice. CYP88D6 catalyses the oxidation of β-amyrin to 11-oxo-β-amyrin when expressed in yeast (Seki et al. 2008).

28.3.3 Glycosyltransferases

Glycosylation of saponins is generally important for the biological activity of these compounds, as discussed above. To date, few of the enzymes responsible for saponin glycosylation have been identified (Bowles et al. 2006; Townsend et al. 2006). Activity-based protein purification studies have been successfully applied to some saponin glycosyltransferases. For example, a UDP-galactose:tomatidine galactosyltransferase has been purified from tomato leaves (Zimowski 1994), and a solanidine glycosyltransferase (SGT) from potato has also been purified (Stapleton et al. 1991). These enzymes both catalyse the transfer of sugar moieties onto steroidal glycoalkaloid aglycones. Unlike triterpene aglycones, the steroidal alkaloid aglycones solanidine and tomatidine have potent antifungal activity (Moehs et al. 1997; Simons et al. 2006). This property

was exploited to clone a solanidine glycosyltransferase (SGT) gene from potato by expressing a potato cDNA library in yeast, plating the transformants onto medium containing solanidine and looking for colonies that had increased solanidine tolerance (Moehs et al. 1997). This led to the cloning of the potato SGT1 enzyme, which catalysed the transfer of glucose to the solanidine aglycone (the first committed step in the synthesis of the steroidal glycoalkaloid, α-chaconine) *in vitro*. The role of SGT in steroidal glycoalkaloid biosynthesis *in planta* was investigated through antisense RNA-mediated gene silencing (McCue et al. 2005). Silencing of *SGT1* did not result in the expected reduction in α-chaconine levels. However, the levels of a different steroidal glycoalkaloid, α-solanine, were substantially reduced in *SGT1*-silenced plants, suggesting that *SGT1* functions as a galactosyltransferase *in planta* and not as a glucosyltransferase. Indeed, subsequent biochemical characterisation showed that the SGT1 enzyme has a preference for UDP-galactose over UDP-glucose *in vitro* (McCue et al. 2005). A second potato glycosyltransferase SGT2 was subsequently identified as the primary UDP-glucose:solanidine glucosyltransferase (McCue et al. 2006). More recently, a rhamnosyltransferase implicated in the extension of the sugar chains of solanidine-derived steroidal glycoalkaloids has also been reported (McCue et al. 2007). Solanidine glycosyltransferases have been characterised from aubergine (eggplant; *Solanum melongena*) (Paczkowski et al. 1997; Zimowski 1997). Also, a steroidal saponin glucosyltransferase has been purified from the medicinal herb *Withania somnifera*, and the corresponding cDNA cloned (Madina et al. 2007).

Bioinformatics-based approaches to the identification of saponin glycosyltransferases have also been adopted. *Medicago truncatula* accumulates a range of triterpene saponins in response to elicitor treatment (Suzuki et al. 2002, 2005). Transcriptome analysis has been used to identify transcripts for predicted glycosyltransferases on the basis of co-expression with a cloned β-amyrin synthase gene. Subsequent biochemical characterisation revealed that two glycosyltransferases identified in this way were able to catalyse the glucosylation of triterpene aglycones (Suzuki et al. 2002, 2005; Achnine et al. 2005) and a crystal structure has been obtained for one of these enzymes (Shao et al. 2005). However, these glycosyltransferases had very broad substrate specificity *in vitro* and were able to glycosylate phenolic compounds more effectively than saponins (Suzuki et al. 2005; Shao et al. 2005). This highlights a common concern associated with analysis of the properties of enzymes *in vitro* – namely, that data gained from *in vitro* studies may not reflect the true properties of these enzymes *in planta* (Suzuki et al. 2005; Bowles et al. 2006). Comparison of the kinetic properties of enzymes *in vitro* with the availability of substrates *in planta* offers one means of providing further evidence of likely function in plants. However, the presence of other compounds *in planta* may modulate the substrate specificity of glycosyltransferases. For example, phospholipids of varying types, while not serving as substrates, have been shown to markedly alter the substrate preference of the aubergine solanidine glycosyltransferase (Paczkowski et al. 2001). It is interesting to note that the glycosyltransferases from *M. truncatula* that have been implicated in saponin glycosylation are phylogenetically distinct, and each shows similarity to different characterised glycosyltransferases from other species that act on quite different groups of compounds (Gachon et al. 2005).

28.3.4 Acylation of Saponins

Avenacins are acylated at the C-21 carbon with *N*-methyl anthranilate or benzoate (e.g. avenacin A-1; Fig. 28.1). Acylation at the C-21 position in particular has been suggested to be an important factor in the biological activity of saponins (Podolak et al. 2010). Acylation of avenacins is catalysed by a serine carboxypeptidase-like (SCPL) enzyme (AsSCPL1) which is encoded by the *Sad7* gene (Mugford et al. 2009; Mugford and Osbourn 2010). SCPL acyltransferases have previously been identified in dicotyledonous species with roles in the acylation of a range of plant natural products (Milkowski and Strack 2004).

Acyl groups have been identified in a number of saponins from a range of plant species (Fig. 28.1) (Warashina et al. 1991; Kudou et al. 1993; Yoshikawa et al. 1994, 1997, 2000; Yoshikawa M et al. 2005; Germonprez et al. 2004; Zou et al. 2005). Examples of triterpenoid saponins acylated with aromatic side chains are found in purple salsify (*Tragopogon porrifolius*) (Warashina et al. 1991), *Stephanotis lutchuensis* (Yoshikawa et al. 1994, 1997) and the Vietnamese medicinal species *Maesa balansae* (Germonprez et al. 2004). Warashina et al. (1991) isolated 18 tragopogonsaponins – all glycosides of echinocystic acid acylated with the phenylpropanoids *p*-coumarate, ferulate, 4-hydroxyphenyl proponoate or 4-hydroxy, 3-methoxyphenyl proponoate. Yoshikawa et al. (1994, 1997) have identified a number of anti-sweet acylated triterpenoid saponins – sitakisosides – including some that, like avenacin A-1, are acylated with *N*-methyl anthranilate. Germonprez et al. (2004) identified five forms of triterpenoid saponins from *Maesa balansae*, collectively known as maesabalides, which contain cinnamate and benzoate acyl groups. The maesabalides were found to exhibit anti-leishmanial activity.

Some saponin acyl groups have been ascribed a biological function through the comparison of acylated saponins and their unacylated counterparts. Avenacin-deficient oat mutants that are defective in avenacin acylation have been identified (Papadopoulou et al. 1999; Qi et al. 2004). These mutants have enhanced susceptibility to fungal pathogens, indicating that acylation is important for disease resistance, although the significance of this modification for the stability and antifungal activity of avenacins is not yet known. Biological activity of theasaponins from tea (*Camellia sinensis*) has been shown to be dependent upon acylation. Theasaponins are acylated at both the C-21 and C-22 positions by angelate or tiglate ((*Z*)-or (*E*)-2-methylbut-2-enoate, respectively) groups (Yoshikawa et al. 2005). Yoshikawa et al. (2005) showed that the gastro-protective effect offered by these compounds against ethanol toxicity was dependent on the presence of these acyl groups. The α-pyranosyl triterpenoid saponin chromosaponin I from pea is conjugated with a 2,3- dihydro-2, 5-dihydroxy-6-methyl-4 H-pyran-4-one (DDMP) group by an ether linkage (Fig. 28.1). In addition to its effects on plant growth and development (Tsurumi and Ishizawa 1997, 2000), chromosaponin I also has strong antioxidative capacity (Tsujino et al. 1994). Soya also produces triterpenoid saponins conjugated with DDMP, and the antioxidative capacity of these compounds has been shown to be largely due to the presence of the DDMP group (Yoshiki et al. 1998), suggesting an important contribution of DDMP modification to saponin activity.

The different steps in the synthesis of saponins are likely to occur in different subcellular locations. The early steps in saponin synthesis (mediated by OSC and CYP450 enzymes) are most probably associated with the endoplasmic reticulum (Ruf et al. 2004; Qi et al. 2006; Seki et al. 2008), while glycosyltransferases are typically found in the cytoplasm (Bowles et al. 2006). However, avenacins are sequestered in the vacuole (Mylona et al. 2008), suggesting that at least one transport step is required for their synthesis. Future work should lead to the identification of transporters that are required for saponin synthesis and accumulation.

28.4 Genetics and Evolution

While biological activities have been ascribed for many saponins, the demonstration of the importance of these compounds *in planta* is a difficult matter to resolve, requiring isogenic (or near isogenic) lines that differ solely in ability/inability to produce saponins. So far, the application of reverse genetics-based approaches for investigation of saponin biosynthesis and function has been limited. Transgenic potato plants that have reduced α-solanine content by antisense-mediated silencing of the solanidine glycosyltransferase gene *SGT1* have been generated (McCue et al. 2005). This work identified a different function for the enzyme than had been predicted from biochemical analysis *in vitro*, highlighting the importance of genetic tests of function *in planta*. These findings are of commercial relevance since

they open up opportunities for reducing steroidal glycoalkaloid levels in plants with ensuing benefits for human health. The impact of this modification for broader environmental interactions between potato plants and other organisms was not investigated.

The strong blue fluorescence of avenacin A-1 in oat root tips under UV illumination enables the direct visualisation of the presence of the compound *in planta* and has provided a facile screen for isolation of avenacin-deficient oat mutants (Papadopoulou et al. 1999). A total of 92 saponin-deficient (*sad*) mutants with reduced root fluorescence have been identified to date (Papadopoulou et al. 1999; Qi et al. 2006; Qin et al. 2010). These mutants, which represent at least six independent saponin biosynthesis (*sad*) loci, have enhanced susceptibility to disease, consistent with a role for avenacins in plant protection (Papadopoulou et al. 1999). *Sad1* encodes β-amyrin synthase, the OSC that catalyses the first committed step in avenacin synthesis (Haralampidis et al. 2001). Remarkably, four of the other loci that have been defined by genetic analysis as being required for avenacin synthesis co-segregate with *Sad1*, indicating that the avenacin biosynthetic genes are clustered (Qi et al. 2004). Physical clustering of avenacin pathway genes was confirmed by the recent cloning of *Sad2,* (Qi et al. 2006) and of *Sad7* (Mugford et al. 2009). The three genes are adjacent and lie within 140 kb of each other.

The finding that the genes for the avenacin pathway form an operon-like gene cluster was surprising, given our current understanding of eukaryotic genome organisation (Osbourn 2010). Metabolic gene clusters are common amongst the fungi, where there are many examples of gene clusters for natural product pathways (Keller and Hohn 1996; Bok et al. 2006; Keller et al. 2005). However, there are an increasing number of examples of gene clusters for metabolic pathways in plants. Other examples include the cyclic hydroxamic acid (2,4-dihydroxy-1,4-benzoxazin-3-one, DIBOA) pathway in maize (Frey et al. 1995, 1997; Gierl and Frey 2001) and the diterpenoid momilactone cluster in rice (Shimura et al. 2007). Both DIBOA and momilactones are implicated in plant defence. Gene clusters for triterpenoid synthesis have also been recently discovered in the model plant *Arabidopsis thaliana* (Field and Osbourn 2008; Field et al. 2011). Significantly, the triterpenoid gene clusters in oat and *Arabidopsis* have evolved recently and independently, suggesting that there is selection for clustering of genes for triterpenoid pathways (Qi et al. 2004; Field and Osbourn 2008; Osbourn 2010). Gene clustering will favour inheritance of the genes for the pathway in its entirety by minimising the chances of recombination occurring within the cluster during meiosis, which will provide a selective advantage if the pathway end products confer broad-spectrum disease resistance. There is also evidence to indicate that interference with the integrity of natural product gene clusters can lead to the formation of toxic intermediates (Mylona et al. 2008), so providing further selection pressure to maintain the cluster as a whole. Similarly, the biosynthetic intermediates of some other plant saponins are known to exhibit toxicity to fungi at least and may also have phytotoxic effects (Moehs et al. 1997; Simons et al. 2006). It has been observed that the early steps in several of the pathways encoded by known gene clusters are closely related to various hormone biosynthetic pathways and that this might be a factor in the evolution of the clusters (Chu et al. 2011). Additionally, the clustering of genes may facilitate tight co-ordinate regulation of gene expression at the level of chromatin (Qi et al. 2006; Shimura et al. 2007; Field and Osbourn 2008). The genes belonging to these metabolic clusters do show highly co-ordinated expression. For example, expression of the rice momilactone genes is co-ordinately induced upon treatment with elicitors or UV light (Shimura et al. 2007). The oat avenacin gene cluster and the *A. thaliana* thalianol gene cluster are both co-ordinately regulated in specific cell types within the roots and are expressed during normal growth and development (Qi et al. 2004, 2006; Field and Osbourn 2008). The genes within the 2,4-dihydroxy-7-methoxy-1,4-benzoxazin-3-one (DIMBOA) gene cluster in maize are expressed in the shoots of young seedlings (Frey et al. 1995), although some members of this gene cluster are

also expressed in other tissues (von Rad et al. 2001). However, one would expect the genes required for metabolic pathways to be co-ordinately regulated regardless of physical clustering, and there are many instances of co-ordinate regulation of genes that are not clustered but that belong to a single metabolic pathway (e.g. Hemm et al. 2004). Thus, gene clustering is not essential for co-ordinate expression.

Research into the chemical diversity of saponins is well documented (Hostettmann and Marston 1995), and the molecular genetics underlying the biosynthesis of these compounds is gaining ground. Forward genetics, bioinformatics-based approaches and genome browsing have led to the characterisation of new saponin biosynthetic genes and enzymes (Papadopoulou et al. 1999; Suzuki et al. 2002, 2005; Qi et al. 2004, 2006; Achnine et al. 2005; Seki et al. 2008). The current acceleration in gene discovery will yield biotechnological toolkits (genes, enzymes, regulators, transporters) that will be invaluable in designing strategies for quantitative and qualitative manipulation of saponin content in plants and for production of high-value compounds for commercial use. Future work will also shed further light on the ecological significance of saponins, on the relationship between structure and biological activity and on the mechanisms through which these compounds exert their effects on living cells.

References

Abbott DG, Field K, Johnson EI (1960) Observation on the correlation of anticholinesterase effect with solanine content of potatoes. Analyst 85:375–377

Abe I (2007) Enzymatic synthesis of cyclic triterpenes. Nat Prod Rep 24:1311

Achnine L, Huhman DV, Farag MA, Sumner LW, Blount JW, Dixon RA (2005) Genomics-based selection and functional characterization of triterpene glycosyltransferases from the model legume *Medicago truncatula*. Plant J 41:875–887

Agrell J, Oleszek W, Stochmal A, Olsen M, Anderson P (2003) Herbivore-induced responses in alfalfa (*Medicago sativa*). J Chem Ecol 29:303–320

Arase Y, Ikeda K, Murashima N, Chayama K, Tsubota A, Koida I, Suzuki Y, Slaitoh Y, Kobayashi M, Kumada H (1997) The long term efficacy of glycyrrhizin in chronic hepatitis C patients. Cancer 79:1494–1500

Armah CN, Mackie AR, Roy C, Price K, Osbourn AE, Bowyer P, Ladha S (1999) The membrane-permeabilizing effect of avenacin A-1 involves the reorganization of bilayer cholesterol. Biophys J 76:281–290

Arneson PA, Durbin RD (1967) Hydrolysis of tomatine by *Septoria lycopersici*: a detoxification mechanism. Phytopathology 57:1358–1360

Arneson PA, Durbin RD (1968a) Studies on the mode of action of tomatine as a fungitoxic agent. Plant Physiol 43:683–686

Arneson PA, Durbin RD (1968b) The sensitivity of fungi to α-tomatine. Phytopathology 58:536–537

Attele AS, Wu JA, Yuan C-S (1999) Ginseng pharmacology. Biochem Pharmacol 58:1685–1693

Barr IG, Sjölander A, Cox JC (1998) ISCOMs and other saponin based adjuvants. Adv Drug Deliv Rev 32:247–271

Basyuni M, Oku H, Inafuku M, Baba S, Iwasaki H, Oshiro K, Okabe T, Shibuya M, Ebizuka Y (2006) Molecular cloning and functional expression of a multifunctional triterpene synthase cDNA from a mangrove species *Kandelia candel* (L.) Druce. Phytochemistry 67:2517–2524

Begley MJ, Crombie L, Crombie WML, Whiting DA (1986) The isolation of avenacin A-1, A-2, B-1 and B-2, chemical defences against cereal "take-all" disease. Structure of their "aglycones", the avenestergenins, and their anhydro dimers. J Chem Soc Perk Trans 1:1905–1915

Bok JW, Noordermeer D, Kale SP, Keller NP (2006) Secondary metabolic gene cluster silencing in *Aspergillus nidulans*. Mol Microbiol 61:1636–1645

Bones AM, Rossiter JT (1996) The myrosinase-glucosinolate system, its organisation and biochemistry. Physiol Plantarum 97:194–208

Bourab K, Melton R, Peart J, Baulcombe D, Osbourn A (2002) A saponin-detoxifying enzyme mediates suppression of plant defences. Nature 418:889–892

Bowles D, Lim E-K, Poppenberger B, Vaistij FE (2006) Glycosyltransferases of lipophilic small molecules. Annu Rev Plant Biol 57:567–597

Bowyer P, Clarke BR, Lunness P, Daniels MJ, Osbourn AE (1995) Host range of a plant pathogenic fungus determined by a saponin detoxifying enzyme. Science 267:371–384

Burkhardt HJ, Maizel JV, Mitchell HK (1964) Avenacin, an antimicrobial substance isolated from *Avena sativa*. II. Structure. Biochemistry 3:427–431

Carter JP, Spink J, Cannon PF, Daniels MJ, Osbourn AE (1999) Isolation, characterization, and avenacin sensitivity of a diverse collection of cereal-root-colonizing fungi. Appl Environ Microbiol 65:3364–3372

Chu HY, Wegel E, Osbourn AE (2011) From hormones to secondary metabolism: the emergence of metabolic gene clusters in plants. Plant J 66:66–79

Chung E, Cho C-W, Kim K-Y, Chung J, Kim J-I, Chung Y-S, Fukui K, Lee J-H (1994) Molecular characterization of the *GmAMS1* gene encoding β-amyrin synthase in soybean plants. Russ J Plant Physiol 54:518–523

Cinatl J, Morgenstern B, Bauer G, Chandra P, Rabenau H, Doerr HW (2003) Glycyrrhizin, an active component of licorice roots, and replication of SARS-associated coronavirus. Lancet 361:2045–2046

Connolly JD, Hill RA (2007) Triterpenoids. Nat Prod Rep 24:465–486

Crombie WML, Crombie L (1986) Distribution of the avenacins A-1, A-2, B-1 and B-2 in oat roots: their fungicidal activity towards take-all fungus. Phytochemistry 25:2069–2073

Crombie L, Crombie WML, Whiting DA (1984) Structure of the four avenacins, oat root resistance factors to take-all disease. J Chem Soc Chem Commun 244:246–248

Dang TY, Prestwich GD (2000) Site-directed mutagenesis of squalene-hopene cyclase: altered substrate specificity and product distribution. Chem Biol 7:643–649

Dao L, Friedman M (1994) Chlorophyll, chlorogenic acid, glycoalkaloid and protease inhibitor content of fresh and green potatoes. J Agric Food Chem 42:633–639

Dixon R (2001) Natural products and disease resistance. Nature 411:843–847

Dixon RA, Sumner LW (2003) Legume natural products: understanding and manipulating complex pathways for human and animal health. Plant Physiol 131: 878–885

Ebizuka Y, Katsube Y, Tsutsumi T, Kushiro T, Shibuya M (2003) Functional genomics approach to the study of triterpene biosynthesis. Pure Appl Chem 75:369–374

Fenwick GR, Price KR, Tsukamoto C, Okubo K (1992) Saponins. In: D'Mello JPF, Duffus CM, Duffus JH (eds) Toxic substances in crop plants. The Royal Society of Chemistry, London, pp 285–327

Field B, Osbourn AE (2008) Metabolic diversification – independent assembly of operon-like gene clusters in different plants. Science 320:543–547

Field B, Jordán F, Osbourn A (2006) First encounters – deployment of defence-related natural products by plants. New Phytol 172:193–207

Field B, Fiston-Lavier AS, Kemen A, Geisler K, Quesnevillec H, Osbourn AE (2011) Formation of plant metabolic gene clusters within dynamic chromosomal regions. Proc Natl Acad Sci USA 108:16116–16121

Francis G, Kerem Z, Makkar HPS, Becker K (2002) The biological action of saponins in animal systems: a review. Br J Nutr 88:587–605

Frey M, Kliem R, Saedler H, Gierl A (1995) Expression of a cytochrome P450 gene family in maize. Mol Gen Genet 246:100–109

Frey M, Chomet P, Glawischnig E, Stettner C, Grün S, Winklmair A, Eisenreich W, Bacher A, Meeley RB, Briggs SP, Simcox K, Gierl A (1997) Analysis of a chemical plant defense mechanism in grasses. Science 277:696–699

Friedman M (2002) Tomato glycoalkaloids: roles in the plant and in the diet. J Agric Food Chem 50: 5751–5780

Friedman M (2006) Potato glycoalkaloids and metabolites: roles in the plant and in the diet. J Agric Food Chem 54:8655–8681

Friedman M, McQuistan T, Hendricks JD, Pereira C, Bailey GS (2007) Protective effect of dietary tomatine against dibenzo[a, l]pyrene (DBP)-induced liver and stomach tumors in rainbow trout. Mol Nutr Food Res 51:1485–1491

Gachon CM, Langlois-Meurinne M, Saindrenan P (2005) Plant secondary metabolism glycosyltransferases: the emerging functional analysis. Trends Plant Sci 10:542–549

Germonprez N, Van Puyvelde L, Maes L, Van Tri M, De Kimpe N (2004) New pentacyclic triterpene saponins with strong anti-leishmanial activity from the leaves of *Maesa balansae*. Tetrahedron 60:219–228

Gierl A, Frey M (2001) Evolution of benzoxazinone biosynthesis and indole production in maize. Planta 213:493–498

Goodwin RH, Pollock BM (1954) Studies on roots. I. Properties and distribution of fluorescent constituents in *Avena* roots. Am J Bot 41:516–520

Grenby TH (1991) Intense sweeteners for the food industry: an overview. Trends Food Sci Technol 2:2–6

Gurfinkel DM, Rao AV (2003) Soyasaponins: the relationship between chemical structure and colon anticarcinogenic activity. Nutr Cancer 47:24–33

Halkier BA, Gershenzon J (2006) Biology and biochemistry of glucosinolates. Annu Rev Plant Biol 57:303–333

Hanausek M, Gaensh P, Walaszek Z, Arntzen CJ, Slaga TJ, Gutterman JU (2001) Avicins, a family of triterpenoid saponins from *Acacia victoriae* (Bentham), suppress H-*ras* mutations and aneuploidy in a murine skin carcinogenesis model. Proc Natl Acad Sci USA 98: 11551–11556

Hansen AA (1925) Two fatal cases of potato poisoning. Science 61:340–341

Harada S (2005) The broad anti-viral agent glycyrrhizin directly modulates the fluidity of plasma membrane and HIV-1 envelope. Biochem J 329:191–199

Haralampidis K, Bryan G, Qi X, Papadopoulou K, Bakht S, Melton R, Osbourn AE (2001) A new class of oxidosqualene cyclases directs synthesis of antimicrobial phytoprotectants in monocots. Proc Natl Acad Sci USA 98:13431–13436

Haralampidis K, Trojanowska M, Osbourn AE (2002) Biosynthesis of triterpenoid saponins in plants. Adv Biochem Eng Biotechnol 75:32–47

Haridas V, Higuchi M, Jayatilake GS, Bailey D, Mujoo K, Blake ME, Arntzen CJ, Gutterman JU (2001a) Avicins: triterpenoid saponins from *Acacia victoriae* (Benthem) induce apoptosis by mitochondrial perturbation. Proc Natl Acad Sci USA 98:5821–5826

Haridas V, Arntzen CJ, Gutterman JU (2001b) Avicins, a family of triterpenoid saponins from *Acacia victoriae* (Bentham), inhibit activation of nuclear factor-κB by inhibiting both its nuclear localization and ability to bind DNA. Proc Natl Acad Sci USA 98:11557–22562

Haridas V, Kim S-O, Nishimura G, Hausladen A, Stamler JS, Gutterman JU (2005) Avicinylation (thioesterification): a protein modification that can regulate the response to oxidative and nitrosative stress. Proc Natl Acad Sci USA 102:10088–10093

Haridas V, Li X, Mizumachi T, Higuchi M, Lemeshko VV, Colombini M, Gutterman JU (2007) Avicins, a novel plant-derived metabolite lowers energy metabolism in tumor cells by targeting the outer mitochondrial membrane. Mitochondrion 7:234–240

Hartmann T (2007) From waste products to ecochemicals: fifty years of research of plant secondary metabolism. Phytochemistry 68:2831–2846

Hayashi H, Hirota A, Hiraoka N, Ikeshiro Y (1999) Molecular cloning and characterization of two cDNAs for *Glycyrrhiza glabra* squalene synthase. Biol Pharm Bull 22:947–950

Hayashi H, Huang P, Kirakosyan A, Inoue K, Hiraoka N, Ikeshiro Y, Kushiro T, Shibuya M, Ebizuka Y (2001a) Cloning and characterization of a cDNA encoding β-amyrin synthase involved in glycyrrhizin and soyasaponin biosynthesis in licorice. Biol Pharm Bull 24:912–916

Hayashi H, Huang P, Inoue K, Hiraoka N, Ikeshiro Y, Yazaki K, Tanaka S, Kushiro T, Shibuya M, Ebizuka Y (2001b) Molecular cloning and characterization of isomultiflorenol synthase, a new triterpene synthase from *Luffa cylindrica*, involved in biosynthesis of bryonolic acid. Eur J Biochem 268:6311–6317

He J-X, Akao T, Nishino T, Tani T (2001) The influence of commonly prescribed synthetic drugs for peptic ulcer on the pharmacokinetic fate of glycyrrhizin from Shaoyao-Gancao-tang. Biol Pharm Bull 24: 1395–1399

Hemm MR, Rider SD, Ogas J, Murry DJ, Chapple C (2004) Light induces phenylpropanoid metabolism in Arabidopsis roots. Plant J 38:765–778

Heng L, Vincken J-P, van Koningsveld GA, Legger A, Gruppen H, van Boekel T, Roozen J, Voragen F (2006) Bitterness of saponins and their content in dry peas. J Sci Food Agric 86:1225–1231

Hiradate S, Yada H, Ishii T, Nakajima N, Ohnishi-Kameyama M, Sugie H, Zungsontiporn S, Fujii Y (1999) Three plant growth inhibiting saponins from *Duranta repens*. Phytochemistry 52:1223–1228

Hlywka JJ, Stephenson GR, Sears MK, Yada RY (1994) Effects of insect damage on glycoalkaloid content in potatoes (*Solanum tuberosum*). J Agric Food Chem 42:2545–2550

Hostettmann KA, Marston A (1995) Saponins: chemistry and pharmacology of natural products. Cambridge University Press, Cambridge

Huang X, Renwick JAA, Sachdev-Gupta K (1994) Oviposition stimulants in *Barbarea vulgaris* for *Pieris rapae* and *P. napi oleracea*: isolation, identification and differential activity. J Chem Ecol 20:423

Ito S, Takahara H, Kawaguchi T, Tanaka S, Kameya-Iwaki M (2002) Post-transcriptional silencing of the tomatinase gene in *Fusarium oxysporum* f. sp *lycopersici*. J Phytopathol 150:474–480

Ito S, Eto T, Tanaka S, Yamauchi N, Takahara H, Ikeda T (2004) Tomatidine and lycotetraose, hydrolysis products of α-tomatine by *Fusarium oxysporum* tomatinase, suppress induced defense responses in tomato cells. FEBS Lett 571:31–34

Ito S, Ihara T, Tamura H, Tanaka S, Ikeda T, Kajihara H, Dissanayake C, Abdel-Motaal FF, El-Sayed MA (2007) α-Tomatine, the major saponin in tomato, induces programmed cell death mediated by reactive oxygen species in the fungal pathogen *Fusarium oxysporum*. FEBS Lett 581:3217–3222

Jayatilake GS, Freeberg DR, Liu ZJ, Richheimer SL, Blake Nieto ME, Bailey DT, Haridas V, Gutterman JU (2003) Isolation and structures of avicins D and G: in vitro tumor-inhibitory saponins derived from *Acacia victoriae*. J Nat Prod 66:779–783

Ji Y-H, Moog C, Schmitt G, Luu B (1990) Polyoxygenated sterols and triterpenes: chemical structures and biological activities. J Steroid Biochem 35:741–744

Kawano N, Ichinose K, Ebizuka Y (2002) Molecular cloning and functional expression of cDNAs encoding oxidosqualene cyclases from *Costus speciosus*. Biol Pharm Bull 25:477–482

Keller NP, Hohn TM (1996) Metabolic pathway gene clusters in filamentous fungi. Fungal Genet Biol 21:17–29

Keller NP, Turner G, Bennett JW (2005) Fungal secondary metabolism – from biochemistry to genomics. Nat Rev Microbiol 3:937–947

Kensil CR, Patel U, Lennick M, Marciani D (1991) Separation and characterisation of saponins with adjuvant activity from *Quillaja saponaria* molina cortex. J Immunol 146:431–437

Keukens EA, deVrije T, Fabrie CH, Demel RA, Jongen WM, deKruijff B (1992) Dual specificity of sterol-mediated glycoalkaloid induced membrane disruption. Biochim Biophys Acta 1110:127–136

Keukens EA, deVrije T, van den Boom C, de Waard P, Plasman HH, Thiel F, Chupin V, Jongen WM, deKruijff B (1995) Molecular basis of glycoalkaloid induced membrane disruption. Biochim Biophys Acta 1240:216–228

Kitagawa I (2002) Licorice root. A natural sweetener and an important ingredient in Chinese medicine. Pure Appl Chem 74:1189–1198

Konoshima T, Kokumai M, Kozuka M et al (1992) Anti-tumor-promoting activities of afromosin and soyasaponin I isolated from *Wisteria brachybotrys*. J Nat Prod 55:1776–1778

Korpan YI, Nazarenko EA, Skryshevskaya IV et al (2004) Potato glycoalkaloids: true safety or false sense of security? Trends Biotechnol 22:147–151

Kudou S, Tonomura M, Tsukamoto C et al (1993) Isolation and structural elucidation of DDMP-conjugated soyasaponins as genuine saponins from soybean seeds. Biosci Biotechnol Biochem 57:546–550

Kushiro T, Shibuya M, Masuda K, Ebizuka Y (2000a) A novel multifunctional triterpene synthase from *Arabidopsis thaliana*. Tetrahedron Lett 41:7705–7710

Kushiro T, Shibuya M, Masuda K, Ebizuka Y (2000b) Mutational studies on triterpene synthases: engineering lupeol synthase into β-amyrin synthase. J Am Chem Soc 122:6816–6824

Lavie Y, Harel-Orbital T, Gaffield W, Liscovitch M (2001) Inhibitory effect of steroidal alkaloids on drug transport and multidrug resistance in human cancer cells. Anticancer Res 21:1189–1194

Lee K-R, Kozukue N, Han J-S, Park J-H, Chang E-Y, Baek E-J, Chang J-S, Friedman M (2004) Glycoalkaloids and metabolites inhibit the growth of human colon (HT29) and liver (HepG2) cancer cells. J Agric Food Chem 52:2832–2839

Lemeshko VV, Haridas V, Quijano Pérez JC, Gutterman JU (2006) Avicins, natural anticancer saponins, permeabilize mitochondrial membranes. Arch Biochem Biophys 454:114–122

Lenhart A, Weihofen WA, Pleschke AE, Schulz GE (2002) Crystal structure of a squalene cyclase in complex with the potential anticholesteremic drug Ro48-8071. Chem Biol 9:639–645

Li Y, LiangW ZX, Liu F, Zhu X (2004) Allelopathic activity of root saponins of alfalfa on wheat, corn and barnyardgrass. Allelopathy J 15:119–123

Lodeiro S, Segura MJ, Stahl M, Schulz-Gasch T, Matsuda SPT (2004) Oxidosqualene cyclase second-sphere residues profoundly influence the product profile. ChemBioChem 5:1581–1585

Lodeiro S, Xiong QB, Wilson WK, Kolesnikova MD, Onak CS, Matsuda SPT (2007) An oxidosqualene cyclase makes numerous products by diverse mechanisms: a challenge to prevailing concepts of triterpene biosynthesis. J Am Chem Soc 129:11213–11222

Madina BR, Sharma LK, Chaturvedi P, Sangwan RS, Tuli R (2007) Purification and characterization of a novel glucosyltransferase specific to 27β-hydroxy steroidal lactones from *Withania somnifera* and its role in plant stress responses. Biochim Biophys Acta 1774: 1199–1207

Maizel JV, Burkhardt HJ, Mitchell HK (1964) Avenacin, an antimicrobial substance isolated from *Avena sativa*. I. Isolation and antimicrobial activity. Biochemistry 3:424–426

Martin-Hernandez AM, Dufresne M, Hugouvieux V, Melton R, Osbourn AE (2000) Effects of targeted replacement of the tomatinase gene on the interaction of *Septoria lycopersici* with tomato plants. Mol Plant Microbe Interact 13:1301–1311

Matsui S, Matsumoto H, Sonoda Y, Ando K, Aizu-Yokota E, Sato T, Kasahara T (2004) Glycyrrhizin and related compounds down-regulate production of inflammatory chemokines IL-8 and eotaxin 1 in a human lung fibroblast cell line. Int Immunopharmacol 4: 1633–1644

McCue KF, Shepherd LVT, Allen PV, Maccree MM, Rockhold DR, Corsini DL, Davies HV, Belknap WR (2005) Metabolic compensation of steroidal glycoalkaloid biosynthesis in transgenic potato tubers: using reverse genetics to confirm the in vivo enzyme function of a steroidal alkaloid galactosyltransferase. Plant Sci 168:267–273

McCue KF, Allen PV, Shepherd LVT, Blake A, Whitworth J, Maccree MM, Rockhold DR, Stewart D, Davies HV, Belknap WR (2006) The primary in vivo steroidal alkaloid glucosyltransferase from potato. Phytochemistry 67:1590–1597

McCue KF, Allen PV, Shepherd LVT, Blake A, Maccree MM, Rockhold DR, Novy RG, Stewart D, Davies HV, Belknap WR (2007) Potato glycosterol rhamnosyltransferase, the terminal step in triose side-chain biosynthesis. Phytochemistry 68:327–334

McManus OB, Harris GH, Giangiacomo KM et al (1993) An activator of calcium-dependent potassium channels isolated from a medicinal herb. Biochemistry 32:6128–6133

McMillan M, Thompson JC (1979) An outbreak of suspected solanine poisoning in schoolboys: examinations of criteria of solanine poisoning. Q J Med 48:227–243

Melton RE, Flegg LM, Brown JKM, Oliver RP, Daniels MJ, Osbourn AE (1998) Heterologous expression of *Septoria lycopersici* tomatinase in *Cladosporium fulvum*: effects on compatible and incompatible interactions with tomato seedlings. Mol Plant Microbe Interact 11:228–236

Meyer MM, Xu R, Matsuda SPT (2002) Directed evolution to generate cycloartenol synthase mutants that produce lanosterol. Org Lett 4:1395–1398

Milgate J, Roberts DCK (1995) The nutritional and biological significance of saponins. Nutr Res 15: 1233–1249

Milkowski C, Strack D (2004) Serine carboxypeptidase-like acyltransferases. Phytochemistry 66:517–524

Moehs CP, Allen PV, Friedman M, Belknap WR (1997) Cloning and expression of solanidine UDP-glucose glucosyltransferase from potato. Plant J 11:227–236

Mondy NI, Leja M, Gosselin B (1987) Changes in total phenolic, total glycoalkaloid, and ascorbic acid as a result of bruising. J Food Sci 52:631–633

Morrissey JP, Osbourn AE (1999) Fungal resistance to plant antibiotics as a mechanism of pathogenesis. Microbiol Mol Biol Rev 63:708–724

Mugford ST, Osbourn A (2010) Evolution of serine carboxypeptidase-like acyltransferases in the monocots. Plant Signal Behav 5:193–195

Mugford ST, Qi X, Bakht S et al (2009) A serine carboxypeptidase-like acyltransferase is required for synthesis of antimicrobial compounds and disease resistance in oats. Plant Cell 21:2473–2484

Mujoo K, Haridas V, Hoffmann JJ et al (2001) Triterpenoid saponins from *Acacia victoriae* (Bentham) decrease tumor cell proliferation and induce apoptosis. Cancer Res 61:5486–5490

Mylona P, Owatworakit A, Papadopoulou K et al (2008) *Sad3* and *Sad4* are required for saponin biosynthesis and root development in oat. Plant Cell 20:201–212

Nelson DR, Schuler MA, Paquette SM et al (2004) Comparative genomics of rice and Arabidopsis. Analysis of 727 cytochrome P450 genes and pseudogenes from a monocot and a dicot. Plant Physiol 135:756–772

Noma H, Tanaka H, Noguchi H et al (2004) Enzymatic formation of an unnatural novel tetracyclic sesterterpene by β-amyrin synthase. Tetrahedron Lett 45:8299–8301

Oda K, Matsuda H, Murakami T et al (2003) Relationship between adjuvant activity and amphipathic structure of soyasaponins. Vaccine 21:2145–2151

Ohana P, Delmer DP, Carlson RW et al (1998) Identification of a novel triterpenoid saponin from *Pisum sativum* as a specific inhibitor of the diguanylate cyclase of *Acetobacter xylinum*. Plant Cell Physiol 39:144–152

Ohmoto T, Ikuse M (1970) Triterpenoids of the gramineae. Phytochemistry 9:2137–2148

Oleszek W, Jurzysta M (1987) The allelopathic potential of alfalfa root medicagenic acid glycosides and their fate in soil environments. Plant Soil 98:67–80

Osbourn AE (1996) Saponins and plant defence- a soap story. Trends Plant Sci 1:4–8

Osbourn AE (2010) Secondary metabolic gene clusters: evolutionary toolkits for chemical innovation. Trends Genet 26:449–457

Osbourn AE, Clarke BR, Lunness P, Scott PR, Daniels MJ (1994) An oat species lacking avenacin is susceptible to infection by *Gaeumannomyces graminis* var. tritici. Physiol Mol Plant Pathol 45:457–467

Osbourn AE, Qi X, Townsend B, Qin B (2003) Dissecting plant secondary metabolism- constitutive chemical defences in cereals. New Phytol 159:101–108

Osbourn AE, Goss RJM, Field RA (2011) The saponins-polar isoprenoids with important and diverse biological activities. Nat Prod Rep 28:1261–1268

Paczkowski C, Kalinowska M, Wojciechowski ZA (1997) UDP-glucose:solasodine glucosyltransferase from eggplant (*Solanum melongena L.*) leaves: partial purification and characterization. Acta Biochim Pol 44:43–53

Paczkowski C, Kalinowska M, Wojciechowski ZA (2001) Phospholipids modulate the substrate specificity of soluble UDP-glucose:steroid glucosyltransferase from eggplant leaves. Phytochemistry 58:663–669

Papadopoulou K, Melton RE, Leggett M, Daniels MJ, Osbourn AE (1999) Compromised disease resistance in saponin-deficient plants. Proc Natl Acad Sci USA 96:12923–12928

Pareja-Jaime Y, Roncero MIG, Ruiz-Roldán MC (2008) Tomatinase from *Fusarium oxysporum* f. sp *lycopersici* is required for full virulence on tomato plants. Mol Plant Microbe Interact 21:728–736

Phillips DR, Rasbery JM, Bartel B, Matsuda SPT (2006) Biosynthetic diversity in plant triterpene cyclization. Curr Opin Plant Biol 9:305–314

Podolak I, Galanty A, Sobolewska D (2010) Saponins as cytotoxic agents: a review. Phytochem Rev 6: 425–474

Price KR, Johnson IT, Fenwick GR (1987) The chemistry and biological significance of saponins in foods and feedstuffs. Crit Rev Food Sci Nutr 26:27–135

Qi X, Bakht S, Leggett M, Maxwell C, Melton R, Osbourn A (2004) A gene cluster for secondary metabolism in oat – implications for the evolution of metabolic diversity in plants. Proc Natl Acad Sci USA 101:8233–8238

Qi X, Bakht S, Qin B, Leggett M, Hemmings A, Mellon F, Eagles J, Werck-Reichhart D, Schaller H, Lesot A, Melton R, Osbourn A (2006) A different function for a member of an ancient and highly conserved cytochrome P450 family: from essential sterols to plant defence. Proc Natl Acad Sci USA 103:18848–18853

Qin B, Eagles J, Mellon FA, Mylona P, Peña-Rodríguez L, Osbourn AE (2010) High throughput screening of mutants of oat that are defective in triterpene synthesis. Phytochemistry 71:1245–1252

Rahman A, Ahamed A, Amakawa T, Goto N, Tsurumi S (2001) Chromosaponin I specifically interacts with AUX1 protein in regulating the gravitropic response of Arabidopsis roots. Plant Physiol 125:990–1000

Rick CM, Uhlig JW, Jones AD (1994) High α-tomatine content in ripe fruit of Andean *Lycopersicon esculentum* var. *cerasiforme*: developmental and genetic aspects. Proc Natl Acad Sci USA 91:12877–12881

Roddick JG (1979) Complex formation between solanaceous steroidal glycoalkaloids and free sterols in vitro. Phytochemistry 18:1467–1470

Roddick JG (1989) The acetylcholinesterase-inhibitory activity of steroidal glycoalkaloids and their aglycons. Phytochemistry 28:2631–2634

Roddick JG, Drysdale RB (1984) Destabilization of liposome membranes by the steroidal glycoalkaloid α-tomatine. Phytochemistry 23:9–25

Ruf A, Müller F, D'Arcy B et al (2004) The monotopic membrane protein human oxidosqualene cyclase is active as monomer. Biochem Biophys Res Commun 315:247–254

Sandrock RW, Van Etten HD (1998) Fungal sensitivity to and enzymatic degradation of the phytoanticipin α-tomatine. Phytopathology 88:137–143

Sandrock RW, Van Etten HD (2001) The relevance of tomatinase activity in pathogens of tomato: disruption of the β2-tomatinase gene in *Colletotrichum coccodes* and *Septoria lycopersici* and heterologous expression of the *Septoria lycopersici* β2-tomatinase in *Nectria haematococca*, a pathogen of tomato fruit. Physiol Mol Plant Pathol 58:159–171

Sato T, Hoshino T (2001) Catalytic function of the residues of phenylalanine and tyrosine conserved in squalene-hopene cyclases. Biosci Biotechnol Biochem 65:2233–2242

Segura MJ, Meyer MM, Matsuda SPT (2000) *Arabidopsis thaliana* LUP1 converts oxidosqualene to multiple triterpene alcohols and a triterpene diol. Org Lett 2:2257–9225

Segura MJR, Lodeiro S, Meyer MM, Patel AJ, Matsuda SPT (2002) Directed evolution experiments reveal mutations at cycloartenol synthase residue His477 that dramatically alter catalysis. Org Lett 4:4459–4462

Segura MJR, Jackson BE, Matsuda SPT (2003) Mutagenesis approaches to deduce structure-function relationships in terpene synthases. Nat Prod Rep 30:304–317

Seki H, Ohyama K, Sawai S et al (2008) Licorice β-amyrin 11-oxidase, a cytochrome P450 with a key role in the biosynthesis of the triterpene sweetener glycyrrhizin. Proc Natl Acad Sci USA 105:14204–14209

Shan H, Segura MJR, Wilson WK, Lodeiro S, Matsuda SPT (2005) Enzymatic cyclization of dioxidosqualene

to heterocyclic triterpenes. J Am Chem Soc 127: 18008–18009

Shao H, He X, Achnine L, Blount JW, Dixon RA, Wang X (2005) Crystal structures of a multifunctional triterpene/flavonoid glycosyltransferase from *Medicago truncatula*. Plant Cell 17:3141–3154

Shibuya M, Hoshino M, Katsube Y, Hayashi H, Kushiro T, Ebizuka Y (2006) Identification of β-amyrin and sophoradiol 24-hydroxylase by expressed sequence tag mining and functional expression assay. FEBS J 273:948–959

Shibuya M, Xiang T, Katsube Y, Otsuka M, Zhang H, Ebizuka Y (2007) Origin of structural diversity in natural triterpenes: direct synthesis of *seco*-triterpene skeletons by oxidosqualene cyclase. J Am Chem Soc 129:1450–1455

Shimura K, Okada A, Okada K et al (2007) Identification of a biosynthetic gene cluster in rice for momilactones. J Biol Chem 282:34013–34018

Shinoda T, Nagao T, Nakayama M et al (2002) Identification of a triterpenoid saponin from a crucifer, *Barbarea vulgaris*, as a feeding deterrent to the diamondback moth, *Plutella xylostella*. J Chem Ecol 28:587–599

Shinozaki J, Shibuya M, Masuda K, Ebizuka Y (2008a) Dammaradiene synthase, a squalene cyclase, from *Dryopteris crassirhizoma* Nakai. Phytochemistry 69: 2559–2564

Shinozaki J, Shibuya M, Masuda K, Ebizuka Y (2008b) Squalene cyclase and oxidosqualene cyclase from a fern. FEBS Lett 582:310–318

Simons V, Morrissey JP, Latijnhouwers M, Csukai M, Cleaver A, Yarrow C, Osbourn A (2006) Dual effects of plant steroidal alkaloids on *Saccharomyces cerevisiae*. Antimicrob Agents Chemother 50:2732–2740

Sparg SG, Light ME, van Staden J (2004) Biological activities and distribution of plant saponins. J Ethnopharmacol 94:219–243

Stapleton A, Allen PV, Friedman M, Belknap WR (1991) Purification and characterization of solanidine glucosyltransferase from the potato. J Agric Food Chem 39:1187–1193

Steel CS, Drysdale RB (1988) Electrolytic leakage from plant and fungal tissues and disruption of liposome membranes by α-tomatine. Phytochemistry 27:1025–1030

Suleman P, Tohamy AM, Saleh AA, Madkour MA, Straney DC (1996) Variation in sensitivity to tomatine and rishitin among isolates of *Fusarium oxysporum* f. sp. *lycopersici*, and strains not pathogenic on tomato. Physiol Mol Plant Pathol 48:131–144

Suzuki H, Achnine L, Xu R, Matsuda SPT, Dixon RA (2002) A genomics approach to the early stages of triterpene saponin biosynthesis in *Medicago truncatula*. Plant J 32:1033–1048

Suzuki H, Reddy MSS, Naoumkina M et al (2005) Methyl jasmonate and yeast elicitor induce differential transcriptional and metabolic re-programming in cell suspension cultures of the model legume *Medicago truncatula*. Planta 220:696–707

Suzuki M, Xiang T, Ohyama K et al (2006) Lanosterol synthase in dicotyledonous plants. Plant Cell Physiol 47:565–571

Takahara T, Watanabe A, Shiraki K (1994) Effects of glycyrrhizin on hepatitis B surface antigen: a biochemical and morphological study. J Hepatol 21:601–609

Tansakul P, Shibuya M, Kushiro T, Ebizuka Y (2006) Dammarenediol-II synthase, the first dedicated enzyme for ginsenoside biosynthesis, in *Panax ginseng*. FEBS Lett 580:5143–5149

Taylor WG, Fields PG, Sutherland DH (2004) Insecticidal components from field pea extracts: soyasaponins and lysolecithins. J Agric Food Chem 52:7484–7490

Thoma R, Schulz-Gasch T, D'Arcy B et al (2004) Insight into steroid scaffold formation from the structure of human oxidosqualene cyclase. Nature 432:118–122

Townsend B, Jenner H, Osbourn A (2006) Saponin glycosylation in cereals. Phytochem Rev 5:109–114

Tsujino Y, Tsurumi S, Yoshida Y, Niki E (1994) Antioxidative effects of dihydro-γ-pyronyl-triterpenoid saponin (chromosaponin-I). Biosci Biotechnol Biochem 58:1731–1732

Tsurumi S, Ishizawa K (1997) Involvement of ethylene in chromosaponin-induced stimulation of growth in lettuce roots. Plant Cell Physiol 38:668–675

Tsurumi S, Wada S (1995) Chromosaponin-I stimulates the elongation of cortical-cells in lettuce roots. Plant Cell Physiol 36:925–929

Tsurumi S, Takagi T, Hashimoto T (1992) A γ-pyronyl triterpenoid saponin from *Pisum sativum*. Phytochemistry 31:2435–2438

Tsurumi S, Ishizawa K, Rahman A et al (2000) Effects of chromosaponin I and brassinolide on the growth of roots in etiolated Arabidopsis seedlings. J Plant Physiol 156:60–67

Turner EM (1960) The nature of the resistance of oats to the take-all fungus. J Exp Bot 11:403–412

Turner EM (1961) An enzymic basis for pathogenic specificity in *Ophiobolus graminis*. J Exp Bot 12: 169–175

Vincken J-P, Heng L, de Groot A, Gruppen H (2007) Saponins, classification and occurrence in the plant kingdom. Phytochemistry 68:275–297

von Rad U, Hüttl R, Lottspeich F, Gierl A, Frey M (2001) Two glucosyltransferases are involved in detoxification of benzoxazinoids in maize. Plant J 28:633–642

Waller GR, Jurzysta M, Thorne RLZ (1993) Allelopathic activity of root saponins from alfalfa (*Medicago sativa* L.) on weeds and wheat. Bot Bull Acad Sinica 34:1–11

Warashina T, Miyase T, Ueno A (1991) Novel acylated saponins from *Tragopogon porrifolius* L. Isolation and the structures of tragopogonsaponins A-R. Chem Pharm Bull 39:388–396

Wu TK, Chang CH (2004) Enzymatic formation of multiple triterpenes by mutation of tyrosine 510 of the oxidosqualene-lanosterol cyclase from *Saccharomyces cerevisiae*. Chembiochem 5:1712–1715

Wu TK, Griffin JH (2002) Conversion of a plant oxidosqualene-cycloartenol synthase to an oxidosqualene-lanosterol cyclase by random mutagenesis. Biochemistry 41:8238–8244

Wu TK, Liu YT, Chang CH (2005) Histidine residue at position 234 of oxidosqualene-lanosterol cyclase from *Saccharomyces cerevisiae* simultaneously influences cyclization, rearrangement, and deprotonation reactions. Chembiochem 6:1177–1181

Wu TK, Yu MT, Liu YT, Chang CH, Wang HJ, Diau EW (2006) Tryptophan 232 within oxidosqualene-lanosterol cyclase from *Saccharomyces cerevisiae* influences rearrangement and deprotonation but not cyclization reactions. Org Lett 8:1319–1322

Xiang T, Shibuya M, Katsube Y et al (2006) A new triterpene synthase from *Arabidopsis thaliana* produces a tricyclic triterpene with two hydroxyl groups. Org Lett 8:2835–2838

Yoshikawa K, Taninaka H, Kan Y, Arihara S (1994) Antisweet natural products. X: structures of sitakisosides I-V from *Stephanotis lutchuensis* kodiz. var. *japonica*. Chem Pharm Bull 42:2023–2027

Yoshikawa K, Mizutani A, Kan Y, Arihara S (1997) Antisweet natural products. XII: structures of sitakisosides XI-XX from *Stephanotis lutchuensis* Kodiz. var. *japonica*. Chem Pharm Bull 45:62–67

Yoshikawa K, Hirai H, Tanaka M, Arihara S (2000) Antisweet natural products. XV: structures of jegosaponins A–D from *Styrax japonica* Sieb. et Zucc. Chem Pharm Bull 48:1093–1096

Yoshikawa M, Morikawa T, Li N, Nagatomo A, Li X, Matsuda H (2005) Bioactive saponins and glycosides. XXIII. Triterpene saponins with gastroprotective effect from the seeds of *Camellia sinensis* -theasaponins E3, E4, E5, E6, and E7. Chem Pharm Bull 53:1559–1564

Yoshiki Y, Sigemitsu K, Okubu K (1998) Relationship between chemical structures and biological activities of triterpenoid saponins from soybean. Biosci Biotechnol Biochem 62:2291–2299

Zhang H, Shibuya M, Yokota S, Ebizuka Y (2003) Oxidosqualene cyclases from cell suspension cultures of *Betula platyphylla* var. *japonica*: molecular evolution of oxidosqualene cyclases in higher plants. Biol Pharm Bull 26:642–650

Zimowski J (1994) Characterization of UDP-galactose:tomatidine galactosyltransferase from tomato (*Lycopersicon esculentum*) leaves. Acta Biochim Pol 41:202–204

Zimowski J (1997) Synthesis of γ-chaconine and γ-solanine are catalyzed in potato by two separate glycosyltransferases: UDP-glucose:solanidine glucosyltransferase and UDP-galactose:solanidine galactosyltransferase. Acta Biochim Pol 44:209–214

Zou K, Tong W-Y, Liang H, Cui J-R, Tu G-Z, Zhao Y-Y, Zhang R-Y (2005) Diastereoisomeric saponins from *Albizia julibrissin*. Carbohydr Res 340:1329–1334

Cardenolide Aglycone Formation in *Digitalis*

29

Wolfgang Kreis and Frieder Müller-Uri

Abstract

Recent developments and the state of knowledge concerning the biosynthesis of the steroid part of cardenolides in the genus *Digitalis* (including *Isoplexis*) are reviewed. Substrate specificities and kinetic properties of native and recombinant enzymes are reported and discussed. Special emphasis is put on enzymes and genes involved in early pregnane metabolism. Evidence is provided that cardenolides are not assembled in one straightforward process but may be synthesised instead via a complex multidimensional metabolic network grid employing highly substrate-promiscuous enzymes.

Keywords

Digitalis • *Isoplexis* • Plantaginaceae • Biosynthesis • Cardenolides • Cardiac glycosides • Enone reductase • Oxidoreductase • Hydroxysteroid dehydrogenase • Short-chain dehydrogenase/reductase family • SDR • Cytochrome P450 • Molecular cloning • Gene expression • Phylogeny

29.1 Introduction

Cardenolide glycosides are still valuable drugs in the medication of patients suffering from cardiac insufficiency. *Digitalis* species are the major sources of the cardiac glycosides most frequently employed in medicine. Most of the cardiac glycosides found in *Digitalis* (incl. *Isoplexis*) belong to the group of 5β-cardenolides that are characterised by a steroid nucleus with its rings being connected *cis-trans-cis*, possessing a 14β-hydroxyl group, and substituted at C-17β with an unsaturated five-membered lactone ring. At position 3β, a sugar side chain with up to five carbohydrate units is attached containing glucose and various rare 6-deoxy, 2,6-dideoxy and 6-deoxy-3-methoxy sugars, such as D-fucose, D-digitoxose or D-digitalose (Fig. 29.1). A putative, one-dimensional biosynthetic

W. Kreis (✉) • F. Müller-Uri
Lehrstuhl für Pharmazeutische Biologie,
Friedrich-Alexander-Universität Erlangen-Nürnberg,
Staudtstr. 5, 91058 Erlangen, Germany

ECROPS, Erlangen Center of Plant Science,
Schlossplatz 4, 91054 Erlangen, Germany
e-mail: wkreis@biologie.uni-erlangen.de

T.J. Bach and M. Rohmer (eds.), *Isoprenoid Synthesis in Plants and Microorganisms: New Concepts and Experimental Approaches*, DOI 10.1007/978-1-4614-4063-5_29,

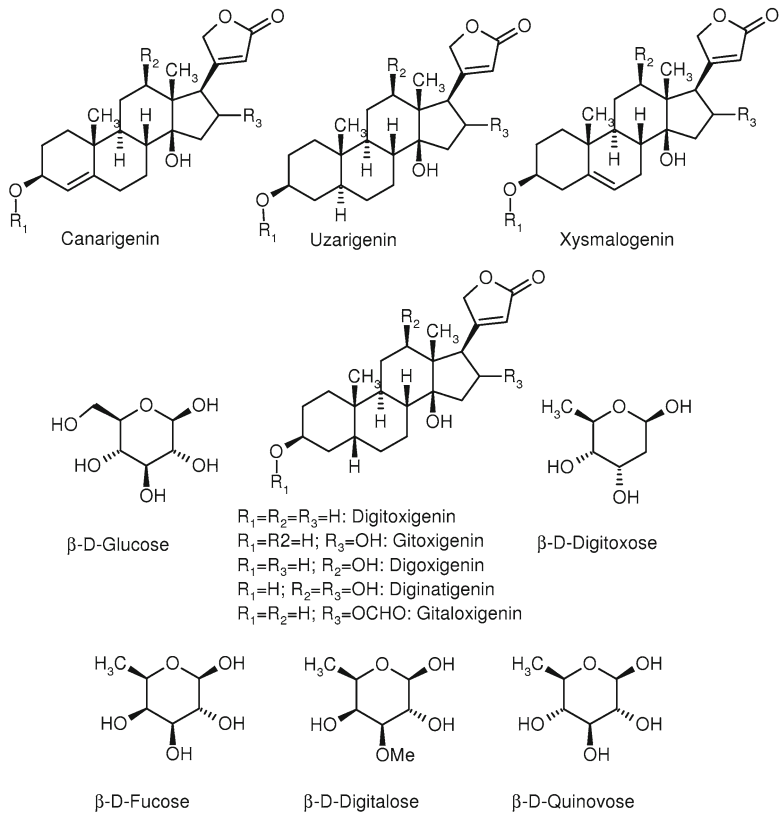

Fig. 29.1 Cardenolide structures mentioned in the text

pathway leading to the cardenolides is outlined in Fig. 29.2. For more details, the reader is referred to previous reviews (Kreis et al. 1998; Kreis and Müller-Uri 2010).

The paradigms, developments and achievements in plant secondary metabolism research were recently reviewed and discussed by Hartmann (2007). He also described a number of interesting perspectives for future research and pointed out that a network of plant research is needed to investigate plant secondary metabolism in more depth. The progress in the investigation of different fields, from the genome to the proteome and metabolome, will open new insights into plant secondary metabolite formation. Up to now, only little is known about how the pathways leading to plant secondary metabolites are regulated. However, the analysis of the different pathways is going on and will give first hints how to study their regulation in the future (Grotewold 2005).

The identification and characterisation of enzymes involved in pregnane and cardenolide metabolism has now also allowed new insight into the pathway that leads to cardenolides. In this review, emphasis is put on cardenolide formation, gene expression, molecular cloning and substrate preferences of enzymes probably involved in cardenolide formation.

So far, only few investigations have focussed on the formation of the sugar side chain of the cardenolides, especially the point of time when the characteristic 2,6-dideoxysugars are attached to the cardenolide genin. The hypothetical pathway implies that the various sugars are attached at the cardenolide aglycone stage although it cannot be ruled out that pregnane glycosides are obligate intermediates in cardenolide formation. Cardenolide genin glycosylation was discussed in more depth and detail in a previous review (Kreis et al. 1998) but has not been studied much since then. Hence, the enzymes involved in the

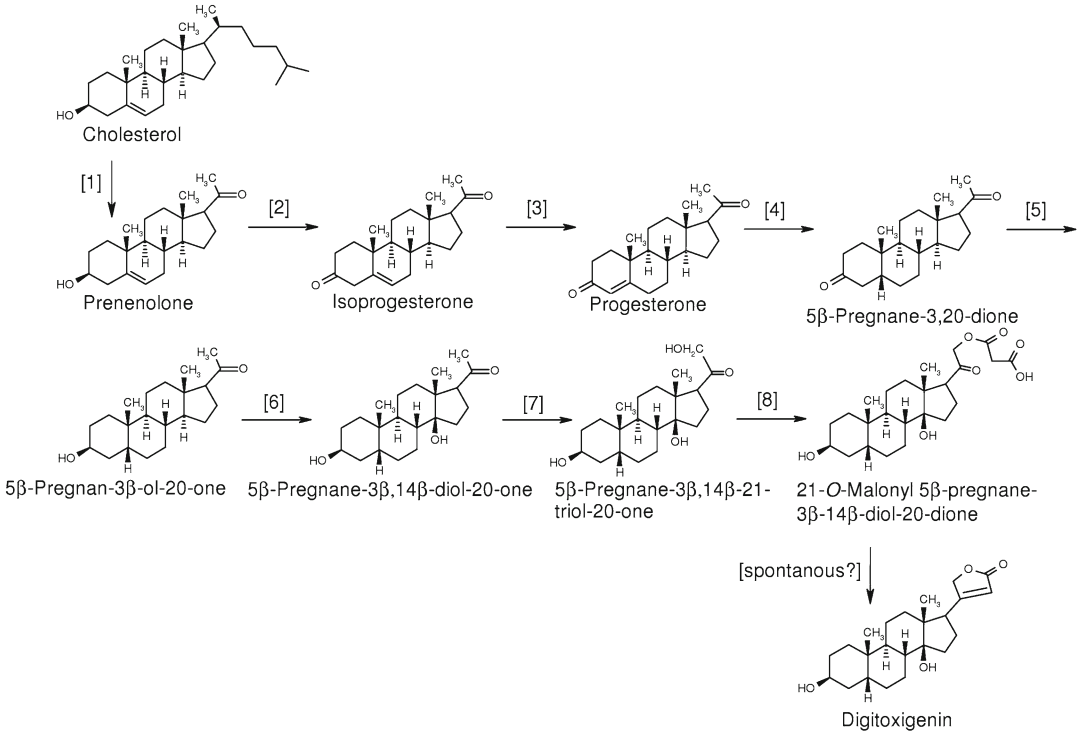

Fig. 29.2 Early steps in cardenolide biosynthesis. A putative two-dimensional pathway. [*1*] cholesterol side-chain cleaving enzyme (SCCE), [*2*] NAD: 3β-hydroxysteroid dehydrogenase (3β-HSD), [*3*] Δ^5-Δ^4-ketosteroid isomerase, [*4*] NADPH: progesterone 5β-reductase (5β-POR), [*5*] NADH: 3β-hydroxysteroid dehydrogenase (3β-HSD), [*6*] pregnane 14β-hydroxylase (hypothetical), [*7*] 14β-hydroxypregnane 21β-hydroxylase (hypothetical), [*8*] malonyl-coenzyme A:21-hydroxypregnane 21-*O*-malonyltransferase (21MAT), [*9*] spontaneous or enzymatically catalysed butenolide ring formation

formation of the sugar side chains will not be discussed here. Instead, the interested reader is referred to the review of Kreis et al. (1998) and the *Digitalis* monograph (Luckner and Wichtl 2000). The most recent achievements in this area were the cloning and heterologous expression of cardenolide glucohydrolase I (CGH I) in *Escherichia coli* and hairy roots obtained from *Agrobacterium-rhizogenes*-infected explants of *Cucumis sativus* (Shi and Lindemann 2006).

29.2 The Starting Point

Cardenolides are steroids and thus supposed to be derived from mevalonic acid via triterpenoid and phytosterol intermediates. As early as 1960, it was found that 2-^{14}C-mevalonic acid is incorporated into the steroid part of digitoxin (Ramstad and Beal 1960). Later on, degradation experiments revealed that the label of 2-^{14}C-mevalonic acid appeared in C-1, C-7 and C-15 of the cardenolide genin (Gros and Leete 1965), which is consistent with a biosynthetic route via the mevalonic acid pathway.

Since cholesterol is a major sterol in *Digitalis* plants and cell cultures (Tschesche 1970; Helmbold et al. 1978), it was hypothesised that pregnanes used for the formation of cardenolides may be derived from cholesterol. Indirect evidence for a favoured route not involving cholesterol was provided by studies with a specific inhibitor of 24-alkyl sterol biosynthesis. On one hand, feeding of 25-azacycloartanol led to an increase of endogenous cholesterol in *D. lanata* shoot cultures. On the other hand, the content of 24-alkyl sterols was dramatically reduced, as was the content of cardenolides (Milek et al. 1997),

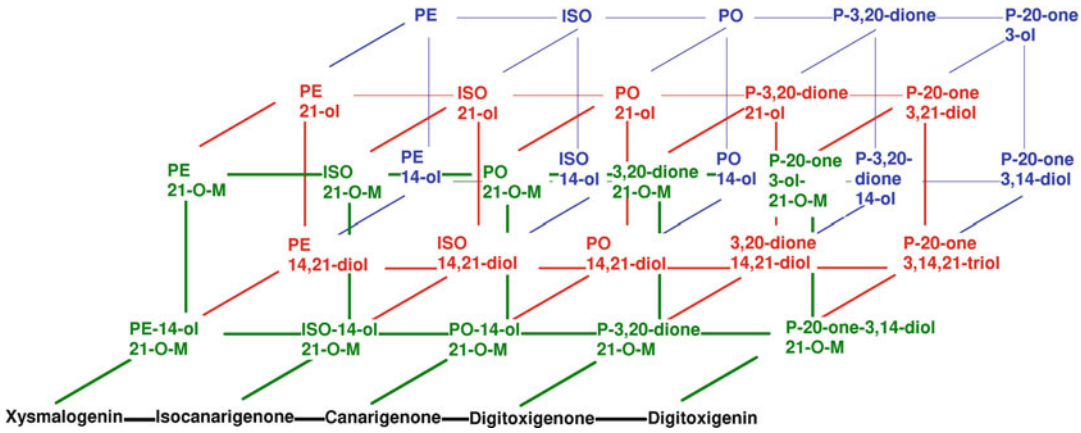

Fig. 29.3 Simple metabolic grid proposed for cardenolide formation. Abbreviations: *PE* pregnenolone, *ISO* isoprogesterone, *PO* pogesterone, *M* malonyl hemiester, *P* pregnane (C_{21}). The model does not include 3-*O*-glycosylation reactions which may modify any 3-hydroxypregnane structure in the grid

indicating a route via typical phytosterols, such as campesterol or β-sitosterol.

It was found that the carbon atoms C-22 and C-23 of the butenolide ring of the cardenolides are not derived from mevalonic acid (Gregory and Leete 1969). It was thus concluded that a pregnane has to be condensed with a C_2 donor, such as acetyl-CoA or malonyl-CoA, to yield the cardenolide genin. This route was termed the "pregnane pathway" of cardenolide formation. Intra- or intermolecular nucleophilic attack at the C-20 carbonyl of an appropriately activated acetate or malonate is proposed as one possible mechanism of attaching C-22 and C-23 to the pregnane skeleton. The formation of the butenolide ring system can then be accomplished by formal elimination of water and lactonization. Experimental evidence for these steps is still lacking, and recently, a different mechanism of butenolide ring formation has been suggested, involving the formation of a pregnane 21-O-malonyl hemi-ester with subsequent intramolecular condensation under decarboxylation and dehydratisation (Stuhlemmer and Kreis 1996a; Pádua et al. 2008).

Independent of the sterol precursor assumed, pregnenolone may be considered as the starting point for cardenolide formation via the "pregnane pathway" (Tschesche and Lilienweiss 1964). Since 3α-H of [3α-^{3}H, 4-^{14}C]-pregnenolone was lost in 5β-cardenolide formation, it was inferred that 3-oxosteroids, such as progesterone, are intermediates of the cardenolide pathway. Interestingly, the occurrence of progesterone in plants has only been demonstrated unambiguously after isolation and thorough structure elucidation by NMR (Pauli et al. 2010). *Digitalis* (incl. *Isoplexis*) cardenolides can be of four different types, namely, xysmalogenin ($\Delta^{4,5}$-cardenolides), canarigenin ($\Delta^{3,4}$-cardenolides), uzarigenin (5α-cardenolides) or digitoxigenin (5α-cardenolides). The isomerisation of 5α-pregnanes to 5β-pregnanes has never been reported, and 5α-pregnanes were the only products formed from exogenous progesterone in cardenolide-free suspension cultures and white dark-grown shoot cultures (Hagimori et al. 1983; Stuhlemmer et al. 1993). The cardenolides used in therapy, such as digoxin and digitoxin, are all 5β-configured. 5β-Pregnane-3,20-dione was converted to 5β-pregnan-3β-ol-20-one and *vice versa* (Tschesche et al. 1970), indicating the occurrence of reversible redox reactions in the cardenolide pathway (Fig. 29.3). Both compounds were incorporated into digitoxigenin by *D. lanata* leaves (Tschesche et al. 1970; Deluca et al. 1987) and shown to stimulate cardenolide production in *D. lanata* shoot cultures (Stuhlemmer et al. 1993; Haussmann et al. 1997).On the other hand, feeding experiments with labelled C_{23} steroids revealed that 23-norcholanic acids can serve as cardenolide precursors. It has been shown that

the radioactivity of side-chain label appears in the butenolide ring, thus indicating the incorporation of the C_{23} steroid without degradation (Maier et al. 1986). When 21-[^{3}H]-2β,20ξ-dihydroxy-23-nor-5β-cholanic acid was administered together with 21-[^{14}C]-3β-hydroxy-5β-pregnane-20-one, the so-called norcholanic acid pathway was even the preferred route for cardenolide formation (Deluca et al. 1989).

The 14β-hydroxyl group is an important structural feature of all cardiac glycosides including the 5β-cardenolides. Neither 14α-hydroxysteroids (Caspi and Lewis 1968) nor 5β-pregn-8(14)-en-3,20-dione (Deluca et al. 1987; Aberhart et al. 1973) was incorporated into cardenolides, and it was thus concluded that a route via Δ^{8}(14) or Δ^{8}(9) pregnenes or an 8,14-epoxide as once postulated (Tschesche and Kleff 1973) does not seem not to be operative. 14β-Hydroxyprogesterone was incorporated into cardenolides, and it was concluded that 14β-hydroxylation must occur prior to the formation of the butenolide ring (Haussmann et al. 1997). It still remains unclear whether pregnane 14β-hydroxylation precedes 21-hydroxylation or *vice versa*. Steroid 12β-hydroxylation and 16β-hydroxylation can occur at the pregnane, the cardenolide genin and the glycoside level (Tschesche 1971; Furuya et al. 1970; Reinhard 1974).

29.3 Enzymes Involved in the Formation of the Cardenolide Aglycone

The putative pathway of cardenolide formation led to the investigation of the enzymes described here. The results achieved until the year 2000 are summarised and discussed in the *Digitalis* monograph compiled by Luckner and Wichtl (2000).

29.3.1 Cholesterol Side-Chain Cleaving Enzyme (SCCE)

Cholesterol is supposed to be a precursor of cardenolides during the formation of which the side chain of cholesterol has to be cleaved between C-20 and C-22. The reaction converting sterols into pregnenolone is thought to be catalysed by a mitochondrial cytochrome P450-dependent side-chain cleaving enzyme (P450scc) (Lindemann and Luckner 1997) although no evidence of such a P450 (CYP11A in animals) has been found in plants as yet (Ohnishi et al. 2009). The enzyme activity was determined by measuring either the decrease of cholesterol, the radioactivity of the C_{6} fragment formed from the cleavage of [26-^{14}C]-cholesterol or the quanti fication of the product pregnenolone released from cholesterol and other phytosterols by GC-MS (Lindemann and Luckner 1997). As the enzyme may be part of a protein complex in the mitochondria, more effort was directed to study the possible interaction partners, especially the peripheral-type benzodiazepine receptor (Papadopolous et al. 2006; Koch 2002) and the acyl-CoA-binding protein (ACBP) by Metzner et al. (2000). The ACBPs bind to the peripheral-type benzodiazepine receptor (PBR) present in the envelope of mitochondria (Garnier et al. 1994). This interaction stimulates the transport of cholesterol into mitochondria (Papadopolous and Brown 1995; Papadopolous et al. 1997). Because of its interaction with PBR, ACBP is also described as diazepam-binding inhibitor or endozepine. Some isoforms of the latter were isolated and characterised from *D. lanata* (Metzner et al. 2000).

29.3.2 NAD: 3β-Hydroxysteroid Dehydrogenase/Δ^{5}-Δ^{4}-Ketosteroid Isomerase (3β-HSD/KSI)

The conversion of pregnenolone into progesterone is composed of two steps: The first reaction is the NAD-dependent oxidation of the 3-hydroxy group yielding Δ^{5}-pregnen-3-one catalysed by the Δ^{5}-3β-hydroxysteroid dehydrogenase. The double bond then shifts from position 5 to position 4. The animal enzyme (EC 1.1.1.145/EC 5.3.3.1) involved in the conversion of progesterone to androgens catalyses two steps, namely, the oxidation of the steroid substrate (3β-HSD activity) and the subsequent isomerisation of the intermediate (KSI activity). The isomerase reaction is irreversible,

and the NADH produced during the 3β-HSD reaction is needed for the activation of the isomerase activity of the same enzyme protein.

29.3.2.1 NAD: 3β-Hydroxysteroid Dehydrogenase (3β-HSD)

A plant 3β-HSD was isolated from *D. lanata* cell suspension cultures as well as from shoot cultures and leaves of *D. lanata* plants (Seidel et al. 1990). NAD is the preferred proton acceptor. The 3β-HSD exhibited maximal activity at pH 8.0 and around 50°C. The apparent K_m values were 12.5 μM and 82 μM for pregnenolone and NAD, respectively. The enzyme was purified, and its molecular mass was 80–90 kDa as determined by size exclusion chromatography (Finsterbusch et al. 1999).

Attempts to isolate the plant *3β-HSD* gene have been reported by Lindemann et al. (2000). Deduced oligonucleotide primers from peptide fragments obtained from the digestion of the 3β-HSD isolated from *D. lanata* leaves (Finsterbusch et al. 1999) were used for the amplification of 3β-HSD gene fragments. Subsequently, Lindemann et al. (2000) amplified and sequenced a 700-nucleotide cDNA fragment for a putative 3β-HSD. Based on these reports, Herl et al. (2007) generated primers for PCR amplification of the *D. lanata 3β-HSD* gene. The full-length clone was generated using two synthetic oligonucleotide primers deduced from the published nucleotide sequence of the *3β-HSD* gene (GenBank Acc.-Nr. AJ345026). PCR amplification of the fragments was performed with DNA templates from several *Digitalis* species (Acc.-Nr. DQ466890, AY844960, AY789449-453, AY844959). All genes were found to be of similar size, and they did not differ much from each other or from their genomic fragments. The genomic sequences contained a 90 bp intron at the 3' end of the gene causing the differences in size.

The *Digitalis* 3β-HSDs show sequence similarities with microbial hydroxysteroid dehydrogenases and contain a conserved putative short-chain dehydrogenase (SDR) domain (Lindemann et al. 2000). The *Digitalis* 3β-HSD genes also share some similarities with putative alcohol dehydrogenase genes of *Arabidopsis thaliana*, *Lycopersicon esculentum*, *Oryza sativa*, *Nicotiana tabacu*m and *Solanum tuberosum* (BLAST alignment) and, even more exciting, (−)-isopiperitenol dehydrogenase from *Mentha x piperita* (Ringer et al. 2005) and secoisolariciresinol dehydrogenase from *Forsythia x intermedia* (Xia et al. 2001). No obvious similarities with the animal 3β-HSD/KSI were seen.

Molecular cloning and heterologous expression of the Δ^5-3β-hydroxysteroid dehydrogenase (3β-HSD) from *D. lanata* was achieved by Herl et al. (2007). The recombinant 3β-HSD (r*Dl*3β-HSD) had a pH optimum of 8.5, and its activity was highest at 55°C. These findings confirm the results of Seidel et al. (1990) and Finsterbusch et al. (1999), who investigated crude protein extracts and partially purified 3β-HSD from *D. lanata* cell cultures, respectively. The isoelectric point (pI) of r*Dl*3β-HSD was 6.5. In *Digitalis*, 3β-HSD is a soluble enzyme and shares this property with other members of the SDR family (Janknecht et al. 1991; Oppermann and Maser 1996). In the presence of NAD, r*Dl*3β-HSD converts pregnenolone to isoprogesterone. Progesterone was produced too, probably as a result of non-enzymatic isomerisation of isoprogesterone. Besides pregnenolone, several steroids with 3β-hydroxy group were tested. 5β-Pregnan-3β-ol-20-one, 5α-pregnan-3β-ol-20-one, 21-hydroxypregnenolone (C_{21}-steroids) and 5-androsten-3β-ol-17-one (a C_{17}-steroid) were all well accepted, whereas cholesterol was not. The quite long lipophilic side chain of the latter might have been responsible for this effect. Steroids with a 3α-hydroxy group were tested as well. Interestingly, 5β-pregnan-3α-ol-20-one was accepted, whereas 5α-pregnan-3α-ol-20-one was not. Testosterone (4-androsten-17β-ol-3-one), a C_{17}-steroid with a 3-carbonyl group and a 17β-hydroxy group, was converted to 4-androstene-3,17-dione. This indicates that r*Dl*3β-HSD possesses 3β- as well as 17β-dehydrogenase activity. Only recently, it was demonstrated that 23-nor-5,20(22)*E*-choladienic acid-3β-ol and other intermediates of the putative norcholanic acid pathway of cardenolide biosynthesis are used as substrates by recombinant 3β-hydroxysteroid

dehydrogenase, indicating that a "norcholanic acid pathway" for cardenolide formation (see above) may be operative in cardenolide-producing plants (Schebitz et al. 2010). A 3β/17βHSD with a broad substrate spectrum was also reported to occur in the bacterium *Comamonas testosteroni*, whereas other HSDs may display stricter substrate specificities (see Benach et al. 2002 for more details).

The r*Dl*3β-HSD was also able to catalyse the reduction of 3-ketosteroids when NADH was used as co-substrate. Pregnane-3,20-diones without Δ^4- or Δ^5-double bond like 5β-pregnane-3,20-dione and 5β-pregnane-3,20-dione were accepted. 4-Androstene-3,17-dione was also accepted as a substrate but not the 3-keto although the 17-keto function was reduced. Isomerisation of Δ^4- or Δ^5-double bond was not observed under these conditions. A clear preference for NAD (NADH for reduction) as co-substrate(s) was observed. NADP and NADPH, respectively, were also accepted but were less efficient. In many aspects, the r*Dl*3β-HSD behaves like the hydroxysteroid oxidoreductases supposed to be involved in cardenolide metabolism (Warneck and Seitz 1990; Seitz and Gärtner 1994). It was presumed (Finsterbusch et al. 1999; Herl et al. 2007) that 3β-HSD catalyses at least two steps in cardenolide biosynthesis, namely, the dehydrogenation of pregnenolone and the reduction of 5β-pregnane-3,20-dione (Fig. 29.2). The occurrence of 3β-HSD in species not accumulating cardenolides indicates that the enzyme may also be involved in other metabolic pathways (Seidel et al. 1990).

Dehydrogenase activity could clearly be separated from a ketosteroid isomerase (KSI, see below), indicating that r*Dl*3β-HSD is related to microbial 3β-HSDs of the short-chain dehydrogenase/reductase (SDR) family but not to mammalian 3β-HSDs which are multifunctional enzymes.

29.3.2.2 Δ^5-Δ^4-Ketosteroid Isomerase (3-KSI)

Δ^5-3-Ketosteroid isomerase catalyses the allylic isomerisation of the 5,6 double bond of Δ^5-3-ketosteroids to the 4,5 positions by stereospecific intramolecular transfer of a proton. The enzyme has been isolated from bacteria, and especially, the KSIs from *Comamonas testosteroni* and *Pseudomonas putida* biotype B have been investigated (Benisek et al. 1980). The structural gene coding for the KSI of *Pseudomonas putida* biotype B has been cloned and its nucleotide sequence determined. The molecular mass of this bacterial KSI is 14.5 kDa (Kim et al. 1994).

It was shown that KSI activity was present in crude protein extracts prepared from a *D. lanata* cell suspension culture and leaves. From the latter source, it was partially purified, and it was found that KSI did not co-purify with 3β-HSD. The molecular mass of the enzyme is about 15 kDa as determined by SDS-PAGE (Meitinger 2011). However, it is not yet finally clear whether KSI activity is also associated with the 3β-HSD although circumstantial evidence implies that this is not the case. The spontaneous isomerisation of 4-pregnene-3,20-dione represents a crucial problem, and this may explain why 5-pregnene-3,20-dione was also found when 5-pregnene-3β-ol,20-one was used as substrate for the *D. lanata* HSD (Finsterbusch et al. 1999) or recombinant HSD (Herl et al. 2006b). Since the occurrence of KSI has been demonstrated unambiguously, the isomerase step is now included in the cardenolide pathway as an individual biosynthetic step (Figs. 29.1 and 29.3).

29.3.3 NADPH: Progesterone 5β-Reductase (P5βR)

The progesterone 5β-reductase (P5βR, EC 1.3.1.23) catalyses the transformation of progesterone into 5β-pregnane-3,20-dione (Gärtner et al. 1990). Optimal enzyme activity was seen at 30°C and at pH 8.0. The P5βR requires NADPH as the co-substrate, which cannot be replaced by NADH. The enzyme was purified 770-fold to homogeneity from the cytosolic fraction of shoot cultures of *D. purpurea*. The molecular mass as determined by SDS-PAGE was 43 kDa. The purified enzyme had a K_m value of 6 μM for NADPH and 34 μM for progesterone. The relative conversion rates for other steroids such as testosterone, cortisone and cortisol were much lower.

29.3.3.1 Molecular Cloning and Expression

Progesterone 5β-reductase is sometimes referred to as a key enzyme in the biosynthesis of 5β-cardenolides. It catalyses the conversion of progesterone to 5β-pregnane-3,20-dione. The enzyme has been partially sequenced (Gärtner et al. 1994). The gene for 5β-POR of *Digitalis obscura* (*Dop5βr;* AJ555127) was first identified by Roca-Pérez et al. (2004). Herl et al. (2006) reported the cloning and heterologous functional expression of P5βR (*Dl*P5βR) from leaves of *D. lanata* Ehrh. and the biochemical characterisation of the recombinant enzymes.

P5βR cDNAs were isolated, cloned and sequenced from 21 species of *Digitalis* (Herl et al. 2008) and were shown to be highly conserved and also present in a cardenolide-free *Digitalis* species. PCR amplification with genomic DNA as the template revealed that the gene contained a small intron about 100 bp down the start codon. It seems as if the P5βR genes are highly conserved within the genus *Digitalis.* The deduced P5βR protein sequences were found similar to those of, e.g. *Oryza sativa* (about 58%) and *Populus tremuloides* (about 64%) and many other proteins annotated as P5βR (Bauer et al. 2010) but bear no structural homology to its mammalian counterpart, which is a member of the aldo-keto reductase (AKR) superfamily (Gavidia et al. 2007). No obvious similarities were found with the pulegone reductase of *Mentha x piperita*, described as a medium-chain dehydrogenase/reductase (Ringer et al. 2003), implying very different evolutionary origins in spite of the similarity of the reactions catalysed or even substrates used. Using progesterone as a substrate, pH and temperature dependencies of the purified enzyme were investigated. Recombinant P5βR activity was optimal at pH 7.8. The enzyme worked best at around 40°C. The pI of the r*Dl*P5βR was 6.5.

Besides the putative natural substrate progesterone, other steroid substrates were tested and the respective kinetic constants determined (Herl et al. 2006b, 2007, 2009). The r*Dl*P5βR did not only accept progesterone but also testosterone, 4-androstene-3,17-dione, cortisol and cortisone. Moreover, 23-nor-4,20(22)*E*-choladienic acid-3-one, which would be an intermediate in the so-called norcholanic acid pathway of cardenolide formation (see above), was also found to be a substrate of *rDlP5βR*. Steroids not bearing a carbonyl-activated C=C double bond, such as pregnenolone, 21-OH-pregenenolone and isoprogesterone, were not accepted by r*Dl*P5βR. Besides steroids, small progesterone mimics, e.g. 2-cyclohexen-1-one, isophorone and ethyl acrylate were also accepted as substrates by the recombinant *Dl*5βRs of *Digitalis* (Burda et al. 2009) and from other plant species (Bauer et al. 2010, Munkert et al. 2011). Some of these small enones were converted much faster than progesterone. NADPH is the only co-substrate and cannot be replaced by NADH. For r*Dl*P5βR, the K_m value for progesterone was 120 μM; for NADPH, it was 8 μM. The K_m values determined for the enzyme isolated from *D. purpurea* leaves (Gärtner et al. 1994) were very similar. P5βR was chosen as a new molecular marker (Herl et al. 2008) to infer phylogenetic relationship and compared to the previously applied nuclear *ITS* and plastid *trnL-F* sequences (Bräuchler et al. 2004). The results from separate analysis on the basis of almost identical plant material show high congruence within the genus *Digitalis* and support the conclusion that all species of *Isoplexis* have a common origin and are embedded now in the genus *Digitalis*.

29.3.3.2 Crystallisation and Structural Modelling of P5βR

Gavidia et al. (2007) predicted on the basis of *in silico* sequence alignments that the P5βR is a member of a novel subfamily of extended SDRs (Oppermann et al. 1997; Persson et al. 2009) or a new SDR family. Egerer-Sieber et al. (2006) reported on the purification and crystallisation of recombinant P5βR from *D. lanata*. Later on, (Thorn et al. 2007, 2008) fully characterised the crystal structure of P5βR and found that the progesterone reductase from *D. lanata* defines a novel class of short-chain dehydrogenases/reductases. The architecture of the active site was unprecedented since none of the standard catalytic residues are structurally conserved. The active sites and amino acid residues of the substrate-binding pocket of several P5βRs were modeled using the *D. lanata* P5βR (2V6G) structure

as template. As in the previously characterised P5βR-like proteins (Thorn et al. 2008; Herl et al. 2009), conserved Y179 and K147 residues were located in the active site. Another five conserved amino acids were found within the catalytic pocket. Some of them do not appear in any of the known sequence motifs but yet have a pronounced effect on the shape of the binding site (Bauer et al. 2010).

29.3.4 NADPH: Progesterone 5α-Reductase (P5αR)

Progesterone 5α-reductase, which catalyses the reduction of progesterone to 5α-pregnane-3,20-dione, probably in a competition situation to the progesterone 5β-reductase, was isolated and characterised from cell cultures of *D. lanata* (Wendroth and Seitz 1990). Optimal conditions for the progesterone 5α-reductase were at pH 7 and 40°C. At temperatures below 45°C, the product of the enzyme reaction, 5α-pregnane-3,20-dione, was enzymatically reduced to 5α-pregnan-3β-ol-20-one (see below). The enzyme requires NADPH as a co-substrate, which cannot be replaced by NADH. By means of linear sucrose gradient fractionation of the cellular membranes, progesterone 5α-reductase was found to be located in the endoplasmic reticulum. The apparent K_m values for NADPH and progesterone were 130 μM and 30 μM, respectively. Recently, it was found that the addition of finasteride, an inhibitor of animal and human testosterone-5α-reductase, at 180 μM inhibited P5αR activity of *D. lanata* completely but left P5βR activity of the same source unaffected (Grigat 2005).

29.3.5 NADPH: 3-Hydroxysteroid 5-Oxidoreductases

29.3.5.1 3β-Hydroxysteroid 5α-Oxidoreductase

This enzyme activity was first demonstrated in *D. lanata* cell suspension cultures by Warneck and Seitz (1990). The enzyme catalyses the conversion of 5α-pregnane-3,20-dione to 5α-pregnan-3β-ol-20-one. The enzyme worked best at pH 8.0 and 25°C. An increase in the temperature to 27°C already resulted in a marked reduction of 3β-hydroxysteroid oxidoreductase activity. Apparent K_m values for 5α-pregnane-3,20-dione and NADPH were 18.5–20 μM and 50–120 μM, respectively.

29.3.5.2 3β-Hydroxysteroid 5β-Oxidoreductase

This enzyme catalyses the conversion of 5β-pregnane-3,20-dione to 5β-pregnan-3β-ol-20-one (Gärtner and Seitz 1993). Optimal enzyme activity was found at pH 6.5 and at around 40°C. NADPH was the preferred co-substrate. The apparent K_m values for NADPH and 5β-pregnane-3,20-dione were 0.8 μM and 17.1 μM, respectively. When using 5β-pregnan-3β-ol-20-one and NADP as substrate and co-substrate, respectively, the reverse reaction was observed, yielding 5β-pregnane-3,20-dione. The K_m value for 5β-pregnan-3β-ol-20-one was 31.7 μM.

29.3.5.3 3α-Hydroxysteroid 5β-Oxidoreductase

This enzyme catalyses the conversion of 5β-pregnane-3,20-dione to 5β-pregnan-3α-ol-20-one. 3α-Cardenolides have never been described in the genus *Digitalis*, and the final products of a putative 3α-pregnane pathway are not yet known. Interestingly, protein extracts from light-grown *D. lanata* shoots were shown to reduce 5β-pregnane-3,20-dione almost exclusively to 3α-hydroxy-5β-pregnan-20-one when 0.05 M $MgCl_2$ was present in the incubation mixture (Stuhlemmer and Kreis 1996b). These conditions were inhibitory for the formation of 3β-hydroxy-5β-pregnan-20-one. The enzyme activity was found in microsomal preparations. Optimal enzyme activity was observed at pH 7.0 and 42°C. NADPH was the preferred co-substrate, but NADH was accepted as well. SH reagents were essential for enzyme activity. The enzyme seems to be specific for 5β-pregnane-3-ones, 5α-pregnane-3-ones or Δ^4/Δ^5-pregnenes were not accepted as substrates.

Finsterbusch et al. (1999) already discussed that some if not all of these reactions may also be catalysed by the 3β-HSD (see above) although

they were assigned to putative individual enzymes. This issue has to be examined further (e.g. Herl et al. 2007) before clear conclusions concerning the role of the mentioned enzymes in the cardenolide pathway can be drawn.

29.3.6 Pregnane 21-Hydroxylation and 14β-Hydroxylation

The enzymes involved in pregnane 21-hydroxylation and pregnane 14β-hydroxylation in the course of cardenolide formation have not been described yet. In animals, steroid 21-hydroxylation catalysed by a cytochrome P450 enzyme (CYP21) is an important reaction in cortisol biosynthesis (New 1995). The mycelium of the fungus *Curvularia lunata* displays steroid 14-hydroxylase activity, an observation which may lead to the isolation of the respective gene (Iaderets et al. 2007).

29.3.7 Malonyl-Coenzyme A: 21-Hydroxypregnane 21-O-Malonyltransferase (21MAT)

As far as the formation of the butenolide ring is concerned, it is supposed that the condensation of 5β-pregnane-3β,14β,21-triol-20-one with a dicarbon unit yields digitoxigenin. When 5β-pregnane-14β,21-diol-20-one 3-β-*O*-acetate was incubated together with malonyl-coenzyme A in a cell-free extract of *D. lanata* leaves, a product was formed, which was identified as the malonyl hemi-ester of the substrate (Stuhlemmer and Kreis 1996a). The compound decarboxylates easily and forms two products, namely, 5β-pregnane-14β-ol-20-one 3β-*O*-,21-*O*-diacetate and digitoxigenin 3-*O*-acetate. Hence, butenolide ring formation may be a non-enzymatic step in cardenolide biosynthesis. Malonyl-coenzyme A and acetoacetyl-coenzyme A were accepted as co-substrates. CoA inhibited the malonylation reaction. 5β-Pregnane-14β,21-diol-20-one 3β-*O*-acetate and 5β-pregnane-3β,14β,21-triol-20-one were the most suitable substrates for the transferase reaction. 21-Hydroxypregnenolone, 21-hydroxyprogesterone, 5β-pregnane-21-ol-3,20-dione and 5β-pregnane-3β,21-diol-20-one were only very poor substrates. The enzyme could so far only be detected in cardenolide-producing plants (Stuhlemmer and Kreis 1996a).

Kuate et al. (2008) reported the purification and characterisation of malonyl-coenzyme A: 21-hydroxypregnane 21-*O*-malonyltransferase (*Dp*21MaT) from leaves of *Digitalis purpurea* L. Optimised fresh plant material (leaves) has been used for the purification protocol including four column chromatography steps. Gel filtration and native SDS-PAGE analysis showed that Dp21MaT exists as a monomer with a molecular mass of 27 kDa. Its pI was 4.66 and the enzyme showed maximal activity at pH 6.5 when incubated at 42°C. Dp21MaT was purified 252-fold and the K_m values for 3β-benzoyloxy-5β-pregnane-14β,21-dihydroxy-20-one and malonyl-CoA were 99 μM and 28.4 μM, respectively.

29.3.8 Digitoxigenin 12β-Hydroxylase

This microsomal cytochrome P_{450}-dependent monooxygenase is capable of converting digitoxigenin-type cardenolides to their corresponding digoxin-type ones (Petersen and Seitz 1985). The enzyme was first isolated from cell suspension cultures of *D. lanata*, where the enzyme was found to be located in the endoplasmic reticulum. The pH optimum was at pH 7.5 and the temperature optimum at 20°C. Digitoxin, β-methyldigitoxin and α-acetyldigitoxin as well as digitoxigenin-type cardenolides with shorter or no sugar side chain were hydroxylated (Petersen et al. 1988). Gitoxigenin, *k*-strophanthin-β and cymarin, on the other hand, were not accepted as substrates. The K_m values for β-methyldigitoxin and digitoxin were 7.1 μM and 10 μM, respectively. NADPH is essential for the catalytic activity, with an optimum NADPH concentration of 1 mM. The apparent K_m value was 26 μM for NADPH.

29.4 Concluding Remarks

About 20 enzymes affecting the formation of cardenolides (Fig. 29.1) have been identified in the past years. Only few of the corresponding genes have been cloned and over-expressed in *Escherichia coli* for the production of decent amounts of the recombinant enzymes. So far, the x-ray structure of only one of the enzymes probably involved in cardenolide biosynthesis was elucidated. The resulting structural three-dimensional models opened new understanding of the mechanism of the enzyme reaction and the application of this enzyme in organic chemistry. The studies reviewed here and in other places (Kreis et al. 1998; Luckner and Wichtl 2000; Kreis and Müller-Uri 2010) allowed modifying the text book biosynthetic scheme (Fig. 29.2). The discovery of even more enzymes involved in cardenolide formation may help to clarify the pathway further, and detailed analyses of these enzymes are necessary for approaching the regulation and engineering of the metabolic grid/network of cardenolide formation (Fig. 29.3) and to understand the evolution of the cardenolide trait. The enzymes characterised in some detail all show a rather relaxed substrate specificity. Assuming that the enzymes described above are involved in cardenolide formation, we propose that an appropriate set of substrate-promiscuous enzymes may promote the (transient) realisation of different metabolic pathways. They may thus be regarded as pontoon elements that can be "utilised" for the "scouting" and "pioneering" of new pathways (Munkert et al. 2011). A specific pathway may establish itself promoted by the feedback of its end products, providing the producer with a selective advantage. Thus, promiscuous enzymes may contribute an important driving force in pathway evolution and diversity. SDRs, such as the P5βR and 3β-HSD described here, and the diverse pathways they are involved will serve as good examples to demonstrate the role of substrate promiscuity in pathway evolution.

Acknowledgements The authors thank Gabriele Fischer for her help preparing the manuscript.

References

Aberhart DJ, Lloyd-Jones JG, Caspi E (1973) Biosynthesis of cardenolides in *Digitalis lanata*. Phytochemistry 12:1065–1071

Bauer P, Munkert J, Brydziun M, Burda E, Müller-Uri F, Gröger H, Muller YA, Kreis W (2010) Highly conserved progesterone 5β-reductase genes (P5βR) from 5β-cardenolide-free and 5β-cardenolide-producing angiosperms. Phytochemistry 71:1495–1505

Benach J, Filling C, Oppermann UCT, Roversi P, Bricogne G, Berndt K, Jörnvall H, Ladenstein R (2002) Structure of bacterial 3β/17β-hydroxysteroid dehydrogenase at 1.2 Å resolution: a model for multiple steroid recognition. Biochemistry 41:14659–14668

Benisek WF, Ogez JR, Smith SB (1980) Recent studies on steroid isomerase from *Pseudomonas testosteroni* and *Pseudomonas putida*. Ann N Y Acad Sci 346:115–130

Bräuchler C, Meinberg H, Heubl G (2004) Molecular phylogeny of the genera *Digitalis* L. and *Isoplexis* (Lindley) Loudon (Veronicaceae) based on ITS- and *trnL-F* sequences. Plant Sys Evol 248:111–128

Burda E, Krausser M, Fischer G, Hummel W, Müller-Uri F, Kreis W, Gröger H (2009) Recombinant Δ4,5-steroid 5β-reductases as biocatalysts for the reduction of activated C=C double bonds in monocyclic and acrylic molecules. Adv Synth Catal 351:2787–2790

Caspi E, Lewis DO (1968) Biosynthesis of plant sterols – IV. An investigation of a possible mode of 14β-hydroxylation in digitoxigenin. Phytochemistry 7:683–691

Deluca ME, Seldes AM, Gros EG (1987) The 14β-hydroxylation in the biosynthesis of cardenolides in Digitalis purpurea The role of 3β-hydroxy-5β-pregn-8(14)-en-20-one. Z Naturforsch 42c:77–78

Deluca ME, Seldes AM, Gros EG (1989) Biosynthesis of digitoxin in *Digitalis purpurea*. Phytochemistry 28:109–111

Egerer-Sieber C, Herl V, Müller-Uri F, Kreis W, Muller YA (2006) Crystallization and preliminary crystallographic analysis of selenomethionine-labelled progesterone 5β-reductase from *Digitalis lanata* Ehrh. Acta Cryst F62:186–188

Finsterbusch A, Lindemann P, Grimm R, Eckerskorn C, Luckner M (1999) Δ5-3β-hydroxysteroid dehydrogenase from *Digitalis lanata* Ehrh. – a multifunctional enzyme in steroid metabolism? Planta 209:479–486

Furuya T, Hirotani M, Shinohara T (1970) Biotransformation of digitoxin by suspension callus culture of *Digitalis purpurea*. Chem Pharm Bull 18:1080–1081

Garnier M, Dimchev AB, Boujrad N, Price JM, Must NA, Papagopoulos V (1994) *In vitro* reconstitution of a functional peripheral-type benzodiazepine receptor from mouse Leydig tumor cells. Mol Pharmacol 45:201–211

Gärtner DE, Keilholz W, Seitz HU (1994) Purification, characterization and partial peptide microsequencing of progesterone 5β-reductase from shoot cultures of *Digitalis purpurea*. Eur J Biochem 225:1125–1132

Gärtner DE, Seitz HU (1993) Enzyme activities in cardenolide-accumulating, mixotrophic shoot cultures of *Digitalis purpurea* L. J Plant Physiol 141:269–275

Gärtner DE, Wendroth S, Seitz HU (1990) A stereospecific enzyme of the putative biosynthetic pathway of cardenolides. Characterization of a progesterone 5β-reductase from leaves of *Digitalis purpurea* L. FEBS Lett 271:239–242

Gavidia I, Tarrio R, Rodriguez-Trelles F, Perez-Bermudez P, Seitz HU (2007) Plant progesterone 5β-reductase is not homologous to the animal enzyme. Molecular evolutionary characterization of P5βR from *Digitalis purpurea*. Phytochemistry 68:853–864

Gregory H, Leete E (1969) Progesterone: its possible role in the biosynthesis of cardenolides in *Digitalis lanata.* Chemistry and Industry, London, UK, 30: 1242–1243

Grigat R (2005) Die Progesteron-5α-Reduktase. Dissertation, Universität Erlangen-Nürnberg

Gros EG, Leete E (1965) Biosynthesis of plant steroids. J Am Chem Soc 87:3479–3484

Grotewold E (2005) Plant metabolic diversity: a regulatory perspective. Trends Plant Sci 10:1–6

Hagimori M, Matsumoto T, Obi Y (1983) Effects of mineral salts, initial pH and precursors on digitoxin formation by shoot-forming cultures of *Digitalis purpurea* L. grown in liquid media. Agric Biol Chem 47:565–571

Hartmann T (2007) From waste products to ecochemicals: Fifty years research of plant secondary metabolism. Phytochemistry 68:2831–2846

Haussmann W, Kreis W, Stuhlemmer U, Reinhard E (1997) Effects of various pregnanes and two 23-nor-5-cholenic acids on cardenolide accumulation in cell and organ cultures of *Digitalis lanata*. Planta Med 63: 446–453

Helmbold H, Voelter W, Reinhard E (1978) Sterols in cell cultures of *Digitalis lanata*. Planta Med 33: 185–187

Herl V, Fischer G, Bötsch R, Müller-Uri F, Kreis W (2006a) Molecular cloning and expression of progesterone 5β-reductase (5β-POR) from *Isoplexis canariensis*. Planta Med 72:1163–1165

Herl V, Fischer G, Müller-Uri F, Kreis W (2006b) Molecular cloning and heterologous expression of progesterone 5β-reductase from *Digitalis lanata* Ehrh. Phytochemistry 67:225–231

Herl V, Frankenstein J, Meitinger N, Müller-Uri F, Kreis W (2007) Δ5-3β-Hydroxysteroid dehydrogenase (3βHSD) from *Digitalis lanata* Ehrh. Heterologous expression and characterisation of the recombinant enzyme. Planta Med 73:704–710

Herl V, Albach DC, Müller-Uri F, Bräuchler C, Heubl G, Kreis W (2008) Using progesterone 5β-reductase, a gene encoding a key enzyme in the cardenolide biosynthesis, to infer the phylogeny of the genus *Digitalis*. Plant Syst Evol 271:65–78

Herl V, Fischer G, Reva VA, Stiebritz M, Müller-Uri F, Muller Y, Kreis W (2009) The VEP1 gene (At4g24220) encodes a short-chain dehydrogenase/reductase with 3-oxo-Δ4,5-steroid 5β-reductase activity in *Arabidopsis thaliana* L. Biochimie 91:517–525

Iaderets VV, Andriushina VA, Bartoshevich IE, Domracheva AG, Novak MI et al (2007) A study of steroid hydroxylation activity of *Curvularia lunata* mycelium. Prikl Biokhim Mikrobiol 43:695–700

Janknecht R, de Martynoff G, Lou J, Hipskind RA, Nordheim A, Stunnenberg HG (1991) Rapid and efficient purification of native histidine-tagged protein expressed by recombinant vaccinia virus. Proc Natl Acad Sci USA 88:8972–8976

Kim SW, Kim CY, Benisek WF, Choi KY (1994) Cloning, nucleotide sequence, and overexpression of the gene coding for Δ^5-3-ketosteroid isomerase from *Pseudomonas putida* biotype B. J Bacteriol 21: 6673–6676

Koch A (2002) Identifizierung eines am Steroid- und Tetrapyrroltransport beteiligten Proteins in Pflanzen. Dissertation, Halle/Saale

Kreis W, Hensel A, Stuhlemmer U (1998) Cardenolide biosynthesis in foxglove. Planta Med 64:491–499

Kreis W, Müller-Uri F (2010) Biochemistry of sterols, cardiac glycosides, brassinosteroids, phytoecdysteroids, and steroid saponins. In: Wink M (ed) Biochemistry of Plant Secondary Metabolism, vol 40. CRC Press, Sheffiled, pp 304–363

Kuate SP, Padua RM, Poumale HMP, Kreis W (2007) Synthesis of a putative substrate for malonyl-coenzymeA:21-hydroxypregnane 21-*O*-malonyltransferase and development of an HPLC method for the quantification of the enzyme reaction. J Chromatogr B 860:195–201

Kuate SP, Padua RM, Eisenbeiss WF, Kreis W (2008) Purification and characterization of malonyl-coenzymeA:21-hydroxypregnane21-*O*-malonyltransferase (*Dp*21MaT) from leaves of *Digitalis purpurea* L. Phytochemistry 69:619–626

Lindemann P, Luckner M (1997) Biosynthesis of pregnane derivatives in somatic embryos of *Digitalis lanata*. Phytochemistry 46:507–513

Lindemann P, Finsterbusch A, Pangert A, Luckner M (2000) Partial cloning of a Δ^5-3β-hydroxysteroid dehydrogenase from *Digitalis lanata*. In: Okamoto M, Ishimura Y, Nawata H (eds) Molecular Steroidogenesis, proceedings Yamada Conference LII, vol 29 – XXIV, Frontiers Science Series. Universal Academy Press, Tokyo, pp 333–334

Luckner M, Wichtl M (2000) Digitalis. WV GmbH, Stuttgart

Maier MS, Seldes AM, Gros EG (1986) Biosynthesis of the butenolide ring of cardenolides in *Digitalis purpurea*. Phytochemistry 25:1327–1329

Meitinger N (2011) Reinigung und Charakterisierung der 3-Ketosteroidisomerase aus *Digitalis lanata*. Dissertation, Erlangen-Nürnberg

Metzner M, Ruecknagel KP, Knudsen J, Kuellertz G, Mueller-Uri F, Diettrich B (2000) Isolation and characterization of two acyl-CoA-binding proteins from proembryogenic masses of *Digitalis lanata* Ehrh. Planta 210:683–685

Milek F, Reinhard E, Kreis W (1997) Influence of precursors and inhibitors of the sterol pathway on sterol and cardenolide metabolism in *Digitalis lanata* Ehrh. Plant Physiol Biochem 35:111–121

Munkert J, Bauer P, Burda E, Müller-Uri F, Kreis W (2011) Progesterone 5β-reductase of *Erysimum crepidifolium*: cDNA-cloning, expression in *Escherichia coli*, and reduction of enones with the recombinant protein. Phytochemistry 72:1710–1717

New MI (1995) Steroid 21-hydroxylase deficiency (congenital adrenal hyperplasia). Am J Med 98:2S–8S

Ohnishi T, Yokota T, Mizutani M (2009) Insights into the function and evolution of P450s in plant steroid metabolism. Phytochemistry 70:1918–1929

Oppermann UCT, Filling C, Berndt KD et al (1997) Active site directed mutagenesis of 3β/17β-hydroxysteroid dehydrogenase establishes differential effects on short-chain dehydrogenase/reductase reactions. Biochemistry 36:34–40

Oppermann UCT, Maser E (1996) Characterization of a 3β-hydroxysteroid dehydrogenase/carbonyl reductase from the gram-negative bacterium *Comamonas testosteroni*. Eur J Biochem 241:744–749

Pádua RM, Waibel R, Kuate SP, Schebitz PK, Hahn S, Gmeiner P, Kreis W (2008) A simple chemical method for synthesizing malonyl hemiesters of 21-hydroxypregnanes, potential intermediates in cardenolide biosynthesis. Steroids 73:458–465

Papadopolous V, Amri H, Boujrad N, Cascio C, Culty M, Garnier M, Hardwick M, Li H, Vidic B, Brown AS, Reversa JL, Bernassau JM, Drieu K (1997) Peripheral-type benzodiazepine receptor in cholesterol transport and steroidogenesis. Steroids 62:21–28

Papadopolous V, Baraldi M, Guilarte TR, Knudsen TB, Lacapère JJ, Lindemann P, Norenberg MD, Nutt D, Weizman A, Zhang MR, Gavish M (2006) Translocator protein (18 kDa): new nomenclature for the peripheral-type benzodiazepine receptor based on its structure and molecular function. Trends Pharmacol Sci 27:402–409

Papadopolous V, Brown AS (1995) Role of the peripheral-type benzodiazepine receptor and the polypeptide diazepam binding inhibitor in steroidogenesis. J Steroid Biochem Mol Biol 53:103–110

Pauli GF, Friesen JB, Gödecke T, Farnsworth NR, Glodny B (2010) Occurrence of progesterone and related animal steroids in two higher plants. J Nat Prod 73:338–345

Persson B, Kallberg Y, Bray JE, Bruford E, Dellaporta SL, Favia AD, Duarte RG, Jörnvall H, Kavanagh KL, Kedishvili N, Kisiela M, Maser E, Mindnich R, Orchard S, Penning TM, Thornton JM, Adamski J, Oppermann U (2009) The SDR (short-chain dehydrogenase/reductase and related enzymes) nomenclature initiative. Chem Biol Interact 178:94–98

Petersen M, Seitz HU (1985) Cytochrome P-450-dependent digitoxin 12β-hydroxylase from cell cultures of *Digitalis lanata*. FEBS Lett 188:11–14

Petersen M, Seitz HU, Reinhard E (1988) Characterization and localization of digitoxin 12β-hydroxylase from cell cultures of *Digitalis lanata* Ehrh. Z Naturforsch 43c:199–206

Ramstad E, Beal JL (1960) Mevalonic acid as a precursor in the biogenesis of digitoxigenin. J Pharm Pharmacol 12:552–556

Reinhard E (1974) Biotransformation of plant tissue cultures. In: Street HD (ed) Tissue Culture and Plant Science. Academic, London, pp 443–459

Ringer KL, Davis EM, Croteau R (2005) Monoterpene metabolism. Cloning, expression, and characterization of (−)-isopiperitenol/(−)-carveol dehydrogenase of peppermint and spearmint. Plant Physiol 137: 863–872

Ringer KL, McConkey ME, Davis EM, Rushing GW, Croteau R (2003) Monoterpene double-bond reductases of the (-)-menthol biosynthetic pathway: isolation and characterization of cDNAs encoding (-)-isopiperitenone reductase and (+)-pulegone reductase of peppermint. Arch Biochem Biophys 418:80–92

Roca-Pérez L, Boluda R, Gavidia I, Pérez-Bermúdez P (2004) Seasonal cardenolide production and *Dop5* gene expression in natural populations of *Digitalis obscura*. Phytochemistry 65:1869–1878

Schebitz P, Nothdurft L, Hensel A, Müller-Uri F, Kreis W (2010) Norcolanic acids as substrates for recombinant 3β-hydroxysteroid dehydrogenase and progesterone 5β-reductase, enzymes of the 5β-cardenolide biosynthesis. Tetrahedron Lett 51:367–370

Seidel S, Kreis W, Reinhard E (1990) Δ5-3β-Hydroxysteroid dehydrogenase/Δ5-Δ4-ketosteroid isomerase (3β-HSD), a possible enzyme of cardiac glycoside biosynthesis, in cell cultures and plants of *Digitalis lanata* Ehrh. Plant Cell Rep 8:621–624

Seitz HU, Gärtner DE (1994) Enzymes in cardenolide-accumulating shoot cultures of *Digitalis purpurea* L. Plant Cell Tissue Organ Cult 38:337–344

Shi H-P, Lindemann P (2006) Expression of recombinant *Digitalislanata*Ehrh.Cardenolide16'-*O*-glucohydrolase in *Cucumis sativus* L. hairy roots. Plant Cell Rep 25:1193–1198

Stuhlemmer U, Kreis W (1996a) Does malonyl coenzyme A: hydroxypregnane 21-hydroxy malonyltransferase catalyze the first step in butenolide ring formation? Tetrahedron Lett 37:2221–2224

Stuhlemmer U, Kreis W (1996b) Cardenolide formation and activity of pregnane-modifying enzymes in cell suspension cultures, shoot cultures and leaves of *Digitalis lanata*. Plant Physiol Biochem 34:85–91

Stuhlemmer U, Kreis W, Eisenbeiss M, Reinhard E (1993) Cardiac glycosides in partly submerged shoots of *Digitalis lanata*. Planta Med 56:539–545

Thorn A, Egerer-Sieber C, Jäger CM, Herl V, Müller-Uri F, Kreis W, Muller Y (2007) The crystal structure of progesterone 5β-reductase from *Digitalis lanata* defines a novel class of short-chain dehydrogenases/reductases. J Biol Chem 283:17260–17269

Thorn A, Egerer-Sieber C, Jäger CM et al (2008) The crystal structure of progesterone 5β–reductase from *Digitalis lanata* defines a novel class of short chain dehydrogenases/reductases

Tschesche R (1970) Advances in the chemistry of antibiotics substances from higher plants: Pharmacognosy and phytochemistry. In: Proceeding of the 1st International Congress, Munich

Tschesche R (1971) Zur Biogenese der Cardenolid- und Bufadienolidglykoside. Planta Med Suppl 4: 34–39

Tschesche R, Hombach R, Scholten H, Peters M (1970) Neue Beiträge zur Biogenese der Cardenolide in *Digitalis lanata*. Phytochemistry 9:1505–1515

Tschesche R, Kleff U (1973) Beiträge zur biochemischen 14β-Hydroxylierung von C21-Steroiden zu Cardenoliden. Phytochemistry 12:2375–2380

Tschesche R, Lilienweiss G (1964) Cardenolid-Biosynthese aus Pregnenolonglucosid. Z Naturforsch 19b:265–266

Warneck HM, Seitz HU (1990) 3β-Hydroxysteroid oxidoreductase in suspension cultures of *Digitalis lanata* Ehrh. Z Naturforsch 45c:963–972

Wendroth S, Seitz HU (1990) Characterization and localization of progesterone 5α-reductase from cell cultures of foxglove (*Digitalis lanata* Ehrh.). Biochem J 266:41–46

Xia Z-Q, Costa MA, Pélissier HC, Davin LB, Lewis NG (2001) Secoisolariciresinol dehydrogenase purification, cloning, and functional expression. Implications for human health protection. J Biol Chem 276: 12614–12623

Biosynthesis of Isoprenoid Precursors in Arabidopsis

30

Manuel Rodríguez-Concepción, Narciso Campos, Albert Ferrer, and Albert Boronat

Abstract

Isoprenoids are the most functionally and structurally diverse group of plant metabolites reported to date. Many of them participate in essential processes, like respiration (ubiquinone), photosynthesis (carotenoids, chlorophylls, plastoquinone), and regulation of growth and development (cytokinins, brassinosteroids, gibberellins, abscisic acid). However, most plant isoprenoids are considered as secondary metabolites and play key roles in mediating the interactions of plants with their environment. Some plant isoprenoids also have biotechnological interest. Despite their structural and functional diversity, all isoprenoids derive from the same five-carbon precursors, isopentenyl diphosphate (IPP) and its isomer dimethylallyl diphosphate (DMAPP). Plants contain two pathways for the synthesis of IPP and DMAPP: the mevalonate pathway (located in the cytosol/endoplasmic reticulum) and the methylerythritol 4-phosphate pathway (located in the plastids). A limited exchange of IPP and/or prenyl diphosphates is known to take place between these compartments in plant cells. In recent years, the use of the model plant *Arabidopsis thaliana* in genetic and biochemical approaches has allowed the identification of all the genes and enzymes from both pathways and has accelerated the flow of information on their

M. Rodríguez-Concepción
Department of Molecular Genetics,
Centre for Research in Agricultural Genomics (CRAG),
CSIC-IRTA-UAB-UB, Campus UAB Bellaterra,
E-08193 Barcelona, Spain

N. Campos • A. Ferrer • A. Boronat (✉)
Department of Molecular Genetics,
Centre for Research in Agricultural Genomics (CRAG),
CSIC-IRTA-UAB-UB, Campus UAB Bellaterra,
E-08193 Barcelona, Spain

Department of Biochemistry and Molecular Biology,
Faculty of Biology, University of Barcelona,
08028 Barcelona, Spain
e-mail: aboronat@ub.edu

T.J. Bach and M. Rohmer (eds.), *Isoprenoid Synthesis in Plants and Microorganisms: New Concepts and Experimental Approaches*, DOI 10.1007/978-1-4614-4063-5_30,

regulation. A major challenge now is to understand how the production of common isoprenoid precursors in different subcellular locations conveys the information required to coordinate the fluxes of the two pathways. Here we review the current knowledge on these matters deduced mainly from work carried out in Arabidopsis.

Keywords
Arabidopsis • Dimethylallyl diphosphate • Isopentenyl diphosphate • Isoprenoid • Methylerythritol 4-phosphate • Mevalonate • Terpenoid

30.1 Introduction

Isoprenoids, also known as terpenoids, are the most functionally and structurally diverse group of plant metabolites reported to date. They are produced in all living organisms, but their abundance and variety in plants are unparalleled. From the tens of thousands of plant isoprenoid compounds, only a few can be considered as "primary" metabolites, i.e., those that are essential for plant function and are therefore common to all plant species. These include compounds that participate in respiration (ubiquinone), photosynthesis (carotenoids, chlorophylls, plastoquinone), and regulation of growth and development (cytokinins, brassinosteroids, gibberellins, abscisic acid). The rest are "secondary" metabolites, non-essential compounds whose biosynthesis is usually restricted to specific plant families or even to particular plant species. They typically function in protecting plants against herbivores and pathogens, in attracting pollinators and seed-dispersing animals, and as allelochemicals that influence competition among plant species (cf. Croteau et al. 2000; Bouvier et al. 2005). A large number of secondary isoprenoid metabolites have a commercial value as flavors, pigments, polymers, or drugs.

Despite the structural and functional diversity among isoprenoids, they all derive from the same five-carbon (C_5) precursors, isopentenyl diphosphate (IPP) and its isomer dimethylallyl diphosphate (DMAPP), also called isoprene units (Fig. 30.1). Addition of IPP units to DMAPP generates prenyl diphosphate molecules of increasing size such as geranyl diphosphate (GPP, C_{10}), farnesyl diphosphate (FPP, C_{15}), and geranylgeranyl diphosphate (GGPP, C_{20}). These are the starting points for the production of the huge variety of isoprenoids found in plants. Consistent with the compartmentalization of most plant metabolic pathways in plants (Lunn 2007), different steps of plant isoprenoid biosynthesis can take place in different plant tissues and subcellular compartments. Most notably, all plants use two different pathways for the production of the same universal isoprenoid precursors (Fig. 30.1). The mevalonic acid (MVA) pathway synthesizes cytosolic IPP for the production of sterols, brassinosteroids, sesquiterpenes, polyprenols, dolichols, and prenyl moieties used for protein modification. MVA-derived IPP is also transported to mitochondria for the biosynthesis of ubiquinone (Disch et al. 1998). Plastidial IPP and DMAPP precursors for the production of carotenoids, abscisic acid, gibberellins, monoterpenes, isoprene, and the side chain of chlorophylls, tocopherols, phylloquinones, and plastoquinone are synthesized by the methylerythritol 4-phosphate (MEP) pathway. A limited exchange of IPP and/or prenyl diphosphates is known to take place between these compartments in plant cells (Rodríguez-Concepción and Boronat 2002; Bouvier et al. 2005). In recent years, the use of the model plant *Arabidopsis thaliana* in genetic and biochemical approaches has allowed the identification of all the genes and

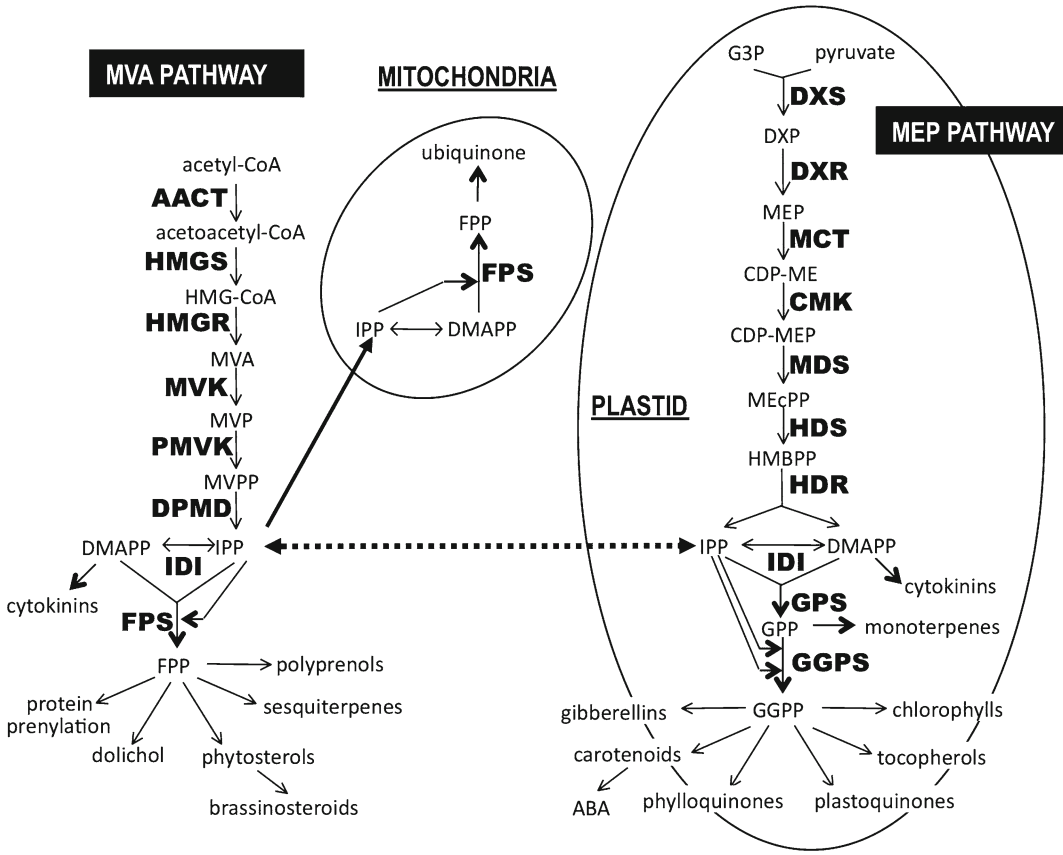

Fig. 30.1 *Organization and compartmentalization of isoprenoid biosynthesis in plants*. *HMG-CoA* 3-hydroxy-3-metylglutaryl coenzyme A, *MVA* mevalonate, *MVP* 5-phosphomevalonate, *MVPP* 5-diphosphomevalonate, *IPP* isopentenyl diphosphate, *DMAPP* dimethylallyl diphosphate, *FPP* farnesyl diphosphate, *G3P* D-glyceraldehyde 3-phosphate, *DXP* 1-deoxy-D-xylulose 5-phosphate, *MEP* 2-*C*-methyl-D-erythritol 4-phosphate, *CDP-ME* 4-(cytidine 5′-diphospho)-2-*C*-methyl-D-erythritol, *CDP-MEP* 4-(cytidine 5′-diphospho)-2-*C*-methyl-D-erythritol phosphate, *MEcPP* 2C-methyl-D-erythritol 2,4-cyclodiphosphate, *HMBPP* 4-hydroxy-3-methylbut-2-enyl diphosphate, *GPP* geranyl diphosphate, *GGPP* geranylgeranyl diphosphate. Enzymes are *AACT* acetoacetyl-CoA thiolase, *HMGS* HMG-CoA synthase, *HMGR* HMG-CoA reductase, *MVK* MVA kinase, *PMVK* MVP kinase, *DPMD* MVPP decarboxylase, *IDI* IPP isomerase, *DXS* DXP synthase, *DXR* DXP reductoisomerase, *MCT* CDP-ME synthase, *CMK* CDP-ME kinase, *MDS* MEcPP synthase, *HDS* HMBPP synthase, *HDR* HMBPP reductase

enzymes from both pathways and has accelerated the flow of information on their regulation. A major challenge now is to understand how the production of common isoprenoid precursors in different subcellular locations conveys information between compartments in order to coordinate fluxes through both pathways. Here we review the current knowledge on these matters deduced mainly from work carried out in *Arabidopsis*.

30.2 Historical Perspective

Until relatively recent times, it was believed that IPP was synthesized from acetyl-CoA via MVA and then isomerized to DMAPP in all living organisms (Chappell 1995; McGarvey and Croteau 1995). The MVA pathway, discovered in the 1950s, was soon found to function in plant cells (Goldstein and Brown 1990). However, inconsistent data suggesting the existence of a

MVA-independent pathway in bacteria and plant plastids grew stronger until the early 1990s, when compelling new evidence for the existence of a completely novel pathway for the production of IPP and DMAPP was shown (reviewed in Lichtenthaler et al. 1997; Eisenreich et al. 1998; Lichtenthaler 1999; Rohmer 1999, 2008). It was soon established that the new pathway, currently known as the MEP pathway after what it is believed to be its first committed precursor in bacteria (following the same rule used to name the MVA pathway), was the only one present in most eubacteria and apicomplexan protozoa such as the malaria parasite. Following the first biochemical approaches, genetics and genomics (database searches) demonstrated the existence of the pathway in several plants, including *Arabidopsis*. By 2002, all the genes encoding MEP pathway enzymes in *Arabidopsis* had been identified (cf. Rodríguez-Concepción and Boronat 2002). Genomic tools also led to identify all the *Arabidopsis* genes potentially encoding MVA pathway enzymes, as well as those putatively involved in other isoprenoid biosynthetic pathways (Lange and Ghassemian 2003).

30.3 The MVA Pathway in *Arabidopsis*

The MVA pathway (Fig. 30.1) starts with the sequential condensation of three molecules of acetyl-CoA to yield 3-hydroxy-3-methylglutaryl CoA (HMG-CoA) catalyzed by the enzymes acetoacetyl-CoA thiolase (AACT) and HMG-CoA synthase (HMGS). HMG-CoA is then converted to MVA in a functionally irreversible reaction catalyzed by HMG-CoA reductase (HMGR). MVA is sequentially phosphorylated and decarboxylated to generate IPP by the enzymes mevalonate kinase (MVK), 5-phosphomevalonate kinase (PMVK), and 5-diphosphomevalonate decarboxylase (DPMD). IPP along with DMAPP, formed by the action of isopentenyl diphosphate isomerase (IDI), represent the building blocks for the synthesis of isoprenoid end products and derivatives in the cytosol, endoplasmic reticulum (ER), and mitochondria. With the only exception of PMVK, the rest of the MVA pathway enzymes have been characterized at the biochemical and genetic level in *Arabidopsis*.

AACT catalyzes the reversible Claisen-type condensation of two acetyl-CoA molecules to form acetoacetyl-CoA. *Arabidopsis* contains two genes encoding AACT, *ACT1* (At5g47720) and *ACT2* (At5g48230). These genes encode two closely related AACT isoforms, designated as AACT1 and AACT2 respectively, located in different cell compartments (Ahumada et al. 2008). While AACT1 is found in peroxisomes, AACT2 is localized in the cytosol and the nucleus. The peroxisomal localization of AACT1 depends on the presence of a C-terminal peroxisomal targeting sequence 1 (PTS1) motif (Ser-Ala-Leu) not previously found in other organisms (Ahumada et al. 2008). However, targeting of AACT1 to peroxisomes has also been associated to an N-terminal extension (PTS2) present in a splicing variant of the protein (Carrie et al. 2007). *ACT1* and *ACT2* genes are differentially expressed. Whereas *ACT2* expression is relatively high in all parts of the plant, the expression of *ACT1* is much lower and restricted to roots and inflorescences (Ahumada et al. 2008). The expression of *ACT2* is induced by light during seedling development (Ahumada and Boronat, unpublished results).

Although the metabolic role(s) of AACT1 and AACT2 has not yet been unequivocally assigned, the characterization of *Arabidopsis* knockout mutants defective in the *ACT1* or *ACT2* genes suggests that only AACT2 is actually involved in isoprenoid biosynthesis. T-DNA insertion mutants affected in the expression of the *ACT2* gene are embryo-lethal, whereas null alleles of *ACT1* are viable and have no apparent growth phenotypes (Jin and Nikolau 2007). The metabolic function of AACT1 is not clear at present, although its particular peroxisomal localization might exclude a role in isoprenoid biosynthesis, and rather argues for its implication in β-oxidation of fatty acids, catalyzing the last step.

HMGS catalyzes the condensation of acetyl-CoA with acetoacetyl-CoA to produce HMG-CoA. A cDNA encoding HMGS was cloned by Montamat et al. (1995) and corresponds to the

only gene coding for this enzyme in *Arabidopsis* (*HMS*, At4g11820). Although HMGS behaves as a cytosolic enzyme, immunocytochemical analysis has shown that the enzyme is mainly found associated with the ER, the Golgi apparatus, and unknown globular structures (Díez and Boronat, unpublished results). *HMS* transcripts have been detected in all plant tissues, although they are particularly abundant in the hypocotyl and the root elongation zone of young seedlings and in the roots and the inflorescences of adult plants (Díez and Boronat, unpublished results). In contrast to other MVA pathway genes, the expression of *HMS* is not regulated by light (Díez and Boronat, unpublished results). A more detailed kinetic analysis has been done with HMGS1 from the closely related plant *Brassica juncea* (Indian mustard, Nagegowda et al. 2004). In this plant, four stress-inducible genes exist, encoding closely related isozymes (Alex et al. 2000), which are differentially expressed in the plant (Nagegowda et al. 2005).

HMGR has a well-recognized regulatory role in isoprenoid biosynthesis and is the best characterized enzyme of the MVA pathway. In *Arabidopsis*, the genes *HMG1* (At1g76490) and *HMG2 (*At2g17370) encode three HMGR isoforms (HMGR1S, HMGR1L, and HMGR2) (Caelles et al. 1989; Enjuto et al. 1994; Lumbreras et al. 1995). HMGR1S and HMGR1L isoforms only differ in their N-terminal region and derive from two mRNAs transcribed from two alternative promoters in the *HMG1* gene. The presence of an in-phase upstream AUG start codon in the HMGR1L mRNA results in the synthesis of the HMGR1L isoform that has 50 additional amino acid residues at its N-terminal end with respect to the HMGR1S isoform (Lumbreras et al. 1995). The three HMGR isoforms are primarily targeted to the ER and have the same topology in the membrane (Campos and Boronat 1995; Lumbreras et al. 1995). Like all known plant HMGRs, four regions have been defined in HMGR1S, HMGR1L, and HMGR2: the N-terminal region (highly divergent), two conserved membrane-spanning targeting sequences, the linker region (also highly divergent), and the catalytic domain, which is highly conserved among eukaryotic HMGRs. The N-terminal region and the catalytic domain are located in the cytosol, whereas only a short stretch of amino acids of the membrane-spanning domain are facing the ER lumen. In *Arabidopsis* epidermal cells, HMGR was immunolocalized in the ER, as expected, but also in spherical structures of the endomembrane system, 0.2–0.6 μm in diameter, that may represent a specific subcompartment for isoprenoid biosynthesis (Leivar et al. 2005). In a more recent study, using tobacco BY-2 cells expressing GFP proteins to which the membrane domains of two major HMGR isoforms were N-terminally fused suggested an association with the cytoskeleton of one form, which could be interconverted into the other one forming aggregates by just one amino acid exchange in a putative phosphorylation motif (Merret et al. 2007). The HMGR1S transcript is found in all tissues, but at fairly higher levels during the first stages of development and in the inflorescences (Enjuto et al. 1994). HMGR1L and HMGR2 transcripts are detected only in seedlings, roots, and inflorescences, and their abundance is much lower than that of the HMGR1S mRNA (Enjuto et al. 1995; Lumbreras et al. 1995). In transgenic tobacco plants harboring a *HMG2*: *GUS* quimeric gene, GUS expression was restricted to meristematic and floral tissues (Enjuto et al. 1995). Promoter analysis has revealed that sequence elements of the 5′ transcribed-untranslated region (5′-UTR) are important for expression in both *HMG1* and *HMG2* (Enjuto et al. 1995; Lumbreras et al. 1995). These observations suggest a housekeeping role for HMGR1S and a more specialised function for HMGR1L and HMGR2, which might be required in particular cell types or at specific developmental stages. In agreement with this, the analysis of an *Arabidopsis* null mutant affecting *HMG1* (*hmg1-1*) confirms the essential role of this gene on growth and development (Suzuki et al. 2004). Mutant *hmg1-1* plants show dwarfism, early senescence, and male sterility. In contrast, the disruption of *HMG2* does not affect the phenotype or the fertility of the plant under normal growth conditions (Ohyama et al. 2007). The *hmg1-1* mutant has a severe reduction in sterol and triterpenoid content, which was proposed to be related with

the observed phenotype (Suzuki et al. 2004). Consistently, the phenotype of the *hmg1-1* mutant was rescued by the exogenous application of MVA or squalene (Suzuki et al. 2004).

MVK catalyzes the phosphorylation of MVA to yield 5-phosphomevalonate. A cDNA encoding *Arabidopsis* MVK was cloned by functional complementation of a yeast mutant defective in this enzyme activity (Riou et al. 1994). *Arabidopsis* contains a single gene encoding MVK that is widely expressed throughout plant development, although the highest level of expression is detected in roots, predominantly in the meristematic region, and in floral organs. The *MVK* gene (At5g27450) expresses three major mRNA populations, which most likely encode the same protein, but have different 5′ ends. The 5′-UTR of the MVK transcripts includes several ATG codons located upstream of the MVK translation start codon, which suggests that MVK protein levels might be regulated at both transcriptional and translational levels (Lluch et al. 2000).

PMVK, the enzyme that phosphorylates 5-phosphomevalonate to produce 5-diphosphomevalonate, has not yet been characterized in plants. A putative gene encoding PMVK (At1g31910) has been annotated in the *Arabidopsis* genome by similarity to known eukaryotic PMVK gene sequences. Expression data available at the eFP Browser database indicate that the putative *PMK* gene is constitutively expressed.

The formation of IPP from 5-diphosphomevalonate, catalyzed by DPMD, represents the last step of the MVA pathway. A cDNA coding for DPMD was cloned in *Arabidopsis* by complementation of a yeast mutant strain defective in the DPMD enzyme (Cordier et al. 1999). *Arabidopsis* contains two annotated genes encoding DPMD, *MVD1*(At2g38700) *and MVD2* (At3g54250). *MVD1* encodes the DPMD isoform cloned by Cordier et al. (1999). The *MVD2* gene has not yet been characterized. Data available at the eFP Browser database show a similar and almost overlapping pattern of expression for the *MVD1* and *MVD2* genes, which are constitutively expressed.

A recent report has shown that both *Catharanthus roseus* and *Arabidopsis* PMVK and DPMD fused to YFP are targeted to peroxisomes in transfected *C. roseus* cells (Simkin et al. 2011). This, together with the previous finding that *Arabidopsis* IDI can also be targeted to peroxisomes in tobacco protoplasts (Sapir-Mir et al. 2008), has led to propose that the final steps of the MVA pathway are localized in peroxisomes.

30.4 The Plastidial MEP Pathway in *Arabidopsis*

The MEP pathway enzymes are encoded by nuclear genes and targeted to plastids. The initial reaction of the MEP pathway, catalyzed by deoxyxylulose 5-phosphate (DXP) synthase (DXS), involves the condensation of (hydroxyethyl)thiamine derived from pyruvate with the C1 aldehyde group of glyceraldehyde 3-phosphate (GAP) to produce DXP (Sprenger et al. 1997; Lange et al. 1998; Lois et al. 1998), a compound that may also serve as a precursor for the biosynthesis of vitamin B_1 (thiamine) (Julliard and Douce 1991). In the second step, an intramolecular rearrangement and reduction of DXP by the enzyme DXP reductoisomerase (DXR) yields MEP (Takahashi et al. 1998; Lange and Croteau 1999; Schwender et al. 1999). MEP is converted into methylerythritol 2,4-cyclodiphosphate (MEcPP) in three enzymatic steps (Fig. 30.1), catalyzed by 4-diphosphocytidyl-methylerythritol (CDP-ME) synthase (MCT), CDP-ME kinase (CMK), and MEcPP synthase (MDS) enzymes. A reduction of MEcPP catalyzed by hydroxymethylbutenyl diphosphate (HMBPP) synthase (HDS) produces HMBPP, which the enzyme HMBPP reductase (HDR) finally converts to a 5:1 mixture of IPP and DMAPP (reviewed in (Rodríguez-Concepción and Boronat 2002; Eisenreich et al. 2004; Bouvier et al. 2005). Rules for the nomenclature of the *Arabidopsis* MEP pathway genes, enzymes, and mutants have been recently proposed (Phillips et al. 2008).

DXS is encoded by more than one gene in several plants, particularly in those with an active secondary metabolism (Walter et al. 2002; Paetzold et al. 2010; Walter et al. this volume). It has been proposed that class 1 DXS would have a housekeeping function, whereas class 2 enzymes

might participate in the biosynthesis of secondary isoprenoids. No genes encoding class 2 DXS enzymes have been found in *Arabidopsis*, whose genome contains three open reading frames encoding sequences with homology to class 1 DXS isoforms (Rodríguez-Concepción and Boronat 2002). From these three putative isoforms, tentatively named DXS1 (At4g15560), DXS2 (At3g21500), and DXS3 (At5g11380), evidence of a role in the MEP pathway is only available for DXS1. Overexpression of DXS1 in transgenic plants leads to a higher production of MEP-derived isoprenoids (Estévez et al. 2001; Botella-Pavía et al. 2004; Carretero-Paulet et al. 2006; Muñoz-Bertomeu et al. 2006) and complements the pigmentation and developmental defects of DXS1-defective mutants (Crowell et al. 2000). Growth of *cla1* plants can also be rescued by adding deoxyxylulose (DX, the dephosphorylated product of DXS activity) to their growth medium (Estévez et al. 2003). Similarly, the decreased accumulation of plastidic isoprenoid pigments and the pale variegated phenotype of mutants such as *chs5* (*dxs-3*) and *lvr111* (*dxs-4*), which harbor point mutations in the gene encoding DXS1, was partially rescued with DX supplementation or DXS1 overexpression (Araki et al. 2000; Crowell et al. 2003). In contrast to the relatively high expression level of the *DXS1* gene, only a few ESTs from the *DXS2* and *DXS3* genes are available (Rodríguez-Concepción and Boronat 2002), suggesting that their expression is low and most likely restricted to particular tissues or developmental stages. The differential expression pattern could explain why the mutations in the *DXS1* gene are not rescued by the other two putative DXS isoforms. Alternatively, it is possible that DXS2 and DXS3 do not have DXS activity, as deduced from the fact that the predicted mature proteins lack amino acid residues that are conserved in all the bacterial and plant DXS (Rodríguez-Concepción and Boronat 2002; Phillips et al. 2008).

The rest of the *Arabidopsis* MEP pathway enzymes appear to be encoded by a single gene (Rodríguez-Concepción and Boronat 2002). Experimental data have confirmed that all the MEP pathway enzymes harbor N-terminal sequences that target them to plastids (Araki et al. 2000; Carretero-Paulet et al. 2002; Querol et al. 2002; Hsieh and Goodman 2005; Hsieh et al. 2008). A screening for *Arabidopsis* seedling-lethal mutants from T-DNA collections identified albino mutants being disrupted in the genes encoding DXS1 (At4g15560), DXR (At5g62790), and MCT (At2g02500). These lines have been renamed *dxs-2*, *dxr-1*, and *mct-3*, respectively (Phillips et al. 2008). The same phenotype displayed by these and the DXS-defective *cla1* (*dxs-1*) mutant (Mandel et al. 1996; Estévez et al. 2000) was found in loss-of-function mutants of the genes encoding CMK (At2g26930), MDS (At1g63970), HDS (At5g60600), and HDR (At4g34350) in *Arabidopsis* (Gutiérrez-Nava et al. 2004; Guevara-García et al. 2005; Hsieh and Goodman 2005; Hsieh and Goodman 2006; Hsieh et al. 2008). These mutants typically display chloroplasts with virtually no development of thylakoids and almost undetectable levels of photosynthetic pigments (chlorophylls and carotenoids). As expected, the accumulation of these and other plastidic isoprenoids is reduced in partial loss-of-function mutants and antisense lines with reduced activity levels of DXS, CMS, or HDS (Araki et al. 2000; Okada et al. 2002; Crowell et al. 2003; Flores-Pérez et al. 2008b). Most interestingly, some of these lines have unveiled connections between the MEP pathway and other metabolic pathways and cell processes. For instance, the *csb3* (*hds-3*) mutant, which harbors a point mutation in the gene encoding HDS (Gil et al. 2005) and causing a decreased production of isoprenoid pigments (Flores-Pérez et al. 2008b), was unexpectedly found in a search for mutants resistant to biotrophic pathogens, suggesting the involvement of the MEP pathway in defense responses. Also unexpectedly, the decreased DXS activity in the pale *lvr111* (*dxs-4*) mutant correlates with an enhanced resistance to the block of the MVA pathway with lovastatin (also known as mevinolin), a specific inhibitor of HMGR (Crowell et al. 2003), suggesting a crosstalk between the two pathways leading to the production of isoprenoid precursors.

30.5 Crosstalk Between Pathways and Exchange of Common Pathway Products

Mutant *Arabidopsis* seedlings with a block in the MEP pathway have been shown to still accumulate low levels of plastid isoprenoids such as chlorophylls and carotenoids, suggesting an import of cytosolic MVA-derived isoprenoid precursors to the plastids (Araki et al. 2000; Estévez et al. 2000; Nagata et al. 2002). Labeling experiments have demonstrated that a bidirectional exchange of common isoprenoid precursors between cell compartments takes place in *Arabidopsis*. For example, gibberellins are formed from precursors derived mostly from the MEP pathway, but also from the MVA pathway (Kasahara et al. 2002). The exchange rate, however, is not high enough to rescue the production of all types of isoprenoids when one of the two pathways is pharmacologically or genetically blocked in *Arabidopsis*. The extent of the exchange can be increased by feeding of intermediates of the MVA or the MEP pathways and by metabolic, environmental, or developmental cues (Kasahara et al. 2002; Nagata et al. 2002; Schuhr et al. 2003; Rodríguez-Concepción et al. 2004). Together, these results suggest a coordination of the activities of the MVA and MEP pathways to ensure the availability of precursors for the plethora of isoprenoid end products synthesized in plant cells. The nature of the mechanisms involved, however, has remained largely unknown.

Factors responsible for the inter-pathway crosstalk are now being identified using molecular, genetic, and genomic approaches. A recent analysis of transcriptional profiles of genes of the MVA and MEP pathways under various experimental conditions could not detect a close connection between these pathways, suggesting that the crosstalk at the transcriptional level may be restricted to single genes in both pathways (Wille et al. 2004). In particular, the gene encoding HMGR1, the most widely distributed HMGR isoform in *Arabidopsis* (Enjuto et al. 1994), appeared as a good candidate for inter-pathway crosstalk since it had few connections to the MVA pathway and was found to be negatively correlated to the module of fully connected genes in the MEP pathway (those encoding DXR, MCT, CMK, MDS, and HDS), suggesting a mutually exclusive pattern of expression.

A second module of MEP pathway genes was formed by *DXS1* and *HDR*, which were only connected to each other.

A complementary approach to investigate the crosstalk between the MVA and MEP pathways is the isolation and characterization of mutants resistant to a block of these pathways. The specific block of the MVA pathway with mevinolin (MEV, an inhibitor of HMGR) or the MEP pathway with fosmidomycin (FSM) in *Arabidopsis* results in a developmental block at the seedling stage (Rodríguez-Concepción et al. 2004). A strategy based on the isolation of *Arabidopsis* mutants capable of overcoming the inhibition of the MVA pathway with MEV which could also survive in the presence of FSM resulted in the identification of *rim1*, which was shown to be defective in phytochrome B, the major light stable photoreceptor of red light in *Arabidopsis* seedlings. The MEV-resistant phenotype of *rim1* seedlings was shown to be caused by increased levels of HMGR enzyme activity due to an activation of gene expression, whereas the FSM-resistant phenotype of mutant seedlings was proposed to derive from an enhanced intake of MVA-derived isoprenoid precursors by the plastid (Rodríguez-Concepción et al. 2004). The analysis of FSM resistance of mutants being impaired in light perception and signal transduction indicated that the light-triggered signaling pathway eventually leading to downregulation of the cytosol-to-plastid transport of prenyl diphosphates is initiated by phytochromes, but did not require the participation of other factors required for HMGR upregulation and MEV resistance, thereby revealing the existence of distinct light perception and signaling pathways for the control of the MVA pathway and the exchange of common products of the MVA and MEP pathways. The identification and characterization of other mutants resistant to a block in the MVA or the

MEP pathways should provide further insights into the molecular networks coordinating inter-pathway crosstalk in plants.

30.6 Regulation of the Metabolic Flux Through the MVA Pathway

Several lines of evidence sustain that HMGR has a key role in the regulation of the MVA pathway. The first indications in this direction came from studies on the distribution of HMGR activity in pea and radish seedlings (Brooker and Russell 1975; Grumbach and Bach 1979; Bach et al. 1980; Bach and Lichtenthaler 1984) and HMGR transcripts in wheat and *Arabidopsis* (Aoyagi et al. 1993; Enjuto et al. 1994; Enjuto et al. 1995; Lumbreras et al. 1995). Both the enzymatic activity and transcript levels are high in rapidly growing parts of the plant, such as apical buds and roots, where very active sterol biosynthesis occurs, and low in more mature structures. In agreement, the levels of HMGR activity tightly correlate with the rate of sterol production in developing seeds of rape and tobacco (Harker et al. 2003a). HMGR activity and transcript levels are also high in actively dividing *Arabidopsis*, tomato and tobacco culture cells (Lumbreras et al. 1995; Jelesko et al. 1999; Hemmerlin and Bach 2000; Hemmerlin et al. 2004). On the other hand, it was found that the challenge of some solanaceous species with pathogens or elicitor treatment induces sharp increases in HMGR activity and transcript levels, that precede the accumulation of sesquiterpenoid phytoalexins (Suzuki et al. 1975; Ôba et al. 1985; Chappell and Nable 1987; Yang et al. 1991). Thus, the regulatory role of HMGR in the MVA pathway seems to be important not only for normal plant growth and development but also for the adaptation to challenging environmental conditions.

More conclusive evidence in favor of the limiting role of plant HMGR in the biosynthesis of MVA-derived isoprenoid products has been obtained by expression of different variants of this enzyme in homologous and heterologous systems. The level of total phytosterols was increased about eightfold in leaves of tobacco plants by constitutive expression of either the *Hevea HMG1* gene (Schaller et al. 1995) or the catalytic domain of hamster HMGR (Chappell et al. 1995). The overexpression of the *Arabidopsis* HMGR isoforms in transgenic *Arabidopsis* plants also led to higher accumulation of leaf phytosterols (González 2002; Manzano et al. 2004; Leivar et al. 2005). The increase was moderate with ectopic expression of HMGR1L and HMGR2 (1.3- and 1.5-fold, respectively) and more prominent with HMGR1S (2.5-fold). However, the highest success in the homologous *Arabidopsis* system was achieved by expression of the catalytic domain of either HMGR1 (11.5-fold phytosterol increase) or HMGR2 (fivefold). Higher phytosterol accumulation in tobacco leaves and seeds was also obtained when the catalytic domain of Hevea HMGR1 was expressed instead of the complete protein (Harker et al. 2003b). In all the above-mentioned systems, the HMGR activity correlates positively with the phytosterol production level. Therefore, the cumulative data indicate that plant HMGR activity is downregulated by its membrane domain. The elimination of this domain allows deregulation of HMGR and more active phytosterol biosynthesis. However, regulation of downstream enzymes in the phytosterol pathway still limits the production of end-of-chain phytosterols, and the excessively accumulated intermediates are largely esterified with fatty acids and accumulate as lipid droplets in the cytosol of HMGR overexpressing plant cells (Schaller et al. 1995).

Additional proof of the limiting role of HMGR in plant isoprenoid biosynthesis was obtained by the overexpression of cytosolic or mitochondrial FPP synthase in *Arabidopsis* plants (Masferrer et al. 2002; Manzano et al. 2004; Manzano et al. 2006). High levels of FPP synthase activity without a concomitant increase of MVA production led to a reduction of isoprenoid precursors for cytokinin biosynthesis, the formation of necrotic lesion, and premature senescence. A strict control of the level of isoprenoid intermediates is thus required to avoid deleterious effects on plant growth and development (Manzano et al. 2004). All these observations underline the

importance of plant HMGR in the control of the metabolic flux to cytosolic and mitochondrial isoprenoid products. In sharp contrast, no evidence has been provided to date in support of such a regulatory role for other enzymes of the MVA pathway.

In agreement with its fundamental role in the control of the MVA pathway, plant HMGR is modulated by a variety of developmental and environmental signals such as phytohormones, calcium, calmodulin, light, wounding, elicitor treatment, and pathogen attack (cf. Stermer et al. 1994). The response to these factors involves a complex regulatory network that operates at both transcriptional and post-translational level. It has been proposed that the major changes in HMGR activity would be determined at the transcriptional level, whereas the posttranscriptional control would allow a finer and faster adjustment (Chappell 1995). In *Arabidopsis*, development and light have major effects on HMGR transcript and activity levels. The expression of the *Arabidopsis HMG1* gene is triggered by germination, and the *HMG1* mRNA levels increase rapidly as the seedling develops (Learned and Connolly 1997). In rosette leaves, HMGR activity declines with age (Manzano et al. 2004), but *HMG1* and *HMG2* expression is induced in the inflorescences (Enjuto et al. 1994; Enjuto et al. 1995; Lumbreras et al. 1995). This alternating profile of HMGR levels, encompassing seedling, leaf, and inflorescence development, is not exclusive of *Arabidopsis*, but occurs in other plant systems as well (Brooker and Russell 1975; Aoyagi et al. 1993; Moore and Oishi 1993; Korth et al. 1997; Jain et al. 2000; Korth et al. 2000). Light is a negative regulator of *Arabidopsis HMG1* gene expression (Learned 1996). This control is exerted at the transcriptional level and depends on the fluence rate, time of illumination, and spectral quality. In agreement, genetic evidence was provided showing that phytochrome and cryptochrome are required for downregulation of *Arabidopsis HMG1* and *HMG2* transcript levels (Rodríguez-Concepción et al. 2004). The *HMG1* promoter was activated by light deprivation in immature *Arabidopsis* leaves, but not in roots, indicating differential responsiveness in different organs (Learned and Connolly 1997). Direct control by light and the light-dependent developmental program likely contribute to the higher HMGR activity and transcript levels observed in etiolated seedlings versus light-exposed seedlings of several plant species (Brooker and Russell 1975; Bach 1986; Ji et al. 1992; Enjuto et al. 1994).

Evidences showing posttranscriptional regulation of plant HMGR are still scarce. Pioneering work in pea indicated that phytochrome can repress HMGR activity at the posttranslational level (Brooker and Russell 1979; Wong et al. 1982). Downregulation of potato HMGR occurring along development and in response to light is most likely mediated by protein degradation (Korth et al. 2000). It has been shown that the increase or reduction of the flux through the sterol pathway in tobacco cell culture and *Arabidopsis* seedlings causes compensatory response in HMGR activity, which is regulated at the posttranslational level (Wentzinger et al. 2002; Nieto et al. 2009). The block of sphingolipid biosynthesis in *Arabidopsis* also led to post-translational repression of HMGR activity and concomitant reduction in the sterol content, indicating a regulatory crosstalk between the two lipid biosynthetic pathways (Nieto et al. 2009). In microsomal preparations from pea seedlings, addition of increasing nanomolar concentrations of calcium caused a proportional reversible decrease of HMGR activity (Russell et al. 1985). This effect was not mediated by direct action of Ca^{2+} on HMGR, Ca^{2+}-induced proteolysis or interaction with calmodulin. Reversible inhibition of HMGR activity by calcium was also observed in *Arabidopsis* extracts (Antolín and Campos, unpublished results), thus indicating that a still unknown mechanism for calcium-dependent regulation of enzyme activity might be conserved in plants. It has been shown that *Arabidopsis* HMGR1 can be phosphorylated at a conserved serine residue (Ser577 in the HMGR1S sequence) by SnF1-related kinase (SnRK1) of cauliflower and spinach cell-free extracts (Dale et al. 1995; Sugden et al. 1999). This modification completely inactivates the HMGR enzyme and could, therefore, determine the flux through the MVA pathway. In fact, phytosterol levels in

transgenic tobacco seeds are higher when a variant of *Arabidopsis* HMGR1S without the phosphorylation site is used instead of the unmodified enzyme (Hey et al. 2006). However, the gain in phytosterol content (19 % increase, with respect to the non-transformed control, and 10 % increase, with respect to tobacco expressing the original HMGR1S) was moderate in comparison with that obtained after constitutive expression of single copy HMGR catalytic domain (170 % increase) (Harker et al. 2003b). Thus, further work is required to reinforce the view that phosphorylation of plant HMGR catalytic domain has a major role in the posttranslational control of the MVA pathway.

Protein phosphatase 2A (PP2A) was recently identified as a multilevel regulator of HMGR in *Arabidopsis* (Leivar et al. 2011). Both HMGR1L and HMGR1S interact with PP2A through B″ regulatory subunits of PP2A, which are also Ca^{2+}-binding proteins (Leivar et al. 2011). Whereas the *Arabidopsis* B″β variant is involved in the posttranscriptional repression of HMGR in unchallenged seedlings, B″α modulates HMGR transcript, protein, and activity levels in response to salt challenge (Leivar et al. 2011). When *Arabidopsis* seedlings were transferred to salt-containing medium, B″α and PP2A mediated the decrease and subsequent increase of HMGR activity, which resulted from a steady rise of *HMG1* transcripts levels and an initial sharper reduction of HMGR protein level (Leivar et al. 2011). A similar biphasic profile of HMGR activity was previously observed when bright yellow-2 tobacco cells were subjected to a block with mevinolin (Hemmerlin et al. 2003) or when potato tubers were subjected to wounding (Yang et al. 1991), suggesting that these responses might be also mediated by PP2A through B″ regulatory subunits. Since PP2A is involved in auxin, abscisic acid, ethylene, and brassinosteroid signaling and the B″-PP2A subunit is a Ca^{2+}-binding protein, these observations uncover the potential of PP2A to integrate developmental and Ca^{2+}-mediated environmental signals in the control of plant HMGR (Antolín-Llovera et al. 2011).

30.7 Regulation of the Metabolic Flux Through the MEP Pathway

The first two and the last two enzymes of the MEP pathway (DXS, DXR, HDS, and HDR) were first proposed as potential control points of the metabolic flux to plastidial isoprenoids. Pioneer studies in tomato supported such a role for DXS and HDR, but not for DXR or HDS, mainly based on the correlation between the accumulation of transcripts and proteins from these genes and the production of MEP-derived products (carotenoids) during fruit ripening (Lois et al. 2000; Rodríguez-Concepción et al. 2001; Rodríguez-Concepción et al. 2003; Botella-Pavía et al. 2004). During light-induced de-etiolation of *Arabidopsis* seedlings, high IPP and DMAPP levels are also required to support an increased production of plastid isoprenoids such as carotenoids and chlorophylls. But the analysis of transcript accumulation in de-etiolating *Arabidopsis* seedlings has shown that all the genes encoding MEP pathway enzymes are upregulated after the light treatment (Mandel et al. 1996; Botella-Pavía et al. 2004; Rodríguez-Concepción 2006; Hsieh et al. 2008; Cordoba et al. 2009). More compelling evidence for the role of DXS, DXR, HDS, and HDR in controlling plastidial IPP and DMAPP production came from the analysis of transgenic *Arabidopsis* plants in which their levels had been altered (Estévez et al. 2001; Botella-Pavía et al. 2004; Carretero-Paulet et al. 2006; Flores-Pérez et al. 2008b). Transgene-mediated upregulation and/or downregulation of DXS, DXR, or HDR levels in *Arabidopsis* correlated with concomitant changes in the levels of MEP-derived isoprenoid end products such as chlorophylls and carotenoids (Estévez et al. 2001; Botella-Pavía et al. 2004; Carretero-Paulet et al. 2006). Similarly, transgenic tomato fruit overexpressing a bacterial DXS enzyme showed a significant increase in the production of carotenoids (Enfissi et al. 2005), whereas peppermint plants overexpressing DXR also accumulated enhanced levels of MEP-derived monoterpenes (Mahmoud and Croteau 2001).

By contrast, no effect on the accumulation of MEP-derived isoprenoids was observed in transgenic lines overexpressing HDS (Flores-Pérez et al. 2008b). These results demonstrate that not all the MEP pathway enzymes cause a significant change in the pathway flux when their concentration is altered, supporting the metabolic control analysis (MCA) conclusion that several enzymes can share control over the flux of the pathway, with different enzymes exhibiting different degrees of control (Thomas and Fell 1998; Libourel and Shachar-Hill 2008). Based on the overexpression studies described above, the control of flux through the MEP pathway should be shared by the rate-determining enzymes DXS, DXR and HDR, whereas the contribution of HDS to overall flux appears to be comparatively much lower. Nothing is known yet about the relative contribution of the rest of MEP pathway enzymes (MCT, CMK, and MDS) to flux control. A thorough examination of the relevant MCA parameters, including a detailed study of the effect of the overexpression of each enzyme of the MEP pathway on the activity of the rest, is now needed to identify what enzymes besides DXS, DXR, and HDR are "rate-determining" (a MCA term used when changes in the concentration of an enzyme cause a change in the pathway flux) and to assign which steps have greater influence in regulating flux to IPP and DMAPP. This analysis is particularly important for the rational design of metabolic engineering approaches aimed to overproduce MEP-derived isoprenoids in plant systems.

Changes in gene expression appear to act as a coarse control to regulate the MEP pathway enzyme levels, but they do not always lead to similar changes in protein levels and, most importantly, enzyme activities and metabolite production (Rodríguez-Concepción 2006). For instance, the partial block of the MVA and MEP pathways in *Arabidopsis* seedlings grown in the presence of sublethal concentrations of specific inhibitors causes a reduction in derived isoprenoid levels without changes in gene expression (Laule et al. 2003). The levels of DXS protein, but not transcripts, are upregulated in FSM-treated *Arabidopsis* seedlings, and a posttranscriptional increase of DXS and HDR protein levels has been recently shown to occur specifically in *Arabidopsis* null mutants of the MEP pathway (Guevara-García et al. 2005). Posttranscriptional events also appear to modulate the accumulation of MEP pathway proteins during seedling development, resulting in discrete changes on protein levels despite strong upregulation of gene expression (Guevara-García et al. 2005). These and other results have led to suggest that the accumulation of at least some MEP pathway enzymes (including flux-controlling DXS and HDR) in *Arabidopsis* might be regulated by changes in the metabolic flux through the pathway. Further experiments are, however, required to ascertain the importance of this type of potential regulation.

The identification of *Arabidopsis* mutants that are resistant to FSM (*rif* mutants) has recently unveiled a mechanism for the posttranscriptional accumulation of active MEP pathway enzymes in plastids (Sauret-Güeto et al. 2006; Flores-Pérez et al. 2008a). The characterization of the *rif1* and *rif10* mutants showed that their FSM resistance phenotype was the result of upregulated DXS and DXR levels without major changes in the expression of the corresponding (nuclear) genes. Both RIF1 (Flores-Pérez et al. 2008a) and RIF10 (Sauret-Güeto et al. 2006) proteins are required for the proper expression of the plastid genome (plastome), and their loss of function in *rif1* and *rif10* lines cause a reduction in the production of plastome-encoded proteins linked to the posttranscriptional accumulation of DXS, DXR, HDS, and HDR in mutant plastids. Mutant seedlings were shown to have altered levels of the plastome-encoded ClpP1 protein, one the catalytic subunits of the stromal Clp protease complex (Peltier et al. 2004), likely resulting in a decreased proteolytic activity of the entire complex as a consequence of impaired subunit stoichiometry (Sjögren et al. 2006). Consistent with a role of this protease in the regulation of MEP pathway enzyme levels, mutants with a decreased Clp protease activity also showed an increased accumulation of active DXS and DXR enzymes, leading to FSM resistance (Flores-Pérez et al. 2008a). The presence of similar Clp protease core

complexes in all plastid types, their abundance, and the essential character of the catalytic subunits suggests that it plays a central role in plastid homeostasis and biogenesis, similar to that of the ubiquitin-proteasome system for plant development (Sjögren et al. 2006). However, little is currently known concerning the specific function of this stromal protease or its protein substrates in higher plants. Although the participation of the Clp protease in the degradation of at least some of the MEP pathway enzymes within plastids is clear (Flores-Pérez et al. 2008a), current evidence does not allow to conclude whether these proteins, which are also localized in the stroma (Carretero-Paulet et al. 2002; Oudin et al. 2007), are direct targets (actual substrates) of this protease. Thus, it is possible that downregulation of Clp activity in plastids results in changes that are ultimately responsible for the observed accumulation of DXS, DXR and/or the other proposed substrates of this proteolytic complex. In summary, the metabolic flux through the MEP pathway appears to be controlled by several enzymes (with a major contribution of DXS and HDR) regulated at transcriptional and posttranscriptional levels in response to metabolic (feedback regulation), environmental (light), and developmental cues.

Acknowledgments Work from our groups was supported by grants from the Spanish Ministerio de Ciencia e Innovación (MICINN) (BIO2011-23680 to MRC, BFU2006-14655 to NC, BIO2009-06984 to AF, and BIO2009-09523 to AB, all including FEDER funds) and the Generalitat de Catalunya (GC) (grant 2009SGR-26) and carried out within the Centre CONSOLIDER on Agrigenomics (CSD2007-00036) funded by MICINN and Xarxa de Referencia en Biotecnologia funded by GC.

References

Ahumada I, Cairó A, Hemmerlin A, González V, Pateraki I, Bach TJ, Rodríguez-Concepción M, Campos N, Boronat A (2008) Characterization of the gene family encoding acetoacetyl-CoA thiolase in Arabidopsis. Funct Plant Biol 35:1100–1111

Alex D, Bach TJ, Chye ML (2000) Expression of *Brassica juncea* 3-hydroxy-3-methylglutaryl CoA synthase is developmentally regulated and stress-responsive. Plant J 22:415–426

Antolín-Llovera M, Leivar P, Arró M, Ferrer A, Boronat A, Campos N (2011) Modulation of plant HMG-CoA reductase by protein phosphatase 2A. Positive and negative control at a key node of metabolism. Plant Signal Behav 6:1127–1131

Aoyagi K, Beyou A, Moon K, Fang L, Ulrich T (1993) Isolation and characterization of cDNAs encoding wheat 3-hydroxy-3-methylglutaryl coenzyme-A reductase. Plant Physiol 102:623–628

Araki N, Kusumi K, Masamoto K, Niwa Y, Iba K (2000) Temperature-sensitive *Arabidopsis* mutant defective in 1-deoxy-D-xylulose 5-phosphate synthase within the plastid non-mevalonate pathway of isoprenoid biosynthesis. Physiol Plant 108:9–24

Bach TJ (1986) Hydroxymethylglutaryl-CoA reductase, a key enzyme in phytosterol synthesis? Lipids 21:82–88

Bach TJ, Lichtenthaler HK (1984) Application of modified Lineweaver-Burk plots to studies of kinetics and regulation of radish 3-hydroxy-3-methylglutaryl-CoA reductase. Biochim Biophys Acta 794:152–161

Bach TJ, Lichtenthaler HK, Rétey J (1980) Properties of membrane-bound 3-hydroxy-3-methylglutaryl coenzyme A reductase (EC. 1.1.1.34) from radish seedlings and some aspects of its regulation. In: Mazliak P, Benveniste P, Costes C, Douce R (eds) Biogenesis and function of plant lipids. Elsevier, Amsterdam, pp 355–362

Botella-Pavía P, Besumbes O, Phillips MA, Carretero-Paulet L, Boronat A, Rodríguez-Concepción M (2004) Regulation of carotenoid biosynthesis in plants: evidence for a key role of hydroxymethylbutenyl diphosphate reductase in controlling the supply of plastidial isoprenoid precursors. Plant J 40:188–199

Bouvier F, Rahier A, Camara B (2005) Biogenesis, molecular regulation and function of plant isoprenoids. Prog Lipid Res 44:357–429

Brooker JD, Russell DW (1975) Properties of microsomal 3-hydroxy-3-methylglutaryl coenzyme A reductase from *Pisum sativum* seedlings. Arch Biochem Biophys 167:723–729

Brooker JD, Russell DW (1979) Regulation of Microsomal 3-hydroxy-3-methylglutaryl coenzyme-A reductase from pea seedlings – rapid posttranslational phytochrome-mediated decrease in activity and *in vivo* regulation by isoprenoid products. Arch Biochem Biophys 198:323–334

Caelles C, Ferrer A, Balcells L, Hegardt FG, Boronat A (1989) Isolation and structural characterization of a cDNA encoding *Arabidopsis thaliana* 3-hydroxy-3-methylglutaryl coenzyme-A reductase. Plant Mol Biol 13:627–638

Campos N, Boronat A (1995) Targeting and topology in the membrane of plant 3-hydroxy-3-methylglutaryl coenzyme A reductase. Plant Cell 7:2163–2174

Carretero-Paulet L, Ahumada I, Cunillera N, Rodríguez-Concepción M, Ferrer A, Boronat A, Campos N (2002) Expression and molecular analysis of the *Arabidopsis* DXR gene encoding 1-deoxy-D-xylulose 5-phosphate reductoisomerase, the first committed enzyme of the

2-*C*-methyl-D-erythritol 4-phosphate pathway. Plant Physiol 129:1581–1591

Carretero-Paulet L, Cairo A, Botella-Pavia P, Besumbes O, Campos N, Boronat A, Rodríguez-Concepción M (2006) Enhanced flux through the methylerythritol 4-phosphate pathway in *Arabidopsis* plants overexpressing deoxyxylulose 5-phosphate reductoisomerase. Plant Mol Biol 62:683–695

Carrie C, Murcha MW, Millar AH, Smith SM, Whelan J (2007) Nine 3-ketoacyl-CoA thiolases (KATs) and acetoacetyl-CoA thiolases (ACATs) encoded by five genes in *Arabidopsis thaliana* are targeted either to peroxisomes or cytosol but not to mitochondria. Plant Mol Biol 63:97–108

Chappell J, Nable R (1987) Induction of sesquiterpenoid biosynthesis in tobacco cell-suspension cultures by fungal elicitor. Plant Physiol 85:469–473

Chappell J, Wolf F, Proulx J, Cuellar R, Saunders C (1995) Is the reaction catalyzed by 3-hydroxy-3-methylglutaryl coenzyme A reductase a rate-limiting step for isoprenoid Biosynthesis in Plants. Plant Physiol 109:1337–1343

Chappell J (1995) Biochemistry and molecular biology of the isoprenoid biosynthetic pathway in plants. Ann Rev Plant Physiol Plant Mol Biol 46:521–547

Cordoba E, Salmi M, León P (2009) Unravelling the regulatory mechanisms that modulate the MEP pathway in higher plants. J Exp Bot 60:2933–2943

Cordier H, Karst F, Bergès T (1999) Heterologous expression in *Saccharomyces cerevisiae* of an *Arabidopsis thaliana* cDNA encoding mevalonate diphosphate decarboxylase. Plant Mol Biol 39:953–967

Croteau R, Kutchan T, Lewis N (2000) Natural products (secondary metabolites). In: Buchanan B, Gruissem W, Jones R (eds) Biochemistry and molecular biology of plants. American Society of Plant Biologists, Rockville, pp 1250–1268

Crowell DN, Packard CE, Pierson CA, Giner JL, Downes BP, Chary SN (2003) Identification of an allele of *CLA1* associated with variegation in *Arabidopsis thaliana*. Physiol Plant 118:29–37

Dale S, Arró M, Becerra B, Morrice NG, Boronat A, Hardie DG, Ferrer A (1995) Bacterial expression of the catalytic domain of 3-hydroxy-3-methylglutaryl-CoA reductase (isoform Hmgr1) from *Arabidopsis thaliana*, and its inactivation by phosphorylation at Ser577 by *Brassica oleracea* 3-hydroxy-3-methylglutaryl-CoA reductase kinase. Eur J Biochem 233: 506–513

Disch A, Hemmerlin A, Bach TJ, Rohmer M (1998) Mevalonate-derived isopentenyl diphosphate is the biosynthetic precursor of ubiquinone prenyl side chain in tobacco BY-2 cells. Biochem J 331:615–621

Eisenreich W, Bacher A, Arigoni D, Rohdich F (2004) Biosynthesis of isoprenoids via the non-mevalonate pathway. Cell Mol Life Sci 61:1401–1426

Eisenreich W, Schwarz M, Cartayrade A, Arigoni D, Zenk MH, Bacher A (1998) The deoxyxylulose phosphate pathway of terpenoid biosynthesis in plants and microorganisms. Chem Biol 5:R221–R233

Enfissi EMA, Fraser PD, Lois LM, Boronat A, Schuch W, Bramley PM (2005) Metabolic engineering of the mevalonate and non-mevalonate isopentenyl diphosphate-forming pathways for the production of health-promoting isoprenoids in tomato. Plant Biotech J 3:17–27

Enjuto M, Balcells L, Campos N, Caelles C, Arró M, Boronat A (1994) *Arabidopsis thaliana* contains two differentially expressed 3-hydroxy-3-methylglutaryl-CoA reductase genes, which encode microsomal forms of the enzyme. Proc Natl Acad Sci USA 91:927–931

Enjuto M, Lumbreras V, Marin C, Boronat A (1995) Expression of the Arabidopsis *HMG2* gene, encoding 3-hydroxy-3-methylglutaryl coenzyme A reductase, is restricted to meristematic and floral tissues. Plant Cell 7:517–527

Estévez JM, Cantero A, Reindl A, Reichler S, León P (2001) 1-Deoxy-D-xylulose-5-phosphate synthase, a limiting enzyme for plastidic isoprenoid biosynthesis in plants. J Biol Chem 276:22901–22909

Estévez JM, Cantero A, Romero C, Kawaide H, Jiménez LF, Kuzuyama T, Seto H, Kamiya Y, León P (2000) Analysis of the expression of *CLA1*, a gene that encodes the 1-deoxyxylulose 5-phosphate synthase of the 2-*C*-methyl-D-erythritol-4-phosphate pathway in *Arabidopsis*. Plant Physiol 124:95–103

Flores-Pérez U, Sauret-Güeto S, Gas E, Jarvis P, Rodríguez-Concepción M (2008a) A mutant impaired in the production of plastome-encoded proteins uncovers a mechanism for the homeostasis of isoprenoid biosynthetic enzymes in *Arabidopsis* plastids. Plant Cell 20:1303–1315

Flores-Pérez U, Pérez-Gil J, Rodríguez-Villalón A, Gil MJ, Vera P, Rodríguez-Concepción M (2008b) Contribution of hydroxymethylbutenyl diphosphate synthase to carotenoid biosynthesis in bacteria and plants. Biochem Biophys Res Commun 371:510–514

Gil MJ, Coego A, Mauch-Mani B, Jordà L, Vera P (2005) The *Arabidopsis csb3* mutant reveals a regulatory link between salicylic acid-mediated disease resistance and the methyl-erythritol 4-phosphate pathway. Plant J 44:155–166

Goldstein JL, Brown MS (1990) Regulation of the mevalonate pathway. Nature 343:425–430

González V (2002) Caracterización funcional de la 3-hydroxi-3-metilmetilglutaril CoA reductasa de *Arabidosis thaliana*. Ph.D. Thesis. Department of Biochemistry and Molecular Biology. University of Barcelona

Grumbach KH, Bach TJ (1979) The effect of PSII herbicides, amitrol and SAN 6706 on the activity of 3-hydroxy-3-methylglutaryl-coenzyme A reductase and the incorporation of (2-^{14}C) acetate and (2-^{3}H) mevalonate into chloroplast pigments of radish seedlings. Z Naturforsch 34c:941–943

Guevara-García A, San Román C, Arroyo A, Cortés ME, Gutiérrez-Nava ML, León P (2005) Characterization of the *Arabidopsis clb6* mutant illustrates the importance of posttranscriptional regulation of the methyl-D-erythritol 4-phosphate pathway. Plant Cell 17:628–643

Gutiérrez-Nava ML, Gillmor CS, Jiménez LF, Guevara-García A, León P (2004) *CHLOROPLAST BIOGENESIS* genes act cell and noncell autonomously in early chloroplast development. Plant Physiol 135:471–482

Harker M, Hellyer A, Clayton JC, Duvoix A, Lanot A, Safford R (2003a) Co-ordinate regulation of sterol biosynthesis enzyme activity during accumulation of sterols in developing rape and tobacco seed. Planta 216:707–715

Harker M, Holmberg N, Clayton JC, Gibbard CL, Wallace AD, Rawlins S, Hellyer SA, Lanot A, Safford R (2003b) Enhancement of seed phytosterol levels by expression of an N-terminal truncated *Hevea brasiliensis* (rubber tree) 3-hydroxy-3-methylglutaryl-CoA reductase. Plant Biotechnol J 1:113–121

Hemmerlin A, Bach TJ (2000) Farnesol-induced cell death and stimulation of 3-hydroxy-3-methylglutaryl-coenzyme A reductase activity in tobacco cv bright yellow-2 cells. Plant Physiol 123:1257–1268

Hemmerlin A, Gerber E, Feldtrauer JF, Wentzinger L, Hartmann MA, Tritsch D, Hoeffler JF, Rohmer M, Bach TJ (2004) A review of tobacco BY-2 cells as an excellent system to study the synthesis and function of sterols and other isoprenoids. Lipids 39:723–735

Hemmerlin A, Hoeffler JF, Meyer O, Tritsch D, Kagan IA, Grosdemange-Billiard C, Rohmer M, Bach TJ (2003) Cross-talk between the cytosolic mevalonate and the plastidial methylerythritol phosphate pathways in tobacco bright yellow-2 cells. J Biol Chem 278:26666–26676

Hey SJ, Powers SJ, Beale MH, Hawkins ND, Ward JL, Halford NG (2006) Enhanced seed phytosterol accumulation through expression of a modified HMG-CoA reductase. Plant Biotechnol J 4:219–229

Hsieh MH, Goodman HM (2005) The *Arabidopsis* IspH homolog is involved in the plastid nonmevalonate pathway of isoprenoid biosynthesis. Plant Physiol 138:641–653

Hsieh MH, Goodman HM (2006) Functional evidence for the involvement of *Arabidopsis* IspF homolog in the nonmevalonate pathway of plastid isoprenoid biosynthesis. Planta 223:779–784

Hsieh MH, Chang CY, Hsu SJ, Chen JJ (2008) Chloroplast localization of methylerythritol 4-phosphate pathway enzymes and regulation of mitochondrial genes in *ispD* and *ispE* albino mutants in Arabidopsis. Plant Mol Biol 66:663–673

Jain AK, Vincent RM, Nessler CL (2000) Molecular characterization of a hydroxymethylglutaryl-CoA reductase gene from mulberry (*Morus alba* L.). Plant Mol Biol 42:559–569

Jelesko JG, Jenkins SM, Rodríguez-Concepción M, Gruissem W (1999) Regulation of tomato *HMG1* during cell proliferation and growth. Planta 208:310–318

Ji W, Hatzios KK, Cramer CL (1992) Expression of 3-hydroxy-3-methylglutaryl coenzyme A reductase activity in maize tissues. Physiol Plant 84:185–192

Jin H, Nikolau BJ (2007) Genetic, biochemical and physiological studies of acetyl-CoA metabolism via condensation. In: Benning C, Ohlrogge J (eds) Current advances in the biochemistry and cell biology of plant lipids. Aardvark Global Publishing Company, LCC, Sal Lake City, p 177

Julliard JH, Douce R (1991) Biosynthesis of the thiazole moiety of thiamin (vitamin B1) in higher-plant chloroplasts. Proc Natl Acad Sci USA 88:2042–2045

Kasahara H, Hanada A, Kuzuyama T, Takagi M, Kamiya Y, Yamaguchi S (2002) Contribution of the mevalonate and methylerythritol phosphate pathways to the biosynthesis of gibberellins in *Arabidopsis*. J Biol Chem 277:45188–45194

Korth KL, Stermer BA, Bhattacharyya MK, Dixon RA (1997) HMG-CoA reductase gene families that differentially accumulate transcripts in potato tubers are developmentally expressed in floral tissues. Plant Mol Biol 33:545–551

Korth KL, Jaggard DAW, Dixon RA (2000) Developmental and light-regulated post-translational control of 3-hydroxy-3-methylglutaryl-CoA reductase levels in potato. Plant J 23:507–516

Lange BM, Croteau R (1999) Isoprenoid biosynthesis via a mevalonate-independent pathway in plants: cloning and heterologous expression of 1-deoxy-D-xylulose-5-phosphate reductoisomerase from peppermint. Arch Biochem Biophys 365:170–174

Lange BM, Ghassemian M (2003) Genome organization in *Arabidopsis thaliana*: a survey for genes involved in isoprenoid and chlorophyll metabolism. Plant Mol Biol 51:925–948

Lange BM, Wildung MR, McCaskill D, Croteau R (1998) A family of transketolases that directs isoprenoid biosynthesis via a mevalonate-independent pathway. Proc Natl Acad Sci USA 95:2100–2104

Laule O, Fürholz A, Chang HS, Zhu T, Wang X, Heifetz PB, Gruissem W, Lange M (2003) Crosstalk between cytosolic and plastidial pathways of isoprenoid biosynthesis in *Arabidopsis thaliana*. Proc Natl Acad Sci USA 100:6866–6871

Learned RM (1996) Light suppresses 3-hydroxy-3-methylglutaryl coenzyme A reductase gene expression in *Arabidopsis thaliana*. Plant Physiol 110: 645–655

Learned RM, Connolly EL (1997) Light modulates the spatial patterns of 3-hydroxy-3-methylglutaryl coenzyme A reductase gene expression in *Arabidopsis thaliana*. Plant J 11:499–511

Leivar P, González VM, Castel S, Trelease RN, López-Iglesias C, Arró M, Boronat A, Campos N, Ferrer A, Fernàndez-Busquets X (2005) Subcellular localization of *Arabidopsis* 3-hydroxy-3-methylglutaryl-coenzyme A reductase. Plant Physiol 137:57–69

Leivar P, Antolín-Llovera M, Ferrero S, Closa M, Arró M, Ferrer A, Boronat A, Campos N (2011) Multilevel control of *Arabidopsis* 3-hydroxy-3-methylglutaryl coenzyme A reductase by protein phosphatase 2A. Plant Cell 23:1494–1511

Libourel IGL, Shachar-Hill Y (2008) Metabolic flux analysis in plants: from intelligent design to rational engineering. Annu Rev Plant Biol 59:625–650

Lichtenthaler HK (1999) The 1-deoxy-D-xylulose-5-phosphate pathway of isoprenoid biosynthesis in plants. Annu Rev Plant Physiol Plant Mol Biol 50:47–65

Lichtenthaler HK, Rohmer M, Schwender J (1997) Two independent biochemical pathways for isopentenyl diphosphate and isoprenoid biosynthesis in higher plants. Physiol Plant 101:643–652

Lluch MA, Masferrer A, Arró M, Boronat A, Ferrer A (2000) Molecular cloning and expression analysis of the mevalonate kinase gene from *Arabidopsis thaliana*. Plant Mol Biol 42:365–376

Lois LM, Rodríguez-Concepción M, Gallego F, Campos N, Boronat A (2000) Carotenoid biosynthesis during tomato fruit development: regulatory role of 1-deoxy-D-xylulose 5-phosphate synthase. Plant J 2: 503–513

Lois LM, Campos N, Putra SR, Danielsen K, Rohmer M, Boronat A (1998) Cloning and characterization of a gene from *Escherichia coli* encoding a transketolase-like enzyme that catalyzes the synthesis of D-1-deoxyxylulose 5-phosphate, a common precursor for isoprenoid, thiamin, and pyridoxol biosynthesis. Proc Natl Acad Sci USA 95:2105–2110

Lumbreras V, Campos N, Boronat A (1995) The use of an alternative promoter in the *Arabidopsis thaliana HMG1* gene generates a mRNA that encodes a novel 3-hydroxy-3-methylglutaryl coenzyme A reductase isoform with and extended N-terminal region. Plant J 8:541–549

Lunn JE (2007) Compartmentation in plant metabolism. J Exp Bot 58:35–47

Mahmoud SS, Croteau RB (2001) Metabolic engineering of essential oil yield and composition in mint by altering expression of deoxyxylulose phosphate reductoisomerase and menthofuran synthase. Proc Natl Acad Sci USA 98:8915–8920

Mandel MA, Feldmann KA, Herrera-Estrella L, Rocha-Sosa M, Leon P (1996) *CLA1*, a novel gene required for chloroplast development, is highly conserved in evolution. Plant J 9:649–658

Manzano D, Fernández-Busquets X, Schaller H, González V, Boronat A, Arró M, Ferrer A (2004) The metabolic imbalance underlying lesion formation in *Arabidopsis thaliana* overexpressing farnesyl diphosphate synthase (isoform 1S) leads to oxidative stress and is triggered by the developmental decline of endogenous HMGR activity. Planta 219:982–992

Manzano D, Busquets A, Closa M, Hoyerova K, Schaller H, Kaminek M, Arró M, Ferrer A (2006) Overexpression of farnesyl diphosphate synthase in *Arabidopsis* mitochondria triggers light-dependent lesion formation and alters cytokinin homeostasis. Plant Mol Biol 61:195–213

Masferrer A, Arró M, Manzano D, Schaller H, Fernández-Busquets X, Moncaleán P, Fernández B, Cunillera N, Boronat A, Ferrer A (2002) Overexpression of *Arabidopsis thaliana* farnesyl diphosphate synthase (FPS1S) in transgenic *Arabidopsis* induces a cell death/senescence-like response and reduced cytokinin levels. Plant J 30:123–132

McGarvey DJ, Croteau R (1995) Terpenoid metabolism. Plant Cell 7:1015–1026

Merret R, Cirioni J, Bach TJ, Hemmerlin A (2007) A serine involved in actin-dependent subcellular localization of a stress-induced tobacco BY-2 hydroxymethylglutaryl-CoA reductase isoform. FEBS Lett 581:5295–5299

Montamat F, Guilloton M, Karst F, Delrot S (1995) Isolation and characterization of a cDNA encoding *Arabidopsis thaliana* 3-hydroxy-3-methylglutaryl-coenzyme A synthase. Gene 167:197–201

Moore KB, Oishi KK (1993) Characterization of 3-hydroxy-3-methylglutaryl coenzyme-A reductase activity during maize seed development, germination, and seedling emergence. Plant Physiol 101:485–491

Muñoz-Bertomeu J, Arrillaga I, Ros R, Segura J (2006) Up-regulation of 1-deoxy-D-xylulose-5-phosphate synthase enhances production of essential oils in transgenic spike lavender. Plant Physiol 142:890–900

Nagata N, Suzuki M, Yoshida S, Muranaka T (2002) Mevalonic acid partially restores chloroplast and etioplast development in *Arabidopsis* lacking the non-mevalonate pathway. Planta 216:345–350

Nagegowda DA, Bach TJ, Chye ML (2004) *Brassica juncea* 3-hydrox-3-methylglutaryl (HMG)-CoA synthase 1: expression and characterization of recombinant wild-type and mutant enzymes. Biochem J 383: 517–527

Nagegowda DA, Ramalingam S, Hemmerlin A, Bach TJ, Chye ML (2005) *Brassica juncea* HMG-CoA synthase: localization of mRNA and protein. Planta 221:844–856

Nieto B, Forés O, Arró M, Ferrer A (2009) *Arabidopsis* 3-hydroxy-3-methylglutaryl-CoA reductase is regulated at the post-translational level in response to alterations of the sphingolipid and the sterol biosynthetic pathways. Phytochemistry 70:58–64

Ôba K, Kondo K, Doke N, Uritani I (1985) Induction of 3-hydroxy-3-methylglutaryl CoA reductase in potato tubers after slicing, fungal infection or chemical treatment, and some properties of the enzyme. Plant Cell Physiol 26:873–880

Ohyama K, Suzuki M, Masuda K, Yoshida S, Muranaka T (2007) Chemical phenotypes of the *hmg1* and *hmg2* mutants of *Arabidopsis* demonstrate the *in-planta* role of HMG-CoA reductase in triterpene biosynthesis. Chem Pharm Bull 55:1518–1521

Okada K, Kawaide H, Kuzuyama T, Seto H, Curtis IS, Kamiya Y (2002) Antisense and chemical suppression of the nonmevalonate pathway affects *ent*-kaurene biosynthesis in *Arabidopsis*. Planta 215:339–344

Oudin A, Mahroug S, Courdavault V, Hervouet N, Zelwer C, Rodríguez-Concepción M, St-Pierre B, Burlat V (2007) Spatial distribution and hormonal regulation of gene products from methyl erythritol phosphate and monoterpene-secoiridoid pathways in *Catharanthus roseus*. Plant Mol Biol 65:13–30

Paetzold H, Garms S, Bartram S, Wieczorek J, Urós-Gracia EM, Rodríguez-Concepción M, Boland W, Strack D, Hause B, Walter MH (2010) The isogene 1-deoxy-D-xylulose 5-phosphate synthase 2 controls

isoprenoid profiles, precursor pathway allocation, and density of tomato trichomes. Mol Plant 3:904–916

Peltier JB, Ripoll DR, Friso G, Rudella A, Cai Y, Ytterberg J, Giacomelli L, Pillardy J, van Wijk KJ (2004) Clp protease complexes from photosynthetic and non-photosynthetic plastids and mitochondria of plants, their predicted three-dimensional structures, and functional implications. J Biol Chem 279:4768–4781

Phillips MA, León P, Boronat A, Rodríguez-Concepción M (2008) The plastidial MEP pathway: unified nomenclature and resources. Trends Plant Sci 13:619–623

Querol J, Campos N, Imperial S, Boronat A, Rodríguez-Concepción M (2002) Functional analysis of the *Arabidopsis thaliana* GCPE protein involved in plastid isoprenoid biosynthesis. FEBS Lett 514:343–346

Riou C, Tourte Y, Lacroute F, Karst F (1994) Isolation and characterization of a cDNA encoding *Arabidopsis thaliana* mevalonate kinase by genetic complementation in yeast. Gene 148:293–297

Rodríguez-Concepción M, Ahumada I, Diez-Juez E, Sauret-Güeto S, Lois LM, Gallego F, Carretero-Paulet L, Campos N, Boronat A (2001) 1-Deoxy-D-xylulose 5-phosphate reductoisomerase and plastid isoprenoid biosynthesis during tomato fruit ripening. Plant J 27:213–222

Rodríguez-Concepción M, Boronat A (2002) Elucidation of the methylerythritol phosphate pathway for isoprenoid biosynthesis in bacteria and plastids. A metabolic milestone achieved through genomics. Plant Physiol 130:1079–1089

Rodríguez-Concepción M, Querol J, Lois LM, Imperial S, Boronat A (2003) Bioinformatic and molecular analysis of hydroxymethylbutenyl diphosphate synthase (*GCPE*) gene expression during carotenoid accumulation in ripening tomato fruit. Planta 217:476–482

Rodríguez-Concepción M, Forés O, Martínez-García JF, González V, Phillips MA, Ferrer A, Boronat A (2004) Distinct light-mediated pathways regulate the biosynthesis and exchange of isoprenoid precursors during *Arabidopsis* seedling development. Plant Cell 16:144–156

Rodríguez-Concepción M (2006) Early steps in isoprenoid biosynthesis: multilevel regulation of the supply of common precursors in plant cells. Phytochem Rev 5:1–15

Rohmer M (1999) The discovery of a mevalonate-independent pathway for isoprenoid biosynthesis in bacteria, algae and higher plants. Nat Prod Rep 16:565–574

Rohmer M (2008) From molecular fossils of bacterial hopanoids to the formation of isoprene units: discovery and elucidation of the methylerythritol phosphate pathway. Lipids 43:1095–1107

Russell DW, Knight JS, Wilson TM (1985) Pea seedling HMG-CoA reductases: regulation of activity *in vitro* by phosphorylation and Ca^{2+}, and posttranslational control *in vivo* by phytochrome and isoprenoid hormones. In: Randall DD, Blevins DG, Larson RL, Kagawa T (eds) Current topics in plant biochemistry and physiology. University of Missouri-Columbia, Columbia, pp 191–206

Sapir-Mir M, Mett A, Belausov E, Tal-Meshulam S, Frydman A, Gidoni D, Eyal Y (2008) Peroxisomal localization of *Arabidopsis* isopentenyl diphosphate isomerases suggests that part of the plant isoprenoid mevalonic acid pathway is compartmentalized to peroxisomes. Plant Physiol 148:1219–1228

Sauret-Güeto S, Botella-Pavía P, Flores-Pérez U, Martínez-Garcia JF, San Román C, León P, Boronat A, Rodríguez-Concepción M (2006) Plastid cues posttranscriptionally regulate the accumulation of key enzymes of the methylerythritol phosphate pathway in *Arabidopsis*. Plant Physiol 141:75–84

Schaller H, Grausem B, Benveniste P, Chye ML, Tan CT, Song CT, Chua NH (1995) Expression of the *Hevea brasiliensis* (Hbk) Mull Arg 3-hydroxy-3-methylglutaryl-coenzyme A reductase-1 in tobacco results in sterol overproduction. Plant Physiol 109:761–770

Schuhr CA, Radykewicz T, Sagner S, Latzel C, Zenk MH, Arigoni D, Bacher A, Rohdich F, Eisenreich W (2003) Quantitative assessment of crosstalk between the two isoprenoid biosynthesis pathways in plants by NMR spectroscopy. Phytochem Rev 2:3–16

Schwender J, Müller C, Zeidler J, Lichtenthaler HK (1999) Cloning and heterologous expression of a cDNA encoding 1-deoxy-D-xylulose-5-phosphate reductoisomerase of *Arabidopsis thaliana*. FEBS Lett 455:140–144

Simkin AJ, Guirimand G, Papon N, Courdavault V, Thabet I, Ginis O, Bouzid S, Giglioli-Guivarc'h N, Clastre M (2011) Peroxisomal localisation of the final steps of the mevalonic acid pathway in planta. Planta 234:903–914

Sjögren LL, Stanne TM, Zheng B, Sutinen S, Clarke AK (2006) Structural and functional insights into the chloroplast ATP-dependent Clp protease in *Arabidopsis*. Plant Cell 18:2635–2649

Sprenger GA, Schorken U, Wiegert T, Grolle S, de Graaf AA, Taylor SV, Begley TP, Bringer-Meyer S, Sahm H (1997) Identification of a thiamin-dependent synthase in *Escherichia coli* required for the formation of the 1-deoxy-D-xylulose 5-phosphate precursor to isoprenoids, thiamin, and pyridoxol. Proc Natl Acad Sci USA 94:12857–12862

Stermer BA, Bianchini GM, Korth KL (1994) Regulation of HMG-CoA reductase activity in plants. J Lipid Res 35:1133–1140

Sugden C, Donaghy PG, Halford NG, Hardie DG (1999) Two SNF1-Related protein kinases from spinach leaf phosphorylate and inactivate 3-hydroxy-3-methylglutaryl-coenzyme A reductase, nitrate reductase, and sucrose phosphate synthase *in vitro*. Plant Physiol 120:257–274

Suzuki H, Ôba K, Uritani I (1975) Occurrence and some properties of 3-hydroxy-3-methylglutaryl coenzyme A reductase in sweet-potato roots infected by *Ceratocystis fimbriata*. Physiol Plant Pathol 7:265–276

Suzuki M, Kamide Y, Nagata N, Seki H, Ohyama K, Kato H, Masuda K, Sato S, Kato T, Tabata S, Yoshida S, Muranaka T (2004) Loss of function of *3-hydroxy-3-methylglutaryl coenzyme A reductase 1 (HMG1)* in *Arabidopsis* leads

to dwarfing, early senescence and male sterility, and reduced sterol levels. Plant J 37:750–761

Takahashi S, Kuzuyama T, Watanabe H, Seto H (1998) A 1-deoxy-D-xylulose 5-phosphate reductoisomerase catalyzing the formation of 2-*C*-methyl-D-erythritol 4-phosphate in an alternative non-mevalonate pathway for terpenoid biosynthesis. Proc Natl Acad Sci USA 95:9879–9884

Thomas S, Fell DA (1998) The role of multiple enzyme activation in metabolic flux control. Adv Enzyme Regul 38:65–85

Walter MH, Hans J, Strack D (2002) Two distantly related genes encoding 1-deoxy-D-xylulose 5-phosphate synthases: differential regulation in shoots and apocarotenoid-accumulating mycorrhizal roots. Plant J 31:243–254

Wentzinger L, Bach TJ, Hartmann M-A (2002) Inhibition of squalene synthase and squalene epoxidase in tobacco cells triggers an up-regulation of 3-hydroxy-3-methylglutaryl coenzyme A reductase. Plant Physiol 130:334–346

Wille A, Zimmermann P, Vranová E, Fürholz A, Laule O, Bleuler S, Hennig L, Prelic A, von Rohr P, Thiele L, Zitzler E, Gruissem W, Bühlmann P (2004) Sparse graphical Gaussian modeling of the isoprenoid gene network in *Arabidopsis thaliana*. Genome Biol 5:R92. doi:10.1186/gb-2004-5-11-r92

Wong RJ, McCormack DK, Russell DW (1982) Plastid 3-hydroxy-3-methylglutaryl coenzyme A reductase has distinctive kinetic and regulatory features – properties of the enzyme and positive phytochrome control of activity in pea-seedlings. Arch Biochem Biophys 216:631–638

Yang ZB, Park HS, Lacy GH, Cramer CL (1991) Differential activation of potato 3-hydroxy-3-methylglutaryl coenzyme A reductase genes by wounding and pathogen challenge. Plant Cell 3:397–405

Understanding the Mechanisms that Modulate the MEP Pathway in Higher Plants

31

Patricia León and Elizabeth Cordoba

Abstract

The methyl-D-erythritol 4-phosphate (MEP) pathway is responsible for the biosynthesis of an impressive number of natural compounds of biological and biotechnological importance. In recent years, this pathway has become a clear target to develop new herbicides and antimicrobial drugs. Additionally, the production of a variety of compounds of medical and agricultural interest may be possible through genetic manipulation of this pathway. To this end, a full understanding of the molecular mechanisms that regulate this pathway is of tremendous importance. Our work has shown that the MEP pathway is subjected to multiple levels of regulation, some of them being conserved among different plant species. In this chapter, we describe some of these regulatory mechanisms.

The first enzyme of this anabolic route is the 1-deoxy-D-xylulose 5-phosphate synthase (DXS). Our work has provided evidence of the strategic role that this enzyme plays in the overall regulation of the pathway. DXS is encoded by a small gene family, between two or three members, that belong to three major groups maintained through evolution. In some plants (e.g., maize), each of the *DXS* genes exhibits a unique expression pattern, supporting a particular function for each gene product during plant development. One of the most interesting regulatory events identified is the modulation of the DXS protein level in response to a blockage or decrease of the pathway flow. This regulation is conserved among plants, suggesting that it is an important feedback mechanism for the proper response of this pathway to the plant's metabolic demand.

P. León (✉) • E. Cordoba
Departamento de Biología Molecular, Instituto de Biotecnología Universidad Autónoma de México, Av. Universidad 2001 Chamilpa Cuernavaca, Morelos 62210, Mexico
e-mail: patricia@ibt.unam.mx

T.J. Bach and M. Rohmer (eds.), *Isoprenoid Synthesis in Plants and Microorganisms: New Concepts and Experimental Approaches*, DOI 10.1007/978-1-4614-4063-5_31,

Keywords
Isoprenoids • Chloroplasts • MEP pathway • DXS enzyme • Gene family • Maize • Arabidopsis

31.1 Introduction

The isoprenoid family of compounds includes on the order of 30,000 natural products present in all living organisms. These compounds have overwhelmingly diverse structures and functions, many of them essential in growth and development. All isoprenoid compounds are synthesized through the condensation of different numbers of two universal 5-carbon precursors: isopentenyl diphosphate (IPP) and dimethylallyl diphosphate (DMAPP). Among living organisms, two non-related biosynthetic routes exist for the synthesis of these two basic building blocks which use different precursors (Bouvier et al. 2005). One is the mevalonate pathway where IPP and DMAPP are synthesized from mevalonic acid (MVA). The other is the methyl-D-erythritol 4-phosphate (MEP) pathway that uses as precursors pyruvate and glyceraldehyde 3-phosphate for the synthesis of IPP and DMAPP. The existence of the MEP pathway as an alternative route for the biosynthesis of IPP and DMAPP was demonstrated about 18 years ago (Rohmer et al. 1993; Sprenger et al. 1997; see also elsewhere in this volume), and since this discovery, remarkable advances in the understanding of this pathway have been made. Today, each of the biosynthetic steps of the MEP pathway is known, as well as some aspects of the enzymatic properties of the corresponding proteins.

The MEP pathway is distributed in most eubacteria, including pathogenic species, and represents the only route for the production of the isoprenoid compounds in these organisms. It is also present in eukaryotes including apicomplexa parasites such as plasmodium and in all photosynthetic organisms. This pathway, however, is absent from other eukaryotes, including yeast and humans. This distribution makes the MEP pathway an attractive target to develop new antibacterial and antiparasitic drugs and herbicides by identifying compounds that inhibit or block their enzymatic activities or that affect their regulation (Zeidler et al. 2000; Rodríguez-Concepción 2004; Rohdich et al. 2005).

In plant cells, the isoprenoid universal precursors IPP and DMAPP are derived from both the MVA and the MEP pathways. These two pathways are located in different subcellular compartments; the MVA pathway is present in the cytoplasm and the MEP pathway in plastids. Although there is clear evidence that demonstrate an exchange between the two pathways, this appears to be rather limited and it is not sufficient to rescue the production of several cytoplasmic or plastidial isoprenoids when the corresponding pathway is absent or inhibited (Estévez et al. 2000; Carretero-Paulet et al. 2006; Flores-Perez et al. 2010). As a consequence of this compartmentalization, the synthesis of a number of medically and biotechnologically important isoprenoid compounds is largely through the MEP pathway, and many of these represent important targets for future manipulation. Examples of those include commonly used antioxidants such as carotenoids and tocopherols as well as anticancer drugs such as paclitaxel (Dubey et al. 2003; DellaPenna and Pogson 2006). This pathway is also responsible for the biosynthesis of several major plant hormones including gibberellins, abscisic acid, and even the recently discovered strigolactones (Umehara et al. 2008; see also elsewhere in this volume). In consequence, studies that advance understanding of the regulatory mechanisms that govern this pathway, as well as those biosynthetic steps that limit this route, are of major importance.

In this chapter, we summarize some of our work that aims to identify the major mechanisms that regulate the function of MEP pathway and that limit the pathway flux. We hope that these findings will contribute to a better understanding of this central pathway and will shed light on unprecedented regulatory mechanisms that modulate this metabolic route.

31.2 DXS: A Flux-Controlling Enzyme for the MEP Pathway

The first step of the MEP pathway is catalyzed by the 1-deoxy-D-xylulose 5-phosphate synthase (DXS). This enzyme catalyzes a transketolase-like decarboxylation reaction using the precursors pyruvate and glyceraldehyde 3-phosphate to form 1-deoxy-D-xylulose 5-phosphate (DXP) (Sprenger et al. 1997; Lois et al. 1998). In bacteria, this enzymatic reaction appears to not be exclusively dedicated to the MEP pathway, as it is also required for the synthesis of the vitamins thiamin and pyridoxal (Julliard and Douce 1991). However, ever increasing experimental evidence exists for DXS playing a critical role in the synthesis of IPP and DMAPP in plants. In Arabidopsis transgenic lines that express higher (overexpressors) DXS levels, the concentration of various isoprenoid final products including chlorophyll, carotenoids, tocopherols, and ABA is increased in direct correlation to the DXS content. Similar findings are observed in lines that express lower (anti-sense) levels of DXS (Estévez et al. 2001). Comparable results were observed in other plants including tomato (Lois et al. 2000), potato (Morris et al. 2006), and *Ginkgo biloba* (Gong et al. 2006). These data support that in plants, DXS enzyme catalyzes a rate-limiting step in the synthesis of the IPP and DMAPP building blocks and behaves as an important control of the pathway flux. The limiting activity of DXS enzyme has also been reported in eubacteria (Harker and Bramley 1999; Kuzuyama et al. 2000). Thus, DXS represents one of the obvious targets for manipulation of this metabolic route.

31.3 DXS, an Enzyme Subjected to Multiple Levels of Regulations

The molecular characterization of the *Arabidopsis* DXS has shown that unlike other genes in this pathway, three putative *DXS*-like genes exist. Activity as a DXP synthase has only been demonstrated for one of the corresponding enzymes: DXS1/CLA1 (Estévez et al. 2000). Knockout mutations in the Arabidopsis *DXS1* gene (At4g15560), initially reported as *CLA1*, result in albino plants, with severely affected chloroplasts that are unable to synthesize photosynthetic pigments (Mandel et al. 1996). The phenotype observed corroborates that DXS1 is essential for plant survival. The phenotype also demonstrates that the other *DXS*-like genes present in the Arabidopsis genome do not have redundant functions. Arabidopsis *DXS1* is sufficient to support photosynthetic pigment (chlorophyll and carotenoid) biosynthesis. Although the other *DXS*-like genes are apparently expressed during specific developmental stages, their function remains unclear and this characterization represent a target for future investigations (see also Walter et al., this volume).

The presence of multiple genes that potentially encode DXS is not restricted to Arabidopsis. Many plant species, including conifers, dicots, and monocots, contain several putative *DXS* genes. In maize and rice, three potential *DXS* genes exist (Cordoba et al. 2009; Vallabhaneni and Wurtzel 2009). Multiple *DXS* genes have been found also in *Medicago truncatula* and *Picea abies* (Chahed et al. 2000; Walter et al. 2000; Walter et al. 2002; Kim et al. 2005; Paetzold et al. 2010). Phylogenetic analysis demonstrates that the different DXS proteins clustered into three independent clades. Representative genes belonging to each of these groups have been maintained during evolution in several species, which supports a particular function for each of them (Cordoba et al. 2011). An exception to this is Arabidopsis in which, although three different *DXS*-like genes exist, the proteins encoded by the *DXS/CLA1* (At4g15560) and *DXS2* (At3g21500) genes cluster into the same clade (clade 1). The other Arabidopsis DXS-like protein encoded by the gene referred to as *DXS3* groups together with other DXS type 3 proteins such as DXS3 from maize. Thus, in Arabidopsis, no *DXS*-like type 2 gene seems to exist (Cordoba et al. 2011).

31.4 Differential Expression of the *DXS* Genes in Plants

Expression analysis of different *DXS* genes in plants demonstrates particular expression patterns for each family member. In Arabidopsis, the

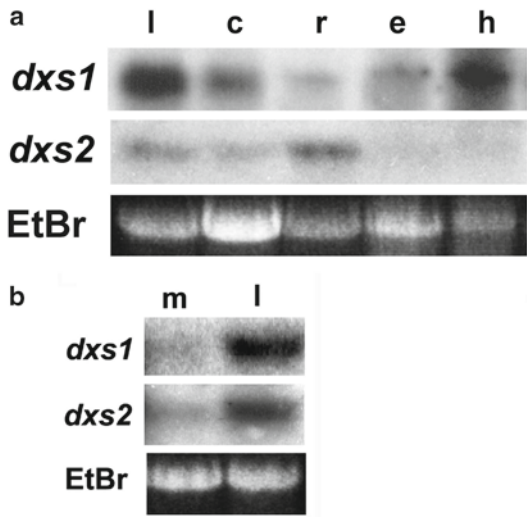

Fig. 31.1 *dxs1* and *dxs2* are differentially expressed in maize tissues. (**a**) Northern blot analysis of total RNA (20 μg) extracted from 8-day-old leaves (*l*), 6-day-old dark-grown coleoptiles (*c*), 6-day-old roots (*r*), immature ears (*e*), and husks (*h*) from 4-month-old plants. (**b**) Northern blot analysis of mesophyll protoplasts (*m*) and second leaf blade (*l*) from 12-day-old seedlings. The ethidium bromide (*EtBr*) rRNAs are shown as loading controls. The membrane was hybridized sequentially with specific probes for *dxs1* and *dxs2* genes. The ethidium bromide (*EtBr*) stained gel is shown as the loading control

DXS/CLA1 gene is highly expressed in photosynthetic tissues, where high levels of photosynthetic pigments are required. In contrast, based on public expression data (www.genevestigator.com/gv/doc/plant_biotech.jsp), the transcript accumulations of the other *DXS* genes appear to be restricted to particular tissues (Fig. 31.1). In maize, the *dxs1* gene accumulates at high levels in photosynthetic tissues (Cordoba et al. 2011; Walter et al. 2002), displaying a similar pattern to *DXS1/CLA1* in Arabidopsis. The other *dxs* genes are expressed at lower levels in different tissues. The transcript of a second gene (*dxs2*) predominantly accumulates in roots and in yellow kernels, suggesting a role for this protein in nongreen tissues. Previous reports described that in maize roots, *dxs2* transcripts strongly accumulate upon colonization by mycorrhizal fungi and in concordance with the increase in apocarotenoid compounds (Walter et al. 2002). The present analysis, however, demonstrates that the expression of *dxs2* in maize is not only restricted to mycorrhiza fungi colonization but is also detected at considerable levels during early root development. There are two distinct of mRNA products derived from the *dxs2* gene in maize that differ around 30 amino acids at their amino termini. Analysis of the subcellular localization of these two transcripts using maize protoplasts demonstrates that the differences in the amino acid composition between these two transcripts change their subcellular localization. Only the protein encoded by the transcript referred to as T1 is localized into chloroplasts, where it is expected to perform its function (Cordoba et al. 2011). The product of the T2 transcript remains in the cytoplasm. Each of these transcripts has a differential expression pattern; for example, the T1 transcript accumulates in roots and ears but apparently not (or at very low levels) in mature leaves. It is also possible that this transcript species might be the result of a cryptic transcription initiation site in the absence of specific regulators present in particular tissues. At the moment, the precise function, if any, for the *dxs2* transcript T2 remains unknown.

The product of a third maize gene that we refer to as *dxs3* clusters with DXS type 3 proteins from other plants. The *dxs3* gene is detected at lower levels than the other two *dxs* genes in most tissues, but its highest expression is observed in unfertilized ovules (Vallabhaneni and Wurtzel 2009; Cordoba et al. 2011). Based on the expression level and the expression profile of the *dxs3* maize gene, we speculate that a possible function for this gene might be related to the synthesis of particular isoprenoids that are required at low levels, like hormones (GA and ABA), essential for plant survival. Complementation analysis of a *dxs* mutant in *E. coli* demonstrates that the protein products derived from the three *dxs* genes from maize are functional as true DXS proteins. These data further support a particular function for each of the different family members in plants.

31.5 The Expression of the MEP Genes Is Regulated by Multiple Signals

Expression analysis of the MEP pathway genes in Arabidopsis under various growth conditions has shown that the accumulation of their transcripts is modulated by multiple signals. In Arabidopsis, transcript levels of all genes from the pathway accumulate upon exposure to light (Cordoba et al. 2009). We have also observed that the expression of all genes from the pathway is high in the early stages of seedling development, during the establishment of the first true leaves (Guevara-García et al. 2005). This regulation is also observed at the protein level for several of the enzymes of the pathway (Fig. 31.2). Our interpretation of this expression pattern is that during early development, there is an elevated demand for photosynthetic pigments that results in the increased expression levels of all genes of the pathway. We also corroborated a circadian regulation for all genes of the pathway. In this case, the transcripts for all MEP genes fluctuate following the same phase, reaching their highest levels just before dawn (Cordoba et al. 2009). An interesting outcome of these analyses is that several of the responses analyzed at the transcriptional level argue for a coordinated regulation between all genes of the pathway in response to several signals including light, development, and circadian. Similar results have been obtained by other groups (Hsieh and Goodman 2005). Future work in this area is needed to fully interpret those factors that are involved in the pathway's regulation.

The characterization of mutants in MEP pathway genes has been important to confirm the functionality of each of these genes. In Arabidopsis, mutants for each of the genes that constitute the pathway (with the exception of the *DXS-like 2* and *DXS-like 3* genes) have been characterized. Knockout mutations in any of the genes in the pathway result in an albino phenotype, with profound alterations in chloroplast development (Mandel et al. 1996; Gutiérrez-Nava et al. 2004). The only exception to this is the IPP isomerase (*IDI*) gene, which appears to be nonessential for the function of the pathway (Phillips et al. 2008). Phenotypic characterization during embryogenesis of the mutants being affected in the last two steps in the pathway, *HDS* and *HDR* (that code for 4-hydroxy-3-methylbut-2-enyl diphosphate synthase and 4-hydroxy-3-methylbut-2-enyl diphosphate reductase enzymes, respectively), showed that these genes act in a non-cell autonomous way. In the developing embryos of both mutants, partial complementation of chlorophyll accumulation is observed, and this is attributed to import of a yet unknown precursor from

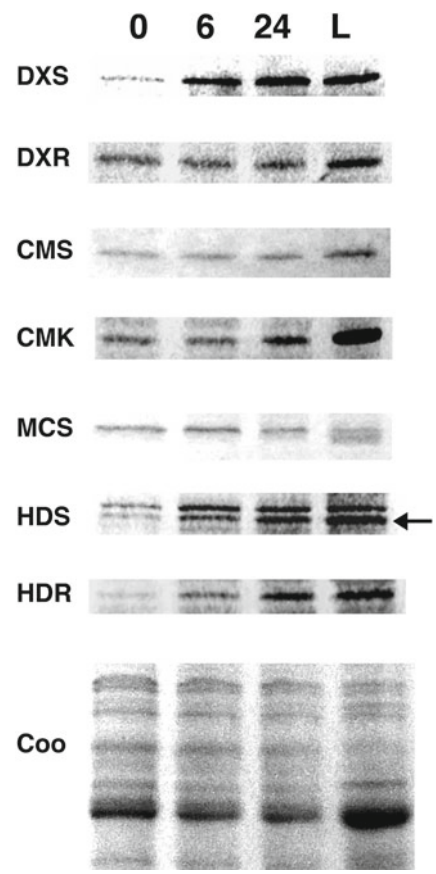

Fig. 31.2 Light regulation of the MEP pathway enzymes. 8-day-old seedlings grown in the dark for 5 days and exposed to light for 0, 6, and 24 h or grown in a 16:8 light:dark cycle. Immunoblots were performed with antibodies against the specified enzymes. Each lane contains 10 μg of total protein extracts. A Coomassie blue-stained gel (*Coo*) is shown as a loading control. The *arrow marks* the specific HDS protein

maternal origin (Gutiérrez-Nava et al. 2004). In addition, these mutants have been useful to identify other regulatory signals that modulate this pathway at both the transcript and protein levels (Guevara-García et al. 2005).

The expression of all genes in this pathway is regulated by retrograde chloroplast to nuclear signaling. In mutants that affect chloroplast development, the accumulation level of the different MEP pathway gene transcripts is reduced in comparison to wild-type plants. Although the transcript level in all MEP genes is reduced, some of them appear particularly sensitive to this regulatory signal. This regulation is observed in unrelated albino mutants not affected in the MEP pathway, which suggests that this regulation results from the arrested chloroplast development (Guevara-García et al. 2005).

To understand additional regulatory events that modulate the MEP pathway, our work has focused on the accumulation of the proteins in this pathway. In collaboration with the group of Dr. Kamiya (RIKEN, Yokohama), a set of antibodies specific for each of the proteins of the pathway were obtained. Using these antibodies, we confirmed that the mutations in any of the genes from the pathway resulted in a low accumulation of all transcripts and proteins of the pathway (Guevara-García et al. 2005). The only exception to this is the first enzyme of the pathway (DXS). In this case, the DXS protein accumulates to high levels despite its transcript being dramatically reduced. These DXS levels are considerably higher than those present in wild-type seedlings at a similar developmental stage. This accumulation is not exclusive to a specific mutation, but is observed in mutations that affect all the different biosynthetic steps of the route. Moreover, analysis of DXS protein levels in two unrelated albino mutants (*clb5* and *chl1*) demonstrates that this regulation is particular to mutants in the MEP pathway, not a more general result of the lack of pigments. These results suggested that this response represents a biologically relevant regulation of the DXS protein. An increase of DXS protein levels is also observed when applying specific inhibitors of the MEP pathway: Wild-type plants treated with fosmidomycin, which blocks the second enzymatic step of the pathway, also accumulate high levels of the DXS protein. Taking this data together, we propose that this represents a feedback regulatory mechanism that can modulate the flow of the pathway in response to the fluctuating demand for the final pathway products, IPP and DMAPP.

Additional data that further support that the accumulation of DXS protein acts as a regulatory response to changes in the pathway flow is that it is conserved among plants. We observed that after fosmidomycin treatment of maize seedlings, the level of DXS protein that accumulates is similar to that in Arabidopsis (Cordoba et al. 2011). This protein accumulation does not result from a higher transcript level of any of the three genes that code for this enzyme in maize. Thus, a posttranscriptional event similar to that in Arabidopsis appears to be responsible for this regulation. These data show that changes in the DXS protein levels in response to perturbations of the pathway flow are not exclusive to Arabidopsis, but are conserved among dicot and monocot plants. Taken together, these studies have demonstrated an important posttranscriptional mechanism that modulates the levels of DXS, a critical enzyme of the MEP pathway, which has a limiting role in the pathway flux.

31.6 Conclusion and Perspectives

In recent years, our group has used diverse approaches including genetic, molecular, and biochemical techniques, to gain a better understanding of the regulation of the MEP pathway in higher plants. Our results have contributed to uncovering a novel regulation of the first enzyme of this pathway (DXS) at the protein level. Interestingly, this regulation operates inversely to its transcript accumulation. This example highlights the need to be alert and suspect of the common practice of extrapolating protein levels based on transcript accumulation. Although other examples like this have been reported in the literature, and it is likely that more will follow, this regulation is unusual. In fact our group, in collaboration with the group of Dr. Rodríguez-Concepción, has found a similar regulation for DXR, the second step of the pathway (Sauret-Güeto et al. 2006).

Today, the MEP pathway represents one of the most promising targets to develop new herbicides and antiparasitic drugs (cf. Gerber et al. 2009). To achieve this, elucidation of the mechanisms that regulate this biosynthetic route is critical. The molecular mechanisms of this regulation at the protein level are still largely unknown and provide a promising target for future manipulations of this important pathway that will certainly be explored in the near future. It will be also important to identify the factors that are involved in the particular accumulation of the DXS protein.

Acknowledgments We thank Dr. Analilia Arroyo and Carolina San Román for contributing with experimental data and Dr. Mari Salmi for her critical review of this chapter. Financial support for this work has been provided by Dirección General de Asuntos para el Personal Académico-UNAM (IN208211), CONACYT (127546), and the Howard Hughes Medical Institute.

References

Bouvier F, Rahier A, Camara B (2005) Biogenesis, molecular regulation and function of plant isoprenoids. Prog Lipid Res 44:357–429

Carretero-Paulet L, Cairó A, Botella-Pavía P et al (2006) Enhanced flux through the methylerythritol 4-phosphate pathway in *Arabidopsis* plants overexpressing deoxyxylulose 5-phosphate reductoisomerase. Plant Mol Biol 62:683–695

Chahed K, Oudin A, Gh N, Hamdi S, Chénieux J-C, Rideau R, Clastre M (2000) 1-Deoxy-D-xylulose 5-phosphate synthase from periwinkle: cDNA identification and induced gene expression in terpenoid indole alkaloid-producing cells. Plant Physiol Biochem 38:559–566

Cordoba E, Salmi M, León P (2009) Unravelling the regulatory mechanisms that modulate the MEP pathway in higher plants. J Exp Bot 60:2933–2943

Cordoba E, Porta H, Arroyo A, San Roman C, Medina L, Rodriguez-Concepcion M, León P (2011) Functional characterization of the three genes encoding 1-deoxy-D-xylulose 5-phosphate synthase in maize. J Exp Bot 62:2023–2038

DellaPenna D, Pogson BJ (2006) Vitamin synthesis in plants: tocopherols and carotenoids. Annu Rev Plant Biol 57:711–738

Dubey VS, Bhalla R, Luthra R (2003) An overview of the non-mevalonate pathway for terpenoid biosynthesis in plants. J Biosci 28:637–646

Estévez JM, Cantero A, Reindl A, Reichler S, León P (2001) 1-Deoxy-D-xylulose-5-phosphate synthase, a limiting enzyme for plastidic isoprenoid biosynthesis in plants. J Biol Chem 276:22901–22909

Estévez JM, Cantero A, Romero C et al (2000) Analysis of the expression of *CLA1*, a gene that encodes the 1-deoxyxylulose 5-phosphate synthase of the 2-*C*-methyl-D-erythritol-4-phosphate pathway in *Arabidopsis*. Plant Physiol 124:95–103

Flores-Pérez U, Pérez-Gil J, Closa M et al (2010) PLEIOTROPIC REGULATORY LOCUS 1 (PRL1) integrates the regulation of sugar responses with isoprenoid metabolism in *Arabidopsis*. Mol Plant 3:101–112

Gerber E, Hemmerlin A, Hartmann M et al (2009) The Plastidial 2-*C*-Methyl-D-Erythritol 4-Phosphate Pathway Provides the Isoprenyl Moiety for Protein Geranylgeranylation in Tobacco BY-2 Cells. Plant Cell 21:285–300

Gong YF, Liao ZH, Guo BH, Sun XF, Tang KX (2006) Molecular cloning and expression profile analysis of *Ginkgo biloba DXS* gene encoding 1-deoxy-D-xylulose 5-phosphate synthase, the first committed enzyme of the 2-*C*-methyl-D-erythritol 4-phosphate pathway. Planta Med 72:329–335

Guevara-García AA, San Roman C, Arroyo A, Cortés ME, Gutiérrez-Nava ML, León P (2005) The characterization of the *Arabidopsis clb6* mutant illustrates the importance of post-transcriptional regulation of the methyl-D-erythritol 4-phosphate pathway. Plant Cell 17:628–643

Gutiérrez-Nava ML, Gillmor CS, Jiménez LF, Guevara-García A, León P (2004) *CHLOROPLAST BIOGENESIS* genes act cell and noncell autonomously in early chloroplast development. Plant Physiol 135:471–482

Harker M, Bramley PM (1999) Expression of prokaryotic 1-deoxy-D-xylulose-5-phosphatases in *Escherichia coli* increases carotenoid and ubiquinone biosynthesis. FEBS Lett 448:115–119

Hsieh MH, Goodman HM (2005) The *Arabidopsis IspH* homolog is involved in the plastid nonmevalonate pathway of isoprenoid biosynthesis. Plant Physiol 138:641–653

Julliard JH, Douce R (1991) Biosynthesis of the thiazole moiety of thiamin (vitamin B1) in higher plant chloroplasts. Proc Natl Acad Sci USA 88:2042–2045

Kim BR, Kim SU, Chang YJ (2005) Differential expression of three 1-deoxy-D-xylulose-5-phosphate synthase genes in rice. Biotechnol Lett 27:997–1001

Kuzuyama T, Takagi M, Takahashi S, Seto H (2000) Cloning and characterization of 1-deoxy-D-xylulose 5-phosphate synthase from *Streptomyces sp*. strain CL190, which uses both the mevalonate and nonmevalonate pathways for isopentenyl diphosphate biosynthesis. J Bacteriol 182:891–897

Lois LM, Rodríguez-Concepción M, Gallego F, Campos N, Boronat A (2000) Carotenoid biosynthesis during tomato fruit development: regulatory role of 1-deoxy-D-xylulose 5-phosphate synthase. Plant J 22:503–513

Lois LM, Campos N, Rosa-Putra S, Danielsen K, Rohmer M, Boronat A (1998) Cloning and characterization of

a gene from *Escherichia coli* encoding a transketolase-like enzyme that catalyzes the synthesis of 1-deoxy-D-xylulose 5-phosphate, a common precursor for isoprenoid, thiamin, and pyridoxol biosynthesis. Proc Natl Acad Sci USA 95:2105–2110

Mandel MA, Feldmann KA, Herrera-Estrella L, Rocha-Sosa M, León P (1996) *CLA1*, a novel gene required for chloroplast development, is highly conserved in evolution. Plant J 9:649–658

Morris WL, Ducreux LJ, Hedden P, Millam S, Taylor MA (2006) Overexpression of a bacterial 1-deoxy-D-xylulose 5-phosphate synthase gene in potato tubers perturbs the isoprenoid metabolic network: implications for the control of the tuber life cycle. J Exp Bot 57:3007–3018

Paetzold H, Garms S, Bartram S et al (2010) The isogene 1-deoxy-D-xylulose 5-phosphate synthase 2 controls isoprenoid profiles, precursor pathway allocation, and density of tomato trichomes. Mol Plant. 3:904–916

Phillips MA, D'Auria JC, Gershenzon J, Pichersky E (2008) The *Arabidopsis thaliana* type I isopentenyl diphosphate isomerases are targeted to multiple subcellular compartments and have overlapping functions in isoprenoid biosynthesis. Plant Cell 20:677–696

Rodríguez-Concepción M (2004) The MEP pathway: a new target for the development of herbicides, antibiotics and antimalarial drugs. Curr Pharm Des 10: 2391–2400

Rohdich F, Bacher A, Eisenreich W (2005) Isoprenoid biosynthetic pathways as anti-infective drug targets. Biochem Soc Trans 33:785–791

Rohmer M, Knani M, Simonin P, Sutter B, Sahm H (1993) Isoprenoid biosynthesis in bacteria: a novel pathway for the early steps leading to isopentenyl diphosphate. Biochem J 295:517–524

Sauret-Güeto S, Botella-Pavía P, Flores-Pérez U et al (2006) Plastid cues posttranscriptionally regulate the accumulation of key enzymes of the methylerythritol phosphate pathway in *Arabidopsis*. Plant Physiol 141:75–84

Sprenger GA, Schörken U, Wiegert T et al (1997) Identification of a thiamin-dependent synthase in *Escherichia coli* required for the formation of the 1-deoxy-D-xylulose 5-phosphate precursor to isoprenoids, thiamin and pyridoxol. Proc Natl Acad Sci USA 94:12857–12862

Umehara M, Hanada A, Yoshida S et al (2008) Inhibition of shoot branching by new terpenoid plant hormones. Nature 455:195–201

Vallabhaneni R, Wurtzel ET (2009) Timing and biosynthetic potential for carotenoid accumulation in genetically diverse germplasm of maize. Plant Physiol 150:562–572

Walter M, Fester T, Strack D (2000) Arbuscular mycorrhizal fungi induce the non-mevalonate methylerythritol phosphate pathway of isoprenoid biosynthesis correlated with accumulation of the yellow pigment and the other apocarotenoids. Plant J 21:571–578

Walter M, Hans J, Strack D (2002) Two distantly related genes encoding 1-deoxy-D-xylulose 5-phosphate synthases: differential regulation in shoots and apocarotenoid-accumulating mycorrhizal roots. Plant J 31: 243–254

Zeidler J, Schwender J, Müller C, Lichtenthaler HK (2000) The non-mevalonate isoprenoid biosynthesis of plants as a test system for drugs against malaria and pathogenic bacteria. Biochem Soc Trans 28: 796–798

Functional Analysis of HMG-CoA Reductase and Oxidosqualene Cyclases in *Arabidopsis*

32

Toshiya Muranaka and Kiyoshi Ohyama

Abstract

In plants, more than 200 triterpenes with various carbon skeletons have been found, of which some triterpenes are biologically active. Here we show recent detailed analyses on the biosynthetic genes and the mechanism of triterpene biosynthesis characteristic of higher plants. The studies presented here employed molecular genetic tools and organic chemistry methods to focus on the function of HMG-CoA reductase, the triterpene biosynthesis rate-limiting enzyme, and oxidosqualene cyclase, the enzyme catalyzing the formation of the cyclic triterpene skeletons.

Keywords

Arabidopsis • Lanosterol • Mevalonate • Mutant • NMR • Oxidosqualene cyclase • Sterol • Triterpenoid

32.1 Introduction

Triterpenes, natural organic compounds consisting of six isoprene units (C_5), are found among various plant and animal species. Some of them, such as sterols, are essential for biological activities as structural component of cell membranes and as precursors of plant and animal steroid hormones. Most are polycyclic, having carbon skeletons with (steroid type) four or five rings. Various cyclization and modification reactions of the common precursor squalene and oxidosqualene (C_{30}) can lead to extremely diverse structures. In particular, more than 200 triterpenes with varying carbon skeletons have been identified in plants (Xu et al. 2004; Connolly and Hill, 2007, 2008, 2010; Hill and Connolly 2011, 2012). Various compounds with quite diverse carbon skeletons are further metabolized by oxidation and glycosylation reactions being frequently unique to plant species, and the resulting entities are further diversified to serve in various

T. Muranaka (✉)
Department of Biotechnology, Graduate School of Engineering, Osaka University, 2-1 Yamadaoka Suita, Osaka 565-0871, Japan
e-mail: muranaka@bio.eng.osaka-u.ac.jp

K. Ohyama
Department of Chemistry and Materials Science, Tokyo Institute of Technology, Meguro, Tokyo 152-8551, Japan

T.J. Bach and M. Rohmer (eds.), *Isoprenoid Synthesis in Plants and Microorganisms: New Concepts and Experimental Approaches*, DOI 10.1007/978-1-4614-4063-5_32,

metabolic and physiological processes. Many of them are used as active ingredients of drugs and supplements (Mahato and Garai 1998; Lacaille-Dubois and Wagner 2000; Aleth and Dubois 2005; Aldo and Pinarosa 2006). Among the triterpenes, primary metabolites like cell membrane sterols and brassinosteroids have been long studied, as well as the biosynthetic pathways involved, including the functional elucidation of the corresponding genes. Although steroids contain many compounds that show important pharmacological activities, the biosynthesis of other compounds, such as triterpenols and triterpenoids, is complex and mostly unknown.

Here we show mainly our recent results focusing on triterpene biosynthesis regulation and the processes that diversify triterpenes: (1) HMG-CoA reductase, the rate-limiting enzyme in triterpene biosynthesis, and (2) oxidosqualene cyclases catalyzing the formation of cyclic triterpene skeletons in plants.

32.2 HMG-CoA Reductase, an Enzyme Responsible for the Rate-Limiting Step in Plant Triterpene Biosynthesis

The isoprene units, isopentenyl diphosphate (IPP) and dimethylallyl diphosphate (DMAPP) are synthesized through the mevalonic acid (MVA) pathway that commonly occurs in the eukaryotic cytoplasm. In plants, in addition to the MVA pathway, isoprene units are synthesized via the mevalonic acid-independent bacterial isoprenoid biosynthesis pathway, which occurs in the plastid. Although cross talk between pathways at the metabolic level occurs (Kasahara et al. 2002; Nagata et al. 2002; Hemmerlin et al. 2003), triterpenes are mainly synthesized by the MVA pathway (Lichtenthaler 1999). IPP and DMAP synthesized by the MVA pathway condense by a head-to-tail coupling reaction to form farnesyl diphosphate (FPP) that subsequently dimerizes by a tail-to-tail coupling reaction to form the triterpene intermediate, squalene. Squalene then oxidizes to form oxidosqualene, and various triterpene skeletons are synthesized through stereospecific cyclization reactions. Oxidation and glycosylation of these skeletons will in turn form cell membrane sterols, steroid hormones, and other triterpenoids. HMG-CoA reductase (HMGR) catalyzes the initial step of the MVA pathway and is understood to be the key enzyme in the pathway (Bach 1987; Goldstein and Brown 1990). In animals, HMGR is a rate-limiting enzyme in the cholesterol biosynthesis pathway and is highly regulated during transcriptional and post-transcriptional mechanisms (Goldstein and Brown 1990). In plants, HMGR constitutes a multigene family: two genes (*HMG1*, *HMG2*) encode HMGR in Arabidopsis (*Arabidopsis thaliana*) (Enjuto et al. 1994), three genes in potatoes (*Solanum tuberosum*) (Korth et al. 1997), and four genes in tomatoes (*Solanum lycopersicum*) (Daraselia et al. 1996), whereas in animals a single gene encodes HMGR. Differences in gene expression pattern between *HMG1* and *HMG2* in Arabidopsis have been reported. Although *HMG1* is expressed throughout all plant tissues, *HMG2* is only expressed in floral and meristematic tissues (Enjuto et al. 1994, 1995). *HMG1* expression is also controlled by light (Learned 1996; Learned and Connolly 1997). In potatoes, elicitor treatment inhibits *HMG1* expression and induces *HMG2* expression (Choi and Bostock 1994). These results indicate that biochemically seen HMGR is simply a catalyst that reduces HMG-CoA in plants. However, inside the plant body, each HMGR has its own unique function, and the functions of HMGRs are believed to vary from developmental to defensive processes.

The molecular mechanism on how these various HMGRs affect each downstream metabolites and how they distribute the functions was unknown. However, these mechanisms could be analyzed by using T-DNA insertional mutations in both *HMG1* and *HMG2* genes present in Arabidopsis. The *hmg1* mutant showed multidimensional phenotypes such as dwarfism, premature senescence, and male sterility (Suzuki et al. 2004). These phenotypes suggested the involvement of HMGR in isoprenoid type hormones such as cytokinins and brassinosteroids. However, the *hmg1* mutants did not contain decreased cytokinin levels and photomorphogenesis effects in the dark

that are characteristic of brassinosteroid-deficient mutants; therefore, defects in the balance of plant hormones are believed to be causative of growth effects in *hmg* mutants (Suzuki et al. 2004). The observation that the *hmg1* mutant phenotype can be rescued by administration of squalene, an acyclic triterpene (Suzuki et al. 2004), and being characterized by the decrease in sterols and triterpenols down to approximately 50% of the wild-type (Ohyama et al. 2007) indicates that triterpenes are involved in pleiotrophic, yet important phenomena such as dwarfism, early senescence, and male sterility. In contrast, although the *hmg2* mutants did not show any morphological phenotypes under normal growth conditions, the total sterol level was 18% and total triterpenol level was 27% less than that of the wild-type (Ohyama et al. 2007). Because *HMG1* expression levels are higher than *HMG2* expression levels (Enjuto et al. 1994), the differences in the gradually reduced sterols and triterpenols content between *hmg1* and *hmg2* mutants are believed to be due to such differences in their relative expression levels. However, because both *hmg* mutants showed a phenotype at the molecular level, even some marginal synthesis of 20% of sterols and triterpenols does not dramatically affect the biological activity. It is also interesting that there was a difference in the decreasing rate between sterol and triterpenol levels. In general, sterols are compounds that help to constitute the cell membrane, which is the minimum requirement for plant maintenance. Triterpenols are biosynthetic intermediates of the secondary metabolite triterpenoids, but their function is not well known. There may be some developmentally regulated mechanism to maintain essential internal sterol levels, and therefore, this may be the reason for the difference between sterol and triterpenol levels.

32.3 Cyclic Triterpene Skeleton Formation Catalysis by Oxidosqualene Cyclases

We have just seen that the two HMGRs of Arabidopsis are involved in sterol and triterpenol synthesis and that these triterpenes participate in pleiotrophic biological phenomena. What type of reaction pathways occurs downstream of HMGR for the synthesis of various triterpenes? Here, we review oxidosqualene cyclase (OSC), an enzyme responsible for the synthesis of various carbon skeletons.

32.3.1 Discovery of the Lanosterol Biosynthetic Gene in Plants

Sterols and triterpenols are synthesized by the cyclization of 2,3-oxidosqualene. The cyclization step catalyzed by oxidosqualene cyclase (OSC) is believed to be the initial conversion process that differentiates the sterol skeleton formation in plants from that in animals and yeasts (Abe et al. 1993). Although animals, yeasts, and plants synthesize oxidosqualene through the MVA pathway, oxidosqualene is subsequently metabolized to cholesterol in animals and ergosterol in yeasts, both through lanosterol as key intermediate. (From here on, sterol synthesis pathways via lanosterol will be referred to as the lanosterol pathway).

In plants, however, oxidosqualene is cyclized into cycloartenol (Benveniste et al. 1966, 1969; Ehrhardt et al. 1967; Rees et al. 1968; Heintz and Benveniste 1970) and subsequently metabolized to sterols (from here on, sterol biosynthesis through the intermediate cycloartenol will be referred to as the cycloartenol pathway) and have been described in text books. These results are mostly from tracer experiments using radiolabeled acetate, mevalonate, squalene, cycloartenol, and lanosterol (Grunwald 1975). Furthermore, *OSC* gene isolation from plants resulted in the isolation of a cycloartenol synthase gene (*CAS*) (Corey et al. 1993; Hayashi et al. 2000); *OSC* gene isolation from animals and yeasts resulted in the isolation of lanosterol synthase genes (*LAS*) (Baker et al. 1995; Corey et al. 1996). No contradictory results have yet been reported, thereby supporting the results of the tracer experiments.

When the entire genome of Arabidopsis was sequenced, it was found to contain 13 genes encoding *OSC* (Husselstein-Muller et al. 2001). The function of some of those genes was

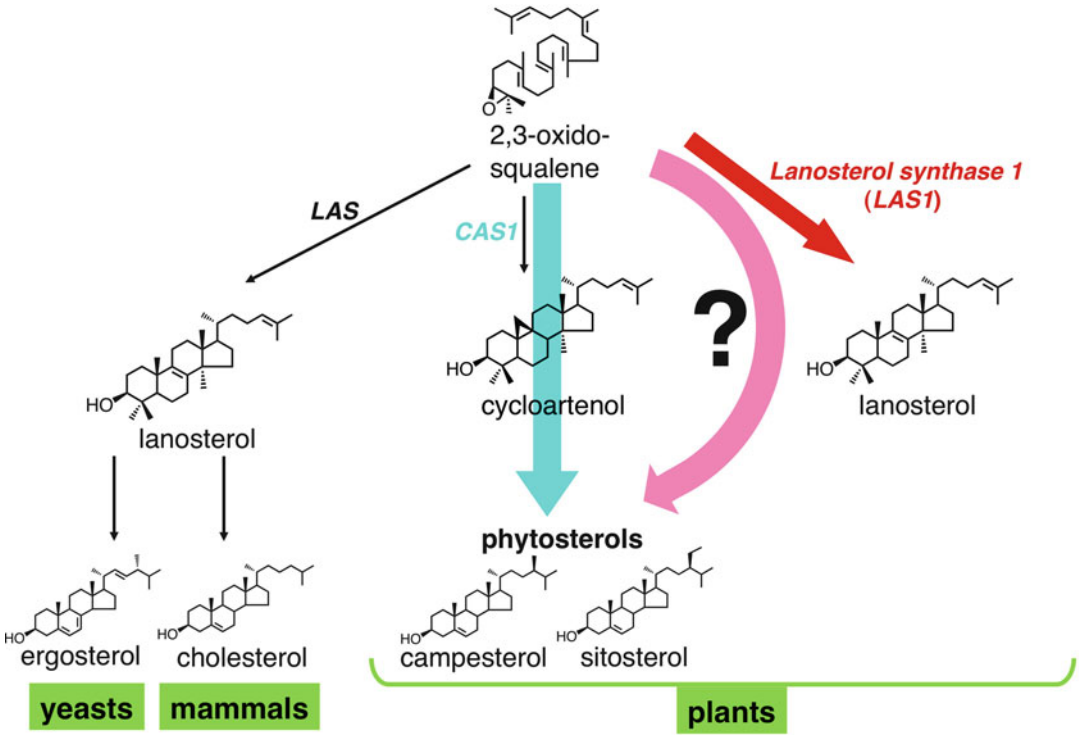

Fig. 32.1 Cyclization step of oxidosqualene in yeasts, mammals, and plants

elucidated by expression analyses in yeast (Phillips et al. 2006). A multifunctional enzyme that carries out multiple cyclization reactions, albeit being encoded by a single gene, has already been discovered. This enzyme is believed to catalyze a complex reaction mechanism. The assumption that an enzyme that synthesizes an unidentified triterpenol from Arabidopsis, which was elucidated by heterologous expression analysis in yeast, is valid; this could not be validated by plant metabolite analysis. Thus, some caution must be taken in the interpretation of results obtained with such plant enzymes expressed in yeast cells. Results obtained by bioinformatic analysis are still useful for identifying gene functions in plants.

Of the 13 genes, Arabidopsis is believed to have two enzyme genes (*At2g07050*, *At3g45130*) involved in the cyclization reaction of sterol skeletons. *At2g07050* was identified to be a cycloartenol synthase (*cycloartenol synthase 1* (*CAS1*)) by gene expression analysis in yeast (Fig. 32.1) (Corey et al. 1993). In contrast, although At3g45130 has a high amino acid sequence identity (64%) to CAS1, and its gene is therefore annotated as coding for a putative cycloartenol synthase, however, the activity has not been experimentally investigated. CAS and LAS use oxidosqualene as a substrate and similarly catalyze the synthesis of cyclic compounds through a protosteryl cation. Therefore, their primary structure is extremely similar, as presumably their secondary structure too. CAS has been reported to (Lodeiro et al. 2005) gain the ability to synthesize lanosterol on substitution of only one amino acid (Hart et al. 1999; Matsuda et al. 2000; Segura et al. 2002), and substitution of two amino acids (converts 481 isoleucine to valine, 477 histidine to asparagine) allows lanosterol to be selectively synthesized. When CAS1 and LAS1 were aligned to the peptide sequence of At3g45130, 481st and 477th residue corresponded to valine and asparagine, respectively. From these results, we concluded that *At3g45130*

does not encode the predicted cycloartenol synthase, but actually codes for a lanosterol synthase, which had not yet been isolated from plants.

Experiments conducted by using a yeast strain that cannot synthesize lanosterol indicated that *At3g45130* could functionally complement the lanosterol synthesis defect. When an extract from this yeast was analyzed by GC-MS and ^{1}H-NMR, lanosterol was found and thus, *At3g45130* was named *LAS1* (*LANOSTEROL SYNTHASE* 1) (Suzuki et al. 2006). Furthermore, the apparent accumulation of lanosterol in hairy roots highly expressing *At3g45130* indicated that LAS1 could synthesize lanosterol in plants. At the same time, Kolesnikova et al. (2006) also performed an expression analysis in yeast and presented evidence that *At3g45130* codes for a lanosterol synthase gene that was named *LSS* (*Lanosterol Synthase*). In addition, Sawai et al. (2006a) reported the isolation of a lanosterol synthase gene (*OSC7*) from *Lotus japonica*. Interestingly, all genes identified so far that code LAS enzymes originate from dicotyledonous plants. As by now, no *LAS* genes from monocotyledonous plants, for instance from rice as a model plant with a sequenced genome, have been reported.

32.3.2 Lanosterol Synthase Gene Was Isolated and Identified from Plants: Are Plant Sterols Synthesized from Lanosterol?

Studies on sterol biosynthesis were widely conducted from 1960 to 1970. Tracer experiments using radiolabeling, isolation, and identification of the putative intermediates were the principal methods employed in these studies. Although plants and cultures from algae (*Ochromonas malhamensis*) and plant tissues from tobacco (*Nicotiana tabacum*), pine trees (*Pinus pinea*), and peas convert [^{14}C]cycloartenol and [^{14}C] lanosterol into sterols, the precursor molecules [^{14}C]acetate and [^{14}C]MVL are converted only to cycloartenol, and detecting lanosterol from these cultures was difficult if not impossible, and therefore, its involvement could not be confirmed (Grunwald 1975).

These results indicated that plant sterols are synthesized through cycloartenol and lanosterol is converted to plant sterols because the C24 methylation and the C4 methyl group demethylase possess low substrate specificity. However, after adding high levels of exogenous lanosterol, it was believed to get it converted into plant sterols because of an "enzyme error" (Hewlins et al. 1969; Grunwald 1975). In contrast, lanosterol isolation in *Euphorbia* species has been reported in several studies (Ponsinet and Ourisson 1967, 1968a, b; Sekula and Nes 1980; Giner and Djerassi 1995; Giner et al. 2000). In such Euphorbia species, [^{14}C]acetate is metabolized to lanosterol, and [^{14}C]lanosterol is metabolized to sterols (Ponsinet and Ourisson 1968b; Baisted et al. 1968). However, the existence of a metabolic pathway converting cycloartenol to lanosterol has also been assumed (Ponsinet and Ourisson 1968b; Grunwald 1975). Even in *Euphorbia lathyris*, where lanosterol has been detected, the direct cyclization of oxidosqualene to lanosterol and its further being metabolized into downstream sterols has not yet been established.

Cycloartenol and lanosterol are believed to be synthesized through protonation and cyclization passing through a protosteryl cation intermediate. Proton elimination of the C19 methyl of this protosteryl cation forms cycloartenol, whereas the elimination of the C9 methine proton forms lanosterol. Therefore, for the formation of cycloartenol, a proton is eliminated from the C26 methyl group of oxidosqualene forming a cyclopropane, and for the formation of lanosterol, the methyl group is retained. Analyses focusing on the difference between these biosynthesis mechanisms were performed by Seo et al. (Seo et al. 1987, 1988, 1991).

Seo et al. distinguished the two pathways by observing the number of deuterium atoms in the C19 methyl group of the collected sterol by tracer experiments using [2-^{13}C^{2}H$_{3}$] acetate. By administering [2-^{13}C^{2}H$_{3}$] acetate and observing the number of deuterium in the C19 methyl group, they were able to identify the pathway that was followed for the synthesis. If a molecular species with three deuterium atoms is detected, it will be considered as being synthesized directly from oxidosqualene cyclization through lanosterol instead of being

formed through the cycloartenol pathway. In contrast, if a molecular species with two deuterium atoms is detected, it will be considered as synthesized through cycloartenol. The number of deuterium atoms in the C19 methyl group can be detected by isotope shifts in ^{13}C-NMR spectra. Upfield isotope shift due to the presence of deuterium is known to occur for approximately 0.3 ppm per 1 substitution and has additive effects (Sympson 1987). Observing upfield shifts of 0.6 ppm (two ^{2}H) or 0.9 ppm (three ^{2}H) for the C19 methyl group, thus, clarifies the pathway through which the sterol was synthesized. In normal ^{13}C-NMR (proton decoupled ^{13}C-NMR: ^{13}C-{^{1}H}NMR), coupling from ^{13}C and ^{2}H fractionates the signal and the spectra become complex and hard to analyze. The proton deuterium double decoupled ^{13}C-NMR (^{13}C-{^{1}H}{^{2}H}NMR) method reported by Seo et al. is an effective method. On this basis, Seo et al. demonstrated that in *Trichosanthes kirilowii* (Cucurbitaceae) tissue culture, yeast, and dog liver cells, plant sterols are synthesized through the cycloartenol pathway and the dominant sterols of yeasts (ergosterol) and of animals (cholesterol) are synthesized via the lanosterol pathway (Seo et al. 1987, 1988, 1991). However, when performing a [2-^{13}C^{2}H$_3$] acetate tracer experiment, one needs to consider that deuterium is inevitably substituted by solvent hydrogen before oxidosqualene cyclization and the isotope dilution comes from the chemical equilibrium when acetate is converted into MVA, mainly caused by the keto-enol tautomerization of acetoacetyl-CoA, accompanied by the exchange of protons. Therefore, when the contribution ratio of lanosterol pathway was found low, there existed some probability that the 0.6 ppm upfield shift (two ^{2}H held) could not be detected. We actually followed the method reported by Seo et al. and performed the [2-^{13}C^{2}H$_3$] acetate tracer experiments using Arabidopsis seedlings. The data obtained made clear that sterols were also synthesized through the cycloartenol pathway in this plant. However, a sterol biosynthesis pathway through lanosterol could not be established. These results predict that even if a lanosterol pathway existed, its contribution ratio to sterol biosynthesis was extremely low and suggested that an increase in sensitivity was necessary to identify this pathway.

The improvements that are necessary to increase sensitivity consist in eliminating the deuterium dilution outside the oxidosqualene cyclization and increasing the substrate incorporation rate. It has been revealed that the hydrogen of the C6 methyl group of MVA is not substituted during the pathway involving oxidosqualene (Goodwin 1979; Ramos-Valdivia et al. 1997). In addition, Kasahara et al. (2002) obtained sterols of approximately 80% higher labeling index by simultaneous application of [2-^{13}C]MVL and a HMG-CoA reductase inhibitor like lovastatin (= mevinolin). Therefore, it was assumed that sterol of higher labeling degree could be obtained and easier to be analyzed by simultaneously incubating with [6-^{13}C^{2}H$_3$]MVL in the presence of lovastatin (Fig. 32.2). Furthermore, in [6-^{13}C^{2}H$_3$] MVL tracer experiments, deuterium substitution is limited to the cyclization step, and therefore, the contribution of cycloartenol and lanosterol pathways in sterol biosynthesis can be traced down simultaneously. For that reason [6-^{13}C^{2}H$_3$] MVL was synthesized and a tracer experiment was performed (Ohyama et al. 2009).

Wild-type Arabidopsis seedlings were cultured in a liquid medium, supplemented with [6-^{13}C^{2}H$_3$]MVL and lovastatin. Sitosterol, a plant sterol present in high concentration, was isolated using HPLC and analyzed by ^{13}C-{^{1}H}{^{2}H} NMR. The results show that compared to the sitosterol sample signal, C18, C21, and C27 methyl group signals show an upfield shift of 0.88, 0.94, and 0.96 ppm, respectively, and in the C19 methyl group, an upfield shift of 0.59 ppm was detected. Three ^{2}H atoms were bound to C18, C21, and C17 methyl groups and two ^{2}H atoms were bound to C19, respectively. These results made clear that most phytosterols are synthesized through the cycloartenol pathway in Arabidopsis. However, careful observation of the C19 signal detected another signal from three bound ^{2}H atoms (upfield shift at 0.87 ppm) in addition to the signal from two bound ^{2}H atoms (upfield shift at 0.59 ppm). This peak had approximately 1.5% of the peak strength caused by two^{2}H atoms. To verify the significance of this peak, [6-^{13}C^{2}H$_3$] MVL tracer experiments were performed using plants overexpressing *LAS1* and plant with a *las1* mutation to analyze the C19 methyl group signal.

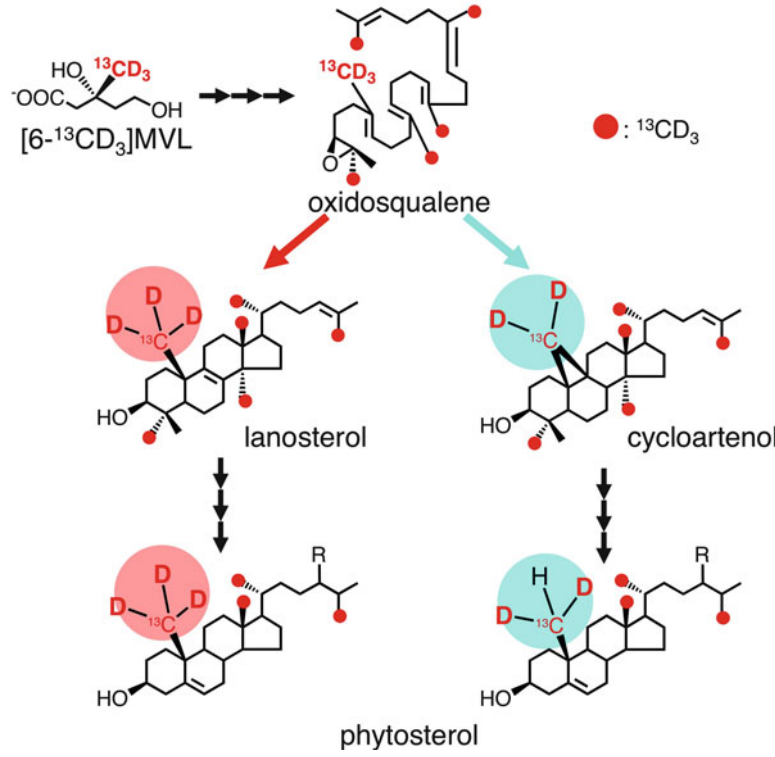

Fig. 32.2 Labeling pattern of phytosterol in the feeding experiment

From those results, the C19 signal of sitosterol isolated from the plant overexpressing *LAS1* showed an upfield shift to 0.87 ppm, which was three times more intense than that of the signal of the wild-type. This peak was not detected in sitosterol isolated from *las1* mutants. These results strongly suggest that sitosterol is also synthesized to some extent through the lanosterol pathway depending on the expression levels of *LAS1* (Ohyama et al. 2009).

Expression analysis of *CAS1* in yeasts revealed approximately 1% synthesis of lanosta-9(11),24-dien-3β-ol (parkeol), in addition to cycloartenol (Hart et al. 1999). Parkeol is thought to be synthesized when the proton at the C11 methyl group of protosteryl cation is eliminated. Therefore, should a pathway for the synthesis of this compound exist in plant sterol biosynthesis, three ^{2}H atoms would be detected at the C19 methyl group in [6-$^{13}C^{2}H_3$]MVL tracer experiments. Although parkeol has not yet been identified in Arabidopsis, from the above-mentioned experiments, the possibility that sitosterol with three ^{2}H at the C19 methyl group can be synthesized from parkeol cannot be eliminated. From the results of tracer experiments using *las1* mutants, the upfield shift of signal to 0.87 ppm, which was marked, could not be detected. From the above results, it is clear that the signal showing an upfield shift at 0.87 ppm was detected because it was the first cyclic intermediate synthesized during cyclization of oxidosqualene to lanosterol. This was the first result to directly indicate that the lanosterol pathway existed in plants (Ohyama et al. 2009).

32.3.3 Physiological Significance of the Lanosterol Pathway in Plants

A plant sterol biosynthesis pathway depending on lanosterol as the first cyclic intermediates has been shown to exist. However, why do two sterol skeleton formation pathways via cycloartenol and via lanosterol occur in plants? *CAS1* usually shows a constant level of expression in all plant organs

throughout development, but *LAS1* shows a slightly stronger expression in sheaths, stems, and roots. *CAS1* and *LAS1* are mildly expressed in inflorescences or leaves (Suzuki et al. 2006). Furthermore, when treated by methyl jasmonate, a compound involved in combating plant injury or disease, or when infected with *Pseudomonas syringae, LAS1* expression is stimulated, whereas *CAS1* expression levels remain constant (Arabidopsis eFP Browser: http://www.bar.utoronto.ca/efp/cgibin/efpWeb.cgi; TAIR: http://www.arabidopsis.org/). From such observations, it seems reasonable to assume that the activity of LAS and its reaction product lanosterol are involved in plant defense mechanisms (Kolesnikova et al. 2006).

Hence, plants produce triterpene compounds with various skeletons, some of which are believed to be involved in plant defense mechanisms. Although OSC in animals and yeasts are restricted to LAS, it is believed that plants evolved further OSC enzymes to form various triterpene skeletons. From amino acid sequence analysis, these OSCs are believed to have evolved from CAS (Zhang et al. 2003). LAS is phylogenetically located between OSC triterpenol and CAS (Sawai et al. 2006b). Therefore, LAS, similar to the other OSCs in plants, is believed to be recruited for secondary metabolite synthesis, being functional in defense mechanisms. Therefore, lanosterol-dependent pathways were postulated to be primarily involved in synthesis of steroid compounds as secondary metabolites, independent of some contribution to plant sterol synthesis. Previous analyses of Solanaceae and Lamiaceae plants showed, for instance, that under normal growth conditions, contributions of sterol/steroids synthesized through the lanosterol pathway are low and that steroid compounds are synthesized primarily through the cycloartenol pathway (Ohyama et al. unpublished). It will be necessary to understand the contribution of the lanosterol pathway in steroid biosynthesis by using plants stimulated from damage or disease, such as with methyl jasmonate.

Acknowledgements This work was supported in part by Grants-in-Aid for Scientific Research and Bilateral Program from JSPS, Japan, and Strategic International Cooperative Program from JST, Japan.

References

Abe I, Rohmer M, Prestwich GD (1993) Enzymatic cyclization of squalene and oxidosqualene to sterols and triterpenes. Chem Rev 93:2189–2206

Aldo T, Pinarosa A (2006) Chemical and biological activity of triterpene saponins from Medicago species. Nat Prod Commun 1:1159–1180

Aleth M, Dubois L (2005) Bioactive saponins with cancer related and immunomodulatory activity: recent developments. Stud Nat Prod Chem 32:209–246

Bach TJ (1987) Synthesis and metabolism of mevalonic acid in plants. Plant Physiol Biochem 25:163–178

Baisted DJ, Gardner RL, McReynolds LA (1968) Phytosterol biosynthesis from lanosterol in *Euphorbia peplus*. Phytochemistry 7:945–949

Benveniste P, Hirth L, Ourisson G (1966) La biosynthèse des stérols dans les tissus de tabac cultivés *in vitro*—II. Particularités de la biosynthèse des phytostérols des tissus de tabac cultivés *in vitro*. Phytochemistry 5:45–58

Benveniste P, Hewlins MJE, Fritig B (1969) La biosynthèse des stérols dans les tissus de tabac cultivés *in vitro*. Cinétique de formation des stérols et de leurs précurseurs. Eur J Biochem 9:526–533

Baker CH, Matsuda SPT, Liu DR, Corey EJ (1995) Molecular-cloning of the human gene encoding lanosterol synthase from a liver cDNA library. Biochem Biophys Res Commun 213:154–160

Choi D, Bostock RM (1994) Involvement of de novo protein synthesis, protein kinase, extracellular Ca^{2+}, and lipoxygenase in arachidonic acid induction of 3-hydroxy-3-methylglutaryl coenzyme A reductase genes and isoprenoid accumulation in potato (*Solanum tuberosum L.*). Plant Physiol 104:1237–1244

Connolly JD, Hill RA (2007) Triterpenoids. Nat Prod Rep 24:465–486

Connolly JD, Hill RA (2008) Triterpenoids. Nat Prod Rep 25:794–830

Connolly JD, Hill RA (2010) Triterpenoids. Nat Prod Rep 27:79–132

Corey EJ, Matsuda SPT, Baker CH, Ting AY, Cheng H (1996) Molecular cloning of a *Schizosaccharomyces pombe* cDNA encoding lanosterol synthase and investigation of conserved tryptophan residues. Biochem Biophys Res Commun 219:327–331

Corey EJ, Matsuda SPT, Bartel B (1993) Isolation of an *Arabidopsis thaliana* gene encoding cycloartenol synthase by functional expression in a yeast mutant lacking lanosterol synthase by the use of a chromatographic screen. Proc Natl Acad Sci USA 90:11628–11632

Daraselia ND, Tarchevskaya S, Narita JO (1996) The promoter for tomato 3-hydroxy-3-methylglutaryl coenzyme A reductase gene 2 has unusual regulatory elements that direct high-level expression. Plant Physiol 112:727–733

Ehrhardt JD, Hirth L, Ourisson G (1967) Études sur les triterpènes précurseurs des phytostérols. Recherche du

cycloarténol et du lanostérol dans diverses espèces végétales. Phytochemistry 6:815–821

Enjuto M, Balcells L, Campos N, Caelles C, Arró M, Boronat A (1994) *Arabidopsis thaliana* contains two differentially expressed 3-hydroxy-3-methylglutaryl-CoA reductase genes, which encode microsomal forms of the enzyme. Proc Natl Acad Sci USA 91:927–931

Enjuto M, Lumbreras V, Marín C, Boronat A (1995) Expression of the *Arabidopsis HMG2* gene, encoding 3-hydroxy-3-methylglutaryl coenzyme A reductase, is restricted to meristematic and floral tissues. Plant Cell 7:517–527

Giner J-L, Berkowitz JD, Andersson T (2000) Nonpolar components of the latex of *Euphorbia peplus*. J Nat Prod 63:267–269

Giner JL, Djerassi C (1995) A reinvestigation of the biosynthesis of lanosterol in *Euphorbia lathyris*. Phytochemistry 39:333–335

Goldstein JL, Brown MS (1990) Regulation of the mevalonate pathway. Nature 343:425–430

Goodwin TW (1979) Biosynthesis of triterpenoids. Annu Rev Plant Physiol 30:369–404

Grunwald C (1975) Plant sterols. Annu Rev Plant Physiol 26:209–236

Hart EA, Hua L, Darr LB, Wilson WK, Pang J, Matsuda SPT (1999) Directed evolution to investigate steric control of enzymatic oxidosqualene cyclization. An isoleucine-to-valine mutation in cycloartenol synthase allows lanosterol and parkeol biosynthesis. J Am Chem Soc 121:9887–9888

Hayashi H, Hiraoka N, Ikeshiro Y et al (2000) Molecular cloning and characterization of a cDNA for *Glycyrrhiza glabra* cycloartenol synthase. Biol Pharm Bull 23:231–234

Heintz R, Benveniste P (1970) Cyclisation de l'époxyde-2,3 de squalène par des microsomes extraits de tissus de tabac cultivés *in vitro*. Phytochemistry 9:1499–1503

Hemmerlin A, Hoeffler JF, Meyer O et al (2003) Cross-talk between the cytosolic mevalonate and the plastidial methylerythritol phosphate pathways in tobacco bright yellow-2 cells. J Biol Chem 278:26666–26676

Hewlins MJE, Ehrhardt JD, Hirth L, Ourisson G (1969) The conversion of [^{14}C]cycloartenol and [^{14}C]lanosterol into phytosterols by cultures of *Nicotiana tabacum*. Eur J Biochem 8:184–188

Hill RA, Connolly JD (2011) Triterpenoids. Nat Prod Rep 28:1087–1117

Hill RA, Connolly JD (2012) Triterpenoids. Nat Prod Rep 29:780–818

Husselstein-Muller T, Schaller H, Benveniste P (2001) Molecular cloning and expression in yeast of 2,3-oxidosqualene-triterpenoid cyclases from *Arabidopsis thaliana*. Plant Mol Biol 45:75–92

Kasahara H, Hanada A, Kuzuyama T, Takagi M, Kamiya Y, Yamaguchi S (2002) Contribution of the mevalonate and methylerythritol phosphate pathways to the biosynthesis of gibberellins in *Arabidopsis*. J Biol Chem 277:45188–45194

Kolesnikova MD, Xiong Q, Lodeiro S, Hua L, Matsuda SPT (2006) Lanosterol biosynthesis in plants. Arch Biochem Biophys 447:87–95

Korth KL, Stermer BA, Bhattacharyya MK, Dixon RA (1997) HMG-CoA reductase gene families that differentially accumulate transcripts in potato tubers are developmentally expressed in floral tissues. Plant Mol Biol 33:545–551

Lacaille-Dubois MA, Wagner H (2000) Bioactive saponins from plants: an update. Stud Nat Prod Chem 21: 633–687

Learned RM (1996) Light suppresses 3-hydroxy-3-methylglutaryl coenzyme A reductase gene expression in *Arabidopsis thaliana*. Plant Physiol 110:645–655

Learned RM, Connolly EL (1997) Light modulates the spatial patterns of 3-hydroxy-3-methylglutaryl coenzyme A reductase gene expression in *Arabidopsis thaliana*. Plant J 11:499–511

Lichtenthaler HK (1999) The 1-desoxy-D-xylulose-5-phosphate pathway of isoprenoid biosynthesis in plants. Annu Rev Plant Physiol Plant Mol Biol 50:47–65

Lodeiro S, Schulz-Gasch T, Matsuda SPT (2005) Enzyme redesign: two mutations cooperate to convert cycloartenol synthase into an accurate lanosterol synthase. J Am Chem Soc 127:14132–14133

Mahato SB, Garai S (1998) Triterpenoid saponins. Indian Institute of Chemical Biology, Calcutta, India. Prog Chem Org Nat Prod 74:1–196

Matsuda SPT, Darr LB, Hart EA et al (2000) Steric bulk at cycloartenol synthase position 481 influences cyclization and deprotonation. Org Lett 27:2261–2263

Nagata N, Suzuki M, Yoshida S, Muranaka T (2002) Mevalonic acid partially restores chloroplast and etioplast development in *Arabidopsis* lacking the non-mevalonate pathway. Planta 216:345–350

Ohyama K, Suzuki M, Kikuchi J, Saito K, Muranaka T (2009) Dual biosynthetic pathways to phytosterol via cycloartenol and lanosterol in *Arabidopsis*. Proc Natl Acad Sci USA 106:725–730

Ohyama K, Suzuki M, Masuda K, Yoshida S, Muranaka T (2007) Chemical phenotypes of the *hmg1* and *hmg2* mutants of *Arabidopsis* demonstrate the *in-planta* role of HMG-CoA reductase in triterpene biosynthesis. Chem Pharm Bull 55:1518–1521

Phillips DR, Rasbery JM, Bartel B, Matsuda SPT (2006) Biosynthetic diversity in plant triterpene cyclization. Curr Opin Plant Biol 9:305–314

Ponsinet G, Ourisson G (1967) Biosynthèse *in vitro* des triterpènes dans le latex d'*Euphorbia*. Phytochemistry 6:1235–1243

Ponsinet G, Ourisson G (1968a) Etudes chimiotaxonomiques dans la famille des Euphorbiacées 3. Répartition des triterpenes dans les latex d'*Euphorbia*. Phytochemistry 7:89–98

Ponsinet G, Ourisson G (1968b) Aspects particuliers de la biosynthèse des triterpènes dans le latex d'*Euphorbia*. Phytochemistry 7:757–764

Ramos-Valdivia AC, Van der Heijden R, Verpoorte R (1997) Isopentenyl diphosphate isomerase: a core enzyme in isoprenoid biosynthesis. A review of its biochemistry and function. Nat Prod Rep 14:591–603

Rees HH, Goad LJ, Goodwin TW (1968) Studies in phytosterol biosynthesis. Mechanism of biosynthesis of cycloartenol. Biochem J 107:417–426

Sawai S, Akashi T, Sakurai N et al (2006a) Plant lanosterol synthase: divergence of the sterol and triterpene biosynthetic pathways in eukaryotes. Plant Cell Physiol 47:673–677

Sawai S, Shindo T, Sato S et al (2006b) Functional and structural analysis of genes encoding oxidosqualene cyclases of *Lotus japonicus*. Plant Sci 170:247–257

Segura MJR, Lodeiro S, Meyer MM, Patel AJ, Matsuda SPT (2002) Directed evolution experiments reveal mutations at cycloartenol synthase residue His477 that dramatically alter catalysis. Org Lett 4: 4459–4462

Sekula BC, Nes WR (1980) The identification of cholesterol and other steroids in *Euphorbia pulcherrimma*. Phytochemistry 19:1509–1512

Seo S, Saito H, Uomori A, Yoshimura Y et al (1991) Biosynthesis of cholesterol and lanosterol in isolation dog hepatocytes: Incorporation of [1,2-$^{13}C_2$]- and [2-$^{13}C^2H_3$]-acetate, and [1-^{13}C]acetate and [1-$^2H_2$] ethanol. J Chem Soc Perkin I. 2065–2072

Seo S, Uomori A, Yoshimura Y, Takeda K et al (1987) Stereospecificity in the side-chain formation of 24β-ethylsterols in tissue cultures of *Trichosanthes kirilowii*. J Chem Soc Chem Commun. 1876–1878

Seo S, Uomori A, Yoshimura Y, Takeda K et al (1988) Biosynthesis of sitosterol, cycloartenol, and 24-methylenecycloartanol in tissue cultures of higher plants and of ergosterol in yeast from [1,2-$^{13}C_2$]- and [2-$^{13}C^2H_3$]-acetate and [5-$^{13}C^2H_2$]MVA. J Chem Soc Perkin I. 2407–2414

Suzuki M, Kamide Y, Nagata N, Seki H et al (2004) Loss of function of *3-hydroxy-3-methylglutaryl coenzyme A reductase 1* (*HMG1*) in *Arabidopsis* leads to dwarfing, early senescence and male sterility, and reduced sterol levels. Plant J 37:750–761

Suzuki M, Xiang T, Ohyama K, Seki H et al (2006) Lanosterol synthase in dicotyledonous plants. Plant Cell Physiol 47:565–571

Sympson TJ (1987) Applicaton of multinuclear NMR to structural and biosynthetic studies of polyketide microbial metabolites. Chem Soc Rev 16:123–160

Xu R, Fazio GC, Matsuda SPT (2004) On the origins of triterpenoid skeletal diversity. Phytochemistry 65: 261–291

Zhang H, Shibuya M, Yokota S, Ebizuka Y (2003) Oxidosqualene cyclases from cell suspension cultures of *Betula platyphylla* var. *japonica*: molecular evolution of oxidosqualene cyclases in higher plants. Biol Pharm Bull 26:642–650

Systems Understanding of Isoprenoid Pathway Regulation in *Arabidopsis*

33

Eva Vranová

Abstract

Recent technological advancement in molecular biosciences makes it possible to study biological processes at the systems level. At present, two main biological systems approaches are recognized: top-down and bottom-up. Top-down approach uses the "omics" data to characterize the system in a comprehensive way. Result of this approach is a topological or phenomenological molecular network. A bottom-up approach, on the contrary, uses an already defined network and kinetic properties of the individual network components to build a model with the predictive value. Systems understanding of plant isoprenoid pathway regulation is at present largely dominated by top-down approaches, as building of a complete dynamic model of isoprenoid pathway regulation requires prior identification of all elements of the isoprenoid pathway network and an associated regulatory network. In this chapter, an overview is given on the progress in systems biology research on isoprenoid pathway in a model plant *Arabidopsis thaliana.* First, an overview on existing resources to obtain *Arabidopsis* isoprenoid pathway gene network is presented. Second, available methods to obtain quantitative "omics" data with the focus on isoprenoid pathway are discussed. And lastly, systems biology approaches and their application to isoprenoid pathway research are shown.

Keywords

Arabidopsis • Isoprenoid gene network • Systems biology

E. Vranová (✉)
Department of Plant Biotechnology,
Institute of Plant Sciences, ETH Zurich, Zurich,
CH-8092, Switzerland
e-mail: evranova@ethz.ch

T.J. Bach and M. Rohmer (eds.), *Isoprenoid Synthesis in Plants and Microorganisms: New Concepts and Experimental Approaches*, DOI 10.1007/978-1-4614-4063-5_33,

33.1 Introduction

The isoprenoid pathway is a source of many essential plant metabolites that participate in diverse physiological processes. For example, the plant hormones gibberellins, abscisic acid, cytokinins, brassinosteroids, and apocarotenoids modulate developmental processes; chlorophyll and carotenoids are photosynthetic pigments; phytosterols are structural components of the membranes; ubiquinone, plastoquinone, and phylloquinone function as electron carriers; and dolichol phosphate as a sugar carrier during protein glycosylation. Moreover, many isoprenoids are mediators of plant-plant and plant-pathogen interactions. It is therefore expected that fluxes through the isoprenoid metabolic network will be controlled by environmental and developmental cues. In order to fully understand the regulation of the isoprenoid pathway, it is essential to study the behavior of the pathway in its entity and within a context of cellular metabolic and regulatory networks. With the availability of sequenced genomes and development of post-genomic technologies and high-throughput data analysis tools, the study of complex metabolic and regulatory networks is becoming feasible.

An ultimate goal of systems biology is to quantitatively describe responses of all the components of the living system with the vision to build predictive models. A complete systems biological approach requires the following: (1) a (complete) characterization of an organism in terms of what its molecular constituents are, with which molecules they interact, and how these interactions lead to cell function; (2) a spatiotemporal molecular characterization of a cell (e.g., component dynamics, compartmentalization, vesicle transport); and (3) a thorough analysis of the "molecular response" of a cell to external and internal perturbations. In addition, information from (1) and (2) must be integrated into mathematical models to enable knowledge testing by formulating predictions (hypotheses), the discovery of new biological mechanisms, calculation of the system behavior obtained under (3), and, finally, development of rational strategies for control and manipulation of cells (Bruggeman and Westerhoff 2007).

At present, we are still far from such systems modeling, and rather systems biology nowadays is dominated by development of methods and techniques to obtain and analyze the "omics" data, for example, transcriptome, proteome, and metabolome data. This approach is regarded as top-down approach, and its goal is to identify all molecular components of the system and to study molecular interaction networks on the basis of correlated molecular behavior or direct molecular interactions (Bruggeman and Westerhoff 2007; Bais et al. 2010).

Taking an isoprenoid pathway and its regulation as a system under study, the top-down approach will bring about information on structural components of the isoprenoid metabolic and regulatory network and on the interaction between the individual components of the system. Additionally, information on the interaction of this subsystem with the whole molecular network will be revealed.

33.2 Isoprenoid Pathway Gene Network Structure

Systems analysis of isoprenoid pathway regulation requires prior knowledge of the isoprenoid pathway gene network structure. Once the pathway network structure is defined, different modeling approaches can be applied to understand pathway regulation and integration into the cellular molecular networks. At present, the *Arabidopsis* isoprenoid pathway gene network is the most complete among the plant isoprenoid pathway gene networks and can be obtained from several resources. Gene networks originating from different resources vary in their comprehensiveness and the quality of the gene and pathway annotations (Table 33.1).

The most comprehensive and high-quality *Arabidopsis* isoprenoid pathway gene network has been constructed recently by Vranová et al. (2011; "*Arabidopsis thaliana* isoprenoid pathway database – AtIPD"). The list of *Arabidopsis* isoprenoid pathway genes underlying this network was created by compilation of data on pathways

Table 33.1 Characteristics of different *Arabidopsis* isoprenoid pathway gene networks

Arabidopsis isoprenoid pathway gene network	BioPathAt	AraCyc	KEGG	AtIPD
General features				
Reference database used to build isoprenoid pathway gene network	Expert-constructed database of isoprenoid pathway genes	MetaCyc	KEGG	BioPathAt
Homology search criterium	Sequence	Annotation	EC number	None
Manual curation	Fully	Partly	Partly	Fully
Pathways				
Methylerythritol phosphate pathway	x	x	x	x
Mevalonate pathway	x	x	x	x
Biosynthesis of prenyl PP (C10-Cn)	x	x	x	x
Plastoquinone biosynthesis	x	x	x	x
Chlorophyll biosynthesis	x	x	x	x
Tocopherol biosynthesis	x	x	x	x
Phylloquinone biosynthesis	x	x	x	x
Carotenoid biosynthesis	x	x	x	x
Apocarotenoid biosynthesis		x		x
Abscisic acid biosynthesis	x	x	x	x
Gibberellic acid biosynthesis	x	x	x	x
Monoterpenoid biosynthesis	x	x	x	x
Cytokinin biosynthesis		x	x	x
Sterol biosynthesis	x	x	x	x
Brassinosteroid biosynthesis	x	x	x	x
Triterpenoid biosynthesis	x	x		
Ubiquinone biosynthesis	x	x	x	x
Protein prenylation	x	x		x
Sesquiterpenoid biosynthesis	x	x		x
Diterpenoid biosynthesis	x			x

and pathway genes from Lange and Ghassemian (2003, 2005), from the KEGG (the "Kyoto Encyclopedia of Genes and Genomes"; Ogata et al. 1999; http://www.genome.jp/kegg) and the AraCyc (Mueller et al. 2003; Zhang et al. 2005; http://www.arabidopsis.org/biocyc) databases, and from the literature. Lange and Ghassemian (2003, 2005) isoprenoid gene database was used as a starting point because it represented the most curated version of the isoprenoid pathway database. Old pathway models were replaced and novel genes were added when their function or their homology to functional proteins had been demonstrated either in the literature or in case of genes annotated by homology, at least in TAIR (http://www.arabidopsis.org). In the last case, sequence alignments were inspected manually for the quality of hits. Compared with other available pathway databases, AtIPD is the best-annotated isoprenoid gene database. The database provides intuitive pathway maps and embedded information on subcellular localization, which can be searched or browsed, and provides links to the source information related to pathway models, enzyme activities, or subcellular enzyme localizations.

Information on the *Arabidopsis* isoprenoid pathway gene network can also be extracted from public online metabolic pathway databases like AraCyc and KEGG. The advantage of both pathway network repositories is that a pathway and gene database is regularly updated. The drawback

on the other side is that many reaction steps in the pathway are still missing and are wrongly annotated or coded for nonfunctional proteins. Moreover, complete pathway branches are often missing. This problem is inherent to the way how these pathway databases were created. AraCyc was computationally predicted using annotation terms as a criterion (Mueller et al. 2003), while KEGG used EC numbers as a homology search criterion (Ogata et al. 1999). Both were therefore dependent on the quality of gene annotations. Moreover, reference databases in both cases initially contained mainly metabolic pathways from non-plant organisms that generally lack plant-specific pathways such as hormone or secondary metabolite biosynthetic pathways. Although both plant metabolic pathway databases are being manually curated, the process is not yet completed. Additional disadvantage in some instances can be redundancy in pathway models (especially in AraCyc database) as different models are retained in the database. Although this type of redundancy is advantageous in discovery-oriented research, it does not help system-oriented research in which a system and its elements should reflect reality as closely as possible.

33.3 Acquirement of Quantitative Data

33.3.1 Transcriptome

Systems understanding of isoprenoid pathway regulation requires quantitative data on all elements of the cellular molecular network and that of the isoprenoid network in particular.

Genome-wide gene expression analysis was the first available method to obtain "omics" information. Nowadays, microarray analysis is considered a well-established method, and Affymetrix ATH1 genome arrays and more recently *Arabidopsis* Tiling 1.0R arrays are used to obtain *Arabidopsis* transcriptome data. In the last years, new generation sequencing (NGS) technologies are being used. Unlike microarrays, NGS technologies are not limited to sequenced genomes because they generate tags independently of knowledge of gene annotation. Genome-wide gene expression does not suffer substantially from the dynamic range problems and quantitative data for almost all gene network elements, including those of isoprenoid pathway genes can be obtained.

33.3.2 Proteome

Quantitative proteomics provides an excellent tool for the global characterization of protein abundance; however, standard methods are often limited by their sensitivity. This is a result of the high redundancy of protein identifications in nontargeted proteomics approaches, in which the same set of abundant proteins is repeatedly identified, while low-abundance proteins escape their detection. While the lack of analytical depth is a serious problem, undirected quantitative protein profiling is unbiased and provides insights into global proteome reorganizations. Such an undirected and unbiased approach may therefore reveal dependencies in the metabolism that were not expected.

Table 33.2 gives an overview of the different methods for protein quantification. Two different quantitative proteomics approaches can be distinguished: relative and absolute protein quantification. Absolute quantification provides information about the exact concentration of a given protein in a cell and can be based on protein staining methods or stable-isotope-based mass spectrometric approaches. Relative quantification reveals those proteins whose abundance changes in response to a signal. High-throughput relative protein quantification methods include two-dimensional gel electrophoresis, stable isotope techniques such as isotope tagging for relative and absolute quantification (iTRAQ) or isotope-coded affinity tag (ICAT), and label-free relative quantification approaches via peptide total ion current in LC-chromatograms.

Despite its importance, there is currently no robust high-throughput method for the reliable absolute quantification of proteins in complex mixtures. Because peptides differ widely in their ionization efficiencies and flight properties, ion current readout as used for the relative quantification

Table 33.2 High-throughput quantification methods used in proteomics (reviewed in Baginsky 2008)

Protein quantification	Procedure	Rationale
Relative quantification		
Two-dimensional gel electrophoresis (2D-PAGE)	The protein complement of 2 or more differentially treated samples is compared, either between different gels or on the same gel after differential labeling (DIGE)	Proteins that are affected by the treatment decrease or increase in abundance (determined by staining), and modified proteins will be shifted in molecular mass and/or isoelectric point
Isotope-coded affinity tag (ICAT)	Isotope labeling at Cys, mixing of two samples	Intensity read-back (TIC) comparison of isotopically labeled and unlabeled peptide
Isotope tagging for relative and absolute quantitation (iTRAQ)	Isotope labeling at primary amine groups, mixing of up to eight samples	Intensity read-back (TIC) comparison of reporter ions dissociated from differentially labeled peptides
Total ion current (TIC) comparison	Peptide's TIC read-back in two different samples	Identical ionization properties of identical peptides allow TIC comparison between different LC runs (neglects ion suppression effects)
Metabolic labeling	Labeling of de novo synthesized proteins by growing cells on ^{15}N-containing media as the only nitrogen source	Proteins from cells grown with ^{15}N as the only nitrogen source can be distinguished from those of other cells by a mass shift in MS, quantification by intensity read-back ratio (TIC)
Stable isotope labeling with amino acids in cell culture (SILAC)	Similar to metabolic labeling, but instead of inorganic ^{15}N, labeled amino acids are provided	Proteins from cells grown with labeled amino acids can be distinguished from those of other cells by a mass shift in MS, quantification by intensity read-back ratio (TIC)
Absolute quantification		
Spiking isotopically labeled peptide into sample (absolute quantification; AQUA)	Isotope labeling of selected peptides, spiking into sample	Comparison of native peptide to TIC of labeled peptide with known concentration
Peptide count (absolute protein expression index; APEX)	Counting identified peptides per protein, normalization to expected peptides or MW and overall sampling depth	Number of detected peptides is proportional to protein abundance
Staining methods combined with gel electrophoresis	Intensity, combined with MS-based protein identification	Staining intensity is proportional to protein abundance

is unsuitable for absolute quantification purposes. In order to circumvent this limitation, Gerber and colleagues (2003) suggested spiking stable-isotope-labeled peptides at known concentrations into a complex peptide mixture, followed by screening for pairs of native and spiked peptides in the mass spectrometry measurement (Fig. 33.1 and Table 33.2). The detection of such a pair allows inferring the concentration of the native peptide by calculating the ion current ratio between spiked and native peptide (Gerber et al. 2003). Because most mass spectrometers are also excellent mass filters, this approach can be performed in a peptide-specific manner, in which the complete analysis is focused only on a set of peptides of interest (i.e., those that were used for spiking). Those peptides that unambiguously identify a protein and are most likely to be detected in a complex mixture can be selected from existing proteome maps and used for such a quantitative proteome survey (presented in Kuster et al. 2005). Proof of concept for this strategy in the plant proteomics field came from the quantification of sucrose synthase in a highly complex leaf proteome sample by multiple reaction monitoring (Wienkoop and Weckwerth 2006).

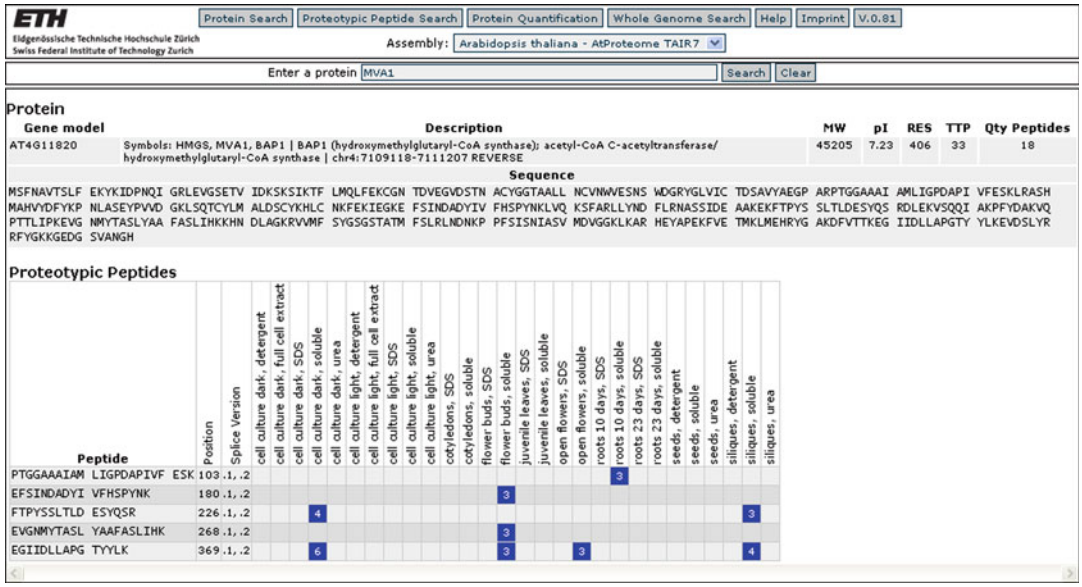

Fig. 33.1 Selection of proteotypic peptides for absolute protein quantification via multiple reaction monitoring (MRM). The detectability of proteotypic peptides not only depends on intrinsic peptide characteristics such as ionization and dissociation properties but also on the dynamic composition of the proteome sample. Thus, the optimal selection of proteotypic peptides is difficult to predict, and therefore, public proteomics data repositories should be consulted before designing a MRM experiment. The example presented above is taken from AtProteome (Baerenfaller et al. 2008), which provides information about organ-specific proteotypic peptides, in this case for HMGS (At4g11820). The numbers in the highlighted boxes furthermore indicate the number of spectra that were identified for the indicated peptide in the respective organ

Such a scenario is excellently suited for the characterization of enzymes active in an individual pathway, because it permits focusing the analysis on a number of selected peptides, which allows a mass spectrometer to operate at an optimal duty cycle. This renders the analysis highly sensitive, and also, low-abundance components in metabolic pathways can be detected and quantified. In order to select a set of peptide markers that are most likely detectable in complex samples, some information about the peptide traceability and the composition of the proteome sample is necessary. *Arabidopsis thaliana* is sufficiently well characterized for targeted proteomics surveys, because high-density organ-specific proteome maps have become available for this organism. With the availability of comprehensive information about proteotypic peptides, targeted quantitative measurements of enzymes in a pathway can be performed. Peptides are selected for the desired proteins (e.g., from www.atproteome.ethz.ch), synthesized with an isotope tag, and spiked into a complex proteome sample. The mass spectrometric survey is then designed in a way that in MS1 only the mass range of the spiked peptides and in MS2 the transition to one specific product ion for each peptide is scanned and analyzed.

With the procedure detailed above, the absolute abundance of the enzymes involved in isoprenoid biosynthesis can be measured under a number of different conditions. Additionally, quantitative information about the protein constituents of a pathway can be used to build a kinetic model of the pathway.

33.3.3 Metabolome

While comprehensive analysis of transcriptome and proteome is quite advanced, a truly comprehensive analysis of metabolome remains a vision

for the future. The highly diverse chemical properties of metabolites present the crucial limiting factor. This high diversity impedes comprehensive metabolomics with single analytical technologies. Thus, the current developments in metabolomic technologies focus on establishment and optimization of minimally overlapping, broad-spectrum metabolite profiling methods (Steinhauser and Kopka 2007). Additionally, metabolome quantification is hindered by the lack of simple extraction methods that would recover all plant metabolites with the same efficiency, and nowadays, different classes of compounds are rather extracted through the use of optimized solvents. Moreover, for the low abundant compounds, enrichment methods, such as solid phase extraction, are used (Sumner et al. 2007).

Profiling of isoprenoids also suffers from the diverse chemical composition of the compounds and from the low abundance of many of them. The most comprehensive coverage of isoprenoid compounds so far was achieved by Fraser et al. (2000). Carotenoids, tocopherols, quinones, and chlorophylls were simultaneously extracted, separated, and quantified. Chloroform (compared to hexane, light petroleum, diethyl ether, and ethyl acetate) proved to be the most suitable solvent to efficiently extract this broad range of isoprenoids.

Another approach focused on concomitant profiling of several classes of isoprenoid compounds, namely, on phytohormones. Several plant hormones are synthesized by isoprenoid pathway. Chiwocha et al. (2003) established method in which at least three of them – abscisic acid, gibberellic acid, and cytokinins – are detected and quantified simultaneously. In addition to end-product analysis, a few approaches were undertaken to analyze broad range of intermediates, mainly prenyl diphosphates and mevalonate (MVA) and methylerythritol phosphate (MEP) pathway intermediates (McCaskill and Croteau 1993; Lange et al. 2001; Henneman et al. 2011).

Further optimization is required to establish a method for the simultaneous and comprehensive analysis of isoprenoid compounds. Ideally, concomitant analysis of isoprenoids, together with other secondary and primary metabolic compounds, would be best appreciated to understand isoprenoid pathway regulation in the whole genome context. Extraction and analytical methods that can accommodate the wide range of chemical properties represented by the different classes of compounds must be developed. Furthermore, the analytical method must be extremely selective to enable quantification of the relatively lower level metabolites in the presence of more abundant compounds. The enhanced interest in plant secondary metabolism and further improvement in sensitivity of analytic instruments will certainly bring about major improvements in obtaining "omics" data for complete metabolome profiling in a near future.

33.4 Top-Down Systems Biology Approaches and Their Application to Isoprenoid Pathway Research

Top-down systems biology emerged with the introduction of the "omics" technologies as a predominant systems biology approach. It starts from a bird's eye view of the behavior of the system – from the top or the whole – by measuring genome-wide experimental data and aims to discover and characterize biological mechanisms closer to the bottom – that is, the parts and their interactions. In the early stages, the experiments aim to discover the identity of the components. Later, the main objective is to determine correlations between concentrations of molecules, and in the end, hypotheses are formulated concerning co- and inter-regulation of groups of those molecules (Bruggeman and Westerhoff 2007).

33.4.1 Post-genomic Data Visualization Tools

Simple visualization of the relative or absolute expression values by using one of the post-genomic data visualization tools can be a first step to evaluate the behavior of the system. There are several bioinformatic tools allowing visualization of one or multiple post-genomic data sets

Table 33.3 Post-genomic data visualization tools

Tool name/URL	Pathway gene database	Modularity		
		Multiple data viewer	User "omics" data	User pathway
KaPPA-View http://kpv.kazusa.or.jp/kpv3/guestIndex.jsp	Lange and Ghassemian 2003, 2005 – updated OR KEGG	Yes	Yes	Yes
Pathway tools omics viewer http://www.arabidopsis.org:1555/expression.html	AraCyc	Yes	Yes	No
KeggArray http://www.genome.ad.jp/kegg/expression/	KEGG	Yes	Yes	No
Genevestigator http://www.genevestigator.ethz.ch/	Lange and Ghassemian 2003	No	No	No
MapMan http://gabi.rzpd.de/projects/MapMan/	Few pathways OR AtIPD	Yes	Yes	Yes
MetNet http://metnet.vrac.iastate.edu/	AraCyc	Yes	Yes	No

directly on the biochemical pathway maps (Table 33.3). Currently, the best way to visualize isoprenoid metabolic pathway data is the use of the MapMan tool (http://mapman.gabipd.org/web/guest/mapman; Thimm et al. 2004) together with the pathway images, image annotation files, and mapping file from the AtIPD database (http://www.atipd.ethz.ch). The advantages are as follows: (1) an expert-curated isoprenoid gene database; (2) user-friendly, intuitive, simple graphical representation; (3) embedded information on subcellular localization; and (4) possibility to customize pathway images to visualize other quantitative protein or metabolite data or to add structural and regulatory network elements.

Another tool where post-genomic data for isoprenoid pathway can be displayed is KaPPA-View (http://kpv.kazusa.or.jp/kpv4/; Tokimatsu et al. 2005). An advantage is that in addition to transcriptomic, metabolomic data can be displayed and the tool allows also gene-to-gene and/or metabolite-to-metabolite relationships such as co-expression correlations. A disadvantage of the tool is that the gene network is based on either the Lange and Ghassemian (2003, 2005) gene database or KEGG (the "Kyoto Encyclopedia of Genes and Genomes"; Ogata et al. 1999; http://www.genome.jp/kegg) gene databases that are less accurate and there is no subcellular localization displayed on the maps.

Post-genomic data for isoprenoid pathway can be displayed also with Pathway Tools Omics Viewer (Mueller et al. 2003). The advantage of this tool is that it is easy to handle and that it provides a bird's eye view on changes in all metabolic pathways. The disadvantage compared to above-mentioned tools is that the annotation quality of the underlying database (AraCyc) and visualizations are not optimal. For example, individual pathways are not interconnected, not all isogenes are displayed on the overview image, and there is no information on subcellular localization displayed. Another web tool allowing visualization of post-genomic data on the isoprenoid metabolic gene network is KegArray (Kanehisa et al. 2002). The KegArray tool is based on the KEGG database where coverage of the isoprenoid network is quite good, but a drawback is, as mentioned earlier, the nonoptimal pathway gene annotation and no easy way to visualize the data.

Other visualization tools such as MetNet (Wurtele et al. 2003) are using AraCyc database and MapMan (Thimm et al. 2004; Usadel et al. 2005) and possess only limited own gene network information related to the isoprenoid pathway.

An alternative to visualize post-genomic expression data is Genevestigator (http://www.genevestigator.ethz.ch/; Zimmermann et al. 2004; Zimmermann et al. 2005) that has isoprenoid pathway gene network based on the Lange and Ghassemian (2003) pathway gene annotation. A disadvantage is that own expression data cannot be uploaded, and only data stored in the reference expression database can be displayed.

33.4.2 Network Analysis

The construction of molecular networks based on quantitative "omics" data is an advanced form of post-genomic data analysis. Data are not solely visualized; rather, casual relationships among them are sought out. Gene expression networks are so far the most common types of networks inferred using the post-genomic data, because mRNA levels are the easiest to measure at genome-wide scale. Gene expression networks, as other intracellular networks, can be analyzed at different levels (Schöner et al. 2007).

33.4.2.1 Cluster Identification

Clustering is the simplest way of network analysis and is primarily targeted to find group of co-expressed genes; thereby co-regulated or functionally related genes may be identified. The main advantage of this approach is the general applicability and the availability of efficient – and for the biological community! – easily understandable algorithms. A disadvantage is that clustering usually provides only a rough picture of the underlying network, and other methods are needed for inferring more specific network characteristics (Schöner et al. 2007).

The goal of clustering is to find group of genes that have similar expression patterns. Genes with similar expression fall into the same cluster, whereas dissimilar items fall into different clusters. A simple and easy-to-read description of similarity measures and clustering algorithms can be found in short review of D'Haeseleer (2005). Briefly, most clustering algorithms use a matrix of a pair-wise distance between genes as input. So far, most clustering studies in the gene expression literature use either Euclidean or Pearson correlation between expression profiles as a distance measure. Based on the calculated distance measure, genes are assigned to different clusters. There are two types of clustering algorithms: hierarchical and partitional. Hierarchical algorithms find successive clusters using previously established clusters (hierarchical clustering), whereas partitional algorithms determine all clusters at once (*k*-means and self-organizing maps).

Gene expression clustering is first of all used for simple visualization of gene expression profiles. Beyond that, clustering is used to identify *cis*-regulatory sequences in the promoters of tightly co-expressed genes. Gene expression clusters also tend to be significantly enriched for specific functional categories – which may be used to infer a functional role for unknown genes in the same cluster (D'Haeseleer 2005).

Clustering proved to be a useful tool in identification of different regulatory mechanisms in regulation of isoprenoid pathway genes in *Arabidopsis* during de-etiolation. Ghassemian et al. (2006) applied genome-wide gene expression profiling to evaluate the regulation of biochemical pathways during photomorphogenesis. Etiolated *Arabidopsis thaliana* seedlings were irradiated with continuous red light (Rc), which led to rapid greening, or continuous far-red light (FRc), which did not result in visible greening. Interestingly, exposure to FRc resulted in enhanced expression of all pathway genes similarly to Rc-irradiated plants. To evaluate the transcriptional regulation in a detailed way, *k*-means cluster analysis was applied to genes significantly deregulated over the time course. Five clusters with the same genes were identified in both Rc- and Frc-irradiated seedlings. Despite very similar time course of expression between the Rc- and Frc-irradiated seedlings, genes in three clusters displayed different dynamics of induction. Chlorophyll and carotenoid biosynthetic genes were present in these clusters. Such subtle but potentially important differences in the regulation of isoprenoid pathway genes by experimental treatments (in this case Rc and FRc) could not be readily identified if gene clustering would not be applied to analyze gene expression.

33.4.2.2 Topology Inference

Topology inference is another method to find group of co-regulated genes. The main advantage of topology inference over clustering is a graphical representation of expression relationships between the genes in the network. Genes are here defined as nodes. Edges, called also links, are drawn between the nodes in case of mutual co-expression relationship. Expression topology networks are assembled according to co-regulation of genes and the magnitude of regulation (Aoki et al. 2007). In comparison with cluster analysis, genes are not only grouped into the clusters, which are here defined as modules, but relationship of genes across modules is also displayed. As such, modules of densely connected nodes that have a sparsely connected periphery are generated (Fig. 33.2).

Currently, the most widely used computational method to calculate expression relationship involves calculating standard Pearson correlation coefficients between pairs of genes (Ma et al. 2007). A pair of genes with a Pearson correlation coefficient larger than a preselected threshold is considered to reveal functional interaction, influence, or dependence, and links are drawn between such genes (nodes). Correlation coefficients between genes are calculated using the own expression data sets. Alternatively, researchers can retrieve correlation coefficients from public databases using various data mining tools such as AthCoR@CSB.DB – The A. thaliana co-response database (http://csbdb.mpimp-golm.mpg.de/csbdb/dbcor/ath.html; Steinhauser et al. 2004), ATTED-II – *Arabidopsis thaliana trans*-factor and *cis*-element prediction database (http://atted.jp; Obayashi et al. 2007), and BAR-Expression Angler (http://bbc.botany.utoronto.ca/; Toufighi et al. 2005). Usually, large-scale expression data from multiple experiments are used, as information originating from multiple experiments is more robust and not biased towards a specific experiment. It has been calculated that in order to obtain a robust co-expression network, more than hundred arrays should be used to calculate correlation coefficient. After finding the co-expression module, the validity of the module is evaluated by a statistical test, based on random sampling or permutation (Aoki et al. 2007). To visualize co-expression, network viewers such as Pajek (http://vlado.fmf.uni-lj.si/pub/networks/pajek/), BioLayout (http://www.biolayout.org/), or Cytoscape (http://www.cytoscape.org) are used.

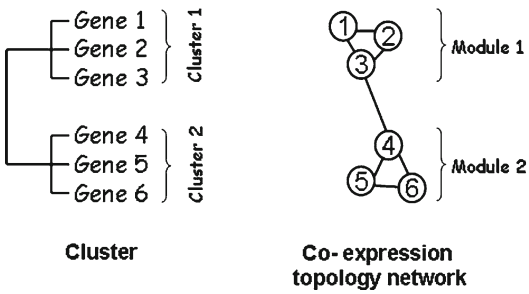

Fig. 33.2 Comparison of cluster analysis and topology network inference in co-expression analysis. While in cluster analysis genes are "forced" to be part of clusters and only the "relationship" between different clusters is displayed (here, clusters 1 and 2), in co-expression topology network inference, the relationship between individual genes in modules is retained (here, genes 3 and 4 represent connection between modules 1 and 2, respectively)

In principle, there are two approaches to build a co-expression topology network: In a first approach, the targeted approach, bait genes or group of genes related to the biological question are used to calculate correlation coefficients. In a second, the knowledge-independent approach, correlation coefficients are calculated between all genes taken for the analysis. While the first approach is primarily focused to search genes that are functionally related to the bait genes, the second approach aims to find novel modules of functionally related (co-expressed) genes in the entire co-expression network(Aoki et al. 2007).

In the simplest form, co-expression analysis is used to annotate metabolic genes with unknown topology. It has been demonstrated for several organisms, including *Arabidopsis*, that metabolic pathways are enriched for co-expressed genes, and genes involved in the same metabolic pathway are co-expressed to a greater degree than genes involved in different pathways (Ihmels et al. 2004; Wille et al. 2004; Wei et al. 2006). Yet overrepresentation of genes from one metabolic pathway among the co-expressed genes points out to which pathway an unknown gene belongs.

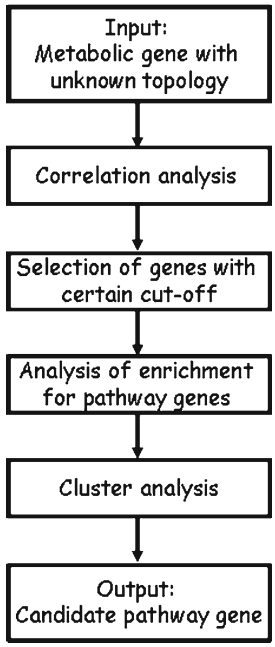

Fig. 33.3 Experimental flow chart of co-expression analysis to annotate metabolic genes with unknown topology. Gene of interest is used as a bait to calculate pair-wise correlation coefficient with other metabolic pathway genes. Once the correlation coefficient is calculated, a cut-off is made arbitrarily. In general, genes with the correlation coefficient higher than 0.6 are selected for the analysis, and the gene list is screened for the presence of pathway genes. Enrichment for genes of the certain pathway is evaluated empirically or using an appropriate statistical test (Ehlting et al. 2008). Once the pathway genes are selected, original expression profile of selected genes is displayed. This is to ensure that selected genes are "truly" co-expressed genes and that the high correlation coefficient is not a result from co-expression of otherwise "silent" genes that are expressed only under a few conditions (Aoki et al. 2007)

Typical experimental flow chart for such analysis is presented in Fig. 33.3. Co-expression analysis was, for example, used to annotate an acetoacetyl-CoA thiolase AACT2 (At5g48230) as a thiolase active in mevalonate pathway (Carrie et al. 2007; Ahumada et al. 2008) and to map number of cytochrome P450 monooxygenases to isoprenoid pathways (Ehlting et al. 2008).

Acetoacetyl-CoA thiolase encodes an enzyme that catalyzes the first committed step in the mevalonic acid pathway, synthesis of acetoacetyl-CoA from acetyl-CoA. In *Arabidopsis*, five structurally similar thiolase genes are present in the genome. Based on similarities with mammalian and yeast genome, they are, besides mevalonate biosynthesis, implicated in lipid and amino acid catabolism (Carrie et al. 2007). The probable function of three of these five thiolases (KAT2, KAT5, ACAT2) was examined by analysis of gene co-expression in microarray data from *Arabidopsis* (Carrie et al. 2007). The Expression Angler correlation tool from the Botany Array Resource (BAR; Toufighi et al. 2005) was used to find the most co-expressed genes based on microarray hybridization data on *Arabidopsis* 22 K gene chips. Twenty-five genes with highest correlation coefficient were inspected for the presence of relevant metabolic genes. Mevalonate pathway genes were found only in the group of genes co-expressed with *AACT2* (At5g48230). To confirm the co-expression groups, genes and their cohort of metabolic co-expressed genes were clustered using different series of microarray data, in this case Genevestigator (Zimmermann et al. 2004) tissue-specific expression data. The bootstrapped cluster tree confirmed results of co-expression analysis, placing *AACT2* (At5g48230) and co-expressed mevalonic acid (MVA) pathway genes in separate clade of the tree.

Cytochrome P450 monooxygenases play prominent roles in a diverse set of metabolic pathways, but the function of most of these enzymes remains obscure. Ehlting et al. (2008) used publicly available large-scale expression data sets to perform co-expression analysis comparing the expression vector of each P450 with 4,130 *Arabidopsis* genes that were annotated as metabolic pathway genes in various pathway annotation databases. Co-expressed genes with a correlation coefficient of more than 0.5 were selected. At least 79 new candidate pathway genes were co-expressed with the plastidial isoprenoid pathway genes, and 63 P450s were co-expressed with the triteprene, sterol, and brassinosteroid metabolic genes. Many P450s identified by co-expression analysis have been previously shown *in vivo* to be part of the isoprenoid biosynthetic pathway (Helliwell et al. 2001; Kim et al. 2005; Kim and DellaPenna 2006), demonstrating that co-expression analysis is a powerful tool to annotate metabolic gene with unknown topology.

In the above-mentioned approaches, a single gene was used as bait. To find genes associated with the group of the functionally related genes, such as, for example, pathway genes, Wei et al. (2006) proposed some modification to the correlation analysis. Genes for the network are selected not solely on their correlation coefficient or similar measure but also on the number of links to the individual pathway genes. As a rule, genes are considered related to the pathway when multiple (more than one) members of a given pathway are correlated to them.

Nontargeted co-expression network analysis has been performed using 1,330 *Arabidopsis* metabolic pathway genes from AraCyc database, including genes from the isoprenoid pathway (Wei et al. 2006). Similar to the analysis in other organisms (Ihmels et al. 2004), *Arabidopsis* genes associated with the same metabolic pathway were, on average, more highly co-expressed than genes from different pathways. It was also demonstrated that pathways involved in core metabolic pathways such as glycolysis, tricarboxylic acid (TCA) cycle, and the pentose phosphate pathway, which produce precursors for many other pathways, were more tightly co-regulated as noncore or peripheral biochemical pathways. From pathways associated with isoprenoid metabolism, carotenoid and chlorophyll biosynthetic pathways displayed the tightest level of transcriptional coordination. In addition, Wei et al. (2006) also demonstrated that similarly to yeast (Magwene and Kim 2004), distribution of co-expression links per gene is highly skewed, with a small but significant number of genes having numerous co-expression partners, but most having fewer than ten. Genes with multiple connections (hubs) tend to be single-copy genes, while genes with multiple paralogs are co-expressed with fewer genes, on average, than single-copy genes. No untargeted analysis was performed with isoprenoid pathway genes only.

To create a topology network using the correlation coefficient is quite easily performed and therefore very popular. The disadvantage, however, is that such networks may lead to ambiguous results, especially when the network is heavily connected (Ma et al. 2007). An alternative method, the graphical Gaussian model (GGM; Whittaker 1990), uses partial correlations as the source for a robust assessment of a direct interaction between any gene pair. Different from Pearson correlation that records correlation between gene pairs without regard to other genes, partial correlation between two genes measures the degree of correlation remaining after removing the effects of other genes (Ma et al. 2007). This means that direct interactions are distinguished from indirect interactions, and therefore, partial correlation coefficients do provide a strong measure of dependence. Recent studies have demonstrated that GGM is a useful tool to infer conditional dependency structure and to reconstruct network-like associations among genes (Li and Gui 2006; Wille et al. 2004; Wille and Bühlmann 2006; Ma et al. 2007).

GGM has been used by Wille et al. (2004) to infer gene co-expression network in the isoprenoid pathway (Fig. 33.4). Data from 118 *Arabidopsis* GeneChip microarrays were used, and a network of 40 isoprenoid-related genes associated with both mevalonate (MVA) and methylerythritol phosphate (MEP) pathway was modeled.

In the MEP pathway, the genes *DXR* (At5g62790), *MCT* (At2g02500), *CMK* (At2g26930), and *MECPS* (At1g63970) were shown to be almost fully connected. Similarly, the genes *AACT2* (At5g48230), *HMGS* (At4g11820), *HMGR2* (At2g17370), *MK* (At5g27450), *MPDC1* (At2g38700), *FPPS1* (At4g17190), and *FPPS2* (At5g47770) share many edges in the MVA pathway. This is in agreement with the result from the *Arabidopsis* metabolic network analysis, which showed that genes associated with the same metabolic pathway are, on average, more highly co-expressed (Wei et al. 2006).

From the group of MEP pathway genes, there were a few edges to genes in the MVA pathway. Among these genes, *AACT1* (At5g47720) and *HMGR1* (At1g76490) form candidates for cross talk between the MEP and the MVA pathway because they have no further connection to the MVA pathway. Their correlation to MEP pathway genes is always negative. From the MVA pathway genes, edges were found to *IPPI1* (At3g02780) and *GGPPS12* (At4g38460) in the MEP pathway. Whereas *IPPI1* (At3g02780) is

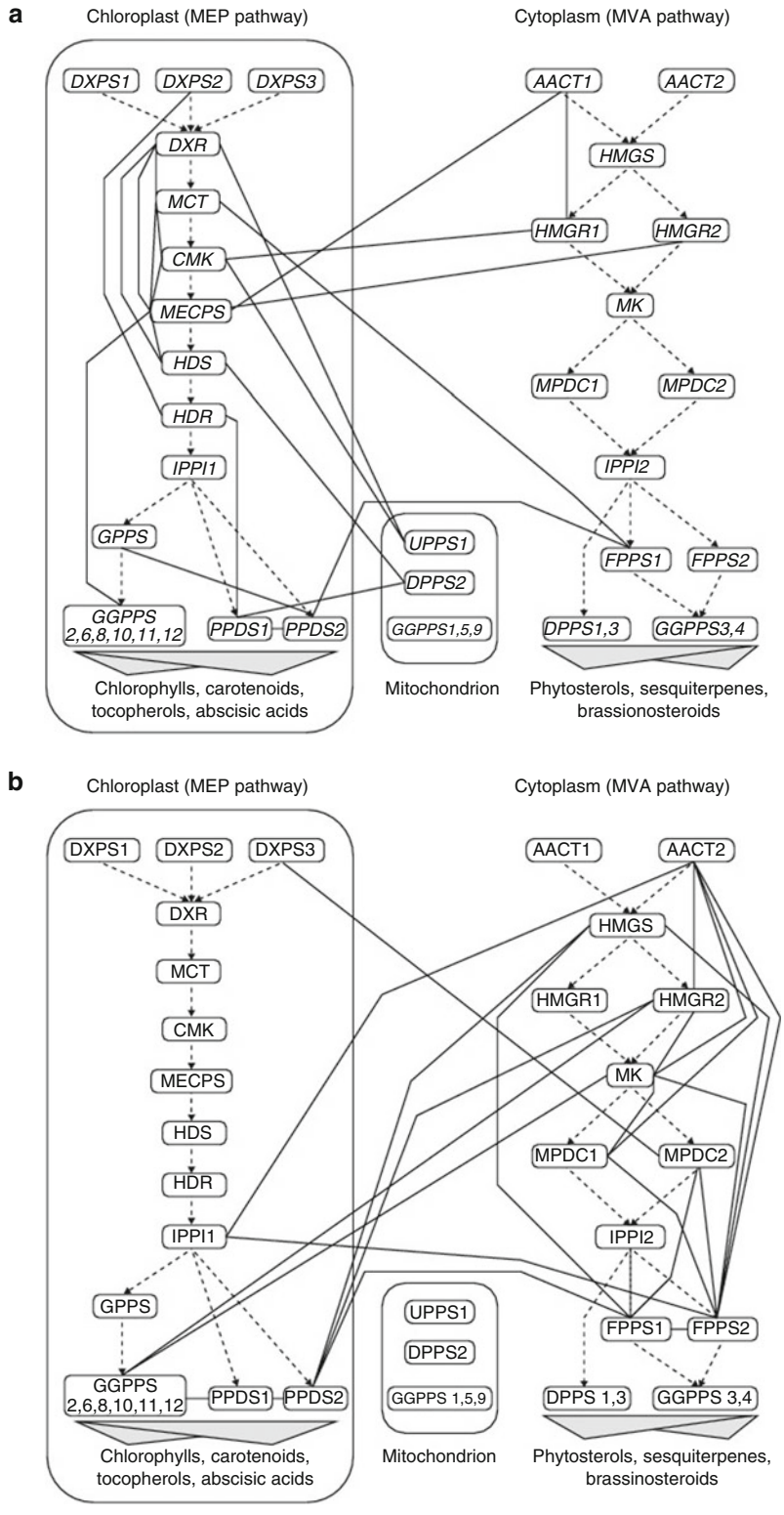

Fig. 33.4 Dependencies between genes of the isoprenoid pathways according to the frequentist modified GGM method (Wille et al. 2004). (**a**) Subgraph of the gene module in the MEP pathway and (**b**) subgraph of the gene module in the MVA pathway. The solid undirected edges connecting individual genes (in *boxes*) represent the GGM. *Dotted* directed edges mark the metabolic network and are not part of the GGM. The *gray* shading indicates metabolic links to downstream pathways

positively correlated with MVA pathway genes, *GGPPS12* (At4g38460) displays negative correlation. Interestingly, although *IPPI1* (At3g02780) gene product was generally considered to be localized in the plastids, it was recently shown that it also localizes to the cytosol (Okada et al. 2008; Phillips et al. 2008). This demonstrates the power of predictive function for co-expression network inference.

Following construction of the isoprenoid gene network, 795 additional genes from 56 metabolic pathways were incorporated. Among these were genes from pathways downstream of the two isoprenoid biosynthesis pathways, such as phytosterol biosynthesis, mono- and diterpene metabolism, porphyrin/chlorophyll metabolism, carotenoid biosynthesis, and plastoquinone biosynthesis, for example. Interestingly, from all 56 metabolic pathways considered, predominantly genes from isoprenoid downstream pathways fitted well into the isoprenoid network. These results suggested a close regulatory connection between isoprenoid biosynthesis genes and groups of downstream genes. On the one hand, strong connections were found between the MEP pathway and the plastoquinone, the carotenoid, and the chlorophyll pathways. On the other hand, the plastoquinone and phytosterol biosynthesis pathways appear to be closely related to the genetic network of the MVA pathway.

33.4.3 Integration of "Omics" Data

Integration of different "omics" data is useful to reveal at what molecular level regulatory routes of organism contribute to the pathway behavior. As to obtain quantitative genome-wide protein and metabolite data is still not possible at present, only a few studies describe integration of different "omics" data in the analysis of isoprenoid pathway regulation, using data of limited size.

Laule et al. (2003) applied genome-wide gene expression profiling to reveal a cross talk between the mevalonate (MVA) pathway and methylerythritol (MEP) pathway following inhibition of either of them. Gene expression analysis was accompanied by analysis of chlorophylls, carotenoids, and sterols. Treatment of seedlings with lovastatin (inhibitor of the MVA pathway) resulted in a transient decrease in sterol levels and a transient increase in carotenoid as well as chlorophyll levels. After the initial drop, sterol amounts in lovastatin-treated seedlings recovered to levels above controls. As a response to fosmidomycin treatment (MEP pathway block), a transient increase in sterol levels was observed, whereas chlorophyll and carotenoid amounts decreased dramatically when compared with controls. Ninety-six hours after fosmidomycin addition, the levels of all metabolites assayed (sterols, chlorophylls, and carotenoids) were substantially lower than in controls. Interestingly, these inhibitor-mediated changes were not reflected in altered gene expression levels of the genes involved in sterol, chlorophyll, and carotenoid metabolism. The lack of correlation between gene expression patterns and the accumulation of isoprenoid metabolites indicates that posttranscriptional processes may play an important role in regulating the flux through isoprenoid metabolic pathways.

In the de-etiolation experiment with *Arabidopsis thaliana* seedlings, described earlier in this chapter, Ghassemian et al. (2006) used genome-wide gene expression profiling in combination with metabolite analysis to evaluate the regulation of biochemical pathways during photomorphogenesis. Irradiation of etiolated *Arabidopsis thaliana* seedlings with continuous red light (Rc) led to rapid greening, whereas continuous far-red light (FRc) did not result in visible greening. The process of de-etiolation in seedlings irradiated with Rc was associated with the accumulation of chlorophylls a and b, xanthophylls, β-carotene, phylloquinone, and α-tocopherol, and enhanced accumulation of metabolites was associated with enhanced gene expression of the respective pathway genes. Interestingly, exposure to FRc resulted in enhanced expression of all genes similarly to Rc-irradiated plants, but chlorophyll a, chlorophyll b, β-carotene, and xanthophylls were not synthesized, suggesting that transcriptional regulation is not sufficient to control flux via isoprenoid pathways in this case.

Both examples clearly demonstrate how integration of different molecular data, in this

case changes in the transcript and metabolite abundances, enhances the level of understanding of isoprenoid pathway regulation.

33.4.4 Concluding Remarks and Outlook

Dynamic network inference represents the ultimate goal of network analysis. Here, the focus is on network dynamics, which is essential for understanding and predicting the system's behavior. Building a complete dynamic model of isoprenoid pathway regulation would first require identification of all elements of isoprenoid pathway network and associated regulatory network. This can be achieved by improvement of quantitative proteomics and metabolomics technologies and by building phenomenological models using these "omics" data. Later, bottom-up modeling approaches should be used to extend such model to dynamic regulatory and metabolic network model (Rios-Estepa and Lange 2007). Some initial studies to obtain kinetic models of isoprenoid metabolism (although on small network scale) have already been initiated (Sielewiesiuk and Gruszecki 1991; Latowski et al. 2000; Zimmer et al. 2000; Rios-Estepa et al. 2008), and it is likely that both top-down and bottom-up approaches will evolve simultaneously to ultimately merge and give a systems understanding of isoprenoid pathway regulation.

Acknowledgments I thank Sacha Baginsky for his contribution and critical comments on this chapter.

References

Ahumada I, Cairó A, Hemmerlin A et al (2008) Characterization of the gene family encoding acetoacetyl-CoA thiolase in *Arabidopsis*. Funct Plant Biol 35:1100–1111

Aoki K, Ogata Y, Shibata D (2007) Approaches for extracting practical information from gene co-expression networks in plant biology. Plant Cell Physiol 48:381–390

Baerenfaller K, Grossmann J, Grobei MA et al (2008) Genome-scale proteomics reveals *Arabidopsis thaliana* gene models and proteome dynamics. Science 320:938–941

Baginsky S (2008) Plant proteomics: concepts, applications and novel strategies for data interpretation. Mass Spectrom Rev. doi:10.1002/mas.20183

Bais P, Moon SM, He K et al (2010) PlantMetabolomics.org: a web portal for plant metabolomics experiments. Plant Physiol 152:1807–1816

Bruggeman FJ, Westerhoff HV (2007) The nature of systems biology. Trends Microbiol 15:45–50

Carrie C, Murcha M, Millar A et al (2007) Nine 3-ketoacyl-CoA thiolases (KATs) and acetoacetyl-CoA thiolases (ACATs) encoded by five genes in *Arabidopsis thaliana* are targeted either to peroxisomes or cytosol but not to mitochondria. Plant Mol Biol 63:97–108

Chiwocha SDS, Abrams SR, Ambrose SJ et al (2003) A method for profiling classes of plant hormones and their metabolites using liquid chromatography-electrospray ionization tandem mass spectrometry: an analysis of hormone regulation of thermodormancy of lettuce (*Lactuca sativa* L.) seeds. Plant J 35:405–417

D'Haeseleer P (2005) How does gene expression clustering work? Nat Biotech 23:1499–1501

Ehlting J, Sauveplane V, Olry A et al (2008) An extensive (co-)expression analysis tool for the cytochrome P450 superfamily in *Arabidopsis thaliana*. BMC Plant Biol 8:47. doi:10.1186/1471-2229-8-47

Fraser PD, Pinto MES, Holloway DE et al (2000) Application of high-performance liquid chromatography with photodiode array detection to the metabolic profiling of plant isoprenoids. Plant J 24:551–558

Gerber SA, Rush J, Stemman O et al (2003) Absolute quantification of proteins and phosphoproteins from cell lysates by tandem MS. Proc Natl Acad Sci USA 100:6940–6945

Ghassemian M, Lutes J, Tepperman JM et al (2006) Integrative analysis of transcript and metabolite profiling data sets to evaluate the regulation of biochemical pathways during photomorphogenesis. Arch Biochem Biophys 448:45–59

Helliwell CA, Chandler PM, Poole A et al (2001) The CYP88A cytochrome P450, *ent*-kaurenoic acid oxidase, catalyzes three steps of the gibberellin biosynthesis pathway. Proc Natl Acad Sci USA 98:2065–2070

Henneman L, van Cruchten AG, Kulik W, Waterham HR (2011) Inhibition of the isoprenoid biosynthesis pathway; detection of intermediates by UPLC-MS/MS. BBA – Mol Cell Biol L 1811:227–233

Ihmels J, Levy R, Barkai N (2004) Principles of transcriptional control in the metabolic network of *Saccharomyces cerevisiae*. Nat Biotechnol 22:86–92

Kanehisa M, Goto S, Kawashima S et al (2002) The KEGG databases at GenomeNet. Nucleic Acid Res 30:42–46

Kim J, DellaPenna D (2006) Defining the primary route for lutein synthesis in plants: the role of *Arabidopsis* carotenoid β-ring hydroxylase CYP97A3. Proc Natl Acad Sci USA 103:3474–3479

Kim G-T, Fujioka S, Kozuka T et al (2005) CYP90C1 and CYP90D1 are involved in different steps in the brassinosteroid biosynthesis pathway in *Arabidopsis thaliana*. Plant J 41:710–721

Kuster B, Schirle M, Mallick P et al (2005) Scoring proteomes with proteotypic peptide probes. Nat Rev Mol Cell Biol 6:577–583

Lange BM, Ketchum REB, Croteau RB (2001) Isoprenoid biosynthesis. Metabolite profiling of peppermint oil gland secretory cells and application to herbicide target analysis. Plant Physiol 127:305–314

Lange BM, Ghassemian M (2003) Genome organization in *Arabidopsis thaliana*: a survey for genes involved in isoprenoid and chlorophyll metabolism. Plant Mol Biol 51:925–948

Lange BM, Ghassemian M (2005) Comprehensive post-genomic data analysis approaches integrating biochemical pathway maps. Phytochemistry 66: 413–451

Latowski D, Burda K, Strzalka K (2000) A mathematical model describing kinetics of conversion of violaxanthin to zeaxanthin *via* intermediate antheraxanthin by the xanthophyll cycle enzyme violaxanthin de-epoxidase. J Theor Biol 206:507–514

Laule O, Fürholz A, Chang H-S et al (2003) Crosstalk between cytosolic and plastidial pathways of isoprenoid biosynthesis in *Arabidopsis thaliana*. Proc Natl Acad Sci USA 100:6866–6871

Li H, Gui J (2006) Gradient directed regularization for sparse Gaussian concentration graphs, with applications to inference of genetic networks. Biostatistics 7:302–317

Ma S, Gong Q, Bohnert HJ (2007) An *Arabidopsis* gene network based on the graphical Gaussian model. Genome Res 17:1614–1625

Magwene P, Kim J (2004) Estimating genomic coexpression networks using first-order conditional independence. Genome Biol 5:R100. doi:10.1186/gb-2004-5-12-r10

McCaskill D, Croteau R (1993) Procedures for the isolation and quantification of the intermediates of the mevalonic acid pathway. Anal Biochem 215:142–149

Mueller LA, Zhang P, Rhee SY (2003) AraCyc: a biochemical pathway database for *Arabidopsis*. Plant Physiol 132:453–460

Obayashi T, Kinoshita K, Nakai K et al (2007) ATTED-II: a database of co-expressed genes and *cis* elements for identifying co-regulated gene groups in *Arabidopsis*. Nucleic Acids Res 35:D863–D869

Ogata H, Goto S, Sato K et al (1999) KEGG: Kyoto encyclopedia of genes and genomes. Nucleic Acids Res 27:29–34

Okada K, Kasahara H, Yamaguchi S et al (2008) Genetic evidence for the role of isopentenyl diphosphate isomerases in the mevalonate pathway and plant development in *Arabidopsis*. Plant Cell Physiol 49: 604–616

Phillips MA, D'Auria JC, Gershenzon J et al (2008) The *Arabidopsis thaliana* type I isopentenyl diphosphate isomerases are targeted to multiple subcellular compartments and have overlapping functions in isoprenoid biosynthesis. Plant Cell 20:677–696

Rios-Estepa R, Lange BM (2007) Experimental and mathematical approaches to modeling plant metabolic networks. Phytochemistry 68:2351–2374

Rios-Estepa R, Turner GW, Lee JM et al (2008) A systems biology approach identifies the biochemical mechanisms regulating monoterpenoid essential oil composition in peppermint. Proc Natl Acad Sci 105: 2818–2823

Schöner D, Barkow S, Bleuler S et al (2007) Network analysis of systems elements. In: Baginsky S, Fernie AR (eds) Plant systems biology. Birkhäuser, Basel

Sielewiesiuk J, Gruszecki WI (1991) A simple model describing the kinetics of the xanthophyll cycle. Biophys Chem 41:125–129

Steinhauser D, Kopka J (2007) Methods, applications and concepts of metabolite profiling: primary metabolism. In: Baginsky S, Fernie AR (eds) Plant systems biology. Birkhäuser, Basel

Steinhauser D, Usadel B, Luedemann A et al (2004) CSB. DB: a comprehensive systems-biology database. Bioinformatics 20:3647–3651

Sumner L, Huhman D, Urbanczyk-Wochniak E et al (2007) Methods, applications and concepts of metabolite profiling: Secondary metabolism. In: Baginsky S, Fernie AR (eds) Plant systems biology. Birkhäuser, Basel

Thimm O, Blasing O, Gibon Y et al (2004) Mapman: a user-driven tool to display genomics data sets onto diagrams of metabolic pathways and other biological processes. Plant J 37:914–939

Tokimatsu T, Sakurai N, Suzuki H et al (2005) KaPPA-View. A web-based analysis tool for integration of transcript and metabolite data on plant metabolic pathway maps. Plant Physiol 138:1289–1300

Toufighi K, Brady SM, Austin R et al (2005) The Botany Array Resource: e-northerns, expression angling, and promoter analyses. Plant J 43:153–163

Usadel B, Nagel A, Thimm O et al (2005) Extension of the visualization tool MapMan to allow statistical analysis of arrays, display of corresponding genes, and comparison with known responses. Plant Physiol 138:1195–1204

Vranová E, Hirsch-Hoffmann M, Gruissem W (2011) AtIPD: a curated database of *Arabidopsis* isoprenoid pathway models and genes for isoprenoid network analysis. Plant Physiol 156:1655–1660

Wei H, Persson S, Mehta T et al (2006) Transcriptional coordination of the metabolic network in *Arabidopsis*. Plant Physiol 142:762–774

Whittaker J (1990) Graphical models in applied multivariate statistics. Wiley, New York

Wienkoop S, Weckwerth W (2006) Relative and absolute quantitative shotgun proteomics: targeting low-abundance proteins in *Arabidopsis thaliana*. J Exp Bot 57:1529–1535

Wille A, Bühlmann P (2006) Low-order conditional independence graphs for inferring genetic networks. Stat Appl Genet Mol Biol 5: Article 1. http://www.bepress.com/sagmb/vol5/iss1/art1. Accessed 4 Jan 2006

Wille A, Zimmermann P, Vranová E et al (2004) Sparse graphical Gaussian modeling of the isoprenoid gene network in *Arabidopsis thaliana*. Genome Biol 5:R92. doi:10.1186/gb-2004-5-11-r92

Wurtele E, Li J, Diao L et al (2003) MetNet: software to build and model the biogenetic lattice of *Arabidopsis*. Comp Funct Genom 4:239–245

Zhang P, Foerster H, Tissier CP et al (2005) MetaCyc and AraCyc. Metabolic pathway databases for plant research. Plant Physiol 138:27–37

Zimmer W, Bruggemann N, Emeis S et al (2000) Process-based modelling of isoprene emission by oak leaves. Plant Cell Environ 23:585–595

Zimmermann P, Hennig L, Gruissem W (2005) Gene-expression analysis and network discovery using Genevestigator. Trends Plant Sci 10:407–409

Zimmermann P, Hirsch-Hoffmann M, Hennig L et al (2004) GENEVESTIGATOR. *Arabidopsis* microarray database and analysis toolbox. Plant Physiol 136: 2621–2632

Index

T.J. Bach and M. Rohmer (eds.), *Isoprenoid Synthesis in Plants and Microorganisms: New Concepts and Experimental Approaches*, DOI 10.1007/978-1-4614-4063-5,

Q

R

S